UNCLASSIFIED

AD NUMBER
AD221585
CLASSIFICATION CHANGES
TO: **UNCLASSIFIED**
FROM: **CONFIDENTIAL**
LIMITATION CHANGES
TO: **Approved for public release; distribution is unlimited.**
FROM: **Distribution authorized to U.S. Gov't. agencies and their contractors; Administrative/Operational Use; 1946. Other requests shall be referred to Office of Scientific Research and Development, Washington, DC 20301.**
AUTHORITY
SOD memo dtd 2 Aug 1960; SOD memo dtd 2 Aug 1960

THIS PAGE IS UNCLASSIFIED

UNCLASSIFIED

SUMMARY TECHNICAL REPORT
OF THE
NATIONAL DEFENSE RESEARCH COMMITTEE

This document contains information affecting the national defense of the United States within the meaning of the Espionage Act, 50 U.S.C., 31 and 32, as amended. Its transmission or the revelation of its contents in any manner to an unauthorized person is prohibited by law.

This volume is classified CONFIDENTIAL in accordance with security regulations of the War and Navy Departments because certain chapters contain material which was CONFIDENTIAL at the date of printing. Other chapters may have had a lower classification or none. The reader is advised to consult the War and Navy agencies listed on the reverse of this page for the current classification of any material.

UNCLASSIFIED

TECHNICAL LIBRARY
BLDG 313
ABERDEEN PROVING GROUND, MD.
STEAP-TL

UNCLASSIFIED

Manuscript and illustrations for this volume were prepared for publication by the Summary Reports Group of the Columbia University Division of War Research under contract OEMsr–1131 with the Office of Scientific Research and Development. This volume was printed and bound by the Columbia University Press.

Distribution of the Summary Technical Report of NDRC has been made by the War and Navy Departments. Inquiries concerning the availability and distribution of the Summary Technical Report volumes and microfilmed and other reference material should be addressed to the War Department Library, Room 1A–522, The Pentagon, Washington 25, D. C., or to the Office of Naval Research, Navy Department, Attention: Reports and Documents Section, Washington 25, D. C.

Copy No.

This volume, like the seventy others of the Summary Technical Report of NDRC, has been written, edited, and printed under great pressure. Inevitably there are errors which have slipped past Division readers and proofreaders. There may be errors of fact not known at time of printing. The author has not been able to follow through his writing to the final page proof.

Please report errors to:

JOINT RESEARCH AND DEVELOPMENT BOARD
PROGRAMS DIVISION (STR ERRATA)
WASHINGTON 25, D.C.

A master errata sheet will be compiled from these reports and sent to recipients of the volume. Your help will make this book more useful to other readers and will be of great value in preparing any revisions.

[redacted]

UNCLASSIFIED

UNCLASSIFIED

SUMMARY TECHNICAL REPORT OF DIVISION 1, NDRC

VOLUME 1

HYPERVELOCITY GUNS AND THE CONTROL OF GUN EROSION

OFFICE OF SCIENTIFIC RESEARCH AND DEVELOPMENT
VANNEVAR BUSH, DIRECTOR

NATIONAL DEFENSE RESEARCH COMMITTEE
JAMES B. CONANT, CHAIRMAN

DIVISION 1
L. H. ADAMS, CHIEF

WASHINGTON, D.C., 1946

UNCLASSIFIED

NATIONAL DEFENSE RESEARCH COMMITTEE

James B. Conant, *Chairman*
Richard C. Tolman, *Vice Chairman*

Roger Adams	Army Representative[1]
Frank B. Jewett	Navy Representative[2]
Karl T. Compton	Commissioner of Patents[3]

Irvin Stewart, *Executive Secretary*

[1]*Army Representatives in order of service:*

Maj. Gen. G. V. Strong
Maj. Gen. R. C. Moore
Maj. Gen. C. C. Williams
Brig. Gen. W. A. Wood, Jr.
Col. L. A. Denson
Col. P. R. Faymonville
Brig. Gen. E. A. Regnier
Col. M. M. Irvine
Col. E. A. Routheau

[2]*Navy representatives in order of service:*

Rear Adm. H. G. Bowen
Capt. Lybrand P. Smith
Rear Adm. J. A. Furer
Rear Adm. A. H. Van Keuren
Commodore H. A. Schade

[3]*Commissioners of Patents in order of service:*

Conway P. Coe
Casper W. Ooms

NOTES ON THE ORGANIZATION OF NDRC

The duties of the National Defense Research Committee were (1) to recommend to the Director of OSRD suitable projects and research programs on the instrumentalities of warfare, together with contract facilities for carrying out these projects and programs, and (2) to administer the technical and scientific work of the contracts. More specifically, NDRC functioned by initiating research projects on requests from the Army or the Navy, or on requests from an allied government transmitted through the Liaison Office of OSRD, or on its own considered initiative as a result of the experience of its members. Proposals prepared by the Division, Panel, or Committee for research contracts for performance of the work involved in such projects were first reviewed by NDRC, and if approved, recommended to the Director of OSRD. Upon approval of a proposal by the Director, a contract permitting maximum flexibility of scientific effort was arranged. The business aspects of the contract, including such matters as materials, clearances, vouchers, patents, priorities, legal matters, and administration of patent matters were handled by the Executive Secretary of OSRD.

Originally NDRC administered its work through five divisions, each headed by one of the NDRC members. These were:

Division A—Armor and Ordnance
Division B—Bombs, Fuels, Gases, & Chemical Problems
Division C—Communication and Transportation
Division D—Detection, Controls, and Instruments
Division E—Patents and Inventions

In a reorganization in the fall of 1942, twenty-three administrative divisions, panels, or committees were created, each with a chief selected on the basis of his outstanding work in the particular field. The NDRC members then became a reviewing and advisory group to the Director of OSRD. The final organization was as follows:

Division 1—Ballistic Research
Division 2—Effects of Impact and Explosion
Division 3—Rocket Ordnance
Division 4—Ordnance Accessories
Division 5—New Missiles
Division 6—Sub-Surface Warfare
Division 7—Fire Control
Division 8—Explosives
Division 9—Chemistry
Division 10—Absorbents and Aerosols
Division 11—Chemical Engineering
Division 12—Transportation
Division 13—Electrical Communication
Division 14—Radar
Division 15—Radio Coordination
Division 16—Optics and Camouflage
Division 17—Physics
Division 18—War Metallurgy
Division 19—Miscellaneous
Applied Mathematics Panel
Applied Psychology Panel
Committee on Propagation
Tropical Deterioration Administrative Committee



NDRC FOREWORD

As events of the years preceding 1940 revealed more and more clearly the seriousness of the world situation, many scientists in this country came to realize the need of organizing scientific research for service in a national emergency. Recommendations which they made to the White House were given careful and sympathetic attention, and as a result the National Defense Research Committee (NDRC) was formed by Executive Order of the President in the summer of 1940. The members of NDRC, appointed by the President, were instructed to supplement the work of the Army and the Navy in the development of the instrumentalities of war. A year later, upon the establishment of the Office of Scientific Research and Development (OSRD), NDRC became one of its units.

The Summary Technical Report of NDRC is a conscientious effort on the part of NDRC to summarize and evaluate its work and to present it in a useful and permanent form. It comprises some seventy volumes broken into groups corresponding to the NDRC Divisions, Panels, and Committees.

The Summary Technical Report of each Division, Panel, or Committee is an integral survey of the work of that group. The first volume of each group's report contains a summary of the report, stating the problems presented and the philosophy of attacking them, and summarizing the results of the research, development, and training activities undertaken. Some volumes may be "state of the art" treatises covering subjects to which various research groups have contributed information. Others may contain descriptions of devices developed in the laboratories. A master index of all these divisional, panel, and committee reports, which together constitute the Summary Technical Report of NDRC, is contained in a separate volume, that also includes the index of a microfilm record of pertinent technical laboratory reports and reference material.

Some of the NDRC-sponsored researches which had been declassified by the end of 1945 were of sufficient popular interest that it was found desirable to report them in the form of monographs, such as the series on radar by Division 14 and the monograph on sampling inspection by the Applied Mathematics Panel. Since the material treated in them is not duplicated in the Summary Technical Report of NDRC, the monographs are an important part of the story of these aspects of NDRC research.

In contrast to the information on radar, which is of wide-spread interest and much of which is released to the public, the research on subsurface warfare is largely classified and is of general interest to a more restricted group. As a consequence, the report of Division 6 is found almost entirely in its Summary Technical Report, which runs to over 20 volumes. The extent of the work of a division cannot therefore be judged solely by the number of volumes devoted to it in the Summary Technical Report of NDRC: account must be taken of the monographs and available reports published elsewhere.

Division 1, under the leadership of its Chief, L. H. Adams, conducted a program of research in the field of hypervelocity guns. Its main responsibility was to study the effects of gun erosion and the erosive qualities of the common propellants, in order that means could be found for prolonging the life of guns firing at muzzle velocities higher than the pre-war maximum of 3,000 feet per second.

The contractor of the Division developed several highly erosion-resistant materials, and means were found for the preparation of these alloys in forms suitable for use as bore-surface material. Stellite, one of these alloys, when applied to caliber .50 machine-gun barrels as a short breech liner, increased their life several fold under severe conditions, especially when the bore surface ahead of the liner was chromium plated. As the war came to an end, an experimental 90-mm gun (to fire at a muzzle velocity of at least 4,000 fps) was being developed, and further work on it was turned over to the Army, while the Navy was able to take over the plans for the fabrication of a molybdenum liner for its new 3-inch/70-caliber gun.

The Summary Technical Report of Division 1, prepared under the direction of the Division Chief, and authorized by him for publication, is a record of this work, and a comprehensive review of the state of the art. It also stands as a testimonial to the energy and resourcefulness of the personnel of the Division, whose contributions to the war effort are worthy of grateful appreciation.

Vannevar Bush, Director
Office of Scientific Research and Development

J. B. Conant, Chairman
National Defense Research Committee



FOREWORD

A FOUR-YEAR program of research and development in which experienced investigators from leading universities, from other academic institutions, and from commercial organizations with competent research and engineering departments work together on a series of closely integrated problems is almost certain to uncover a variety of interesting facts and generalizations. In the case of a broad assignment, like that of Division 1, NDRC, involving a number of fields in chemistry, physics, metallurgy, mathematics, and engineering, it is especially desirable for the new knowledge to be consolidated in the form of a Summary Technical Report, as specified by OSRD, for the benefit of those who in the future may wish to pursue further the problems that were attacked. Although the findings of Division 1 are covered in great detail by a series of 144 formal reports on various subjects, in addition to numerous interim reports submitted by the 29 different contractors, it was decided by Division 1 that its Summary Technical Report should be more than merely a collection or a condensation of previous reports. Instead, as is brought out in the Editor's preface, it deals systematically, although briefly, with the subject of hypervelocity and the control of gun erosion in relation to work of the Division. It is intended that by the selection of results and conclusions, as well as by the sequence of topics, the Report should tell a story of an interesting adventure in scientific collaboration.

In formulating the program and in supervising the work of the various groups, it was deemed essential that a well-rounded series of investigations, including research as well as development and testing, be set up. It was felt that even in wartime, fundamental research is essential for real progress. No small part of whatever success Division 1 may have attained in a field requiring fresh ideas and novel procedures was largely a result of the attitude of NDRC toward research. In conformity with the fixed policy of that agency of the Government with reference to the handling of contracts, particular care was exercised in Division 1 not to have Government officials substitute their own ideas for those of the skilled scientists in the associated research groups. Rather, the investigators, engaged as they were in exploring the unknown, were given the utmost freedom of action consistent with focusing their efforts on the central problem.

The results of those efforts are outlined in this volume. It may be seen that the accomplishments are mainly of two kinds: First, the obtaining of a better understanding of gun erosion and the means of combatting it; and second, the development and testing of specific methods for the solution of the hypervelocity problem. As a by-product of the main investigation, there was obtained a notable improvement in machine gun barrels—the need for which was not visualized when the original program was formulated.

To all those who collaborated or otherwise aided in this undertaking, the Division Chief is deeply indebted: the contractors' employees who worked together energetically and harmoniously in the common cause; the Division staff members who performed patiently and effectively a variety of difficult tasks; and the technical representatives of our British and Canadian allies who gave encouragement and valuable advice. It is a pleasant duty to record also the debt of gratitude that Division 1 owes to those individuals in the Navy Department and the War Department, acting formally or informally in a liaison capacity, with most of whom constant and almost daily contact was maintained: In the Navy Bureau of Ordnance, among others, Captain G. L. Schuyler, Captain J. S. Champlin, Commander E. A. Junghans, Mr. C. B. Green, and especially Lieutenant Commander B. D. Mills, Jr.; in the Army Ordnance Department Major H. A. Ellison, Mr. B. E. Anderson, Mr. M. C. Miller, Mr. G. E. Stetson, and especially Mr. S. Feltman; at Aberdeen Proving Ground Mr. R. H. Kent; and at Watertown Arsenal, Dr. P. R. Kosting. Above all, without the wise counsel and unfailing patience of Colonel S. B. Ritchie, progress would have been much more difficult.

Special credit is due Dr. J. S. Burlew, the Editor of this volume. His skill in arranging for the orderly presentation of the joint efforts of a large group of authors is matched only by his energy and enthusiasm in carrying the undertaking through to the end.

L. H. ADAMS

Chief, Division 1



PREFACE

ONE OF THE SIGNIFICANT FEATURES of the investigation by Division 1, NDRC, of the mechanism of gun erosion and of means of attaining hypervelocity was the close integration of its various phases. Not only were the several major projects made up of interrelated subprojects, but also there were many aspects that were common to two or more of the major projects. This situation has been reflected in the Division's Summary Technical Report.

The report was planned as a logical exposition of the different aspects of the main problem denoted by its title "Hypervelocity Guns and the Control of Gun Erosion." In relating the final status of the investigation, no attention has been paid to the way in which the program had been organized by projects or assigned to different contractors, for such divisions were useful only during the administration of the program. Instead, chapters have been allotted to those subjects considered to be of principal importance. Thus, the report is a unified one rather than merely an assemblage of separate documents.

At the same time, it is realized that the Summary Technical Report is intended to be consulted as a reference work, as well as to be read in its entirety. Hence an attempt has been made to have each chapter nearly an independent unit. For this reason there is some duplication of material, since occasionally it has been desirable to consider the same subject from more than one point of view. Frequent cross references to other parts of the volume have kept such duplication to a minimum.

The entire report was planned in advance and the topics to be included in each chapter were specified. The order of treatment of these topics and the emphasis to be placed on each, however, usually were left to the authors. When a topic assigned to one chapter was very closely related to the subject matter of another, the more appropriate place was not always apparent until both chapters had been written. In some cases the editor, with the authors' permission, moved material from one chapter to another. One feature that is common to many chapters is that the first section not only serves to introduce a new subject but also furnishes a résumé of the chapter.

The chief source material for the Division 1 STR consists of the 143 formal reports, listed in the first part of the Bibliography, which were prepared for issuance in mimeographed format for the Division by the Technical Reports Section of NDRC. These classified reports, in which is presented the essential information gained by Division 1 contractors, have been deposited in a number of Service libraries and copies of them are available as microfilms. Because of lack of funds and personnel during the final stage of the demobilization of OSRD, it was not possible to have all these reports mimeographed. Consult the paragraph at the beginning of the Bibliography concerning their availability. In some instances supplementary details, such as dimensioned drawings or additional experimental data, may be found in the monthly progress reports or the interim reports from contractors. If so, appropriate reference is made in the formal report concerning the location of the complete files of these reports.

Every important topic covered by the Division 1 formal reports is mentioned in the STR (with a reference to the appropriate report), so that it is a key to the entire work of Division 1 and its contractors. Because of the close dependence of the STR on this body of Division 1 reports, it has not seemed necessary to use quotation marks in those cases where sentences have been lifted bodily or whole sections have been paraphrased, especially when the author of a chapter of the STR was also author of the report on which it was based. Even when this is not the case, it is hoped that citation of the original report will suffice to give proper credit to its author.

The other sources for the STR are also listed in the Bibliography under appropriate headings that indicate the organization issuing the report. All these reports are referred to specifically in the text of STR, except for British reports[a] that summarize the work of Division 1.

The principal objective sought in the preparation of the STR has been the integration of the knowledge gained by Division 1 in its broad investigation of erosion and hypervelocity, in order to orient the reader with respect to the work described in the formal reports from the Division. Chapter 16 on erosion-resistant materials is an especially striking example of this feature. It presents results from many sources and shows how all of them fit into a single program of investigation. Furthermore, the preparation of the STR has given opportunity for

[a]These reports are listed as the following items in the Bibliography: 356, 360, 400, 407, 408, 409, 410.

some of the investigators to review and re-evaluate the results of their work as a whole, whereas previously it had been reported piecemeal.

In keeping with the general purpose of the Summary Technical Reports of NDRC, an effort has been made to have as many as possible of the chapters present the "state of the art" with respect to the subject treated therein. There is considerable variability in this respect. Thus, at one extreme, Chapter 5, which deals with the heating of guns during firing, is based on Army, Navy, and British reports to as great an extent as it is on Division 1 reports and therefore approaches a summary of the state of the art. Although Chapters 22, 23, and 24 are limited to a recital of Division 1's experience, they present the state of the art with respect to the development of improved machine gun barrels, for the Division has been the only contributor in the field. On the other hand, a number of the chapters, notably Chapters 4, 8, 9, 26, 27, and 28, deal with only that limited aspect of a general subject that was applicable to Division 1's program.

Because so many of the mathematical equations have been taken from reports already issued, a considerable diversity in notation has been introduced. It was considered not worth while to make the equations uniform, for after an equation had been modified, a reader might find it difficult to compare it with related ones in an original report. Therefore a uniform system of notation has not been adopted.

Many of the illustrations used in the STR have been taken from previously issued reports of Division 1 as indicated by the bibliographical reference numbers included in the legends. A few of the illustrations have been taken from reports issued by the Office of the Chief of Ordnance, to which appreciation is expressed for permission to reproduce them. For some chapters special illustrations were prepared by their authors. A number of other figures were executed by Mr. Ernest Albert of the H. L. Yoh Company, Philadelphia, Pennsylvania.

The editor wishes to record the fine spirit of cooperation displayed by the 25 other authors who contributed to the Division 1 STR. These authors, whose names are listed in the Contents of this volume, either had taken part in some of the investigations or else were members of the Division staff. One of the greatest values of the book is the careful appraisal they have made of the vast quantity of experimental data accumulated by Division 1 contractors during its 4-year period of investigation. To each of these authors the editor is indebted personally for the privilege of having worked with them.

In addition to having been reviewed by the Division Chief, nearly every chapter has been reviewed by at least one other person who has an intimate knowledge of the subject matter, either through having been associated with the investigation itself or through having followed the work closely. The valuable suggestions made by these reviewers are hereby acknowledged. The persons who served Division 1 in this way and the chapters that they reviewed are included in the following list.

	CHAPTER
W. S. Benedict, National Bureau of Standards	5, 11
F. A. Biberstein, The Catholic University of America	27
H. L. Black, Technical Aide, Division 1, NDRC	6
W. Blum, National Bureau of Standards	23, 25
P. H. Brace, Westinghouse Research Laboratories	18
H. C. Cross, War Metallurgy Committee	16
C. L. Faust, Battelle Memorial Institute	20
L. H. Germer, Bell Telephone Laboratories	21
J. W. Greig, Geophysical Laboratory, C. I. W	23, 24, 29
K. F. Herzfeld, The Catholic University of America	7
J. O. Hirschfelder, (formerly) Geophysical Laboratory, C. I. W	2, 3, 6
F. H. Horn, The Johns Hopkins University	14
W. F. Jackson, E. I. du Pont de Nemours and Company	4, 14
H. S. Jerabek, (formerly) Geophysical Laboratory, C. I. W	12, 16, 19
R. H. Kent, Aberdeen Proving Ground	8
J. F. Kincaid, (formerly) Explosives Research Laboratory (Division 8, NDRC)	15
Z. Kopal, Massachusetts Institute of Technology	8
V. Lamb, National Bureau of Standards	23, 25
J. J. Lander, Bell Telephone Laboratories	12

CHAPTER

J. P. Magos, Crane Company 22, 24

J. W. Marden, Westinghouse Lamp Division . . 18

H. E. Merwin, Geophysical Laboratory, C. I. W. 10, 12, 13

L. W. Nordheim, Consultant, Division 1, NDRC 5

E. F. Osborn, (formerly) Geophysical Laboratory, C. I. W. 24, 25

B. B. Owen, Yale University 21

R. M. Parke, Climax Molybdenum Company . . 17

J. F. Schairer, Special Assistant, Division 1, NDRC 17, 18, 20, 21, 26

F. R. Simpson 11

N. H. Smith, The Franklin Institute 15, 28

W. E. Story, Liaison Office, OSRD 32

CHAPTER

W. F. G. Swann, Bartol Foundation, The Franklin Institute 9

J. A. TenBrook, Special Assistant, Division 1, NDRC 28

E. G. Townes, Editor, Technical Reports Section, NDRC 8

W. D. Urry, Geophysical Laboratory, C. I. W. 11

W. A. Wissler, Union Carbide and Carbon Research Laboratories 19

N. H. Ziegler, Crane Company 19

E. G. Zies, Geophysical Laboratory, C. I. W. 10, 13

Finally, it is a great personal pleasure to acknowledge the devoted services rendered by both Miss Charlotte A. Marsh and Miss Helen M. Watson in helping to edit this volume.

JOHN S. BURLEW

Editor

[redacted]

CONTENTS

CHAPTER		PAGE
	Summary	1
	PART I	
	INTRODUCTION	5
1	The Problem of Hypervelocity by *L. H. Adams*	7
	PART II	
	BALLISTICS	19
2	Properties of Powder Gas by *F. C. Kracek*	21
3	Interior Ballistic Calculations by *William S. Benedict*	54
4	Instrumentation for Experimental Ballistic Firings by *H. B. Brooks*	76
5	Heating of Guns During Firing by *H. L. Black* and *G. Comenetz*	98
6	Bore Friction by *William S. Benedict*	129
7	Band Pressure and Related Stresses by *H. L. Black*	152
8	Exterior Ballistics of Hypervelocity projectiles by *A. H. Stone*	163
9	Terminal Ballistics of Hypervelocity Projectiles by *H. S. Roberts* and *Walker Bleakney*	180
	PART III	
	GUN EROSION	193
10	Description of Eroded Gun Bores by *Lloyd E. Line, Jr.*	195
11	Laboratory Methods of Studying Gun Erosion by *Lloyd E. Line, Jr.*	219
12	The Products of Gun Erosion by *E. G. Zies* and *C. A. Marsh*	244
13	The Causes of Gun Erosion by *C. A. Marsh* and *J. N. Hobstetter*	260
	PART IV	
	EROSIVE ACTION OF PROPELLANTS	281
14	Effects of Constituents of the Powder Gases on Gun Steel by *W. D. Urry*	283
15	Erosion of Gun Steel by Different Propellants by *J. N. Hobstetter*	308
	PART V	
	EROSION RESISTANT MATERIALS	329
16	Selection of Erosion Resistant Materials for Gun Bores by *J. F. Schairer*	331

CHAPTER PAGE

17 Chromium and Chromium-Base Alloys by *Helen M. Watson* 356
18 Molybdenum by *F. Palmer* 370
19 Stellites and other Cobalt Alloys by *J. F. Schairer* 391
20 Electroplating by *William Blum* 408
21 Vapor-Phase Plating of Molybdenum, Tungsten, and Chromium by *C. A. Marsh* 419

PART VI

IMPROVED MACHINE GUN BARRELS 441

22 Stellite-Lined Machine Gun Barrels by *J. F. Schairer* 443
23 Nitrided and Chromium-Plated Machine Gun Barrels by *E. F. Osborn* 458
24 Barrels both Stellite-Lined and Chromium-Plated by *J. F. Schairer* 473
25 Pilot Plants for Chromium-Plating Caliber .50 Barrels by *V. Wichum* and *C. A. Marsh* 485

PART VII

HYPERVELOCITY GUNS AND PROJECTILES 501

26 Short Liners and other Design Features of Gun Tubes by *William H. Shallenberger* 503
27 Design Features of Projectiles by *F. R. Simpson* and *H. L. Black* 518
28 Automatic Gun Mechanism by *William H. Shallenberger* 538
29 Sabot-Projectiles by *J. S. Burlew* 557
30 Tapered-Bore Guns and Skirted Projectiles by *Edwin L. Rose* 569
31 Pre-Engraved Projectile with Chromium-Plated Bore by *Nicol H. Smith* 591
32 The Fisa Protector and Chromium-Plated Bore by *Nicol H. Smith* 609
33 Practical Hypervelocity Guns by *L. H. Adams, J. S. Burlew,* and *E. L. Rose* 615

Glossary 631
Bibliography 633
OSRD Appointees 652
Contracts 653
Service Projects 656
Index 657

CONFIDENTIAL

SUMMARY

HYPERVELOCITY PROBLEM

DURING RECENT DECADES there has been a tendency to use more guns of high power. There has not been, however, a corresponding increase in the maximum muzzle velocity in common use. This maximum has remained at about 3,000 fps, for if a higher velocity is used, the rate of erosion is excessive and gun life is correspondingly short.

When, in the summer of 1941, the National Defense Research Committee undertook to investigate means of making higher velocity guns practical, it was recognized that one of the principal hurdles would be the control of gun erosion. At the same time it was deemed desirable to investigate other possible means of attaining this end simply by circumventing erosion by a change in design of the gun or projectile. Division 1, NDRC, followed concurrently these two courses of action, accompanying them by such investigations of interior ballistics as were needed to supplement existing knowledge.

EROSION STUDIES

The novel approach that was adopted for the study of gun erosion was, in effect, to learn the history of the bore surface of different guns that had been fired under various conditions. Considerable information was obtained from examination of the erosion products found on the bore surfaces of guns worn out in service. Of equal importance was the knowledge gained from special experiments in which a new gun was fired a relatively few rounds and then examined, so that the course of the erosion process could be followed. A special caliber .50 hypervelocity erosion-testing gun was developed to make possible many routine firings under a variety of conditions. One important series of such experiments involved a determination of the relative erosiveness of all the common propellants.

Another group of erosion experiments was undertaken to observe the effect on a steel bore surface of the individual constituents of the powder gases. By use of the techniques of physical chemistry it was demonstrated that several of the principal constituents react readily with steel at the temperatures and pressures prevailing in guns. Mixtures of the products resulting from these reactions have a lower fusion range than gun steel itself.

The evidence from these two types of erosion experiments has led to the conclusion that the erosion of a steel gun tube results from the reaction of a thin layer of steel at the bore surface with the powder gases, followed by removal of the reaction products. The bore-surface temperature plays a predominant role in determining what type of product is formed, although the chemical nature of the propellant also is a factor. Furthermore, the higher the bore-surface temperature the greater the extent to which the altered bore-surface material is softened and even fused, and hence more readily removed both by the powder gases and by the projectile. In the case of a hypervelocity gun fired with a very hot propellant, fusion of the gun steel itself occurs, and the molten material is blown out of the bore by the powder gases.

EROSION-RESISTANT MATERIALS

Early in the course of the erosion studies some inkling of the process delineated in the previous paragraph was obtained. Thereupon it was tentatively concluded as a working hypothesis (which subsequent experience confirmed) that severe erosion is inevitable in a steel gun tube, regardless of the type of steel, when fired under hypervelocity conditions with present-day propellants. Thereupon a search was begun for nonferrous materials that might be erosion resistant. It was soon found that resistance to erosion by the powder gases is a property of only a few pure metals—in particular, chromium, molybdenum, tungsten, and tantalum—and of certain of their alloys. It was also learned that a very intensive effort would be required to prepare any one of these metals in a form suitable for use as a bore-surface material.

Two of the erosion-resistant materials ultimately developed by Division 1 were applied to caliber .50 aircraft machine gun barrels that were used in combat in the latter months of the war in the Pacific. The one was stellite, applied as a short breech liner, which increased the velocity life of the barrel because of its high temperature strength and superior erosion resistance. The other was chromium electroplate applied to the hardened bore surface of the barrel, which increased the accuracy life in long



bursts because it was applied in such a way that the muzzle end of the bore was "choked" and therefore did not become oversize so quickly from the heat of firing. After improved barrels of each of these types had been in use for a short time, a "combination" barrel having choked-muzzle chromium plate ahead of a stellite breech liner was developed. This barrel had a life at least tenfold greater than that of a steel barrel when fired in long bursts (as, for example, in strafing) and about a threefold greater life when fired in very short bursts.

A stellite liner was also applied to the Ordnance Department's experimental caliber .60 machine gun barrel which has a muzzle velocity of 3,500 fps. The use of such a liner may be expected to be mandatory for all future machine gun barrels until a superior bore surface material is developed. One possible superior material is a chromium-base alloy which can be fired with double-base powder, whereas a stellite liner melts under these conditions. This alloy requires further development to improve its ductility.

The most promising material so far developed for the bore surface of a hypervelocity medium-caliber gun is hardened molybdenum. The problem has been to learn how to fabricate pieces of ductile molybdenum large enough for use as gun liners, and how to harden the metal sufficiently so that it will withstand the swaging action of a projectile during engraving. This goal was achieved in liners for the caliber .50 erosion-testing gun. Plans were then developed for equipment with which to apply the same techniques to the fabrication of pieces large enough for liners for a 3-in. gun. After OSRD's contracts had been terminated, the Bureau of Ordnance, Navy Department continued this work.

BALLISTIC STUDIES

In the study of the fundamental causes of gun erosion, knowledge of the physical conditions existing in the gun bore during firing was important. Hence the process of the burning of powder was studied, a means was developed for measuring the temperature of the powder gases, and the chemical composition of these gases was determined.

Two other series of measurements dealt with the heat input to the bore surface of a gun during firing and with the rise of temperature of the bore walls, especially of a machine gun barrel during the firing of a long burst. From these experimental data it was possible to arrive at much closer approximations to the bore-surface temperature than had been heretofore possible. These results were of inestimable value in the formulation of the final explanation of the process of erosion.

Theoretical determinations of bore-surface temperatures required the development of an improved system of interior ballistic calculations. After the groundwork in the development of this system had been laid, its usefulness for other purposes was realized and additional work was done to simplify the computations. One advantage of this system over others commonly used is that various empirical factors can be allowed for explicity. As additional information is gained, it can easily be incorporated in the system with a resulting improvement in accuracy. This system proved to be useful not only in routine ballistic calculations but also in analyses of the ballistic factors that enter into a consideration of an increase in muzzle velocity.

Experimental ballistic firings were conducted in an effort to obtain more precise information about the effect on the behavior of a gun of variables such as the weight and composition of the powder charge and the projectile band diameter. A new device, termed the "microwave interferometer" was developed for measurement of projectile movement down the gun bore.

Strain-gauge measurements made on the exterior of the gun barrel during these experimental firings were correlated with static measurements from a study of band pressure. The results were applied to both projectile design and gun design.

Exterior ballistics and terminal ballistics of hypervelocity projectiles were subjects of corollary interest but were not investigated extensively by Division 1. The theory of the motion of a cone moving at high velocity was extended to take into account the effect of yaw. Observations were made of the disruptive effect of a hypervelocity projectile upon entering a liquid.

SUBCALIBER PROJECTILES

The muzzle velocity of any existing gun can be increased considerably by firing from it a subcaliber projectile. It seems to be a fairly safe assumption, although not actually demonstrated by experiment, that the rate of erosion of such a gun is considerably less than the rate of erosion of a conventional gun firing a standard projectile at the same velocity. Hence the use of a subcaliber projectile is a means of



attaining hypervelocity without a marked increase in erosion.

For this reason Division 1 sponsored the development of a sabot-projectile, which is one type of subcaliber projectile. Considerable attention was paid to the use of plastics in such projectiles for the purpose of reducing weight; but dimensional instability of plastics when exposed to variations in atmospheric conditions made it impossible to develop a satisfactory design. Preliminary tests of the final design of an all-steel 90-mm sabot-projectile with an 8-lb tungsten carbide core, which were made just before the work was terminated, indicated that by the use of such a projectile the muzzle velocity of the standard gun was raised from 2,700 to 3,700 fps. The projectile's accuracy was as good as that of the standard 90-mm projectile.

Another type of subcaliber projectile is a skirted one, to be fired from a tapered-bore gun. Experiments with tapered-bore guns of different proportions showed that the most successful type is one having a short unrifled tapered section at the muzzle end. The simplest way to provide such a tapered section is by attaching a short muzzle adaptor to an existing gun. A satisfactory means of doing this for a 57-mm gun was developed, together with a design of an armor-piercing tungsten carbide-cored projectile which had a muzzle velocity of 4,200 fps. In this case, also, preliminary tests showed that the accuracy was at least as great if not greater than that of the standard round fired at a velocity of 2,800 fps from the same gun without a muzzle adaptor.

LINERS AND OTHER FEATURES OF GUN DESIGN

The development of erosion-resistant materials naturally led to efforts to utilize them to best advantage. With respect to machine-gun barrels, it was demonstrated that the utilization of the full potentialities of stellite liners and of chromium electroplates demanded a barrel having a slightly greater wall thickness and made of steel having greater strength at high temperatures. In preliminary tests such an improved barrel showed a severalfold increase in life compared with an assembly consisting of the ordinary barrel with the same liner.

Experience in the application of short breech liners to medium-caliber guns was obtained by the development of a successful design of replaceable steel liner for a 90-mm gun. Such a liner was considered originally as an emergency means of prolonging the life of a steel barrel subjected to severe firing conditions. Later it was demonstrated by trial of a 37-mm stellite liner that some features of this design were useful as a means of applying an erosion-resistant material to a gun bore.

Although chromium is highly erosion resistant, it is difficult to keep an electroplate of chromium on a steel gun bore surface. One of the major causes of its removal is the high stress concentration set up during engraving of the projectile. Two means of preventing this action were tried in an effort to enhance the usefulness of chromium plate. One was the "Fisa protector," which is a thin steel sleeve attached to the neck of the cartridge case and extending forward over the projectile as far as the bourrelet. It covers the origin of rifling during engraving and then is extracted with the cartridge case. This device has not yet been perfected.

The second means of avoiding undue stress on a chromium-plated bore surface is a pre-engraved projectile. Its successful utilization requires a convenient way of orienting the projectiles prior to chambering. One self-orienting arrangement that made use of pointed lands in the gun was tried in an experimental hypervelocity 37-mm gun (velocity: 3,500 fps). The severe erosion that occurred at the origin of rifling in this particular gun tube might be prevented by the use of a thicker chromium plate.

A gun design project that was separate from the rest of the Division's activities was the development of an improved mechanism for a 20-mm automatic cannon. Although a completely satisfactory design had not been developed by the time the project was terminated, firing tests of the latest model indicated the hope that one might be achieved eventually.

EXPERIMENTAL HYPERVELOCITY GUN

After Division 1's investigations had yielded a rational explanation of the phenomenon of gun erosion and had pointed the way toward the development of erosion resistant materials, an attempt was made to apply this new knowledge to the development of a practical hypervelocity gun. The first step in this direction was to have been an experimental 90-mm gun firing at a muzzle velocity of at least 4,000 fps. Two tubes for this gun, chambered and bored but not rifled, were prepared before the termination of the Division's activities and then were turned over to the Army Ordnance Department for further develop-

ment. According to the original plans these tubes were to have been chromium plated and were to have fired pre-engraved projectiles, and thus make use of the experience gained in the trial of the 37-mm tubes.

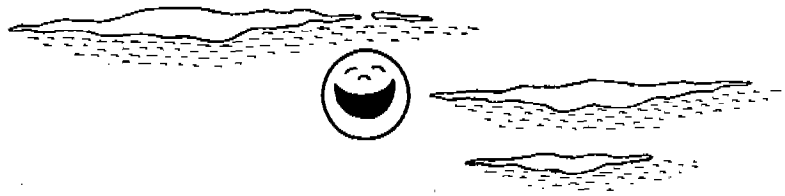
The next step in this program was to have been the insertion of a molybdenum liner in another tube having the same ballistic characteristics. As a preliminary, plans were made for the fabrication of a molybdenum liner for the Navy's new 3-inch/70-caliber gun. Upon cessation of Division 1's sponsorship, this project was taken over by the Navy Bureau of Ordnance.

Means are thus at hand for an immediate study of some of the characteristics of medium-caliber hypervelocity guns. What is needed next is a careful evaluation of the possible ways of utilizing erosion-resistant materials in such guns by actual trial of them. Firings should be conducted to determine the optimum ballistic conditions, particularly means of increasing the density of loading. Finally, then, by combining such information with that concerning the effects on different targets of hypervelocity projectiles, it should be relatively simple to decide on a design of gun best adapted to serve any particular Service requirement.

[redacted]

PART I

INTRODUCTION





On what strange stuff ambition feeds!
—Eliza Cook
"Thomas Hood"

Chapter 1

THE PROBLEM OF HYPERVELOCITY

By *L. H. Adams*[a]

IT IS THE PURPOSE of this chapter to indicate briefly the nature of the hypervelocity problem, to summarize the advantages of and the difficulties with higher muzzle velocities in guns, to indicate the methods by which some of the difficulties have been obviated, and to outline the various means that have been employed to make guns of greatly increased performance practicable. Throughout the volume as a whole these same broad topics form the basis of detailed presentation. The present chapter concludes with some remarks comparing the status of the hypervelocity problem in 1946 with that in 1941.

1.1 NATURE OF THE PROBLEM

1.1.1 Some Elementary Considerations

A gun is a device for converting the chemical energy of a powder charge into mechanical energy of a moving projectile and for launching the projectile toward a target in an accurately specified direction. Thus, it serves two principal purposes. As an engine, its mechanical efficiency compares favorably with the best turbines and internal combustion engines. For example, a representative gun with a 3-in. bore and a muzzle velocity of about 2,700 fps converts 29 per cent of the powder energy into kinetic energy of the projectile. (Compare Table 7, Chapter 6.) Of the remaining 71 per cent, about 9 per cent is accounted for by heat conducted into the gun barrel, the remainder being accounted for mainly by the heat and kinetic energy of the hot gases ejected from the gun.

Under favorable conditions, a greater proportion of the powder energy may be converted into energy of the projectile; but in a gun operating at extreme muzzle velocities, the mechanical efficiency is lower, mainly because more energy is lost in the effluent gases. Fortunately, this falling off in efficiency does not become important until velocities very much higher than conventional ones are reached. For example, the calculated value for a 90-mm gun operating at 4,250 fps is only about 10 per cent lower than that for an existing gun of the same caliber operating at 2,700 fps. At still higher velocities, the mechanical efficiency of a gun begins to drop more rapidly, and at 6,000 fps muzzle velocity would not exceed two-thirds of that of existing guns, the velocity of which seldom exceeds half this magnitude.

A variety of complex factors, discussed in Chapters 2, 3, 5, and 6, determine the overall efficiency and hence the energy and muzzle velocity of a given projectile when shot from a given gun with a given powder charge. Without going into details, it suffices for the moment to note that within the range of customary designs and for a specified powder, the muzzle velocity depends primarily on the ratio of powder weight to projectile weight, and may be varied within wide limits simply by changing this ratio. That is, with a given gun, higher velocities may be obtained either by providing for more powder capacity or by decreasing the weight of the projectile. Contrary to what has sometimes been assumed, the limiting velocity of a projectile is not the velocity of sound in the powder gas at the temperature and pressure existing in the gun during firing; velocities of 9,000 fps (about three times the pertinent sound velocity) have been obtained experimentally. (See Section 3.5.2.) Rather, the limit is a practical one, imposed by other considerations which are listed and discussed briefly in Section 1.3.

In order that the gun may fulfill satisfactorily its second principal purpose, namely, that of a projectile launcher, it is necessary that the projectile be ejected with a predetermined velocity and direction. For projectiles stabilized in flight by spinning, there is the added requirement that the rate of spin be adequate for stabilization. That modern guns have a remarkable accuracy may be emphasized by comparing their precision with that of the human eye. The best guns, under favorable conditions, show a mean dispersion at the target of less than one-half mil, or about 1 min of arc, which happens to be the same as the limit of resolution of the eye under conditions of good lighting and normal vision. Thus, with a good gun, the gunner should be able to see only with difficulty the separate hits on the target at any range.

When a gun is fired, the bore surface deteriorates, and the consequent alteration of the above-mentioned

[a] Chief, Division 1, NDRC. (Present address: Geophysical Laboratory, Carnegie Institution of Washington.)

ballistic factors gradually impairs the accuracy and finally brings the gun to the end of its useful life. It was stated in the preceding paragraph that, viewed as an engine, a gun is an efficient mechanism. But, whereas the operating life of a gasoline engine is measured in thousands of hours, that of a gun is measured in minutes or even seconds. This follows from the circumstance that a gun is actually operating only while the projectile is passing down the bore. In a 12-in. gun of the usual design the travel time in the bore is about 30 msec; and if we multiply this time interval by 350 (a reasonable estimate for the useful life of a 12-in. gun) we obtain approximately 10 sec as the operating life. It is a curious fact that the corresponding figure for guns of various sizes is of the same order of magnitude, provided that the muzzle velocity remains approximately constant and the gun is fired slowly; for with smaller guns the travel time of the projectile down the bore is shorter, and (ordinarily) the usable number of rounds is correspondingly greater. It appears, therefore, that a gun is an efficient thermodynamic machine but that its life, whether measured in number of rounds or time of operation, may be discouragingly small. All efforts to make guns more effective must take into account the element of useful life.

1.1.2 Trend of Muzzle Velocities in the Past

Cannon were in use as early as the 14th century, at which time stone shot were fired from wrought iron barrels, the propellant being a crude form of black powder. Little information is available concerning the performance of these weapons, but it is unlikely that the muzzle velocities were more than a few hundred fps. Beginning in 1520, cast iron round shot began to be used and muzzle velocities were gradually increased. Records of Italian guns of 1746 show muzzle velocities in excess of 1,600 fps. A notable advance in ordnance began to take place about 1850 with the discovery and application of progressive-burning powders. Somewhat later, black powder, which had held the field in artillery for over 500 years, was displaced by nitrocellulose powder. During this same period, elongated rifled projectiles were developed, and by the year 1900 several nations were employing large-sized guns with muzzle velocities of 3,000 fps. Subsequent to that year, there has been little or no change, except perhaps the use of a greater proportion of high-velocity guns.

It may be instructive to note the rate of change of muzzle velocities for cannon throughout the past. For the 500 years ending in 1850 the average increase was about 5 fps per year, while for the 50 years following that date the average increase was of the order of 30 fps per year. During the 4 decades subsequent to 1900, the change was essentially zero.

In this connection, it is pertinent to take note also of the increase in rate of fire that has accompanied the increase in velocity.[510] The primitive guns were muzzle loading and required many minutes to reload and fire. With the advent of breech loading, and later of cased ammunition, the time per round was significantly reduced; and in the fairly recent past, automatic mechanisms have greatly increased the rate of fire. We now have 5-in. cannon firing at 20 rounds per minute and small arms (machine guns) firing at rates of 1,200 rounds per minute. Contrasted with muzzle velocity, rate of fire does not seem to have reached a corresponding state of stagnation. As mentioned in Section 1.3.2, these two aspects of improved gun performance involve features that are closely interrelated.

1.1.3 The Term Hypervelocity

There has been a tendency to make a rough division of artillery into low-velocity and high-velocity guns, the former class including velocities not much higher than 2,000 fps and the latter running up to 3,000 fps or a little above. Partly because there seemed to be unusual difficulties in the practical attainment of guns operating at muzzle velocities much in excess of 3,000 fps, it has been deemed convenient to use a special designation for guns of very high velocities. The term *hypervelocity* has been used; and in this volume hypervelocity guns are considered by definition to be ones operating at muzzle velocities of 3,500 fps or higher.[b]

1.1.4 The Problem Defined

A study of the past almost inevitably arouses our curiosity as to whether the long upward trend in muzzle velocities has properly come to an end, or whether further advances are both possible and profitable. We are confronted with a problem, the basis of which may be formulated by a series of questions as follows.

[b] This usage follows that adopted by the Ordnance Board of Great Britain, the limiting velocity having been set at 3,500 fps by the Hypervelocity Panel at its meeting on May 28, 1942.

(1) What are the advantages of hypervelocity guns?

(2) What obstacles are in the way of attaining higher muzzle velocities than have heretofore been considered practicable?

(3) What are the physical and chemical factors in such limitations?

(4) By what new knowledge can the difficulties be resolved?

(5) How can the results of such knowledge be translated into weapons of increased effectiveness?

Anticipating at this point some of the conclusions mentioned in the following paragraphs and explained more fully elsewhere in other chapters, we may note that hypervelocity does have worthwhile advantages and does involve serious difficulties; and that of the latter the outstanding one is erosion of the gun bore. The core of the problem is erosion. As implied by the title of this volume, if we can find the cause and cure of gun erosion and other deteriorations of the bore surface—or, if not a cure, a means of obviating the effects—we shall have gone a long way toward the complete solution of the hypervelocity problem.

1.2 A PRIORI ADVANTAGES OF HIGHER PROJECTILE VELOCITIES

1.2.1 General

It should be fairly obvious that a projectile at high velocity will outperform one at low velocity. Not so obvious perhaps is the increased effectiveness, in several respects, for the same energy or for the same weight of equipment. More exactly, the comparison is made between two projectiles of different calibers, either having the same muzzle energy or being fired from two guns having the same total weight, including associated equipment. As a means of summarizing the advantages of hypervelocity, it is convenient to group them in three categories: greater range; increased armor penetration; and increased probability of hitting the target. (Compare Section 33.2.)

In addition to these principal advantages, there are others, less well defined, that may merit careful evaluation. For example, as explained in Section 9.1, hypervelocity bullets show a strange disruptive effect when impinging on a vessel filled with liquid. For each of the aspects of hypervelocity, there is a limiting velocity beyond which, for practical reasons, it is not profitable to go, but it is now quite certain that the limit is well above the velocities that have been used heretofore.

1.2.2 Greater Range

In the ideal case of negligible air resistance, the trajectory is a simple parabola and the maximum range of a projectile varies as the square of the initial velocity.[c] This applies to both the horizontal and the vertical range. Actually, the relationship is a very complex one, owing to the large retarding effect of the atmosphere on the projectile; but the range nevertheless increases rapidly with increase of initial velocity and for a 50 per cent increase in muzzle velocity the maximum range of a large gun would be extended by something like a ratio of two to one. If a comparison is made on the basis of maximum *effective* range, it is usually found that this quantity also increases rapidly with muzzle velocity.

Even a moderate increase of horizontal range might be of great value if the guns of an enemy could thereby be outranged. Moreover, greater vertical range would clearly be of great value in coping with high-flying airplanes. These advantages are of course to be assessed against a variety of tactical situations, but it is likely that under some conditions the advantages would offset a considerable increase in weight and bulk of equipment.

1.2.3 Improved Armor Penetration

Measurements of the penetration of armor plate by projectiles of various sizes and types have shown that the thickness of plate that can be penetrated increases more rapidly than the striking velocity, being proportional to approximately the three-halves power of the velocity. This relation is known to hold approximately up to velocities somewhat above 3,000 fps, provided that the projectile does not shatter upon impact, as brought out in Section 9.2. With steel projectiles, such shattering without penetration is likely to take place at velocities somewhat above the velocities at

[c] Constant force of gravity and a plane reference surface is assumed also. Under these ideal conditions, a shot at an angle of elevation of 45 degrees and an initial velocity of 3,000 fps would travel to a distance of 54 miles, and a shot projected vertically upwards with the same initial velocity would reach a height of 27 miles; but the effect of air resistance is so great that for a standard 4.7-in. projectile, with a muzzle velocity of 3,000 fps, the maximum horizontal range is only about 15 miles (attained with an angle of elevation of 47½ degrees). The corresponding maximum vertical range is 11 miles.

which they would just perforate the plate.[d] At still higher velocities, the projectiles may penetrate even though they shatter, but there may be a range of distances (and striking velocities) at which a particular projectile is ineffective against armor. This might appear to limit seriously the usefulness of hypervelocity guns. But it should be noted that at all except short distances from target to gun, the striking velocity usually will have diminished to such an extent that it will be well below the velocity at which shattering takes place.

Further encouragement is afforded by the behavior of projectiles having cores of cemented tungsten carbide. Such projectiles show greater penetrating power than ordinary steel projectiles, as may be seen from an Ordnance Department test of a 1.5-in. (37-mm) projectile having a tungsten carbide core, which penetrated a 3⅝ plate of Class "B" armor at 20 degrees incidence at a velocity of 3,440 fps, whereas a projectile of similar design, but having a steel core, did not penetrate the same plate at a striking velocity of over 4,000 fps. Above a certain velocity, tungsten carbide cores break up when passing through armor plate. The older cores disintegrated into fine particles, but it is now known that cores can be fabricated in such a way that on passing through armor they break up into a moderate number of fragments which for antitank use are effective in putting the tank out of action.

Results of experiment and calculation indicate that, by the use of hypervelocity projectiles, materially increased effectiveness is achieved for the same total weight of gun and mount. Put in another way, it is readily practicable to obtain a desired effect with about one-half the total weight of the usual equipment, and thus with a corresponding increase in mobility.[190]

1.2.4 Increased Probability of Hitting Target

Higher velocities mean shorter times of flight and flatter trajectories; both factors are important because they increase the chance of hitting the target. In antitank warfare,[145] a flatter trajectory is advantageous because the resulting decrease in the angle of impact reduces the chance of missing the target through imperfect knowledge of the range. If an error is made in estimating the distance from gun to target, the flatter the trajectory the less will be the vertical distance from the point of aim. This may well make the difference between hitting an object of a given height and missing it altogether. As an example, we may note that for a tank 8 ft high and for a conventional 75-mm projectile with a muzzle velocity of 2,030 fps, the allowable error in estimating the range at 1,500 yd is only 100 yd, while with a tungsten carbide subcaliber projectile shot from the same gun with a muzzle velocity of 3,550 fps, owing to the flatter trajectory, the allowable error at the same range is 400 yd.

A reduction of the "lead" required in aiming at a moving target is one consequence of the shorter time of flight. For the two projectiles just referred to, the respective leads to be applied by the gunner in the case of a tank at 1,500 yd moving at a speed of 30 mph are 105 ft as compared with 60 ft. In the case of aircraft gunnery, the reduction of lead is also important; but here the advantages of hypervelocity are difficult to assess, because of various factors, especially the limitation in weight of equipment.[146,325,375]

Short times of flight are particularly desirable in firing at fast-moving targets such as airplanes, the advantage being most noteworthy when the target resorts to dodging tactics.[164] Many mathematical analyses have been made of the probability of hitting a plane from the ground in relation to the velocity of the projectiles. The answer depends upon the assumed conditions of the problem. Depending on these conditions, the number of hits for a given number of shots is found to be proportional to a power of the velocity that varies from the third to the sixth for targets moving in three dimensions. Even on the most conservative basis, that is, variation with the third power, a 50 per cent increase in velocity more than triples the number of hits.

1.3 FACTORS LIMITING USABLE MUZZLE VELOCITY

1.3.1 Individual Problems to be Solved

As indicated above, there is no particular difficulty in obtaining projectile velocities very much greater than those in conventional guns; but there are certain practical considerations that seriously limit the velocities that can be usefully employed. Among these factors, the immediately obvious is the wearing away of the material at the bore surface, especially when

[redacted]

[d] Recently, steel armor piercing projectiles of improved design have been shown to penetrate armor 3 calibers in thickness, without shattering, at velocities in the neighborhood of 4,800 fps at an angle of 30 degrees. (See Section 9.2.1.)

muzzle velocities are much above 3,000 fps. Other effects such as the overall heating of the gun barrel, the decreased mechanical efficiency of the gun, and the loss of projectile velocity in flight, add to the complexities of the hypervelocity problem. Means must be found to combat them all by solving separately the problems that arise, for the deleterious phenomena are rapidly enhanced whenever an attempt is made to achieve higher muzzle velocities.

At each stage in the history of ordnance some one or more of the factors that limit the usefulness of a gun has been predominant. As improvements in materials and in methods of fabrication have led to better ways of making guns and their ammunition, it has been necessary for the gun designer periodically to re-evaluate the problem in the light of the tactical needs of the moment. On the basis of such analyses compromises have been reached in the design of guns for particular purposes. Thus shortly before World War II design studies were made at Aberdeen Proving Ground as to the best means of improving the effectiveness of antiaircraft guns[550] and of antitank guns.[205,551] Although these studies indicated that considerable advantage would be gained in both applications by increasing the muzzle velocity to well above 3,000 fps, the new guns that were built later for these purposes perforce had lower velocities. Lack of a means of erosion control still prevented the use of otherwise superior designs.

1.3.2 Erosion[e]

During the firing of a gun, the powder burns and is converted into white-hot gas, under high pressure, which propels the projectile down the bore. At the same time, the mass of compressed gas mainly follows the projectile; and what may be called a condensed, swiftly-moving flame heats, chemically alters, and scours the bore surface. Some gas may leak past the projectile and produce locally intensified effects. In addition, the rubbing of the projectile, or its rotating band, against the inner wall of the gun tube may abrade the surface; and other actions such as abrasion by unburned powder grains may take place.

After a few rounds at high muzzle velocities, or after many rounds at lower velocities, enlargement of the bore becomes readily evident. The effects are more noticeable at the two ends of the barrel, but are not confined to these localities. At or near the origin of rifling, the damage to the bore surface is a maximum. This "origin erosion"—or, as it is sometimes called, "breech-end erosion"—may amount in a worn gun to several per cent of the bore diameter. Although the erosion per round is measured in fractions of a thousandth of an inch, or at most, a very few thousandths, the amount of metal lost is sometimes impressive, particularly in large guns. For example, in a 12-in. gun firing at 2,600 fps, nearly a pound of material may be removed from the bore surface during a single round. The erosion drops off rapidly in the forward direction and rarely is significant beyond about 10 calibers distance from the origin. With either separate-loading or fixed ammunition, a gun in an eroded condition produces less muzzle velocity unless the powder charge is increased. Another disadvantage results when the ammunition is of the "fixed" type, for with such ammunition, the initial free run of the projectile in a badly eroded gun may cause stripping of the rotating band and damage to the fuze.

Origin erosion in a given gun is directly related to the weight of powder and only indirectly to the muzzle velocity, but, in general, larger charges are necessary for higher velocities; and for only a 50 per cent increase in muzzle velocities, say from 2,800 fps to somewhat above 4,000, it can be expected that origin erosion will be increased by several times with a corresponding decrease in gun life unless means are found to cope with the erosion.

Near the muzzle, the total erosion is notably different in character and magnitude. It is greatest at the muzzle where the radial extent is usually only a small fraction of the origin erosion in the same gun, and it decreases in the rearward direction, usually becoming zero at a distance one-third or more of the distance to the breech. Although the enlargement of the bore at the muzzle is small in comparison with that at the breech end of the tube, muzzle erosion (sometimes called muzzle wear) nevertheless may lead to troublesome dispersion of shots by producing an initial yaw of the projectile. It is now known as a result of studies undertaken by Division 1 that the rate of muzzle erosion increases exponentially with the muzzle velocity; and it is probable that at very high velocities this type of erosion rather than the more familiar origin erosion constitutes the more serious limitation.

1.3.3 Heating of Gun Barrel[f]

By transfer of heat from the powder gases, the

[e] This subject is discussed at length in Part IV.

[f] See Chapter 5 for further details.

[redacted]

temperature of the gun barrel rises to an extent dependent on a variety of conditions. The temperature rise is, of course, greatest at the inner surface, where a resulting high temperature not only enhances all erosive effects but also may soften the inner layers of the wall so that the lands are flattened by action of the projectile, and the rifling no longer imparts the proper spin to the projectile. When successive shots are fired at short intervals, there is an accumulation of heat so that the barrel wall as a whole may be overheated. In machine guns after prolonged bursts even at conventional velocities, the temperature of the barrel may increase to as much as 800 C; so that the barrel may swell and eventually blow up. In rapid-fire guns of all calibers, operating at hypervelocities, the heating of the gun barrel is one of the major difficulties to be overcome before such guns become entirely practicable. From what has been said, it is evident that the high rate of fire intensifies the difficulties encountered with hypervelocity; and it is therefore not practicable to separate completely these two aspects of the broader problem.

1.3.4 Projectile Stabilization[g]

Ordinarily, projectiles are afforded stability in flight by being given a rapid spinning motion which is caused by the engagement of helical rifling grooves of the gun with a rotating band on the projectile. It can be shown both theoretically and experimentally that in order to obtain the usual rates of spin (varying from several thousand revolutions per minute in large guns to over 100,000 rpm in small ones), the stresses set up in the banding material by its interaction with the rifling often are close to the maximum strength of the commonly used materials for rotating bands. Moreover, for a given projectile, the requisite rate of spin for stability in flight is very nearly proportional to the velocity. It follows, therefore, that with conventional projectiles band failure is likely to limit the muzzle velocities that can be usefully employed, and that the broad hypervelocity problem includes among its subsidiary problems that of providing adequate stability.

1.3.5 Other Mechanical Limitations

In the usual high power guns for military application, internal pressures of the order of 50,000 psi are employed. The design of hypervelocity gun tubes would be simplified if still higher pressures could be used. (Section 33.3.9) This would require tubes with higher strength materials or with thicker walls, or both. Higher velocities for a projectile of a specified weight require larger powder charges unless a more powerful propellant is used. As noted in the preceding text, very high muzzle velocities are attained at the cost of lessened efficiency at which the energy of the powder is converted into kinetic energy of the projectile, and therefore powder weight and powder-chamber capacity increase faster than the muzzle energy. A more troublesome limitation is introduced by the fact that larger powder charges almost inevitably require longer, heavier, and more cumbersome gun tubes. Clearly, the overall weight of the tube and mount is an important factor that enters into considerations involving the advantages of hypervelocity and into the design of guns having optimum effectiveness.

It is evident that when all, or a sufficient number, of the individual problems have been solved and the limiting factors properly taken account of, there remains a careful balance between conflicting elements of design, if a satisfactory use is to be made of hypervelocity.

1.4 STATUS OF PROBLEM IN 1941

1.4.1 Divergent Views on Advantages of Hypervelocity

To those scientists and engineers who in 1941 made their first acquaintance with ordnance matters, the most striking aspect of the situation was the lack of agreement among qualified observers as to the advantages of guns having muzzle velocities much higher than those being currently employed. On the one hand, there were circumstances[425] that indicated pronounced advantages, as brought out in Section 1.2; while on the other hand, certain lines of reasoning indicated that higher velocities would offer little or no improvement in overall performance.[146,325]

The need for increased range, both horizontal and vertical, had been urged in certain quarters, and in particular it was evident that a higher vertical range would be desirable as a protection against airplanes which were flying at ever-increasing altitudes.[550]

Prior to 1941, some attention had been given to the presumable advantages of machine guns with higher muzzle velocities. The need for such guns had not

[g] Compare Section 8.3.

been clearly formulated nor had the desirability of developing machine guns that would fire long bursts without becoming useless been recognized.

1.4.2 Imperfect Understanding of Nature of Erosion

Despite the numerous investigations over a period of years on gun erosion, some of which were conducted with great skill and perseverance, there was little real understanding of the processes by which the bore of a gun is eroded during firing. To be sure, a number of suggestions had been put forward as to the principal causes of erosion.[15,16] Among these were abrasion of the surface by unburned powder grains, a scouring of the surface by the blast of powder gases, a melting of the surface material and subsequent blowing away, chemical action by the constituents of the hot gases, friction between the bore and projectile, and a variety of other factors. The results of previous efforts to reduce erosion had not been encouraging. In the belief that materials other than steel were not practicable for gun barrels, most of the efforts had been devoted to the development of steels of better performance. It was thought in those days that an improvement of something like 5 per cent in erosion resistance would represent a worthwhile goal.[244]

The general attitude prior to the war may be characterized as a tendency to take a somewhat pessimistic view of the erosion problem and to minimize the advantages of the higher velocities that would be practicable if erosion could be cured or by-passed.

1.4.3 NDRC Attacks Problem in Comprehensive Way

Initially, the National Defense Research Committee [NDRC] undertook projects of direct and immediate applicability to military needs. Although there was an obvious need for guns having better performance, it was generally known that serious difficulties stood in the way of realizing guns with higher muzzle velocities, and NDRC quite naturally hesitated to spend time, effort, and money on problems of uncertain value for the current emergency or for the impending war. Gun erosion was the key to the situation, and preliminary consideration of the whole matter raised grave doubts as to whether it would be proper or profitable for NDRC to attempt to engage upon a program for the solution of the age-old erosion problem. It is not to be wondered at that the Armed Services should have had little hope that this problem could be satisfactorily solved or should offer only faint encouragement for taking up a hypervelocity project as a wartime measure.

The situation eventually crystallized in a decision, largely as a result of the views of the British, who strongly urged that NDRC undertake broad problems in ordnance and placed as number one on their list of projects the practical attainment of hypervelocity guns and projectiles. In particular, for antiaircraft use, they emphasized the need for a gun that would fire a projectile having a time of flight of only 3 sec to 10,000 ft—which would require a muzzle velocity of from 4,000 to 5,000 fps.

In the summer of 1941, NDRC decided to embark on a broad program, and for this purpose, Section A-A, later Division 1, was created, its assignment being "gun erosion and other ordnance problems," a title intended to camouflage the real objective, which was the development of practical hypervelocity guns and in general the improvement of gun performance. The program was intended to be a long-range one with the initial emphasis on basic research, with the understanding that the immediate trial of promising devices and even the playing of hunches were not to be excluded. This ambitious venture was entered into with the full knowledge of the complexities of the subject, and a realization of the difficulties that even experienced investigators would encounter, if they undertook to solve problems in a field with which they were not familiar and in which ordnance experts had made little progress for many years. But it was the duty as well as the privilege of NDRC to concern itself with ordnance projects of any kind that seemed worthwhile, and it was evident that a thorough exploration of the possibilities of vastly improving the existing guns was a necessary "hedge" against a long-continuing war, the hypervelocity program being in the nature of essential insurance against the adverse effects of increasing technical proficiency on the part of our potential enemies.

1.5 APPROACHES TO PRACTICAL ATTAINMENT OF HYPERVELOCITY

1.5.1 Classification of Methods

Higher velocities ordinarily are accompanied by greater erosion. The practical attainment of hypervelocity therefore involves principally the discovery

CONT[redacted]

and application of methods for avoiding or circumventing erosion so that the gun may have a reasonably long life. Several lines of attack were apparent as the program of research and development began to be formulated. Erosion may be combatted by an erosion-resistant liner or coating. A suitable protection might also be given by a film of some sort applied to the bore surface. Inasmuch as the most seriously eroded part of the bore is near the origin of rifling, this part of the bore surface could be protected from the powder gases by a thin sleeve attached to and extracted with the cartridge case. Lightweight projectiles may be used in a standard gun, a procedure which partially solves the erosion problem. Finally, propellants that have a lower flame temperature and less chemical activity might significantly diminish the erosive effect. The specific devices and methods that, after preliminary inspection of the problem by Division 1, seemed promising for investigation are given in the following paragraphs and are described in detail in other chapters of this volume.

1.5.2 Replaceable Steel Liners

It was said somewhat facetiously in the early days of Division 1 that the way to solve the hypervelocity problem was to let the gun wear out, throw it away, and get a new one. More seriously, a liner could be discarded; and it was judged worthwhile to investigate thoroughly the practibility of developing a short steel liner, which could be inserted in the bore at the breech end and, when badly worn, promptly replaced by a new one. This development is described in Section 26.3.

1.5.3 Erosion-Resistant Liners and Coatings

The selection and development of materials that will resist gun erosion obviously require a knowledge of the nature of gun erosion and the principles by which it is possible to combat it. Parts III and IV of the present volume are taken up with the description of the basic research applied to this part of the problem. It was necessary to have better information concerning the behavior of the powder gases in a gun and concerning other features of interior ballistics. As a result of the intensive studies on erosion, it was possible at an early stage of the investigation to define accurately the physical, chemical, and mechanical requirements for usable erosion-resistant substances, and to make a preliminary selection of erosion-resistant materials for development and trial. As will be shown in Parts V and VI, primary attention was focused on chromium, on molybdenum, on alloys containing dominant amounts of these metals, and also on high-cobalt alloys. Some of these, as for example chromium, seemed more suitable for application as electroplated coatings. Others were more promising for application as liners.

1.5.4 "Fisa" Protector

A suggestion that came from abroad formed the basis of another approach to the practical attainment of hypervelocity. This took the form of a thin sleeve to be attached to the forward end of the cartridge case enclosing the rear portion of the projectile and extracted with the case after firing. This device seemed worth developing because the erosion in a gun is most noticeable near the origin of rifling. Accordingly, the protection of the bore surface for even a short distance in this region would be advantageous and it therefore seemed worth while to evaluate this device. Designs and performance are discussed in Chapter 32.

1.5.5 Pre-Engraved Projectiles

It soon became evident that the interaction between the rotating band and the bore surface was an important source of deterioration of the surface. The stresses arising from the engraving of the band are likely to damage the surface, particularly by flattening the lands; and the frictional heat superimposed upon that derived from the hot powder gases will obviously augment all adverse thermal effects. By using pre-engraved projectiles, that is ones on which "teeth" had previously been formed for engaging with the rifling grooves, these mechanical effects are obviated.

Furthermore, a pre-engraved projectile was found to be a valuable research tool because it offers the opportunity of separating some of the effects due to the powder gas and those due to the rotating band. As the development proceeded, it became evident that the practical value of pre-engraved projectiles is much enhanced by using them in conjunction with a bore surface protected from the powder gases. The chromium plate is inert to the powder gases; and the pre-engraved projectiles do not cause mechanical deterioration of the plate, as engraving-type projectiles do. The device, as finally put in the practical form described in Chapter 31, consisted of the combination

of pre-engraved projectile and chromium-plated bore surface.

1.5.6 Sabot-Projectiles

A sabot offers a convenient means of using a lightweight projectile and therefore obtaining hypervelocity in a standard gun. Sabot-projectiles do not represent a new idea, having been tried out many years ago; but, because they offered a possibility of quick solution of the hypervelocity problem, it seemed worth while to make a serious attempt to develop a practical projectile of this kind. Fundamentally, such a projectile consists of a subcaliber core, of either steel or tungsten carbide, supported in the bore by a sabot, which is a framework of some sort, including a base that fits the bore and carries a rotating band. Upon being fired, the projectile proceeds with the velocity appropriate to the weight of the assembly in relation to the powder charge. Shortly after leaving the gun, the base and auxiliary parts fly off by centrifugal action or air resistance, and the core goes on toward the target. It was recognized that a considerable amount of research and development would be necessary in order to meet various requirements such as stability of the projectile and in general the requisite accuracy of the shots. (See Chapter 29.)

It is not immediately obvious that the sabot is a true solution of the hypervelocity problem, in the sense of providing higher velocities with reasonable gun life. Although it is a convenient method for combining large powder charges with projectiles of relatively light weight, it might appear at first glance that erosion would offer the same limitation as it does in conventional guns. It turns out, however, that the more noticeable variety of erosion in a gun, namely that near the breech end, depends more on the ratio of powder charge to bore surface than on the weight of the projectile. Consequently, with a lightweight projectile, the erosion may be expected to be much less than would be encountered with conventional guns and projectiles operating at corresponding muzzle velocities. For this reason, such devices are properly considered among the fundamental approaches to the practical realization of hypervelocity.

1.5.7 Tapered-Bore Guns

Another method for practical utilization of a lightweight projectile that has a sufficiently high sectional density is represented by the tapered-bore gun. This device was known to have been developed in Germany prior to World War II. Remarkable results were credited to a 28/20-mm tapered-bore gun used by the Germans in the African campaign against the British. A projectile with flanges, or skirts, is reduced in diameter as it passes through the bore, of which all or a part is tapered so as to decrease in diameter in the direction of the muzzle. The further investigation of such guns clearly was a necessary part of the hypervelocity program. Little was generally known about the principles of design of such projectiles for most effective performance, or of the performance of guns with the bore tapered in various ways. Results of the investigations by Division 1 on tapered-bore guns and projectiles will be found in Chapter 30.

1.5.8 Other Devices and Processes

There are several other approaches that were given consideration by Division 1 but were not actively explored by that organization, although some of them are discussed in various chapters of this volume. A propellant of decreased erosiveness would obviously be of great advantage, for improved action might result from lower flame temperature or lessened chemical activity. Furthermore, a powder of greater energy for a given bulk would simplify appreciably the design of hypervelocity guns. Successful methods for cooling the bore surface or the entire barrel would counteract the tendency to erosion and would minimize other difficulties with high-power guns, especially those operating at a high rate of fire. Inasmuch as a part of the troubles arising from high velocities are due to the action of conventional rotating bands on the bore surface, improved rifling and banding are desirable subjects for investigation. Still another in the list of devices for appraisal and investigation was the "booster" projectile, for which added velocity is given to the projectile near the end of its course by a rocket attached to the base.

1.6 STATUS OF PROBLEM IN 1946

1.6.1 Clarification of Advantages of Hypervelocity

As one of the results of the comprehensive series of investigations undertaken by Division 1 and as the result also of the various tactical and strategic situations occurring during the past 5 years, the advantages of hypervelocity now stand out in much sharper

relief than heretofore. (For an analysis of these advantages, see Section 33.2.) In comparison with the attitude in 1941, there is now little doubt as to the reality of the advantages of projectiles with velocities in what we call the hypervelocity range, that is, those in excess of 3,500 fps.

For antitank warfare, for other ground use, for antiaircraft applications, or for aircraft armament, there is now little division of opinion as to need for improving conventional guns. Greater range, improved armor penetration, and increased probability of hitting a target, more especially a fast-moving airplane, add up to an advantage that few will ignore. In 1946, the problem is not so much to evaluate the merits of hypervelocities, but rather to find the best means of achieving them.[h] One would now indeed be conservative not to visualize the "gun of the future" as one firing projectiles with an initial velocity of more than 4,000 fps, and quite possibly more than 5,000. It can be claimed fairly that the war period has clarified our notions on this subject.

1.6.2 New Knowledge Concerning Nature of Gun Erosion

The scientific groups who undertook to find quickly the cause and cure of gun erosion, who somewhat naïvely approached with confidence the task of making real progress in a field new and strange to them, a field in which significant advances had not been made for many years, have the satisfaction of knowing that they now have a picture of gun erosion that is clearly outlined, although not complete in all its details. They can visualize the several steps in gun erosion, and they can differentiate between the nature and probable cure of origin erosion on the one hand and muzzle erosion on the other. It is now quite definite that of the various possible factors in the erosion of guns, thermal effects, including melting, aided and abetted by chemical action, are the general regulators of origin erosion, and it is also apparent how other factors, such as stress and frictional heat associated with rotating bands, enter the erosion problem. In addition, a useful distinction has been drawn between the origin erosion of high-power, slow-fire guns where the overall effect is a loss of the material from the bore, and the deterioration of machine guns firing long bursts at moderate velocities where the outstanding factor in bringing the gun to the end of useful life is a flattening of the lands on the softened bore surface.

We now perceive that the erosion problem has several aspects, each of which in reality presents a separate problem. The first may be called the "high-power gun" or the "big-gun problem," which is solved either by diminishing the heat to each unit of the bore surface or by supplying a liner or coating that is sufficiently chemically inert and at the same time is refractory enough to withstand, without melting, the intense heat applied over a short interval of time. The second, the "machine-gun problem," finds its solution in the knowledge that here the *desideratum* is hot-hardness and in the use of a liner or a coating of adequate hot-hardness, or a combination of liners and coatings, in the protection of the bore surface. To these problems we may add a third, which relates to the cure of muzzle erosion. Although in 1941 the extent to which muzzle erosion was prevalent in guns was not well known, and even its existence generally in guns was a subject for frequent debate, it is now known to vary in an orderly fashion with muzzle velocity and caliber. Indeed, its variation with muzzle velocity is well enough understood for us to predict confidently that at muzzle velocities of 4,000 fps or more it will begin to be of commensurate importance with origin erosion, and may even be the dominating factor. We also have sufficient understanding of the nature of muzzle erosion to afford promising leads for the avoidance of the difficulty.

These various conclusions on the nature of erosion emanated partly from well selected tests and partly from basic research in a closely integrated series of investigations.

1.6.3 Development of Several Solutions of the Hypervelocity Problem

The investigations of Division 1 provided new knowledge that was not only interesting and suggestive but also of practical value, as is demonstrated by the fact that the results and conclusions led to the successful development of six useful, or potentially useful, solutions of the hypervelocity problem. At the time Division 1 discontinued its activities, various devices embodying these solutions either had been offered to the Services or were in an advanced state of development. These were the following devices already described briefly in Section 1.5: The replaceable short steel liner, a variety of erosion-resistant liners and coatings, the pre-engraved projectile with

[h] A statement of the British point of view on this subject was prepared in the summer of 1944.[395]

chromium-plated bore, the Fisa protector with chromium-plated bore, sabot projectiles, and the tapered-bore gun with skirted projectiles. In the category of erosion-resistant liners are ones of hardened molybdenum, which offers a gratifying solution of the high-power gun problem, and those of Stellite No. 21, which in the caliber .50 machine gun has given a solution of the machine-gun problem that was successful to the point of being spectacular. Stellite-lined machine guns were in large production at the close of the war.

Other approaches to the practical attainment of hypervelocity were given some consideration by various civilian and military groups, but Division 1 did not participate actively in the investigation of those methods, including the ones mentioned in Section 1.5.8.

1.6.4 Demonstration of Successful Method for Attacking Difficult Ordnance Problem

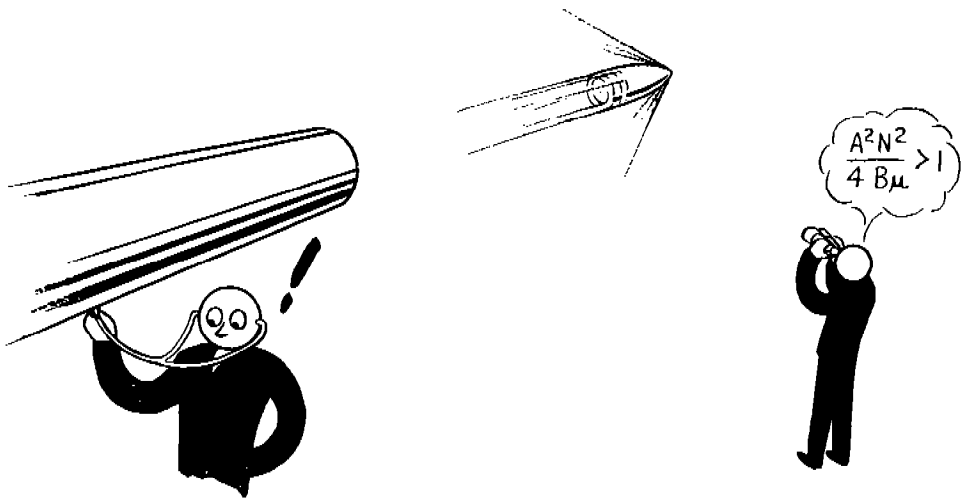
That the task undertaken by the Division 1 in 1941 was one of formidable complexity, few will deny; and we think it fair to claim that the outcome was reasonably satisfactory. It might even be claimed that whereas the group of investigators, upon first acquaintance with the field of gun erosion and hypervelocity, found it a frozen subject, they left it a fluid one. The procedure that was followed might therefore serve as a pattern for future investigations in the same fields or in ones of similar difficulties and scope. We feel that whatever success may have been attained was largely due to two factors.

The first was the inclusion of an adequate amount of fundamental research. In the broad program of Division 1 neither research nor engineering development was neglected. There was at all times a judicious combination of effort in these two directions, the former being the fruitful source of new ideas and the latter the means to a useful end. For example, as soon as promising results were obtained with stellite liners, plans were put into effect for the production of caliber .50 machine-gun barrels with such liners; while at the same time further investigations were conducted in order to learn more about the fundamental behavior of this material under various conditions.

The second essential factor was the constant preservation of an open mind as to the possibilities of success of any development no matter what the apparent obstacles might be, and a refusal to be swayed unduly by unpromising results of various lines of attack in the past. The guiding philosophy might perhaps be described as a resolution to "lean neither to foolish optimism nor to unreasoning conservatism."

PART II

BALLISTICS



Who should decide when doctors disagree
And soundest casuists doubt like you and me.
—*Alexander Pope*
"Moral Essays"

Chapter 2

PROPERTIES OF POWDER GAS

By *F. C. Kracek*[a]

2.1 INTRODUCTION

THE CHEMICAL SYSTEM of powder and gas presents a complex in which chemical reactions occur at high speed with remarkable precision. The free energy of powder gas is much less than that of powder, and the reaction between them, when once initiated, goes forward rapidly—in common parlance, the powder burns. The gas is never in equilibrium with the powder; the powder must first be "vaporized," the intermediate products then react further, and under suitable conditions, the final products come to equilibrium with each other as powder gas at a high temperature. These intermediate steps are of interest both theoretically and in practice, for they lead to a better understanding of the use of powder to give a push on a projectile or a rocket.

Modern propellants are composed of certain principal constituents, explosive in nature, and other added constituents used as plasticizers, stabilizers, or solvents to modify the physical properties of the explosives and make the resulting substance safe for handling as a propellant. The principal explosives used are cellulose nitrate (nitrocellulose, NC) and glycerol nitrate (nitroglycerine, NG); others more recently introduced are nitroguanidine (NQ) and hexamethylene trinitramine (cyclonite, RDX). All are compounds of carbon, hydrogen, oxygen, and nitrogen, and contain enough oxygen in the reactive $-O-NO_2$ (nitrate), or $-NO_2$ (nitro) groups for internal combustion.

This combustion, the completeness of which depends upon the ratio of oxygen to carbon and hydrogen, produces a quantity of heat, known as the heat of explosion, and results in the conversion of the solid powder to a gas composed principally of nitrogen, carbon dioxide, carbon monoxide, water, and hydrogen. The relative proportions of these gases in the final products are determined by (1) the relative contents of carbon, hydrogen, oxygen, and nitrogen in the propellant, and (2) the temperature and pressure developed in the process of burning. Additional gaseous constituents are present in the powder gas, as a result of dissociative high temperature reactions, or of secondary reactions which occur on cooling. These are relatively unimportant, and will be considered only incidentally.

It is important to note that explosives are inherently unstable at all temperatures, and can be prepared and kept only because the decomposition reactions proceed exceedingly slowly at ordinary temperatures. The initiation of the decomposition requires a certain activation energy which may be supplied by heating or by impact. The resulting decomposition may be burning or detonation, the two being distinguished by the speed with which the process takes place; the rate of detonation is about a thousand times that of burning. The detonation of explosives was studied intensively in other divisions of the NDRC; the burning, particularly of propellants, falls within the scope of the work of Division 1 and is treated in the following pages.

Recent investigations have enabled us to put labels on the intermediate steps in the conversion of powder to the final products. The rates at which these steps occur are connected with the mechanism; some experimental evidence on this is also available. These problems are treated in the second section of this chapter. The next section takes up the problem of equilibrium, and evidence is presented to show that at least so far as the final reaction in powder gas is concerned, equilibrium is maintained among the final products.

Internal ballistics is concerned with the conversion of the "latent" energy of the powder into mechanical energy through the medium of powder gas. The chemical thermodynamics of this process are presented briefly in Section 2.4. Experimental methods for determining the temperature of powder gas, discussed in the last two sections, present an experimental check on the theoretically calculated temperatures, and together with measurements of pressure, enable the ballistician to discuss the state of powder gas.

2.2 THE BURNING OF POWDER

2.2.1 The Overall Burning Process

When a propellant is ignited in a closed chamber at a high density of loading, and suitable measurements

[a] Physical Chemist. Geophysical Laboratory, Carnegie Institution of Washington.

are taken, it is noted that soon after ignition is initiated, the pressure begins to rise and then reaches a peak value in times of the order of milliseconds. Simultaneously with the development of pressure, the contents of the chamber begin to emit radiation the intensity of which, like the pressure, reaches a peak value.[44]

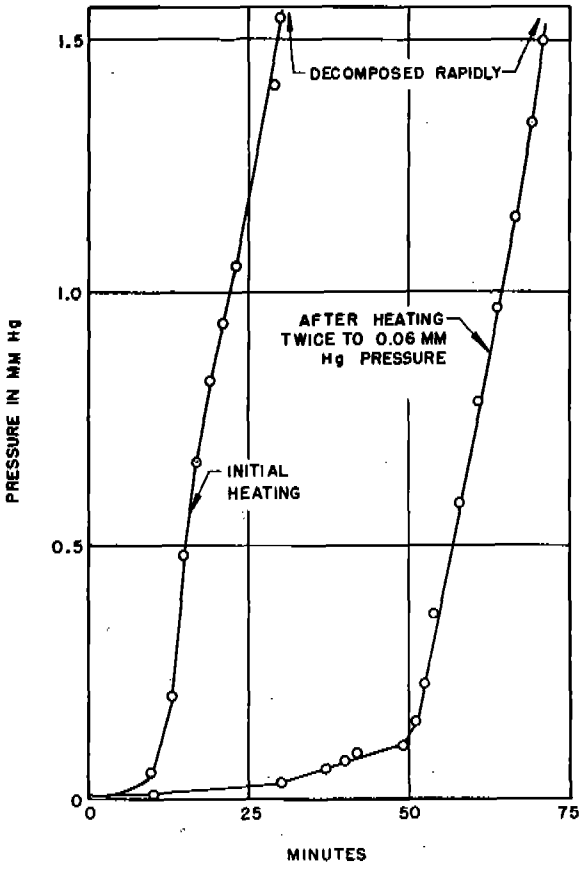


FIGURE 1. Decomposition of nitrocellulose at pressures below 1.75 mm Hg. Reaction becomes self-sustaining at higher pressures. (This figure has been redrawn from Chart No. I in Ballistic Research Laboratory Report No. 353, Aberdeen Proving Ground.)

The radiation at high densities of loading is continuous in the visible and near infrared regions of the spectrum; at very low densities of loading, discrete lines appear in the spectrum. These are due to inorganic constituents or impurities. The radiation at high densities is found to be not only continuous but also to have a distribution of intensities with respect to wavelength such as would be typical of a black body at a temperature T which is somewhat lower, because of the heat losses, than the adiabatic flame temperature T_0, characteristic of the propellant. As example, typical values of T_0 are 2650 K for NH, 2440 K for FNH-M1, 3525 K for FNH-M2 powders. The temperature T has been identified as the temperature of the powder gas.

The instants of time at which the peak of the radiation and the peak of pressure occur coincide closely and denote the conclusion of the process of burning. After the attainment of the peak values, heat continues to be given off to the walls as the gas cools; in a gun, the gas is cooled not only by such heat transfer but also by conversion of a part of its thermal energy to kinetic energy of the projectile. The distribution of the energy of the powder is discussed in Section 6.5, in which the relation of the gas temperature to the energy is shown.

The details of the burning of the powder cannot be analyzed in such experiments as described above and must be investigated in other ways, but the overall kinetics of the burning process can be learned from the measurement of the rate of pressure increase, at times preceding the attainment of maximum pressure.

Experimentally, it is known that powders do not ignite until the surface is raised to a temperature near 200 C; the self-sustaining reaction probably maintains the surface at about 1000 K.[160] This burning may be extinguished upon sudden reduction of pressure, as this causes appreciable cooling of the gas at the surface. This suggests that stable burning requires heat to be transferred to the surface by the hot gases in an amount sufficient to maintain the surface layer hot enough for rapid decomposition of the powder to take place.

The amount of heat transferred to the surface may be expected to depend upon at least two factors; (1) the intensity and type of radiation which falls upon it, and (2) the number of molecules of high energies which collide with it per unit time. The part played by radiation, which is difficult to evaluate, will be discussed later.

The number of colliding molecules will be nearly proportional to the pressure, but their average energies cannot be estimated without detailed knowledge of the reactions involved in the process of burning. If we assume, as a first approximation, that the entire reaction process takes place at the powder surface, then the gas molecules have energies corresponding to the flame temperature T_0. On this assumption, the burning rate may be expected to be high for powders whose flame temperature is high, and this is at least qualitatively confirmed by experiment. As we shall see, the reactions liberating the energy of the powder

take place only partly at the surface, but mainly in the gas space, probably separated from the surface by a more or less thin layer of cooler gas. This reduces the rate of heat transfer but does not necessarily alter the relative order of burning rates for hot and cool powders.

2.2.2 The Stepwise Mechanism of Burning

Before considering the *rates of burning* of powder it is desirable to present an outline of the reactions involved in the *process of burning*.[b]

As long ago as 1907, it was demonstrated[457,458] that an early step in the decomposition of nitrocellulose and nitroglycerine is the splitting off of NO_2 from the molecules of the explosives, and that the NO_2 is quickly reduced to NO when the gas is allowed to remain in contact with the decomposing substance. Recent experiments[194] have shown that at very low pressures (below 1.75 mm Hg) the decomposition reaction of nitrocellulose is endothermic with the evolution of gas, and may be stopped and restarted at will by controlling the heating (see Figure 1). At pressures above this value, the reaction becomes exothermic and hence self-sustaining; it proceeds with the evolution of gas and sublimation of a white solid. At still higher pressures and with a chemically indifferent gas present (about 40 mm Hg), there is produced a resinous red liquid that gives the chemical reaction for aldehydes. This evidence indicates that the original cellulose nitrate molecule has been attacked, most probably at the points of attachment of the nitrate groups.

The liquefaction of nitrocellulose has also been observed[350] at a pressure of about 50 mm Hg of nitrogen, in experiments on controlled thermal decomposition. At 1-atmosphere pressure with air in the apparatus, liquefaction was not complete before an explosive inflammation occurred; the ignition was preceded by an induction period which was shorter at higher temperatures. The activation energies deduced from the variation of the induction period with temperature, and of the rates of gas evolution during the quiescent preignition decomposition agree provisionally with the activation energies for the splitting of the $-O-NO_2$ bond, which is known from other data to be 40–50 kcal.

The exothermic heat effect up to the point of consumption of the red substance has been measured to be near 500 cal/g, about one-half of the full heat of explosion of nitrocellulose. Similar experiments yield approximately the same values with double-base powders (rocket compositions, cordite S.C.). The gas produced at this stage contains the nitrogen of the powder principally as nitric oxide (NO); other gases present are CO_2, CO, H_2O, with very little H_2 and no NO_2. Upon inflammation, H_2 definitely appears in the gases, and the full heat of explosion tends to be realized. (See Figure 2.)

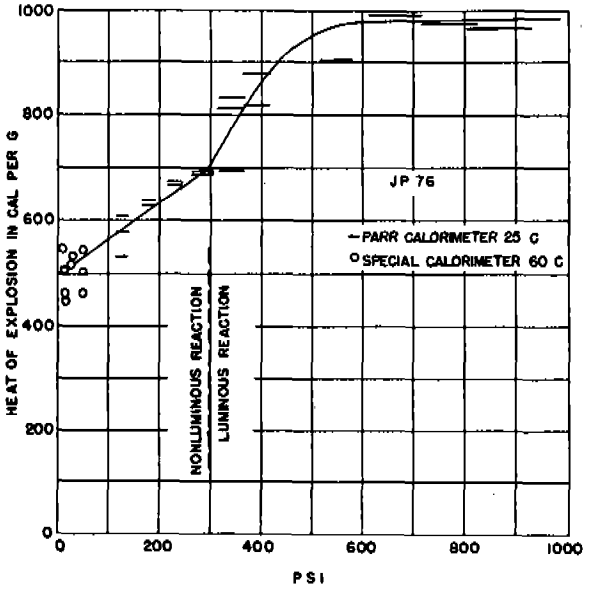


FIGURE 2. Heat of explosion as a function of gas pressure showing the course of the curve in the region of the transition from nonluminous to luminous burning of propellant JP76. (This figure is based on Table VI of NDRC Report A-268.)

Visual observation of the formation of flame from the burning of double-base rocket powder in nitrogen under pressure[161] shows a transition from nonluminous to luminous burning at pressures near 300 psi. The flame, when first formed at the lowest pressure, is at some distance from the stick of powder, but approaches it as the pressure is raised, as shown in Figure 3. The transition from nonluminous to luminous burning in the gas phase marks the beginning of disappearance of NO from the gas. It is accompanied by an increase of the heat evolved with increasing pressure; the full heat of explosion is reached at about 700 psi. At this pressure the NO in the gas virtually dis-

[b] Most of the data upon which this outline is based has been accumulated during the war years by investigations at the Ballistic Research Laboratory, Aberdeen Proving Ground, [194,198,243,548,549] by contractors of Divisions 1 and 3, NDRC, [107,159–163,547] and by investigators working for the British Ministry of Supply.[334,335,345,350,364,396]

appears. At the higher pressures the gas contains N_2 and the water gas reaction gases CO, CO_2, H_2, and H_2O in chemical equilibrium at the flame temperature. The gases of the nonluminous zone are not in equilibrium, and probably contain fragments of the original molecules; thus C_2H_2 has been detected in quenched gas from nonequilibrium burning.[107] The temperature of this zone has been estimated[e] to be about 1200 K.

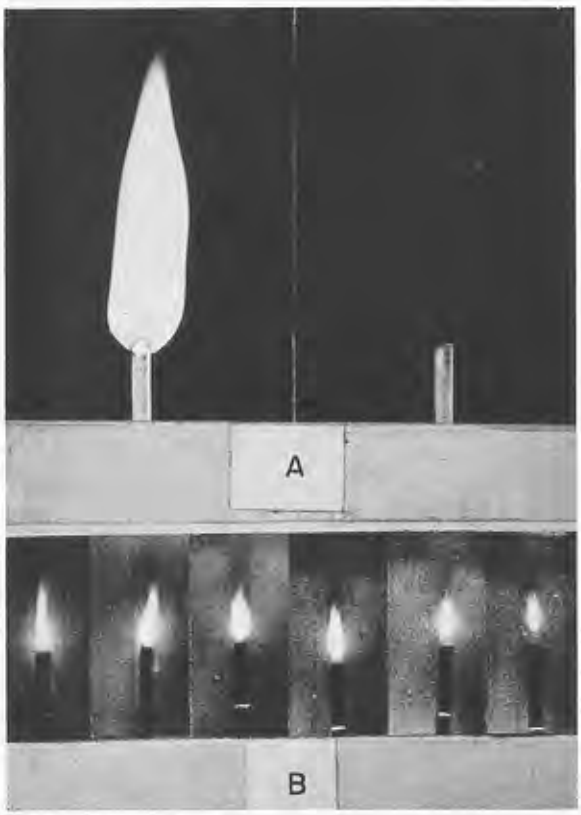


FIGURE 3. Nonluminous to luminous transition in the burning of double-base powder. (A) Luminous and nonluminous burning of powder HES 4016. (B) Variation in thickness of the dark zone, powder HES 4196 burning in nitrogen (25 C) at pressures (left to right) 410, 365, 310, 280, 255 and 225 psi. (These figures have appeared as Figures 1, 2, and 3 of NDRC Report A-268.)

SUMMARY

The foregoing stages of burning may be summarized somewhat as follows:

Stage A: Initial Decomposition. Through heat supplied from the outside or from subsequent reactions, the surface of the powder grain is brought to a temperature at which gases are just evolved at a rate determined by the heat supply. This endothermic stage may be the activation of decomposition of the $-O-N$ bond. The gas may contain NO_2.

Stage B: Secondary Decomposition. The highly reactive gaseous products of Stage A react with one another or with the material on the surface of the powder, with the evolution of heat (which makes the reaction self-sustaining) and of further gases, and a volatile solid or aldehydic liquid, depending upon the pressure at which the reaction occurs.

Stage C: Gasification of Intermediate Products. This reaction is a continuation of Stage B. It results in further evolution of heat and production of not fully reacted gases containing much of the nitrogen of the powder as NO, and the C, H, and O as CO_2, CO, and H_2O. Little H_2 is present. The net thermal effect of Stages A, B, and C is an evolution of about one-half of the full heat of explosion. It is probable that only part of the condensate of Stage B has reacted at this point.

Stage D: Final Reaction. Oxidation of the remaining combustible products by nitric oxide, with the formation of N_2 and of the water gas reaction gases, CO, CO_2, H_2, and H_2O, in chemical equilibrium at the temperature of the flame, releases the second half of the energy of the overall reaction. It appears to be very sluggish, and is believed to have no effect on the rate of the overall reaction other than that due to the increased temperature of the powder surface.

Stage E: Postburning Stage. After all of the energy of the powder has been liberated and the final products evolved, the gas cools with a readjustment of the equilibrium of the water gas reaction, and production of secondary reactions, such as the formation of methane from CO and H_2. These reactions occur with changes in energy which are small in comparison with the heat of explosion.

Thus the steel of the bore surface of a gun is in contact with a variety of gases other than those found by an analysis of the relatively cool gases ejected at the muzzle. This situation, although vaguely suspected, had not yet been experimentally demonstrated when Division 1 began its investigation of gun erosion. It helps to explain the existence of some of the products of erosion found on the bore surface, which are described in Chapter 12.

2.2.3 The Rate of Burning

From the preceding discussion it appears that the rate of burning is controlled, not by the rate of forma-

[e] Personal communication from Capt. J. H. Frazer, BRL.

CONFIDENTIAL

tion of the final products in the gas phase (Stage D), but rather by the rates of the reactions taking place at or near the surface of the powder, Stages A, B, and C of the process of burning. Stage D contributes to the rate insofar as the heat liberated in the gas phase reaches and penetrates through the surface and thus heats the solid powder. The thermal conductivity of the powder being low, and the times at disposal short, this penetration is exceedingly shallow.

Rates of burning have been studied largely by measurements of the rate of change of pressure after ignition. Early experiments of this sort showed that the pressure increases slowly at first, both in closed chambers and in guns during the period before the projectile starts to move, and then more and more rapidly, the pressure-time curve somewhat resembling a hyperbola or a parabola.

The powder is believed to burn at the surface in parallel layers, it being assumed that all the surface is ignited at the same time, and burns at the same rate. This rate may be defined as the rate r at which the parallel layers are removed in the direction normal to the surface. The rate of "recession of the surface" may be related to the mass burned up to any instant by means of form functions derived from the geometry of the various types of granulations.[520] The functions proposed to express r in terms of the pressure P are of two general types, as given in equations (1) and (2).

$$r \equiv \frac{dx}{dt} = a + bP^m \qquad (1)$$

$$r \equiv \frac{dx}{dt} = cP^n \qquad (2)$$

in which dx/dt is $-W(df/dt)$, W being the web thickness and f the fraction of the web which remains unburnt at any time. The coefficient c in equation (2) is denoted B in the Division 1 system of ballistics described in Chapter 3. Equation (2), was proposed by Vieille in 1893. He recognized that the exponent n varies for different types of powder, having values from about 0.75 to 0.95. The rate equation (2) with a fractional exponent is difficult to handle in interior ballistics equations, and the general practice has been to adopt $n = 1$ and make a judicious adjustment in the value of c.[26]

For closed chamber firings, equation (1) has been rewritten[436,439] in the form of equation (1′).

$$r = a + bP \qquad (1')$$

This equation of a straight line with an intercept is a good approximation to the experimental results in the higher pressure range, above perhaps 1,500 psi, as has been shown by measurements[141] for the range of pressure up to and beyond 20,000 psi.

At lower pressures, such as are attained in rockets (600–6,000 psi) the exponential form, equation (2), is a better fit; in fact, with certain rocket powder compositions, the exponent n is so small (about 0.5) as to rule out the linear form altogether.[161] At very much lower pressures, in the neighborhood of 1 atm, the experimental curve shown in Figure 4 indicates a break in the curve of burning rate vs pressure, as if the mechanism of burning here suddenly changed. Fortunately this region is of no interest for ballistics.

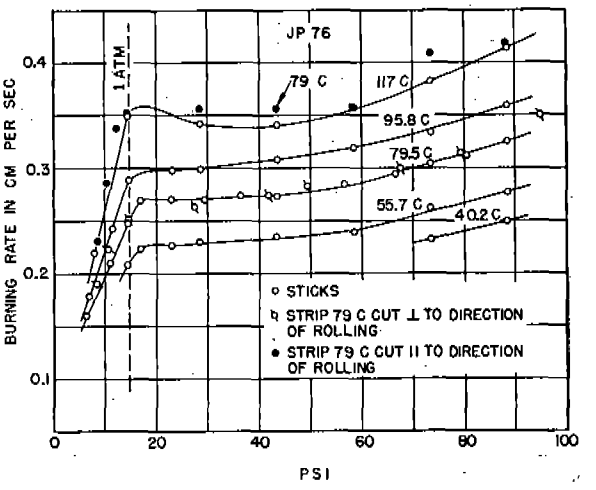


FIGURE 4. The course of burning rate versus pressure for JP76 at different low pressures and temperatures showing the break at about 1 atm. (This figure has been based on Figure 19 of NDRC Report A-268.)

In the intermediate pressure range (up to 2,000 psi) the rate of recession of burning powder was observed[161] visually and photographically in a chamber equipped with a glass window. This direct measurement yields lower values for the burning rate than the indirect measurement from a pressure-time curve secured[159] in a rocket motor. The discrepancy is ascribed to a more rapid consumption of powder in the rocket than in a closed chamber by removal of the products of combustion, and by erosion.

A comparison of the burning rate r as a function of the pressure for the straight-line law with an intercept, and the simple power law is given in Figure 5. The data represented by the straight line are those for the closed chamber burning of a powder containing 58% NC, 40% NG, 1% centralite, 0.2% diphenylamine, and 0.9% volatiles at a loading density of 0.1. For the purpose of the comparison, the straight

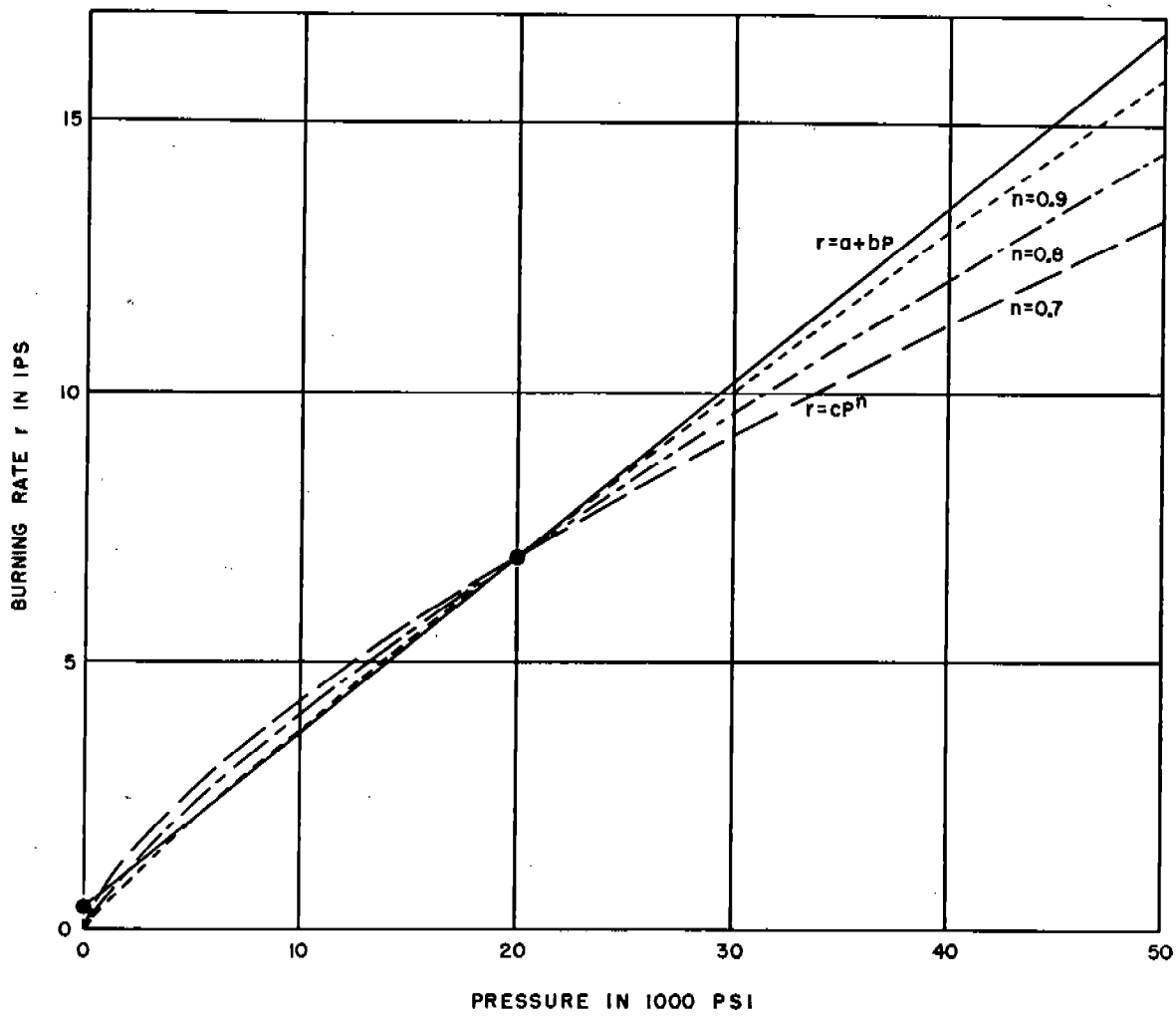


FIGURE 5. Comparison of the course of the burning rate versus pressure for the linear law (with intercept) and the exponential law. (This figure is based on the data for Powder A-20 contained in Appendix II of OSRD Report 4382.)

line is extrapolated beyond the 19,500 psi measured, to 50,000 psi. The curves representing the power-index law are drawn for $n = 0.7$, 0.8, and 0.9, respectively, adjusted to coincide with the straight line at 20,000 psi. It will be noted that over the measured interval of about 1,000 to 20,000 psi, the error would not be great, whether the data were represented by the power-index law with $n = 0.8$ or 0.9, or by the straight-line law, although, over an extended range of pressure the four curves deviate from each other appreciably.

A further comparison of the two burning-rate laws is afforded by the firings of the 3-in. Navy gun, and the 37-mm gun, T47 at the Taylor Model Basin.[39,65,131,132] (These guns are described in Sections 4.2.2 and 4.2.3, respectively.) The burning rates, which have been discussed in two Division 1 reports,[113,116] are represented in Figure 6 as a function of pressure. It is seen that it would do considerable violence to the data to represent them by the pressure-index law. The values of the constants a (in./sec) and b (in./sec/klb/in.^{2}) for equation (1′) applied to these data are given in Table 1. The values of the constant a are somewhat erratic, and considerably higher than might be expected from the closed chamber firings on which Figure 5 was based.

This anomaly is undoubtedly due to ignition effects. Localization of the early burning in a portion of the powder may result in a considerable local pressure increase and high burning rate at a time when the average pressure is still low. This effect is also evidenced by a 40 per cent reduction in the value of a

TABLE 1. Values of burning-rate constants for powders used in 3-in. Navy gun and in 37-mm gun T47, as obtained from ballistic data.[113]

Powder*	Class†	in./sec‡	in./sec/klb/in.²*	[a-(25b)/25]§
NH		1.35	0.260	0.314
Pyro		1.97	.242	.321
M1	1	2.59	.239	.343
M1	4	1.57	.255	.318
M5	6	2.01	.458	.538
M5	10	1.49	.483	.543
M5	12	1.85	.451	.525

* NH and Pyro were fired in the 3 in.

† Classes: (1) short primer, 1.62-lb projectile (medium)
(4) long primer, 1.62-lb projectile (short)
(6) short primer, 1.62-lb projectile (medium)
(10) short primer, 1.34-lb projectile (short)
(12) short primer, 1.92-lb projectile (medium).

‡ From Reference 113.

§ The last column gives the "effective" b at 25 klb for comparison with Hirschfelder's c referred to in the text.

in the firings of the 37-mm gun, resulting from the use of a long primer that favored even ignition. The constant b has about the same value for all three single-base powders (0.250 ± 0.007), and is nearly 80 per cent greater for the double-base M5 powder.

The use[26] of the approximation of $c = 0.36$ for single-base and 0.51 for double-base powder in the first power burning law without intercept (Section 3.2.5) can be reconciled[113] with these data when it is noted that the rather large term in a compensates for the lower values of b; the rates given by the two laws agree to within 10 per cent at 25 klb/in.². In actual use, the constants in the Division 1 system of ballistics would be adjusted by fitting the firing data for either the maximum pressure, or muzzle velocity.

2.2.4 Effect of Various Factors on the Rate of Burning

Temperature of the Powder

Powders burn at a rate which causes the surface to recede so fast that very little heat is conducted below the surface and the bulk of the powder, therefore, does not change in temperature during the burning. The initial temperature of the powder has been found to increase the rate by 3 to 6 per cent for every 10 centigrade degrees rise in the powder temperature. For burning in rockets, the effect of the initial temperature could be expressed [163] by equations (3 and 4)

$$r = \frac{a' + b'P}{t_1 - t_p} \tag{3}$$

$$r = \frac{c'P^n}{t_1 - t_p} \tag{4}$$

where t_p is the (centigrade) temperature of the powder; t_1 is a constant whose value is typical of each powder, and varies from 200 to over 300 degrees for rocket compositions, being larger for powders showing smaller dependence of the rate on temperature.

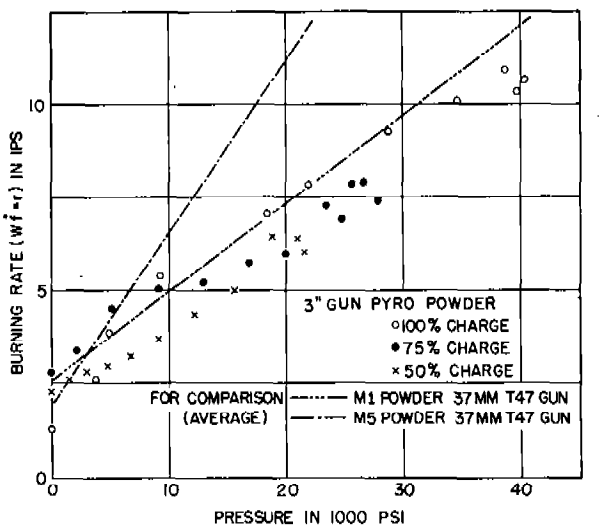


FIGURE 6. Burning rates in 3-in. Navy gun and 37-mm gun T47, for different powders showing the inapplicability of the exponential rate law to gun results.

Composition of the Powder

The burning rates are higher for powders which liberate larger amounts of energy on burning. The meager data available indicate that for burning at gun pressures, the burning rate constant b is increased 0.03 to 0.05 (in./sec/klb/in.²) for every 100 Kelvin degrees rise in the adiabatic flame temperature. More consistent burning rate data are needed, both for closed chambers and guns.

Volatile constituents of powders serve as coolants, and lower the burning rate by some 10 per cent for every 1 per cent of solvent and moisture present.[162]

Radiation

An increase in the radiation received by the powder increases the rate of burning. This has been shown for firings in a pressure vessel with reflecting walls. Previous experiments[160] had shown that a double-base rocket powder (40% NG) burning in open air emits strong radiation, possibly due to chemiluminescence from vibrationally excited molecules of CO_2 and H_2O, at 2.8 and 4.4 μ, superimposed on weak black body radiation. In a pressure vessel with a

quartz window, the 2.8 μ band was found also at 2,000 psi pressure (the 4.4 μ band was blanked out by the opacity of the window).

Potassium salts incorporated in powders have been known to increase the burning rate. When powders containing several per cent of potassium salts were burned in air at atmospheric pressure, a strong emission was found at the red line of potassium, 7660 A. The black body radiation intensity was negligible in these experiments. Burning the powders in the pressure vessel with a window, with freshly polished walls, at pressures up to 1,600 psi, the burning rate was increased about 30 per cent over that observed with absorbing surroundings. Sodium salts did not seem to have such an effect.

It is not known what effect this discrete radiation has under gun conditions, but it must be greatly subordinated to that of the black body radiation, inasmuch as all the discrete lines in the visible and near infrared spectrum merge into a continuum of emissivity approaching unity at density times pathlength of the order of 0.06 g per sq cm.[44]

The radiation, regardless of its nature, if it penetrates into the powder, gradually raises the powder temperature and the burning rate. This effect is especially important with transparent powder near the end of burning when the interior of the web may be heated by radiation from both sides. In rockets, this may cause a marked progressiveness of the rate of burning and a sharp upward rise in pressure near the tail end of burning. It may be counteracted by incorporating darkening agents in the powder, such as lampblack or nigrosene dye which prevents the radiation from penetrating to any depth into the powder.

Little attention has been given to radiation effects in guns. It may be mentioned that irregularities of ignition have been counteracted by treating the powder with an aqueous solution of paraphenylenediamine which blackens the surface uniformly; if an alcoholic solution is used, the blackening penetrates throughout the body of the powder, and the burning rate may rise dangerously high.[243] These effects undoubtedly arise at least partly from absorption of radiation at the surface.

Further investigation of this phenomenon is highly desirable, because of its possible application to hypervelocity guns.[d] In the past the density of loading for cannon has been limited to about 0.7 because the use of higher densities has resulted in irregularities in ignition. The use of blackened powder combined with a long primer may represent a simple means of overcoming this difficulty and permitting the use of the higher densities of loading that are essential if hypervelocities are to be achieved with existing propellants.

[d] Such an investigation had been planned by Division 1, NDRC, in connection with its development of a hypervelocity 90-mm gun, described in Chapter 33.

2.2.5 Stepwise Mechanism in Relation to Rate of Burning

According to the stepwise mechanism of burning the gases resulting from the incomplete burning in Stages A, B, and C accumulate in the space around the powder and are ignited in Stage D with heating of the products to the flame temperature. Although the average rate of burning of the powder shows no sudden change in the corresponding region of pressure, there is evidence that local irregularities in the rate occur.

High frequency variations in dP/dt have been observed, especially with perforated powder, beginning at pressures of the order of those at which the appearance of visible flame has been observed[161] or at slightly higher pressures. This so-called "hash" on the oscillograph trace may be due to earlier ignition in the perforations caused by local pressure excess. Experiments[198] in which dP/dt was directly measured as a function of time with unperforated, very smoothly burning powder showed that the dP/dt vs t curve exhibits a hump in the corresponding pressure region, as shown in Figure 7. The irregularity is too small to be observed in the curve of P vs t. The irregularity in dP/dt is believed to be the result of the sudden ignition of the intermediates to form the final products at the beginning of Stage D.

2.3 CHEMICAL EQUILIBRIUM IN POWDER GAS

2.3.1 Reactions During the Cooling of Powder Gas

Questions arise as to the state of the powder gas both while burning is in progress and afterwards. If equilibrium among the various constituents prevails, the composition may be expected to vary with the temperature according to the thermodynamic laws. Because of the heats of reaction, this modifies the energy relationships; other properties of the gas also vary with the compositions. All these questions have a bearing on the calculations of interior ballistics. As



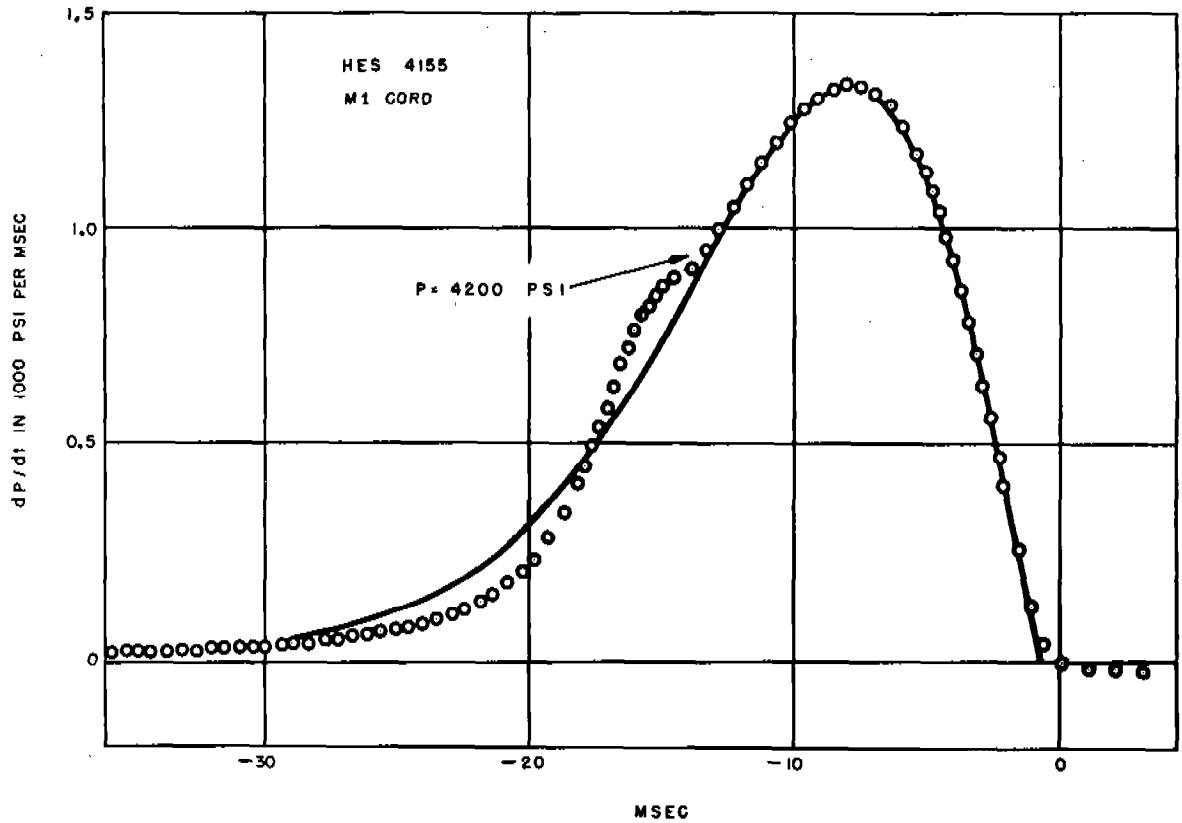


FIGURE 7. Comparison of experimental (circles) and average calculated dP/dt versus time curves for a very smoothly burning cord powder. Arrow indicates the conclusion of the irregularity in the burning rate. (This figure appeared as Figure 20 in Ballistic Research Laboratory Report No. 456, Aberdeen Proving Ground.)

will be shown in this section, there is reason to believe that equilibrium is maintained in the gas, at least during the postburning period. Such a conclusion is, of course, anticipated by the success with which interior ballistic calculations predict the behavior of powder in guns.

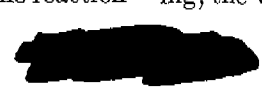
The principal chemical reaction among the gases in a gun after the powder is burnt is the readjustment of the concentrations of the water gas constituents. During the burning the energy liberated heats the products to a temperature somewhat below the adiabatic flame temperature, the deficiency being accounted for by heat losses. As the gas cools afterwards, the water gas reaction components continue to react with each other and if the rate of this reaction is high enough to maintain equilibrium, the relative composition at any temperature T is given by the equilibrium "constant"

$$K_1 G_1 = \frac{C_{CO} C_{H_2O}}{C_{CO_2} C_{H_2}} = K(\Delta, T) \qquad (5)$$

where K_1 is the equilibrium constant for the reaction in terms of ideal gases and the factor G_1, which is unity for ideal gases accounts for the gas imperfection at the prevailing density.[24] The equilibrium constant K_1 increases with the temperature, and its values have been tabulated.

When powder gas after cooling to room temperature is analyzed, the relative concentrations of the water gas constituents do not correspond to a value of K_1 characteristic of room temperature, but rather to one for a higher temperature, which is of the order of 1000 K or higher; the observed constant $K_1 G_1$ depends upon the rate at which the gas was cooled and decreases with increasing density of loading, as may be shown from data[443] secured in massive chambers. This indicates that at the temperature corresponding to the observed value of $K_1 G_1$ the rate of reaction had become negligible in comparison with the rate of cooling, and the observed gas composition had been frozen-in. (See also Section 2.3.4.)

Numerous analyses of powder gases have been performed, with little attention paid to the rate of cooling; the values of the equilibrium constant calculated



from such analyses are of little significance for our purpose. The first systematic study[451] of the influence of rapid cooling on the gas composition showed that powder gas cooled in an explosion vessel chilled to −120 C contained more CO than gas in a vessel heated to 90 C, and also that powder gas quickly expanded from a rifle whose barrel was cut off at various lengths contained more CO near the origin of rifling than at the muzzle[452] where the gas arrived cooler. These changes of composition will be seen to correspond to the expected changes in the freezing-in of equilibrium under the stated conditions.

2.3.2 Quenching of Powder Gas Reactions

An extended series of experiments on the freezing-in of equilibrium in powder gases, or "quenching," as it is more conveniently called, was performed for Division 1 at the Geophysical Laboratory.[107] In these experiments an effort was made to obtain as rapid cooling as possible, by expanding the gases from a small firing chamber through a nozzle into a much larger expansion chamber. The expansion ratio was about 230:1.

If the nozzle performed adiabatically, the gas would first be cooled on entrance into the throat in the ratio $T_t/T_c = 2/(\gamma - 1)$ where T_t and T_c are the temperatures of the gas in the throat and the firing chamber, respectively, and γ is the ratio of the specific heats of the gas. On the exit side further cooling by expansion into an evacuated chamber should reduce the temperature momentarily in the ratio $T/T_t = (P/P_t)^{\gamma/(\gamma-1)}$ where the subscript t refers to the values in the throat of the nozzle. Unfortunately, this momentary cooling is not permanent, as the gas reheats in the expansion chamber by recompression to the final low pressure (about 1 atm). In the meantime, however, much heat is given up to the walls, and the net effect is a relatively rapid cooling. It will be instructive to note that the walls of the chamber that was used should absorb about 0.2 to 1 cal/cm² (depending on the energy of the powder) per gram of powder fired, in the time the firing chamber is emptied, in order to cool the gas quickly to about 1500 K.

In a second method of quick cooling, the incoming powder gas was mixed with an inert gas (usually argon) in the expansion vessel. This permitted the heat to be distributed and delivered to the walls more slowly. The momentary temperature attained by the mixture before any heat is given up to the walls is expressed by

$$T = \frac{n_1c_1T_1 + n_2c_2T_2}{n_1c_1 + n_2c_2}, \qquad (6)$$

where n, c, and T are the number of moles, the heat capacity, and the temperature of the gases which are distinguished by the subscripts 1 and 2. The method therefore is an attractive one; however, because of imperfect mixing, its full value is not realized in practice.

The pressure at which the powder gas was released for expansion was controlled by using rupture disks of selected thickness to close off the exit of the firing vessel; it varied from 500 to 1,850 atm.

A large variety of powder was used, ranging from single-base NH and FNH and cool RDX powders at one extreme to very hot, double-base powders such as Hercules ballistite in fine granulation at the other, T_0 ranging from 2420 to 3860 K. With powders of low flame temperature, the quenched gas had compositions yielding values of K_1 of the order of 3.5 to 5[e] corresponding to quenching temperatures of 1700 to 2000K for experiments in which nearly all the powder was burnt before breaking of the rupture disk. Gas from powders of very high flame temperature usually gave lower values of K_1, about two to three, which may be interpreted to mean that the additional heat delivered into the expansion chamber by the gas could not be dissipated as rapidly as in the previous case, so that the gas cooled more slowly and had its equilibrium quenched at a lower temperature.

For both these extremes, there was little difference in the results whether the gas was expanded into an evacuated chamber, or into a chamber filled with argon. On the other hand, with fine silver coils in the expansion chamber as cooling agent, quenching occurred more efficiently in expansions into a vacuum than into an argon atmosphere. For example, with an NH powder, K_1 (vacuum) was 4.9, where K_1 (argon) was 4.3, corresponding to temperatures of 2040 and 1870K, respectively. The lower value observed in argon may have been due to imperfect mixing of the two gases.

When the amount of powder fired exceeded appreciably that to produce rupture, the results differed according to conditions. As outlined in the next paragraph for the NH powder, $T_0 = 2651$ K.

[e] The equilibrium was quenched always on the exit side of the nozzle where the pressure was of the order of 1 atm and where therefore the gas imperfection was negligible, so that $K_1G_1 = K_1$, the value determined for ideal gases.

Pressure at Rupture: Above 1,000 Atm, NH Powder

At these pressures, the observed values of K_1 did not differ appreciably, whether the amount of powder loaded and burnt just sufficed to produce rupture, or whether an excess of powder was used; in either case, they averaged about 3.8. However, with excess powder, somewhat less of the carbon of the powder than before was accounted for in the gas as CO and CO_2, indicating a tendency toward less complete burning. Often acetylene, and in some cases, small quantities of nitric oxide were found in the quenched gas.

Pressure at Rupture: 500 Atm, NH Powder

Three different regions of loading density could be distinguished when the pressure at rupture was 500 atm.

Region 1. Powder all burnt at rupture (0.6 g, caliber .30 nozzle, $\Delta_0 = 0.061$). Values of K_1 were near 5.0, corresponding to a quenching temperature somewhat in excess of 2000 K. This is believed to be a normal value, as the quantity of gas is small, and heat should therefore be dissipated quickly, the process giving rise to efficient quenching.

Region 2. Powder not all burnt at rupture (0.6 to > 3.0 g powder, caliber .30 nozzle, $\Delta_0 = 0.061$ to 0.37).

1. With *argon* in the expansion chamber the values of K_1 obtained were anomalously high (about 8 or more) and corresponded to quenching temperatures in excess of the flame temperature. (See Figure 8.) Although little or no unburnt powder was recovered from the apparatus, the carbon of the powder accounted for in the gas was uniformly low, often below 70 per cent. The percentage of H_2 in the gas was very low. C_2H_2 and much NO were present in the gas, NO often accounting for half of the nitrogen. Tarry residue accumulated in the apparatus. The powder consumed after rupture evidently did not burn completely by the reactions of the last stage of burning, but rather decomposed only partially beyond the stage of the red liquid and nitric oxide. This interpretation is favored also by the fact that the small percentage of H_2, commonly found in incomplete burning, was largely responsible for the high values of K_1 determined, for the CO/CO_2 ratio usually had a slightly lower value than in normal, complete burning.

2. When the expansion chamber was originally *evacuated* and the pressure at release was 500 atm, the values of K_1 were somewhat high, but not as anomalous as when argon was present in the chamber; however, C_2H_2 and NO were present, and the excess powder burned incompletely. It is believed that the more anomalous burning found in the presence of argon is the result of local quenching in the gas mixture, argon acting as diluent.

Region 3. Powder not all burnt at rupture, (3.5 g powder or more, caliber .30 nozzle, Δ_0 greater than 0.37). In expansions either into argon or a vacuum, these charges gave normal values of K_1, and both

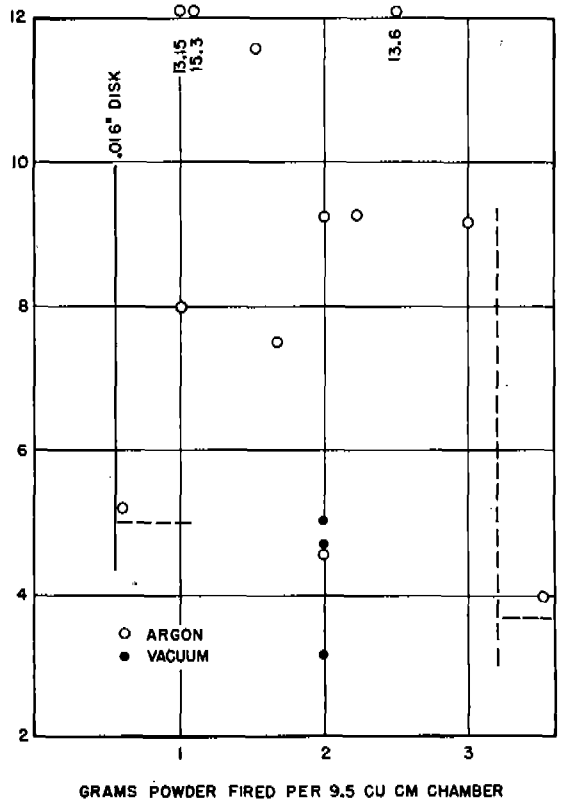


Figure 8. Values of the water gas reaction constant K_1G_1 for NH powder gas quenched by pressure release at 500 atm into argon (open circles) and into a vacuum (full circles), with increasing excess charge of powder.

C_2H_2 and NO were absent from the gas. The C, H, and O of the powder were fully accounted for in the gas, so that all indications point to a complete burning of the water gas constituents and N_2. The apparent explanation for this sharp return to normal burning with release at 500 atm pressure and a very large excess of powder loaded is that, at these increased densities of loading, the friction encountered in the nozzle by the increased volume of the products maintains a back pressure in the ignition chamber high

enough for the rate of burning to remain above the value for incomplete burning.

Following the instant of rupture, the pressure undoubtedly falls sharply from the 500 atm value at rupture to a lower value; in view of the observations on the variation of the rate of burning discussed in Section 2.2.5, the minimum pressure reached must not be much lower than about 60 atm if the final stage of burning is to be maintained. This means that soon after the initial drop in pressure a steady state must be established in the nozzle such that the rate at which discharge takes place is balanced by the rate at which gases are produced.[163] On this explanation, the steady state is never quite reached in Region 2 of loading densities.

The anomalous values of K_1 at releasing pressures of 500 atm were not obtained with fast-burning powders of moderate and high flame temperatures. It may be suggested that, at rather low releasing pressures, a Region 2 of loading densities would also be realized with such powders. At such low pressures, the burning rate would be low at release and subsequent readjustment of the rates of burning and of discharge would allow the pressure to fall below the critical value for complete burning. This contention is supported by experiments performed without using rupture disks, the burning powder evolving gases freely into the expansion chamber without obstruction. Argon at 1 atm pressure was used to provide the initial pressure necessary for ignition. In such experiments, all powders gave values of K_1 in excess of 10, sometimes in excess of 50; H_2 concentration in the gas was always low, that of NO was high, and consumption of the carbon of the powder only near 50 per cent.

2.3.3 Occurrence of Methane, Acetylene, and Nitric Oxide in Quenched Gas

Methane is usually assumed to be formed in powder gas as the result of secondary reactions, such as for example, $CO + 3H_2 = CH_4 + H_2O$, or $2CO + 2H_2 = CH_4 + CO_2$. Acetylene has not been systematically reported by other investigators. In the quenching experiments described in Section 2.3.2, chemical tests showed that when nitric oxide was present in the gas, the hydrocarbon constituents in the quenched gas contained acetylene, but when nitric oxide was absent, acetylene also was usually absent.

The nitric oxide was present, as already mentioned, in experiments with excess powder, and particularly when the pressure at release was low. It is believed to be the result of primary decomposition in the early stages of burning. The presence of acetylene in the same experiments indicates that it likewise is a product of the early stages. Neither acetylene nor nitric oxide formed under such conditions would be expected to survive the high temperatures prevalent in the final stage, for thermodynamic considerations show that both these gases, if formed at high temperatures, would tend to decompose in a cooling gas. Methane on the other hand is expected to form in increasing quantities as the temperature falls. This, of course, does not preclude methane being formed also as a product of the primary decomposition. Some evidence on this point is given in Section 2.3.5.

2.3.4 Water Gas Reaction Equilibrium in Quenching

The foregoing discussion of quenching experiments gives no indication whether the concentrations of the water gas reaction components determined corresponded to equilibrium values for the reaction at the quenching temperatures. To obtain this information, it is necessary to compare the experimental results with values expected from the powder composition.[107] Such a comparison can conveniently be made in the following manner.

The expected gas composition can be calculated[24] from the powder composition converted to moles of atoms of C, H, O, and N per unit weight of powder, and an assumed value of K_1G_1 ($= K_1$ at ordinary pressure) corresponding to some chosen gas temperature. The values of CO/CO_2 were evaluated for $K_1 = 3.5$ ($T = 1687$ K) for the various powders studied, and plotted against the adiabatic flame temperature, as in Figure 9. In order to make the desired comparisons with the quenching data, the observed gas compositions from the quenching experiments likewise were recalculated to $K_1 = 3.5$ from whatever value of K_1 given by the experiment, and the corresponding values of the CO/CO_2 ratios were evaluated. Only data in which the evidence pointed to complete burning of the powder were utilized for these comparisons. Thus, none of the experiments for which K_1 was anomalously high, or in which appreciable concentration of NO was found, were included.

The plot of observed and expected values of the CO/CO_2 ratios vs the flame temperatures is given in Figure 10. It is seen from this figure that the agreement between observed and expected is fair, especially when it is remembered that (1) the nominal powder

compositions do not always represent the actual powder compositions, by reason of variations in the volatiles, etc., (2) the efficiency of quenching is only moderate, and (3) the gas analysis, in the hands of even the best experimenters [443] makes an accounting which may vary as much as 10 per cent from the mean for a series of experiments on the same powder. It may, therefore, be concluded that within the experimental error, the concentrations of the water gas components readjust themselves with the temperature as rapidly as the temperature changes occur down to the instant of quenching.

2.3.5 Equilibrium Among the Carbon Atoms

As we have already seen, powder gas may contain products of incomplete combustion or of secondary reactions in addition to the water gas reaction constituents. With the discovery of induced radioactivity, a direct means has become available for testing the distribution of any one element among the different gaseous species of which the element is a constituent, by using its radioactive isotope as a tracer. From such experiments conclusions may be drawn concerning the state of equilibrium in the gas as a whole. This can be done for carbon by using preferably its radioactive isotope (C^{14}) which is long lived and hence lends itself particularly well for use as a tracer element.

The principle of such an experiment is portrayed by Figure 11. The powder charge is coated with a small quantity of a dissociable carbon compound containing the radiocarbon, as indicated by the red lines outlining the powder grains in the upper part of the figure. The carbon atoms in the powder itself are not radioactive. When the powder is burned, the radiocarbon atoms in the coating are converted to gas along with those from the powder grains. Exchange reactions take place among them and some of the resulting carbon monoxide and carbon dioxide molecules become radioactive from the presence of tracer atoms of radiocarbon as shown by the red circles in the lower part of the figure. The proportion of carbon monoxide and carbon dioxide molecules that become radioactive can be determined by recovering the powder gases and measuring their specific activity.

The first experiment [244] of this sort, performed at Aberdeen Proving Ground, demonstrated that tracer atoms (of heavy carbon C^{13} instead of radiocarbon C^{14}) were uniformly distributed between the molecules of carbon monoxide and carbon dioxide recovered from a caliber .30 rifle after firing. This result indicated that these two gases had been in mutual equilibrium in the powder gas.

Later a more extensive investigation [61] was undertaken with the quenching apparatus referred to in Section 2.3.2, with radiocarbon (C^{14}) as tracer added to the powder. When the conditions of burning were such that the powder burned to the water gas constituents and nitrogen, the earlier results with respect to carbon monoxide and carbon dioxide were confirmed. It was found in addition that methane present in powder gas resulting from complete burning is in equilibrium with the CO and CO_2, and therefore, must be the result of secondary reactions after burning.

In experiments with incomplete burning at the instant of release of pressure (compare Section 2.3.2), none of the carbon gases were in mutual equilibrium. The methane present was essentially inactive, and, therefore, presumably a product of primary decomposition of the organic residues. The acetylene always carried about a half of the proportionate activity of CO or CO_2, which would indicate that it was a product of CO or CO_2 with a hydrocarbon fragment

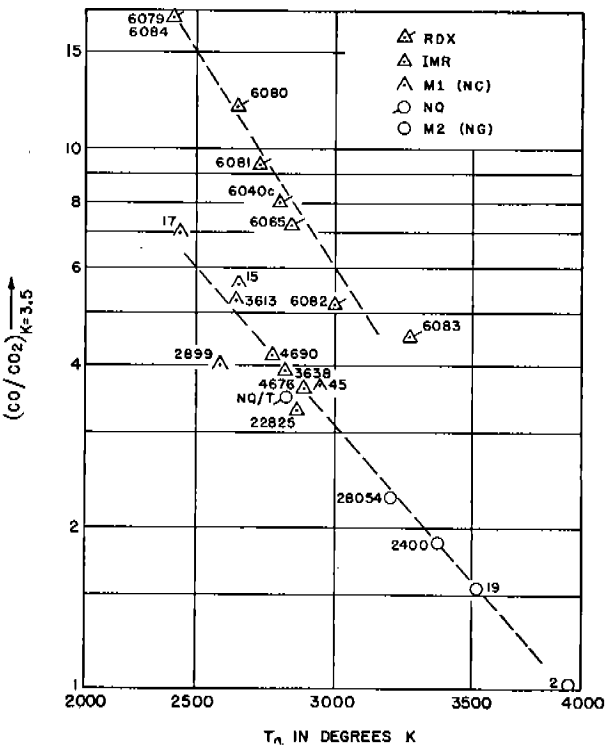


FIGURE 9. Values of CO/CO_2 in the gas from various powders at $K_1G_1=3.5$, calculated from powder analysis, and plotted versus the adiabatic flame temperature.

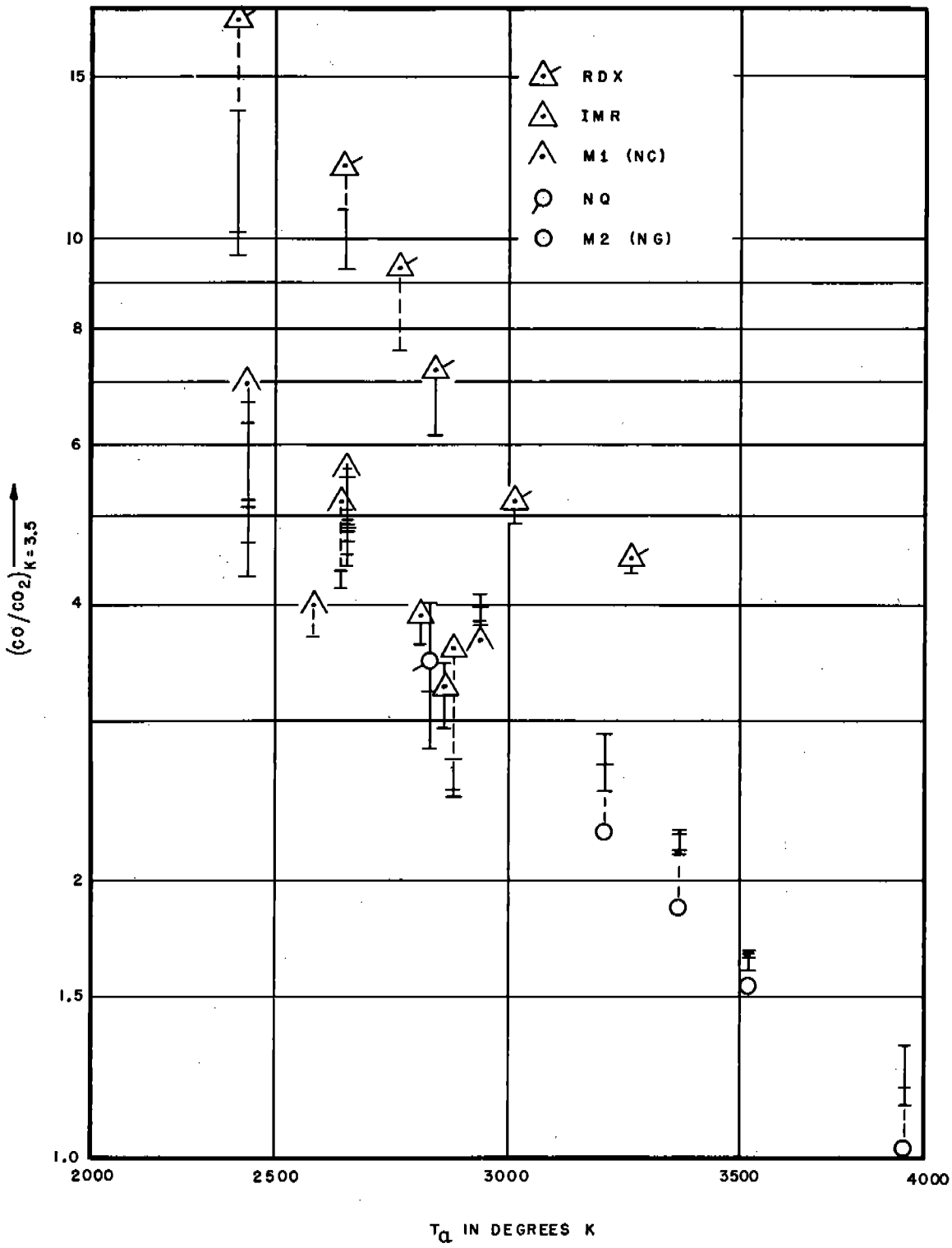


FIGURE 10. Values of CO/CO_2 in the gas from various powders at $K_1G_1=3.5$, versus the adiabatic flame temperature, comparing values calculated from powder analysis with values deduced from the quenched gas compositions. The calculated values are the same as those shown in Figure 9.

formed in the primary decomposition of excess powder already stripped of its radiocarbon. The lack of mutual equilibrium of CO and CO_2 in the incomplete burning is the result, most probably, of the excess powder being decomposed at low pressure to the products of the early stages of burning described in Section 2.2.2.

2.3.6 Equilibrium in Powder Gas—Conclusions

The definite conclusions concerning the state of equilibrium in powder gas that can be given at this time are the following.

The agreement of the observed and expected values of CO/CO_2 ratios from quenching experiments with complete high-pressure burning indicates that changes in chemical equilibrium among the water gas constituents closely follow the changes of temperature during the postburning stage, down to about 1500 K at pressures above 60 atm.

The carbon gases are in mutual equilibrium in high-pressure burning, both during the active-burning and the postburning stages.

When burning occurs at reduced pressure, equilibrium is maintained only when a certain minimum pressure (about 60 atm) is exceeded; below this, water gas reaction equilibrium is not established. This is shown by the results of quenching experiments both with and without tracer radiocarbon in the powder.

One more piece of evidence may be noted here. Measurements of the temperature of the powder gas show[44] that when a reasonable allowance is made for heat losses, the measured temperature closely agrees with the calculated adiabatic flame temperature. This temperature is calculated by thermodynamic methods from known energy data, and for products in thermal and chemical equilibrium. The agreement between the calculated and observed temperatures, therefore, indicates that the full calculated energy of the powder is liberated by an equilibrium process in the high-pressure burning.

2.4 THERMODYNAMICS OF POWDER GAS

2.4.1 The Thermodynamic Problem

When powder burns, a certain amount of energy is liberated by the combustion reaction. In a closed vessel, if the process occured adiabatically, this energy would heat the gas to the *adiabatic flame temperature* T_0. In the actually realizable process, some of the energy is expended in heating the chamber, and, in the case of a gun, in doing external work. As a result, the energy available for heating the gas is less, and the final gas temperature T is lower than the adiabatic temperature T_0. The energy lost by the gas to the surroundings may be termed the *energy released*. Thermochemically, it is the energy stored in the powder (per gram) less the energy stored in the gas in its final state of temperature T, density Δ.

The thermodynamic problem is, then, to evaluate these energies and the related thermodynamic functions such as the heat content, the entropy, and the heat capacities for the actual gases and their mixtures as they occur in powder gas. Since the properties of the mixture depend upon the composition, and this in turn depends upon the equilibrium of each component reaction, the equilibrium constants and their variations with the temperature and the density must be known. The properties of the gases at high densities also depart widely from those of the ideal gas. In thermodynamics these properties are treated most simply by considering the properties the gas would have if it were ideal, and applying corrections for

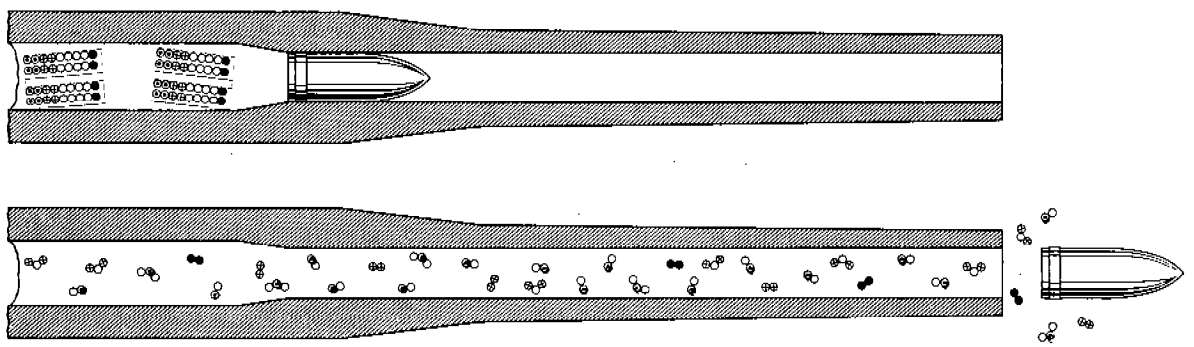


FIGURE 11. Equilibrium among the carbon atoms of the powder gases has been demonstrated by radioactive tracer experiments.



departures from this state. For this approach, an adequate equation of state is necessary.

Outstanding contributions to this thermodynamic problem have been made by several investigators.[24,340,435,440,441,480] The treatment of the problem given here is necessarily brief, and the reader is referred for details to an NDRC report[24] in which is given a full discussion with applications and tabulated functions of the various quantities needed in computation.

Conventions

The notation employed is that of Lewis and Randall.[511] The standard state chosen for elements is zero energy at 0 K, and for gases, that of the ideal gas. It may be noted that *energies* of formation (constant volume) and not *heats* of formation are employed throughout. The energies are obtained from conventional heats of formation Q_f by equation (7), in which

$$-\Delta E_T^\circ = Q_f + \Delta nRT \tag{7}$$

Δn is the net increase in the number of moles of gases for the unit reaction. Thus, for the formation of water according to equation (8)

$$H_2(g) + \tfrac{1}{2}O_2(g) = H_2O(l). \tag{8}$$

$\Delta n = -1.5$ and $\Delta E_{298.16}^\circ = -(68{,}318.1 - 1.5 \times 1.9871 \times 298.16) = -67{,}429.4$ cal/mole.

Approximations

It is assumed that there is no energy or volume change of mixing of powder gas constituents. Powder gas is thus treated as a perfect solution, and its properties are computed additively from those of the individual gases. Powder itself is treated as a simple mixture. These assumptions greatly simplify the work of computation; moreover, the contributions due to interactions of unlike molecules, although they are not too well known, are small for gas mixtures, except perhaps at extremely high densities. Experience shows that at densities of gas such as prevail in guns, the assumption of simple additivity is fully justified.[113]

2.4.2 The Equation of State for Powder Gas

Actual gases at high pressures deviate greatly in their P-V-T relationships from the ideal gas. For application to the problem of internal ballistics, a modified van der Waals' equation in the form proposed by Abel, shown in equation (9), has been usually employed.

$$P(1 - \eta\Delta) = n\Delta RT. \tag{9}$$

Here Δ is the density of the gas, $1/v$, and η is the *covolume* which corrects for the apparent volume of the molecules. The equation neglects the van der Waals' correction for the attractive forces between the molecules, as these may be expected to play only a minor role at the temperature of powder gas.

For exact thermodynamic studies of powder gas such an equation does not reproduce the P-V-T relations with sufficient accuracy. Of the numerous equations of state proposed, equation (10), which is a van der Waals' equation expanded in increasing powers of $1/V$, was selected for Division 1's thermochemical calculations.[24]

$$\frac{PV}{RT} = 1 + \frac{b - a/RT}{V} + \frac{5}{8}\left(\frac{b}{V}\right)^2 + 0.2869\left(\frac{6}{V}\right)^3 + 0.1928\left(\frac{b}{V}\right)^4. \tag{10}$$

The quantities a and b are the van der Waals constants. The coefficients of the second and third power terms in (b/V) were calculated[534,535,536,537] to account for triple and higher collisions among the molecules. The fourth power term was added[454] to make the equation merge smoothly into the limiting form for high densities, given by equation (11),

$$\frac{PV}{RT} = \frac{-a}{VRT} + \left[1 - 0.6962\left(\frac{b}{V}\right)^{1/3}\right]^{-1} \tag{11}$$

in which the coefficient 0.6962 is calculated for face-centered close packing of rigid spheres. For a body-centered lattice, the value would be 0.7163, and for simple cubic packing, 0.7816.

The van der Waals a appears in these equations in the fraction a/VRT. Its effect on the pressure is small when T is high, and is ignored in ballistic applications. High temperature values of b have been evaluated by statistical mechanics;[455,456,501,506] they are not strictly independent of T, but because the temperature coefficient is small, they are assumed constant and equal to their values at 3600 K in the ballistic equation of state. Their values differ somewhat from the conventional van der Waals b's derived from the properties of the critical state. Such values are listed in Table 2 for powder gas constituents.

The covolume η in equation (9) has been evaluated[173] by analysis of the data[440] on uncooled pressures

[redacted]

for the N(1) powder referred to in Section 2.4.5 and Table 4. A value of (1.074 ± 0.021) cc per g was recommended.

TABLE 2. Van der Waals constants for constituents of powder gas.

Constituent	a Conventional* 10^6 atm$\left(\frac{cm^3}{mole}\right)^2$	b Conventional* $\frac{cm^3}{mole}$	b High temp† $\frac{cm^3}{mole}$
CO_2	3.60	42.8	63.0
CO	1.486	39.9	33.0
H_2	0.245	26.6	14.0
N_2	1.346	38.5	34.0
H_2O	5.47	30.5	10.0
NH_3	4.17	37.1	15.2
CH_4	2.26	42.8	37.0
NO	1.341	27.9	21.2
N_2O	3.79	44.1	63.9
O_2	1.361	31.8	30.5

*Derived from critical constants.
†Calculated by means of statistical mechanics.

For a mixture of gases, the gas imperfection correction may be computed additively by the introduction of equation (12) or (13),

$$b_{mix} = \sum_i x_i b_i, \tag{12}$$

$$b' = \sum_i n_i b_i, \tag{13}$$

where x_i and n_i are the mole fraction and the number of moles of gas i in the mixture for 1 g of powder, respectively; b' is defined as the *covolume*.

Important applications of the equation of state occur in the exact calculation of the pressure, composition, and energy of powder gas. The correction for the *energy* of gas imperfection is small and may be neglected in the simplified calculation of the adiabatic flame temperature. The corrections for the pressure and the composition, on the other hand, are large, and neglecting them would lead to serious errors.

THE CHANGE OF INTERNAL ENERGY WITH DENSITY FOR GASES

The internal energy of actual gases, unlike that of an ideal gas, varies with the volume (or the density). The contribution is relatively small, and arises almost exclusively from the temperature coefficient of $b - a/RT$. By statistical mechanical considerations, it has been evaluated for constituents of powder gas by equations of the type of equation (14),

$$E\ (\text{gas imp.})_i = \Delta'(A_i - B_i \log T - CT_i), \tag{14}$$

where, for a given gas, the energy of gas imperfection is defined by equation (15),

$$E\ (\text{gas imp.}) = E\ (\text{actual}) - E\ (\text{ideal}). \tag{15}$$

For a mixture of gases, the energy of gas imperfection (in calories per gram of powder) is given by

$$E\ (\text{gas imp.})_{mix} = \sum_i n_i E\ (\text{gas imp.})_i. \tag{16}$$

The contribution to the energy of the gas from this cause rarely exceeds 10 cal/g at powder gas temperatures.

THE PRESSURE OF POWDER GAS

Assume the covolumes to be additive in a mixture of gases ($b_{mix}/V = b'\Delta$) and define further a fictive density according to equation (17),

$$\Delta' = 22.98n\Delta, \tag{17}$$

where n is the total number of moles of gas per gram of powder. Then the equation of state (10) can be solved for the pressure in atmospheres in accordance with equation (18),

$$P = 3.571\Delta' T[1 + D(P,T)] \tag{18}$$

in which the numerical coefficient 3.571 is the value of $R/22.98$ in atm/cc/degree/mole and the function $D(P,T)$, which is the gas imperfection correction, stands for the sum of the terms on the right-hand side of equation (10) minus 1.

COMPOSITION OF POWDER GAS AS A FUNCTION OF TEMPERATURE

The composition of powder gas varies with the temperature and density as a result of shifts in the equilibriums of the chemical reactions. For a given reaction, the equilibrium constant K^0 for an ideal gas is related to the standard free energy change ΔF^0 for the reaction by equation (19).

$$R \ln K^0 = \frac{-\Delta F_T^0}{T} = -\frac{\Delta(F_T^0 - E_0^0)}{T} - \frac{\Delta E_0^0}{T}. \tag{19}$$

The second expression on the right of this equation is the more convenient to use because tabulated free energy changes are usually referred to the energy of the standard reaction at 0 K.

Because the gas imperfection correction is different for different gases, values of K as ordinarily defined in terms of partial pressure, concentration, or mole frac-

tion x, vary with the density of the gas. The partial pressure P_i of gas i, for example, is equal to x_iP for an ideal gas, where P is the total pressure. For actual gases at high pressure this is no longer true, but instead we may write equation (20),

$$\gamma_i \equiv \frac{\gamma_i P_i}{x_i P} = \frac{f_i}{x_i P}. \tag{20}$$

in which γ_i, the activity coefficient for gas i, and f_i, the fugacity of gas i, contain the correction for the gas imperfection, as expressed by equation (21),

$$\ln \gamma_i = \ln \frac{f_i}{x_i P} = \int_0^P \frac{D_i(P,T)\,dP}{P} = -\int^{\infty} \frac{D_i}{P}\left(\frac{\partial P}{\partial V}\right)_T d\,V. \tag{21}$$

The indicated integral may be evaluated from the equation of state; values of $\ln \gamma$ thus derived have been tabulated[24] for values of Δ' up to 0.5.

The equilibrium constants may be written in terms of the fugacities $f_i \equiv \gamma_i P_i$ and related to K_p, the equilibrium constant in terms of partial pressures, in accordance with equation (22),

$$K_f = K_p K_\gamma = K_p{}^0. \tag{22}$$

K_f then retains, at all pressures, the values of K_p characteristic of the ideal gas. The correction for gas imperfection, contained in K_γ is conveniently introduced by equation (23).

$$K_p = KG = \frac{K_f}{K_\gamma} = \frac{K_p{}^0}{K_\gamma}. \tag{23}$$

Values of G for the various reactions that may occur in powder gas as calculated from the values of γ_i obtained by equation (21) have been tabulated.[24]

When it is desired to evaluate the composition of a gaseous mixture at a given temperature T and density Δ, it is convenient to deal with K_n, the equilibrium constant in terms of the relative numbers of moles of a constituent per gram of powder rather than with K_p. The two constants are related by

$$K_n = K_p\left(\frac{P}{n}\right)^a, \tag{23'}$$

where a is the sum of the number of moles of the products less the number of moles of reactants in the chemical equation.

2.4.3 The Adiabatic Flame Temperature

The Energy Released in the Burning of Powder

The energy released per gram of powder is the energy given up to the surroundings when 1 gram of powder at 15 C is burned to form the (gaseous) products at T K and density Δ g/cm^3, as shown in equation 24.[f]

$$\begin{aligned} E_{\text{rel}}(T^0\text{K},\Delta) = {} & E \text{ (powder, 15 C)} \\ & - E^0 \text{ (elements, 15 C)} && E(1) \\ & + (E^0{}_{15}\text{C} - E_0{}^0) \text{ elements} && E(2) \\ & - [E^0 \text{ (products 0 K)} \\ & \quad - E^0 \text{ (elements 0 K)}] && E(3) \\ & - (E_T{}^0 - E_0{}^0) \text{ products} && E(4) \\ & - E \text{ (gas imp.)} && E(5). \end{aligned} \tag{24}$$

The terms $E(1)$ and $E(2)$ together represent the energy of formation of powder at 15 C from the elements at 0 K; $E(3)$ is the negative of the energy of formation of the products from the elements, both at 0 K; $E(4)$ is the negative of the energy required to heat the products in their standard states from 0 K to T K; and $E(5)$, which is the negative of the energy due to gas imperfection, represents the energy necessary to convert the products from the standard state of ideal gas to the actual state. $E(1)$ and $E(2)$ are computed additively from the energies of formation of powder constituents referred to the elements at 0 K. $E(3)$, $E(4)$, and $E(5)$ are similarly computed additively from the corresponding energies for the gaseous products. For this purpose, knowledge of the composition of powder gas at T K and Δg/cm^3 is obtained from the values of KG, as outlined in the last paragraph of Section 2.4.2, and from the composition of the powder in terms of moles of its elements per gram of powder.

Simplified Calculation of the Adiabatic Flame Temperature

It will be noted that the highest temperature that can be attained adiabatically by the products is the temperature when the energy released is zero. This temperature is called the adiabatic flame temperature T_0. It is an important constant for each powder. Its

[f] In NDRC Report A-116[24] (p 32) the quantity represented here by the sum of $E(1)$ and $E(2)$ is called the negative of the energy of formation of powder from the elements at 0 K; and the term $E(3)$ is designated as $-E_0{}^0$.

evaluation by the general method just outlined is exceedingly laborious, and a shorter method is desirable. It was found[23] that, since the energies are all computed additively, a considerable simplification could be achieved if a suitable compensation could be made for changes in the composition of the powder gas. It was noted that, while the gas composition varies considerably at a given temperature for different densities, the energy released and the specific heat at constant volume are not greatly influenced by the density except at very high temperatures, when account must be taken of energy-rich minor constituents. For the large group of powders with T_0 not greater than 3000 K, equation (25) was proposed.

$$T_0 = 2500 + \sum_i \frac{y_i E_i}{y_i C_{vi}}. \qquad (25)$$

In it y_i is the weight fraction of constituent i of the powder.

The numerator of the fraction in equation (25) represents the energy released at 2500 K, and the denominator the average value of C_v over the range of temperatures 2500 ± 500 K, both computed additively from the composition of the powder. The energy released at 2500 K and the C_v were evaluated, first for the case of no CO_2 in the powder gas and second, for the case of no H_2O. It was noted that typical powder gas at the temperatures and densities prevalent in guns contains 77 moles H_2O for every 23 moles of CO_2. The mean energy released at 2500 K was therefore taken to be made up of the two extreme values in the ratio of 77 : 23. C_v has a slightly larger value than would be expected on this basis, and a ratio of 1 : 1 of the two extreme values was found to give more nearly representative results.

At temperatures above 3000 K it is necessary to correct the energy released for the effect of dissociative equilibriums; when such a correction is made, equation (26) results.

$$T_0 = 3000 - 6046A + 6046\,(A^2 + B)^{1/2}. \qquad (26)$$

In this equation A and B have the values given by equations (27) and (28), respectively.

$$A = \sum_i y_i C_{vi} + 0.01185. \qquad (27)$$

$$B = 0.0003308\left(\sum_i y_i E_i - 500\sum_i y_i C_{vi}\right). \qquad (28)$$

The values of T_0 obtained by this approximate method usually agree very closely with those obtained by the accurate method. Table 3 gives values of the additive constants of powder constituents, C_{vi}, E_i (2500 K), n_i and η_i for reference.

TABLE 3. Molar additive constants of powder constituents per gram of powder for computation of adiabatic flame temperature.*

Constituent i	C_{vi}	E_i	n_i	η_i
Nitrocellulose †	0.3421 (0.006Y)	274.6 (−142Y)	0.03920 (−0.00218Y)	27.56 (+1.00Y)
Nitroglycerine	0.3439	951.9	0.03083	22.78
Diphenylamine	.3475	−3009.7	.10637	65.44
Dibutylphthalate	.4261	−2694.7	.09700	56.97
Dinitrotoluene	.3213	− 708.4	.06040	40.44
Water	.6507	−1567.6	.05551	24.60
Acetylene	.3755	−1374.0	.11523	69.30
Acetone	.5107	−2842.5	.10331	57.22
Ethyl alcohol	.6085	−2784.8	.10854	56.35
Ethyl ether	.5980	−3073.7	.12142	64.06
Centralite	.3909	−2873.7	.10444	62.60
Nitroguanidine	.3711	− 60.5	.04804	31.77
Cyclonite (RDX)	.3415	622.3	.0405	28.5
PETN	.3485	724.1	.0348	24.9
Vaseline	.5983	−4175.1	.142	65.6
Diamylphthalate	.4408	−2809	.1013	58.8
Trinitrotoluene	.3035	− 110.1	.0484	34.3
Triacetin	.4191	−1973	.07331	43.77
Graphite	.1349	−3223.8	.08326	60.53
NH_4NO_3	.4424	405.1	.03748	22.83
KNO_3	.2158	25	.00989	23.61
$Ba(NO_3)_2$	.1574	131	.00765	15.34
K_2SO_4	.1250	− 860	.00574	9.36

* Taken from NDRC Reports A-101[23] and A-142.[26] The values of E_i for nitrocellulose, dinitrotoluene, centralite, and nitroguanidine have been recalculated by W. S. Benedict from thermal data furnished by F. D. Rossini.[561,562] Values for ether have also been added. The values of n_i have been checked and modified when necessary.

† $Y = 13.15 - \%N$.



2.4.4

Other Thermodynamic Properties of Powder Gas

For completeness it is desirable to evaluate the enthalpy, the entropy, and the specific heats of powder gas.

The Enthalpy

The enthalpy (also called the "heat content" or "total heat") H is defined by equation (29).

$$H = E + PV \tag{29}$$

When referred to its value at 0 K, the enthalpy represents the heat that must be added to raise the temperature of the gaseous products from 0 K to T K, the products being maintained in thermal and chemical equilibrium throughout, at the equilibrium pressure $P(T)$ corresponding to the given density Δ g per cu cm. The E term in the definition is $-[E_{\text{rel (0 K)}} - E_{\text{rel }(T\text{ K})}]$, taken negative because the energy released is given up by the system. The PV term is zero at 0 K, since the equilibrium pressure at this temperature is zero at all densities. Accordingly the enthalpy at 0 K, H_0 equals $-E_{\text{rel (0 K)}}$, and the enthalpy H at any temperature T referred to its value at 0 K is given by equation (30),

$$H - (H_T - H_0) = E_{\text{rel (0 K)}} - E_{\text{rel }(T\text{ K})} + 0.024214nPV, \tag{30}$$

which may be written as equation (31)

$$H = H_1 - E_{\text{rel }(T\text{ K})} + 0.024214\,\frac{P}{\Delta} \tag{31}$$

in order to introduce the symbols used in the Division 1 system of ballistics (Section 3.1), H being expressed in calories per gram and P in atmospheres.

The Specific Heats

The ratio of specific heats, $\gamma = C_p/C_v$, rather than the separate values of C_p or C_v, finds extensive use in the calculations of interior ballistics. It will be evident that, when the energies released and the enthalpies are tabulated for different values of T and Δ, C_v and C_p may be obtained from equations (31) and (32).

$$C_v = -\left(\frac{\partial E_{\text{rel}}}{\partial T}\right)_{\Delta} \quad \text{cal/g.} \tag{32}$$

$$C_p = \left(\frac{\partial H}{\partial T}\right)_{p} \quad \text{cal/g.} \tag{33}$$

The ratio of the specific heats for the gaseous products in the state of the ideal gas (γ^0) is given by equation (34), in which $C_v{}^0$ in calories per mole may be obtained from tabular differences of $n_i(E_T{}^0 - E_0{}^0)_i$ at two different temperatures T, summed up for the separate powder gas constituents i.

$$\gamma^0 = 1 + \frac{nR}{C_v{}^0} \tag{34}$$

At high densities and pressures, where the energy of gas imperfection may become significant, an accurate value of γ may be obtained from equation (35),

$$\gamma^{-1} = 1 - \left\{\frac{0.024214\,T}{C_p\Delta^2}\right\}\left\{\left(\frac{\partial\Delta}{\partial T}\right)_p^2\left(\frac{\partial P}{\partial\Delta}\right)T\right\}, \tag{35}$$

in which C_p is given in cal/g/degree K, P is in atmospheres, and the other symbols have their usual significance. The derivatives are obtained from graphs of (Δ vs $P)_T$ and of $(P/\Delta$ vs $T)_p$ by use of the relation expressed by equation (36).

$$-2.303\left[\partial\log_{10}\left(\frac{P/\Delta}{\partial T}\right)\right]_p = \frac{1}{\Delta}\left(\frac{\partial\Delta}{\partial T}\right)_p. \tag{36}$$

An effective ratio of the specific heats (γ_{eff}) may be obtained on the assumption of equation (37) combined with equation (38),

$$(C_p - C_v) = nR \tag{37}$$

$$\gamma_{\text{eff}} = 1 + \frac{(F)(T_0 - T)}{\overline{E}_{\text{rel}}T_0}, \tag{38}$$

where (F) is the "force" or impetus, nRT_0. It may be noted here that the influence of pressure on the specific heats or their ratio is small, and arises from the small temperature coefficient of the energy of gas imperfection.

The Entropy

The entropy, aside from its intrinsic value, has use in the construction of Mollier diagrams. Equation (39) expresses the entropy for the mixture represented by powder gas.

$$S = \frac{E_T{}^0 - E_0{}^0}{T} + \frac{E\,(\text{gas imp.})}{T} - \frac{F_T{}^0 - E_0{}^0}{T} - nR[\ln(3.571\,T\Delta') + \textstyle\sum_i x_i \ln x_i + \Phi - 1]. \tag{39}$$

In using this equation $(E_T{}^0 - E_0{}^0)$ and $(F_T{}^0 - E_0{}^0)$ are obtained additively on multiplying the number of moles n_i and the respective energies for the different gases, and Φ is given by equation (40).

$$\Phi = b'\Delta + 0.3125(b'\Delta)^2 + 0.09563(b'\Delta)^3 + 0.0482(b'\Delta)^4. \tag{40}$$

2.4.5 Applications of Thermodynamics to Powder Gas

Thermodynamics has been applied[24] to the calculation of properties of powder gas from a number of different propellants. Space does not permit considering these in detail. Types of results obtained are illustrated in Figure 12, giving the energy released for a nitrocellulose powder [designated[440] "N(1)"], similar to the U.S. Navy Pyro powder, an FNH powder, lot No. 1358 (designated "D") and a cordite [designated[440,538] "C(1)"] containing 28.7% nitroglycerine. In each case the E_{rel} is given for two densities, as indicated in the figure. At the lower temperatures, E_{rel} is not a sensitive function of the density, but near 3000 K and higher the dissociation of the main products, which is influenced by the density, becomes appreciable, and the energy released reflects this. The adiabatic flame temperatures T_0 for these powders are the temperatures at $E_{rel} = 0$. They are for $\Delta = 0.25$, 2915 K for powder N(1), 2575 K for powder D, and 3735 K for powder C(1). The values calculated by a short method[23] are 2899, 2577, and 3727 K. Calculated values of the thermodynamic properties of British powders have been tabulated.[9]

2.4.6 Comparison of Calculated Thermodynamic Properties with Experimental Ones

Pressures

The pressures calculated thermodynamically are the uncooled pressures—that is, no allowance is made for heat loss to the walls. Measured pressures are lower. A method[191] of correcting observed pressures for heat loss has been derived at Aberdeen Proving Ground. A comparison of the calculated pressures at T_0 with corrected observed pressures for powder gas from powder N(1) are given in Table 4.

Table 4. Comparison of calculated uncooled pressures for N(1) powder gas with experimental values of Crow and Grimshaw as corrected by Kent and Vinti.[191]

Density Δ (g/cm³)	P_0(calc) (kg/cm²)	P_0(expt) Large chamber (kg/cm²)	P_0(expt) Small chamber (kg/cm²)
0.2479	3368	3403	3391
.2211	2911	2946	2934
.2049	2647	2690	2729
.1819	2288	2288	2336
.1546	1883	1907	1896
.1344	1597	1614	1618
.1066	1225	1232	1209
.0755	835	826	823
.0585	633	632	636
.0420	446	435	442
.0263	274	270	266

Heat of Explosion

The heat of explosion, per gram of powder, as observed in a closed chamber calorimeter is equal to the energy released at the calorimeter temperature (water liquid). It is of interest to determine the influence of the gas composition on the energy released, and compare the result with a measured heat of explosion. The powder selected for this is powder N(1), for which a calorimetric value[440] at a density of loading 0.1 is 936 cal per g (water liquid, no gas analysis is given). In making the calculations we have adopted 300 K as the calorimeter temperature and assumed the water gas equilibrium to freeze at a series of temperatures T_0' from 300 to 3000 K. In view of the quenching results discussed in Section 2.3, the values for $T = 2000$ K and above obviously have no physical significance and are included for another purpose to be made evident shortly. The results, considering water gas constituents and nitrogen only at densities $\Delta' = 0$, 0.1, 0.25, and 0.4 are given in Table 5, for water gas-

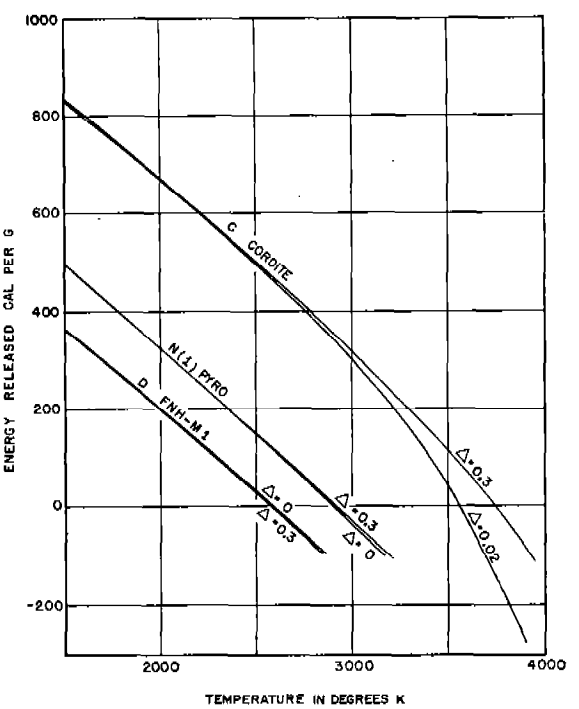


Figure 12. Energy released versus temperature for three different powders. (This figure is based on data in NDRC Report A-116.)

TABLE 5. Energy released at 300 K for Crow and Grimshaw's[440] N(1) powder, calculated for the indicated values of Δ', and T_g', water-gas constituents only. ($\Delta = 1.05943\Delta'$ for this powder.)

T_g'/Δ'	300	1000	1500	2000	2500	3000
0	(911.4)*	(858.2)	(830.7)	(819.7)	(814.3)	(811.4)
	911.4†	911.8	912.0	912.2	912.2	912.2
0.1	(922.1)*	(863.7)	(835.9)	(825.0)	(819.7)	(816.9)
	922.1†	921.6	921.2	921.1	921.1	921.0
0.25	(938.3)*	(864.7)	(837.7)	(827.7)	(823.0)	(820.6)
	938.3†	935.5	934.4	934.1	933.8	933.8
0.40	(954.4)*	(854.8)	(832.1)	(824.6)	(821.3)	(819.6)
	954.4†	948.0	946.5	946.0	945.8	945.7

* $E_{\text{rel 300 K}}$ water gaseous.
† $E_{\text{rel 300 K}}$ water liquid.

eous (in parentheses) and for water liquid. The feature to be noted is the negligible effect of T_g' and hence, of the shift of the water gas equilibrium on the energy released (water liquid).

The value of the heat of explosion calculated for $\Delta = 0.10$ ($\Delta' = 0.0944$ with $n = 0.041075$ mole/g) for $T_g' = 1500$ K is 92.07 cal/g. The methane formed and its influence on the properties of the gas at 1500 K had been calculated[24] previously. The presence of methane, because of the large amount of heat evolved in its formation, increases the energy released. If its equilibrium quantity at 1500 K were formed, and the equilibrium froze at this temperature, $E_{\text{rel 300 K}}$ at $\Delta = 0.10$ would be increased by 18 cal/g, making a total of 939 cal/g, in comparison with the measured heat of explosion of 936 cal/g. The agreement is excellent. Actually the methane equilibrium tends to freeze-in at a T_g' of about 1800 K, which would mean a somewhat lower than equilibrium concentration at 1500 K, and a lower contribution to the energy released.

The use of a *rational* heat of explosion, defined as the amount of heat liberated per gram when the powder gas cools from the adiabatic flame temperature to room temperature without a change in composition has been advocated.[539] The rational heat is identical with the E_{rel} at the calorimeter temperature, (water gaseous), with $T_g' = T_0$, $\Delta = \Delta_0$ (density of loading), provided all the powder burns. For N(1) powder gas at $T_g' = T_0 = 2915$ K and $\Delta = 0.10$ it is 817.5 cal/g, as interpolated from Table 5, values in parentheses (water gaseous).

Among the many applications of thermodynamics to powder gas that might be mentioned, an outstanding example is given by an interpretation of the chemical thermodynamics of gun erosion.[60] In this work the powder gas is assumed to be quenched at a series of temperatures T_g' as defined earlier in this section, and the free energy of the reaction of the quenched gas with the surface of the bore at its surface temperature T_s is calculated. The work is presented in detail in Sections 12.2.4 and 13.3.3, together with a slightly different approach[138] to the same problem.

2.5 POWDER GAS RADIATION AND TEMPERATURE

2.5.1 Temperature Determinations from Radiation Measurements

Thermodynamic calculations for powder gas yield, as is shown in Section 2.4, a value for the uncooled pressure P_0, and the adiabatic flame temperature T_0. In interior ballistic calculations certain simplifying assumptions based on experience are made concerning the burning rate, heat, and frictional loss, and these with a simplified equation of state for the gas enable the course of the pressure and temperature to be computed as a function of the time or travel as described in Chapter 3. On the experimental side, the advent of the piezoelectric and the electrical-resistance strain gauges make possible a measurement of the pressure as a function of time as described in Chapter 4.

Until recently, however, there has been no reliable measurement of the temperature for powder gas. In the past, attempts to measure the temperature have been made with thermocouples, and by inclusion in the propellant of metals in thin sheets or in pulverized form. These methods have failed to supply adequate information for reasons which need not be discussed here. More recently studies were made in England of the spectral distribution of the emitted radiation, generally at low density of loading.[352,358,393] These have shown a continuous background radiation together with lines of Na, K, and CaO bands.

In an investigation[44] at the Geophysical Laboratory for Division 1 experimental methods were developed for precise measurements of the radiation from burning propellants at densities of loading corresponding to those in guns. The stumbling-block in making radiation measurements at high densities has been the lack of a strong enough window. Successful use was made at pressures up to 50,000 psi of fused quartz windows of the Poulter type[540] in which a plane polished window surface is brought in contact with a

plane polished surface of a hardened steel supporting plug.

The first results of this investigation showed that at a sufficiently high density of loading (0.03 minimum, with a path length of 1.75 cm) the radiation is not only continuous, but has a spectral distribution closely resembling that of a black body,[g] and that hence, a powder gas temperature can be determined from measurements of the radiation intensity.

This principle was then applied to the development of the photoelectric pyrometer described in Section 2.5.4. With it studies have been made of the temperature of powder gas in small closed chambers, in a jet propulsion motor, and in the 3-in. gun at Carderock described in Section 4.2.2. The results are presented briefly in Section 2.5.5. Preparations[109,110] were made for similar measurements to be carried out during the firing of a 90-mm gun, M1A1 at Carderock (Section 4.1).

2.5.2 Spectral Characteristics of Powder Gas Radiation

Spectra of radiation emitted by powder gas at very low densities of loading or at early times in firings at intermediate and high densities of loading in a closed chamber consist of discrete lines and bands superimposed upon a continuous background. In specific experiments the discrete features observed had their origin in resonance transitions of potassium, sodium, calcium, (and calcium oxide), barium, iron, chromium, nickel, and vanadium, in the order of their prominence. A hydroxyl (OH) band at 3064 A was observed in absorption, and a faint band near 8150 A may be a vibrational band of water. The chromium, nickel, and vanadium, together with some of the iron, probably came from the nichrome wire igniter; the other substances were present in powders either as impurities, or as a deliberate addition to make the powders "flashless."

The intensity of the continuous radiation increases with the gas density and length of path; as the density increases some of the stronger discrete lines may appear in reversal. The sole origin of the lines and bands in resonance transitions, and the intensity of the continuum are evidence that the spectra are thermally excited.

None of the major constituents of powder gas emit strongly enough in the visible and the near infrared, in comparison with the inorganic impurities, to make a detectable contribution to the spectrum, with the possible exception of water vapor. Among the free radicals, only OH, CN, CH, and NH might be detectable.

The continuous spectra may have their origin in (1) recombination of free radicals which would not lead to black body distribution of intensities, or (2) glowing "soot" or inorganic particles. The latter alternative is much the more probable. It has been shown that particles of diameter 1 μ or less assume the temperature of the gas in times of the order of 0.1 msec. The radiation in such a case would have a distribution closely approximating that of a black body at the temperature of the gas.

A characteristic spectrum obtained with a moving film spectrograph at a density of loading 0.082 of Hercules No. 2 pistol powder is shown in Figure 13. Microphotometer traces of this and similar spectra, together with comparison spectra of the tungsten filament heated at known color temperatures, are reproduced in Figure 14, where the legend explains the various experimental conditions. It will be noted that as time, and hence the gas density, increases during a firing, the relative prominence of the sharp peaks corresponding to line structure decreases until all the tracings assume the same general shape. The coincidence of the tungsten strip and the powder gas spectra is a strong indication that, as the density increases, the spectral distribution of the continuous radiation approaches that of a black body, at least for the wavelength range 4000 to 6400 A observed in the experiments.

Measurements of the emissivity and absorptivity of powder gas at various densities also showed that unit emissivity is rapidly approached at values of the density times the length of path about 0.06 g/cm^2. The actual value of the density at which a stated emissivity ϵ is reached depends on the mass emissivity k characterizing the gas from a particular powder, as given in equation (41),

$$\ln (1 - \epsilon) = - k\Delta l \qquad (41)$$

where Δ is the gas density and l the length of path.

Values of k found for NH and FNH-M2 powder gas, for example, were 34 and 120 cm^2/g. In a gun at a time when $\Delta = 0.2$ g/cm^3, $\epsilon = 0.9$ would be expected to be reached with such powders in thicknesses of gas 0.34 and 0.095 cm, and $\epsilon = 0.99$, in 0.68 and 0.19 cm, re-

[redacted]

[g] The black body characteristics of powder gas radiation were earlier studied by Col. Libesart[487] who, however, does not appear to have carried the matter further.

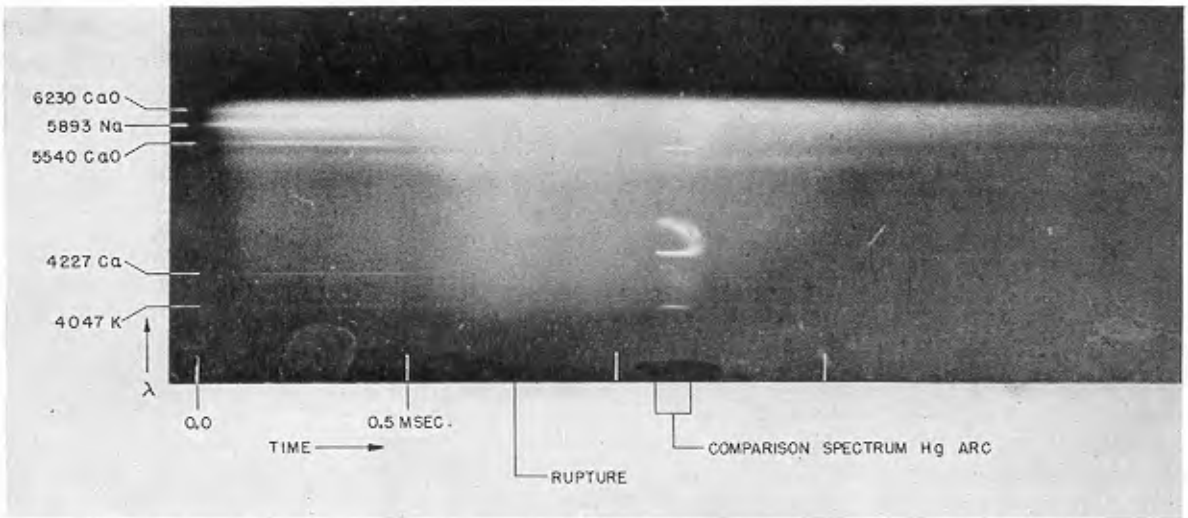


FIGURE 13. Spectrum of burning powder photographed with a moving-film spectrograph, length of path 1.75 cm. Hercules No. 2 pistol powder, loading density 0.082, a comparison spectrum of the mercury arc appears superposed on the shot. (This figure has appeared as Figure 15 in NDRC Report A-252.)

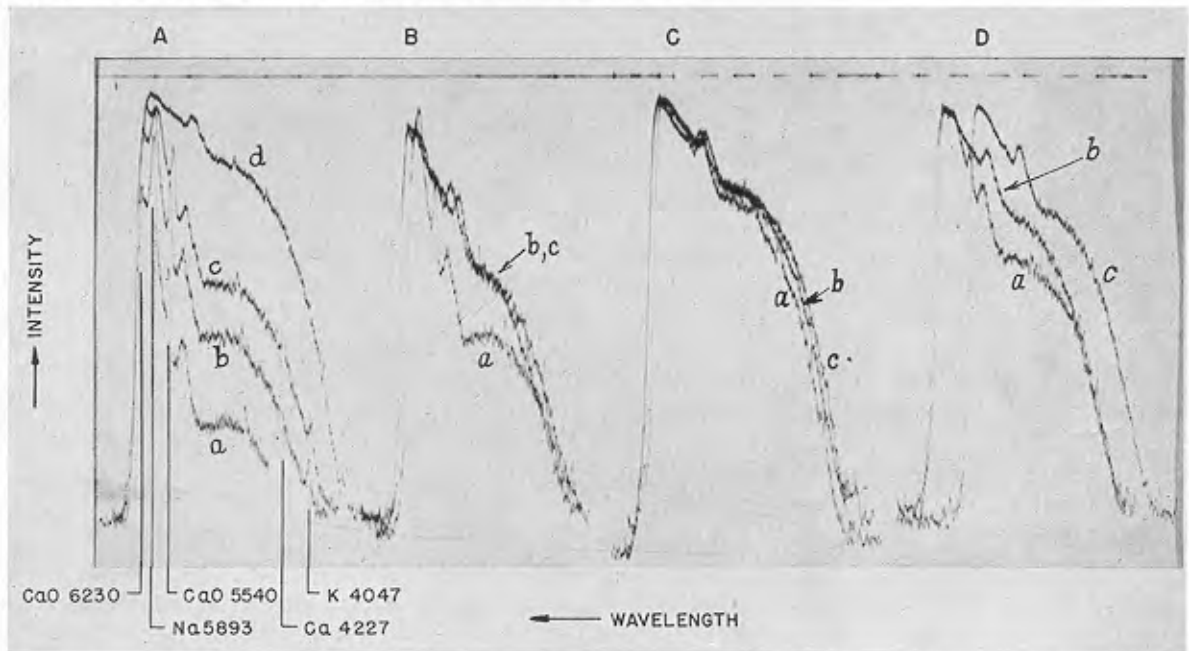


FIGURE 14. Four sets of microphotometer traces from the spectra obtained with the rotating drum spectrograph, principally from Figure 13, together with comparison spectra of a tungsten strip-filament at known color temperatures. All the films were developed at the same time. (This figure has appeared as Figure 16 in NDRC Report A-252.)

Set	Trace	Source	Time (msec)
A	a	Shot, Powder (2), Δ_0 = 0.082	0.1
A	b	Shot, Powder (2), = .082	.25
A	c	Shot, Powder (2), = .082	.5
A	d	Shot, Powder (2), = .082	.75 (max)
B	a	Shot, Powder (2), Δ_0 = 0.082	0.3
B	b	Shot, Powder (2), = .082	1.3
B	c	Tungsten, T_c = 3120 K	
C	a	Shot, Powder (2), Δ_0 = 0.082	0.60
C	b	Shot, Powder (2), = .082	1.00
C	c	Tungsten, T_c = 3240 K	
D	a	Shot, Powder (2), Δ_0 = 0.082	0.45
D	b	Shot, Powder (2), = .082	1.05
D	c	Shot, Powder (19), = .179	(max)

CONFIDENTIAL

spectively. Gases from powders containing large amounts of inorganic constituents tend to be characterized by high values of k.

2.5.3 Characteristics of Radiation

Black Body Radiation

The intensity of radiation emitted by a body in thermal and radiative equilibrium $J(\lambda, T)$, at the absolute temperature T and at the wavelength λ is accurately expressed by the well known Planck distribution law; for temperatures below 4000 K and wavelengths in the ultraviolet, visible, and near infrared, it is expressed without appreciable error (less than 5 degrees) by the simpler Wien equation, equation (42), in which $c_1 = 2\pi hc^2 = 3.740\times10^{-5}$ erg cm^2/sec^{-1} and $c_2 = hc/k = 1.436$ cm/deg.

$$J(\lambda, T) = c_1\lambda^{-5} \exp \frac{-c_2}{\lambda T}, \qquad (42)$$

Equation (42) has been confirmed by prior experiments for wavelengths in the visible and ultraviolet regions, even at the highest temperatures.

Radiation from Actual Bodies

As a consequence of reflection and the possible failure of Lambert's cosine law for solids or liquids, or of low mass emissivity k for gases, real bodies may radiate less than a black body. The ratio of the surface brightness $B(\lambda, T)$ to that of a black body $B_0(\lambda, T) = J(\lambda, T)$ is given by the spectral emissivity $\epsilon(\lambda, T)$ which in general is less than unity and varies with both the temperature and the wavelength. The spectral distribution of brightness for such bodies therefore differs from that of a black body.

For any one selected wavelength λ_i it is possible, however, to define an apparent *brightness temperature* S_i, by Wien's law such that a black body at S_i has the same brightness as the real body at T, as shown in equation (43)

$$B(\lambda_i, T) = c_1\lambda_i^{-5} \exp \frac{-c_2}{\lambda_i S_i}. \qquad (43)$$

S_i will in general be different for every λ_i.

It is also possible to seek a second apparent temperature, the *color temperature* T_c, such that a black body at T_c has the same spectral distribution as the real body at T, as expressed by equation (44).

$$B(\lambda, T) = c_1\lambda^{-5} \exp \frac{-c_2}{\lambda T_c}. \qquad (44)$$

Such a color match may not be possible for all wavelengths, but it can be made for two selected ones, such as 6650 and 4670 A customarily used in pyrometry. The apparent temperature T_{cij} thus defined is usually termed the *two-color* or the *red-blue* color temperature. The three temperatures, S_i, T_{cij} and T, the spectral emissivity ϵ_i and the two-color emissivity ϵ_{cij} are connected by the relation given in equation (45).

$$\begin{aligned} B(\lambda_i, T) &= c_1\lambda_i^{-5} \exp \frac{-c_2}{\lambda_i S_i} \\ &= c_1\epsilon_i\lambda_i^{-5} \exp \frac{-c_2}{\lambda_i T} \\ &= c_1\epsilon_{cij}\lambda_i^{-5} \exp \frac{-c_2}{\lambda_i T_{cij}}. \end{aligned} \qquad (45)$$

where S_i is defined for any one λ_i, T_{cij} for any two λ_i and λ_j and T for all values of λ.

In particular, the ratio of the brightness at two wavelengths λ_r and λ_b for a body at the temperature T is given by equation (46).

$$\begin{aligned} \ln \frac{B(\lambda_r, T)}{B(\lambda_b, T)} &= 5 \ln \frac{\lambda_b}{\lambda_r} + \ln \frac{\epsilon_r}{\epsilon_b} + \frac{c_2}{T}\left(\frac{1}{\lambda_b} - \frac{1}{\lambda_r}\right) \\ &= 5 \ln \frac{\lambda_b}{\lambda_r} + \frac{c_2}{T_{crb}}\left(\frac{1}{\lambda_b} - \frac{1}{\lambda_r}\right). \end{aligned} \qquad (46)$$

From this equation it is evident that $T_c = T$ if $\epsilon_r/\epsilon_b = 1$ even though ϵ_r and ϵ_b separately are not unity. Since the ratio ϵ_r/ϵ_b for two fixed wavelengths λ_r and λ_b is only a weak function of the temperature, it may be assumed constant without an appreciable error; equation (46) may then be expressed by the simpler equation (47),

$$\ln \frac{B(\lambda_r, T)}{B(\lambda_b, T)} = A' + \frac{c_2 B}{T} = A + \frac{c_2 B}{T_c}, \qquad (47)$$

which is linear in reciprocal T or T_c.

As has already been stated, the emissivities of powder gas approximate unity in a sufficiently thick layer of gas even at quite low densities; when this is true, the brightness, color, and the true temperature should coincide. For substances having relatively low emissivities, however, the differences may be quite large, and dependent on wavelengths. Thus, for tungsten, which is of interest because it is used in making calibrations, it is found at $T = 2500$ K, with $\lambda_r = 6650$ A, $\lambda_b = 4670$ A and $\epsilon_r = 0.4250$, $\epsilon_b = 0.4620$, that $S_r = 2275$ K, $S_b = 2352$ K, $\epsilon_c = 0.349$ and $T_c = 2558$ K. If, on the other hand, $\lambda_r = 9000$ A, $\lambda_b = 4500$ A with $\epsilon_r = 0.3610$, $\epsilon_b = 0.4655$, then $S_r = 2156$ K, $S_b = 2359$ K, $\epsilon_c = 0.2800$, and $T_c = 2604$ K.

2.5.4 Photoelectric Pyrometer for Powder Gas

Design Principles

In the burning of powder in closed chambers and guns the total time in which a quantitative measurement of the radiation must be secured is of the order of a few milliseconds, and it is desirable to have a frequency response up to 10^5 c. Among the possible methods of securing such a measurement, the most advantageous appears to be the use of vacuum-type photocells to observe the radiation, combined with oscillographic recording of the photocell response, as a function of time. In photocells the response is instantaneous, directly proportional to the intensity of radiation over a wide range, and moreover, cells are available with spectral sentivities such that different spectral regions may be explored.

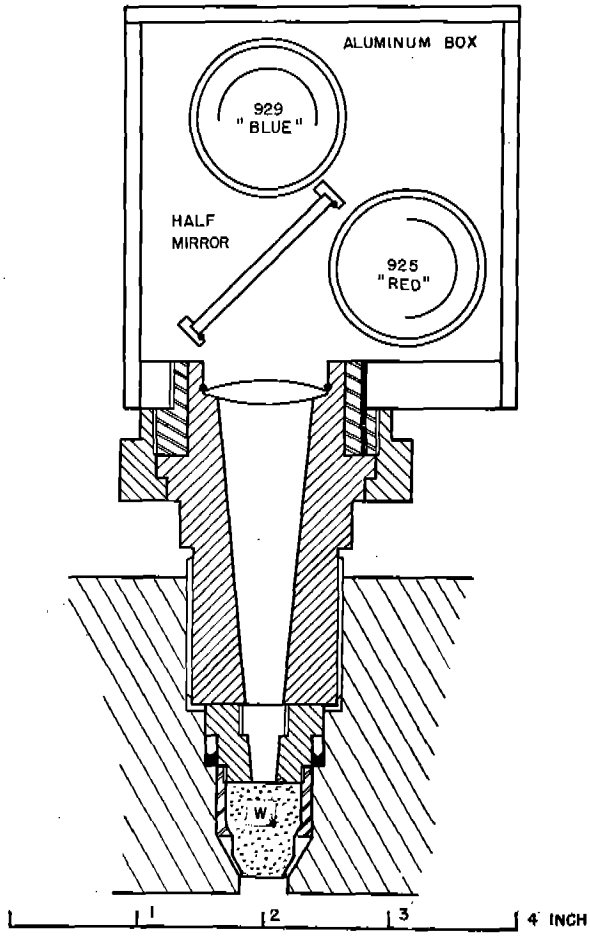


Figure 15. A two-color photoelectric pyrometer for mounting on a 3-in. gun. (This figure has appeared as Figure 26 in NDRC Report A-323.)

Measurements for calculating the brightness temperature S_i [defined by equation (43)] may be made with single cells; it is more desirable, however, to make measurements with two cells simultaneously for determining the color temperature T_c [defined by equation (44)], inasmuch as many factors which assume undue importance in the single-cell measurements balance out when two cells are used. This is especially true concerning the absorption of radiation by the window, the transmission through which varies with time owing to the deposition of smoke particles.

The isolation of wavelengths or wavelength ranges transmitted to the photocells can be made by a monochromator or by filters. Because of the usual small aperture of monochromators the oscillograph deflection is very small unless the photocell response is overamplified; for application to recoiling guns their use would be unworkable. The method was tested, however, and for research purposes with instruments of high light-gathering power, is deserving of further trial, particularly with low-density firings when deviations from black-body conditions may be important.

For routine measurements wavelength ranges may be isolated by appropriate glass or gelatine filters. Suitable combinations for the two-color measurement are the RCA phototube 922 or 925 with Wratten filter 87, giving an effective λ of 9000 A and 8600 A respectively, and an RCA phototube 929 with filter 556 effective λ 4450 A; with filter 511, effective λ 4200 A; or with filter 43, effective λ 4800 A. Cell 929 can also be used without a filter when its effective λ is 5000 A.

Apparatus

For photoelectric measurements by the two-color method, the radiation as it emerges from the window in the pressure vessel or gun must be divided so that separate beams may reach simultaneously the red-sensitive and blue-sensitive photocells. This may be done by a spectrograph (provided with two emergent slits) or better, by a semitransparent mirror. One of the "pyrometers" incorporating this feature and designed for mounting on a 3-in. gun is illustrated in Figure 15. (See Section 4.4.13.)

In this installation the radiation from the window W passes through a condensing lens of suitable focal length, and is divided by the mirror so that part of the beam is reflected to the "red" cell, and part transmitted to the "blue" cell. Gelatine filters are wrapped around the phototubes. Since the pyrometer recoils

with the gun, relative vibration of the photocell elements may be objectionable. To minimize this, the aluminum box holding the cells is arranged to swivel around the retaining plug so it may be oriented for the axes of the cells to be parallel to the direction of motion.

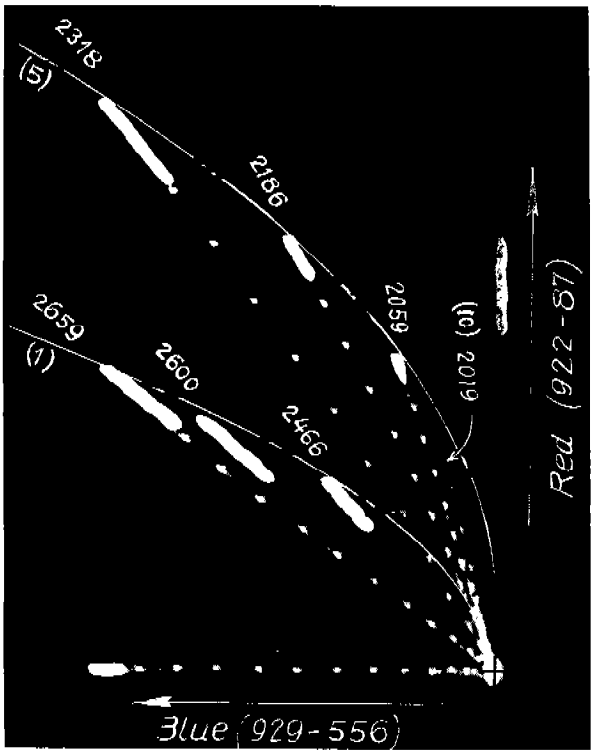


FIGURE 16. Oscillographic calibration record for the two-color photoelectric pyrometer, giving traces corresponding to the stated color temperatures of a tungsten strip-filament, at three amplifications in the ratio 1:5:10. As the temperature increases, the blue/red ratio increases. The dot and dash curves are curves of constant emissivity for the two lower amplifications. (This figure has appeared as Figure 10 in NDRC Report A-252.)

The output of the photocells is led first to a preamplifier giving fixed gains adjustable in steps, and then to a cathode ray oscillograph. The output of each photocell may be recorded separately as a function of time by a rotating drum camera or by using a recurrent sweep and a still camera. For the two-color measurement, the outputs of the two cells are connected individually to the X- and Y-axes of the oscillograph; the spot then moves at an angle which is a measure of the ratio of the two amplified photocurrents, and thereby, becomes an index of the color temperature. The amplitude of the motion of the spot is similarly a measure of the emissivity of the gas; the absolute value of the emissivity may be determined from the ratio of the observed photocurrent to that which would be produced under like conditions by a black body at the same temperature.

The calibration[44] of the instrument is carried out by comparison with a tungsten-strip lamp operated at known brightness temperatures, calibrated with reference to an optical pyrometer. A typical calibration

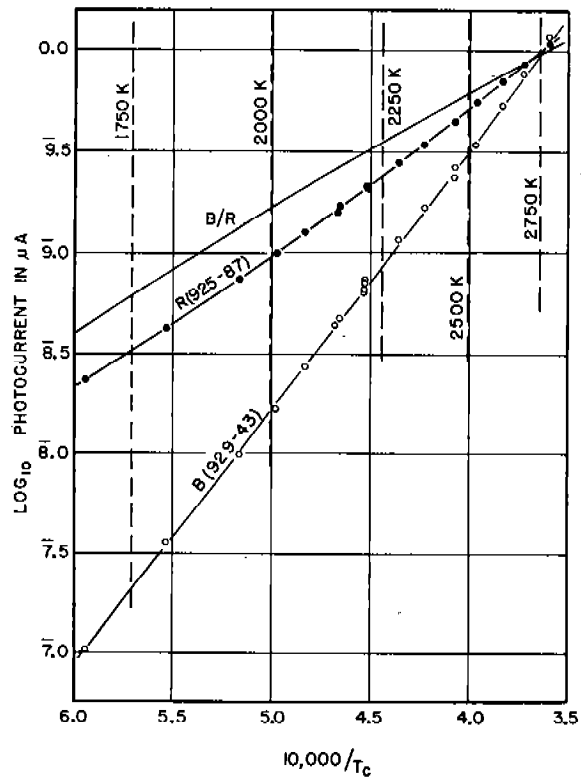


FIGURE 17. Results of a series of calibration records made by the two-color photoelectric pyrometer. The photocurrent is plotted versus the color temperature of the tungsten filament. Circles represent experimental points; the slopes of the R and B lines were calculated from the phototube sensitivities and filter transmissions in combination with the Wien formula and the known emissivity of tungsten. Vertical adjustment of the curves is made to fit the individual sensitivities of phototubes used. (This figure has appeared as Figure 11 in NDRC Report A-252.)

record obtained with the two-color pyrometer is reproduced in Figure 16, and a plot of a series of calibrations is given in Figure 17, where the logarithms of the photocurrents of the red and the blue cells and their ratios are plotted against the reciprocals of the color temperature T_c.

[redacted]

2.5.5 Determinations of Powder Gas Temperatures

Firings in Closed Vessels

During the course of development of the photoelectric pyrometer, many firings with four typical propellants (NH, FNH-M2, single-base pistol, double-base pistol) were made at loading densities from below 0.01 to more than 0.25 in closed vessels provided with windows. Only one series of six shots at $\Delta = 0.20$ with NH powder, designed to test the reproducibility, will be discussed here briefly.

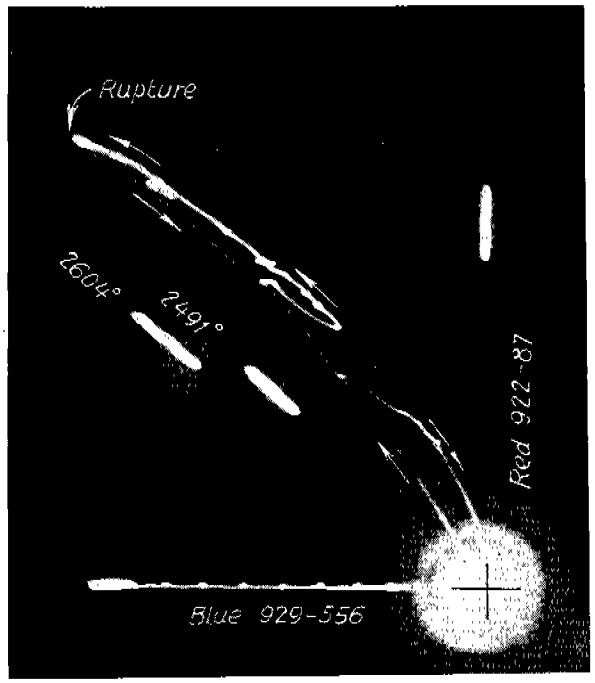


Figure 18. Oscillographic temperature record in a closed chamber firing taken with a two-color photoelectric pyrometer. Arrows indicate the advance of time. Calibration traces at color temperatures of 2491K and 2604 K are superposed.

Figure 18 gives a two-color oscillograph record for the first shot in the series, with three superimposed calibration traces. The direction of motion of the oscillograph spot is indicated by the arrows. Timing dots on the trace give a correlation of events with pressure-time, and with red (or blue) radiation intensity-time traces taken simultaneously with other oscillographs. From measurements of the ordinates and abscissas at any point on the trace the photocurrents and their ratios are evaluated, and from these, with reference to the calibration chart, the temperatures. Once the temperatures are known, the apparent relative emissivities $(\epsilon_r)_T$ or $(\epsilon_b)_T$ can be calculated by comparing the photocurrent in firing with the photocurrent in calibration for the particular value of T.

The results for the six shots in the series are summarized in Figure 19 which gives the pressures and the emissivities, referred to their values at rupture (release of pressure), and the individual values of the two-color temperature T_c for the various firings. The pressures appear to be reproducible to within 2 per cent of the average curve. The emissivities show a much greater variation, but in general they rise to the saturation value before the pressure rises to 20 per cent of its final value.

The general course of the temperature with time is shown to be similar for all the six shots: with individual variations, there is an initial peak followed by a drop, and then a more gradual rise to the final value. It will be noted that part of the time the emissivity exceeds unity. This appears to be common for ϵ_r while the powder is actively burning, and may be due to the same causes as the strong infrared emission observed in a separate investigation[160] already referred to in Section 2.2.4. The individual variations in temperature may arise partly as the result of irregular ignition and burning of powder grains; more specifically they emphasize the inherent variations in the local temperature of gas in turbulent motion. When the gas is comparatively opaque (high mass emissivity k), the radiation which is emitted comes from a comparatively thin layer next to the window which may be cooler than the average, and whose temperature may be varying because of local pressure inequalities and other sources of imperfect thermal equilibrium.

Firings in 3-in. Gun

As part of the comprehensive series of internal and external ballistics measurements with the 3-in. gun at Carderock, described in Section 4.2.2, measurements for determining the powder gas temperature were taken, first through holes into the chamber alone, and later, in two other positions, one 10 in. and the other 51 in. ahead of the forcing cone (see Section 4.3.16). Firings were made with Navy "SPDN" and "SPD" powders (NH and pyro, respectively) at full charge, and at fractional charges down to 0.50 of full charge. The details are given in separate reports.[39,65,132] Here it is possible to reproduce only two examples of the

results obtained. Measurements were taken with the two-color pyrometers, and with single-color pyrometers; the temperatures were determined as the two-color temperature T_c or the single-color brightness temperatures T_R or T_B.

Figure 20 gives a correlation of the temperature,

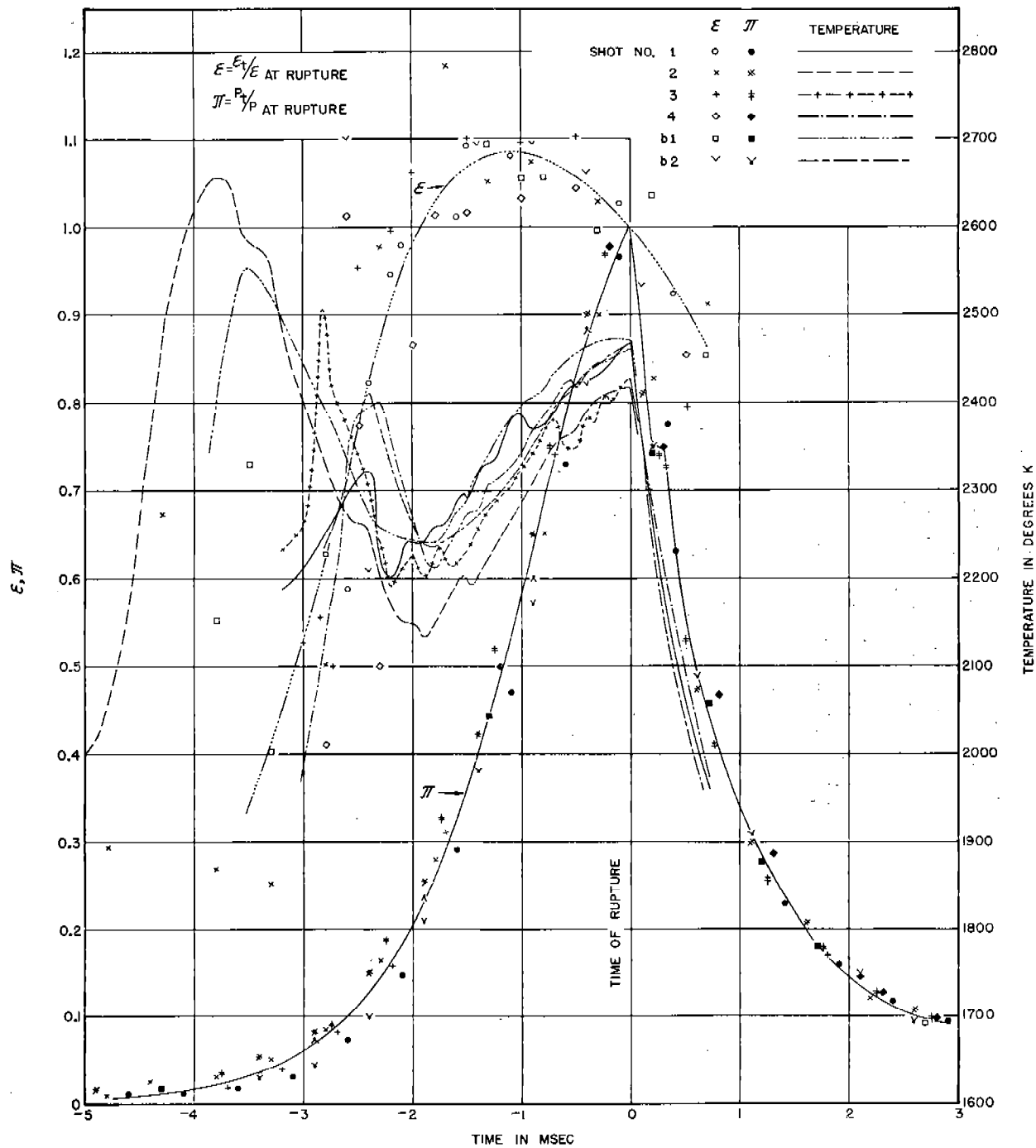


FIGURE 19. A diagram illustrating the reproducibility of results in six consecutive firings in a closed chamber, with NH powder. The absolute temperature T, the relative emissivity ($\epsilon = \epsilon t/\epsilon r$), and the pressure ($\pi = Pt/Pr$) are plotted as functions of time. The emissivities and pressures are expressed in terms of their values at rupture. Single curves are drawn to represent average ϵ and π for all shots; the T's are sketched individually up to the time of rupture; thereafter they are roughly parallel. (This figure has appeared as Figure 24 in NDRC Report A-252.)

[redacted]

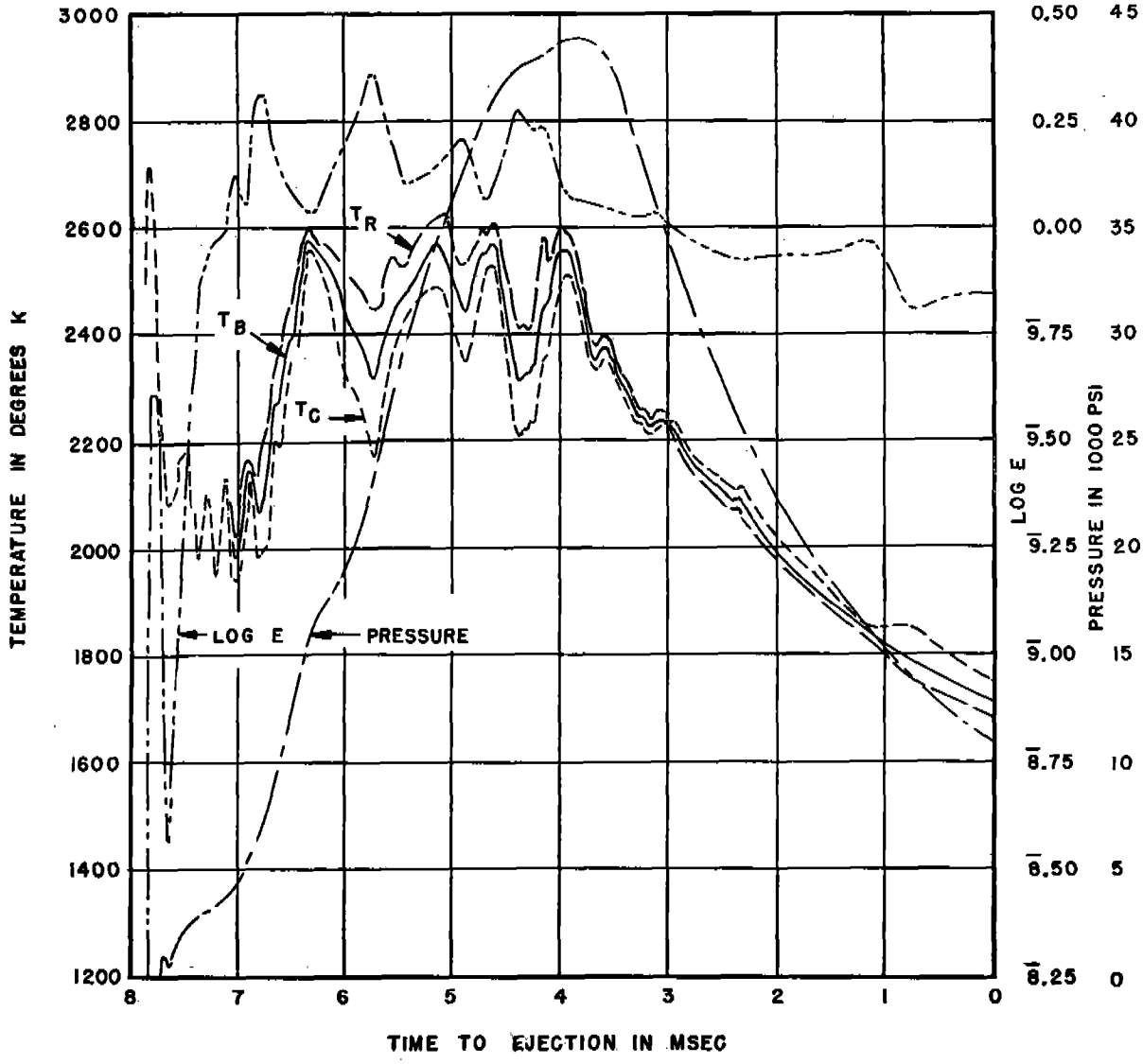


FIGURE 20. Powder gas temperature, pressure and emissivity curves for a 100 per cent round with SPDN (NH) powder in 3-in. gun, plotted as functions of time. Temperatures represented are those observed through a window into the chamber of the gun. Note the large differences between T_R, T_B, and T_c while the powder is actively burning, resulting from ϵ_r being greater than unity. (This figure has appeared as Figure 58 in NDRC Report A-323.)

the pressure, and the emissivity for one round with SPDN powder from measurements taken at the chamber position. It will be seen that during the early stages of burning there is a parallelism between the results in the gun and those obtained in the closed vessel (Figure 19). The outstanding difference between the two lies in the course of the emissivity with time. Again ϵ_r exceeds unity and also exceeds ϵ_b, hence $T_R > T_B > T_c$; however, the emissivity builds up faster to saturation in the gun than in the closed vessel. This is largely because of the presence of black powder in the gun primer; the mass emissivity k for black powder gas being much higher than that for NH powder gas, the gas in the gun becomes more emissive earlier in the shot.

Figure 21 presents the course of the temperature with time, averaged for 13 full-charge rounds, with measurements taken at all three positions on the gun. It will be noted that the temperatures measured in the chamber (position 1) are higher than the other two throughout the round, and that, hence, there is a large gradient of temperature between the chamber and the bore. There is a similar but not so pronounced, gradient of pressure. The temperature gradient is

greater than can be accounted for quantitatively on simple ballistic theory.[65,113] It is believed that transfer of heat to the walls must be largely responsible, inasmuch as heat transfer between the forward portions of the gas and the walls takes place much faster than that between the forward and rear portions of the gas itself. Because of the high opacity of the gas, and the high rate of heat transfer to the walls, the temperatures measured are those of a relatively thin layer of gas cooler than the average, near the window; at the forward holes, this effect is likely to be much more pronounced than in the chamber, and hence the observed temperature gradient may be more apparent than real.[113]

Firings in a Jet Propulsion Motor

Firings in an experimental jet propulsion motor, 2½ in. inside diameter and 9 in. long, equipped with two diametrically opposite windows placed near the nozzle end were made with six different rocket powders, both salted and unsalted. The pressures ranged up to 3,000 psi. Measurements were taken with a two-color photoelectric pyrometer through one window, and spectra were photographed through the other, on stationary or moving plates, with a small Bausch and Lomb quartz spectrograph.

The experimental findings showed that with salted powders even at fairly low pressures of gas, and with unsalted powders at pressures above 1,000 psi the radiation was near-black-body in distribution, and characteristic of temperatures considerably lower than the (isobaric) adiabatic temperature. At low pressures the spectral features, photographed from 7000 A to shorter wavelengths, were emission lines and bands due to resonance transitions in K, Na, Ca, CaO, Fe, Cu, and CuH, together with a continuous background. No nonresonance lines or bands were

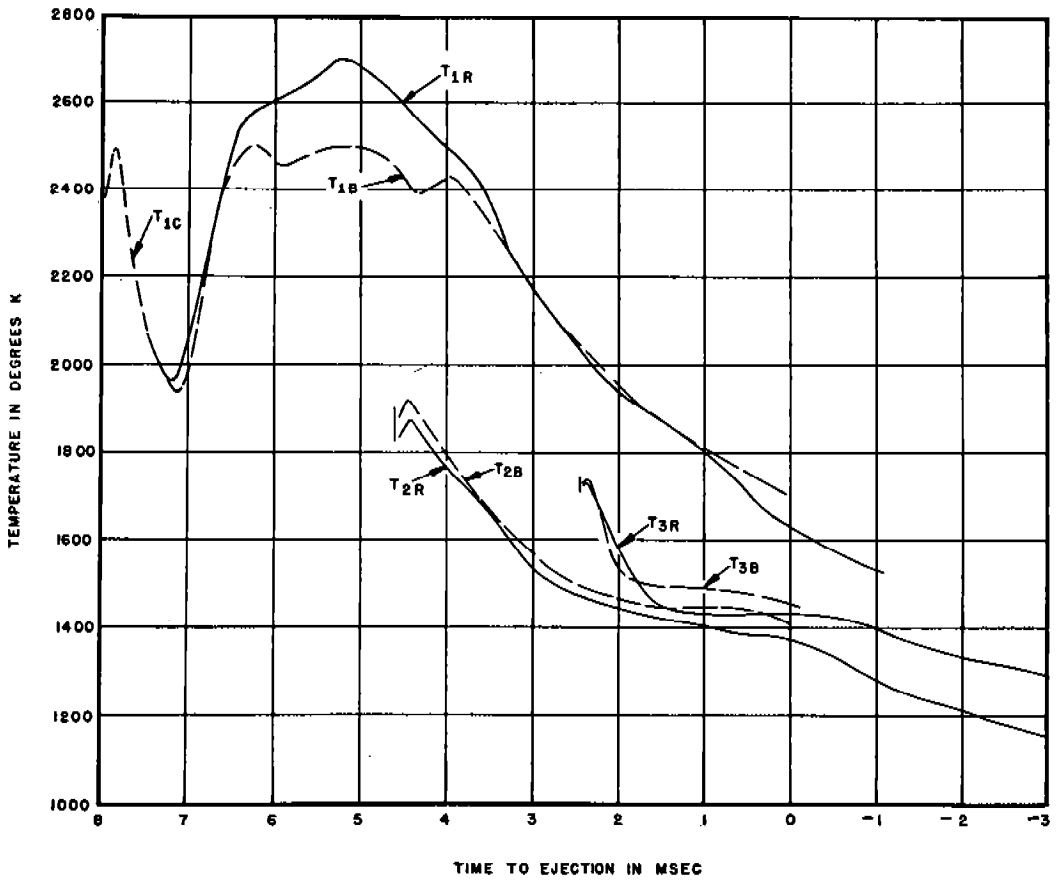


Figure 21. Gas temperature versus time curves averaged for 13 rounds at 100 per cent charge with SPDN powder in a 3-in. gun. The temperatures were observed at three positions: T_1, chamber; T_2, 10 in. ahead of origin of rifling; T_3, 51 in. ahead of origin of rifling. Note the large apparent gradient of temperature between hole 1 and holes 2 and 3. (This figure has appeared as Figure 58 in NDRC Report A-323.)

[redacted]

found, nor any due to free radicals, such as CH, C_2, NH, and CN. At all pressures after the early stages of firing, strong reversal was observed at the positions of Na 5896 A and K 4046 A, as well as in some cases at the CaO bands and Ca lines (the plates used were not sensitive beyond 7000 A, hence the K 7665-7699-A doublet was not observed). The reversal of these intense lines is indicative of a cooled layer of gas near the windows; it was strongest when the windows were recessed and not flush with the inner wall of the motor.

As already stated, the temperatures observed were much below the adiabatic; as an extreme case, unsalted ballistite 14400, T_0 (isobaric) = 3200 K, gave T_c about 2700 K at 1,000 psi, windows flush, and about 2300 K at 2,100 psi, windows recessed 1½ in. The emissivity in the red, ϵ_r, tended to be greater than ϵ_b, as in the results for the closed vessels and for the 3-in. gun. There was also observed considerable fluctuation of both the color temperature and the emissivity even when the pressure was moderately steady. This was due presumably to the great turbulence of gas in the motor.

The early course of the temperature is of interest in connection with the discussion of Section 2.2; at pressures below 100 psi, the temperatures appeared to be below 2000 K, and then rose sharply to near the maximum temperature at the time the pressures reached the range 300 to 700 psi.

2.5.6 Concluding Remarks

Anomalous Emissivities

In the foregoing brief discussion of the radiation emitted by powder gas, and the determination of powder gas temperature from the intensity of its radiation, it has been indicated that, while the gas appears to have high mass emissivity (values ranging up to about 100 cm^2/g for certain powders) and hence should in a thick enough layer radiate as a black body, there are certain discrepancies observed, particularly when the powder is in an active state of burning. The persistent tendency toward excessive emissivity in the red region of the spectrum, especially where the burning goes on at moderate and high densities when black body conditions should be most nearly fulfilled, leads to the supposition that some processes other than thermal ones may be involved in the spectral excitation, even though all the observed spectra in the visible and near infrared regions appear to have their origin in thermal excitation alone.

It seems significant that the anomalous emissivities become normal when the burning is completed. It would seem profitable to extend the studies of the radiation as far into the infrared as may be practicable, in view of the highly intense bands already observed[160] in that region. While at the low pressures and short path lengths used in those studies the con-

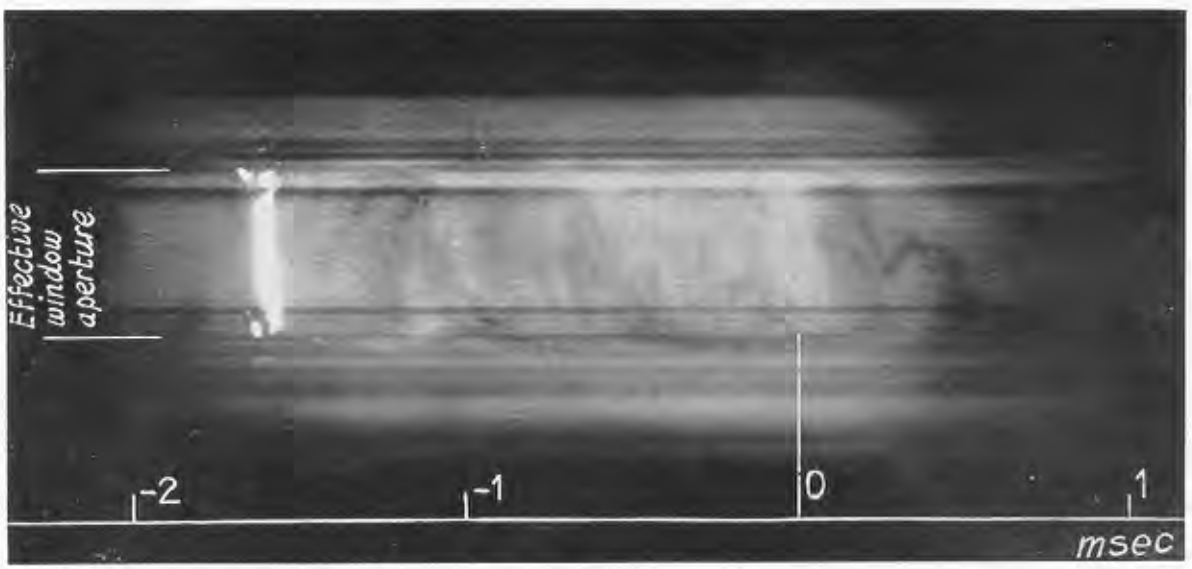


Figure 22. Enlargement of a photograph of the luminosity and turbulence of powder gas in a closed vessel, taken with a rotating drum camera on Super XX film. The time scale is referred to the instant of release of pressure by rupture. Powder—FNH-M2; loading density—0.18. Image of the slit is superposed.

CONFIDENTIAL

tinuous radiation intensity was very low in comparison with that of the observed bands, it is possible that the bands, if suprathermally excited, may remain more intense than the continuous background even at gun pressures.

The errors in temperature introduced by departures of the emissivities of powder gas from unity are evident from equations (48) and (49), which are obtained by recasting equations (42), (43), and (44).

$$\frac{1}{S_i} - \frac{1}{T} = \frac{\lambda_i \ln \epsilon_i}{c_2} \tag{48}$$

$$\frac{1}{T_c} - \frac{1}{T} = \frac{+\lambda_r \lambda_b \ln \epsilon_r/\epsilon_b}{c_2(\lambda_r - \lambda_b)} \tag{49}$$

Thus, if $\epsilon_b = 1$, $\epsilon_r > 1$, the blue brightness temperature is the correct temperature, the red, S_r (or T_r) is too high, and T_c is too low. As an orienting calculation taking $\lambda_r = 9000$ A, $\lambda_b = 4500$ A, $T = 2500$ K, $\epsilon_r = 2$, $\epsilon_b = 1$, we find $T_b = T = 2500$ K, $T_r = 2800$ K, and $T_c = 2250$ K. This would be an extreme case, as red emissivities as high as 2 are not frequently found.

Absorption of Radiation

Errors may occur in calibration, and in evaluating the records. These are of minor magnitude, however, and depend upon the care with which the work is done. A more serious possibility of error lies in the absorption of radiation by dirt deposited on the window. A study of this has shown that such deposits appear to be re-evaporated in successive firings, and condense only after the gas has cooled appreciably.[44] The deposits do not appear to be spectrally selective, and would not, therefore, affect adversely the determination of the color temperature. It is recommended that fresh windows be used in each firing, nevertheless, in order to minimize any errors from this source.

Gas Turbulence

It must be remembered that powder gas is relatively opaque to radiation coming from considerable depths in consequence of the high mass emissivities k, as given by equation (41). As a result, the radiation characteristics measured are those of a relatively thin layer of gas near the window, which may not be representative of the bulk of the powder gas insofar as its temperature is concerned because of cooling by the walls, and uneven turbulence.[44] The effect of turbulence is strikingly demonstrated in Figure 22. It is largely responsible for the individual minor variations of the observed temperature presented by Figure 19. It is likewise responsible for the lack of strict reproducibility of temperature in guns; thus, when the radiation in the 3-in. gun was observed simultaneously at two diametrically opposed holes in the positions 1, 2, or 3 in a firing, only the major variations in temperature were found common to both, the minor fluctuations differing by as much as 100 K at any instant.[65]

Temperature Gradient

The observational difficulties pointed out here may, similarly, make the apparent gradient of temperature between the chamber and bore of a gun greater than the real gradient associated with gas flow and heat transfer in the gas and between the gas and the walls.

Chapter 3

INTERIOR BALLISTIC CALCULATIONS

By *William S. Benedict*[a]

3.1 INTRODUCTION

THE SUBJECT of interior ballistics, interpreted broadly, would include all the phenomena that take place inside a gun when it is fired. In the more limited sense with which this chapter is concerned, interior ballistics calculations are those systematized mathematical methods whereby the motion of the projectile in the gun is related to the state of the powder and its gaseous products of burning, and to the design of the gun. More specifically it is concerned with the following variables: the travel of the projectile, L, the velocity of the projectile, V, the pressure of the powder gas, P, the temperature of the powder gas, T, and the time, t. These depend upon the dimensions of the gun: its chamber volume, v_c, its bore diameter, D, its length, X_m; upon the projectile: its weight, M, and reaction with the bore; upon the powder: its weight, C, chemical composition, and granulation; and upon other factors, such as ignition and the temperature of both the gun and the powder.

We may mention some of the practical reasons why the entire course of these variables should be known. The muzzle velocity is one of the most important properties of a gun, and should be accurately reproducible. The pressure-travel curve must be known both in order to design a gun of the minimum weight that will not burst and also in order to determine whether it is safe to use a prospective powder in an existing gun. The pressure-time and temperature-time data must be known in considering gas-operated rapid-fire devices, and in making calculations for recoilless guns. The temperature plays an important role in understanding the thermal and chemical processes causing erosion. The pressure and temperature at the muzzle affect the blast and flash.

The ultimate aim of interior ballistic theory must be to make predictable in every detail the outcome of firing any designated gun with any designated ammunition. In view of the large number of variables involved—and we have not named them all—this aim is not likely to be achieved. More modestly, however, we may hope to so reduce the problem, with the aid of reasonable assumptions and approximations, that the art of gun operation and design is based securely on scientific fact.

A historical survey of the development of interior ballistic theory falls beyond the scope of this chapter. A good summary of the earlier advances is given in Cranz's textbook.[144,505] Methods used by the Army and Navy in recent years are described in the Service textbooks.[509,515,520] There have been two main lines of approach. In one, the theoretical, the aim is to base the largest possible number of relations upon the general laws of physics and upon independently determined properties of the powder and gun. In this way a complete prediction might be made without firing a shot. In the second, or empirical, approach, the observed pressure-travel-velocity relations for various guns firing various charges are correlated so as to give a good representation of the overall process, without inquiring into the detailed mechanism. Such tables as those of Le Duc,[509,515] Röggla,[180] and Bennett[553] result from the second approach; these are highly useful in predicting the behavior of the conventional types of guns and powders, firings of which were used in compiling the tables.[18]

In making a fundamental attack on the problems of hypervelocity and gun erosion, the first approach is obviously to be preferred. The various interrelated physical processes are to be given the mathematical expression that is in best accord with present-day theoretical and experimental knowledge. The resulting set of equations is then to be solved, with the aid of simplifying assumptions, and approximations, in as general a manner as possible. The dependence of the variables of interest upon a large number of parameters is thus obtained.

A formalized method of setting up and solving the equations is referred to as a system[b] of interior ballis-

[a] Geophysical Laboratory, Carnegie Institution of Washington, and National Bureau of Standards.

[b] The system was developed in a series of formal Division 1 reports (listed in the bibliography as items 26, 30, 33, 35, 37, 55, 66), later consolidated and revised into a single report.[69] During the same period of time improvements[353,354,374] made in the standard British system of ballistics[431] caused it to have some of the same advantages as the Division 1 system. At Aberdeen Proving Ground, interest in ballistic systems has been directed lately toward the development of functions to be used with a differential analyzer.[654]

tics. Such a system has been developed at the Geophysical Laboratory as a part of the Division 1 program. For brevity we shall refer to this formulation as the Division 1 system.[c] Although work of this nature does not lend itself readily to summarization, we attempt in this chapter to state the fundamental principles and chief achievements of the Division 1 system, with emphasis upon the physical content rather than the mathematical details. Frequent references are made to equations and tabular matter that cannot be reproduced here, for which the interested reader must consult the original papers, particularly the consolidated report.[69]

There is nothing radically novel in the Division 1 system; its advantage over previous systems consists primarily in the large number of factors given explicit consideration, and related a priori to the powder composition. Naturally the use of a large number of parameters leads to rather complicated expressions. In its complete form the Division 1 system has been aimed toward accuracy and flexibility rather than convenience. For certain applications, on the other hand, ease of use has been achieved by the excision or limitation of variables; and it has been possible to prepare various sets of tables that greatly reduce the difficulty of solving many types of problems.

3.2 THE FUNDAMENTAL EQUATIONS OF INTERIOR BALLISTICS

3.2.1 The Basic Processes

What happens in a gun? The charge, consisting of a number of small nearly identical grains of smokeless powder, of a definite geometrical shape, is ignited. The solid powder liberates gas at a high temperature, T_0, and a definite rate, dN/dt, that depends on the pressure, P. The pressure in turn depends on the quantity of gas, N, its temperature, T, and the available volume, v, which is initially the volume of the chamber, v_c, less the volume of the solid powder C/ρ. The pressure exerted on the base of the projectile causes the projectile of mass M/g to move down the bore with a velocity V, thus increasing the volume. The energy acquired by the moving projectile $MV^2/2g$, as well as heat lost to the walls of the chamber and bore, comes from the powder gas, thus decreasing its temperature. The pressure increase due to burning of powder to gas is opposed by the two effects just mentioned, and a maximum pressure is attained, usually when the volume has about doubled. Thereafter the pressure falls, slowly at first, then more rapidly after the powder is completely burned. The projectile velocity continues to increase, but at a decreasing rate, until it reaches the muzzle.

There are thus four relationships among the variables that are of fundamental importance. These are: (1) the equation of motion of the projectile, relating its velocity and position to the gas pressure; (2) the equation of energy, relating the velocity to the gas temperature and quantity; (3) the equation of state, relating the gas pressure, temperature, quantity, and volume; (4) the equation of burning, relating the gas quantity and the pressure.

Figure 1 attempts to portray schematically the nature and interrelation of these four fundamental equations. Of the six variables portrayed, only five are independent, the gas volume being linked to the projectile position and quantity of gas (or solid powder). We might also consider the time as a primary variable in place of the projectile position or velocity. By combining the four fundamental equations among the five variables, it is possible to arrive at a single equation between two variables. It is found most convenient to use the velocity as the primary independent variable. In the following sections we will state the four fundamental equations in their most general form, and then indicate how, with the aid of certain assumptions and approximations, these are cast into a form suitable for combining into the single equation, and the nature of the solution of that equation, in the Division 1 system.

3.2.2 The Equation of Motion

The equation of motion is Newton's law, which states that the acceleration of the projectile times its mass equals the net force exerted upon it. The accelerating force is the difference between the pressure exerted by the gas on the base of the projectile, P_X, and the retarding pressure due to friction, P_r, multiplied by the area of the bore, A. The acceleration of motion may thus be put in the form of equation (1).

$$(P_X - P_r)A = \frac{MV}{g}\frac{dV}{dX}. \qquad (1)$$

In the succeeding equations we are less concerned with P_X than with P, the average pressure of the

[c] This system has been familiarly referred to as the "Hirschfelder System" after Dr. J. O. Hirschfelder, who was in charge of the group that developed it.

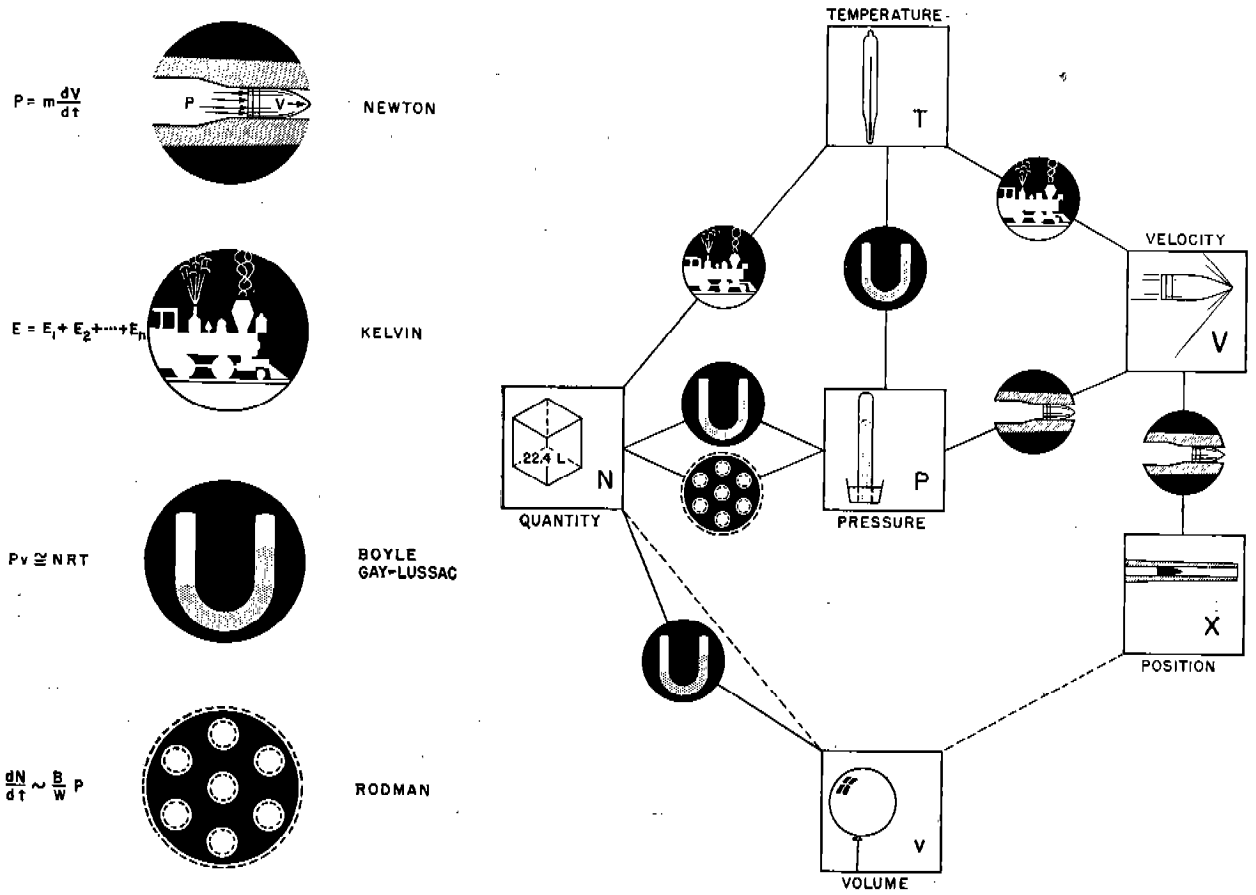


FIGURE 1. The four fundamental equations of interior ballistics are interrelated by the properties of the powder gases and by the velocity and position of the projectile.

powder gas. These are not identical, because a pressure gradient will develop in a column of gas of which one end (at the breech) is stationary, and the other (at the projectile) is accelerated. In a gun there may also be pressure waves due to irregular ignition. A complete solution of the problem of pressure and energy distribution of the powder gas moving in a gun according to the laws of hydrodynamics has not been found.[69,113] The theory due to Kent,[500] which must be a good approximation to the truth after the projectile is well advanced in the bore, and which has experimental confirmation (Section 6.2.4), relates the pressure drop to the ratio of the weight of charge to that of the projectile through equation (2).

$$P = P_X \frac{(M + C/\delta)}{M} \tag{2}$$

The factor δ, depending on C/M, is very close to 3 except for hypervelocity guns. Although equation (2) may not be exact in the early stages of projectile motion, both because of the approximate nature of the Kent theory and the increased importance of ignition pressure waves at that period, it is the best available relation and is incorporated in the Division 1 system.[26]

The other uncertain term in equation (1), the friction P_r, is discussed in more detail in Chapter 6, in which equation (1) is a variant of equation (1) of Chapter 3. It is there pointed out that P_r is in general not a simple function of any principal variable. It is, however, large compared to P_x only at the start of motion when the projectile is being engraved; thereafter it is comparatively small. The assumption expressed by equations (3a) and (3b) is, therefore, made in the Division 1 system (and generally in other systems). In these equations

$$P_r = P_X (P_X < P_0), \tag{3a}$$

$$P_r = \frac{c}{1 + c} P (P_X > P_0), \tag{3b}$$

c, a constant of the order of 0.04, and P_0, the starting

pressure, are adjustable parameters of the particular firing in question.

With these approximations, and defining m, the effective mass of the firing, by

$$m = (M + C/\delta)\frac{(1+c)}{g}, \tag{4}$$

the equation of motion may be put in the form

$$P = \frac{mV}{A}\frac{dV}{dX}. \tag{5}$$

3.2.3 The Equation of Energy

The equation of energy is simply the law of conservation of energy, as applied to the interior ballistic process, as expressed in equation (6).

$$E_{\text{rel}} = \frac{MV^2}{2g} + E_g + E_f + h. \tag{6}$$

The individual terms in this equation are discussed below.

1. The first one, E_{rel}, is the energy released when the burned powder gas cools from its adiabatic "flame temperature" T_0 (defined in Section 2.4.3 as the temperature that would be attained if all the energy of the chemical rearrangement was expended in heating the powder gas) to the actual temperature T, which is lower than T_0 because energy is expended in the processes summarized by the terms on the right-hand side of equation (6). The dependence of E_{rel} on the chemical composition of the powder, and on the density, state of chemical equilibrium, and temperature of the gas, has been discussed in outline in Section 2.4. Calculations of the type described and illustrated there show that E_{rel} is nearly independent of density and nearly a linear function of T. In the Division 1 system these approximate properties are assumed to hold generally, which leads to equation (7),

$$E_{\text{rel}} \equiv N\int_{T}^{T_0} C_v dT = \frac{NF}{\gamma - 1}\left(1 - \frac{T}{T_0}\right), \tag{7}$$

in which F, the "impetus" (called "force" in most earlier ballistic systems), is defined as nRT_0, n being the number of moles of gas generated per unit weight of powder, and R the gas constant. The ratio of specific heats $\gamma \equiv C_p/C_v$, is defined as nR/C_v.

2. Of the expended energy terms, $MV^2/2g$, the kinetic energy of the projectile, is the largest. The energy of rotation of the projectile and of recoil of the gun are proportional to it, and relatively small, and may be included by adjusting M.

3. E_g is the kinetic energy of the powder and powder gas. Its exact value is slightly uncertain. A good approximation is given by equation (8), which is based on the same Kent solution for the motion of the powder gas that leads to the assumed pressure distribution.

$$E_g = \frac{CV^2}{2g\delta}. \tag{8}$$

4. E_f is the energy expended in overcoming friction. Under the assumptions (3) for the friction, it is given by equation (9).

$$E_f = \int P_r dX = \frac{c}{1+c}\int P dX \leqq \frac{(M + C/\delta)c}{2g}V^2. \tag{9}$$

5. h is the energy lost as heat, principally by forced convection from the gas, to the walls of the chamber and bore. It is discussed in detail in Section 5.2. The theoretical analysis of the problem leads to the result that h is approximately proportional to the travel L, which in turn is nearly proportional to the kinetic energy. Hence the assumption is made that the heat loss is proportional to the kinetic energy,

$$h = \beta\frac{mV^2}{2}. \tag{10}$$

Defining the effective ratio of specific heats, $\bar{\gamma}$, by equation (11),

$$\bar{\gamma} - 1 = (\gamma - 1)(1 + \beta), \tag{11}$$

incorporating the assumptions of equations (7) to (10) into equation (6), and remembering the definition in equation (4), the energy equation becomes

$$NF\left(1 - \frac{T}{T_0}\right) = \tfrac{1}{2}(\bar{\gamma} - 1)mV^2. \tag{12}$$

3.2.4 The Equation of State

The equation of state of powder gas is discussed in Section 2.4.2. Again, it is necessary to recast the equation (10), developed there as the most accurate equation, into a form more suited to ballistic calculations. The Abel equation (13)

$$P\left(\frac{1}{\Delta} - \eta\right) = nRT = \frac{FT}{T_0}, \tag{13}$$

is the same as equation (10) of Chapter 2 except that only one of the virial coefficients is retained. In the ballistic equation the covolume η is considered to be independent of density and temperature, and is set

approximately equal to $0.9b'$ in order to compensate for the effect of the higher terms in b' at the average density prevailing in guns,[69,113] 0.2 g/cm³ = 0.0072 lb/in.³.

The density Δ depends on the weight of gas N, the weight of charge C, the density of solid powder ρ, the chamber volume $v_c = AX_0$, and the position of the projectile, $X = X_0 + L$, as expressed by

$$\Delta = \frac{N}{AX - (C - N)/\rho}. \tag{14}$$

Defining the loading density $\Delta_0 \equiv C/v_c$, and the term $a \equiv (\eta - 1)/\rho$, the equation of state becomes

$$Pv_c\left(\frac{X}{X_0} - \frac{\Delta_0}{\rho} - \frac{a\Delta_0 N}{C}\right) = \frac{NFT}{T_0}. \tag{15}$$

3.2.5 The Equation of Burning

The laws governing the burning of propellants are discussed in Section 2.2.3. It is assumed that each surface of each grain is ignited simultaneously, and that the burning of each surface proceeds normal to the surface, at a rate dependent on the average pressure. As a consequence, the fraction of powder burned, N/C, is related to the fraction f of the original web thickness W remaining unburned. The relation, known as the form function, depends solely on the geometry of the grain. It may in general be approximated by a quadratic function (16).

$$\frac{N}{C} = k_0 - k_1 f + k_2 f^2. \tag{16}$$

In the simplest case (sheet, long strips, or long single-perforated grains) of constant-burning-surface powder, $N/C = 1 - f$. In our derivation of the equations we shall confine ourselves to this case, although the equations for grains of any shape have been worked out in the Division 1 system. With seven-perforated powders, it is necessary to use two sets of constants k, the first until splintering occurs, the second to describe the burning of the splinters.

The experimental evidence adduced in Section 2.2 led to equations (17a and b) for the pressure-dependence of the burning rate:

$$-W\frac{df}{dt} = a + bP, \tag{17a}$$

or

$$-W\frac{df}{dt} = BP^n. \tag{17b}$$

The value of the exponent n in equation (17b) is from 0.8 to 0.9. Neither equation (17) can be fitted into a ballistic system without great computational difficulties. Accordingly in the Division 1 system equation (17b) is used, with $n = 1$. The equation of burning, for constant-burning-surface powder, thus becomes

$$\frac{dN}{dt} = \frac{CBP}{W}. \tag{18}$$

3.2.6 The Fundamental Equation and Its Solution

The four fundamental equations, in their simplified forms, equations (5), (12), (15), and (18), may now be combined. There will be different equations for the interval of burning, when $N < C$; and after burning is complete, when $N = C$, and equation (18) no longer is needed.

Interval of Burning

During the interval of burning, we first combine equations (5) and (18), and integrate, obtaining equation (19).

$$N = N_0 + \frac{Cm}{A}\frac{B}{W}V. \tag{19}$$

The constant of integration N_0 is the quantity of powder burned at the time of start of projectile motion; by the definition (3a) and the equation of state (15) it depends on the starting pressure P_0 according to equation (20).

$$N_0 = \frac{P_0 v_c(1 - \Delta_0/\rho)}{F + aP_0}. \tag{20}$$

By simple linear substitutions we may now eliminate P, T, and N from equations (5), (12), (15), and (19), leaving the fundamental ballistic equation (21) for the interval of burning (for the case of constant burning surface).

$$\frac{\bar{\gamma} - 1}{2} mV^2 = FC\frac{N_0}{C} + \frac{mB}{AW}V - \frac{v_c m}{A}\frac{X}{X_0} - \Delta_0\left(\frac{1}{\rho} + \frac{aN_0}{C} + \frac{amBV}{AW}\right)V\frac{dV}{dX}. \tag{21}$$

This is a differential equation in which the velocity V is the independent variable and the position of the projectile X the dependent variable. All the other quantities that enter into the equation are constants of the firing. Its solution is facilitated by introducing the following abbreviations, z, y, q, and r, expressed by equations (22) to (25).

1. Z, a dimensionless variable proportional to the velocity:

$$Z \equiv \frac{A}{FC}\frac{W}{B}V. \tag{22}$$

2. y, a dimensionless variable related to the travel:

$$y \equiv \frac{X}{X_0} - \Delta_0\left(\frac{1}{\rho} + \frac{\alpha N_0}{C}\right) \equiv \frac{X}{X_0} - \alpha. \tag{23}$$

3. q, a dimensionless parameter related to the starting pressure:

$$q \equiv \frac{A^2N_0}{FC^2m(B/W)^2}. \tag{24}$$

4. r, a dimensionless parameter related to the gas imperfection:

$$r \equiv \Delta_0 FCm(B/AW)^2\alpha. \tag{25}$$

With these abbreviations, equation (21) becomes

$$\frac{dy}{dZ} = \frac{Z(y - rZ)}{q + Z - \frac{1}{2}(\bar{\gamma} - 1)/Z^2}. \tag{26}$$

The solution of this linear differential equation is

$$y = J(1 - \alpha) + r(Z - S), \tag{27}$$

where

$$J = \exp\int_0^Z \frac{ZdZ}{q + Z - \frac{1}{2}(\bar{\gamma} - 1)/Z^2}. \tag{28}$$

and

$$S = J\int_0^Z \frac{dZ}{J}. \tag{29}$$

The integrals J and S have been evaluated numerically and tabulated[69] for a large range of the parameters q and $u = \frac{1}{2}(\bar{\gamma} - 1)$, and for closely spaced values of the independent variable, the reduced velocity Z. In addition, closed expressions have been given by which they may be calculated for other values of the parameters.

The other variables during the interval of burning are related in a straightforward manner to the variables Z and y, the tabulated functions J and S, and the parameters r, s, and u. They are:

The travel

$$L = \frac{v_c}{A}[y + \alpha - 1] = \frac{v_c}{A}[(J - 1)(1 - \alpha) + r(Z - S)]; \tag{30}$$

the pressure

$$P = \frac{m}{v_c}\frac{C^2F^2}{A^2}\left(\frac{B}{W}\right)^2 Z\frac{dZ}{dy} = \frac{m}{v_c}\frac{C^2F^2}{A^2}\left(\frac{B}{W}\right)^2 \frac{q + Z - uZ^2}{J(1 - \alpha) - rS}. \tag{31}$$

the velocity

$$V = \frac{FC}{A}\frac{B}{W}Z; \tag{32}$$

the time since the start of motion

$$t = \frac{m}{v_c}\int_0^V \frac{dV}{P} = \frac{mCF}{A^2}\frac{B}{W}\int_0^Z \frac{dZ}{P}; \tag{33}$$

the gas temperature

$$T = T_0\left(1 - \frac{uZ^2}{q + Z}\right); \tag{34}$$

and the fraction burned

$$\frac{N}{C} = \frac{N_0}{C} + \frac{mBV}{AW} = \frac{N_0}{C} + \frac{mFC}{A^2}\left(\frac{B}{W}\right)^2 Z. \tag{35}$$

Equations (30) through (35) express all the variables in terms of the independent variable Z, which runs from zero to its value when all the powder is burned ($N/C = 1$); from equations (19) and (32) this is

$$Z_b = \frac{(1 - N_0/C)A^2}{mFC(B/W)^2} \tag{36}$$

All functions at the point of complete burning are denoted by the subscript b. The maximum pressure, usually reached before the end of the burning interval, occurs at the point

$$Z_p = \frac{1}{\bar{\gamma}}\left(1 + \frac{a}{F}P_p\right). \tag{37}$$

All functions at the point of maximum pressure are denoted by the subscript p. Although Z_p depends on the maximum pressure P_p, the term $(a/F)P_p$ is small compared to unity, so that equations (37) and (31) may readily be solved to find the maximum point and pressure. If the solution yields Z_p greater than Z_b it means that the maximum point occurs at Z_b.

Interval after Burning

The fundamental ballistic equation (38) for the interval after burning is derived by combining equations (5), (12), and (15):

$$\frac{\bar{\gamma} - 1}{2}mV^2 = FC - v_c m\left(\frac{X}{X_0} - \eta\Delta_0\right)V\frac{dV}{dX}. \tag{38}$$

Its solution, the velocity-travel relation, is

$$V^2 = \frac{2FC}{(\bar{\gamma}-1)m}\left[1 - Q\left(\frac{X}{X_0} - \eta\Delta_0\right)^{1-\bar{\gamma}}\right]. \quad (39)$$

in which Q, the constant of integration, depends on the velocity and position at the point of complete burning, as expressed by equation (40),

$$Q = \left[1 - \left(\frac{\bar{\gamma}-1}{2}\right)\left(1 - \frac{N_0}{C}\right)Z_b\right]\left(\frac{X_b}{X_0} - \eta\Delta_0\right)^{\bar{\gamma}-1}. \quad (40)$$

The other variables in this interval are relatively simple functions of Q and X; as given by equations (41), (42), and (43):

$$P = F\Delta_0 Q\left(\frac{X}{X_0} - \eta\Delta_0\right)^{-\bar{\gamma}}, \quad (41)$$

$$t = t_b + \frac{v_c}{A}\sqrt{\frac{(\bar{\gamma}-1)X}{2CF}}\int_{X_b/X_0-\eta\Delta_0}^{X/X_0-\eta\Delta_0}(1 - Q\lambda^{1-\bar{\gamma}})^{-1/2}d\lambda, \quad (42)$$

$$T = T_0 Q\left(\frac{X}{X_0} - \eta\Delta_0\right)^{1-\bar{\gamma}}. \quad (43)$$

The values at the time the projectile reaches the muzzle, denoted by the subscript m, are readily obtained by using the above equations and the overall length of the gun, X_m.

3.2.7 Discussion of the Solution

Nature of the General Solution

The equations of the preceding section, together with the tables for J and S, permit the calculation of the complete ballistic solution for any gun using any powder of constant burning surface, in terms of the parameters F, $\bar{\gamma}$, η, ρ, Δ_0, T_0, P_0, m, B, and W. For powders of other granulation, the solution is functionally very similar, except that the additional parameters k_0, k_1, and k_2 are involved; with seven-perforated powders there are two sets of k's, the second being used in the additional burning period, that of the powder splinters, during which the fundamental velocity parameter varies from Z_b to Z_s. Because of the large number of parameters, and the complication of the equations, it is rather difficult to evaluate the importance of any one variable. The importance of each is to some extent brought out in succeeding sections; continued use of the system in various ballistic applications is, however, needed for full appreciation of the factors.

In Section 3.3 we present the suggested methods whereby numerical values of the parameters may be obtained. In Section 3.4 are given methods whereby, by limitation of some of the parameters to their most usual numerical values, the influence of other parameters, which depend upon the choice of the gun dimensions and powder type, may be more clearly seen. These are illustrated by numerical examples. In Section 3.5 are given some applications of these simplified methods to problems of design of hypervelocity guns.

Simplest Possible Particular Case

We may point out here how the solution in the burning interval becomes particularly simple if two additional restrictions are made on the parameters: (1) If the covolume of the powder gas equals the specific volume of the solid powder (about 17 in.^{3}/lb), the constant a and its associated parameter r equal zero. This results in the elimination of the integral S from the solution; (2) if the starting pressure and its associated parameter q is zero, the integral J is much simplified, as expressed by equation (44).

$$J = (1 - uZ)^{-1/u}. \quad (44)$$

Under these conditions all velocity-travel, pressure-travel, and temperature-travel curves are alike, and their dependence on the gun and powder parameters can be more readily seen. In particular, we have equation (45) for the pressure-travel curve.

$$P = \frac{m}{V_c}\frac{C^2F^2}{A^2}\left(\frac{B}{W}\right)^2\frac{(1-y)^{-\frac{1}{2}(\bar{\gamma}-1)}y^{-\frac{1}{2}(\bar{\gamma}-1)}}{(\bar{\gamma}-1)/2(1-\eta\Delta_0)}. \quad (45)$$

The reduced volume at the time of maximum pressure is then dependent only on $\bar{\gamma}$, as given by equations (46) and (47):

$$y_p = \left(\frac{2\bar{\gamma}}{\bar{\gamma}+1}\right)^{2(\bar{\gamma}-1)}, \quad (46)$$

$$P_p = \frac{m}{V_c}\frac{C^2F^2}{A^2}\left(\frac{B}{W}\right)^2\frac{1}{1-\eta\Delta_0}\frac{(\bar{\gamma}-1)(\bar{\gamma}+1)}{4\bar{\gamma}^2(2\bar{\gamma}/\bar{\gamma}-1)^{2(\bar{\gamma}-1)}}. \quad (47)$$

Since the functions of $\bar{\gamma}$ in equations (46) and (47) do not vary greatly over the range of values of $\bar{\gamma}$ usually encountered, to this degree of simplification all pressure-travel curves are similar.

This much-simplified ballistics has been used in a number of Aberdeen Proving Ground reports[196,204] and was also used by Nordheim[48] in his calculations of the heating of guns, as described in Section 5.4.1.

TABLE 1. Nominal values of powder constants.

Powder	Pyro	FNH (85/10/5)	NH (87/10/3)	FNH-M2 (20% N.G.)	IMR (Small arms)
T_0 (K)	2320 + 7/W*	2480	2425 + 10/W	3560	2800
C_v (cal/g-deg.)	.3653 − .00022/W	.3456	.3520 − .00025/W	.3439	.3460
n (moles/g)	.0466 − .00007/W	.04482	.0461 − .0001/W	.03873	.04301
F (ft)	300,000 + 500/W	310,000	309,000 + 500/W	384,000	334,000
γ	1.252 − .0002/W	1.258	1.256	1.223	1.246
η (in.^{3}/lb)	29.70	30.57	30.49	26.95	29.32
ρ (lb/in.^{3})	.0560	.0567	.0571	.0596	.0578
α (in.^{3}/lb)	13.72	12.93	12.98	10.17	12.02

* (W = powder web in inches.)

3.3 EVALUATION OF THE PARAMETERS IN THE BALLISTIC EQUATIONS

3.3.1 Powder Constants

The powder parameters—the impetus ("force") F, the adiabatic flame temperature T_0, the ratio of specific heats γ, and the covolume η—are calculable from the chemical composition of the powder. The assumptions which make this distinctive feature of the Division 1 system possible (in earlier systems such constants were estimated from closed-chamber measurements) have been outlined in Sections 2.4.3, 3.2.3, and 3.2.4. In case the exact composition of a particular powder lot is not available, or in making general calculations, it is useful to have "nominal" values of the powder constants, based on the average composition of the particular type of powder in question. Table 1 presents such recommended values. Since the volatile and moisture content of certain powders varies with the web, the constant W enters into the results.

For a comparison of the approximate methods of calculation of powder parameters with more exact methods, and with experimental results, the original papers[6,23,24,43,113,116] must be consulted. Except possibly for times near ejection, when the gas composition is uncertain, the nominal parameters will be quite accurate.

3.3.2 Heat and Friction Losses

The parameters $\bar{\gamma}$, m, and P_0, which take into account the energy losses and travel delay due to heating of the gun and friction between projectile and bore, may not always be known a priori. If ballistic results on a given gun are available, it may be possible to adjust these parameters so as to obtain the best fit. A closer discussion of the processes of heat loss and friction, and of some typical numerical results, is given in Chapters 5 and 6. The following generalizations from these results may be used to estimate the parameters when no experimental knowledge is available.

The factor β, the ratio of heat loss (prior to ejection) to kinetic energy, which relates the effective $\bar{\gamma}$ to the true γ [equation (11)] is a function principally of the caliber of the gun, being lower for larger guns. It also increases with the flame temperature of the powder, and with the length of the gun. It, in general, decreases as the maximum pressure and muzzle velocity are increased by increasing the density of loading in an existing gun. Some typical theoretical values[48] are shown in Table 2.

TABLE 2. Theoretical values of ballistic heat loss, typical guns.*

Gun	Powder	β	$\bar{\gamma}$
Caliber .50	IMR	0.40	1.35
37-mm	FNH-M1	0.27	1.33
3-in.	FNH-M1	0.25	1.32
4.7-in.	FNH-M1	0.19	1.31
8-in.	FNH-M1	0.17	1.30
16-in.	FNH-M1	0.13	1.29

* The values of β have been taken from Table XXVII of NDRC Report A-262[48] and the values of $\bar{\gamma}$ have been computed from them by equation (11). (Compare Table 2 in Chapter 5, in which the total heat loss to the gun tube for these same guns is presented.)

The most recent experimental evidence (for the 37-mm and 3-in. guns at Carderock)[106] would indicate that the values of Table 2, and those given by the following formula [equation (48)] recommended in an early report,[30]

$$\beta = \frac{0.09(T_0 - T_s)^{4/3} CLD^{-4/3}}{\frac{1}{2} m V_m^2}, \qquad (48)$$

are from 10 to 25 per cent too high. For an average powder and an average caliber gun (from 37 mm to 5 in.), $\bar{\gamma}$ will be close to 1.30. This rounded value is

TABLE 3. Approximate values of burning rate constant, typical powders.

Powder	FNH-M1	NH	Pyro	IMR	FNH-M2
B (in. per sec/psi)	.00033	.00036	.00036*	.00040	.00050

* For W < .05 in.; W = .00034. When W > .05 in., W = .00042.

generally used in the construction of many tables in the Division 1 system, and in all following calculations of this chapter, unless otherwise specified. It may be used without introducing gross errors for all except the smallest caliber guns (caliber .50 or smaller).

The parameter P_0 cannot be directly correlated with its physical meaning of the starting pressure. The over-simplification of friction and of the burning law destroy the exact correspondence of P_0 with the results of static push tests, which may roughly be expressed as a function of caliber in accordance with equation (49),

$$P_0 = 2500\, D^{-1/3} \text{ psi}, \qquad (49)$$

which may be used if firing data are lacking.

It is also permissible to take a starting pressure corresponding to $N_0/C = .01$. The latter assumption is used in most of the following calculations of this chapter. When pressure-travel data are available, P_0 should be determined from them. In general, in addition to the variation with caliber, P_0 decreases with increased loading density and increased run-up of the projectile before engraving starts.

The parameter m, the effective mass, depends upon

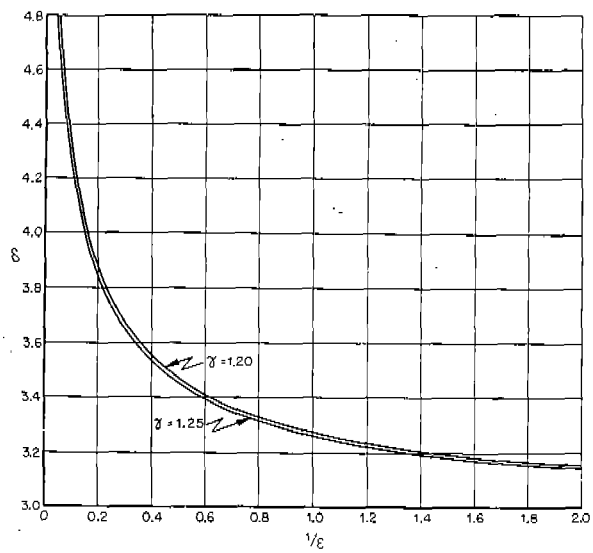


FIGURE 2. The dependence of δ on C/M. (This figure has appeared as Figure 15-2 in NDRC Report A-397)

two auxiliary parameters, the friction factor c, and the pressure-drop factor δ. Factor c may normally be taken equal to .04. It may be somewhat higher in high-velocity guns, and also when the velocity is reduced in normal guns by reduction of charge; and somewhat lower in shorter guns. Factor δ may be taken as 3 in all cases unless the ratio of charge to projectile weight exceeds 0.5; for very large ratios $\epsilon = C/M$ its variation is as shown in Figure 2, based on the Kent-Hirschfelder theory.

3.3.3 Burning Rates

The burning constant B is of prime importance in determining the maximum pressure, as is clear from equation (47). It is, however, difficult to correlate values of B determined from closed-chamber firings with those obtained in guns. Hence whenever possible B should be determined from the observed maximum pressure or muzzle velocity. Lacking such data the values of B presented in Table 3 may be used. These correspond to a P_p of the order of 40,000 psi and $N_0/C = .01$. For higher maximum pressures and starting pressures the nominal B decreases somewhat. B varies with the initial temperature of the powder; the tabulated values refer to 25 C. The average temperature coefficient dB/dT is about 0.004 per degree centigrade.

3.4 SIMPLIFIED NUMERICAL METHODS OF BALLISTIC CALCULATIONS

3.4.1 Construction of Tables

The solution of the ballistic equations, as given in Section 3.2, followed the happenings within the gun in logical sequence from the start of burning to shot ejection. In a very large number of ballistic problems, however, one final result, the muzzle velocity, and one intermediate occurrence, the maximum pressure, are the two quantities of greatest interest. These may either be given, as the most readily determinable measurements, or are the most important results to be calculated. It is therefore desirable to simplify the ballistic system in such a way that these two quanti-

ties may be most readily correlated with the other parameters. This entails some recasting of the equations. Then, by fixing certain of the parameters, tables may be constructed which facilitate the solution of all the principal equations.

A complete description of the methods is given in Chapters IV and V of Interior Ballistics Consolidated;[69] Tables III - XV of that report comprise the principal results. They are based on the following values of the parameters: *Heat loss*, $\bar{\gamma} = 1.30$ ($u = 0.15$); *Starting pressure*, $N_0/C = .01$; *Powder constants*, those given in Table 1 of the present chapter for nominal FNH-M1 powder (the tables may readily be adapted to other powders, since only the ratio F/a enters into the equations); *Granulation*, two cases are considered, (1) constant burning surface, (2) seven-perforated grains, with a ratio of grain length to diameter of 2.5, and grain diameter to perforation diameter of 10.

There are five fundamental parameters or auxiliary variables that enter into the simplified tables. These are:

1. The reduced velocity at the completion of burning,

$$Z_b = .99\frac{A^2}{CF}m\left(\frac{B}{W}\right)^2$$

(for constant-burning grains), (50a)

$$Z_s = 1.369\frac{A^2}{CF}m\left(\frac{B}{W}\right)^2$$

(for seven-perforated grains). (50b)

2. The pressure function:

$$P_0 = \left(\frac{F}{a}\right)_{M1}\cdot\frac{a}{F}P = 2.3969 \times 10^4\frac{a}{F}P. \quad (51)$$

3. The travel function:

$$\xi = \frac{a\Delta_0}{(X/X_0) - \eta\Delta_0}. \quad (52)$$

4. The density-of-loading function:

$$\phi = \frac{a}{(1/\Delta_0\ (-)\ 1/\rho)}. \quad (53)$$

5. The velocity function for the period after burning is complete

$$\Gamma(Z_b,P_p^0) = (1-.1485Z_b)\ \xi_b^{-0.3}. \quad (54)$$

In terms of these functions the velocity after burning, including the muzzle velocity, is

$$V^2 = \frac{CF}{.15m}(1 - \Gamma\xi^{0.3}). \quad (55)$$

Since q, r, and u have been fixed by assigning definite values to P_0, a, and $\bar{\gamma}$, the point of maximum pressure, Z_p, is a function only of the maximum pressure, as expressed by equation (56).

$$Z_p = \frac{1}{1.3}(1 + 3.4767 \times 10^{-6}P_p^0). \quad (56)$$

Hence the entire ballistic solution is fixed when P_p and either ϕ or Z_b is specified. For example, there is a relationship among the three principal variables for the constant-burning case, stated in equation (57).

$$\phi^{-1} = \frac{.99}{Z_bJ_p}\cdot\left[S_p + \frac{2.8763\times10^5(.0101Z_b + Z_p - .15Z_p^2)}{P_p^0}\right] \quad (57)$$

The simultaneous solution of equations (56) and (57) is given in tabular form, one variable being tabulated as function of pairs of arguments: $\phi(Z_b,P_p)$, $Z_b(\phi,P_p)$. The travel at the end of the burning period is given by equation (58).

$$\zeta_b^{-1} = J_b(\phi^{-1} - .01) - .99\frac{S_b}{Z_b}. \quad (58)$$

From this equation and equation (54) Γ, and hence V_m, is related to P_p, Z_b, and ϕ. Additional tables express Γ as a function of pairs of arguments. By an extension of these methods the pressure, velocity, and temperature may be found as functions of time as well as of travel of the projectile.

3.4.2 Generalized Pressure-Travel Curves

Equations (30) and (31) together give the pressure-travel curve for the interval of burning, parametrically in terms of Z, and are exact, but involve a number of constants. If, as in the preceding section, the constants N_0/C, $\bar{\gamma}$, and the powder constants η and ρ are fixed, the relation between the pressure, in terms of its ratio to the maximum pressure P/P_p, and the travel, in terms of the volume expansion ratio X/X_0, depends only on the loading density Δ_0 and the fundamental burning parameter Z_b. The latter moreover enters only in the less important terms q and r. Hence, if one substitutes in these terms for Z_b the value Z in the region of the pressure-travel curve from the maximum pressure to the completion of burning, and the value at the maximum, Z_p, for lower values of the travel, a family of pressure-travel curves are obtained which are approximately valid under all conditions, and which depend only on one parameter, the loading density.



The most applicable family of such curves, drawn for $\bar{\gamma} = 1.30$, $N_0/C = 0.01$, and the values of η and ρ characteristic of FNH-M1 powder (the curves are nearly equally valid for other powders) are shown in Figure 3. The loading density Δ_0 is in units of g/cm³. In order to use these curves the gun constants must be known, together with the values of P_p and Z_b; if the latter are not given with the problem, they may be determined from the loading density and muzzle velocity by the methods described in the preceding section. These curves apply up to the value X_b/X_0 corresponding to Z_b, when the burning period is complete.

In the region from X_b/X_0 to the muzzle, X_m/X_0, the pressure, relative to its value at X_b/X_0, is, according to equation (41) dependent only on Δ_0, $\bar{\gamma}$ and η being fixed. The general family of pressure-travel curves for this region, for the same values of Δ_0 as were used in Figure 3, are shown in Figure 4. They are applied by suitable vertical adjustment of the pressure axis to join with the curve from the burning interval at X_b/X_0.

3.4.3 Numerical Examples

The original reports describing the Division 1 system are liberally studded with numerical examples, in which each step in the solution of the various types of problems considered is worked out in detail.[d] We choose to illustrate the methods by calculations based on the 3-in. gun at Carderock, on which extensive ballistic measurements were made, as described in Chapter 4 and further discussed in Section 6.3.

The gun constants are:

$$A = 7.30 \text{ in.}^2; \; v_c = 223.1 \text{ in.}^3;$$
$$L_m = 126.2 \text{ in.}; \; M = 12.79 \text{ lb.}$$

The constants for NH powder were:

$$C = 4.02 \text{ lb}; \; T_0 = 2636 \text{ K}; \; F = 321{,}800 \text{ ft};$$
$$\eta = 30.06 \text{ in.}^3/\text{lb}; \; \rho = 0.0571 \text{ lb/in.}^3.$$

The web of the seven-perforated grain is 0.0355 in.; we shall carry out the simplified computation in which a constant-burning-surface grain is considered, with web W = 0.0452 in.

[d] In addition to the general reports listed in footnote b, separate reports were issued concerning the free-run-up of a projectile[29] and recoilless guns.[36] Also some features of the Division 1 system were used extensively by investigators in Section H of Division 3 in calculations of the ballistics of rockets.[163]

The following are the principal derived constants:

$$\Delta_0 = \frac{C}{v_c} = .01802 \text{ lb/in.}^3;$$

$$X_0 = \frac{v_c}{A} = 30.56 \text{ in.};$$

$$\frac{X_m}{X_0} = 1 + \frac{L_m}{X_0} = 5.1296;$$

$$a = \eta - \frac{1}{\rho}$$

$$= 12.54 \text{ in.}^3/\text{lb};$$

$$m = 1.04\frac{M + C/3.14}{g}$$

$$= 0.4548 \text{ lb-sec}^2/\text{ft} \text{ (assuming } c = .04).$$

First Computation. To calculate the burning constant B from the muzzle velocity $V_m = 2{,}700$ fps, using the assumptions and simplified method outlined in Section 3.4.1. From equation (53),

$$\phi = \frac{12.54}{(55.50 - 17.52)} = 0.3302. \tag{59}$$

From equation (52),

$$\zeta_m = \frac{12.54 \times .01802}{(5.1296 - 0.5417)} = 0.04925. \tag{60}$$

From equation (55),

$$\Gamma = \frac{1 - (.15mV_m^2/CF)}{\zeta_m^{0.3}} = 1.5189. \tag{61}$$

The value of P_p^0 corresponding to the above values of ϕ and Γ is located in Table VI of Report A-397; it is 35,420 psi. For the powder in question this gives, according to equation (51),

$$P_p = \frac{321{,}800P_p^0}{12.54 \times 23{,}969} = 37{,}920 \text{ lb/in.}^2. \tag{62}$$

The value of Z_b corresponding to the above values of P_p^0 and ϕ is located in Table IV of Report A-397; it is 1.0397.

From equation (50a)

$$B = W(.99A^2/CFm\,Z_b)^{1/2}$$
$$= .000420 \text{ in.}^3/\text{lb/sec}. \tag{63}$$

Second Computation. Using the value of B just derived, to calculate the complete ballistics, by the detailed methods of Section 3.2.6: By assumption, $u = 0.15$ and $N_0/C = 0.01$. From equation (23)

$$\alpha = .01802\,(1/.0571 + .125) = 0.3179. \tag{64}$$

From equation (24)

$$q = .01\,Z_b/.99 = 0.0105. \tag{65}$$



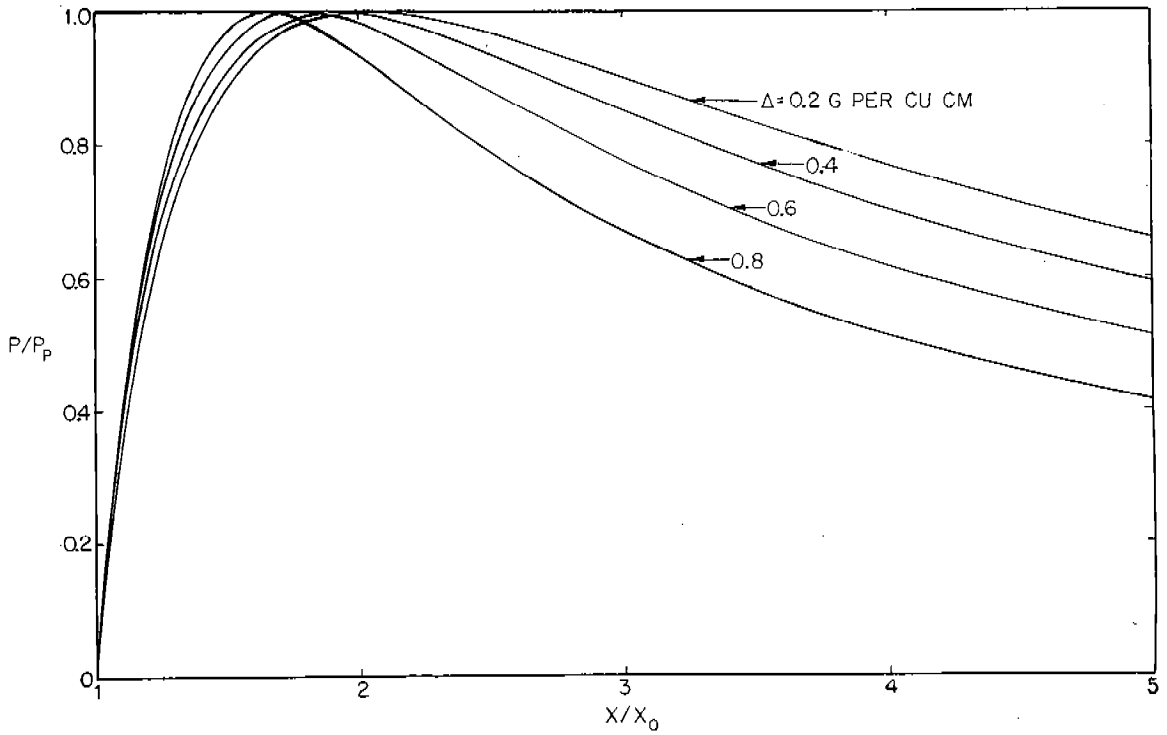


FIGURE 3. Generalized pressure-travel curves, interval of burning. (This figure has appeared as Figure 6-1 in NDRC Report A-397)

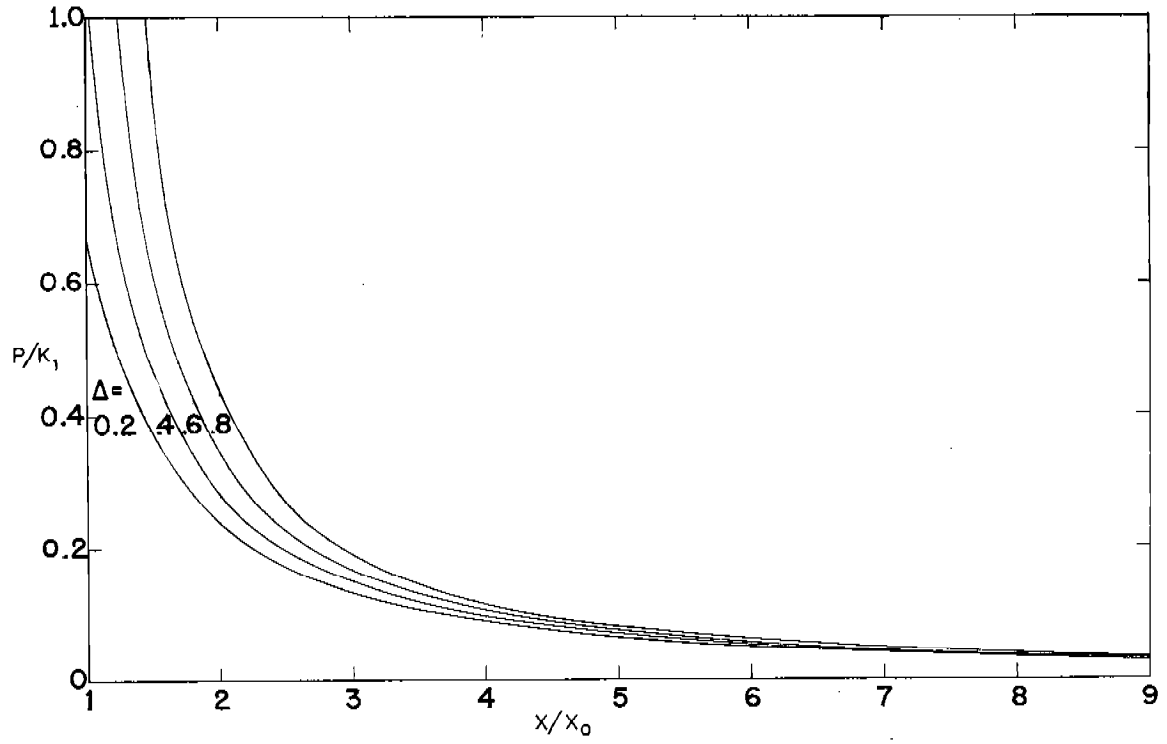


FIGURE 4. Generalized pressure-travel curves, interval after burning. (This figure has appeared as Figure 6-2 in NDRC Report A-397)



From equation (25)

$$r = .99a\Delta_0/Z_b = 0.2152. \quad (66)$$

The remainder of the computation is summarized in Table 4. The principal parameter in the burning interval, Z, runs from 0 to $Z_b = 1.0397$. In the afterburnt interval the principal parameter, X/X_0, runs from $X_b/X_0 = 2.1404$ to $X_m/X_0 = 5.1296$. The auxiliary parameter Q is found from equation (40),

$$Q = (1 - .1485\,Z_b)\,(2.1404 - 0.5417)^{0.3} = 0.9732. \quad (67)$$

The results, for the pressure, velocity, temperature, and fraction burned, are plotted against the time to the muzzle in Figure 5. The pressure and velocity are plotted against travel in Figure 6.

Third Computation. The detailed calculation is repeated, using the same values of B and the same parametric assumptions, except that the actual seven-perforated grain with W = .0355 in. is considered. Inasmuch as the equations for this case have not been presented in this chapter, we will give no details. The procedure is similar to that shown in Table 4, except that the first period ends with the splintering of the grains, at $Z_s = 0.8886$, $N/C = 0.8487$, and is followed by a second burning period. The results, as pressure-travel and velocity-travel curves, are shown in Figure 6.

It is not within the scope of this chapter to discuss the correspondence between such theoretical curves as those given in Figures 5 and 6 with the experimental findings, such as are illustrated in Figures 2 and 3 of Chapter 4. The agreement of the pressure-time curves is good but far from perfect, because the theoretical curves are based on fixed values of the parameters P_0, c, and $\bar{\gamma}$, and an oversimplified burning law. Further numerical comparisons of the Division 1 theory with ballistic experiments are given in two reports.[113,116]

3.5 INTERIOR BALLISTICS OF HYPERVELOCITY GUNS

3.5.1 Introduction

The equations and tables previously presented and discussed in this chapter are quite general. According to them, and to common sense considerations as well, for a gun of given caliber the muzzle velocity may be increased in a number of ways. We may increase the length X_m; increase the charge C; decrease the mass of the projectile M; or increase the impetus of the powder F.

In this section we present some of the contributions that the Division 1 system has made to the theory of design of hypervelocity guns. Three questions are considered. First, is there any theoretical limit to the

TABLE 4. Illustrative numerical example of complete ballistic calculation, 3-in. gun.*

Quantity—	Z	J	S	L	P	V	t	T	N/C
Units—				in.	klb/in.^{2}	ft/sec	msec	K	
				Interval (a)—Burning					
	0	1.0000	0.0000	0.00	1.01	0	0.00	2636	0.0100
	.1	1.0786	0.1044	1.62	10.06	165	2.53	2600	0.1052
	.2	1.1864	0.2198	3.78	17.66	329	3.31	2561	0.2004
	.4	1.4517	0.4908	8.88	28.74	658	4.19	2482	0.3909
	.6	1.7932	0.8291	15.14	35.03	987	4.83	2403	0.5813
	.8	2.2342	1.2567	22.89	37.47	1317	5.39	2324	0.7618
	1.0	2.8068	1.8036	32.63	37.05	1646	5.95	2245	0.9622
	1.0397	2.9399	1.9298	34.85	36.71	1711	6.06	2229	1.0000
Source—		Table	Table	Eq (30)	Eq (31)	Eq (32)	Eq (33)	Eq (34)	Eq (35)
	X/X_0			Interval (b)—After-burnt					
Source—					Eq. (41)	Eq. (39)	Eq. (42)	Eq. (43)	
	2.1404			34.85	36.71	1711	6.060	2229	
	2.5417			47.11	27.50	1993	6.614	2084	
	3.0417			62.39	20.58	2224	7.218	1949	
	3.5417			77.67	16.23	2385	7.771	1845	
	4.0417			92.95	13.29	2508	8.290	1762	
	4.5417			108.23	11.17	2605	8.788	1693	
	5.1296			126.20	9.35	2698	9.352	1624	

*The value of α used in calculating this table was 0.3134 instead of 0.3179 as given by equation (64).

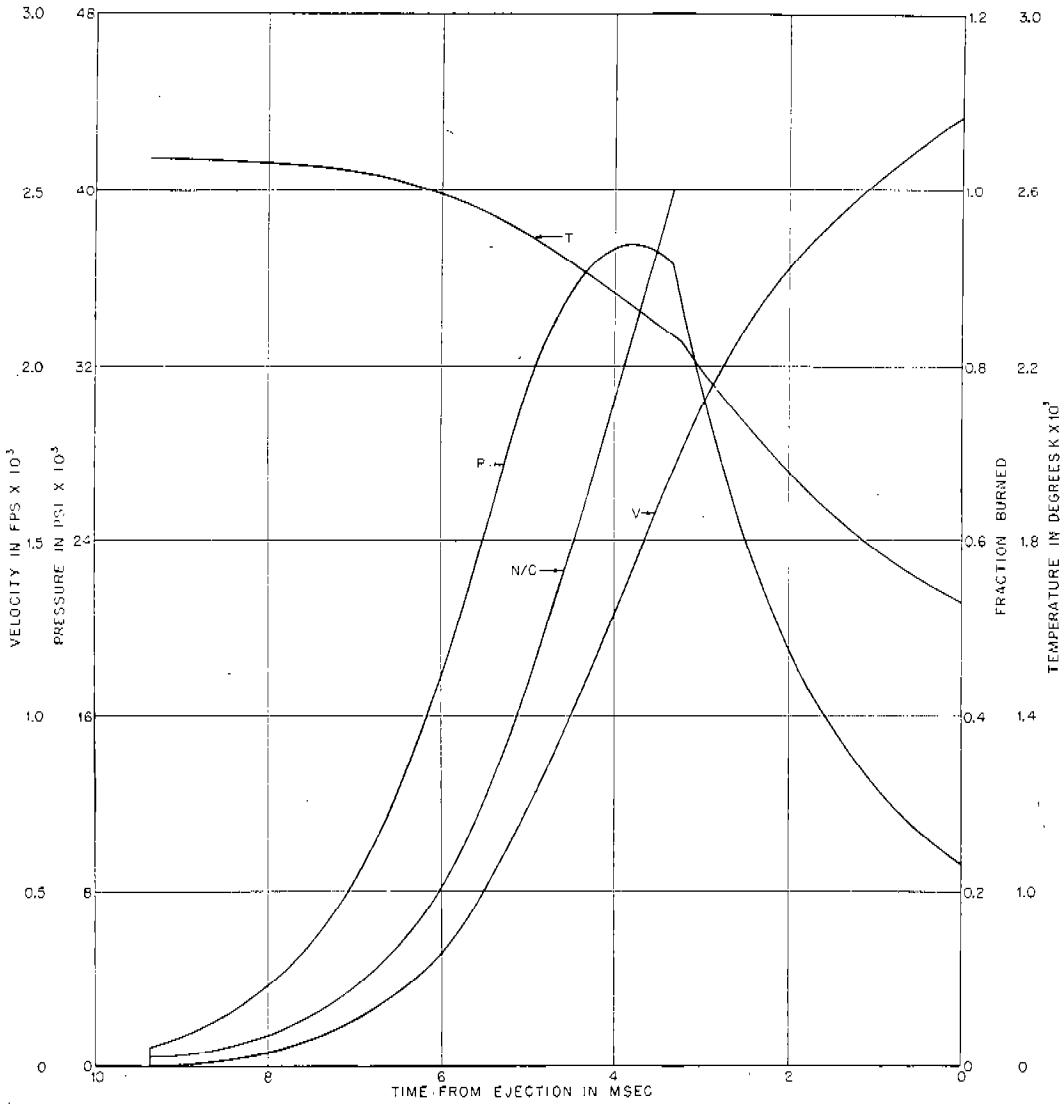


FIGURE 5. Theoretical ballistic curves, 3-in. gun at Carderock.

velocity that may be attained in a gun, laying aside all thought of practicality? Second, in a gun of given total volume firing a projectile of given weight, what are the theoretically optimum conditions to produce the maximum velocity? Finally, what practical considerations govern the use of modification of the theoretical optimum in gun design?

3.5.2 The Upper Limit to Muzzle Velocity

The existence of an upper limit to muzzle velocity is required, because as the charge-to-mass ratio (C/M) increases, the kinetic energy of the powder gas, $CV^2/2\delta g$, becomes large by comparison with the kinetic energy of the projectile, $MV^2/2g$. As may be seen from Figure 2, as C/M approaches infinity, δ approaches a finite limiting value, $(3\gamma - 1)/(\gamma - 1)$.

The equation for the muzzle velocity (39) may be rewritten as equation (68), where μ and s are defined by equations (69) and (70), respectively.

$$V_m^2 = \frac{200gF\Delta_0(1 - c)(1 - \Gamma\zeta_m^{\bar{\gamma}-1})}{(\bar{\gamma} - 1)(X_m/X_0)(\mu - s)}. \tag{68}$$

$$\mu = \frac{100M}{AX_m}. \tag{69}$$

$$s = \frac{100\Delta_0}{\delta(X_m/X_0)}. \tag{70}$$

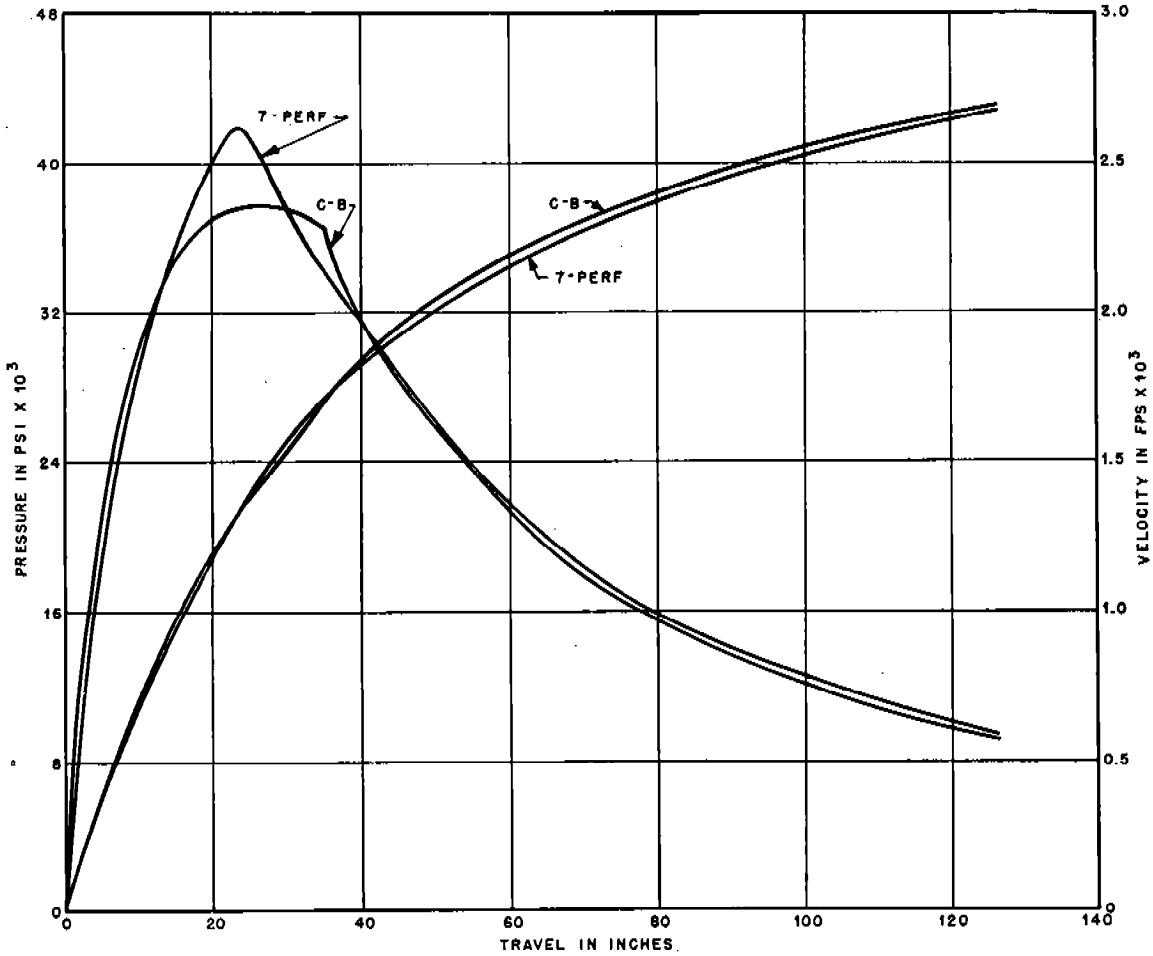


FIGURE 6. Theoretical pressure-travel curves, 3-in. gun at Carderock.

As M approaches zero, the muzzle velocity approaches the limit given by equation (71).

$$V_m^2 \longrightarrow \frac{2(1-c)gF\delta}{(\bar{\gamma}-1)}(1-\Gamma\zeta_m^{\bar{\gamma}-1}). \qquad (71)$$

Using the limiting value for δ, and considering the most favorable case of an infinitely long gun ($\zeta_m = 0$) with no friction or heat loss, the limiting muzzle velocity $V_{\lim}$ is expressed by equation (72).

$$V_{\lim} = \frac{[2gF(3\gamma-1)]^{1/2}}{\gamma-1}. \qquad (72)$$

Equation (73),[26] shows the relation between the limiting velocity for a projectile and V_s, the velocity of sound in the gas at the adiabatic flame temperature, which would be the velocity of efflux of a gas through an orifice into a vacuum.

$$V_{\lim} = \left[\frac{2(3\gamma-1)}{\gamma(\gamma-1)^2}\right]^{1/2} V_s. \qquad (73)$$

Assuming the F corresponding to FNH-M2 powder in equation (72) leads to a value of 36,400 fps for the limiting muzzle velocity. Friction and heat losses increase with increasing velocity to such an extent that the actual limiting muzzle velocity for even the hypothetical projectile of zero mass probably would not exceed 20,000 fps. For an actual gun firing a projectile of useful weight, of course, the possible velocity is much less.[498] (See Section 33.2.2.)

3.5.3 The Optimum Conditions

Considering equation (68) from a more practical angle, it will be observed that the muzzle velocity depends on μ, X_m/X_0, P_p, Δ_0, $\bar{\gamma}$, and the powder composition. The main problem in gun design is the determination of the best values of these quantities that will yield a desired muzzle velocity. It is clear that for any values of the other quantities, μ can be

chosen to give any velocity up to the impractically high limit. Tables[69] have been prepared, based on the simplified ballistic tables described in Section 3.4.1, that shows the values of μ required to give velocities up to 5,000 fps at various values of P_p, X_m/X_0, and Δ_0, for a typical single-base and a typical double-base powder of constant burning surface. An illustrative portion of the tables, for $V_m = 4{,}000$ fps, is reproduced as Table 5. The variation of μ with V_m is presented in Table 6. Figures 7 and 8 illustrate the dependence of the velocity on the loading density and on the volume ratio for various fixed values of μ.

The most efficient gun at a given velocity and caliber has the highest value of μ (greatest kinetic energy of projectile, least length of gun). Conversely, at a given μ it is desirable to maximize the muzzle velocity.

The optimum density of loading, $(\Delta_0)_1$, is therefore defined as the density of loading that gives the highest muzzle velocity for a given powder, at a preassigned value of the maximum pressure, projectile mass, and total gun volume. It is obtained by differentiating equation (68) with respect to Δ_0 and equating to zero. Since Γ, ζ_m, and s are all functions of Δ_0, the resulting equation is a complicated function of P_p, X_m/X_0, and $\mu/(\mu + s) = M/(M + C/\delta)$; it may be solved numerically. $(\Delta_0)_1$ has been computed and tabulated under the usual simplified ballistic assumptions. In a precisely similar manner, one defines and obtains the optimum volume ratio $(X_m/Z_0)_2$.

The double optimum, $(\Delta_0)_3$ and $(X_m/X_0)_3$, is defined as the combination of loading density and gun length that gives the maximum muzzle velocity for any given value of the maximum pressure, projectile mass, total gun volume, and powder type. It is obtained by

TABLE 5. Values of $\mu = \dfrac{100M}{A X_m}$ lb/in.^{3} for $V_m = 4.000$ fps.

Powder	FNH-M1			FNH-M2		
Δ_0, (g/cm^3)	0.6	0.7	0.8	0.6	0.7	0.8
X_m/X_3			P_p = 50,000 psi			
3	.6026	.6386	.5982*	.6744	.6641	.6126*
4	.6091	.6746	.6814	.7046	.7462	.6917*
5	.5716	.6431	6726	.6714	.7383	.7235
6	.5281	.5989	.6376	.6260	.6904	.7041
8	.4512	.5158	.5589	.5406	.6047	.6348
10	.3917	.4495	.4916	.4722	.5322	.5669
			P_p = 60,000 psi			
3	.6645	.7456	.7670	.7662	.8202	.7909*
4	.6508	.7464	.8049	.7666	.8523	.8799
5	.6025	.6961	.7635	.7173	.8087	.8585
6	.5523	.6404	.7085	.6620	.7318	.8096
8	.4677	.5440	.6071	.5652	.6466	.7066
10	.4039	.4705	.5274	.4905	.5633	.6203

* Powder not all burned when projectile leaves muzzle.

TABLE 6. Values of $\mu = \dfrac{100M}{A X_m}$ lb/in.^{3} for $P_p = 50{,}000$ lb/in.^{3} and $X_m/X_0 = 5$.

Powder	FNH-M1			FNH-M2		
Δ_0, (g/cm^3)	0.6	0.7	0.8	0.6	0.7	0.8
V_m (fps)						
1,500	4.8594	5.5005	5.8426	5.5688	6.1204	6.2046
2,000	2.6766	3.0277	3.2106	3.0756	3.3764	3.4143
2,500	1.6662	1.8831	1.9924	1.9215	2.1063	2.1227
3,000	1.1174	1.2613	1.3306	1.2947	1.4163	1.4211
3,500	0.7864	0.8865	0.9316	0.9167	1.0003	0.9981
4,000	0.5716	0.6431	0.6726	0.6714	0.7383	0.7235
4,500	0.4244	0.4763	0.4951	0.5032	0.5452	0.5353
5,000	0.3190	0.3570	0.3681	0.3829	0.4128	0.4006



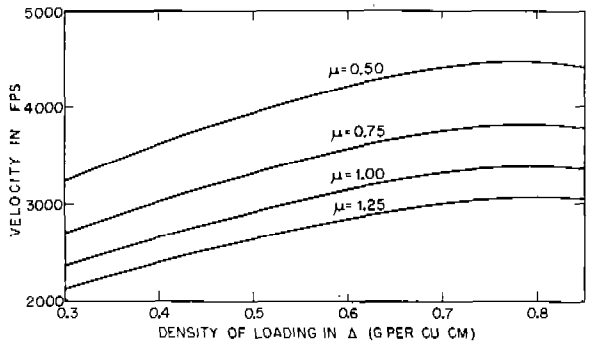


FIGURE 7. Curves of velocity versus density of loading at constant μ for $X_m/X_0=5$ and $P_p=50{,}000$ psi. (This figure has appeared as Figure 7-5 in NDRC Report A-397.)

TABLE 7. Conditions for the double optimum.

Powder	FNH-M1		FNH-M2	
P_p (psi)	$(\Delta_0)_3$ (g/cm³)	$(X_m/X_0)_3$	$(\Delta_0)_3$ g/cm³	$(X_m/X_0)_3$
10,000	.284	4.70	.248	4.69
20,000	.465	4.27	.413	4.33
30,000	.594	3.93	.540	4.05
40,000	.689	3.66	.640	3.83
50,000	.764	3.45	.720	3.65
60,000	.823	3.29	.786	3.49

simultaneous solution of the maximizing equations for $(\Delta_0)_1$ and $(X_m/X_0)_2$. The double-optimum density is independent of the muzzle velocity, but $(X_m/X_0)_3$ is weakly dependent on V_m. Some values of the double optimum are listed in Table 7; the values of X_m/X_0 are the limiting values at $V_m = 0$. The values of the mass/volume parameter μ that correspond to these double-optimum conditions, in the hypervelocity range 3,000 to 5,000 fps are listed in Table 8.

It must be emphasized that the calculations leading to these theoretically optimum conditions are based upon the simplified ballistic assumptions of Section 3.4. They serve therefore only as an orientation to the approximate dimensions to choose in seeking the best design. They must be modified by practical considerations long familiar to the gun designer, as is outlined in the next section. After deciding upon the approximate optimum dimensions, calculations by the detailed ballistics may be made, and further tested for the optimum conditions, by the methods sketched here.

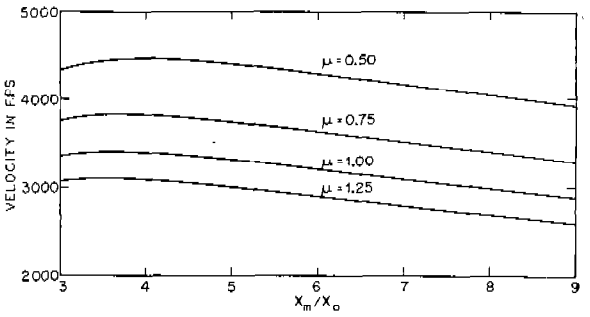


FIGURE 8. Curves of velocity versus X_m/X_p at constant μ for $\Delta_0=0.7$ g per cu cm and $P_p=50{,}000$ psi. (This figure has appeared as Figure 7-4 in NDRC Report A-397.)

3.5.4 Practical Considerations in the Design of Hypervelocity Guns

Limiting Density of Loading

There are various considerations that limit and modify the attainment in actual practice of the optimum conditions. It is clear from the tables of the preceding section that guns with higher maximum pressures, which lead to higher muzzle energies, are most efficiently operated at high loading densities. The loading density cannot, however, be increased indefinitely; it is limited by the density of solid powder and by the geometry of the grains and the chamber, to values near 1.0 g/cm³.

At such high densities it is, moreover, impossible to operate a gun with any degree of safety, because

TABLE 8. Values of $\mu = \dfrac{100M}{AX_m}$ lb/in.³ at the double optimum.

Powder	FNH-M1			FNH-M2		
P_p (psi)	40,000	50,000	60,000	40,000	50,000	60,000
V_m (fps)						
3,000	1.142	1.382	1.665	1.208	1.477	1.735
3,500	0.788	0.960	1.158	0.841	1.037	1.218
4,000	0.561	0.688	0.832	0.609	0.749	0.884
4,500	0.409	0.499	0.604	0.451	0.552	0.651
5,000	0.302	0.369	0.448	0.344	0.414	0.490

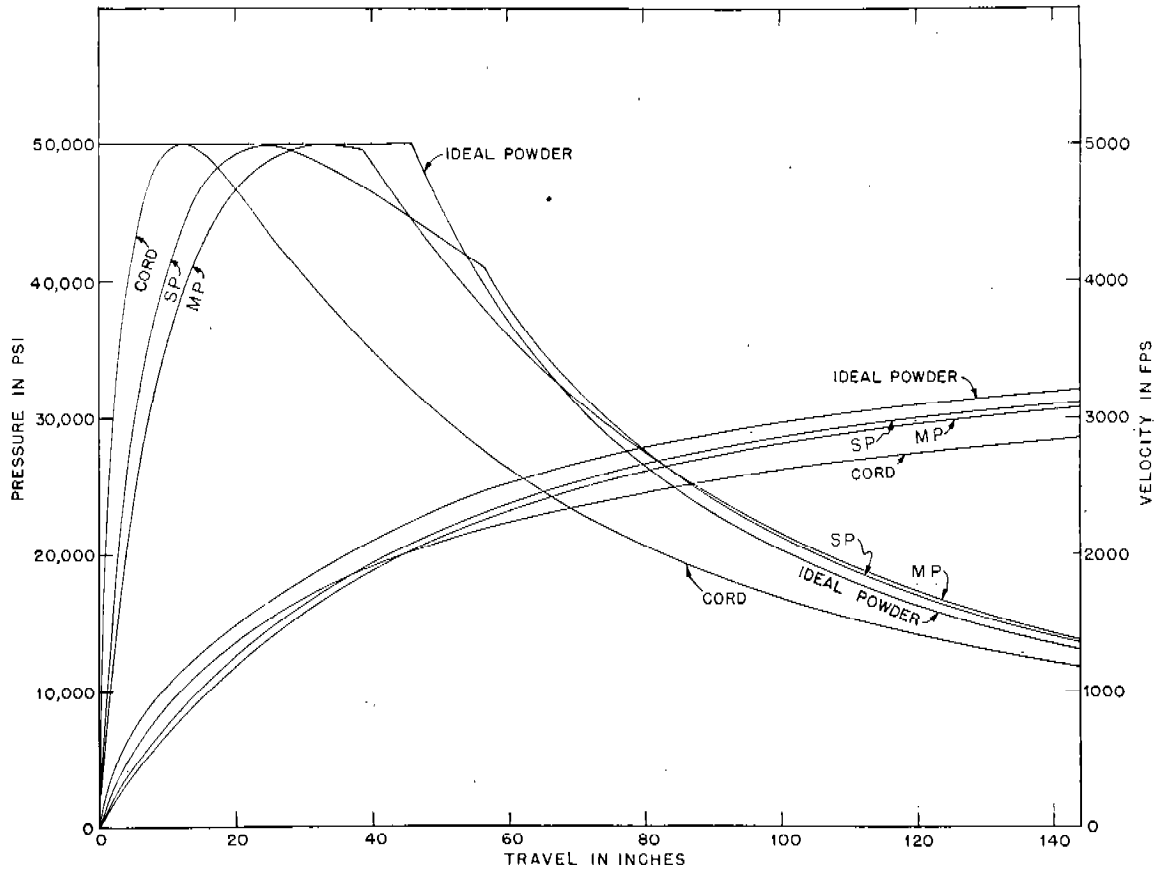


FIGURE 9. Pressure-travel and velocity-travel curves for various shapes of powder grains. (This figure has appeared as Figure 7-7 in NDRC Report A-397.)

when the free volume in the chamber is small, the pressure and velocity become very sensitive to small variations in the web, burning rate, or charge weight of the powder. Thus the changes in these properties that are inevitable in the processing of powder and its storage under field conditions may lead to unsafe variations in the pressure. Furthermore, at high loading densities pressure waves and other erratic results, usually attributable to ignition difficulties, are frequently encountered.

Hence the upper practical limit, using present-day powders and igniters, can rarely exceed 0.8 g/cm³ (except for small arms). This limit may be increased somewhat by improved methods of ignition, such as are provided by the use of long primers.

LIMITING PRESSURE

As mentioned above, an increase in the maximum pressure, limited by the safe strength of the gun, which in turn is limited by the properties of the gun metal and the tactical considerations that do not permit any superfluous bulk in weapons, is in general desirable. Equally important in attaining a high value of μ is an increase in the effective pressure, which is defined as the pressure on the base of the projectile averaged over the travel:

$$P_{\text{eff}} = \frac{6MV_m^2}{gAL} = \frac{.06V_m^2}{g(1 - X_0/X_m)}\mu. \qquad (74)$$

The ratio P_{eff}/P_p is a convenient measure of the efficiency of a gun. At a given density of loading the maximum P_{eff}/P_p occurs at the P_p that corresponds to the optimum density of loading. Higher pressures can be reached only if the pressure-travel curve has a peak near the origin of travel, and hence a comparatively low P_{eff}/P_p. It is therefore inefficient to use a maximum pressure much above that for which the loading density is optimum. Since at present this is limited as just mentioned to about 0.8 g/cm³, it is usually not desirable to aim for maximum pressures much

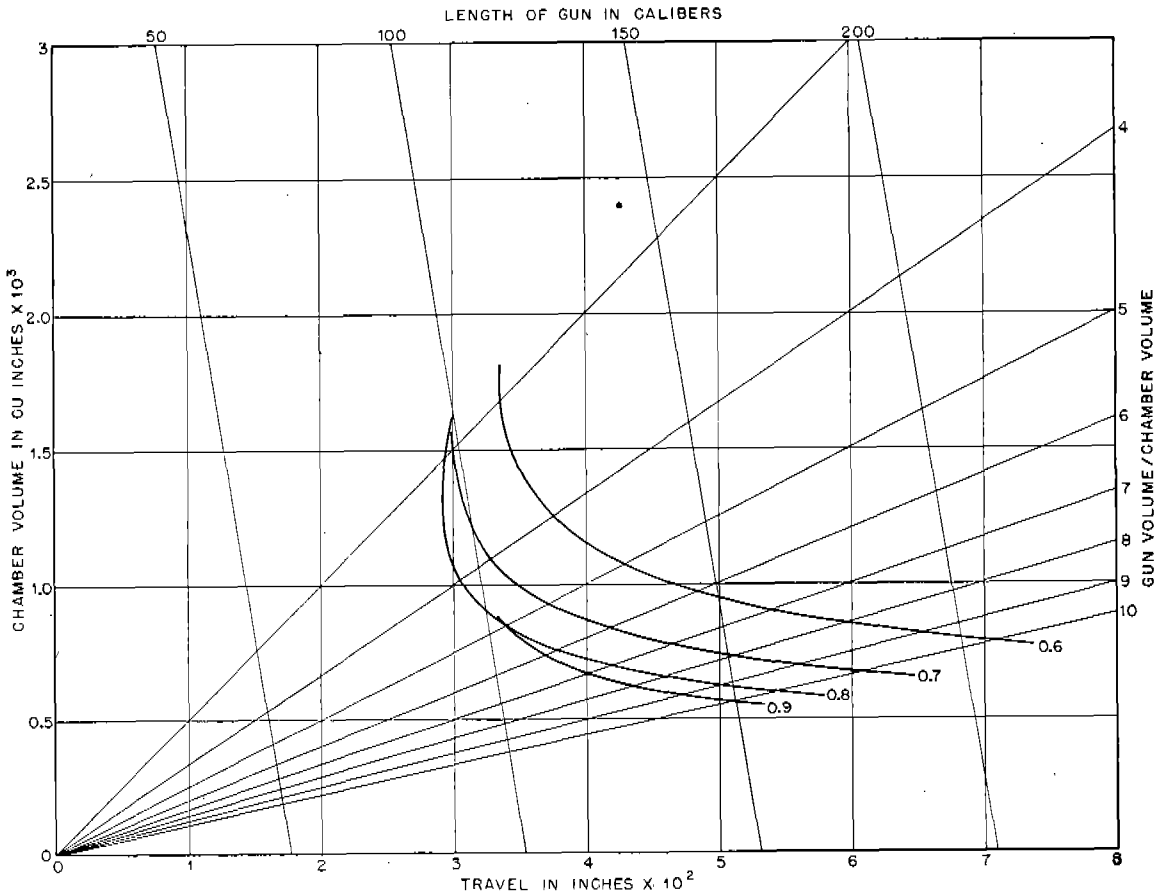


FIGURE 10. Relations between chamber volume and gun length, for a 90-mm gun at $P_p = 60{,}000$ psi, $V_m = 4{,}500$ fps; FNH-M1 powder. (This figure has appeared as Figure 12-3 in NDRC Report A-397.)

above 60,000 psi. It is for this reason that Tables 7 and 8 are not carried beyond that limit. Thus new advances in the strength of gun steels, while very desirable in reducing the weight of the weapons, might not permit a great extension of the present-day limitations on ballistic design, unless accompanied by an increase in the density of loading.

PREFERRED VOLUME RATIO

The optimum volume ratio $(X_m/X_0)_3$ usually corresponds to a comparatively large chamber and short travel. However, as is clear from the flat maximum in Figure 8, an increase in X_m/X_0 by one or two units above the optimum value does not decrease the velocity greatly, and implies a considerably smaller chamber, for the same total volume. This in turn means a decreased charge and a more efficient utilization of the powder.

As a typical numerical example, we note from Tables 5, 6, and 7 that at $V_m = 4{,}000$ fps and $P_p = 50{,}000$ psi the optimum loading density for M1 powder is 0.764, corresponding to $\mu = 0.688$ and $X_m/X_0 = 3.45$. At that density an increase to $X_m/X_0 = 5.0$ would lower μ only to 0.661. That is, the same muzzle velocity and maximum pressure could be obtained with a decrease in chamber volume and powder charge of 27 per cent, at the expense of an increased total gun volume of only 4 per cent. Thus, unless tactical considerations demand either an unusually short gun or an unusually light charge, the best volume ratio is one or two units above the theoretical optimum.

There is another strong reason for using a gun length greater than the optimum in most cases; namely, the larger the gun, the lower are the temperatures and pressures of the powder gas when the projectile leaves the muzzle. Too high muzzle temperatures and pressures result in considerable muzzle flash, muzzle blast, and increased velocity dispersion.

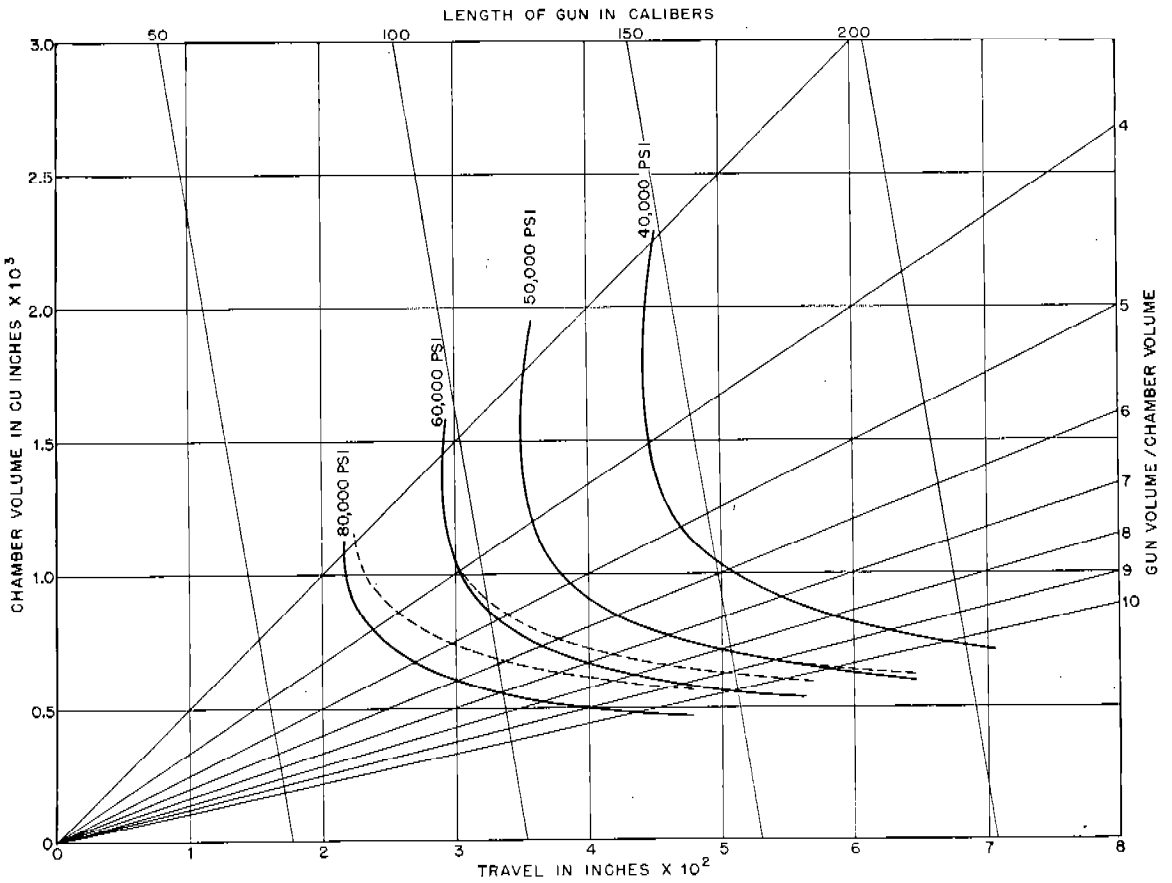


FIGURE 11. Relations between chamber volume and gun length at optimum density of loading, for a 90-mm gun at V_m = 4,500 fps; FNH-M1 powder. (This figure has appeared as Figure 12-6 in NDRC Report A-397.)

CHOICE OF POWDER

The comparison between FNH-M1 and FNH-M2 powders in the tables in this section shows that the double-base powder, with an impetus ($F = nRT_0$) greater by almost 25 per cent, gives an increase in muzzle energy, under optimum conditions at the same maximum pressure and muzzle velocity, of about 10 per cent. Because an increase in impetus nearly always connotes an increase in gas temperature, which in turn leads to much greater erosion, it is rarely desirable to make use of the slight gain in ballistic efficiency provided by double-base powders.[c] It would, however, be clearly advantageous to develop powders with a high n but low T_0.

[c] A study at Aberdeen Proving Ground of the dependence of muzzle velocity on the potential and on the force of powder showed that at optimum conditions the muzzle velocity depends much less on the energy properties of the powder than on the maximum pressure or the length of the gun.[204]

GRANULATION OF POWDER

All the previous discussion in this section has been based on the simplest powder granulation, that of constant burning surface. The maximum ballistic efficiency would be obtained from a very progressive powder; that is one whose surface would increase with burning in such a way that the amount burned would increase proportionately with the available volume, resulting in a uniform pressure until the powder was completely burned, with a correspondingly high P_{eff}/P_p.

A mixed charge, consisting of a small amount of a very fine granulation, to burn rapidly and establish the constant high pressure, and the remainder of single-perforated tubes of very small inside diameter, fireproofed to burn only on the inside, would approach this ideal granulation. The seven-perforated powders in common use are only very slightly progressive; it has been shown that they are practically equivalent

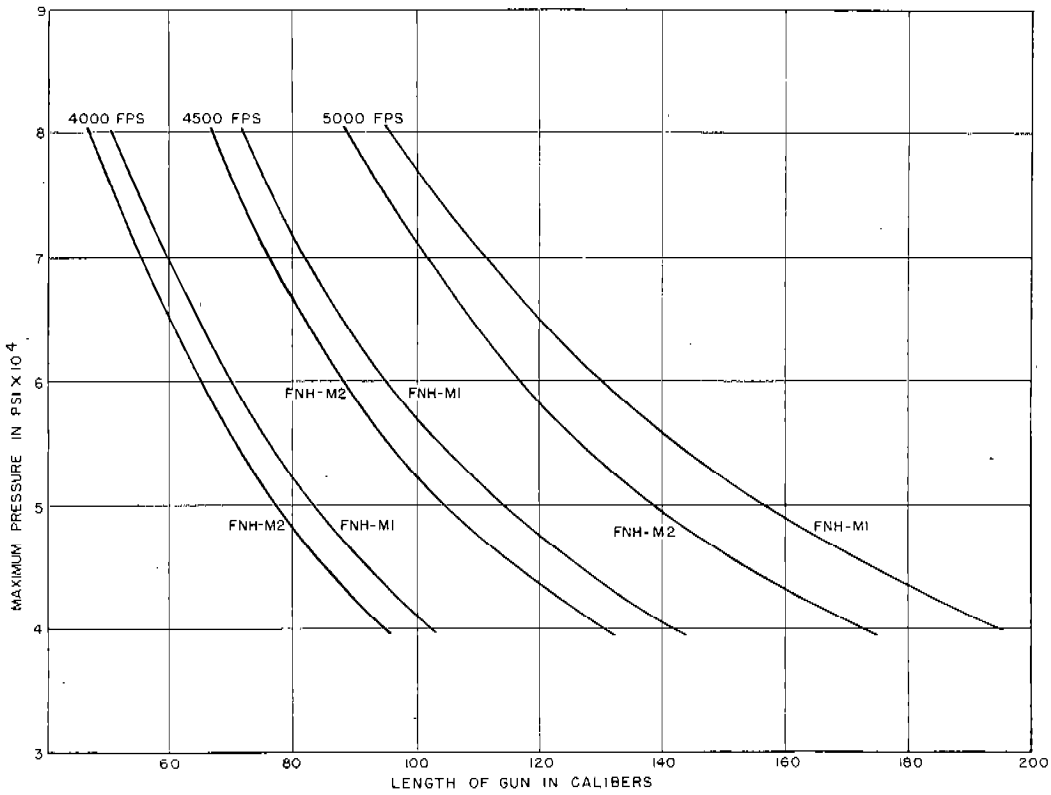


FIGURE 12. Relations between gun length and muzzle velocity at double-optimum conditions for a 90-mm gun, firing a projectile of normal weight (24 lb) at various muzzle velocities with either FNH-M1 or FNH-M2 powder. (This figure has appeared as Figure 12-11 in NDRC Report A-397.)

ballistically to constant-surface powder of 27 per cent greater web, the advantage of increasing surface before splintering being counterbalanced by the rapidly decreasing surface after splintering. Cord granulation, used extensively in British guns, is very degressive, and hence ballistically less efficient; it can, however, be loaded and ignited controllably at higher densities of loading than other powders, and thus has many advantages.

The effect of granulation on gun performance has been calculated. A typical example of the differences in pressure-travel and velocity-travel curves resulting from changes in grain shape is shown in Figure 9.

3.5.5 The Design of a Hypervelocity 90-mm Gun

To illustrate the types of calculations described in Section 3.5.3, a number of curves have been drawn[69] for the 90-mm gun described in Section 33.1.4 (A = 10 in.^{2}), firing a projectile of 24 lb. We then have

$$\mu = \frac{2400}{v_c X_m/X_0},$$

$$L = 0.1 v_c (X_m/X_0 - 1).$$

Taking the cross-sectional area of the chamber to be three times that of the bore, the total length of gun, $L_g = L + 0.033\, v_c$. Hence from the tables of μ we may plot v_c against X_m/X_0 or L, at various muzzle velocities, maximum pressures, and densities of loading. Such a curve for V_m = 4,500 fps, P_p = 60,000 psi, the listed densities of loading, and FNH-M1 powder, is reproduced as Figure 10. The optimum density of loading is that corresponding to the shortest gun at each value of X_m/X_0. The optimum densities, for various maximum pressures, are shown in Figure 11. The shortest gun for each maximum pressure and the corresponding density of loading are the double-optimum conditions. The velocity and gun length corresponding to these are plotted, for two powder types, and several maximum pressures, in Figure 12. It must be remembered that in practice one would use

a somewhat smaller chamber, smaller density of loading, and longer gun than are given by Figure 12; but the curves give a good idea of the effect of changing maximum pressure, powder type, or required muzzle velocity, in designing a 90-mm gun. The application of these calculations to a specific case is described in Section 31.8.

3.5.6 Interior Ballistics of Gun Firing Subcaliber Projectiles

The preceding discussion, the principal results of which are depicted in Figure 12, illustrate how difficult it is, even with all improvements in theoretical and practical gun design, to increase the velocity of conventional guns firing conventional projectiles into the range of 5,000 fps, unless very long weapons are used.

In order to attain velocities this high without lengthening the gun to 100 calibers or more, one must find other means of decreasing μ. To use a projectile that is light for its caliber makes for poor exterior-ballistic stability, as is brought out in Chapter 8. If, however, a small-caliber projectile can be fired from a large-caliber gun, good exterior ballistics may be obtained together with a lowered value of μ. As the tables indicate, if μ can be reduced to one-quarter of its normal value, by firing a projectile of half the caliber of the gun, the velocity increase will be of the order of 2,000 fps.

If the decreased caliber of the projectile is obtained by means of a sabot (Chapter 29), there is some decrease in ballistic efficiency, in that a portion of the energy of the powder is used in providing kinetic energy to the sabot that is subsequently discarded. An alternate means of obtaining a subcaliber projectile with good ballistic form is to fire a deformable projectile from a tapered-bore gun, as is described in Chapter 30. The methods and tables of the earlier sections of this chapter may be applied to the guns firing these unconventional projectiles.

Chapter 4

INSTRUMENTATION FOR EXPERIMENTAL BALLISTIC FIRINGS

By *H. B. Brooks*[a]

4.1 THE ROLE OF EXPERIMENTAL BALLISTICS

SOME OF THE PROBLEMS in interior ballistics that face the designer of a hypervelocity gun have been outlined in Chapter 3. Their solution requires more exact knowledge of the behavior of guns and projectiles during firing than has been available in the past, especially under conditions of hypervelocity. Division 1, NDRC, working through the National Bureau of Standards and the Geophysical Laboratory of the Carnegie Institution of Washington, attempted to obtain some of that knowledge by setting up a ballistic range and making physical measurements with laboratory precision during the firing of guns.

The present chapter deals primarily with the instrumentation developed for this purpose. It comprises a general description of the firing range, an outline of the ballistic events recorded during the firing of a gun, and a condensed description of the apparatus used to record them.[b] A sketch is also given of a separate development at the Geophysical Laboratory of techniques and instruments for measuring ballistic quantities directly by means of apparatus attached to the projectile while it is moving in the bore of a gun.

Although certain instruments have been used for many years at proving grounds for some routine ballistic measurements, many others had to be developed especially for these firings. This development was carried out during the first two series of firings of a 3-in. naval gun. Even though this is not a hypervelocity gun, a third series of firings was made with it not only for the sake of checking the performance of the instruments but also for the sake of obtaining ballistic data that could be used in elucidating some aspects of ballistic theory. The principal results are presented under appropriate subject headings in Sections 2.5.5, 5.2.2, 6.3, and 7.4.

The first hypervelocity gun to which this instrumentation was applied was the 37-mm, T47 (Section 31.7), firing pre-engraved projectiles at a muzzle velocity of approximately 3,500 fps. These firings represented the first recorded systematic study of the interior ballistics of a medium-caliber gun with pre-engraved projectiles. The results are summarized in Sections 5.2.2, 6.4, and 7.4.

An important feature of the later stage of Division 1's program was the development of a hypervelocity 90-mm gun, firing pre-engraved projectiles at a muzzle velocity of 4,000 fps, as outlined in Section 31.8. It was planned that eventually one of these guns would be used in a series of ballistic firings. As a preparation for that investigation, and especially in order that there would be available a firm basis of comparison, plans were made for conducting a series of firings with a 90-mm gun, M1A1. The gun was procured through the cooperation of the Army Ordnance Department and its tube was modified to accommodate measuring instruments just as the 3-in. gun had been. When Division 1's sponsorship of this work had to be withdrawn near the close of 1945, the Bureau of Ordnance of the Navy Department supported its continuance by the National Bureau of Standards.

4.2 THE CARDEROCK RANGE AND THE GUNS

4.2.1 Range and Laboratory

The ballistic range, including the associated laboratory, was constructed for Division 1 on the grounds of the Navy Department's David W. Taylor Model Basin at Carderock, Maryland, a few miles from the District of Columbia. The range is 500 ft long and is horizontal. Concrete piers for the support of velocity solenoids are located at 50-ft intervals along the range. A set of ducts extends along the range from the laboratory with a manhole opposite each pier and one near the gun. Through these ducts wires extend to the laboratory from each pier and from the gun. At the distant end of the range there is a sand-filled butt with heavy concrete walls and a removable concrete block for a cover.

The laboratory is a one-story frame structure located about 50 ft behind the gun. It has two rooms,

[a] National Bureau of Standards and Geophysical Laboratory, Carnegie Institution of Washington.

[b] Complete descriptions are given in a series of NDRC reports listed as the following items in the Bibliography: 39, 44, 65, 108, 131, 132.

one 18 by 18 ft, the other 12 by 18 ft. It is possible to make the laboratory light-tight, as is necessary when the very sensitive films are to be placed on or removed from the recorder drums. A ventilating system operates through the attic, and heat is supplied by a system of thermostatically-controlled electric heaters. The wiring connections to the laboratory apparatus are suspended from hooks in the ceiling. An interior view of the larger laboratory room is shown in Figure 1.

4.2.2 The 3-in. Gun and its Mount

A 3-in./50-cal. gun, Mark 3, Mod. 7 and mount were provided by the Bureau of Ordnance, Navy Department. Very few shots had been fired from the gun since it was relined. The primary support for the gun was a heavily reinforced concrete slab 20 ft sq and 4 ft thick. Steel foundation bolts, cast into the concrete slab, extended up through a cushioning layer of 2-in. plank and through a piece of 2-in. armor plate to which the gun mount was bolted. About 1 ft beneath the gun and forward from the mount was a concrete pier with a top about 2 by 3 ft. This pier supported the apparatus which was connected directly to the gun for the purpose of measuring displacement, velocity, and acceleration of recoil.

Some modifications were made in the gun in the shops of the Taylor Model Basin before the ballistic firings were started. The firing mechanism was modified so that the gun could be fired electrically. Two holes were bored into the powder chamber at opposite ends of a diameter to allow the pressure and temperature of the powder gas to be measured at each instant. Two bands with projecting arms were fitted to the gun so that recoil apparatus could be readily attached to the gun barrel. A muzzle plate with a suitable clamp was fitted to the gun to permit the instant of ejection of the projectile to be determined.

After eleven rounds had been fired, three additional pairs of holes were drilled through the barrel between



FIGURE 1. Interior of larger laboratory room at ballistic range.

CONFIDENTIAL

the powder chamber and the muzzle. The two holes composing each pair were at opposite ends of a horizontal diameter.

4.2.3 The 37-mm Gun

One of the experimental 37-mm, T47 guns described in Section 31.7 was provided by Division 1 through the Franklin Institute. This gun fired a 1.62-lb preengraved projectile at a muzzle velocity of about 3,500 fps. Its chromium-plated tube had been made by boring a 40-mm tube for 37-mm and chambering it for a standard 40-mm cartridge case necked down to accommodate a 37-mm projectile.

In order to prepare this tube for ballistic firings, a collar about 6 in. long was shrunk on the barrel, near the base of the powder chamber, and two holes were drilled through this collar into the powder chamber to receive powder-pressure gauges. The flash hider was replaced with a muzzle plate carrying muzzle fingers, an optical ejection indicator, and the antennas for the microwave interferometer.

Six types of projectiles, two types of powder, and three types of primers were used in the ballistic firings.

4.3 EVENTS RECORDED AND QUANTITIES DETERMINED

4.3.1 Method of Measurement

The important events which occur when a gun is fired are recorded on photographic films as oscillograph traces and in other ways by means of the instruments described in Section 4.4. From these records the quantities involved in interior ballistic calculations are determined. Some of the events involve only time, such as the time the firing pin strikes the primer or the time the projectile passes the muzzle of the gun. Other events require the determination of a quantity as a function of time, such as the temperature or the pressure of the powder gases. The measurement of each event requires special consideration.

4.3.2 Firing Pin Strikes the Primer

The firing pin of the 3-in. gun carried two spring contact devices, normally closed. The free end of each spring was loaded to increase its inertia. These contact devices faced in opposite directions. When the firing pin started to move, the inertia of one of the loaded springs broke its contact and thus recorded this event on the oscillograph trace. The inertia of the other loaded spring, however, held its contact more tightly closed until the firing pin struck the primer, when the inertia of its loaded spring opened this contact and thus made its record. The average time of travel of the firing pin was about 15 msec, which was about 5 msec longer than the time from the ignition of the primer to the ejection of the projectile, when full service charge was used.

4.3.3 Start of Powder Pressure

The time at which the powder pressure started was obtained from a film by determining the time at which the trace for the pressure in the powder chamber showed the first sign of curving. Because of the slow rise of pressure at the beginning, the time at which it started could not be determined precisely. The uncertainty in the time of start of pressure in the 3-in. gun did not often exceed 0.2 or 0.3 msec in a total time to ejection of about 8 msec.

4.3.4 Start of Radiation

The time at which radiation from the powder gas started was obtained from its trace on the film by determining the time at which the trace started to curve. The initial rise in radiation was quite rapid so that the time at which it started could be determined within 0.1 msec. The start of radiation usually occurred slightly before the start of pressure.

4.3.5 Start of Recoil

The start of recoil of the gun was indicated by the opening of a contact on the recoilmeter (Section 4.4.7), which was designed to operate when the gun had moved less than 0.001 in. The operation of this contact produced a step on the film traces the time of which could be determined to 0.01 msec. The start of recoil usually occurred before the measured start of pressure or of temperature of the powder gas. It is of interest to note that the recoil was initiated in the 3-in. gun by the forward motion of the powder charge before the projectile started to move.

4.3.6 Start of Projectile

The time of the start of the projectile was originally recorded on the oscillograph film by an inertia con-



tact-breaking device located within the projectile. This device transmitted its starting signal when the projectile had moved only a few thousandths of an inch. It required a wire stretched between the projectile and the muzzle. It had to be discarded when the microwave interferometer (Section 4.4.15) was installed. However, the approximate time at which the projectile started to move could be obtained from the microwave interferometer method by observing when the trace started to curve.

4.3.7 Travel of Projectile in Gun

For the 3-in. gun the travel of the projectile was observed by three independent methods. In the first method the instant was recorded at which the rotating band made contact with each of several insulated pins inserted in radial holes along the gun barrel. This method is probably the most precise of the three, but is limited by the necessarily small number of holes. The second method uses wire-resistance strain gauges (Section 4.4.10) to determine the instant at which the projectile passes given transverse planes, as discussed in Section 7.4.1. Variations in the ratio of band pressure to powder pressure introduce uncertainties in the interpretation of results. The third method locates the projectile by the microwave interferometer (Section 4.4.14). This method gives a large number of points along the gun barrel but at the disadvantage of requiring elaborate apparatus. It was the only method used in determining the motion of the projectile in the 37-mm gun.

4.3.8 Velocity of Projectile in Gun

Several methods have been used experimentally for measuring this quantity. The preferred method consists in plotting the curve of projectile position as a function of time, as obtained from the data yielded by the microwave interferometer (Section 4.4.14), and graphically differentiating this curve to obtain the curve of velocity as a function of time.

4.3.9 Acceleration of Projectile in Gun

The acceleration-time curve for the projectile has been obtained by graphical differentiation of the velocity-time curve. No direct method of measuring the projectile acceleration was used in the Carderock firings. A method tried in a 20-mm gun is described in Section 4.5.

4.3.10 Muzzle Velocity

Approximate values of the muzzle velocity for the 3-in. gun have been determined by two independent methods, one of which involves the extrapolation of the range velocity backward to the muzzle, the other the extrapolation of the velocity in the gun forward to the muzzle. The extrapolation required in the first method can be more accurately performed, but the value obtained for the muzzle velocity requires a correction for the effect of the blast. This correction has not been determined directly, and the uncertainty in its value as found by approximate procedures constitutes the chief limitation on the accuracy of the method. Presumably the blast accelerates the projectile, and hence the first approximate value of muzzle velocity given by extrapolation of the range velocity will be too large. The muzzle velocity for the 37-mm gun was obtained by this method of extrapolation.

4.3.11 Velocity of Projectile on Range

For both guns the velocity of the magnetized projectile was measured by recording on an oscillograph film the times at which the projectile passed through solenoids located at measured positions along the range (Section 4.4.11). It was estimated that the average velocity between any pair of solenoids was determined with an accuracy of at least 1 fps.

The observed values for the 3-in. gun extend from 1,730 fps with 50 per cent of service charge to 2,730 fps with 100 per cent charge. For the 37-mm projectiles the velocities range from 3,260 to 3,870 fps for projectiles weighing 1.92 to 1.34 lb.

4.3.12 Deceleration of Projectile on Range

The deceleration of 3-in. projectiles on the range has been computed for each successive trio of solenoids, and for the first and the last pair of solenoids. Observed values range from 178 ft/sec^2 for 50 per cent of service charge to 380 ft/sec^2 for 100 per cent of service charge. It was found that for 3-in. projectiles having identical rotating bands the deceleration α, in ft/sec^2, is given with reasonable accuracy by

$$\alpha = 0.194V - 157. \qquad (1)$$

For the 37-mm projectiles the observed values of deceleration range from 600 to 1,250 ft/sec^2.



4.3.13 Displacement of Gun in Recoil

The displacement of the 3-in. gun in recoil as a function of time has in most instances been directly determined by the step-by-step recoilmeter; in a few rounds the continuous recoilmeter has been used (see Section 4.4.7). Other methods, used in a few cases, are (1) the integration of the velocity-time curves of the velocimeters, and (2) the double integration of the acceleration-time curves of the accelerometers. Theoretically, all the records of the motion of the gun in recoil can be compared through differentiation or integration of the curves drawn by the various instruments.

4.3.14 Velocity of Gun in Recoil

The velocity of the 3-in. gun in recoil as a function of time has been measured by three different methods, namely, (1) direct measurement with a velocimeter (Section 4.4.8); (2) differentiation of a displacement-time curve; and (3) integration of an acceleration-time curve. The method that has been most extensively used is the graphical differentiation of the displacement-time curve given by the step-by-step recoilmeter (Section 4.4.7). However, this method does not work well when the velocity and the displacement are small, and other methods are at least of equal accuracy for the first part of the curve.

4.3.15 Acceleration of 3-in. Gun in Recoil

The acceleration of this gun in recoil has been recorded directly by the crystal accelerometer, and by differentiators operating on the current from a velocimeter (Section 4.4.9). It has been obtained indirectly by the differentiation of a velocity-time curve and by the double differentiation of a displacement-time curve.

The acceleration of the gun at a given point consists of two parts, namely, its basic acceleration, and the acceleration resulting from vibrations in the gun structure. The accelerometers may have a very rapid response, indicating all the sudden changes in acceleration (including those resulting from vibrations); the graphical-differentiation methods, on the other hand, are suitable only for giving average values covering about 0.1 msec. Both types of method have their uses.

Maximum values of acceleration in recoil for the 3-in. gun range from nearly 7,000 ft/sec^2 for 100 per cent of service charge down to about 2,000 ft/sec^2 for 50 per cent charge. For 100 per cent and 90 per cent of service charge the maximum acceleration in recoil occurs about 4.5 msec before ejection. For the lower values of charge the maximum occurs at longer intervals before ejection, the interval for 50 per cent charge being about 7 msec.

4.3.16 Pressure of Powder Gas

The pressure of the powder gas was usually measured at four positions along the 3-in. gun by the gauges described in Section 4.4.12. The data from the pressure-time curves of each round have been combined with the data from the displacement-time curve of the projectile for that round to give the pressure in each hole as a function of the position of the projectile. The displacement-time curve of the projectile, as determined by the microwave interferometer, has been used in all rounds when available, but in other rounds it was obtained either from strain-gauge data or computed from measurements of the recoil of the gun. The pressure on the base of the projectile as a function of projectile displacement has been determined from the pressures at the several holes and plotted for each round. Figure 2 shows the pressure-time curve for 100 per cent charge in round 65, as measured at each of four holes. Figure 3 relates to the same round but shows the pressure as a function of projectile travel.

The values of maximum pressure obtained in the various rounds may have been influenced by at least three factors, namely, condition of the interior surface of the gun barrel, the initial position of the projectile, and the temperature of the gun barrel and the powder. There is a definite indication that the maximum pressure is lowest with the projectile in its normal position and the interior surface of the barrel greased. The maximum pressure is somewhat greater if the gun barrel is dry; it is a little greater if the gun barrel is greased and the projectile is advanced so that it is seated against the rifling; and it is greatest when the projectile is advanced and the inner surface of the gun barrel is dry.

Maximum values of powder pressure in the powder chamber of the 3-in. gun for service charge ranged from 38 to 49 kilopounds psi. Maximum pressures in the 37-mm gun ranged from 52 to 64 kilopounds psi.

4.3.17 Temperature of Powder Gas

Measurements of the temperature of the powder gas were made by observing the intensity of the emit-



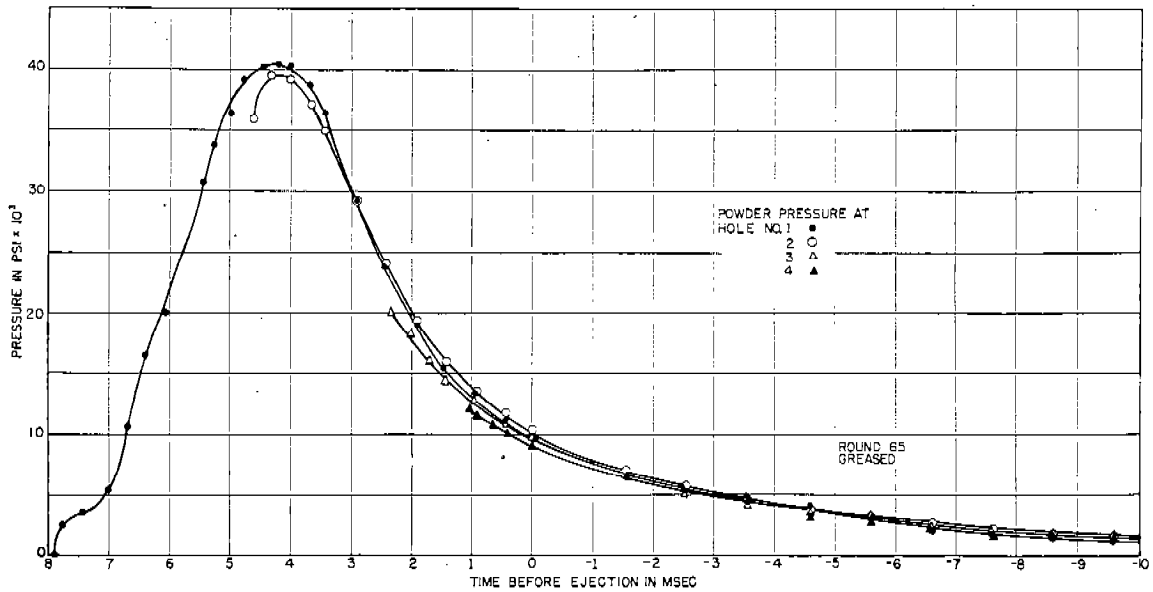


FIGURE 2. Pressure-time curves for 100 per cent charge, 3-in. gun.

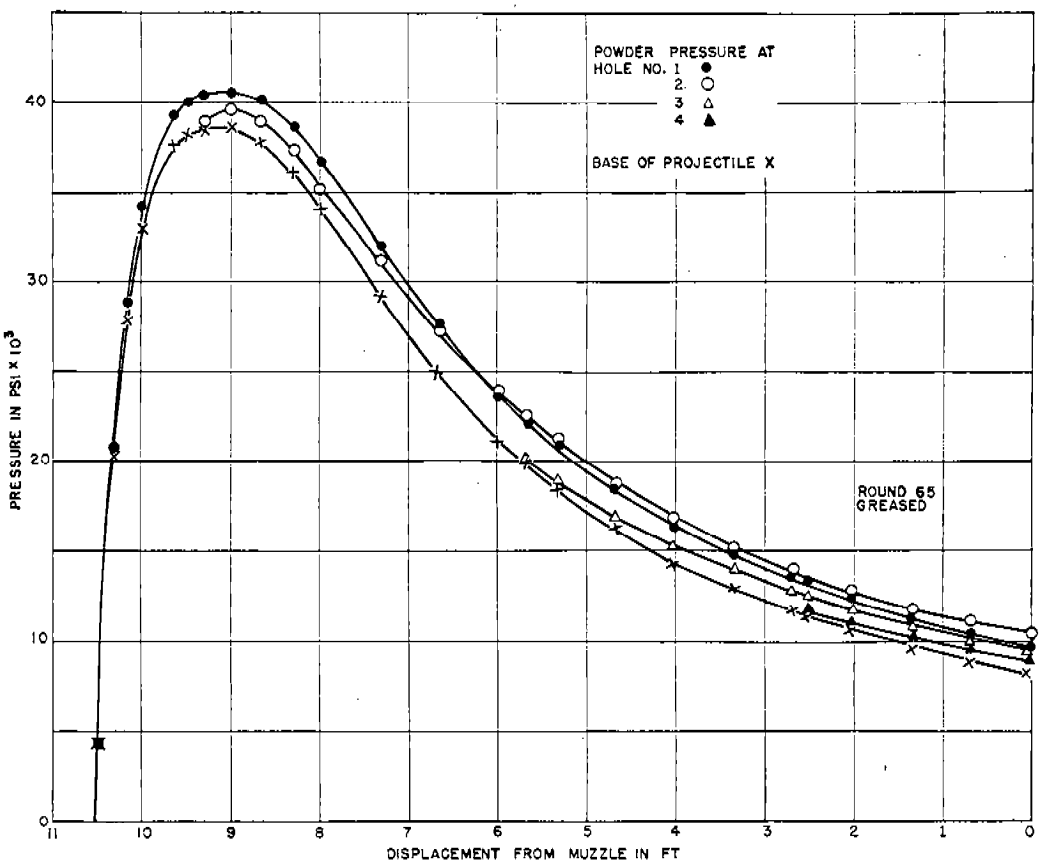


FIGURE 3. Curves of pressure versus projectile displacement for 100 per cent charge, 3-in. gun.

[redacted]

ted radiation as described in Section 2.5.4. One-color and two-color pyrometers (Section 4.4.13) have been used on the 3-in. gun in various combinations at hole positions 1, 2, and 3, as far as the limited number of recording channels permitted. Unfortunately, it appears that the temperature is far from uniform throughout the powder chamber or along the bore of the gun and the results for any one round at any instant give the temperature of only a small local volume in front of the window, rather than the average temperature at that instant throughout the chamber or across the diameter at the position of the hole. For this reason, together with the fact that the limited supply of recording apparatus restricts the types of measurements made in any one round, the typical rounds chosen for the report must not be thought of as in any sense typical of the complete body of the data, but merely as examples. The results of the temperature measurements are summarized in Section 2.5.5.

In the holes opening into the powder chamber it has been found that for service charge (1) radiation is first observed at or shortly before the start of pressure; (2) a brief flash of high-temperature radiation (about 2300 K) coinciding with the first sharp rise of pressure to about 1,000 psi, is followed by rapid cooling to about 1900 K, and then by a gradual rise toward a maximum; (3) the maximum temperature of 2550 ± 100 K is reached at about 5 msec before ejection; the maximum pressure occurs about 1 msec after the maximum temperature; (4) as further expansion of the gas continues, the temperature drops rapidly until at ejection it is near the limit of measurement (1600 K).

4.3.18 Strain Measurements on the Gun

Strain measurements[65] made by means of the gauges described in Section 4.4.10, which were placed on the external surface of the 3-in. gun barrel, have been of two kinds: (1) qualitative measurements which served to determine the time of passage of the projectile, and (2) quantitative measurements, used in studying the forces acting on the gun tube, in order to determine their influence on the friction between the gun and the projectile. This evaluation is a difficult problem, as is brought out in Chapter 7 (especially Section 7.4).

4.3.19 Jump of Gun

The jump of the 3-in. gun as a function of time was measured for all but one of the first 11 rounds.[39] The measurements showed that the muzzle of the gun started to move upward at about 1 msec before ejection and had moved nearly 2 mm at ejection.

4.3.20 Pressure in Recoil Cylinders

Measurements of pressure in the recoil cylinder of the 3-in. gun were made under two conditions. In the first, the recoil cylinders were filled with fluid to the vent hole, whereupon the pressure began to rise several milliseconds before ejection. In the later rounds the cylinders were first filled and then a small quantity (½ pt in most cases) was removed. Under these conditions the initial rise of recoil-cylinder pressure occurred after ejection. This delay simplified the correlation of the motions of the gun and the projectile because the opposing force exerted by the recoil cylinders is zero throughout the interval considered. The distance the gun recoiled was not changed appreciably by the removal of the liquid.

4.3.21 Ejection of Projectile

Two methods of recording the ejection of the projectile were tried. One depended upon the mechanical contact in an electric circuit while the other was an optical method. An ejection signal was recorded when the front of the rotating band made contact with a muzzle finger mounted on the muzzle plate. Complete ejection occurred slightly later, as about 2 in. of the projectile was still in the muzzle of the gun when the signal was recorded.

An optical system was developed with the expectation that a signal would be obtained when the nose of the projectile intercepted a beam of light passed in front of the muzzle and which activated a photoelectric cell. As explained in Section 4.4.15, this optical method of determining ejection did not work well because the beam was obscured by compressed gases and smoke 0.6 to 1.0 msec before the nose of the projectile arrived at the beam.

4.3.22 Pictures of Muzzle Smoke and Flash

The smoke and gases emerging from the muzzle of the gun and the flash were photographed by the high-speed cameras described in Section 4.4.16. Gases emerging from the muzzle usually obscured the projectile so that it did not become visible until it was several feet in front of the muzzle. The pic-

tures showed the development of the flash over the ball of emerging gases. It usually started at several different points at about the same time and then merged into a single ball of flame. The different powders produced about the same type of flash when service charges were used; but the flash developed with different speeds when reduced charges were used.

4.3.23 Intensity of Muzzle Flash

The intensity of the muzzle flash from the 37-mm gun was measured with the flashmeter described in Section 4.4.17. Measurements were made at several positions in front of the muzzle. The results show no significant correlation with powder classes except for the marked difference between M-1 powder (low flash-intensity) and M-5 powder (high flash-intensity).

4.3.24 Pictures of Projectile in Flight

On several rounds pictures of the 37-mm projectiles in flight were made about 75 ft in front of the gun by illuminating the projectile with a "microflash" (Section 4.4.18). In some cases two cameras were placed so that the angle between their lines of sight was 90°, thus making it possible to measure the yaw of the projectile. However, the cameras that were used were so small that the measurements of yaw were not precise. In other cases the two cameras were placed a short distance apart on a line parallel to the path of the projectile and stereoscopic pictures were obtained.

4.3.25 Shock Waves

A shock wave is initiated as a pulse at the muzzle of the gun when the projectile is ejected and is propagated outward from the muzzle in the form of a spherical shell. A zone of the sphere lying along that great circle which is perpendicular to the sun's rays refracts the rays to produce a shadow of that great circle on the ground or other background. Some of these shadows have been photographed by the projectile camera. They were not observed in the first examination of the pictures made with the 3-in. gun. They were first observed in one of the pictures taken in a continuation of this research. A re-examination of the pictures from the 3-in. gun showed the shadows of the waves quite distinctly.

4.4 INSTRUMENTATION[c]

4.4.1 General Outline

The instruments located on or attached to the gun produce electric signals that are transmitted to the laboratory and control the deflection of the electron beams of cathode-ray oscillographs. Because a rather high voltage on the deflecting plates is required to deflect these beams, an amplifier is built into each oscillograph to increase the voltage of the transmitted signals. Other electronic equipment between the instruments and the oscillographs is mainly for mixing circuits or for matching impedance. In all but the temperature measurement, the records are made on a rapidly moving film mounted on a drum. Temperature measurements are recorded by small cameras rigidly mounted in front of the oscillograph screen, with a sweep circuit to produce the horizontal motion of the oscillograph spot.

The timing of the moving film or of the motion of the sweep circuit is accomplished by giving to the electron beam a small vertical deflection every millisecond. The speed of the moving film is such that these millisecond pulses are about 1.5 cm apart. On the film of the still cameras the distance between timing pulses is about 9 mm. A common-time signal is recorded on each trace when the firing pin begins to move (Section 4.3.2). This signal makes it possible to correlate the times of events recorded on different films. For some of the events only the time of occurrence needs to be recorded. Other phenomena require the measurement of quantities that vary with time, for which purpose two types of recording instruments have been used. One gives a continuous record, the other a step-by-step record.

4.4.2 Instruments for Making the Records

The instruments for making the records were oscillographs, recorders, and auxiliary equipment. The latter includes the wiring for operating the recorders, the devices for making a definite base line on the film, and the calibrating apparatus. Figure 4 shows an assembly of recording apparatus including two details of special parts.

The two oscillographs are of the DuMont Type

[c] The experience of the Geophysical Laboratory in recording explosion pressures[3] by means of oscillographs[7] was available in planning the installation at Carderock.



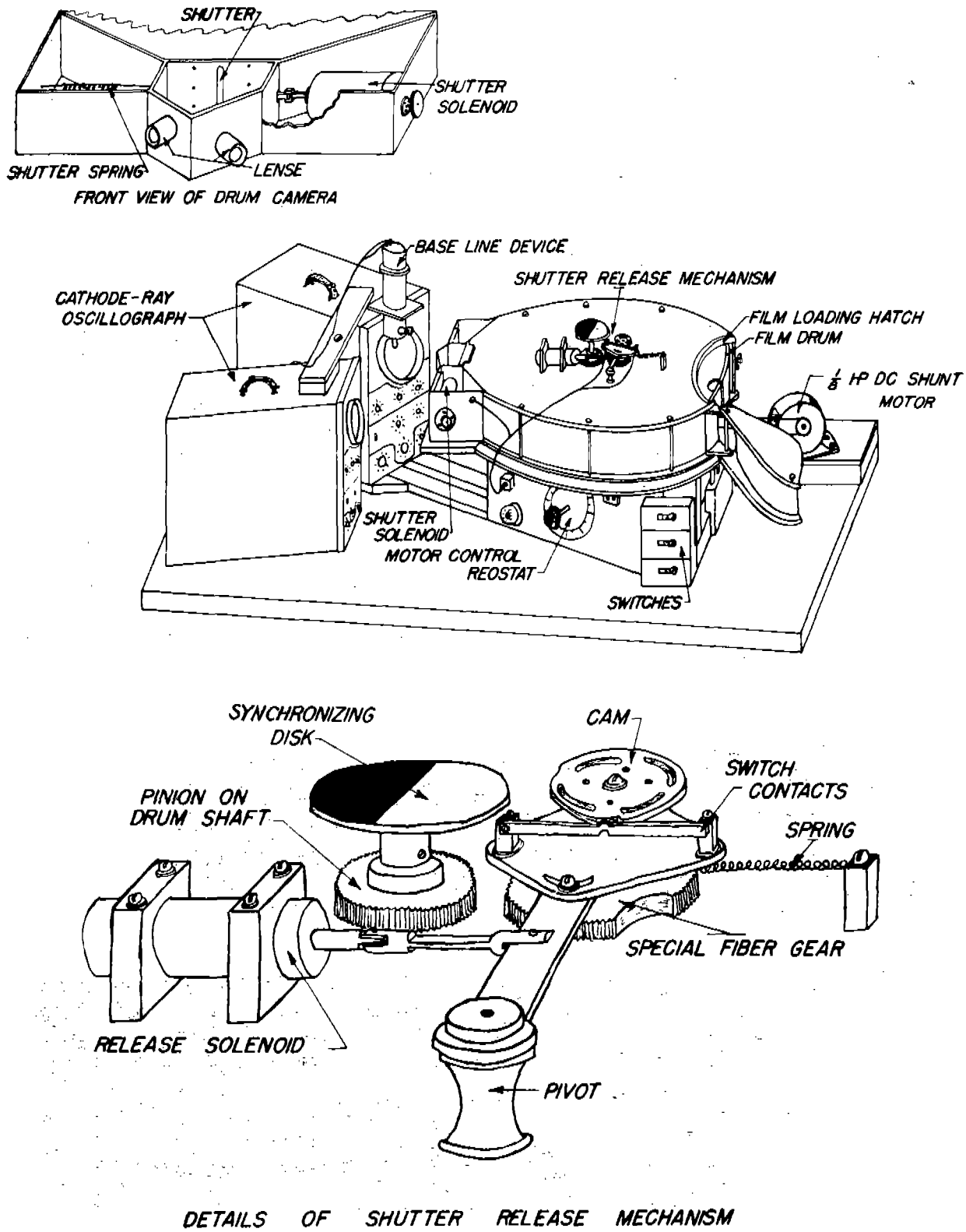


FIGURE 4. Recording apparatus for ballistic measurements.

208. Directly in front of them is the recorder, which is essentially a light-tight housing enclosing an aluminum drum 19 in. in diameter with a 4-in. face. The drum is belt-driven by a d-c motor. The housing can be opened to permit the mounting of a photographic film on the drum. An electrically operated shutter controls the exposure of the film. The shutter opening is wide enough so that the two oscillographs may record on a single film. A release magnet opens the shutter circuit and allows the shutter to close after any desired number of revolutions not exceeding 5. The optical system requires a lens to focus the spot of each oscillograph on the film.

The drums were synchronized with each other and with the firing mechanism of the gun so that the shutters of all the drums opened immediately after the slot holding the ends of the film passed the shutter. One drum was used as a master drum and a contact on it operated the firing mechanism. This same contact flashed lights on the other drums which allowed the operators to synchronize their drums with the master drum by observing the stroboscopic motion of a disk mounted on the drum shaft. By this arrangement the record always appeared in the central portion of the film.

Two types of records were obtained, one in which the time of an event is indicated by an abrupt displacement of the trace, the other, in which the ordinate of the curve at any time is proportional to the magnitude of the quantity measured. In Figure 5 the lowest trace of (A) is an example of the former type of record, and the trace of (B) illustrates the latter type. For both traces the number above the trace is the number of milliseconds from a common time signal not shown in the figure. The figures below trace (A) indicate the steps on a recoilmeter. The other traces of (A) will be referred to later.

4.4.3 Oscillograph Calibrators

The oscillograph calibrators break up the measuring trace into a definite series of short sections, stair-step fashion, the ordinate of each step corresponding to a definite value of the quantity that has just been recorded by the trace. The unique feature of these calibrators is the switching mechanism, in which an electrically released falling weight opens a series of switches, connected to a special network, to produce the steps on the film by changes of either resistance or voltage. This feature is shown in Figure 6. An important feature of these calibrators is the fact that all switches are *opened* to produce changes in resistance or voltage. This feature of operation insures that no chattering of contacts can occur, even when they are

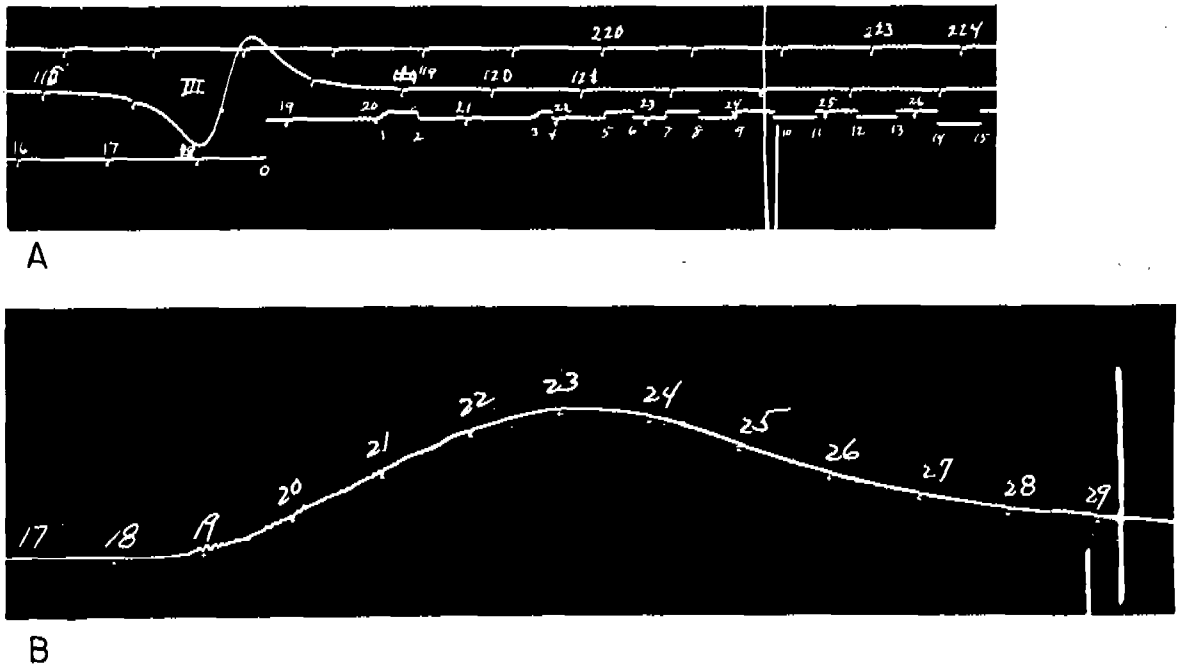


FIGURE 5. Types of traces obtained in ballistic measurements with 3-in. gun.

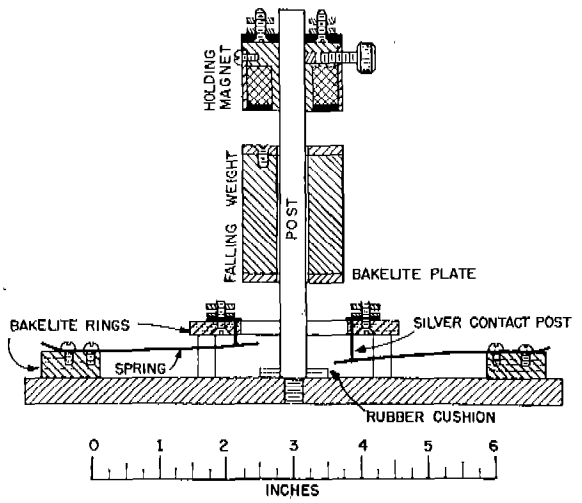
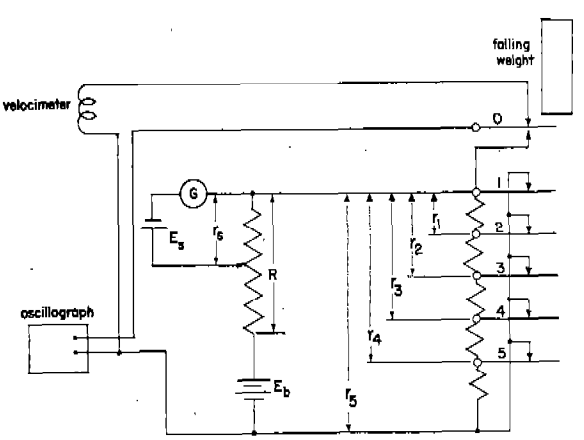


FIGURE 6. Switching device of the oscillograph calibrator. The switches are actuated by a falling weight.

opened at the rate of one every millisecond. Figure 7 is a diagram of the circuit of the calibrator used with the velocimeter.

4.4.4 Timing of Film

The timing of each film is accomplished by recording on it a continuous series of pulses that occur at intervals of 1 msec. These timing pulses may be seen on the traces shown in Figure 5. The same series is recorded on all the traces of the films that are exposed at any one time. The series on the different traces of a set are correlated by having one or more distinctive events, called the *common time*, recorded on each trace. The timing pulses for the films are initiated by a 1,000-c fork and are impressed on the oscillograph circuit by electronic devices called "pulsers." In the course of the investigation these devices have undergone improvements which make the pulses appear simultaneously on all the oscillographs and increase the precision of reading the position of the pulses on the film. The description in the next section is limited to the improved form as used in the third series of firings with the 3-in. gun.[132]



R is total resistance in battery circuit when all switches are closed.
0, 1, 2, . . . 5 are switches opened by falling weight.
$r_1, r_2, \ldots r_5$, are resistances added to circuit by opening of switches 1, . . . 5
E_b is voltage of battery and E_s that of standard cell.
G is galvanometer.

FIGURE 7. Oscillograph calibrator circuit for velocimeter.

4.4.5 Pulsers

The timing-pulse generator is designed to convert the 1,000-c output of the tuning fork (and related assembly) into a series of pulses in which the voltage rises sharply, remains nearly constant for about 25 μsec, then decreases just as sharply to zero. The distance on the film between the rising side of the pulse and the descending side is such that the cross hair of the reading microscope may be accurately set midway between the two sides. This condition enables accurate settings to be made. An identifying signal, inserted in the trace of each film by the firing-pin contact, provides a common-time origin for all the films. This feature, in connection with the simultaneity of the timing pulses, makes possible very accurate coordination of the times of all recorded events.

4.4.6 Developing of Films

The exposed films required special handling and developing because of the stringent requirements for the finished negatives.[39] The development and initial fixing were carried out in the dark because the film was too sensitive to permit the use of even red light. The observed differential shrinkage ranged from 0.4 per cent to nearly 1 per cent and the resulting error in time measurements did not exceed 5 μsec and was usually less.

4.4.7 Recoilmeters

Two forms of recoilmeters have been used to measure the displacement of the gun in recoil (Section

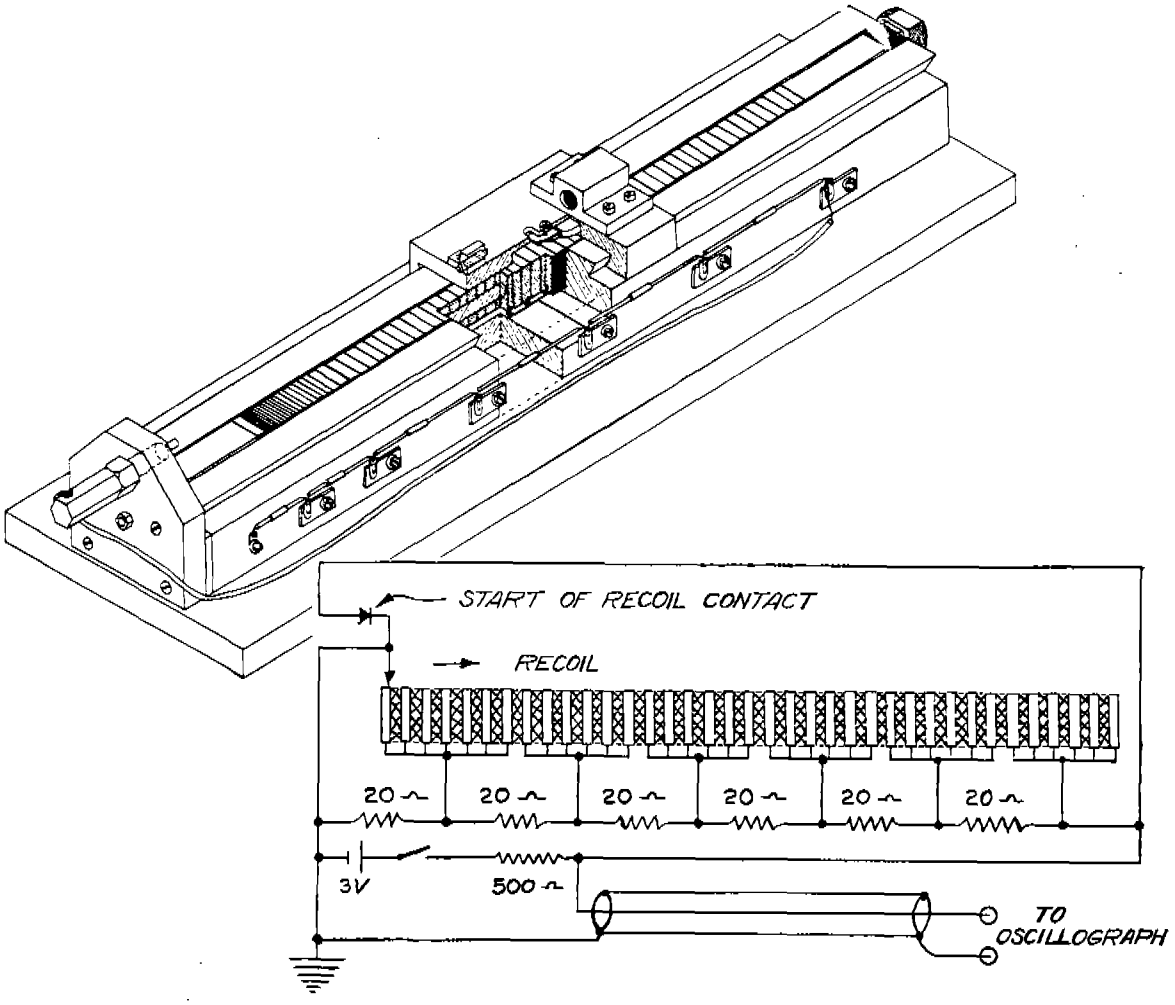


FIGURE 8. Recoilmeter for measuring amount of recoil of a gun.

4.3.13). Both operate on the same general principle, namely, the variation of resistance in a circuit by the motion of a sliding contact. In the first recoilmeter the motion of the gun drives the slider along over a series of silver contact segments between which resistors are connected. Figure 8 shows this instrument with a part cut away to show details. The step-by-step record obtained with this instrument gives a precise indication of the time at which the displacement of the gun attains certain values. The slider of this recoilmeter is connected to the gun by a steel tube. Provision is made for indicating the start of recoil (Section 4.3.5) by the separation of two contacts, one attached to the slider and the other to the base of the recoilmeter.

The second recoilmeter operates on the same general principle but the series of discrete contacts is replaced by a slide wire. Because of the form of the record given by this instrument, it is called the continuous recoilmeter. Its slider is carried by the dovetail slide of the step-by-step recoilmeter, and the slide-wire assembly is fastened to the side of the base of the step-by-step recoilmeter.

4.4.8 Velocimeters

Two forms of velocimeters have been used for determining the velocity of recoil of the gun (Section 4.3.14). In the first one used in this investigation the linear motion of the gun causes the armature of a small a-c generator to rotate. This requires intermediate mechanical means to convert the linear recoil of the gun into rotary motion of the armature. In the second form the linear motion of a coil of wire in a radial magnetic field is nominally identical with the motion of the gun and the mechanical connection

of the velocimeter to the gun is therefore much simpler.

Rotary Velocimeter

The rotary velocimeter is a magneto-type bipolar a-c generator constructed to have a substantially linear relation between angular velocity and electromotive force over about 110° of each half-cycle. Figure 9 is a view of the generator. The stationary field magnet is composed of five Alnico magnets of the type used in General Electric Type DP-9 d-c ammeters. The armature, which is a single narrow coil wound on a bakelite tube, revolves around a stationary iron core located coaxially between the polepieces of the magnets and supported by pedestals attached to the ends of the base plate. The ends of the armature coil are connected to silver slip rings mounted on the bakelite tube. With no current in the armature, no armature reaction can occur, and because the armature core does not rotate, there is no reaction from it that can affect the field flux either in magnitude or distribution. The instantaneous induced electromotive force is accurately proportional to the instantaneous angular velocity, and the wave form for any constant angular velocity is independent of the magnitude of this velocity.

Because the generator must be mounted and used near the gun, and consequently be exposed to outdoor temperatures, the dependence of its induced electromotive force on the temperature of the generator is important. It was found that an increase of 1 centigrade degree in its temperature lowered its induced electromotive force by 0.014 per cent.

The armature of the generator is rotated by the gun by means of two thin steel tapes that wind in grooves in a sheave attached to the tubular armature "shaft." As the gun recoils, one tape unwinds from the sheave and the other winds up. During counter-recoil the functions of the two tapes are interchanged. If vibrations in the driving system of the armature are neglected, the angular velocity of the armature of the generator is proportional to the linear velocity of the gun. The velocity of the gun was obtained from the mechanical dimensions of the driving system and the electrical calibration of the generator. The electrical calibration was obtained by rotating the armature at a known uniform speed and determining the gener-

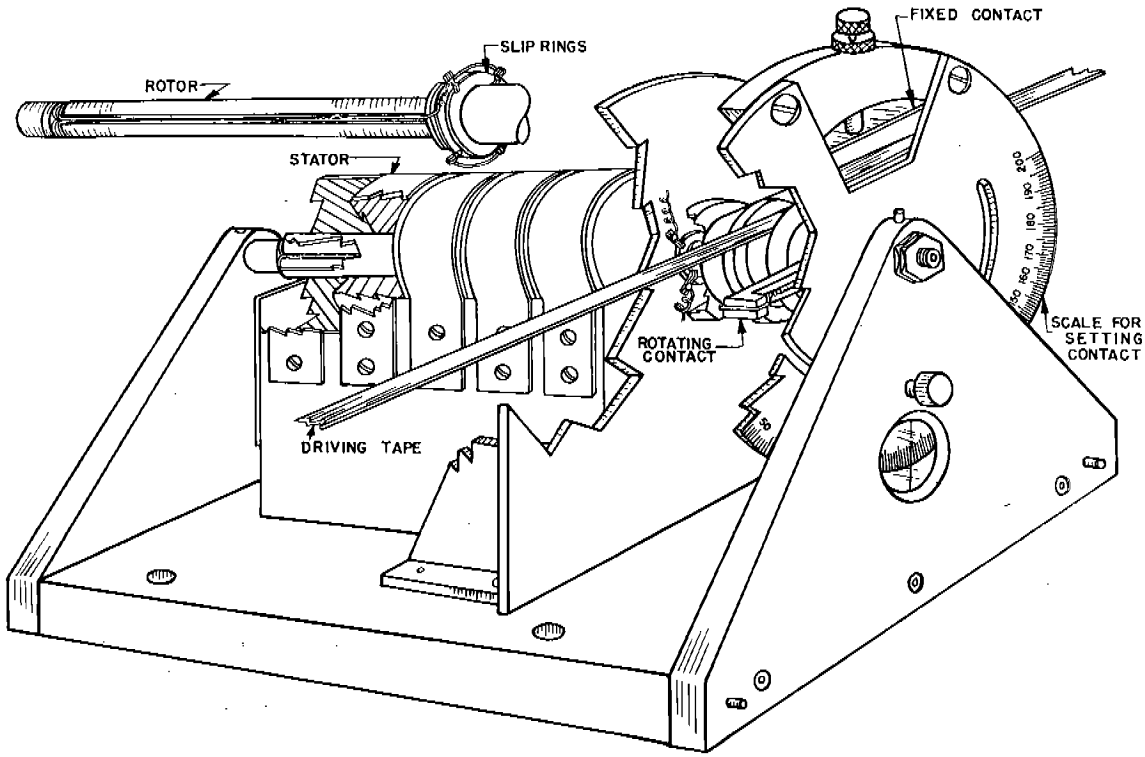


Figure 9. Rotary velocimeter for measuring velocity of recoil of a gun.

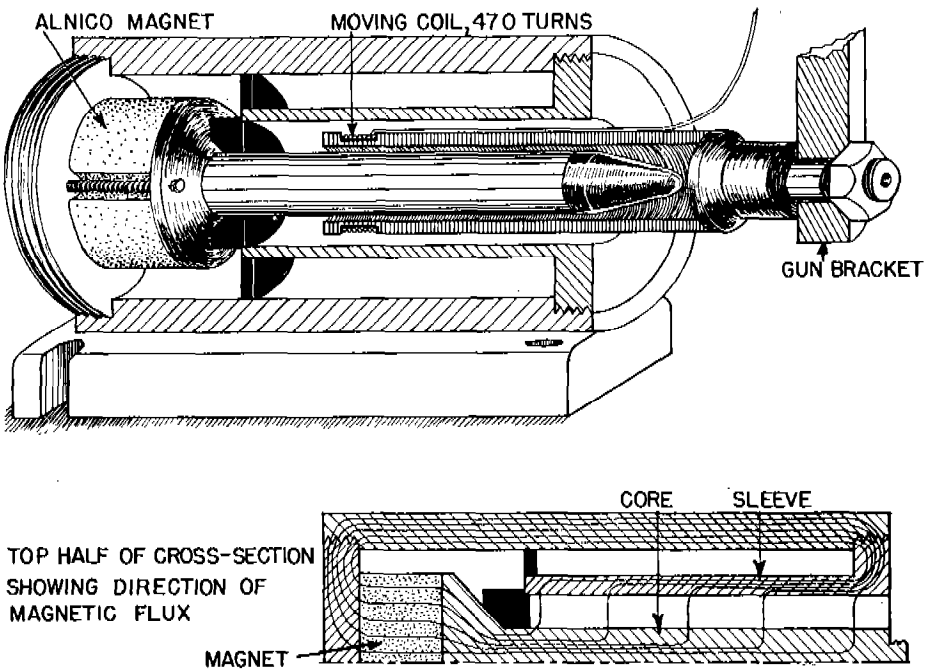


FIGURE 10. Linear velocimeter for measuring velocity of recoil of a gun.

ated electromotive force during the portion of the cycle when it was uniform. Thus the relationship between the recorded electromotive force and the velocity of the gun was obtained.

LINEAR VELOCIMETER

In the linear velocimeter, shown in Figure 10, a helical coil of wire, which can move only in its axial direction, is located in the radial magnetic field between an iron rod and the inner surface of an outer coaxial iron tube. The coil is wound in an annular groove cut in a bakelite tube that slides on the iron rod. The magnetic flux is set up by an Alnico magnet. This flux is uniform in the axial direction for about 6 cm. This uniformity was checked by observing that equal deflections of a ballistic galvanometer were obtained when the coil was suddenly moved through small equal distances throughout this region. These deflections along with known constants of the system were used to determine the voltage which was induced when the coil was moved with unit velocity. The magnetic structure of the accelerometer is fastened to the gun pier and the bakelite tube is attached to the gun barrel in such a manner that when the gun recoils, the velocimeter coil is drawn through the magnetic field without any physical contact between the coil tube and the iron structure.

4.4.9 Accelerometers

DIFFERENTIATORS FOR VELOCIMETER

In addition to the use of the crystal accelerometer described later in this section, gun acceleration was measured with instruments which are in effect devices for differentiating the electromotive force generated by the velocimeter. Two types have been considered and tried, one of which employs a mutual inductance, the other a capacitance in series with a resistance.

Figure 11 is the circuit diagram of the mutual-inductance accelerometer. The principle involved is that the voltage induced in the secondary of a pure mutual inductance is directly proportional to the time-rate of change of current in the primary. Except for some disturbing elements, the output voltage of the generator is directly proportional to the velocity of recoil. The output voltage of the generator is fed into the grid circuit of a 6J7 tube, the plate circuit of which includes the primary of the mutual inductor. The tube is so biased that, for the range of input signal voltage used, the waveform of the plate current is a faithful reproduction of the waveform of the input voltage. Hence the current in the primary of the mutual inductor has the same waveform as the voltage induced in the velocimeter. The voltage induced in the secondary of the mutual inductor is di-

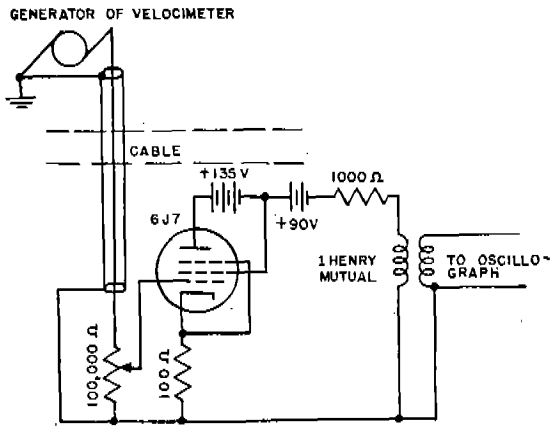


FIGURE 11. Mutual-inductance accelerometer for measuring acceleration of recoil of a gun.

rectly proportional to the time-rate of change of the plate current, and hence the deflection of the oscillograph at any instant is theoretically proportional to the acceleration of the gun. However, difficulties were encountered in the use of this method during the firings of the first 11 rounds.[39]

These difficulties were caused by distributed capacitances in the air-core mutual inductor used. Since then, this inductor has been replaced by an inductor with a magnetic core which had a winding of fewer turns and hence smaller distributed capacitance. A filter was connected between the inductor and the oscillograph to suppress high-frequency oscillations. The resulting improved differentiator has been used as an accelerometer to obtain a continuous record of acceleration from a voltage that at every instant is proportional to the velocity of recoil. It has also been used to record the velocity of recoil from the drop in potential across a slide-wire, namely, the continuous recoilmeter described in Section 4.4.7. Satisfactory records have been obtained.

The type of differentiator using a capacitance in series with a resistance was used on a very limited number of rounds so that insufficient data were obtained to determine its usefulness. However the mutual inductance type had the advantage of being much more simple to construct and use than the capacitance-resistance type. For this reason the mutual inductance type was used in most cases.

CRYSTAL ACCELEROMETER

The crystal accelerometer consists of a piezoelectric crystal having its electrodes connected to a capacitor. The crystal is so cut and mounted that the quantity of electricity developed on its electrodes is proportional to the acceleration to which the crystal and any associated load are subjected. The potential drop over the parallel capacitor is equal to the quotient obtained by dividing the quantity of electricity developed by the sum of the capacitances of the crystal, the line, and the parallel capacitor respectively. The accelerometer impresses on the oscillograph a voltage which is partly the result of the instantaneous acceleration at the point of attachment to the gun and partly the result of the vibrations of the crystal and those of the gun, each at its individual resonant frequency. As the voltages caused by the acceleration of these resonant vibrations may at any instant be several times as large as the voltage produced by the nonvibratory acceleration of the gun, it is necessary to use a filter in the oscillograph circuit to suppress the voltages produced by the resonant vibrations.

The crystal accelerometer embodied a crystal unit made of a newly developed material,[d] ammonium diphenyl phosphate (ADP). The details of its construction and attachment to the gun, the method of calibration of the crystal, and a block diagram of connections of the crystal, cathode follower, filter and oscillograph have been described.[65]

4.4.10 Strain Gauges for Projectile Displacement in the 3-in. Gun

As the projectile passes any given section of the gun, the barrel expands. If the time of occurrence of this expansion is recorded for a number of points along the barrel, a displacement-time curve can be plotted. A record of barrel expansion, as obtained in this manner, is shown in Figure 12. Two types of wire-resistance strain gauges have been used in this project. The first was the Baldwin-Southwark Type C-1, SR-4 gauge, in which the active wire is mounted on a thin paper backing that can be cemented to the

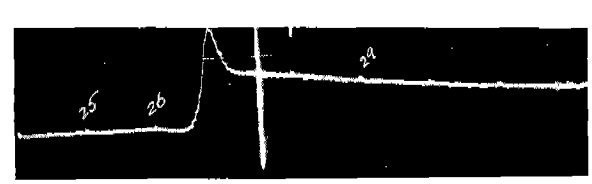


FIGURE 12. Record of strain gauge mounted on the gun barrel.

[d] Furnished by A. C. Keller of the Bell Telephone Laboratories.

surface of the gun. For the purpose of measuring the expansion of the bore, these gauges were mounted so that the long dimension lay in a plane perpendicular to the axis of the bore.

Gauges of the other type were made up directly on the gun, of 1-mil enameled Advance wire, one or two turns of which were wound around the gun and cemented to hold them in place. The principal advantage of this second type of gauge might be that its position can be determined more precisely because it occupies only 0.001 in. of the length of the gun, as compared with 0.16 in. for the C-1 gauge. This was not a practical advantage, however, because the effects of the gun jacket on the strain records make it unnecessary to know the linear position of a gauge more accurately than to 0.3 in.

These strain gauges were used also for measurements of band pressure during rounds 61 through 77. Tangential and axial strains were measured at 90 in. and at 121.2 in. from the muzzle. Measurements of strain were made on the 37-mm gun.

An important limitation of the strain-gauge method, as it concerns the 3-in. gun, is the fact that important parts of the gun tube are covered by the gun slide and the locking ring. The records obtained show that if it were possible to locate the strain gauges 6 in. apart all along the barrel, the signals from all of them could be recorded on one film. The connection of several strain gauges to a single oscillograph requires special design of the electric circuits.[39]

4.4.11 Solenoids for Projectile Velocity on Range

The method used for determining the velocity of the magnetized projectile after ejection is a modification of the camera-chronograph method described in *Army Ordnance Proof Manual*.[289] The changes consist in making the record with a cathode-ray oscillograph instead of a galvanometer, and in passing the transient currents from the solenoids through suitable mixing circuits so that other phenomena can be recorded on the same oscillograph trace.

Each solenoid, of nominally 30 in. diameter, contained 7 layers, of about 35 turns per layer, of No. 26 AWG cotton-enamel magnet wire, impregnated with insulating varnish and baked. Each solenoid was rigidly supported by a wooden frame mounted on one of the concrete piers of the range. In the earlier stages of the investigation four solenoids were used, their distances from the muzzle being 100, 200, 350, and 450 ft.; later, two more were added, one 50 ft, the other 500 ft from the muzzle.

In a few of the later rounds two solenoids, 10 in. in diameter were used. With these solenoids the same deflection of the trace was obtained with the important advantage of considerably fewer turns and hence much less inductance.

In Figure 5, the second curve from the bottom of (A) shows the form of the recorded signal produced by the passage of the magnetized projectile through a solenoid.

4.4.12 Gauges for Powder Pressure

Resistance gauges were usually used to measure powder pressure. In one form of these gauges the longitudinal compression of a piston by the powder pressure changes the resistance of a winding of fine wire cemented to the piston. This winding is preferably applied so that the reflexed wires are parallel to the axis of the piston, as shown in Figure 13. In this type of gauge the effect of the pressure is to decrease the resistance of the winding, the relation between pressure and decrease of resistance being closely linear.

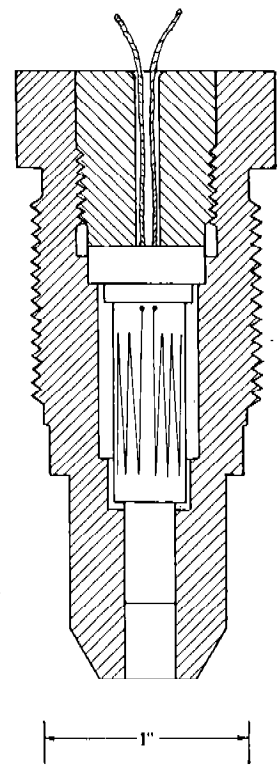


FIGURE 13. Resistance gauge for powder pressure measurements.

Gauges with the winding applied as a helix around the piston are easier to construct but so much less sensitive that a preamplifier was required between the gauge and the oscillograph. In this type of gauge the resistance of the winding increases linearly with the applied pressure.

In a third type of gauge, used for lower pressures (that near the muzzle and in the recoil cylinders), the pressure to be measured is applied to the inside of a thin-walled steel tube having an external helical winding. These gauges were calibrated by applying a known load to the piston and measuring the change of resistance of the winding.

In the early stages of the investigation some use was made of piezoelectric pressure gauges also. After round 19 it was found expedient to use the resistance gauge exclusively because of its greater ruggedness and convenience in calibration. The records obtained from the resistance-type gauges and the piezoelectric-type gauge may be compared by referring to Figure 47 of NDRC Report No. A-229.[39]

4.4.13 Radiation Pyrometer for the Measurement of Powder-Gas Temperature

The method of measuring the temperature of the powder gas is given in Section 2.5.5. Both the two-color pyrometers and single-color pyrometers described in Section 2.5.4 were used. The single-color pyrometers required less recording apparatus than the two-color. At least two oscillographs and their recorders were required for each two-color pyrometer, whereas a single oscillograph and recorder sufficed for the single-color pyrometer. In any given round, the number of locations at which temperatures were recorded was usually limited by the number of oscillographs available.

4.4.14 Microwave Interferometer

The motion of the projectile in the bore has been studied by means of a microwave interferometer,[108] with which the distance from the projectile to the

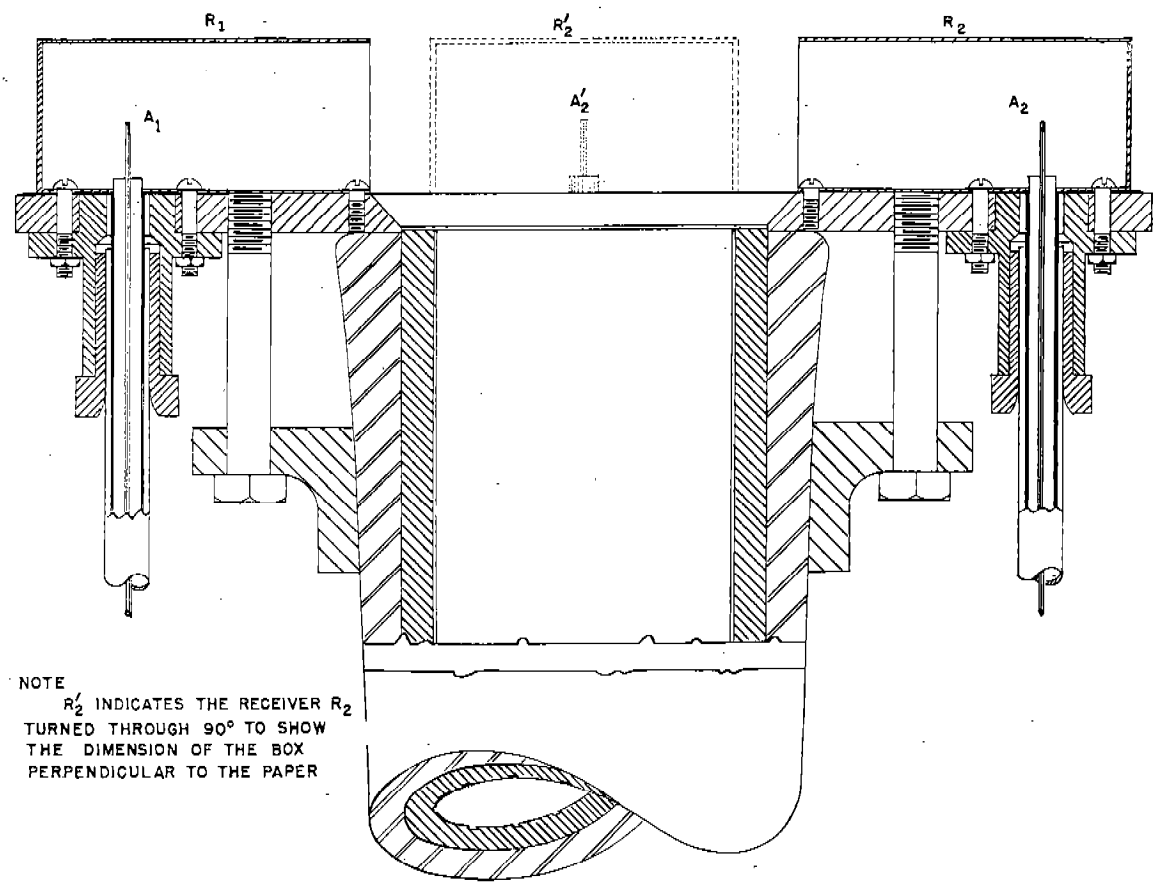


FIGURE 14. The radiator (R_1) and receiver (R_2) of the microwave interferometer, with their antennas (A_1 and A_2), attached to the muzzle of a gun.

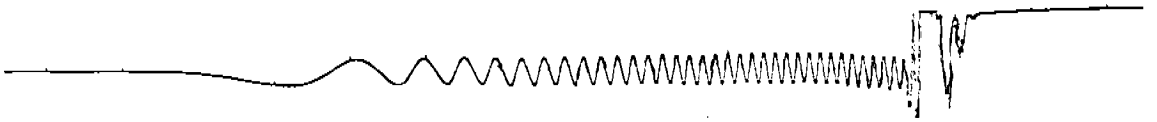


FIGURE 15. Oscillograph trace of microwave interferometer.

muzzle is measured continuously by reflected electromagnetic waves several centimeters in wavelength. A beam of radiation is directed across the muzzle from a simple radiator, R_1, to an identical receiver, R_2, shown in Figure 14. A_1 and A_2 are antennas. Part of the beam enters the gun and travels down to the projectile; here it is reflected and returns to the muzzle, where it is picked up by the receiver. If at this point the reflected wave is in phase with the direct wave, the received signal is a maximum; if it is opposite in phase the signal is a minimum. Thus while the projectile is moving along the bore the signal passes through a series of maxima and minima as the path of the reflected beam is shortened. The signal from the receiver is demodulated by a crystal detector and applied to an oscillograph. Figure 15 shows a sample of the resulting record.

The calibration of the microwave interferometer was done by placing the projectile manually at definite positions in the gun and reading the deflection of the galvanometer in the receiving circuit. This was done in steps of 0.01 or 0.02 ft from an arbitrary reference point. The abscissa at each maximum and minimum of the oscillograph trace obtained in a firing gave the time of arrival of the projectile at a position which is given by the abscissa at the corresponding maximum or minimum of the appropriate calibration curve. Additional points were also obtained at intermediate points, especially near the start of motion. From the positions of the maxima and minima about 70 values of position and of time were obtained.

It is essential, both in calibrating and in firing, that the same sending wavelength and the same type of projectile be used. The shape and structure of the projectile nose modify the waveform of the detector current, the waveform being particularly influenced near the beginning of travel and as the projectile approaches the muzzle.

The use of the microwave interferometer requires that the generator wavelength be within the limits $2.62r$ and $3.42r$, where r is the radius of the bore of the gun:[46] hence the wavelength used was nearly 10.5 cm for the 3-in. gun and 5.0 cm for the 37-mm gun. Outside of these limits, more than one mode of vibration appear, and the pattern is no longer simple.

The interferometer method assumes that the positions of maxima and minima are the same when the gun is fired as they were during the previous calibration. However, when the gun is fired, the gas that is being pushed out of the bore by the projectile is highly compressed and may include some ionized powder gas that has leaked past the projectile. Consequently, the dielectric constant may differ significantly from that of empty space, and the positions of the maxima and minima may be shifted somewhat. The microwave-interferometer values were checked against barrel-contact values and the agreement was always within 0.02 ft.

4.4.15 Optical Ejection Indicator

An optical system was arranged to send a beam of light perpendicular to the axis of the gun and to focus it on the axis a few millimeters in front of the muzzle. This beam was collected by a lens on the opposite side of the muzzle and illuminated the sensitive surface of a photoelectric cell. It was expected that, when the nose of the projectile cut the beam at the focus, the light would be cut off from the photoelectric cell, causing a deflection on the recording trace and indicating the instant of ejection. However, it was found that smoke or other obscuring gases preceding the projectile gave a false indication of ejection. It was discovered in the records on the 37-mm gun that at the time the base of the projectile was ejected, the light from the hot gases produced a very sharp deflection of the record from the photocell.

4.4.16 High-Speed Cameras

The smoke and flash were photographed by two types of cameras. One was a high-speed movie camera run at a speed of 3,000 pictures per second. The other camera was one in which the film was mounted on a rotating drum and which had a set of shutters of the focal-plane type under a row of lenses. A second shutter opened in synchronism with the firing of the gun. Successive pictures of a point were about 3.5 in. apart on the film and the time between pictures was approximately 2.5 msec. The movie camera made

more pictures per second than the drum camera but had to be brought from rest to the correct speed at the correct time to record the desired event, which made synchronizing difficult. It also required intense illumination. The drum camera was more easily handled and did not require as intense illumination as the movie camera.

4.4.17 Flashmeter

The flashmeter used to measure the intensity of the muzzle flash consisted of a radiation pyrometer mounted on the end of a 2-in. tube. The pyrometer is the same as used for the measurement of gaseous radiation from the powder chamber. The tube was pointed at the point where it was desired to measure the flash intensity.

4.4.18 "Microflash" Equipment

The "Microflash" apparatus[e] and cameras were placed inside a small hut which had pipes about 14 in. in diameter extending 18 in. outside in the direction of fire. The projectile passed through the pipes and a microphone actuated by the bow wave of the projectile triggered the microflash when the projectile was in the center of the hut. The shutters of the cameras were opened when the gun fired and remained open until the projectile had passed.

4.4.19 Comparator for Distance Measurements on Films

The data obtained in a firing are recorded in the form of a set of oscillograms from which the times of all events and the magnitudes of certain events must be determined. The time coordinate is determined by making distance measurements along the length of the film and interpolating between the timing pulses. Distance measurements made at right angles to the line of motion of the film give values of those quantities for which there is a continuous record. Both of these kinds of measurement are made with a comparator.

The comparator consists of a heavy metal frame about 120 cm long, 30 cm wide, and 30 cm high, on which a traveling carriage rests at an angle of 45° from the horizontal. The carriage, driven by a screw, has a range of about 90 cm longitudinal motion. Two long glass plates for holding the film, illuminated from below by a green fluorescent light, are set about 6 cm below the carriage and parallel to it. On the carriage itself are the observing microscope, supported on a Gaertner micrometer slide, and an auxiliary microscope moved by a micrometer screw. The slide has a range of 10 cm and a precision of 0.001 cm. All crosswise distance measurements were made with it.

Running along the top of the comparator frame is a scale, 100 cm in length, divided in millimeters. It is not a precision scale, but is more than accurate enough to give the position of the carriage to the nearest millimeter. Below the carriage, in a position such that the auxiliary microscope on the carriage can be focused on it, is an Invar meter bar made by the Geneva Society, divided in millimeters and accurate to within 0.0003 mm at 20 C. The two scales are rectified by setting the carriage approximately on a millimeter division mark on the top scale, setting the cross hair of the auxiliary microscope on a millimeter division of the meter bar and then, while holding the micrometer screw fixed, turning the micrometer scale (which is held by a friction clamp) until the zero mark of this scale coincides with its fiducial mark. The scales remain sufficiently well in alignment over the entire length of the film so that there is no uncertainty.

The micrometer screw attached to the auxiliary microscope has a pitch of 1 mm, and its head is divided into 100 divisions. Thus the longitudinal position of the observing microscope is given to 1 mm by the top scale and to 0.01 mm by the reading of the micrometer screw when the cross hair of the auxiliary microscope is in coincidence with a millimeter division of the meter bar. Although fractions of a hundredth of a millimeter could be estimated on the micrometer screw, the error of setting the cross hair on the divisions of the scale may be as much as 0.01 mm.

4.4.20 Protractor for Differentiating Curves

The instrument shown in Figure 16 furnishes a rapid and simple method for graphical differentiation. A steel protractor, divided in degrees with a vernier reading to 5 min, is equipped with a gear for slow motion. It is attached to the straightedge of a drafting machine. The sheet carrying the curve to be differentiated is placed on the drawing board so that the axis of abscissas is parallel to the straightedge. The center of the protractor circle is placed at the point where the slope is required. The protractor is then turned

[e] Made by the General Radio Company, Cambridge, Massachusetts.

until its edge is tangent to the curve at that point, and the angle is read. The derivative at that point is directly proportional to the tangent of the angle.

4.5 PROJECTILE GAUGES FOR INTERIOR BALLISTIC MEASUREMENTS

4.5.1 Introduction

In addition to the comprehensive ballistic investigations at Carderock, described in the earlier sections of this chapter, Division 1 sponsored the development of techniques and instruments for making ballistic measurements directly on a projectile moving in the bore of a gun. The quantities to be measured were displacement, velocity, and acceleration of the projectile, pressure on the base of the projectile, and friction between the projectile and the barrel.

The basic principles[5] involved had been developed by Section T of Division A, NDRC. Then the Geophysical Laboratory of the Carnegie Institution of Washington undertook to perfect for Division 1 an experimental routine for use with different sizes of projectiles.[46]

4.5.2 Wire-in-Bore Technique[f]

The basic technique for these measurements was that of making contact with the moving projectile by

[f] A similar technique had been developed by the British at about the same time.[337]

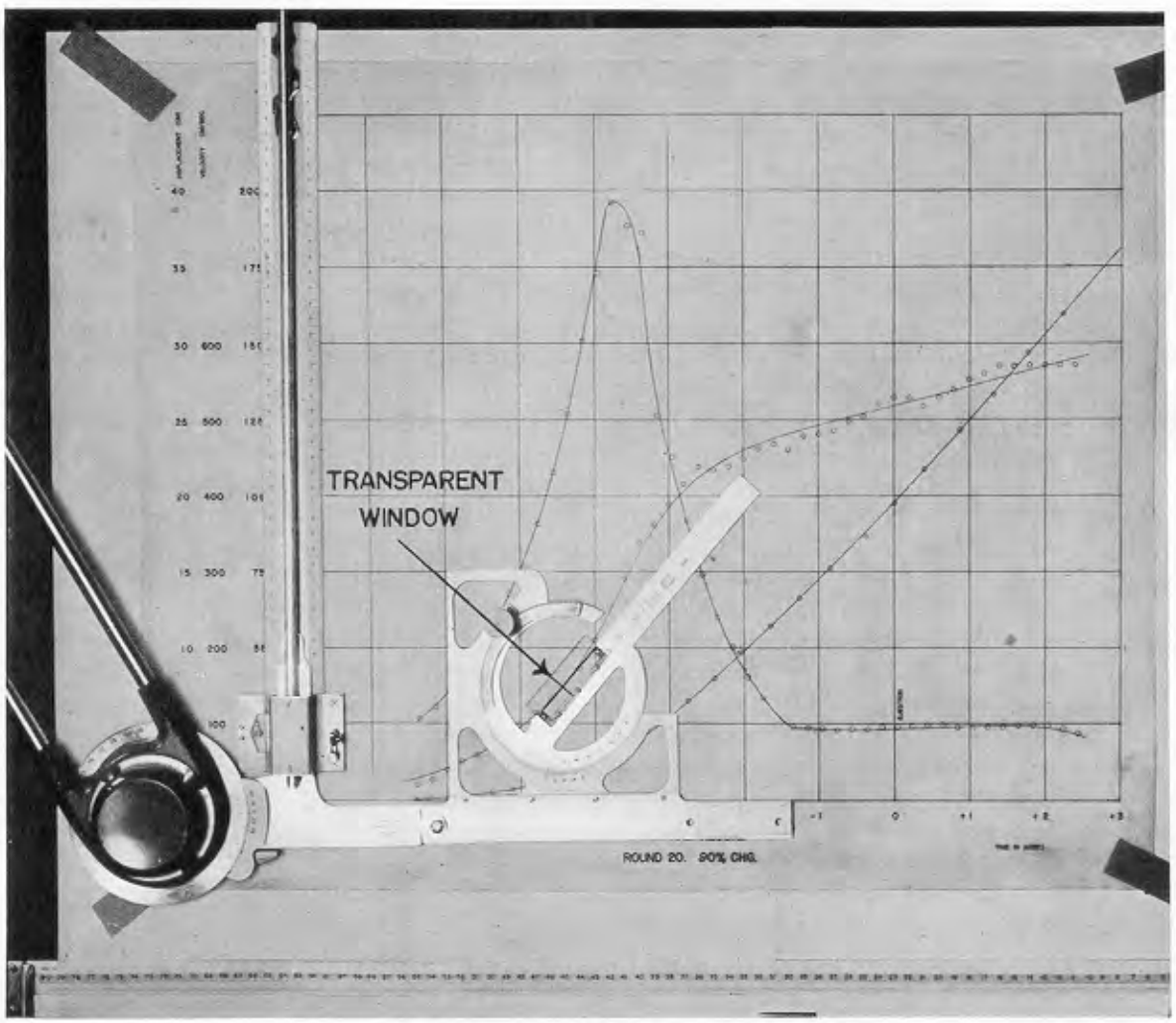


FIGURE 16. Protractor modified for differentiation of a curve.

CONFIDENTIAL

means of a wire stretched coaxially within the bore of the gun from the nose of the projectile to the muzzle and picked up by a "collector cup" on the nose of the projectile. By making electrical contact with the projectile in this way, many types of measurement are possible, for any phenomenon associated with a projectile that can be converted into an electrical signal may be measured.

Projectile Displacement

The simplest application of this technique was to measure the displacement of a moving projectile by measuring the change of resistance of the wire as its length became less. This was done by recording with an oscillograph the variation of the voltage across the ends of the wire while a small constant current was passed through it. A lead lining in the collector on the nose of the projectile was found to be necessary for maintaining good electrical contact. The oscillographic trace showed fluctuations in the resistance of the contact between the projectile and the bore surface before the rotating band was engraved.

Improved Obturation

An apparent decrease in the resistance of the wire at the beginning of motion of the projectile was attributed to heating of the wire by powder gas that had leaked past the projectile. Several methods were undertaken to improve obturation. One method provided, to a degree, an initial seal which was effective only until the band was engraved. It consisted in spinning up one or more skirts of metal from the band with a cutting tool. Thus modified, the projectile had to be forced home in loading. The spun skirts gave no added obturation after the band passed through the forcing cone. The other method for improving obturation was the use of the Bridgman "unsupported-area pressure seal," referred to as a "hydraulic obturator." Various combinations of the two methods of obturation were tried; the most effective was found to be the hydraulic method in combination with two skirts spun up on the band.

With this best method of obturation, various kinds and sizes of wires were tried, in particular those kinds having a low temperature coefficient of resistance. It was found that No. 34 manganin wire gave the best-appearing traces. The magnitude of the overall error in measuring the displacement in the 20-mm gun was estimated as ± 3.2 cm. For comparison, measurements were made using the microwave technique,[g] for which the error was found to be less than one-third as large.

4.5.3 Piezoelectric Crystal Gauges

The wire-in-bore technique described in the previous section made it possible to obtain a signal from a piezoelectric crystal gauge located in a projectile and subjected to various forces associated with the motion of the projectile in the bore of a gun. Such gauges were developed for the measurement of acceleration, base pressure, and bore friction.[5]

The chief difficulty in making these gauges was in designing the component parts small enough to fit into 20-mm projectiles and yet strong enough to withstand the high acceleration (100,000 g) to which they were to be subjected during firing. Thus in order to reduce crystal breakage it was possible to use only one crystal, although a stack of three would have been preferable as far as the strength of the signal was concerned. Mechanical refinements had to be introduced, such as ball-and-socket joints to equalize the pressure over the surface of the crystal.

The general qualitative results obtained by the use of the crystal gauges may be briefly stated as follows. The signal traces obtained from the three types of gauges were consistent in shape during the first one-third of the travel time. The last part of the trace was anomalous in all cases; furthermore, the anomaly was not consistent in size or in shape. Special experiments showed that this part of the signal was associated with the leakage of ionized propellant gas past the projectile as it traveled through the bore. No effective way was found to reduce to an insignificant amount the spurious signals from this cause. For the first fourth of the travel of a 20-mm projectile the maximum error of the acceleration gauge amounted to ± 10 per cent, that of the base-pressure gauge ± 5 to 10 per cent, and that of the bore-friction gauge ± 10 to 20 per cent for starting friction and ± 40 to 60 per cent for running friction.

Preliminary experiments[46] with some 3-in. projectiles fitted with crystal gauges and fired from the

[g] The microwave interferometer described in Section 4.4.14 was an outgrowth of an apparatus developed as part of this project for measurement of the displacement of a projectile in the bore of a 20-mm gun.[46] After the possibility of such a measurement had been suggested by Dr. T. H. Johnson of the Ballistic Research Laboratory, Aberdeen Proving Ground, parallel development of apparatus for the purpose was carried out there and by Division 1 at the Geophysical Laboratory.

3-in. gun at Carderock showed that the leakage of powder gas past the projectile was equally as serious as in the 20-mm gun. The record was unreliable during the last 4 msec of travel time, that is, after the projectile had traveled 50 cm, which is only about one-seventh the length of travel. During the first part of the travel the maximum uncertainty was estimated to be of the same order of magnitude as for the 20-mm gun. Most of this uncertainty was caused by gas leakage. Thus these gauges are not satisfactory unless some more effective means of obturation can be found.



Chapter 5

HEATING OF GUNS DURING FIRING

By *H. L. Black*[a] and *G. Comenetz*[b]

5.1 INTRODUCTION

IN ATTACKING the problem of hypervelocity, the direct approach would seem to be that of increasing the energy of the powder charge. This could be done quantitatively by increasing the amount of powder or qualitatively by using a powder with higher potential. The limitations of the former method are well known. When the latter method is used we encounter higher flame temperatures, and the resulting temperature of the gun bore surface becomes seriously high. If we combine with this increased flame temperature the high rates of fire maintained in automatic weapons, the question of heating of guns during firing is critical. The thermal effects are an important factor in erosion and in addition lower the tensile strength of the gun metal. Division 1 was therefore interested in the study of the heat input to the gun, the distribution of heat in the barrel, the temperature of the bore surface, and in methods of gun cooling.

As a result of these studies, our knowledge concerning heat input from a single round, input from a burst or a series of bursts, temperature attained by the bore surface, critical temperatures in firing, and methods of cooling has been greatly extended. The application of this knowledge in the development of improved machine gun barrels by lining or plating them has been of definite value and will aid in the design of future hypervelocity guns. In particular, these temperature investigations show that to combat the effects of heat input we must look to the development of alloys with physical qualities which will make them satisfactory as liners or coatings for the bore surface at temperatures above the melting point of steel. The search for such alloys is reviewed in Chapter 16.

A better understanding of the heat input from band friction and its combination with that from powder gases is to be desired. Similarly, the effect of thermal stresses taken in combination with band and powder pressures should be more completely analyzed as an aid to the designer. We may expect improved experimental methods of measurement of the bore surface temperature. Finally, methods of cooling under service conditions certainly need to be improved.

5.2 HEAT INPUT TO THE BORE SURFACE

5.2.1 Magnitude of the Energy Loss

A complete analysis of the distribution of the energy of the charge is given in Section 6.5. Here we are particularly concerned with the percentage of the energy expended in heating the gun; for purposes of comparison, however, it is convenient to compare this with the kinetic energy of the projectile at the muzzle. It is customary to consider heat transferred to the cartridge case as going to the barrel.

Experiments[516] as early as 1870, in which rifles using black powder were tested, indicated that from 31.7 to 39.3 per cent of the total energy of the powder was absorbed by the barrel. A later investigation[442] with guns gave a heat input ranging from 4.2 to 17 per cent of the powder potential. The energy balance for one shot fired in a rifle has been determined in a series of carefully controlled experiments.[450]

Since 1936 a number of measurements and calculations of energy distribution have been made. Table 1 presents the results obtained by a number of experimenters for various guns. In Tables 2 and 3 are given calculated values for typical guns in a similar range of calibers.

These tabular percentages do not, of course, represent results which are completely comparable. The powders used vary; however, for the larger guns, all powders have flame temperatures close to 2500 K. In Section 15.5.3 it is shown that heat input is a linear function of the flame temperature of the powder in a caliber .50 gun.

The data available are too limited to draw a valid conclusion as to the functional relationship between caliber and heat input; it is, however, apparent that as caliber increases, the percentage of the powder potential transformed into heat decreases. This is in line

[a] Technical Aide, Division 1, NDRC. (Present address: Department of Mathematics, Michigan State College, East Lansing, Michigan.)

[b] Mathematical Physicist, Geophysical Laboratory, Carnegie Institution of Washington. (Present address: Westinghouse Research Laboratories, East Pittsburgh, Pennsylvania.)

TABLE 1. Percentage of energy of powder lost by heating of gun compared to that acquired by the projectile measured for various guns.

	Cal .30 rifle[450]	Cal .50 MG[182,183] (1)	(2)	3-in. AA, M3[179] (1)	(2)	3-in. Navy[65] gun
K. E. of projectile	33	29	28	29	32	27.7
Heating of gun	22	19	16	11	9	6.3

Note. Caliber .50 MG: (1) water-cooled barrel fired without water-cooling jacket; (2) air-cooled heavy barrel. Three-inch AA, M3: (1) with Pyro powder; (2) with NH powder.

TABLE 2.* Percentage of energy powder lost by heating of gun compared to that acquired by the projectile—calculated for U. S. guns.[48]

Gun	Cal .50	37-mm	3-in.	4.7-in.	8-in.	16-in.
K.E. of projectile	29	32	23	27	25	26
Heating of gun	18	14	8	8	7	5

* Compare Table 2 of Chapter 3 which gives for these same guns corresponding values for the heat loss just to the time of ejection.

TABLE 3.* Percentage of energy of powder lost by heating of gun compared to that acquired by the projectile—calculated for British guns.[348]

Gun	2-pr. (1.57 in.) S.C. Cordite,			25-pr. (3.65 in.) Cordite	8-in. Mk. VIII Cordite
Propellant	slotted tube			W .057	S.C. 205
Travel (calibers)	36.67	55.01	73.32	22.06	43.32
K.E. of projectile	20.7	26.9	31.1	41.8	40.3
Heating of gun	4.7	6.5	8.1	4.6	4.7

* The method of calculation is that described in Section 5.4.1 under "Method of Hicks, Thornhill, and Ware."

with the theory that most of the heat is transferred from a laminar layer of gases relatively close to the bore surface, rather than from the main gas stream, which occupies a larger percentage of the total volume in larger guns.

5.2.2 Sources of Heat Input

Studies of the causes of heat input to the bore surface are numerous in ballistic literature.[144,348,505] The sources may conveniently be classified as follows: (1) radiation from the hot powder gases; (2) input from gas leakage past the rotating band; (3) heat of engraving and friction; (4) transfer from the gases in a laminar layer near the bore surface.

RADIATION

Radiation is an unimportant source of heat input. In the heat transfer equation,

$$Q = \sigma\, \epsilon_1 \epsilon_2\, (T_g^4 - T_s^4). \qquad (1)$$

it has been shown[12] that for a gas temperature of 2500 K above that of the surface, the maximum rate of transfer is 53 cal per sq cm per sec. T_g is the gas temperature, T_s the temperature of the bore surface, ϵ_1 and ϵ_2 are the emissivities, and σ, has the value 1.36×10^{-12} cal per sq cm per sec per fourth power of the degree of temperature. At this rate the bore surface temperature would be raised only about 36 centigrade degrees during the firing of the very largest guns.

HEAT OF ENGRAVING AND FRICTION

There has been a great deal of argument as to the importance of mechanical effects as sources of heat input.[c] Thus as recently as 1925 it was suggested on the basis of extensive experimentation "that the main source of heating of the bore does not lie in the transfer of heat from the powder gas to the wall of the barrel but in the mechanical work (friction, engraving by the rifling, and so on) which is converted into heat." This, however, was a minority opinion, and the review continued: "It is to be hoped that still further investigations may be carried through in order to solve the interesting question as to the causes of the heating of the bore."

With this in mind, it was decided by Division 1 to make experimental determinations of the heat input from engraving and friction using new methods of measurement.[72] Because of the interest in pre-engraved projectiles (Section 27.3), a logical first approach seemed to be by a comparison of the input with ordinary and with pre-engraved projectiles under otherwise identical conditions.

First measurements were made by the calorimetric ring method described in Section 5.4.3, and an early report stated, "Preliminary results show only little variation in the difference of heat input values for standard and pre-engraved M2 bullets measured at

[c] Opinions of some of the writers were summarized by Cranz.[144, 505]

[redacted]

the forcing cone against values of that difference determined in back of the origin of rifling, thus indicating that the heat of engraving is rather small compared with the total heat input to the bore." Later measurements during firings supported this position, but it was considered advisable to attempt a direct determination of the heat of engraving and friction.

For this purpose a falling-weight apparatus was devised. A heavy carriage dropped from a maximum height of 64 ft struck a piston which in turn forced a bullet through an "engraving ring." This was a short section of a caliber .50 barrel placed vertically and supported by a hollow metal cylinder. The ring acted as a calorimeter; from its rise in temperature the heat input from friction and engraving was calculated. Formulas due to Jaeger were used to extrapolate to velocities of the order of those attained in actual firings. The results indicated an input for ball bullets, M2 of approximately 1.3 cal/cm^2 near the beginning of travel, decreasing to 0.6 cal/cm^2 toward the muzzle. This value compares with a total heat input during firing of the order of 10 cal/cm^2.

For reasons which will be discussed in Section 5.4.4, this input does not, however, cause a very large variation in the maximum bore surface temperature. This seeming contradiction explains the varying estimates of the contributions of engraving and friction to heat input. One such estimate[397] of their importance has been given as follows: "During the engraving of the driving band, a short section of the barrel surface near the commencement of rifling may, at worst, be raised to the melting temperature of the band for a small time interval. Temperature calculations are made, including a liberal estimate of this heat transfer, but it is not found to produce sudden large increases to temperatures above the melting point of the barrel, and in the 8-in. gun gives an increase of only 200 centigrade degrees in the maximum surface temperature at the commencement of rifling. This estimate is probably several times too great." This question of the effect of input from the rotating band, in combination with input from the gases, is discussed in Section 5.4.4.

Frictional heat input will continue even after engraving is considered complete. It is generally agreed, however, that this is relatively unimportant and that it causes a negligible increase in maximum bore surface temperatures. Friction does, however, add appreciably to the strains upon the gun.[39,65,113] It is also important to consider the melting of the metal of the rotating band,[556] which causes coppering of the bore. Even here the effect is not so great as might be expected because the higher diffusivity of the common band materials tends to more than counterbalance the lower melting point. This is brought out in the theoretical discussion in Section 6.2.2.

By assuming that the rotating band in a 37-mm gun, M3 rises to a maximum temperature 1000 centigrade degrees above the temperature of engraving, a coefficient of friction of 0.03 was calculated.[45] Based on this value, curves for rates of heat generation and conduction were plotted against time, and for heat transferred to the bore surface as a function of position in the bore. It was concluded that conduction into the bore reached a maximum slightly above 2 cal/cm^2.

Transfer from the Gases in a Laminar Layer Near the Surface[d]

This brings us to the consideration of the source of input now generally considered the most important, transfer from the hot powder gases. The powder gases rush past the bore surface at a velocity of the order of 1,000 fps, and heat is transferred by forced convection. For the gas flow we may use the theory for an incompressible fluid; this is justified on the basis of experiments[496] that showed that the shearing stress on the wall of a pipe (or gun) is the same for compressible as for incompressible fluids at the same Reynolds numbers.

If now we consider the motion of the gases as turbulent, it nevertheless is true that the velocity near the walls remains laminar, although with a large gradient. At some distance δ from the walls, the velocity approaches its midstream value; and although the value of δ is not sharply defined, this laminar layer is referred to as a film. The film thickness and, hence, the rate of heat transfer depend on the condition of the bore surface.

The heat transfer coefficient h may be defined by,

$$Q = h\,(T_g - T_s) \qquad (2)$$

in which Q is the actual rate of heat transfer, while T_g and T_s are, respectively, the temperature of the powder gas (beyond the laminar layer) and of the bore surface. The aim of the hydrodynamic analysis is to

[d] A standard work on heat transfer is that of McAdams;[513] for related hydrodynamic problems, Goldstein[507] may be consulted. Fundamental theory discussed in these works is referred to in NDRC Reports A-87, A-201, and A-262. The following discussion is based largely on these three reports.

evaluate h in terms of the state of the gas and the condition of the bore surface. Because it is difficult to specify the latter precisely, that is, to define the degree of roughness of the particular wall, no purely theoretical formula can be given with perfect confidence. A productive procedure,[48] however, has been to obtain an expression for h with one adjustable constant that is related to the roughness of the wall; and to calculate from the observed heat transfer at various positions in various guns an empirical value of this constant that might be applicable to the bore surface of all guns. This procedure has proved fairly successful, because the heat transfer coefficient is not very sensitive to minor variations in roughness. Measurements of the friction when water flowed through rifled and unrifled caliber .50 barrels showed that the presence of the rifling made only a negligible difference.[105]

The fundamental hydrodynamic expression for h (expressed in calories per square centimeter per second) is given by

$$h = \tfrac{1}{2}\lambda c_p \rho U \tag{3}$$

where c_p is the specific heat, ρ the density, U the velocity of the powder gas, and λ is an empirical constant, the friction factor or Fanning coefficient. λ is related to the bore diameter and to a roughness parameter r, which measures the average size of the irregularities on the bore surface. Different expressions of this relationship are required if the surface is hydrodynamically "smooth" ($r < 10^{-5}$ cm), or "rough" ($r > 10^{-5}$ cm). The latter condition almost certainly applies in guns.

The application of equation (3) to the calculation of bore surface temperatures and heat input is discussed in some detail in Section 5.4.1. The preferred analysis[48] of the most careful measurements[71] of heat transfer near the origin of bore of a caliber .50 barrel leads to the value of λ given by

$$\lambda = (14.2 + 4 \log_{10} D)^{-2} \tag{4}$$

where D is the caliber of the gun in centimeters.

In some computations, described in Section 5.4.1, equation (3) has been simplified. Using an average ballistic value for c_p, and expressing ρ in the convenient units of grams per cubic centimeter, and U' in 1,000 fps, we have for rough pipes,

$$h = 10{,}400 \lambda \rho U'. \tag{5}$$

For smooth pipes, h may be evaluated in terms of $\rho U'$. Tables of the dependence have been given,[12] and the results may be approximated to yield

$$h = 8.9(\rho U)^{0.8}. \tag{6}$$

These last two equations are probably not so adequate as the empirical expression (4), although the results to which they lead, as described in Section 5.4.1, do not differ greatly.

Most of the calculations of bore surface temperature and of heat input, including the one from which equation (4) was derived, have been based on the assumption that input from sources other than transfer from the gases was relatively unimportant. Actual input as determined by measurements by thermocouples (Section 5.3) give approximate figures for the transfer at various positions along the barrel and therefore may be used to check the assumptions. It is perhaps significant that in the cases of the 37-mm gun, T47 and the 3-in. gun at Carderock, described in Chapter 4, the experimental results show a slightly greater decrease toward the muzzle than was calculated by the methods of NDRC report A-262.[48]

For example, in the 3-in. gun, near the origin of rifling, the experimental results[106,113] indicate an input, using two different methods, of 25.8 and 26.7 cal/cm^2, whereas the calculated input was 24.6 cal/cm^2. Nearer the muzzle, however, the calculated inputs were from 20 to 30 per cent *higher* than those observed. In the case of the 37-mm gun, T47, using FNH-M5 powder and firing 1.62-lb projectiles with a muzzle velocity of 3,600 fps, the measured input near the origin averaged 23.5 cal/cm^2 as compared with a calculated value of 24.6; whereas with the cooler M1 powder the actual results were 16.4 cal/cm^2 as against a calculated value of 14.1. Again, nearer the muzzle the observed values fell below those calculated.

These results constitute good confirmation of the general methods employed in calculating the heat input to the bore surface. The divergences between theory and experiment may be due to several causes. Neglect of the frictional contributions to the heating, both in the standard gun from which equation (4) was derived and in other guns, would lead to divergences of the order of 1 to 2 cal/cm^2, if the frictional heat varies relative to the total heat; the ratio of frictional to total heat is certainly greater near the origin. The situation is further confused by the fact that the theoretical basis of Nordheim's tables involves the total heat transfer *from the gases*, whereas the empirical calibration factor that is used to derive equation (4) involves the total transfer from the gases, friction and all other causes.

[redacted]

Variations in surface roughness sufficient to cause variations in heat input may occur between guns, and even at different points along the bore of the same gun. Finally the actual ballistics may differ from those assumed in making the calculations; for example, the theory takes no account of a possible temperature gradient in the powder gas down the barrel, such as has been observed (cf. Section 6.5.1). It is clear that although the fundamental concept that heat transfer is principally due to forced convection is soundly based, a much greater body of experimental data is necessary before we can specify the reliability of the results to a degree which will enable us to separate the effects of the various factors.

5.3 METHODS OF MEASUREMENT OF HEAT INPUT

5.3.1 Overall Calorimetric Methods

The early attempts to measure heat input were largely of a direct calorimetric type. One investigator[516] measured the rise in temperature of mercury with which the bore of a rifle was filled; from this rise the heat input was calculated. In a later experiment[442] the hot gun barrel was put in a water bath.

This method was also employed in a more precise determination described[144,505] as follows: "The barrel of the gun . . . was surrounded by a thin-walled cylindrical sheet-metal jacket of about 4.5-cm diameter, extending from the muzzle almost to the breech . . . during the firing, gun and metal jacket were enclosed in a wooden box. The jacket was filled with 1.2 liters of water, so that the entire barrel was in a water bath. A stirring ring was moved up and down in the water. The water equivalent [thermal capacity] of the whole arrangement was obtained by passing steam through it."

It has been pointed out[144,505] that a rough determination of input is possible with the aid of a machine gun having a cooling jacket; but the hypothetical example given was based on the assumption of constant input per round. This method was applied[475] to a Maxim caliber .30 q.f. rifle, with the following results: "If this quick firing rifle be originally at about 60°F it will boil water after firing about 600 rapid rounds in about 1¼ min.; it will then continue to evaporate water at the rate of 1½ pints per 1000 rapid rounds [about 2.2 minutes]." From these data a heat transmission of 133,363 Btu per square foot of outer surface per hour was computed and it was concluded finally that the heat absorbed was nearly twice the muzzle energy. The corresponding estimate of the maximum bore surface temperature, using Fourier analysis, was only 600 F.

This method may be applied to obtain the approximate input in a water-cooled 40-mm Navy gun on which temperature measurements were taken. Inlet and outlet water temperatures were read for bursts of 50 and 100 rounds under almost identical conditions, and for a 150-round burst with slight variation. Consistent results were obtained in the three cases. Using the first as an illustration, the burst was fired in 25 sec; a peak temperature 25 centigrade degrees above the original was attained almost immediately afterward. Equilibrium inlet and outlet temperatures were reached approximately 3½ min later at a value 14 centigrade degrees above the initial value. The net input per round after this period of cooling is 6.0 cal/cm² of bore surface; if it is assumed that all the water reached maximum temperature, the average input per round is 10.8 cal/cm². It should be remarked that the reduction of input with successive rounds is not so great as in a gun without water-cooling.

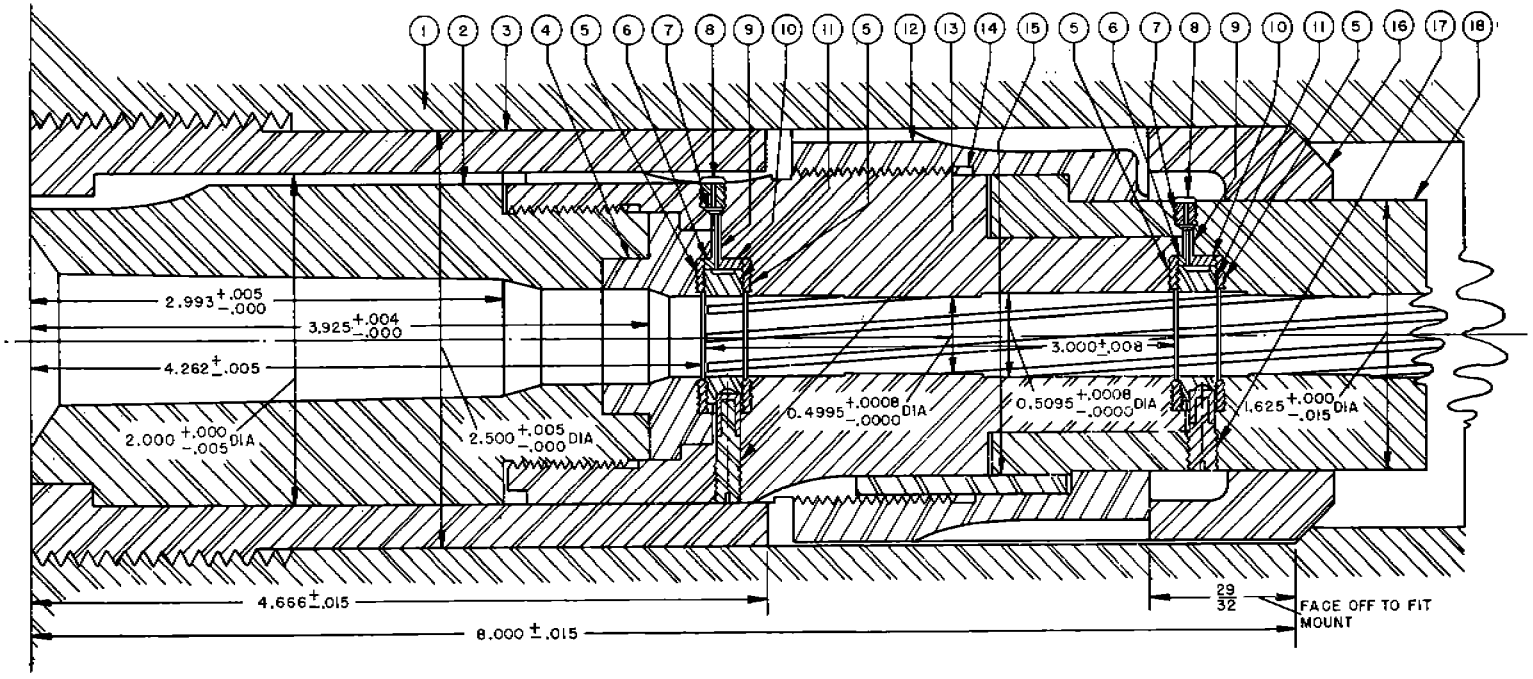
In studies[182,183] at Aberdeen Proving Ground of the heat transferred to the cartridge cases of caliber .50 machine guns, both air-cooled and water-cooled, the temperature rise of a quantity of water into which the cases were dropped during the firing was measured by means of a mercury thermometer.

5.3.2 Artificial Heating of the Barrel

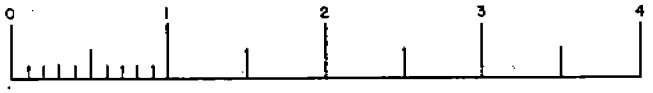
A natural approach to the study of heat input during firing is to reproduce by other methods the temperature distributions that have been observed during firings. Such an investigation[450] was carried out using a rifle barrel itself as a resistance thermometer. A shot was fired every 30 sec until a "quasi-stationary state" was reached, with an average barrel temperature of 122 C. In the second part of the experiment, an insulated manganin wire was passed through the barrel, and then heated by current from a storage battery until an equivalent state was reached by the barrel. The input from the wire was calculated, and from this the heat introduced by one shot was computed to be 624 calories. This represented an average input to the hot barrel.

A refinement of this method has been reported by British investigators.[398] Rounds are fired at a rate such that a steady external temperature distribution





ALL DIMENSIONS IN INCHES UNLESS OTHERWISE SPECIFIED



NO.	NAME OF PART	MATERIAL
1	GUN BARREL MODIFIED	STEEL
2	GUN BREECH	NO.4150 STEEL
3	SLEEVE	STEEL
4	RETAINING RING	NO.4150 STEEL
5	INSULATING GASKET	CLOTH BAKELITE
6	SPACER	CLOTH BAKELITE
7	PACKING GLAND WASHER	NO.5565 FAIRPRENE
8	PACKING GLAND SCREW	DRILL ROD
9	INSULATING TUBING	HARD RUBBER
10	SPACER	CLOTH BAKELITE
11	CALORIMETRIC RING	NO. 4150 STEEL
12	NUT	NO. 4150 STEEL
13	SCREW PIN	STEEL AND BAKELITE
14	BARREL SECTION	NO.4150 STEEL
15	1/8 IN. X 1/8 IN. KEY	COLD-ROLLED STEEL
16	SPACING COLLAR	COLD-ROLLED STEEL
17	SCREW PIN	STEEL AND BAKELITE
18	GUN MUZZLE MOD	NO.4150 MOD (USA-57-107-25)

FIGURE 1. Calorimetric rings in gun. (This figure has appeared as Figure 1 in NDRC Report No. A-399.)

along the barrel surface is established and maintained; this distribution is recorded by means of thermocouples. An electrical heating coil constructed of a spiral of resistance tape on a refractory form is then inserted into the barrel. The spacing of the turns of the tape is adjusted until the same steady external temperatures are obtained. The electrical energy dissipated is measured. From these data, the heat transfer per unit area of the bore surface per round can be deduced. It should again be noted that this will give results for transfer to a "hot" barrel. The method is not satisfactory for points near the origin of rifling.

5.3.3 Calorimetric Ring Method[71]

Several methods of heat input measurement have been developed for Division 1 by the Leeds and Northrup Company. In the first of these a thermally and electrically insulated ring, cut from a barrel of the same caliber as the gun being tested, is set flush with the inside of the bore, as shown in Figure 1. The ring must be thick enough to insure against mechanical deformation. A thermocouple is affixed to its outer wall, with wires leading to the outside of the barrel through thin bakelite tubes. These are sealed against gas leakage by neoprene washers compressed by metal plugs. Fluorocarbon is used as an obturator; insulating gaskets made of linen-base bakelite are subjected to a make-up force of 20 tons during installation.

The first rings were placed behind the origin of rifling; later, rifled rings were installed at locations farther forward. These were carefully aligned with the rifling of the bore and pinned to prevent rotation.

The heat input per unit area of the bore is computed from the formula

$$H = \frac{Emc}{\pi dwP} \tag{7}$$

in which E is the emf output of the thermocouple, P its thermoelectric power, and m, c, d, and w respectively the mass, specific heat, inner diameter, and width of the ring.

Radial thermal equilibrium is reached throughout the ring in less than a second. Heat is lost relatively fast by leakage, particularly through the insulating gaskets. The emf-time curve of the thermocouple reaches a maximum and then falls steadily. To obtain the ring temperature for zero thermal loss, the exponential decay curve can conveniently be extrapolated back to time zero on semilogarithmic graph paper. The problem, for a perfectly insulated ring, has also been approached by calculating the amount of heat stored in the bakelite gaskets.

Consistent results were obtained by the calorimetric ring method. It gives absolute heat input determinations near the origin of rifling, where some other methods fail. Objections to it as compared with methods developed later are the large amount of shop work involved, the lower degree of precision, and deterioration of the insulation resulting from firing.

5.3.4 Calorimetric Section Method[71]

The term "calorimetric section" as used here applies to a relatively long section of the barrel which has been reduced in diameter by removal of an annular ring of metal. The purpose of this machining is to delay and diminish the longitudinal flow of heat to the remaining "thick" sections. As long as the thickness of the barrel wall of the calorimetric section is small as compared with the distance from the measuring thermocouple to the nearest end of the section, the section acts as a calorimeter for a considerable length of time after the heat input through the bore has taken place, and the temperature of the outer surface remains at its maximum value for about a second. Since this temperature is determined only by the amount of heat transferred through the bore surface and the thermal capacity of the section, measurements by this method give absolute values of the heat input.

Since the heat input through the bore is equal to the heat received by the barrel calorimeter, we have

$$H\pi d = \theta c\rho\frac{\pi}{4}\left[(d + 2b)^2 - d^2\right] \tag{8}$$

where H is the heat input per unit area, θ the temperature rise of the section, d the average inside bore diameter, b the wall thickness of the section, c the specific heat of the gun metal, and ρ its density. Solving this equation for H, we obtain

$$H = \frac{E}{P}(bc\rho)\left(1 + \frac{b}{d}\right) \tag{9}$$

in which the symbols E and P have the same meaning as in the preceding section.

5.3.5 Outer Surface Measurements

Thermocouples attached to the outer surfaces of guns have been used in many temperature measure-

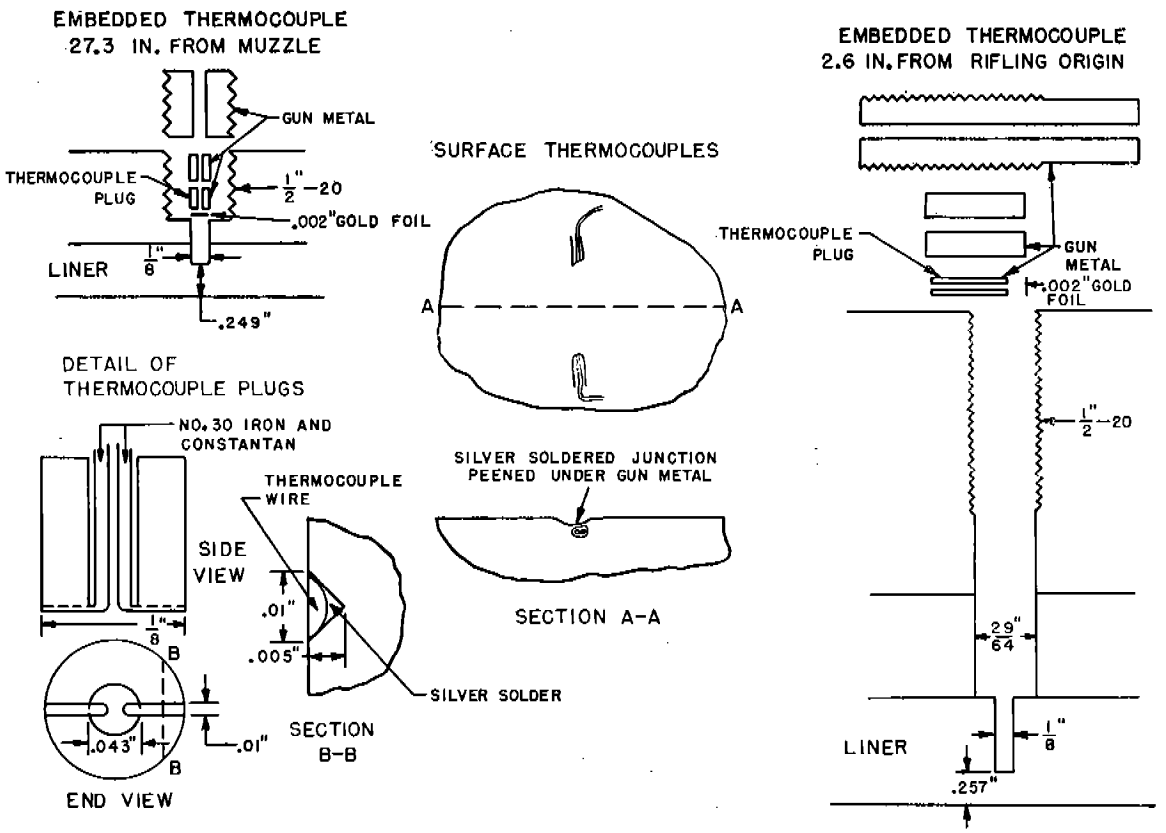


FIGURE 2. Assembly for embedded thermocouple. (This figure has appeared as Figure 2 in NDRC Report No. A-434.)

ments. As examples, the British report using the method in temperature measurements with 20-mm, Mark V (Hispano) guns, 3.7-in. Mark VI AA guns, and 3-in. and 4.2-in. mortars.

The method has also been extensively employed in studies with the caliber .50 machine gun, especially by North American Aviation, Inc., where a large number of heating and cooling curves have been observed.[526] Since this type of measurement can be made under conditions very similar to service ones, there has been great interest in the study of the correlation between outer surface temperature and malfunctioning in machine guns (Section 5.6.4).

The unmodified barrel wall itself may be considered as a calorimetric section in the sense of Section 5.3.4. Although this method is a convenient one for absolute heat input measurements in large caliber guns, it has some disadvantages.[71] The accuracy of measurement is reduced because of the greatly diminished temperature rise in a thick-wall calorimeter; the equilibrium conditions are attained slowly; and the temperature indication of the thermocouple is averaged over a large bore area. This method was used[106] in conjunction with the ballistic firings of the 3-in. and 37-mm guns at Carderock (Section 4.2).

5.3.6 Embedded Thermocouple

At a distance of more than a few hundredths of an inch from the bore surface, the transient rise of temperature as a function of time when a single round is fired depends on the shape and material of the barrel and the total heat input from the round, but not sensibly on the rate of heat input as a function of time, because the time during which the heat enters is so short. If the distance from the bore is several times larger than the depth of rifling and at least several times smaller than the distance back to the origin of bore or forward to the muzzle, the time-temperature transient approximates (for some seconds at least) to that produced in a solid having constant thermal coefficients, bounded internally by a circular cylinder and unbounded externally, initially all at a uniform temperature, to which a pulse of heat is supplied instantaneously and uniformly at the initial time all over the inner surface, that surface being

thereafter insulated. The transient is given by

$$\theta = \frac{2H}{\pi \rho c}\int_0^\infty e^{-\alpha u^2 t} \frac{J_1(ua)Y_0(u\tau) - Y_1(ua)J_0(u\tau)}{J_1^2(ua) + Y_1^2(ua)}du \quad (10)$$

in which θ is temperature rise, H is heat input per unit area, ρc is volume specific heat, α ($\equiv k/\rho c$) is diffusivity, t is time, a is mean bore radius, τ is radial distance, and the J and Y are Bessel functions.[542]

A thermocouple assembly[106] designed at the Geophysical Laboratory fitted into a hole of small diameter drilled radially to within a fraction of an inch of the bore of a gun barrel as shown in Figure 2. The junction was formed at the bottom of the hole, and the electrical insulation was made thin in order that the flow of heat should be altered as little as possible. By means of a Leeds and Northrup Speedomax or its equivalent, time-temperature transients were recorded during the firing of single rounds in different guns. The junction was situated about $\frac{5}{16}$ in. from the bore, and a maximum temperature rise ranging from a few degrees to 20 or 30 degrees centigrade was recorded after about 2 sec, depending on the gun, the location of the thermocouple, and the ammunition.

In some cases, although not in all, the recorded curve was matched quite accurately by equation (10) or a similar equation which took into account the finite outside diameter of the barrel. Since the volume specific heat ρc (which occurs in the diffusivity) can be considered known, the equation contains two parameters, H and the thermal conductivity k. Change of H corresponds to a change of temperature scale and change of k to a change of time scale. When the experimental curve is matched by a suitable choice of the two scales, the values of the heat input H and the conductivity k are determined. Of course, if k is known in advance for the particular steel, the determination of H is more precise.

The method of the embedded thermocouple is the simplest for measuring heat input just forward of the origin of bore. However a completely reliable design of embedded thermocouple is still to be sought. In one developed at Purdue University[321] for the Army Ordnance Department the end of the thermocouple junction was at the bore surface, but the thermoelectric voltage produced corresponded to the temperature over a zone of metal several thousandths of an inch thick, which is the zone where the temperature gradient is steepest.

5.3.7 Heat Input by Strain Measurement

During the course of the firings of caliber .50 aircraft barrels at Carderock, described in Section 7.5, thermal strain was observed in the oscillograph records. These showed that after the effect of the gas pressure had subsided, the strain settled down about 15 msec after firing to a value which remained constant for at least 35 msec. This constant strain was considered to be a thermal effect and was used to determine heat input. The method was based on a theorem proved in Section 7.2.3, to the effect that circumferential strain at the outer surface of a hollow cylinder depends only on the quantity of heat in the cylinder and is independent of the (cylindrically symmetrical) distribution of the heat.

It was assumed that this theorem could be applied to the aircraft barrels; final temperature rise was then computed from the thermal strain and the heat input was thus found.[106] The coefficient of linear thermal expansion of the steel was taken as 11.2×10^{-6}/°C, the volume specific heat as 0.86 cal/cm³/°C. Single rounds in a nitrided and chromium-plated barrel gave results shown in Table 4. Since values are correct within 10 per cent, except near the origin of bore where the underlying assumptions of the method are not met, the results were very satisfactory. They could be further improved by testing for thermal strain alone, in which case higher amplification could be used.

TABLE 4. Heat input by strain measurement, nitrided and chromium-plated caliber .50 aircraft machine-gun barrel fired single shot.

Distance from breech (in.)	Heat input (cal/cm²)
4.4	7.4 ± 0.5
10.0	7.6 ± 0.2
14.0	6.5 ± 0.4
24.0	6.5 ± 0.4

5.3.8 Other Methods of Measurement

Of other possible methods of measurement of input or temperature, one that has been of interest recently is measurement by means of temperature-indicating coatings.[412,432,433,529,530,531] Such paints are now available covering a range of 80 to 800 degrees centigrade, well suited to external barrel temperatures. Single, double, and multiple-change colors have been devel-

oped. Those of the first kind change color irreversibly at a fixed temperature; for the double-change type, the first change is a reversible one taking place at a relatively low temperature; continued heating causes a permanent change at a much higher temperature. The multicolored paints show varying irreversible changes at different levels; the regions of color are, however, not so sharply defined. It is claimed that with careful handling, indicated temperatures will be within approximately 5 per cent of the actual ones.

The paints are dependent for effectiveness on time of exposure to heat. Some have been standardized on a basis of 30 min heating, others on 10 min. At temperatures which are high for the particular paint being used, however, the color changes may result from much shorter times of exposure.[433] In the case of Thermindex paint E6 a transition which requires 10 min at 450 C will occur in 4 to 5 sec at 680 C. For this paint it has been shown that, on a graph of temperature versus logarithm of heating time required for a color change, a simple linear relation holds over the time range investigated for the two lower temperature transitions, but that the relation for the upper temperature transition is more complex.

5.3.9 The Thermal Analyzer

Various aids to the study of temperature distributions have been devised; in particular, a thermal analyzer has been developed at the University of California under the auspices of the OSRD Engineering and Transition Office. A network of electrical resistors and capacitors is used to simulate the thermal system. In a typical unit eight radial positions and eight axial positions are provided; impulses are introduced at any one of eight points to represent heat input. The corresponding first eight resistors represent the resistance of the laminar layer next to the surface. Temperatures can be taken at any of 64 network positions at which condensers are attached. All condensers and resistors are variable, making the unit applicable to different guns and firing conditions.

5.4 BORE SURFACE TEMPERATURES[e]

5.4.1 Theoretical Methods of Determination[f]

The temperature of the bore surface may be calculated from the heat input and the known laws of heat flow. In this section are summarized some of the methods and results that various workers have obtained. All are based on the same fundamental assumptions: (1) the principal source of heat transfer is forced convection from the gas, as described in Section 5.2.2; and (2) the heat conduction problem is that of flow through a semi-infinite slab. For this flow we have the fundamental equation

$$\frac{\partial T}{\partial t} = \frac{k}{c\rho_s}\frac{\partial^2 T}{\partial z^2}, \tag{11}$$

where T is the temperature of the gun metal at depth z from the surface and time t, and k, c, and ρ_s are respectively the thermal conductivity, specific heat, and density of the metal of the bore wall. The ratio $(k/c\rho_s)$, which is called the "thermal diffusivity," is considered constant in most applications. To obtain the temperature of the surface T_s, equation (11) is integrated under the boundary conditions

$$\text{At } z = 0,\ \frac{dT_s}{dz} = -\frac{h}{k}(T_g - T_s) \tag{12a}$$

$$\text{At } t = 0,\ T = T_s = T_{s_0} \tag{12b}$$

where h is the heat transfer coefficient discussed in Section 5.2.2. This integration leads to

$$T_s(t) - T_{s_0} = (\pi\rho_s ck)^{-1/2}\int_0^t h(T_g - T_s)(t - m)^{-1/2}dm \tag{13}$$

where m is a variable of integration. This equation shows the characteristic difficulty of the calculation of bore-surface temperature: the heat input as defined in equation (2) is itself dependent on the desired temperature T_s. Hence numerical or other approximate methods of solution must be sought.

The five methods now to be described differ principally in the manner of calculating h, in the values chosen for the thermal constants, and in the methods of approximating the solution of equations (11) and (13).

[e] In the fall of 1943, Section A of Division A, NDRC held a symposium to review the current knowledge about the heat input to the bore surface of guns and the temperatures resulting. The ten papers presented, together with useful contributed comment, were later edited and issued as NDRC Report A-201.[32] Some of this material was later expanded and issued in separate reports which are referred to elsewhere in this chapter.

[f] In general the mathematical notation follows that of the original sources, and therefore is not consistent throughout this chapter. In order to simplify the reading of individual sections, however, some changes have been made. In particular, throughout this section α is used for diffusivity and T for temperature, although in some of the sources other symbols had been used.

Method of Fulcher[32]

In this method of computation the heat transfer coefficient used was that given by equation (6), the simplified theoretical expression for smooth pipes. Then the rate of heat input Q (in calories per square centimeter) was obtained from equation (14), in which U' is the velocity in thousands of feet per second.

$$Q = 8.9(\rho U')^{0.8}(T_g - T_s). \tag{14}$$

Since Q varies regularly with time, equation (13) was approximated by

$$T_s(m) - T_{s0} = 3.4\left(1 + \frac{T_s}{7800}\right)\sum_{5}^{m}\Delta Q\frac{n}{n-1}[mt - (n+f)]^{1/2} \tag{15}$$

in which n is the number of small intervals into which the graph of Q as a function of time is arbitrarily divided and f is a function of the curvature of that graph.

The method of calculation consists in determining ρ, U', and T_g from experimental records of breech pressure and projectile position as functions of time during firing, by using the fundamental gas laws. From the known data graphs are set up for total energy, energy remaining in the powder gas, gas temperatures, and velocity of the powder gas, as partially illustrated in Figure 3. Then the values for ρ, U', and T_g are used with equations (14) and (15) by the method of successive approximations to obtain values for the rate of heat input Q and the surface temperatures T_s at any time and for various positions along the bore.

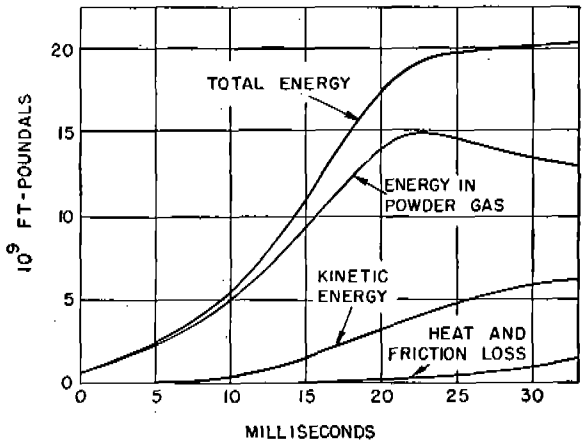


Figure 3. The total kinetic energy which the powder gas would have had if it had lost no energy, versus time (upper curve). This curve is determined by summing the energies as indicated on the three lower curves. (This figure has appeared as Figure 3 in NDRC Report No. A-201.)

An important advantage of this method of calculation is that it is readily adaptable to different experimental conditions. Thus it is not limited to any particular assumption about variation of gas density or gas temperature, and it is possible to take preheating (as by engraving) into account.

Method of Hirschfelder, Kershner, and Curtiss[32]

In this method the smooth pipe approximation for h was used, in the form of equation (5), with the exact theoretical expression for h. The ballistic variables ρ, U', and T_g were obtained by the detailed theoretical methods of calculation described in Chapter 3. A constant value of 3.4 was adopted for the term $2(\pi\rho_s ck)^{-1/2}$ and equation (13) was approximated by

$$T_s(t_m) - T_0 = 3.4\sum_{j=1}^{m}Q(t_{j-1})(\sqrt{t_m - t_{j-1}} - \sqrt{t_m - t_j}). \tag{16}$$

That is, the time was divided into m small intervals, and the rate of heat transfer assumed constant through each interval. A step-by-step computation was carried out, using the value of $Q(t_{j-1})$ calculated on the basis of the T_s at the beginning of the interval.

The more general case for temperature T_x at a distance x from the bore surface was solved on the basis of an analogous equation. The resulting step-by-step summation method of solution is indicated by equation (17)

$$T_x(t_m) = T_x(0) + \sum_{j=1}^{m}\delta T_s(t - t_{j-1})\cdot\left[E\left(\frac{x}{2\sqrt{\alpha t_j}}\right) - E\left(\frac{x}{2\sqrt{\alpha t_{j-1}}}\right)\right], \tag{17}$$

in which α is diffusivity and the function $E(y)$ is the error integral defined by

$$E(y) = \frac{2}{\sqrt{\pi}}\int_0^y e^{-u^2}du\,. \tag{18}$$

Existing data were similarly fitted to empirical relations to give equation (19) for total input to entire barrel up to time of ejection (h_1)

$$h_1 = \frac{0.09(T_0 - 300)^{4/3}LC}{D^{4/3}}\text{cal/round} \tag{19}$$

and equation (20) for average heating per square inch of bore surface per round.

$$\frac{h_1}{\pi D X_m} = \frac{L/D[.09(T_0-300)^{4/3}]\,\Delta D^{2/3}}{4\times 27.68\left(\frac{X_m}{X_0}\right)} \qquad (20)$$

In these equations T_0 is flame temperature on the absolute temperature scale, L projectile travel in inches, C the charge in pounds, D caliber in inches, Δ loading density in g/cm^3, X_m is equivalent length of chamber in inches and X_m/X_0 the ratio of gun volume to chamber volume. Equation (20) makes clear the well-known relation that for guns and loading such that L/D, X_m/X_0, and Δ are the same, the heating per unit area per round varies as the two-thirds power of the caliber.

In connection with these methods of calculation it is of interest to note approximate results for *near-surface* temperatures that have been found by the classical theory of heat flow in a semi-infinite solid. Heat input values suitable for normal guns and machine guns and thermal constants generally accepted for gun steel were used. The temperature rise at distances near enough to the bore surface to make $x/4\alpha t < 0.01$ are shown in Figure 4. The maximum temperatures attained by points at various distances from the surface are shown in Figure 5, together with the elapsed time to the maximum. The functions used in these calculations are, of course, discontinuous at the bore surface itself.

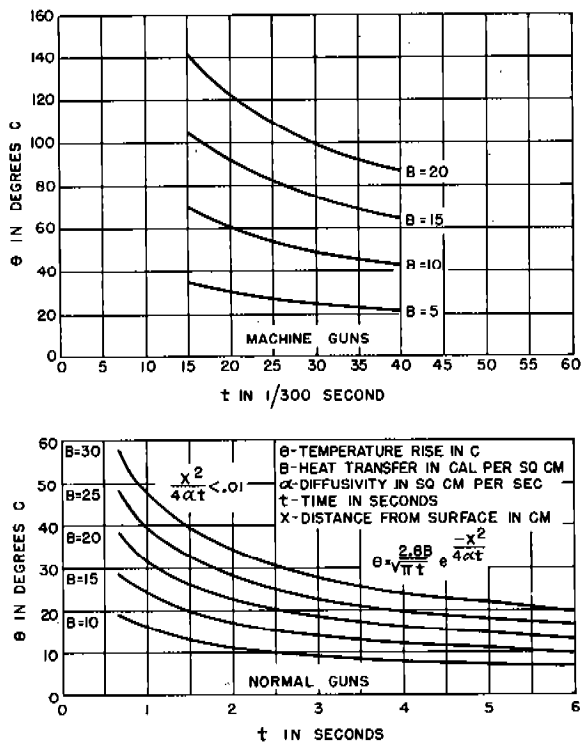


FIGURE 4. Temperature rise near the bore surface after firing of one round.

NORDHEIM'S METHOD[48]

This method uses the preferred expression, equation (4), for heat transfer in a rough tube, in which the constant λ is fitted empirically to the experimental results for heat transfer. The ballistic parameters are derived theoretically from the simplified ballistic system described in Section 3.2.7. For this system, all velocity-time curves are the same if described in terms of a reduced-time variable τ. It then becomes possible to solve equation (13) in terms of this reduced-time variable and a corresponding reduced-depth variable ζ, so that the results are applicable to guns of varying sizes and conditions of firing. The simplifications in the ballistic system cause relatively small changes in the calculated heat transfers and surface temperatures.

Fundamental experiments on erosion vents[27,260,479] also formed part of the basis for the analysis. A knowledge of an experimental value of the heat input to at least one gun is required. From such a measurement values of the friction factor λ in guns of different calibers were derived. Because the measurements[71] of

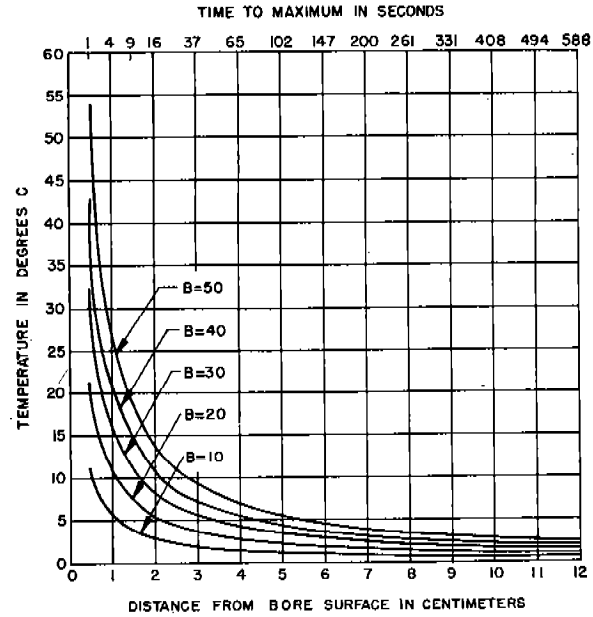


FIGURE 5. Maximum temperature attained from firing of one round.

heat input were still in progress when this method of calculation was developed, two values of the heat input were introduced, so that interpolation might be made later on the basis of more accurate experimental determinations.

In the computations it was further assumed that the density of the propellant gases is constant throughout the whole space behind the projectile. Constant values of k, c, and ρ_s were chosen, so that the value of the ratio $2/(\pi\rho_s ck)^{1/2}$ was 3.16.

The simplified or reduced ballistic system permitted the development of formulas and tables independent of the absolute size of the gun, relatively insensitive to variations in loading density lying within the normal range from 0.5 to 0.7 g per cc, and to other ballistic variables. The results[48] depend essentially on two parameters. The first is the "burning parameter" E which fixes the position of the projectile when the powder is all burnt. E may be calculated from the powder and gun constants, and then the position y_b at all-burnt is given by equation (21),

$$\frac{y_b}{y_0} = [1/(1 - E)]^{2/(\bar{\gamma}-1)} \tag{21}$$

in which y is a reduced-position variable, the subscript 0 indicating the initial position of the projectile. In preparation of the tables,[48] a value of 1.36 was used for $\bar{\gamma}$, although as pointed out in Section 3.3.2 a somewhat lower value would be preferable.

The second fundamental parameter is the "heating parameter" L. This variable is independent of time, contains the friction factor λ, and may otherwise be calculated from the gun and powder constants by equation (22), where the symbols have their usual ballistic significance (Chapter 3).

$$L = \left[\frac{43.1\lambda c_p C^{3/4}}{\sqrt{kc}\rho_s(m^{1/4}A^{1/2}F)}\right]\left[\frac{1 - \Delta_0\rho_p}{\Delta_0}\right]^{3/4} P_p^{5/4} \tag{22}$$

There are three periods of time which have special significance in temperature studies—prior to all-burnt, after the burning of the powder but preceding ejection of the projectile, and after the ejection. For positions back of y_b, the heat input is greatest during the first period, smaller in the second, and relatively slight after ejection. For positions toward the muzzle from y_b, heating begins in the second period and is important in the third. It has been remarked that uncertainties as to the behavior of the gas stream following ejection make the figures given in NDRC report A-262 less reliable; they have, however, compared reasonably well with experimental results, as brought out at the end of Section 5.2.2.

On the reduced basis the fundamental heat-transfer equations (11) and (12) become equations (23) and (24),

$$\frac{\partial T}{\partial \tau} = \frac{1}{2}\frac{\partial^2 T}{\partial \zeta^2}, \tag{23}$$

$$\frac{\partial T}{\partial \zeta} = -H(T_g - T_s) \tag{24}$$

The reduced heat-transfer coefficient $H(\tau)$ is the product of three factors, as shown in equation (25).

$$H(\tau) = \left(\frac{X_s}{X_0}\right)Lf(\tau) \tag{25}$$

These factors are, respectively, the position in the gun X_s/X_0, the time-independent heating parameter L, and the general function $f(\tau)$, which depends only on the burning parameter E. Thus a general solution of the problem has been obtained.

The heat-transfer function $f(\tau)$ plotted against τ gives an asymmetric bell-shaped curve. A simplified method of finding approximate maximum temperatures near the beginning of travel involves use of a straight line to replace this curve between the origin and the point corresponding to "all-burnt." In most cases results obtained by this method will be within 30 centigrade degrees of those given by the full tabular method, usually considerably closer.

Tables have been issued[48] for the temperature rise corresponding to various values of L, assuming flame temperatures of 2500 K for "normal" guns and 2795 K for machine guns. A slightly different treatment was used for machine guns because their ballistics are somewhat different from those of larger guns. These tables contain values corresponding to different depths below the bore surface. Separate tables are given for times prior to all-burnt and after burning has been completed.

The main tables are based on the assumption that the unburned powder grains are distributed uniformly in the space behind the projectile. An auxiliary table can be used to obtain values corresponding to the assumption that all the unburned powder remains in the chamber.

Correction functions are presented for changes in the flame temperature of the powder and the initial temperature of the bore surface. It has been pointed out,[113] however, that it is undesirable to extrapolate beyond a flame temperature of 3000 K for normal guns. In several cases results for hotter powders that

have been compared with those obtained by numerical integration have shown larger variations (as much as 100 degrees than for cooler powders.

Method of Hicks, Thornhill, and Ware

In developing this method the heat transfer coefficients were assumed known from the smooth-pipe expression and empirical values of the ballistic quantities. By application of the boundary conditions given by equations (26),

$$\left.\begin{array}{ll} t = 0, & T = T_0 \\ z = 0, & \partial T/\partial z = -(h/k)(T_g - T) \\ z \to \infty & T \to 0 \end{array}\right\} \quad (26)$$

a convenient numerical solution[348] of the heat conduction equations (11) and (12) was obtained. As originally described it may be outlined as follows:

Dividing up the time interval over which heat transfer takes place into a number of equal small intervals δt, equation (11) may be replaced approximately during one of these intervals by equation (27),

$$\frac{T_1(Z) - T_0(Z)}{\delta t} = (1/2)\frac{k}{c\rho_s}\frac{\partial^2}{\partial Z^2}[T_0(Z) + T_1(Z)], \quad (27)$$

where the T's are the temperature-space distributions at the beginning and end of the interval. By applying the definition of q given by equation (28)

$$q^2 = \frac{2c\rho_s}{k\delta t}, \quad (28)$$

equation (27) reduces to equation (29).

$$\frac{\partial^2}{\partial Z^2}(T_0 + T_1) = q^2(T_0 + T_1) - 2q^2 T_0. \quad (29)$$

After proper consideration of the boundary conditions, the temperature distribution at the beginning of the $(n + 2)$nd interval δt may be written

$$T_0(Z) = e^{-qz}[a_0 + a_1(2qz) + \cdots + \frac{a_n}{L_n}(2qz)_n]. \quad (30)$$

The temperature at the end of this interval is given by a similar relation with coefficients b_0 to b_{n+1}. Coefficient b_0 may be expressed in the form

$$\frac{h_0 T_{g0} + h_1 T_{g1}}{h_1 + kq} - \frac{h_0 + kq}{h_1 + kq}a_0 + \frac{kq}{L_a + kq}[a_0 + a_1 + \cdots a_n] \quad (31)$$

The other b's are functions of the a's alone. Starting from the initial temperature $T_0(Z) = 0$, these recurrence relations enable one to calculate the temperature distribution at the end of any subsequent interval.

If instead of using the varying values of $h(t)$ and $T_g(t)$ and integrating by a step-by-step method we assume that these quantities may be replaced by some form of average values h and T_g, the heat conduction equation may be solved analytically, as shown by Thornhill and Ware[398,403] and by Hobstetter.[124] The latter has written the result in the form

$$\frac{T - T_g}{T_0 - T} = \mathrm{Erf}\left(\frac{Z}{2\sqrt{\alpha t}}\right) + e^{\frac{h}{k}Z + \frac{h^2}{k^2}\alpha t}\left[1 - \mathrm{Erf}\left(\frac{Z}{2\sqrt{\alpha t}} + \frac{h}{k}\sqrt{\alpha t}\right)\right]. \quad (32)$$

In this equation α is the diffusivity and h the average heat transfer coefficient. The abbreviation Erf stands for the error function;[521] for example,

$$\mathrm{Erf}\frac{Z}{2\sqrt{\alpha t}} = \frac{2}{\sqrt{\pi}}\int_0^{Z/2\sqrt{\alpha t}} e^{-u^2}du. \quad (33)$$

T_g is likewise taken as an average; the other symbols are as previously introduced.

In applying this method, Thornhill and Ware have considered time to projectile ejection as time of transfer of heat, the average T_g to be the mean of the initial and final gas temperatures, and the average h to be half the maximum numerical value of $h(t)$. As compared with their more accurate method outlined above, they have found the values for heat transfer to be correct within a few per cent, and the maximum surface temperatures to be about 15 per cent too low. Since the calculations were made for the origin of rifling, the input after ejection is a minor factor; however for points farther down the barrel, ignoring this would lead to a considerable error.

Hobstetter's Method[124]

In an effort to obtain a truer picture of the situation by a different choice of parameters, the analytic expression of the previous method was combined with the heat transfer coefficient and other ballistic quantities as calculated by Nordheim's simplified system described above. For points near the origin of rifling, and under the assumption of equal distribution of unburnt powder, the gas temperature decreases slowly and therefore it was concluded that a good approximation is given by taking this equal to the flame temperature of the powder.

For the duration of heating the time to maximum temperature was expressed graphically in terms of the burning parameter E. Finally, for the heat transfer coefficient equation (34) was adopted. In it h is the transfer coefficient used by Nordheim,

$$h' = h\sqrt{\frac{\alpha k c \rho_s}{2}} \tag{34}$$

α is the ratio τ/t between Nordheim's reduced time and time in the ordinary scale, k, c, and ρ_s have the same meaning as in equation (11).

This method was applied to studies of caliber .50 and 37-mm guns. The former computations were carried out in conjunction with metallographic studies of bore surface erosion, which are discussed in Chapter 13.

Comparison of the Methods

A comparison of the results by the different methods is desirable; it has been difficult to find guns for which calculations have been made by all the methods. For two guns the values given in Table 5 have been

Table 5. Bore surface temperatures calculated by various methods.

Gun	Method			
	Simplified Nordheim	Nordheim tabular	Hobstetter	Hirschfelder Kershner et. al.
37-mm M3	570 C	590 C	532 C	555 C
8-in. Mk VI	1017 C	1022 C	1014 C	1210 C

calculated. It may be remarked that in general, results are not so consistent as the 37-mm gun temperatures would imply; on the other hand, the Hirschfelder results are usually in better agreement than the 8-in. gun results would indicate.

5.4.2 Temperature in Continued Fire

The preceding section on calculation of bore surface temperature dealt with actual instantaneous temperature, and had in view chiefly a single round. In the firing of a continuous burst a concept of importance is *average temperature*. It is best defined as the temperature that would be produced if the heat of each round entered in a uniform way over the whole time between that round and the next, instead of almost at once after the instant of firing. The average temperature rises smoothly and steadily as the burst goes on whereas the actual temperature at or near the bore surface rises far above the average almost immediately after a round is fired and falls below the average during most of the time between rounds. At a distance from the bore surface the actual and average temperatures are practically the same in rapid fire.[106] The progress of heating of the whole barrel is described at some length in Section 5.5.

The average temperature in the neighborhood of the bore surface tells the general temperature level, as distinguished from the momentary sharp peak of temperature after each round. The latter is important chiefly for chemical effects and bore surface melting, the former rather for deeper mechanical effects following upon bullet impact, as described in Section 13.1.2.

Average bore surface temperature can be determined from measurements of temperature during a burst taken at several distances from the bore. Such measurements were made in caliber .50 barrels at the Geophysical Laboratory by means of the embedded thermocouples described in Section 5.3.5. The readings were taken by photographing millivoltmeters and a clock, or by pen and ink recorders. In one case, four thermocouples were inserted at the origin of bore, at distances from the bore ranging from 1/16 in. to the outer surface. Soon after the beginning of the burst, temperatures were rising at nearly the same rate at all four thermocouples (see Figure 8, couples 4.35 in. from breech). The heat input H per unit time, through a bore surface area of unit length axially and extending one radian circumferentially, could then be calculated by equation (35),

$$H = \frac{\dot{\Theta}(r_1) - \Theta(r_2) + \int_{r_1}^{r_2} \frac{1}{k\sigma} \int_a^\sigma \rho c s \frac{\partial \Theta}{\partial t} ds d\sigma,}{\int_{r_1}^{r_2} \frac{d\sigma}{k\sigma}} \tag{35}$$

in which Θ is temperature, r_1 and r_2 are the distances from the axis of two thermocouples, k is conductivity, a is bore radius, ρc is volume specific heat, and t is time. The average bore surface temperature was given by

$$\Theta(r_1) + H\int_a^{r_1} \frac{d\sigma}{k\sigma} - \int_a^{r_1} \frac{1}{k\sigma} \int_a^\sigma \rho c s \frac{\partial \Theta}{\partial t} ds d\sigma. \tag{36}$$

In these two formulas the effect of any possible flow of heat in the axial direction has been neglected. If axial flow is not neglected, additional terms appear in both formulas. An estimate of the axial flow can be made from the readings of three thermocouples.[106]

The principal term in the numerator of equation (35)

in the calculation of the rate of heat input H is $\Theta(r_1) - \Theta(r_2)$, the temperature difference at a given moment between thermocouples at two different distances from the bore. In the example cited above the difference amounted to about 80 degrees centigrade between $\frac{1}{16}$ in. and $\frac{1}{8}$ in. from the bore. It is doubtful, however, whether the embedded thermocouples were capable of measuring such a difference very accurately.

The amount by which the average bore surface temperature exceeds the actual temperature just before a new round may be estimated by $1.46B\times(n/\pi\rho ck)^{\frac{1}{2}}$, in which B is the heat input of the new round per unit area and n is the rate of fire of the burst.[106]

It is possible to calculate average temperatures in a burst, and for that matter actual temperatures not too close to the bore, by in effect accumulating the temperatures of the separate rounds as expressed in equation (10) or analogous equations, provided the section in question is not too close to the origin or the muzzle, and the outer surface of the barrel is nearly cylindrical in the neighborhood of the section. Besides the dimensions of the barrel and the thermal coefficients of the steel, it is necessary only to have some knowledge of the heat input per round. This can be gained from measurement at the outer surface during a burst; or from measurement of the input of a single round coupled with the assumption that heat input decreases in proportion as average bore temperature approaches a fixed "limit temperature" of about 1000 C; or finally, without measurement, from Nordheim's tables or an equivalent theoretical calculation (see Section 5.4.1).

Figure 6 shows calculated average temperatures in a 3-in. gun firing 90 rounds at a rate of 6 rounds per minute. These temperatures are drawn in full line, for the bore surface and the outer surface, at a position near the muzzle and another about midway along the barrel. Measured outer surface temperatures at the same positions are drawn in dotted lines. The calculations were based on measurements of single round heat input, and the assumption of a limit temperature of 1000 degrees near the middle of the barrel and 700 degrees near the muzzle. It was assumed also that no heat escaped from the outer surface. If an allowance had been made according to known rules for the escape of heat there, the calculated and measured outer surface temperatures would have come very near to agreement.[106]

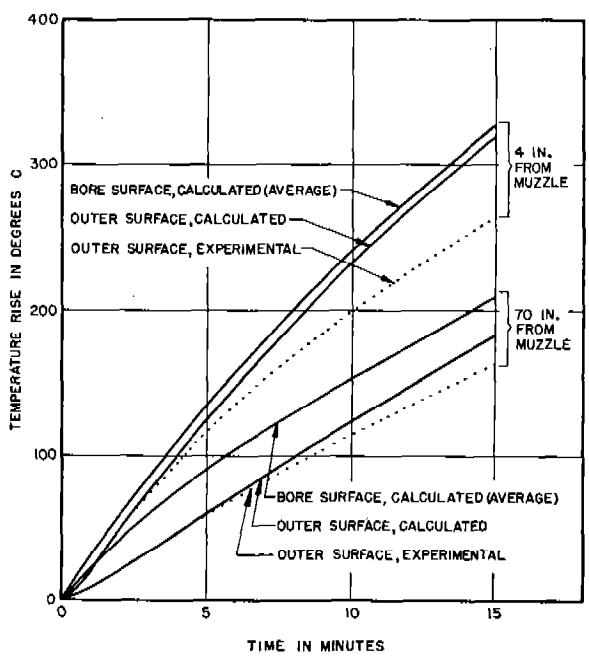


FIGURE 6. Calculated and experimental temperatures in 3-in./50-cal. Mark 22 Naval gun firing 90 rounds at the rate of 6 rounds per minute. Allowance is not made in the calculation for heat loss through the outer surface. (This figure has appeared as Figure 70 in NDRC Report No. A-434.)

5.4.3 Experimental Methods of Determination

Bore Surface Thermocouple

A means of recording the transient temperature at the bore surface of a gun was devised by a German investigator.[492] The measurement was made with a thermocouple assembly that could be inserted in a gun wall so that the thermo-element formed part of the gun bore surface. This thermo-element consisted of an oxidized nickel wire that passed down a fine hole in a steel plug and a thin layer of nickel that had been plated on the exposed end. This layer of nickel bridged the layer of nickel oxide that insulated the wire from the plug, in which it was a tight fit. There is not available any record of the extent to which this method was used.

Fusion Temperature of Erosion Products

Many of the chemically altered erosion products that occur on the bore surface give evidence of having been liquefied, as is brought out in Section 12.6. Hence a determination of the temperature of incip-

ient fusion of such materials gives a lower limit to the temperature of the bore surface. An experimental method for such a determination has been worked out in a preliminary way.[105]

A few milligrams of the bore surface deposit were sealed in a very small, thin-walled, well-evacuated silica-glass container whose volume was about 20 mm^3. The container was heated in a vertical electric furnace (2.5 cm bore), which had been preheated to the temperature at which it was desired to heat the charge.

The furnace temperature was measured with a platinum-platinrhodium thermocouple junction located a few millimeters above the bottom of a 7-mm silica glass tube, closed at its lower end, which was placed at the hottest part of the furnace.

The sample in its evacuated container was lowered on a platinum wire to the bottom of the silica tube, left there for a certain number of seconds (long enough to attain a temperature which was certainly not more than 5 or 10 degrees lower than the furnace temperature), and was then lifted out and the contents examined for signs of melting. If no melting had taken place, a new sample was used for the next trial at a higher temperature. Suitable criteria for melting had to be found for each substance studied. X-ray examinations were made of the phases in the material before and after melting.

Interpretation of the results is difficult because of the limited amount of experimental data. A residue from decoppering (see Section 11.4.3) showed a fusion temperature of 1160 ± 40 C. As now set up, the method unfortunately cannot be used for temperatures above 1250 C. because of softening of the silica glass container.

5.4.4 Applications to Conditions of Firing

Effect of Preheating

As stated in Section 5.2.2, the methods of calculation just discussed have ignored heat input from sources other than transfer from the hot gases. However, an indication of the effects from engraving and frictional forces has been given there and in Section 5.3.8.

The reality of a high temperature at the interface between a projectile and the gun bore has been demonstrated in the case of caliber .50 bullets.[72] By using the gilding metal of the bullet jacket in contact with the steel of the bore surface as a sliding thermocouple, measurements of the temperature of the interface were made while the bullet was in motion in a shortened caliber .50 barrel. A temperature of 860 C was recorded for the apparent average temperature over the area of contact between the bullet and the bore; and very likely some spot reached a higher temperature.

The question naturally arises as to the effect of such preheating[κ] on the bore surface temperature. When the time of preheating is very small (less than half the burning time) as in the case of preheating resulting from either engraving or bore friction, the increase of maximum temperature due to gas heating is relatively low.[48] For a 37-mm gun the increase per preheating unit of 1 cal/cm^2 for the neighborhood of the origin of rifling is 25 degrees centigrade. As mentioned at the end of Section 5.3.8, one set of assumptions led to an estimate of approximately two such units for the maximum preheating input. Therefore, we may be safe in saying that for this gun the increase of maximum bore surface temperature from preheating due to the rotating band does not exceed 50 degrees centigrade and it is probably considerably less.

Effect of Bore Surface Material

When a liner is inserted in a gun, or when the bore surface is plated, heat input and resulting bore surface temperature are correspondingly affected. The metals now of most interest as liner materials are chromium-base alloys (Chapter 17), molybdenum (Chapter 18), and Stellite No. 21 (Chapter 19). The one commonly used in plating is chromium (Chapter 20).

In plated guns it is essential to have the depth of plating sufficient to prevent thermal alteration of the underlying steel (see Section 13.3 and Section 31.5). When this is the case it is necessary in calculating heat input to the bore surface from a single round to consider only the thermal constants of the plated metal and its surface roughness as compared with gun steel. After a few rounds have been fired in a gun there appears to be little difference between metals in regard to the latter factor.

[κ] It is important to note that the correction functions given in Table 38 of NDRC Report A-262[48] and applied in formula 6.16 of that report applies to initial temperatures that are fairly uniform throughout a layer of the bore surface considerably thicker than the maximum depth considered in the tables. This preheating might be from a previous round or from an external source, such as the sun.

Since liners are much thicker than plating, it is sufficient for purposes of comparison of temperatures at the bore surface to base calculations entirely on the thermal constants of the metals occurring there. Unfortunately these are not too well established, even for gun steel. Also, since both conductivity and volume specific heat are functions of temperature, there is always some question as to what values to adopt. Values for steel and stellite are given in Table 3 of Chapter 19. Values for chromium and molybdenum may be derived from data given in Chapters 17 and 18. The melting temperature of molybdenum is so high, 2620 C, that liners made of this metal will not melt with any propellants now in service.

If average values for the constants are assumed, calculations indicate that the bore surface temperatures reached in gun steel and in stellite-lined guns differ by very little. For the caliber .50 erosion testing gun (Section 11.2.1), calculated[124] values using FNH-M2 powder are 1670 C and 1680 C, respectively, for the temperature after a single shot. Surface melting was observed in both cases.[76,77] With IMR powder the calculated results are 1310 C and 1325 C. Here it is important to note that the lower end of the fusion range of stellite is exceeded slightly while the melting point of gun steel is not reached; but yet surface melting of the stellite was not observed after 500 rounds. Gun steel did not melt when one round of IMR powder was fired, but liquefaction of the steel which had been chemically altered by the powder gases occurred after a number of rounds.[124] It is not surprising that, in the case of continued fire with IMR powder, steel melts while stellite does not, for the melting range of altered gun steel is much lower than that of stellite, as is brought out in Section 12.5.3.

The bore surface temperatures for a stellite-lined 37-mm gun for three FNH-powders have also been similarly computed. The estimates are 980 C for M1, 1310 C for M5, and 1330 C for M2; the last powder is considerably hotter than M5, but a smaller charge is sufficient to give the desired velocity of 2,900 fps. These figures predict melting of the stellite when the hot powders are used; this has been verified experimentally in firings of a 37-mm stellite liner at Aberdeen, as described in Section 33.2.

Temperatures in a nitrided, chromium-plated aircraft barrel, or in one containing a 9-in. stellite liner, are not remarkably different from those in a steel barrel, especially at the higher levels. Chromium plate permits more heat to enter in a single round or a short burst, but in longer-continued fire it has a contrary effect. Average temperature at the bore of a stellite liner, at the origin, is at first considerably higher than in steel, but by the 200th round of a long burst, the difference is in great part erased.[106]

Effect of Obturation

The "blow-torch" effect of gas leakage resulting from imperfect obturation is particularly likely to occur in worn guns. For banded projectiles, the danger of gas washing is greatest at the beginning of the travel of the projectile, before the rotating band has been engraved.[48] Later the band forms a more effective seal, and the increased velocity of the projectile reduces the time for gas washing. There are two chief reasons for the relatively large effect of the escaping gases; first, that the velocity of the gas stream is very high—equal to the velocity of sound—and second, that the friction is large in narrow and irregular slits. The result of gas washing is localized melting leading to scoring of a gun, as discussed in Section 13.4.1.

It is clear that in the case of pre-engraved projectiles the possibility of gas leakage is always present, and that this would be accentuated by any imperfections in their manufacture. Experiments with caliber .50 projectiles, described in Section 31.4.2, indicated an increase in erosion with increased leakage area. Whether the same conclusion holds for larger projectiles is not yet known. The only experimental evidence is that obtained with the 37-mm gun, T47 (Section 31.7). Erosion was disappointingly rapid; but it is not certain that gas leakage was an important factor.

5.5 RATES OF HEATING UNDER RAPID FIRE

5.5.1 Machine Guns

The heating of the caliber .50 machine gun barrel has been studied far more than that of any other gun. In part, this is because the caliber .50 was used as a laboratory test piece through which the cause and cure of erosion in other guns might be understood, and in part for its own importance as an aircraft weapon. The study included both the 28-lb, 45-in. heavy barrel and the 10-lb, 36-in. aircraft barrel; nitrided and chromium plated and stellite lined barrels as well as steel barrels; single rounds, bursts, and continued fire under various firing schedules; different positions on the outer surface and inside the barrel wall; different ammunition; and different methods of

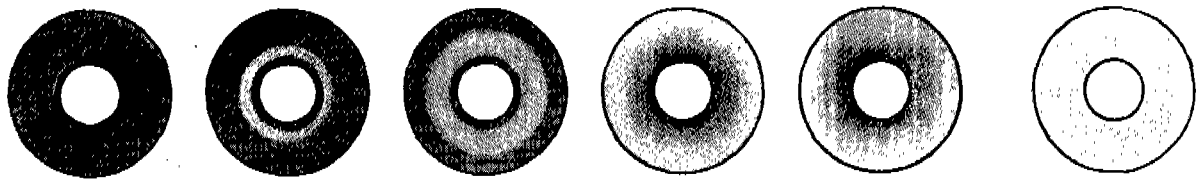


FIGURE 7. Diagrammatic representation of the successive stages of heating of a cross section of a machine gun barrel, during the firing of a single long burst. At first the high temperature is limited to a thin annulus at the bore surface. The heat spreads out radially with a very steep gradient continuing close to the bore surface. If the barrel is allowed to cool for a short time (last diagram on the right), the steep gradient disappears and the temperature becomes almost uniform throughout the cross section.

cooling. The work was done at Aberdeen Proving Ground, the Crane Company, the Geophysical Laboratory, Leeds and Northrup Company, the Naval Bureau of Aeronautics, North American Aviation Corporation, the University of California and at several places by the British.[h]

The process of heating, which is shown diagrammatically in Figure 7, is as follows: With each round that is fired through a caliber .50 barrel, heat enters through the bore surface. At the first round the input amounts to about 5 cal/cm^2 per round at the muzzle, increasing at first slowly and then nearer the breech more rapidly to about 10 cal/cm^2 per round at the origin. In the half inch or so of space between the origin and the mouth of the cartridge case the input may considerably exceed 10 cal/cm^2 where the bore surface is inclined to the axis of the barrel, forming part of the surface of a cone instead of a cylinder. From the mouth of the cartridge case back to the breech, a distance of nearly 4 in., the walls of the chamber receive little or no heat directly, for the cartridge case is ejected so quickly that not much heat can pass through its walls. (In fact, once the gun becomes hot, it may be that the net effect of each freshly loaded cold cartridge is to extract heat from the chamber walls. The input may then be positive in one direction from the cartridge case mouth and negative in the other.) The rounds after the first convey decreasing amounts of heat to the barrel; the input to a barrel at 500 C is everywhere roughly half what it is to one at room temperature.

It takes a matter of seconds for any considerable part of a pulse of heat received at the bore surface to make its appearance at the outer surface. On the other hand at least 6 or 7 rounds per second are fired in the heavy barrel, and as many as 20 rounds per second in the aircraft barrel in the M3 gun. The average temperature (Section 5.4.2) therefore builds up rapidly near the bore surface, and may exceed the temperature at the outer surface by hundreds of degrees centigrade. During firing the greatest flow of heat is therefore radial, directly outward from the axis of the barrel, under the influence of these steep gradients. To a less extent flow parallel to the axis also takes place, especially from the region of the origin back toward the thermally shielded chamber walls, and wherever the outer contour of the barrel changes abruptly.

For a barrel firing in still air, the escape of heat through the outer surface is always small compared with the rate of entry through the bore, even when the outer surface is as hot as 800 C. If the barrel is cooled by a strong air blast, however, the rates may become nearly equal at such high temperatures.

Within a few seconds after firing stops the radial temperature differences subside almost completely, especially in still air or where the barrel wall is thin. Axial differences on the other hand, the equalization of which would require flow through a long path of metal, may remain considerable for minutes. In particular, in still air, the origin section may continue 250 centigrade degrees cooler than the forward part of an aircraft barrel for 3 min after a long burst.

The temperature levels attained at a given section depend chiefly on the heat input per round, the number of rounds, and the wall thickness at the section. The aircraft barrel, as it happens, is so tapered that wall thickness is in fairly constant ratio to heat input along most of the length. From a few inches beyond the origin to a few inches short of the muzzle, therefore, average temperatures after a given number of rounds are fairly uniform. They are lower toward the origin because of the flow to the chamber walls, and toward the muzzle because of the bulge in the last 3 in. of the barrel's length. In the heavy barrel, temperatures are much lower in the rear half of the length than in the corresponding part of the aircraft barrel because of the much greater wall thickness. In fact

[h] For references see the bibliography in Report A-434.[106]

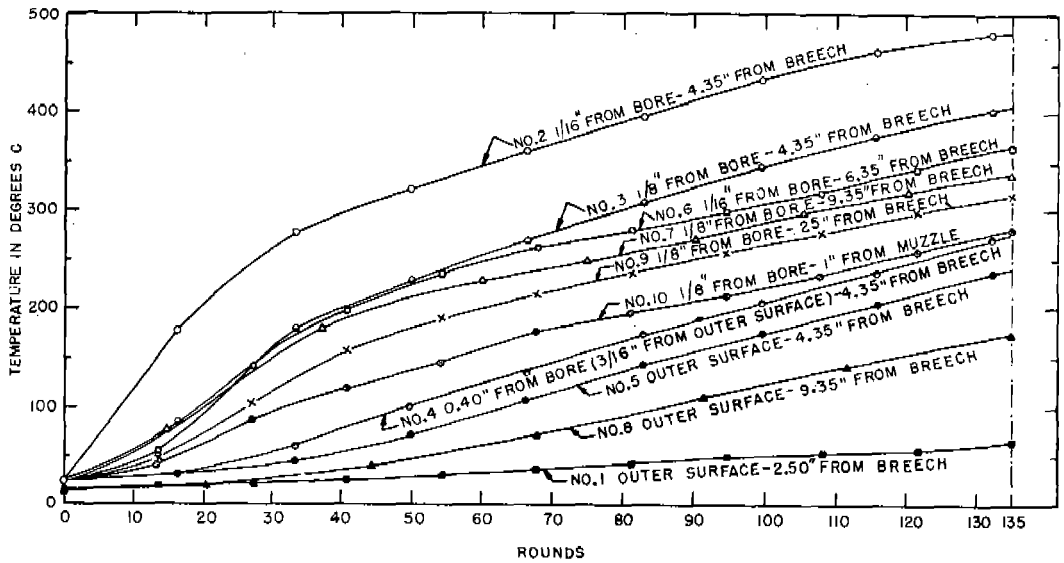


FIGURE 8. Temperature measurements at 10 different positions in a caliber .50 heavy machine gun barrel firing a burst of 135 rounds of AP ammunition, M2. (This figure has appeared as Figure 34 in NDRC Report No. A-434.)

the bulges in that region were no doubt placed there largely as thermal sinks.

Figure 8 shows measurements of temperatures at 10 different positions in a caliber .50 heavy barrel firing a burst of 135 rounds of AP ammunition, M2. These were made with thermocouples attached at the surface and others embedded as described in Section 5.3.5. The barrels were either solid steel or contained short steel liners. The figure is a composite of several firings at rates ranging from 400 to 500 rounds per minute, but the temperatures are plotted as functions of the round instead of the time, for a more equal comparison. One thermocouple was at the outer surface, 2.50 in. from the breech, over the chamber; four were at different distances from the bore at 4.35 in. from the breech (the origin of bore section); two were at 9.35 in. from the breech; and one was embedded at 6.35, 25, and 44 in. from the breech. The figure illustrates, among other things, the low temperatures over the chamber; the manner in which the temperature differentials at any one section are established in the first 40 or 50 rounds of a burst and are thereafter maintained rather constant; and the magnitude of these differentials.

An example[106] of maximum temperatures at different points of a steel aircraft barrel after firing five 100-round bursts with a 2-min cooling interval between bursts is given in Figure 9. Maximum temperatures (centigrade degrees) after five 100-round bursts, with 2-min cooling between bursts, from a barrel initially at 20 C, are written on the figure at 16 places. The distances of these places from the breech are 4.35 in. (origin of rifling), 8.35 in., 24.00 in., and 35.00 in. (1 in. from muzzle). The distances from the bore are

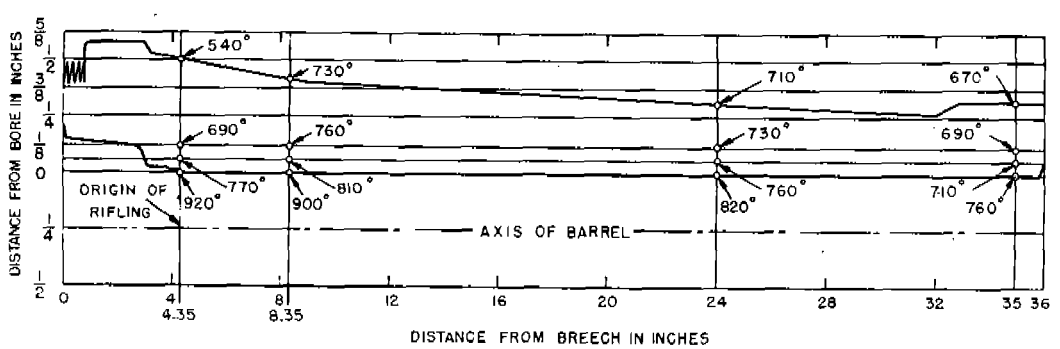


FIGURE 9. Maximum temperatures at different points of a steel aircraft barrel after firing five 100-round bursts, with 2-min cooling between bursts. (This figure has appeared as Figure 57 in NDRC Report No. A-434.)

0.01 in., 1/16 in., 1/8 in. and the outer surface distance. The temperatures 1/16 in. from the bore at 4.35 and 8.35 in. from the breech are experimental and are 770 C and 810 C, respectively. The others are estimated on the basis of other firings. The accuracy is ±30 degrees centigrade. At the same four distances from the bore, temperatures are nowhere more than 40 degrees higher than those shown. Maximum temperature much closer to the bore than 0.01 in. is not at present known accurately.

Here may be seen the uniformity of temperature over the middle two-thirds of the barrel; the lower overall level at the origin and muzzle; and the decrease forward from the origin of difference between average temperature at the outer surface and 0.01 in. from the bore owing to decrease in heat input per unit area and in wall thickness. These maximum temperatures were not reached simultaneously. At 0.01 in. from the bore the time interval by which they followed the passage of the last of the 500 bullets was about 0.008 sec, at 1/16 in. 0.1 sec, at 1/8 in. 0.4 sec, and at the outer surface from 2 to 5 sec, depending on the wall thickness.

The very high value of 920 C for maximum temperature 0.01 in. from the bore at the origin is noteworthy. This is a calculated rather than an experimental value. The highest temperature actually measured at the Geophysical Laboratory in a caliber .50 steel barrel was the 810 C shown 4 in. forward of the origin at 1/16 in. from the bore. The highest temperature measured in any caliber .50 barrel was 900 C, 1/16 in. from the bore at the origin of rifling of an aircraft barrel having a stellite liner, at the end of a continuous burst of 440 rounds.[106]

Forced cooling is discussed in Section 5.7. It may be remarked here that the various methods (external liquid cooling excepted) are effective in reducing average barrel temperatures principally in intermittent fire. In a continuous burst it is not easy to take heat from the barrel and remove it to a distance or convert it to a less objectionable form of energy, as rapidly as it is supplied through the bore surface.

Temperature in caliber .30 machine guns has been studied at Aberdeen Proving Ground,[175] and in a 0.303 in. Bren gun by the British.[398]

5.5.2 Automatic Cannon

The British reported[428] heating rates in a 20-mm Hispano Mark V gun, in connection with cook-off trials. Average rise in external chamber temperature for a given number of rounds, fired automatically at a rate of approximately 140 rpm, is shown in Table 6.

TABLE 6. Heating of chamber of 20-mm Hispano gun, Mark V, fired long bursts at approximately 140 rpm.

No. of rounds	175	200	225	250	275	300
Temperature rise (C)	234	279	302	325	349	382

These figures may be compared with temperatures recorded when firing 25-round bursts at 1-min intervals. The equivalent of 24 such bursts produced a peak temperature of 239 C; 15 led to a figure of 202 C.

Tests by the Bureau of Ordnance with 20-mm AA guns, while not giving specific temperatures, indicated that 120 rounds of automatic fire result in a dangerously high temperature. For 40-mm air-cooled guns, 45 rounds fired in 8-round bursts with 15 sec pauses between bursts resulted in a temperature too high for safety.

For 40-mm water-cooled guns, tests made at the Naval Proving Ground gave the results shown in Table 7 for increase in temperature of the coolant. A change in gun elevation from 0 to 60 degrees reduced the firing rate slightly but had little effect on the water temperature.

TABLE 7. Temperature of coolant of water-cooled 40-mm gun after having been fired bursts of different lengths.

No. of rounds	50	80	100	150
Time in seconds	25	45	50	80
Temperature rise (C)	25	41	55	70

5.5.3 Medium Caliber Guns

ABERDEEN PROVING GROUND TESTS

The heating of guns of medium caliber has been studied for a number of years at Aberdeen Proving Ground.[i] In one investigation temperatures resulting from rapid fire in a 105-mm AA gun, M1, were measured.[178] Following 20 preliminary rounds, series of 58, 66, 28, and 16 rounds were fired at varying rates. Temperatures were recorded by means of thermocouples welded to the gun barrel at distances of 0.95, 7.35, and 13.7 ft, respectively, from the muzzle. Maximum values reached were 285 C, 300 C, and 280 C, respectively. The overall time for the 168 rapid-fire rounds was approximately 42 min.

[i] These studies have been summarized and discussed in Ballistic Research Laboratory Report No. 104.[186]

From the heating effects, the temperature rise of the gun for rates of fire of 5, 10, and 15 rpm was computed and the results plotted. The times for the temperatures to reach 600 degrees centigrade above atmospheric near the origin of rifling were found to be approximately 100, 35, and 25 min, respectively.

Similar tests were made with a 3-in. AA gun M3.[179] Two thermocouples were welded to the gun, at 1.08 and 5.21 ft from the muzzle. After 129 rounds had been fired in about 8 min, these had attained temperatures of 320 C and 240 C, respectively. After 4 min, during which these remained practically unchanged, firing was resumed. One hundred and eighteen rounds fired over a period of 15 min resulted in temperatures of 430 C and 360 C, attained 2 min after the close of firing. At rates of fire of 5, 10, 15, and 20 rpm, the estimated times for the temperature near the breech to rise 500 degrees centigrade were found to be respectively 100, 38, 25 and 18 min.

For a 75-mm gun, M1897E3, temperature-time graphs were obtained by means of thermocouples 12, 36, and 55½ in. from the muzzle when 300 rounds were fired at a mean rate of 16 rpm.[181] Maximum temperatures recorded were almost identical, being 320 C, 328 C, and 328 C. It was calculated that at the thermocouple nearest the breech, rates of 10, 15, and 20 rpm would result in a temperature of 400 C, in 55, 28 and 19 min, respectively.

British Experiments

The British have conducted a temperature investigation[427] with the quick-firing 3.7-in. gun Mark VI. The data are graphed in Figure 10. The firing was in bursts of 10 rounds fired automatically; the rate of fire during a burst being 20 rpm. However, the bursts were fired at irregular intervals, as shown by the figure. In all 140 rounds were fired in about an hour.

A spring-loaded thermocouple was used at the muzzle; for chamber measurements two spring-mounted thermocouples were fastened to a steel tube; this was inserted so that contact was made by the thermocouples with the wall at the commencement of rifling and at the neck of the cartridge case. Temperatures were taken at the end of each burst. The relatively rapid heating and cooling at the muzzle are clearly shown in the figure. The air temperature was 10 C, and a high cold wind assisted in cooling the muzzle section. It must be noted that the opening of the breech for the insertion of the thermocouples had a marked cooling effect. Maximum temperatures were

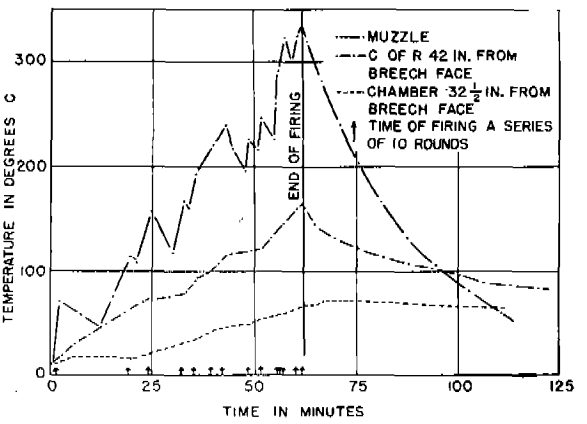


FIGURE 10. Temperature measurements in 3.7-in. AA gun, Mk VI. (From Proceedings of the Ordnance Board No. 27,604.)

333 C at the muzzle, 165 C at the commencement of rifling, and 73 C in the second chamber position.

These experimental results have been compared[401] with computations made by Hicks and Thornhill by their method outlined in Section 5.4.1, using an assumed average rate of fire of 2⅓ rpm. Since the early firings were at a slower, and the later ones at a faster average rate than this, the calculated temperatures for the muzzle are high from the second burst till near the end of firing, when they agree well with the measurements. Computed and measured temperatures near the commencement of rifling agree well throughout.

U. S. Naval Guns

This theory was extended,[401] although with necessary qualifications, to the estimation of temperatures in a proposed U. S. Naval 3-in./70-cal. gun to fire at a rate of 90 rpm. Upper and lower bounds for heat input were assumed. The resulting estimated temperature-time-rounds relations are shown in Figure 11. It is to be noted that temperatures near the origin of rifling are calculated for operation with and without a cooling jacket. The results indicate hypothetical mean barrel temperatures, and give no idea of the temperature gradients across a barrel section. It was tentatively concluded that general softening of the bore might occur near the muzzle, but would not be likely near the origin of rifling; and that it is unlikely that more than two or three bursts of 75 rounds each could be fired before the condemning limit of wear would be reached.

A more complete study of the same 3-in./70 cal.

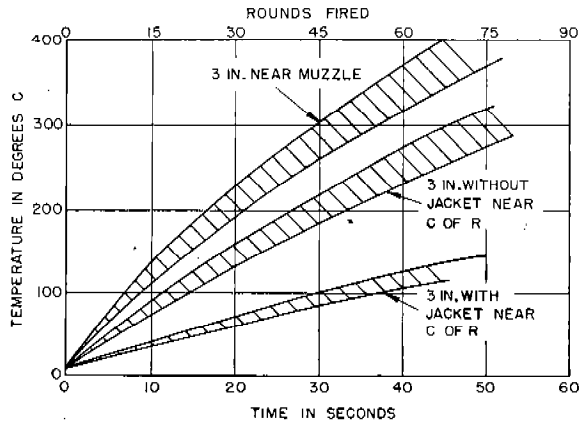


FIGURE 11. Estimated temperatures in proposed 3-in./70-cal. naval gun. (From report to Bureau of Ordnance, Navy Department, from E. P. Hicks and C. K. Thornhill.[401])

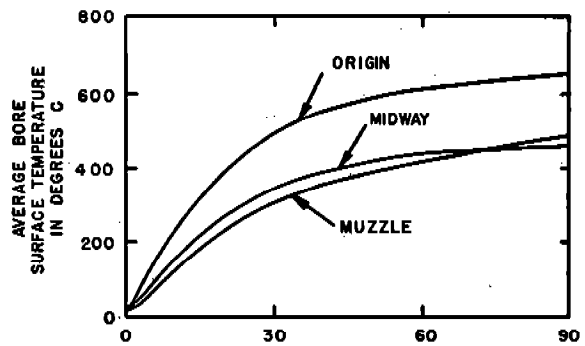


FIGURE 12. Average bore surface temperature of 3-in./70-cal. gun firing at rate of 90 rounds per minute, uncooled. (This figure has appeared as Figure 72 in NDRC Report No. A-434.)

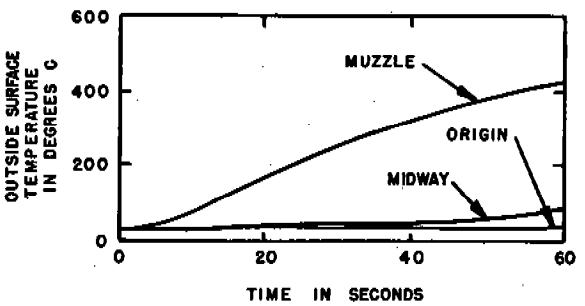


FIGURE 13. Outside surface temperature of 3-in./70-cal. gun firing at rate of 90 rounds per minute, uncooled. (This figure has appeared as Figure 73 in NDRC Report No. A-434.)

gun was later made at the Geophysical Laboratory by methods that did take into account position within the barrel wall (see Section 5.4.2). The principal results are shown in Figures 12, 13, and 14. At the

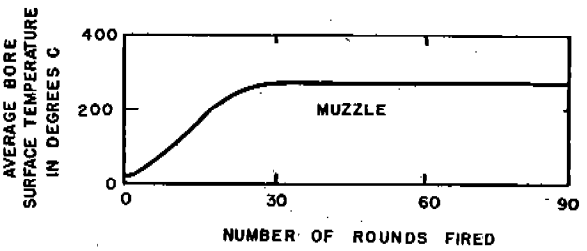


FIGURE 14. Average bore surface temperature of 3-in./70-cal. gun firing at rate of 90 rounds per minute, water-cooled. The origin and midway temperatures are practically the same as in Figure 12 of Chapter 5. (This figure has appeared as Figure 75 in NDRC Report No. A-434.)

muzzle, where the wall is thin, the average temperature for an uncooled gun is little larger at the bore than at the outer surface (Figures 12, 13). Therefore at either position the temperature is nearly equal to the mean muzzle temperature, and the agreement with Figure 11 is good. But toward the breech, where the wall is thicker, the mean temperature across a section does not give the essential picture. At the end of 90 rounds fired in 1 min, the average temperature at the bore near the origin of rifling reaches 650 C, while at the outer surface it has not begun to rise. It follows that external water cooling has no effect at the origin during this time, contrary to what appears in Figure 11.

The Bureau of Ordnance of the Navy Department has measured external temperatures near the muzzle of 5-in. guns during periods of rapid fire. For a 5-in./38-cal. gun, fired 151 rounds in 12½ min, a rise of temperature amounting to 375 degrees centigrade was observed. For a 3-in./50-cal. gun the temperature rose 275 degrees centigrade after 98 rounds had been fired in about 16 min. The rise of temperature during the latter firing is shown in Figure 6 in comparison with calculated values discussed at the end of Section 5.4.2. Similar calculations have also been made for the same gun fired at 40 and 45 rounds per minute[99,106] and for 3-in. and 90-mm guns fired with different powders at 20 rounds per minute.

5.6 RESULTS OF HIGH TEMPERATURES

5.6.1 Erosion

The temperature of the bore surface is the general regulator of the changes there which, taken together, constitute erosion, as is discussed in detail in Chapter 13. One of those changes is liquefaction of the surface. In this connection it is important to keep in mind that

the liquefied material on the surface of a steel barrel is a reaction product having a fusion temperature considerably lower than that of steel, as is brought out in Section 12.5.3. Therefore there is no essential conflict between the observations summarized in Section 12.6 and the calculations of bore surface temperatures that had led to the conclusion[48] that "the maximum temperature of the bore for all small guns (at conventional velocities) remains definitely below the melting point of steel, even with the hot FNH-M2 powder and under conditions of rapid firing."

5.6.2 Danger of Cook-Offs

A cook-off may be defined as an explosion of the fuze, projectile filler, or propellant that results from a high temperature reached by a round after standing for some time in the chamber of a hot gun.

Experimental evidence regarding the danger of cook-offs has been gathered from two sources—tests definitely set up to determine conditions under which cook-offs occur, and studies of the phenomenon as it took place fortuitously in the course of experiments designed for other purposes or under actual service conditions. Temperature measurements in the various trials reported were made by thermocouples attached to the outer surface of the guns.

Tests on the caliber .30 Colt-Browning MG firing ball, M1 ammunition, and on the caliber .50 Browning MG were conducted in England.[381] For air-cooled guns, cook-offs of detonator, filling, or propellant were shown to result after long bursts. Bursts of 100 to 200 rounds caused cook-offs of the fuze and shell-filling; bursts of 250 and more rounds led to cook-offs of all three components. In water-cooled guns no cook-offs resulted.

In experiments[526] with cooling of the caliber .50 machine gun, gun temperature against time to cook-off were plotted for 14 observed cases. This showed that the time decreases with temperature. No cook-offs were observed at temperatures below 900 F, which was considered a critical temperature.

In a study of the 20-mm Hispano Mark V gun, tests were again made for cook-offs of the various components. Several different fillings and propellants were tested. Some cases of explosions in the lips of the belt feed mechanism were reported. As a result of these trials, although bursts of 175 rounds caused no cook-offs, a maximum of 150 rounds was recommended for complete safety. However, in a test of 20-mm AA guns conducted by the Navy, Bureau of Ordnance, a cook-off occurred after the firing of only 120 rounds. This may have been due to a very high rate of fire.

Results also vary with 40-mm guns. The lowest reported number of rounds causing a cook-off of U. S. ammunition, starting with a cold gun, is 94. Firings in England using British guns and ammunition, have been reported to give cook-offs 3 min after the firing of 50 rounds, with an initially cold gun. As to water-cooled guns, a Bureau of Ordnance letter states "it is believed that relatively small danger of a cook-off exists in the water-cooled gun when the cooling system is operating properly."

The British have also conducted trials for propellant cook-offs in the 3.7-in. gun, Mark VI, and the quick-firing 3.7-in. AA guns, Marks I and III. It was concluded that one of the cooler propellants would not cook-off in a round left in the gun after a series of firings at a rate of 20 rounds per minute and that the hotter ones would be unlikely to do so under most circumstances.

Relatively little information is available on cook-offs in larger guns, most of this having been gleaned from field experience or in tests set up for other purposes. Taking into consideration the dependence of heat input on caliber, the following rule-of-thumb for heating has been stated by British authorities: [544]

> The number of rounds of continuous fire with full charges that will bring guns to the conditions described as "hot" will vary with rate of fire and may be taken to be approximately as follows:
>
> | | |
> |---|---|
> | 6-inch and above | 80 rounds |
> | Below 6-inch | 30 rounds |
>
> If a gun has not reached this critical condition no special precaution need be observed in leaving a round chambered.

5.6.3 Effect of Temperature on Ballistics

Accuracy Drop from Expansion of Bore

When a gun barrel wall reaches high temperatures as the result of rapid fire, the metal expands. If this expansion is sufficiently great, the engagement of the rotating band of the projectile with the rifling of the bore diminishes until proper spin is no longer imparted to the projectile, when tumbling begins.

It is interesting to compare the ballistic behavior of a barrel with the expansion computed from a measured rise of temperature. This has been done for a caliber .50 aircraft barrel with a 9-in. stellite liner.[106] During the firing of a 425-round burst, tumbling became persistent after about round 350. At this time the outer surface temperature at a distance of 24.0 in.

from the breech was 735 C, and the temperature 0.14 in. from the bore surface was 765 C. Assuming an average barrel temperature of 750 C, and a coefficient of linear thermal expansion of 16×10^{-6}, the increase in bore diameter amounted to 0.006 in. Since the depth of rifling in this barrel is only 0.005 in., the amount of spin imparted to the bullet would be small because of "skidding," an effect that is illustrated in Figure 12 of Chapter 27.

At less extreme temperatures there is still some loss of spin, accompanied by balloting and increasing yaw within the gun, resulting in greater external yaw and loss of accuracy. This effect in a caliber .50 machine gun barrel has been counteracted to a large extent by using a "choked muzzle" obtained by means of chromium plate of tapering thickness, as described in Chapter 23.

Pressure and Velocity Changes from Heated Propellant

In ballistic tables, pressure and muzzle velocity are calculated for a powder temperature of 70 F (21 C). It has long been known, however, that an increase in temperature increases the potential and the burning rate of the powder (Section 3.3.3), giving a greater muzzle velocity.[509,515] Pressures are also greater. Since it was recognized that in service a powder might be fired at ambient temperatures varying from −50 F to +150 F, this problem was studied by the Army Ordnance Department.

Tests were made [286] with FNH-M1 powder manufactured for 3-in. guns fired in a 76-mm gun, M1. The special interest in this experiment was in the low temperatures, since service experience had shown that dangerous sporadic pressures may arise under conditions of extreme cold. However, the tests at 0 F and above, while considered "satisfactory and normal," showed a definite linear trend of increased pressure with rising temperature, as shown in Figure 15. In the course of these tests a procedure was developed and used for ten 76-mm guns, whereby the 115 per cent pressure proof-firing was performed, using rounds heated to 135 F rather than by increasing the charge. If we assume that the linear trend exhibited in Figure 15 would continue, a powder temperature of 265 F (129 C) would yield a dangerously high pressure of 145 per cent normal. This temperature might well be reached by a round left for a considerable time in the chamber of a hot gun.

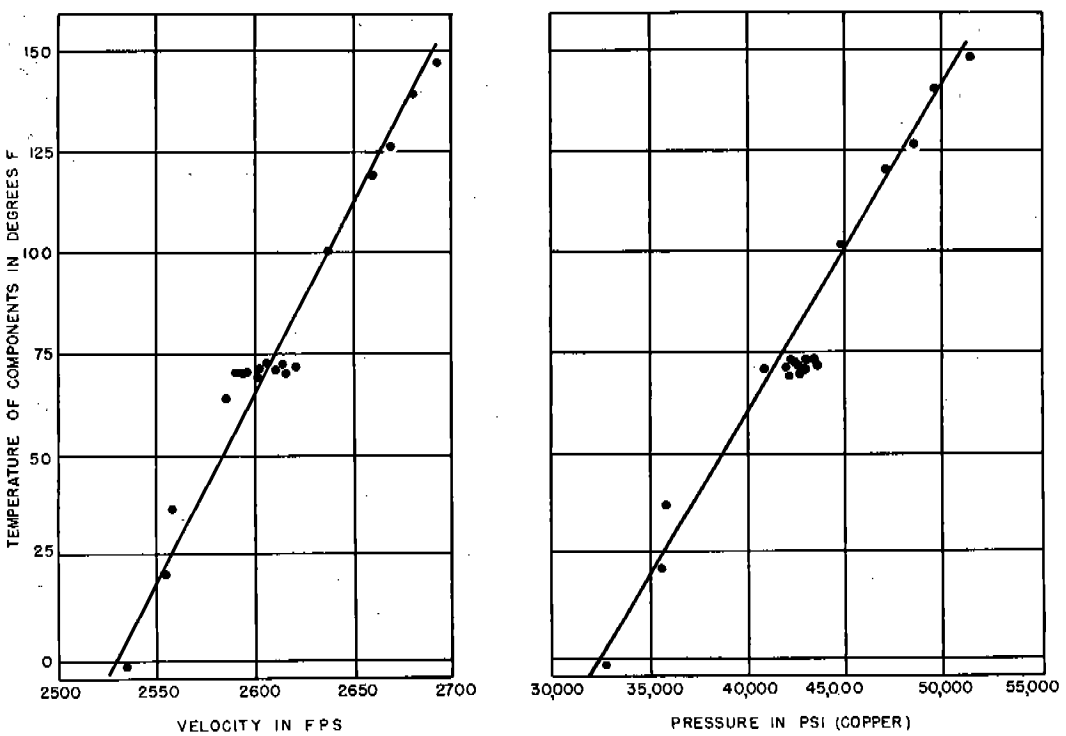


Figure 15. Average velocity and pressure vs temperature for 76-mm gun, M1. (By courtesy of War Department Technical Division; *High and low temperature ballistic research*, 1st Progress Report.[286])

These experiments were continued with a 37-mm gun, T28 (ballistically the same as the M3) and with a 20-mm gun, AN-M2.[j] In the latter case, using IMR powder, it was demonstrated that the change in pressure was approximately linear and equal to 49 psi per degree Fahrenheit change in temperature. For the 37-mm gun tests were carried out with both FNH-M5 and FNH-M2 powders. Equations (37) and (38) were developed in the two cases for the change in pressure in pounds per square inch as a function of Fahrenheit temperature T.

$$(P_T - P_{68}) = -3421 + 42.5T - .008T^2 + .0018T^3 \quad (37)$$

where $P_{68} = 45{,}300$ psi when $T = 68$ F for FNH-M5

$$(P_T - P_{68}) = -2584 + 22.8T + .066T^2 + .0023T^3 \quad (38)$$

where $P_{68} = 43{,}100$ psi when $T = 68$ F for FNH-M2.

For muzzle velocity in the 76-mm gun, the indicated increase per degree Fahrenheit was shown to be approximately 1 fps. For the 20-mm gun, the velocity change was a linear function of the temperature equal to 1.2 fps per degree Fahrenheit. In the 37-mm gun, the trends were found to be nonlinear, as in the case of the pressure, equations (39) and (40) having been developed to express the data.

$$(V_T - V_{68}) = -81.7 + 1.416T - .00599T^2 + .0000417T^3 \quad (39)$$

with $V_{68} = 2{,}894$ fps for $T = 68$ F for FNH-M5.

$$(V_T - V_{68}) = -59.1 + .89T - .00304T^2 + .000040T^3 \quad (40)$$

with $V_{68} = 2{,}842$ for $T = 68$ F for FNH-M2.

5.6.4 Weakening of the Barrel Wall

That high temperature attained in a gun can result in weakening of the barrel wall has long been well known. The sequence of events in long bursts of automatic fire in a steel barrel appears to be as follows. During the early rounds the conduction from the bore surface is rapid; the barrel as a whole heats slowly with slight and generally favorable effects on ballistics. After the mass temperature of the barrel becomes relatively high, thermal expansion permits some balloting of the projectile. At the same time the heated bore surface begins to be austenitized and the lands to be swaged. The swaging combined with further thermal expansion weakens the engagement of the rifling, increasing internal yaw of the projectile and making obturation less effective. Origin erosion with consequent blow-by of gases results in reduced muzzle velocity and still higher bore surface temperature.

The process continues and the bullets pursue erratic courses in the hot bore. If a short section at the muzzle has a small enough diameter and sharp rifling (as in a barrel with choked muzzle chromium plate), the bullet may receive sufficient spin to be stable after

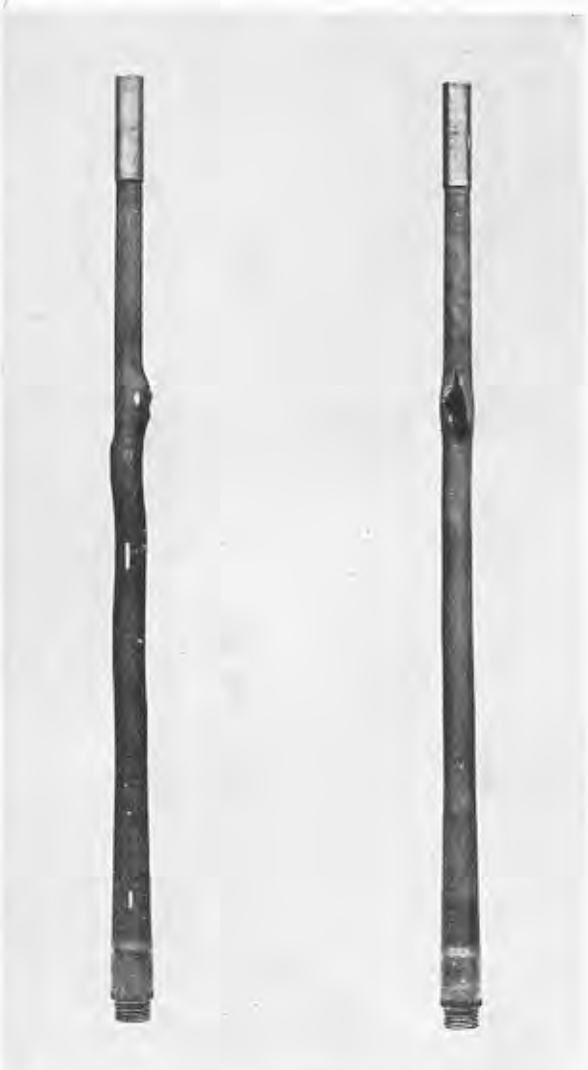


FIGURE 16. Caliber .50 aircraft barrel distorted during firing. Note that bulging is confined essentially to one plane; the two photographs were taken at right angles to each other.

[j] Private communication from B. E. Anderson, Office of the Chief of Ordnance.

CONFIDENTIAL

leaving the barrel. Otherwise tumbling occurs. Finally, at very high temperatures the tensile strength of the gun steel fails, the barrel warps and the gun jams; in extreme cases the bullet plows into, or even through, the barrel wall, as is illustrated in Figure 16. In the case of a stellite-lined barrel, origin erosion is inappreciable and tumbling (keyholing) begins rather suddenly, with no great drop in muzzle velocity.

In the case of larger guns, this problem of the effect of temperature on yield strength has received careful consideration. In rapid-fire tests of a 3-in. AA gun, calculations were made to determine maximum temperatures permissible at various distances from the breech.[179] These were determined from the expected pressures and the yield points of the gun-steel at elevated temperatures. On the basis of these computations, it was decided to have the crew take cover when a welded thermocouple 5.21 in. from the muzzle indicated an external barrel temperature of 250 C. The actual temperature there at which bursting might have been expected was approximately 475 C. Although the former temperature was maintained for a considerable length of time, the latter was not reached during the firing, the highest temperature recorded by this thermocouple having been 360 C. This temperature was attained 2 min after the firing of 118 rounds in 15 min; previous firing had already preheated the gun to 245 C.

Similar calculations were made for the 105-mm AA gun, M1. Dangerous external temperatures ranged from 405 C at 165 in. to 565 C at 40 in. from the muzzle. This gun has a liner with a clearance tapering from 0.007 in. at the muzzle to 0.003 in. at the breech. Most of this space is filled with mixed grease and powdered graphite when the liner is inserted.

A number of mechanical effects of raised temperatures in guns have been listed by the British Gun Design Committee.[333] A first statement is "The temperatures attained (a maximum external value of 322 C) would not permanently affect the yield point of the ordinary gun steels because they are far below the tempering temperatures employed, but the yield point of the steels when stressed at the raised temperature would be lower than at normal temperatures."

It was also remarked that uniform heating would not substantially reduce internal stresses due to autofrettage or to shrinkage, but "The heating is, of course, not uniform and a steep temperature gradient might have more pronounced effects on stress distribution. Temperature gradients through the wall may be very irregular in guns which have been cooled after rapid fire."

In conclusion there was considered the possibility of longitudinal stress. It was pointed out that a temperature difference of 100 degrees centigrade between the inner and outer tubes of a built up gun might lead to protrusion of the liner at the muzzle. This, together with circumferential cracking, has been observed in 8-in. howitzers, Mark VII; they were, however, considered to be poorly designed. It has also been considered in connection with the design of a 16-in. gun.[429] It is stated that a difference of 400 degrees Fahrenheit may cause a loose liner to protrude as much as 2 in. This may cause the liner to bell-mouth thus affecting accuracy. It may later prove difficult to remove the liner. Additionally, appreciable hoop stresses may be caused by the liner being wedged into the taper seating by reason of its longitudinal extension and diametrical expansion.

5.7 COOLING OF GUNS[k]

5.7.1 Rates of Cooling

Having examined the rates and sources of heat input to the gun bore, and considered the distribution of the heat in the barrel wall, we turn our attention to the corresponding cooling conditions; in particular, we shall look for methods by which the temperatures may be held within limits which will prevent the occurrence of the most serious results of overheating.

There is no doubt that some heat loss takes place from the bore surface; the opening of the breech of the gun causes some forced convection there, and ejection of the projectile has some effect at the muzzle. But in the case of very rapid fire there is little chance for the gases within the gun to cool, and although as has been pointed out,[348] there is some reversal of heat

[k] Division 1, NDRC did not undertake any extensive experimental investigation of the cooling of guns, but limited its activities largely to interpreting data obtained elsewhere, in an effort to apply them to the problem of increasing muzzle velocity without decreasing barrel life. In an effort to facilitate the crossflow of information it organized, at the instance of the Army and Navy, a special Advisory Committee on the Cooling of Guns, made up of representatives of the Army Ordnance Department, the Air Ordnance Office, the Navy Bureau of Ordnance, the Navy Bureau of Aeronautics, two Division 1 contractors (Geophysical Laboratory and Crane Company), and Division 1 staff. This committee held three meetings during 1945 and two during 1946. Much of the material in this section was presented and discussed at those meetings.

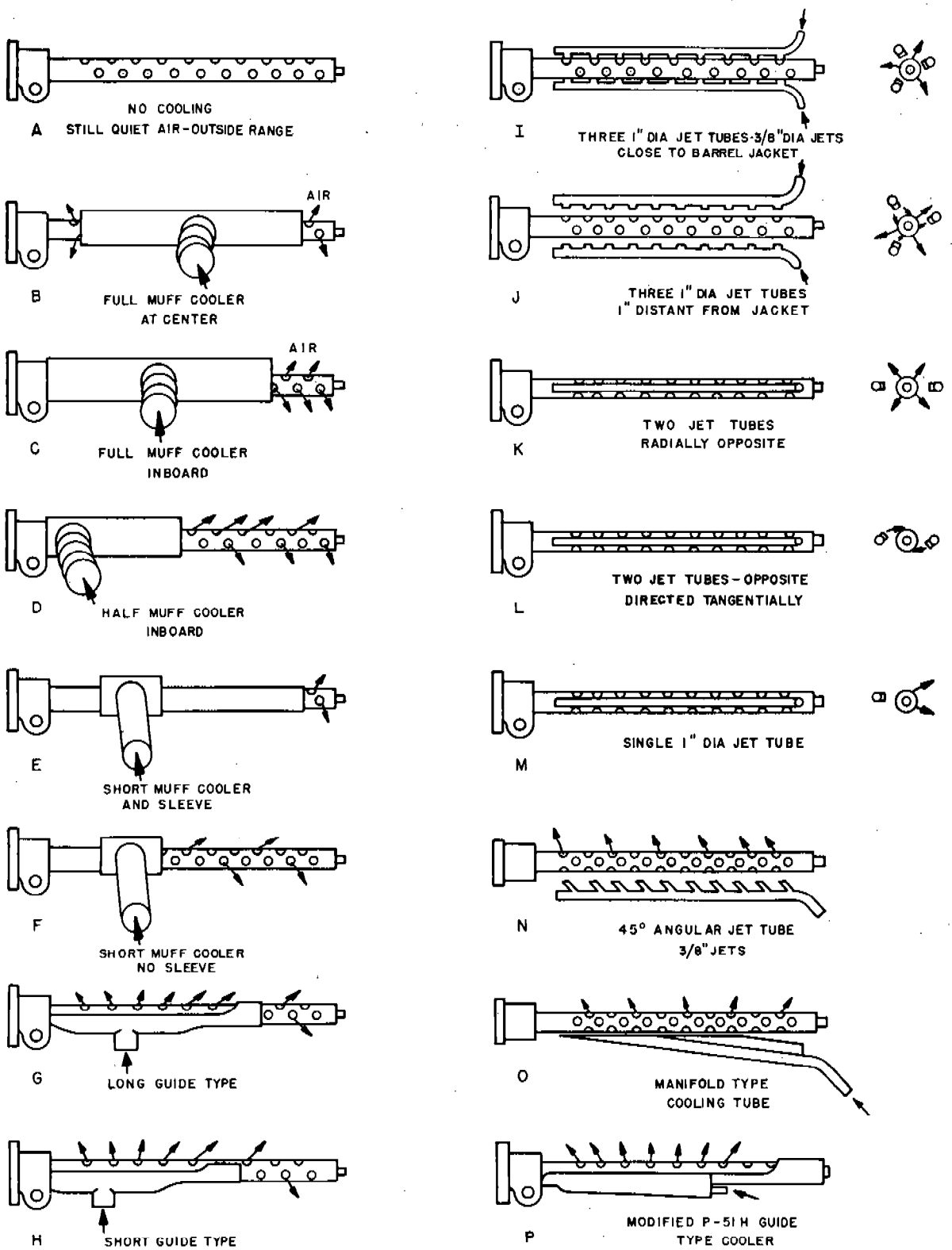


FIGURE 17. Various types of cooling devices tested on ground (by permission of North American Aviation, Inc.; Report No. NA-8568, *Performance and design criteria for caliber .50 gun barrel coolers for aircraft*).

[redacted]

flow, this must have very slight effect and we may continue to consider the flow as one-directional.

On the external surface of the gun there is longitudinal variation in temperature; commonly the thinner muzzle section heats more rapidly at first, but as flow continues through the wall the greater heat input near the origin of rifling results in higher temperatures in that region. For our purposes it is convenient to consider the whole outer surface as being at approximately the same temperature. Cooling then takes place by radiation, and by free or forced convection.

Radiation plays an important part in cooling. It has been estimated[187] that "on a windless day, with the gun at a temperature of 330 C almost 80% of the heat loss is by radiation." The intensity of radiation is given by the Stefan-Boltzmann law, equation (41),

$$I = \sigma(T_G^4 - T_A^4)\epsilon_s, \tag{41}$$

in which T_G is the absolute temperature of the gun surface, T_A is ambient temperature, and ϵ_s is the emissivity of the barrel surface. If I is in calories per second per square centimeter, the value of σ is 1.36×10^{-12}. For the example just given, we find $I = 0.18$ cal/cm^2. If this rate were maintained, a gun with a heat input of 18 cal/cm^2 in one round would have its heat dissipated in about 50 sec if we assume a wall ratio of 2 and ignore the time of conduction through the barrel. Of course the radiation rate drops rapidly with temperature; but this emphasizes the importance of cooling by radiation at high temperatures.

Cooling by convection is fundamentally exponential. Since the cooling rate is proportional to the difference between surface and ambient temperature, as given by equation (42),

$$\frac{dT}{dt} = -k(T_G - T_A), \tag{42}$$

we obtain the temperature-time equation (43):

$$\frac{T_G - T_A}{T_0 - T_A} = e^{-kt}. \tag{43}$$

Since cooling actually results from the two causes acting simultaneously, various empirical relations have been adopted to represent the situation. One assumption[187] was that cooling is proportional to the 1.23 power of the temperature difference. Another investigator [181] assumed the power to be 5/4 and made experimental determination of the proportionality factor for the 75-mm gun, pointing out that this is dependent on wind velocity. The resulting graphs indicated cooling of approximately 280 centigrade degrees in 80 min. The temperature at the thermocouple nearest the breech did not drop this rapidly, indicating greater heat storage in that section. Increase in thickness of the barrel wall giving greater heat storage has long been known to diminish maximum temperature. The limitation of the method is obvious; the added weight is particularly undesirable in aircraft guns.

5.7.2 Methods of Cooling

Air blasts. The noticeably improved cooling rate occurring during firings made in strong winds suggested the desirability of using artificial air blasts. The weight of other types of cooling equipment, combined with the obvious possibilities of forced convection in flight, made this the natural method for aircraft. Extensive studies of this type of cooling were made both in Britain and in this country.

The cooling system[302,411,419,420,430] developed in Britain by the Naval Air Fighting Development Unit consists of a 2½-in. diameter steel tube surrounding the barrel of the caliber .50 gun and open at both ends. An auxiliary tube 1 in. in diameter enters the rear portion of the tube and extends to the outside of the lower wing surface. One assembly weighs approximately 5 lb. The assemblies have been adapted for use with a number of types of fighter-planes. When a firing cycle of 3-sec bursts at 1-min intervals is used, the N.A.F.D.U. cooling tube doubles the accuracy and velocity life of chromium-plated barrels and gives marked improvement in standard unplated barrels. It will not, however, be of benefit if continuous bursts of 300 rounds are fired.

A comprehensive program of tests for performance of a variety of cooling devices was carried out[525,526] for the Army Air Forces at North American Aviation, Inc. Thermocouples were fastened to the barrels at five points spaced at 5-in. intervals along the barrel, beginning at a point 5 in. from the face of the receiver. Temperatures at these positions were graphed for various times during the firings. These records were made for a number of firing schedules with the several cooling installations. The cooling devices tested are shown diagrammatically in Figure 17.

The second of the thermocouple positions was adopted as a temperature index for performance; occasionally more than one thermocouple were placed there. The performance factor for a given cooler represents the number of rounds that can be fired each

minute through a barrel that has already reached a temperature of about 900 F, without further raising its temperature appreciably. Numerical and graphical methods were established for determining this point. Some typical values of the performance factor are given in Table 8. An empirical linear relation between this factor F and the length I of the permissible initial burst is given by equation (44).

$$I = 125 + 0.65F \qquad (44)$$

A single jet cooler was decided upon as most effective.

Water Jackets. Cooling of gun barrels by means of water circulating through a jacket over the barrel was considered and adopted many years ago. Where this type of installation is feasible, it has proved to be very effective. Water-cooled machine guns have operated under severe schedules without overheating. In some cases the heat of vaporization is utilized by permitting boiling off of the water.

The objections to water-cooling are weight, size of installation necessary, and under some conditions, difficulty in securing water for the purpose.

Tests have recently been made at the Naval Proving Ground on the cooling of 40-mm guns by this method, as referred to in Section 5.5.2. In addition, as mentioned in Section 5.6.2, service reports indicate no dangerously high temperatures in these guns.

In the 5-in./38-cal. gun tests mentioned in Section 5.5.3, the effect of external water-cooling by hoses was tried. After the close of firing, a projectile was inserted in the breech. Temperatures under the band and under the bourrelet rose for about 6 min after the water was applied, then fell off as it continued to play.

Special Coolants. The use of special coolants has often been considered. Preliminary tests of a cooling device which injects liquefied CO_2 into the chamber of a caliber .50 barrel during firing were made at the Geophysical Laboratory.[110] One hundred-round bursts, with a 2-min interval between bursts, were fired in a new steel aircraft barrel, using AP-M2 ammunition. The rate of fire averaged 810 rpm. Results showed apparent improvement over a similar barrel without cooling, but a direct comparison with earlier firings was impossible because of three short stoppages in the second burst. The amount of CO_2 used during the firing of 500 rounds was 4.6 lb.

Injection Sprays. Cooling of the bore by wet swabs is traditional; and it has been suggested that for smaller caliber cannon, the tube might be cooled by pumping water through the bore between bursts. The general problem of utilization of the latent heat of vaporization of water has been frequently studied, and injection-cooling has now been developed.

The initial work in this development was done with caliber .50 barrels by Purdue University for the Army Ordnance Department, using a nonaqueous cooling liquid. Although considerable improvement in the performance of steel aircraft barrels was found,[294] it was not as great as that gained by the use of either a stellite liner (Chapter 22) or choked-muzzle chromium plate (Chapter 23). Some tests by the Ordnance Department with stellite-lined barrels and chromium-plated barrels delivered by Division 1 showed still further improvement in the former by the use of this device, but the result was not obtained in general with chromium-plated barrels. Furthermore, the device was erratic in its performance[1] and decreased the cyclic rate of the gun.

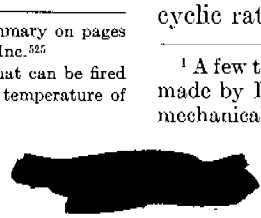
TABLE 8. Performance factors of air-cooling devices for caliber .50 aircraft machine gun barrels fired 200-round bursts in still air on the ground.*

Type of cooler (See Figure 17)	Performance factor†
A. (No cooling)	10
B. Full muff cooler, at center	19
C. Full muff cooler, inboard (Cooler against gun trunnion collar)	14
D. Half muff cooler, inboard (Air inlet near body)	17
E. Short muff cooler and sleeve	64
F. Short muff cooler without sleeve	37
G. Long guide type cooler	40
H. Short guide type cooler	51
I. Triple jet tube cooler, close to barrel jacket	48
J. Triple jet tube cooler, 1-in. distant from jacket	32
K. Two jet tubes, radially opposite	41
L. Two jet tubes opposite, directed tangentially	42
M. Single jet tube	
Jets aimed at barrel jacket holes	55
Jets aimed at solid jacket	28
Jets aimed between holes in jacket	53
Jets aimed at holes, with P-51H guide	55
N. 45° angular jet tube	
Jets aimed opposite thermocouple	45
Jets aimed at thermocouple	31
O. Manifold type cooling tube	
Touching jacket, $5\frac{1}{8}$ in. from collar	56
Touching jacket, $3\frac{1}{4}$ in. from collar	49
One inch from jacket, 11 in. from collar	20
One-half inch from jacket, $3\frac{1}{4}$ in. from collar	33
P. Modified P-51H guide type cooler	29

* This table has been taken by permission from the summary on pages 59 and 60 of Report NA-8568, North American Aviation, Inc.[525]

† The "Performance Factor" is the number of rounds that can be fired each minute through a barrel that has already reached a temperature of about 900 F, without raising its temperature appreciably.

[1] A few tests on special barrels using this cooling device were made by Division 1 at the Geophysical Laboratory,[81,110] but mechanical difficulties prevented any comprehensive testing.



A similar injection-cooling device that was more satisfactory mechanically was developed by Purdue University[545] for the 90-mm gun, M1A1, and the 155-mm gun, M1. For bores this large it was possible to impart rotation to the spray in an attempt to disperse any tendency toward "film" conditions. These cooling devices were tested at Aberdeen Proving Ground.

The nozzle was manually positioned. Water was injected at a gauge pressure of 200 psi. For the 90-mm gun a weight of 0.47 lb of water proved satisfactory for a rate of fire of 10 rounds per minute. This held the temperature to 260 F with very slight temperature gradient. For a higher cyclic rate, 0.60 lb of water seemed preferable. For the 155-mm gun, 1 lb of water was injected in a 2-sec cycle. At the time of writing the tests were being continued. They indicated favorable results for this method of cooling as a means of reducing erosion.



Chapter 6

BORE FRICTION

By *William S. Benedict*[a]

6.1 INTRODUCTION

6.1.1 Nature and Importance of Bore Friction

THE IDEAL GUN would be one in which all the available energy of the powder was transformed into kinetic energy of the projectile. Unhappily, as pointed out in the discussion of the general problem of hypervelocity (Chapter 1) and more particularly in Section 3.5, actual guns fall far short of the ideal, and even short of the more attainable goal of an efficient thermodynamic engine, in several respects. One principal source of inefficiency, thermal losses to the bore, has been discussed in the preceding chapter. Another most important cause of diminished performance in new guns, a factor of some importance in their erosion, and a prime factor in their erratic behavior, is the subject of the present chapter, bore friction.

Under the heading of bore friction it is customary to include all the forces that oppose the acceleration of the projectile, counter to the force exerted on the base of the projectile by the pressure of the powder gas. We will express the friction as the force per unit area that resists the accelerating pressure on the base of the projectile, and denote it by P_r, usually in units of thousands of pounds per square inch, klb/in.^{2}. If the inertial mass of the projectile is m, the cross-sectional area of the bore A, X, the coordinate of the projectile relative to the gun, and P_X the pressure on the base of the projectile when it is at X, equation (1) is the fundamental one by which we define the friction.

$$P_r = -\frac{m}{A}\frac{d^2X}{dt^2} + P_X. \qquad (1)$$

The largest portion of this chapter is concerned with the methods of determining the accelerating pressure, the base pressure, and their difference, which is the resisting pressure or bore friction; and in describing the results obtained in measuring these quantities in the ballistic firings carried out as part of the program of Division 1 at Carderock (Chapter 4). As a preliminary, we shall discuss in general terms the nature of the various forces that may be expected to contribute to the resisting pressure.

[a] Geophysical Laboratory, Carnegie Institution of Washington, and National Bureau of Standards.

6.1.2 Component Forces Appearing as Bore Friction[342]

Engraving Forces

At the commencement of motion, in guns employing conventional banded projectiles, the resisting pressure will be high compared to the accelerating pressure. At the very start, with fixed ammunition, the projectile must be released from the case into which it is crimped. Then follows the engraving period. The force required to engrave the rotating band, as determined from "static" tests in which the projectile is slowly forced through the rifling in a testing machine, ranges from 2 to 20 klb/in.^{2}. The force is required to "engrave" the soft metal of the band by the process described in Section 7.3.5 and to overcome surface-to-surface friction between the band and the bore surface. In guns in which the projectile is rammed home against the forcing cone these engraving resisting forces will be operative at the very start, so that the velocity of the projectile is zero as it enters the forcing cone, and the starting friction during firing should be equivalent to that determined statically; in most guns with fixed ammunition, however, the projectile will have traveled on the order of a tenth of a caliber and have acquired an appreciable velocity before engraving begins. In all cases the velocity will increase during engraving. With increased velocity the resistance to plastic deformation will decrease, and hence the engraving friction will fall below that found statically.

Band-to-Bore Friction

After the deformation of the band to fit the grooves of the rifling is complete, the passive resistance generated at the band decreases greatly, being now due principally to surface friction. (In guns with increasing twist engraving continues throughout the travel; in most guns it is virtually complete after the rear

of the band has entered the region of constant land diameter.) The surface component of friction P_{rs} is proportional to P_b, the pressure of contact of the surfaces (band pressure), as expressed by

$$P_{rs} = \frac{4fbP_b}{D}, \tag{2}$$

where b is the length of band, D the tube diameter, and f the coefficient of friction. As discussed in Chapter 7, P_b depends only to a slight extent on the powder pressure; it is more a function of the relative dimensions of band and tube, and is nearly constant over the length of the gun, decreasing somewhat towards the muzzle. For most bands P_b is of the order of 50 to 70 klb/in.^{2}. The coefficient of friction f, as is well known,[617] tends to decrease rapidly below its static value (which for copper-steel is of the order of 0.1) with increasing velocity; it should also depend on the condition of the bore and band, being decreased by lubrication of the bore, and decreasing further if a surface layer of the band should melt. The theory of the heating of rotating bands[45] indicates that melting of the band surface occurs in many guns; this is confirmed by the known facts of coppering of the bore surface (Section 10.5.4) and by direct measurements[72] of the interface temperature. Thus, f and P_{rs} will be comparatively low for much of the travel; the latter probably below 1 klb/in.^{2}.

Body Engraving

As the projectile acquires velocity, however, other factors will enter to increase P_r. With increasing wear on the band, and especially in partially eroded guns, the projectile cannot remain centered in the tube. The bourrelet will come in contact with the bore at irregular intervals and with varying intensity. In extreme cases this leads to "body engraving," wherein impressions of the rifling are found to considerable depth. (The relation of this phenomenon to muzzle erosion and gun performance is discussed in Section 10.4.10.) Such bourrelet-bore and body-bore contacts result in contributions to P_r, whose magnitude cannot be estimated in advance, but which may vary considerably in time and intensity from round to round.

Back Pressure of Gas

As the projectile moves down the tube, it compresses the gas ahead of it, both the originally present atmosphere and any powder gases that may have leaked past. The compressed gas will flow out of the muzzle, but its rate of flow cannot exceed the velocity of sound (1,100 fps when unheated by compression). Hence after the projectile velocity exceeds 1,100 fps the back pressure due to the gas becomes increasingly important; for an average gun, with a muzzle velocity of 2,500–3,000 fps, the resisting pressure due to compressed gas at ejection may be of the order of several hundred pounds per square inch.

6.1.3 Typical Friction Curves

In most systems of interior ballistics (Section 3.2.2) it is found convenient to divide P_r into two portions. The relatively large resisting pressure during engraving is set equal to the starting pressure P_0; it is assumed that no motion of the projectile occurs until $P_X = P_0$. Thereafter it is assumed that P_r is a constant fraction c of P_X. It is apparent from the discussion given that this represents a considerable oversimplification of the true course of the friction-time or friction-travel curve. The situation is illustrated graphically in Figure 1. A typical pressure-time and pressure-travel curve for the 3-in. gun are there presented. The friction, as determined by methods which are described later, is seen to follow the general course outlined in the preceding discussion. When plotted as a function of travel, the high engraving friction is followed by a rapid decrease to a much lower level. The conventional friction, with $P_0 = 4$ klb/in.^{2} and $c^f = 0.04$, is plotted as the dashed curves. It is seen that while there is considerable difference in the friction-time curves, the areas under the friction-travel curves, which determines the energy expended in overcoming friction, as given by

$$E_f = A\int P_r dX, \tag{3}$$

are not greatly in divergence. It is further to be noted that except during engraving the friction is very small relative to the pressure, and that therefore, in order to determine it with any degree of accuracy, all the experimental factors entering into its calculation must be known with great precision.

6.2 METHODS OF DETERMINING FRICTION

6.2.1 General Discussion of Available Methods

Having sketched the general features of the problem of bore friction, we now discuss the methods by

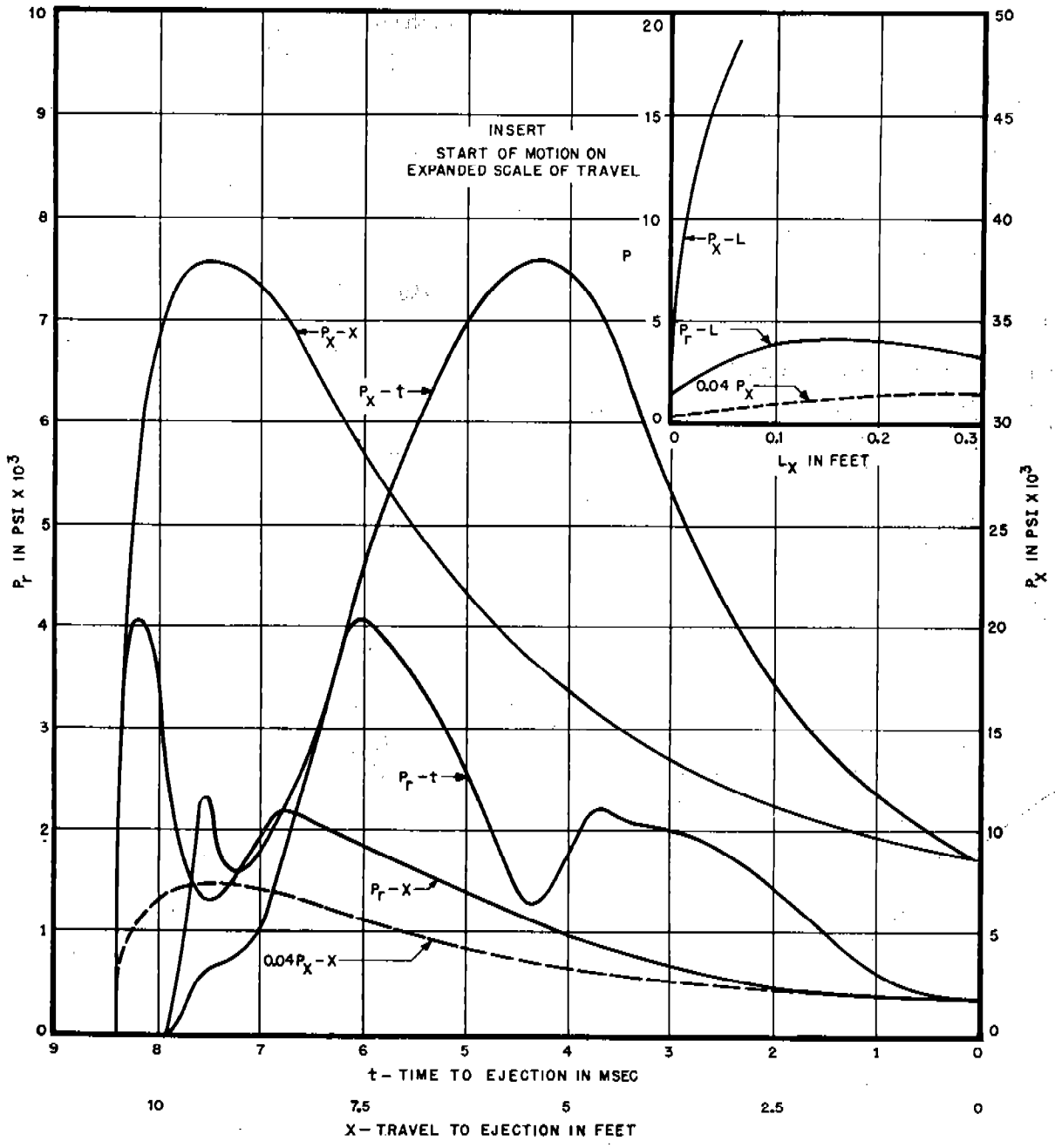


FIGURE 1. Typical curves of pressure and friction versus time and travel, 3-in. gun.

which it may be determined. The most satisfactory method would be by direct application of equation (1), measuring the base pressure, the acceleration, or their difference, by suitably loaded gauges mounted in the projectile. Such measurements have been attempted[46] but reliable results have not been attained. Not quite so direct, but apparently capable of greater precision, are other methods based on equation (1), in which the base pressure is inferred from pressure measurements made by gauges located at several positions along the bore of the gun, and the acceleration is determined from differentiations of a curve by locating the projectile with great accuracy as a function of the time. Finally there are indirect methods, by which the friction, possibly averaged over a portion of the gun, is inferred from other measurements,

such as the heat input to the bore surface or the strains in the tube wall. In using these indirect methods a distinction must be drawn between nonballistic conditions, in which the frictional forces may be isolated for study, and ballistic conditions; only in the latter are the results truly meaningful for the firing process, but it is extremely difficult to separate the observable results due to friction from those due to the action of the powder.

6.2.2 Indirect Methods

Static Push Tests and Strain Measurements

The study of band pressure and related stresses is described in more detail in Chapter 7, and need only be mentioned at this point. The quasi-static push tests,[64,114,115] of 37-mm and 75-mm projectiles of various band designs are of fundamental importance in relating the magnitude of the engraving friction to the band dimensions and design, but give only an upper limit for the actual values of P_r to be encountered in firings. The mathematical theory[13,17,58] of the stresses in a gun tube during firing contains relations from which the friction may be deduced from simultaneous measurements of the axial and tangential strain in the barrel as is described in Section 7.1.4. The friction is, however, a second-order effect and no estimates of its magnitude of any accuracy have as yet been obtained from available strain data.

Falling Weight Tests

Measurements[72] of the temperature rise in the barrel and at the band-bore interface have been made when standard ball M2 bullets were forced through sections of caliber .50 barrels. Both nonballistic tests, in which a falling weight and piston arrangement forced the bullet through the bore at velocities up to 60 fps, and ballistic firings, with standard and reduced charges of IMR powder, were performed as described in Section 5.2.2. Their principal aim was to evaluate the contribution of the frictional heat to the observed heat input in caliber .50 guns; but it also appears possible to determine the resisting pressure from experiments of this type, as may be seen from the following considerations, based on a report[45] on the theory of the heating of rotating bands.

The energy of friction E_f, defined by equation (3), will appear as heat generated at the interface, to the extent that P_r represents bore-band friction. It will flow into the bore (which is cold at the moment the band reaches it) at a rate dQ_{fb}/dt and into the band (which rapidly heats up) at a rate dQ_{fp}/dt. The temperature of the interface or band surface, T_p, depends on these rates and the thermal constants and history of both surfaces. Considering the interface to be a smooth cylinder, of diameter D and band length b, the rate of heat production per unit area of interface,

$$\frac{dQ_f}{dt} = \frac{1}{\pi Db}\frac{dE_f}{dt} = \frac{AP_rV}{\pi Db} = \frac{DP_rV}{4b} = \frac{dQ_{fb}}{dt} + \frac{dQ_{fp}}{dt}. \tag{4}$$

The amount of heat produced at any point equals the rate times the contact time, b/V. In the customary English units (Q in cal/in.^{2}–sec; P_r in klb/in.^{2}), this is

$$Q_f = Q_{fb} + Q_{fp} = 1.046DP_r. \tag{5}$$

If the friction is not produced uniformly at the interface (it will be greater along the top and driving surface of the lands than in the grooves in all guns), equation (4) must be modified, but equation (5) will hold. Assuming the band to be a source of uniform temperature T_p, we have

$$\frac{dQ_{fb}}{dt} = 2\sqrt{\frac{(kc\rho)_b}{\pi}}\sqrt{\frac{V}{b}}\,T_p, \tag{6}$$

and T_p in turn is determined by the integral

$$T_p = \frac{1}{\sqrt{\pi(kc\rho)_p}}\int_0^t \frac{dQ_p(W)}{dt}(t-W)^{1/2}dW. \tag{7}$$

The simultaneous solution of equations (4), (6), and (7), given P_r and V as functions of t, permits the determination of T_p, Q_{fb} and Q_{fp}; conversely, if T_p and V are known, P_r and the Q's may be determined.

In the falling-weight tests, V, T_p, and Q_{fb} were determined, the two last being in agreement under the theory just sketched. We find that under the conditions of these experiments Q_{fb} and Q_{fp} are nearly equal, so that the average

$P_r = \dfrac{2Q_{fb}}{.5 \times 1.046} = 3.8Q_{fb}$. At $V = 40$ fps, $P_r = 15$ klb/in.^{2}; and at $V = 60$ fps, $P_r = 12$ klb/in.^{2}.

In the ballistic firings T_p was measured, but since the time-travel relations of the projectile are only approximate, and pressure data are lacking, it is not possible to say more about the friction than that it was sufficient to raise the maximum temperature in

the interface to the melting point, which would correspond to a P_r of 3 to 10 klb/in.^{2} during engraving. Further determinations of interface temperatures in conjunction with other ballistic and heat-input data might lead to valuable results in evaluating friction.

6.2.3 Direct Determination by Projectile Gauges

Piezoelectric gauges[5,46] for the direct measurement of bore friction, acceleration, and base pressure and their methods of use are described in Section 4.5.3. Further mention should here be made of the bore friction gauge, which was essentially a pressure gauge mounted in the base of the projectile. An accelerated pressure gauge will measure not the pressure applied to the piston, but the difference between the pressure and the force per unit area needed to overcome the inertia of the piston. By constructing the piston so that the ratio of its mass to cross section equals that of the projectile, the force exerted by the piston on the crystal becomes proportional to the difference between the acceleration of the projectile and the pressure exerted on its base, that is, to the friction. Acceleration and base pressure gauges were similar, with effectively infinite and zero mass of the piston, respectively.

The performance of the gauge did not equal the excellent principle of its construction, mainly because of distortion of the signal. Some numerical results for the friction in a 20-mm Hispano-Suiza AA gun were obtained; the maximum P_r for a number of rounds averaged 9.4 klb/in.^{2}, and the friction quickly fell from this peak value attained in the first millisecond of travel to about 1.4 klb/in.^{2}. These numbers are extremely uncertain; the friction-time curve was not reproducible from round to round, and showed several sharp peaks, dropping nearly to zero, during the engraving period. If the difficulties of preventing spurious gauge vibrations and false signal pickup due to ionization could be overcome, these methods might be of considerable use.

6.2.4 Semidirect Determination from Ballistic Firings

The classical method of determining friction remains the best current one; that of analyzing ballistic data concerning the pressure of the powder gas and the position of the projectile. One prime objective of the ballistic firings[39,65,108,116,131,132] at Carderock of a Naval 3-in. gun, Mark VII, and of an experimental 37-mm gun, T47, was the determination of the friction. These firings are described in Chapter 4; we will here recapitulate the methods of obtaining and interpreting the data relative to the friction. The subsequent sections of this chapter present and discuss a few of the results.

Determination of Projectile Acceleration

The acceleration of the projectile was determined from either the position of the projectile, or the position, velocity, and acceleration of the gun in recoil. The recoil is proportional to the displacement of the projectile if the powder and powder gas move uniformly and if there is no resistance due to the recoil brake while the projectile remains in the gun.

Analysis of the recoil data, as obtained by the various instruments, leads to the conclusion that the differentiating instruments (rotary velocimeter, linear velocimeter, mutual inductance differentiator, crystal accelerometer) do not give results that may be applied to the determination of friction, probably because of vibrations in the gun or instruments. The step-by-step recoilmeter, however, gives results that are in excellent linear relationship to the best determination of projectile position, after the first 6 in. of projectile travel, indicating that the recoil is essentially free and that the powder and gas are essentially uniformly distributed.

The recoilmeter data, while of good accuracy, are not so extensive as the displacement data obtained by the microwave interferometer. Hence the latter are to be preferred in computing friction, when they have been obtained with good reliability, as in the 3-in. gun; but the recoilmeter appears to be a simple and useful instrument, by which a number of points on the displacement-time curve may be obtained.

The microwave interferometer gives essentially a continuous record of the projectile displacement, without modifying the projectile or gun in any significant way. In the 3-in. gun the projectile position was located at over 100 points per round from the start of travel to about 1 ft from the muzzle, with a relative accuracy of about 0.003 ft. The absolute accuracy as judged from the agreement of the microwave with the position given by barrel and ejection contacts may be no better than 0.02 ft; however the relative accuracy is the more significant in determining the acceleration. The time of arrival of the projectile at each point can be measured with an accuracy of 2 microseconds.

From these data it should be possible to determine the acceleration with an accuracy of about 3 per cent ($\pm$ 10 ft/sec–msec). This corresponds to an uncertainty in P_r of $\pm$ 0.5 klb/in.^{2}. It is obviously necessary and desirable to reduce to a minimum the personal factor and the accidental introduction of error in carrying out the double differentiation of the displacement-time data. Various methods of graphical, numerical, and analytical differentiation have been tested on the data for consistency and reliability. These are described in detail in the original reports and cannot be evaluated here. It is believed that least error is introduced when the displacement data are plotted as deviations from a "master curve" whose first and second time derivatives are known with absolute accuracy. Inasmuch as all similar rounds in a gun show nearly identical displacement-time curves, the deviations in displacement for any given round may be plotted on a greatly expanded scale, permitting increased accuracy in smoothing the experimental points and in differentiation of the smoothed curve. The smoothed curve may be drawn so that the velocity at the muzzle equals the velocity as determined by measurements down the range. A correction of 1 per cent or less, which may be attributed to the accelerating effect of the gaseous blast after the projectile has passed the muzzle contact, must sometimes be applied in order to bring the internal and external velocities into best agreement. The smoothed curve may be located by least-squares methods, in regions where a simple analytical function may be used to represent the travel, as for example when the pressure-time, and hence the acceleration-time, curve is a linear or quadratic function. After the smoothed curve has been located on the deviation plot, its first and second time derivatives are found by graphical or numerical methods; these added to the known first and second derivatives of the master curve give the velocity and acceleration of the projectile.

Determination of Base Pressure

In the 3-in. gun, the gas pressure was measured simultaneously at four points along the barrel. The pressure on the base of the projectile is determinable by an extrapolation of the pressure-displacement curve from the gauge positions to the base. According to the Kent-Hirschfelder theory of gas flow and pressure distribution in guns referred to in Section 3.2.2, and according to a large number of similar theories to a degree of approximation small compared with the experimental uncertainty, the ratio of pressure at any point to the base pressure P_X is given by equation (8),

$$\frac{P}{P_X} = 1 + \frac{C}{2M}(1 - y^2), \tag{8}$$

in which C is the weight of the charge, M is the weight of the projectile, and y is the ratio of volume between the point and the breech to the total volume between breech and projectile. By equation (8) we may thus calculate P_X from the observed P at any gauge, and the known position of that gauge, as a function of the position of the projectile. When several gauges are recording simultaneously, the average calculated value of P_X may be used. In case the observed pressures at the several gauges consistently disagree with equation (8), a similar relation, with an empirical constant $r(y)$ replacing $C/2M$ may be used.

Having obtained the acceleration and the base pressure by the methods just sketched, the friction follows immediately by equation (1). Care must be taken to adjust the mass m of the projectile for the rotation of the projectile and the recoil of the gun, if the accelerations are computed relative to the gun.

6.2.5 Smoothed Determination from Ballistic Measurements

When applied to most existing sets of ballistic data, the procedures of Section 6.2.4 yield results for the friction which are quite erratic in time, and negative values, which are physically absurd, are often encountered. This is the natural result of having to determine, even from data of quite high accuracy, a small difference between two much larger quantities, when there is some arbitrariness in determining one of these (the acceleration). In order to arrive at more reasonable values of the friction, it is frequently desirable to apply the following procedure, which has been termed the "integration method."

The "free velocity" V_f, which is the velocity the projectile would acquire were there no retarding force,

$$V_f(t) = \frac{gA}{M}\int_0^t P_X dt \tag{9}$$

may be accurately evaluated from P_X by equation (9). Then the corresponding "free travel" L_f may be found from it by means of equation (10)

$$L_f(t) = \int_0^t V_f(t)dt. \tag{10}$$



The "retardation," defined by equation (11), is

$$X_r = L_f - L \tag{11}$$

much smaller (from .05 − .25) than the observed travel L, but may be calculated with equal precision. By plotting against time not the observed travel but the retardation, we obtain both a smoothing of the travel data, by increase of scale, and the assurance that the friction will be everywhere positive, if we draw the curve through the observed points always concave upwards. Two differentiations of the smooth retardation-time curve give in turn the "retardation velocity" V_r and the friction P_r, in accordance with equations (12) and (13), respectively.

$$V_r = \frac{dX_r}{dt} = V_f - V, \tag{12}$$

$$P_r = \frac{M}{gA}\frac{dV_r}{dt} = P_x - \frac{M}{gA}\frac{dV}{dt}. \tag{13}$$

That is, by subtracting out the base pressure *before* plotting and doubly differentiating the travel we effectively smooth the data. Hence this method would appear to be the preferred means of determining friction.

6.2.6 Determination of Average Friction

It is to be noted that two principal determining parameters of the retardation-time curve, namely, its value X_{rm} and limiting slope V_{rm} at ejection, do not depend on any internal travel data, but are given by the pressure-time curve, the known length of the gun, and the observed muzzle velocity. Hence two constants that characterize the average friction may be determined from these data alone, if a constant time relationship for the friction-time curve may be assumed. Similarly three constants characterizing the average friction may be calculated from the pressure-time curves, the muzzle velocity, and one internal travel point.

For example, it was found[113] that a fairly good approximation to the friction in the 3-in. gun was obtained by expressing it in terms of three constants, the engraving friction P_{re}, the intermediate friction P_{ri}, and the muzzle friction P_{rm}. These are consistent functions of the reduced time t', the fraction t/t_0 of the observed time to the total time t_0 from start to ejection. The assumed functions are given in equations (14). The three P_r's may be calculated from X_{rm}, V_{rm} and X_r at $t' = 0.5$.

$$\left.\begin{aligned} P_r &= P_{re}t'/0.15 && (0 < t' < 0.15)\\ &= P_{re} && (0.15 < t' < 0.25)\\ &= P_{re} - (P_{re} - P_{ri})(t' - 0.25)/0.15 && (0.25 < t' < 0.40)\\ &= P_{ri} - (P_{ri} - P_{rm})(t' - 0.4)/0.3 && (0.4 < t' < 0.7)\\ &= P_{rm} && (0.7 < t' < 1.0) \end{aligned}\right\} \tag{14}$$

A function similar to (14), with $P_{ri} = P_{rm}$ is suggested as a suitable two-constant equation of general applicability, to calculate the friction from the pressure-time curve and the muzzle velocity. The equations yielding the P_{re} and P_{rm} are then:

$$P_{re} = \frac{MV_m}{gAt_0}8.675\frac{X_{rm}}{V_m t_0} - 2.940\frac{V_{rm}}{V_m}, \tag{15}$$

$$P_{rm} = \frac{MV_m}{gAt_0}2.570\frac{V_{rm}}{V_m} - 3.213\frac{X_{rm}}{V_m t_0}. \tag{16}$$

6.2.7 Correlation of Friction with Other Ballistic Measurements

In Section 6.2.2 it was pointed out how the friction may be roughly inferred from measurements of strain or heat input. The more accurate methods may be checked against such measurements. For example, if friction has been determined by the methods of Sections 6.2.4 or 6.2.5, from the results we may calculate the heating and melting of the rotating band; this in turn should correlate with observations on the band pressures and the coppering of the gun. The heat input due to friction may be calculated, and is to be considered in any theoretical accounting for the observed total heat input, as determined either by direct measurement of the temperature rise at various positions along the gun, or by indirect calculation of the energy losses from the powder gas.

If a series of projectiles of varying band diameter is fired, there should be a correlation with both the observed friction and band pressures. Any irregularity of the bore diameter as revealed by star-gauging should be reflected in the friction at that point. Thus in any comprehensive series of ballistic measurements the observation and correlation of these interlinked factors should be sought.

6.3 RESULTS—3-IN. GUN

6.3.1 Experimental Conditions

The apparatus and methods by which were obtained the data necessary for the determination of friction in a 3-in. gun have been described in detail in

[redacted]

Chapter 4. The constants of the gun have been listed in Section 3.4.3. The rifling of the gun was of twist increasing from zero at the origin of rifling to one turn in 25 calibers at the muzzle.

Of the 87 rounds fired from this gun at Carderock, approximately 35 were suitable for the determination of friction by the methods outlined in Sections 6.2.4 and 6.2.5, in that experimentally reliable pressures were obtained at four positions along the gun, the position of the projectile was accurately located by the microwave interferometer, and the muzzle velocity was known from the range solenoids. These rounds may be classified by the type of powder (NH, fired in the "Second Series"[65] from October 1943–May 1944, or Pyro, fired in the "Third Series"[132] from October 1944–April 1945); by the fractional weight of service charge (1.0, 0.9, 0.8, 0.7, 0.6, and 0.5 for NH; 1.0, 0.75, and 0.5 for Pyro); by the condition of the bore surface ("greased" when the surface was covered with a thin coating of heavy gun grease between firings; "dry" when the surface was untreated between rounds, which were fired at intervals of from two hours to several days, with no "warm-up" rounds); or by the initial position of the projectile ("advanced" when it was uncrimped from the shell case so that the rotating band was rammed against the forcing cone; "normal" when it was left in place, giving it about 0.4 in. of run-up). Each change in these conditions altered to some extent the pressure-travel curves and the muzzle velocity, and hence the friction. Among rounds with identical conditions, variations also appeared.

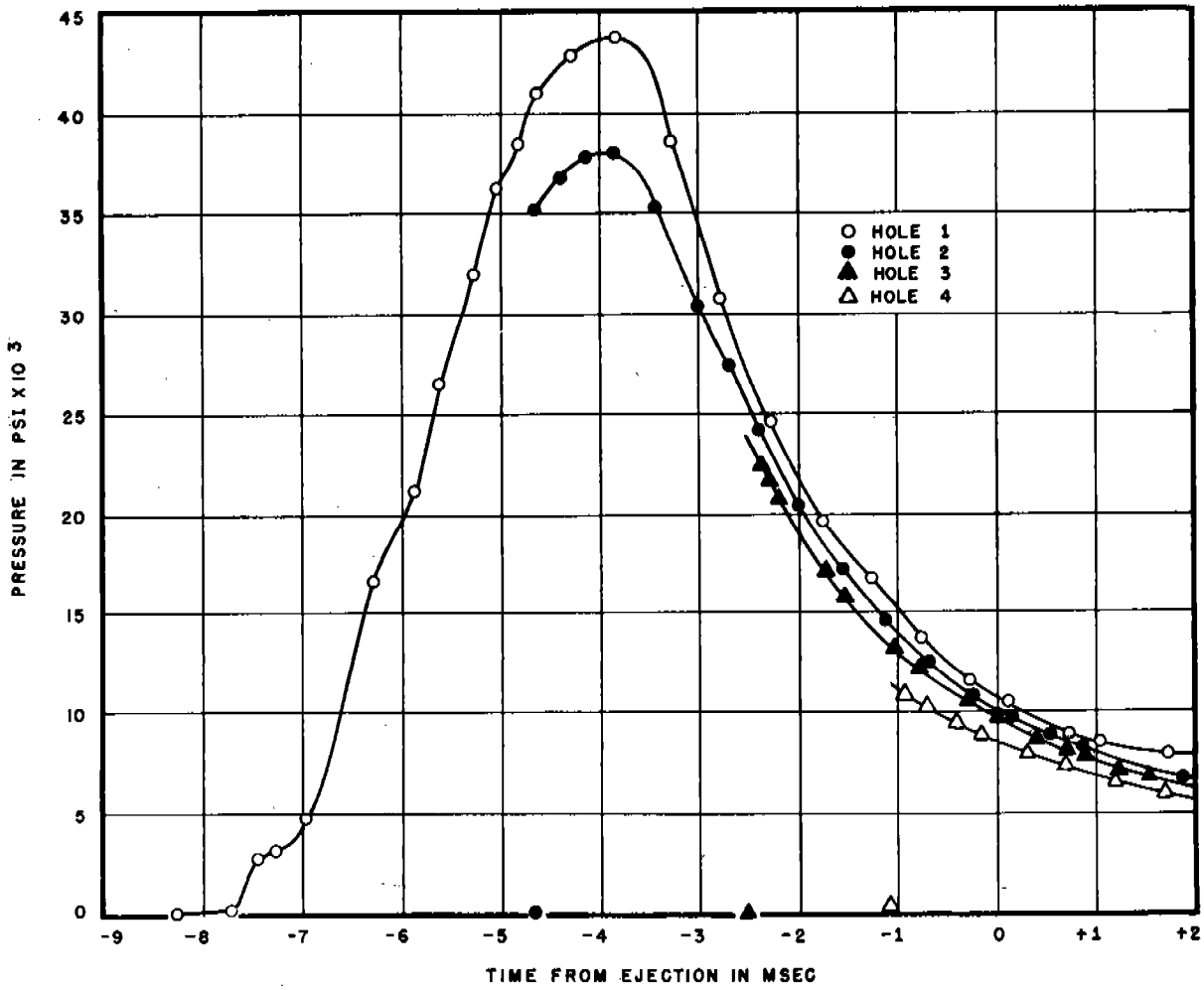


FIGURE 2. Pressure-time curves for a greased round, full charge, second series in 3-in. gun. (NDRC Report A-323, Figure 47.)

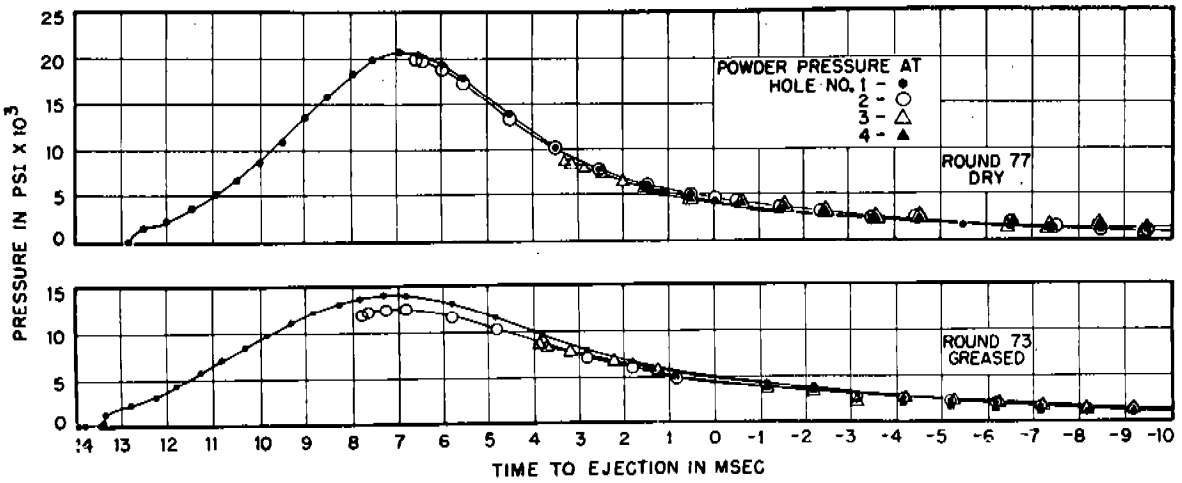


FIGURE 3. Pressure-time curves for greased and dry rounds, 50 per cent charge, third series in 3-in. gun. (NDRC Report A-460, Figure 36.)

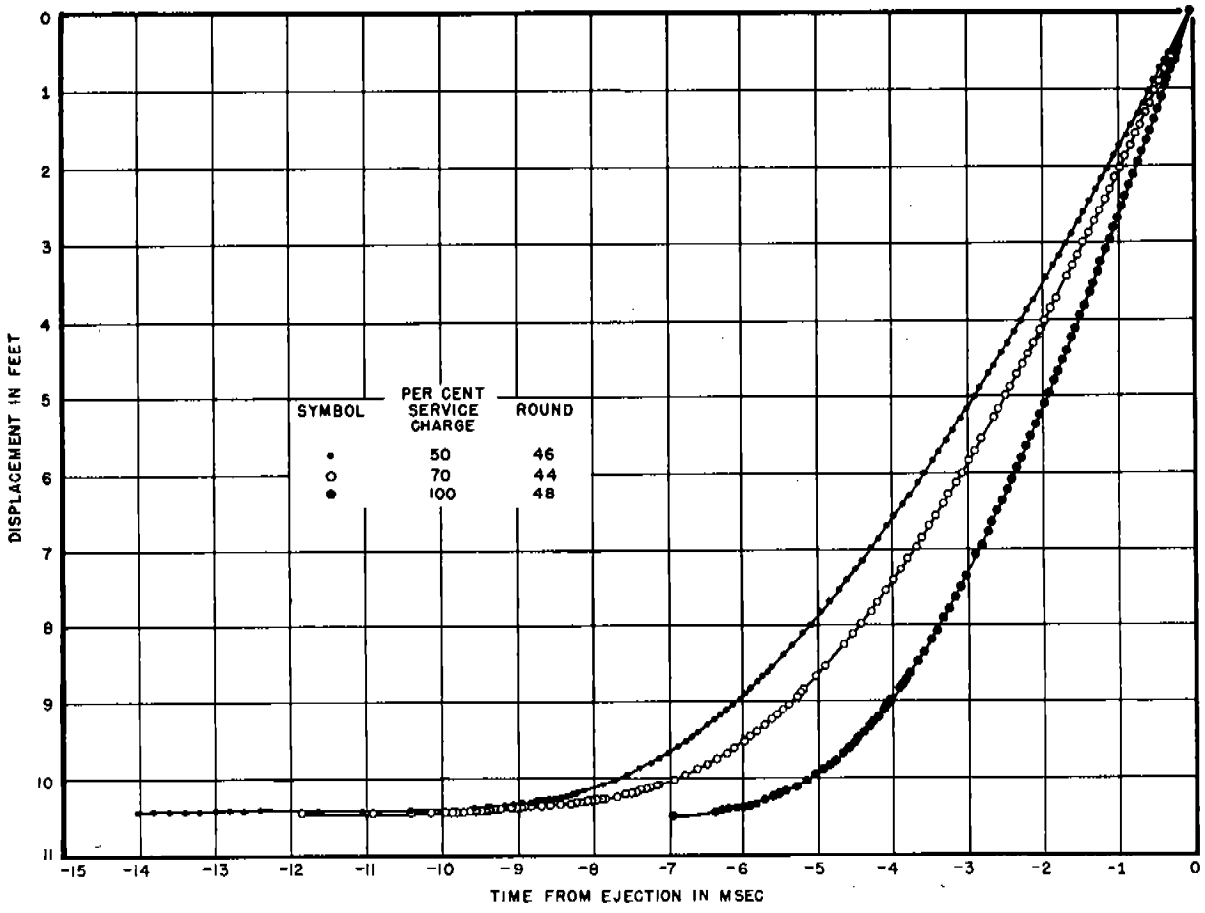


FIGURE 4. Projectile displacement-time curves, microwave data, second series in 3-in. gun. (NDRC Report A-323, Figure 32.)

[redacted]

6.3.2

Typical Basic Data

The basic data for the determination of friction are the pressures and the projectile displacement. The pressures were measured at hole 1, located in the chamber, 12.3 in. from the breech; at hole 2, 8.9 in. beyond the start of rifling or 116.9 in. from the muzzle; at hole 3, 75.3 in. from the muzzle; and at hole 4, 35.0 in. from the muzzle. The pressures were read from the oscillograph records at intervals of 0.3 msec or less, and have been graphed as smooth pressure-time curves. A typical set of such curves, for a full-charge "dry" round of the third series, has already been presented as Figure 2 of Chapter 4; additional typical sets, for a full charge "greased" round of the second series, and 50 per cent dry and greased rounds of the third series, are exhibited in Figures 2 and 3.

A reproduction of the oscillographic recording of the microwave interferometer for a 70 per cent dry round of the second series, has been shown as Figure 15 of Chapter 4. A plot of displacement from the muzzle versus time, for dry 100 per cent, 70 per cent, and 50 per cent rounds of the second series, is shown in Figure 4. From plots of the type illustrated the pressure and displacement may be read at evenly spaced time-intervals, and pressure-travel curves plotted, or

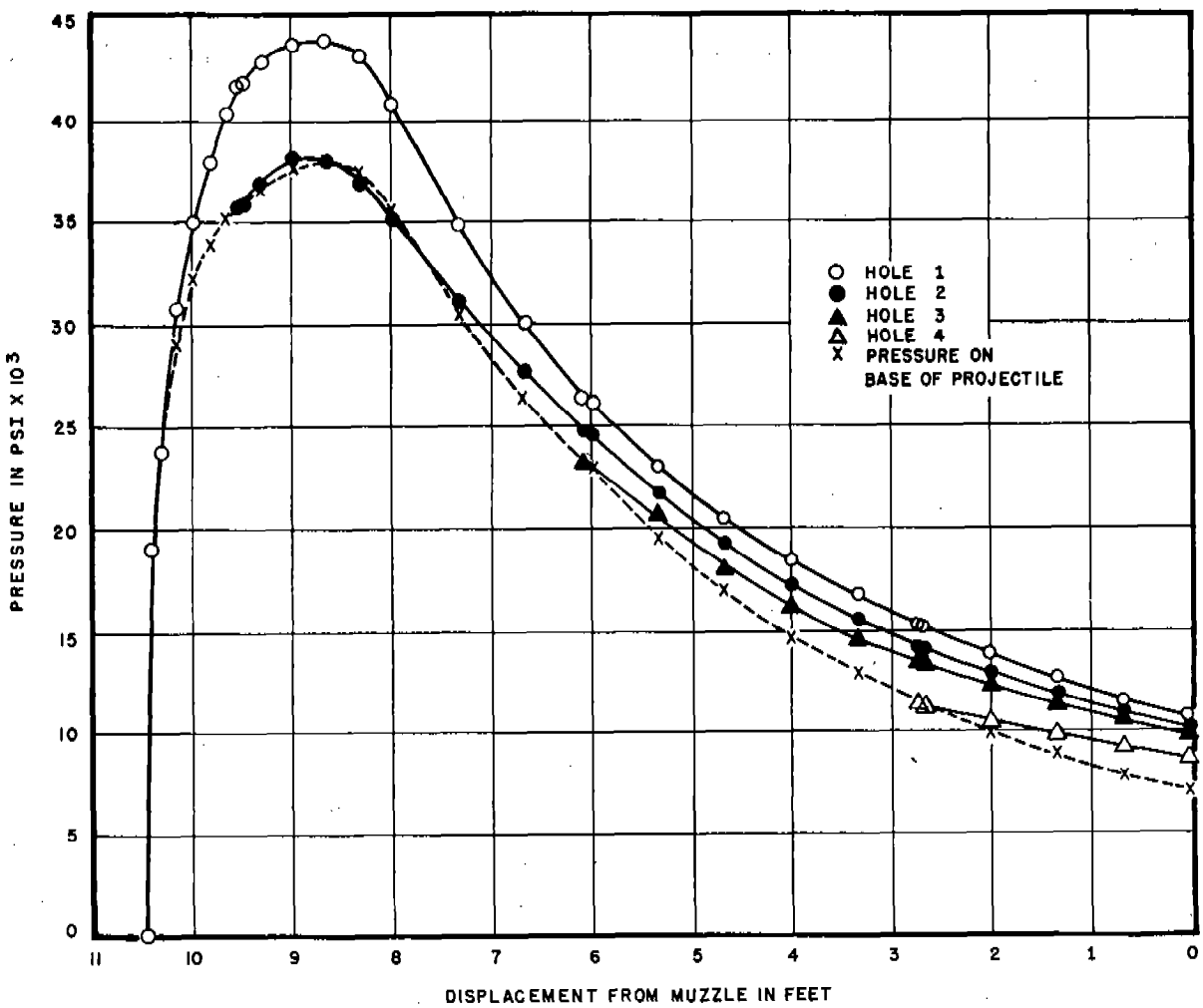


FIGURE 5. Pressure-travel curves for same round as Figure 2. (NDRC Report A-323, Figure 52.)

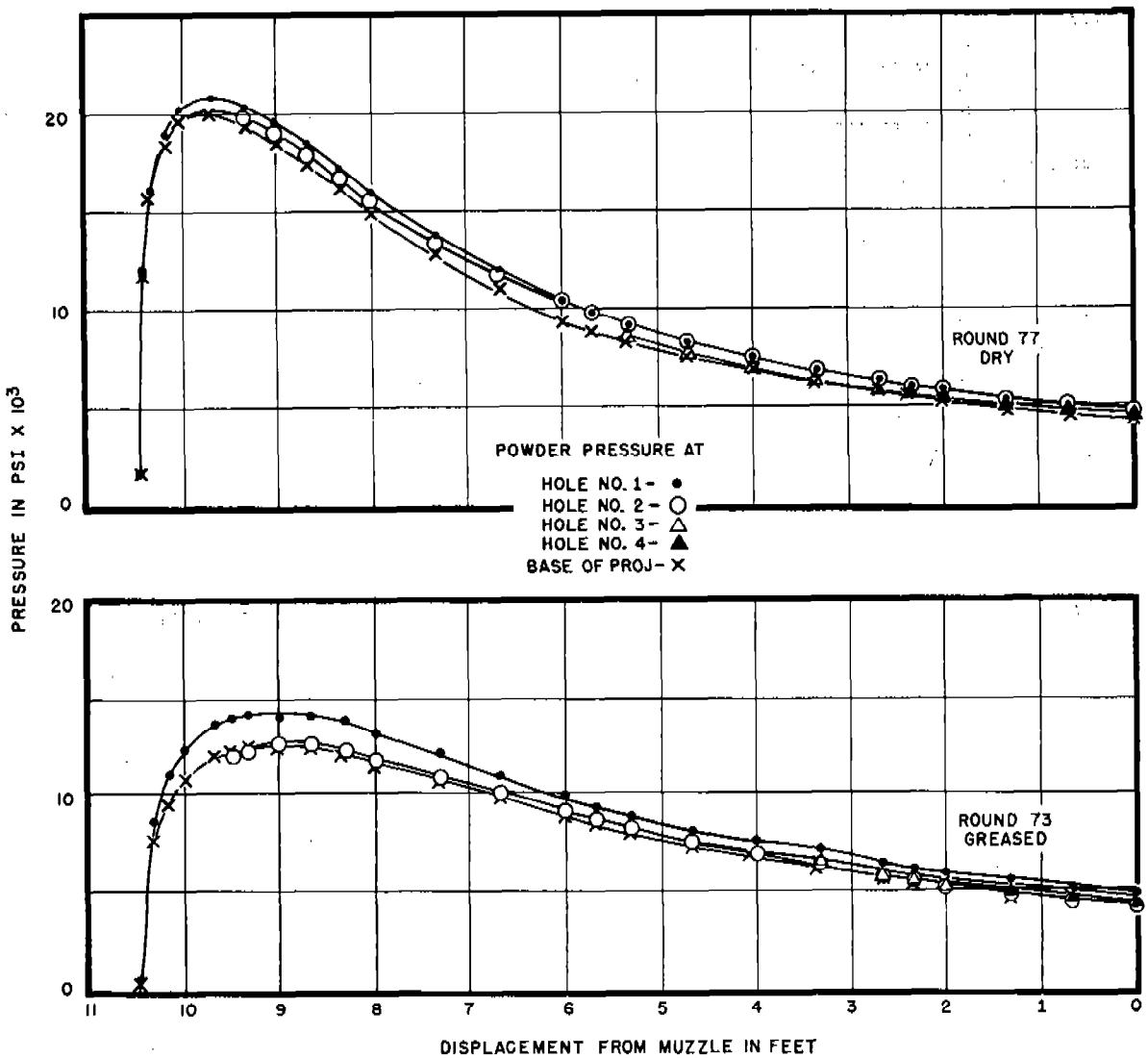


FIGURE 6. Pressure-travel curves for same rounds as Figure 3. (NDRC Report A-460, Figure 39.)

tables[b] of both functions constructed. The pressure-travel curves for the rounds illustrated by Figures 2 and 3 are exhibited as Figures 5 and 6.

As the first step in computing friction from the basic data, the pressure must be extrapolated from the observing gauge positions to the base of the projectile. It is clear from a comparison of Figure 3 in Chapter 4 and Figure 5 of this chapter that there was a considerable difference in the magnitude of the pressure drop down the barrel between the two rounds depicted. This difference recurred consistently between rounds of the second series, in which, for example, the average ratio P_1/P_4 for all full-charge rounds when the projectile was 2 ft from the muzzle was 1.31, and rounds of the third series, in which the corresponding ratio was 1.14. The average pressure ratios for the two series are plotted against projectile travel, and compared with the simple theory [equation (8)] in

[b] Tables in which the pressure and displacement from the muzzle are given at intervals of 0.5 msec are given in NDRC Reports A-323[65] and A-460;[132] those reports also list the times of arrival of the projectile at the displacements corresponding to each of the 71 maxima and minima of the microwave, for several rounds. For some purposes, for example in applying the "integration" method for determining friction, it is more convenient to have the pressure and travel from the starting position tabulated at a fixed number of even time-intervals. Such tables may be found in NDRC Report A-441,[113] at 20 values of the reduced time t' evenly spaced from the starting time to ejection.

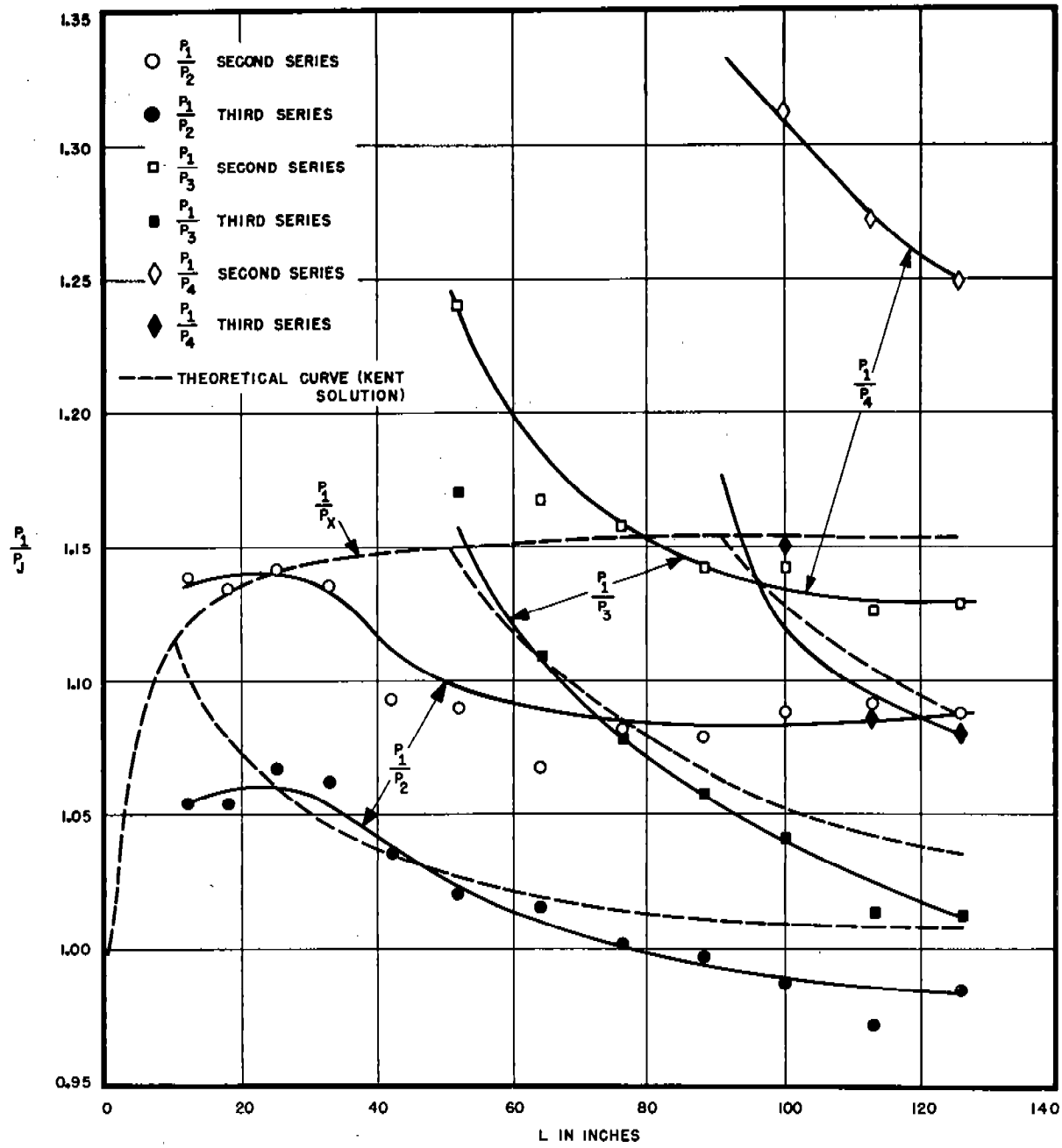


FIGURE 7. Pressure ratios versus travel, 3-in. gun, second and third series. (NDRC Report A-441, Figure 1.)

Figure 7. The theory represents the results of the third series quite well, and is used for the extrapolation to the base of the projectile; for the second series an empirical extrapolation was required. Since no theoretical explanation of the wide discrepancy in the pressure-drop behavior in the two series has been offered, it is most probable that there is an experimental uncertainty in one set of data, although the error should not have exceeded 5 per cent or 1,000 psi. Tables of P_X have been issued.[113]

6.3.3 Typical Results for Friction

A determination of friction by the method which appears most reliable, namely the integration method of Section 6.2.5, is illustrated for a typical 100 per



cent dry round of the third series in Figure 8. The retardation X_r is plotted in two segments in order to permit a more expanded scale. The first segment runs from the start, at about 8 msec before ejection, to 4 msec, when the free travel is 1.966 ft, the observed travel 1.633 ft, and hence the retardation 0.333 ft. The retardation velocity V_r has increased from 0 to 172 fps in this interval. From 4 msec to ejection V_r further increases to 271 fps, corresponding to V_m = 2,728 fps; in this time interval instead of X_r we plot $X_r' = X_r - 271t$. Each measured microwave point is plotted; these fall closely upon the smooth, concave-upward curves drawn to represent X_r. The deviations in X_r are less than 0.005 ft, except for a few points nearest the muzzle. The curve, however, does not intersect the X_r' axis at $t = 0$; the deviation of 0.024 ft, equivalent to 9 msec, represents a typical experimental discrepancy between the location of the projectile as given by the microwave and by the muzzle contact. The retardation velocity V_r is obtained by graphical differentiation of X_r, and is probably accurate to 3 fps, except near the muzzle, where an

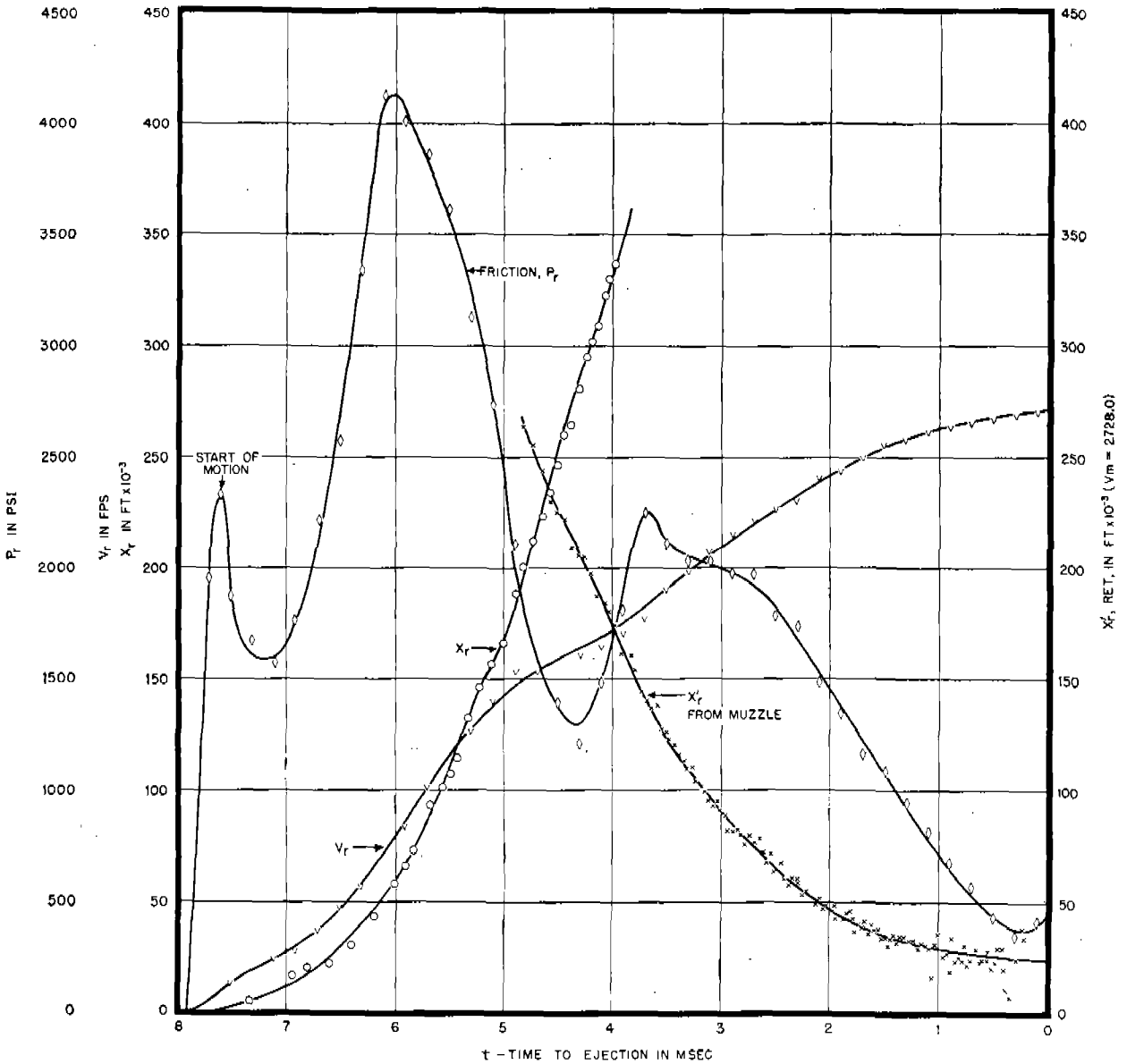


FIGURE 8. Determination of friction, integration method; 3-in. gun, third series, round 75, dry, full charge. (NDRC Report A-441, Figure 4.)

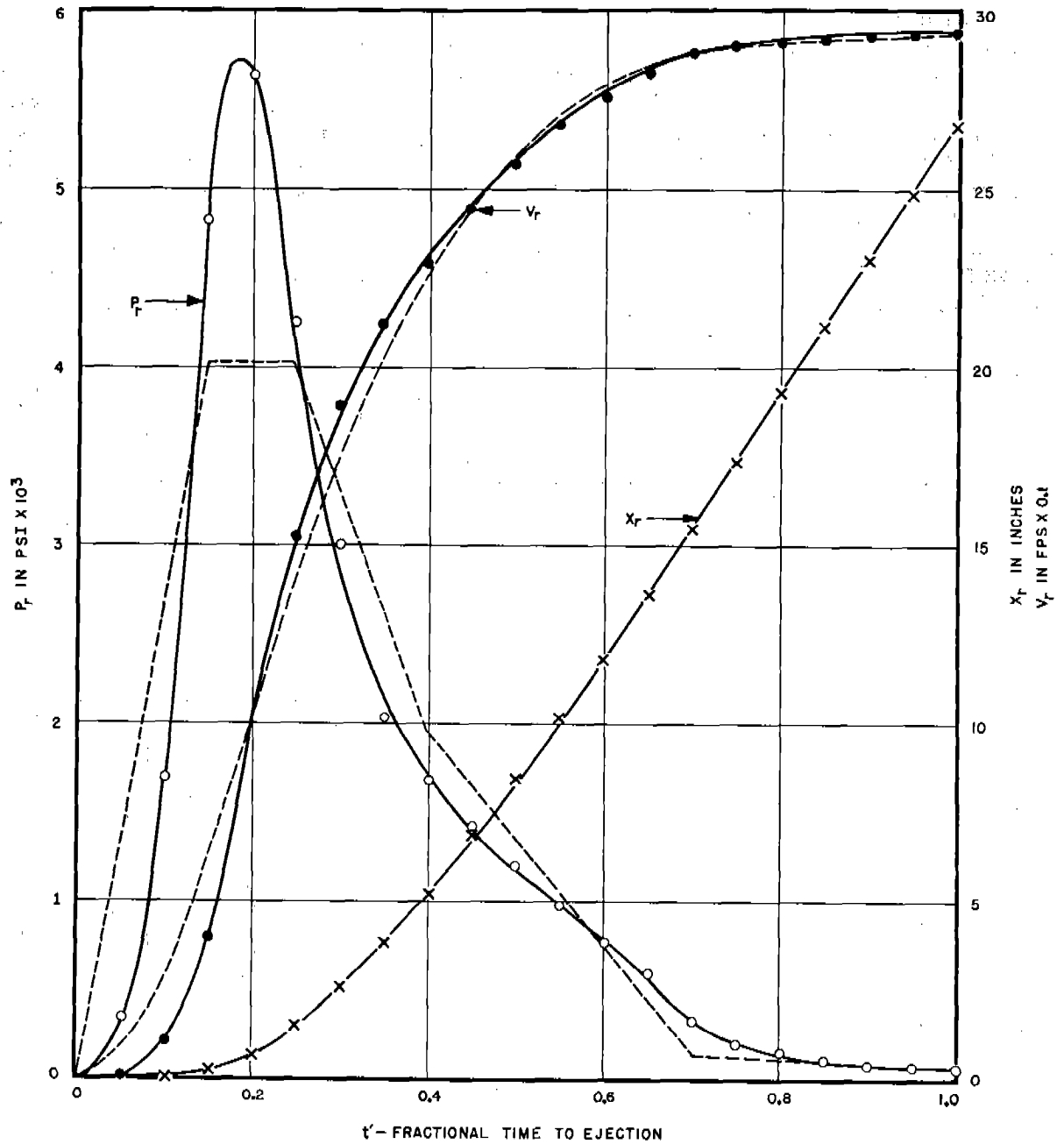


FIGURE 9. Simplified determination of friction, integration method; 3-in. gun, second series, round 44, dry, 70 per cent charge. (NDRC Report A-441, Figure 6.)

uncertainty of 10 fps may occur. The curve is drawn to agree with the extrapolated range velocity, assuming no acceleration of the projectile after leaving the muzzle. Graphical differentiation of V_r yields the friction P_r; the probable error here may not exceed 5,000 ft/sec^2 in dV_r/dt, or 300 psi in P_r. However any uncertainty in P_X must also be taken into account. Hence, the secondary rise in friction near 3 msec, although clearly required by the travel data as plotted, may not be real although it may be related to coppering (Section 10.5.4). The course of P_r versus time is typical of the third series; it has already been exhibited, compared with the pressure, and plotted against the travel, in Figure 1.

A typical friction determination for the second series (70 per cent dry) is presented in Figure 9. Here the

reduced time scale t' is used, and the X_r curve is based not on the individual microwave points, but on smoothed values of the travel at 20 intervals of t'. In addition to the V_r and P_r curves obtained by graphical differentiations of X_r, there are shown (dashed lines) the V_r and P_r resulting from application of the three-constant approximation equation (14). The simplified averaging method is seen to give a fairly good approximation to the detailed results.

The energy of friction E_f for the two rounds illustrated, and the corresponding ratios c of E_f to the total kinetic energy of projectile and powder, are given in Table 1.

TABLE 1. Typical frictional energies and ratios for 3-in. gun.

Reduced time t' —	.25	.5	.75	1.0
Round 75 E_f(10^3 ft-lb) —	2.94	26.5	79.4	107.5
(Third Series) c —	0.207	0.062	0.067	0.065
Round 44 E_f(10^3 ft-lb) —	4.81	22.5	39.0	42.6
(Second Series) c —	0.997	0.119	0.058	0.042

The heating of the rotating band in round 75 has been calculated from the friction by the methods sketched in Section 6.2.2. The result is that about 60 per cent of E_f is expended in heating the bore, 15 per cent in heating the band, and 25 per cent in melting the band, the melting occurring at travels from 5 to 12 in. and 18 to 85 in. This is in general accord with the observed coppering of the gun, which is noticeable at hole 2 (9 in. travel) but much heavier at hole 3 (50 in. travel). The calculated amount of melting in the second period appears to be too high, leading to the conclusion either that the experimental P_r is too high (due to error in P_X), or that retarding forces other than band-bore friction, such as body engraving, are operative.

Other typical results, such as graphical depiction of friction-time and friction-travel data for other rounds, and tabulations of P_r at 20 time-intervals and E_f and c at four time-intervals for many rounds, may be found in the detailed reports.[65,113,132]

6.3.4 Summary and Discussion of Results

The principal results of the firings of the 3-in. gun, as related to bore friction, are summarized in Table 2. This gives, averaged for rounds of each type fired, the muzzle velocity V_m relative to the gun; the maximum pressure in the chamber P_p; the travel at maximum pressure L_p; the friction averaged over the engraving period, from 0.2 to 2 in. travel, P_{re}; the friction averaged over the intermediate range of travels from 2 to 25 in., P_{ri}; the friction averaged over the rest of the bore to the muzzle, P_{rm}; the total energy of friction, E_{fm}; and the final ratio of frictional to kinetic energy, c_m.

From Table 2 the effect of changing the conditions of firing may be seen. The effect on engraving friction

TABLE 2. Summary of results pertaining to bore friction from firings of 3-in. gun.

Powder	Charge	Bore†	V_m fps	P_p klb/in.^{2}	L_p in.	P_{re} klb/in.^{2}	P_{ri} klb/in.^{2}	P_{rm} klb/in.^{2}	E_{fm} 10^3 ft-lb	c_m
Pyro	1.0	G	2698	40.2	17.2	2.5	1.81	1.51	121.7	.0749
Pyro	1.0	D	2712	41.6	15.7	2.9	2.30	1.41	123.9	.0757
Pyro	0.75	D	2269	27.9	14.2	6.6	2.18	1.03	97.6	.0726
Pyro	0.5	G	1730	15.0	16.2	3.3	1.55	0.68	68.8	.1144
Pyro	0.5	D	1867	21.4	9.8	7.0	2.29	0.87	91.7	.1246
NH	1.0	G	2730	43.6	20.9	1.9	−0.1?	0.30	26.4	.0160
NH	1.0	D	2748	47.1	19.1	4.2	0.6	0.43	45.3	.0267
NH	1.0	G*	2713	39.2	26.2	1.1?	−0.5?	0.1?	0 ?	.0 ?
NH	1.0	D*	2724	42.0	20.1	0.3	−0.4?	0.03	−17.5?	−.0106?
NH	0.9	G*	2504	31.1	25.9	1.0	−0.1?	0.32	16.1	.0117
NH	0.9	D	2571	40.0	16.0	4.7	1.6	0.55	47.9	.0330
NH	0.8	G	2315	27.0	22.0	2.1	1.35	0.94	73.9	.0634
NH	0.8	D	2387	32.3	18.2	3.3	0.7	0.67	57.9	.0468
NH	0.7	G	2125	21.4	21.0	2.5	0.8	0.33	31.3	.0322
NH	0.7	D	2150	24.5	20.8	4.1	1.55	0.32	42.6	.0424
NH	0.6	G	1954	18.1	20.0	2.3	0.72	0.46	40.5	.0498
NH	0.6	D	1986	21.0	17.3	4.2	1.78	0.60	63.9	.0760
NH	0.5	G	1774	16.1	15.0	2.7	1.35	0.52	54.0	.0813
NH	0.5	D	1842	18.0	13.2	4.7	1.38	0.27	33.6	.0467

* Projectile in normal position; 0.3-in. free run-up.
†G = greased; D = dry



is particularly to be marked, this being the only frictional parameter determined with any great accuracy, since the error may reach 1.0 klb/in.^{2}. In both the second and third series P_{re} was lower for rounds with greased bore than with dry bore, and lower for those few rounds with run-up than when the projectile was initially advanced against the forcing cone.

The effect of decreased velocity entering the forcing cone on increasing the engraving friction is further shown by the increase of P_{re} with decreasing charge. This effect is especially noticeable in some of the 50 per cent dry rounds, where the friction exceeds the powder pressure at a travel of 0.3 to 0.5 in. to such an extent that the projectile decelerates and nearly comes to a stop. That the engraving friction has a profound influence on the subsequent ballistic course is demonstrated by the fact that when P_{re} is high there are higher maximum pressures, reached at shorter travels, and resulting in higher muzzle velocities. The same result is observed for individual rounds within a type; Table 3 shows the variation in the 75 per cent rounds of the third series.

TABLE 3. Variation of results associated with engraving friction (P_{re}) 75 per cent dry rounds, third series, 3-in. gun.

Round No.	V_m fps	P_p klb/in.^{2}	L_p in.	P_{re} klb/in.^{2}
64	2244	25.5	16.6	3.8
68	2262	28.0	16.2	5.1
76	2308	30.2	14.8	6.4

The intermediate and muzzle frictions P_{ri} and P_{rm} are less accurately known, and are of less ballistic consequence, except that they are the principal contributors to the energy of friction. There does not appear to be any marked correlation of the bore friction with the state of the bore surface; with decreasing charge the energy loss decreases slightly but the ratio of frictional to kinetic energy increases markedly. The most marked effect is the difference between the second and third series, but this is hardly likely to be a real effect, being most probably due to the same experimental uncertainty that gave rise to the unexplained difference in the pressure drop. For this reason it is hard to say what the best average value of c for the gun may be; since the high frictions of the third series lead to implausibly large amounts of band melting, that series may be too high; but the second series bore frictions are likewise implausibly low for a gun with increasing twist. The most probable result, for full charge, probably lies between the two extremes, namely $c = .05 \pm .03$.

6.4 RESULTS, 37-MM GUN WITH PRE-ENGRAVED PROJECTILES

6.4.1 Experimental Conditions

The 37-mm gun, T47, is described in Sections 4.2.3 and 31.7. The six lands for the pre-engraved projectile had a constant twist of 24 calibers per turn. The chamber volume was 31.43 cu in.; the travel of the projectile from seating to ejection, 73.96 in. Forty-three rounds were fired, at least three in each of 12 classes, which differed in the type of charge and projectile, as listed in Table 4.

TABLE 4. Conditions of firing 37-mm gun, T47.

Class	Powder Type*	Powder Weight lb	Primer†	Projectile‡ Weight lb	Projectile‡ Length in.	
1	M1	0.819	S	1.62	6.25	
2	M1	0.819	S	1.62	6.25	PL
3	M1	0.819	M	1.62	5.75	
4	M1	0.819	L	1.62	5.75	
5	M1	0.797	S	1.62	6.44	Obt
6	M5	0.828	S	1.62	6.25	
7	M5	0.828	S	1.62	6.25	PL
8	M5	0.828	L	1.62	5.75	
9	M5	0.803	S	1.62	6.44	Obt
10	M5	0.850	S	1.34	5.75	
11	M5	0.839	S	1.62	6.25	
12	M5	0.794	S	1.92	6.25	

* Some powder properties were:

	T_0 K	F ft-lb/lb	γ	W in.
M1	2406	302,100	1.2505	.0231
M5	3278	363,380	1.2284	.0403

† The primers were: S = Short, M23A2, length 1 in.
M = Medium, M38B2, length 2.8 in.
L = Long, T34, length 7.7 in.

‡ Two special types of projectiles were included: PL = Parco-Lubrized, that is surface treated with iron phosphate coating; Obt = Obturated, with a 1-mm copper skirt near the base.

Pressure-time records were obtained by two gauges located at opposite ends of the same diameter in the chamber, at about four-fifths of the distance from the breech to the seated projectile. The gauges served as experimental checks on each other, but gave no information concerning the pressure gradient down the barrel. It was therefore necessary to compute the base pressure by the theoretical equation (8). The displacement, velocity, and acceleration of the projectile were determined by the microwave interferometer; in this gun the records were at times disturbed, possibly due to ionized gases that had leaked past the

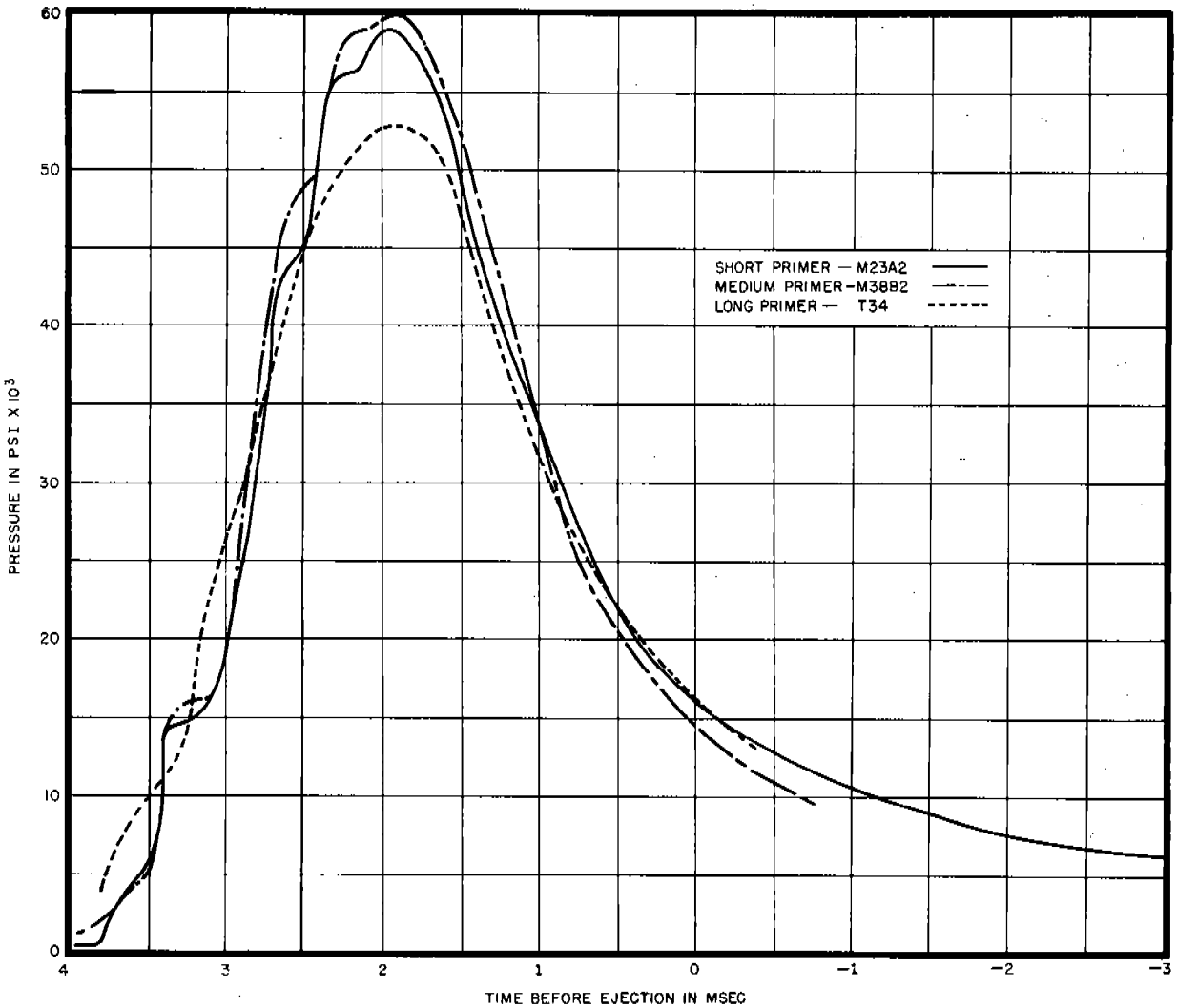


FIGURE 10. Pressure-time curves for M1 powder, three classes of primers in 37-mm gun. (NDRC Report A-459, Figure 2.)

projectile. An unexplained dependence of the type of microwave record on the type of projectile also occurred, the results being most satisfactory for classes 10 and 12, least for classes 1, 9, and 11. Typical pressure-time curves for M1 powder, showing how ignition waves are reduced by increasing the primer length, are presented in Figure 10. Typical microwave records of five classes are shown in Figure 11.

6.4.2 **Results and Discussion**

Because of the uncertainty in base pressure (of the order of ± 2 klb/in.^{2}) imposed by the use of only one gauge position and the experimental error at that point, and in projectile displacement and acceleration caused by the erratic microwave records, the results of friction determinations in the 37-mm gun, T47 are not of high accuracy. The results for a typical round of class 12, as determined by the integration method (Section 6.2.5), are shown in Figure 12. The individual microwave points scatter rather widely about the smooth curve drawn to represent X_r, the average deviation being 0.008 ft. In view of the shorter time intervals in this gun, this would lead to a probable error of about $\pm$ 15 fps in V_r, and $\pm$ 30,000 ft/sec^2 in dV_r/dt or $\pm$ 1 klb/in.^{2} in P_r. For classes of rounds in which the microwave record was less satisfactory, the scatter and resulting inaccuracy are greater. There is, however, one consistent feature of the results which is illustrated in this typical round, namely, that the friction is low at the start, which is the reason that pre-engraved projectiles reduce

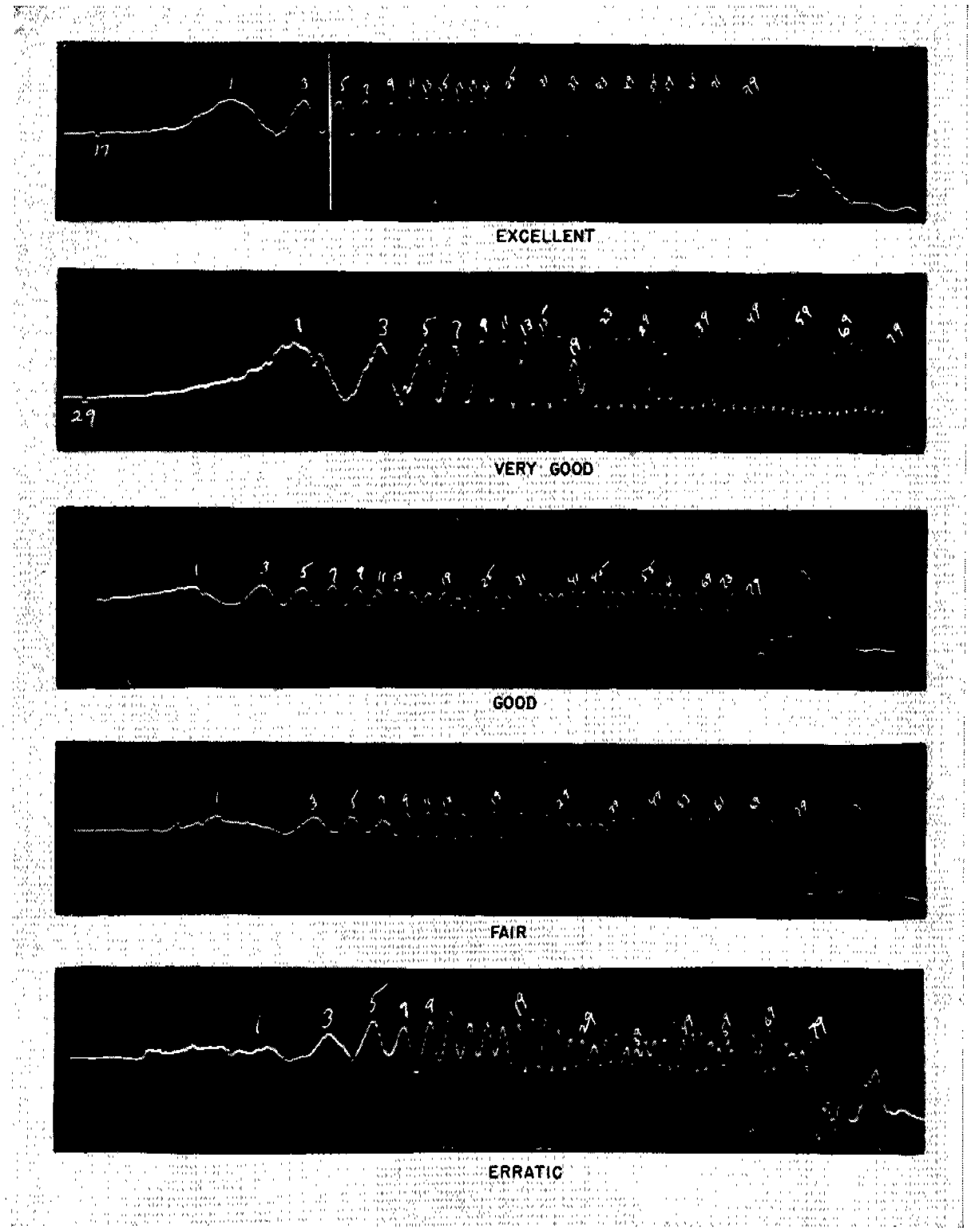


FIGURE 11. Microwave records for five classes of projectiles in 37-mm gun: Excellent—Class 10; very good—Class 4; good—Class 2; fair—Class 5; erratic—Class 9. (This appears as Figure 4 in NDRC Report A-459.)

[redacted]

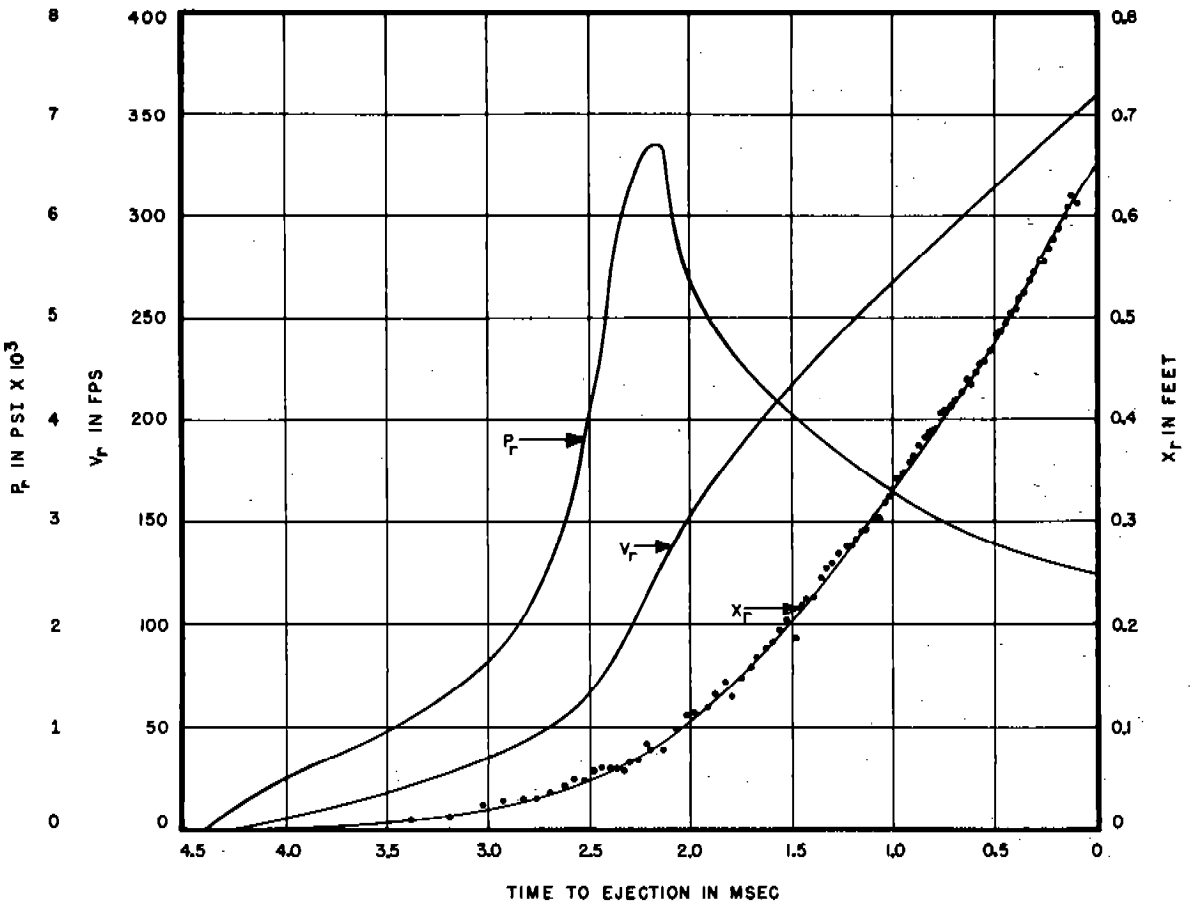


FIGURE 12. Determination of friction, integration method, round E 14 (37-mm gun, M5 powder, 1.92-lb projectile). (NDRC Report A-441, Figure 8.)

erosion (Chapter 31). The friction reaches a maximum near the time of maximum acceleration or later. The difference from the results in the 3-in. gun, due to the absence of the rotating band, is marked.

A summary of the results is presented in Table 5. This gives, averaged for each class, the time from start of pressure to ejection, the muzzle velocity, the maximum pressure, the friction averaged at 0.5 msec intervals, and the final ratio of frictional to kinetic energy.

Within the limited accuracy of the results, no definite correlation can be made between the friction and the type of projectile. Very little change in the overall ballistics is caused by "Parco-Lubrizing" the projectile surface, or by adding the thin obturating ring. The comparatively high resisting pressures found with all classes can hardly be due entirely to projectile-bore friction. The observed heat transfers were not anomalously high, nor did they show a maximum near the point of maximum acceleration, indicating that the large apparent P_r did not give rise to a correspondingly large heat of friction. The high values

TABLE 5. Summary of results pertaining to friction, 37-mm gun.

Class*	t_0 msec	V_m fps	P_p klb/in.^{2}	$P_{r,\,(av.)}$ klb/in.^{2}	e_m
1	3.86	3348	57.8	1.7	.071
2	3.92	3347	58.7	2.1	.070
3	3.96	3328	57.4	2.5	.087
4	4.48	3261	52.0	2.4	.087
5	3.96	3290	55.3	2.8	.098
6	4.15	3588	63.1	2.5	.092
7	3.98	3595	63.4	3.4	.099
8	4.07	3604	63.5	2.9	.074
9	4.04	3513	56.6	1.7	.050
10	3.74	3868	59.2	1.7	.063
11	3.90	3631	64.1	2.1	.081
12	4.33	3302	64.3	3.1	.096

* See Table 4 for a definition of each class of rounds.

found may be due in part to errors in measurement and calculation of P_X; or in part it may represent a resisting pressure on the part of the projectile caused by the leakage of gases. Several lines of evidence, notably photographs of the muzzle before the projectile has emerged, point to a considerable quantity of such gas.

6.5 DISTRIBUTION OF ENERGY OF THE POWDER

6.5.1 Methods of Determining Energy Balance

The Energy Equation

Another important result of a complete set of ballistic measurements, such as those carried out at Carderock, is that several lines of experimental evidence are brought to bear on the problem of the energy distribution of the powder. A theoretical discussion of the ballistic energy equation is given in Section 3.2.3; for the present purposes we may write the fundamental equation (17), which is essentially the same as equation (6) of Chapter 3,

$$E_{\text{rel}} = \frac{NF}{\gamma - 1}\left(1 - \frac{T}{T_0}\right) - E_u$$
$$= \frac{M}{2g}V^2 + \frac{C}{2\delta g}V^2 + E_f + h. \quad (17)$$

This equation expresses the fact that the extent by which the gas temperature T falls below the flame temperature T_0 is a measure of the energy released as work or heat, or unexpended due to incomplete burning; the terms on the second line distribute the released energy among the kinetic energy of the projectile, the kinetic energy of the powder and gas, the energy of overcoming friction, and the heat transferred to the walls. In the Carderock firings all the terms of equation (17) were determined, directly or indirectly; a more detailed analysis than the brief summary to be presented here may be found in the original reports, especially A-441[113] and A-444.[116]

The powder constants F, γ, and T_0 have been calculated by both the detailed and approximate (additive) methods sketched in Section 2.4. The inaccuracy introduced by use of the simpler approximate method is less than 3 per cent, except at times near shot ejection, when the temperature is below 1750 K and secondary gas reactions leading to methane formation become of importance.

The kinetic energy terms, which constitute the largest fraction of the expended energy, may readily be calculated from the projectile velocity, which was determined as a function of time by the methods described in Section 6.2. The factor δ may be taken as 3, the theoretical value, with sufficient accuracy, except at times near the start of travel when the turbulent velocity of the unburned powder considerably exceeds the projectile velocity. E_f may also be calculated by the methods described in Section 6.2.

The problem of determining energy balance thus depends on a knowledge of N, T, E_u, and h. At times near shot ejection, the powder is completely burned, and $N = C$. At such times, with rare exceptions to be mentioned in the next section, E_u may be neglected. Hence the problem is solved if either T or h may be determined or calculated.

Average Temperature

The average temperature T of the gas throughout the gun volume may be estimated from the experimentally determined temperatures (Sections 2.5 and 4.3.17), but the results are of limited accuracy, except at position 1, in the powder chamber. Even there, because of the high degree of turbulence and temperature inhomogeneity in the gas, values averaged over a number of rounds are needed to obtain representative results. The observed temperatures at the forward positions appear to be considerably lower than the average temperature at those points, due to cooling by the walls.

The average temperature T may be approximated roughly by the chamber temperature T_1 and also it may be calculated from the observed average pressure [computed from the observed pressures by the use of equation (8) or other empirical representation of the pressure gradient] and travel, by means of the equation of state, equation (15) of Chapter 3. The experimental value of T_1 (or of h) may be used to check the covolume η; in general it is better to assume that η is accurately calculable by the methods of Section 2.4, and to use the equation of state to check the experimental self-consistency of P, T_1, and h, or to calculate T and h from P.

Heat Input (h)

The heat h transferred from gas to bore may be calculated by the methods described in Section 5.3. The computation may either follow the detailed method

based on the fundamental equation (18),

$$\frac{dQ}{dt} = \tfrac{1}{2}\lambda(T_g - T_s)C_p\Delta v, \qquad (18)$$

using an assumed value for the friction factor λ, and the observed ballistic data for the gas temperature T_g, density Δ and velocity v, or use may be made of tables [48] based on the observed muzzle velocity and an assumed simple ballistics. It has been shown [116] that the two methods of calculation of h were in good agreement for the 3-in. gun, and that h was very nearly a linear function of the travel L.

The quantity h may also be derived from experimental determinations of heat input at various points along the gun, as described in Section 5.4. This also requires theoretical calculations concerning the contributions to the observed total heat input of the heat of friction and of the heating by the gases after ejection. Using either ballistic data or theoretical computations regarding the state of the powder gas after ejection, the result is obtained that the heat input up to ejection, h_m, is approximately 0.64 of the total heat input. For times before ejection, a linear dependence of h on L is assumed; the alternative assumption, equation (10) of Chapter 3, made in the theoretical ballistics, may also be used.

Energy Balance During Burning

At times before the powder is completely burned, any two of the three quantities P, T, and h must be known in order to calculate N/C from equations (18) in this chapter and (15) in Chapter 3, if E_u is assumed negligible; or all three must be known to calculate E_u. In general the best procedure is to make use of P and h, assuming $E_u = 0$; if T calculated in this way is within 100 Kelvin degrees of the observed T, the energy balance is reasonably reliable. If the observed T falls below the calculated by more than 100 degrees, it must be associated with an $E_u > 0$.

6.5.2 Energy Balance during Firing of 3-inch Gun

At Ejection

To illustrate the results of the different possible experimental and theoretical approaches to the computation of the energy balance at the time of ejection, there are presented in Table 6, for various conditions of firing, values of T calculated by the following methods.

1. The experimentally determined temperature in the chamber;

2. Values calculated from the experimentally determined average pressure, using alternatively:

   a. The approximate additive equation of state (15) in Chapter 3,
   b. The more exact equation (10) of Chapter 2;

3. Values calculated from the energy balance equation (17) of this chapter, assuming $E_u = 0$, and using alternatively:

   a. The approximate method of calculation of E_{rel} and the observed value of h,
   b. The exact calculation of E_{rel}, and the observed value of h,
   c. The exact E_{rel} and the value of h calculated using the simplified ballistics given in Section 3.2.7 and the value of λ corresponding to $Q = 10.2$ cal/cm^2 in the caliber .50 gun.

From Table 6, supported by the more detailed computations not reproduced here, the following conclusions may be drawn.

1. The various experimental results do not lead to identical values of T, but the disagreement is not more than $\pm$ 5 per cent, and hence is attributable to experimental error in the determination of temperature and pressure.

2. The differences between calculations based on

Table 6. Average values of gas temperature at shot ejection, 3-in. gun.

Powder—	NH	NH	NH	Pyro	Pyro	Pyro	Pyro
Charge—	1.0	0.7	0.5	1.0	0.75	0.5	0.5
Bore—(G=greased; D=dry)	G-D	D	D	G-D	D	D	G
Source and method of calculation of T, (K)							
1. Experimental	1634	1740	1518	1696	1752	1650	1590
2a. Pressure, approx eqn of state	1689	1682	1575	1721	1686	1642	1675
2b. Pressure, exact eqn of state	1706	1690	1579	1737	1692	1646	1678
3a. Energy, approx calc; h obs.	1610	1683	1639	1597	1640	1680	1732
3b. Energy, exact calc; h obs.	1651	1707	1653	1626	1657	1687	1737
3c. Energy, exact calc; h theor.	1629	1677	1611	1603	1624	1642	1697

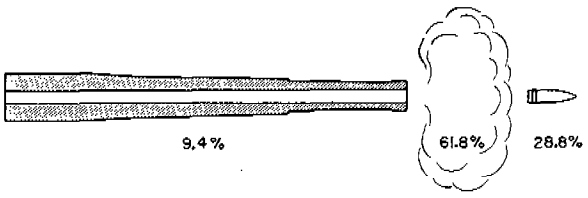


FIGURE 13. Energy distribution of powder, 100 per cent charge, 3-in. gun.

the approximate and detailed computation of covolume and energy release are less than the differences between the several experimental methods; hence more exact measurements are needed before an experimental determination of the covolume, or other checks on the finer points of the calculations can be made.

3. For all rounds except at 50 per cent charge, better agreement with the other temperatures is obtained by using the experimental rather than the theoretical values of h; that is, the other results reinforce the experimental heat inputs and suggest that in this gun a value of λ from 20 to 25 per cent lower than that found in the caliber .50 gun was operative.

4. For the 50 per cent rounds, and most markedly for the greased Pyro rounds that gave the lowest P_p and V_m (Table 2), the energy balance gives temperatures that exceed the experimental temperatures by amounts greater than the probable error. Hence in these cases there is an energy deficit E_u to be attributed to incomplete reaction of the powder. In such rounds an E_u of similar magnitude is also found at times before ejection, by methods stated in Section 6.5.1.

The energy distribution at ejection is summarized in Table 7. The various energies are expressed as percentages, first of the total potential energy the powder could liberate if cooled to 0 K, and second of the kinetic energy of the projectile. The total heat transmitted to the gun, which includes in addition to h_m the contributions of frictional and post-ejection heating, is also listed. Figure 13 illustrates the overall result.

BEFORE EJECTION

At times before ejection, the energy distribution is roughly similar to that just discussed. Some values of the ratio c of frictional to kinetic energy have been presented in Table 1. The ratio β of heat loss to kinetic energy [see equation (11) of Chapter 3 in Section 3.2.3] in general shows a minimum at times near $t' = 0.6$. Some typical results are presented in Table 8. This gives, for the average full-charge firing of NH powder, at various times, the temperature as observed, and as calculated from the observed pressure, travel, and heat loss using the experimental value of h and two different assumptions for a constant ratio β. The

TABLE 8. Observed and calculated gas temperatures—100 per cent charge NH powder, 3-in. gun.

	Values of T, K				
t'	Exp.	Calc. h	Calc. $\bar{\gamma} = 1.275$	Calc. $\bar{\gamma} = 1.30$	N/C
0.05	2045	2636	2636	2636	0.0278
0.10	1948	2635	2636	2636	0.0467
0.15	2267	2631	2634	2634	0.0969
0.2	2520	2621	2625	2624	0.1650
0.3	2528	2569	2574	2569	0.3120
0.4	2413	2448	2451	2436	0.5358
0.5	2373	2296	2295	2268	0.7691
0.6	2192	2156	2155	2118	0.9700
0.7	2010	1984	1988	1934	0.9882
0.8	1869	1839	1856	1785	1.0033
0.9	1760	1716	1749	1768	1.0004
1.0	1634	1605	1662	1573	1.0157

TABLE 7. Distribution of energy of the powder, 3-in. gun.

Type of energy		100 Per cent charge			50 Per cent charge		
		E 10^3 ft-lb	Per cent of total	Per cent of $(KE)_p$	E 10^3 ft-lb	Per cent of total	Per cent of $(KE)_p$
Total potential of powder	$CF/(\gamma - 1)$	5144	100.0	.....	2572	100.0	.....
Released at ejection	$CF(1 - T_m/T_0)/(\gamma - 1)$	1984 ± 100	38.6	135.1	1016 ± 100	39.5	160.0
Kinetic of projectile	$(KE)_p$	1469 ± 20	28.6	100.0	635 ± 60	24.7	100.0
Kinetic of powder gas	$(KE)_g$	148 ± 20	2.87	10.1	32 ± 5	1.24	5.0
Kinetic of recoil	$(KE)_r$	11	0.21	0.7	4.0	0.16	0.6
Rotation of projectile	E_{rot}	12	0.23	0.8	5.3	0.21	0.8
Frictional	E_f	80 ± 30	1.56	5.4	65 ± 20	2.53	10.2
Gaseous heat transfer	h	264 ± 100	5.13	18.0	181 ± 80	7.04	28.5
Unreleased potential	E_u	0	0.	0.	94 ± 90	3.65	14.8
Total heat to gun	H	482 ± 50	9.37	32.8	338 ± 40	13.14	53.2

fraction burned as calculated in this way is also listed. It is seen that the usual ballistic assumption of constant β does not lead to wide errors in the calculated temperature; the experimental results for both T and h favor a lower ratio than was usually adopted for ballistic calculation, as suggested in Table 2 of Chapter 3.

A noteworthy feature of Table 8 is the large extent by which the experimental T falls below the theoretical at early times. This has been attributed partly to an incomplete burning term E_u, and partly to an increase in the kinetic energy of the solid powder moving turbulently in the chamber. This temporarily lost energy is recovered by the gas as burning proceeds.

The values of N/C obtained in this way were used in the calculation of burning rates, as discussed in Section 2.2.

6.5.3 Approximate Results for 37-mm Gun, T47

In the 37-mm gun, T47, the gas temperature was not measured, and so there is one less check on the consistency of the results. At ejection the temperatures calculated from the pressure averaged 9 per cent above those calculated from the energy balance with observed values of h. This adds additional weight to the possibility that the experimental pressures, and the friction calculated therefrom, were too high. Hence no very reliable results for the energy distribution are at hand. The average value of the effective specific heat ratio $\bar{\gamma}$ was 1.317 for M1 powder and 1.289 for M5 powder, corresponding to $\beta = 0.24$, again somewhat lower than suggested in Table 2 of Chapter 3.

6.6 CONCLUSIONS

The general conclusions regarding bore friction and related problems, that may be drawn from the experimental results and theoretical discussion of this chapter, may be summarized briefly. It appears that even with the data at hand, which in precision and completeness compared very favorably with any previous ballistic results, it is difficult to obtain reliable results for such a small differential effect as the friction. It has however been demonstrated that the engraving friction in a 3-in. gun varies with the conditions of firing from 2 to 10 klb/in.^{2}, or from 5 to 50 per cent of the maximum pressure, the variations in some cases being without assignable cause, and that these variations are reflected in the maximum pressure and muzzle velocity.

The engraving friction bears a relation to the parameter P_0, the starting pressure, that appears in interior ballistic calculations, but is not identical with it, inasmuch as the theoretical quantity is influenced by the various simplifying assumptions that are made concerning friction and burning rate. (See Section 3.2.2.) The coefficient of bore friction c in this gun varies with the travel and the firing conditions, but in general appears to exceed the average value of 0.04 assumed in the Division 1 theoretical ballistics. The energy distribution of the powder likewise varies with the travel; at early times and in low-density firings there is some additional energy deficit due to incomplete evolution of powder energy. Otherwise the relations are fairly in accord with theory, with the heat loss being somewhat lower than usually assumed.

Further work of the kind described in this and the preceding chapters, using a variety of guns firing conventional and experimental projectiles and powders, is needed. Only in this way will it be possible to establish the general laws relating bore friction and powder energy distribution to interior ballistic theory and to gun design and performance.



Chapter 7

BAND PRESSURE AND RELATED STRESSES

By *H. L. Black*[a]

7.1 THEORY OF POWDER GAS AND BAND STRESSES IN GUNS

7.1.1 Introduction

DURING WORLD WAR II it became clear from actual failures of guns and shells during testing that the effect of rotating band pressure had not been given proper consideration in the design of either guns or shells. In addition, there developed a tendency to fire guns with powder pressures exceeding those for which they were originally intended. As a result a great deal of attention has been given to the problem of the stresses in a gun tube under combined band and powder pressures and the corresponding stresses in the wall of a shell.

In this country this work has been carried on by the Army in the Office of the Chief of Ordnance[307,308] at Watertown Arsenal,[249–256] for the Navy at Dahlgren Proving Ground[330] and at the Massachusetts Institute of Technology,[326,327] and for Division 1, NDRC, at both the Catholic University of America[117] and the National Bureau of Standards.[58,65,132] In Britain an earlier interest in the subject was continued.[302,366,370,376,377,378,424]

As a result of the theoretical and experimental work discussed in the present chapter, important progress has been made in the determination of band pressure and of its effects in combination with powder pressure and thermal stresses. The knowledge gained will be a valuable aid to the designer of hypervelocity guns. If muzzle velocities are to be pushed to levels formerly considered impossible, there is need of further study, particularly of the cause of pressure waves that may impose dangerously high sporadic stresses on the tube.

The application of these results to improvements in the design of projectiles is taken up in Chapter 27. Some attention is given there to the first efforts to reduce band pressure, a change that would appear to be a prerequisite to the use of the higher powder pressures that are required in hypervelocity guns.

[a] Technical Aide, Division 1, NDRC. (Present address: Department of Mathematics, Michigan State College, East Lansing, Michigan.)

7.1.2 Fundamental Assumptions

In considering stresses in a gun tube, it is customary to make certain assumptions.

1. The gun is a smooth-walled, hollow cylinder.

2. The tube is sufficiently long (or the projectile base is considered at a sufficient distance from an end of the tube) to make end effects negligible.

3. Band and powder pressures give axially symmetric radial stresses.

4. Under uniform radial pressures, the stress distribution follows the equations of Lamé, given in equations (1) to (3),

$$\text{Radial stress: } \widehat{rr} = \frac{E}{1-\mu^2}\left(\frac{\partial w}{\partial r} + \mu\frac{w}{r}\right) \qquad (1)$$

$$\text{Hoop stress } \widehat{\theta\theta} = \frac{E}{1-\mu^2}\left(\mu\frac{\partial w}{\partial r} + \frac{w}{r}\right) \qquad (2)$$

$$El = \frac{-\mu}{1-\mu}\left(\frac{\partial w}{\partial r} + \frac{w}{r}\right) \qquad (3)$$

in which E is Young's modulus, μ the Poisson ratio, w the radial deformation, r the distance from the axis of the tube, and l a constant of integration determined by boundary conditions.

5. The generally accepted criterion for failure is that of Mises-Hencky, according to which the equivalent stress, S_e, can be expressed by equation (4). If S_e exceeds the tensile strength of the gun steel, failure of the gun is to be expected.

$$2S_e^2 = (\widehat{\theta\theta} - \widehat{rr})^2 + (\widehat{rr} - \widehat{xx})^2 + (\widehat{xx} - \widehat{\theta\theta})^2 \qquad (4)$$

6. Stresses are algebraically additive. If, for example, the simultaneous stresses caused by powder pressure and by band pressure at a given point are known, the combined stress is given by their sum. In particular, if the two stresses are graphed against position in the gun, the resultant stress may be obtained by composition of ordinates. This principle of superposition can be extended to any number of stresses and is a valuable tool in developing the theory of stress distribution.

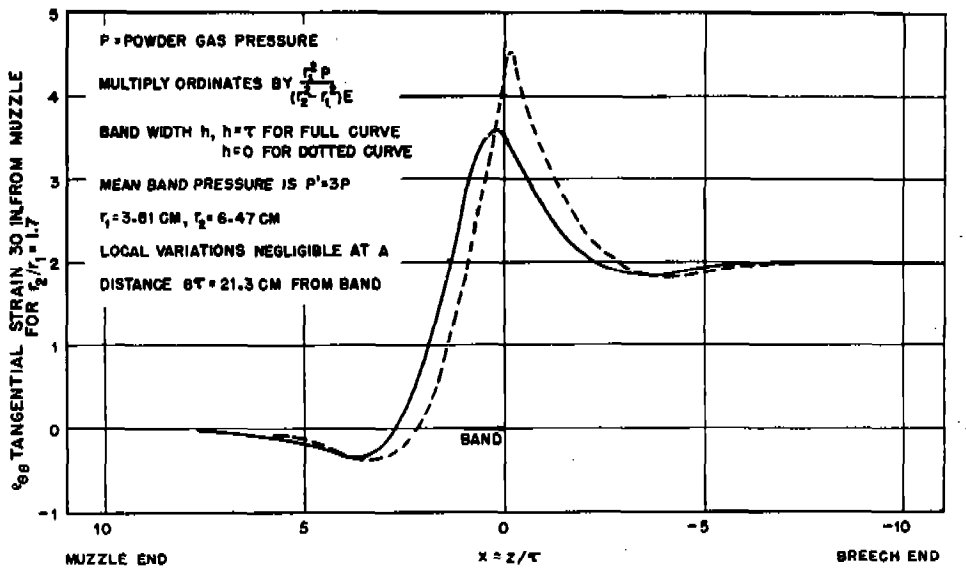


FIGURE 1. Tangential strain in 3-in. gun tube as a function of distance from the band. (Figure 13, NDRC Report A-298.)

7.1.3 Integrated Stresses in the Tube

During the engraving of the rotating band of the projectile by the rifling of the gun, pressure is highly concentrated on a narrow strip, in width actually less than the band. However, stresses exist over the whole length of the tube, tending toward zero at the ends. Lamé's formulas for the deformation and the stresses resulting from uniform pressure are valid in this case also, if the uniform deformation is replaced by the integral of the deformation over the length of the tube and the uniform stresses by the integrals of the stresses taken over the length of the tube.[10] The resulting formulas are the analogues of equation (1), (2), and (3), with w, $\widehat{rr}$, and $\widehat{\theta\theta}$ replaced respectively by W, R, and Θ where $W = \int w dx$, $R = \int \widehat{rr}_\theta dx$, and $\Theta = \int \theta\theta dx$.[b]

An important principle employed in the development of this theorem is that every axially symmetric load distribution can be built up by superposition of half-infinite uniform radial loads.

During engraving of the projectile the longitudinal stress in the gun tube is practically that for a closed chamber, but later it is less, and as the projectile nears the muzzle, the more nearly the stress problem approaches that of the open tube case. Formulas have been developed[13] for the axial stress at points between the projectile and the muzzle, between the projectile and the breech, and above the powder chamber while the projectile is moving down the bore.

[b] Somewhat similar theorems have been presented by other writers.[512,557]

7.1.4 Methods of Determining Frictional Force from Band Pressure

Three methods have been suggested[13] for determining the frictional force[c] between a projectile and the gun barrel from a measurement of the strains in the barrel caused by band and powder pressure. The formulas used to determine the frictional force are based on the elementary solution of the stress equations for an infinite, circular, cylindrical shell. The gun tube is acted on by both the uniform powder pressure P and a uniform longitudinal traction of total amount F.

The analysis for one of the methods was extended[33] and calculations were made to see whether it would be applicable to the 3-in. gun at Carderock, described in Section 4.2. The strain components on the outer surface of the tube may be represented by equations (5) for gauge positions behind the projectile.

$$e_{\theta\theta} = \frac{r_1^2}{[r_2^2(z) - r_1^2]E}\left\{2P - \frac{\mu[F + M(z)\ddot{Y}]}{\pi r_1^2}\right\},$$
$$e_{zz} = \frac{r_1^2}{[r_2^2(z) - r_1^2]E}\left\{-2\mu P + \frac{F + M(z)\ddot{Y}}{\pi r_1^2}\right\}, \quad (5)$$

Here, r_1 and $r_2(z)$ are the inner and outer radii of the gun tube, $M(z)$ is the mass of the tube between any plane z and the muzzle, $\ddot{Y}$ is the positive acceleration of recoil of the gun, E is Young's modulus, and μ is the Poisson ratio. These two equations are the equivalent of equation (6), which gives the friction,

$$F = \frac{E\pi[r_2^2(z) - r_1^2]}{1 - \mu^2}[\mu e_{\theta\theta} + e_{zz}] - M(z)\ddot{Y}, \quad (6)$$

[c] This subject is dealt with more broadly in Section 6.2.

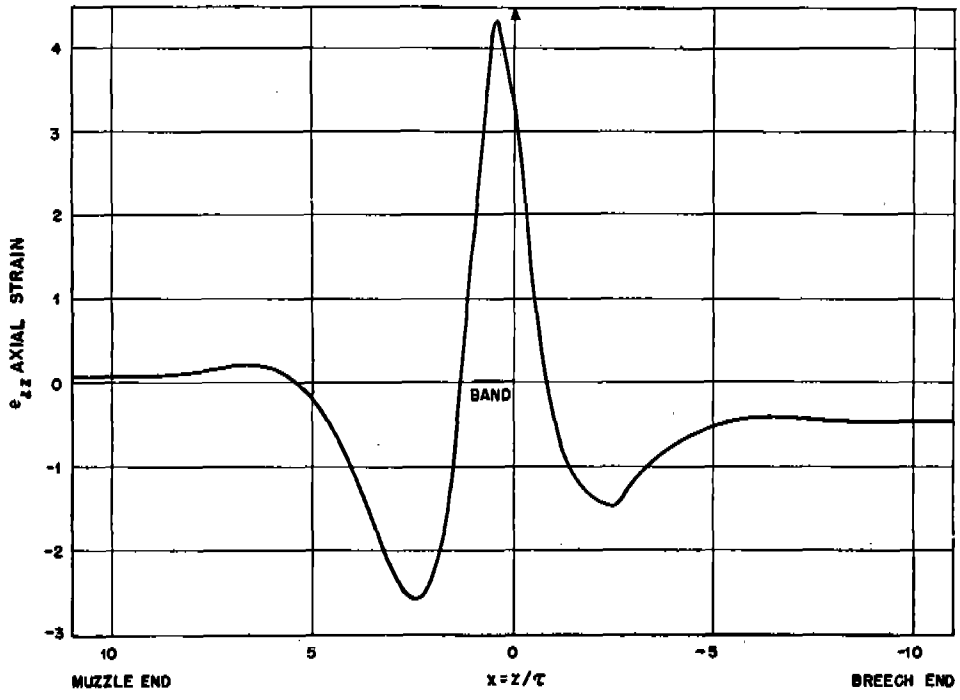


FIGURE 2. Axial strain in 3-in. gun tube as a function of distance from the band. (Figure 14, NDRC Report A-298.)

and equation (7),

$$\pi r_i^2 P = \frac{E\pi[r_2^2(z) - r_i^2]}{2(1-\mu^2)}[e_{\theta\theta} + \mu e_{zz}] \qquad (7)$$

which gives the pressure on the base of the projectile directly from two measurements of strain behind the projectile.

Equations (5) may be replaced by similar expressions in which the acceleration of recoil is expressed in terms of a "gauge constant." This gauge constant was evaluated empirically from the firings of the 3-in. gun at Carderock, and then the curves shown in Figures 1 and 2 were drawn for the tangential strain and axial strain, respectively, at a distance of 30 in. from the muzzle.[d] It was found that the curve for the tangential strain would be unchanged if the friction were assumed to be zero and that even in the curve for axial strain the contribution from the friction is not large enough to be determined accurately.

Therefore, it was concluded that friction cannot be determined directly from strain gauge measurements by this method. It was pointed out, however, that the use of strain gauges as pressure gauges should be satisfactory, and that acceleration of recoil might be evaluated in this manner.

The other two methods[13] for determining friction from band pressure have not been similarly analyzed in terms of experimental conditions. The one involves the use of two longitudinal strain gauges set close together over the powder chamber in a gun having a uniform wall thickness in this region. The other method uses one such strain gauge and a recoilmeter.

7.2 THERMAL STRESSES IN THE BARREL WALL

7.2.1 Stresses at a Point

If a nonuniform temperature distribution results during the heating or cooling of a solid body, the cooler portions of the body exert a restraint upon the expansive tendencies of the warmer portions and the mutual interference causes thermal stress which may be superposed upon any existing stress system within the body. This theory has been applied[151] in the case of a long, hollow cylinder unrestrained at the ends. It is assumed that plane sections far from the ends remain plane and that the temperature field is axially symmetric and uniform along the axial coordinate x. The coefficient of thermal expansion α, the Poisson

[d] It was pointed out that, allowing for certain differences in the experimental conditions, these curves agreed well with some obtained[196] in the firing of a 76-mm gun, M1E2 at Aberdeen Proving Ground.

TABLE 1. Compressions at interface between a 1/16-in. stellite liner and steel caliber .50 machine gun barrel.[151] Case I, 100-round burst; Case II, 250-round burst. Each case postulated for two situations: (a) moderate bore surface temperature; (b) very high bore surface temperature.

Compression	Case I (a) (10^3 psi)	Case I (b) (10^3 psi)	Case II (a) (10^3 psi)	Case II (b) (10^3 psi)
Radial stress	15	20	24	26
Maximum shear	15	12	21	20
Tangential stress	45	47	67	62

ratio μ, and the modulus of elasticity E are assumed invariant with temperature. With the boundary condition $\sigma_r = 0$, at $r = a$ and at $r = b$, where a and b are respectively the inner and outer radii, equations (8) and (9) are obtained for the stresses at a point r units from the axis.

$$\sigma_r = \frac{E}{1-\mu}\left[\frac{1}{r^2}\int_a^r \alpha T r dr + \frac{r^2 - a^2}{r^2(b^2 - a^2)}\int_a^b \alpha T r dr\right]. \quad (8)$$

$$\sigma_\theta = \frac{E}{1-\mu}\left[\frac{1}{r^2}\int_a^r \alpha T r dr + \frac{r^2 + a^2}{r^2(b^2 - a^2)}\int_a^b \alpha T r dr - \alpha T\right]. \quad (9)$$

Here T is the temperature excess over the lowest value in the body.

7.2.2 Application to Caliber .50 Machine Gun

Generalized stress equations were developed for composite hollow cylinders and the results were applied to the computation of stress in a stellite-lined caliber .50 machine gun barrel (Chapter 22). Two temperature distributions based on experimental firings (of the sort described in Section 5.5.1), were used; Case I, resulting from a 100-round burst, and Case II from a burst of 250 rounds. For each case two situations, (a) and (b), were postulated within the liner; distribution (b) assumes a higher bore surface temperature and a steeper gradient than (a). Under the four sets of conditions, the thermal stresses in a gun with a 1/16-in. liner were exhibited graphically for three values of the Poisson ratio in the stellite. Case I (a) and Case I (b) were also graphed for a liner of thickness 1/32-in.

Optimum stellite liner thicknesses, considering thermal stresses only, are given as 1/16-in. for the 100-round burst and 1/9-in. for the 250-round burst. If barrel strength also is considered, the former figure remains unchanged, but the latter increases to 3/10 in. The order of the thermal stresses (compressions) at the interface of the 1/16-in. liner is shown in Table 1.

These thermal stresses are accordingly significant in design problems, as discussed in Section 26.5.2. It should be remembered, however, that they exist for only a small fraction of the time of a round.

7.2.3 Circumferential Strain at Outer Surface

A method of determining heat input by strain measurement is mentioned in Section 5.3.7. The proof of the underlying theorem, which applies to strains in a heated barrel, is outlined in the present section.

The circumferential strain at the outer surface of a heated cylinder depends only on the quantity of heat in the cylinder and is independent of the cylindrically symmetrical distribution of the heat, provided that axial shear strain is neglected, and the specific heat and the expansion coefficient are assumed to be independent of temperature. It is assumed that from a tube of inner radius a and outer radius b, an inner cylindrical barrel section of radius r is removed, heated, and then reinserted in the outer cool section by a shrink fit. By equating the two formulas for the resulting interface radius, equation (10) is obtained.

$$r + r\alpha\theta - \frac{p}{E}r\left(\frac{r^2 + a^2}{r^2 - a^2} - \mu\right) = r + \frac{p}{E}r\left(\frac{b^2 + r^2}{b^2 - r^2} + \mu\right). \quad (10)$$

Then, if the temperature rise θ results from a heat input B per unit area, equation (11) for p can be obtained.

$$p = \left(\frac{E\alpha B}{\rho C}\right)\left(\frac{a(b^2 - r^2)}{r^2(b^2 - a^2)}\right). \quad (11)$$

The corresponding external expansion W_e is given by equation (12),

$$W_e = \left(\frac{pb}{E}\right)\left(\frac{2r^2}{b^2 - r^2}\right), \quad (12)$$

[redacted]

which by combination with equation (11) is simplified to equation (13),

$$W_e = \frac{2\alpha B}{\rho c} \frac{K}{K^2 - 1}, \qquad (13)$$

in which K is the wall ratio. The expansion W_e, is therefore independent of r, and is equal to the expansion of the tube when the heat is uniformly distributed. If the heat has any cylindrically symmetrical distribution, the proof follows from the principle of superposition, since the equations are linear.

7.3 STATIC MEASUREMENTS WITH 37-MM AND 75-MM PROJECTILES

7.3.1 Purpose of the Investigation

The theoretical studies referred to in Sections 7.1.3 and 7.1.4 were accompanied by static measurements with 37-mm and 75-mm projectiles. The aim of this investigation was [64] to arrive at an understanding of the physical processes occurring during and after engraving, so that the behavior of shells during engraving might be predicted for cases in which measurement is impossible.

7.3.2 Apparatus and Method

The early work consisted in setting up apparatus and developing methods for measuring the total radial load due to band pressure, and also the width of the pressure band, that is, the width of that portion of the actual rotating band on which most of the radial load is impressed. For a "thin" tube, with wall ratio 1.5, a radial deflection scanner, pictured in Figure 3, was employed. This method was a refinement of the inspection method of checking tube diameters by means of a 60-degree steel V-block under a dial gauge. The three contact points were the dial plunger and two spherical anvils set 120 degrees apart. The dial reading then gave the sum of the radial changes on profiles 120 degrees distant. Accuracy of readings was improved by maintaining a controlled temperature.

A section of steel tube cut from a 37-mm barrel was placed in the scanner and an "initial scan" with no pressure applied was obtained by taking dial readings at 0.05-in. intervals. The tube section was then removed from the scanner and pressure applied to the middle of the tube section, either by a band of known width, or by the rotating band of a projectile pushed in by a testing machine. A second scan was then made. Finally the tube was removed, the pressure released, and final scans made to determine whether a permanent set had been produced in the tube. This was likely to have occurred with tubes having low wall ratios.

Curves were then drawn plotting three times the radial deformation against distance along the cylinder. A typical graph is shown in Figure 4. Similar curves for known band widths were used in calibrating deflections observed during the actual push tests, while the pressures were found by the method of Section 7.1.3.

For a "thick" 37-mm tube, with wall ratio 2.18, and for sections of larger guns, a different type of scanner was necessary. The cylinder was supported horizontally in a machinist's lathe, and a ring carrying a dial gauge and anvils to measure the deforma-



FIGURE 3. A radial-deflection scanner. (From figure 1, NDRC Report A-312.)

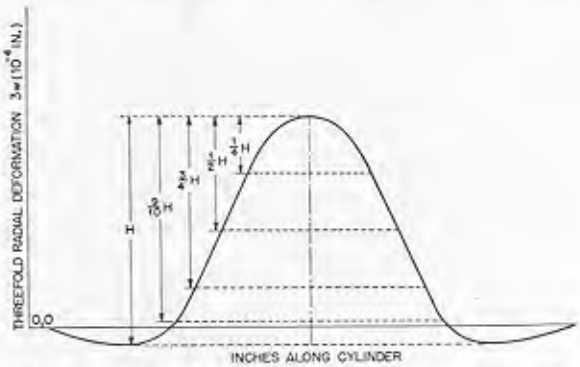


FIGURE 4. Threefold radial deformation. (Figure 3, NDRC Report A-312.)

CONFIDENTIAL

tions was so mounted that it could be moved along the cylinder in measured steps.

7.3.3 Evaluation of Band Pressure

Effective Area of Interference (EAI). The early tests were carried out with solid 37-mm shot, and band pressure was measured at a point in the tube about 3 in. beyond that at which engraving takes place. It was indicated that the pressure is small on the foremost part of the band and that it increases toward the back. In analyzing the results of these tests, the concept of "rectangular interference" was used. Since this quantity ignores the depth of rifling, it was later decided to use "Effective Area of Interference," hereinafter abbreviated EAI.[114] This function may be defined as the quotient obtained by dividing the volume of band metal, expressed in cubic inches, that would be scooped out in passing through the bore if tube and shot were rigid, by the bore circumference. It will be noted that the method of evaluating EAI differs according to whether band diameter is smaller or larger than the groove diameter.

Band Pressure per Inch Circumference. In these static studies it was found convenient to use band pressure per inch circumference (designated by P), rather than pressure(per square inch). It is found by integrating the deformation curve over the length of the gun and applying the theorem on radial deformation given in Section 7.1.3. The key equations are

$$\int w\,dx = \frac{2r_2}{E(\rho^2 - 1)} \int p\,dx \qquad (14)$$

and

$$P = \int p\,dx = \frac{1}{3}\frac{E}{2r_2}(\rho^2 - 1) \int 3w\,dx \qquad (15)$$

in which $2r_2$ is the band width, ρ the wall ratio, and p the pressure in pounds per square inch.

Friction Coefficient. A third quantity of particular interest in these static tests is a friction coefficient, defined as the ratio of the axial load to the product of P and the bore circumference. The axial load necessary to move the projectile can be measured directly on the testing machine. In the 37-mm solid shot, friction coefficients were found to vary from 0.117 to 0.270, clustering around 0.230.

7.3.4 Prediction of Band Pressures

The theory of thin tubes was considered in relation to the observed deformations. It was found that reasonably good agreement could be obtained by a suitable adjustment of parameters.

Probably the most significant results of the study lie in the comparison of radial load with EAI. A linear relationship appears to exist for 37-mm shot, and reasonably good predictions of load can be made from EAI. It is necessary, however, to consider wall ratio and tightness of band seat.[114] The great variation that was observed in the tightness of seating of the rotating bands of 37-mm shot caused a corresponding variation in the apparent EAI. In a final series of tests[115] with 75-mm AP shot and HE shell, the projectiles were subjected to push tests in a used 75-mm, M1897 barrel. For the solid shot it was found that radial load P is proportional to EAI, as is shown in Figure 5. The average ratio was 78 pounds per inch circumference for 10^{-5} sq in. EAI, but the ratio increased for very small bands. The main part of the pressure appeared to be concentrated in a narrow part of the rotating band. The behavior of the bands as far as P/EAI was concerned was practically duplicated with a punch moving radially inward against the band.

For the 75-mm HE shell, P/EAI was approximately 37 for intermediate band sizes, with an increase of the ratio for very small bands. For very large ones, P became practically constant. In this connection consideration was given to the elastic deformation of the shell, and also to the firmer seating of the band during engraving. When allowance was made for these factors, the ratio P/EAI was increased, even beyond the value for AP shot. For values of EAI in excess of 0.011 sq in., P remained essentially constant, which indicated that plastic deformation of the shell wall had occurred.

An extension of the study of band pressures in 37-mm projectiles led to interest in band design giving low stresses,[114] as summarized in Section 27.4.

Calculations of P/EAI were made for guns of a number of different sizes based on firing tests at Aberdeen Proving Ground and push tests at Watertown Arsenal.[117] They showed that P/EAI is independent of the size and design of the rotating band, except that this ratio is larger for very small bands. It was found that in general the value of P/EAI in firing tests is 10 to 30 per cent higher than in push tests. Also, it was found that P/EAI for HE shells is much lower than for solid shot in small calibers, but that in larger calibers the values approach each other.

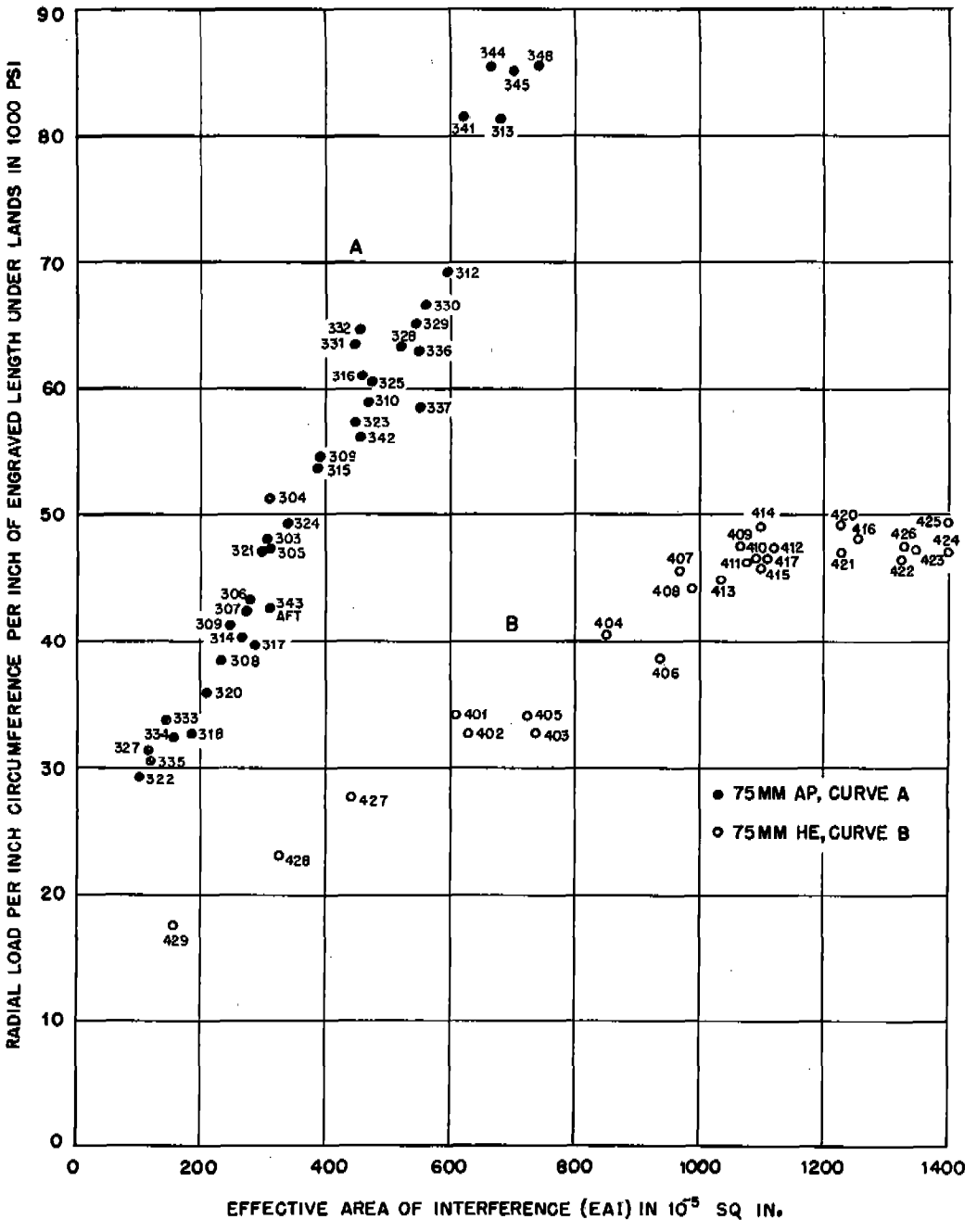


FIGURE 5. Band pressure as function of EAI for 75-mm AP and HE projectiles. (Figure 62, NDRC Report A-443.)

7.3.5 The Process of Engraving

The static test measurements were also used to study the process of engraving.[114] At the beginning of the test, that is, at zero penetration, the conic taper of the band rested against the forcing cone. The projectile was then pushed into the tube by 0.2-in. steps, deformations being measured after each step. In a new 37-mm tube with standard forcing cone, radial load was shown to rise smoothly with shot travel. The average radial pressure P was fairly constant during engraving. In a moderately-eroded 37-mm tube, engraving continued over a considerable distance. It was found that the radial load at a given position of the shot had the same value it would have in a new tube for a correspondingly smaller band.

[redacted]

The axial load behaved very irregularly, depending on the tube. A maximum of from 110 to 200 per cent of the value found after engraving usually occurred near the end of engraving.

Tests were made on a forcing "cone" of 90-degree angle. The resulting radial loads were found to be only one fifth to one sixth of those for a standard forcing cone. The rifling in this case acted like an axial punching tool. For purposes of comparison, the load for a circular punch penetrating a thick plate was measured as a function of penetration. The behavior in the two cases was quite similar.

Mechanism of Engraving

It was concluded[114] that axial shearing is not the principal mechanism involved in the engraving of a rotating band by a forcing cone of small angle, such as in a Service gun. It seems that the principal effect is a radial pressure toward the axis of the projectile, resulting in plastic flow of the band material normal to the radius. Because of the angle of the taper this flow results in considerable displacement of metal rearward, as is shown in Figure 6. Any shearing that occurs is only at the sides of the lands in a radial direction. In addition to the motion radially inward and axially backward, band metal also flows sideways from the space to be occupied by the lands to the space under the grooves of the rifling.

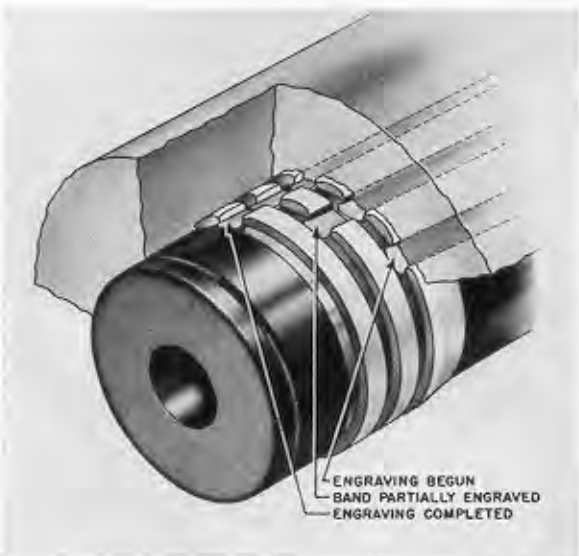


Figure 6. The three stages in the engraving of the rotating band of a projectile.

It appears probable that the angle of the forcing cone does not matter as long as it is sufficiently small. If it approaches 90 degrees, however, then the square ends of the rifling can act like a punching tool in an axial direction, which causes shearing across the rotating band.

7.4 DYNAMIC MEASUREMENTS DURING FIRING OF 3-IN. AND 37-MM GUNS

7.4.1 Firings with 3-in. Gun

Strain measurements on the external surface of the gun barrel were taken during the firings of the 3-in. gun at Carderock, as described in Section 4.4.10. Components of tangential strain due to gas pressure and band pressure may be computed from tables issued by Watertown Arsenal.[251] By suitable interpolation and extrapolation, these tables may be used for any wall ratio. Formulas employed for this transformation are given as equations (16) and (17), where w is the wall ratio (ratio of outer diameter), e_t is the tangential strain on the outer surface of the gun, Z is the distance along the gun, in calibers, and the subscripts 1 and 2 refer respectively to the "unknown gun" and to the "known gun" for which values are tabulated.

$$e_{t_1} = e_{t_2}\left(\frac{w_2^2 - 1}{w_1^2 - 1}\right). \tag{16}$$

$$Z_1 = Z_2\sqrt{\frac{w_1^2 - 1}{w_2^2 - 1}}. \tag{17}$$

A tangential strain gauge was placed on the surface of the 3-in. gun at a point 32 in. from the muzzle. Curves for this gauge compiled from the Watertown tables are shown in Figure 7.

In computing the band pressure, it is assumed that friction and acceleration produce negligible components of tangential strain, and that if the component due to gas pressure is subtracted from the measured strain, the value of the band strain is obtained. From this the band pressure is calculated.

From observed data, strain was plotted against projectile displacement. (See Figure 8.) Gas pressure P was determined by assuming that the strain e measured for abscissas from 14 to 29 in. from the muzzle was entirely due to this pressure, which was then calculated by the Lamé equation (18) where E is Young's modulus and w is the wall ratio.

$$e = \frac{2P}{E(w^2 - 1)}. \tag{18}$$

CONFIDENTIAL

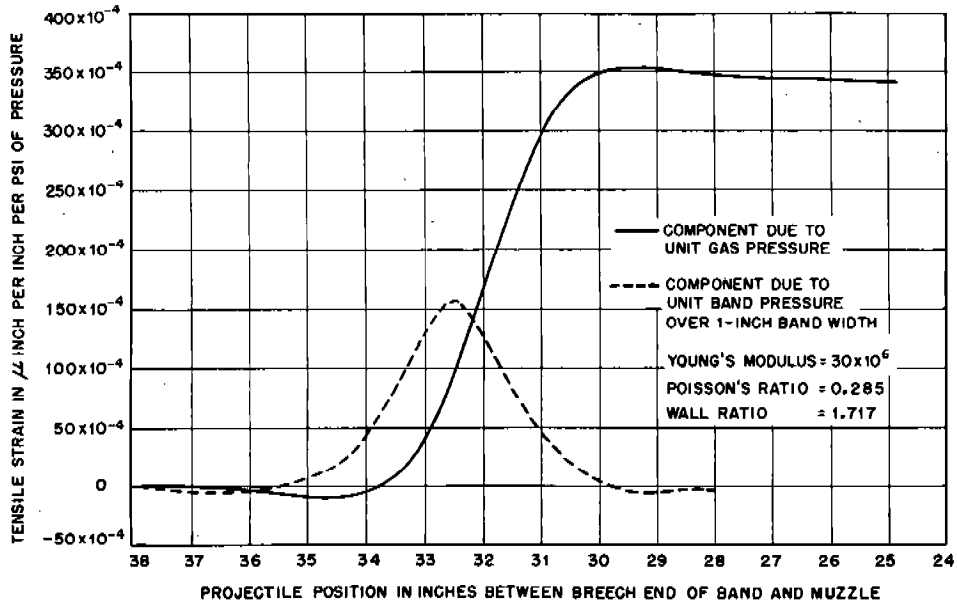


FIGURE 7. Computed tangential strain per unit pressure on surface of 3-in. gun at 32 in. from the muzzle. (Figure 61, NDRC Report A-323.)

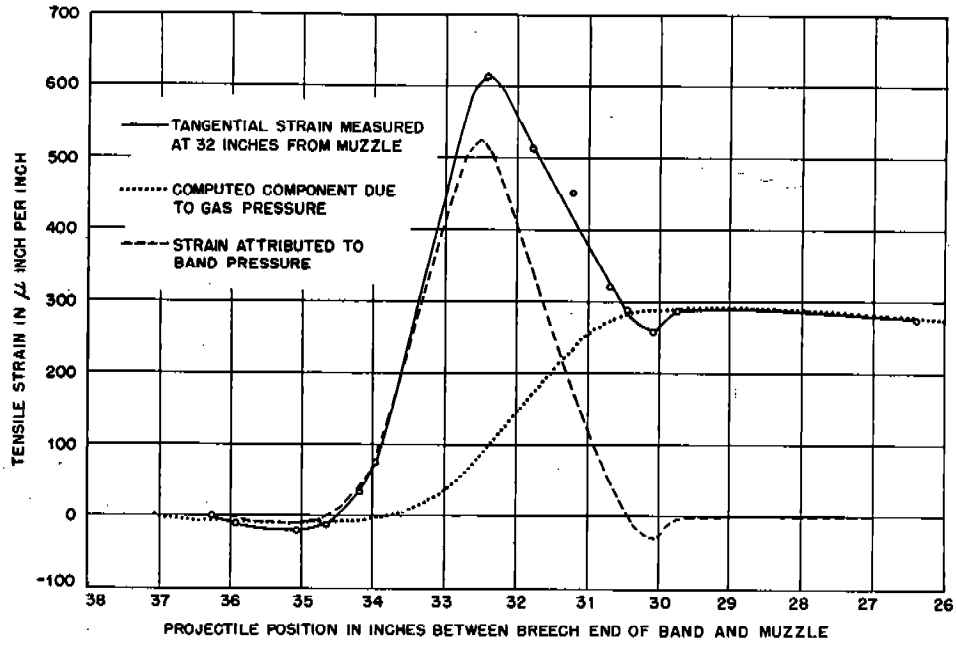


FIGURE 8. Graphical determination of band-pressure strain at gauge 32 T (round 43) of 3-in. gun. (Figure 62, NDRC Report A-323.)

Assuming linear pressure variation, these values of P were extrapolated to projectile positions 29–37. Multiplying them by the corresponding strains per unit pressure shown in Figure 7, the component of strain due to gas pressure resulted, as shown by the dotted curves in Figure 8. This was then subtracted from the measured tangential strain, to give strain due to band pressure. Band pressure in pounds per square inch was found by dividing the peak value of this curve by that of the dashed curve in Figure 7.

[redacted]

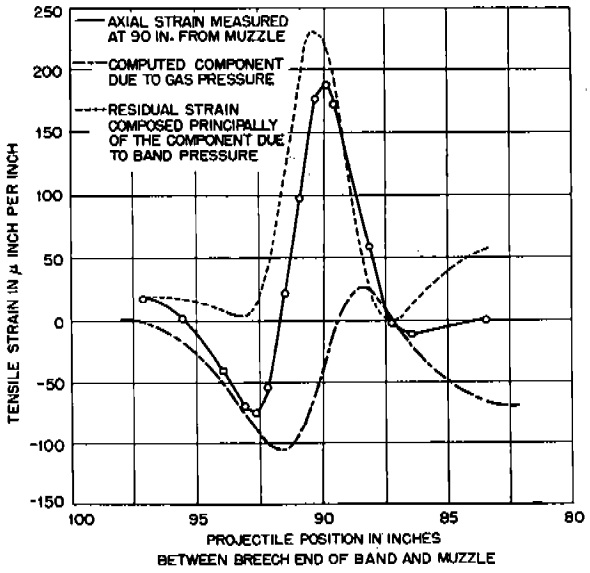


FIGURE 9. Graphical determination of band-pressure strain at gauge 90 A (round 61) of 3-in. gun. (Figure 42, Third Carderock Report, A-460.)

A somewhat similar method was used for computing band pressure at gauge 121.2 T, placed only 4.6 in. from the origin of rifling. However, the gas pressure was derived from that at the breech, using a different assumption as to pressure distribution.

The results of these measurements indicate a band pressure, for a 100 per cent charge round, of from 20,000 to 30,000 psi near the muzzle, compared with a pressure of from 60,000 to 70,000 psi near the origin. For reduced-charge rounds the latter pressure shows little variation from that for the 100 per cent charge, but the pressure farther along the barrel is decreased to only about 40,000 psi. These band pressures exceed the yield point of cold-worked copper, the material of the rotating bands used in the firings.

An interesting special measurement was that of strains in the vicinity of a hole in the gun bore which had been drilled at right angles to the axis for the introduction of a pressure gauge. Eleven strain gauges were cemented to the surface of the gun barrel around the hole, one of them being an axial gauge at its edge. The typical curve of axial strain illustrated in Figures 8 and 9 was modified, the tension peak being chopped off about half way up by a jagged line which corresponded to the time the rotating band was passing under the hole. Axial gauges 2 in. from the hole's edge showed this phenomenon to a lesser degree. This reduction in strain is attributed to local reduction in band pressure over that portion of the band which passes under the hole.

7.4.2 Studies With Army 37-mm Field Gun

High-speed strain-recording equipment for use in general stress research has been developed in recent years at the Massachusetts Institute of Technology. It was tested at Watertown Arsenal[249] in firings of a 37-mm field gun, and characteristic firing strain records were obtained.[166]

Eight strain gauges of the same type as was used later on the 3-in. gun at Carderock were used in combination with a special three-element film-recording oscillograph. Two gauges were placed tangentially over the powder chamber, and pairs of tangential and axial gauges were placed near the origin of rifling, midway down the barrel, and near the muzzle. The firing-strain records of the two gauges near the powder chamber rose smoothly to maxima and then decreased gradually. Gauges 3, 4, 5, and 6 exhibited curves similar to those of Figures 1 and 2.

Gauge 7 indicated some vibrational effect, but this was much more pronounced for gauge 8, the tangential gauge near the muzzle. These vibratory strains developed earlier and were greater in amplitude when the projectile had a muzzle velocity of 2,650 fps than when the velocity was 2,520 fps. At 2,000 fps the effect was hardly noticeable.

Later a detailed study of band pressures in these firings was made.[327] The computed band pressure reached a maximum of 78,100 psi. This value is of the same order of magnitude as that found for the 3-in. gun used in experiments described in Section 7.4.1, when the bore was greased.

Several types of theoretical analysis were introduced in this study. The first is a modified shear analysis, which gave good results for band pressures during firing when taken in conjunction with oscillograph records of firing strains. When this distortion was later combined with bending, agreement with experiment was again good, except for maximum stresses, which checked better with full shear analysis.

Two general methods were employed in interpreting the firing data. The first method[339] assumes that the rotating band acts like a narrow band of high pressure moving down the barrel, followed by the powder pressure. The crest of the transient would occur at the instant the center of the rotating band passes the gauge location, if powder pressure is neglected. For gauges 6, 12, 15, 18, and 24 in. from the muzzle of the 3-in. gun this assumption gave excellent agreement.[39] Gauges farther from the muzzle gave readings not readily interpreted because of other

factors involved. The second method[327] is a modification[341,346] of the relaxation procedure of analysis introduced by the British, which is described in Section 27.2.3.

7.5 DYNAMIC MEASUREMENTS DURING FIRING OF CALIBER .50 MG BARRELS

7.5.1 Experimental Conditions

Strain measurements were made during the firing of four caliber .50 aircraft machine gun barrels. Two of the barrels were fitted with 9-in. liners of Stellite No. 21, as described in Section 22.3. The third was a nitrided, chromium-plated barrel, in which the plating was slightly tapered toward the muzzle, as described in Chapter 23. The fourth barrel was a regular steel one.

Four types of ammunition were used: API-M8, a common combat round; AP-M2, the ammunition ordinarily used in the erosion tests of caliber .50 machine gun barrels; Tr-M1, which previous experiences had shown to give the least erosion; and Tr-M10, which previously had given the most erosion in caliber .50 aircraft barrels. (See Chapter 23.) The largest and smallest diameter AP-M2 bullets were especially fired for purposes of comparison.

7.5.2 Measurements and Computations

Strains were measured with resistance gauges cemented circumferentially at chosen locations on the outer surface of the barrel, the results being recorded by the oscillographs described in Section 4.4.2. Maximum tangential stresses were then tabulated. Starting at the origin of rifling, these ranged from 10,000 psi up to values approaching 20,000 psi at 10 in. from the breech, then decreased as the bullet approached the muzzle. This was not characteristic of stresses when oil was present in the bore, however.

In addition to the determination of tangential stresses, calculations were made for five other quantities:

1. Maximum bore stresses, computed from the outer surface stresses by the Lamé formula given in equation (19

$$P_B = P_0^{w^2 - 1/2} \tag{19}$$

in which P_B and P_0 are the bore and surface stresses, and w is the wall ratio.

2. Gas pressures, similarly computed from the strain-gauge records, after the band pressure peak had passed.

3. Band pressure, computed by a method developed at Watertown Arsenal.[249] The band width was assumed to be 1.6 calibers.

4. Bore expansion, e_{tam}, calculated from the wall ratio w and the maximum external tangential strain, e_{tm}, according to the Lamé theory as expressed in equation (20) in which μ, the Poisson ratio, is taken to be 0.3.[249]

$$e_{tam} = \frac{(1 - \mu) + (1 + \mu)W^2}{2} e_{tm}. \tag{20}$$

5. Heat input, by the method discussed in Section 5.3.7. (See also Section 7.2.3.)

7.5.3 Discussion of Results

In a nitrided and chromium-plated barrel with tapered plating, the band-pressure peak disappeared at a point between 14 and 24 in. from the breech; in the stellite-lined barrel this occurred around the end of the liner, at about 12 in. from the breech.

Band pressure, when present, was greater than the gas pressure. When the bore was oily, these band pressures, except at the origin of rifling, were higher and lasted for a greater distance down the barrel.

Outer surface stresses on the chamber section of a lined barrel were smaller than on a monobloc barrel. The more erosive ammunitions produced the greatest strains. Maximum gas pressures ranged from 45,000 to 53,000 psi and maximum band pressures from 51,000 to 75,000 psi. The bore expansion was of the order of from 0.001 to 0.002 in.

Chapter 8

EXTERIOR BALLISTICS OF HYPERVELOCITY PROJECTILES

By *A. H. Stone*[a]

8.1 INTRODUCTION

HYPERVELOCITY PROJECTILES have many advantages, as far as exterior ballistics is concerned, as indicated in Chapter 1, provided that they can be designed so as to satisfy two conflicting requirements. These are: (1) stability (so that the yaw is kept small), and (2) high ballistic coefficient (i.e., low air resistance). Calculations, confirmed by firings, show that these requirements can be met satisfactorily by subcaliber projectiles and evaluate their advantages.

Much research was involved in these developments. Simplified methods have been devised for predicting the behavior of projectiles in the hypervelocity range. The stability and the optimum proportions of subcaliber projectiles have been investigated for a selected minimum value of the stability factor. Since experimental ballistic data at high velocities were lacking for a series of projectiles having a systematic variation of dimensions, a theoretical attack was made on the behavior of the drag and the stability at high velocities through the application of the dynamics of compressible fluids. The theory also makes possible an estimation of the effects of varying ogive lengths. The analysis of the results of firings is greatly simplified by the development of a photographic method of trajectory determination. Finally, the effects of various design features have been studied by systematic firings carried out with the cooperation of Aberdeen Proving Ground.

While attention was focused on hypervelocities and in particular on subcaliber projectiles, the results obtained are of value for exterior ballistics in general.

8.2 FLIGHT CHARACTERISTICS OF HYPERVELOCITY PROJECTILES

8.2.1 Hypervelocity and Energy Loss

Hypervelocity projectiles differ in their exterior ballistics from standard projectiles in two respects: (1) there is an effect caused purely by their higher velocity; (2) the projectiles themselves are generally different from the standard type, and in the cases of greatest interest are subcaliber.

The first effect can be described by saying that a given projectile overcomes air resistance more efficiently at hypervelocity than at conventional speeds. The drag force d resisting the motion of a projectile is expressible as [176,509]

$$d = \rho K_D D^2 U^2, \tag{1}$$

where ρ is the air density in pounds per cubic foot, D is the diameter of the projectile in feet, and U is its velocity in feet per second. The dimensionless coefficient K_D is, for any one projectile, a function of the velocity (or, more accurately, of the ratio U/a_1 where a_1 is the velocity of sound). In the supersonic range, K_D is found to decrease gradually from a maximum in the neighborhood of the velocity of sound. Figure 1 illustrates a typical case. [Systematic data are lacking at velocities above 4,000 fps and extrapolation is used; but theoretical considerations (Section 8.5) show that this is not likely to cause much error.] Thus while increasing U increases the drag it also decreases the ratio of the drag to the kinetic energy of the pro-

TABLE 1. Remaining velocities (RV) and energy losses (EL) of G_8-type projectile traveling over various ranges.

Muzzle velocity (fps)	Range (yd) 500 RV (fps)	500 EL (per cent)	1,000 RV (fps)	1,000 EL (per cent)	1,500 RV (fps)	1,500 EL (per cent)	2,000 RV (fps)	2,000 EL (per cent)
5,000	4,710	12	4,430	22	4,160	31	3,890	40
4,000	3,730	13	3,470	25	3,210	35	2,960	45
3,000	2,750	16	2,510	30	2,270	43	2,040	54
2,000	1,780	21	1,570	38	1,380	52	1,200	64

[a] Geophysical Laboratory, Carnegie Institution of Washington. (Present address: Cambridge University, Cambridge, England.)

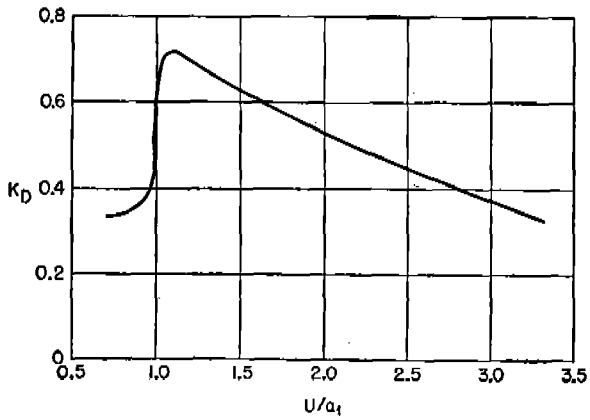


FIGURE 1. The drag coefficient K_D for a projectile of type G_8. (This figure is based on Figure 1 of Ballistic Research Laboratory Report No. 409, Aberdeen Proving Ground.)

jectile. Consequently, in traveling over a given range, a projectile at hypervelocity retains not only a greater kinetic energy, but a greater proportion of its original kinetic energy as compared with the same projectile at a lower but still supersonic velocity. This effect is seen in Table 1, which shows the remaining velocity (RV) and the percentage of the kinetic energy that has been lost (EL) in a typical case, for various muzzle velocities and ranges. The table has been computed for a projectile[b] of type G_8 and ballistic coefficient 1.0 when fired horizontally.

8.2.2

Range and Time of Flight at High Speeds[c]

Hypervelocity has a further advantage to the exterior ballistician, in that it permits simplification of computations, particularly over ranges short enough for the curvature of the trajectory to be neglected (as is usually the case with hypervelocity projectiles in practice). If correction factors for variations in air density and air velocity are omitted, the retardation $(-dU/dt)$ produced by the drag of the projectile can be expressed[509] by equation (2),

$$-\frac{dU}{dt} = \frac{\rho U F(U)}{C}, \tag{2}$$

in which for a given standard projectile shape, $F(U)$ is a definite function of the velocity (or, more exactly, of the Mach number, U/a_1), and C, the ballistic coefficient, is defined by

$$C = m/iD^2, \tag{3}$$

where m is the mass of the projectile and i is the "form factor"[172,188]—a number usually close to 1 that corrects for the deviation of the actual projectile shape from the standard one to which F strictly applies. In equation (3) and subsequent equations based on it, the projectile diameter D is measured in inches, instead of in feet, as in equation (1). For ranges that are short enough for the curvature of the trajectory to be neglected, equation (2) leads to

$$R = -C\int_{U_0}^{U} \frac{dU}{\rho F(U)}, \tag{4a}$$

$$t = -C\int_{U_0}^{U} \frac{dU}{\rho U F(U)}, \tag{4b}$$

where the projectile velocity falls from U_0 to U in traversing a distance R in a time t. Now, over the hypervelocity range, the function $F(U)$ is very "smooth," partly because it is obtained by extrapolation, and can be approximated sufficiently well by the linear expression

$$F(U) = AU + B, \tag{5}$$

where A and B are suitably chosen constants, easily determined graphically. For example, it has been calculated that in the range $3{,}800 \leqq U \leqq 6{,}000$, if $A = 0.0001$ and $B = 0.0123$, the error is less than one-third percent. Here the projectile[d] is of type G_1, and the velocity is measured in feet per second. In a wider velocity range, $2{,}400 \leqq U \leqq 6{,}000$, if $A = 0.00009$ and $B = 0.06$, the error is less than 3 per cent.[42] The substitution of $AU + B$ for $F(U)$ in equations (4) enables the integration to be carried out explicitly. Thus

$$R \text{ (in yards)} = \frac{1}{3}\frac{C}{A}\ln\left(\frac{U_0 + B/A}{U + B/A}\right), \tag{6}$$

$$t \text{ (in seconds)} = \frac{C}{B}\ln\left(\frac{U_0(U + B/A)}{U(U_0 + B/A)}\right), \tag{7}$$

and the relation between t and R can be obtained.[42] Equations (6) and (7) also enable C to be determined

[b] The G_8 type of projectile is characterized by a cylindrical base and a long ogive (radius of curvature: 5 to 10 calibers). It is the standard British projectile form.

[c] Based on a memorandum, not available for general circulation, from C. W. Beck and K. F. Herzfeld, Catholic University, to the Chief of Division 1, NDRC, 1942. See also pp 67–75 of NDRC Report A-234.[42]

[d] The G_1 type of projectile is characterized by a square base and a blunt ogive (radius of curvature: 2 calibers). It was one of the types fired at Gâvre.

from a firing of the projectile. For this purpose it is found that a single firing over a long trajectory gives more accurate results than several firings over shorter distances.

8.2.3 Subcaliber Projectiles

The effect of replacing a standard projectile by one of subcaliber can now be considered. It is evident from equation (3) that scaling down a full-caliber projectile to one of subcaliber tends to decrease the ballistic coefficient C, because the mass varies as the cube of the caliber. Thus, a comparison between the two types of projectile shows that

$$C_1/C_2 \leqq D_1/D_2,$$

where the subscript 1 refers to the subcaliber projectile, and the subscript 2 refers to the one of full caliber; hence, the retardation of the subcaliber projectile will be at least D_2/D_1 times the retardation of the full-caliber projectile. This effect is accentuated by the fact that, in practice, requirements of stability (see Section 8.3) may oblige the subcaliber projectile to be shorter in proportion, which results in a further lowering of its mass and in an increase in the form factor.

To investigate how far this effect may offset the advantage of the higher velocity of the subcaliber projectile, calculations have been carried out for the least favorable case, namely, that of the sabot-projectile (described in Chapter 29), for which the kinetic energy of the sabot is wasted. Using the method just described, it has been shown[42] that over short ranges the ratio of the times of flight t_1 and t_2 for a typical sabot-projectile and a full-caliber projectile, respectively, is approximately given by equation (8),

$$\frac{t_1}{t_2} = \frac{C_1 \ln \{[F(U_1) - Be^{AR/C_1}]/AU_1\}}{C_2 \ln \{[F(U_2) - Be^{AR/C_2}]/AU_2\}}, \qquad (8)$$

in which R is the range, U_1 and U_2 are the muzzle velocities of the two projectiles, and A and B are as in equation (5). From equation (8) the times of flight of a 57/75-mm sabot-projectile and a 75-mm full-caliber projectile fired from the same gun have been calculated for various ranges as shown in Figure 2, using $C_1 = 2.0$, $C_2 = 2.6$, $U_1 = 2{,}805$ fps, and $U_2 = 2{,}050$ fps.

It will be seen that up to a range of 5,000 ft, the time of flight of the sabot-projectile is only about three-quarters of the time of flight of the corresponding full-caliber projectile. Furthermore, over this range the two projectiles have nearly equal kinetic energies; and since the sabot-projectile has its energy concentrated over a smaller area, it has the advantage in armor-piercing ability, as discussed in Section 9.2.2.

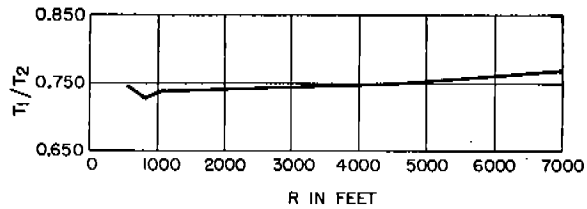


FIGURE 2. Ratio of time of flight of 57/75-mm sabot-projectile to that of a full-caliber projectile fired from the same gun to various ranges. (This figure has appeared as Figure 18 of NDRC Report A-234.)

The above calculations refer to an extreme case. In practice a compromise is often made by increasing the mass of the subcaliber projectile, usually by giving it a core of tungsten carbide. This results in a lower initial velocity but a more favorable ballistic coefficient, and, moreover, tungsten carbide leads to improved armor penetration, for the reasons given in Section 9.2.2. Another reason for this compromise is the need for stability, which will now be considered.

8.3 STABILITY OF SUBCALIBER PROJECTILES

8.3.1 General Theory

The requirement of stability is crucial for subcaliber projectiles, especially sabot-projectiles. Accordingly the following account begins by briefly reviewing the general considerations involved.

In general, a spinning projectile in flight does not point exactly in the direction of its motion, but yaws in an oscillatory way; and it is important that the yaw should be damped out, or at least should not increase. The projectile is then said to be stable.

In the first instance, the situation may be simplified by disregarding the more complicated features of air resistance and considering only a short portion of the trajectory, so that the retardation of the projectile and the effect of gravity can be disregarded. The air resistance acting on the projectile is then equivalent to a single force f, which can be resolved into two components: (1) the axial drag d acting along the axis of the projectile, and (2) a force L perpendicular to the axis, acting through a point P on the axis

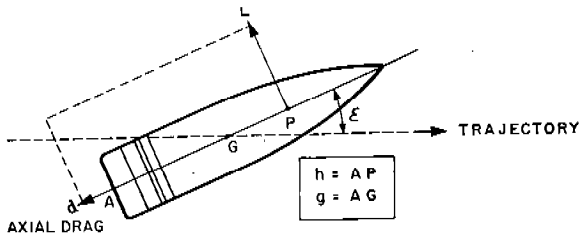


FIGURE 3. Simplified representation of the forces that act on a spinning projectile in flight. The air resistance is considered as a single force having two components: the axial drag d acting along the axis of the projectile and a force L perpendicular to the axis, acting through the center of pressure P. For a spin stabilized projectile, P is in front of the center of gravity G. The angle of yaw is ϵ.

called the center of pressure (see Figure 3). For spin-stabilized projectiles, the center of pressure P is in front of the center of gravity G.

The moment tending to overturn the projectile is then $M = LD\ (h-g)$, where g and h are the distances (in calibers) from the base A to the centers of gravity and pressure, respectively, and D is the caliber of the gun.

It is found that L/ϵ and h are nearly independent of the yaw ϵ (measured in radians), provided ϵ is not too large; hence

$$M = LD(h-g) = \mu\epsilon, \tag{9}$$

where μ can, for the moment, be regarded as constant. The condition for stability[184,199,509] is then $s > 1$, where s, the stability factor, is defined by

$$s = \frac{A^2N^2}{4\mu B}, \tag{10}$$

in which A is the axial moment of inertia of the projectile, B is the moment of inertia about the transverse axis through the center of gravity, and N is the axial spin of the projectile (in radians per second). If the condition that the stability factor is a constant greater than unity is satisfied, the motion of the nose of the projectile as seen from the center of gravity will be epicyclic. For the simplified set of forces shown in Figure 3, the motion is that of a simple epicycle, which is the path traced by a point attached to a fixed point by two jointed links, each of which rotates uniformly, as illustrated in Figure 4A.

8.3.2 Stability Under Actual Conditions

If now the full effects of the air resistance are allowed for, the situation becomes more complicated. There are forces and couples present caused by the Magnus effect, by the frictional resistance to the spin of the projectile, and even by the yawing oscillations themselves. The complete theory[197,444] shows that if $s > 1$ the nose of the projectile oscillates in much the same way as before, but the lengths of the epicyclic arms are exponentially damped, that is, are multiplied by factors of the form e^{-cR}, where R is the range and c is a parameter that is nearly constant. This damping causes the path described by the nose of the projectile as seen from the center of gravity to be that shown in Figure 4B.[509]

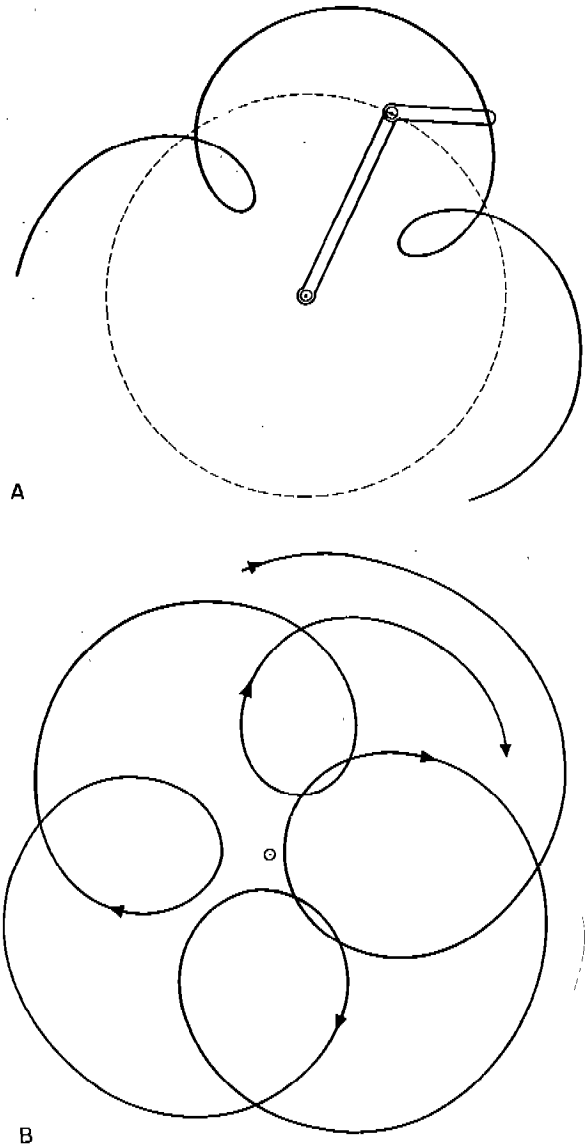


FIGURE 4. Epicyclic motion of the nose of a projectile: A. Retardation and effect of gravity disregarded. B. Full effects of air resistance considered.

Moreover, it is possible for this damping to be negative, so that the yaw can actually increase, even if $s > 1$.[e] The condition for positive damping of the yaw is found[f] to be

$$s > \frac{(1+t')^2}{4t'},$$

where

$$t' = \frac{\frac{A}{B}K_H - \frac{1}{2}(K_A - 2K_T)}{\frac{A}{mD^2}K_L + \frac{1}{2}(K_A - 2K_T)}, \qquad (11)$$

in which D is the diameter of the projectile, m its mass, A and B the moments, and K_H, K_L, K_A, K_T, are various dimensionless coefficients, all nearly constant. Equation (11) is more restrictive than the condition $s > 1$. The coefficients involved are difficult to measure; but, using the best estimates[e] available, s should be at least 1.2 for projectiles of conventional type if the yaw is to be damped at all, and should preferably be at least 1.5 for rapid damping, namely, a shrinkage of both epicyclic arms to one-half of their initial value in 3,000 calibers of travel. A value of s of 1.3 may be taken as a minimum. For unusually long projectiles, e.g., rockets, the limit for s is larger; and very long projectiles may possibly be incapable of stabilization by spin.

8.3.3 Stability Over Long Arcs of the Trajectory

The foregoing applies only to a short arc of the trajectory. Over longer arcs, the variation of μ must be taken into account. The "moment coefficient" μ can be expressed[509] by equation (12),

$$\mu = \rho K_M D^3 U^2 = \rho K_N D^3 (h-g) U^2 \qquad (12)$$

(where $K_N = L/\rho D^2 U^2 \epsilon$); here, as before, ρ denotes the air density, U the velocity, and D the caliber of the projectile. The dimensionless coefficients K_M and K_N are, for a given projectile shape, functions of U (or rather U/a_1); K_M does not vary greatly in the relevant range (see Figure 5).[509] Along the trajectory, U decreases faster than the spin N; hence, from equations (10) and (12), s increases along the trajectory. Thus if a projectile is initially stable, it will remain so.

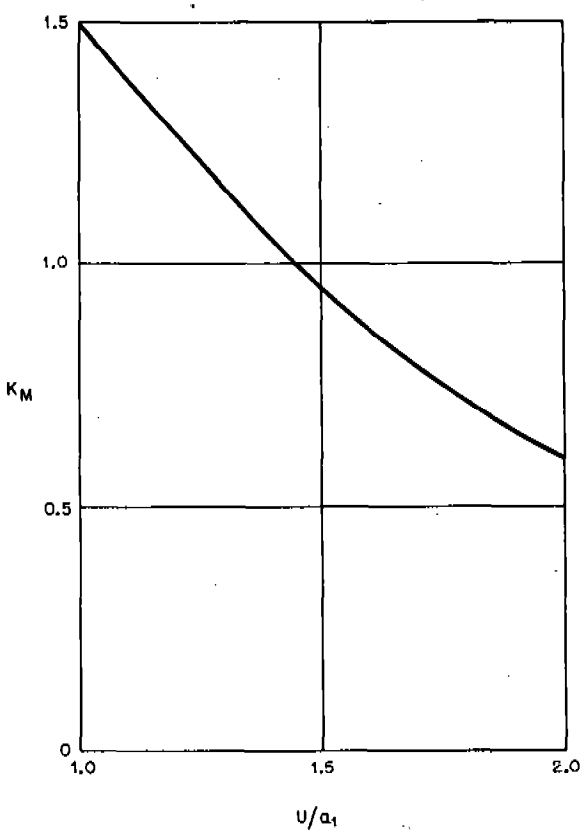


FIGURE 5. The coefficient K_M in equation (12) as a function of the velocity for a projectile of type J. (Reprinted by permission from *Elements of Ordnance* by T. J. Hayes, published by John Wiley and Sons, Inc. This figure is based on Figure 223 in that work.)

Equation (12) shows also that the stability of a projectile depends on the weather. A projectile fired into denser (e.g., colder) air than standard will have a larger moment coefficient, and hence a smaller stability factor, than when fired under standard conditions. To allow for this, and to provide a margin of safety, the stability factor of a projectile when tested under standard conditions should be at least 1.5.

8.3.4 Stability As Affected By Special Conditions

Under special circumstances, this limit for s may be modified.

[redacted]

[e] Personal communication from I. E. Segal, Ballistic Research Laboratory, Aberdeen Proving Ground, as given in his memorandum to R. N. Thomas, September 28, 1944. An example was given in that memorandum.

[f] This equation is based on one published by Kent and McShane[199] (equation 31). A substantially equivalent condition, in the notation of Fowler[444] is:

$$s > \frac{(h+k)^2}{4(h+\gamma)(R-\gamma)}$$

Small Initial Yaw

If the initial yaw can be kept very small, a lower value of s may be used; even if the yaw increases at first, the increase of s along the trajectory may lead to damping of the yaw before it reaches an unduly large value. This consideration applies to most deformable projectiles (Chapter 29) and to pre-engraved projectiles with wide rotating bands (Section 27.3) since both types acquire very little yaw in the gun.

Projectile Fired From a Plane

However, a larger value of s may be needed to moderate the yaw of a projectile fired from an airplane,[174,193] where there may be a large effect caused by head wind and crosswind combined.

Firing Ahead. The head-wind effect on stability is at its worst when the fire is straight ahead, for then the initial velocity relative to the air is increased from U to $U + w$ (where w is the velocity of the plane) without a compensating increase in the spin, N. From equations (10) and (12) the value of ϵ must be multiplied by $U/(U + w)^2$. In a representative case, $w = 300$ fps, $U = 2{,}500$ fps, hence the stability factor is decreased by nearly 20 per cent from its value when the projectile is fired from rest.

Firing Abeam. The crosswind effect is at its worst when the fire is abeam. The projectile will then have an initial yaw of approximately w/U (radians) and a first maximum yaw of approximately $w/U\sqrt{1 - 1/s}$.[174] In the case just cited, with $s = 1.5$, the yaw is about 12 degrees, which is undesirably large. An increase in s is desirable on this account, to accelerate the damping of the yaw. (It also decreases the first maximum yaw, but only slightly.) The way in which this damping depends on s is given by equation (13),[193]

$$\epsilon^2 = \epsilon_0^2 \left(\frac{s - 1/2}{s - 1}\right) e^{-2\rho R(a+a')}, \qquad (13)$$

where ϵ is the mean yaw, ϵ_0 the initial yaw, R the distance traveled, ρ the air density, a is a constant (the "damping constant") and $a' = D^2K_D/2(s - 1)m$. This equation is based on the assumption that the damping rates on the two epicyclic arms of Figure 4B are equal.

Thus a satisfactory value of the stability factor for a projectile to be fired from an airplane is about 1.7.

Effect of Hypervelocity. Finally, one may inquire into the effect of hypervelocity as such on stability. As Figure 5 suggests, the indications are that K_M should be slightly smaller in the hypervelocity range than at standard muzzle velocities. This means that a given projectile has a higher stability factor at hypervelocity than at standard velocities, in other words, that hypervelocity has to some extent a stabilizing effect. However, though systematic experimental data are lacking in the hypervelocity range, theoretical considerations (which are dealt with in Section 8.4.6) indicate that this effect is small at best, and may be reversed at still higher velocities. Thus on firing from a stationary gun, the stability factor is substantially independent of the muzzle velocity.

However, in connection with fire from airplanes, hypervelocity has an obvious advantage, since in effect it reduces the relative importance of the velocity of the airplane. For example, doubling U would halve the effects considered in the preceding subsection.

Summary. To sum up, an acceptable value of the stability factor is in general 1.5, but it can be lower if the initial yaw is kept very small, or if the projectile is not to be used under conditions of high air density, and it should be higher if the projectile is to be fired from an airplane, though this last effect is less important for hypervelocity projectiles.

8.3.5 Methods of Obtaining Stability

From equations (10) and (12),

$$s = \frac{A^2N^2}{4\rho K_N D^3(h-g)U^2B}. \qquad (14)$$

This expression makes obvious several general methods[14] for modifying the design of a spin-stabilized projectile so as to increase its stability.

1. The twist of the rifling in the gun can be increased. This increases s very effectively (by increasing N), but was virtually excluded during World War II by the great desirability of retaining standard guns, a consideration that might still have weight in the future with new guns for the sake of using standard projectiles.

2. The projectile can be shortened, thereby increasing A^2/B. This has the drawback of decreasing the ballistic coefficient defined by equation (3).

3. The density of the projectile can be increased. Here both A^2/B and the ballistic coefficient are increased. There is the disadvantage that the increased mass leads to some loss of muzzle velocity.

4. A compromise version of the preceding methods is possible whereby the projectile can be given a core of denser material, such as tungsten carbide. This has

the advantage that the optimum combination for armor penetration can be selected.

5. If a core is used, it may (if geometrically possible) be set forward. This moves the center of gravity closer to the center of pressure, that is, it decreases $(h-g)$ and so increases s without affecting the ballistic coefficient.

6. Finally, fins or tail surfaces may be used to move the center of pressure closer to the center of gravity. As has been pointed out,[14,42] this method would be especially suitable for sabot-projectiles. It has been tried by the Germans and deserves further investigation.

8.3.6 Stability of Deformable Projectiles[g]

Consider first a deformable projectile which, after deformation, is equivalent to a scaled-down version of the full-caliber projectile. We use the subscript 0 to refer to the deformable projectile before deformation, the subscript 1 to refer to it after deformation, and the subscript 2 to refer to the full-caliber projectile. From equations (10) and (12),

$$s_1 = \frac{A_1^2(N_1/U_1)^2}{4\rho K_M D_1^3 B_1}, \tag{15}$$

and since the conservation of angular momentum shows that $A_1N_1 = A_0N_0$ (if frictional losses are, for the moment, neglected), this can be written

$$s_1 = \frac{(A_0/A_1)^2 A_1^2 (N_0/U_1)^2}{4\rho K_M D_1^3 B_1}. \tag{16}$$

Similarly

$$s_2 = \frac{A_2^2(N_2/U_2)^2}{4\rho K_M D_2^3 B_2}. \tag{17}$$

Now, $N_0/U_1 = N_2/U_2$, both being determined by the pitch of rifling of the gun. Further, if both projectiles have the same density, $A_1/A_2 = D_1^5/D_2^5 = B_1/B_2$. Hence,

$$\frac{s_1}{s_2} = \left(\frac{A_0}{A_1}\right)^2\left(\frac{D_1}{D_2}\right)^2. \tag{18}$$

Since $A_0 > A_1$, while $D_1 < D_2$, the factors on the right tend to cancel. For example, in the 57/40-mm deformable projectile described in Section 30.2, $A_0/A_1 = 1.35$, $D_1/D_2 = 40/57$, hence $s_1/s_2 = 0.90$. Here the deformable projectile would be nearly as stable as the full-caliber projectile, except that frictional losses have been so far neglected. The friction in the muzzle adaptor will change U_1 only a little, since it is offset by the continued pressure of the powder gases; but it will slow down the angular spin. Experiments indicate[128] that in a new adaptor about 10 per cent of the angular momentum is lost in this way. (In an old adaptor the loss rises to 25 per cent.) Thus A_1N_1 is equal to only (0.9) A_0N_0, and equation (18) must be replaced by approximately

$$\frac{s_1}{s_2} = 0.8\left(\frac{A_0}{A_1}\right)^2\left(\frac{D_1}{D_2}\right)^2, \tag{19}$$

for a new tube, the constant factor falling to 0.5 in a worn tube.

The full-caliber projectile ordinarily has enough excess stability for the deformable projectile to be sufficiently stable, particularly since deformable projectiles ordinarily have small initial yaws. Furthermore, attention has been concentrated on deformable projectiles with tungsten carbide cores; and, as was pointed out in Section 8.3.5, this feature increases s, and may be made to increase it still further by advancing the core. This effect is borne out, on the whole, by the data[456] shown in Table 2.

TABLE 2. Stability factors of some 57/40-mm deformable projectiles.

Type No.	Distance from rear of core to rear of container (in.)	Distance of center of gravity from rear of container (in.)	Stability factor
1932	1.50	2.70	2.3
1936	1.44	2.66	4.9
1938	1.37	2.61	4.8

Thus there is no difficulty in obtaining sufficient stability for deformable projectiles without undue sacrifice of muzzle velocity or ballistic coefficient.

8.3.7 Stability of Sabot-Projectiles[14,42]

As before, we begin by comparing the stability factors of a standard full caliber projectile and a scaled-down sabot-projectile. Using subscripts 1 and 2 to refer to the sabot-projectile and the full-caliber projectile, respectively, equations (15) and (17) are again applicable. Suppose the projectiles have densities λ_1 and λ_2; then $A_1A_2 = \lambda_1 D_1^5/\lambda_2 D_2^5 = B_1/B_2$. In the present case, $N_1/U_1 = N_2/U_2$, both being equal to $2\pi/\eta D_2$ where η calibers per turn is the pitch of the rifling. Hence

$$\frac{s_1}{s_2} = \frac{\lambda_1}{\lambda_2}\left(\frac{A_0}{A_1}\right)^2\left(\frac{D_1}{D_2}\right)^2. \tag{20}$$

[redacted]

[g] Compare Chapter 30. In that chapter the adjective "skirted" is used rather than "deformable."

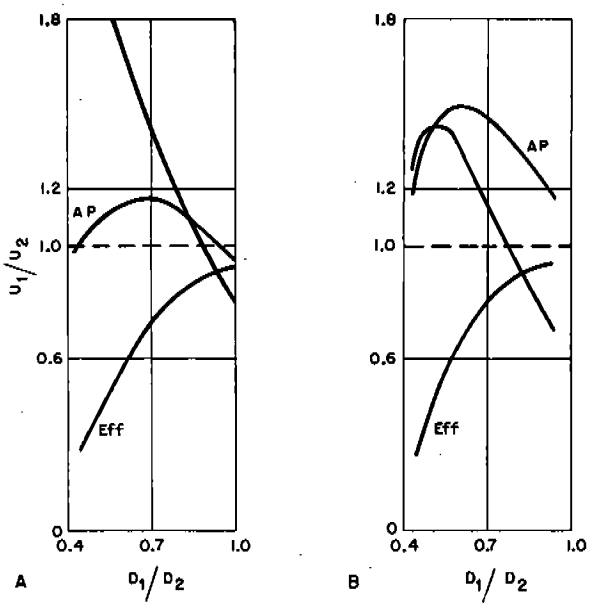


FIGURE 6. The ratios of muzzle velocities (U_1/U_2), armor penetration (AP), and efficiency (proportion of work done by powder which goes into projectile) relative to the standard, as functions of D_1/D_2, for (A) a steel sabot-projectile and (B) a tungsten carbide sabot-projectile. (This figure is based on Figures 3(a) and 4(a) of NDRC Report A-88.)

If the densities are the same, the requirement of stability imposes a severe limitation on the reduction D_1/D_2, particularly since sabot-projectiles tend to have appreciable initial yaws, and hence should have stability factors of at least 1.5. This difficulty can be overcome in part by choosing a standard projectile with a high stability factor s_2 for a model, and by increasing the density.

The validity of equation (20) is confirmed by some firings of 75/57 mm and 75/40 mm projectiles,[42,100] in which, however, the subcaliber projectile was simply a standard projectile of lower caliber, and thus was not designed for optimum results.

To explore the possibilities more fully, calculations were undertaken[14] to determine the best scaled-down projectile to be used in the 37-mm cannon for sabot-projectiles made of (1) steel and (2) tungsten carbide (for which λ_1/λ_2 is nearly 2). In each case, the value of the scaling-down ratio D_1/D_2 was chosen to give the greatest armor penetration at point-blank range consistent with a stability factor of at least 1.5. Since the stability factor of the standard AP shot in this gun is 3.0, equation (20) shows that D_1/D_2 cannot be less than $1/\sqrt{2} = 0.71$ in case (1), nor less than $\frac{1}{2}$ in case (2). The analysis leads to the results exhibited in Figure 6, which shows that these ratios are in fact almost exactly those that give maximum penetration.

The effect of modifying the body length of the projectile was also considered, with the final result that the sabot-projectiles giving optimum armor penetration in the 37-mm cannon were found to be as follows:

1. Sabot-projectiles of steel should be scaled down from the standard 37-mm AP projectile in the ratio $D_1/D_2 = 0.7$; thus the subcaliber is 26 mm. The proportions of the projectile are then about the same as those of the standard, except that the body is 10 per cent shorter. The muzzle velocity is 40 per cent higher than that of the standard, and the armor penetration is increased by 18 per cent. The ballistic coefficient is lower than that of the standard projectile; thus the improvement applies only to short ranges.

2. Sabot-projectiles of tungsten carbide should be scaled down from the standard 37-mm AP projectile in the ratio $D_1/D_2 = 0.5$. The proportions are the same as for standard projectiles; the muzzle velocity is increased by 33 per cent, and the armor penetration by 50 per cent. Furthermore, the ballistic coefficient is the same as that of the standard projectile, so that the reduction in time of flight, and the gain in velocity and armor penetration apply throughout the trajectory. If tungsten carbide is used merely in the form of a core, the results are intermediate.

8.4 MOTION OF A SLIGHTLY YAWING CONE MOVING AT SUPERSONIC SPEEDS[h]

8.4.1 Idealization

A purely theoretical determination of the effects produced upon the flight of a projectile by yaw was carried out in a case which, while necessarily idealized, is sufficiently close to actuality to be useful. This is the case in which the projectile has a conical head. The theory determines with exactness the air flow past the conical head, and the forces on the head. It then can be applied to give estimates of the forces on the entire conical-headed projectile. While the results do not apply exactly to the ogival-headed projectiles used in service, they indicate the way in which the moment coefficient (and thus the stability) of an actual projectile can be expected to vary with varying ogive lengths and velocities. They also pave the way for an eventual complete theoretical study of projectile aerodynamics.

[h] This section is based on NDRC Report A-358.[68]

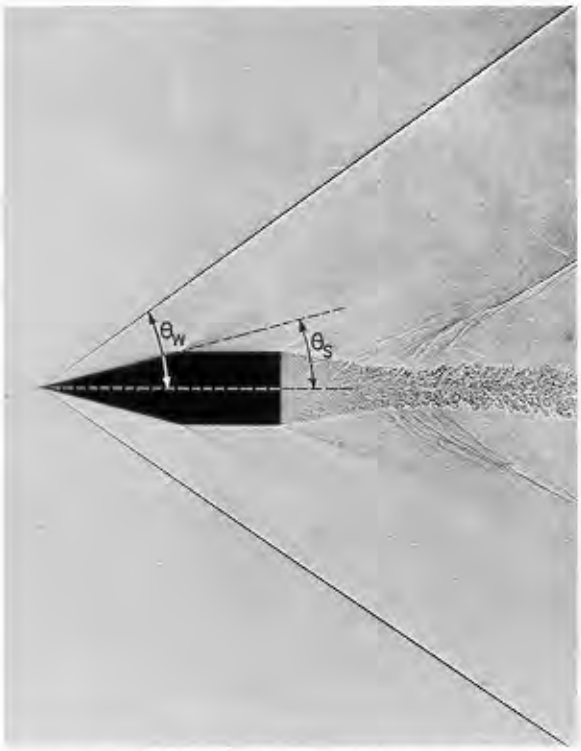


FIGURE 7. The conical shock wave set up in air by a 20-mm projectile in flight, velocity 2,112 fps. (Photograph by courtesy of Ballistic Research Laboratory, Aberdeen Proving Ground.)

The mathematical problem is simplified by noting that the air flow in the neighborhood of the conical head is the same as if the cone were to extend to infinity. This is because at the speeds considered, the alterations in the flow that are produced by altering the length of the projectile cannot "catch up" to the head.

8.4.2 Nonyaw Theory

If the conical-headed projectile (which may for the present purposes be regarded as an infinite circular cone) has zero yaw, the mathematical solution has been known for some years.[437,438,495] At supersonic speeds, a shock wave travels ahead of the cone. If the semiangle of the cone, denoted by θ_s, is not too large (the upper limit being about 56 degrees) and the velocity U of the cone is somewhat larger than the velocity a_1 of sound (the limit depending upon θ_s, if $\theta_s = 15$ degrees, U/a_1 should be greater than 1.2), the shock wave is also conical, and is attached to the projectile at the vertex (see Figure 7). The semi-angle of the shock-wave cone is denoted by θ_w.

An important feature of the flow of air relative to the projectile is that it is "conical." This means that, besides being symmetric about the axis of revolution of the projectile, the air velocity components, (such as the pressure and density) are the same at all points on any one ray through the vertex. The flow relative to the projectile is also steady, since only a short portion of the trajectory is being considered, so that the changes in magnitude and direction of U can be disregarded.

In the papers of Taylor and Maccoll,[437,438] the pressure (and hence the drag) on the conical head, the velocity components of the flow, and the shock angle θ_w, have been determined as functions of θ_s and the Mach number U/a_1 in excellent agreement with experiment.

8.4.3 Yaw Theory

If the projectile in flight yaws through a small angle ϵ, the conical shock wave will also yaw, although through a different angle δ. It can be proved[68] that it is otherwise unaltered, that is, it remains a circular cone of semi-angle θ_w, attached to the vertex of the conical head. (See Figure 8.) The flow, as before considered relative to the projectile, is no longer symmetrical but one can still assume that the flow is steady, and that it is the same at all points on any one ray through the vertex.

The problem is now one of the steady flow of a compressible ideal gas. The lack of axial symmetry presents the following complications: (1) there is no velocity potential, that is, the flow is not "irrotational"; (2) the entropy change produced by the shock surface varies from streamline to streamline because of the ack of symmetry, that is, the flow is not "isentropic";

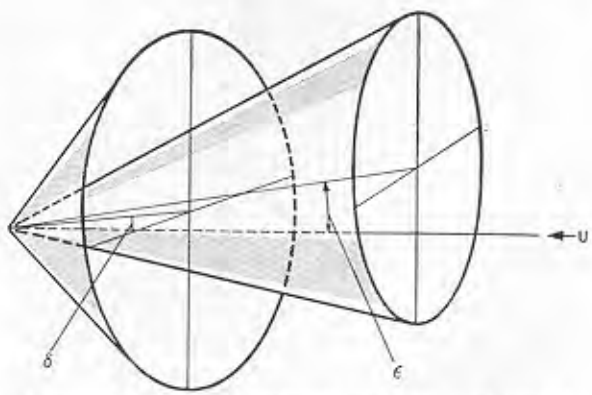


FIGURE 8. Yaw ϵ of projectile and yaw δ of conical shock wave.

CONFIDENTIAL

and (3) at ballistic speeds the entropy variations and the rotation of the flow are small, but they may become appreciable at hypervelocities.

The method adopted is to regard the flow as differing from the nonyaw flow only by a small "perturbation." Products of the perturbation terms are neglected; this amounts to assuming that ϵ^2 (the square of the yaw, measured in radians), can be neglected, or that ϵ does not exceed (say) 5 degrees. A number of cruder approximate[i] treatments have been suggested,[47,434,445,485,494] some applicable to arbitrary slender bodies of revolution; however, they do not a priori seem accurate enough for the present purpose.

Without entering into details, the method can be described as follows. The air is considered to move with velocity U relative to the stationary cone. Spherical coordinates (r,θ,ϕ) are used as indicated in Figure 9. The velocity components of the air relative to the

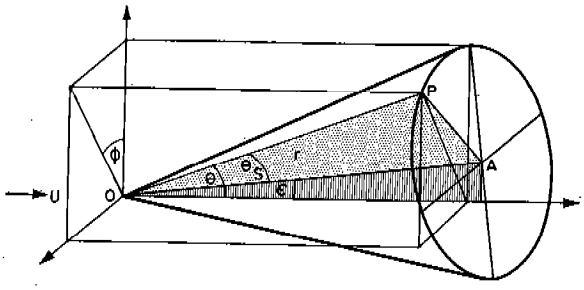


FIGURE 9. Coordinates used to describe the motion of a supersonic cone having a slight yaw ϵ. (This figure has appeared as Figure 2 of NDRC Report A-358.)

conical head in the directions of increasing r, θ, and ϕ, respectively, are denoted by u,v,w. The air density at the point (r,θ,ϕ) is denoted by ρ, and the pressure by p. The nonyaw values of these quantities are indicated by barred letters $\bar{u}$, $\bar{v}$, etc.; from symmetry, $\bar{w} = 0$. The differences, such as $u-\bar{u}$, can be expanded as Fourier series in ϕ. It is found that only the "first harmonics" are significant, and that one can write (for the flow between the shock wave and the conical head)

$$u = \bar{u} + \epsilon x \cos\phi, \quad v = \bar{v} + \epsilon y \cos\phi, \quad w = \epsilon z \sin\phi,$$
$$p = \bar{p} + \epsilon\eta \cos\phi, \quad \rho = \bar{\rho} + \epsilon\xi \cos\phi, \qquad (21)$$

where x, y, z, η, ξ are (for given θ_s and Mach number) unknown functions of θ only.

Five linear differential equations for these five unknowns are obtained (neglecting ϵ^2) from Newton's equations of motion, the "equation of continuity" (expressing the conservation of mass), and the requirement that the flow, once past the shock wave, must be adiabatic—that is, $p/\rho\gamma$ (where γ is the ratio of the specific heats) must be constant for each air particle, although it varies from particle to particle because of the variation in entropy. These equations can be greatly simplified since various combinations of the unknowns can be integrated exactly; and one finally obtains a linear second order differential equation for x/d as a function of θ, d being an unknown constant. When the conditions at the shock wave are introduced into the standard Rankine-Hugoniot equations, the values of x/d and $d(x/d)/d\theta$ when $\theta = \theta_w$, can be derived from the resulting equations. The quantity x/d is now determined; and the values of d, x, and all the other unknowns are settled by the final requirement that the flow must be tangential to the conical head.

8.4.4 Experimental Verification

A valuable check on the theory is provided by the fact that it determines the ratio δ/ϵ of the shock yaw to the projectile yaw. Thanks to the cooperation of the Ballistic Research Laboratory of Aberdeen Proving Ground, this ratio was computed in one case ($\theta_s = 15$ degrees, $U/a_1 = 1.901$) and compared with the actual values as shown by measurements of spark photographs (Figure 7) of conical-headed projectiles in flight. The results are shown in Figure 10.[j] Since the departures from the theoretical line are all within experimental error, the agreement is satisfactory.

A further check is given by the fact that theoretically the yaw should be independent of the shock angle θ_w. This also holds within experimental error, but it is less conclusive since θ_w is rather sensitive to variations in Mach number in this range and is hard to measure exactly.

8.4.5 Normal Force and Center of Pressure

From the theory, also the forces on the conical head can be calculated. The force on the head normal to the projectile axis, say L_H, is expressible as

$$L_H = \rho K_{NH} D^2 U^2, \qquad (22)$$

[i] A closer analysis shows that the results are substantially valid if only ϵ^3 is negligible.[111] The results should thus apply for yaws up to 10 degrees.

[j] The values given for δ and ϵ are, strictly, not δ and ϵ but their projections on the plane of the photographic plate. However, it can be shown that the projections have the same ratio as δ and ϵ, so the comparison still is valid.

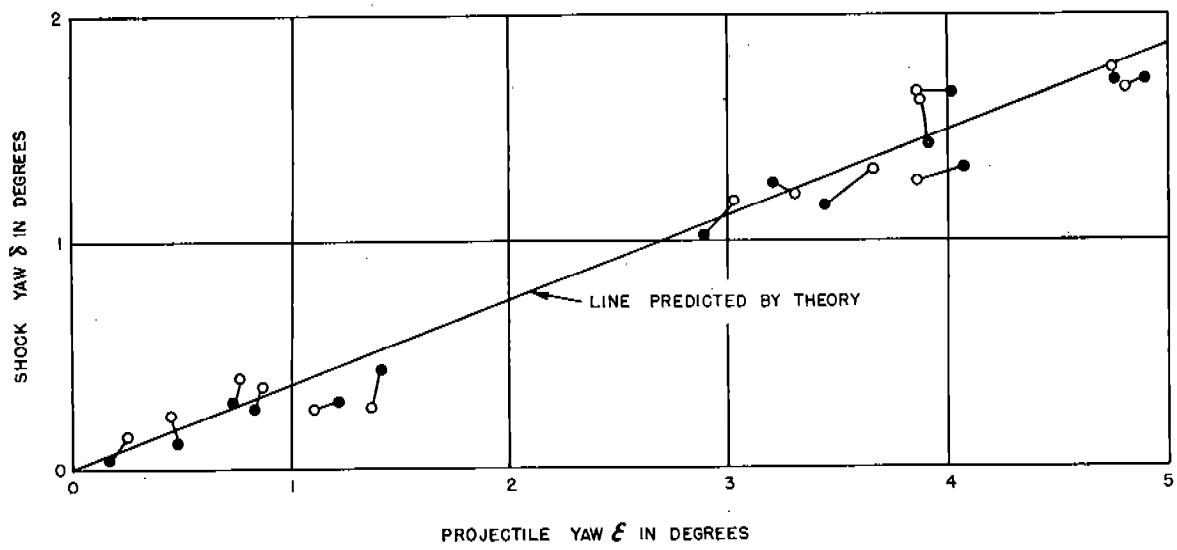


FIGURE 10. Ratio of shock yaw to projectile yaw, for $\theta_s = 15°$ and $U/a_1 = 1.9$. The yaw on each photographic plate is represented by ○——●, where ○ and ● are the values read by two observers. (This figure is used by courtesy of Ballistic Research Laboratory, Aberdeen Proving Ground.)

where K_{NH}, the contribution of the head to the total normal force L, is determined by

$$K_{NH} = -\frac{\pi}{8}\cot\theta\left[\bar{u}x + \frac{d}{2\gamma}(c^2 - \bar{u}^2)\right]\bar{\rho}/\rho U^2, \qquad (23)$$

evaluated with $\theta = \theta_s$. Here γ is the ratio of specific heats ($= 1.405$), $c^2 = U^2 + 2a_1^2/(\gamma - 1)$, and ρ is the density of the stationary air.

This normal force L_H acts at a "center of head pressure" at a distance $\frac{2}{3}l \sec^2\theta_s$ from the vertex, where l is the perpendicular distance from the vertex to the base of the conical head (see Figure 11).

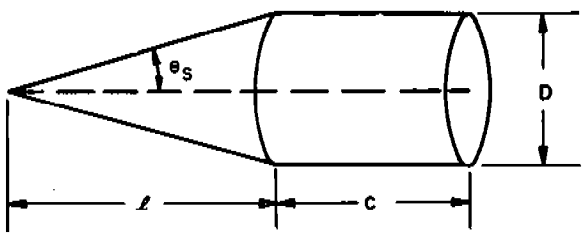


FIGURE 11. Idealized conical-headed projectile. (This figure is based on Figure 4 of NDRC Report A-358.)

The axial drag on the head is also determined from the present theory. It is, however, the same as in the nonyaw theory of Taylor and Maccoll,[437] since the change produced in it by the yaw, though significant, is proportional to ϵ^2. Its determination is discussed in the next section.

Estimates can now be made of the normal force, center of pressure, and overturning moment for the entire projectile. For this purpose the simplest assumptions are made: namely (a) the projectile has a cylindrical body of length c (see Figure 11), (b) the pressure on its base is zero (which is very nearly the case at high velocities), and (c) the perturbation in the pressure produced by the yaw is assumed to vary linearly along the cylindrical body. The resulting estimates can be improved when more accurate knowledge of the air flow along the body of the projectile becomes available. It is found that, approximately,

$$K_N \doteq K_{NH}\left(1 + \frac{c}{l}\right); \qquad (24)$$

that the distance from the vertex to the center of pressure is approximately

$$j \doteq \tfrac{1}{3}(2l + c) + \frac{D^2}{6(l + c)}, \qquad (25)$$

(in which the last term is usually negligible); and, finally, that the overturning moment coefficient K_M, if the projectile is homogenous (in particular, with no windshield), is roughly given by equation (26)

$$K_M \doteq K_{NH}\left(\frac{l + 2c}{12D} + \frac{cl}{4D(l + 3c)}\right)\left(1 + \frac{c}{l}\right). \qquad (26)$$

Equation (25) for the center of pressure is compared in Table 3 with experimental values for conical-headed 3.3-in. shells,[177] excluding shell types for which the values are uncertain. There is agreement to within a

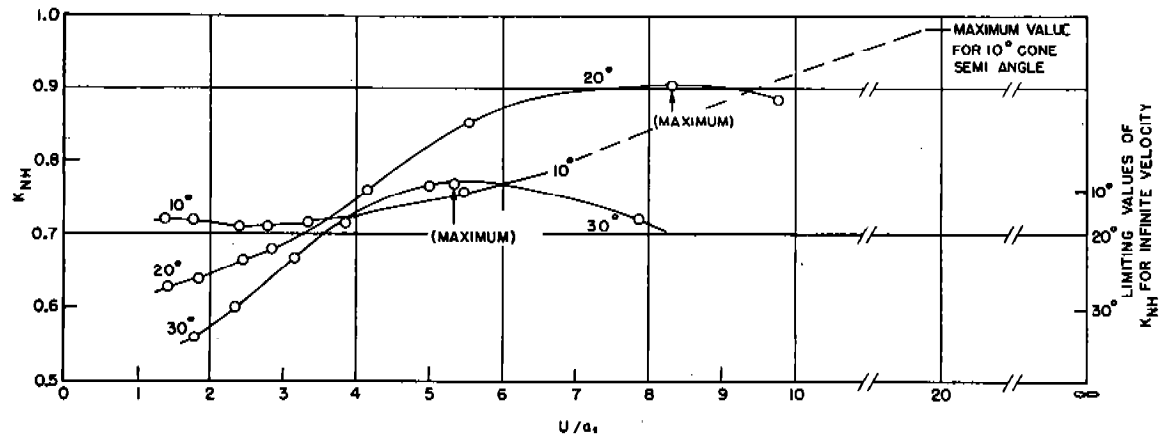


FIGURE 12. Normal head force coefficient K_{NH} for projectiles with conical heads having various cone semi-angles, as a function of the Mach number U/a_1.

TABLE 3. Comparison of estimated and experimental positions of center of pressure. (3.3-in. conical-headed shells: j = distance from vertex of cone to center of pressure. All distances measured in calibers.)

Shell type	l	L	Experimental j	Estimated j	Discrepancy
111	3.26	2.49	2.68	3.03	+0.35
112	3.26	2.49	3.05	3.03	−0.02
123	3.56	2.49	3.30	3.23	−0.07
125	3.26	1.49	3.10	2.71	−0.39
168	2.58	1.76	2.25	2.31	+0.06
169	2.94	1.76	2.72	2.59	−0.13

probable error of 0.15 calibers, which is not unreasonable in view of the experimental errors and the roughness of the estimate leading to equation (25). It should be noted that all but the last two shell types in Table 3 had varying amounts of boat-tail, the effect of which is apparently considerable, though it has been neglected in making the estimate.

8.4.6 Values of K_{NH} and δ/ϵ

The values[k] of the normal head force coefficient K_{NH} and yaw ratio δ/ϵ are shown for various cone semi-angles θ_s as functions of the Mach number U/a_1 in Figures 12 and 13. From equation (26), K_M should vary with the velocity in roughly the same way as K_{NH} for a given conical-headed projectile; thus Figure 12 indicates roughly how the moment coefficient K_M may be expected to vary with the velocity for supersonic projectiles in general. It should be remarked that there are *two* values of K_{NH} and δ/ϵ theoretically possible for each velocity. This is because the Taylor-Maccoll nonyaw theory shows that *two* regimes are theoretically possible in the nonyaw case, having different values of θ_w, and leading to different drags on the conical head; however, only *one* of them is observed in actual firings. The other possibility (not shown in Figures 12 and 13) was long believed to represent an unstable condition of the projectile, but it recently has been observed in carefully controlled wind-tunnel experiments. The present theory provides a partial explanation. It is found that the yaw ratio δ/ϵ (and also K_N) is large in the second nonyaw regime, so that the yaw always present in projectiles as fired would lead to impossibly large shock-wave yaws. This shows that the second regime, though stable for very small yaws, is unstable for the yaws that occur in ballistic practice.

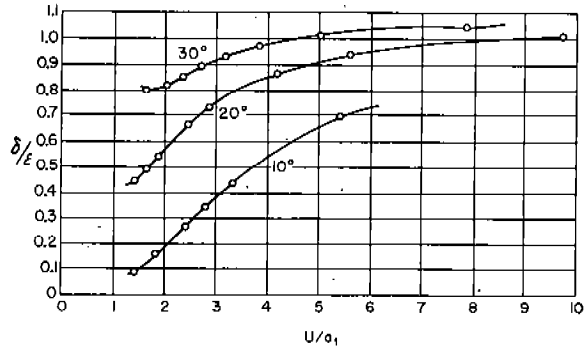


FIGURE 13. Ratio of shock-wave yaw δ to projectile yaw ϵ for projectiles with conical heads having various semi-cone angles, as a function of the Mach number U/a_1. See Figure 8 for a representation of the two angles.

[k] These values are based on extensive computations on this theory that have been carried out recently by the Department of Electrical Engineering of Massachusetts Institute of Technology, under the auspices of the Navy Department.[331]

As pointed out above, Figure 12 shows in a general way how the moment coefficient K_M may be expected to vary with the velocity for pointed projectiles in general although experimental observations are needed to verify these relations. Figure 13 reveals the interesting feature that at extremely high speeds the shock yaw δ becomes larger than the projectile yaw ϵ. Calculations show that the limiting values of δ/ϵ (approached as the speed becomes infinite) are: 1.06 for $\theta_s = 10$ degrees, 1.07 for $\theta_s = 20$ degrees, and 1.08 for $\theta_s = 30$ degrees.

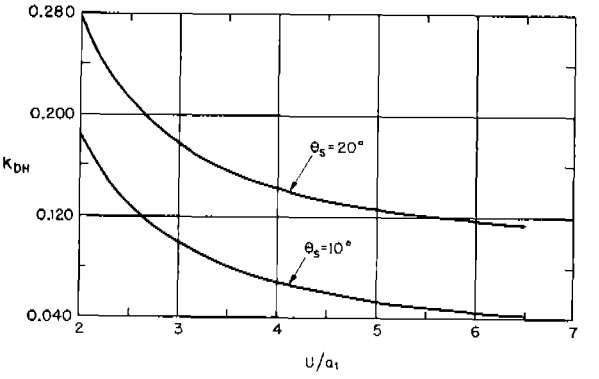


FIGURE 14. The head drag coefficient K_{DH}, as a function of the Mach number U/a_1, according to the approximate theory. (This figure has appeared as Figure 3 in NDRC Report A-126 where the coefficient was designated as K_D.)

8.5 THE DRAG COEFFICIENT FOR A CONE MOVING WITH HIGH VELOCITY

8.5.1 Simplification of Nonyaw Theory

As has been noted in Section 8.4, the theory of Taylor and Maccoll determines the air flow in the neighborhood of the head of a projectile, if the head is conical and the yaw is zero. It does not, however, lead to explicit formulas for the velocity components $(\bar{u},\bar{v})$ of the flow, or for the drag on the head of the projectile, etc.; and such explicit formulas would be convenient for both practical and theoretical purposes. A simplified approximate treatment was devised which achieves such explicit formulas.[1] The differential equation of Taylor and Maccoll is replaced by an approximate equation that can be solved explicitly. This is done by disregarding the variation in air density in the flow behind the shock. In this way it is found that

$$\bar{u}/\bar{u}_s = \sin^2\theta_s + \cos\theta_s\cos\theta + \sin^2\theta_s\cos\theta\ln\frac{\tan 1/2\theta}{\tan 1/2\theta_s}, \qquad (27)$$

(where $\bar{u}_s$ denotes the value of $\bar{u}$ for $\theta = \theta_s$) with similar formulas for $\bar{v}$, etc. The drag on the conical head can be expressed as

$$\rho K_{DH} D^2 U^2 \qquad (28)$$

and K_{DH} is likewise determined approximately. Its values, for varying Mach numbers U/a_1, are shown for two cone semi-angles ($\theta_s = 10$, 20 degrees) in Figure 14.

Theoretical estimates of the error produced by this approximation show that $\bar{u}$ and K_{DH} should be accurate to within 1 percent for Mach numbers of over 2.5 and cone angles of 10 degrees or over, and the accuracy is much greater for large Mach numbers. However, the approximations to $\bar{v}$ and θ_w will be less accurate, as confirmed by numerical calculation.

It is known that,[189,555] roughly,

$$K_D = 3K_{DH}, \qquad (29)$$

where K_D is the drag coefficient for the entire projectile. In this way K_D can be estimated, using Figure 14, for velocities higher than those for which direct experimental determinations have been carried out.

8.5.2 Effect of Yaw[111]

The theoretical evaluation of the extent to which the yaw of a conical-headed projectile increases the drag on the head is in principle similar to the determination of the other yaw effects described in Section 8.4. It is necessary, as shown there, to consider the second approximation on the assumption that the first approximation is now known. It can be shown that the desired second approximation (now neglecting ϵ^3, where ϵ is the yaw in radians) is expressible in the form

$$\begin{aligned} u &= \bar{u} + \epsilon x\cos\phi + \epsilon^2(u_0 + u_2\cos 2\phi),\\ v &= \bar{v} + \epsilon y\cos\phi + \epsilon^2(v_0 + v_2\cos 2\phi),\\ w &= \epsilon z\sin\phi + \epsilon^2 w_2\sin 2\phi,\\ p &= \bar{p} + \epsilon\eta\cos\phi + \epsilon^2(p_0 + p_2\cos 2\phi),\\ \rho &= \bar{\rho} + \epsilon\xi\cos\phi + \epsilon^2(\rho_0 + \rho_2\cos 2\phi), \end{aligned} \qquad (30)$$

where the ten unknowns u_0, u_2, etc., are functions of θ alone for given θ_s and U/a_1. For the determination of the drag, only the unknowns with subscript 0 need to be considered. The equations connecting them are de-

[1] Slight changes in the notation used in NDRC Report A-126[25] have been made in the present summary.

rived and simplified in essentially the same way as before (in the first approximation). Two complications arise, however. First, the equations, though of the same general character as before, are decidedly more complicated. Second, several of the unknowns apparently become infinite when $\theta = \theta_s$. This is because in these equations $\epsilon^3/\bar{v}$ is neglected rather than ϵ^3, and since $\bar{v} = 0$ when $\theta = \theta_s$, the equations are no longer valid approximations for values of θ close to θ_s. Fortunately the unknown (p_0) needed for the effect of yaw on the drag is not affected in this way. Finally, it is shown that the drag on the head of the projectile (i.e., the component of the air resistance *along the trajectory*, rather than along the axis of the projectile) is expressible as

$$K_{DH}(1 + K_{DYH}\epsilon^2)\rho D^2 U^2, \tag{31}$$

where ρ is the free air density and K_{DYH}, the "head-yaw drag coefficient," is expressed in terms of the solutions of two linear second order differential equations with simple boundary conditions but with complicated coefficients.[111]

8.5.3 Estimate for Entire Conical-Headed Projectile

Using the idealized projectile shown in Figure 11, it is assumed (for a rough approximation) that the yaw does not appreciably change either the pressure on the base (which is nearly zero, in any case, at high velocities) or the skin friction. From equation (31), it now follows that the *total* drag on the conical-headed projectile is expressible as

$$K_D(1 + K_{DY}\epsilon^2)\rho D^2 U^2, \tag{32}$$

where K_{DY}, the "yaw drag coefficient" (often also denoted by $K_D\delta^2$) is given roughly by

$$K_D \doteqdot \frac{1}{3}\left(K_{DYH} + \frac{\eta_s}{\bar{p}_s}\,\frac{c}{D}\right), \tag{33}$$

where c/D is the length of the projectile, exclusive of head, in calibers, and η_s and $\bar{p}_s$ denote the values of η and $\bar{p}$ when $\theta = \theta_s$ (known from the first approximation considered in Section 8.4).

The computation of K_{DYH} in a typical case ($\theta_s = 15$ degrees, $U/a_1 = 1.954$) has been undertaken by the Department of Electrical Engineering at Massachusetts Institute of Technology, under the auspices of the Bureau of Ordnance, Navy Department. As reported, it is known[509] that for standard projectiles $K_{DY} \doteqdot 20$.

8.5.4 Suggestions for Further Research

Different Head Shapes

It would be very desirable to have a theoretical study of more realistic head shapes than the conical. Progress has been made in this direction under the auspices of the Armed Forces. One method[332] is based on the fact that *any* pointed ogive can be closely approximated by a cone in the neighborhood of its tip, and the airflow past the ogive is derived as a perturbation from the theoretical flow past the cone. This seems to give a good approximation to the flow around part, at least, of the ogive. Another proposed method[202] is to start with a plausible shape for the shock wave (which is hard to predict exactly for ogives other than conical) and then determine the ogive that would give this shock wave, and the resulting airflow. By repeating this computation with several shock-wave shapes, the flow for a given ogive could be obtained by interpolation. The computations are necessarily laborious, since now *partial* differential equations must be solved.

Drag Function

Once the flow around the head of a (nonyawing) projectile has been determined, it is possible, in principle, to extend the calculations to give the flow around the body of the projectile. If this is practicable, it would enable the drag function of the projectile to be calculated by theory alone, long a dream of ballisticians. As mentioned in Section 8.4.3, the approximate methods previously published do not seem to be sufficiently precise. Grave difficulties would have to be overcome (particularly in view of the boundary-layer effect and turbulence), and a combination of theoretical and experimental work may be the most effective.

Stability Factor

It should be possible to extend the determination of the effects of yaw on the flow, which has been carried out for conical heads, to general ogives or even to the entire projectile. The stability factor of a projectile would then be predictable by theory alone, with obvious advantages to the projectile designer.

Other Aerodynamic Coefficients

Finally, it may be possible to calculate the effects produced by other features of the air resistance (involving the "yawing moment due to yawing," the



Magnus effect, etc.) on the flow past a cone, an ogive, or even the complete projectile. A major difficulty here is that the airflow (relative to the projectile) could no longer be regarded as steady, but if this problem can be solved, the more recondite aerodynamic coefficients (which are difficult to measure) would be determined, and such things as the drift of the projectile and the rate of damping of its yaw, would be predictable.

Effect of Higher Powers of Yaw

It seems neither desirable nor practicable to repeat the method of successive approximations to take into account the effects produced by higher powers of the yaw. These effects are small in practice; and, moreover, the method would probably break down on account of the infinities introduced by the method of approximation. If the way in which K_N (say) varies with the yaw were desired theoretically, the nonlinearity of the fundamental differential equations would have to be faced.

8.6 TRAJECTORY DETERMINATION BY TRACER PHOTOGRAPHY[m]

8.6.1 General Method

A simple and convenient method of obtaining ballistic data from firings was developed at the University of New Mexico, the original purpose being to investigate the relatively unexplored hypervelocity region. The method, however, is of general applicability as far as velocity is concerned, but is limited to projectiles equipped with tracers. The tracer projectile is photographed in flight at night, using an ordinary (still) camera. A vibrating "chopper" in front of the open lens provides an automatic time scale, and the resulting photograph gives the complete trajectory and enough data to compute the velocities, retardations, and ballistic coefficient of the projectile.

8.6.2 Experimental Details

The setup is illustrated in Figure 15, which is not drawn to scale. The projectile is fired from the gun G in a vertical plane through the horizontal line MNQ. Lights are placed at fixed points M and N, to provide

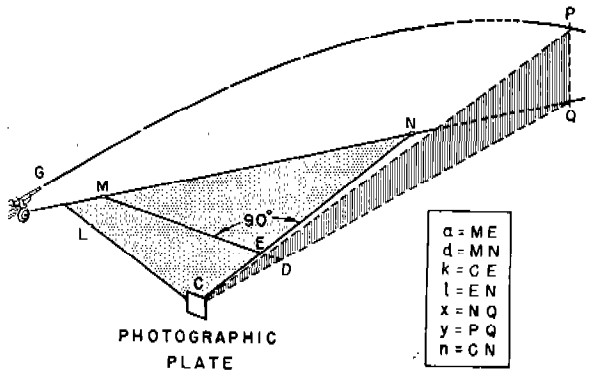


FIGURE 15. Setup for trajectory determination by tracer photography. (This figure is a perspective interpretation based on Figures 3 and 4 of NDRC Report A-283.)

reference points on the photographic image. The camera and chopper are set up at C, with the plane of the photographic plate perpendicular to a vertical plane through the line CN. The plane $CQNM$ is horizontal and CQP is vertical. A third light at L, placed near G in the plane $CQNM$, provides an additional reference point and enables the beginning of the trajectory to be located precisely. The chopper is set vibrating just before the gun is fired, each period of the chopper giving two occlusions of the image.

The camera lens should have as flat a field as possible, although it is possible to correct for a moderate amount of distortion. The chopper used was simple, consisting essentially of a weighted spring anchored to a heavy block; but it worked very well, its period (0.0936 sec) varying by less than 0.2 per cent with temperature (from -2 C to $+27$ C) and amplitude. The chopper and camera were mounted separately, to avoid transmitting vibrations to the camera. With the layout chosen, ranges up to 2,500 yd were photographed; but ranges several times greater could be used with proper choice of lens, chopper, and geometry. The errors can be made negligible for low-angle fire and high accuracy can be obtained by introducing extra lights marking reference points; but in high-angle fire it is difficult to correct for lens distortion, although this error is not serious with a good lens. In designing the layout, it should be borne in mind that many tracers do not reach full brilliance until nearly ¼ sec after leaving the gun.

8.6.3 Reduction of the Experimental Data

The coordinates x and y (see Figure 15) of the position P of the projectile corresponding to a point P' of the photographic image (see Figure 16) are found to

[m] This section is based on NDRC Report A-283,[57] which should be consulted for complete details of the method and for a discussion of the possible sources of error.

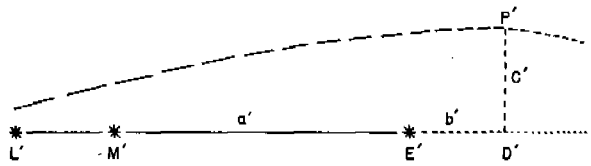


FIGURE 16. Measurements on the photographic plate in trajectory determination by tracer photography. (This figure is based on Figure 5 of NDRC Report A-283.)

be given by

$$x = \frac{nd}{\frac{a'}{b'}k - l}; \quad y = \frac{na}{\frac{a'}{b'}k - l} \cdot \frac{c'}{b'}. \tag{34}$$

The distances a, d, k, l, and n are identified in Figure 15, and the lengths a', b', and c' are shown in Figure 16. In that figure L', M' and E' are the images of the three lights at L, M, and N which define the baseline. The point D' is obtained for successive positions along the trajectory by dropping a perpendicular from P' to the baseline. The horizontal range R is then $x + GN$, and the vertical height Y of P above G is obtained by subtracting from y the height of G above the line MN.

In practice, the positions chosen for P' are the ends of the intervals into which the trajectory is divided by the chopper. To smooth the results, these points are grouped into fours (each four corresponding to a complete oscillation of the chopper so that the successive groups are accurately timed), and for every group of four the values of R and Y are averaged and taken to correspond to the average time. These average values of R and Y are then plotted, and the smooth curve, upon which the points are found to lie with remarkable precision, gives the trajectory. (See Figure 17.)

To determine with accuracy the velocity as a function of the time, some smoothing process must be employed. The adopted procedure, which works well for low-angle short-range trajectories, is to begin by drawing an accurate time-distance curve based on the trajectory record of Figure 17, the distance traveled being taken equal to R, to a sufficient approximation. From this curve, the average velocity over each chopper period is calculated. These average velocities are plotted against the time, and the resulting points should lie close to, but by no means on, a smooth curve. A smooth curve is drawn close to these points, and is checked by comparing the areas under it with the ordinates of the R, t-curve, since

$$\int_{t_1}^{t_2} U dt = R_2 - R_1.$$

The curve is then adjusted until the agreement is sufficiently close, and then it constitutes an acceptable U, t-curve.

The procedure can be repeated to give an r, t-curve (where r is the retardation) or an r, U-curve, using the fact that

$$\int_{u_1}^{u_2} dU/r = t_2 - t_1.$$

In this way the law of resistance for the projectile can be established, and its ballistic coefficient can be determined.

This method of determining the resistance function has an advantage over the customary chronograph methods, since one firing here covers a range of velocities, so that comparatively few firings at different muzzle velocities cover the whole velocity range desired.

It is estimated that, over a 2,000-yd segment of trajectory, the position-versus-time data are accurate to within less than ± 1 per cent, and the velocities are accurate to within ± 2 per cent. The retardations

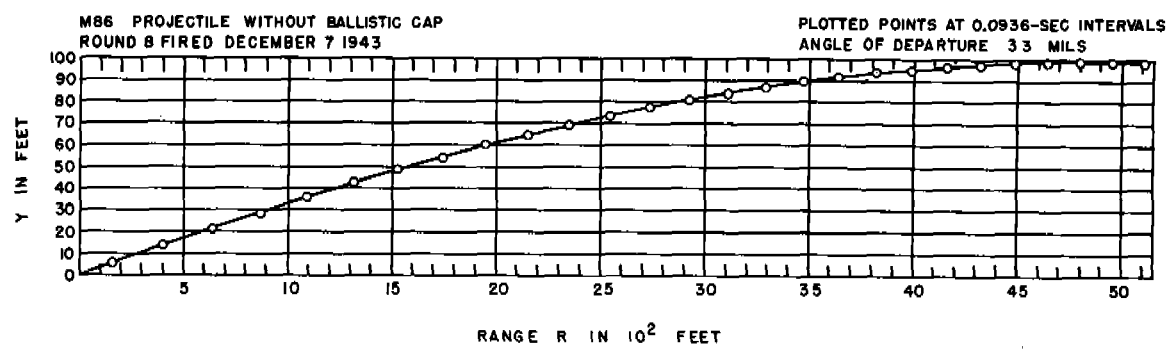


FIGURE 17. A trajectory determined by tracer photography. (This figure has appeared as Figure 6 of NDRC Report A-283.)



are less accurate, because of the necessary differentiations. Longer trajectories could be covered by using a number of cameras disposed along the trajectory so as to record successive segments. The accuracy could be increased at the cost of making the setup more elaborate.

6.7 FIRINGS OF CALIBER .50 PROJECTILES

To investigate the effects of changes in details of the design on the ballistic coefficient and the stability factor, an extensive series of firings of caliber .50 bullets was carried out through the cooperation of Aberdeen Proving Ground in connection with an investigation of pre-engraved projectiles.[n] The results are analyzed in detail in Section 27.3. In brief, it may be noted here that:

1. The various changes made in number, position, shape and width of rotating bands, in radius of ogive, and in boat-tailing (but without greatly affecting the overall proportions of the projectiles), altered the moment coefficient K_M very little, but had significant effects upon the drag.[211] Thus, roughly speaking, once the proportions and balance of the projectile are such that it is adequately stable, other changes in the design do not greatly change the stability factor, and hence can be aimed solely at reducing the drag.

2. Abrupt leading edges of the rotating band, or wider or double bands, and similar features increase the drag; a boat-tail reduces the drag, even at hypervelocity.

3. Features, such as double rotating bands, that decrease the yaw in the gun are very effective in keeping the external yaws small, even if the stability factor is decreased.

[n] This general investigation was carried out by Division 1 at the Franklin Institute. See Chapter 31.



Chapter 9

TERMINAL BALLISTICS OF HYPERVELOCITY PROJECTILES

By *H. S. Roberts*[a] and *Walker Bleakney*[b]

9.1 DISRUPTION OF A LIQUID BY A HYPERVELOCITY PROJECTILE[c]

9.1.1 Introduction

The interest of Division 1 in the problem of the disruption of a liquid by a hypervelocity projectile was aroused by a British report[126] concerning the effects produced when a 20-mm projectile, having a muzzle velocity of about 4,550 fps, penetrated a self-sealing gasoline tank, half filled with water. The tank exploded with surprising violence.[d] Since such an explosion might have considerable tactical importance, it seemed desirable to investigate the phenomena.

9.1.2 Firings into Cans of Liquid

In the initial experiments, several empty tin cans about 2½ in. in diameter and 3¾ in. high were filled with water and penetrated by bullets of different velocities. The ones used were 9.8-g bullets from a caliber .30 Springfield rifle, muzzle velocity about 2,800 fps, and 2.5-g "half hard" Phosphor bronze bullets from a caliber .22 Swift rifle, muzzle velocity about 4,200 fps. The caliber .30 bullets in some cases opened up the seams of the cans but in other cases the seams held and little damage was done except for the entrance and exit holes and a slight bulging of the sides. The caliber .22 bullets, however, invariably burst the cans tearing them not only at the seams but often elsewhere.

Since the kinetic energy of the caliber .30 bullets was nearly twice that of the caliber .22, it is evident that velocity, which was 50 per cent greater in the case of the smaller bullets, is a more important factor in disruption than is kinetic energy. Some of the cans were filled with gasoline in place of water and were fired on with the Swift rifle in the expectation that the gasoline might ignite. This did not take place and the damage was apparently the same as it would have been if the cans had been filled with water.

In a separate series of experiments automobile gasoline tanks having a capacity of 16 gal were penetrated by caliber .50 bullets weighing 49 g. Figure 1 is a photograph of one of the original tanks. Figure 2 shows the same tank after being filled with water and traversed by the caliber .50 bullet fired with a muzzle velocity of 3,500 fps. The tank exploded, that is, the disruptive impulse must have been considerably greater than was needed to split the tank and it must have been applied so suddenly that the inertia of the water prevented the first split from relieving the pressure elsewhere. Consequently cracks developed in many places and the "follow up" was sufficient to tear the tank into several pieces and to distribute most of the water over a wide area.

The experiment was repeated using half the charge of powder; the result is shown in Figure 3. This tank was torn chiefly at the seams and it remained in one piece. In both cases the 2-in.x6-in. plank on which



FIGURE 1. Automobile gasoline tank before firing.

[a] Deceased; formerly physicist, Geophysical Laboratory, Carnegie Institution of Washington. Author of section 9.1.

[b] Deputy Chief of Division 2, NDRC, and a Member of Division 1. (Present address: Department of Physics, Princeton University.) Author of Section 9.2.

[c] The experiments described in this section were performed by H. S. Roberts at the Geophysical Laboratory under Contract OEMsr-51 in 1942 and by D. T. MacRoberts and associates at the University of New Mexico under Contract OEMsr-668 in 1942 as corollaries to broader developments of hypervelocity projectiles. They were described in informal progress reports submitted by those contractors to Division 1, but have not been included in any formal reports. The experiments with caliber .50 bullets described in Section 9.1.2 and the shock-wave photographs described in Section 9.1.4 were made at the University of New Mexico, the others at the Geophysical Laboratory. The mathematical analysis presented in Section 9.1.6 is based on two memoranda prepared by W. F. G. Swann, Director of the Bartol Research Foundation of the Franklin Institute, and submitted on December 29, 1943, and February 28, 1945, to the Chief of Division 1 under Contract OEMsr-533 with the Franklin Institute.

[d] A similar phenomenon occurs when a high-velocity projectile penetrates soft animal tissue. It has just been learned that this aspect of wound ballistics was studied by the Department of Biology of Princeton University for the Division of Surgery of the Committee on Medical Research. (*Editor's note.*)

CONFIDENTIAL



FIGURE 2. Tank shown in Figure 1 after having been filled with water and traversed by a caliber .50 bullet, velocity 3,500 fps.

the tank rested was broken. A third tank, only half full of water, exploded when a full-charge bullet penetrated it at a considerable depth below the water line; but a fourth tank, also half full, failed to explode when the bullet entered at, or just below, the water line.



FIGURE 3. Tank similar to one shown in Figure 2 after having been filled with water and traversed by caliber .50 bullet fired at half powder charge.

9.1.3 Motion Pictures of Jets During Disruption

Some motion pictures were made of paper tanks fired on by the caliber .30 Springfield and by the caliber .22 Swift rifles. The tanks, which were paper bags 6 in. square, were filled with water to a depth of 5½ in. so that the volume of water was approximately a 6-in. cube. The bullet entered horizontally about the center of one face from a direction approximately parallel to the adjacent faces. The tank stood on a wooden box placed near the center of a heavy plank spanning two logs. The camera was set up about 90 degrees from the line of fire and took 16 pictures per second.

Figure 4 shows the effect of a 2.5 g caliber .22 Phosphor bronze bullet, velocity about 4,200 fps. The gun was outside the picture to the left. The half frame at the top shows the tank on the wooden box just before firing. The other three frames show most of the water being expelled in five jets, approximately normal to each of the five free faces of the cube. In the last two frames the vertical jet has reached the top of the picture, about 11 ft above the top of the tank. The pattern on the ground showed that water had been thrown about 20 ft toward the gun and about 15 ft to the sides. These lobes were nowhere more than 4 ft wide and there was no water in the 45-degree positions except quite close to the tank. A downward impulse on the bottom of the tank was shown by the fact that the resilience of the plank caused the wooden box to be thrown a foot or so upward.

The effect of a standard 9.8-g caliber .30 bullet, velocity about 2,800 fps, is shown in Figure 5. In the half frame at the top the bullet evidently struck toward the end of the exposure. There is a jet about 4 ft long directed away from the gun and some evidence of a jet starting toward the camera; but the vertical jet has not yet appeared. In the last frame the vertical jet has reached its maximum height of only 4 or 5 ft.

9.1.4 Shock Waves in Water Penetrated by a Bullet

Spark photographs were made of caliber .22 lead bullets, velocity 1,200–1,400 fps, passing through water in various glass containers. In every case the bullet entered through a paper closure at the mouth of the container and not through the glass. In Figure 6 the bullet has entered at the left and has traveled

CONFIDENTIAL



FIGURE 4. Motion picture of a paper tank penetrated by a caliber .22 bullet, velocity 4,200 fps.



FIGURE 5. Motion picture of a paper tank penetrated by a caliber .30 bullet, velocity 2,800 fps.

CONFIDENTIAL

two thirds of the way to the end of the jar. The shock wave that precedes the bullet has cracked the glass in many places but there is no evidence that the fragments have moved, except that thin sheets of water are seen emerging from the cracks at the top of the picture.

Following the bullet is a "conical" disturbance whose nature has not been determined. Its velocity of propagation in the water was estimated to be about 66 fps. The sharply defined reflecting surface of this disturbance was interpreted to indicate the presence of either a definite liquid-vapor interface or else an extremely fine emulsion.

That these phenomena do not depend on the shape of the container was shown by firings into other vessels. Figure 7 shows a spherical container not quite full of water in which the bullet has nearly reached the far wall. The glass is cracked much as it was in Figure 6, the fragments remain in place and the water level has not been disturbed. In Figure 8A taken just before firing, we have a large glass tube filled with water except for a small bubble near the right hand end. Figure 8B shows the bullet about half way through. The conical disturbance has reached the wall of the container, and glass and water are moving outward with a velocity much greater than that at which the conical disturbance was propagated. The bubble has moved a few millimeters away from the bullet.

Previously published photographs[486] of shock waves in water penetrated by a bullet showed that the shock wave will not damage a flexible tank wall but will damage a rigid one. A curved shock wave was reflected from a cellophane wall of a small tank without damage to the cellophane.



FIGURE 6. Spark photograph of a glass jar filled with water being traversed by a caliber .22 bullet, velocity 1,200–1,400 fps.



FIGURE 7. Spark photograph of a spherical glass tank not quite full of water being traversed by a caliber .22 bullet, velocity 1,200–1,400 fps.

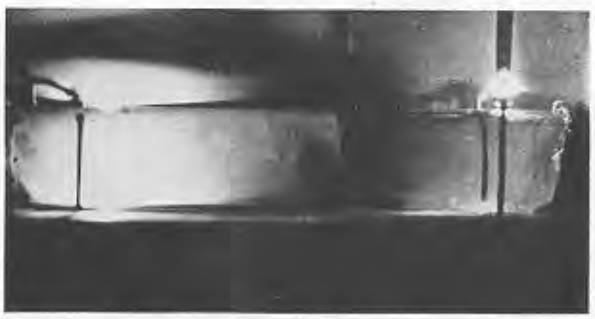


FIGURE 8A. Spark photograph of a large glass tube filled with water; before firing.



FIGURE 8B. Same tube as in Figure 8A; caliber .22 bullet part way through, velocity 1,200–1,400 fps.

CONFIDENTIAL

9.1.5

Transient Pressures in Water Penetrated by a Bullet

Measure of the Bursting Strength of a Tank

These purely qualitative experiments have shown (1) that the disruptive effect increases rapidly with the velocity of the bullet and that the velocity is a more important factor than the kinetic energy; and (2) that there are two phenomena, (a) a shock wave which originates when the bullet enters the liquid and travels with the velocity of sound (about 4,800 fps in water), and (b) a secondary disturbance of unknown nature which travels much more slowly. They show further that much more energy is associated with the secondary disturbance than with the shock wave, at least at low bullet velocities.

The ability of the container to resist disruption by a uniform pressure (such as might be applied by a pump) can be expressed either (1) as the pressure just before the tank bursts, or (2) as the work that must be done to stretch the tank to the bursting point. The latter is the better concept for our purpose because we have, in the shock wave, pressures that may be far greater than the bursting pressure of the tank but of such short duration that the work they can do may be inadequate.

We can imagine two tanks of the same size, one of glass and the other of rubber, with the wall thickness so proportioned that they will burst at the same pressure. Once the tank is filled, a single stroke of the pump might be sufficient to burst the glass tank while many strokes might be required for the rubber tank. As we have seen, the pressures we are dealing with are nonuniform. Even so, the work done on the walls, or on one wall, of a particular container should be a measure of the relative effectiveness of the same type of bullet fired at different velocities; although there is the possibility that this method may fail to indicate significant changes in pressure distribution.

Experiments with Water Ballistic Pendulum

The Pendulum. These considerations led to the construction of a water ballistic pendulum, shown in Figure 9. The body, B, of the pendulum was a 16-in. length of a worn 3-in. steel gun liner having walls about 1-in. thick. The back (right hand end in the figure) was closed by a heavy steel plate P, held on by eight ½-in. cap screws and made watertight by a rubber gasket. The front of the body was closed by a disk of tar paper held in place by the flanged nozzle N.

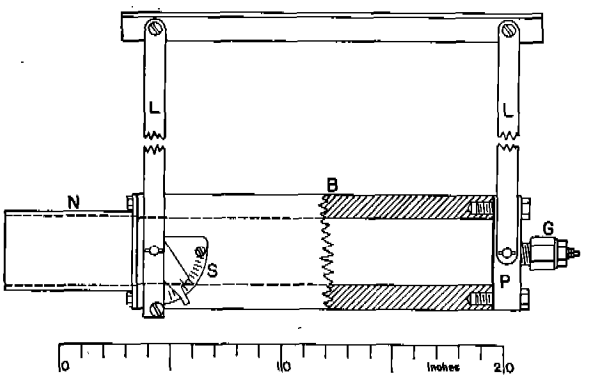


Figure 9. Water ballistic pendulum.

The purpose of the nozzle was to confine the expelled water to a narrow cone so that the momentum of the empty pendulum would be substantially equal to the total momentum of the water.

The pendulum was hung from the ceiling by four strap iron links L and its angular deflection was indicated by a friction pointer which was moved over a scale S by a pin in an extension of one of the links. A piezoelectric pressure gauge G fitted into a hole in the rear plate was connected to an oscillograph to give a permanent record of the water pressures. The pendulum body could be filled completely with water by disengaging the rear links so that the body hung vertically.

Procedure. The bullet was fired through the tar paper disk as nearly as possible along the axis of the body. Practically all of the water was expelled violently, taking the bullet with it. Thus, if we assume that no energy was lost in stretching the pendulum, (or the cap screw) the kinetic energy, e_p, imparted to it is given by equation (1)

$$e_p = Wr(1 - \cos\theta) \text{ foot-pounds} \qquad (1)$$

where W is the weight of the empty pendulum plus two of the links (71 lb); r is the radius of the links (5.65 ft) and θ is the angle of deflection.

Very short bullets weighing only 1.8 g were made of "half hard" Phosphor bronze, and by modifying the powder charge a range of velocities up to 5,800 fps was obtained. Only 2 rounds were fired at this highest velocity because the powder pressures were found to have been dangerously high. Bullet velocity was determined for each round by means of two screens of 0.003-in. copper wire placed 8 ft apart; the velocities are believed to be accurate to about 2 per cent.

Measurements of Pressure and Kinetic Energy. The

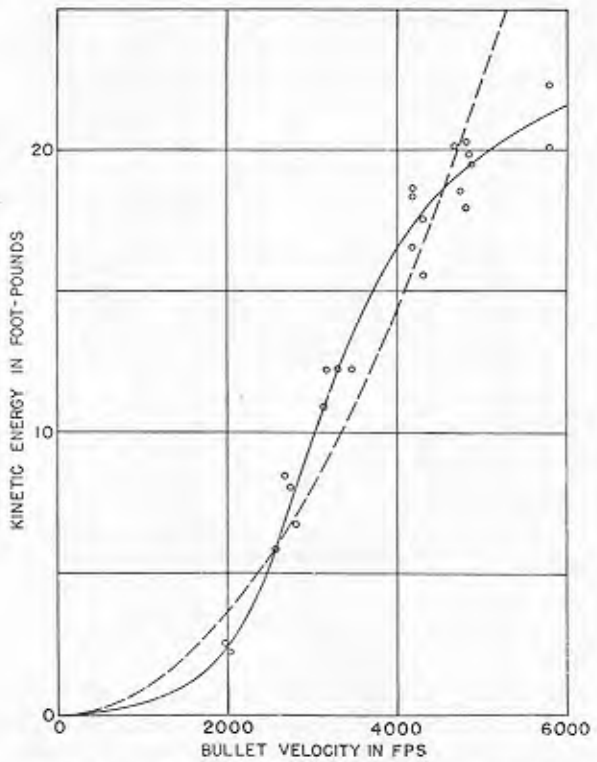


FIGURE 10. Kinetic energy of water ballistic pendulum (full curve) and 0.0145 times the kinetic energy of the bullet (dashed curve), as functions of the bullet velocity.

pressure gauge was designed originally for recording powder gas pressures; its natural frequency, about 70,000 c was too low to permit adequate representation of the shock waves. Thus its indications may have been considerably lower than the actual peak pressures. They should, however, provide a basis for comparison. In Figure 10 the kinetic energy imparted to the pendulum is plotted against the velocity of the bullet. The ordinates of the dashed curve are proportional to the kinetic energy of the bullet. Below 2,000 fps the efficiency (e_p/e_b) is quite low after which it rises to a flat maximum at about 3,500 fps and then falls off. There seems to be no reason to expect a maximum efficiency to occur in general at 3,500 fps. Its position may be due to the shape, dimensions, or rigidity of the pendulum and may be very different for an actual gasoline tank.

In Figure 11 are two pressure oscillograms for the ballistic pendulum. They were made with a still camera, the oscilloscope operating with a 500-c recurrent sweep; the records are thus 2 msec long, time being read from left to right. Since the camera shutter was open for 1/25 sec the base line was swept over many times before and after the shot and the heavy fogging covers up the record of the lower pressures. For *A* the bullet velocity was 2,580 fps and the peak pressure of the first pulse to arrive was 10,800 psi. In *B* the velocity was 5,800 fps and the peak pressure of the first pulse 78,000 psi. The presence of a series of shock waves can best be explained by multiple reflections from the wall of the tube. In Figure 12 the peak pressure of the first shock wave is plotted against bullet velocity for several experiments. The pressure begins to increase rapidly at about 2,000 fps and appears to go through a definite maximum at the velocity of sound, 4,800 fps.

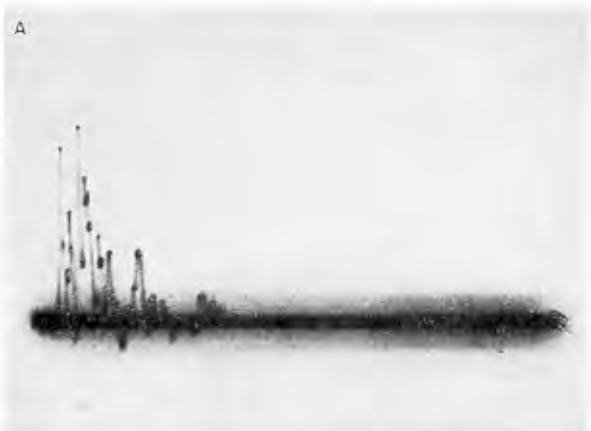


FIGURE 11A. Pressure oscillogram, water ballistic pendulum; bullet velocity 2,580 fps, first pressure pulse 10,800 psi.

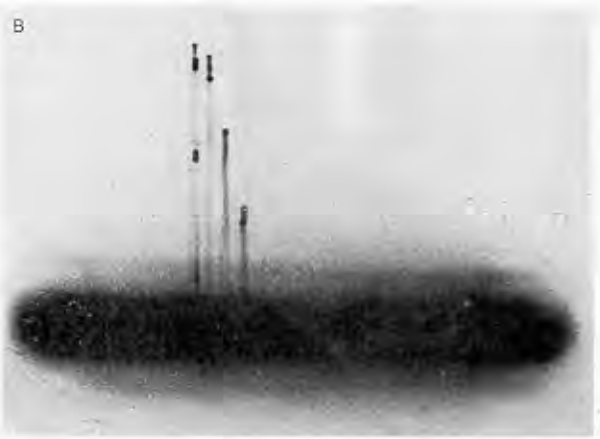


FIGURE 11B. Pressure oscillogram, water ballistic pendulum; bullet velocity 5,800 fps, first pressure pulse, 78,000 psi.

CONFIDENTIAL

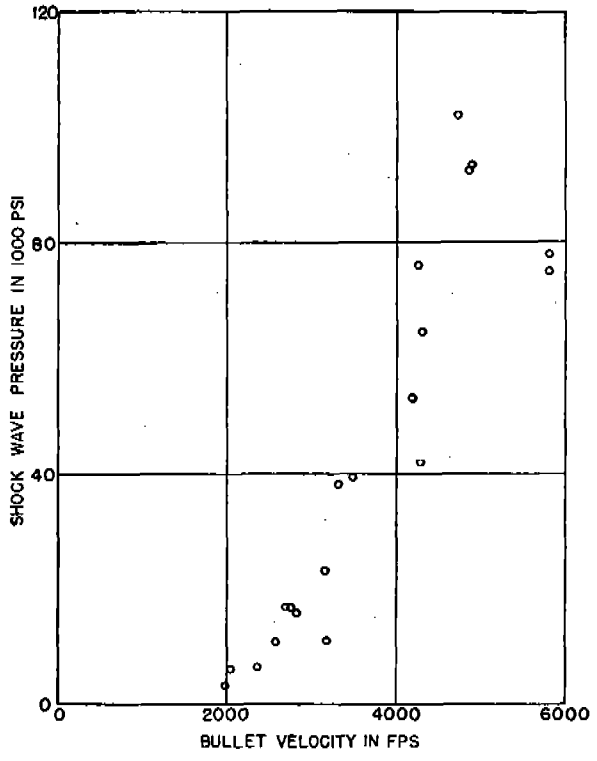


FIGURE 12. Shock-wave pressure as a function of bullet velocity, water ballistic pendulum.

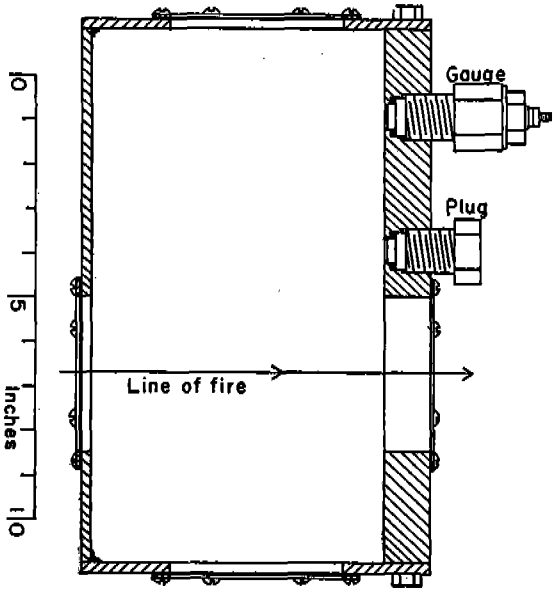


FIGURE 13. Rectangular steel tank.

EXPERIMENTS WITH A HEAVY STEEL TANK

Before the water ballistic pendulum was built some work was done with a rectangular steel tank, Figure 13. The front sides, top and bottom were ¼-in. thick and the back 1-in. thick. The ¼-in. plates were welded to each other but were bolted to the back plate. Four circular windows were provided to fire through and were closed by disks of tar paper. There were two holes in the back plate for the pressure gauge; the one used was 5¾ in. from the line of fire. A considerable number of experiments were planned for this tank, but the first shot opened up the weld at the bottom of the front face. The tank was kept in operation for a while by calking the leak with putty, but when the side seams began to open up its use was abandoned.

Figure 14 is a pressure oscillogram for a 3.1-g soft nose bullet fired from the caliber .22 Swift with a velocity of 3,000 fps. The pressure reading for the initial shock wave is 7,800 psi. There is a rather violent oscillation of the gauge, or of the back plate, but the average pressure remains close to zero until a second shock wave arrives about 0.4 msec after the first. The average pressure remains in the neighborhood of 1,000 psi for nearly a millisecond; and then there is another short period of somewhat lower pressure beginning near the end of the sweep and continuing over into the early portion of the following sweep.

CONCLUSIONS FROM THE PRESSURE AND ENERGY MEASUREMENTS

The early deductions from the qualitative experiments were, on the whole, confirmed by the records of energy and pressure. The work done on the water ballistic pendulum increases about sevenfold as the bullet velocity is raised from 2,000 to 4,000 fps; above 4,000 fps the increase is less rapid. The pressure of the initial shock wave may be very high, but the pulse is of such short duration that it has little energy. The shock wave is followed by an interval during which the pressure is close to zero; then the pressure rises to a moderate value which is sustained for some time. It is believed that disruption of a flexible tank is caused by this later, sustained pulse. The mechanism by which this pulse is produced was not determined.

It is quite possible that the water ballistic pendulum may be too unlike the self-sealing gasoline tanks we are interested in. A better representation might be given by a paper tank in which the surface of the water was covered with floating cubes of wood roughly corresponding to an upper, horizontal wall of the tank. The height to which one of these blocks is

thrown, multiplied by the weight of the block, would be somewhat less (due to air resistance) than the work done on the base of that particular block.

Recommendations. In a continuation of this investigation it would be desirable to study the disruptive effects of different types and weights of bullet fired from the same gun, modifying the powder charge, if necessary, because of changes in weight. The means for evaluating the disruptive effect may be rather crude (the wood blocks already referred to should be adequate) because the effect is likely to vary considerably from round to round. It should be remembered that in combat the bullet has to travel for considerable distance through air and may have to pierce the armored skin of the airplane before it reaches the gasoline tank.

9.1.6 Partial Analysis of the Phenomena

Before these experiments were begun it was known that the impact of a high velocity bullet on a body of liquid would produce a shock wave in the liquid and that if the striking velocity of the bullet were increased, the intensity of the shock wave would be increased, probably reaching a maximum intensity when the striking velocity equals the propagation velocity of the shock wave. The following analysis has to do with the mechanism by which this initial shock wave, presumably, is produced. Since the analysis takes no account of the velocity with which the shock wave is propagated it does not predict the maximum observed in the data of Figure 12 at the velocity of sound. Later, when the experiments began to indicate that the initial shock wave may have very little to do with the disruption of a flexible tank, an independent analysis of the disturbance set up in the liquid as the bullet travels through it was attempted. This later analysis was foredoomed to failure because the nature of the disturbance was not, and is not, known. It seems worth while however to include the first analysis even though the initial shock wave does not appear to be directly relevant to the subject at hand.

Generation of the Initial Shock Wave

For the initial shock wave, the fundamental consideration is the speed with which the projectile makes room for itself in the container by compressing the liquid. If it were inserted very slowly, the ultimate pressure created would be uniform throughout the liquid. It would amount to $(w/W)E$, where w is the volume of the projectile, W the volume of the liquid, and E the bulk modulus of the liquid. For water E is taken as 2×10^{10} dynes per square centimeter. Thus if a caliber .22 bullet (volume about $\frac{1}{2}$ cm^3) entered a liter of water slowly, the contraction would be about 1 part in 2,000 and the pressure required would be about 10 atmospheres.

When the bullet enters the liquid in a time short compared with the time necessary for elastic waves to reach all parts of the surface of the liquid, the pressure is locally much larger than for the case of slow compression. This is true because the amount of liquid that suffers the compression is much less, being in fact, merely that liquid in the immediate vicinity of the bullet through which the sound wave has passed during the time of penetration of the bullet.

In order to arrive at an approximate expression for the pressure in the liquid we may consider the simplified situation consisting of a bullet of radius a in the center of a container of radius b. Suppose that the radius of the bullet suddenly increases at a rate v cm per sec. The increase in size of the bullet need last only an instant in order to generate a pressure wave, although the longer it lasts the greater will be the extent of the wave. The radial displacement ζ of a particle of the liquid caused by this acoustical wave obeys the differential equation

$$\frac{1}{c^2}\frac{\partial^2\zeta}{\partial t^2} = \frac{\partial^2\zeta}{\partial r^2} + \frac{2}{r}\frac{\partial\zeta}{\partial r}, \qquad (2)$$

where r is the distance of the particle from the center



FIGURE 14. Pressure oscillogram for water in a steel tank fired into by a caliber .22 bullet at 3,000 fps; first pressure pulse: 7,800 psi.

CONFIDENTIAL

of the container, c is the velocity of an acoustical wave in the liquid, and t is the time.

The general solution of equation (2) is given by equation (3),

$$\zeta = \frac{1}{r}f(ct - r) + \frac{1}{r}F(ct + r), \tag{3}$$

in which f and F are arbitrary functions. For outgoing waves only f applies, so that equation (3) may be replaced by equation (4)

$$\zeta = \frac{1}{r}f(ct - r). \tag{4}$$

It is well known that for such a system the pressure p at any point is given by equation (5),

$$p = \left(\frac{\zeta}{r} + \frac{\partial\zeta}{\partial r}\right)E, \tag{5}$$

where E is the elastic modulus of the liquid. By combining equations (4) and (5), the pressure may be expressed by equation (6), where ρ is the density.

$$p = \rho c\frac{d\zeta}{dt}. \tag{6}$$

In the case of the spherical bullet that suddenly begins to increase in radius at the rate v, the pressure at a radius a is given by equation (7).

$$P_a = \rho cv. \tag{7}$$

In order to obtain the pressure at a later time t at a radius r, equation (4) may be differentiated with respect to time and then evaluated for $t = 0$ to give the velocity of particles at radius a and for $t = (r-a)/c$ to give the velocity of the particles at radius r. The resulting expressions are given by equations (8) and (9),

$$\left(\frac{d\zeta}{dt}\right)_a = \frac{c}{a}\frac{df}{dt}(-a), \tag{8}$$

$$\left(\frac{d\zeta}{dt}\right)_r = \frac{c}{r}\frac{df}{dt}(-a), \tag{9}$$

which, when combined with equations (6) and (7) give equation (10) for the pressure at radius r.

$$p_r = \rho cv\left(\frac{a}{r}\right). \tag{10}$$

The pressure at the wall of the container of radius b, when the pulse reaches it, is given by equation (11).

$$p_b = \rho cv\left(\frac{a}{b}\right). \tag{11}$$

If $d\zeta/dt$ is of the order of magnitude of the velocity of the bullet, say 3,000 fps, and if $a/b = 1/15$ (a ratio that is valid for the cans used in the experiments described in Section 9.1.2), p_b would be about 6 tons per square inch. If a rigid container wall is perpendicular to the plane of the wave front, the wave will be reflected back along the path by which it came, and during reflection the incident and reflected waves will combine to give a pressure twice that just stated.

Equation (11) indicates that for given values of b and v the pressure at the wall of the container is proportional to a, and hence to the cube root of the mass of the bullet. Equation (11), however, does not show why the hypervelocity caliber .22 bullets fired at a velocity of 4,000 fps were so much more damaging than the caliber .30 ones fired at 2,700 fps. The calculated pressure in the former case was only 9 per cent greater than in the latter.

Transfer of Momenta

Another feature of the experiments described in the foregoing sections is that when a bullet is fired into water there is a very large transfer of momenta if the water is free to move. Thus in the case of the experiments with the ballistic pendulum the momentum P_1 imparted to the pendulum in the direction of flight of the bullet was from 13 to 19 times the original momentum of the bullet. Because of the law of conservation of momentum, the amount of momentum P_2 imparted to the water in the opposite direction must have been equal to P_1 less the original momentum of the bullet.

Such a large transfer of momentum, although it is not frequently encountered, is merely a special case of a general relationship that may be expressed in the following terms. Suppose that a mass m having a velocity v is permitted to share its momentum with two other masses. For simplicity in computation suppose further that these two masses are equal, and hence may be designated by M. For the sake of generality, suppose that only a fraction α of the original kinetic energy of the first body is conserved as observable kinetic energy, the remainder being converted into heat; and further, that of the kinetic energy lost by this body, only a fraction β is conserved as observable kinetic energy in the two masses M, the remainder being converted into heat.

These two conditions are expressed by equation (12) and the conservation of momentum by equation (13).

$$\frac{1}{2}MV_1^2 + \frac{1}{2}MV_2^2 = \frac{1}{2}\beta(1-\alpha)mv^2 \qquad (12)$$

$$MV_1 + MV_2 = \alpha mv. \qquad (13)$$

Equations (12) and (13) may be solved for the momenta of the two large masses, as given in equations (14), in which M' represents $[2\beta(1-\alpha)Mm - \alpha^2m^2]^{1/2}$

$$MV_1 = \frac{\alpha mv}{2} + \frac{M'v}{2} \qquad (14a)$$

$$MV_2 = \frac{\alpha mv}{2} - \frac{M'v}{2} \qquad (14b)$$

Thus by making M sufficiently large, we can make the momentum MV_1 as large as we please; but by whatever amount it exceeds $\alpha mv/2$, there is always a corresponding amount of negative momentum in the other mass. It should be remembered that by putting a finite amount of *momentum* into a very large mass, we endow it with only an infinitesimal amount of *energy*, whereas by putting a finite amount of energy into a very large mass, we endow it with a very large momentum, an infinite amount in the limiting case of an infinite mass.

9.2 ARMOR PERFORATION[e]

9.2.1 Specific Limit Energy

It is convenient to discuss the perforation of armor plate in terms of the "specific limit energy," which is defined by the expression WV_l^2/d^3, where W is weight of projectile; d is diameter of projectile, that is, the caliber; and V_l is limit velocity. By "limit velocity" is meant the minimum velocity required to defeat[f] the plate. Most experimental results may be described for practical purposes by formulas expressing WV_l^2/d^3 as a function of e/d and θ, where e is plate thickness, e/d is plate thickness in calibers, and θ is obliquity, that is, the angle between the trajectory and the normal to the plate.

One way to systematize the observations is to make a chart in which WV_l^2/d^3 is plotted against e/d. The results for a particular combination of projectile and plate material and a particular angle θ will be found to lie along a curve or band, the width of the band representing the uncontrollable scatter in the data. For a different angle θ a different band will be found. The advantage of such a choice of variables is that it reduces the results obtained with all sizes of projectiles to a common basis. The fact that extensive investigation has shown that this procedure is possible without much error means that there is very little "scale effect" in armor perforation. However, this scale effect, while small, is nevertheless real and is in the direction of decreasing WV_l^2/d^3 with increasing d. A chart such as that discussed in the preceding paragraphs is presented in Figure 15 where the shaded bands indicate the actual performance attained with practical projectiles having armor-piercing cores of tungsten carbide. It will be noted that the weight and diameter refers to this core only, without regard to any jacket or cap material.

A very carefully controlled series of laboratory experiments[158] with nonshattering shot at normal incidence is represented by equation (15). The units are the same as those in Figure 15.

$$\frac{WV_l^2}{d^3} = 158\times10^6\left(\frac{e}{d}\right)^{1.26} \qquad (15)$$

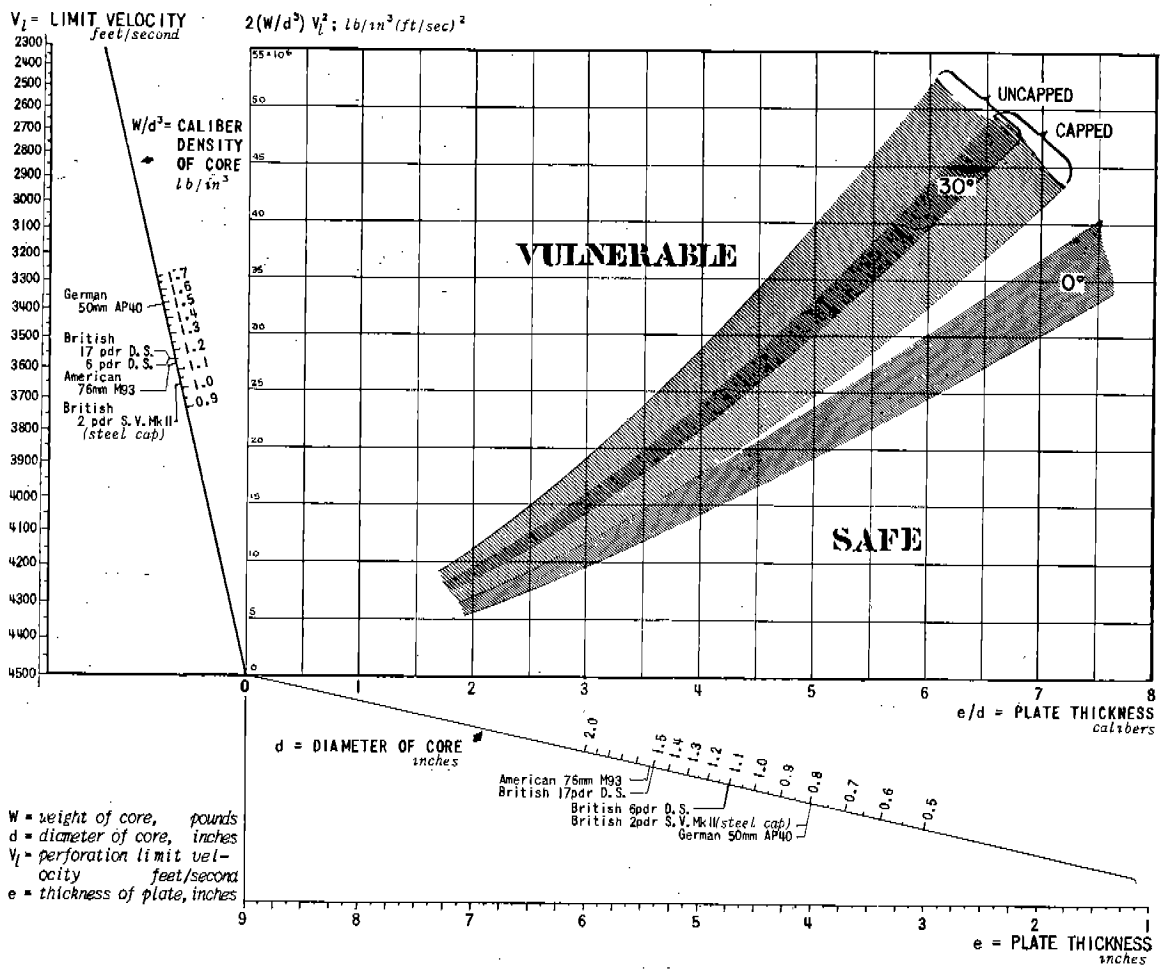
For the caliber (0.244 in.) and the armor used, this represents something very close to the ultimate in projectile performance and therefore represents a boundary beyond which we do not expect to go with conventional projectiles. The boundaries for other obliquities have not as yet been so clearly defined. It may appear that some limit energies obtained from Figure 15 are less than those given by the above relation. This discrepancy may be related to two circumstances, (1) the small scale effect which favors the larger projectiles and (2) the fact that the data plotted in Figure 15 refer to the core only whereas the carrier in many cases contributes to the penetration by giving the core a boost from behind when it strikes the plate.

It has been found that most observations on armor perforation in which the projectiles are but little de-

[redacted]

[e] Only a short description is given here of the perforation of armor by hypervelocity projectiles since the subject is covered much more extensively in the Summary Technical Report of Division 2, where a bibliography will be found.

[f] The term "defeat" as used here may be defined in various ways. The limit velocity for complete perforation of the plate by the entire projectile constitutes defeat in Navy terminology, whereas a pinhole made by the very tip of the missile represents defeat in Army parlance. Limit velocities for bulging, spalling, cracking, plugging, may likewise be defined. The discussion given here applies regardless of which kind of "defeat" is under consideration but quantitative and numerical results refer to the complete perforation of the plate by the armor-piercing core of the projectile.

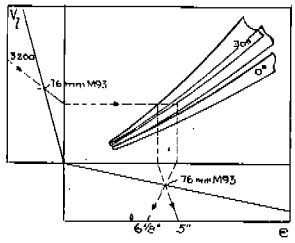


The chart shows the way in which limit velocity for complete perforation is related to thickness of homogeneous armor (BHN 220-330) perforated by capped and uncapped tungsten carbide cored projectiles striking at normal incidence and at 30° to the normal. The data represent projectiles having cores ranging from 0.65 to 1.52 inches in diameter. Indicated on the nomogram scales are projectiles with cores standardized for field use.

Because of inherent scatter of firing data, results are presented as bands. For each obliquity, the band was drawn to include 90% of the points. Capped and uncapped projectiles at 0° scatter randomly through the band; at 30° there is an evident separation as indicated. Tungsten carbide cores usually break up on impact. If there is complete disintegration of the core, perforation of the indicated thickness may not be attained.

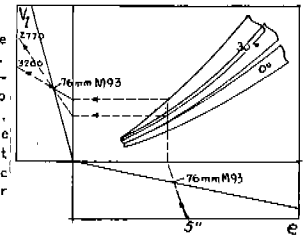
EXAMPLE A

Given an uncapped American 76 mm M93 projectile striking at 30° with a velocity of 3200 ft/sec, two values of plate thickness, about 5 inches and $6\frac{1}{8}$ inches, are read by following the line to each of the two borders of the band. It is reasonable to assume that plate thicknesses greater than $6\frac{1}{8}$ inches will be safe against this projectile, while thicknesses less than 5 inches will be vulnerable.



EXAMPLE B

Similarly, for the same projectile (see Example A) fired at a plate about 5 in. thick, two values of the striking velocity are read by following the line to each of the two borders of the band, namely 3200 and 2770 ft/sec. The plate referred to is likely to be safe against striking velocities less than 2770 ft/sec and vulnerable to velocities greater than 3200 ft/sec.



SOURCE: Based on experiments by American, British and Canadian military establishments.

FIGURE 15. Perforation of homogeneous armor by tungsten carbide cored projectiles. (From OSRD Report No. 6053, *Weapon data: fire, impact, explosion*, Division 2, NDRC.)



formed in the process can be represented fairly well at obliquities near the normal by a relation of the form of equation (16),

$$\frac{WV_l^2}{d^3} = R\left(\frac{e}{d}\right)^n, \tag{16}$$

where R is determined chiefly by the strength of the plate material and n has a value between 1 and 2. If n is given the value 1.5 the De Marre formula in use by the Army Ordnance Department is the result. The value $n = 1$ gives essentially the Thompson formula used extensively in the Navy Bureau of Ordnance. Neither of these forms fits the observations over a very wide range without changing R. In fact, for a given projectile and plate material, the behavior cannot be represented over extreme ranges of V_l and e/d by any one set of values for R and n. Equation (15) has the form of equation (16) and n lies between the Thompson and De Marre values.

The preceding discussion has been concerned with projectiles which suffered little deformation on impact with armor plate or in other words "successful" projectiles. If the shape of the missile, or more particularly, its armor-piercing core, is seriously changed on impact, the penetration is drastically reduced. There is a common belief in ordnance circles that at very high velocities, deformation of the bullet is unimportant. Experiment has shown that this idea in general is false. The greatest limitation by far on the use of hypervelocity in armor penetration is the difficulty in avoiding the shatter of the projectile. Considerable progress has been made in this direction by the addition of caps, pads, and other parts which aid in introducing the core into the armor without shatter.

The value of an armor-piercing cap is illustrated by Figure 16, which shows a caliber .80 steel projectile and the hole it made in a piece of homogeneous armor (Brinell hardness: 250) 2.5 in. thick, which it had struck at a velocity of about 4,800 fps at an angle of 30 degrees from the normal. The projectile had been equipped with an armor-piercing cap that disintegrated in the process. A similar steel projectile without the cap was severely deformed by the impact and did not perforate the plate.

This example illustrates the fact that steel shot, if properly designed, stands up against this type of target under hypervelocity conditions. Steel suffers in comparison with tungsten carbide in having lower density and lower hardness but may be preferred in some hypervelocity applications because of its availability and ease of fabrication. Experience indicates that tungsten carbide can be made to outperform steel at hypervelocities but nevertheless steel has given a creditable performance in experimental firings under these conditions. It is not yet certain that steel projectiles made by customary mass-production procedures will do so.

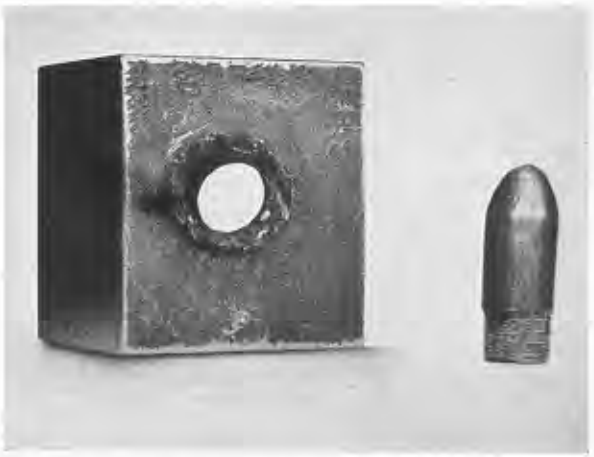


FIGURE 16. Perforation of homogeneous armor 3.1 calibers thick by a caliber .80 steel projectile at 30° obliquity. (Photograph by courtesy of Princeton University Experiment Station, Division 2, NDRC.)

The design of practical projectiles to meet conditions of impact at high obliquities, spaced armor, face-hardened armor and combinations of these factors is very complicated and largely empirical at the present time. More extensive discussion of these problems is beyond the scope of this short review.[8]

9.2.2 Armor Perforation by Hypervelocity Projectiles

It is impossible to separate the fields of interior, exterior, and terminal ballistics; solve their problems separately; and obtain the best overall answer to the ballistic problem. Nevertheless it is helpful to make an approximate separation in order better to organize our thinking. If perforation of armor is the only consideration and the discussion is based on equal energies of the projectiles when striking the plate, the following conclusions may be made as a result of investigation in the hypervelocity field.

1. *A nondeformable projectile gives maximum performance.* Failing to meet this requirement in its en-

[8] They are treated in Chapter 6 of the Summary Technical Report of Division 2, NDRC.

CONFIDENTIAL

tirety the statement still applies to the armor-piercing core. If concession must be made to deformability the amount of deformable material should be held to a minimum. There may be exceptions to these statements under special circumstances, such as impact on thin armor at high obliquity.

2. *It is advantageous to concentrate the energy in a packet of small dimensions.* It is easier to punch a small hole through a given plate than it is to punch a large one. However, a needle is not practicable because of the difficulty in satisfying condition (1). It is desirable, therefore, to make the armor piercing projectile of material having the highest possible density and the highest possible strength. The best material so far developed for the purpose is tungsten carbide. To be sure, this material usually suffers some fractures, but if properly designed, its penetration properties and destructive power on emerging from the plate are such as to make it a formidable weapon.

3. *If two identical projectiles are fired with different energies the faster one will pierce the thicker armor at zero range and its advantage over the other will increase with range.* The indications are that if two similar projectiles of different caliber are fired with the same energy, the smaller will pierce more armor and its advantage will (percentagewise) increase with range. This important conclusion must be suitably qualified. The energies must be below the shatter point for the projectile but above the velocity of sound. The sweeping generalization that one sometimes hears, "very high velocities are unprofitable because the rate of loss in velocity is so high," is false from this point of view.

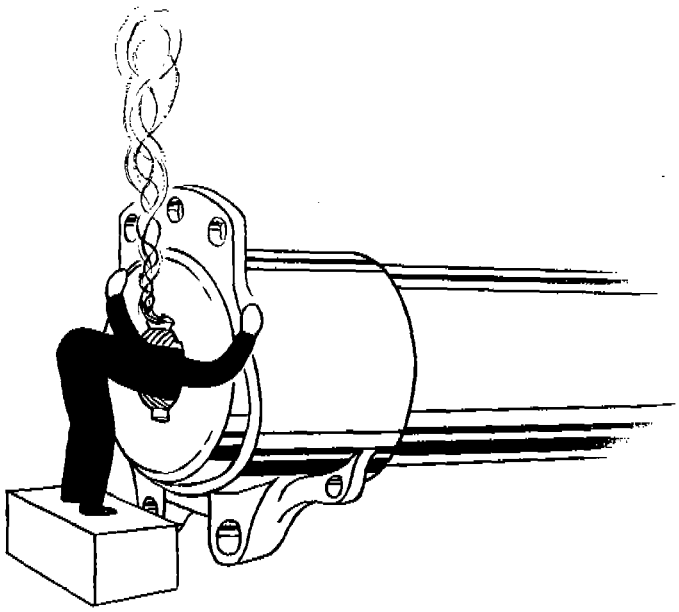
4. *Muzzle velocities above the critical shatter velocity will improve the armor piercing capabilities beyond the range where the velocity drops below the shatter point.* It has been amply demonstrated that a projectile will shatter under certain conditions if the striking velocity is above a critical value and fail to pierce the plate, whereas at a lower velocity perforation will be achieved.

All of these conclusions point to the fact that for a conventional gun as it is used at present the armor-piercing performance can be improved by adopting a tungsten carbide subcaliber projectile with a carrier of minimum weight. A successful design of such a projectile mounted in a sabot is described in Chapter 29 and a design of one mounted in a projectile for a tapered bore gun is described in Chapter 30.



PART III

GUN EROSION



Attempt the end, and never stand to doubt
Nothing's so hard but search will find it out
—*Robert Herrick*
"Seek and Find"

[redacted]

Chapter 10

DESCRIPTION OF ERODED GUN BORES

By *Lloyd E. Line, Jr.*[a]

10.1 DEFINITION OF TERMS

ENLARGEMENT of the bore of a gun by erosion radically affects the flight of the projectile. In general, erosion at the breech end decreases the range of the gun and erosion at both ends decreases its accuracy. For these reasons it is important to seek means of mitigating or controlling bore enlargement.

This chapter contains a description of eroded guns with respect to the superficial effects of the eroding process that are deduced from physical measurements of bore dimensions and from visual examination of the surface. More fundamental effects of gun erosion will be described in Chapter 12.

For the purposes of this Summary Technical Report, the term "gun erosion" is defined as the gradual changes in bore dimensions as a result of normal firing[b] and the changes in character of the bore surface and walls that lead to these changes in dimensions. Such a definition would satisfy the metallographer who might detect a slight flow of gun metal or the presence of a thermally altered layer after the firing of only one round. It would also satisfy a star gauger who measures changes in bore diameter or a ballistician who notes the effect of such changes on gun performance.

In any case, by "gun erosion" we mean a *result* and not the process that produces the result. In Sections 10.3 and 10.4, entitled "Origin Erosion" and "Muzzle Erosion," respectively, the term "erosion" is used in a macroscopic sense; that is, it is synonomous with the enlargement observable with the eye or with star and plug gauges. In Section 10.5, entitled "Nature of the Eroded Surface," many of the microscopic changes in the bore surface, such as liquefaction of surface material and pebbling, will also be included in the term "erosion" because these changes definitely lead to the macroscopic changes in dimensions that ultimately affect gun performance.

If we measure the bore diameter near the origin of rifling across several of the lands of a gun that has been fired an appreciable number of rounds, we find that this diameter is greater than that of a new gun; a similar result will be noted for the grooves. We express this *land erosion* and *groove erosion* as the diametral enlargement across the lands and grooves, respectively.

The erosion of a gun is not uniform along its length but is localized in the region of the origin of rifling in all guns, and it is localized also in the region of the muzzle in many guns (particularly those of relatively high velocity). The former type of erosion we call *origin erosion*, the latter we call *muzzle erosion*. As is described in detail in Sections 10.3.2 and 10.4.3, the origin erosion decreases toward the muzzle and the muzzle erosion in most cases increases toward the muzzle, so that in practically all cases *origin erosion* and *muzzle erosion* occur in two distinct regions. Between them there frequently occurs a region several calibers long where the bore is constricted, which is usually attributed to *coppering*, that is, the deposition of material from the rotating band of the projectile. This phenomenon is described briefly in Section 10.5.4.

In *origin erosion* we find both *land erosion* and *groove erosion*, the former being some two or three times as great as the latter; in *muzzle erosion* we find, for all practical purposes, only *land erosion*. Figure 1 shows how the land and groove erosion vary along the bore for the 4.7-in. gun, T2, No. 2. The origin erosion here is typical of guns in general. Not only do we speak of *erosion* as general enlargement of a region of the bore, but we often wish to speak of erosion at a particular position along the bore. Thus we speak of *erosion at the origin of rifling, erosion at the muzzle*, and so forth.

As will be seen later (Sections 10.3.6 and 10.4.8), erosion at a particular position is not always circularly symmetrical. In referring to this fact we employ the term *asymmetric erosion*. Muzzle erosion is usually asymmetric. (In the literature, the terms *oval, elliptic*, and *eccentric* are often used to indicate asymmetry. Star gaugers at Army establishments use the term *out-of-round*.)

[a] Technical Aide, Division 1, NDRC. (Present address: Chemistry Department, University of Tennessee, Knoxville, Tenn.)

[b] This definition is not intended to include the increase in bore diameter that results from excess powder pressure, either during proof firing or later.

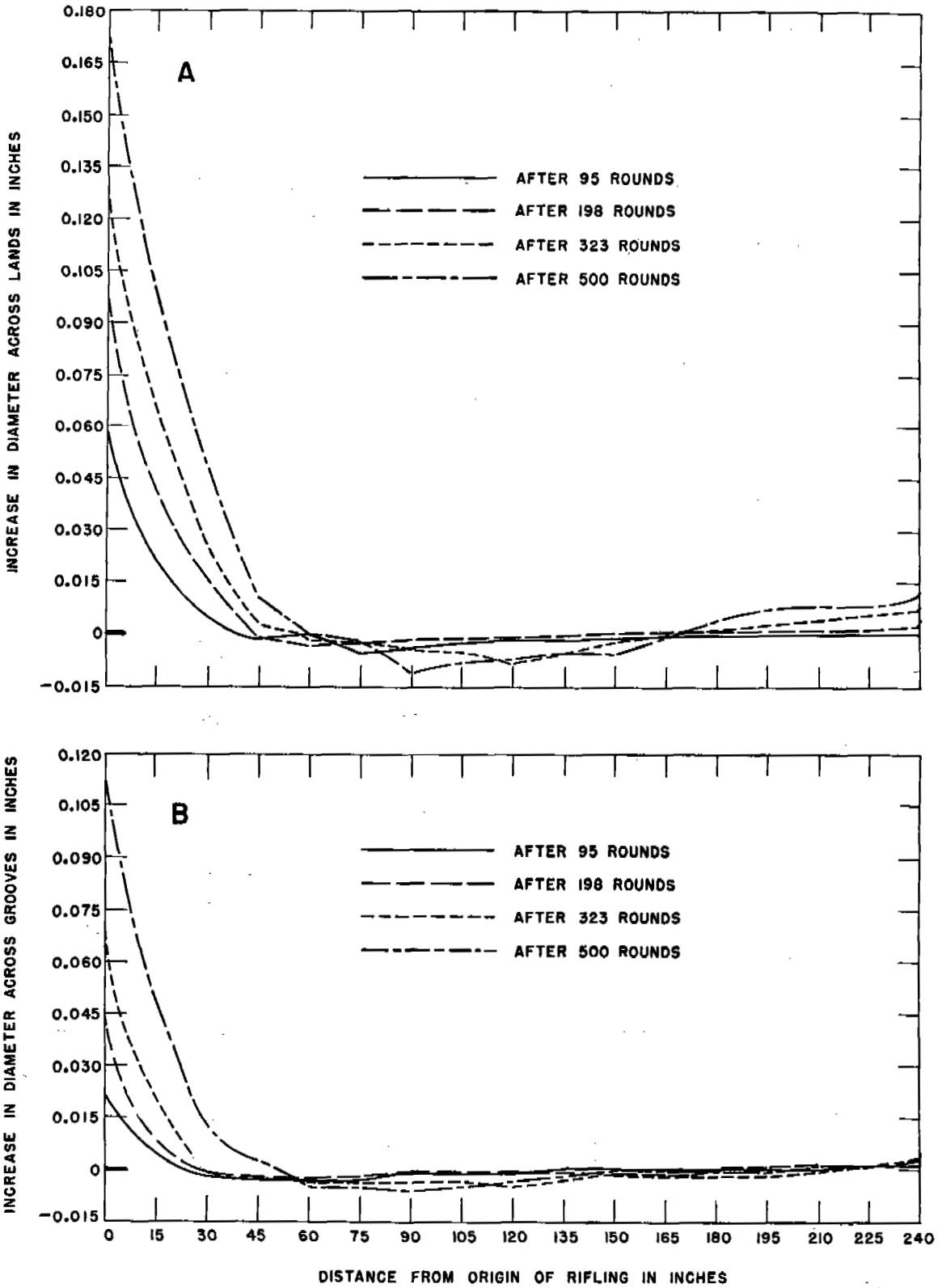


FIGURE 1. Star-gauge curves for 4.7-in. gun.



Asymmetric erosion gives configurations, such as an oval, a circle with a localized region of erosion (pocket), or perhaps a circle eccentric with the original bore. In any case the configuration has some orientation (such as 7 o'clock, breech time) with respect to the mounting of the barrel. If, along the bore, the orientation of the configuration twists more or less with the rifling, as seems to be the case for muzzle erosion, we say the erosion "follows the rifling" or is of the *spiral* type. In some large guns spiral erosion is immediately evident to the observer.

The high cost of guns and of ammunition has precluded the firing of any large number of medium or large-caliber guns just for the sake of obtaining erosion data. Even in the case of small arms extensive testing under a large variety of conditions was not carried out until World War II. Then the diversion of an insignificantly small proportion of the millions of caliber .50 machine gun barrels being produced provided ample quantities for testing purposes. Such tests were performed at Purdue University for the Army Ordnance Department[294] as well as at Aberdeen Proving Ground. In Great Britain a long series of firings under a great many different conditions was made under the auspices of the Barrel Life Panel.[405,406]

10.2 MEASUREMENT OF GUN EROSION

10.2.1 Star Gauges

The ways in which a change in bore diameter may be brought about are (a) removal or displacement of bore surface material, (b) distortion of rifling, (c) barrel expansion or contraction, and (d) coppering. A star gauge gives no indication of the predominant change; it merely registers a change in diameter due to one or more of the above causes. It is therefore well to bear in mind these considerations in studying star gauge data. As will be seen later, measurement of the bore diameter with plug gauges also has certain limitations.

At Army and Navy establishments gun erosion and bore enlargement in general (for cannon) are measured by a star gauge. This instrument measures the bore diameter of a gun across lands and across grooves. The points of the gauge are extended radially in a plane by the movement of a handle at the opposite end of a long staff until they contact the surfaces of the lands (or the grooves, as the case may be). The diameter is read from a vernier scale on the handle.

There are several kinds of star gauges, the details of which may be found elsewhere.[288] Essentially they may be classified according to whether they have two measuring points 180 degrees apart or three measuring points 120 degrees apart. At Army establishments these are called *two-point* and *three-point* gauges, respectively.

It is the practice at Army establishments to make two measurements of diameter with a star gauge in order to take asymmetric erosion into account. In the case of a two-point star-gauge, the diameter is measured in two planes perpendicular to each other, and the two measurements are averaged. This average represents contact by the points with the lands (or grooves, as the case may be) at four places, 90 degrees apart. Similarly, with the three-point star gauge, the diameter is measured, first with the "Y" in one position, and then with the "Y" rotated 180 degrees, and the two measurements are averaged. This average represents contact by the points of this gauge with the lands (or grooves) at six places, 60 degrees apart. Thus the measurement of erosion by a star gauge yields a fairly average diametral change at a particular position along the bore.

At Army establishments, bore diameters are usually measured at a number of positions with intervals no greater than 5 in. It is the practice to star gauge the gun from muzzle to the breech with the measuring points of the star gauge resting on the same lands or grooves, as the gauge moves down the bore. A plot of the diameter or increase of diameter of a gun as a function of distance from some fixed point, such as the origin of rifling, is called a *star gauge curve*. At the Naval Proving Ground such a curve for the lands is called a *bore profile*. Usually a star gauge curve represents the average diametral increase given by the gauge in two positions, as previously described. Sometimes, however, the "horizontal" and "vertical" or the "Y-up" and "Y-down" readings are plotted separately to show asymmetric erosion. These positions, at Army establishments, have reference to the position of the gauge when a reading is taken at the origin of rifling.

Most star gauges can be read accurately to 0.001 in., and an experienced operator can duplicate his measurements with an error no greater than 0.001 in. But among different operators, including experienced and inexperienced ones, there might be variations of 0.005 in. or more in the measurement of the same diameter.

A limitation of the ordinary star gauges, especially with regard to muzzle erosion, should now be pointed

out. As previously mentioned, erosion is often asymmetrical. Since a star gauge measures a diameter instead of a radius, it gives no information concerning erosion at different positions around the periphery. Furthermore, the average of the diameters indicated by the two positions of the star gauge may be somewhat different from the true average diameter that would be given by an average of the readings with the gauge in a large number of positions around the bore. Especially may this be true in cases where the asymmetry is characterized by erosion in a rather narrow region of the periphery.

10.2.2 Plug Gauges

Another way in which erosion is measured is by means of the advance of a plug gauge having a cylindrical, conical, or other type of head. Such a gauge has been used both to obtain the bore profile of a gun and to indicate the end of life.

In studies with the Franklin Institute caliber .50 erosion-testing gun (Section 11.2.1) plug gauges having cylindrical heads ranging from 0.490 in. to 0.516 in. in diameter (in steps of 0.002 in.) were used to measure diameters across lands. Also rifled plug gauges ranging from 0.511 in. to 0.529 in. in diameter (in steps of 0.002 in.) were used to measure diameters across grooves. Thus gauge diameters plotted against distance of the head from the breech gave the profile of the bore.

Such gauges were found to have the advantages of simplicity and speed, but they could be used only in measuring the erosion of materials, such as gun steel, the erosion of which produced a bore that tapered in only one direction. They were not reliable in measuring the erosion of bore surfaces which had been plated with a resistant coating, such as molybdenum or chromium (Section 16.4). A small block of resistant material adhering to the surface (beyond which measurable erosion has occurred) easily stops the advance of a plug gauge.[122]

Because of erosion in the neighborhood of the origin of rifling, the forcing cone does not retain its original position; it gradually moves forward. The advance of the forcing cone is measured with a special tapered plug gauge that is inserted through the breech until it is stopped by contact with the "new" forcing cone.[288] Accompanying the advance in forcing cone is a loss of muzzle velocity, so that such an advance gives some indication of the gun performance with respect to muzzle velocity. (See Section 10.3.7 and 23.1.4.)

As the measurement of the forcing cone advance is much simpler than a star-gauge measurement, it is more readily performed in the field. Although the relation between muzzle velocity loss and forcing cone advance is nonlinear for most guns, it nevertheless can be used as a criterion of the end of life. This was done in World War I by the French and subsequently by the AEF when using French guns.[16] During World War II studies were carried out by the Army and Navy on cannon with gauges having different types of heads.[c]

10.3 ORIGIN EROSION

10.3.1 Relative Erosion of Lands and Grooves

In general, land erosion is greater than groove erosion at any stage in gun life or at any position along the bore. Usually it is two or three times as great in medium and large caliber guns. The relative rates of erosion, however, seem to depend on land height and on degree of land erosion. At the origin of rifling the lands at first erode much faster than the grooves, but the rates tend to equalize and become nearly uniform as the land and groove diameters approach equality.

In seven barrels of five different calibers, 37-mm to 8-in., selected because of best uniformity of firing, the lands, which varied in height radially from 0.02 to 0.14 in., eroded down to their original bases while the grooves deepened almost a fixed amount (0.020 ± 0.005 in., radially). The subsequent rates of erosion of the lands of each gun were scarcely greater than of the grooves and both were nearly uniform. Possibly in 37-mm guns and in ones of smaller caliber, under "mild" conditions of firing, the lands and grooves would erode almost equally from near the start. In guns of larger caliber the three-sided exposure of the high-standing lands above relatively narrow grooves would be expected to favor rapid erosion.[75]

The prime importance of the protrusion of the lands into the gas stream on heat transfer, as related to flame temperature and thermally altered layers, which was shown in studies[124] with the caliber .50 erosion-testing gun (Section 11.2.1), is discussed in Section 15.3.3.

[c] Information received by the author on visits to Aberdeen Proving Ground and the Naval Proving Ground.

10.3.2 Variation Along the Bore

In cannon, the erosion of both lands and grooves is highest at the origin of rifling. Toward the muzzle it drops off rapidly at first, with the rate of change becoming progressively less, so that at several calibers from the origin of rifling there is no measurable enlargement, but cracking is extensive. In most cases this variation along the bore is regular; that is, a smooth curve can be drawn through the points representing increases in diameter, and the curves of all guns are quite similar in form. Typical star-gauge curves for origin erosion are given in Figure 1. In chromium-plated guns the extension of the origin erosion toward the muzzle is less than in nonplated ones, other things being equal. Ordinarily, groove erosion does not extend as far as land erosion.

For equivalent rounds fired in the caliber .50 erosion-testing gun (Section 11.2.1), the extension of land erosion with hot (double-base) powders was greater than with cooler (single-base) powders.[123] The extension of land erosion forward from the origin of rifling in chromium-plated guns is less than it is for a nonplated gun after the same number of rounds, as evidenced by the fact that after 83 rounds with double-base powder, the extension in 90-mm guns for chromium-plated bores was about 10 in. from the origin of rifling whereas it was about 50 in. for the nonplated ones. There was little difference in the magnitude of erosion at the origin of rifling between the plated and nonplated guns.[d]

There is often conspicuous erosion in guns behind the origin of rifling. This has received but little attention. Because the thermal factors in the cause of erosion are more important here than the mechanical, as is brought out in Section 13.2.5, chromium plate offers considerable protection.

In a case gun, erosion between the position of the mouth of the case and the origin of rifling is often about as much as in the adjacent grooves. In a badly worn bag gun, there is a gradual decrease of erosion rearward one to three calibers from the origin of rifling. An eroded, pebbled surface gives place to a cracked surface.[16]

For small arms fired in bursts, origin erosion extends over a much greater proportion of the barrel than in cannon, particularly if the bursts are long. For example erosion extended to the muzzle in a caliber .50 machine gun after it had been fired one continuous burst of 250 rounds.[406] Serious effects resulting from the weakening, and expansion and contraction, of the whole barrel wall as a result of continued fire are the subject of Sections 5.6.4 and 10.5.3.

[d] Author's observation from data supplied by Aberdeen Proving Ground.

10.3.3 Development of Origin Erosion with Firing

The extent of origin erosion in a gun is ordinarily indicated numerically by the increase in diameter of the lands Δd_0 at the origin of rifling or immediately in front of it. In standard nonplated guns of medium or large caliber firing banded projectiles the land erosion at the origin of rifling and positions forward of it begins perhaps with the first round, its rate being higher initially than during later rounds. For 14-in./50-cal. guns this variation of erosion Δd_0 with the number of rounds N has been expressed by the Bureau of Ordnance, Navy Department, as an exponential function[16] according to equation (1).

$$\Delta d_0 = 0.349\ (1 - e^{-0.01065N}). \qquad (1)$$

Studies of such curves have shown that in some guns the erosion rate eventually becomes nearly constant,[75] as exemplified by Figure 2, for 4.7-in. gun, T2, No. 2.

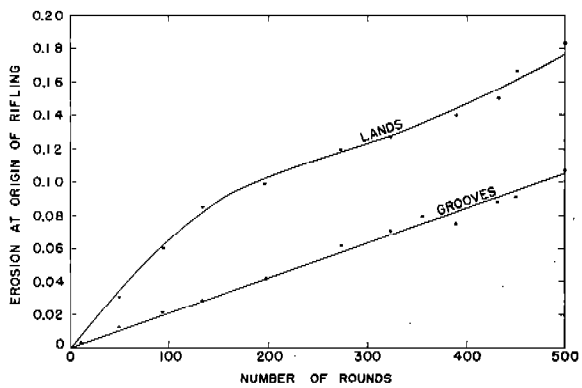


FIGURE 2. Erosion at origin of rifling versus number of rounds for 4.7-in. gun.

A cursory examination by the author of curves of many Naval guns in which origin erosion was plotted against E.S.R. (equivalent service rounds)[e] showed a

[e] In the U. S. Navy for the purpose of tabulation, warming rounds or any other rounds fired at other than the standard charge are converted into equivalent service rounds by means of the formula E.S.R. = $(W/W_s)^6$, where W is the weight of the charge actually used and W_s is the weight of the service charge.

falling off of the erosion rate with E.S.R. and straight portions of curves beginning at a value of land erosion roughly twice the land height. The attainment of a constant rate is considered in Section 10.3.1.

That the erosion rate eventually becomes constant was shown also by studies of erosion with the caliber .50 erosion-testing gun.[122] The progress of erosion observed in some of these tests is given in Section 15.3.1. A study of erosion rates using pre-engraved projectiles (Chapter 31) showed that once erosion started, the rate was about the same as that shown by the straight portion of the erosion curve for banded bullets of the artillery type. This result led to a rough distinction between gas erosion and erosion caused by the forces of engraving, e.g. friction and swaging (see Section 13.4.2). Thus the feature of the gradual diminishing of the erosion rate of the lands to a constant value during the life of a gun may be related to a diminishing of the mechanical forces in engraving, as the amount of the engraving lessens in the worn gun.

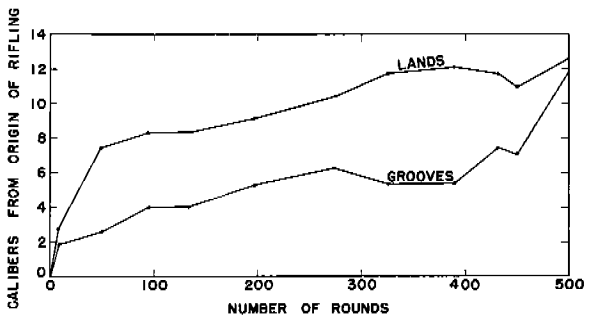


FIGURE 3. Extension of origin erosion for 4.7-in. gun.

Not only does the origin erosion rate decrease with the number of rounds, but also the same holds true roughly for the rate of forward extension of the erosion. A typical example of this variation is given in Figure 3 for 4.7-in. gun tube, T2, No. 2.

Thus we see that in origin erosion a sort of "cone" of wear develops, extending toward the muzzle from the origin of rifling. Both the "base" and the "height" enlarge with firing, at first rapidly and later more slowly. In many guns, while origin erosion is developing, muzzle erosion is developing in the forward portion of the barrel. (This will be described in Section 10.4.) In connection with the falling off of the rate of general erosion there is a similar occurrence with respect to velocity loss. Thus, Figure 4, which is typical of guns in general, shows that the velocity drops at first rapidly and later more slowly.

10.3.4 Dependence on Caliber

The erosion per round and also the maximum of erosion at the end of life increase very greatly with increase of caliber. Representative values of the former quantity for several guns of about the same muzzle velocity but different calibers are given in Table 1. It should be remembered that the variation in the rate of erosion of guns of the same caliber and muzzle velocity is quite large, and that therefore the values given in Table 1 should not be considered as establishing functional relation between erosion and caliber. They are merely illustrative of possible values.

TABLE 1. Comparison of average erosion per round for guns of different caliber: velocity, 2,500 to 2,750 fps.[16]

Gun	Rounds	Erosion Rate* Lands	Grooves
37-mm M3 Tube No. 22708	902 to 1472	0.000047	0.000026
3-in. AA Gun M3 No. 640	326 to 528	0.00017	0.00012
8-in. M1888 MII No. 56	62 to 127	0.00035	0.00027
14-in. M1920 MII No. 11	123 to 154	0.0011	0.00096
16-in. M1919 MII No. 2	123 to 152	0.0028	0.0014

*Average erosion rate at origin of rifling in inches per round.

A functional relationship between erosion or erosion rate and caliber might possibly be established if data on guns (fired in a uniform manner) that are more or less scale models of each other could be assembled.

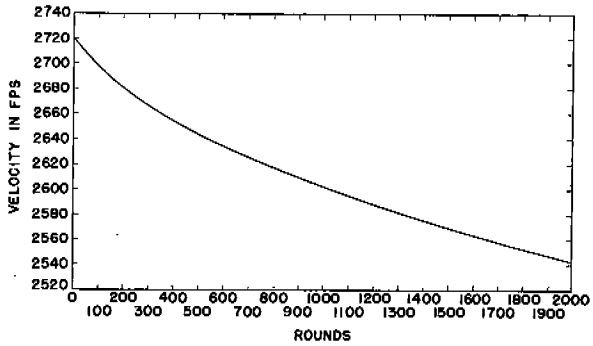


FIGURE 4. Muzzle velocity versus number of rounds for 90-mm guns. (Average of several guns.)

10.3.5 Dependence on Muzzle Velocity

It has long been known that the rate of origin erosion increases very rapidly with an increase in muzzle velocity. This fact has prohibited the employment of muzzle velocities for standard guns much beyond about 3,000 fps. Some idea of the relation of muzzle velocity to origin erosion may be obtained from Table 2.

[redacted]

TABLE 2. Relation of muzzle velocity to origin erosion.*

Gun	Proj. wt. (lb)	Charge (lb)	Service velocity (fps)	Average origin erosion† Nonplated guns 400 E.S.R.	Nonplated guns 800 E.S.R.	Chromium plated guns 400 E.S.R.	Chromium plated guns 800 E.S.R.
5-in./25-cal.	53.55	9.75	2175	0.055(1)	0.090(1)	0.041(5)	0.068(5)
5-in./38-cal.	54.9	15.0	2600	....	....	0.076(94)	0.116(94)
5-in./51-cal.	50.0	27.0	3150	0.141(7)	0.225(1)	0.127(12)	0.155(6)

* These data were furnished by the Naval Proving Ground.
† A number in parenthesis indicates the number of guns for which the value was averaged

The erosion rate, of course, is not fundamentally related to muzzle velocity. Most likely, it is related to the powder charge, which ordinarily is increased to increase the velocity. This may be seen from the fact that there was little difference in the erosion of a 45-in. barrel (muzzle velocity 3,458 fps) and of an 85-in. barrel (muzzle velocity 4,200 fps) when fired with about the same charge (400–405 grains) of double-base (FNH-M2) powder and pre-engraved projectiles in the caliber .50 erosion-testing gun. The rate of land erosion at 0.5 in. from the origin of rifling was of the order of 20×10^{-5} in. per round.[122]

Aside from the size of the powder charge, erosion rate depends also on the type of powder used, as evidenced by the fact that different propellants fired in the caliber .50 erosion-testing gun at the same muzzle velocity ($3{,}300 \pm 50$ fps) gave different erosion rates.[123] This subject is dealt with in Chapter 15.

10.3.6 Asymmetry of Erosion

Origin erosion is usually not circularly symmetrical, although asymmetry of origin erosion is ordinarily less than that of muzzle erosion. It is usually detected in the course of star gauging by the difference between "horizontal" and "vertical" or "Y-up" and "Y-down" readings. Table 3 is illustrative of asymmetry encountered in Service guns. The writer has observed that in the majority of cases, especially in Army 155-mm guns, M1, the vertical erosion is greater than the horizontal erosion.

10.3.7 Effect of Origin Erosion on Gun Performance

As has been mentioned, origin erosion decreases the range and accuracy of a gun. To some extent these effects are interrelated, but they will be separated for purposes of discussion.

The decrease in range is due in a large measure to the loss in muzzle velocity that accompanies origin erosion. Such a loss is progressive, its rate being greater in the early stages of firing than in the later stages. A typical curve showing the variation of the muzzle velocity with the number of rounds for several 90-mm guns is given in Figure 4.

Perhaps the most important effect of origin erosion on muzzle velocity is that the projectile is more easily moved forward during the early stages of burning; that is, the starting pressure [P_0 in equations (3a) and (3b) of Chapter 3] is less than for a new bore. As a result, the rate of burning of the powder is changed in such a way that the average pressure developed over the length of the bore is less, with a consequent loss in muzzle velocity. Moreover, in a bag gun the projectile is rammed farther forward than normally, thus reducing the maximum pressure.

TABLE 3. Asymmetry of origin erosion in several Service guns.

Gun	Designation	Rounds fired	Erosion (in.) Lands "Horizontal"	Lands "Vertical"	Grooves "Horizontal"	Grooves "Vertical"
4.7-in.	T2, No. 3	93	0.061	0.057	0.019	0.027
155-mm	M1A1, No. 18	1148	0.057	0.086	0.016	0.032
6-in.	B.L. Mk XXIII*	....	0.100	0.075	....	....
8-in.	M1, No.20	572	0.250	0.263	....	....
12-in./45-cal.	Mk V	183	0.350	0.386	....	....

*British gun.



It has been suggested[509] that leakage of gas past the projectile accounts in some measure for pressure and velocity loss, but this has been questioned.[515] However, tests in the caliber .50 erosion-testing gun with obturated and unobturated pre-engraved projectiles and projectiles of the base-cup type, which are described in Section 31.4.2, seem to indicate that gas leakage is important in this respect.[122]

Loss in range is also due to interior ballistic conditions caused by origin erosion. For example, the origin erosion may reach a stage wherein the lands are removed over a considerable length of the barrel. As a result the rifling may fail to impart sufficient rotational spin to the projectile causing it to wobble in its flight with consequent loss in range. Also, the rotating band may be sheared instead of engraved, so that practically no spin is imparted to the projectile.

As a gun is fired, its muzzle velocity diminishes, so that its accuracy diminishes progressively in the sense that it cannot hit the target at a given distance. However, in addition, the erosion apparently gives rise also to a dispersion of the shots. Usually the dispersion is greater in range than in azimuth.

Part of the dispersion in range is related to the dispersion in the muzzle velocity due to erratic burning of the powder and other interior ballistic effects. In addition, the geometry of the worn gun has an effect. As previously mentioned, the rifling may be so worn that insufficient spin or no spin at all (due to stripping of the rotating band) may result for a large number of shots. Also, a worn bore may allow gas to leak by the projectile in an indeterminate fashion from round to round causing the bullet to tip in the bore with consequent dispersion.[f] In the caliber .50 erosion-testing gun (Section 11.2.1) the base-cup type of bullet (designed for better obturation) gave a mean radius of dispersion at 45 ft of 0.6 in. whereas the standard ball bullet, M2 gave a dispersion of 2.2 in. under the same test conditions.[122] Furthermore, the worn condition of the bore, especially if it extends forward appreciably, may allow the projectile to tip or ballot in the bore so that it emerges from the muzzle with an initial yaw.

While velocity loss occurs progressively, excessive dispersion develops more or less abruptly. This is especially true in the burst firing of caliber .50 machine guns in which keyholing occurs rather suddenly. Part of this, however, is attributable to the expansion of the gun due to the heating caused by the burst firing. Because of this expansion, the effect of temperature on gun performance, discussed in Section 5.6.3, is similar to the effect of erosion. The sequence of events as the machine gun barrel wall weakens during rapid fire is given in Section 5.6.4.

At the Naval Proving Ground range dispersion of a gun is said to develop rather abruptly in the course of firing.[102]

10.3.8 Erosion Ahead of a Liner Joint

The use of short breech gun liners (discussed in Parts VI and VII) has added a new feature to gun erosion. When a gun containing a steel liner at the breech is fired, the bore diameter increases just ahead of the liner as well as at the origin of rifling. This phenomenon, which is attributed to increased gas turbulence, was studied first with the caliber .50 erosion-testing gun (Section 11.2.1).

Two liners were inserted in tandem in the barrel so that two liner joints at different places in the bore would be exposed simultaneously to the powder gases from the same charge. The main purpose was to determine the effectiveness of different methods of sealing the joint so that the powder gases would not penetrate behind the liner. A lapped joint was found to be preferable to one employing a gasket. In addition it was observed that erosion was much greater just beyond the liner joint than just behind it.

The same effect was observed during the firing of the 90-mm gun, T19, containing a replaceable steel liner (Section 26.3). As may be seen from Figure 8 of Chapter 26, erosion just beyond the joint was appreciable long before the origin erosion had extended as far forward as the liner joint. The rate of this erosion was a linear function of the total number of rounds fired, independent of the condition of the origin of rifling. This result clearly demonstrated that this type of erosion is almost entirely attributable to the powder gases.

A machine gun barrel containing an erosion-resistant liner presents a different situation with respect to erosion beyond the liner joint. In this case the liner makes it possible to fire the gun so much longer than is possible with a plain steel barrel that powder-gas erosion of the steel section beyond the liner presents a serious problem. The enlargement of the bore and obliteration of the rifling there contribute to the eventual failure of the barrel through both inaccuracy and loss of muzzle velocity. After the

[f] Gas leakage is also believed to be responsible for some cases of body engraving. (See Section 10.4.10.)

enlargement becomes great enough for blow-by of the powder gases (Section 13.4.1), the increased heating of the bore surface further accelerates the erosion there and also increases the undesirable effects on ballistics from general heating of the barrel wall, discussed in Section 5.6.4.

10.4 MUZZLE EROSION

10.4.1 Introduction

The importance of muzzle erosion has become apparent only in recent years. While origin erosion occurs in all guns, muzzle erosion occurs only in some guns, particularly those of relatively high muzzle velocity. This kind of erosion has not been studied as thoroughly as origin erosion. One reason for this is that in most instances it is not nearly so conspicuous as is origin erosion; hence its effects on the life of present Service weapons have been considered of secondary importance, if any. However, it seemed to Division 1, whose ultimate goal was the achievement of hypervelocity guns, that muzzle erosion might well limit the life of a gun firing at a muzzle velocity in excess of 4,000 fps even though the problem of origin erosion were solved.

In order to have a body of knowledge that would clarify this situation and perhaps point to possible ways of eliminating muzzle erosion, a survey[67] of existing information was made. Following this general survey, a collection[102] of previously unpublished data at the Naval Proving Ground was made. Then a careful study was made of the bore surface of the muzzle sections of some typically eroded guns: a 57-mm Army gun, an 8-in. Army gun, and a 14-in. Naval gun liner. The results[130] supported the conclusion, tentatively stated in the earlier survey,[67] that the mechanism of muzzle erosion is different from that of origin erosion in that, whereas the primary mechanism of the latter involves the powder gases, that of the former involves mechanical action of the projectile (chiefly rubbing) on the muzzle lands.

The following description of muzzle erosion, which parallels that of origin erosion in Section 10.3, is based on the three reports[67,102,130] just mentioned. The very paucity of the previous information on this subject makes it desirable to present the available data here in more detail than for origin erosion, for the benefit of those who are likely to undertake studies of muzzle erosion in the future.

10.4.2 Relative Erosion of Lands and Grooves

The relative erosion of lands and grooves at the muzzle differs greatly from that at the origin of rifling. At the muzzle, when the increase in diameter across the lands is small, say of the order of 10^{-3} in., the corresponding increase in diameter across the grooves is of the same order of magnitude. But when the increase in diameter across the lands is relatively large, say of the order of 10^{-2} or 10^{-1} in., the corresponding increase across the grooves is still no greater than 10^{-3} in. It is sometimes negative, owing presumably to copper from the rotating band. Thus, groove erosion at the muzzle is practically negligible. Therefore muzzle erosion ordinarily refers to erosion of the lands. These tendencies are shown by Tables 4 and 5.

TABLE 4. Land erosion at the muzzle versus corresponding groove erosion when land erosion is slight, as indicated by measurements of average bore diameter with a star gauge.[67] Measurements taken at or very near the muzzle face.

Gun			Number of rounds fired	Erosion at the muzzle, change in diameter (in.)	
Caliber	Designation	Number		Lands	Grooves
37-mm	M1A2	313	5375	0.005	0.003
37-mm	M3	2110	6082	0.004	0.004
90-mm	M1	35	302	0.006	0.005
4.7-in.	T2E1	2	188	0.004	0.004
155-mm	M1918M1	842	812	0.007	0.005
12-in.	M1895	40	157	0.006	0.004

TABLE 5. Land erosion at the muzzle versus corresponding groove erosion when land erosion is large as indicated by measurements of average bore diameter with a star gauge.[67] Measurements taken at or very near the muzzle face.

Gun			Number of rounds fired	Erosion at muzzle, change in diameter (in.)	
Caliber	Designation	Number		Lands	Grooves
57-mm	M1	1941	556	0.042	−0.001
3-in.	M3	909	1269	0.017	0.001
6-in.	Brown		88	0.045	−0.012
8-in.	Mk VI, Mod 3A2	173L2	295	0.054	−0.002

10.4.3 Variation Along the Bore

Muzzle erosion is usually found over a considerable length of the bore at the muzzle end of the gun—some 15 or 20 calibers in most cases. Unlike origin

erosion, its variation along the bore is not uniform among different guns. The shapes of the curves are varied. Some of the types that have been observed are shown in Figure 5. Curve D illustrates the extreme case of measurable erosion throughout the length of the bore.

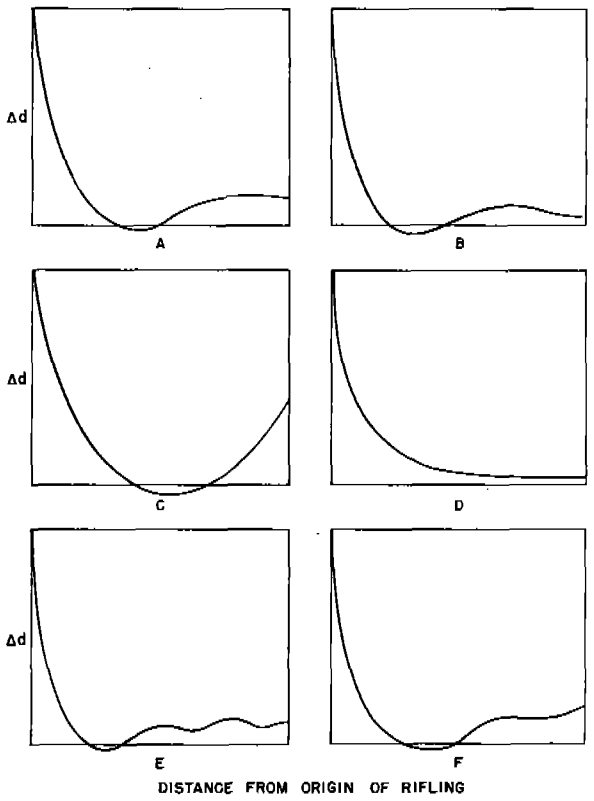


FIGURE 5. Types of bore profiles. (Schematic.)

In terms of diametral change, muzzle erosion is almost never as great as origin erosion. But in terms of total volume change, as judged from the areas under the star gauge curves, the erosion at the muzzle end is often greater than that at the breech end. In most worn guns, the muzzle erosion decreases less rapidly toward the breech than does origin erosion toward the muzzle.

10.4.4 Development of Muzzle Erosion with Firing

For most guns, the maximum muzzle erosion is at or very near the muzzle face. This quantity is generally taken as a measure of the degree of muzzle erosion. In this chapter it is denoted by Δd_m where d is the bore diameter and m refers to the muzzle.

Information received from Naval Ordnance personnel based on erosion data accumulated at the Naval Proving Ground indicates that Δd_m is approximately a linear function of the number of actual rounds N, beginning with the first round, provided the charge for each round is the same. Thus about the same amount of muzzle erosion may be said to accompany the firing of each round, and we may ascribe to the muzzle erosion of a particular gun a characteristic rate $\Delta d_m/N$, which is more or less independent of the stage of life of the gun. Some exceptions to this generalization have been found.

The linear relationship is said to apply also to chromium plated guns, but in these guns the muzzle erosion is delayed by the presence of chromium so that the linear function does not begin with the first

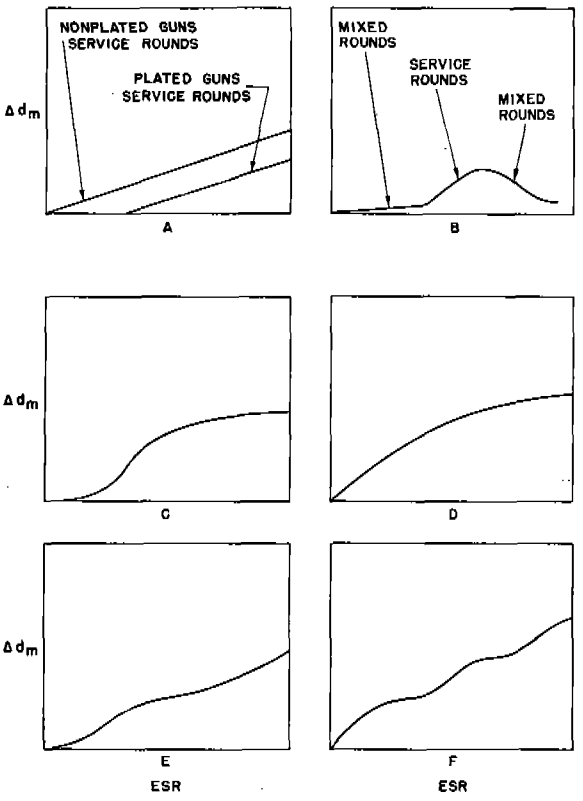


FIGURE 6. Variation of erosion at the muzzle versus E.S.R. for Naval guns.

round. It is said, however, that when the muzzle erosion begins, its rate is very nearly the same as that of the corresponding nonplated gun. (See Figure 6A.)

Plots of muzzle erosion vs E.S.R., when the charges are not the same for each round, do not give straight lines through the origin of coordinates. The curves

are varied in form. This may be due to coppering of the muzzle end when low-charge rounds are fired.

Thus, it has been observed at the Naval Proving Ground that in guns fired with mixed rounds, i.e., groups of service rounds alternated with groups of low-charge rounds, the muzzle erosion is slight. If after firing mixed rounds, service rounds only are fired, the muzzle erosion becomes appreciable, its rate being the same as would be the case if the gun had fired only service rounds. If the firing of mixed rounds is resumed, the muzzle enlargement actually decreases. These phenomena, illustrated schematically by Figure 6B, are explained by the assumption that the firing of low-charge rounds tends to copper the muzzle, which protects it from erosion, and the firing of service rounds removes the copper, thus exposing the surface to erosive influences.[102]

Studies of star gauge curves have shown that muzzle erosion is not usually confined to a relatively short section of one or two calibers, as is often thought to be the case. In fact, it may extend as far back as 15 to 30 calibers from the muzzle. Furthermore, such ex-

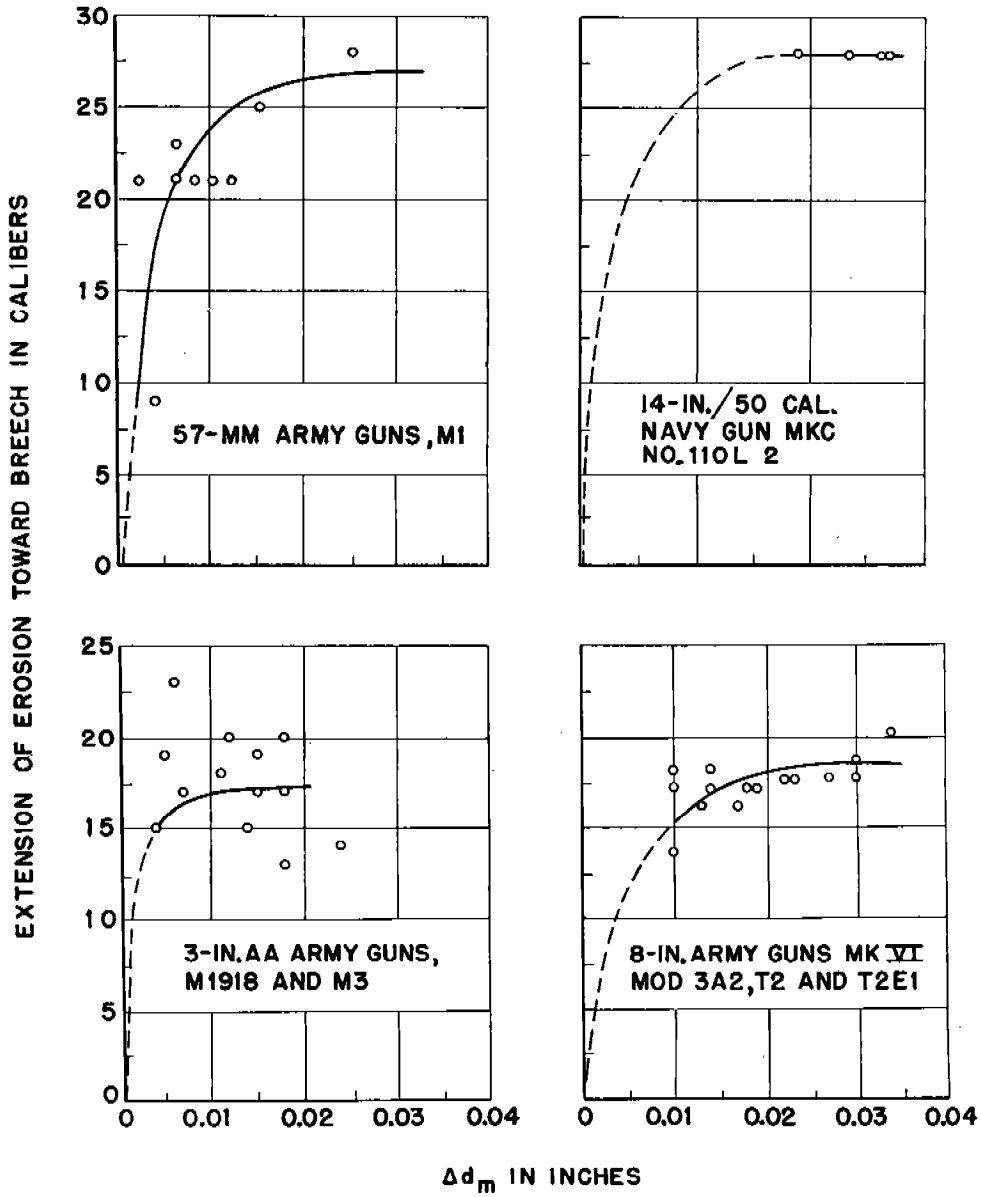


FIGURE 7. Correlation of extension toward the breech of muzzle erosion with Δd_m. (This figure has appeared as Figure 7 of NDRC Report No. A-357.)

tension of erosion seems to be reached relatively quickly, as exemplified by Figure 7. Thus when Δd_m for the 8-in. guns was only 0.01 in., erosion could be detected as far back as 15 calibers from the muzzle. But with further increase in diameter up to 0.03 in. there was little extension of the erosion.

10.4.5 Dependence on Caliber

It is usually said that muzzle erosion occurs only in large-caliber guns. While it is true that it is most conspicuous in those guns, examination of star gauge data shows that some muzzle erosion occurs in practically all guns. It has been shown[67] that the muzzle erosion rate $\Delta d_m/N$ varies approximately as the square of the bore diameter for standard guns of different calibers fired at about the same level of muzzle velocity with projectiles of normal weight for their caliber. (Such projectiles are characterized by having $W/d^3 \cong .5$, where W is projectile weight in pounds and d is bore diameter in inches.) This approximation is illustrated by Figure 8.

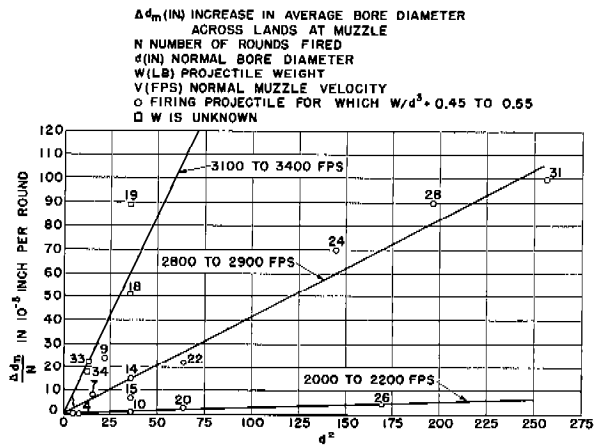


FIGURE 8. Approximate linear dependence of muzzle erosion rate on the square of the bore diameter for guns fired at three nominal muzzle velocity levels. (This figure has appeared as Figure 4 of NDRC Report No. A-357.)

10.4.6 Dependence on Muzzle Velocity

Whether a gun erodes seriously at the muzzle seems to depend largely on its muzzle velocity. Qualitatively it has been known for some years to ordnance personnel that guns of relatively low muzzle velocity (say, < 2,500 fps) are eroded at the muzzle only slightly, if at all, while guns of relatively high muzzle velocity (say, > 2,800 fps) are conspicuously eroded.

It has been shown[67] that the quantity $\Delta d_m/Nd^2$, (constant for guns of different calibers fired at about the same muzzle velocity) varies exponentially with the muzzle velocity, as represented by equation (2),

$$\Delta d_m/Nd^2 = Ce^V, \qquad (2)$$

where V is the muzzle velocity, C is a constant, and e is the base of natural logarithms. A plot of log $\Delta d_m/Nd^2$ against V gave a straight line as shown in Figure 10. Figure 9 is the exponential form of the curve derived from the dashed line of Figure 10. Thus the early qualitative ideas regarding the effect of muzzle velocity on muzzle erosion are confirmed in a more quantitative way.

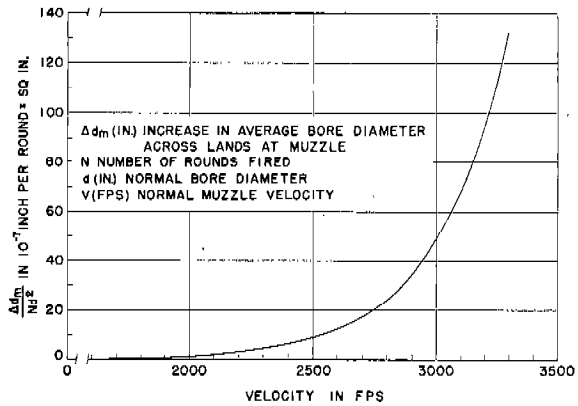


FIGURE 9. Muzzle erosion rate divided by square of the bore diameter ($\Delta d_m/Nd^2$) for nonplated guns fired at different muzzle velocities. (This figure has appeared as Figure 6 of NDRC Report No. A-357.)

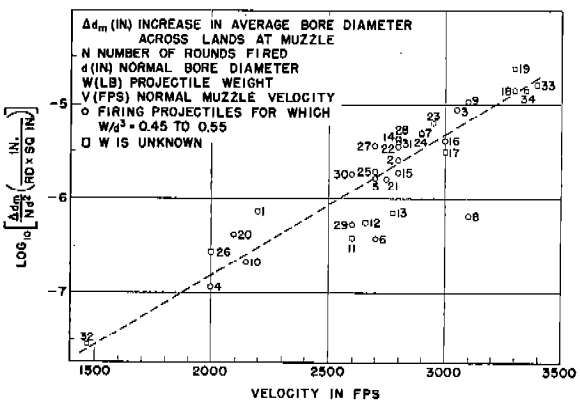


FIGURE 10. Log ($\Delta d_m/Nd^2$) for nonplated guns fired at different muzzle velocities. (This figure has appeared as Figure 5 of NDRC Report No. A-357.)

[redacted]

10.4.7 Correlation of Muzzle Erosion and Origin Erosion

It should be emphasized that the foregoing description of muzzle erosion and the correlations of muzzle erosion with the number of rounds, bore diameter, and muzzle velocity refer to the normal case in which origin erosion progresses simultaneously with muzzle erosion. What the rate of extension of muzzle erosion would be if origin erosion were prevented (as for example by the use of some erosion-resistant material or sufficiently cool powder) is difficult to predict.

It has been suggested that muzzle erosion is "symptomatic" of origin erosion, owing to the possible influence of the latter on the mode of behavior of the projectile in the bore. While this hypothesis seems reasonable, the information at hand [67,102] shows that muzzle erosion is not well correlated with origin erosion. The data of Table 6 illustrate the slight relationship between muzzle erosion and origin erosion. The muzzle erosion of different guns of the same caliber varies widely when the extent of origin erosion is about equal. This means that factors other than origin erosion are also responsible for the growth of muzzle erosion. Therefore it would seem reasonable to suppose that the two kinds of erosion occur to some extent independently and that if origin erosion were eliminated the problem of muzzle erosion might still exist.

TABLE 6. Muzzle erosion of guns having the same degree of erosion at the origin of rifling, as indicated by measurements of average bore diameter with a star gauge.[67]

Gun			Erosion, increase in diameter across lands (in.)		
Caliber	Designation	Number	At origin of rifling Δd_0	At muzzle Δd_m	Number of rounds fired
155-mm	M1	11	0.152	0.002	1070
155-mm	M1	12	0.112	0.014	1081
155-mm	M1A1	409	0.124	0.041	944
8-in.	Mk VI Mod 3A2	190L2	0.173	0.024	70
8-in.	Mk VI Mod 3A2	173L2	0.169	0.054	295

10.4.8 Asymmetry of Muzzle Erosion

Perhaps the most characteristic feature of muzzle erosion is its asymmetry, that is, the unevenness of the land erosion around the periphery at a given cross section and the tendency for the erosion to be confined largely to a group of adjacent lands. These effects are sometimes so great that they are readily noticeable on looking into the muzzle of a gun.

Figure 11[g] shows the variation of land erosion around the periphery for three 14-in./45 cal. Naval guns, Mk VIII, at three stages of erosion. In these guns "pockets" of erosion have formed and the peak erosion is very nearly opposite the minimum erosion. Note that the peak erosion shifts in a clockwise direction (viewed from the breech) with the number of rounds fired. The curves are symmetrical and are very nearly like normal frequency distribution curves.

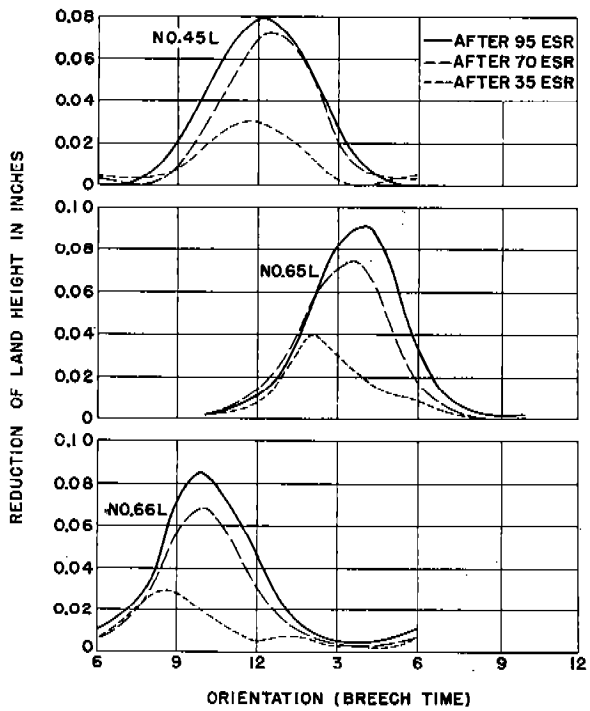


FIGURE 11. Asymmetrical muzzle erosion in 14-in./45-cal. Naval guns, Mk VIII. (This figure has appeared as Figure 8 of NDRC Report No. A-357.)

These curves, however, are not to be taken as necessarily typical of 14-in. guns. Recent study of the muzzle of a 14-in. Naval gun after some 500 rounds showed two maxima and two minima in erosion rather than one maximum and one minimum as shown by the guns referred to in Figure 11.[130]

Figure 12 shows the variation of land erosion around the periphery for four 8-in. Army guns. These

[g] In this figure and in Figure 12 breech time refers to positions around the periphery, as viewed from the breech end, that correspond to those of a clock.

curves are different from those of the 14-in. guns. Note the lack of symmetry of the curves and the tendencies toward formation of secondary peaks, most prominent in the Mk VI, gun Mod 3A2 at the 6 o'clock position. The curve for the M1 gun, No. 20 shows that the erosion is very nearly uniform around the periphery. Few instances of such uniform muzzle erosion have been found.

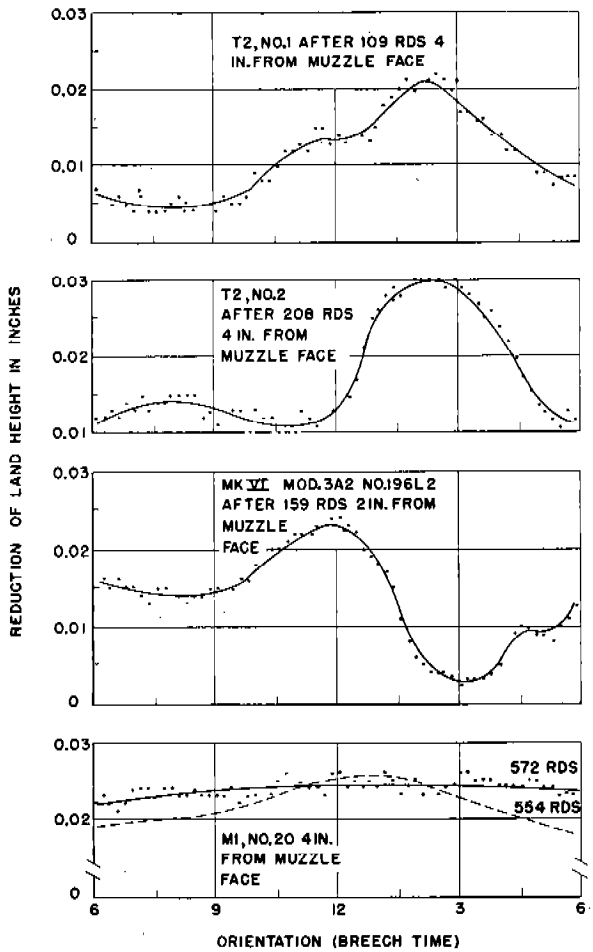


FIGURE 12. Asymmetrical muzzle erosion in 8-in. Army guns. (This figure has appeared as Figure 10 of NDRC Report No. A-357.)

It is not true, as is generally supposed, that the orientation of the peak erosion is always in a certain clock position or quadrant. Neither is it true that the lands included in the eroded sector are always those which are in the 6 o'clock position at the origin of rifling. However, Table 7 shows that the orientations of the peak erosion when referred to the origin of rifling are most frequently in the neighborhood of 6 and 12 rather than 3 and 9 o'clock. This would seem to support the view that the position of asymmetric erosion is predetermined by the asymmetric positioning of the projectile at the start of travel due to gravity.

The asymmetry of muzzle erosion supports the theory that muzzle erosion is largely a result of mechanical action of the projectile as distinguished from powder gas erosion. As the powder gases do not spin they would not be expected to produce the preferential erosion of a group of lands such as is usually observed in the muzzle end of a gun. Also, in 8-in. gun T2 No. 2, 8-in. gun Mk VI, Mod 3A2 and the 14-in./50-cal. gun, the secondary erosion peaks are nearly opposite the primary ones, which would be expected from projectiles with the base bearing on one group of lands and the bourrelet bearing on opposite lands.

A comparison of the peaks for the 14-in. guns Mk VIII and for the 14-in. guns Mk VIII Mod A is instructive. The peaks of the Mk VIII guns fall in the upper half of the bore circumference (9 to 3 o'clock) while those of the Mk VIII Mod A gun fall in the lower half (3 to 6 o'clock). The two types of guns differ in nominal land height (which would not be expected to determine orientation of erosion) and rifling twist. However, the eroded lands at the origin of rifling for both types of guns are in the lower half of the bore (3 and 9 o'clock) at the origin of rifling. This fact suggests that the rifling twist is one factor that governs the orientation of erosion and adds to the evidence that mechanical action of the projectile is of chief importance in muzzle erosion.

10.4.9 Effect of Muzzle Erosion on Gun Performance

Owing to the fact that origin erosion exists along with muzzle erosion, it is difficult to separate the effects of the two kinds of erosion on gun performance. An attempt was made to effect such a separation by analysis of erosion and range data at the Naval Proving Ground but the data were found to be inadequate.[102] However, a general statistical method of attacking the problem was formulated which should prove useful if a considerable amount of adequate data is made available.

We may, however, state some of the probable effects of muzzle erosion on gun life. The maximum angle of yaw of a projectile is proportional to the yaw in the gun due to clearance between the projectile and the bore.[509] As muzzle erosion usually develops over a



TABLE 7. Orientation of asymmetric muzzle erosion in ten major-caliber guns. Compiled from measurements of land height near the muzzle.[67]

Gun	Rifling twist (turns/cal.)	Approx. length of bore (in.)	No. of turns from muzzle to origin of rifling	Number of rounds	Orientation* of "peak" muzzle erosion	Orientation* at origin of rifling of "peak" muzzle erosion
8-in., T2, No. 1	1/25	328	1.64	109	2:00	6:30†
8-in., T2, No. 2	1/25	328	1.64	190	2:30	7:00†
8-in. Mk VI, Mod 3A2, No. 196L2	1/25	289	1.44	159	12:00	6:30†
14-in./45-cal. Mk VIII No. 45L	1/32	533	1.19	35 E.S.R.	11:30	9:00‡
				70 E.S.R.	12:30	10:00
				95 E.S.R.	12:00	9:30
14-in./45-cal. Mk VIII No. 65L	1/32	533	1.19	35 E.S.R.	2:00	11:30‡
				70 E.S.R.	3:30	1:00
				95 E.S.R.	4:00	1:30
14-in./45-cal. Mk VIII No. 66L	1/32	533	1.19	35 E.S.R.	8:30	11:00‡
				70 E.S.R.	10:00	12:30
				95 E.S.R.	10:00	12:30
14-in./45-cal. Mk VIII Mod A No. 22L2	1/25	533	1.52	23 E.S.R.	4:30	10:30
				63 E.S.R.	No peak	
				103 E.S.R.	6:30	12:30
				128 E.S.R.	6:30	12:30
14-in./45-cal. Mk VIII Mod A No. 13L2	1/25	533	1.52	23 E.S.R.	3:00	9:00
				63 E.S.R.	5:00	11:00
				103 E.S.R.	6:00	12:00
				128 E.S.R.	6:00	12:00
14-in./45-cal. Mk VIII Mod A No. 15L3	1/25	533	1.52	25 E.S.R.	No peak	
				65 E.S.R.	6:00	12:00
				104 E.S.R.	7:30	1:30
				129 E.S.R.	7:30	1:30
14-in./50-cal.§ Mk G, No. 110L2	1/25	607	1.74	209 E.S.R.	1:00	4:00
16-in./45-cal.§ Mk VI, No. 202	1/25	617	1.54	140 E.S.R.	9:00	2:30
				200 E.S.R.	9:00	2:30

* Breech time.
† See Figure 12.
‡ See Figure 11.
§ Chromium-plated.

considerable length of the forward end of the bore, it is reasonable to expect that such erosion will affect the value of the first maximum yaw.

The results of a life test at Aberdeen Proving Ground of a chromium-plated 155-mm gun (M1A1E1, No. 3052), with a nonplated 155-mm gun (M1A1, No. 1069) as a control, seem to disclose the effect of muzzle erosion on yaw and yaw dispersion. Some 2,000 rounds were fired in each gun, each round with the HE projectile, M101, and with a charge of single base propellant calculated to give a muzzle velocity of about 2,800 fps in a new gun.

For the first 1,000 rounds the erosion of the chromium-plated gun at every measured position in the region of the origin of rifling was less than that of corresponding positions in the nonplated gun. However, in the neighborhood of the muzzle, the erosion of the chromium-plated gun was considerably greater than that of the nonplated gun. Measurements of yaw showed a consistently greater yaw for the chromium-plated gun than for the nonplated gun. Moreover the dispersion in yaw and the probable error in range were greater. These results (except for the probable error in range) are summarized in Figure 13.

Muzzle erosion probably also increases the dispersion in range because of possible leakage of gas past the projectile as it enters the enlarged area. A theory involving the following conditions in the bore has been proposed.[h]

[h] Personal communication from Dr. L. T. E. Thompson, Director of Research, Development and Test Organization, U. S. Naval Ordnance Test Station (Inyokern, California); formerly Chief Physicist, U. S. Naval Proving Ground (Dahlgren, Virginia).

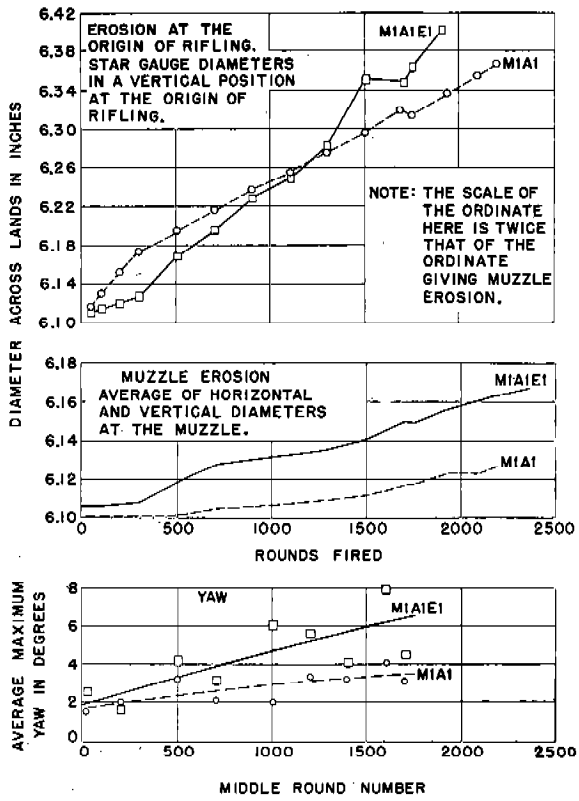


FIGURE 13. Erosion and yaw for 155-mm guns, M1A1, No. 1069 (nonplated) and M1A1E1, No. 3052 (chromium plated). (This figure has appeared as Figure 2 of NDRC Report No. A-357.)

The motion of the projectile is unstable in the presence of high-pressure loading on the base. The axis of the projectile and the axis of the bore do not coincide because of clearance between the projectile and the bore. Since the rotating band is engraved by and fits closely the bore surface, there may be a point near the base of the projectile through which the instantaneous longitudinal axis of the projectile always passes (approximately). In general, and particularly in a worn bore, the longitudinal axis and the axis of angular momentum will not coincide and a sort of Poinsot motion may be expected.

Under these circumstances, the bourrelet may roll in a spiral motion with considerable contact pressure along one section of the lands as the projectile moves toward the muzzle. When the projectile reaches the enlarged muzzle, the powder gases may escape past it in asymmetric fashion. As the projectile leaves the muzzle, the gas stream enveloping the projectile can be sufficiently asymmetric with respect to the projectile to introduce moments tending either to increase or decrease the yaw. If they tend to decrease the yaw, the flight of the projectile may be good. If they tend to increase it, a bad flight may be set up and it may last over a considerable portion of the early part of the trajectory depending on the extent to which damping is effective. According to this theory, when shots are fired successively from a gun with a badly eroded muzzle, some will have good flight, others bad flight. The result is a dispersion in range.

Recent studies at the Naval Proving Ground of range and erosion data failed to establish muzzle erosion as affecting range dispersion. On the other hand they did not demonstrate that muzzle erosion was unimportant.[102]

It has been suggested that in addition to the effect of the enlargement of yaw and the effect of the muzzle blast in producing dispersion of yaw, the enlarged muzzle probably gives rise to an indeterminate angle and direction of departure of the center of gravity from the axis of the bore. Some evidence to support this suggestion has been adduced.

Two experiments have been suggested to gain more exact information concerning the importance of muzzle erosion apart from origin erosion: (a) that the performance of a new gun be compared to one in which the muzzle has been artificially eroded or to one in which the muzzle has been eroded by firing (the comparison to be made with the origin of rifling restored with a replaceable liner such as described in Section 26.3); and (b) that the performance be compared of two eroded guns having about the same bore contour at the origin of rifling, the one having considerable muzzle erosion produced in firing, the other having no muzzle erosion. The possibility of having the latter experiment (together with other controlled experiments to obtain further information on muzzle erosion) carried out by the Navy Department has been suggested by Division 1 to the Bureau of Ordnance.

10.4.10 Muzzle Erosion and Body Engraving

A phenomenon that may be associated with muzzle erosion is *body engraving*. In some guns and under certain conditions the recovered projectiles are found to be more or less deeply marked by the rifling at the base above and below the rotating band. In practically all guns there is light marking of the bourrelet. Available information on the subject of body engraving has been summarized in a recent NDRC report.[67] In Appendix B of this report[67] appears a translation of

what was perhaps the first summary of information on this subject: "Note sur les empreintes des projectiles au tir," by P. Regnauld, Chief Engineer of French Naval Artillery, 1923.

It has not been shown conclusively that body engraving occurs in the muzzle, but available evidence is in agreement with such an assumption. In any case it appears that both body engraving and muzzle erosion are symptomatic of a common malady, namely a motion of the projectile in the bore which ultimately results in balloting or rubbing in the muzzle end or both. These two phenomena cause both an erosion of the muzzle and the marking of the projectile (body engraving). Figure 14 is an attempt to show what may be the separate effects of body engraving and muzzle erosion on the performance of the gun. It would seem that the only effect of body engraving *per se* would be the increased drag (and thus the loss of range) occasioned by the marking. The importance of this effect does not seem to have been evaluated.

The effect of muzzle erosion is probably to increase the yaw and the dispersion of yaw (loss of range and dispersion of range) indirectly through leakage of gas according to the theory of Thompson (Section 10.4.9) and to increase the dispersion in range and lateral dispersion by a direct geometric effect, i.e., the effect of the enlargement itself on the angle of departure of the center of gravity of the projectile.

If Figure 14 represents the relation between body engraving and muzzle erosion, it is clear that apart from correcting the behavior of the projectile in the bore, the correcting of body engraving may not correct muzzle erosion and vice versa. Thus if we should protect the projectile against body engraving by use of a harder steel for the projectile, we might reduce body engraving, but there would still be wear or deformation of the lands by the projectile and the muzzle erosion would give rise to the effects suggested by Figure 14. On the other hand, if we should protect the bore against erosion, as for example by a satisfactory liner or coating, we might solve the problem of erosion; but if the behavior of the projectile in the bore is bad, the projectile will still be body-engraved and perhaps emerge with a significant yaw. Therefore, as Figure 14 suggests, perhaps a consideration of the more fundamental problems of the motion of the projectile in the bore[192] will lead to a solution of both the problems of body engraving and muzzle erosion.

In Figure 14 the various factors that are shown as contributing to the motion of the projectile in the bore and to muzzle erosion are only in the nature of suggestions. The importance of each has been discussed elsewhere.[67] The evidence presented there indicates that muzzle erosion is related more to the motion of the projectile than to the powder gases, abrasion by powder grains and other particles, and oxidation

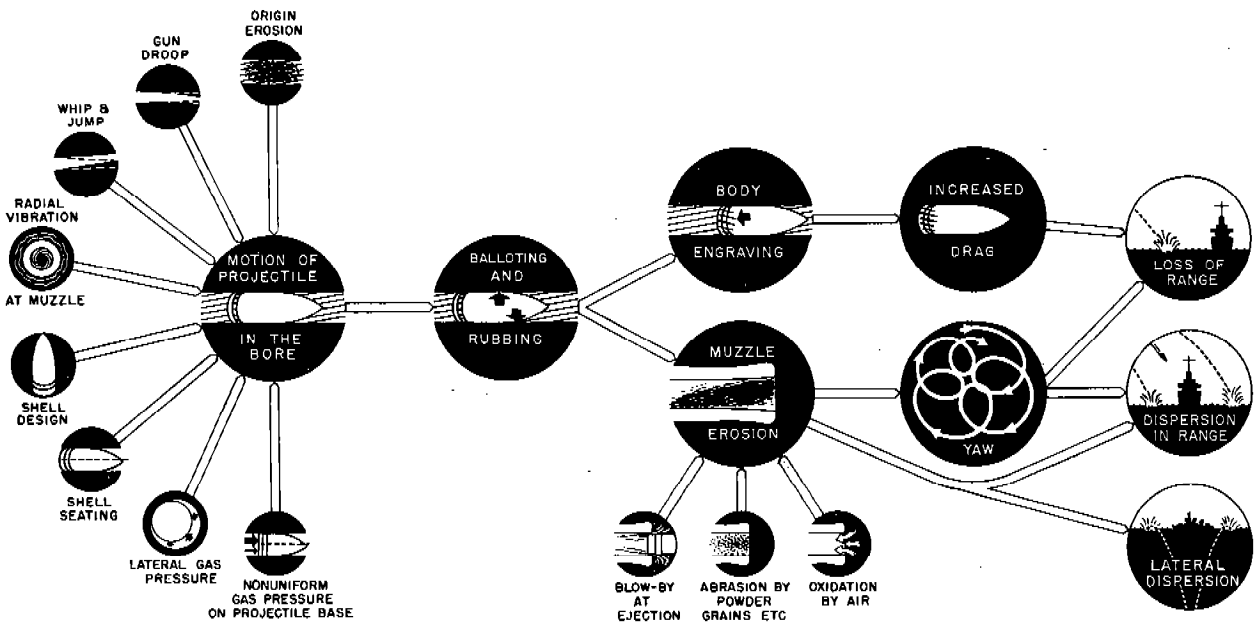


FIGURE 14. Suggestions as to the influence of the motion of the projectile in the bore on body engraving and muzzle erosion and the effects of these two phenomena on gun performance.

by air after expulsion of the projectile, although the latter effects may contribute to some extent.

10.5 NATURE OF THE ERODED SURFACE

We have described the general erosion of guns in terms of the changes in the dimensions of the bore. We now turn to a detailed description of the eroded surface such as would be gained by examination with the naked eye or with the microscope.

10.5.1 Cracking

Perhaps the first thing that is noticed in examining the bore surface of a worn gun is the crack pattern, an example of which is given in Figure 15. Cracking always accompanies erosion in steel guns; the extent of their interrelation, however, is not clear. This subject and the general one of the causes of cracking are discussed at length in Section 13.5.

In advanced stages of wear, it is usually found that the widest and deepest cracks are longitudinal in the grooves and transverse on the lands. Circumferentially, cracks are usually deepest where lands meet grooves on the driving side. Longitudinally, they become shallower toward the muzzle. The depth of cracks varies considerably in different guns, but without any apparent regularity. A technique has been developed[98] whereby the three dimensional aspect of the crack system of an eroded bore specimen may be revealed by making a cast of the bore surface, as described in Section 11.4.4.

The few laboratory studies that have been made of the muzzle ends of guns indicate that the depth of cracking bears no relation to the variation of erosion along the bore in the muzzle end. Thus, in 14-in. Naval gun, Mk VII, Mod 1, No. 188L ($\Delta d_m = 0.16$ in.) cracking diminished while erosion continuously increased toward the muzzle.[130]

Development of Crack Patterns

Microscopic studies of a number of worn guns of different calibers[19,112] have indicated that the development of the characteristic crack pattern near the origin of rifling in guns is about as follows. The initial pattern is largely controlled by the machine marks of the surface, which usually run transversely on the lands and longitudinally in the grooves. These areas of disturbed metal etch and crack minutely, with parallel grooves joined crosswise by little cracks, forming a brickwork pattern. As firing progresses, the little areas assume a roughly domed surface and become nearly equal in size while some of the cracks, in becoming wider and deeper, form irregular shaped poly-

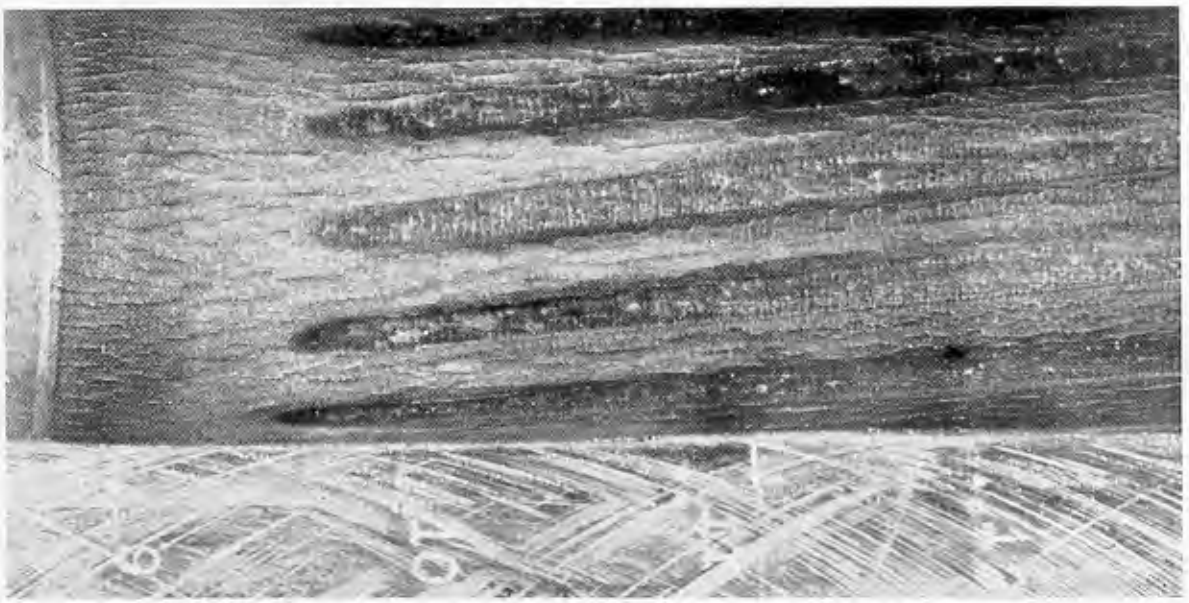


FIGURE 15. Section of the bore surface at the origin of rifling of a 37-mm Browning automatic gun, M1, after 8,032 rounds. (This figure has appeared as Figure 5 of NDRC Report No. A-91, for which use it had been furnished by Watertown Arsenal.)

CONFIDENTIAL

gons bounding the smaller units. In a still later stage, distinct zigzag cracks more or less following the rifling are developed. Often the edges of the transverse cracks are modified (the side of the transverse crack toward the muzzle tending to be the lower).

The development of the crack pattern and erosion has also been studied for chromium-plated guns.[86] In chromium-plated guns, firing weakens the bore by opening microscopic cracks originally present when the plate was deposited, by producing and developing new cracks such as those that form in steel barrels, and by effecting corrosion of the steel thus exposed. The sequence of events which leads to failure of a plated gun is given in Section 20.2.1.

10.5.2 Liquefaction of the Bore Surface

Examination of worn guns fired with single- and double-base powders has revealed so much evidence of liquefaction[1] of the surface during firing that there is little doubt that this phenomenon is one of the most important factors in the erosion of guns as they are fired today. This evidence appears under the stereoscopic microscope as "ripples," "tongues," and smears of metal, gouges, and other irregularities.[112] Metallographic examination of bore cross sections gives supporting evidence, summarized in Section 12.6, to liquefaction phenomena.[112, 124] Melting of a number of nonferrous alloys used experimentally for gun bores has also been observed.[124]

In the muzzle section of a gun there is very little evidence of liquefaction except of the coppering. The erosion of this area seems to be the result chiefly of abrasion.[130]

The liquefied material may remain in place, may be deposited elsewhere, or may be swept out of the barrel. Whether it remains in place or is transported depends upon its mobility and the forces exerted upon it. A "pebbled" appearance is characteristic of a surface where the partially liquefied metal has solidified in place; tongues which stand out clearly in relief consist of material that had flowed as a "mush;" and relatively smooth, rippled surfaces, which may be covered with slender tongues of low relief, are evidence that melting had produced a liquid of high mobility. The last, although sometimes observed in guns fired with single-base powder (Section 12.5.3), is characteristic of guns that have been fired with double-

[1] The term "liquefaction" is preferable to "melting" since it appears that in many cases the melting that occurs is not of the original steel but of chemically altered steel.

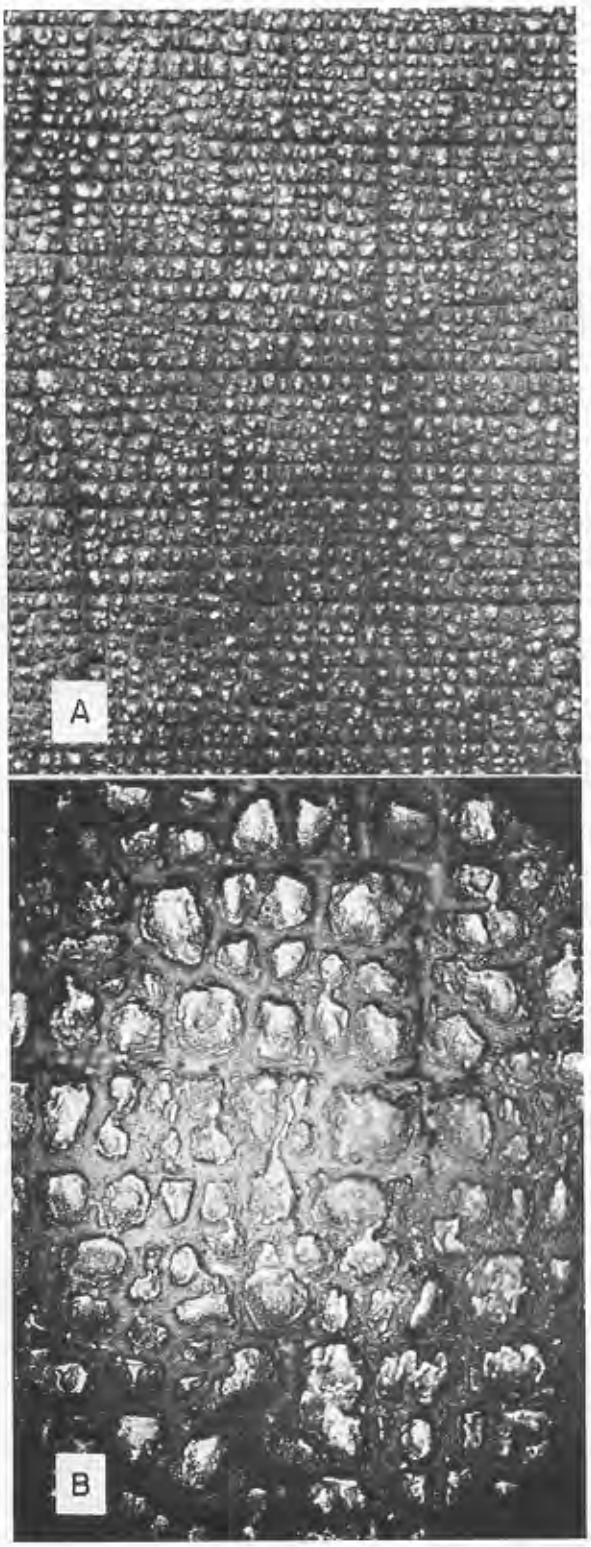


FIGURE 16. Pebbling in chamber of 5-in./51-cal. Naval gun liner, No. 806L2: Single-base powder; (a) *10X*, (b) *35X*. [Figure 19 (a,c) of NDRC Report A-440.]

CONFIDENTIAL

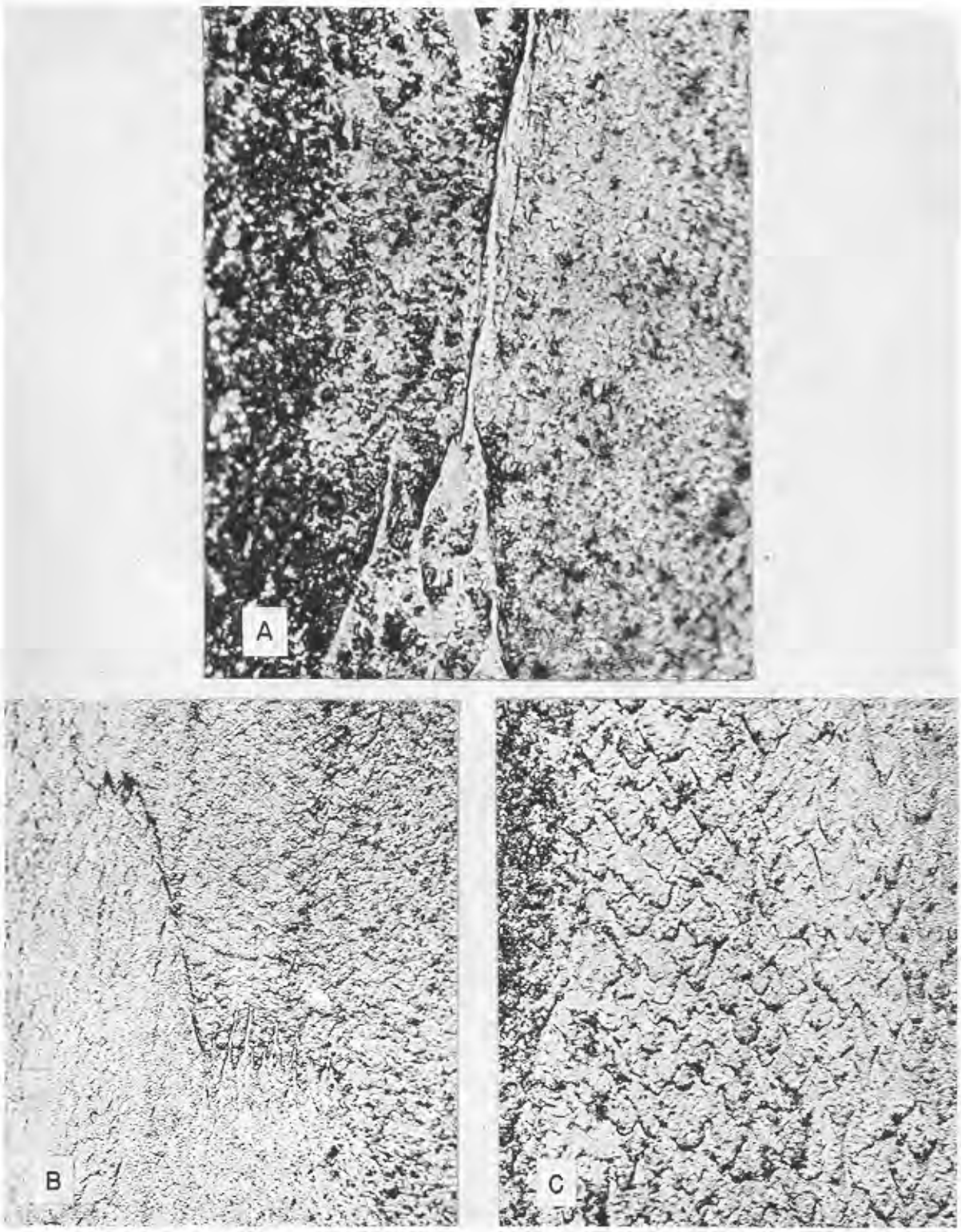


FIGURE 17. Wind-rippled surfaces on which the tops of some ripples were blown forward into tongues and splashes (76-mm Army gun M1A1, Tube No. 1425; single-base powder). (a) 14½-in. from origin of rifling, *1000X*, (b) 6½ in. from origin of rifling, *250X*, (c) 14½ in. from origin of rifling, *500X*. [Figure 9 (a, b, c), NDRC Report A-440.]

CONFIDENTIAL

base powders. Liquefaction resulting from the firing of these two different types of powder is discussed more fully in Section 13.2.4.

Pebbling

In the forward part of the chamber of a bag gun, where the surface is most exposed to the sweep of the powder gases, a brickwork crack pattern develops, such a pattern being started along the lines of the machine marks. The heat of the powder gases softens the metal in each little area bounded by cracks, and reactions with the powder gases (Section 13.3) lower the fusion range so that incipient liquefaction may occur. The metal tends to draw itself into a globule, with the result that a pebblelike pattern develops, as shown in Figure 16. In the chamber, the bulk-velocity of the propellant gases is not high and there is no rubbing by the projectile; hence molten and previously molten material tends to remain in place.

Forward of the origin of rifling, the pebblelike pattern may be somewhat obscured by the deposition of transported material over the cracks, in which case the rounding of the edges of the cracks in the original steel surface by liquefaction can be observed better in cross section. Metallographic examination has revealed that the inner white layer, which, as is described in Section 12.1.2, follows the contour of the steel around the edges of the cracks, is probably material that had been liquefied but not transported.

Removal and Deposition of Liquefied Material

Striking evidence of deposition of molten material has been found in a variety of guns. These deposits appear as splashes, tongues, and smears, often "buttered" over the cracks, on the surface and mixed in the coppering as sheets, scales, and pellets. Examples of such deposits are shown in Figures 17 and 18. In the case of a "dirty" gun steel, an inclusion is often melted and "exploded out" in the direction of the gas stream, leaving a pit and becoming quenched as branched tongues just ahead of the pit, as shown in Figure 19. Sometimes streamlining "trails" are formed by crystals that did not go into solution in the partially liquefied metal.

When liquefied material is transported, the direction is not always axially toward the muzzle but may be affected by localized, turbulent flow of the gases. A discussion of deposits which show this is given in Section 13.4.1. Gouges and pits, direct evidence of the removal of material, are features that are pronounced also because of localized conditions. As was mentioned above, pits are left by the fluxing of inclusions; gouges, shown in Figure 20, are evidence of

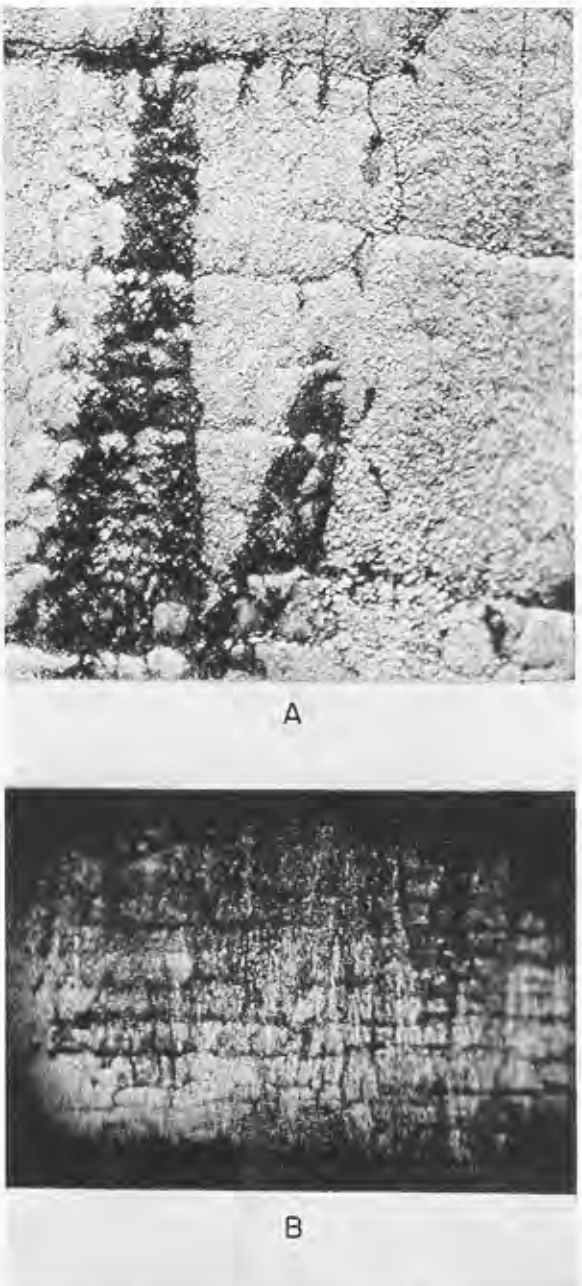


Figure 18. Examples of smeared metal: (A) 3-in gun liner No. 1460, *50X*; (B) Steel liner in a caliber .50 heavy-barrel machine gun, *75X*. (These figures have appeared as Figures 10(a) and 3(a) of NDRC Report No. A-440.)

CONFIDENTIAL

scoring produced by localized gas leakage, which is discussed more fully in Section 13.4.1. The deposits ahead of gouges appear to have been sprayed from a jet.

10.5.3 Distortion of Rifling

Careful microscope, boroscope, and star gauge examinations of a number of chromium-plated liners in caliber .50 machine gun barrels have given a clear picture of how such barrels erode when fired with ball ammunition in moderately long bursts.[50,85] Although the chromium that was applied to the barrels offered remarkable protection from the action of the powder gases, the diameter across the lands at the origin of rifling increased almost as rapidly as if no chromium had been present. Owing to the mechanical action of the bullet the steel of the lands during firing had moved in three directions: (1) forward, (2) laterally, and (3) downward with lateral movement into the grooves. The forward movement resulted in a piling up of steel forward of the enlarged area. The lateral movement was a flattening of the lands, in some cases widening them by as much as 50 per cent. Polished cross sections across the lands showed that the lands had spread out at the top, overthrusting onto the grooves, the top layer of steel carrying the chromium with it. The downward movement of the lands caused a decrease in the diameter across the grooves. Figure 21 is a sketch showing these effects of swaging of the rifling.



FIGURE 19. Erupted surface with tongues of metal carried forward from pits left by the fluxing of inclusions in barrel fired with double-base powder in caliber .50 erosion-testing gun, *150X*. (This figure has appeared as Figure 7(d) of NDRC Report No. A-440.)



FIGURE 20. An example of gouging from blow-by in 20-mm gun, M1, No. 18709 fired with single-base powder, *6X*. (This figure has appeared as Figure 6(a) of NDRC Report No. A-440.)

Although the importance of swaging of the lands was first appreciated in the examination of chromium plated machine gun barrels, later evidence has indicated that swaging plays a part in the erosion of large-caliber chromium-plated guns. It is now believed to be a general phenomenon, the result of which is frequently obscured in nonplated guns by

the fact that metal is removed simultaneously by powder-gas erosion.

The swaging of the lands as related to the austenization of steel bore surfaces is discussed in Section 13.4.2. The recognition of the importance of this thermal transformation as a factor in erosion has had considerable influence in orienting the search for erosion-resistant materials described in Chapter 16.

In some guns firing long bursts at a rapid rate the bore is subject to heating in such a manner that enlargements and constrictions associated with differential plastic deformations develop in the barrel. In extreme cases ricocheting bullets batter the bore and even perforate the barrel, as shown in Figure 16 of Chapter 5.

10.5.4 Coppering

Coppering is the term used to describe the deposition of material from the copper or gilding metal rotating bands or jackets of projectiles onto the bore surfaces of guns. It varies in an irregular manner from round to round. It is commonly greatest in the central portion of the bore. The amount is usually insignificant at the origin of rifling unless the firing conditions have been relatively mild. Only in the case of machine guns which have been subjected to severe conditions is extensive coppering found at the muzzle. In a given gun the copper deposit is usually thicker in the grooves than on the lands.

As was mentioned in Section 6.1.2, it was found in studies of bore friction[72] that the temperature of the interface between a bullet and the bore surface was above the melting point of copper, which indicates that thin films of the band metal are applied to the bore in a fused state. Thick deposits of copper are probably not remelted during successive rounds, but their configuration may be easily changed by the swaging action of the projectile. In the case of a 14-in. gun, a dark, spongy variety of copper appeared to have been sprayed into place beyond the region of maximum coppering and to have been slightly oxidized in the process.[98]

No coppering is found where general melting of the bore surface has taken place. In fact, it appears that relatively thick deposits cannot be built up when the bore-surface temperatures are much higher than the melting point of copper or gilding metal. Qualitative estimates were made of the amount and distribution of coppering relative to the bore-surface temperatures of the caliber .30 barrels used in the investigation described in Section 14.2. They showed that, with an increase in the bore-surface temperature during firing, there is a consistent tendency for the coppering to be displaced toward the muzzle.[99] Copper has been observed to have dripped out of the muzzle end of a caliber .50 machine gun barrel during the firing of a severe schedule.

Relatively thick deposits of copper not only obscure the crack systems in gun bores but are rooted in the cracks, a fact which was at one time used as a partial basis for formulating a theory of the cause of gun erosion.[476]

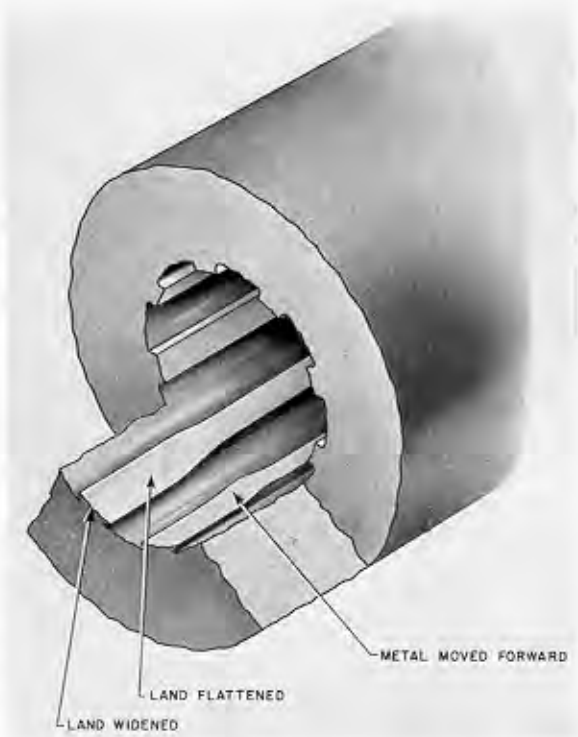


FIGURE 21. The lands of a caliber .50 machine gun barrel move in three directions when they are swaged by the impact of the bullet.

The presence of coppering is more extensive than a superficial examination might indicate, for its surface is frequently blackened by copper oxide.[16] Moreover, it is sometimes so thoroughly contaminated with debris, such as dark, powdery, erosion products and carbonaceous matter, that it may be completely coated over with dark material.[98] The fact that it entraps such substances makes it possible to study erosion products that might otherwise have been blown out of the gun. The technique of segregating these com-

CONFIDENTIAL

pounds by dissolving the copper is described in Section 11.4.3.

Coppering is considered by the U.S. Navy to be so important in its effect on ballistics that it employs decoppering agents and also specifies liberal bore-bourrelet clearances.[515] One of the decoppering methods is to add lead foil to the powder charges. Another[j] involves the use of a solution containing chromic and sulfuric acids.

[j]The details of this method were worked out for the Naval Gun Factory by the Geophysical Laboratory.



Chapter 11

LABORATORY METHODS OF STUDYING GUN EROSION

By *Lloyd E. Line, Jr.*[a]

11.1 INTRODUCTION

THE MOST IMPORTANT laboratory methods of studying erosion that have been used or developed in the course of the work of Division 1 may be divided broadly into two classes: (1) Methods developed and employed to study the fundamental causes of gun erosion or to isolate and study separate effects, such as the effect of heat alone or of a single gaseous component on the surface of gun steel; and (2) methods used to test different liner materials, projectiles, and powders for their possible use in guns.

The surest and most direct way to test a given material for erosion resistance, as is brought out in Section 16.2.5, is to incorporate the material in a gun of the same caliber and design that calls for improvement in durability. Indeed, this test should be performed ultimately, but less costly and less time-consuming methods are necessary to determine the materials that are most likely to prove the least erodible, so that final proving in larger calibers will involve a few carefully chosen materials.

The caliber .50 erosion-testing gun was developed to serve both purposes mentioned above. Insofar as possible, this gun, together with its projectiles, was designed as a scaled-down model of a cannon. It fired at velocities above 3,500 fps. Such a gun was found to have wide applicability. In addition to its usefulness for testing the erosion of steel barrels and of liners of many materials with various propellants, it was employed for the development of pre-engraved projectiles (Chapters 27 and 31) and of the Fisa protector (Chapter 32), for studies of body engraving of projectiles, and for studies of the fundamental causes of gun erosion. This gun and its uses are described in Section 11.2.1.

The caliber .50 machine gun of standard design has been used extensively for testing metals and alloys (particularly stellite and chromium plate) described in Part V. The chief object of these experiments was the improvement of the caliber .50 weapon itself with the results described in Part VI. A description of the method of testing is given in Section 11.2.2.

Erosion vent plugs have been used to test both bore surface materials and propellants and to study the causes of erosion. Thus vents of circular cross section have been used for testing alloys and powders (Section 11.2.3), for studies of the erosivity of different gases heated by adiabatic compression (Section 11.3.1), and for testing the effect of stress on erosion (Section 11.2.5).

Two types of apparatus using vents of D-shaped cross section were developed to study the chemical changes and the cracking that takes place when gun steel is exposed to powder gases. These are described in Section 11.2.4.

The methods mentioned so far are not novel in principle. Several new procedures have been developed to study various phases of the erosion problem. For example, as described in Section 11.2.6, filings of metallic or other specimens were mixed with the powder charge for a caliber .30 round. The rifle was fired into an evacuated glass tube. Some of the filings were recovered from a deposit in the walls of the glass tube and the nature of the alteration produced by the powder gases was examined by x-ray diffraction.

Although it turned out that cavitation erosion bore no relation to erosion in guns, some experiments were early carried out in which different metals and alloys were subjected to magnetostriction oscillation in air-free water. The apparatus is described in Section 11.3.3.

In an effort to evaluate the causative influence on erosion of the high bore-surface temperature apart from any chemical causes, a method was developed (Section 11.3.2) in which the surface of a small sample of gun steel or other material was bombarded by bursts of electrons. In this way a very thin layer at the surface of the specimen was subjected to a very high temperature for a period of time comparable to the time of passage of a projectile in a gun bore.

In addition to these laboratory methods of producing gun erosion or some particular feature of erosion, special techniques were developed to study the products of erosion in guns and in the devices enumerated above. The methods used to disengage and to

[a] Technical Aide, Division 1, NDRC. (Present address: Chemistry Department, University of Tennessee, Knoxville, Tennessee.)

segregate products of erosion are described in Section 11.4. The use of the methods of chemistry, metallography, and physics (x-ray and electron diffraction, radioactive tracers) in studying the products of erosion are discussed in Section 11.5.

11.2 LABORATORY FIRING TESTS

11.2.1 Caliber .50 Erosion-Testing Gun[122]

Prior to 1942 most of the laboratory methods to determine the erosiveness of powders and the resistance to erosion of various materials were of the vent-plug type, which do not completely simulate gun conditions. Therefore in the early days of the work of Division 1 there seemed to be a need for (a) an erosion-testing gun which could be used to test materials under normal and hypervelocity conditions, (b) a hypervelocity gun that would provide data translatable to guns of larger calibers, and (c) a standardized erosion test in which all resistant materials and propellants would be examined under identical conditions.

Design of Gun

With this end in view the caliber .50 erosion-testing gun was developed by the Franklin Institute for Division 1, NDRC. This gun was composed of three major units (a) the receiver and mount, (b) the firing mechanism, and (c) the test barrel.

The test barrel was a standard 45-in. monobloc barrel modified as shown in Figure 1. The chamber, origin of rifling, and bullet seat were shaped to receive a 20-mm cartridge case necked down to hold a caliber .50 bullet. The depth of rifling was made 0.010 in. instead of the usual 0.005 in. The enlarged chamber permitted a greater powder charge for attainment of high velocities and the increased depth of rifling provided a greater area of contact between the rotating band of the bullet and the rifling, a necessary condition because of the high velocities used.

Of many of the materials tested, it would have been difficult to make a full-length barrel. Furthermore, since erosion is confined to the region of the origin of rifling, this was unnecessary. Accordingly, a special gun-barrel assembly was developed into which short liners could be inserted. The assembly consisted of three units as shown in Figure 2: (a) the chamber section, (b) the breech, and (c) the muzzle section. The liner was 8 in. in length and was pressed into the breech. This gun was very economical because the various units could be used many times.

Firing Conditions

The firing conditions were chosen so as to impart a muzzle velocity of 3,500 to 3,750 fps to a 710-grain projectile fired from the 45-in. barrel. This required a powder charge of 476 grains of double-base (20% nitroglycerin) powder of a web size that would keep the maximum pressure in the range 56,000 to 58,000 psi (copper). Occasionally a single-base (IMR) powder was employed to observe effects with a cooler powder at the same muzzle velocity.

The resistance to erosion of different materials and the gun performance with those materials were studied with three principal types of projectiles: (a) the caliber .50 ball bullet, M2, (b) a copper-banded artillery-type bullet, and (c) a steel pre-engraved projectile. The ball bullets were used with steel barrels of standard depth of rifling for erosion tests when the accuracy life was not of any interest.

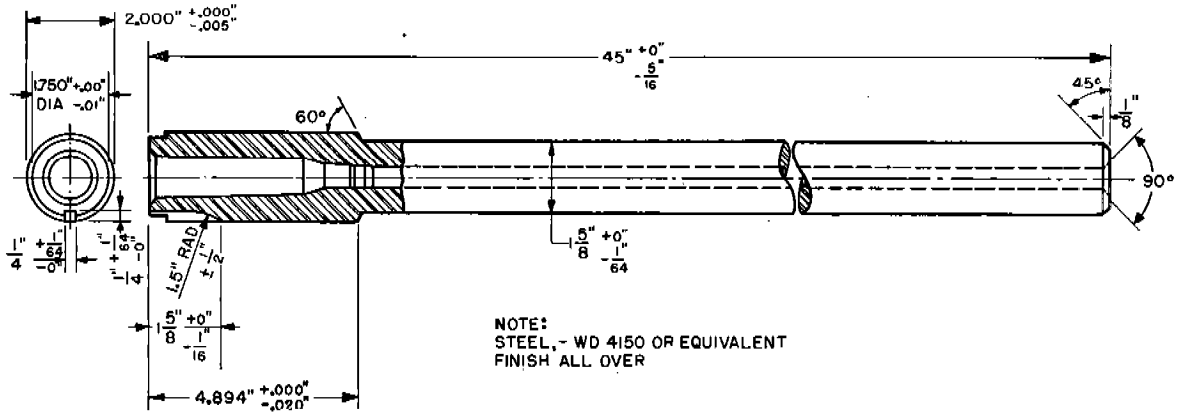


Figure 1. Barrel for caliber .50 erosion-testing gun. (This figure has appeared as Figure 4 of NDRC Report No. A-450.)

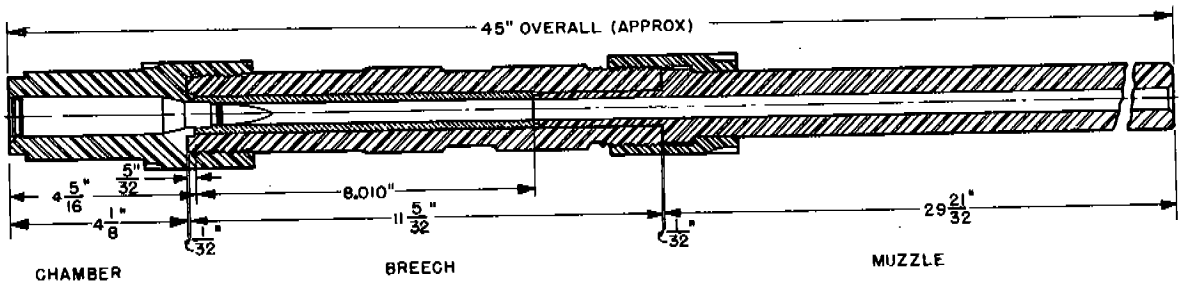


FIGURE 2. Liner-barrel assembly for caliber .50 erosion-testing gun. (This figure has appeared as Figure 7 of NDRC Report No. A-450.)

The artillery-type bullets were fired at hypervelocity to determine velocity-life and accuracy-life of a liner assembly. This bullet, shown in Figure 3A, was so designed that accuracy would not be too critically affected by erosion at the origin of rifling and so as to produce minimum interference of the band with the grooves. A band width of 0.50 in. was found to be necessary in order to yield sharp engraving without widening of the grooves.

The steel pre-engraved projectile in Figure 3B,

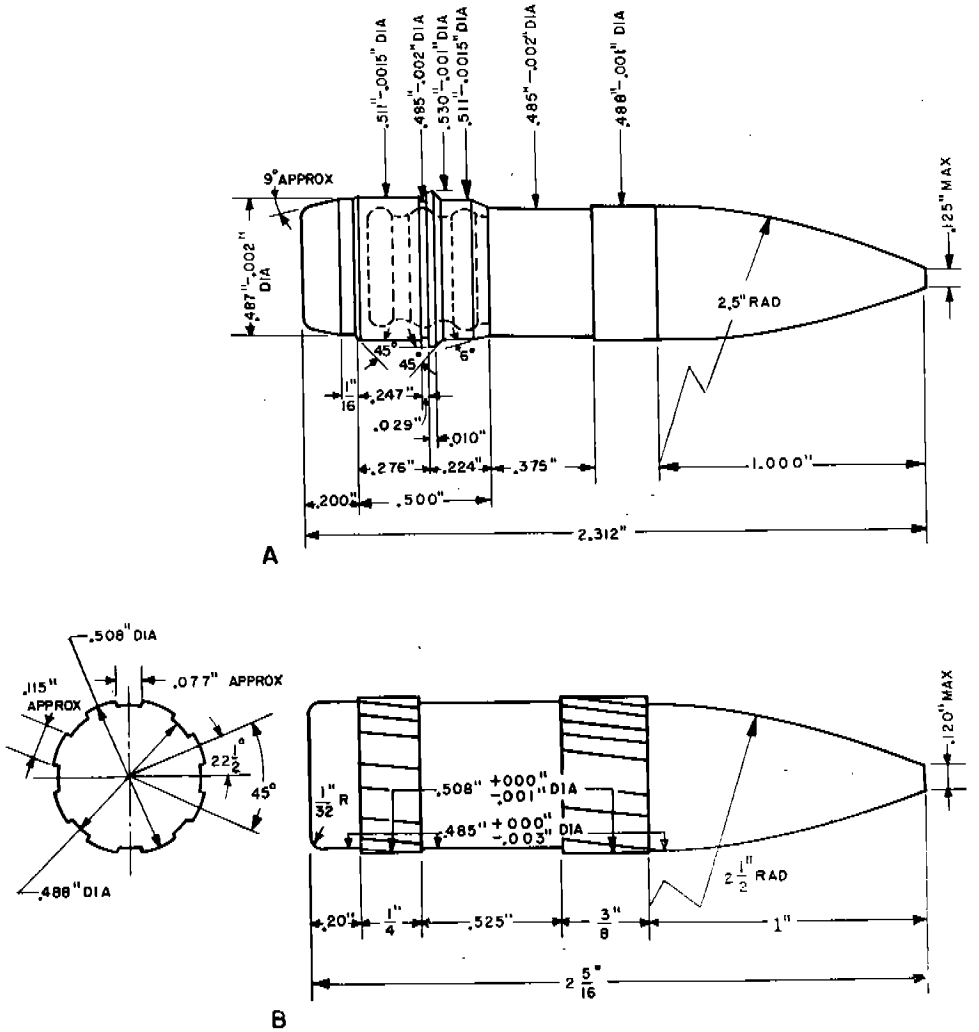


FIGURE 3. Artillery-type (A) and pre-engraved projectiles (B) for caliber .50 erosion-testing gun. (This figure has appeared as Figures 11 and 12 of NDRC Report No. A-450.)

which is discussed in detail in Chapter 27, was used in special tests when it was desired to study the behavior of a liner or bore surface coating in the nearly complete absence of engraving forces and friction.

Three firing schedules were standardized permitting a choice of the severity of the conditions. These schedules and their uses are given in Table 1. After each group of 35, 70, or 140 rounds, respectively, the gun was plug gauged and star gauged, examined with a boroscope, and the bore surface photographed. In most cases the liners or barrels were examined metallographically.[77,124] Control tests were made with gun steel barrels (SAE 4150, modified) for each of three firing schedules.

Criteria for Barrel Failure

Gun barrels or liner assemblies were considered to have failed when (a) velocity had dropped 200 fps, (b) the mean radius of dispersion at 100 ft had increased to three times its initial value or when bullets produced keyholes, or (c) the liner material had changed in some way that prevented further firing.

Maximum powder gas pressures were measured with a crusher gauge of the copper cylinder type. Velocity was determined with two screens 37 ft apart connected to an Aberdeen chronograph, the first screen being 8 ft from the muzzle. The mean radius of dispersion was calculated, in many of the tests, from targets placed at 100 ft.

Erosion on the lands was followed with a set of plug gauges which would give readings in steps of 0.002 in. from 0.490 to 0.516. Erosion across the grooves could be measured with a set of rifled plug gauges by steps of 0.002 in. from 0.511 in. to 0.529 in. These measurements were plotted as bore profiles at various stages of erosion. These gauges were very satisfactory as far as simplicity and speed were concerned, but they could be used only in measuring uniformly tapered erosion. They were not suitable, for example, in measuring the erosion of bore surfaces which had been plated. A small area of the resistant material adhering to the surface would easily stop the advance of the plug gauge. To avoid this difficulty a star gauge was constructed that could measure land and groove diameter within 0.0002 in.

The progress of erosion was also followed by both visual and photographic examination of the bore surface through a boroscope. For many tests, barrel temperatures were ascertained by attaching iron–constantan thermocouples on the outside of the barrel at $10\frac{1}{2}$ in. from the breech face.

Projectiles were recovered in screened sawdust after each group of rounds. Measurements of band diameter, width and depth of engraving, and observation of body engraving indicated the effect of erosion on the behavior of the projectile in the bore.

Uses of Erosion-Testing Gun

The caliber .50 erosion-testing gun had a wide range of usefulness as a research tool. Although primarily designed and most extensively used for the first of the problems listed below, it has been employed to study many others.

(1) Determination of the erosion-resistance of materials under hypervelocity conditions (Section 16.3.5).

(2) Determination of the erosiveness of various propellants at 3,300 fps (Chapter 15).

(3) Design and behavior of projectiles for hyper-

Table 1. Firing schedules used with caliber .50 erosion-testing gun.

Schedule	Cycle	Use
I	(1) 10 rounds to determine pressure and velocity (2) 20 rounds at 4 rounds per min for erosion (3) 5 rounds for projectile recovery	For preliminary test of a new material for erosion resistance, with ball bullets M2; rifling depth 0.005 in.
II	(1) 10 rounds to determine pressure and velocity (2) 55 rounds at 4 rounds per min for erosion (3) 5 rounds for projectile recovery	Adopted as standard for barrels with rifling depth of 0.010 in. and PE projectiles, for testing erosiveness of powders and erosion resistance of liners and coatings.
III	(1) 10 rounds to determine pressure and velocity (2) 130 rounds at 6 rounds per min for erosion	Adopted as a standard for testing liners and coatings more resistant to erosion than gun steel, using ball bullets, M2 and a rifling depth of 0.010 in.



velocity guns, particularly of pre-engraved projectiles (Chapters 27 and 31).

(4) Design and behavior of the Fisa protector (Chapter 32).

(5) The fundamental causes of erosion (Chapter 13).

(6) Erosion at the joints of liners (Section 10.3.8); and

(7) The causes of body engraving (Section 10.4.2).

At about the same time that the caliber .50 erosion testing gun was planned, the Army Ordnance Department was interested in a device for accelerated erosion tests. What was termed an "erosion gauge" was developed by Frankford Arsenal[313] in cooperation with Aberdeen Proving Ground and Watertown Arsenal. This device was similar in principle to the caliber .50 erosion-testing gun, but differed in that the bore was caliber .30. Experience in its use,[314, 315] indicated that the smaller size offered no marked advantage and some disadvantages. Thereupon it was decided by the Army Ordnance Department that its establishments should use the type of erosion-testing gun developed by the Franklin Institute.

11.2.2 Caliber .50 Machine Guns

Introduction

The hypervelocity caliber .50 erosion-testing gun just described had one serious limitation, which was that rapid-fire tests could not be made with it.[b] The only reliable machine guns available for such tests were the Browning caliber .30 and caliber .50. Preliminary trials with the caliber .30 gun (Section 16.3.7) indicated that the rate of erosion was too slight, and therefore attention was concentrated on the caliber .50. At first it was hoped that by control of the barrel temperature of this gun through variation of the rate of fire it would be possible to simulate the conditions of erosion in a gun of higher velocity and larger caliber, such as the 120-mm gun, M1. For this purpose the special firing schedule (designated as "GL-135" in Section 23.1.3) was developed.[49]

Subsequent experience in the testing of materials by this and other schedules led to the conclusion that it is not possible to evaluate completely hypervelocity performance in this way. Nevertheless the caliber .50 machine gun proved to be a useful tool for the study of erosion in two ways. The observations made on steel barrels, both plain and chromium plated, after they had been fired in this gun, formed the basis for some of the conclusions expressed in Chapter 13 concerning the causes of erosion. This was especially true with respect to the phenomenon of swaging of the rifling, described in Sections 10.5.3 and 13.4.2.

In the second place, this gun served well for tests of the erosion resistance of metals and alloys, as outlined in Section 16.3.8. For this purpose they were prepared either as short breech liners or as coatings on a steel barrel or steel liner. Eventually it became possible to improve the life of caliber .50 machine gun barrels by the use of stellite liners (described in Chapter 22), of tapered chromium plate applied on a hardened steel bore surface (Chapter 23), and finally by a combination of these two improvements (described in Chapter 24).

Geophysical Laboratory Liner Design[81]

The first type of liner assembly was developed at the Geophysical Laboratory, CIW in 1942 and 1943, for testing the erosion resistance of a number of metals and alloys that appeared promising as a result of erosion vent plug tests (Section 11.2.3). The heavy barrel[c] was selected for this purpose because its large wall thickness near the breech end facilitated the insertion of a liner.

The design of liner assembly shown in Figure 4 proved to be the most satisfactory one for inserting a liner in a heavy barrel. The liner was inserted by pressing it into the middle piece on a taper. The other two pieces were screwed to the middle one, as shown, to form the completed assembly. The liner was usually 5 in. long but a 9-in. liner was sometimes inserted.

If the barrel was not subjected to too severe a firing schedule, the assembly could be used for another test by inserting a new liner. Although it was found that the press fit was sufficient to prevent the rotation of a liner under normal conditions, it was usually secured against rotation by a pin extending from the outside of the barrel into the liner to within $\frac{1}{16}$ in. from the bore.

Since the joint at the rear end of the liner was covered by the cartridge case, no special method of seal-

[b] It had been planned to overcome this deficiency by adapting a 20-mm automatic gun mechanism to use the barrel of the caliber .50 erosion testing gun. Some preliminary tests were made with Model I of the mechanism described in Chapter 28 shortly before Division 1's contracts were terminated.

[c] By "heavy barrel" is meant the 45-in. barrel weighing 28 to 30 lb. Barrels made according to four different drawing numbers have been used: D28253-11, D28253A, D28253-A3, and D28269-8X. These differ only in small variations of outside contour.

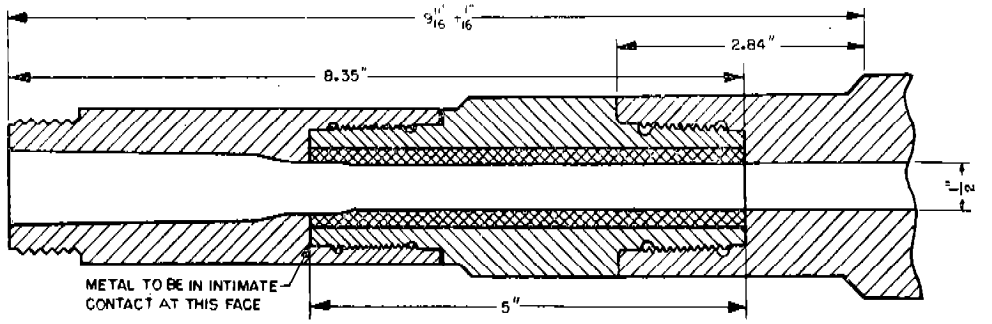


FIGURE 4. Design of liner for caliber .50 heavy machine gun barrel used at Geophysical Laboratory for test of materials. (This figure has appeared as Figure 2 of NDRC Report No. A-409.)

ing was used there. In order to prevent the powder gases from leaking through the forward joint into the space between the liner and the barrel, a washer was inserted at this junction. This washer is not shown in Figure 4.

It was desirable to use as thin a liner as possible, first, because it was very difficult to obtain thick rods of some of the materials, and second, in order to leave as great a thickness of gun steel as possible so as not to weaken the barrel unduly. A minimum wall thickness for the liner of ⅛ in. was decided upon following the failure of a liner made of caliber .50 gun steel which was but 1/16 in. thick.

As described in Part VI these liners were used to test electroplates of chromium and other metals, coatings of the bore surface, gun steel, special steels, molybdenum, Stellite No. 21, and other materials. It was necessary to modify the assembly described above in order to test certain materials, particularly molybdenum.

CRANE COMPANY LINER DESIGN[30]

The design of liner for the heavy barrel just described was also used by the Crane Company in its first experiments with testing erosion-resistant materials. Then, when stellite was introduced, it was found necessary to develop a new design of liner having a flange, as described in Section 22.2. This design, which used a liner 9 in. long, shrink-fitted into a steel barrel and held in place by a steel retainer, is shown in Figure 1 of Chapter 22.

The later success of this type of liner adapted to caliber .50 aircraft barrels[d] and its production in large quantities had the important advantage, as far as further erosion investigations were concerned, that a source of barrels recessed to receive liners greatly simplified the testing of a wide variety of bore-surface materials with the results described in Section 16.4.

A modification of the Crane design of liner, which differed in that it did not use a shoulder flange, was used for chromium-base alloys, as described in Section 17.4.3.

TEST PROCEDURE

The firing schedules to which both these liner assemblies were subjected varied according to the information desired. For example, in comparing liners of metals showing high resistance to erosion, relatively severe schedules had to be employed. The various schedules that were used, and the applicability of each, are summarized in Section 23.1.3.

The performance of the liner assemblies was judged by the muzzle velocity and accuracy. Other data, such as gauge measurements, hardness, microscopic observation, and some temperature measurements, were obtained in a routine manner. Ballistic data for caliber .50 ammunition have been summarized in a report[312] from Frankford Arsenal.

11.2.3 The Erosion Vent Plug

GENERAL DESCRIPTION

Vent-plug tests have long been used by a large number of investigators as a means of studying gun erosion. A number of summaries[16, 260, 479] of the vent-plug method have appeared.

The explosion vessel that is commonly used for erosion vent-plug tests is arranged with three openings. One is fitted with some means of firing the charge, such as an electric connection for firing the powder by

[d] By "aircraft barrel" is meant the 36-in. barrel weighing about 10 lb made according to Ordnance Department drawing D35348A or D28272.

heating a wire to incandescence; a second opening is fitted with a pressure gauge; and the third is arranged so that a cylindrical test-plug with a small axial hole can be inserted in it. The gases formed when a charge of powder is fired in the explosion vessel escape through this hole with high velocity and enlarge its diameter by removal of metal. The extent of vent-plug erosion is usually determined by measuring the loss of weight of the plug.

Improved Vent-plug Apparatus

A vent-plug apparatus, employing less severe conditions than those used by earlier investigations has been developed.[27] The use of precise laboratory techniques contributed to the reproducibility of the results, which was achieved through better control of the rate of burning of the powder by closing the muzzle end of the vent with a rupture disk. The disk allowed the powder gases to be released always at the same predetermined pressure.

The apparatus, shown in Figure 5, consisted of a cylindrical steel block having four holes that met at the center, into each of which was screwed a steel plug. When a charge of propellant was exploded inside the block, pressure was built up until a copper or brass disk ruptured and released the gas through the vent. In this apparatus there was provision for both a crusher gauge and a piezoelectric gauge. The erosion plug A was a cylinder ½ in. in outside diameter and ⅝ in. long.

Two sets of test conditions were adopted in testing with this apparatus: (1) A vent 1/16 in. in diameter subjected to the action of the gases from double-base powder (4.3 g, loading density 0.187 g/cc, which produced maximum pressures in the neighborhood of 35,000 psi with a new vent); (2) A vent ⅛ in. in diameter and a charge of single-base powder chosen to yield the same maximum pressure as above. Conditions (1) are more severe than those of (2). The latter give erosion rates for steel samples that are roughly equivalent to the rate of increase in groove diameter per round found in certain medium-caliber guns.[75]

The vent plug has been used for comparing the erosion of many metals and alloys both with single-base and double-base powders, as recorded in Chapter 16. The erosiveness of various propellants was compared by means of vent plugs of gun steel, as described in Chapter 15.

There are several objections to using the data obtained from vent-plug tests, without further consideration, to evaluate the expected performance of a barrel or liner made of a new material. For instance, such tests do not indicate resistance to mechanical wear such as by abrasion and swaging. The question of the interpretation of the results of vent-plug tests from the viewpoint of gun erosion has been discussed elsewhere.[16]

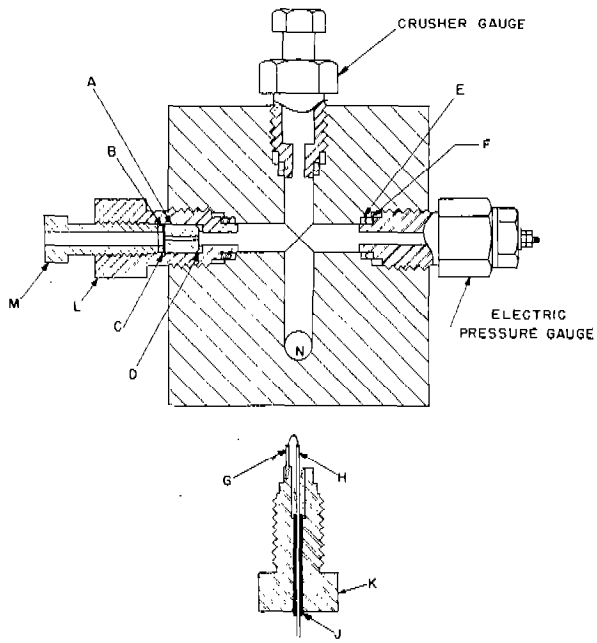


Figure 5. Erosion vent-plug apparatus. The ignition plug K, which carried a platinum filament for electric ignition, was screwed into the horizontal hole N after the powder had been placed in that hole. (This figure has appeared as Figure 1 of NDRC Report No. A-148.)

Rifle Barrel Used as a Vent

The vent plug, in an apparatus very similar to that described above, was used to study erosion by mixtures of carbon monoxide and carbon dioxide.[62] Carbon monoxide and oxygen in various proportions were introduced under pressure into the explosion chamber and ignited electrically. A series of ratios of carbon monoxide to dioxide in the eroding gases was obtained by varying the oxygen content of the exploding mixture. These tests and their results are discussed in Section 14.3.

One of the objects of this research was to ascertain the possible importance of the formation of iron carbonyl in erosion.[63] In order to recover a detectable amount of iron carbonyl it was necessary to increase greatly the area of the surface exposed to the gases over that of the standard vent plug. This was accomplished by using the bore of a B-17 Enfield rifle as a

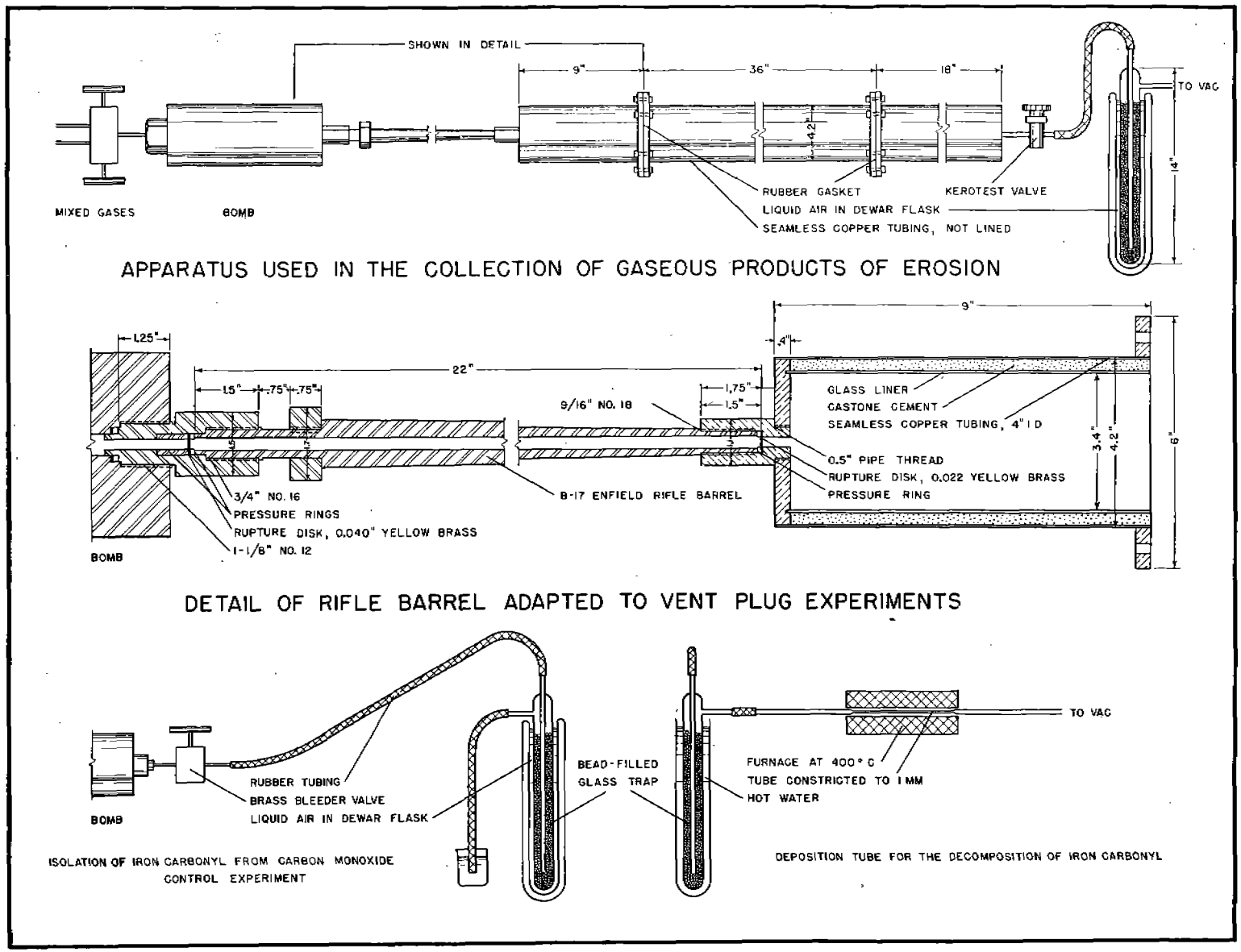


FIGURE 6. Apparatus used in the collection of the gaseous products of erosion of a rifle barrel adapted to vent-plug experiments. (This figure has appeared as Figure 31 of NDRC Report No. A-311.)

vent. The apparatus is shown in Figure 6. The explosive mixture of oxygen and carbon monoxide was contained in a pressure vessel of 62.5-ml volume. The rifled portion of an Enfield barrel was machined to thread directly into the pressure vessel. The breech end was closed with a rupture disk which would burst at a piezo pressure of 25,500 psi. A thinner rupture disk which would burst at 10,500 psi closed the muzzle end.

The muzzle end was machined for attachment, in a vacuum-tight manner, to a large sealed tube of copper called the muzzle tube. The first 9 in. of this tube were lined with glass.

The muzzle tube was connected through a Kerotest valve to a glass trap cooled in a bath of liquid air. Volatile products of erosion were condensed in this trap. The original report[63] contains complete descriptions of the development of the above arrangement, of many pieces of auxiliary apparatus, such as that used to purify the carbon monoxide from iron pentacarbonyl, and of analytical apparatus for identifying the presence of volatile iron compounds, in particular the carbonyl, in the products condensed in the cooled trap.

In performing the experiment the muzzle tube and trap were well evacuated. The Kerotest valve was closed momentarily while the mixture of carbon monoxide and oxygen, or in some experiments a standard solid propellant, was ignited. The resulting gases and vapors were then slowly pumped out through the trap. The trap was sealed off and removed about 30 min later, and the volatile products were transported through a heated capillary tube with a carrier gas while the trap was slowly warmed. A deposit of dark-colored material in the fine capillary, illustrated in Figure 11 of Chapter 14, indicated the presence of a volatile iron compound. If, when the material was decomposed, analysis of the gaseous product indicated the presence of carbon monoxide, the volatile compound was taken to be iron carbonyl.

The identification of iron carbonyl among the erosion products in these experiments with gas mixtures and solid propellants and a description of the various solid deposits in different parts of the apparatus is fully described in Section 14.3.4.

11.2.4 Erosion Vents with D-shaped Cross Section

Studies of Cracking and Mild Erosion

An apparatus similar in principle to that employed with the usual vent plug, described in Section 11.2.3, was devised[51] to study surface changes such as cracking. The surfaces were to be observed and the effects to be photographed with a comparison microscope. It was desirable to follow the course of surface changes through many rounds. The apparatus was designed, therefore, so that removable specimens with flat surfaces could be used. The use of this method to evaluate metals and alloys with respect to erosion resistance is mentioned in Section 16.3.1.

Figure 7 shows a cross section of the apparatus. The "gun" G in which the charge was burned was the receiver of a caliber .30 Army rifle, M1903, and the

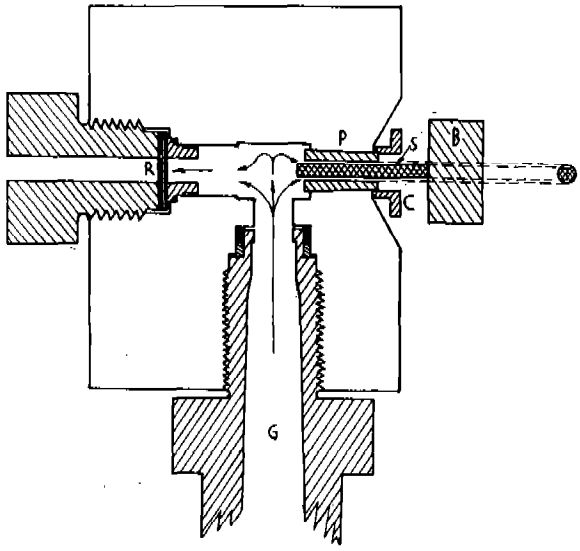


Figure 7. Modified erosion vent apparatus (with D-shaped vents) for study of surface cracking. (This figure has appeared as Figure 1 of NDRC Report No. A-271.)

charges were prepared in caliber .30 cartridge cases. The test specimen S was made from machined round stock. Two flat surfaces were milled on diametrically opposite sides of the rod which was inserted with a good fit into the hole in the cone-shaped plug P. The removable steel bridge B prevented the specimen from being ejected as a projectile from the explosion vessel. The apparatus could function without the collar C but this was found to prevent occasional loosening of the cone-shaped plug in the wall of the vessel. Maximum pressure was controlled by a brass rupture disk R. When inserted, the specimen provided D-shaped vents through which the hot powder gases passed over the flat surfaces. The surfaces were of different widths; hence the cross sections of the vents were different and two sets of conditions could be

studied simultaneously. The exposed wall of the hole in the plug P was, of course, also subjected to erosion. The plug P had to be replaced from time to time to keep the conditions in the vents constant.

The amount and kind of powder used, and the thickness of the rupture disk controlled the time-temperature relation, the composition of the eroding gases, the maximum pressure, and the rate of rise of pressure. All these things were important in obtaining the desired conditions. Because the D-shaped orifices had a much smaller cross-sectional area than the hole punctured in the rupture disk most of the gas went out through the rupture disk when it broke. The fraction of the total gas that passed over the test surfaces depended on the rate of rise of pressure before the rupture disk broke and the maximum pressure which was attained at the moment when the disk ruptured. With this arrangement it was possible to erode the test surfaces at rates much more comparable with erosion rates in guns than is practicable with the conventional vent plug. Erosion rates with this apparatus are plotted in Figure 13 of Chapter 14.

In order to study cracking, it was necessary to select a powder and size of charge that would not cause surface melting but would be severe enough to exhibit cracking after a few rounds. It was found that the conditions with 2.5 g of caliber .45 pistol powder and a $\frac{1}{16}$-in. rupture disk caused noticeable cracking of SAE 4140 gun steel in four rounds; these conditions were chosen as standard. In order to rate the different materials, the procedure was to fire a certain number of rounds and compare the degree of cracking. The results obtained with a variety of metals and alloys are reported elsewhere.[51]

Although the conditions of temperature and pressure as a function of time and the composition of the eroding gases were quite similar to those encountered in guns there were two departures from gun-firing conditions which may be important in the study of cracking. To some extent, the powder gases streamed over the test surfaces during the period in which the pressure was building up, whereas in guns the gases come over as a single blast when the projectile passes. This probably does not constitute a radical departure because in a similar vessel it could be shown that, with a powder burning as quickly as pistol powder, the major portion of the gas issuing through the D-vents does so after maximum pressure is attained.

A more radical departure from the conditions in a gun occurs because of the lack of any wiping action. Thus a coating of the products of a reaction between the specimen and the powder gases builds up at the test surface. This coating is not subject to removal as it would be in a gun by the passage of a projectile. A film of thermal insulation may thus be established when several rounds are ignited in succession, and, in fact, a difference in the degree of cracking was observed between a specimen cleaned off after every few rounds and one subjected to from 20 to 30 rounds without removing the reaction products.

The apparatus described above was also used in the study by a radioactive tracer technique, discussed in Section 14.4, of the effect of sulfur and other components of black powder on the erosion of gun steel. The flat surfaces of the test rods facilitated the beta-ray measurements.[53]

Apparatus Used in Studies with X-Ray and Electron Diffraction

Much information concerning the chemical alteration of surfaces exposed to powder gases was obtained by means of x-ray and electron diffraction (Section 11.5.2). For some of this work an explosion vessel, shown in Figure 8, was designed in which the pressure and temperature as a function of time corresponded approximately to those in a medium-caliber gun.[31] This method, like the one described above, was also used to a limited extent to test materials (given in Section 16.3.1) for erosion resistance.

Following ignition of the powder, the gases passed over two sides of a rectangular specimen of gun steel (0.1x0.2x0.8 in.), held in a cylindrical opening, and escaped from the vessel through a vent plug. The size of the orifice in the vent plug, usually $\frac{1}{16}$ in. in diameter, and the amount and type of powder were the factors which determined the pressure in the explosion chamber. With 3.5 and 2.5 g FNH-M1 powder the measured maximum pressure was 51,000 and 37,000 psi respectively; with 2.5 g of a specially prepared double-base powder the maximum pressure was 43,000 psi.

Scrupulous care was taken to prevent contamination of the test rods with the result that no foreign material, particularly inorganic salts, was detectable in the diffraction patterns obtained from the surfaces of control specimens.

In such studies it is naturally necessary to avoid melting, but it is also necessary to obtain a certain minimum thickness of reaction products even though under ideal conditions it is possible to obtain good electron diffraction patterns with layers only a few



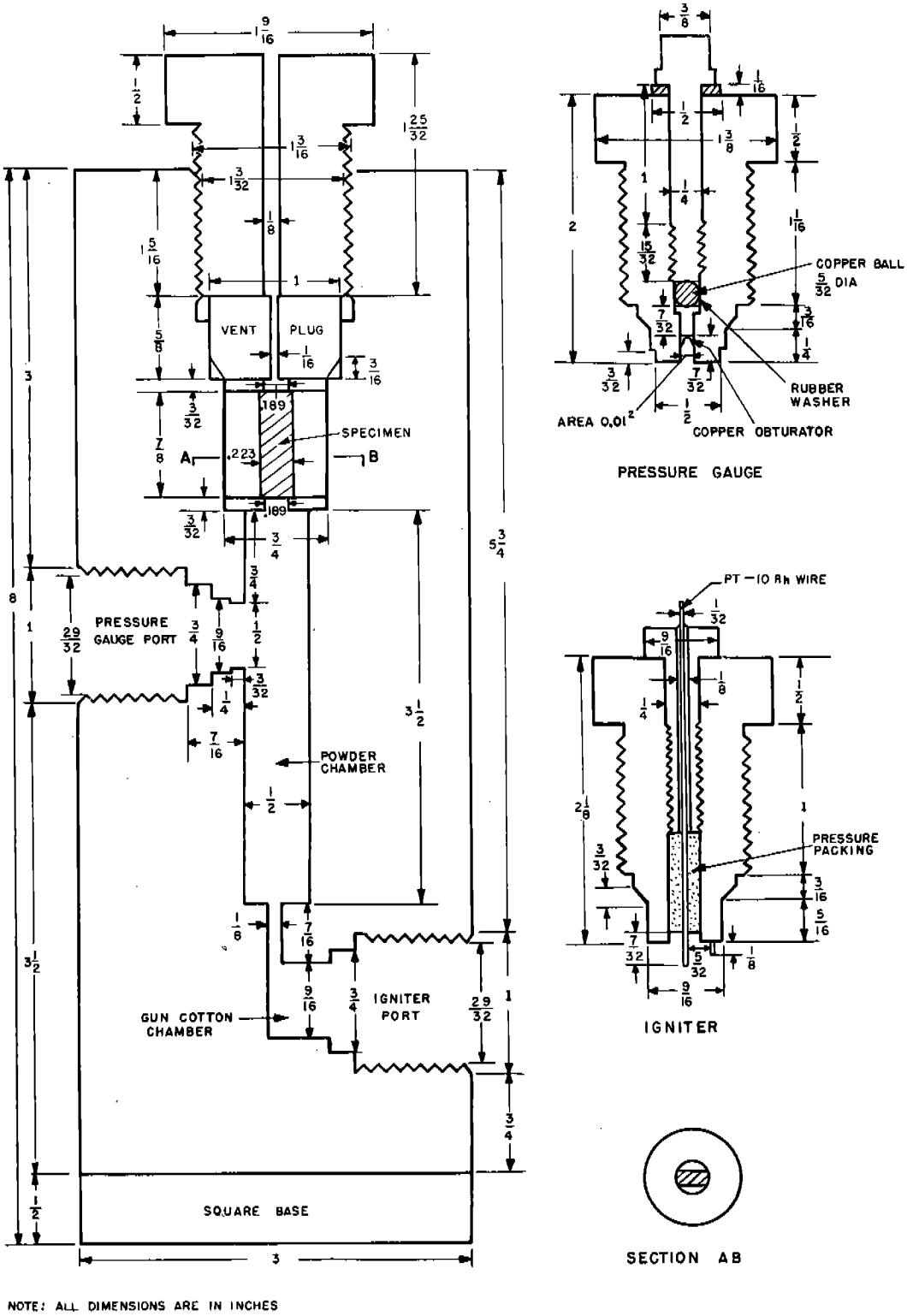


FIGURE 8. Second explosion vessel using D-shaped vents. (This figure has appeared as Figure 1 of NDRC Report No. A-199.)

tens of molecules thick. Blocks of gun steel held in recesses in the side walls of the explosion vessel, for example, acquired such thin films of reaction products that even fair diffraction patterns were extremely difficult to obtain.

The results of the studies on blocks of gun steel are given in Section 12.2.2.

11.2.5 Circular Vents in Stressed Blocks

Stresses in guns might facilitate erosion by exposing fresh metal surfaces to the powder gases. Conceivably, this might result in continuously renewed chemical reaction or absorption of the powder gases. An experiment was set up to test such a possibility.[103]

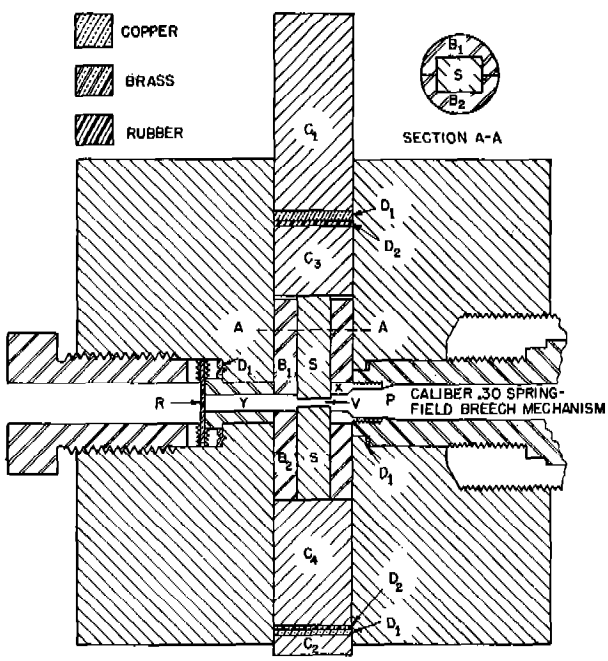


FIGURE 9. Stressed erosion-vent apparatus. (This figure has appeared as Figure 1 of NDRC Report No. A-431.)

Figure 9 shows a cross section of the apparatus in which a type of vent plug was used. The explosion vessel was cylindrical about the vertical axis. Each section shown, except that of the specimen, is cylindrical about either the vertical or the horizontal axis of the containing chamber. All parts were made of steel except the brass rupture disk R and the copper and rubber obturating disks D_1 and D_2. Pressure was applied from a hydraulic press to the parts in the vertical chamber and was transmitted to the ends of the specimens through the hardened steel cylinders C_1 and C_2, the copper and rubber obturating disks D_1 and D_2, and two additional hardened cylinders C_3 and C_4. The specimen was rectangular in cross section, as shown in Section A-A, and the space between it and the cylindrical chamber wall was filled by two steel blocks B_1 and B_2 which occupied almost the entire space but which did not interfere with the compression of the specimen. With this arrangement the cylindrical surface of the hole was in radial compression along the line of intersection with a vertical diametral plane and in radial tension along the intersection with a similar horizontal plane.

The horizontal chamber defined the path of the gas stream. The charge was contained in a caliber .30 cartridge case which was inserted into the powder chamber P of a caliber .30 Springfield breech mechanism attached to one end of the horizontal chamber. A small replaceable plug X narrowed the gas stream and led it to the entrance of the vent V. After passage through the vent, the gases entered a small chamber Y which was terminated by the rupture disk R. The gas pressure built up behind this disk until it broke, permitting the main flow of gas to pass through the vent.

The ballistic conditions chosen for the tests were obtained with a vent of $\frac{5}{32}$ in. diameter, a charge of 2.5 g of powder NH-M1 (for 37-mm gun M1916), a loading density of 0.47 g/cc, and a brass disk that ruptured under a static pressure of 2,000 atm in calibration tests. The applied stresses on the cross section of the specimen corresponded to pressures in the range of 16,600 to 83,100 psi.

After firing, the diameter of the vent in different directions was measured with a traveling microscope. Any differential change in the diameter of the vent in the vertical or horizontal position indicates a different degree of erosion under tension and under compression, respectively.

As further discussed in Section 13.4.1, the measurements showed that there was no appreciable difference in the diameter for surfaces under tension or under compression.

11.2.6 Collection of Particles and Gases

The collection of solid particles and gases discharged from a small-caliber weapon was facilitated with the design of the collection tube[20] shown in Figure 10. This tube, 4 ft long, was made of Pyrex glass with a 0.12-in. wall and 4-in. diameter. It was hermetically sealed at the two ends by heavy brass caps. The muz-

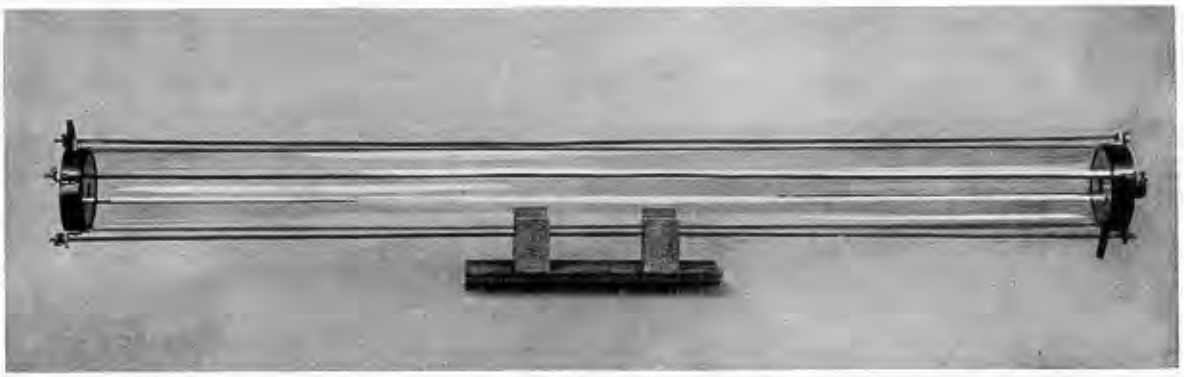


FIGURE 10. Glass tube for collecting gaseous and solid material ejected from the muzzle of a caliber .30 rifle behind the bullet. (This figure has appeared as Figure 1 of NDRC Report No. A-93M.)

zle of a caliber .30 rifle barrel, held in a Mann rest, could be inserted in a gas-tight manner into one cap. When the rifle was fired, the bullet passed down the collection tube and emerged through a renewable disk of thin metal covering a central hole in the cap at the target end of the glass tube. A removable optical system[20] in the bore of the rifle afforded a means of sighting the line of fire with the requisite accuracy.

Exit and entry ports were provided by a radial hole in each of the brass caps. One of these ports was used for evacuating the system. A little heavy grease on the neck of the cartridge case completed the vacuum sealing of the system. The pressure in the collecting tube before firing was reduced to at least 1 cm of Hg, otherwise the mortality rate of the glass tubes was high. In special experiments the pressure was reduced to 1 mm of Hg or less.

The other port could be used to flush out the system with a gas, such as nitrogen, or to permit the collected gases to expand into an evacuated bottle. The latter procedure provided extra room for the gases from high-pressure charges and was used at times in order to collect gas samples. In collecting gas samples the hole left by the bullet was closed immediately by a wad of Plasticene applied by the operator. This procedure was crude, but the apparatus was not designed or used for the refined collection of powder gases.

The chief uses of this apparatus are described in Sections 14.5.3 and 16.3.2. Filings of various metals or nitrides were mixed with the powder charges, otherwise the rounds were standard in all respects. The filings were recovered from the collecting tube, after firing, and examined by x-ray analysis for alteration or formation of reaction products.[28,79]

Some subsidiary experiments were performed with this apparatus in connection with the use of tracers for sulfur[53] and nitrogen.[70] These experiments were devised to study the distribution of the tracer elements in the powder gases, as described in Sections 14.4 and 14.5, respectively.

11.3 OTHER LABORATORY EROSION EXPERIMENTS

11.3.1 Vent Plugs Subjected to Adiabatically Compressed Gases

If a gas at room temperature and 1 atm pressure is compressed adiabatically to about 1,000 atm its temperature will be increased by 1000 C to 3000 C. The actual rise of temperature will depend on the nature of the gas.

This phenomenon opens up the possibility of studying the erosive effect of the individual components of powder gas and also of differentiating between chemical and purely thermal effects by using an inert gas such as argon. With proper design of apparatus it should be possible to control within certain limits the important parameters of time, temperature, and pressure so that they will be of the same order of magnitude as those in a gun.

An apparatus[101] that was used in some preliminary experiments of this nature is illustrated in Figure 11, which shows the assembled compressor and vent plug. The gases were compressed by the piston, which was driven by a falling weight. They were expelled at the bottom of the cylinder through a hole in the side. The bottom of the cylinder was sealed with a piezoelectric gauge protected by a steel disk (not shown). A slot in this disk was lined up with the escape hole so that the piston would not block the efflux of the

CONFIDENTIAL

gases. The escaping gases passed through a vent plug that consisted of a small hole in a washer of the desired material. In some experiments where flat surfaces were desirable, a slit-type vent was formed by mounting two small rectangular blocks of the material to be tested.

The experiments carried out with this apparatus, which are described in Section 14.6, showed its limitations. They also led to a conclusion concerning the desirable form of a more powerful apparatus, which is illustrated in Figure 16 of Chapter 14.

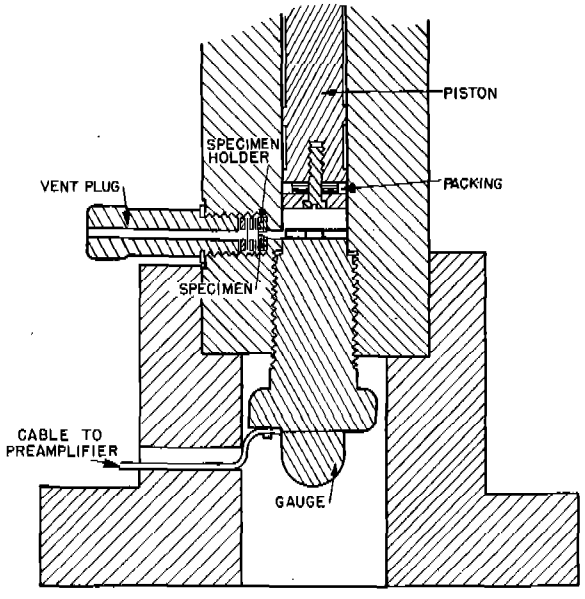


FIGURE 11. Preliminary form of apparatus for adiabatic compression of gases (see Figure 16 in Chapter 14 for proposed improved form). (This figure has appeared as Figure 2 of NDRC Report No. A-429.)

11.3.2 Electron Bombardment Apparatus

An experiment was devised for the purpose of evaluating the effects of heat alone on the bore surface.[104] Electrons from a hot tungsten filament were made to strike a specimen of gun steel or other material causing the surface of the specimen to be heated to a high temperature for a very short time. The use of electron bombardment proved to be amenable to the desired degree of control of time and intensity of heating.

The specimen, mounted on a water-cooled column as shown in Figure 12, was a rod $\frac{5}{32}$ in. in diameter with the end to be exposed carefully polished. This rod formed the anode of a gaseous triode contained in a bell jar under a vacuum of 5×10^{-3} mm of mercury, as shown diagrammatically in Figure 13. The use of nitrogen or argon at these pressures served to reduce the space charge. The specimen was insulated with a Pyrex shield so that only the polished end was effective as the anode. The circuit constants were chosen so that the time of exposure to the bombardment would be about 0.01 sec, which is comparable to the time of exposure of the bore surface to powder gases at the origin of rifling of a 3-in. gun. Electron discharges, usually about 1,000 in number, each lasting about 0.01 sec, were repeated at 3-sec intervals. Power

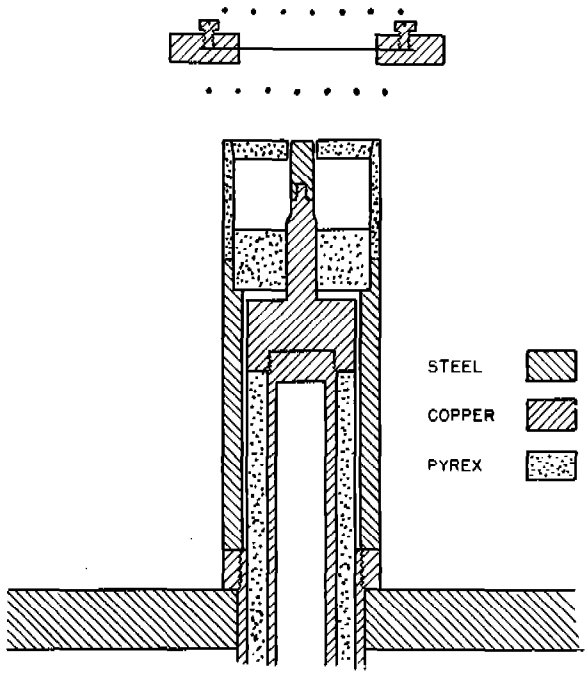


FIGURE 12. Metallic sample mounted as an anode for subjecting it to thermal shock by means of electron bombardment. (See Figure 13 for diagram of electrical circuit of electron bombardment apparatus.) (This figure has appeared as Figure 5 of NDRC Report No. A-432.)

amounting to 20 kw cm^{-2} was applied with each pulse. It was calculated that this amount of energy would be required to raise the surface temperature to the melting point of steel in 0.01 sec.

The results obtained in the course of the development of the apparatus have been reported.[104] It was hoped originally that the bombardment by electrons would provide a simple method for evaluating materials in terms of the purely thermal effect as mentioned in Section 16.3.1. However, an erratic behavior of the discharges, despite very careful control of gas pressure, filament current, and anode voltage, resulted in insufficient accuracy and too poor a degree of repro-

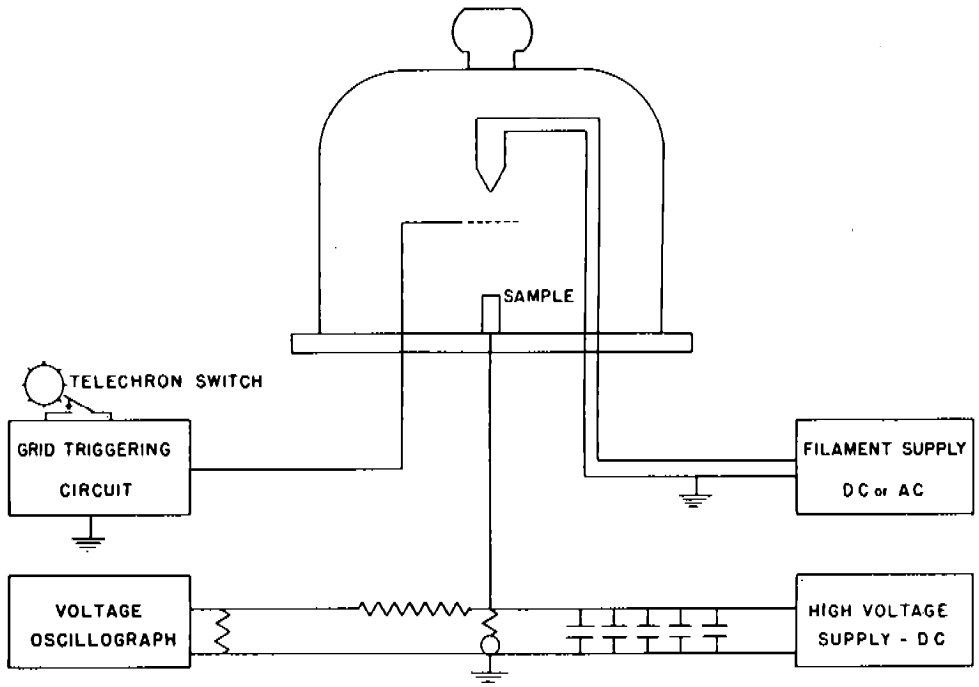


FIGURE 13. Diagram of electrical circuit of electron bombardment apparatus. (See Figure 12 for details of mounting of sample.) (This figure has appeared as Figure 4 of NDRC Report No. A-432.)

ducibility for quantitative evaluation in the hoped-for manner. Better control of the discharge might be obtained with a high-vacuum tube instead of the gaseous triode used.

As a guide to continuation of this work in the future it is well to list the principal difficulties encountered. It was difficult to insulate the specimen, and therefore arcing between the specimen and insulator was a frequently objectionable phenomenon. This probably arose from an accumulation of the electrons which struck the specimen. The discharge did not act uniformly on the surface but tended to concentrate on some areas of the specimen, leaving other parts relatively unaffected. This irregularity vitiated to some extent the calculation of the peak temperature attained by the surface.

Approximately 300 specimens were exposed to electron bombardment. Photographs of the surface and microphotographs of etched cross sections were made. Although the investigation did not result in the development of a simple quantitative method of evaluating materials with respect to the action of heat alone, one result was evident — that, although cracking was observed on specimens fired in nitrogen, none of the specimens exposed showed cracking of the kind observed in guns. This result seems to indicate that the cracking observed on a gun bore surface is not caused by heat alone. This important conclusion is discussed in Section 13.5.3.

11.3.3 Apparatus for Cavitation Erosion

Cavitation erosion was one of the phenomena studied in an attempt to evaluate the erosion resistance of different materials, as described in Section 16.3.3. Apparatus already available at the Armour Research Foundation was used for the purpose.[38] The specimen was submerged in water in the lower end of a nickel tube. This tube was set in vibration by magnetostriction at a frequency of 8,000 c and an amplitude of about 0.05 mm. After a definite length of time, the specimen was dismounted and examined with a binocular microscope to determine the extent of erosion. On the basis of visual examination, the metals were listed according to the degree of resistance to cavitation erosion.

The results showed that the materials that were most resistant to vent-plug erosion, were least resistant to cavitation erosion, and vice versa. The obvious conclusion, therefore, was that vent or gas erosion and cavitation erosion are not related, and that the apparatus is not useful to determine the resistance

of metals and alloys to gas erosion. However, inasmuch as muzzle erosion seems to be the result of mechanical wear, a better correlation might be obtained between cavitation erosion and muzzle erosion. Whether such a correlation exists has not been determined.

11.4 DISENGAGEMENT AND SEGREGATION OF EROSION PRODUCTS[e]

11.4.1 Introduction

In order to make chemical analyses of the products of erosion found on the bore surfaces of guns, it is necessary to disengage them from the unaltered steel. Analysis of the segregated material by a combination of chemical and x-ray techniques gives far more information concerning the nature of the alteration of bore surfaces than does x-ray examination of the products *in situ*, since the latter techniques can only be used to determine what crystalline species are present. Moreover, identification by the x-ray diffraction method of the compounds entrapped in the coppering of guns is not possible unless they are removed from the copper.

In one procedure, described in Section 11.4.2, the bore surface products were dislodged mechanically. In the other two, chemical methods were employed. In one of them the erosion products entrapped in the copper were dislodged by preferentially dissolving the latter, as described in Section 11.4.3. In the other, the erosion products covering the steel surface were dislodged by using a reagent that dissolves the underlying steel. This is discussed in Section 11.4.4.

Preliminary to determining the carbon and nitrogen content of reaction products formed in a gun bore, it was of course necessary to remove grease and particles of unburned powder from the specimens. Ordinarily this was done simply by washing them with petroleum ether to remove grease and with acetone to remove powder particles. The grease was often tenaceously lodged in the fine crack system and was therefore very difficult to remove. In order to insure complete removal it was sometimes necessary to use a Soxhlet extractor. The specimen was removed after each extraction and sufficient time was given for the solvent to seep out of the cracks by capillary action and thus bring the grease to the surface where it could be readily removed by more solvent.

[e] This section has been condensed from sections of NDRC Report A-426,[98] in which complete details for carrying out the different procedures are given.

11.4.2 Mechanical Removal of Erosion Products

The following procedure, which serves as an example of removal of products by mechanical means, was used on two quarter portions of a section of a 3-in. gun liner[98] extending 5.5 to 9 in. from the origin of rifling. The pieces were mounted on a mandrel in a lathe and gun steel was removed from the outside surface until a thickness of 2 mm was obtained. These thin quarter sections were then placed bore surface downward and were flattened out by hammering. The progressive stress-damage cracks (defined in Section 13.5.3) greatly facilitated the operation and, in fact, made it possible to separate the lands and grooves. The specimens were then thoroughly washed with petroleum ether to remove grease and with acetone to remove powder particles, as described above.

Solid reaction products were removed mechanically from areas that formed the walls of these major cracks and were analyzed chemically (for carbon and nitrogen), spectrographically, and by x rays. In addition to removing the crack-filling material, it was possible to dislodge mechanically metallic "beads" that projected over the edges of the cracks. These "beads" were examined by x rays. The results of the analysis of the crack-filling material and of the "beads" are given in Sections 12.4.1 and 12.4.2, respectively.

11.4.3 Removal of Copper and Entrapped Erosion Products

The "copper" that occurs in the central portion of a gun bore, as described in Sections 10.5.4 and 12.3.1, provides a "storehouse" for products of erosion that have been carried forward. A method was developed for removing this copper or gilding metal without attacking the underlying steel or the erosion products. Such a technique not only affords a means of separating the erosion products but also permits examination of the underlying bore surface.

Procedure

Specimens to be decoppered were treated with an ammoniacal solution of ammonium carbonate and hydrogen peroxide at about 5 C. The relative amounts that were found to be expedient were 15 ml ammonia



water (28-29% NH_3), 0.5 g of powdered ammonium carbonate, and 3 ml of 30% hydrogen peroxide. Such a solution is sufficient to dissolve about 0.4 g of copper. It is important that no water be added to the decoppering solution; otherwise attack of the steel takes place. It is also important that the temperature of the solution and steel be held between 0 and 5 C; for if it is inadvertently allowed to warm to room temperature, oxidation of the iron takes place, which is revealed by clouding owing to a precipitation of a hydrated oxide of iron.

Neither steel nor chromium plate was appreciably attacked in a number of experiments as long as the above precautions were observed. Polished specimens were still bright after several hours immersion in the ice-cold solution. Very few of the reaction products formed by the interaction of the powder gases and steel seem to be attacked within the time that they are usually exposed to the solution. Even ferrous oxide, present as wüstite, is not decomposed.

A thin coating of a few microns of copper on a relatively smooth surface was removed in 2 or 3 min, but a coat which is one or more millimeters thick may take many hours and require several treatments with fresh solution. If the surface is deeply eroded, the copper that is lodged in the bottom of the cracks exposes a much smaller surface to the solution than does copper spread out over the bore surface and may require repeated treatment for complete removal.

Treatment of Residues

To recover the gun-erosion products entrapped in the coppering, the mixture was transferred to a container surrounded by ice. The specimen was washed with concentrated ammonia water and treated again, if necessary, with the decoppering solution. The solid particles were promptly separated from the spent solution by centrifuging and were washed in the tube with chilled concentrated ammonia, and finally with "C.P." alcohol. Four washings with each reagent were found to be sufficient. The bulk of the alcohol after centrifuging was decanted as completely as possible, and the remainder removed by cautiously heating at about 55 C, whereupon the tube was placed in a vacuum desiccator. The thoroughly dried residue was then ready for x-ray, microscopic, and chemical analysis. If this procedure is followed, the cementite frequently present in the residues is not attacked, but if the residue is allowed to remain overnight in contact with the decoppering solution at room temperature, it oxidizes and little or no cementite remains.

Analysis of Solutions

The solutions that have been separated from the residue may be evaporated to dryness in a porcelain or platinum basin and any lead, zinc, or sulfate that may be present separated from the copper. Analysis of the solution quickly yields information as to whether the projectiles fired from the gun being examined had had copper or gilding metal rotating bands.

11.4.4 Disengagement of Erosion Products by Attacking the Steel

Another type of segregation of erosion products from the bore surface involved the use of a copper potassium chloride solution. This is a solution which dissolves the ferrite from beneath the erosion products, which may then be analyzed and examined by a combination of techniques. In most instances, as discussed in Section 12.5.2, the products consisted mainly of cementite (Fe_3C). Carbides of alloying elements and nitrides were also found.

Procedure

The reagent was prepared by dissolving 300 g pure copper potassium chloride ($CuCl_2 \cdot 2KCl \cdot 2H_2O$) in a mixture of 65 ml of concentrated hydrochloric acid and about 800 ml of water. The solution was filtered through asbestos and diluted with water to a volume of one liter.

The reagent was used at room temperature and was mechanically stirred to accelerate decomposition of the steel. During this decomposition, copper was deposited on the specimen but was redissolved by the time the ferrite was completely dissolved. Cuprous chloride was also formed; it is soluble in the reagent but somewhat insoluble in water. Washing of all specimens and segregated residues, therefore, was done first with portions of the fresh solution before washing with water.

The reagent was applied directly to the bore surface of a gun section, remaining in contact only long enough to dissolve the immediately underlying steel. The flakes were then picked off. Since the steel was not completely decomposed in this case, the copper deposited in the course of the reaction was not dis-

solved and had to be removed by the decoppering technique previously described in Section 11.4.3.

Relative Insolubility of Compounds in the Reagent

The success that was obtained with such a reagent in segregating cementite and other bore-surface products was due to the fact that they have greater resistance to attack by the reagent than has iron. Thus the erosion products are not "insoluble" in the reagent in the sense that the term "insolubility" is normally used. It is important that the reagent not be allowed to remain in contact with the specimen for too long a time as it dissolves erosion products other than cementite. Eventually even cementite may decompose in the solution.

Products other than cementite were segregated from steel and from eroded bore surfaces by means of this reagent. Thus from a plain carbon steel no cementite was obtained but instead alabandite, a crystalline form of manganese sulfide, together with a highly carbonaceous residue. Nitrides were frequently segregated from the eroded bore surfaces. Their relative insolubility in the reagent is discussed in Section 12.5.2.

Even more erosion products were segregated with a solution of copper potassium chloride to which no acid had been added. However, quantitative analysis of them was made impossible owing to rapid hydrolysis of iron with formation of a presumably hydrated oxide of iron. The non-acid solution, however, was useful when only x-ray analysis of the products was required.

Novel Method of Studying Crack Systems

The crystals of cementite in outer white layers that had been removed by means of the copper potassium chloride solution (see Section 12.5.1) were so coherent that when care was exercised they could be removed as scales which comprised a cast of the reticulated crack system. A refined method of obtaining such a cast consisted of coating with a Vinylite resin the eroded surface of a thin section taken parallel to the bore surface and then dissolving the ferrite away from the other side, whereupon the flakes adhered to the Vinylite. The Vinylite coating and the adherent erosion products was called a "plaque." Stereoscopic photographs of a number of plaques were taken. One of a pair of photographs is reproduced in Figure 14. Plaques may prove useful in studies of crack systems. They should not be confused with the replica films[365] that have been used to study the eroded surface of a gun bore.

11.4.5 Fractionation of Erosion Products

Erosion products disengaged from the bore surface were sometimes separated from one another by elutriation in an organic solvent, such as alcohol. Two refinements of the ordinary elutriation process were employed. The particles stirred up in the liquid were separated (1) by centrifuging the suspensions for different lengths of time, and (2) by holding a magnet near the bottom of the container when decanting the liquid.

11.5 TECHNIQUES USED TO EXAMINE THE PRODUCTS OF EROSION

11.5.1 Visual and Metallographic Examination of Bore Surfaces

The visual examination of eroded bore surfaces is not a technique in the same sense as is examination by x-ray or electron diffraction. Much depends on the acuteness of observation of the investigator, his knowledge of what might be expected to happen in guns, and his general experience in carefully examining gun bores. In short, he must be a detective. His results are not only difficult to describe but also they are sometimes difficult to photograph in such a way as to present to the reader what the investigator himself sees.

The Greenough-type stereoscopic microscope has been used[112] recently to relate the topography of the bore surface with positions in the gun, with various structures and constituents of the surface, and with various processes and stages of erosion. The typical surface features of gun bores are more readily interpreted when observed stereoscopically than when seen in photographs, such as those shown in Section 10.5.2.

Metallographic examination of sections cut normal to the bore surface when polished and etched reveals the character of the surface, particularly the layers which are present. Different etchants have been used to show the constituents present in these layers which are described in Section 12.1.2.

Careful microscopic observation of the altered layer formed in the caliber .50 erosion testing gun



have led to interesting conclusions concerning its role in gun erosion.[124] The salient features of these conclusions are given in Section 13.2.3.

11.5.2 Examination by X-Ray and Electron Diffraction

Relative Advantages of the Two Techniques

Examination of eroded gun bores and test specimens by means of x-ray and electron diffraction has yielded much information concerning chemical substances formed during erosion. The special utility of these methods is due to the fact that only a minute quantity of material is necessary for study.

By the use of electron diffraction notable success has been attained in the identification of films of crystalline material which are too thin to be examined by x-ray diffraction. It was possible to identify successive altered layers on steel blocks exposed to powder gases in the apparatus described in Section 11.2.4 by combining this technique with one developed for the removal of exceedingly thin films.[31]

X-ray examination yields more information when thick films are being examined, as x rays have greater penetrating power than do electrons. X-ray diffraction has been applied more extensively to studies of erosion than has electron diffraction, because a smooth surface is required for the latter method. The cracked bore surfaces of eroded guns are usually too irregular for examination by electron diffraction.

Electron Diffraction Technique [31,137]

In examination by electron diffraction, the eroded specimen is placed in an exhausted container and electrons of uniform energy are caused to impinge on the surface so that they are diffracted from it at a very small glancing angle, about 0.5 degree. The resulting ringlike diffraction pattern is then recorded on a photographic plate. The identity of one or more substances present is established by comparing the measured diameters of the rings with those of standard specimens. Only rough estimates of the relative amounts of the constituents may be obtained from the diffraction pattern.

In order to obtain a good diffraction pattern, the surface must not be microscopically smooth; there must be projections on the surface of small enough dimensions for the electrons to go clear through. Otherwise, refraction of the electrons at the small angle of incidence prevents formation of the diffraction pattern.

Some eroded specimens do not meet this requirement, and it is therefore necessary to resort to some method of roughening the surface in order to obtain a satisfactory diffraction pattern. If the chemically altered layer is thick enough so that there is no danger of removing too much of it, the surface may be scratched with emery. For thin layers, however, scratching with emery paper, brushing with emery powder, or blowing with the powder is unsatisfactory.



Figure 14. Plaque of an area of eroded 3-in. gun liner No. 1460 near the origin of rifling. Groove extends from *A* to *B*, and land from *B* to *C*; *2X*. (This figure has appeared as Figure 1A of NDRC Report No. A-426.)

To overcome this difficulty a ruling machine was built, using a special design of sapphire phonograph cutter so mounted that it digs up the surface in much the same way that a plow digs up the earth. This "microplow" (Figure 15), rules 8,000 "furrows" per inch, as shown in Figure 16, the furrows being of the order of 1 μ in depth.

Thin flakes, removed in etching altered surfaces, were examined by allowing the electrons to pass through them.

Another limitation of the electron-diffraction technique is that the surface on which the electron beam

CONFIDENTIAL

is directed must be flat or nearly so. Thus, in the examination of a section of a ring of the bore surface, the beam cannot be in the plane of the curved specimen. This difficulty diminishes, of course, for guns of larger caliber.

In studies of gun erosion, electron-diffraction examination has been applied to gun specimens, blocks exposed to carbon monoxide-oxygen mixtures (Section 14.3), blocks heated by adiabatically compressed gases (Sections 11.3.1 and 14.6.6), specimens used in the study of the effect of sulfur and other components of black powder (Section 14.4.4), and specimens bombarded with electrons (Section 11.3.2).

X-Ray Diffraction Technique

Examination by x-ray diffraction is a technique similar to that of electron-diffraction analysis, which was described above. Surface layers may be examined *in situ* by the glancing angle method, using an angle of 10 to 30 degrees. Powder photographs may be made of loosely held or dislodged materials.

In some cases where great difficulty in obtaining clear patterns is experienced, it has been recommended that x rays of various wavelengths be used.[137] Variation of the wavelength is obtained by using x-ray tubes having targets of different metals. Each of the elements of the periodic table has a characteristic K absorption wavelength for x rays. If the x rays used to examine a specimen have a wavelength shorter than its K absorption limit, the pattern has a heavy background caused by fluorescence, and the lines of the pattern are weak due to the heavy absorption. If the x rays are just a little longer than the K absorption limit, the resulting pattern has much less background and the pattern stands out clearly.

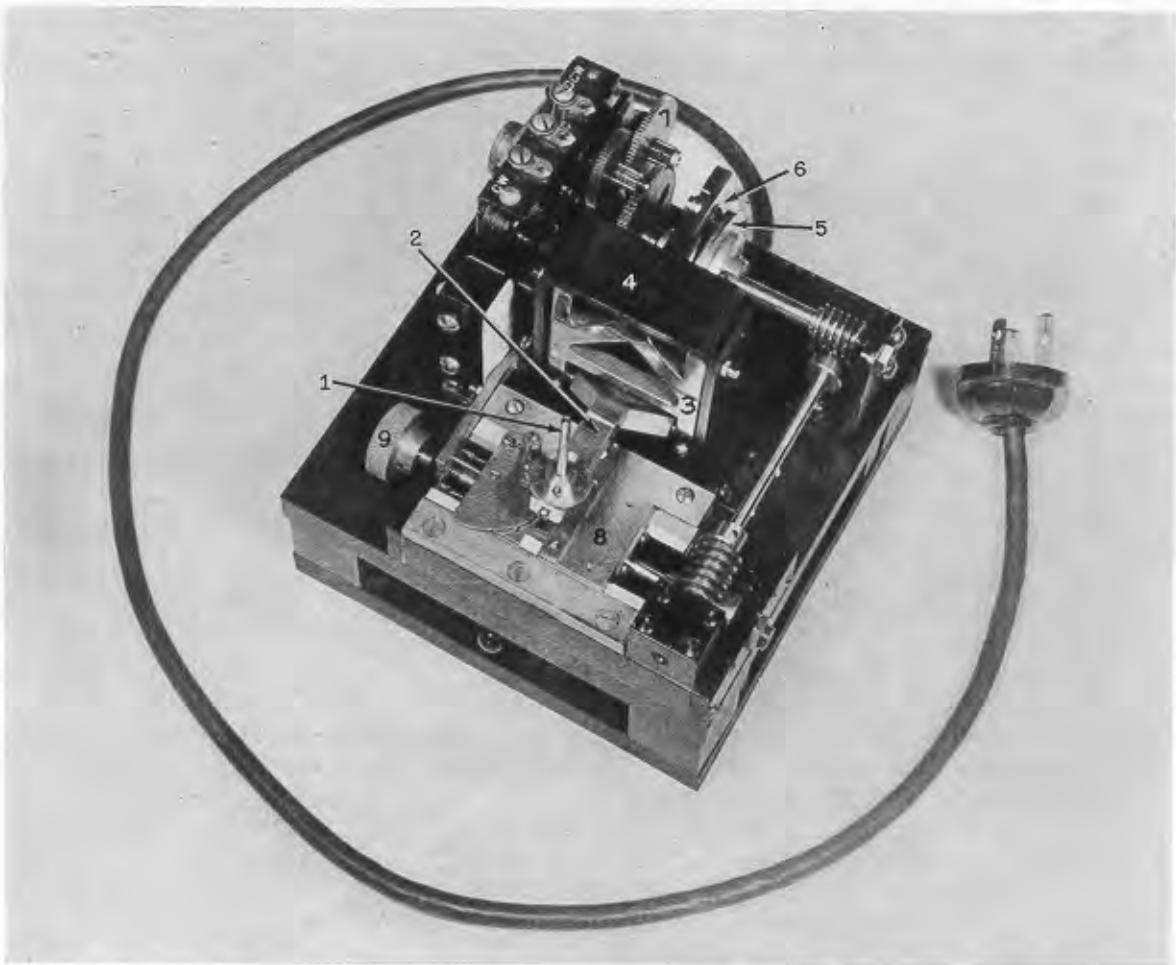


Figure 15. Microplow—an apparatus for ruling a series of fine lines on a specimen of eroded gun steel preparatory to examination by means of electron diffraction. (This figure has appeared as Figure 1 of NDRC Report No. A-465.)

CONFIDENTIAL

As an example of this method of absorption analysis, suppose the specimen is rich in iron, which has a K absorption limit at 1.739 A. If x rays of wavelength 1.539 A from a copper target are used, the resulting pattern is very poor with a heavy background. If, however, radiation of wavelength 1.934 A from an iron target is used, the pattern is stronger with much less background. If it is not known that the specimen is rich in iron, this result only indicates that the specimen is rich in some element with an absorption limit greater than 1.539 A but less than 1.934 A. This restricts the choice to iron, cobalt, and manganese.

The situation is not so clear cut if a pattern obtained with x rays from the copper target is as good as or better than the one taken with iron radiation. About all that can be said in this case is that the specimen is *not* rich in iron, cobalt, or manganese; and if the pattern taken with iron radiation is a good clear one without much background, then the specimen is probably also not rich in chromium, vanadium, titanium, or scandium.

Unidentified Lines. It will be seen in Chapter 12 and elsewhere[28,50,109,123,137,261] that reference is frequently made to the presence of unidentified lines in the photographs obtained by x-ray and electron diffraction. Unfortunately, there are insufficient data at hand to permit one to assign these lines to definite compounds. Then too, the effect of the presence of impurities in causing distortion of lattices also requires further study. When such data have been obtained, x-ray examination will become an even more powerful tool for the examination of eroded specimens, with the result that an even better understanding of the chemical aspects of gun erosion is likely to be obtained than is at present possible.

11.5.3 Chemical Analysis[98]

Introduction

In addition to and in conjunction with analysis of bore-surface products by x-ray and electron diffraction, chemical analysis, both qualitative and quantitative, has been employed. While x-ray and electron diffraction identify particular crystalline phases, chemical analysis tells only what elements and how much of them are present. It is useful however, in showing up elements that give rise to electron and x-ray diffraction patterns that cannot be identified or that are constituents of compounds whose presence cannot be detected by diffraction techniques because they are either amorphous or not present in sufficient quantity. Moreover, analysis by diffraction methods tells nothing about the purity of the compounds identified. For example, in the study of the carbide segregated from the steel of a 3-in. gun liner, x-ray analysis showed that it had the structure of cementite (Fe_3C). Quantitative chemical analysis, however, showed that the carbide from the steel contained appreciable amounts of the alloying constituents, as shown in Table 2 in Chapter 12. Chemical analysis alone only rarely yields sufficient information to permit one to say whether a single substance or a mixture is present.

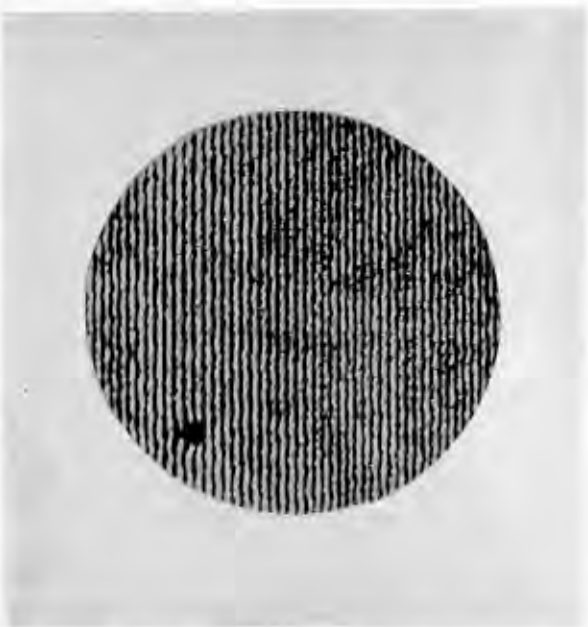


FIGURE 16. Photomicrograph of a ruling made with the microplow shown in Figure 15; 350X. (This figure has appeared in Figure 2 of NDRC Report No. A-465.)

Methods

For quantitative analyses of erosion products, standard methods were employed. When the amounts of available material were small, as they usually were, these methods were modified to bring them within the bounds of semimicro procedures. It was desirable to analyze all segregated products for carbon and nitrogen[49] in order to obtain information on the relative importance of these particular elements in the powder gases in relation to the causes of gun erosion. Very small amounts of iron were determined by potentiometric titration[21] of the electropolishing solutions used in connection with the carbon-penetra-

CONFIDENTIAL

tion studies described in Section 14.2. This procedure was also used for some of the segregated residues. The usual colorimetric methods were used to determine in erosion products the amounts of some of the elements which are used as alloying constituents in gun steel. In order to determine exceedingly small amounts of molybdenum, a considerable refinement of the method[98] was necessary.

The possible role of sulfur in gun erosion, discussed in Sections 12.3 and 14.4, led to the need for a means of determining this element in erosion products. The chemical analysis of a solution or residue can yield information as to the presence of sulfur but does not enable one to identify the compound of which it forms a part. In some cases, however, tests based on reactions in chemically sensitized gelatin-coated papers can be employed to yield a fair amount of information with respect to the presence of sulfides.

Such tests have long been used in metallurgical work to detect the presence of sulfides readily soluble in dilute sulfuric acid. A so-called Baumann print, which is made on silver bromide paper by wetting it with dilute sulfuric acid and then pressing it against the polished surface of the steel, reveals the acid-soluble sulfides by precipitation of silver sulfide in the gelatin coating of the paper. The general principle of the Baumann print may be extended. Thus silver bromide paper soaked in water may be used to detect the presence of water-soluble sulfides; and lead cyanide paper soaked in 5% potassium cyanide may be used to detect copper sulfides.

All three of the above types of contact printing were employed in the study of erosion products. The use of these sensitized papers enabled the detection of sulfides which were not revealed by x-ray or electron diffraction examination.

The physical condition of the sulfide is a controlling factor in obtaining good prints. Thus, precipitated zinc sulfide yields a good print, but the crystalline form, sphalerite, gives no print. The same phenomenon has been observed with precipitated nickel and iron sulfides and their respective crystalline forms, millerite and pyrrhotite.

Details and applications of these printing experiments have been reported.[53,91]

11.5.4 A Method for Determination of the Melting Temperatures of Gun Erosion Products

One of the methods of determining bore-surface temperatures described in Section 5.4.3 was an experimental method[105] based on observations that some of the products of erosion found on gun bore surfaces showed features that indicated they had been in a molten state at some stage during firing. This method was used to determine the incipient melting points of some of the erosion products that were disengaged and segregated by the techniques described in Section 11 4.

11.5.5 Bore Surface Reactions Studied with Isotopic Tracers

The recent methods of concentrating the less abundant isotopes of the elements and of producing radioactive isotopes have provided new and powerful means of tracing individual elements, in particular, nitrogen, carbon, and sulfur, in chemical and physical processes. In some of the experiments on bore surface reactions the ordinary chemical and physical methods would not have provided a solution to several pertinent problems. These problems were successfully studied by the very sensitive method of adding a tracer isotope, either one of the less abundant stable isotopes or a radioactive isotope, as described in Chapter 14.

The work with tracers is largely complementary to the study of eroded bore surfaces described in this chapter because it demonstrated that the process of chemical deterioration of the bore surface is a continuous one commencing with the first firings in a new barrel.

The use of tracers to study the processes of diffusion and reaction of the constituents of the powder gases below fresh bore surfaces of steel is more illuminating than an attempt to demonstrate the course of such processes in badly eroded surfaces. In many of these experiments with new bore surfaces the constituent was present in too small an amount for identification or separation by ordinary chemical procedures.

Demonstration of Equilibrium. For the study of erosion the tracer isotope was introduced into the powder charge for a gun by incorporating it as a coating in the form of a compound which would be completely dissociated when the powder burned. Subsidiary experiments were performed to demonstrate a uniform distribution of a tracer element among the appropriate constituents in the powder gas, a necessary step before interpreting measurements on the bore surface. From one such experiment came a



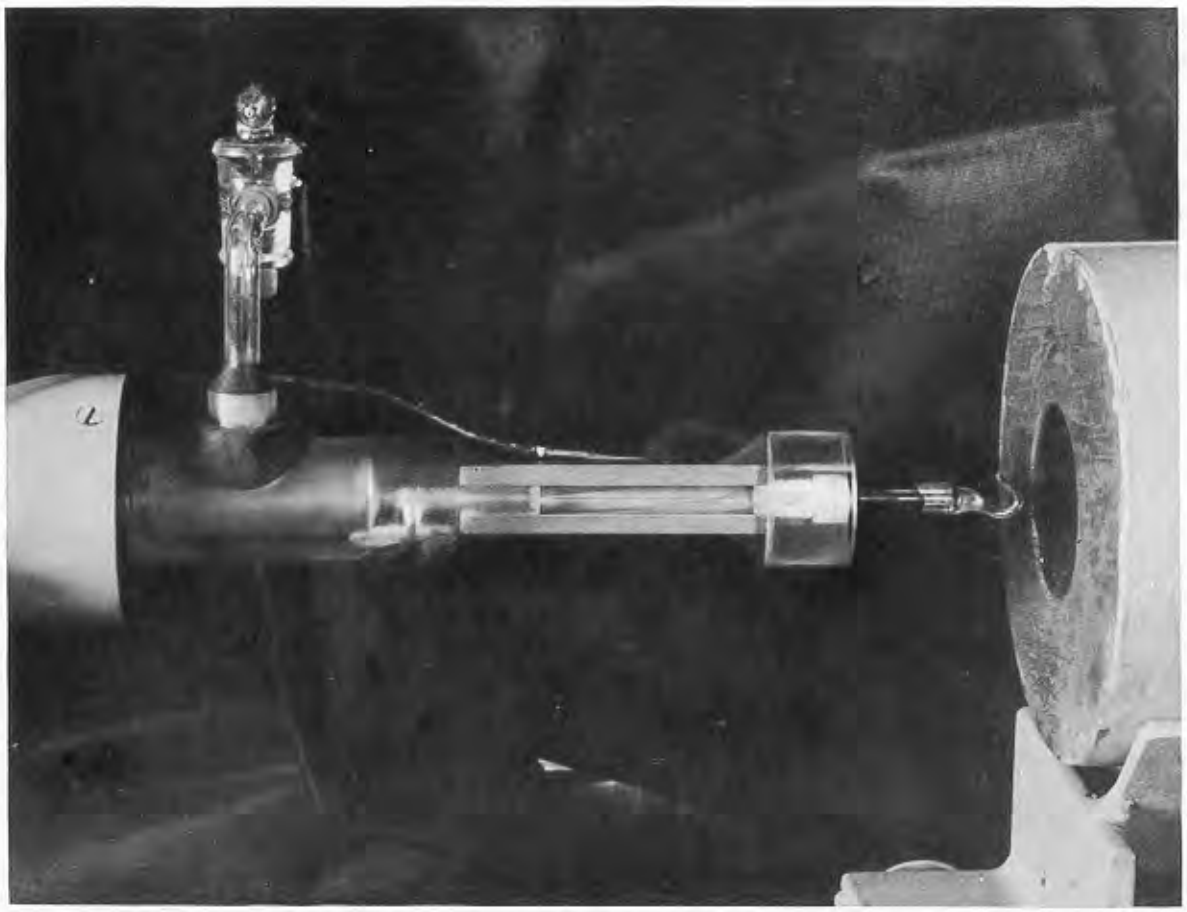


FIGURE 17. A section of a caliber .30 barrel mounted as a Geiger-Mueller counter for measuring the beta ray activity of a radioactive tracer-element incorporated in the bore surface. One half of the section has been cut away to show the Lucite fittings. (This figure appeared as Figure 1 of NDRC Report No. A-427.)

method[61] of determining the state of equilibrium among the carbon atoms of a propellant gas. This is discussed in Section 2.3.5.

Sampling. After the gun had been fired, the tracer atoms that had reacted with the bore surface needed to be recovered so that the proportion of them could be determined. In the study of the penetration of nitrogen, which is described in Section 14.5, thin layers of steel were bored out of a caliber .30 barrel, dissolved in acid, and then analyzed by means of a mass spectrograph. In this way the relative abundance of the rare nitrogen isotope 15, with which the powder charge had been enriched, was determined.

In the study of the reaction of carbon gases with the bore surface, described in Section 14.2, successive layers of the subsurface of the bore, which were often no thicker than $\frac{1}{3}\ \mu$, were removed by a special electropolishing technique in which the iron was preserved for quantitative analysis.[22] The radioactivity of the surface was determined after each such removal, in order to determine the amount of the radioactive tracer, which was the long-lived radioactive isotope of carbon. The carbon content of each layer was thus indexed by the decrease in activity of the radiocarbon. The final result was the construction of a carbon-penetration curve on a microscale. Further details appear in Section 14.2.3.

Isolation of the sample was simplified in one set of experiments[53] on the reaction of sulfur in the powder gases with steel by using steel test rods that were exposed to the powder gases in the apparatus described in Section 11.2.4. How much of the radiosulfur added to the powder charge remained on the surface of the test rod was determined by inserting the test rod directly into a specially designed Geiger-Mueller counter. The extent of the penetration, which is discussed in Section 14.4, was determined by repeating the measurement of radioactivity after successive

CONFIDENTIAL

layers of surface products and steel had been removed on a metallographer's finishing lap, the rods being weighed on a microbalance to determine the amount removed.

Special Geiger-Mueller Counters. An inherent difficulty in many tracer experiments is the tremendous dilution of the tracer isotope. This was particularly the case in the experiments with radiocarbon just mentioned, for the amount of ordinary carbon was fixed by the size of a caliber .30 charge and only very little of the carbon gases penetrated or reacted with the bore wall. Furthermore, radiocarbon emits a very soft beta-ray and the counting of these electrons is very inefficient.

Several of the experiments were possible only because the efficiency of counting the soft beta-rays was maintained at a high level by employing a novel form of Geiger-Mueller counter. A half-section model is illustrated in Figure 17. The cathode of the counter was itself the specimen, namely a short length of the barrel from whose bore surface the beta-rays were emanating. This arrangement may be useful in other studies, as for example in examining the surface effects of commercial carburization.

In an early type of experiment in the study of the penetration and reaction of sulfur, a single round containing radiosulfur was fired from a caliber .30 rifle and the whole barrel was mounted as a Geiger-Mueller counter to measure the soft beta-rays from the radiosulfur. Such a counter worked, but is not to be recommended. Some information concerning the high reactivity of the sulfur gases with gun steel was obtained; but the exact location of the sulfur in the barrel was difficult to find and the amount of penetration could not be satisfactorily established. The procedure developed later for use with radiocarbon, described above, proved far superior. The only advantage in using the whole barrel lies in the fact that its performance as a rifle is not impaired. The same barrel was used alternately in the rifle and as a Geiger counter in studying the effect of subsequently fired rounds.

Temperature of Specimen. There would be little point to studying the penetration of carbon below the

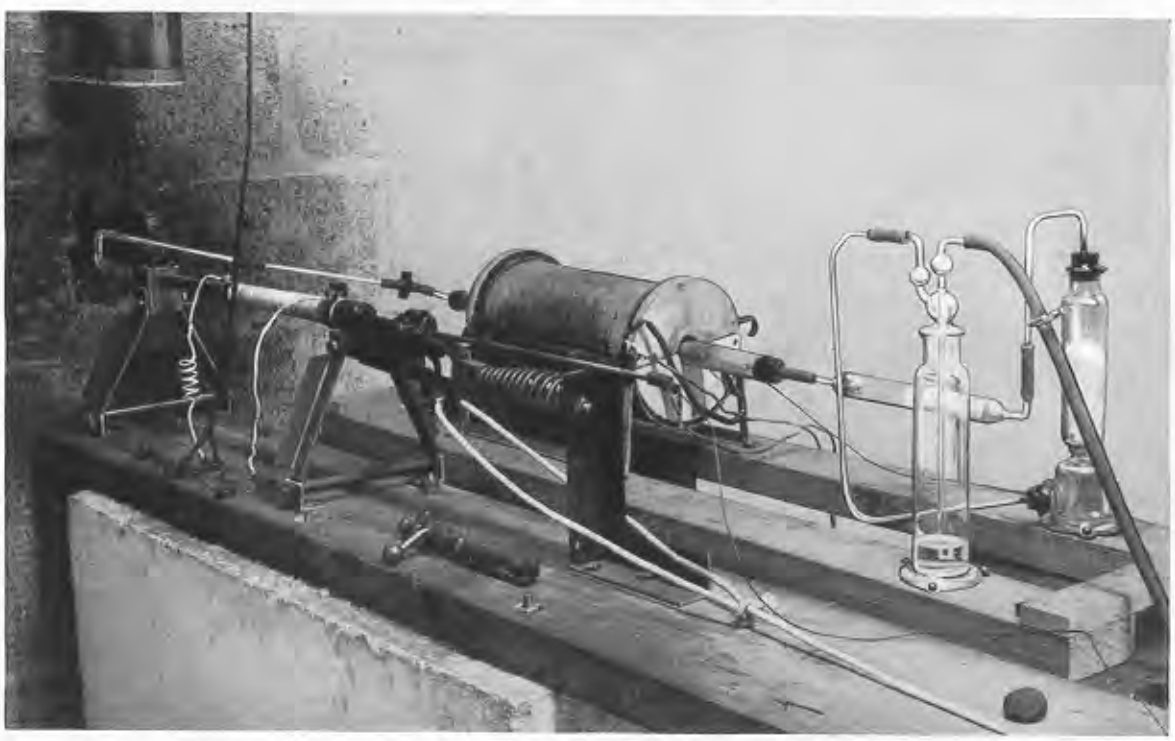


FIGURE 18. Assembly for firing a caliber .30 barrel at elevated initial temperatures. Note the apparatus for passing oxygen-free nitrogen through the barrel in order to protect the bore surface. The glass tube leading to the muzzle was removed about one second before firing. The gunner was protected by a sheet of ½-in. boiler plate, for the experiment was hazardous. Above all, smooth bolt action was imperative, because a "cook-off" would occur after a 2-second contact of the round with the hot chamber. The temperature controls and firing station were in the next room. (This figure has appeared as Figure 4 of NDRC Report No. A-427.)

CONFIDENTIAL

temperature of transition of alpha- to gamma-iron. Because the bore surface of the caliber .30 rifle barrel ordinarily does not reach this temperature, the test barrels were preheated in a protective stream of oxygen-free nitrogen. A photograph of the apparatus is shown in Figure 18.

To gain some idea of the necessary amount of preheat, the question of simulating, in a small caliber barrel, the higher bore-surface temperatures and longer heating times involved in medium and large bore guns, was studied in some detail. Since it seems to be practicable to attain this purpose with respect to temperature and to some extent with respect to the significant times involved, this procedure may constitute a method of approach to other ballistic problems.

Diagrams were prepared to compare the computed temperature-time curves for various guns and propellants with similar curves for preheated caliber .30 barrels.[99] The penetration of carbon and the formation of reaction products containing carbon was studied in the above manner for a number of maximum bore-surface temperatures and propellants. The results are summarized in Section 14.2.2.

Chapter 12

THE PRODUCTS OF GUN EROSION

By *E. G. Zies*[a] *and C. A. Marsh*[b]

12.1 SURFACE LAYERS IN ERODED GUNS

12.1.1 Investigations of Nature of Surface Layers

EXAMINATION OF ERODED GUNS has shown the existence on the bore surface of layers that differ in several respects from the unaltered gun steel. It was soon recognized that in order to know what means could be employed to mitigate the deleterious effect of erosion, it would be necessary to learn what factors are involved in producing the altered bore surface, and how these factors are interrelated, as will be discussed in Chapter 13. An essential part of such a study was a knowledge of the nature of the layers on the eroded bore surfaces.

There are several distinct types of altered layers, not all of which are found in every gun. The layers found depend on a variety of factors. Not all of these variations were recognized by the early investigators; it is quite likely that they were not studying the same types of altered layers.

The methods that have been used to study altered bore surfaces are numerous. They are of value only when the results are coordinated, so that one is sure of what type of altered layer is responsible for the observations. The following techniques were employed by early investigators.

Hardness tests showed that some of the bore surface layers were harder than the unaltered steel. The conclusions reached were that this hardness was due to one or more of the following processes: cold working, martensite formed by quenching, introduction of carbon, introduction of nitrogen. The behavior of the altered layers on tempering led to the conclusion that there was no chemical alteration. Analyses of cuts taken parallel to the bore surface indicated in some instances that a carburized case had formed and in others that a nitrided case had formed. X-ray examinations of eroded bore surfaces revealed the presence of austenite but not of martensite or compounds of iron. The retention of the austenite favored the theory of nitrogen penetration as a cause of erosion.

Metallographic examination seemed to prove the same things that were found by the hardness tests, but etching seemed to show that no cementite was present. Most of the foregoing techniques have been markedly improved since the time they were first employed in the study of gun erosion. This early work has been evaluated elsewhere with respect to the limitations that prevailed at the time it was done.[16,261]

Kosting[261] initiated a truly systematic study of eroded guns. He was the first to show the complexity not only of the altered layers but also of the entire problem of gun erosion. Earlier investigators had used the term "white layer" to designate the whole altered zone, for with the usual, mild etching reagents employed in the metallographic examination of steels, this zone does not appear etched at low magnifications. Kosting restricted the term "white layer" to the outer zone which constitutes only a minor part of the whole altered layer. In order to eliminate confusion, this practice is now generally followed. Moreover, the inner zone sometimes etches dark, thus rendering the term white layer a misnomer when applied to it.

12.1.2 Description of Layers

INTRODUCTION

As was stated above, the layers that may be found in eroded guns vary. In some cases only the thermally altered layer that is common to all eroded guns is present. In the majority of large caliber guns, however, all types of layers may be found if care is exercised to preserve the outermost layers in mounting and polishing the specimens. The following succession of layers is typical for guns of low-alloy steel that have been fired with single-base powders at normal pressures and rates of fire. The succession is from the bore surface inward to the unaltered steel: outer white layer or layers; inner white layer; thermally altered layer; troostite band. These features are shown in Figures 1 and 2.

[a] Chemist, Geophysical Laboratory, Carnegie Institution of Washington.

[b] Assistant Chemist, Geophysical Laboratory, Carnegie Institution of Washington. (Present address: U. S. Geological Survey, Washington, D. C.)

Thermally Altered Layer

The thermally altered layer is common to all steel guns in which the bore surface has been heated above a critical temperature, about 720 C, for a critical length of time.[124] In some cases it is the only altered layer evident. In the usual case, however, it constitutes the bulk of the whole altered zone and over a considerable area of bore surface extends to a uniform depth below the surface. The thickness of this layer depends on many factors, among which may be mentioned the caliber of the gun, the heat input to the bore, and the location in the bore.

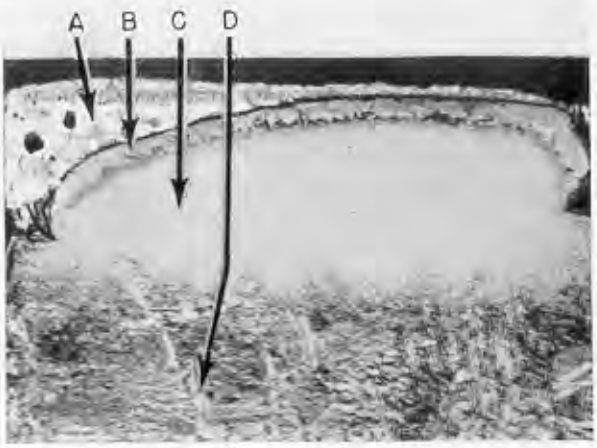


FIGURE 1. The typical succession of layers on the bore surface of an eroded gun: A—outer white layer; B—inner white layer; C—thermally altered layer; D—unaltered steel. [Cross section of 5-in./25-cal. gun tube No. 1982T at the origin of bore. Etched with picral (*500X*)]. (This figure has appeared as Figure 15b in NDRC Report No. A-440.)

The heat input, of course, depends on the flame temperature of the particular powder, the rate of fire, and the amount of powder. The correlation of the thickness of the thermally altered layer, heat input, and flame temperature from available data on tests with the caliber .50 erosion-testing gun is made in Section 15.5.

It was also found in these studies carried out on the erosion-testing gun that the layer was thickest near the origin of rifling and that the thickness decreased muzzleward; in addition, the geometry of the lands caused the layer to be thicker under the land surface than under the groove surface. The depth of the thermally altered layer was practically independent of the number of rounds fired. In the case of chromium-plated barrels tested in this gun, thickness of the thermally altered layer depended on thickness of the chromium plate. As will be described in Section 31.5, experiments were carried out to determine the minimum thickness of chromium plate necessary to suppress the formation of a thermally altered layer.

In some rapid-fire barrels the whole barrel except breech end is so hot and cools so slowly that a definite layer does not result.

The exact nature of the thermally altered layer is still not known. So far no means of isolating it for study has been found. There is good reason for believing that it has essentially the same chemical composition as the steel. For instance, when this layer is tempered, metallographic evidence shows it does not differ from the unaltered sorbitic gun steel.[261] Even a thin chromium plate, so long as it is intact, prevents the penetration of carbon and nitrogen into the steel. Nevertheless, a thermally altered layer can form under this thin plate. Studies of the penetration of carbon[99] and nitrogen[70] into nonplated gun-bore surfaces are discussed in Chapter 14. In the case of carbon, the amount does increase in the thermally altered layer. Presumably the amount of excess carbon is not sufficient to show an appreciable difference between the tempered altered layer and the unaltered steel.

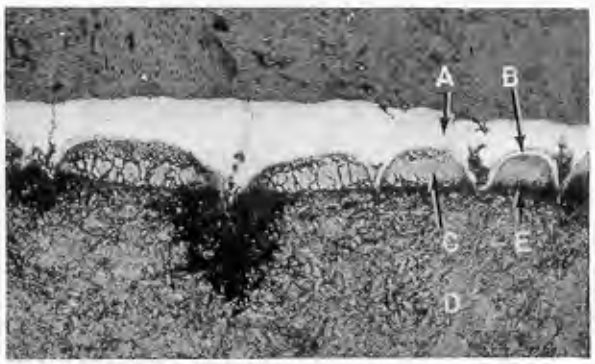


FIGURE 2. The typical succession of layers on the bore surface of an eroded gun. The outer white layer here is unusually thick, and the thermally altered layer has been partially tempered during firing. A—outer white layer; B—inner white layer; C—thermally altered layer; D—unaltered steel; E—troostite band. [Longitudinal cross section of 76-mm gun tube M1A1 No. 1425 at the location of the mouth of the cartridge case. Etched with picral HCl (*1000X*).] (This figure has appeared as Figure 13a in NDRC Report No. A-440.)

Metallographic evidence shows a sharp difference

CONFIDENTIAL

between the thermally altered layer and the unaltered steel, which is usually sorbitic. Since the chemical composition is thought to be the same this must be only a textural difference. The thermally altered layer appears to be structureless when light nital or picral etches are used. When, under certain firing conditions, the layer becomes somewhat tempered, it etches dark with these reagents, as can be seen in Figure 3. With stronger reagents, such as copper potassium chloride, it also etches dark and etches even deeper than the unaltered steel.[98] Furthermore, it can be seen to have a very fine-grained texture.

The evidence cited above together with the fact that the thermally altered layer is harder than the sorbitic gun steel have led to the conclusion that the layer is martensite although the acicular structure characteristic of martensite is not usually observed. It should be mentioned here that needles of some phase have sometimes been observed at the junction of the thermally altered layer and the inner white layer[112,261] as shown in Figure 4. They have not as yet been identified and can be attributed to iron nitride as well as to martensite. Martensite has never been identified by x-ray analysis of eroded bore surfaces, but this is not surprising.

Martensite is a term used by x-ray crystallographers to designate the tetragonal phase of iron containing dissolved carbon. The axial ratio of the iron varies with the carbon content. When the carbon is low the crystal structure is not called tetragonal but is usually referred to as distorted cubic.[49] Nevertheless, it is still considered martensite as long as doublets appear on the x-ray film.

Metallographers, on the other hand, originally used the term martensite in a much less restricted sense. For this reason it is probably permissible to call this altered layer in guns martensitic, especially in view of the fact that even in the case of a slightly tempered martensite layer, the texture and the hardness of the layer would be such that it would obviously be called martensite. Nevertheless, the term thermally altered layer is preferred until more is known about the nature of the layer. The great importance of this layer in relation to the causes of gun erosion is discussed thoroughly in Section 13.2.

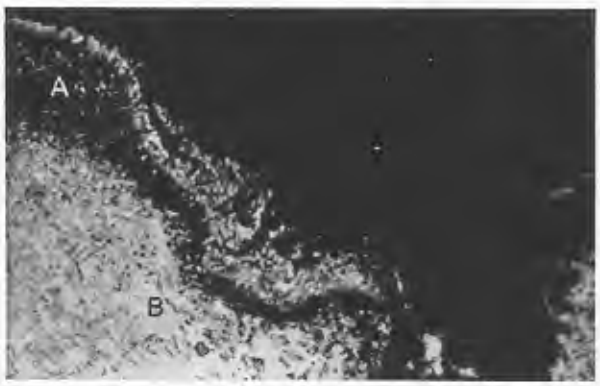


FIGURE 3. A thermally altered layer that has been tempered during firing, and therefore etches dark with picral. A—thermally altered layer; B—unaltered steel. [Cross section of 5-in./51-cal. gun liner No. 806L2 in the bag ammunition chamber. Etched with picral (*1000X*).] (This figure has appeared as Figure 20c in NDRC Report No. A-440.)

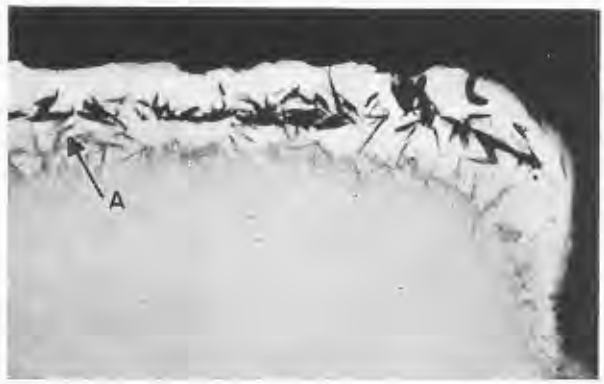


FIGURE 4. An acicular structure (A) at the junction of the thermally altered layer and white layer. A similar structure is seen also within the white layer. [Cross section of 3.7-in. gun tube No. L/2675 at 21 in. in front of the location of the cartridge case. Etched with picral (*1000X*).] (This figure has appeared as Figure 18c in NDRC Report No. A-440.)

It is important to keep in mind that one should not expect to find tetragonal martensite in gun-bore surfaces unless sufficient carbon had penetrated into the thermally altered layer to bring the carbon content of this layer above 0.6%.[c] Iron containing less than this amount of carbon might form tetragonal martensite on being quenched but this would be self-tempering and would transform to cubic martensite, which would appear to be no different from ferrite except that the lines of the pattern would be broad as though the ferrite were badly strained or not well crystallized. Such broadening of the ferrite lines has sometimes been found.[75,123,137]

[c] In the vicinity of resorbing grains of carbide such a concentration might be reached. (Informal communication from H. E. Merwin, June 26, 1946.)

CONFIDENTIAL

Troostite Band

The troostite band is a very narrow band which forms the transition zone between the thermally altered layer and the unaltered gun steel. It is not always sharply defined. Troostite, which is a mixture of iron carbide and alpha-iron in extremely fine dispersion, may be formed by tempering martensite. Since it is a product of thermal transformation, it is really a part of the thermally altered layer. It is described separately because sometimes it is sharply defined due to the fact that it etches darker than the rest of the thermally altered layer.

Inner White Layer

The inner white layer is in some respects more closely related to the thermally altered layer than to the outer white layer. When deep etching is applied and the specimens are viewed under low magnifications the inner white layer is usually sharply defined because it does not etch. When high magnifications are employed, however, the inner white layer and the thermally altered layer are usually seen to grade into each other. In badly cracked and pebbled surfaces the thermally altered layer does not have a uniform thickness but extends to a uniform depth below the general surface, whereas the thin inner white layer actually has a somewhat uniform thickness and follows the contour of the steel around the edges of the cracks.

Usually the inner white layer shows no structure. Sometimes, however, the outermost portion of this layer has the structure usually attributed to austenite,[112,265] as shown in Figure 5. It would seem that, although the thermally altered layer does not take up enough carbon or nitrogen to retain austenite on cooling or even tetragonal martensite, yet the outermost surface of the original steel can dissolve enough carbon or nitrogen to retain austenite. Such an amount of carbon or nitrogen would appreciably lower the melting point of steel. It is believed by some that there is sufficient evidence to show that this surface layer had melted although it had not been transported.[112] In at least one case it was shown that the inner white layer was not radically different in chemical composition from the steel for it could be tempered to have the same type of structure as the steel.[261] Probably, therefore, only a portion of the layer was liquefied at the peak temperature, the phases present being austenite plus melt. Austenite has been consistently identified in the bore surfaces of eroded guns by x-ray analysis. It may be that this retained austenite is actually the dominant constituent of the inner white layer. It should be emphasized that it is possible to identify phases by x-ray analysis that cannot always be readily detected metallographically.

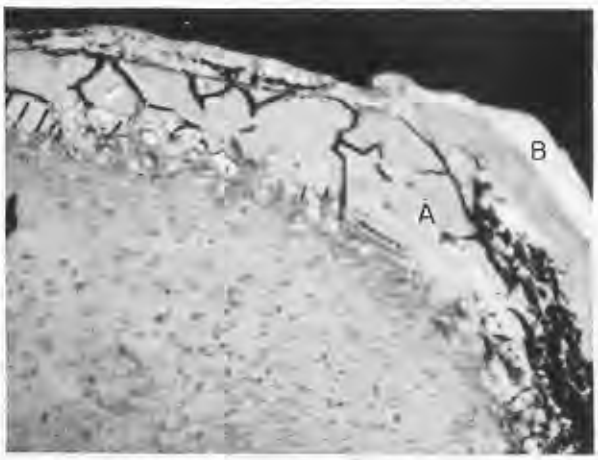


Figure 5. Grain boundaries in an inner white layer. A—inner white layer; B—outer white layer. [Cross section of 5-in./25-cal. gun tube No. 1982T at the origin of bore. Etched with picral (*2000X*).] (This figure has appeared as Figure 16c in NDRC Report No. A-440.)

Outer White Layer

Outer white layers of the type described here are found only in guns that have been fired with single-base powders. It is true that white layers are sometimes found in guns that have been fired with double-base powders and two examples of them are shown in Figures 6 and 7. Their characteristics are somewhat different from the ones about to be described and, unfortunately, they have not been studied in sufficient detail to warrant description here.

The fact that an outer white layer is not found in all guns that have been studied does not necessarily imply that it was never present, for sometimes traces of it can be found in protected areas such as between the lips of cracks, as shown in Figure 6. This layer in the case of single-base powders is hard, brittle, spalls readily, and can thus be easily removed by projectiles during firing. For the same reasons, faulty technique in polishing the specimens for metallographic examination removes it. It is not usually found in guns where general melting[124] of the surface has occurred. With single-base powder, it would probably be found somewhat forward of the region of general melting, and also on the melted surface.

CONFIDENTIAL

When deep etches and high magnifications are used, a considerable amount of detail can be seen in the outer white layer. It is rarely structureless. Blade-like forms, such as are shown in Figure 8, are observed, which are similar to those seen in cast irons.[112] In addition, flow structure can be seen. The thickness of this layer is variable; it bridges cracks and is thickest where it fills up the mouths of cracks, as seen in Figure 2. In these places it can be seen to be complex as though successive flows had piled up on top of one another.

The boundary between the inner and the outer white layers is usually, though not always, sharply defined. The band which separates the layers is sometimes seen to consist of some extraneous substance, perhaps a decomposition product of one of the white



FIGURE 6. An outer white layer in the mouth of a crack in a gun that had been fired with double-base powder. [Longitudinal cross section of 37-mm gun tube No. T-13 in the region ½ to 1½ in. from the origin of bore. Etched with picral (*1500X*).] (This figure has appeared as Figure 18d in NDRC Report No. A-440.)

layers.[261] Some extraneous material, including copper, is often found throughout the outer white layers.[112] This feature is illustrated in Figure 9.[d]

There is no doubt in view of all this evidence that the outer white layers have been at least partially liquefied and flowed into place. (For other evidences of liquefaction of the bore surface, see Section 10.5.2.) There is also no doubt that, whereas the lower altered layers can still be considered steel in various textural modifications, the outer white layers are of quite a different chemical composition than the underlying steel, for experiments have shown that this outer zone does not change on tempering.[261] It is concluded that compounds of iron that are formed by the reaction of powder gases on gun steel are in some manner related to the outer white layers. In recent studies at the Geophysical Laboratory of the products of gun erosion[98] considerable emphasis was placed on finding methods to determine the chemical composition of outer white layers and to identify the constituent phases.



FIGURE 7. An outer white layer in a gun that had been fired with double-base powder. [Cross section of 37-mm gun tube No. 43928 at 1¾ in. in front of the location of the cartridge case. Etched with picral (*1500X*).] (This figure has appeared as Figure 18e in NDRC Report No. A-440.)

12.2 DIFFERENCES BETWEEN GUNS FIRED WITH SINGLE-BASE AND WITH DOUBLE-BASE POWDERS

12.2.1 X-Ray Examinations of Eroded Bore Surfaces

Compounds of iron on the bore surface were first identified by means of x-ray analysis of eroded bore surfaces of Service guns. In the earliest work only ferrite and austenite[e] were found.[183] Later work took cognizance of unidentified lines in the x-ray patterns, in addition to the two modifications of iron contain-

[d] The copper is even more obvious in a Kodachrome[172] of the same field illustrated in the figure.

[e] Ferrite is body centered cubic iron containing carbon, and austenite is face centered cubic iron containing carbon, but in both cases nitrogen can replace some of the carbon. Pure iron undergoes a phase change at 910 C. Below this temperature it is body centered cubic and above this temperature face centered cubic. These two phases of pure iron are called alpha and gamma respectively. These terms are sometimes used by the x-ray crystallographers to designate the structure of the iron even when not pure; however, in this case, the names ferrite and austenite are preferred.

CONFIDENTIAL

ing carbon or nitrogen or both. It was thought that iron nitrides could not account for these lines but the possibility that they might be due to a complex iron cyanide was suggested.[26]

Compounds of iron have recently been identified in eroded bore surfaces for the first time.[28,49] All the examinations were made at or near the origin of rifling. In addition to ferrite and austenite the following compounds were found: wüstite (FeO), cementite (Fe_3C), and the epsilon phase of iron nitride (Fe_2N_z). The first was found in relatively large amounts in guns fired with double-base powder and sometimes in minor amounts in those fired with single-base powder.

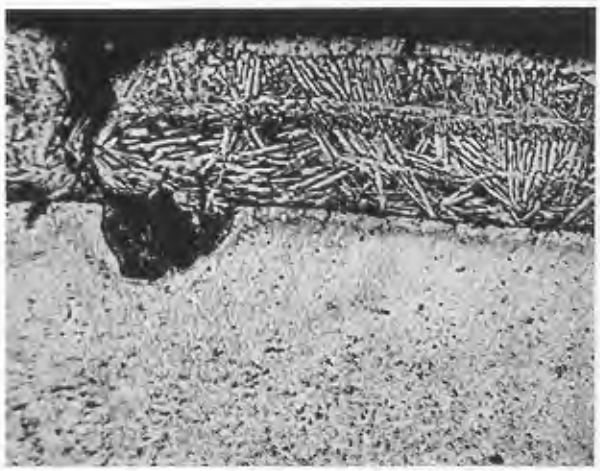


FIGURE 8. The blades of cementite in an outer white layer composed of several superposed flows. [Cross section of 3-in. gun liner No. 1460 at 3½ in. in front of the location of the cartridge case. Etched with picral (*750X*).] (This figure has appeared as Figure 12a in NDRC Report No. A-440.)

The last two were found only in guns that had been fired with single-base powder.

Examples of guns in which wüstite was the only compound identified were a 3.7-in. Canadian gun[28] and a 37-mm M3 gun tube.[50] Examples of guns rich in cementite and epsilon iron nitride were a 90-mm gun tube[49] and the 3-in. gun liner No. 1460.[28] A 5-in./25-cal. gun tube,[28,50] which had been fired with Pyro powder, was found to contain the products characteristic of both single-base and double-base powders.

12.2.2 X-Ray and Electron Diffraction Examinations of Test Blocks

The above differences between the guns fired with single-base and with double-base powders are in agreement with the results obtained on test blocks that were subjected to explosions of powders of these types in the apparatus described in Section 11.2.4.[31]

It was found that a specimen of gun steel that had been exposed to the gases from double-base powder had a layer of wüstite about 0.01 mm thick on the surface. The film on the surface of a specimen that had been exposed to the gases from single-base powder, on the other hand, contained no wüstite but instead consisted largely of cementite. This layer of

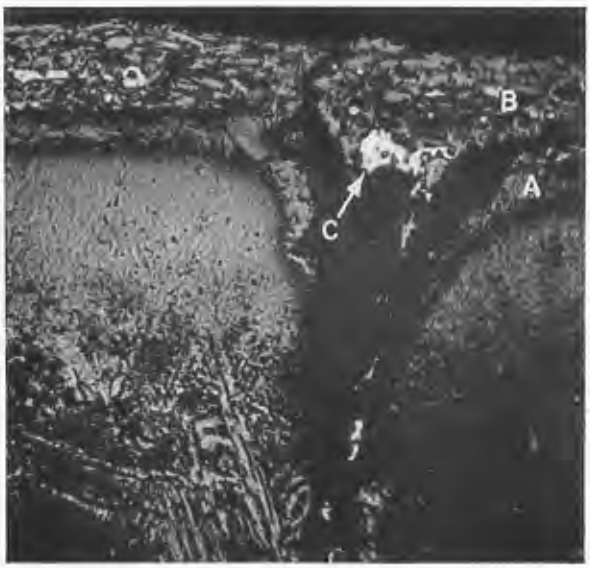


FIGURE 9. Patches of copper within an outer white layer. A—inner white layer; B—outer white layer; C—patches of copper. [Cross section of 5-in./25-cal. gun tube No. 1982T at the origin of bore. Etched with picral (*750X*).] (This figure has appeared as Figure 16a in NDRC Report No. A-440.)

cementite, which in one case was about 0.001 mm thick, was overlaid by a layer of a complex iron cyanide about one-tenth as thick. The cementite layer was removable in large flakes by means of nital, and beneath it was found a considerable amount of additional cementite and still larger amounts of austenite.

12.2.3 X-Ray Examinations of Fired Metal Particles

The results of the examinations of guns were also in accord with those obtained by examining steel filings that had been mixed with the powder charge in a caliber .30 rifle,[28] and fired according to the technique described in Section 11.2.6. Wüstite formed about 90% of the products that resulted from the fir-

CONFIDENTIAL

ing of electrolytic iron with double-base powder. The rest of the material was ferrite together with a small amount of austenite.

Both electrolytic iron and gun steel were fired with IMR, the hottest of the single-base powders. The results were practically the same in both cases. The main products were ferrite and austenite. Fair amounts of epsilon iron nitride and wüstite were also present. No cementite was found. Undoubtedly the particles attained too high a temperature for cementite to be the end product. The metal particles were at a higher temperature for a longer time than the bore surface, which was rapidly cooled by the mass of gun steel.

Iron particles of several different meshes were fired with single-base powder. The larger amounts of wüstite and epsilon iron nitride found in the reaction product when iron of smaller particle size was fired, can be readily accounted for by the increased surface area. These results indicate how much more reactive a bore surface may be once it has acquired an extensive crack system.

12.2.4 Thermodynamic Considerations

The problem of determining the theoretical compounds resulting from the interaction of iron with powder gases was studied in order to explain the differences observed between the results obtained with single-base powders and those obtained with double-base powders. One means of attack[60] employed standard thermodynamic methods to determine, under a number of conditions, the ultimate product, that is, the product that would be formed if chemical equilibrium were established between a finite quantity of iron and an infinite quantity of the powder gas. In a competing series of reactions of gases with iron, the ultimate product is the one that requires the greatest free-energy change for formation directly from iron. All possible equilibriums between the gases and iron are discussed in Section 13.3.3. It seems improbable under gun-firing conditions that the reactions in the gas phase are fast enough to establish the equilibrium composition of the gas at the temperature of the bore surface immediately. Thus the reactions on the surface are those with a gas at the temperature of the surface but having the composition it would have at a somewhat higher temperature.

It was found that for FNH-M1 powder (single-base) the ultimate product at low surface temperatures is Fe_3O_4 if the reacting gas is cooled slowly to the surface temperature, whereas it is Fe_3C if the gas at the surface is cooled rapidly. At higher surface temperatures FeO is formed instead of Fe_3O_4. This accounts for the absence of cementite in the products formed by firing steel or iron filings, mentioned in the preceding subsection.

For FNH-M2 powder (double-base) the ultimate products at low surface temperatures are the same as for single-base powder. At high surface temperatures, however, the product is FeO for a wide range of conditions of cooling of the reacting gas. If 0.1% sulfur is added to either powder, the ultimate product at low surface temperatures is FeS. The presence of sulfur does not affect the products obtained at high surface temperatures.

The formation of iron nitrides was not considered quantitatively because of the paucity of the data. Extrapolation of available data led to the conclusion that formation of iron nitrides is impossible at the temperatures of bore surfaces during firing. Nitrides, however, have been found in guns. It may be that they undergo a transition at temperatures higher than those at which they have been studied, thus invalidating any extrapolation of the data.

In this research the formation of solid solutions could not be considered because of the lack of data. This was unfortunate because the penetration of carbon and nitrogen into the steel, evidence for which is given in Chapter 14, does take place presumably with the formation of solid solutions. It should be borne in mind, however, that once the bore surface has taken up enough carbon or nitrogen or both to liquefy, the formation of solid solutions is of no concern. The liquefied material can dissolve carbon and nitrogen more readily than a solid phase such as austenite.

The other method of attack[138] was an attempt to explain the differences between the results found in the experiments with the test blocks and those in the experiments with the metal filings. Thermodynamic arguments were used to determine the stabilities of the solid phases and also to predict the direction of the chemical reactions. Equilibrium curves were plotted for the reactions to form FeO and Fe_3C from CO_2 and CO and for the reaction to form carbon and carbon dioxide from the monoxide. The curves, shown in Figure 8 of Chapter 13, bounded the regions for the positive and negative free energies of the reactants and the products. The various temperatures considered were those of the bore surface during firing. In this work great care was taken to show that under the conditions of gas flow in the experiments with the

test blocks the assumption that the equilibrium constants to be used for gaseous reactants correspond to a temperature only slightly above the bore surface temperatures is justified. In the use of these equilibrium constants rather than those for higher temperatures this second investigation differed from the first.

A consideration of the effects of pressure and temperature upon the reactions involved led to some important conclusions, which will be discussed in Section 13.3.3. Also the effects of nitrogen and hydrogen upon the system Fe-C-O were considered. Low temperature reactions were discussed in this connection. Some of the conclusions were borne out by experimental evidence.

The following conclusions were drawn from the study of the Fe-C-O system. If the CO/CO_2 ratio is of the order of 2 or 3 and if the temperature at the surface of the specimen does not exceed about 1100 C, Fe_3C is to be expected as the major reaction product, but FeO is to be expected above about 1200 C. If the CO/CO_2 ratio is of the order of unity, then FeO is to be expected as the major reaction product above about 1000 C, but below about 900 C Fe_3C may still be produced in considerable quantity. Increasing the pressure favors Fe_3C while decreasing the pressure favors oxide formation. The higher CO/CO_2 ratio corresponds roughly to single-base powders and the lower ratio to double-base powders.

It should be noted that in this second investigation the products were termed *major* rather then *ultimate*. Nothing is known about the rates of reaction at the temperatures and pressures that are obtained in the firing of guns, but presumably kinetics are of some importance. Therefore, even though all the theoretical ultimate products have been found in guns, it cannot safely be assumed that an actual end product will always be an ultimate product.

12.2.5 X-Ray Examinations of Barrels Fired in the Erosion-Testing Gun

The quantitative determination of the rate of erosion of gun steel with different propellants fired in the caliber .50 erosion-testing gun is thoroughly discussed in Section 15.3. In addition to the general relations between the flame temperature of the powder and the erosion rate and thermal transformation of the steel, the differences in the compounds that were identified on the bore surfaces by x-ray examination are related to the erosiveness of the powder.

The erosiveness depends not only on the flame temperature but to some extent on the composition of the powder. Ferrite and austenite were found in all cases. With double-base powders, the only other constituent identified was wüstite (FeO). Smaller amounts of this substance were found for all the cooler powders with the exception of IMR, the hottest of the single-base powders. Cementite (Fe_3C) and the epsilon phase of iron nitride (Fe_2N_x) in varying amounts were revealed by the x-ray analysis of the barrels fired with most of the cooler powders. In the case of the four coolest powders, an unidentified constituent was found.

In view of the thermodynamic considerations mentioned above, the wüstite and cementite are to be expected in those cases where they were found. The greater complexity of the results is probably due to the fact that other molecules besides those of the water gas reaction are present in the propellent gases. The presence of nitrogen in some form or other accounts for the nitrides that are found.

The dependence of erosion rate on the temperature of the propellent gases in contact with the bore surface and on the compositions of the powders, a major factor in both cases being the CO/CO_2 ratio, has led to the theory that a powder of a certain composition might be found that would be less erosive than any of the present powders. This theory is discussed in Section 15.6.3, and several preliminary experiments along this line are described in Section 15.6.5.

12.3 EROSION PRODUCTS ENTRAPPED IN THE COPPERING[98]

12.3.1 Coppering

The deposits of copper or gilding metal found in guns are rarely clean, since they entrap material eroded from the bore surface, including compounds formed in reactions with the powder gases. For this reason heavily coppered sections of eroded guns have been used as a source of erosion products for study. These compounds were segregated from the copper by dissolving the latter by the technique described in Section 11.4.3. As was stated in Section 10.5.4, the heaviest coppering commonly occurs in the central portion of the bore, thus the deposits that were studied yielded a wealth of material that had been carried forward from the region of the origin of rifling. Frequently a pronounced layered structure was evident, consisting of alternate deposits of reaction products



and other debris and of flows of copper. Because of this mode of deposition, which was likened to alternate ash falls and lava flows from a volcano, it was possible to discern whether or not there was any difference between early and later deposits.

12.3.2 Sulfur in the Coppering

In the study of gun erosion it is the reactions of the powder gases with steel that are of interest; however, the study of the coppering in guns has yielded information regarding other reactions that have taken place. One of these is the reaction of the copper or gilding metal with the sulfur in the powder gases. The fact that copper and zinc react so readily with the sulfur may mitigate the effect of the sulfur components of the powder on the gun steel, which is discussed in Section 14.4.

Copper Sulfides

Both the sulfur which is dissolved in the copper and that which is present in the form of copper sulfides can easily be detected without removing the copper deposit. When coppered bore-surface specimens are heated in hydrogen and the effluent gases are passed into cadmium acetate, a yellow precipitate of cadmium sulfide is formed which indicates the presence of hydrogen sulfide. The presence of copper sulfides can also be indicated by a contact print method in which potassium cyanide is used to etch the specimen. Copper sulfides, such as chalcocite (Cu_2S) and covellite (CuS), are soluble in potassium cyanide. The total sulfur in the copper can be found by removing the deposit with the ammoniacal solution described in Section 11.4.3, and by analyzing both the solutions and the insoluble residues. The solution dissolves the chalcocite and covellite as well as copper; the relatively insoluble copper sulfide, digenite (Cu_9S_5), can sometimes be found in the insoluble residue by x-ray analysis.

Chalcocite has been identified by this method of analysis in the material removed from the cracks near the origin of rifling where there was no copper obvious on the bore surface.

Zinc Sulfides

When gilding-metal (alloy of copper with 10% zinc) rotating bands have been used, zinc sulfides are found in the coppering. These cannot be detected by contact printing methods but can readily be identified by x-ray analysis of residues centrifuged from ammoniacal decoppering solutions (Section 11.4.3), for they are less soluble than the copper sulfides. Both wurtzite (hexagonal ZnS) and sphalerite (cubic ZnS) have been found in eroded guns. In the case of a 75-mm gun a very interesting succession of deposits was found interlayered with the coppering. Wurtzite alone was found in the deposit at the surface, while both sphalerite and wurtzite and also digenite were found nearer the copper-steel interface. Wurtzite and sphalerite are the high- and low-temperature forms of zinc sulfide respectively, the inversion point with the pure sulfide is 1020 C. Digenite (Cu_9S_5) is a low-temperature form of copper sulfide. Presumably, this inversion temperature would enable one to tell what temperatures were reached at and near the bore surface, but the relationships among these sulfides are not simple. The absence of sphalerite does not necessarily mean that the immediate bore surface had reached a temperature of 1020 C since the inversion point may be lowered by the presence of other elements, especially iron, dissolved in the zinc sulfide.[484]

Zinc sulfides are sometimes found in guns that have copper rather than gilding-metal deposits. The zinc in these cases may have been derived from impurities in the copper or what is more likely from the cartridge case. An example of the latter is undoubtedly the wurtzite that was found at the location of the mouth of the cartridge case in a 5-in. gun.[28]

Other Sulfur Compounds

Galena (PbS) has been found in the copper and also on bore surfaces where there was no copper. The lead may be derived from the primers or from lead foil incorporated in the powder charges for the purpose of decreasing the amount of coppering. Metallic lead has been found in eroded guns.[123,137] Barium sulfate and carbonate have been identified in residues centrifuged from decoppering solutions. Potassium sulfate has likewise been identified in bore-surface products. The barium and potassium were both derived from the powders.

Distribution of Sulfur in the Coppering

Very little study has been made of the distribution of sulfur in the coppering of guns. In only one gun, a 5-in. Naval gun tube, have the relations between the amounts of sulfur and copper with respect to the

distance from the origin of rifling been studied. The results are given in Table 1. It can be seen that the

TABLE 1. Copper and sulfur on the bore surface of a 5-in. Naval gun at different distances from the origin of rifling.[98]

Distance from origin of rifling (in.)	Copper (mgs/sq cm)	Sulfur (mgs/sq cm)	S/Cu
1.4– 3.0	6	0.11	0.019
3.6– 5.2	15	0.24	0.016
5.2– 6.8	30	0.15	0.005
11.2–12.8	42	0.25	0.006
11.5–12.8	41	0.20	0.005
13.8–18.8	41	0.12	0.003

amount of copper increased with distance from the origin of rifling, reached a maximum at about 13 in., and apparently decreased slowly from there on. The amounts of sulfur were erratic, but the ratios of sulfur to copper seem to indicate that the sulfur in the powder gases was gradually being exhausted by combination with the copper.

12.3.3

True Erosion Products Entrapped in the Copper

True erosion products are compounds of iron or of any of the alloying constituents in the gun steel. These, as well as the sulfur compounds mentioned above, have been found entrapped in the coppering of guns.

Cementite (Fe_3C) was identified in the decoppering residues from all but one of the guns which had been fired with single-base powders. In the case of the one exception, a 14-in. Naval gun, it may well be that the region studied was too near the muzzle end. In Section 12.2.1 it was pointed out that cementite is a characteristic product at and near the origin of rifling in guns that have been fired with single-base powder.

X-ray analyses of the bore surface had also shown that the epsilon phase of iron nitride (Fe_2N_x) was characteristic of all these guns and that small amounts of wüstite (FeO) were found on some. This iron nitride is unusually resistant, even more so than cementite, to attack by the ammoniacal decoppering solution; thus if present in the copper, it should be found in the residues obtained on decoppering. Epsilon iron nitride was identified in some of the residues in which cementite had been found but was not detected in those from the guns in which wüstite had also been found on the bore surface. This may mean that the iron nitride is less stable than cementite when they are formed under conditions that are favorable for the formation of a small amount of wüstite; and that, while iron nitride is found on bore surfaces together with both wüstite and cementite, it may not be stable when carried away from the bore surface and entrapped in the copper. As was implied in Section 12.2.1 on thermodynamic considerations, the question of the formation and stability of the iron nitrides in guns demands further investigation.

Austenite, as is stated in Section 12.2.1 and 15.3.4, has been found in the bore-surface layers of all eroded guns that were examined by x-ray diffraction, no matter what type of powder had been used. It has not been found in residues obtained on decoppering. As a matter of fact, if it were found, it would be necessary to evaluate the results with great caution since even small amounts of copper contaminating the residue would give the same x-ray diffraction pattern as austenite.

Wüstite (FeO), which is the only iron compound that was found by x-ray diffraction studies of guns fired with double-base powder (see Sections 12.2.1 and 15.3.4), is also the only iron compound identified in decoppering residues obtained from such guns.

Other iron compounds that were not found directly on the bore surfaces have been found entrapped in the copper. One of the most interesting of these was iron-rich, brown "enamel," which was the most outstanding feature of a 5-in. chromium-plated Naval gun. This contained a small amount of crystalline material that could be identified by x-ray diffraction analysis. The compounds identified were potassium copper ferrocyanide $K_2CuFe(CN)_6$, wüstite, barium sulfate, and sphalerite (cubic ZnS). The complex cyanide is, in a sense, a true erosion product for it contains iron. It probably represents the reaction between the copper and a complex iron cyanide formed on the bore surface of the gun. Other indications of complex iron cyanides on surfaces of guns and test specimens have been found.[31,98,261]

Wüstite was identified directly on the bore surface of this gun but the area subjected to the x-ray beam is known to have contained a considerable amount of brown enamel and the wüstite is believed to be closely associated with the brown enamel. Wurtzite (hexagonal ZnS) was found at the location of the mouth of the cartridge case, thus it is not surprising that sphalerite (cubic ZnS) was detected beyond the origin of rifling. These two positions in the bore of this gun are shown in Figures 10 and 11, respectively.

Chemical analysis of the brown enamel revealed its complexity. A fair amount of carbonaceous material was present. Although the enamel was not homogeneous, the following analysis can be given as representative of the ignited material. The constituents are listed on the basis that the material is a silicate: SiO_2 5.8%; BaO 1.9%; PbO 7.8%; CuO 11.2%; Fe_2O_3 64.4%; Cr_2O_3 absent; ZnO 5.5%; Mn_3O_4 0.8%. The sulfur content, which must be referred to the barium sulfate and zinc sulfide, identified by the x-ray analysis, was also determined. Part of the iron must be accounted for by the wüstite and complex iron cyanide, but the bulk of it was probably in the ferrous condition in the amorphous glassy material. It is believed that the wüstite associated with the brown enamel was not derived directly from the interaction of the powder gases with the gun steel but was crystallized out of the iron-rich, brown enamel. How the iron became incorporated in this enamel is not known.[f]



FIGURE 10. Surface of the 5-in./25-cal. gun tube No. 1982 T at the location of the mouth of the cartridge case. (*12X.*) (This figure has appeared as Figure 8b in NDRC Report No. A-440.)

Pyrrhotite (FeS + S) was identified in the decoppering residue from only one gun. The fact that it is seldom found agrees with the results of the thermodynamic calculations which showed that ferrous sulfide is not often likely to be found in eroded guns, since its formation involves a self-inhibiting reaction.[60]

[f] For further details concerning this interesting product the reader should consult the original work.[98]

12.3.4 Complexity of Decoppered Residues

It has been shown above that the brown enamel is a complex substance. This complexity also applies to most of the residues obtained on decoppering. It should be remembered that x-ray analysis reveals the presence of crystalline species but does not reveal their chemical complexity. Furthermore, the application of x-ray analysis[g] was further limited by the fact that many unidentified lines were present in the powder photographs, and it was obvious in some cases that considerable amounts of amorphous materials were present which made it difficult to get good, clear patterns. In addition, chemical analyses, other than the ones of the brown enamel, were made which showed large amounts of carbonaceous matter in some cases and also minor amounts of other substances some of which may have been in solid solution in the compounds which were identified.

12.4 EROSION PRODUCTS SEGREGATED BY MECHANICAL MEANS[98]

12.4.1 Erosion Products Collected in Cracks

The material filling the deep cracks of an eroded 3-in. gun was removed mechanically by the method described in Section 11.4.2 and was subjected to x-ray and chemical analysis. Austenite and magnetite (Fe_3O_4) were identified in addition to sulfides of copper and zinc. Chemical analysis showed that 4.7% of carbon and 0.11% of nitrogen were present.

Since cementite was not detected by x-ray diffraction, the presence of extraneous carbonaceous material must be considered to account for this large amount of carbon. In view of the fact that guns are greased, it is more than likely that this grease, lodged in the major crack system, had been repeatedly subjected to hot gases, had thereby undergone destructive distillation, and had left a coherent coke-like substance in the cracks. It is obvious that if chemical analysis only is used in determining the presence of carbon, no inferences can be drawn with respect to the presence or absence of cementite. The nitrogen content was not large enough to permit the determination of either of the nitrides of iron by x-ray analysis. Moreover, this small amount of nitrogen may have been dissolved in the austenite and thus escaped detection by this method of analysis.

[g] The present limitations in x-ray technique are discussed at the end of Section 11.5.2.

CONFIDENTIAL

The thermochemical calculation referred to in Section 12.2.4 indicated that magnetite (Fe_3O_4) would be the ultimate product resulting from the interaction of the powder gases and the steel at lower temperatures than are attained at the bore surface during firing. Thus, while cementite is formed on the bore surface, magnetite will be formed in the deep cracks which extend well below this surface.



FIGURE 11. A crack filled with a "slag" material that may be the same as the "brown enamel" disengaged from the bore surface of the same gun. A—outer white layer; B—slag-filled crack. [Cross section of 5-in./25-cal. gun tube No. 1982T at origin of bore. Etched with picral (*500X*). (This figure has appeared as Figure 15d in NDRC Report No. A-440.)

12.4.2 Constituents of Surface Layers Removed Mechanically

The outer white layer, which was described in Section 12.1.2, spalls readily and in some cases it is possible to remove portions of this layer mechanically. X-ray analysis of some of this material from a 3-in. gun liner revealed the presence of cementite, austenite, and epsilon iron nitride, the same three products that had been found by examinations of the bore surface, which indicates that the compounds identified on the eroded bore surfaces of guns are definitely constituents of at least the outer white layer. In the case of a 57-mm gun, the layer removed was found to contain cementite and the gamma-prime phase of iron nitride (Fe_4N), whereas the epsilon iron nitride (Fe_2N_x) together with cementite had been found in the decoppering residues.

12.5 CONSTITUENTS OF SURFACE LAYERS REMOVED CHEMICALLY

12.5.1 Introduction

The resistance of the white layers to the usual, mild, etching reagents was discussed in Section 12.1.2. Etching with boiling alkaline sodium picrate, however, showed a concentration of cementite in the outer white layer.[112] In Figure 12 is shown the appearance of this outer layer after etching. The high concentration of cementite is indicated by the intense blackening of the surface portion. This blackening decreases in intensity below the surface and thus indicates a decrease in concentration of cementite.



FIGURE 12. The relative concentrations of cementite in an outer white layer as shown by etching with boiling alkaline sodium picrate. A—thin surface film that has etched entirely black; B—steel. [Cross section of 3-in. gun liner No. 881 at 12 in. in front of location of cartridge case. Etched with boiling alkaline sodium picrate (*880X*).] (This figure has appeared as Figure 12e in NDRC Report No. A-440.)

Since a solution of copper potassium chloride is useful in segregating cementite from gun steel, as described in Section 11.4.4, the use of this reagent to segregate the white layers from the underlying steel was undertaken. That this might be done was first demonstrated by etching a specimen typical of an eroded gun that had a cementite-rich surface layer.[98] Both the thermally altered layer and the unaltered steel were deeply etched, the former more so than the latter, while the white layers were but little attacked.

RESTRICTED

Interstitial material had been dissolved out of the outer white layer leaving the blades of cementite sharply defined. When eroded bore surfaces had been subjected to a solution of copper potassium chloride, coherent flakes could be removed. Metallographic examination showed that the bulk of the material removed in this manner was outer white layer from which the interstitial material had been dissolved by the solution.[112] One of these flakes is shown in Figure 13. By a refinement of this technique, it was possible to obtain casts of the crack systems of eroded guns by the method described in Section 11.4.4.



FIGURE 13. Cross section of outer white layer removed by chemical means. [3-in. gun liner No. 1460 at 3½ in. in front of the location of the cartridge case. Not etched (*500X*).] (This figure has appeared as Figure 17 in NDRC Report No. A-440.)

12.5.2

Study of Cementite-Rich Surface Layers

An extensive study was carried out on flakes removed from a 3-in. gun liner that was typical of guns fired with single-base powder.[98] A moderately thick deposit of flows of outer white layer material had spread out on the bore surface in the area at and near the origin of rifling.[112] These complex flows are shown in Figure 8. X-ray analysis of the flakes revealed that the dominant constituent was cementite (Fe_3C). In addition chromium carbide (Cr_7C_3) and the gamma-prime phase of iron nitride (Fe_4N) were found in the material from the lands and a lesser amount of the latter in that from the grooves. Chemical analyses of the flakes bore out the x-ray results. The quantitative analyses of the material chemically removed from the grooves showed that it was essentially iron carbide as truly represented by the formula (Fe_3C) usually given for cementite. The purity of this cementite contrasted sharply with that of the cementite segregated from the steel. The analyses are given in Table 2. In fact, the cementite from the groove surfaces was actually richer in iron with respect to alloying constituents than was the steel itself, as can be seen from the ratios given in Table 3.

TABLE 2. Analysis of 3-in. gun steel and of carbides segregated from the steel and from the bore surface.[98]

	Gun steel (%)	Carbide from steel (%)	Carbide from surface* (%)
Fe	97.35†	64.67	87.0
Cr	0.90	13.05	0.7
Mn	0.74	4.81	0.2
Mo	0.47	5.03	0.2
V	0.07	2.2	.....
Cu	.....	0.56	None
P	0.009	trace	.....
S	0.019	0.59	.....
Si	0.26	0.09‡	None
C	0.17	6.80	6.8
N	0.007	0.34	0.3

* Average of several samples each of which contained flakes from several grooves. † By difference. ‡ Determined as SiO_2.

TABLE 3. Ratios of alloying constituents to iron for gun steel and for cementite removed from the groove surfaces of a 3-in. gun.[98]

	Gun steel	Cementite
Cr/Fe	0.0093	0.0081
Mn/Fe	0.0076	0.0023
Mo/Fe	0.0048	0.0023

Cementite, of course, had been identified on the bore surface of this gun (Section 12.2.1) and also in the outer white layer that had been removed mechanically (Section 12.4.2). Austenite and epsilon iron nitride (Fe_2N_z) had also been detected in the outer white layer (Section 12.4.2). The austenite was probably a constituent of the interstitial material that had been dissolved during the segregation. It is not surprising that the epsilon iron nitride was not found in the material that was removed from the surface with copper potassium chloride. Experiments showed that this nitride is less resistant to attack by this solution than the gamma-prime phase. This very fact permitted the concentration of the latter so that it could be identified by x-ray diffraction. The exact location of the iron nitrides in the outer white layer is not known.

The chromium carbide that was identified in the material from the land surfaces was not detected by direct examination of the bore surface, and, like the gamma-prime iron nitride, was found by virtue of its

CONFIDENTIAL

being concentrated due to the removal of other substances by the copper potassium chloride solution. This result is not unexpected, since the gun steel contains chromium which is a good carbide-former. Under certain conditions chromium carbide is formed more readily than iron carbide. This chromium carbide was also found at the muzzle end of a 5-in., chromium-plated gun where the plate was essentially still intact except along the driving edges of the lands.[98] The presence of this carbide was revealed by x-ray analysis of the crack material segregated by the technique of Vinylite plaques described in Section 11.4.4.

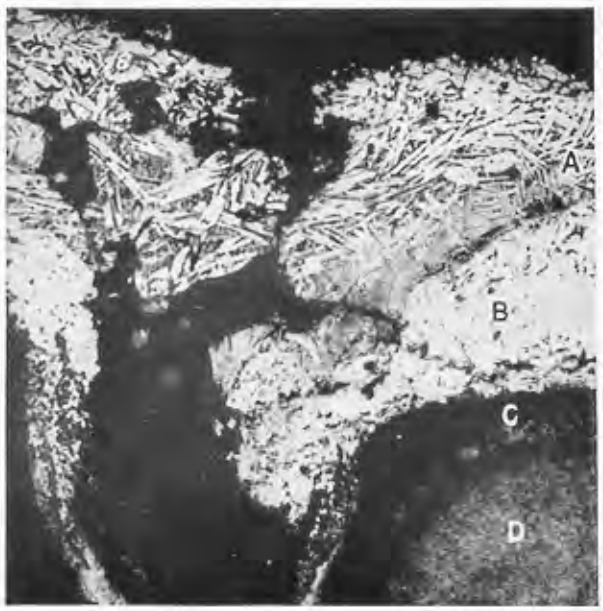


FIGURE 14. A thick white layer which has a well-defined structure only in the outermost portion. A—outermost outer white layer; B—innermost outer white layer; C—inner white layer, which has etched dark with this rather strong etch; D—thermally altered layer. [Cross section of 76-mm gun tube M1A1 No. 1425 at the location of the mouth of the cartridge case. Etched with picral HCl (*1000X*).] (This figure has appeared as Figure 13d in NDRC Report No. A-440.)

Cementite has been found to be the dominant constituent of surface layer flakes from other guns that had been fired with single-base powders.[98]

12.5.3 Study of Austenite-Rich Surface Layer

A 76-mm gun tube that was studied[98,112,265] was found to have a different type of outer layer than the one described above. The steel of this tube contained 4.30% nickel. In front of the location of the mouth of the cartridge case the white layer was unusually thick but forward of this area it was present as a very thin film. Where the layer was thinly spread over the surface, the bore displayed all the features associated with general melting of the bore surface as shown in Figure 17 of Chapter 10. According to metallographic and x-ray evidence, the thick portion of the white layer was not very different from the white layers in other guns that were studied. The outermost portion of the outer white layer had the bladelike forms, which are believed to be the cementite that was identified by x-ray diffraction. The inner portion of the outer white layer seemed structureless. These features are shown in Figure 14. Nickel carbide (Ni_3C) was identified on the surface in addition to cementite. The thin white layer, Figure 15, in the smooth, rippled area, etched a brownish gray but no well-defined structure was apparent. In this region no cementite was detected on the bore surface, but nickel carbide was found here together with austenite.

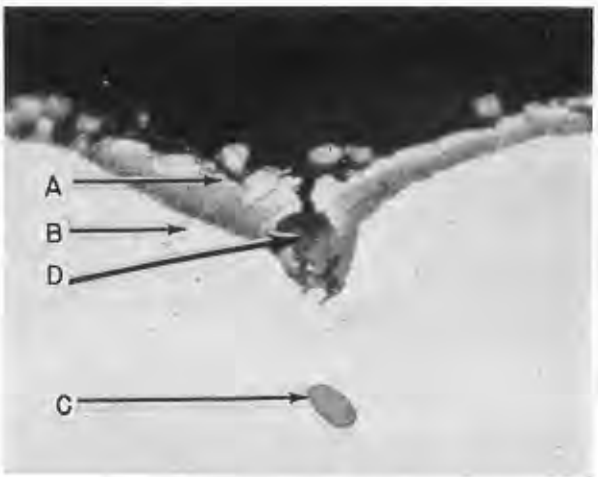


FIGURE 15. A seemingly structureless, thin white layer. A—white layer; B—steel; C—nonmetallic inclusion; D—pocket formed by the fluxing of an inclusion at the bore surface. [Cross section of 76-mm gun tube M1A1 No. 1425 at 14½ in. from the origin of rifling. Etched with picral (*2000X*).] (This figure has appeared as Figure 2b in NDRC Report No. A-440.)

This thin white layer was removed from the bore surface by means of copper potassium chloride solutions. X-ray and chemical analysis showed that the surface layer flakes contained nickel carbide, austenite, approximately 30% of carbon, and a much smaller percentage of nitrogen. There was possibly some

CONFIDENTIAL

gamma-prime iron nitride present, but probably the bulk of the nitrogen was contained in the austenite. The chemical analysis indicated that the nickel carbide did not constitute the bulk of the material in this case as did the iron carbide (cementite) in the case of the white layers in other guns. In this 76-mm gun the surface layer was only slightly enriched in nickel, for the ratio of nickel to iron was not much greater for the surface layer than for the steel.

The incipient melting points of some of the products in this 76-mm gun tube were determined by the method described in Section 5.4.3. There is no doubt that liquefaction of the bore surface took place in this tube and therefore the temperatures at the bore surface during firing must have been above the incipient fusion temperatures of the products. For this reason these melting point determinations are of interest.[105]

The segregated surface layer flakes began to melt at 1150 C. This temperature may be somewhat higher than the actual incipient melting point of the white layer for minor amounts of material may have been dissolved in segregating the layer. Another experiment was carried out which was not subject to this error. Some bore surface material was detached mechanically from the area which had a thick white layer. This began to melt at 1125 C thus indicating that fusion of the reaction products could take place at a temperature at least 300 degrees lower than that of gun steel.

12.6 SUMMARY OF EVIDENCE OF THERMAL AND CHEMICAL ALTERATION

Generalizations concerning the mode of formation of the altered surface layers in eroded gun bores can be drawn from the nature of the erosion products described in the preceding sections of this chapter. The causes of gun erosion, which are discussed in Chapter 13, must take into account a mechanism which is in accord with the observed changes that take place in the bore surface of a gun during firing. The accumulated evidence shows that thermal, chemical, and mechanical factors have all played a role in the alteration of the bore surface. The first two of these are mostly important in producing the types of products that are found. The third is mostly effective in removing them.

The bore surface of a gun is influenced to a greater depth by the heat developed in firing than it is by the chemical action of the powder gases. All but the surface of the altered layer has been shown to differ from the unaltered steel only in texture, not in chemical composition. It is believed, however, that at the very surface the altered layer has dissolved sufficient carbon or nitrogen or both to liquefy partially and to retain austenite on quenching. Thus the first step in the chemical alteration of the bore surface is probably the formation of a surface layer which has the characteristics of the inner white layer when quenched.

Once an *inner white layer* is formed, reactions at the bore surface are with this layer, which is partially liquefied in place during subsequent firing. With increasing chemical complexity of the immediate surface material, the melting temperature is decreased to the point where the material can flow. Material that is of a different chemical composition than the unaltered steel has been observed on many eroded bore surfaces. This forms what is known as the *outer white layer*.

The surfaces of guns having such a layer show features characteristic of liquefaction, as described and illustrated in Section 10.5.2. Metallographic examination of cross sections also gives evidence of liquefaction by revealing laminated structures, as if formed by superposed flows. These structures have been observed for both types of outer white layer. The one that consists essentially of cementite blades that apparently have crystallized out of a melt flows like a mush, whereas the rarer seemingly structureless one without cementite blades apparently flows more easily. Thus all the accumulated evidence indicates that the outer white layer has been liquefied and has flowed into place. Its temperature of liquefaction for one gun has been found to be about 1125 C.

That chemical reactions have taken place between the bore surface and the powder gases is borne out by x-ray studies made of the bore surface and of material found entrapped in the coppering. Further evidence for these reactions has been found by making detailed studies of the outer white layers. The difference in chemical composition between the outer white layer and the underlying steel is obvious from thermal considerations alone: thus the structure of this layer is not obviously changed by tempering; also partial melting of the material at a temperature much lower than that of gun steel as mentioned above indicates that the addition of materials to the surface has lowered the fusion range. In the case of guns fired with single-base powders, the penetration of carbon and nitrogen has been proved, as discussed at length in

Chapters 13 and 14. Chemical analyses of outer white layers removed from bore surfaces by chemical means have confirmed the x-ray evidence that the bulk of the material removed in this manner was essentially a pure iron carbide associated with lesser amounts of iron nitrides. X-ray analysis of material removed by mechanical means showed that austenite, which usually is dissolved when chemical methods of segregation are employed, is an important constituent of the outer white layer.

Guns fired with double-base powders rarely have outer white layers that are as readily amenable to detailed study as those in guns which have been fired with single-base powders. In this case, nevertheless, x-ray analysis of the bore surfaces and of decoppering residues, have shown that ferrous oxide and austenite are the dominant products. Thus reactions do take place between the bore surface and the gases from powders containing nitroglycerin as well as those containing only nitrocellulose.



Chapter 13

THE CAUSES OF GUN EROSION

By *C. A. Marsh*[a] *and J. N. Hobstetter*[b]

13.1 INTRODUCTION

13.1.1 Experimental Approach

THEORIES concerning the causes of gun erosion were formed as early as fifty years ago.[c] Since then many investigators using different techniques have arrived at different conclusions. The lack of agreement may be attributed to several reasons, the most important of which is the fact that most of the early contributors to this study tried to single out the dominant mechanism of erosion and to base their theories of gun erosion upon it alone.

Gun erosion is a complicated process which involves a number of interrelated factors. In spite of their interdependence, which will be stressed in this chapter, different ones of these factors may predominate even in the same gun at certain positions in the bore. Since the early investigators studied several types of guns all with different firing histories, it is not surprising that the dominant mechanisms postulated did not always agree.

Some of the disagreement among the early theories was undoubtedly due both to the techniques employed, some of which are mentioned in Section 12.1.1, and to the fact that in many cases only one line of experimentation was carried out. A variety of methods should be used to study a problem as complicated as gun erosion; furthermore, as many of these as possible should be resorted to in the case of one particular gun. Only after a number of guns have been studied systematically, is it possible to obtain a logical explanation of gun erosion.

Such studies of eroded guns by Division 1 contractors have been described in Chapters 10 and 12. Other pertinent information has been derived from examinations carried out concurrently at Watertown Arsenal on eroded gun tubes of different sizes,[282,283] especially the new 76-mm gun, M1.[247,248,257,259,268] In these examinations special attention[264–267,269] was paid to a type of failure designated as "progressive stress-damage" (Section 13.5.3). In addition, experiments on rifles, liners, vent plugs, test rods, and blocks of steel and other materials, described in Chapters 11, 14, 15, and 16, have yielded a great deal of information that can be fitted together to give a clear and consistent picture of the erosive process in guns.

13.1.2 Principal Factors Involved

It has proved of great value to group the many factors operating in erosion under three general headings: thermal, chemical, and mechanical factors. However, it is not to be assumed that these groups of factors act independently. Rather, it appears that gun erosion is caused by the simultaneous interaction of thermal, chemical and mechanical influences.

Thermal factors, which come about by the transfer of heat from the hot powder gases to the bore walls, are found to contribute to erosion in three important ways. First, the heating causes softening of the bore which makes it more susceptible to the action of mechanical factors. Second, the heating causes the formation at the bore surface of a layer of austenite, which appears to have considerably less resistance to chemical attack by the powder gases than other steel modifications. Third, the heating causes a liquefaction at the bore surface of steel itself, when powders of high flame temperature are fired, or of low-melting mixtures of reaction products, when powders of low flame temperature are fired.

Chemical factors, which come about through chemical interactions of the bore surface and constituents of the powder gases, are controlled as to nature and rate by the temperature obtaining. It is found that the highest range of temperatures favors oxidation, with the formation of FeO, while somewhat lower temperatures favor carburization, with the formation of Fe_3C. Carbon and nitrogen are both found to penetrate the outer skin of the austenitic layer, which is

---

[a] Geophysical Laboratory, Carnegie Institution of Washington. (Present address: U. S. Geological Survey, Washington, D. C.)

[b] Department of Metallurgy, Harvard University. (Present address: Department of Engineering Sciences and Applied Physics, Harvard University.)

[c] The subject of this chapter is one on which extensive studies have been made. Since this was not intended to be a historical account, scarcely any reference has been made to work prior to 1940. Summaries of the early work may be found in three reports[16,261,479] that contain extensive bibliographies.

partly stabilized thereby. Continued reactions and liquefaction of this layer may result in the formation of a complex "white layer" on the bore surface.

Mechanical factors, which involve the stressing of the bore surface by the pressure of the propellant gases and the projectile, effect the actual removal of solid and liquefied material from the bore. Sweeping and scouring action by the gases are found to be important mechanisms. Scoring by gas leakage assumes importance in some cases. Abrasion and swaging by the projectiles are found to contribute appreciably to erosion during whatever time interval the bore experiences softening.

Cracking of the bore is also a factor in causing gun erosion; and the same factors that cause erosion contribute to cracking. Since it is important both as cause and effect, it is treated in a separate section, where its apparent dependence upon very numerous and intricate interrelations among the influences of thermal, chemical, and mechanical shock is described.

The term "shock" has been applied to the chemical as well as to the thermal and mechanical factors to emphasize the briefness of the interval of time in which all three of these factors usually act to alter the bore surface in such a manner that it may be readily removed or distorted.

13.2 THERMAL FACTORS

13.2.1 General Statement

Under the heading of thermal factors are grouped all of the effects directly associated with either the attaining of elevated temperature levels within the bore walls or the changing of those levels during the firing of a gun. Evidently, these effects contribute directly to gun erosion only insofar as they include liquefaction of material at the bore surface. Nevertheless thermal factors play a most important role in erosion when they act in concert with chemical and mechanical factors. Indeed, they may be said to act as overall regulators of the erosive process.

For example, the effect of mechanical stresses depends upon the mechanical properties of the bore wall at the moment when it experiences the stresses. These properties depend in turn on the temperature distribution in the barrel at that moment. Again, the effect of chemical reaction of the bore surface depends on the nature and rate of reactions between the bore material and the constituents of the powder gas. Which of the many possible reactions actually occur at any moment, as well as the rate at which they proceed, depends upon the temperature obtaining at the bore surface at that moment.

It is thus evident that any adequate understanding of the cause of gun erosion must include as a first step a full history of temperature changes experienced by the bore wall. In other words, thermal factors must be quantitatively understood.

13.2.2 Thermal Softening of the Bore

It is well known that the hardness of gun steel drops rapidly if its temperature is raised much above 500 C and that concurrently the strength decreases and the ductility increases. If stresses are applied to the steel when it is in this softened condition, it is obvious that considerably different behavior is to be expected than if they were applied to cold steel. It is important to consider, then, what kinds of stress the bore of a gun experiences when its surface is thermally softened. Two extreme cases can be pictured which bracket the true behavior of any gun: single-shot guns in which cooling is substantially complete between rounds and rapid-fire guns in which the whole bore wall may rise above the softening temperature during prolonged bursts. The first few shots fired in rapid succession from an initially cold machine gun barrel represent an intermediate case: here the whole thickness of the barrel has not yet become hot, but near the origin of rifling a very thin layer of steel beginning at the bore surface remains so hot between rounds that it is soft, and variously transformed on cooling.

Single-Shot Guns

It is not difficult to imagine the history of a single round from among many fired in a single-shot gun. At the moment of firing the bullet begins to move down the bore, passing over a surface bearing the hardened layer which is discussed in Section 13.2.3. This hard layer probably resists adequately the stresses accompanying the engraving and friction of the bullet except that it may become cracked because of the mechanical shock and its low ductility. Such cracking is discussed in detail in Section 13.5.3.

Hot gases follow immediately behind the bullet and heat the bore surface. It has been shown in Chapter 5 that a relatively thin skin at the bore surface is rapidly heated in this way to temperatures far be-



yond the softening temperature. The actual amount of softening that results from this heating increases progressively, since softening is a function of the time at temperature. In any case, as the bore softens it is subjected to scouring action and gas pressure, as described in Section 13.4.1, and is more easily affected by these processes because of deteriorating mechanical properties.

It may be noted that some gases may leak past the bullet and preheat the bore. Friction between the bullet and the bore also cause heating of the bore. Whatever softening accompanies these phenomena, of course, permits an increased superficial deformation of the bore surface during engraving and passage of the bullet, but it seems unlikely that the effect could be large except in extreme cases of faulty obturation.

Finally, the bullet and gases rush from the gun, the heat transferred to the bore surface concurrently diffuses very rapidly into the cold metal of the bore wall, and the hardness of the bore surface is restored.

Rapid-Fire Guns

In principle, the effects accompanying rapid fire are the same as those accompanying single shots except that the heat transfer to the bore surface is effected so frequently, as described in Sections 5.4.2 and 5.5.1, that the whole barrel begins to heat. As is brought out under "Swaging" in Section 13.4.2, a layer extending to a considerable depth below the bore surface may remain in the soft austenitic state. Under these conditions, the bullet passing down the bore encounters only a very soft surface. In addition, the gas pressure may actually dilate the whole softened tube.

13.2.3 Thermal Transformation at the Bore Surface[d]

Development of Austenitization

The methods of calculation outlined in Section 5.4.1 show that the temperature of the bore surface of gun tubes can rise not only above the softening temperature, but above the critical temperature of steel, about 750 C. Indeed, it has been shown that at the hotter parts of the bore surface, a zone more than 0.002-in. thick may experience supercritical temperatures during the firing of a single round. This circumstance suggests very strongly that the bore surface can be transformed to the high-temperature (gamma) modification of iron known as austenite.

That such transformation does actually occur is abundantly demonstrated by the existence of the thermally altered layer which is found in all gun steel tubes, as has been described in Section 12.1.2. It may be mentioned again here that in the caliber .50 erosion-testing gun (Section 11.2.1) this layer is formed by the firing of one round, that its thickness depends almost entirely on the powder and the conditions of firing, as is emphasized in Section 15.5.4, and that it forms under thin protective coatings which prevent direct contact with the powder gases. These facts argue convincingly that the layer is of thermal, not chemical, origin.

Mechanism. Any thermal transformation of this sort depends on time as well as temperature. The transformation in gun steel can be pictured as involving first the formation of austenite from the ferrite (alpha iron modification containing little carbon) and the subsequent solution of carbides in austenite as solvent. Both processes are controlled by the diffusion rate and take time to occur. Of course, it would be proper to speak of austenitization even if the carbide solution process were incomplete, and thermally transformed layers containing undissolved carbides have been observed after the firing of only one round in the caliber .50 erosion-testing gun (Section 11.2.1).

Evidently, the region along the bore surface that is transformed is the region which experiences thermal conditions sufficient to cause austenitization and the rather sharp interface between altered and unaltered steel experiences critical conditions. Because this in-

[d] This section is based on an NDRC report[124] by one of the authors of this Chapter. It uses evidence obtained from a study of eroded gun barrels and liners fired in a particular gun under hypervelocity conditions to support a theory of the interrelations between thermal and chemical factors in the erosion of that gun. There has not been opportunity to determine the extent to which the same approach may be made in the study of other eroded guns. Since this is the first attempt to reduce this important subject to a quantitative basis, it seems desirable to present this point of view in some detail, even though full experimental verification is lacking. Thus the attempted experimental comparison of the relative reactivities of austenite and ferrite is open to the criticism that the observed differences in chemical reactivity can be accounted for on the grounds of differences in temperature and texture. (See Section 12.1.2.) Also examination[86] of some medium-caliber guns fired at conventional velocities has revealed "mushrooming" below chromium plate on a steel surface that had not been thermally altered. It is hoped, at any rate, that future investigators may be stimulated by this account of a new approach to the subject to pursue it further. (Editor's note.)

terface reaches supercritical temperatures during one round, time at temperature must be the limiting factor.

A study was made of the time interval during which the altered layer interface was at supercritical temperatures during single rounds fired with different powders and charges in the erosion-testing gun, which is described in Section 11.2.1. Although the austenitization time could not be definitely evaluated, it seemed to be constant. It was determined, however, that the thermally altered layer was formed in all regions that reached the critical temperature at least 0.0002 sec before the attainment of maximum temperature at the bore surface. This criterion enables the thickness of the altered layer in different guns to be predicted under a wide variety of firing conditions. It also implies that the austenitization time is of the order of 0.5 msec.

Distribution. Thermally altered layers in the gun barrels studied were found to vary in thickness both circumferentially and axially, as described in Section 15.3.3. Thicker layers were found on the protruding lands, particularly on the land corners where heat can enter the metal through two adjacent surfaces. Impoverishment of the heat transfer to the grooves immediately next to the lands was such that the overall heat transfer was inappreciably different from what it would be in unrifled tubes.[18]

The thickness of the layer decreased toward the muzzle. Although the layer formed during the firing of the first round, it thickened progressively with continued single shots except near the origin of rifling. Thus, nearly complete cooling between rounds must have been effected near the origin of rifling by the relatively thick, cold bore walls, whereas toward the muzzle incomplete cooling was effected by the thinner walls.

Reactivity of Austenite

The thermally altered layer in single-shot guns occurs in two modifications, both of which differ from the unaltered steel. The layer is austenite when hot, as described above, and martensite (together with some retained austenite) when it has cooled quickly after the firing of a round, as described below. Either or both of these modifications may be expected to have different chemical properties from the ferrite of the unaltered steel and it is important to consider these properties since, in any round after the first, it is the altered layer that is eroded by the powder gases.

Observation of Greater Reactivity. One of the earliest observations[86,112] relative to the behavior of barrels plated with erosion-resistant coatings was that if the plating were insufficiently thick, it was undercut by considerable erosion of the thermally altered layer that formed beneath it. This behavior is shown quite clearly in Figure 1. The thin coating is chromium plate which has become cracked during firing. The cracks have provided the powder gases access to the thermally altered layer which has, thereupon, developed a pocket-like erosion called "mushrooming."



Figure 1. Pocket-type erosion beneath chromium plate of a steel liner fired in the erosion-testing gun. Nital etch. *200X*. (This figure has appeared as Figure 10 in NDRC Report No. A-452.)

In no case has it been observed that "mushrooming" penetrates the unaltered steel. The increased temperature near the bore surface is insufficient to explain either this greater reactivity or the rather sharp drop in reactivity at the altered layer interface. Accordingly, it may be concluded that the thermally altered layer is in fact much more easily eroded by the powder gases than is unaltered steel.

It remains to show if either or both modifications of the altered layer are easily eroded. The reactivity of the martensitic layer was studied by forming first an altered layer under a thin resistant coating, then protecting this layer with a coating more than critically thick which permitted no further austenitization of underlying steel. (Studies to determine the critical thickness of chromium-plate are described in Section 31.5.) The results are shown in Figure 2 where no evidence of "mushrooming" in the thermally altered layer can be seen. Thus it follows that

CONFIDENTIAL

only in its austenitic state is the altered layer much more easily eroded than ferrite.

Relation to Chemical Erosion. On the basis of these findings it is not difficult to draw a picture of the process of chemical erosion insofar as it is related to thermal factors. Let us consider any one round fired in a single-shot gun. The erosive gases will first strike the bore when it is rather cold and only reactions that can take place at low temperatures may be expected to occur. The bore surface will be heated rapidly, however, first softening and then being transformed



FIGURE 2. Chromium-plated liner fired in the erosion-testing gun. The altered layer was first formed under a thin plate and subsequently protected by the deposition of a very thick plate. Nital etch. *200X*. (This figure has appeared as Figure 11 in NDRC Report No. A-452.)

to austenite. It is believed that during and after this transformation the rates of whatever chemical reactions are going on are enormously accelerated, on one hand by the higher temperature but mostly by the formation of the more reactive phase.

Eventually, the bore-surface temperature reaches its maximum and falls back below the critical temperature whereupon most of the austenite decomposes. The erosive reactions, in turn, become much less violent along with the disappearance of austenite and gradually change character as they revert to the low-temperature type.

The nature of all these reactions is discussed in detail in Section 13.3 on "Chemical Factors."

DECOMPOSITION OF AUSTENITE

The decomposition of austenite which occurs after the peak temperature at the bore surface has been reached may be expected to take place in the same manner as in the ordinary heat treatment of steel. All of the structures that may be obtained by different heat treatments of steel are shown diagrammatically in Figure 3. The mathematical study of wall temperatures given in Section 5.4.1 reveals that the temperature of the bore surface in single-shot guns falls very rapidly indeed. All such very rapid cooling rates suppress completely the isothermal decomposition of the austenitic steel of the composition of gun steels so that pearlites do not form. Instead, the martensite reaction sets in at a very low temperature, which is independent of the cooling rate and the hard, martensitic phase is formed. This phase, then, is what is actually observed when the altered layer is studied metallographically.

It may be noted that the temperature of the beginning of the martensite reaction is generally depressed whenever foreign elements are dissolved in the austenite. Carbon and nitrogen have a pronounced effect in this regard and their presence in the austenite can easily depress the temperature of the martensite reaction below room temperature.

In Chapter 14 it is shown that carbon and nitrogen do penetrate slightly the austenitic layer. In this manner, the immediate surface of the austenite usually becomes stabilized and does not form martensite. This thin skin is usually called the inner "white" layer. The outer "white" layer which is sometimes abundantly found also contains austenite. For a detailed description of the "white" layers see Section 12.1.2 .

13.2.4 Liquefaction of the Bore Surface

Evidence of liquefaction at the bore surface has been presented in Sections 10.5.2 and 12.6. Such a process, assisted by motion imparted mechanically, is the most direct way in which erosion can be brought about by thermal factors. Even so, liquefaction is aided to a very great extent if low-melting mixtures of chemical reaction products are first formed at the bore surface.[6] The nature and the rate of the liquefying process are most easily classified according to the thermal conditions obtaining in the gun and these

[6] An experiment to evaluate the relative importance of melting and chemical attack in the erosion of vent plugs is described in Section 16.4.14.

CONFIDENTIAL

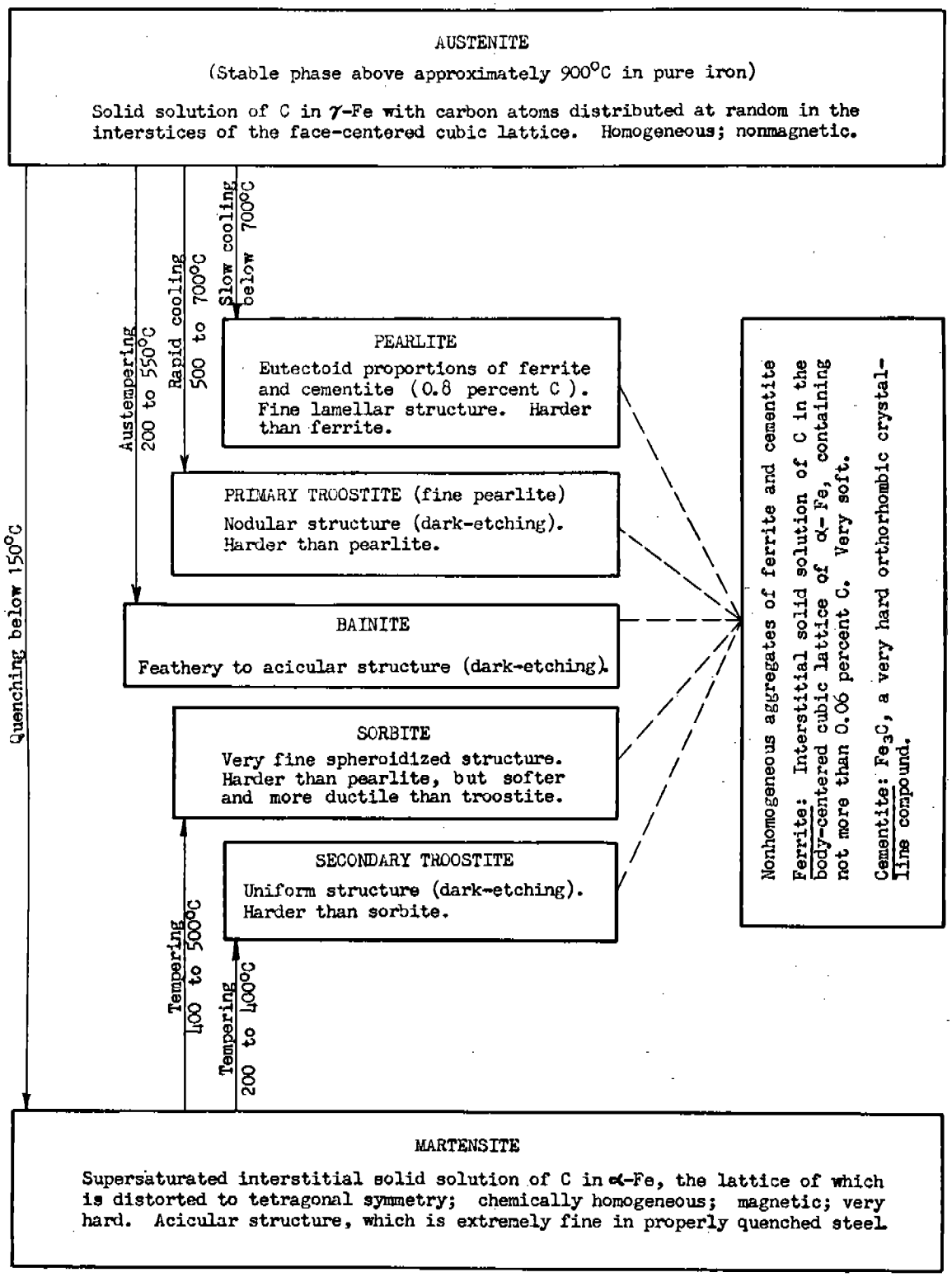


FIGURE 3. The microstructural constituents of steel. (This figure has appeared as Table XX in NDRC Report No. A-91.)

conditions are largely determined by the type of powder fired. The two large classes that can be distinguished are discussed in the following paragraphs.

Liquefaction with Double-Base Powders

It has been found in experiments with the caliber .50 erosion-testing gun (Section 11.2.1) that measurable erosion of gun steel barrels begins with the first round when double-base powders of high flame temperature are fired.[123] Metallographic examination has also shown evidence of liquefaction after the firing of the first round.[123] Furthermore, calculations show that the peak temperature of the bore surface is well above the melting point of steel when such powders are fired.[124] The conclusion that liquefaction of an ordinary gun steel surface takes place when very hot powders are fired is, therefore, inescapable. Any low-melting mixtures of reaction products which may also be formed at the bore surface will, of course, aid the liquefaction, but it would appear that these mixtures are not necessary and that liquefaction can occur in their absence.

It follows, then, that the rate of liquefaction should be limited by the rate at which heat can be transferred to the crystalline part of the bore surface and not by the rate at which chemical reaction products are formed and removed. Erosion may be expected to occur at a rapid rate starting with the first round, which expectation is in accord with observed facts.

Liquefaction with Single-Base Powders

When single-base powders of low flame temperature are fired in the caliber .50 erosion-testing gun, the observed facts of erosion are quite different. Measurable erosion does not begin with the first round, rather there is a lag or "incubation" period.[123] Metallographic evidence of liquefaction is not found until the end of the "incubation" period when pebbling of the surface (Section 10.5.2) begins.[123] Calculations show that the peak bore-surface temperature is less than the melting point of steel.[124] These facts can be explained only on the basis that a mixture of chemical reaction products and not gun steel itself is liquefied. The "incubation" period then becomes a period during which initial reaction products are being formed and the subsequent erosion is limited by the rate of continuing formation and removal of these mixtures and not by the relatively rapid rate of heat transfer that results in their liquefaction.

13.2.5 Importance of Thermal Factors in the Centering Cylinder

Considerable erosion often takes place in the centering cylinders of guns. Here the main cause of erosion is the heat transferred from the powder gases, since the engraving of the projectile has not yet begun. Because of the contour of the chamber, the flow of gases in the centering cylinder is turbulent. Thus more heat is imparted to the walls here than in the bore where the flow of gases, next to the walls at least, is laminar. The type of flow in the different portions of a gun tube is illustrated in Figure 4. The gas stream converges in a *vena contracta* effect when it passes from the large portion of the chamber, and the full force of the turbulent stream thus produced does not strike the tube walls until it reaches an area within the centering cylinder. Here the turbulent gases strike the surface in a radial normal direction and eddy backwards.

Although erosion is produced by these turbulent gases in both bag-fired and case-fired guns, its effects are more noticeable in the latter because erosion of the chamber does not occur in the area protected by

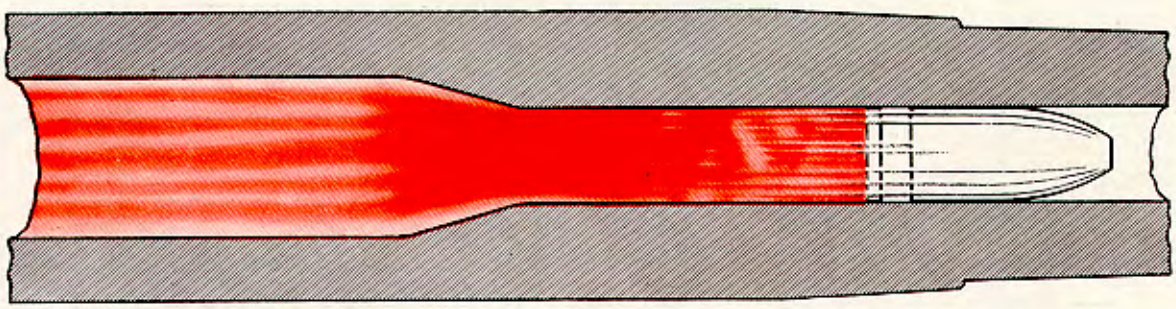


Figure 4. The transfer of heat from the turbulent powder gases to the bore surface is increased by the *vena contracta* effect introduced by chambrage.

the cartridge case. In extreme cases, the centering cylinder, between the origin of rifling and the position of the cartridge case, appears to have been scooped out.

13.3 CHEMICAL FACTORS

13.3.1 Introduction

The discussion of the products of erosion in Chapter 12 has shown that a consideration of the reactions of the constituents of the powder gases with gun steel is of utmost importance in formulating a mechanism of gun erosion. The elements present in the gases resulting from the combustion of all the usual propellants are carbon, oxygen, hydrogen, nitrogen, and sulfur. The effects of separate ones of these constituents has been studied by means of carefully controlled laboratory experiments, the results of which are given in Chapter 14.

It must not be concluded, however, that these elements act independently as such to bring about chemical changes in the bore surfaces of guns during firing. Rather, the powder gases must be considered to consist of a mixture of molecules in which the above elements are combined. Their concentrations depend not only on the type of powder but to a large extent on the temperature of the gas mixture. The type and rate of reactions which take place between the steel and the powder gas depend essentially on the temperature of the bore surface and the composition of the gas, which in turn depends on its temperature. These reactions and the conditions effecting and affecting them are the subject of this section. Insofar as possible they are related to the observations and results described in Chapters 12 and 14.

13.3.2 Penetration of Carbon and Nitrogen

Difference Between Penetration and Surface Reactions

The reactions which produce carbides and nitrides are considered to be the most important of those which contribute to gun erosion. This conclusion was derived not only from the evidence presented in Chapter 12 but from thermodynamic considerations[60] which showed that in guns fired with single-base powders the major product to be expected is cementite (Fe_3C), whereas in guns fired with double-base powders the major product is wüstite (FeO). In the latter case, however, the oxidation of the bore surface is probably of little importance since heat is sufficient to melt the steel under an oxide film, as was mentioned in Section 13.2.4. Furthermore carburization and nitriding of the steel are penetration reactions, whereas oxidation is essentially a surface reaction. Oxide films are easily removed in firing, but the metallic alteration products containing carbides and nitrides may accumulate in some cases to a considerable thickness; hence, in the case of oxidation evidence is not usually as abundant as in the case of penetration of carbon and nitrogen.

These penetrating reactions produce complications in the determination of ultimate products by thermodynamic methods, as is described later, for solid solutions involving carbon and nitrogen are formed, for which there are insufficient data to permit of their treatment. It is believed that an understanding of the systems Fe-C and Fe-N so far as is known is desirable in order to consider the role of carbon and nitrogen in gun erosion.

Iron-Carbon System

A simplified, equilibrium diagram[503] for the iron-carbon system is shown in Figure 5. This might be more truly called a diagram for the iron-iron carbide system since only the high iron end is considered.

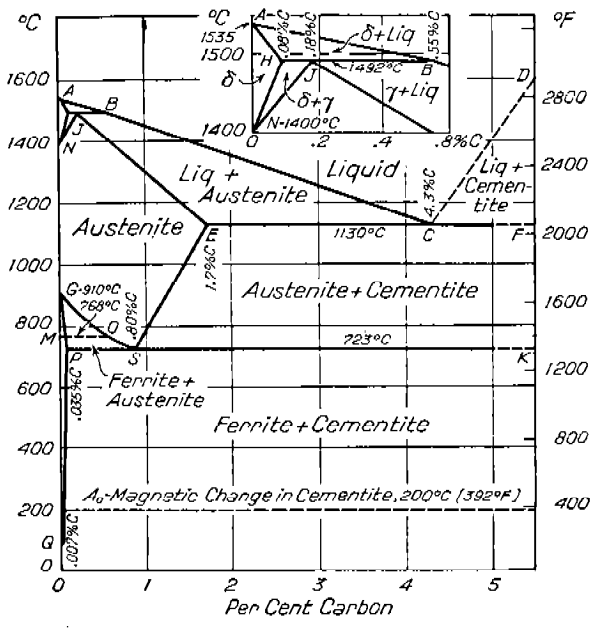


Figure 5. Iron-carbon constitution diagram. (Reproduced from *Metals Handbook*, 1939 ed., p 368, by permission.)

This diagram is simplified in that it gives no indications of the microstructural constituents, which are combinations of the crystalline phases arranged in definite textural patterns that are observed metallographically. For example, the lower half of the diagram shows only the phases ferrite and cementite (6.67% C). In the field designated as "ferrite plus cementite" the microstructural constituents pearlite and ferrite are present to the left of a perpendicular dropped from S; between perpendiculars from S and E, pearlite and cementite are present. Pearlite itself consists of a mixture of ferrite and cementite but in definite proportions and with a characteristic structure.

For those who are not familiar with such constitution diagrams several examples will be given to illustrate the meanings of the various points, lines, and fields. The left edge of the diagram represents pure iron. As the right side of the diagram is approached the composition is that of iron with increasing amounts of carbon. The line $ABCD$, called the liquidus, represents the beginning of solidification on cooling and the end of melting on heating. All points above this line represent alloys in a completely molten condition. All points below $ABCD$ represent alloys partially or completely solid.

The alloy containing 4.3% carbon is the *eutectic alloy* and solidifies entirely at the point C with the simultaneous formation of austenite and cementite. At the eutectic temperature austenite will hold 1.7% carbon. Cementite precipitates out on cooling below this temperature, the limit of solubility of cementite in austenite being represented by the line SE. The point S is called the *eutectoid*. It is similar to the eutectic C except that it is completely surrounded by solid fields.

Any further explanation of this diagram will be postponed until it is referred to in connection with the phenomena associated with gun erosion. Information on microstructures obtained by quenching and by other methods which depart from equilibrium conditions may be obtained from Figure 3.

Iron-Nitrogen System

Several different diagrams for the system iron-nitrogen or iron-iron nitride have been proposed.[503] Molecular nitrogen does not react appreciably with iron; the formation of nitrides is usually carried out through the medium of ammonia. The constitution diagrams do not represent equilibrium conditions but must be considered behavior diagrams. The work on this system is far from complete, but enough has been done to show the similarity between alloys of iron and carbon and alloys of iron and nitrogen.[40] Thus the names of the following constituents that have been found are self-explanatory: nitroferrite, nitroaustenite, and nitromartensite. The eutectoid alloy has been called braunite.

Some of the proposed diagrams were based on experimental work which employed the x-ray diffraction method of analysis. The pertinent data obtained are given here. The eutectoid temperature was found to be 591 C with a nitrogen content of 2.35%. The occurrence of iron nitrides, Fe_4N and Fe_2N_x, has been established. The former, which is called the "gamma-prime phase," has a face-centered cubic structure with a cell size somewhat larger than that of the "gamma phase" (nitroaustenite) when it contains almost as much nitrogen. The latter, which is called the "epsilon phase," has a hexagonal structure and may contain from 8 to 11.3 per cent of nitrogen. The compound Fe_4N is supposed not to be stable at high temperature and to decompose at 650 C into the gamma and epsilon phases.

Further experimental work was carried out on the system iron-nitrogen in connection with the investigation of gun erosion by Division 1. This work[28] is discussed in Section 14.5.3. The experimental results led to the conclusion that since they are not stable under firing conditions, iron nitrides are formed in guns during the cooling stage either by low-temperature reactions with the powder gases or by precipitation from nitroaustenite.

Penetration of Carbon and Nitrogen

If conditions are such during firing that carburizing reactions may take place, then carbon may penetrate the steel bore-surface. Since carbides and nitrides are generally found together in the eroded bore surface and since the two systems of those elements with iron are somewhat similar, it is assumed that nitrogen and carbon penetrate simultaneously. Confirmation in the case of carbon was obtained from the work discussed in Section 14.2 in that carbon penetration was observed, except when FNH-M2 powder was fired, which involved oxidizing conditions.

When austenitization of the bore takes place, as described in Section 13.2.3, it is to be expected that the surface may pick up carbon or nitrogen or both from the powder gases, since the steel does not con-

tain the total amount of carbon or nitrogen that may dissolve in austenite. That carbon actually does penetrate below the layer of reaction products was proved by the experiments with radioactive carbon, the results of which are given in Section 14.2. The carbon did not penetrate to the full depth of the thermally altered layer.

The penetration of carbon or nitrogen or both [at least as far as the bottom of the inner white layer (described in Section 12.1.2) while it remained at the bore surface] is inferred from the fact that this layer is more resistant to mild etches than is the thermally altered layer beneath it. Also, it appears to have been locally slightly liquefied in place, which signifies that the melting point has been lowered by additions of material from the powder gases. The fact that an apparently austenitic structure has sometimes been observed is considered as evidence that austenite was retained in this layer because it had dissolved carbon or nitrogen or both.

The outer white layer, described in Section 12.1.2, although it consists essentially of cementite, is not believed to be merely the result of surface reactions but to constitute evidence of both carbon and nitrogen penetration. It presumably was formed by continued penetration of the inner white layer by the carbon and nitrogen of the powder gases, as described below.

Formation of the White Layers Enriched in Carbon and Nitrogen

Experiments showed in separate instances that both thermal[123] and a minor amount of chemical[99] alteration (carbon penetration) take place during the firing of the first round through a gun.[f] The amount of carbon which has penetrated increases with the number of rounds. By the time the surface has taken up enough carbon to be partially liquefied (see Figure 5 for the boundaries of the field "austenite plus liquid"), there is no longer the question of whether compounds of iron or solid solutions are formed; the powder gases react with the partially liquefied surface which presumably can dissolve more carbon, and possibly nitrogen, than austenite can. The result is an increased "penetration."

[f] It is not known whether this is true for all types of guns. The study of thermal alteration was carried out with the caliber .50 erosion-testing gun; the study of carbon penetration with caliber .30 rifles preheated to different temperatures.

This process continues with a further number of rounds and the melting point is successively lowered until it may reach the eutectic temperature (point C in Figure 5). With the lowering of the melting point, the surface layer may actually flow. The evidence presented in Section 12.6 indicates that the outer white layer is material that has flowed.

It appears in the case of guns that have a white layer in which cementite is the primary constituent that the eutectic composition of carbon was exceeded and that cementite plus liquid (Figure 5) had been present on the surface. Nitrides are found associated with cementite in this layer which means that, whatever the mechanism by which nitrogen was introduced, it did penetrate and nitrides crystallized either out of the melt or out of the austenite which was retained in the interstices between the cementite blades.

For a further discussion of the role of nitrogen in gun erosion see Section 14.5.

13.3.3 Reactions at the Bore Surface During Firing

In the preceding section the systems iron-carbon and iron-nitrogen were discussed to orient the reader with respect to penetration studies. In the reaction of the gun steel with all the constituents of the powder gases, the system involved is Fe-C-O-H-N-S. All the details of this complicated multicomponent system are not necessary in determining what products are likely to be formed on bore surfaces during firing. The thermodynamic methods used to determine the theoretical products of erosion were described briefly in Section 12.2.4. The reactions involved are the subject of this section.

Reactions with the Components of the Water Gas Reaction

The compounds of iron that may be formed on the bore surface under a variety of conditions depend on concentrations of the components of the powder gases under those conditions. At the temperatures obtained during firing, the major components are those of the water gas reaction (1),[107] as is brought out in Section 2.2.2.

$$CO_2 + H_2 \rightleftharpoons CO + H_2O \qquad (1)$$

The equilibrium constant for this reaction, expressed



by equation (2) [which is the same as equation (5) of Chapter 2],

$$K_{wg} = \frac{[CO]\,[H_2O]}{[CO_2]\,[H_2]}, \qquad (2)$$

and the CO/CO_2 ratio decrease with the temperature of the gases. At lower temperatures, soot formation [equation (3)]

$$2CO \rightleftharpoons C + CO_2 \qquad (3)$$

is a competing reaction. The compositions of single-base and double-base propellants, discussed in Section 2.3.4, are such that the flame temperatures of the latter are higher and, for a given value of K_{wg}, the CO/CO_2 ratios are lower. These relationships are represented graphically in Figure 9 of Chapter 2.

Standard thermodynamic methods were used to determine the ultimate products that would be formed if equilibrium were established between a finite quantity of iron and an infinite quantity of the powder gas.[60] In a competing series of reactions, the ultimate product is the one that requires the greatest negative free energy change for formation directly from iron. The compositions of the gas had to be calculated both for the temperature from which it was considered to be quenched and for temperatures approaching those of the bore surface when it was considered to have been cooled slowly so that equilibrium in the gas phase was established at those lower temperatures.

The calculations were made for various gas densities, bore-surface temperatures and pseudo-gas temperatures, which are those from which the gas was considered quenched. The dependence of the ultimate product on the variables just mentioned was represented graphically by the partition of a three-dimensional space diagram. Figures 6 and 7 represent planes cut through such a figure at a certain gas density for single-base and double-base powder respectively.

These graphs show that at the instant of firing the products obtained with single-base and double-base powders are Fe_3C and FeO respectively. When the gases are not quenched, oxides (fields immediately to right of line of unit slope) may be formed in the case of the single-base powders. In both cases Fe_3O_4 is the oxide formed at the low surface temperatures obtained when the bore has cooled somewhat after firing. Thin films of magnetite (Fe_3O_4) have been found by electron diffraction analysis on the bore surfaces of guns fired with both types of powders.[137] The fact that magnetite was the dominant erosion product found in the cracks in an eroded gun was attributed to the steep thermal gradient between the bore and outside of the gun.[98]

It can be seen from the above results and from a consideration of the water gas reaction (1) that at the instant of firing, when the gases are quenched so that the equilibrium constant K_{wg} is high, the reactions that take place in the case of double-base and of

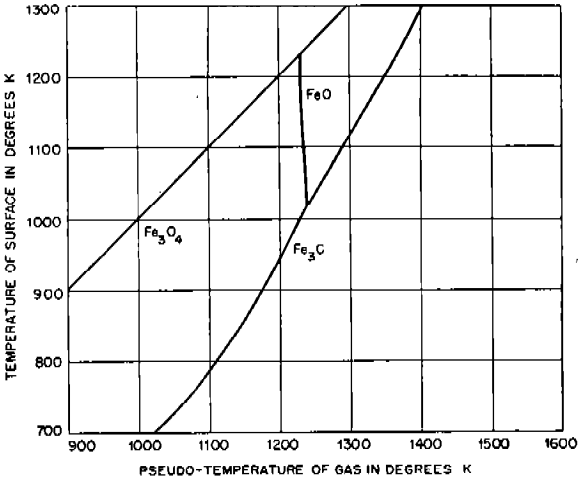


FIGURE 6. The ultimate product for FNH-M1 powder as a function of bore-surface temperature and pseudo-temperature of the gas at a density of 0.2 g per cu cm. (This figure has appeared as Figure 1B in NDRC Report No. A-301.)

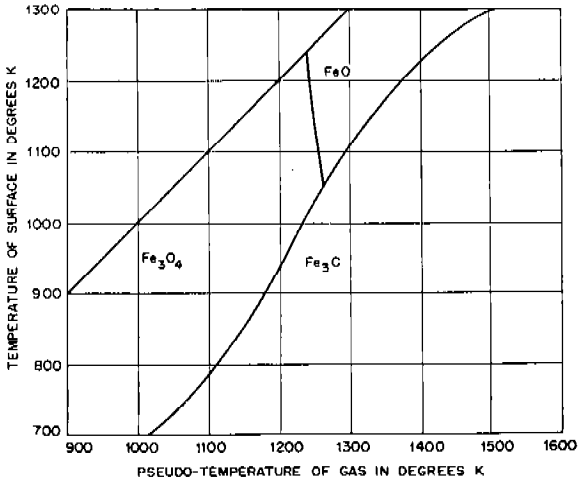


FIGURE 7. The ultimate product of FNH-M2 powder as a function of bore-surface temperature and pseudo-temperature of the gas at a density of 0.2 g per cu cm. (This figure has appeared as Figure 3B in NDRC Report No. A-301.)

[redacted]

single-base powders are probably those represented by equations (4) and (5), respectively.

$$Fe + CO_2 \rightleftharpoons FeO + CO \quad (4)$$
$$3Fe + 2CO \rightleftharpoons Fe_3C + CO_2 \quad (5)$$

Some of the oxide formation may also be attributed to reaction with H_2O by equation (6),

$$Fe + H_2O \rightleftharpoons FeO + H_2, \quad (6)$$

since double-base powders, which have lower CO/CO_2 ratios than single-base powders, have a correspondingly low H_2/H_2O ratio, according to equation (2). The formation of Fe_3O_4 takes place by reaction (7)

$$3Fe + 4CO_2 \rightleftharpoons Fe_3O_4 + 4CO \quad (7)$$

because of the shift in the equilibrium of the water gas reaction with a resulting decrease in the CO/CO_2 ratio. Fe_2O_3, considered a possibility according to equation (8),

$$2Fe + 3CO_2 \rightleftharpoons Fe_2O_3 + 3CO \quad (8)$$

was not found to be an ultimate product under any condition.

The formation of Fe_3C could take place in two stages, first the decomposition of CO into CO_2 [equation (3)] and then the reaction (9)

$$3Fe + C \rightleftharpoons Fe_3C \quad (9)$$

of carbon with iron. The formation of Fe_3C directly from CO according to equation (5), however, is more likely, since Fe_3C is stable with respect to Fe, CO, and CO_2 under conditions such that C is not stable with respect to CO and CO_2.[60]

Kinetics, of course, are not considered in the determination of ultimate products. It is quite likely, however, that they have some importance in the chemistry of gun erosion. Unfortunately nothing is known of the rates of the competing reactions that may take place at the bore surface, but it is considered safe to say that the ultimate products may not always be the major products and perhaps more than one product may result. A reaction that may be of great importance is represented by equation (10).

$$3FeO + 5CO \rightleftharpoons Fe_3C + 4CO_2. \quad (10)$$

A plot of the equilibrium curves for the important equations is shown as Figure 8. Curve *F* represents equation (10). Below curve *B*, the formation of FeO from Fe, the free energy change for FeO is negative. Above curve *E*, the formation of Fe_3C from Fe, the free energy change for Fe_3C is negative. Both FeO and Fe_3C are stable with respect to Fe in the region between these two curves, although not equally stable. The free energy changes for both compounds are equal along curve *F*. In a system corresponding to a point above this curve, Fe_3C will be the major product if equilibrium conditions are fulfilled, and below the curve, FeO will be the major product.

The significance of curve *A* [equation (3)] on this plot is to point out that conditions existing at the surface of the metal may be carburizing even below curve *F* since carbon is precipitated above curve *A*. The rate of diffusion of carbon into iron is higher than that of oxygen; the formation of carbide rather than oxide will certainly be favored at any appreciable distance below the metal surface. With an increase in pressure, the formation of Fe_3C from C [equation (9)] is favored. It can be seen that reactions (3) and (5) also proceed to the right; therefore, no matter by what mechanism Fe_3C is produced, an increase in pressure favors its formation rather than that of FeO for a given CO/CO_2 ratio, since the reaction (4) to form FeO is not dependent on pressure.

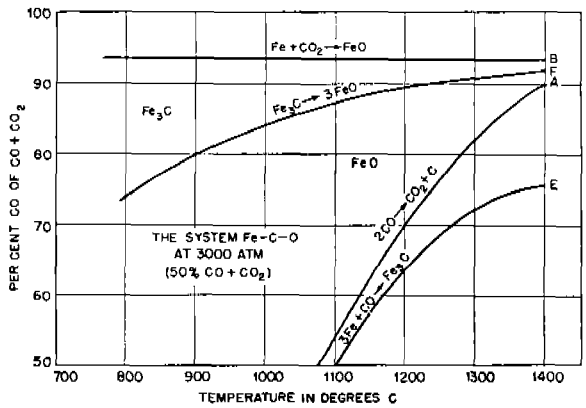


FIGURE 8. Equilibrium curves for reactions involved in the chemical alteration of gun steel by powder gases. (This figure has appeared as Figure 5 in NDRC Report No. A-466.)

REACTIONS WITH HYDROGEN SULFIDE

The only compound of sulfur that is present to any appreciable extent in the powder gases is hydrogen sulfide (H_2S). In the case of guns where coppering of the bore takes place, the copper (and zinc, if gilding metal is used for rotating bands or bullet jackets) takes up essentially all of the sulfur, as described in Section 12.3.2.

Pyrrhotite (FeS_x) has been found only rarely in

eroded guns.[98] Experimental tests showed that iron sulfide was probably formed on steel test rods subjected to powder gases.[53,98] The results of these experiments to investigate the role of sulfur in gun erosion are described in Section 14.4.

The results of the thermodynamic studies[60] led to the conclusion that FeS should be formed only in small quantities in portions of the gun tube not subjected to high temperatures since its formation is self-inhibiting due to the energy of reaction. This is true in spite of the fact that FeS is stable over a large range of conditions found in gun firing.

Reactions Involving Nitrogen Compounds

Probably the most puzzling question with respect to the chemical factors in gun erosion is that of the formation of the iron nitrides identified in eroded guns, which are described in Chapter 12. This subject has been discussed in some detail in Sections 14.5 and 13.3.2. Extrapolation of existing data showed that iron nitrides could not be formed by reaction of the powder gases with the steel at the peak temperatures reached in firing of guns.[60] Experiments showed that iron nitrides are decomposed during firing.[28] From this it is presumed that the nitrides are formed in guns during the cooling stage. It is probably true, however, that nitrogen penetrates the bore surface at the peak pressures and temperatures especially if the surface is partially liquefied. The nitrides may form on cooling by exsolution from a nitrogen-rich phase or by reaction with the cooling gases.

When the powder gases cool slowly, the concentration of ammonia (NH_3) increases. Nitrides may form by reaction of the steel with this component of the gas.[28] The possibility of another reaction has also been proposed[138]—that of the steel with cyanogen (CN) or hydrocyanic acid (HCN). It is believed that the presence of these compounds containing both carbon and nitrogen in the products of combustion of single-base powders may have considerable importance, for complex iron cyanides have been found in cases where an oxide would be expected.[31,138] These compounds, which decompose at relatively low temperatures, have been detected in eroded guns as well as on test rods, as was mentioned in Section 12.2.2.

When the concentration of ammonia in the gases increases, the concentration of hydrocyanic acid should also increase according to data for reaction (11).

$$2CO + NH_3 \rightleftharpoons HCN + CO_2 + H_2 \qquad (11)$$

A concentration of HCN was predicted in the cooling gases from a single-base propellant which might be sufficient to suppress oxide formation and extend the Fe_3C field.[138] In addition the formation of nitrides and complex iron cyanides might result.

Either carbide or nitride may be formed by the reaction of iron with cyanogen. Experiments were carried out to determine what factors were important in determining which compound would be formed.[138] Mixtures of cyanogen and nitrogen were passed over iron filings at different temperatures. Depending on the conditions of the experiment, nitride or carbide or both were formed. It was found that the reactions involved are complicated. Temperature, CN/N_2 balance, relative rates of diffusion of carbon and of nitrogen, and the relative stabilities of cementite (Fe_3C) and of the nitrides are all critical factors in determining the end product.

Conclusions

In this section a number of reactions were discussed in the light of their possible or probable importance in the chemical attack of the bore surfaces of guns by powder gases. It cannot be stated definitely what reactions occur during firing, for the mechanism of the chemical erosion is not thoroughly understood owing to lack of data on the reactions of iron with the constituents of propellant gases at the temperatures and pressures obtained in firing. Nevertheless, a great deal of information has been obtained, as summarized in Chapter 12, which shows that chemical reactions have taken place.

In the case of guns fired with double-base powders, oxidation, with the formation of wüstite (FeO), has been observed. In the case of those fired with single-base powders, penetration of carbon and nitrogen, with the formation in many cases of carbides and nitrides, has occurred. The ultimate products found by thermodynamic calculations agree closely with those found in eroded guns.

13.4 MECHANICAL FACTORS

13.4.1 Powder Gases

Removal of Material from Bore

The final stage in the process of the erosion of steel guns is the removal of material from the bore surface, whereby the bore diameter is increased. This is effect-

ed largely by the stream of powder gases propelling the projectile. Thus the powder gases not only heat the metal and react with it as described in the two preceding sections, but also sweep the surface. The rate and direction of removal of material depends on many factors.

Loose iron oxide films and such solid products as result from reactions within the gases are readily removed. The ease of removal of metal or metallic products depends on whether they are liquefied at the bore-surface temperatures. Chemically altered (Section 13.3.2) steel liquefies at a lower temperature than steel; completely liquefied films are more mobile than "mushy" surface layers which may contain blades of cementite, as shown in Figure 8 of Chapter 12. The higher the velocity of gas, the more effective is the removal of material. A bag-fired gun mentioned in Section 10.5.2. affords a striking example of this relationship. In the chamber, where the velocity of the gas was low, there was much evidence of liquefaction due to the fact that the liquefied material had remained in place as shown in Figure 16 of Chapter 10; whereas in the bore of the gun the liquefied material had been removed by the gas flowing at a higher velocity.[112] When velocities are increased by increasing the powder charge, removal of material is even more effective because the heat input to the bore has been increased and liquefaction takes place more readily.

In general, the liquid and solid products are moved forward by the gas stream because of the strong shearing stress on the walls of the tube in that direction. This effect may be modified by localized turbulent flow. Examinations of eroded guns have shown that peripheral hot gases emerging from the cartridge cases appear to strike the bore area in a nearly radial direction and eddy backward, building up in some cases thick deposits of once-molten material at the location of the mouth of the cartridge case. The importance of the thermal factors in this area is described in Section 13.2.5. The tongues of flowed material in the bores of guns are not always parallel to the bore axis. In the most severely eroded section of a gun showing exaggerated muzzle erosion the tongues pointed somewhat fanwise forward as from a local jet.[130]

Scouring Action

The mechanical action of the propellant gas on the bore surface is aggravated by the presence of solid particles in the gas stream. Some of these, such as unburned powder grains and barium and potassium salts may be directly attributed to the powder itself. In addition, the gases pick up from the eroded surface the hard, brittle products that have been formed by the reaction of the gun steel with the powder gases. These solid particles traveling with high velocity in the gas stream presumably exert an abrasive action on the surface of other parts of the gun bore.

Gas Leakage

Observation of Gas Leakage. Gas leakage is of prime importance as a cause of erosion only in special circumstances, although the escaping of a relatively small amount of gas past the rotating band of the projectile because of imperfect obturation has been observed to be common. In connection with the ballistic measurements with the 3-in. gun described in Section 4.2.2 an attempt was made to determine the time of ejection of the projectile by the cutoff of a beam of light passing across the muzzle and focused on a photo cell. The photocell circuit was interrupted prematurely by the opaque gas which escaped ahead of the projectile, as described in Section 4.3.20. During the development of a gauge for measuring the acceleration of a projectile (Section 4.6), it was discovered that gas leakage occurred soon after the start of travel. High-speed photographs, made at Naval Proving Ground a number of years ago, of a large projectile emerging from the muzzle of a gun showed that a small amount of gas escapes ahead of the projectile.[16] A method was developed for photographing the gas escaping ahead of a caliber .30 bullet when it was fired into an evacuated chamber.[49] A series of pictures was made of the bullet at various positions in the bore. A cloud of gas in advance of the bullet was observed, but it was not possible to tell whether the gas leakage had occurred at the start of travel or later.

Gas Leakage as a Cause of Erosion. A survey of the literature[16] showed that some early writers considered gas leakage one of the dominant causes of gun erosion, but the same survey also revealed that this theory was strongly contested. Most of the arguments, which were often based on observations of eroded vent plugs, were only speculative. The flow of the powder gas in a vent plug, however, is radically different from that in guns. Unless it can be shown that, when gas escapes past the projectile, it flows as through a vent the observations made on vent plugs should not be

applied to the formulation of a theory of gun erosion involving gas leakage.

At present it is believed that the above conditions are met in certain cases in which localized scoring of the bore surfaces of badly eroded guns takes place.[479,541] Where such leakage does occur, relatively large quantities of molten metal are washed from the bore surface. The melting point of steel is easily reached because of the friction developed in the small passageway, as discussed in Section 5.4.4. The molten steel is rapidly washed away because of the very high velocity of the escaping gas. Thus gas leakage under certain conditions is an important cause of erosion from both a thermal and a mechanical standpoint.

A theoretical treatment of the problem was undertaken which showed what critical conditions are exceeded when gas escapes past a projectile as through a vent.[48] The danger of gas washing, according to this study, is greatest at the start of travel before the rotating band of the projectile has been engraved. One of the advantages of a pre-engraved projectile, therefore, is that a much smaller gas pressure is required to start its movement, hence there is not as much opportunity for gas leakage to be effective. A description of some experiments with pre-engraved projectiles having different degrees of gas leakage is given in Section 31.4.2.

Observation of Scoring. In some small- and medium-caliber guns that were examined with a microscope local scoring of the bore surface was observed near the origin of rifling.[112] The gouges produced by gas leakage or "blow-by" are illustrated in Figure 20 of Chapter 10. In some cases the channel evidently developed by enlargement of certain cracks by the main stream of gas. Finally, it reached an optimum width to act like an erosion vent.

In the case of large-caliber guns a channel for escaping gases may be present at the top of the bore before the projectile is fired because of the effect of gravity on its position in the bore. This may lead to severe scoring of the bore surface near the 12 o'clock position in the vicinity of the origin of the bore. Erosion of this type is especially noted in 155-mm guns.[216,284]

Gas leakage occurs and may be a serious cause of erosion at the forward joint of breech liners. The bore ahead of the liner is affected by gas washing. This type of failure occurs regularly in caliber .50 barrels containing stellite liners and is one of the factors that determines the life of such barrels. The practice of chromium plating the bore ahead of a stellite liner mitigates this effect but does not prevent it entirely.

Gas Pressure

Cracking of Bore. The pressure of the powder gases exerts a force on the walls of the gun tube. This is discussed in connection with the theory of tube stresses in Chapter 26. The stress due to gas pressure does not contribute directly to removing material but it does result in cracking of the gun bore which greatly facilitates erosion, as is described in Section 13.5.3.

Bore Expansion. Under conditions of rapid fire, the temperature of a barrel is built up with the result that the steel is weakened, and the barrel may be expanded by the gas pressure, with the resultant bad effects on ballistics described in Section 5.6.4. In the case of barrels containing erosion-resistant liners, expansion in the region of the forward end of the liner imposes a limitation on the length of burst. The methods of mitigating this effect are described in Section 24.2.

Effect of Stress on Powder Gas Erosion. An experiment was carried out to determine whether the stressed condition of a metal surface was related to its erosion by powder gases,[103] using the apparatus described in Section 11.2.5. The measurements did not reveal any appreciable difference between the erosion of surfaces under tension and that of surfaces under compression, for the conditions of this experiment. However, even though the ballistics were regulated so that only a small amount of erosion would take place, plastic flow or melting appeared to be the predominant factor in the erosion, and thus the effect of stress on erodibility was rendered negligible by the larger effect of surface melting.

Occlusion of Gases

Hydrogen, which is an abundant constituent of powder gases, rapidly diffuses through steel at high pressures. It is conceivable that hydrogen diffusing through hot steel may react with the carbon in the steel to form methane, which would exert considerable pressure within the steel. Thermodynamic calculations were made in order to determine if methane pressures could be a contributing factor in gun erosion.[49] From a general relation between the pressures of the gases and the free energy change of the reactions, it was found that, if the gas in contact with the steel under a total pressure of 1,000 atm contained 10% of hydrogen, bubbles of methane at a pressure in excess of 10,000 atm could form within the steel if the temperature were not more than 610 C. There is

no direct evidence, however, to suggest that such a process contributes to erosion.

13.4.2 Projectile

Band Pressure and Engraving Stresses

The rotating band of the projectile exerts pressure on the gun tube as it moves through the bore. The stress exerted on the tube and the resulting deformation is greatest in the vicinity of the origin of rifling because of the force necessary to engrave the band.[422] The band pressure decreases toward the muzzle due to both wear and fusion of the band. This fact makes the design of the rotating band an important factor in the erosion of the gun that fires it.[273] When projectiles become tipped in the bore, so that engraving of the body takes place as described in Section 10.4.10, the erosion of the bore is asymmetric and extends to the muzzle, where it may be greater than elsewhere in the bore.

The study of the stress-strain relationships during the process of engraving, which is discussed in Section 7.3.5, led to the conclusion that the dominant stress in engraving is radial compression. Shearing in a radial direction takes place at the edges of the lands. The greatest deformation usually occurs along the driving edges of the lands because of the force necessary to impart spin to the projectile. Once the rotating band has been engraved, the band pressure is dependent on the size of powder charge, since band wear has been shown to decrease with the velocity of the projectile (Section 7.4.1).

Abrasion

The radial pressure between projectile band and bore produces friction which results in adding heat to the bore, as described in Section 5.2.2, and in abrasion. The abrasion, it should be remembered, is not that of sorbitic steel but of the thermally and chemically altered steel at the bore surface. This material is not resistant to mechanical shock because, even though it is hard, it is brittle. After becoming heated in rapid-fire guns, however, the bore surface is soft and ductile; and swaging, as described in the next subsection, assumes more importance than abrasion. Loose material, such as oxide films, presumably are easily abraded from the bore surface.

The abrasive effect can be minimized by decreasing the radial load, as discussed in Sections 27.3 and 27.4. In particular, when pre-engraved projectiles are employed, erosion is markedly decreased, as is brought out in Section 31.4.3.

Reduction of the coefficient of friction between the projectile and the bore by lubrication has little effect on the abrasion as long as conventional engraving-type projectiles are used. When the radial load is reduced, however, further improvement can be made by reducing the coefficient of friction between the projectile and the bore surface. Thus Parco-Lubrizing pre-engraved caliber .50 projectiles decreased the erosion of the lands, as shown in Figure 11 of Chapter 31.

Swaging

Careful microscope, boroscope, and star gauge examinations of chromium-plated liners which were tested by firing in caliber .50 machine-gun barrels showed how the cracked chromium was removed by the swaging action of the bullets on the steel beneath

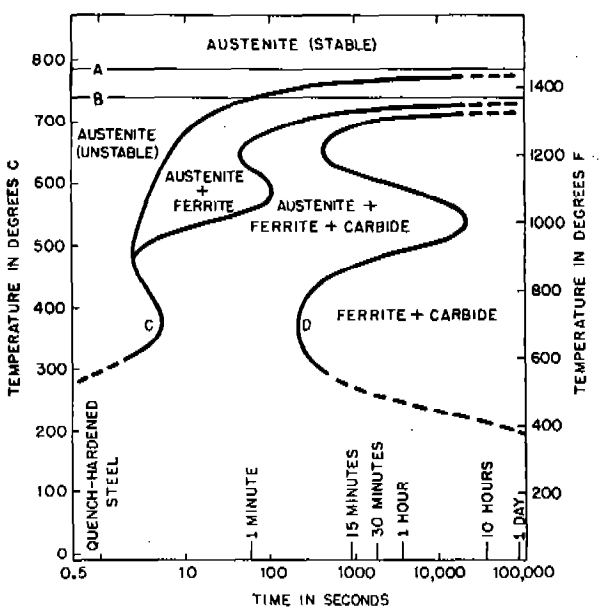


Figure 9. Isothermal transformation diagram (*S* curve) for SAE 4140 steel. Curve *C* represents the start of transformation, curve *D* the end of transformation of austenite when cooled from the austenitizing temperature and held at lower constant temperatures. The temperature represented by line *A* is the critical temperature for the alpha-gamma transformation (line *GS* in Figure 5) of this particular steel and that represented by line *B* is the eutectoid temperature (line *PSK* in Figure 5) for this steel. Austenite is not stable below *B* and ferrite is not stable above *A*. (This figure is based on Figure 6 in NDRC Report No. A-300, which had been made available by courtesy of U. S. Steel Corporation Research Laboratory.)

the chromium.[59] The steel of the lands during firing moved in three directions, as shown in Figure 21 of Chapter 10 and described in Section 10.5.3.

In Section 13.2 the thermal transformation of the steel at the bore surface during firing was discussed. This change is very important in connection with the question of swaging. Temperature measurements made on barrels during long bursts of rapid fire together with *S*-curve data (Figure 9) indicate that the austenite had too little time to transform between



FIGURE 10. Swaged land at 3½ in. from origin of bore in caliber .50 aircraft barrel No. 1194, fired four 100-round bursts with complete cooling between bursts. 25*X*. (This figure has appeared as Figure 8C in NDRC Report No. A-440.)

rapidly fired rounds during the last part of a burst. The steel was in the soft austenitic condition when subjected to the impact of the projectile and was easily swaged.[59] Figure 10 shows a land of a machine gun barrel swaged down the middle as a trough.

In the early rounds of a burst a hardened surface layer begins to form instantaneously during each cooling cycle at about 270 to 300 C, the temperature at which curve *C* in Figure 9 intersects the left-hand edge of the isothermal transformation diagram for SAE 4140 steel, which has a composition approximating that of most gun steels. During the later rounds of a burst, when the minimum temperature for any one round exceeds 300 C, there is not time for the hardened layer to form before the next round is fired, because of the slowness of the transformation. As can be seen from Figure 9, transformation does not even begin above this temperature until several seconds have elapsed and then proceeds slowly (region between curves *C* and *D*).

Swaging is believed to be a general phenomenon but its effects are not always evident in nonplated guns because of the removal of metal by powder gas erosion.

13.4.3 Design of Gun Bore

The design of the gun bore as well as of the projectile is important in determining the stress that is applied to the tube. Rifling (Section 26.6) is essential in order to impart spin to the projectile but its presence means that guns are structurally weak from the very start of their life because of the localization of stresses. Various modifications in the design of the bore have been carried out in order to mitigate erosion and increase accuracy and velocity-life as described in Sections 23.2.1 and 26.6.3.

13.5 CRACKING OF THE BORE SURFACE

13.5.1 Introduction

Generally the most obvious surface feature of eroded bores is the cracked appearance. Cracks are not solely a cause of erosion nor are they solely an effect of erosion. Their relative importance with respect to cause and effect is not known. It can be correctly stated, however, that they always accompany erosion. Because of the complex nature of its role, cracking is treated here in a separate section. It is described first as a factor in aiding erosion. The formation of the cracks is then discussed. The development of certain types of crack patterns is described and illustrated in Section 10.5.1.

13.5.2 Aid to Erosion

POWDER GAS EROSION

Even if it had no other effect, the cracking of the bore surface would increase the rate of powder gas

CONFIDENTIAL

erosion simply because of the increased surface for reaction. The longitudinal cracks act as channelways for the streaming gases and may become enlarged to the extent that localized gas leakage and resultant scoring may develop, as described in Section 13.4.1.

Chromium-Plated Bore Surface. Cracking of the chromium plate is the underlying cause of failure in plated guns,[50,86] as discussed at length in Section 20.2.1. Chromium under gun firing conditions is inert to chemical attack. A continuous coating of this metal protects steel barrels from chemical reaction with the powder gases although it does not, unless thick enough, as mentioned in Section 13.2.3, prevent thermal alteration of the steel. When the chromium plate is cracked due to firing stresses, however, the powder gases have access to the underlying steel and chemical reactions take place, especially if the steel is in the austenitic condition at the time.[124] The steel is eroded from beneath the chromium plate, and the latter, so undermined, is easily removed.

Stress Erosion

Pitting of the bore surface occasionally results when cracks intersect and small blocks of metal are torn away. A serious type of bore damage which fortunately is not common to all types of guns is shearing of the lands. In some badly strained guns, cracks which start at the groove fillets may curve under the lands from both sides and eventually meet, whereupon whole sections of lands may be removed.[277]

13.5.3 Causes of Cracking*

Thermal and Transformation Stresses

During the firing of a gun, the differentially confined bore surface is subjected to volume changes due to rapid heating and cooling and to the thermal transformation of steel (Section 13.2.3). The resulting strains set up in the surface layer may be relieved by cracking. The term "heat checking" has been employed[16] to describe the fine crack system seen in the portions of eroded gun bores where no more than incipient melting of the surface has taken place, since thermally induced stresses would be expected to cause this type of shallow cracking.

Not only the volume changes mentioned above but also the change in mechanical properties resulting from alteration of the bore surface affect the stress-strain relationships in the surface layer. The volume increase accompanying the inversion to austenite was calculated from x-ray data on eroded gun surfaces to be three per cent.[28] The resulting compressive stresses probably cause plastic deformation rather than cracking. Quench-cracking, however, may result when the bulk of the austenite is transformed to a brittle martensitic layer during the rapid cooling by the mass of the gun steel beneath it.[124] In the case of single-shot guns, this type of layer is present before each successive round. It is harder but less ductile than either austenite or the originally sorbitic steel and consequently is more readily fractured by the impact of the projectile.

The thin, complex, outer white layer, discussed at length in Chapter 12, is partially liquefied during firing. It consists of materials only slightly subject to transformation stresses. On cooling it is brittle and tension cracks form in it which are closely in line with the cracks in the steel which the liquefied material has covered.[112]

The evidence which follows seems to show that, even though the thermal and transformation stresses may be of prime importance, heat alone is insufficient to cause the type of cracking referred to as "heat checking."

Studies of Thermal Shock by Electron Bombardment

A study of the effects of thermal shock was made by subjecting gun steel specimens to electron bombardment in the presence of the inert gas argon, according to the procedure described in Section 11.3.2.[104] Additional experimentation was carried out with nitrogen or carbon monoxide substituted for argon. Metallographic examination showed that thermal alteration had taken place; furthermore, analysis by electron diffraction showed that austenite was present in addition to ferrite.[137] Cracking had occurred only on specimens that had been bombarded in nitrogen, but in no case was the crack pattern identical with that observed on eroded gun bores. This evidence shows that "heat checking" is not a characteristic effect of thermal shock alone.

Causes of Cracking of Test Specimens

A testing method was devised in order to determine the resistance of metals to cracking.[51] The polished

* The study of the problem of cracking in gun tubes as manufactured during World War II was undertaken by the War Metallurgy Committee (Division 18, NDRC).[170]

surface of a block of the metal to be tested was exposed to a stream of powder gases in a small explosion vessel, described in Section 11.2.4. The surface was then examined under a microscope.

Cracks that could be attributed to mechanical stresses were observed. In addition, a crack system similar to the so-called "heat checking" in eroded guns was found to start on steel specimens at the place where the hot gases had first come in contact with it and with successive firings to progress "downstream." This type of cracking was not found on an exposed molybdenum surface.



FIGURE 11. Eroded surface of 3-in. gun liner No. 1460 at the location of the mouth of the cartridge case. The pattern on the eroded area was influenced by tool marks. *20X*. (This figure has appeared as Figure 8A in NDRC Report No. A-440.)

The fine crack system did not appear immediately in the case of steel blocks; yet it was apparently related to thermal transformation, which, however, could not be the sole cause of cracking, since the latter did not start until after several firings. This may mean that time was required for sufficient chemical alteration to aid in the formation of the cracks.

Further experiments in which black powder or its components were added to the charge strengthened this idea. The hypothesis was suggested, therefore, that "heat checking" is caused by a combination of thermal and chemical factors. This bears out the conclusion from the electron bombardment experiments just described that "heat checking" is not produced solely by thermal shock.

CAUSES OF "PEBBLING" IN GUNS

Pebbling and heat-checking are terms used to describe the characteristic appearance of an eroded gun bore in which general melting has not occurred; the latter is descriptive of the pattern, whereas the former denotes also the doming of the units of the pattern by liquefaction and erosion as described in Section 10.5.2 and shown in Figure 16 of Chapter 10.[112,124]



FIGURE 12. Elongated pits resulting from fluxing of inclusions on groove surface of 3-in. gun liner No. 1460 at 1 in. from origin of bore. *25X*. (This figure has appeared as Figure 6C in NDRC Report No. A-440.)

Since the cause of this type of cracking has not been found, the use of the term pebbling is preferable in that it does not imply a cause.

The hypothesis mentioned above, namely, that this phenomenon is caused by a combination of thermal and chemical factors, is in agreement with the results of the metallographic examination[124] of the liners used in the powder testing program described in Chapter 15. No pebbling was observed with a small number of rounds with a single-base powder although thermal alteration took place in the first round. The conclusion drawn from this fact was that chemical alteration was necessary before melting of the surface could take place. Furthermore, it is believed that enough carbon or nitrogen or both has to penetrate the steel before austenite formed during firing can be

CONFIDENTIAL

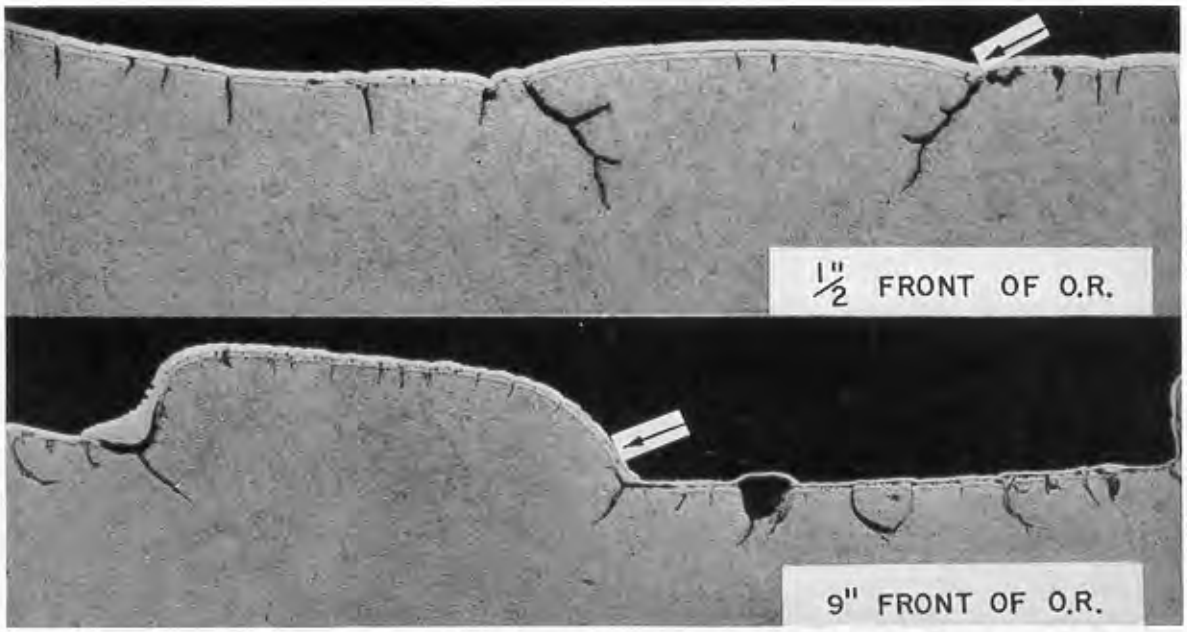


FIGURE 13. Extent of progressive stress-damage in 76-mm M1E5 gun tube No. 2128 after 2,000 rounds. Arrow points to driving side of land. Specimens were nickel-plated prior to polishing. (A) ½ in. ahead of origin of rifling; (B) 9 in. ahead of origin. (This figure has appeared as Figure 7B and 7C of Watertown Arsenal Laboratory Report No. WAL 731/95.)

stabilized. Quenching cracks are inevitable if more carbon than the eutectoid composition is dissolved in the austenite. It would seem then that pebbling may be the result of a combination of quench-cracking and incipient metlting of the surface which tends to draw itself into globules.

STRESS RAISERS

Tool marks have been considered a cause of the cracking in gun tubes when firing stresses are applied, but objections to their importance have been raised in that there are many more cracks in eroded guns than there were tool marks to start with.[16] Tool marks are stress raisers, however, and as such can influence the initiation and direction of cracks as shown in Figure 11.[112] (This figure is also a good illustration of pebbling.)

Inclusions in the steel at the bore surface also influence cracking. This may be a cause of failure in guns made of a dirty steel.[262] The inclusions react with the powder gases and may "explode out" leaving an elongated pit such as those shown in Figure 12 from which cracks may develop in further firing.[112]

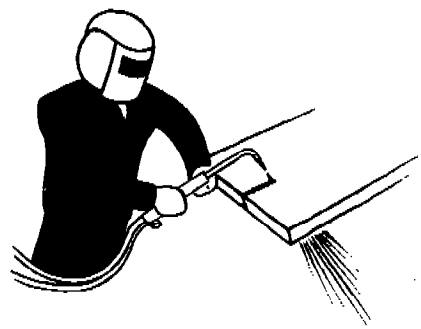
PROGRESSIVE STRESS-DAMAGE

Progressive stress-damage, a term coined at Watertown Arsenal, is defined as "all phenomena associated with the initiation and propagation of cracks in guns as a result of the mechanical stresses imposed by repeated firing."[277] The mechanical stresses are those due to engraving of the rotating bands or of the projectiles themselves, band pressure, and powder gas pressure, all of which are discussed in Section 13.4. Progressive stress-damage cracks are found at places where there were stress raisers. The most serious progressive stress-damage occurs as deep cracks at the groove fillets. An illustration of the extent of progressive stress-damage is shown as Figure 13. The propagation of these cracks may eventually cause failure of the tube by rupturing or by shearing of the lands. The extent of progressive stress-damage in a number of different worn gun tubes,[274,275,277,278,280,281] especially those for the 76-mm gun, M1,[264,265,266,267,269] has been studied in recent years at Watertown Arsenal.

CONFIDENTIAL

PART IV

EROSIVE ACTION OF PROPELLANTS



I were better to be eaten to death with a rust
than scoured to nothing with perpetual motion.
—*William Shakespeare*
"King Henry IV"

Chapter 14

EFFECTS OF CONSTITUENTS OF THE POWDER GASES ON GUN STEEL

By *W. D. Urry*[a]

14.1 INTRODUCTION

THE INVESTIGATIONS described in this chapter were largely complementary to the general study of the nature of eroded bore surfaces, described in Part III, but were intended at the same time to serve a further purpose. It was hoped that they would elucidate the particular role that each of the components of a propellant gas, treated individually insofar as feasible, might play in erosion or in the production of conditions favoring erosion by a more general mechanism. It was even considered at the outset quite possible that such studies would indicate the manner in which the composition of propellants then in use might be modified, perhaps only in a minor respect, in order to mitigate erosion.

The investigations have not demonstrated that the erosion of steel guns can be startlingly diminished by a practical modification of the present powders. Instead they have contributed to the evidence already presented in Chapter 12 that carburization, oxidation, nitriding, reactions of sulfur gases, or possibly the direct removal of iron as a volatile compound like iron carbonyl, present almost insurmountable difficulties if a steel bore surface is to be considered, especially under the conditions of the upswing in ballistic level demanded by modern artillery practice.

The above reactions have been carefully studied under ordnance conditions or in experiments under laboratory conditions simulating one or more of the conditions pertaining to a gun. The experiments may be divided into two general groups in another sense. In the one group the individual constituents of a powder gas were used; in the other the powder gases were employed collectively while studying the role of one particular constituent or element. Only in the latter case, of course, can there be true ordnance conditions.

The constituents of the powder gases that have been studied in relation to reactions with gun steel include carbon monoxide and carbon dioxide, nitrogen, hydrogen, and hydrogen sulfide, some of these gases having been investigated individually, others in various combinations. In other experiments emphasis was placed on a particular element, such as carbon, nitrogen or sulfur, while the gases were present collectively, being obtained from a standard propellant. In this case the minor constituents such as methane and ammonia were present as well as water vapor, which was not otherwise investigated. Black powder, used with the primer, may constitute no negligible fraction of a gun charge. Except in small arms, the sulfur in the black powder is the chief source of the sulfur gases and therefore a study of the reactions with the sulfur gases introduced the question of the effects of the other constituents of black powder, namely, potassium nitrate and charcoal, to which some attention was given.

The chemical factors in the causes of gun erosion and their interrelation with other factors are summarized in Chapter 13. A great many of the conclusions concerning them were derived from or strengthened by the results of the above experiments. A general review of the results of these investigations indicates that many of the undesirable features of the reaction of the powder gases with gun steel can be attributed to the presence of the carbon gases, concerning which little can be done beyond an attempt to adjust their proportions or otherwise attain certain conditions of balance between carburizing and oxidizing states. Nitrogen, perhaps present as the activated molecule or as ammonia, plays its role by forming nitrides. It is difficult to imagine its removal from the propellant. Investigation of the part played by hydrogen is very incomplete. The effects of water vapor, as an individual constituent of the powder gas, have never been studied. There is indirect evidence that its role may be subsidiary because the erosion of vent plugs by artificial gas mixtures free from water vapor is the same order of magnitude as that caused by powder gases derived from standard propellants. Sulfur definitely increases erosion, probably in all cases except where direct melting of the steel is occurring. The exact mechanism whereby the presence of a few tenths of one per cent of hydrogen sulfide can contribute appreciably to the erosion is not completely understood but experiments in three labora-

[a] *Physical Chemist, Geophysical Laboratory, Carnegie Institution of Washington.*

tories show that the elimination of sulfur, largely present in the black powder, lessens the erosion.

Many of the reactions studied, and also the reaction velocities, are strongly favored by increasing the temperature, and insofar as any of these reactions may bear some quantitative relation to the erosion that it causes, either directly or indirectly, the substitution of cooler propellants is worthy of consideration. However, there are some reactions, like the formation of iron nitrides and the oxides Fe_3O_4 and Fe_2O_3, and possibly the production of iron carbonyl, that are strongly favored by lowered temperature. Nevertheless, the substitution of new propellants of lower flame temperature but with unimpaired impetus, for example, the cool albanite and RDX powders,[b] should lead to a mitigation of erosion. Studies of the erosiveness of some of the RDX powders are described in Chapter 15. The slight modification of the older, standard propellant is discussed further in Section 15.6.

14.2 REACTION OF CARBON GASES WITH GUN STEEL

14.2.1 Introduction

Penetration of carbon into the bore surface of guns in both the sense of the formation of carbon compounds and the penetration of the steel may be a factor in erosion. The melting point of the surface material may be lowered from 1450 C to 1135 C by the presence of 4.3% of carbon, as shown in Section 13.3.2. In some experiments with a rifle barrel this amount of carbon was exceeded in nearly all cases close to the surface and near the origin of rifling.[99]

Previous carbon analyses[481,490] are inadequate and interpretation is complicated by the use of completely eroded barrels in which the added carbon may be solely contained in carbonaceous material filling the extensive fissure system, as described in Section 12.4.1, and coating the bore surface. In order to pursue the problem further, it was deemed necessary to develop a technique wherewith the presence of propellant carbon in layers measured in fractions of microns could be detected and measured. It was felt that attention should be confined mainly to the effect of a single round in an unproofed barrel.

Calculations of the probable bore-surface temperature of a caliber .30 barrel indicated that the transition of the iron from the alpha to the gamma phase does not take place when fired single-shot with the barrel at ambient temperatures. Therefore any extensive penetration of carbon into the steel is unlikely. In guns of larger bore this transition does occur, as is brought out in Section 13.2.3. Calculations showed that temperatures, and to some extent, the significant times involved, pertaining to guns up to 90-mm bore, could be simulated in suitably preheated caliber .30 barrels.

14.2.2 Summary of Recent Results

Experiments with preheated caliber .30 barrels showed that carbon from propellant gases can penetrate the bore surface of a gun to a marked degree in two senses. At the immediate surface there are carbon compounds of iron and possibly other elements formed. Below these surface layers carbon penetrates into the steel. These characteristics were found even after firing a single round in unproofed preheated caliber .30 barrels.

Carbon Compounds. The average content of propellant carbon in the reaction products is essentially independent of the bore-surface temperature and of the number of rounds. The distribution of the propellant carbon within this layer is affected by the bore-surface temperature, for example, the carbon content of the part of the layer nearest the surface decreases with increasing bore-surface temperature. A particular feature within the layer of reaction products is the universal occurrence, in these experiments, of a subsurface layer containing more propellant carbon than a layer nearer to the surface that is often almost devoid of carbon. This is in accord with the lamellar structure of the layer of reaction products described below and the bottom of this buried, carbon-rich layer seems to define the boundary between reaction products and steel.

The thickness of the layer of reaction products, for a single round, is almost independent of the bore-surface temperature, particularly near the origin of rifling. The thickness of this layer was increased appreciably by firing more rounds.

A change of propellant causes an important change in the carbon content of the reaction products. A cool RDX powder yielded reaction products that contained much less carbon than the products from IMR powder at the same bore-surface temperature. The products with a hot, double-base powder contained very little carbon near the origin of rifling but a con-

[b] Described in Chapter 6 of Volume 1, Division 8.

siderable amount, although at a very shallow depth, towards the muzzle, by comparison with IMR powder. The average content of propellant carbon and original carbon in any of the tests could produce at the most 30% of cementite in the layer of reaction products, and the introduction of carbon is therefore not the sole cause of the chemical alteration of the bore surface; in fact, with double-base powder it appears to be but a very minor cause.

Penetration into the Steel. There is very little penetration of carbon into the steel below a peak bore-surface temperature of about 900 C. Above this temperature the depth of penetration increases rapidly and the total amount of carbon that has penetrated increases uniformly with increasing temperature. In the caliber .30 barrel there was no evidence of penetration into the steel beyond 20 calibers forward of the origin of rifling.

A change of propellant apparently causes no change in the depth of penetration provided the CO/CO_2 ratio in the powder gases is a carburizing one. If the CO/CO_2 ratio is an oxidizing one and the bore-surface temperatures are high, which is the case with FNH-M2 powder, there is no penetration of propellant carbon into the steel. The dependence of CO/CO_2 on temperature and on composition of powder is discussed in Sections 2.3.4 and 13.3.3.

Relation to Commercial Carburizing. It is very difficult to draw any parallels between carburization phenomena in a gun barrel and observations concerning carburization of steels. The difficulties are manifold: firstly, a lack of understanding of the phenomena in the immediate surface layer of a steel undergoing commercial carburization; secondly, the violent fluctuations in a gun of all the variables that control carburization. Nevertheless, the initial slopes of the carbon depth curves just below the interface between reaction products and steel give diffusion coefficients comparable with values reported in the literature. Carburizing temperatures corresponding to these diffusion coefficients are in reasonable agreement with the theoretical bore-surface temperatures.

Nature of Reaction Products. The nature of the reaction products, concerning which the use of the method to determine carbon content offered no clue, was studied by electron and x-ray diffraction.[137] The cementite (Fe_3C) formed by the firing of IMR powder was separated into a layer removable with nital (5% HNO_3 in alcohol) and a film that adhered to the steel. A very thin film on the surface of the reaction products contained magnetite (Fe_3O_4). In a qualitative manner, this analysis and the order in which the compounds appear correspond well with the distribution of carbon in the layer of reaction products.

The cause of the separation of cementite into two parts, the one removable, the other adherent, appears to be the presence of a noncarbon compound separating the two zones. Evidence for the existence of this separating film is found in the carbon penetration curves. In other work[31] on the nature of the reaction products on blocks of steel exposed to the gases from a single-base powder, the nature of the compounds and the order of their occurrence were the same except that in this case there was evidence for the formation of a thin film of a complex cyanide. The covering of magnetite was particularly a feature of highly heated blocks; a decrease in the carbon content of the immediate surface with increasing initial temperature of the preheated barrels is indicative of the formation of increasing amounts of a noncarbon compound. Carbon penetration curves for the hottest barrels suggest some decarburization following carburization. It is possible that a complex cyanide is momentarily formed but that most of this is lost by oxidation to magnetite. The surface carbon content is high enough in the cold barrel to permit the presence of a cyanide but the nature of the products was not studied.

14.2.3 Experimental Determination of Carbon Penetration[99]

Method

All the carbon components of a powder gas in the act of propelling a projectile under standard ordnance conditions were tagged with radioactive carbon. The barrel was cut up into short lengths after firing and the resulting tubes were mounted in turn to form the hollow-cylindrical cathode of a Geiger-Mueller counter, described in Section 11.5.5. This is an apparatus that measures the passage of any radioactive ray traversing the cylindrical space, in particular the beta-rays emitted from radiocarbon in the surface of the cathode.

Thin layers of the bore surface were removed successively by electropolishing for short periods.[22] The thickness of the layer so removed, controllable from 0.2 micron upwards, was determined by analyzing the electropolishing solution for iron.[21] By alternately electropolishing and measuring the activity of the remaining radiocarbon, the content of propellant carbon in the successive layers was indexed by the fall in activity.

With respect to radioactivity techniques a novel feature of this method is the very efficient use of the specimen, the bore surface, by making it a part of the counter itself. A novel feature as far as analysis is concerned is that preservation of the "cut" for carbon analysis is unnecessary.

Investigation was confined to chromium-molybdenum WD 4150 steel as specified by the U. S. Army for caliber .30 barrels. A special mount for the caliber .30 assembly was necessary in order to fire from initial temperatures up to 700 C. The barrels were preheated by a coil of Nichrome wire wound directly onto a barrel and the bore surface was protected during the preheat period by the passage of nitrogen especially purified to remove oxygen. (See Figure 18 in Chapter 11.)

Validity of Assumptions

Experiments were performed that showed:

1. That the dissociation of the barium carbonate carrying the radiocarbon in the charge was complete.
2. That there was equipartition of this radiocarbon between the carbon monoxide and dioxide so that it was immaterial whether carburization and formation of reaction products proceeded from one or the other.[61] (This phase of the work has been discussed in Section 2.3.5.)
3. That the normal "ballistic level" (muzzle velocity and maximum pressure) is unaffected by the addition of 10 to 30 mg of barium radiocarbonate.
4. That the various experiments were conducted at the same ballistic level for IMR powder and at as nearly the same as possible for FNH-M2 and RDX powders.

Limitation on Interpretation of Results

The results must be interpreted in the light of the following limitations:

1. Measurements were made on surfaces which extended over a 2-in. (6.7 calibers) length of barrel. Consequently areal differences in carbon content were averaged out to this extent. Apart from longitudinal variations a very real difference between lands and grooves was indicated.
2. Carbon concentrations and depths were calculated on the basis of the weight fraction of iron in the steel. Consequently, in that portion of a carbon-depth curve representing reaction products, the carbon content is probably higher than the true value, but not by more than a factor of 1.2. The depth is correspondingly too shallow.
3. The radiocarbon measures only the presence of carbon acquired from the propellant gases. If there is no exchange, that is, simultaneous carburization and decarburization, the total carbon content is given by adding the original carbon (nominally 0.5%) to the amount measured by the tracer and presented in the graphs.
4. Smooth curves are plotted but actually "cuts" of finite thickness were taken. While a sudden change in the carbon content of a very thin layer will show in the analysis, it may not be in true perspective.
5. The abnormal distribution of initial temperature extended that length of bore surface forward of the origin of rifling which was momentarily raised to about the same peak temperature. Carburization appeared to extend further towards the muzzle than it probably does in actual practice.

14.2.4 Bore-Surface Temperatures[99]

The importance of the bore-surface temperatures with particular reference to the temperature of the alpha-gamma transition as controlling carbon penetration has already been mentioned.[c] This temperature is roughly 750 C although there is abundant evidence that a considerably higher temperature is necessary to form an altered layer in guns, probably because of the ultra-short times.[59] Carbon penetration was also found to cease far short of the 750 C isotherm below the surface.

The instantaneous bore-surface temperatures can at present be obtained only from theoretical considerations by the methods described in Section 5.4.1. A few results of a large number of such calculations, including temperatures at depth, having a bearing on the problem of carburization are presented here. Figure 1 illustrates the extent to which a preheated caliber .30 barrel simulates the temperature-time relations in a 3-in. gun. The maximum peak temperature reached in the caliber .30 barrel starting at 27 C is computed to be about 630 C and obviously the part played by carbon in the erosion of caliber .30 rifle barrels in normal usage must be negligible; in fact, there is no erosion problem.

The bore-surface temperatures for four firing tests with a preheated caliber .30 barrel used to determine

[c] The formation of reaction products on the surface is controlled by other temperature considerations not connected with this transition, as discussed in Section 13.3.3.

[redacted]

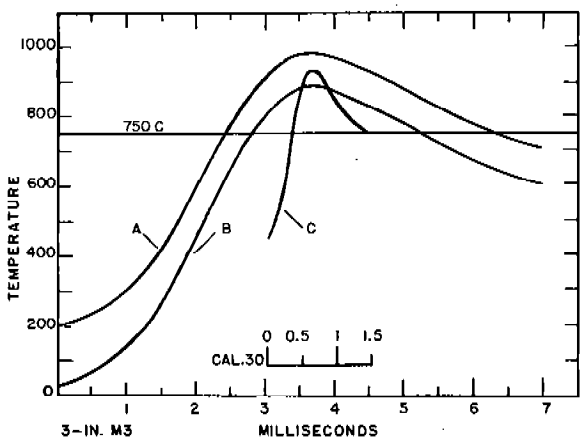


FIGURE 1. A comparison of the calculated bore-surface temperatures near the origin of rifling for a 3-in. AA gun, M3 and a preheated caliber .30 rifle. Curve A—3-in. gun initially at 200 C, e.g., after rapid fire; Curve B—3-in. gun initially at ambient temperature; Curve C—caliber .30 rifle, M1903A1 preheated to 450 C. (This figure was based on Figure 9 of NDRC Report No. A-427.)

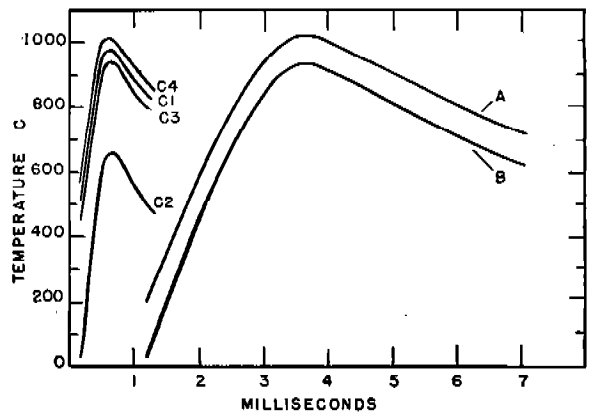


FIGURE 2. A comparison of bore-surface temperatures near the origin of rifling for a 3-in. AA gun, M3 and preheated caliber .30 barrels used in various tests for carbon penetration. Curve A—the 21st round of a burst in a 3-in. gun with NH-M1 powder at 2,750 fps and 20 rounds per minute; Curve B—the first round of the burst in the 3-in. gun; Curves C—caliber .30 barrels at various initial temperatures. (This figure appeared as Figure 11 in NDRC Report No. A-427.)

carbon penetration are compared in Figure 2 with those for a 3-in. gun at the beginning and end of a burst.[106] Figure 3 shows the increase in bore-surface temperature due to a change of propellant from IMR to FNH-M2 in one of the firing tests. Figure 4 shows that the carbon penetration with a cool RDX powder and the hotter IMR powder can be compared when the former is fired at a higher initial temperature to compensate for its lower flame temperature. On firing at the same initial temperature, the RDX powder would produce lower bore-surface temperatures and carburization would be lessened.

The decrease in carburization to be expected in a 90-mm gun by substituting a cool RDX powder for NH-M1 propellant on the basis of these experiments was investigated. It was estimated that the total depth of penetration and the total amount of carbon entering the bore surface might be reduced by at least 50%. The layer of reaction products would contain less carbon, but its thickness would apparently be about the same as with NH-M1 propellant.

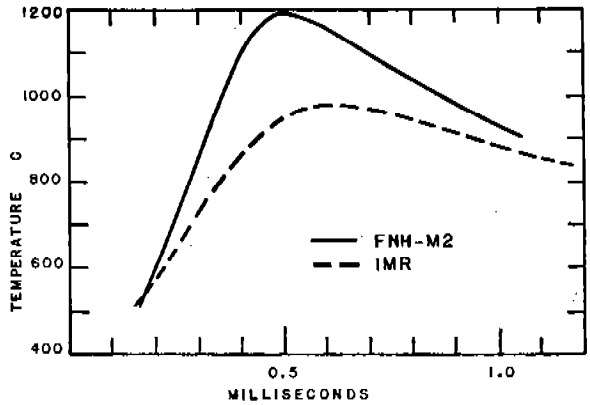


FIGURE 3. A comparison of bore-surface temperatures near the origin of rifling in a preheated caliber .30 rifle for single-base (IMR) and double-base (FNH-M2) propellants. The muzzle velocity was 2,685 fps in each case. (This figure was based on Figure 12 of NDRC Report No. A-427.)

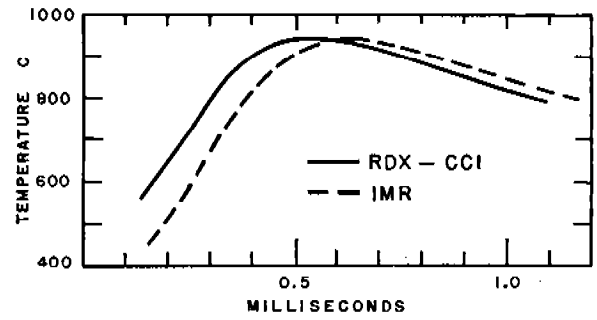


FIGURE 4. The similarity in the temperature-time relations of the bore surface near the origin of rifling in two firing tests, one with an IMR powder, the other with an RDX-CCl powder fired at a higher initial temperature to compensate for its lower flame temperature. (This figure appeared as Figure 15 in NDRC Report No. A-427.)

14.2.5

Carbon Penetration[69]

Measurements of carbon penetration into a caliber .30 barrel initially at room temperature exhibited little more than a veneer of reaction products close to the origin of rifling, although an extremely thin film in the immediate surface had the very high carbon content of 19.3%, indicating possibly a complex cyanide. A typical example of the carbon penetration close to the origin of rifling from firing a single round of IMR powder is to be seen in Figure 5. Carbon penetration was always investigated in two further sections extending to 11 in. forward of the origin of rifling but the penetration was always negligible, being less than 1μ deep and showing none of the peculiarities that occur near the origin of rifling. Thus extensive carbon penetration occurs only in the region of severest erosion.

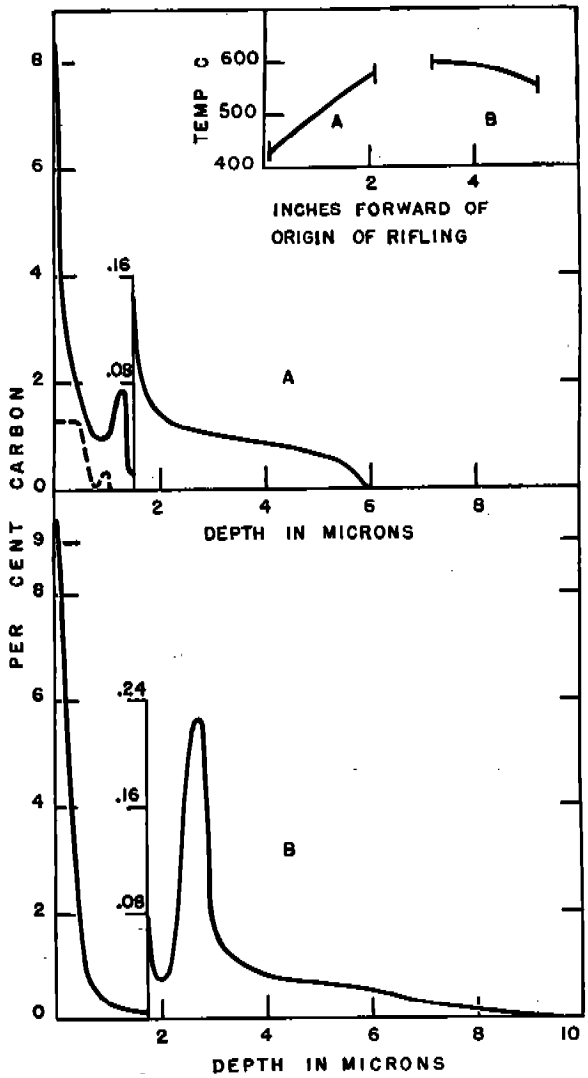


FIGURE 5. The penetration of carbon from propellant gases derived from a single-base powder (IMR), into the bore wall of a preheated, unproofed caliber .30 steel rifle barrel. The inset (upper right) shows the initial temperature of the barrel at different places along its axis and the positions of the specimens. In this figure, and in Figure 6, the curves are actually continuous but the scale for carbon content has been enlarged at an arbitrary depth. The dashed curve for section A shows the small carbon content of the reaction products and lack of any penetration with a double-base propellant (FNH-M2) in another barrel (see Figure 3).

Effects of Temperature

The total depth of carbon penetration increases with increasing temperature of the bore surface. The thickness of the layer of reaction products, however, remains nearly the same for a single round. The content of propellant carbon in the immediate surface decreased from 19.3 to 3.7% in four firings in which the initial temperature was increased from 25 to 565 C.

Effect of Number of Rounds

The firing of ten rounds using IMR powder with radiocarbon in each round caused a considerable thickening of the layer of reaction products, particularly at a point about 3 calibers forward of the origin of rifling; but the depth of penetration into the steel beneath was the same as for a single round. It appears that a given carbon-depth relation is re-established with each round, as might be expected if penetration is chiefly a function of the temperature-time relations during firing. While the depth of penetration into the steel was unchanged, the propellant carbon content was increased in the surface of the steel below the reaction products from 0.2 to 1.9%.

Effect of Propellant

The principal carbon penetration experiments were conducted with a single-base powder of the IMR type. The examination of bore surface materials described in Chapter 12, however, had indicated that in the case of Service guns the type of powder caused a difference in the chemical nature of the erosion product, cementite (Fe_3C) being associated with the firing of single-base powder and wüstite (FeO) with double-base.

Furthermore, thermodynamic calculations[60] (Sec-

tion 12.2.4) indicate that for the bore-surface temperatures shown in Figure 3 and the CO/CO_2 ratio in the gases from a double-base powder, FeO would be the ultimate reaction product. Similar calculations for IMR powder give cementite as the equilibrium product. On the expectation that there might be a difference in the degree and extent of the carbon penetration between firings with single- and double-base propellants, experiments were conducted with both FNH-M2 and RDX powders.

FNH-M2 Powder. A portion of the results obtained in the experiment with FNH-M2 powder are given in Figure 5 for the region near the origin of rifling. A search for carbon to a depth of 8μ revealed none beyond 1μ. Thus carbon plays an insignificant role in the reaction products remaining on the surface with FNH-M2 powder and fails to penetrate the steel at all.

RDX Powder. This powder had the same nominal composition as that used in one of the erosion tests at the Franklin Institute. It caused negligible erosion under certain conditions described in Table 3 of Chapter 15. The bore-surface temperature and the CO/CO_2 ratio are such that chemical thermodynamics would predict a carburizing action. In Figure 6, where a comparison of the carbon penetration is made between IMR and RDX powders for the same bore-surface temperature (see Figure 4), it can be seen that the depths of penetration are the same, although the average content of propellant carbon in the layer of reaction products with RDX powder is only about one-half of that with IMR powder. Other reaction products not containing carbon are presumably present to a greater extent with the cool RDX powder than with IMR powder. This is in accord with the identification of iron nitride (listed in Table 12 of Chapter 15) on the bore surface of a steel barrel that had been fired with this powder in the caliber .50 erosion-testing gun,[123] as described in Section 15.3.4.

14.3 REACTION OF CARBON MONOXIDE WITH GUN STEEL

14.3.1 Introduction

The possibility that the formation of carbonyls of iron might play a role in gun erosion has been care-

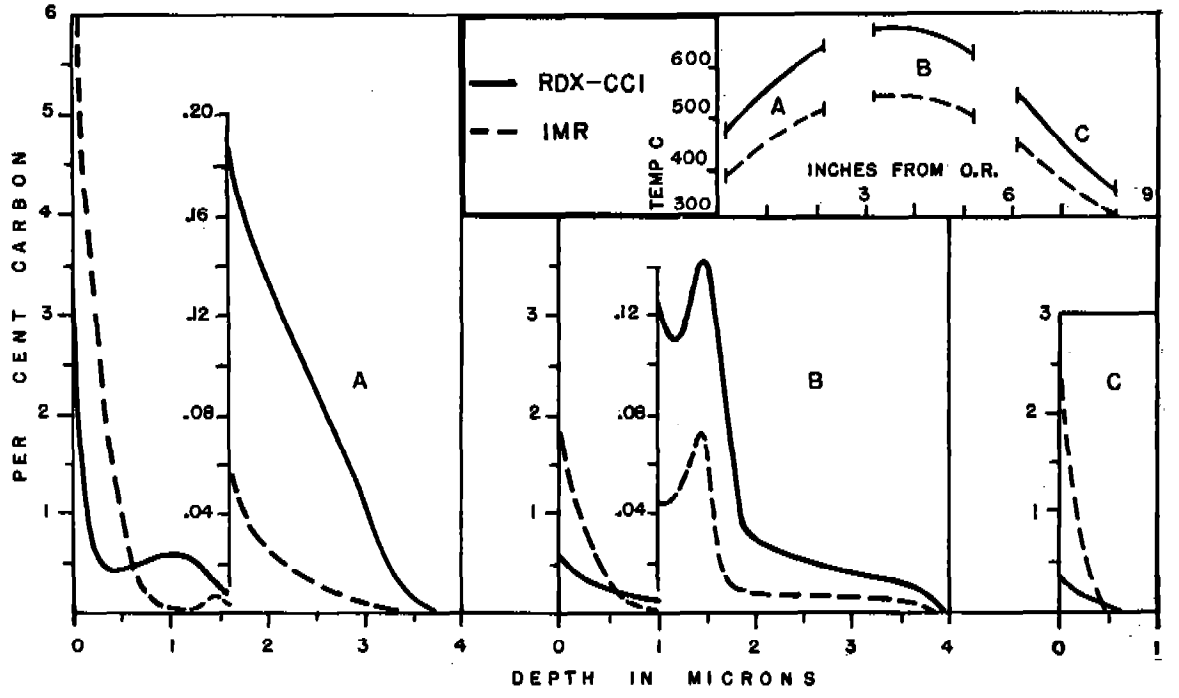


FIGURE 6. The penetration of carbon from propellant gases derived from RDX-CCl powder into the bore wall of a preheated, unproofed caliber .30 steel rifle barrel. These curves are compared with those for the hotter IMR powder at lower initial temperature but same bore-surface temperatures (see Figure 4). The inset (upper right) shows the initial temperatures of the barrels and the positions of the specimens. (This figure appeared as Figure 30 in NDRC Report No. A-427.)

[redacted]

fully studied.[19,62,63] So far only laboratory experiments have been performed. Although a positive identification of a volatile carbonyl under exact ordnance conditions has not been obtained, the work is being continued[d] with this ultimate end in mind. The preliminary studies that can be reported here fall into two groups: measurement of the weight losses of erosion vent plugs subjected to gases resulting from explosions of carbon monoxide-oxygen mixtures and the recovery and identification of volatile iron compounds.

Explosion of the above mixtures produced a mixture of carbon monoxide and dioxide with a small amount of free oxygen due to the dissociation of carbon dioxide. In addition to these gases there were present in the eroding gas mixture the impurities in the original carbon monoxide in either a free or combined state. These consisted of 4 to 5% of nitrogen and 2 to 3% of hydrogen. Especial care was taken to remove the iron carbonyl prevalent in commercial tanks of carbon monoxide. An increase in the oxygen content increased the flame temperature and changed the composition of the eroding gases but the explosion could be modified by the simultaneous addition of carbon dioxide to retain the same composition while lowering the flame temperature by any desired amount.

14.3.2 Summary of Results

The erosion of vent plugs made of gun steel with a 1/16-in. bore diameter was found to be strongly dependent on the flame temperature of eroding gases produced by carbon monoxide-oxygen explosions. The erosion showed little if any dependence on the CO/CO_2 ratio in the eroding gases. The magnitude of the weight losses and the lack of any dependence on this ratio indicates that the steel per se was melted under these experimental conditions, except possibly at the lowest flame temperature. The CO/CO_2 ratios and the character of the reaction products seem to correspond to the conditions for a double-base propellant containing 20% or more of nitroglycerin.

The addition of small amounts of hydrogen sulfide substantially increased the erosion, particularly with the cooler bore surfaces; but when the erosion was extremely severe this effect was relatively small. Hydrogen sulfide is a catalyst for the synthesis of iron carbonyl and increase in erosion might have been caused by the greater production of this volatile compound; but there are other equally feasible explanations.

Iron carbonyl could not be detected in the gases collected after passage through vent plugs. When the bore-surface area was increased by substituting caliber .30 barrels for the vent plugs, iron carbonyl was detected to the extent of a few tenths of 1 per cent of the total iron deposits formed during the explosion of the coolest gas mixture or a solid propellant. The major portion of the iron occurred in iron-bearing deposits in a muzzle tube designed to collect the gases and as a solid unknown material in the cold trap used to condense any volatile iron compound. The amounts of iron measured as carbonyl were insignificant, but it is plausible to assume that a large fraction was decomposed either before it could leave the barrel or in the muzzle tube. So far, it has not been possible to identify these deposits, in part or in whole, with the decomposition products of iron pentacarbonyl.

14.3.3 Vent Plugs[62,63]

Method

The apparatus was identical in principle with that used to study erosion in vent plugs fired with propellants shown in Figure 5 of Chapter 11. The vent plugs were 5/8-in. long with a 1/16-in. bore diameter. They were made of SAE 4140 steel obtained from a liner for a 5-in./25-cal. gun. The bursting pressure of the rupture disk was 25,500 psi which corresponds to the maximum partial pressure of carbon monoxide and dioxide in guns.

Weight Losses

Figure 7 shows that the erosion weight losses are very strongly dependent on the flame temperature of the gases. Figure 8 shows that there is little if any dependence on the $(CO + O_2)/CO_2$ ratio[e] except when the CO_2 greatly exceeds the CO.[f] It is concluded that erosion under the conditions of these vent plug

[d] At the Johns Hopkins University under a contract with the Army Ordnance Department.

[e] For convenience we shall use the expression CO/CO_2. The dissociation of carbon dioxide exceeds 2% only for flame temperatures above 2800 K but it also increases as the pressure drops. The presence of hydrogen lowers the amount of oxygen because of the water-gas reaction.

[f] A ratio of $CO/CO_2 < 1$ in the gases from propellants is unlikely. It might occur with a composition greatly in excess of 40% of nitroglycerin.[107]

[redacted]

experiments was due to melting, with a possible exception for the gases at 2160 K.

X-Ray Analysis

The material collected from the muzzle face of the vent plugs showed in all cases ferrous oxide (FeO), alpha-iron, austenite (gamma-iron containing dissolved carbon), and in some cases magnetite (Fe_3O_4). At 2160 K there was in addition hematite (Fe_2O_3) present. The possibility that aerial oxidation occurred subsequent to the firing was excluded by other experiments. However, since the material was transported from the location of erosion to a position between the muzzle face of the vent plug and the abutting rupture disk, it is not necessarily representative of the actual reaction products of the gas with the gun steel. That the reaction of droplets of molten steel or primary reaction products, with the eroding gas, could well produce these erosion products was demonstrated by experiments with iron filings described in Section 14.5.3. Microanalysis of the erosion products from the muzzle face indicated carbon in excess of the austenite content and not present as a carbon compound in the x-ray analysis. The formation of cementite on the bore surface, later melted and dissociated in the melting and transportation, would yield free carbon and alpha-iron.[g] The investigators preferred to attribute the presence of apparently free carbon to the cracking of the carbon monoxide. The formation of cementite (Fe_3C) does not necessarily require the presence of free carbon,[60] as shown by equations (5) and (10) of Chapter 13.

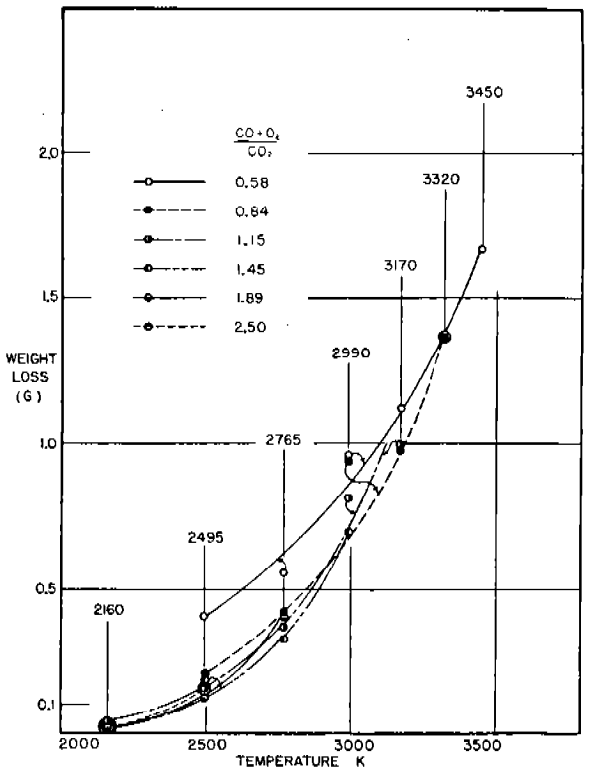


FIGURE 7. The weight losses of 1/16-in. vent plugs subjected to the action of eroding gases of controlled composition and flame temperature resulting from the combustion of oxygen and carbon monoxide. (See Figure 8.) (This figure appeared as Figure 9 in NDRC Report A-310.)

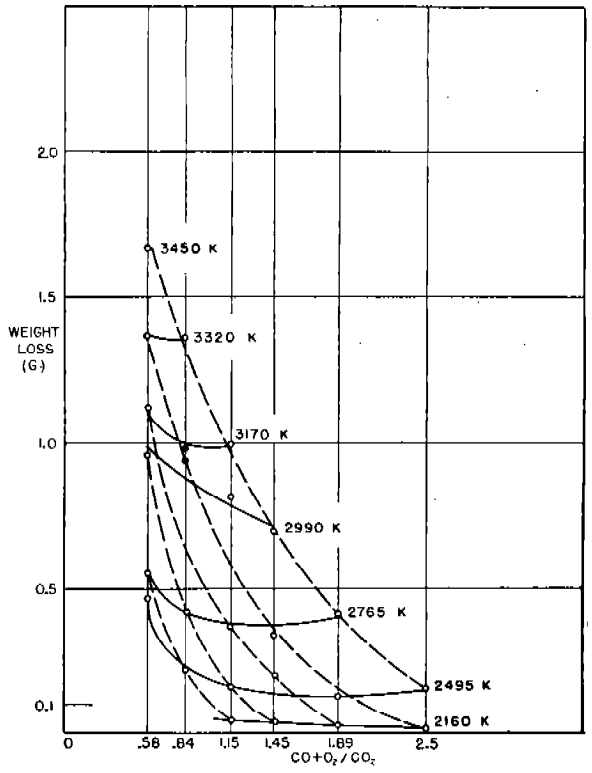


FIGURE 8. The weight losses of the 1/16-in. vent plugs in Figure 7 plotted as a function of the $(CO + O_2)/CO_2$ ration for various flame temperatures. (This figure appeared as Figure 8 in NDRC Report No. A-310.)

Sulfur in the Charge

Sulfur is present to the extent of 0.04 to 0.33% in all gun charges and it is converted almost entirely to

[g] Apparently the solution of carbon in the liberated iron is too slow to stabilize the iron as austenite on cooling even in experiments where the decomposition occurred over a period of several seconds.[105]

hydrogen sulfide (H_2S) in the powder gases, as explained in Section 14.4.1. Catalysts for the formation of iron carbonyl mentioned in the chemical literature are organic and inorganic sulfides, ammonia and hydrogen.[499] Hydrochloric acid and chlorine gas are reported to be inhibitors or destroyers of iron carbonyl.[449]

In some of the vent plug experiments carbon disulfide, or sulfur dioxide or hydrogen sulfide was added to the mixtures of oxygen and carbon monoxide having flame temperatures of 2330 and 2495 K. A continuous layer of iron sulfide was shown to be present on the bore surface of the vent plugs by sulfur prints, examples of which are shown in Figure 9. Carbon disulfide or sulfur dioxide did not essentially alter the erosion, but owing to experimental difficulties this result is not final.

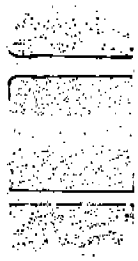


FIGURE 9. Sulfur prints that indicate the formation of a layer of iron sulfide on the bore surface of vent plugs when: (top) carbon disulfide was added to the exploding gas mixture; and (bottom) 1.25% of hydrogen sulfide was added. (This figure appeared as part of Plate VII in NDRC Report No. A-310.)

Hydrogen sulfide, even in amounts as small as a few tenths of 1 per cent, greatly increased the erosion, the increase being proportionately greater the lower the flame temperature and the higher the CO/CO_2 ratio in the eroding gases. A maximum effect was reached at about 5% hydrogen sulfide.

In a series of explosion mixtures that produced eroding gases of increasing flame temperatures, 1.25% of hydrogen sulfide was added. Whereas at the lower flame temperatures the relative effect of the hydrogen sulfide was large and dependent on the flame temperature, the increase in erosion caused by the addition of the hydrogen sulfide for flame temperatures from 2500 to 3320 K was relatively small and practically constant.

These results might be interpreted as indicating an erosion mechanism involving the formation of iron carbonyl particularly during the time that the bore surface is heating up, this reaction being catalyzed by the presence of hydrogen sulfide. Iron carbonyl was not isolated in vent plugs experiments, however, which may have been due to its inability to survive the peak temperatures in sufficient amount.

On the other hand, the reaction

$$Fe + H_2S \longrightarrow FeS + H_2$$

is highly exothermic; the products would be heated to between 600 and 700 C above the reactants in an adiabatic system.[60] It is worth noting that a similar reaction between iron and sulfur dioxide, although not known, should be much less exothermic if not endothermic. Any tendency for the ferrous sulfide (FeS) to be heated above the equilibrium temperature of 1000 to 1100 C will result in its decomposition. If there is a stirring of the surface material, the melting point could be lowered to about 985 C. Such an exothermic reaction could also contribute heat to affect the conditions at the bore surface in several ways. If bore-surface temperatures are just below a critical temperature, such as the melting point of erosion products, the formation of ferrous sulfide could contribute a small amount of heat that would be sufficient to cause this temperature to be reached, or, the rapidity of the temperature rise of the bore surface might be increased by the early formation of ferrous sulfide, thus prolonging the time that the bore surface is at or above some critical temperature.

Both these effects should be particularly noticeable at low gas temperatures. At the higher flame temperatures, however, where melting is almost certainly the principal mechanism of erosion in 1/16-in. vent plugs, the exothermic heat would contribute in a relatively small and rather constant degree in the second manner suggested above.

Some support to the foregoing hypothesis is offered by a few experiments with long vent plugs having a 3/32-in. bore diameter. When the bore surface was coated with ferrous sulfide prior to the explosion, the weight losses were insignificant (1 and 4 mg) but when the surface was not so coated and instead 1.25% of hydrogen sulfide was added to the exploding mixture the vent plug lost 43 mg. It should be emphasized, however, that the data are too meager at present to substantiate either of the above points of view.

X-ray analysis showed a trend to smaller amounts of FeS and larger amounts of FeO in the material from the muzzle face of the plugs as the flame temperature was increased and the CO/CO_2 ratio de-

creased. This can probably be explained by the reaction:

$$FeS + CO_2 \longrightarrow FeO + CO + S$$

Hydrogen sulfide is most effective when the bore surface is but mildly heated. This is illustrated by firings in vent plugs having 1/16-in., 1/8-in., and 3/16-in. bore diameters which showed factors of increase of erosion caused by the addition of 1.25% of hydrogen sulfide equal to 3, 10, and 66 respectively. This is fairly strong evidence that chemical factors are important. A simple explanation would be to assume the catalyzed formation of iron carbonyl, but it is not necessary, and in some cases it would be difficult, to postulate the formation of iron carbonyl to account for any appreciable portion of erosion in the absence of hydrogen sulfide.

Ammonia and Hydrogen in the Charge

The addition of 1 mole % of hydrogen sulfide, or ammonia, or hydrogen to the 2300 K mixture caused the weight losses to increase by more or less the same factor of about 3, from which one might infer that the increased erosion arises from the addition of 1, 1½, and 1 mole % of hydrogen respectively in the above gases. However, later work seems to rule out a common mechanism for the increased erosion. The presence of the above three gases also have a decided effect on the erosion of vent plugs of Armco iron, nickel, and cobalt in the same general manner.

The addition of 1% of chlorine or hydrochloric acid had no effect on the weight losses, which is remarkable in itself. That there was no mitigation of the erosion seems to demonstrate that iron carbonyl formation is insignificant in the absence of the above catalysts but there is no assurance that these inhibitors are acting in the explosion in the manner suggested.

Extreme Severity of Tests

Preliminary investigations were largely confined to the use of 1/16-in. vent plugs rather than the 1/8-in. size later studied. The conditions of erosion were extremely severe with them, the chief part played by the gases being a transport of heat. The CO/CO_2 ratios were all below 2.5 with the one exception of a ratio of about 3. Studies of the composition of quenched powder gases, described in Section 2.3, show that these ratios are about the same as those obtained with double-base powders which range from 1.2 to 2.5. This is a condition which unfortunately cannot be remedied because of the great difficulty of properly exploding such mixtures of carbon monoxide and oxygen that are necessary to give the higher CO/CO_2 ratios.

14.3.4 Isolation and Identification of Iron Carbonyl[63]

The conditions for the synthesis of iron carbonyl are all satisfied in the passage of propellant gases through a gun barrel with the exception of the temperature. For a short period the temperature condition is also satisfied near the origin of rifling and probably for a protracted period near the muzzle.

Experimental Method

The gases emerging from vent plugs 4- to 4½-in. long with 5/32-in. bore diameter, or from a caliber .30 barrel, were collected in an evacuated glass-lined chamber, hereinafter called the *muzzle tube*, shown in Figure 6 of Chapter 11. These gases were later drawn through a *cold trap* maintained at the temperature of liquid nitrogen. Any volatile matter condensed therein was drawn through an analyzing system in which the pentacarbonyl would be decomposed by heat to form a thin mirror of iron-bearing material (analyzed for iron in quantitative work) and to form gaseous products which were analyzed for the presence of carbon monoxide.

The eroding gas mixtures were cool, having been obtained from an explosive mixture of 11 or 12% of oxygen in carbon monoxide. The use of large-bore vent plugs or caliber .30 barrels resulted in a much milder test than those obtained in the erosion tests of vent plugs just described in Section 14.3.3. The bursting pressure of the rupture disk was 25,500 psi. Caliber .30 barrels were fitted with a second 10,000-psi rupture disk at the muzzle.

In order to favor the formation of iron carbonyl, up to 2.5% of hydrogen sulfide was added or the bore surface (of vent plugs only) was converted to ferrous sulfide before the test. A number of different arrangements in the muzzle tube were tried with the object of preserving any iron carbonyl formed.

Location of Erosion Products

Iron-bearing material was found at one or more of

[redacted]

three different positions. Firstly, a consistent feature was the appearance of an adherent iron-bearing deposit on the wall of the muzzle tube in the form of a bright metallic mirror, reminiscent of the decomposition of a volatile metallic compound. This mirror became black if hydrogen sulfide was present in the eroding gases. Secondly, the cold trap usually contained a black sooty iron-bearing material. Thirdly, when iron carbonyl was collected a mirror of iron-bearing material was formed in the heated deposition tube of the analytical apparatus. Analyses for iron in the various deposits showed it to be present (1) as the element, (2) as an oxide, or (3) as a sulfide in cases where hydrogen sulfide or black powder had been used, but no sulfides of iron, or of copper often found in the deposits, were identified by x-ray analysis.

Vent Plugs

Muzzle Tube. X-ray examination of the mirror deposit showed only ferrous oxide (FeO) and austenite. Under certain conditions ferrous oxide can be a product of the decomposition of iron pentacarbonyl but it could have been produced by the passage of hot erosion gases after the iron-bearing deposit was formed. It is, however, difficult to understand the presence of austenite by either of these mechanisms. Whether the deposit in the muzzle tube represents decomposition of iron carbonyl, and if so to what extent, requires further experimentation.

Austenite and ferrous oxide were also obtained with a hydrogen-oxygen explosion but in this case the deposit was but loosely adherent and of different physical appearance. A comparison with the carbon monoxide-oxygen explosion is probably unfair primarily because of the very different thermal conditions.

Cold Trap. The iron-bearing products in the cold trap could not be identified with the possible exception of austenite. The x-ray patterns, except for a single line in one experiment, correspond neither to unidentified lines for the products of thermal decomposition of iron pentacarbonyl nor to lines found in a preparation of a condensed carbonyl, $Fe_3(CO)_{12}$.

Deposition Tube. None of the experiments with steel vent plugs revealed the presence of iron carbonyl condensed in the cold trap. The possibility of its formation is not thereby ruled out, for iron carbonyl introduced into the explosion mixture and fired through a copper vent plug failed to survive the explosion. It was even lost to a marked extent on mere standing in the explosion mixture. Thus, it is quite likely that iron carbonyl may have been formed in the erosion of steel vent plugs in an amount less than the minimum for survival and detection. If mild thermal conditions were to be maintained the only solution was to increase the area of the bore surface. This was accomplished by adapting caliber .30 Enfield barrels to the apparatus as shown in Figure 6 of Chapter 11.

Gas Mixtures in Caliber .30 Barrels

Bore-surface temperatures in the caliber .30 barrels were lower than in the vent plugs and a considerable area of the added surface will reach still lower maximum temperatures. The correspondence between the temperature-time relations for this test and those for ordnance conditions with a projectile present has not been determined.

Table 1. Iron content of deposits after five consecutive firings through caliber .30 barrels used as vent plugs.[63] (Propellant: carbon monoxide and oxygen mixture containing 11% oxygen and a little hydrogen sulfide.)

	Milligrams of iron		
Per cent H_2S	On glass liner of muzzle tube	Solid material in cold trap	From decomposition of condensed iron carbonyl
0.00	0.44	3.02	0.007
0.125	0.87	3.52	0.031
0.25	1.40	5.72	0.063
0.50	1.56	8.53*	0.046*

* Some black material blown out of the cold trap and probably some iron carbonyl also lost. Blank runs on 4,000 psi of carbon monoxide without H_2S and oxygen showed complete absence of iron carbonyl.

No iron carbonyl was detected in a single firing but the usual mirror deposit was found in the muzzle tube. Iron carbonyl was repeatedly found in single firings if 1.25% of hydrogen sulfide was added. A series of firings were made in which small amounts of hydrogen sulfide were added. Analyses for iron in the three deposits yielded the results in Table 1. The addition of hydrogen sulfide, even in the small amounts present in propellant gases, increased the amount of iron recovered from the muzzle tube and cold trap and substantially increased the amount of volatile iron carbonyl recovered.

Standard Propellant in Caliber .30 Barrels

In order to produce the same number of moles of

carbon monoxide[h] as given by the gas mixture. 20.5 g of an NH-M1 powder was burned in the same explosion vessel with and without the addition of black powder. Piezoelectric measurements of the pressure as a function of time, illustrated in Figure 10, showed

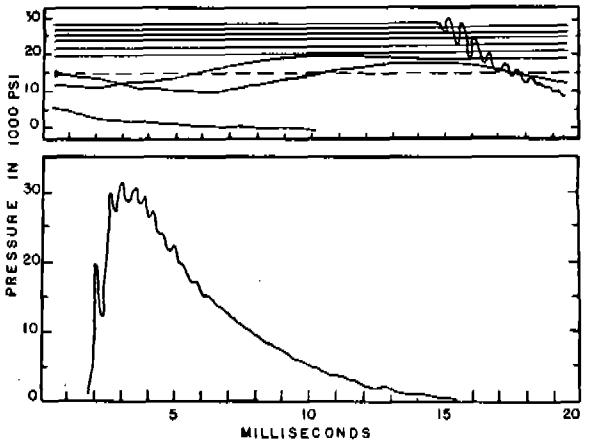


FIGURE 10. Oscillograph record of pressure as a function of time for two types of firing in the same explosion vessel. (Upper part of figure): A typical experiment with the carbon monoxide and oxygen mixture. (Lower part of figure): One of the experiments with the NH-M1 solid propellant. While the combustion of the gas mixture is comparatively very slow, the time of effusion through the barrel after rupture of the disk is the same for the gas mixture and solid propellant. (This figure appeared as Figure 33-1 in NDRC Report No. A-311.)

that the maximum pressure, rate of decrease of pressure, and total time of effusion were about the same for the gas mixture and solid propellant. However, the very slow combustion of the gas mixture compared with the solid propellant is well demonstrated. In experiments with black powder (containing 10 per cent of sulfur) the amount added was the same as that normally present in the charges of a number of medium caliber guns. (See Section 14.4.1.)

The deposits of iron-bearing material produced by the decomposition of the recovered iron carbonyl in the analytical apparatus are illustrated in Figure 11. Analyses for iron in the three deposits, given in Table 2, show that iron carbonyl was formed with the NH-M1 propellant without the addition of sulfur in the form of black powder. The iron content of the deposit in the muzzle tube was increased by the addition of black powder, and most probably the iron present in

[h] The amount of CO present in powder gas at any instant is, unlike the case of gas mixtures, very strongly dependent on the momentary temperature of the water-gas produced by the burning of the propellant. See the discussion in Section 2.3.4.

TABLE 2. Iron content of deposits after five consecutive firings through caliber .30 barrels used as vent plugs.[63] (Propellant: smokeless powder.*)

Addition to powder (g)	Milligrams of iron: On glass liner of muzzle tube	Solid material in cold trap	From decomposition of condensed iron carbonyl
0.0	6.96	38.64	0.078
0.42 black powder	22.33	21.30†	0.058†
1.0 *p*-nitrobenzoyl chloride	16.31	30.71	0.089

* Powder—NH-M1 for 37-mm gun, M1916, Lot 3727.

† Material blown out of the cold trap very probably accompanied by loss of condensed iron carbonyl. Addition of black powder altered the nature of the explosion.

the cold trap as iron carbonyl would have been greater had not the violence of the explosion caused a loss of material. The addition of paranitrobenzoyl chloride, added as a source of chlorine which has been reported to be an inhibitor for the formation of iron carbonyl, failed to reduce the amount of iron carbonyl recovered and produced no change in the total iron from the three sources.

SOLID IRON-BEARING DEPOSITS

The amount of iron recovered as iron carbonyl from the gas mixture or the propellant, in the absence

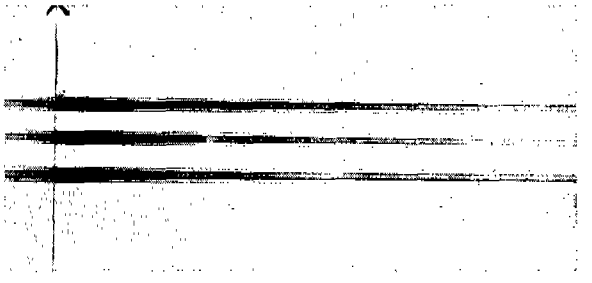


FIGURE 11. Deposits of iron-bearing material from the thermal decomposition of iron carbonyl in the recovered gaseous products from firings of NH-M1 powder with and without the addition of different substances. (Upper) NH-M1 propellant alone; (middle) 2% of black powder added; and (lower) 5% of paranitrobenzoyl chloride added. (This figure appeared as Plate XI in NDRC Report No. A-311.)

of sulfur, was roughly constant at 0.2% of the total iron from all the analyzed deposits. The addition of hydrogen sulfide to the gas mixture increased the iron present as carbonyl to 0.8% of the total. These

amounts are insignificant but it is plausible to assume that a large fraction of the iron carbonyl is decomposed either before it can leave the barrel or in the muzzle tube.

X-ray examination of the bore-surface products near the origin of rifling showed the presence of ferrous oxide, alpha-iron, and sometimes austenite, with a few unidentified lines. For the firings of propellant plus black powder all the lines were attributable to alpha-iron and magnetite (Fe_3O_4). The iron-bearing material in the muzzle tube and cold trap could not be identified; the unidentified pattern, except for one or possibly two lines, is not the same for the various deposits. It is curious that no known sulfides were identified, because their presence was obvious from the chemical analyses.

The thermal decomposition of iron pentacarbonyl is strongly dependent upon the temperature and nature of the carrier gas. In a study of the factors affecting the decomposition one or more of the following products were found: alpha-iron, magnetite, cementite (Fe_3C), always accompanied by unidentified but often different lines. Two of these lines occurred fairly consistently and were possibly the same as the pattern of the two unidentified lines that were the only lines found for the material from a muzzle tube after firing the gas mixture with hydrogen sulfide. Some of the unidentified lines in the decomposition products of iron pentacarbonyl corresponded to a part of the pattern obtained from a synthesized sample of the trimer of iron tetracarbonyl $[Fe(CO)_4]_3$, but this latter pattern could not be repeated.

It is unfortunate that the decomposition of iron pentacarbonyl has so far yielded no distinctive product, because the identified products are ones which might well be expected from reactions taking place in a gun tube quite independently of carbonyl formation. It is thus too early to ascribe the presence of the solid deposits in part or in whole to the decomposition of iron pentacarbonyl.

14.4 REACTION OF SULFUR GASES WITH GUN STEEL

14.4.1 Introduction

In the preceding section it was shown that the addition of a small amount of hydrogen sulfide to the eroding gases produced by the combustion of carbon monoxide and oxygen resulted in a considerable increase in erosion. This section deals with the extent to which sulfur may form reaction products on the bore surface and the degree to which it penetrates the bore wall. If penetration is extensive, the physical properties of the steel can be affected adversely. If iron sulfide is a product of the interaction, the melting point of the bore surface material can be greatly depressed below that of steel.

Elementary sulfur is present in the charges of medium and large bore guns to the extent of 0.04 to 0.33% by weight of the charge,[53] by virtue of the booster and igniter pads of black powder. In small arms the sulfur, present to about the same extent, is all combined in the compounds of the primer. The sulfur goes almost completely to hydrogen sulfide in the powder gases according to a study of the chemical thermodynamics of gun erosion.[60]

The same study indicates that ferrous sulfide (FeS) should be the ultimate product under a great variety of conditions of temperature and gas composition for an interaction between a steel bore surface and powder gases derived from a propellant containing as little as 0.1% of sulfur. However, the formation of ferrous sulfide is self-inhibiting because of the highly exothermic reaction involved in its formation and this probably accounts for the lack of any considerable portion of ferrous sulfide identified in the reaction products at the bore surface of eroded guns described in Chapter 12. Another possibility is a scavenging of the sulfur by the usual deposit of copper in a gun tube,[98] which is discussed in Section 12.3.2.

The extent to which the presence of black powder in a charge of smokeless powder contributes to erosion has been studied in an explosion vessel, but not under ordnance conditions.[53,200,203]

14.4.2 Summary of Results

Sulfur in the reaction products on the bore surface and that which penetrated into the underlying steel was detected and measured by incorporating radioactive sulfur into a charge of single-base powder. This tracer method is sufficiently sensitive so that only a single firing is required and it possesses the advantage that it is often unnecessary to destroy the specimen for a determination of the element in question. Thus it was possible to examine the sulfur content of the bore wall of a caliber .30 rifle barrel by using the whole barrel as a Geiger-Mueller counter in order to detect the emission of beta-rays from the radioactive sulfur. The same barrel could be studied in this man-

ner for the effect of a variety of treatments including the subsequent firing of a number of rounds.

A considerable fraction of the sulfur in a single charge was found to be incorporated in the bore wall. Some of this sulfur may have been associated with the metal-fouling but evidence from various treatments of the barrel was in favor of an association of some of the sulfur with the steel, or an iron-bearing complex coating. Only a small fraction of the sulfur was permanently incorporated and 95% was lost in regularly decreasing amounts during the subsequent firing of 36 rounds. This loss is commensurate with the rate of erosion of caliber .30 barrels. The sulfur permanently incorporated would yield a maximum content of about 0.8% in the altered layer after 1,000 rounds or alternately the crack system might contain material with a 2% sulfur content.

This preliminary work led to further experiments which, while they departed from ordnance conditions, avoid ambiguous interpretations and provide a means of ascertaining the extent of penetration.

Reaction products that were formed by the interaction of propellant gases and the steel surface of test rods (described in Section 11.2.4) contained 12 to 18% of sulfur by weight and this sulfur was shown to be combined with iron. The steel surfaces were chemically attacked by the sulfur components of the powder gases, and the formation of sulfur compounds of iron may contribute to erosion in guns. The evidence from these experiments, and others summarized below, appears to support the idea that the formation of a coating of reaction products in which iron from the steel is transferred to this coating is a necessary intermediate stage in erosion where melting of the steel itself is excluded, the chemical compounds so formed being more susceptible to complete removal than the original steel.

The penetration of sulfur into the steel below the layer of reaction products is extremely shallow, although the sulfur content of this shallow zone is not inconsiderable.

In view of these results a number of test rods were subjected to the action of powder gases derived from a nitrocellulose powder with and without the addition of black powder or its components. The addition of black powder, and of sulfur or potassium nitrate in equivalent amount, increased the rate of erosion of gun steel as measured by weight loss. The addition of charcoal in equivalent amount decreased the rate of erosion and diminished the characteristic cracking of the surface commonly termed "heat checking." While the addition of black powder always increased the erosion, curiously enough it greatly diminished the heat checking and even eliminated it when in sufficient amount. There was abundant evidence that the gun steel per se was not melted in these tests and therefore the above observations could not be so explained.

It was suggested on the basis of these experiments that an effort should be made to remove the sulfur from the charge in an actual firing test and perhaps to incorporate small amounts of charcoal that might mitigate erosion without appreciably lowering the potential of the powder. However, these things have not been accomplished.[i]

14.4.3 Experimental Methods[53]

Rifle Barrel as a Geiger-Mueller Counter

In order to convert a rifle barrel to a Geiger-Mueller counter for detecting the radioactivity of a tracer element incorporated in the bore wall it is only necessary to provide means for stretching a fine tungsten wire along the axis of the tube and to insure electrical insulation of this wire and hermetic sealing of the tube. The location of the sulfur in the tube was determined by inserting glass tubes of appropriate lengths to block the beta-rays emitted by the radiosulfur. Such an arrangement indicated maximum sulfur content of the bore wall over the first six calibers forward of the origin of rifling and a secondary maximum at about 10 calibers behind the muzzle. The propellant was a standard IMR powder for caliber .30 small arms to which 0.07% by weight of native sulfur was added. This sulfur acted as the carrier for the radiosulfur, the two being chemically indistinguishable. The radiosulfur was shown to index not only the added sulfur but all the sulfur in the charge, including that of the primer components.

Penetration Experiments with Test Rods

Small test rods were subjected to the action of straight nitrocellulose caliber .45 pistol powder gases in the apparatus described in Section 11.2.4 for testing the resistance of metals to surface cracking. Test rods were made of SAE 4140 steel in a tempered

[i] The efficiency of certain ignition powders, including modified black powders, that do not contain sulfur has been investigated at Aberdeen Proving Ground. Comparative erosion was studied only in vent plug tests.[200,203]

martensitic state. The rods, 3/16 in. in diameter and 1¼ in. long, were milled to give two diametrically opposite flat surfaces which were highly polished. These flats were subjected to the gases passing through two vents of D-shaped cross section formed by fitting the rods into a round hole in a replaceable cone.

After less than the number of rounds that were established as sufficient to produce cracking had been fired, the rods were introduced into a specially designed Geiger-Mueller counter wherewith the sulfur content of the reaction products and the depth of penetration could be studied by the fall in activity following successive removals of known weights of material with a metallographer's finishing lap. The amount of native sulfur which carried the radiosulfur was between 0.07 and 0.4% by weight of the smokeless powder, corresponding to the amount present in some gun charges.

Cracking and Erosion Tests with Test Rods

The same apparatus, basic charge, and type of steel were used for these tests as for the penetration experiments just described. This kind of test possesses a decided advantage over the usual vent plug experiment in that it is possible to conduct a rapid microscopic examination of the surfaces at any stage before conclusion. The temperature-time relations are more readily controlled because only a portion of the gas passes over the specimen. The conditions were mild, as was confirmed by several observations that were made in order to establish the fact that the steel per se did not melt. Spectrophotometric measurements of the gas temperature of the sort described in Section 2.5.1 showed a maximum increase of 50 C over 2700 C with the addition of 10% of black powder. No change in the pressure-time curve was observed. A maximum weight loss of 12 mg after 85 rounds was recorded with weighings on a microbalance[j] or expressed in ordnance terms these tests correspond to an increase in bore diameter of 0.001 to 0.005 in. in 30 to 60 rounds. This value was obtained by doubling the calculated thickness of metal removed, which is analogous to increase in groove depth. In some experiments black powder was added in amounts varying from 0.5 to 10% by weight; in other tests equivalent amounts of charcoal, sulfur, and potassium nitrate were added.

[j] See Table 13 of Chapter 15 for weight losses of gun steel vent plugs of different sizes fired with different propellants.

14.4.4 Sulfur in Reaction Products[53]

In all these experiments an adherent layer of material was produced on the surface that differed radically from the original steel. The results of some experiments with test rods to determine the role of sulfur in the chemical alteration are given in Table 3. Each charge contained 0.4% of sulfur.

Table 3. Sulfur content of reaction products on the surface of steel test rods subjected to the action of sulfur-containing powder gases.[53]

Number of rounds	Thickness of coating (microns)	Sulfur in coating determined by radioactive tracer (per cent)	Computed as FeS (per cent)
2	0.8	18	50
5	1.8	12	33
2*	0.9	12	33

* The charges were fired electrically in an all-steel system eliminating the possibility of copper, zinc, antimony, lead, or potassium that might have been derived from a caliber .30 case or its primer.

The results in Table 3 do not prove the manner of occurrence of the sulfur. In other experiments no change in the activity of the surfaces was observed after removal of a loose deposit or after immersion in each of the following solvents in turn: ether, carbon disulfide, air-free water, and alcohol. These results indicated the absence of free sulfur in either of its modifications and established that the sulfur compound was not water-soluble or present in combination with carbon and nitrogen in nonmetallic form.

A Baumann or sulfur print affords an extremely sensitive method of detecting the presence of a sulfide[k] of iron or manganese. The surfaces and cross sections of test rods fired with either free sulfur or black powder present in the charges gave very positive sulfur prints similar to those illustrated in Figure 9 for the cross section of a vent plug.

An examination of the products on the surfaces of these test rods by electron diffraction produced a number of patterns which were difficult or impossible to identify, as explained in Section 11.5.2. Moreover, it is believed that some of the products yielded no patterns because they were amorphous.[98] With black powder or sulfur present in the charge the pattern corresponded to a double sulfide with a spinel structure which was possibly violarite [$(Ni,Fe)_3S_4$], al-

[k] The use of this technique and a number of modifications devised to detect other sulfides, with particular reference to erosion products, is described in Section 11.5.3.

though it is likely that manganese or chromium could replace nickel in this compound.[137] There exist only meager data concerning such compounds. Thus, while the exact nature of the sulfur substance remains to be discovered, it has been demonstrated that iron-bearing compounds of sulfur are formed on steel surfaces subjected to propellant gases containing only a small portion of sulfur.

14.4.5 Penetration of Sulfur[53]

The penetration of sulfur into the steel beneath the coating of reaction products is shown in Table 4.

TABLE 4. Penetration of sulfur into steel below the reaction products.[53]

Test rod	Number of rounds	Depth (microns)	Sulfur content (per cent)
5P	2*	0.00 to 0.26	0.28
6D	2†	0.00 to 0.19	0.25
		0.19 to 0.26	0.23
		0.26 to 0.57	0.00
6E	5†	0.00 to 0.16	1.2
		0.16 to 0.24	1.4
		0.24 to 0.31	2.0
		0.31 to 0.39	0.25
		0.39 to 0.66	0.08

* The rounds were fired electrically in an all-steel system. The sulfur content of the charge was 0.4% by weight of the smokeless powder fired.
† The rounds were primer fired from a caliber .30 case which increased the total sulfur content of the charge to 0.5%.

These values are averages for the whole affected area. Localized areas contained slightly more sulfur but not to greater depths, in similar experiments. The slight penetration does not follow the diffusion law. There appears to be a very thin zone of steel that has acquired a roughly constant amount of sulfur. An increase in the number of rounds increases the sulfur content without thickening this zone. The penetration of sulfur is not too significant unless a very thin zone of "hot-short" material is formed which might aid the mechanical removal of the overlying reaction products.

14.4.6 Cracking[53]

A number of test rods were studied with a comparison microscope in order to observe any surface effects caused by the addition of black powder or its components to the charge of smokeless powder. The addition of up to 2% of black powder, i.e., less than the content of the charges for several guns, considerably diminishes the cracking of the surface.[1] This effect persists and is even more noticeable as the number of rounds is increased. With 6 or 10% of black powder, cracking is completely eliminated. With 10% of black powder the cracking is replaced by a pitting that resembles the ripple marks in sand.

The black powder does more than prevent cracking of the surface in a given round because after test rods had been subjected to a number of rounds with 6 or 10% of black powder in the charge they failed to exhibit cracking for a relatively large number of subsequent rounds without black powder present. After a survey of a number of possibilities it was concluded that the phenomenon is caused by a chemical change in the nature of the steel in the surface. This conclusion agrees with the results of other studies discussed in Section 13.5.3. The addition of sulfur alone intensified the cracking as shown in Figure 12. Potassium nitrate was even worse in this respect; but the addition of a third component in the form of powdered willow charcoal to the extent of 0.9% markedly reduced the cracking.

14.4.7 Erosion[53]

The addition of black powder increases the rate of erosion. The results of weighing test rods are given in Figure 13. Similar curves were obtained for the addition of sulfur and potassium nitrate equivalent to the 6% black powder mixture but for the addition of the small equivalent amount of charcoal the erosion by comparison with pure smokeless powder was reduced by a factor of 2. The effects of the components of black powder in increasing the erosion caused by smokeless powder are not simply additive. There is fair agreement with the erosion test with black powder itself for a large number of rounds but a comparison of the initial erosion shows the very serious erosivity at this stage caused by potassium nitrate without its accompanying sulfur and charcoal.

14.4.8 Charges without Sulfur[53]

The foregoing evidence obtained with test rods agrees with that obtained from vent plug tests with carbon monoxide-oxygen mixtures (Section 14.3.3) and from other vent plug tests[200,203] made at Aberdeen Proving Ground with propellant charges, in in-

[1] Such cracking is often termed "heat checking," although this designation infers a cause that does not seem to have been proved. See Section 13.5.3.

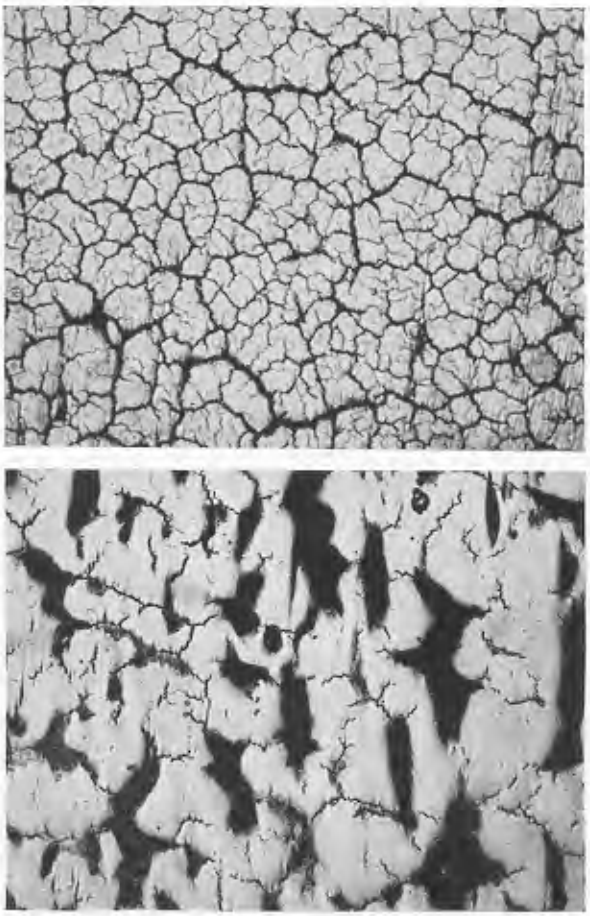


FIGURE 12. The crack systems in the surface of steel test rods subjected to propellant gases, after 85 rounds. (Top): A nitrocellulose pistol powder. (Bottom): The same with 0.6% of native sulfur. Original magnification: *250X*, reduced to about *220X* in reproduction. (This figure has been taken from Figure 18 of NDRC Report No. A-276.)

dicating the desirability of removing sulfur as an element in propellants in order to mitigate erosion, but only if the gun caliber and ballistic level are such that there is no melting of the steel per se. A study of the thermal effects of propellant gases in guns[18] suggests that the latter condition is met for all standard guns, with the exception of the 120-mm gun M1 and the possible exception of 16-in. guns. Therefore the removal of sulfur from the charge should mitigate erosion unless the temperatures are raised by high rates of fire. It would also seem desirable to avoid the presence of potassium nitrate, but it is possible that the correct proportion of the oxidizable component, charcoal, largely eliminates the effects caused by the presence of potassium nitrate alone.

14.5 REACTION OF NITROGEN WITH GUN STEEL

14.5.1 Early Investigations

The role of nitrogen in the production of the features displayed on an eroded bore surface has been discussed for a number of years.[261,421,477,482,483] In these discussions the effect of solution of nitrogen in an austenitic layer was stressed rather than the occurrence of definite nitrides of iron. Before the first paper on the nitrogen theory of erosion appeared, however, it had been suggested[478] that mechanical removal of a brittle nitride layer formed by nitrogenization of the bore surface might be an important mechanism in producing gun erosion.

Nitrogen determinations of layers machined from the bore surfaces of badly eroded caliber .30 machine gun barrels showed an appreciable increase in nitrogen content near the bore surface to a depth of several thousandths of an inch.[481]

14.5.2 Summary of Recent Results

The thermodynamical instability of the iron nitrides at high temperatures would seem to preclude their formation and preservation in a gun tube.[60] Nevertheless, nitrides have been identified in worn Service guns (Chapter 12). Moreover it was shown that hexagonal (epsilon phase) iron nitride (Fe_2N_x) constituted no small portion of the products of interaction between gun steel filings and the gases from a

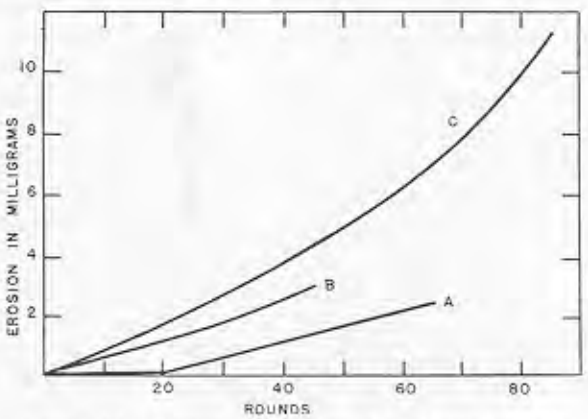


FIGURE 13. The total weight loss of steel from test rods subjected to the action of propellant gases from a nitrocellulose pistol powder to which different amounts of black powder were added. Curve (A) Pistol powder without added black powder; Curve (B) 6% of black powder added; Curve (C) 10% of black powder added. (This figure appeared as Figure 17 in NDRC Report No. A-276.)

CONFIDENTIAL

TABLE 5. X-ray identification of the products of reaction between powder gases and pulverized materials. The numbers indicate only the order of abundance; 1 is the most abundant. Letter d: diminished amount with respect to preceding column; similarly, sd: slightly diminished; and gd: greatly diminished.

	Materials fired with IMR powder (single-base)						Materials fired with FNH-M2 (double-base) powder		
	Electrolytic iron			Gun steel	Fe_4N	Fe_2N_x	Iron	Fe_4N	Fe_2N_x
Product	325 (Mesh)	200 (Mesh)	100 (Mesh)	200 (Mesh)	...	...	325 (Mesh)	...	...
Fe_2N_x	3	2 d	3 sd	2	1	1*		2	2*
Fe_4N					5				
FeO	2	2 gd	3 sd	2	3	2	1†	1‡	1†
Austenite§	1	1	2	1	2	1	3	3	3
Ferrite§	4	1	1	1	4	3	2	3	

* Lower nitrogen content than original. † 90 per cent. ‡ Mostly FeO. § See footnote of Chapter 12 on page 248.

single-base powder fired in the conventional manner from a caliber .30 rifle.[28] With the hotter FNH-M2 powder no iron nitrides were formed. It appears that the nitrides must be formed either very late in a firing or as a secondary product. The main difficulty in establishing the mechanism of their formation is the known inertness of molecular nitrogen. Furthermore, ammonia, which is an active nitriding agent, is present in powder gases in only very small amounts. It is therefore interesting to find in other experiments[70] that while an increase in total nitrogen is confined to the immediate surface, an exchange between the nitrogen of the propellant gases and the original nitrogen of the steel can occur to a very appreciable depth.

14.5.3 Formation of Nitrides[28]

In order to expedite an x-ray study of the erosion products in a gun a very convenient and rapid experimental procedure was devised as described in Section 11.2.6. This consisted of incorporating the pertinent substance in pulverized form in the powder charge for an otherwise normal round of a caliber .30 rifle. The rifle was fired into an evacuated tube from which the products of the explosion were later removed for examination. Such an experiment conforms to ordnance conditions except for one important departure. The temperature of the finely divided material will rise much higher than that of the bore surface which is being simulated by the pulverized substance. The finer particles melted on firing; coarser particles were rounded at the edges only. The results are summarized in Table 5.[m]

[m] Compiled from a description of the results in the NDRC report[28] on this investigation, in which the relative amounts of the products are discussed in greater detail.

Ferrous oxide (FeO) and austenite[n] were common to all the experiments. Ferrous oxide was by far the preponderant product with a nitroglycerin double-base powder. Hexagonal iron nitride formed a lesser, though still appreciable, portion of the total reaction product with IMR powder but was absent with the hotter FNH-M2 powder. This latter relation was fully confirmed in later work on the x-ray and chemical examination of eroded bore surfaces, described in Chapter 12. The conclusion to be drawn from the firings with the iron nitrides is that they are unstable under the temperature and pressure conditions of the experiments. The hexagonal iron nitride found in all the firings of iron and steel particles with single-base powder was therefore presumably formed as a secondary product.

14.5.4 Mode of Formation of Nitrides

The mechanism of the formation of iron nitride on a gun bore surface is far from clear. Iron does not react with molecular nitrogen even at elevated temperatures and pressures; although at a partial pressure of 350 atm, which corresponds roughly to the maximum powder-gas pressure in a gun, the solubility of molecular nitrogen in gamma iron may rise to around 0.4%.[o] Upon cooling and release of pressure some of this nitrogen may be released and form nitrides.

Ammonia reacts rapidly with iron to form nitrides, the reaction proceeding by release of monatomic nitrogen at the surface. The amount of ammonia present in the gases from an FNH-M1 powder has been

[n] See footnote of Chapter 12 on page 248.

[o] There are no experimental data at such pressures. This value was calculated on the basis that the solubility is proportional to the square root of the pressure.

calculated to be roughly 0.2 mole % at a gas temperature of 1800 K and a gas density of 0.3 g per cc, falling to 0.06% at 1000 K and 0.1 g per cc.[60] Gases of these compositions can be in contact with bore surfaces at much lower temperatures because immediately next to the bore wall the gases, although at the bore surface temperature, probably have more nearly the equilibrium composition of the bulk of the gas in the tube. These low ammonia concentrations appear to be unfavorable to the formation of nitrides, particularly if the stability of the nitrides is such that one must assume them to be produced late in the firing. However, the nascent hydrogen released at the surface when any ammonia present dissociates will favor a replenishment of the adsorbed layer of ammonia by reacting with molecular nitrogen. The solubility of nitrogen introduced into gamma iron in this manner need not be limited to the amount of molecular nitrogen that might dissolve.

Well-spheroidized carbides present in an alloy steel proved upon segregation to contain the total nitrogen of the steel, nitrogen being present to the extent of 1 atom to every 23 of carbon. Because it was not possible from x-ray identification to detect the presence of a discrete nitride phase, nitrogen may have been present as replacement or "floating" atoms.[98] The available nitrogen being limited, this experiment does not establish the maximum extent of association of nitrogen with the carbides. This capacity of the carbides to scavenge the nitrogen may be important in reactions at the bore surface, where cementite is a commonly occurring product. The nitrogen thus concentrated, if in sufficient amount, may separate as a discrete nitride phase on cooling, or possibly it may merely change the stability relations of the iron nitrides at the high temperatures reached by gun-bore surfaces. It is generally true that the iron nitrides appear in conjunction with carbide in the reaction products of an eroded bore surface.[98]

While it is difficult with our present knowledge to understand the reason for the formation of nitrides of iron under the temperature conditions encountered during the firing of a gun, the experiments described below indicate a high mobility of original and acquired nitrogen well below the bore surface combined with enrichment close to the surface.

14.5.5 Experimental Determination of Nitrogen Penetration[70]

Studies of badly eroded guns, as mentioned in Section 14.5.1, showed an increase in nitrogen content near the bore surface. It has now been shown in the manner described below that this enrichment is not solely associated with a badly eroded surface but is a feature accompanying the first firings through a new barrel. These experiments were under ordnance conditions.

Method

In order to detect the penetration of nitrogen acquired from the propellant gases into the bore wall, the nitrogen atoms of the propellant were tagged by changing the ratio of the two stable isotopes of nitrogen having masses 14 and 15[p]. This was accomplished by adding to a standard IMR powder for the caliber .30 rifle a small amount of ammonium nitrate that had been enriched in the rarer isotope of mass 15.

A caliber .30 Springfield rifle, M1903A1 was assembled with an unproofed barrel and ten rounds were fired. Each round was standard in all respects except for the addition of 20 mg of the ammonium nitrate enriched with respect to nitrogen 15. The barrels were suitably cleaned and samples were taken by drilling along the axis of the bore. These samples were analyzed for total nitrogen content, following which the residue of ammonium sulfate was treated to recover the nitrogen as the element.

The atomic percentage of nitrogen 15 was then determined in these samples of nitrogen with a mass spectrometer. Ordinary nitrogen (for example, the original nitrogen contained in the steel) has 0.372% of nitrogen 15. The nitrogen in the propellant gases contained, by virtue of the addition of the ammonium nitrate, 0.642% of nitrogen 15. From these values and the atomic analysis of the nitrogen in a given sample it was possible to calculate that fraction of the total nitrogen in the sample which is to be attributed to the presence of propellant nitrogen.

Validity of Assumptions

No experiment was performed to demonstrate definitely a complete dissociation of the ammonium nitrate but it is safe to assume complete dissociation in

[p] The use of a radioactive isotope of nitrogen in the manner described in Section 14.2.3 for tracing carbon would have greatly aided an exploration of very thin layers. The half-life of radio nitrogen (10 min) precluded its use in this type of experiment; also it would have failed to show the features of exchange without enrichment.



view of the experience with barium carbonate described in Section 14.2.4. It was established that the ballistic level was unaffected by the addition of 0.6% by weight of ammonium nitrate in 3.24 g of the IMR powder.

Limitations on Interpretations of Results

The results must be interpreted in the light of the following limitations.

1. Measurements were made on surfaces which extended over one-third to one-half of the length of a barrel. Consequently areal differences in nitrogen content and exchange may be averaged out to a large extent.

2. The depth of any given cut was at least 0.0025 in. (64μ) and therefore a feature of the penetration occurring in a very thin zone would have been largely masked. This is unfortunate with respect to the increase in total nitrogen content of the surface cut, but is unimportant in discussing features of nitrogen exchange.

14.5.6 Bore-Surface Temperatures[70]

No attempt was made to simulate bore-surface temperatures occurring in larger bore guns, as described in Section 14.2.4 for the work on carbon. The calculated maximum peak temperature of the bore surface was therefore around 630 C[99] for barrel *C*. Barrel *B* was fired at the rate of about 1 round per second, which would raise this value for the last round by an estimated 60 C. These temperatures are somewhat in excess of the eutectoidal temperature of the iron-nitrogen system, which is about 600 C.

14.5.7 Nitrogen Penetration[70]

The results of the nitrogen penetration determinations are shown in Figure 14. Barrel *B* was a six-land barrel made of WD 1350 steel containing 1.5% of manganese but no chromium or molybdenum. Barrel *C* was a four-land barrel made of WD 4150 steel. The following points are to be noted.

1. Increase in total nitrogen content is confined to the surface cuts (the first and second bars of the graphs where lands and grooves were separated).

2. Nitrogen from the propellant gases penetrates to a comparatively great depth but merely replaces some of the original nitrogen with no change in the total nitrogen content.

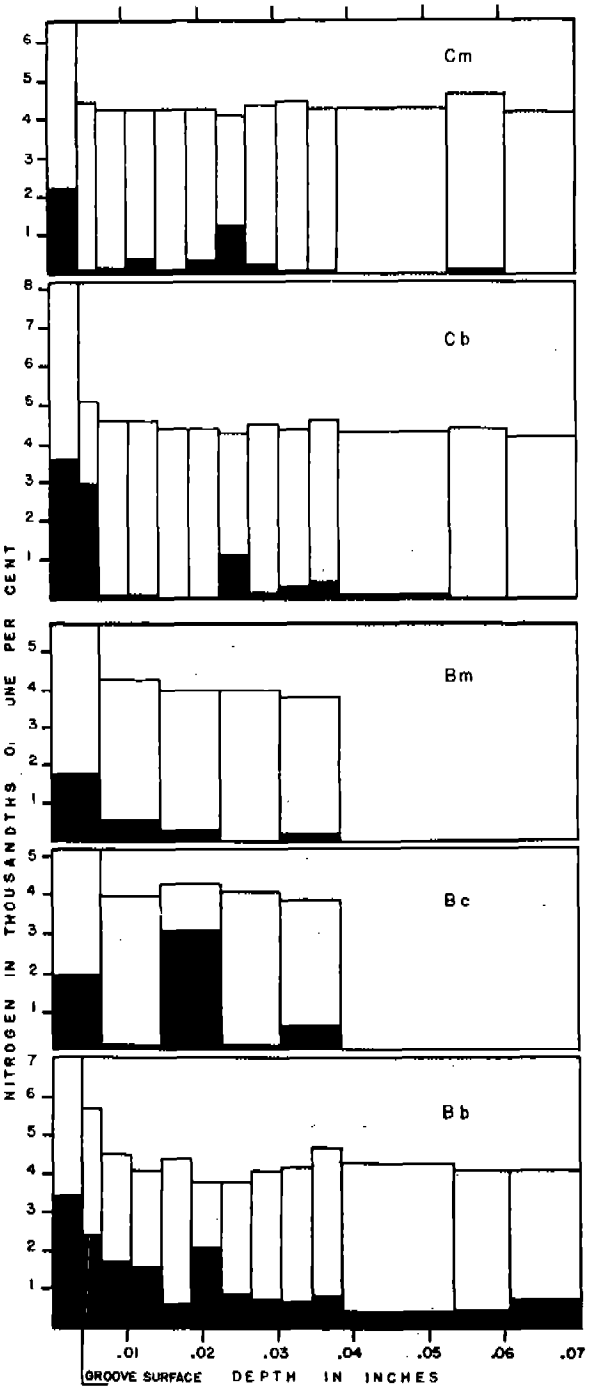


Figure 14. The penetration of nitrogen from propellant gases derived from IMR powder into the bore wall of unproofed caliber .30 steel rifle barrels. The bars indicate total nitrogen content; the black areas show, with a magnification of *5X*, that portion of the total to be attributed to nitrogen acquired from the propellant gases. *Bb*, breech third of barrel *B*, *Bc* center third of barrel *B*, *Bm* muzzle third of barrel *B*, *Cb* breech half of barrel *C*, *Cm* muzzle half of barrel *C*. (This figure was based on Figures 2 and 3 in NDRC Report No. A-398.)

3. Nitrogen from the propellant gases is insufficient to account for the increase in total nitrogen in the surface. It appears that displaced nitrogen below the surface eventually travels counter to the replacing nitrogen and is finally located in the surface. This would provide a mechanism for the late formation of nitrides. In the light of present knowledge, no other explanation can be offered for this increase.

4. In general, the proportion of nitrogen from the propellant gases is highest in the surface cut but there is a secondary maximum at the surprising depth of 0.015 to 0.025 in. (measured from the groove surfaces) without any measurable difference in the total nitrogen content.

5. The depth of the secondary maximum of nitrogen exchange is roughly the same irrespective of the location in the barrel. It occurs somewhat closer to the bore surface in barrel *B* subjected to rapid fire and is absent in the muzzle third. However, this barrel had a different composition from barrel *C*.

6. The total depth of nitrogen exchange is greatest in the breech third of barrel *B*. This depth differs but little for the two halves of barrel *C*. The total depth of nitrogen exchange is greatest, near the breech, in the barrel subjected to rapid fire; but again this difference may be due to the different composition of the steel.

Nitrogen Exchange

The high degree of mobility of nitrogen at relatively low temperatures is well illustrated by these experiments, and yet it appears that there is a strong controlling influence which, while it permits the exchange of nitrogen at depth, precludes any measurable addition of nitrogen except to a layer right at the bore surface. Such an influence might be attributed to the carbides which would be present in fairly constant amount except right at the surface where a considerable increase in carbide content is to be expected on the evidence in Chapter 12 and in Section 14.2. If it is true that in these steels the nitrogen is completely associated with the carbides as was found to be the case in a well-spheroidized alloy steel,[98] then exchange of nitrogen is associated with the carbide grains.

The subsurface maximum of propellant nitrogen is unexplained. At a depth of 0.02 in. the maximum temperature near the origin of rifling during a single firing in a caliber .50 barrel is about 100 C and about 50 C near the muzzle.[106] In a caliber .30 barrel these temperatures will be lower. It therefore appears that some other variable than temperature may be more important in controlling penetration and exchange, perhaps the pressure of the powder gases or the momentary stress configurations set up in the gun tube during firing. (Section 7.1.) The remarkable similarity of the nitrogen exchange over considerable lengths of barrel lends support to this argument.

Nitrogen Increase

It can hardly be supposed that the surface increase in nitrogen is distributed uniformly throughout the surface cut of arbitrary thickness. It seems reasonable to assume that the increase in total nitrogen is largely confined to a layer of the reaction products. In the study of carbon penetration the thickness of this layer could be determined. It was roughly 1μ thick near the origin of rifling for a barrel initially at 27 C.[99] Table 6 indicates that the nitrogen content in such a layer would not be unreasonably large and that the concentration on the lands would be higher than in the grooves. In analyses of surface flakes removed from the eroded bore surface of a 3-in. gun by the method described in Section 11.4.4, the flakes from the lands contained 1.1% nitrogen while the flakes from the grooves showed only 0.3% nitrogen,[98] which yields a ratio roughly the same as for the hypothetical calculation in Table 6 for barrel *C*. It appears that nitride formation is more severe on the lands of a gun than in the grooves. A further discussion of the analyses of the flakes mentioned above may be found in Section 12.5.2.

Table 6. Nitrogen content of a layer of reaction products 1 micron thick if the increase in nitrogen content of the surface cut is confined to such a layer.

Barrel and location		Increase in total nitrogen content of the cut (per cent)	Nitrogen in a surface layer 1 micron thick* (per cent)
Barrel *B*	Lands	0.0029	0.26
Breech third	Grooves	0.0016	0.16
Barrel *C*	Lands	0.0040	0.37
Breech half	Grooves	0.0009	0.08

* Density assumed to be the same as that of the steel.

Metallographic observations of cross sections of barrel *B* showed no development of cracks and no discernible change of structure caused by the firing.

14.6 REACTION OF THE INDIVIDUAL POWDER GAS CONSTITUENTS WITH GUN STEEL

14.6.1 Introduction

The erosive action of a single constituent of the powder gas cannot be studied by attaining the conditions of temperature and pressure directly from the chemical energy of an explosion. An ideal method consists of compressing the gas adiabatically while it is confined by a rupture disk which breaks and releases the gas through the specimen after the necessary temperature and pressure have been reached.[101] This constitutes a radical departure from ordnance conditions, but it is only by experiments of this type that one can appraise the erosive action of an individual constituent and follow the changes of such action with the addition of the other constituents in mixtures of progressively increasing complexity. Further, it should be possible to separate purely thermal effects from chemical effects by the use of an inert gas such as argon.

14.6.2 Summary of Results

A study of erosion and the nature of reaction products that result when appropriate single gases and combinations of these gases are heated by adiabatic compression and passed over the surfaces of gun steel did not provide much information. This was almost certainly due to the limitations of the gas capacity and energy of the available apparatus. Many gases and mixtures were used but only oxygen produced a measurable erosion. Of the several known reaction products (described in Chapter 12) that are found on the bore surface of a gun, only magnetite could be identified by electron diffraction[137] as a product of the gas-steel interaction in these experiments. Other compounds were either debris or unknown substances.

Considerable thought was given to the fundamental requirements and to the design of an apparatus to overcome the limitations of gas capacity and energy. The work was discontinued because of more pressing investigations. A continuation along the lines suggested here should yield valuable information.

14.6.3 Experimental Method[101]

The apparatus for adiabatic compression experiments has been described in Section 11.3.1. Specimens were of two types and were made of SAE 4140 steel obtained from a 5-in./25-cal. gun. For the determination of erosion by weight loss, disks were used which were 0.06 in. thick with center holes, 0.014, 0.022, or 0.031 in. in diameter. For examination by visual, x-ray, or electron diffraction methods the specimen consisted of two small rectangular blocks, with the pertinent surfaces polished, which were clamped in a holder so as to form a slit about 0.010 in. wide. It is important to know the pressure-time relation which, apart from interest in this relation itself, yields the data to calculate gas temperature. A novel form of piezoelectric gauge was incorporated in the apparatus. Experiments were conducted with helium, argon, nitrogen, hydrogen, oxygen, carbon monoxide, carbon dioxide, air, and such mixtures as are indicated in Table 7.

TABLE 7. Maximum temperature and pressure of adiabatically compressed gases in a series of tests for the erosive action on gun steel.[101]

Gas composition (vol %)	Maximum pressure* (atm)	Maximum temperature* (C)
$99\frac{1}{2}N_2$, $\frac{1}{2}O_2$	800–1150	1600–1750
Argon	750–1030	3400–3800
Hydrogen	1200–1800	1750–2000
$99\frac{1}{2}N_2$, $\frac{1}{2}H_2$	900–1100	1650–1750
Hydrogen	1300–3000	1700–2100
98 CO, $2O_2$	1000–1600	1550–1800
A mixture†	1300–2600	1250–1500
$99\frac{1}{2}$CO, $\frac{1}{2}H_2S$	650–1850	1600–2100

* The two values indicate the limit of scatter in 10 shots.

† 36 CO_2, 36 H_2, 17 CO, 11 N_2, which is a mixture with approximately the same atomic composition as nitrocellulose.

14.6.4 Temperature and Pressure

The ratio of the final temperature T_2 of the gas to its initial temperature T_1 is a function of the ratio of the final pressure P_2 to the initial pressure P_1 as expressed by equation (1),

$$\frac{T_2}{T_1} = \left(\frac{P_2}{P_1}\right)\frac{R}{C_v + R}, \tag{1}$$

in which R is the gas constant and C_v the specific heat at constant volume. The final gas pressure is theoretically proportional to the initial pressure for a given gas and a fixed amount of work.

Unfortunately, a difficulty with the available apparatus was a bouncing of the piston and falling weight combination that is well illustrated in a representative pressure-time record in Figure 15. The

gas was sometimes compressed and re-expanded several times, with the result that a major portion of it escaped while the pressure and temperature were low.

Table 7 gives the maximum pressures and temperatures attained by various gases and mixtures and indicates the variation from shot to shot. When the maximum recorded pressures in Table 7 are compared with those of the powder gases,[107] it is found that these pressures exceed the partial pressure of nitrogen and hydrogen in a gun but are about correct for carbon monoxide. The total pressure is somewhat low for the mixture simulating the composition of nitrocellulose. It is important to note, however, from Figure 15 that, whereas the total time of efflux was

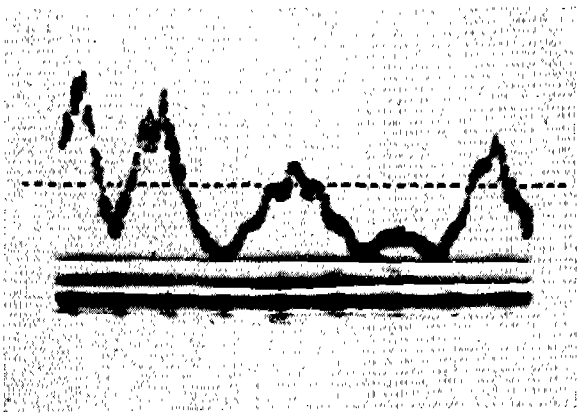


FIGURE 15. Oscillograph record of the pressure as a function of time in the apparatus for compressing gases adiabatically. The dotted line is the 500-atmosphere ordinate. The time signals on the abscissa are 1 msec apart. (This figure appeared as Figure 6 in NDRC Report No. A-429.)

of the desired order of magnitude, these ordnance pressures were sustained for only a fraction of the total time and that the specimen was alternately exposed to cooled gas and gas at the desired temperature and pressure.

It is more difficult to evaluate the appropriateness of the gas temperatures. Spectrophotometric measurements of the gas temperatures in a gun reported in Section 2.5.5 would indicate that the maximum temperatures in Table 7, with the exception of argon, are somewhat lower than desired, particularly for the mixture.

14.6.5 Erosion[101]

Air, helium, nitrogen, hydrogen, carbon dioxide, and carbon monoxide failed to produce a measurable weight loss or increase in bore diameter of the specimens. Oxygen alone gave an appreciable effect. In three shots the bore enlarged from 0.014 to 0.15 in.

14.6.6 Reaction Products

The surfaces of the blocks subjected to the action of the gases in the slit were studied by the methods of x-ray and electron diffraction (Section 11.5.2). The action of nitrogen indicated no change, but with air x-ray patterns of austenite, magnetite (Fe_3O_4), and a trace of ferrous oxide (FeO) were obtained in addition to those of the steel.

Some 18 specimens were studied by electron diffraction[137] including those subjected to the gas mixtures in Table 7. The only product which was probably formed by a gas-steel interaction was magnetite, which was sometimes identified, particularly when small amounts of oxygen were added to the gases. In a study of the action of propellant gases on gun steel, a very thin film of magnetite was often found covering other reaction products,[81] but although the methods devised to expose these subsurface reaction products to the electron beam were applied in detail to the present specimens, no underlying products were identified.

On many of the specimens subjected to multiple firing, 5 to 10 shots, there was evidence of debris in the form of degenerate graphitic carbon, loose magnetite, and organic compounds that resulted from a deterioration of the packing. This undesirable feature was eliminated by firing a single shot.

In many cases part of the pattern was not identified, but this unknown pattern was only identical for three specimens subjected to nitrogen. Of the known substances that result from the interaction of propellant gases with gun steel such as cementite (Fe_3C), iron nitrides (Fe_4N and Fe_2N_x), complex iron cyanides, wüstite or ferrous oxide (FeO), austenite (gamma-iron containing dissolved C or N or both) and magnetite (Fe_3O_4), only magnetite was identified.

The requirements necessary to duplicate the severity of the usual vent-plug test for erosion are outlined below. The tests performed were only about one-tenth as severe and it is apparent that the conditions of these tests were too mild.

14.6.7 Improvements in Apparatus[101]

As a result of the experience gained with the available apparatus and a study of its shortcomings indi-

cated in the preceding sections, the experimenters were able to outline the following requirements for an adequate apparatus and to suggest a possible design of this apparatus.

1. A sixfold increase in the mass of gas.

2. An increase in the energy per unit mass of gas by a factor of 1.5.

3. A means of arresting the compressing mechanism so that the gas is not alternately compressed and re-expanded.

One solution would be to increase the dimensions of the already bulky apparatus by a factor of about 1.8 but a major difficulty would arise in providing for requirement (3) above.

An apparatus which was to have been built is shown schematically in Figure 16. Energy is derived from a solid propellant burning in the cylinder on the left. The gas is compressed in a single-stroke two-stage compressor on the right. The large-bore piston head shears off at the end of the low-pressure stage and permits the small-bore piston to complete the stroke in the high pressure cylinder of much smaller diameter. The piston arrester consists of two wedging blocks that are tripped by the passage of the head of the driving piston and thereupon close together behind this head. The thrust that these blocks must withstand is materially lessened by introducing the small-bore cylinder for the final compression. Such an apparatus should be extremely useful in studying the thermal or chemical effects of gases at high temperature and pressure on a variety of materials when it is desirable to choose a specific gas or a combination of gases other than the qualitatively invariant mixture from a propellant.

14.7 MODIFICATIONS OF PROPELLANTS

Any radical modification of the propellant that might suppress one or more of the undesirable reactions of the constituents of the powder gases with gun steel would require a very extensive research. A few experiments, described in Section 15.6, were performed to test the possibilities of a slight but practical change in the powder. It is now possible to state as a broad principle that double-base powders, which have high flame temperatures and give gases rich in carbon dioxide, cause oxidation of the bore surface, while the cooler single-base powders, which produce more carbon monoxide, are largely carburizing.

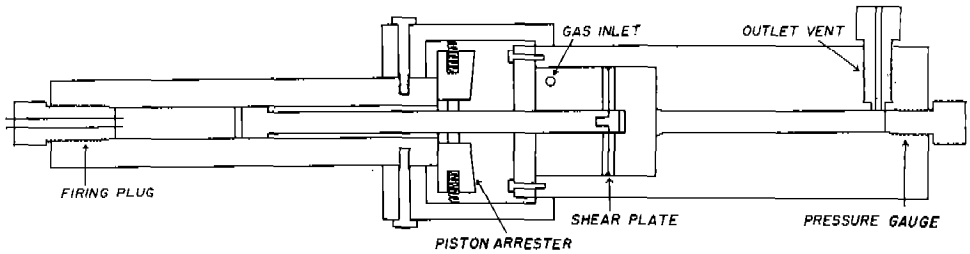


FIGURE 16. Sketch of an apparatus designed to compress gases adiabatically which should perform without the undesirable features inherent in the available compressor. (This figure appeared as Figure 7 in NDRC Report No. A-429.)

Chapter 15

EROSION OF GUN STEEL BY DIFFERENT PROPELLANTS[a]

By *John N. Hobstetter*[b]

15.1 INTRODUCTION

THE TESTING of gun steel with different propellant powders was undertaken by Division 1, NDRC, with a triple aim: to develop accelerated methods for testing and rapid classification of powders according to their erosiveness, to classify many powders on a scale of relative erosiveness, and to discover relationships between observed erosive effects and fundamental properties of the powders. These three aims were amply realized in the course of the extended program of testing.

A survey of the literature[16] had shown that the dependence of the magnitude of erosion on the type of propellant had been suspected as soon as nitrocellulose powders were introduced. Experimental firing had proved the point that not only was double-base powder more erosive than single-base powder but the amount of erosion with each type of powder depended on the barrel temperature. Vent-plug tests, in which erosion was predominantly by melting (as was the case also in the experiments described in Section 14.3.2) had shown a rough correlation between erosion and the flame temperatures of the powders. Division 1 was able, by conducting an extensive series of accelerated tests under carefully controlled conditions of different degrees of severity, to determine quantitative relationships among types of powders, their properties, and the type and magnitude of erosion for many different powders.

Two different approaches were made to the problem of accelerated testing methods. The most direct one was the actual firing of gun steel barrels with the different propellants under conditions of high velocity (3,300 fps) and of hypervelocity (3,600 fps). The less direct approach simulated firing conditions in a gun (except for the effects produced by a projectile) by means of a vent plug. The former provided adequate data on the erosion of gun steel in the course of less than 500 rounds; the latter provided such data in the course of 15 rounds. Agreement between the results of the two methods was in general quite good, although some interpretative difficulty was found in the case of the vent-plug results.

Both methods led to orders of erosiveness among the various powders tested which were in substantial agreement. Generally speaking, the powders were found to fall into three groups: those of low erosiveness, those of intermediate erosiveness and those of high erosiveness. The ordering of the powders within the groups tended to differ somewhat according to the method of testing.

It was found that under conditions giving a constant ballistic level, the observed erosion, particularly the measured dimensional change in a barrel, is related to the flame temperature of the powder or to the heat input to the barrel during firing. The form of the relation is such that a greater and more rapidly increasing erosion rate accompanies higher flame temperatures. Thus, under constant known firing conditions, powders may be classified on a scale of relative erosiveness according to their flame temperatures.

These results should not be taken to mean that the high temperature alone, through melting of the bore surface, provides the erosion mechanism. Rather they mean that temperature is the general regulator of whatever erosion mechanisms do operate, such as chemical attack by the powder gases and deformation and abrasion by the bullets. X-ray diffraction and metallographic studies made of the barrels tested in this program shed considerable light on these mechanisms and their dependence on temperature. They supplied much of the data upon which the discussion of Chapters 12 and 13 is based.

It was considered possible early in the program of Division 1, as was mentioned in Section 14.1, that certain studies might indicate ways in which propellants could be modified in order to mitigate erosion. The results of investigations described in this and the three preceding chapters indicated that some increase in gun life might be possible by only a slight alteration of powder compositions but that no great improvement could be expected in the case of steel guns

[a] This chapter is based in large measure on a comprehensive NDRC report[123] that contains details about the tests of erosiveness of propellants.

[b] Instructor in Department of Metallurgy, Harvard University. (Present address: Department of Engineering Sciences and Applied Physics, Harvard University.)

unless powder compositions were radically changed. The modification of propellants is discussed at the end of this chapter in Section 15.6.

15.2 METHODS OF TEST

15.2.1 Caliber .50 Erosion Testing Gun

Gun Assembly

The caliber .50 erosion-testing gun, described in Section 11.2.1, consists essentially of a monobloc, 45-in. caliber .50 heavy barrel with the origin of rifling and bullet seat shaped to receive a 20-mm cartridge case necked down to hold a caliber .50 bullet. The barrels used in the gun in the testing of different propellants were monobloc barrels made of WD 4150 modified gun steel. Chemical analyses of two representative barrels are given in Table 1.

Table 1. Chemical analyses of two representative barrels used in the caliber .50 erosion-testing gun in per cent.

Element	Barrel D-31	Barrel D-72
Carbon	0.56	0.57
Manganese	0.54	0.54
Phosphorus	0.016	0.016
Sulfur	0.019	0.018
Silicon	0.25	0.25
Copper	0.08	0.08
Nickel	0.19	0.18
Chromium	0.96	0.96
Vanadium	0.004	0.004
Molybdenum	0.25	0.25
Tin	0.013	0.013
Aluminum	0.05	0.05

Bullets

Two types of bullets were fired: pre-engraved and artillery-type, both of which are described in Section 11.2.1. The use of these two types of bullets permitted, by comparison, a considerable separation of the erosive effects of the hot gases from those of engraving stresses and friction. Thus, a good measure of the erosion caused by a given propellant alone could be deduced.

Conditions of Test

Three different series of tests of various powders were carried out with the erosion-testing gun. Two of the series involved the use, respectively, of pre-engraved and artillery-type bullets. The third series was carried out at a higher ballistic level with pre-engraved bullets and included a study of erosion after the firing of 1, 5, 10, and 70 rounds, respectively, for each powder.

Ballistic Levels. Tests with pre-engraved bullets were made with the charges adjusted to give muzzle velocities of 3,300 $\pm$ 50 fps with each powder. This velocity was the highest attainable with a full case of the powder having the lowest potential.

Tests with artillery-type bullets were made with the charges adjusted to give maximum powder pressures of 56,000 to 58,000 psi (copper) with each powder.

Tests at higher ballistic level with pre-engraved bullets were made with charges adjusted to give muzzle velocities of 3,600 fps whenever possible.

Firing Schedules. The same firing schedule was followed in all tests. The rate of fire was 4 rounds per minute, the rounds being divided into three groups: 10 rounds for measurement of pressure and velocity, 55 rounds for erosion, and 5 rounds for bullet recovery. This cycle was repeated until the end of each test.

Measurements

Pressure and Velocity. As shown in Figure 1 of Chapter 11, the chamber of the erosion-testing gun is fitted with a copper crusher gauge for the measurement of maximum powder pressure. The accuracy of this gauge is estimated at 5 per cent, but it is recognized that in the determination of pressure, the values given by such a gauge are considerably lower than the true pressure. Increasing the value of the "copper" pressure by 20 per cent makes it approximately equal to the pressure as measured by a piezoelectric gauge.

Measurements of velocity were made by means of two screens connected to an Aberdeen-type chronograph. The velocities reported are instrumental velocities at 26 ft from the muzzle and it is estimated that the deviation of any single velocity from the mean is no greater than 0.5 per cent.

Erosion Rate. The erosion of the gun barrel was detected or measured in various ways: by dimensional changes in land and groove diameters, by changes in maximum pressure and muzzle velocity, by changes in accuracy, and by the changes in the engraving observed on recovered bullets.

The land and groove diameters were measured by two series of plug gauges. Those for the lands ranged

from 0.490 in. to 0.516 in. in steps of 0.002 in. while those for the grooves were inversely rifled and ranged from 0.511 in. to 0.529 in. in steps of 0.002 in. With these gauges, land and groove profiles were obtained at various stages during the tests.

Pressure and velocity measurements were made during the first 10 rounds of each group of 70 rounds of the firing schedule.

The accuracy was determined at various stages by calculating the mean radius of dispersion on targets made by the 55 erosion rounds at 100 ft from the muzzle.

Bullet recovery was made in sawdust and band diameter and width of engraving were measured. Any body engraving was also noted.

Limited amounts of the special powders tested precluded any exhaustive study of the reproducibility of erosion as measured by these procedures. However, several pairs of check tests were made and they gave results in excellent agreement with one another.

Heat Input. The heat input to the bore was calculated from temperature-time curves which were recorded with thermocouples and Speedomax recorders. Special barrels with wall sections machined down to 5/16 in. near the origins of rifling were used in making these measurements and the thermocouples were placed at several positions along the thin wall, as described in Section 5.3.4. Heat input values were measured[71] for the firing of each of several rounds with loading conditions of the various powders the same as in erosion tests.

Metallographic Changes. Sections of the fired barrels were examined metallographically in order to detect changes in the condition of the bore surface and in the microstructure of the gun steel. These studies were more related to the mechanism of the erosion than to the amount of erosion.

X-Ray Studies. The bore surfaces of the fired barrels were studied by x-ray diffraction in order to identify the erosion products remaining on the bore surfaces. These studies were also related to the erosion mechanism rather than to the amount of erosion.

15.2.2 Erosion Vent Plug

An independent experimental study of the erosiveness of many of the powders which were tested in the erosion-testing gun was made using the vent plug technique described in Section 11.2.3. Results obtained by these two dissimilar methods of study provide corroborative checks on the behavior of the propellants.

Apparatus

The explosion vessel, which could be electrically fired, contained a spherical chamber which communicated with both a detachable erosion vent of cylindrical shape and a piezoelectric pressure gauge. The vent was closed at its muzzle end with a calibrated brass rupture disk. The explosion vessel had a chamber volume of 24.3 cc and, together with its fittings, was made of NE 9450 steel.

Vent Plugs. The cylindrical plugs for the powder testing program were made of SAE 4140 gun steel, heat treated to a hardness of Rockwell C-18 as measured at the extremities of the cylinder axis before drilling of the vent. The length of the plugs was 5/8 in. Since preliminary work showed that the erosion of vents increased with the roughness of the interior vent surface, it was decided to make that surface the smoothest practicable. This aim was accomplished by first reaming the vents 0.0005 in. undersize and then lapping the surface to final dimensions.

Rupture Disks. The rupture disks were stamped from a single sheet of yellow brass having a thickness of 0.042 ± 0.0017 in. and very uniform hardness. The rupture area was 0.049 sq in. These disks were calibrated quite simply by firing increasing charges of FNH-M2 powder and observing the pressure-time curves. It was found that rupture of the 0.042-in. disk occurred at 25,000 ± 1000 psi and the determination was later confirmed through the use of an automatic recording of the instant of rupture on the pressure-time curves. The device consisted of a fine wire stretched before the rupture disk which broke at the instant of rupture and in so doing caused a sudden change in the potential across the recording oscillograph.

Procedure

Ideal operation of the vent-plug apparatus would permit each shot with any powder to build up powder gases to the same maximum pressure, whereupon these gases would suddenly sweep through the vent. In this manner, erosion in the vent would be quite independent of the burning characteristics of the various powders and would reflect only the effect of the gases themselves. In practice this ideal is difficult to achieve primarily because of small variations in



both the maximum pressures and rupture pressures from round to round. Thus, if the charge is so adjusted that the maximum pressure is about the same as the rupture pressure, a large number of failures of disk rupture are encountered. This difficulty was avoided by using charges of the different powders which yielded maximum pressures about 3,000 psi higher than the rupture pressure. Only a very small overlap of burning and erosion times was thus permitted.

Charge Determination. Determination of the proper charges of the various powders tested was made by trial and error. A tendency for the peak pressure to decrease with increasing vent size was noted, but it was felt that the order of magnitude of the variation was too small to have an appreciable effect on the erosion.

Vent Sizes. Ordinarily 4 degrees of severity of test were provided by the use of vents of four different internal diameters: 3/16, 1/8, 3/32 and 1/16 in., in order of increasing severity of test. RDX powders were tested with vents of three different sizes: 5/32, 1/8, and 1/16 in. Tolerances were held to 0.0005 in. for the larger vents and 0.001 in. for the 1/16-in. vent.

Measurements. Erosion was produced by the firing of repeated rounds with various powders at each of the levels of severity afforded by the different vent sizes. Two identical vent plugs of each size were tested with each powder, the plugs being alternated so as to subject them as nearly as possible to equal treatment. These two tests provided checks on one another. Each plug was weighed to the nearest milligram at the completion of 1, 5, 10 and 15 rounds after having been gently scraped, swabbed with acetone and with alcohol, and carefully dried. Erosion was reported in terms of the weight loss of each plug.

Validity of Measurements. It was found that the deviation from the mean weight loss of the two check runs in each pair of tests was quite small, being of the order of 10 per cent for the 1/8-in. vent tests and possibly even smaller for the smaller vents. These deviations were also smaller after 15 rounds than after 5 or 10 rounds. It was inferred, therefore, that reproducibility of these tests was adequate.

The temperature of the explosion chamber varied somewhat from test to test, but it was determined by direct experiment that these variations had negligible effect on the results.

Attention was paid to the possibility that the powder gases might be cooled considerably before coming in contact with the vent plugs and that the extent of such cooling might differ widely in different tests.[c] Accordingly the rate of pressure change with time just after the end of burning of a slow-burning powder was measured at various densities of loading. From these results it was found that the cooling rate for the powder gas was such that its temperature could not have fallen more than 10 C during the 4-msec period required for the burning of this powder prior to the rupture of the disk in one of the erosion vent experiments. Therefore it was assumed that gas temperatures for all the powders at the beginning of erosion were essentially equal to the adiabatic flame temperature.

At any stage after rupture, both experimental and theoretical results indicate that all gas temperatures are similarly related to the respective adiabatic flame temperatures of their powders. It follows, then, that direct comparison of weight losses of the vent plugs permits an accurate determination of the relative erosiveness of the various powders which is dependent only on the flame temperatures and chemical properties of those powders.

15.2.3 Powders Tested

A total of 21 different powders was tested in either the caliber .50 erosion-testing gun or the erosion vent plug, most powders being tested in both. Characteristics of the powders and the methods of testing them are given in Table 2 where they are listed in order of increasing adiabatic flame temperature. The powders were all of standard lots except for those for which the experimental lot numbers are given in column 2. The latter were supplied by Division 8, NDRC. The adiabatic flame temperatures given in column 3 were calculated according to the method described in Section 2.4.3. The numbers in column 4 designate the types of test to which the powders were subjected, as follows:

1. Erosion-testing gun with pre-engraved bullets.
2. Erosion-testing gun with artillery-type bullets.
3. Erosion-testing gun with pre-engraved bullets at high ballistic level.
4. Erosion vent plug.

[c] In experiments conducted at Explosives Research Laboratory under the supervision of Division 8, NDRC, some indication was obtained "that cooling during burning was the same for a large granulation as for a small granulation of the same powder, because the integrated turbulence was the same in each case." (Personal communication from Dr. J. F. Kincaid, formerly of the Explosives Research Laboratory, after having reviewed the manuscript of this chapter, July 24, 1946.)

TABLE 2. Characteristics and methods of test of the various powders.*

Powders	Lot No.	Flame temperature (K)	Tests	Specific heat at constant volume (cal/gram)	Impetus of powder† (ft-lb/lb)
RDX	5060	2320	1	.....	.....
RDX	6079	2465	4	.....	.....
Cordite N	....	2469	1, 2	0.3616	335,000
FNH/P	....	2480	1, 2, 4	0.3456	310,000
FNH-M1	....	2483	1, 2, 3, 4	0.3456	310,000
RDX	5061	2560	1	.....	.....
RDX	6080	2611	4	.....	.....
NH-M1	(3727)‡	2651	4	.....	.....
NH-M1	4974	2696	4	.....	.....
RDX	6081	2713	4	.....	.....
NH-M1	....	2807	1, 2	0.3425	328,010
Pyro	....	2814	1, 2, 4	0.3692	327,490
Cordite NQ	....	2864	1, 2	0.3588	363,000
IMR	....	2938	1, 2, 3, 4	0.3381	344,000
RDX	6082	3003	4	.....	.....
RDX	5059	3080	2	.....	.....
FNH-M5	....	3268	1, 2	0.3445	362,750
RDX	6083	3302	4	.....	.....
FNH-M2	....	3563	1, 2, 3, 4	0.3439	384,000
Ballistite (40% NG)	....	3945	3	0.3393	410,400
Ballistite (60% NG)	....	4300	3	0.3390	441,400

* This table has been compiled from Tables I, II, XXIX, and XXXVa of the NDRC report[123] on this subject, which also gives detailed descriptions of the powders.

† Defined in Section 3.2.3.

‡ Powder for 37-mm gun M1916; standard lot No. 3727.

TABLE 3. Firing conditions for different powders in the erosion-testing gun.

Powder	Web (in.)	Charge (grains)	Loading density (g per cu cm)	Maximum pressure [psi (copper)]	Initial velocity (fps)	Rounds fired
A. Charges to give initial muzzle velocities of about 3,300 fps with pre-engraved bullets.						
RDX-5060	0.019	385	0.762	47,800	3,367	507
Cordite N	0.0186	415	0.822	54,835	3,302	480
FNH-M1	0.0200	420	0.832	55,525	3,335	500
FNH/P	0.0234	425	0.842	52,123	3,300	332
NH-M1	0.0262	415	0.822	55,600	3,365	305
Cordite NQ	0.0181	345	0.683	57,509	3,353	510
RDX-5061	0.025	380	0.752	49,710	3,356	500
Pyro	0.0245	405	0.802	56,100	3,288	360
IMR	0.0318	425	0.842	46,880	3,326	500
FNH-M5	0.0338	360	0.713	46,460	3,305	307
FNH-M2	0.0350	350	0.693	46,600	3,324	220
B. Charges to give maximum pressures of about 57,000 psi (Cu) with artillery-type bullets.						
Cordite N	0.0255	440	0.893	57,920	3,290	557
FNH-M1	0.0241	425	0.862	56,375	3,252	500
FNH/P	0.0240	425	0.862	57,615	3,286	355
NH-M1	0.0294	425	0.862	56,120	3,280	360
Pyro	0.0285	425	0.862	53,000	3,210	360
Cordite NQ	0.0244	420	0.853	55,685	3,434	514
IMR	0.0338	425	0.862	56,700	3,428	515
FNH-M5	0.0454	385	0.782	56,920	3,437	377
FNH-M2	0.0461	400	0.812	57,935	3,458	220
C. Charges to give initial velocities of 3,600 fps with pre-engraved bullets.						
IMR	0.0318	476	0.941	58,000	3,600	
FNH-M2	0.0350	395	0.782	58,000	3,600	
40% NH	0.0490	390	0.762	58,000	3,600	
60% NG	0.0395	330	0.654	58,000	3,600	



Column 5 gives the nominal specific heat at constant volume and column 6 the nominal impetus of the powder. Both were calculated according to the method of Hirschfelder.[26]

The loading conditions in the various tests varied widely so as to maintain the desired ballistic level with each of the different powders. Firing data are given in the three parts of Table 3 for the three series of tests in the erosion-testing gun and in Table 4 for the tests with the erosion vent plug.

TABLE 4. Firing conditions for different powders in the erosion vent plug chamber. Charges to give maximum pressures of 28,000 psi (piezo).

Powder	Web (in.)	Charge (g)	Maximum pressure (for 1/16-in. vent) [psi (piezo)]
RDX-6079	.....	4.0	.....
FNH/P	0.0106	4.4	29,000
FNH-M1	0.0105	4.4	28,500
RDX-6080	.....	3.9	.....
NH-M1*	0.0120	4.18	28,500
NH-M1	0.011	4.2	29,000
RDX-6081	.....	3.8	.....
Pyro	0.0089	4.0	29,000
IMR	0.0099	3.97	28,000
RDX-6082	.....	3.7	.....
RDX-6083	.....	3.4	.....
FNH-M2	0.015	3.6	28,000

* Powder for 37-mm gun M1916; standard lot No. 3727.

15.3 TESTS IN CALIBER .50 EROSION-TESTING GUN

15.3.1 Dimensional Erosion Rate

At frequent intervals in the course of the testing of each powder in the erosion-testing gun the barrel was removed from the gun assembly and measured internally with plug gauges. These measurements were expressed in terms of the observed increase in land diameter ΔL and in groove diameter ΔG at various points along the barrel. Plotting both ΔL and ΔG versus distance from the origin of rifling gave a double erosion-distribution curve for each stage of the test.

The progress of erosion at each point along the barrel was easily obtained by comparing the erosion-distribution curves at different stages during the test. Data taken from these curves permitted the plotting of ΔL and ΔG versus number of rounds for any given position along the barrel.

Distribution of Erosion

Pre-engraved Bullet Series. Separate distributions of land and groove erosion as measured by plug gauges after completion of the various tests are plotted in Figures 1 and 2, respectively. The tests were all carried out at initial muzzle velocities of 3,300 fps, and the numbers of rounds fired in each test are given in the legends.

It will be noted that no erosion was detected in the barrels fired with very cool powders and that the amount of erosion increased generally with the flame temperature of the powder. In every case, erosion was most severe near the origin of rifling and fell off rapidly toward the muzzle. The extension of measured erosion muzzleward increased with the flame temperature of the powder.

Artillery-Type Bullet Series. Similar land and groove erosion distribution curves for all tests with artillery-type bullets are plotted in Figures 3 and 4, respectively. These tests were carried out at maximum pressures of about 57,000 psi (copper). The numbers of rounds fired are given in the legends.

It will be noted that in these tests erosion was detected even when very cool powders were fired. As before, erosion increased in amount and advanced muzzleward as the flame temperature of the powder was increased. In all cases the greatest erosion was found near the origin of rifling.

High Ballistic Level Series. Little attention was paid to distribution of erosion in this series, for which the initial muzzle velocity was 3,600 fps. Pre-engraved bullets were fired. Star gauge measurements were made only at 1/4 in. and 1 in. beyond the origin of rifling to determine the progress of erosion after the firing of 1, 5, 10, and 70 rounds.

Progress of Erosion

Pre-engraved Bullet Series. The progress of land erosion was obtained from the distribution curves by observing the measured land diameter increase at three positions along the barrel at various stages of each test. These data are listed in Table 5. The progress of erosion 1/2 in. from the origin of rifling is plotted for the various tests in Figure 5.

It will be seen that the erosion rate is a constant in these tests; that is, the increase in land diameter ΔL is a linear function of the number of rounds fired. The barrels fired with cooler powders did not start to erode at once, however, so that their curves intersect

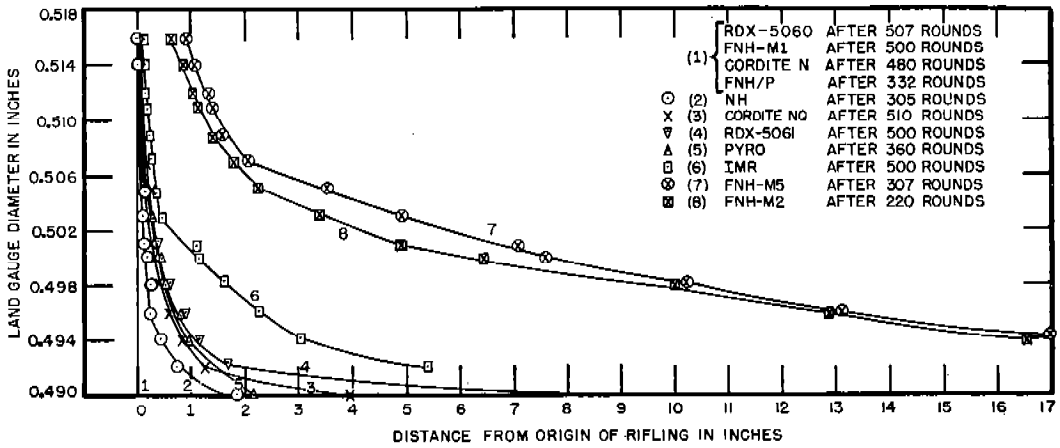


FIGURE 1. Distribution of land erosion for various powders fired with pre-engraved bullets. (This figure has appeared as Figure 8 in NDRC Report No. A-451.)

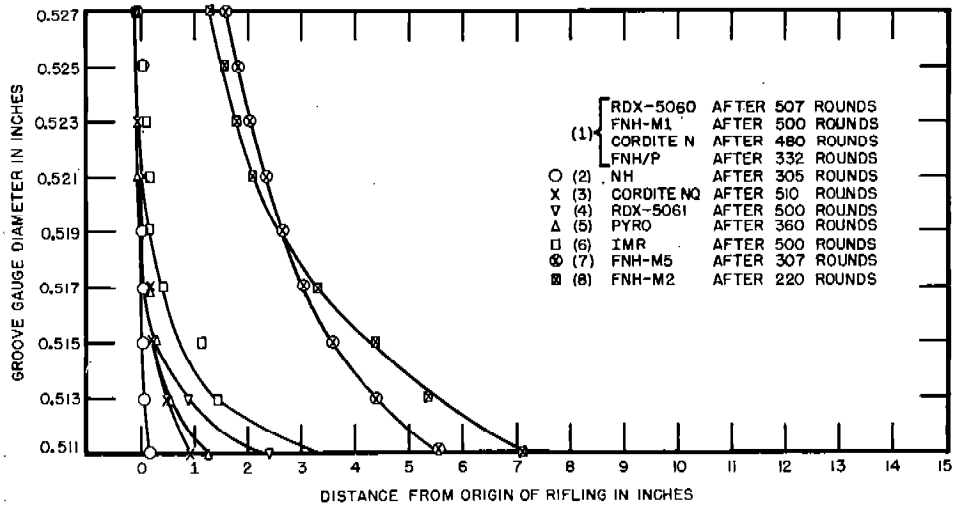


FIGURE 2. Distribution of groove erosion for various powders fired with pre-engraved bullets. (This figure has appeared as Figure 9 in NDRC Report No. A-451.)

TABLE 5. Pre-engraved bullet series. Increase in land diameter found at locations lying ½, 1, and 2 in. beyond the origin of rifling after the firing of 140, 280, and 350 rounds.

Powder	After 140 rounds			After 280 rounds			After 350 rounds		
	½ in. (in.×10⁻³)	1 in. (in.×10⁻³)	2 in. (in.×10⁻³)	½ in. (in.×10⁻³)	1 in. (in.×10⁻³)	2 in. (in.×10⁻³)	½ in. (in.×10⁻³)	1 in. (in.×10⁻³)	2 in. (in.×10⁻³)
RDX-5066	0	0	0	0	0	0	0	0	0
Cordite N	0	0	0	0	0	0	0	0	0
FNH-M1	0	0	0	0	0	0	0	0	0
FNH/P	0	0	0	0	0	0	0	0	0
NH-M1	0.5	0	0	2.6	1.1	0	3.7	1.7	0
Cordite NQ	1.8	0.8	0	3.9	1.7	0.2	5.0	2.2	0.8
RDX-5061	1.5	0.7	0.6	3.9	2.2	1.4	5.0	2.9	1.5
Pyro	2.5	0.6	0	6.6	2.5	0	...	...	...
IMR	3.0	1.3	0	6.8	4.8	2.5	8.9	6.7	3.8
FNH-M5	14.4	12.3	7.6	32.6	22.8	16.6	...	...	...
FNH-M2	17.4	13.2	7.5	....	....	....	...	...	...



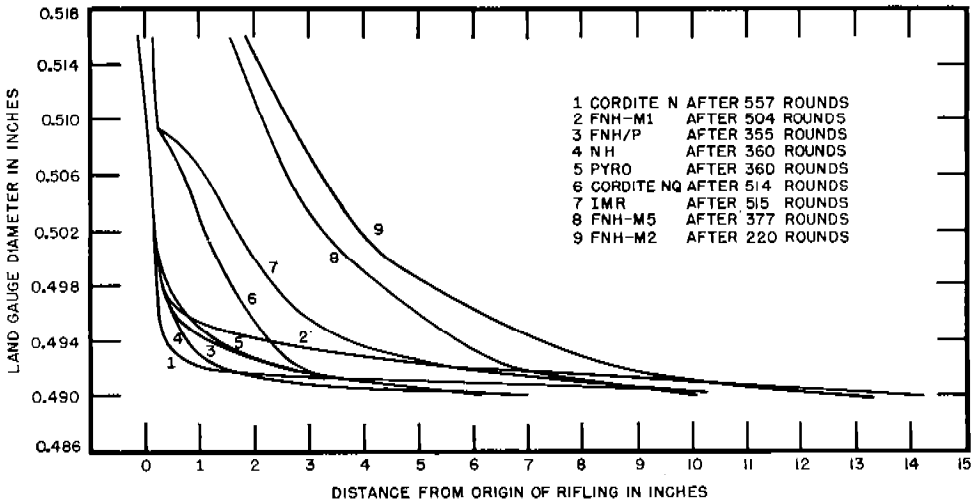


FIGURE 3. Distribution of land erosion for various powders fired with artillery-type bullets. (This figure has appeared as Figure 13 in NDRC Report No. A-451.)

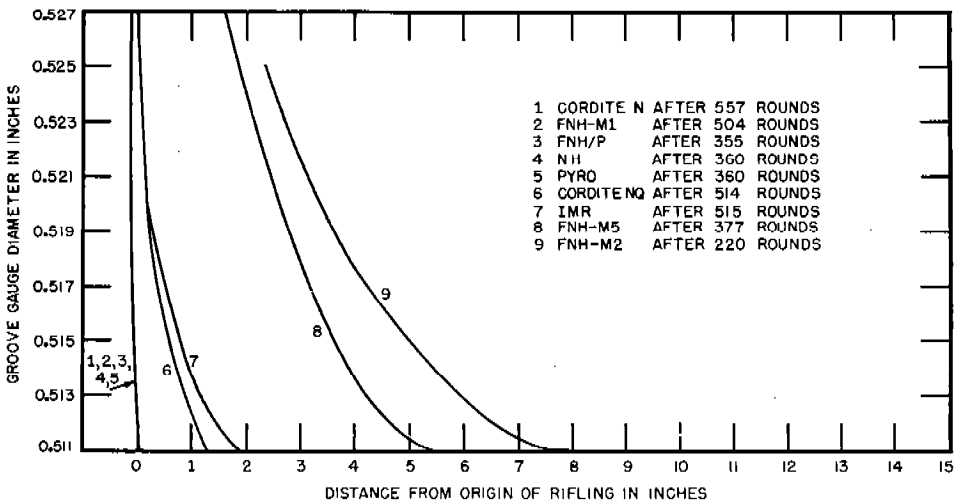


FIGURE 4. Distribution of groove erosion for various powders fired with artillery-type bullets. (This figure has appeared as Figure 14 in NDRC Report No. A-451.)

TABLE 6. Artillery-type bullet series. Increase in land diameter found at locations lying ½, 1, and 2 inches beyond the origin of rifling after the firing of 140, 280, and 350 rounds.

Powder	After 140 rounds			After 280 rounds			After 350 rounds		
	½ in. (in. × 10^{-3})	1 in. (in. × 10^{-3})	2 in. (in. × 10^{-3})	½ in. (in. × 10^{-3})	1 in. (in. × 10^{-3})	2 in. (in. × 10^{-3})	½ in. (in. × 10^{-3})	1 in. (in. × 10^{-3})	2 in. (in. × 10^{-3})
Cordite N	0.2	0	0	2.3	0	0	2.8	0	0
FNH-M1	1.4	0	0	4.5	3.6	2.3	5.4	4.6	3.2
FNH/P	4.2	3.1	1.1	6.1	4.2	2.9	6.6	4.2	3.2
NH-M1	4.4	2.2	0	6.3	3.3	0	6.6	3.0	0
Pyro	5.2	2.1	0	8.5	3.0	0	9.5	3.5	0
Cordite NQ	6.1	4.2	2.1	11.4	1.8	3.7	14.0	9.5	4.4
IMR	9.5	7.7	4.6	14.7	12.3	7.5	16.2	13.7	8.6
FNH-M5	14.8	12.9	7.8	33.0	24.9	15.8	40.0	31.8	19.6
FNH-M2	30.0	24.8	17.5	....	....	....	....	....	....

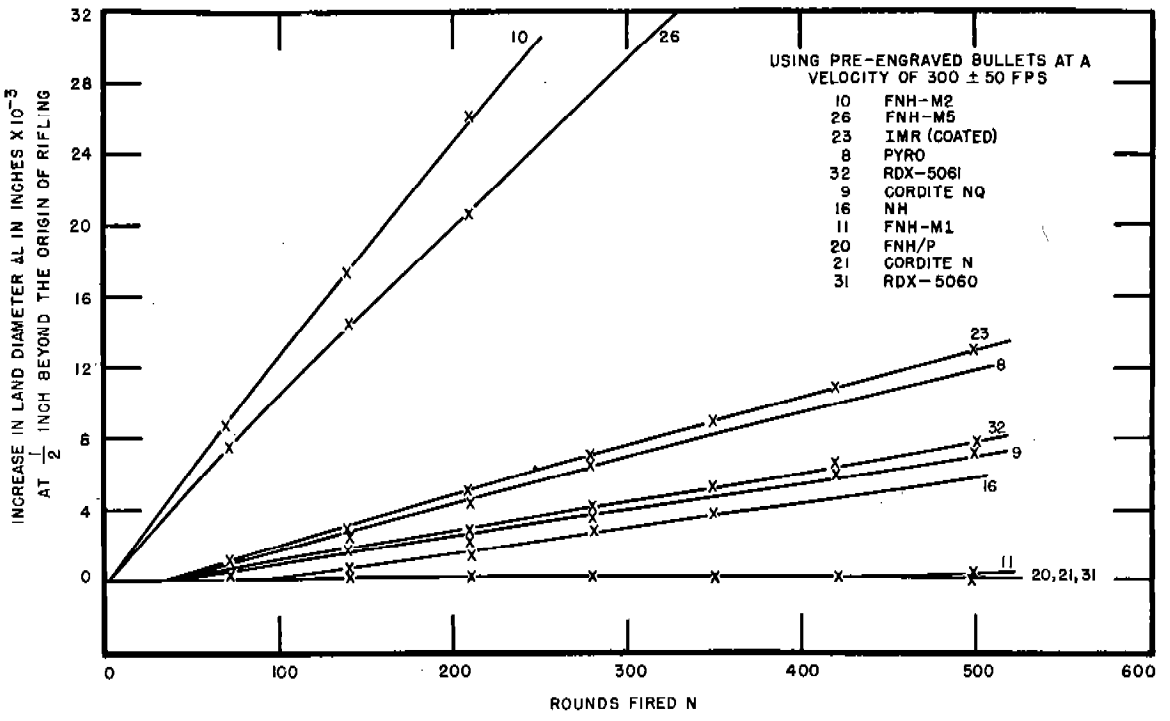


FIGURE 5. Progress of erosion at ½ in. beyond the origin of rifling for various powders fired with pre-engraved bullets. (This figure has appeared as Figure 10 in NDRC Report No. A-451.)

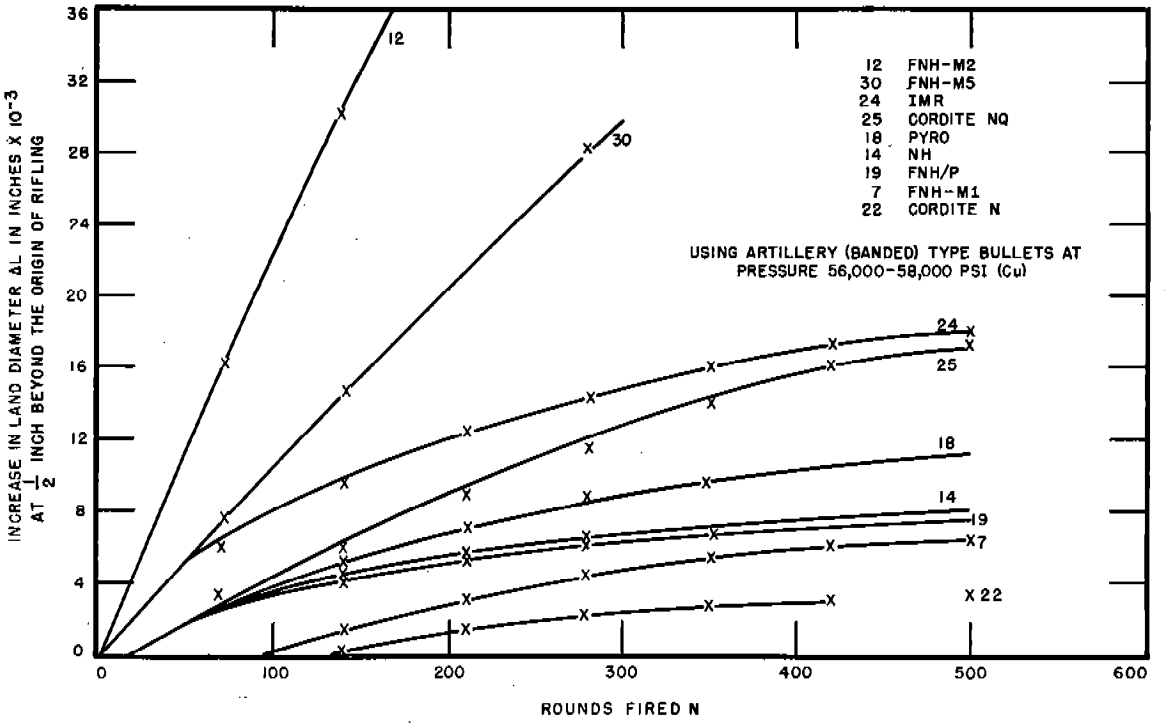


FIGURE 6. Progress of erosion at ½ in. beyond the origin of rifling for various powders fired with artillery-type bullets. (This figure has appeared as Figure 15 in NDRC Report No. A-451.)

the abscissa. The erosion rate increases as the flame temperature of the powder increases.

Artillery-Type Bullet Series. The progress of land erosion was obtained exactly as before, the data being listed in Table 6 and being plotted for points located ½ in. from the origin of rifling in Figure 6.

The erosion rate in these tests will be seen to be no longer constant, but rather to decrease as the test was prolonged. As before, erosion did not start at once in the barrels fired with cooler powders so that their curves intersect the abscissa. The erosion rate at any stage again appears to increase as the flame temperature of the powder increases.

High Ballistic Level Series. Progress of land erosion data at a comparable position along the barrel (½ in. from the origin of rifling) was obtained by interpolation of the star gauge data taken at various stages at positions lying ¼ in. and 1 in. beyond the origin of rifling. The results are listed in Table 7 and are plotted in Figure 7.

TABLE 7. High ballistic level series. Increase in land diameter at ½ inch beyond origin of rifling (interpolated) after the firing of 1, 5, 10, and 70 rounds.

Powder	1 Round (in. $\times 10^{-3}$)	5 Rounds (in. $\times 10^{-3}$)	10 Rounds (in. $\times 10^{-3}$)	70 Rounds (in. $\times 10^{-3}$)
IMR	0	1.2	0.5	6.0
FNH-M2	0	1.2	1.5	21.5
40% NG	0.9	4.5	7.0	48.2
60% NG	0.6	4.8	8.7	66.5

As before in the pre-engraved bullet series (at moderate ballistic level), the erosion rate appears to be constant, but in this series erosion appears to start with the first round. The erosion rate increases with the flame temperature of the powder.

STANDARDIZED MEASURE OF EROSION RATE

The erosion rate characteristic of each of the tested powders should be reduced to a single index if comparisons are to be made easily. This result is easily achieved in the case of tests where pre-engraved bullets are fired, for the erosion rate is a constant in these tests for any definite distance from the origin of rifling. It remains only to note that the erosion rate E (in. per round) is given by equation (1),

$$E = \frac{\Delta L}{N - n} \tag{1}$$

where ΔL is increase in land diameter in inches at some definite distance from the origin of rifling; N is total number of rounds fired; and n is number of rounds fired before measurable erosion occurs. E is, of course, the slope of the progress of erosion curve at the location in question and n is the intercept on the abscissa.

The situation is considerably complicated in the case of the firing of artillery-type bullets, for the erosion rate at any given location is not constant. The reason it is not constant is related to the role played in erosion by the considerable engraving-stresses which accompany the firing of these bullets.

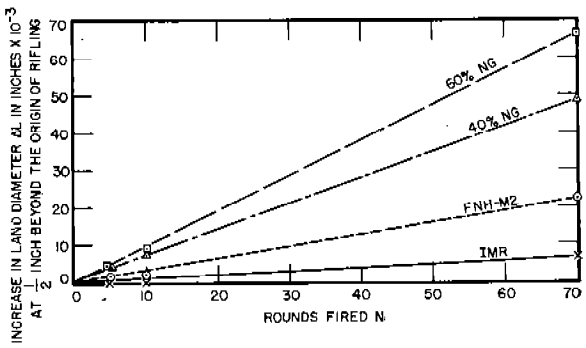


FIGURE 7. Progress of erosion at ½ in. beyond the origin of rifling for propellants of high ballistic level. (This figure has appeared as Figure 19 in NDRC Report No. A-451.)

In a new barrel there is large diametrical interference between the lands and the rotating bands which leads to very severe land wear. This wear, in turn, reduces the land height so that the interference becomes less. Thus, the rate of this mechanical type of land wear is initially large, but decreases as wear proceeds. Superposed upon it is the erosion caused by the powder gases, the sum being the measured erosion.

The erosion rate obtained with artillery-type bullets is properly expressed as the slope of the erosion-progress curve drawn for some given location in the barrel at a given stage of the firing. An average value of this rate might also be reported, but such a figure would be without mechanistic significance.

The best location at which the erosion rate may be specified is where the erosion is most severe; that is, near the origin of rifling. For this reason, the location ½ in. muzzleward from the origin of rifling has been selected. The curves showing progress of erosion for this location have been plotted in Figures 5, 6, and 7.

The best stage of the test at which to specify the erosion rate is probably toward the end of the test,

for at that stage the relative effect of engraving stresses is less and the results are more representative of the effect of powder gases alone. Alternatively, the erosion rate might be specified at such stages that the observed reduction in land height was the same in each of the various tests. It is not certain, however, that the proportion of total erosion resulting from engraving stresses is always the same at given land height independent of other factors.

The erosion rates for the various powders[d] are tabulated in Table 8 by series. The listings for the pre-engraved and the high ballistic level series are, of course, values of E found from the equation given above in this section. The listings for the artillery-type bullet series are slopes of the progress-of-erosion curves for ½ in. beyond the origin of rifling at 300 rounds. Values for the two hottest powders were found by extrapolating their essentially straight, progress-of-erosion curves to 300 rounds.

TABLE 8. Erosion rates observed with various powders in the three firing series.

Powder	Flame temperature (K)	Pre-engraved bullet series (in. per rd $\times 10^{-5}$)	Artillery-type bullet series (in. per rd $\times 10^{-5}$)	High ballistic level series (in. per rd $\times 10^{-5}$)
RDX-5060	2320	0	...	...
Cordite N	2469	0	0.7	...
FNH/P	2480	0	0.8	...
FNH-M1	2483	0	1.2	...
RDX-5061	2560	1.66	...	...
NH-M1	2807	1.42	1.0	...
Pyro	2814	2.60	2.0	...
Cordite NQ	2864	1.52	3.7	...
IMR	2938	2.73	4.0	8.5
FNH-M5	3268	10.22	8.8	...
FNH-M2	3564	12.52	27.0	30.7
40% NG	3945	.....	....	68.8
60% NG	4300	.....	....	95.0

It will be noted that there are some minor differences in order between the erosion rates of the pre-engraved series and the artillery-type bullet series erosion rates. In general, the artillery-type bullet values are more in line with the flame temperatures of the powders and their greater magnitude has permitted ordering of the powders of low erosiveness which produced no measurable erosion with pre-engraved bullets. The relation between the erosion rate and the adiabatic flame temperature is discussed in Section 15.5.2, where the data of Table 8 are presented graphically in Figure 9.

In any event, the groupings of powders are more important than their order within a group. The average of a much larger number of tests would be required to classify the powders in an absolute order of increasing erosiveness. The following groupings are evident, except that it is uncertain whether NH-M1 should be in the first or second group:

RDX-5060, Cordite N, FNH/P, FNH-M1, NH-M1 (?) < RDX-5061, Pyro, Cordite NQ, < IMR < FNH-M5 < FNH-M2 < 40% NG < 60% NG.

15.3.2 Heat Input to the Barrel

The heat input to the barrel was measured according to the method described in Section 5.3.4 at two positions along the barrel: 1.25 in. and 4.50 in. beyond the origin of rifling. These determinations were not made during the tests used to find dimensional erosion, but on specially machined barrels which were fired with equivalent powder charges. Both pre-engraved and artillery-type bullets were fired.

While it is known that the generation of heat accompanying the engraving of artillery-type bullets results in a preheating of the bore, the magnitude of the preheating was too small to be detected by these means. Accordingly, the heat input was found to be characteristic of the powder, but independent of the bullets fired. In Table 9 the measured heat input accompanying the firing of the various powders is

TABLE 9. Flame temperatures of the various powders and heat input as measured at 1.25 in. beyond the origin of rifling of caliber .50 erosion-testing gun.

Powder	Flame temperature (K)	Heat input (cal per sq cm)
RDX-5060	2320	11.7
Cordite N	2469	11.8
FNH/P	2480	11.8
FNH-M1	2483	12.2
RDX-5061	2560	12.8
NH-M1	2807	13.3
Pyro	2814	13.8
Cordite NQ	2864	12.7
IMR	2938	14.4
RDX-5059	3080	14.4
RNH-M5	3268	16.4
FNH-M2	3563	17.1
40% NG	3945	18.5
60% NG	4300	19.2

[d] At Picatinny Arsenal the quickness of standard Pyro and FNH powders has been determined,[316] and thermochemical and physical tests[317] of nitroguanidine powders have been performed.

listed along with the flame temperatures of the powders.

With the exception of the anomalous value for cordite NQ powder, the heat inputs appear to agree with the flame temperatures of the powders. Indeed, as is shown in Section 15.5.3, the relation between flame temperature and heat input appears to be linear except for the hotter powders. These latter are known to cause considerable melting of the bore surface and it seems probable that the absorption of latent heat of fusion accounts for the somewhat low heat input observed during their firing.

The correlation between heat input and erosion rate is discussed in Section 15.5.2.

15.3.3 Metallographic Changes Accompanying Firing

The gun steel barrels of the powder testing program were examined metallographically upon completion of the firing tests and the details of many changes in the nature of the bore surface caused by firing, such as those described in Chapters 10 and 12, were thus revealed. Outstanding among these changes were the cracking of the surface, pebbling of the surface and the development of a layer of transformed steel next to the surface. Relationship between these changes and the flame temperature of the powder was established in several aspects.

Cracking of the Surface

Surface cracking always developed as a network characteristic of the type that has been attributed to thermally induced stresses (Section 13.5.3). The mesh size generally was less as the powder flame temperature was lowered. The apparent width of the cracks appeared to increase directly with the flame temperature and the number of rounds fired. Their depth was rather anomalous, however, being greater in the case of cooler powders.

It seems probable that the incipient melting which occurs during the firing of all but the coolest powders removes stress raisers in the surface with the result that cracks of full depth do not develop. Erosion from the surface also reduces the apparent depth of cracking.

Pebbling of the Surface

The bore surfaces of barrels fired with any but the coolest powders had a pebbled appearance caused by the rounding of the edges of the cracks by liquefaction, as described in Section 10.5.2. Since the pebbling was related to the crack system, it was coarser grained the hotter the powder. It has been shown[124] that the extent of the pebbling can be correlated with the excess of a calculated maximum bore-surface temperature over the melting point of the gun steel, the maximum surface temperature being found, as described in Section 5.4.1, on the assumption that no melting occurs.

When the hottest powders are fired the very coarse pebbling merges smoothly with a general type of melting which produces a rippled surface. This type of melting is presumably a true melting of gun steel, although it is recognized that chemical changes may play a role in lowering the melting point of the steel.

Thermal Transformation of the Surface

The thermal transformation of a gun steel layer next to the bore surface has been discussed in some detail in Sections 12.1.2 and 13.2.3. Much of the quantitative data which has pointed to a possible mechanism of the formation of this layer[124] was obtained from a metallographic study of the barrels fired in the powder testing program. Particularly, the rate of formation and the relation between dimensions of the transformed layer and the flame temperature of the powder were established through this study.

Distribution of the Transformed Layer. The total altered layer on a bore surface is properly divided into at least two distinct parts: a chemically altered, outer layer, to which the term "white layer" is restricted for the reasons given at the end of Section 12.1.1, and an inner layer which has essentially the chemical composition of gun steel but which has been thermally altered. The white layer usually has negligible thickness compared with the thermally altered layer. In the following discussion the thickness reported for the transformed layer is actually the total thickness of both layers, but it is to be understood that this thickness, in the case of the barrels studied in connection with the powder-testing program, is not significantly different from that of the thermally altered layer alone.

By virtue of its well-established independence of chemical effects, it is to be expected that the thickness of the thermally transformed layer will depend on the severity of thermal conditions along the barrel

in which it forms. The expectation is fully confirmed by the distribution of the layer in the barrels studied. In every case the layer was found to be thickest in the neighborhood of the origin of rifling where thermal conditions are most severe and to decrease muzzleward.

This variation presents a minor problem when two or more different test barrels are to be compared. The best point of reference is at the origin of rifling where the layer is thickest, but often the thickness changes so rapidly in this region that minor errors in sectioning the barrel cause large errors in thickness measurement. The problem was solved by determining the thickness at different points away from the origin of

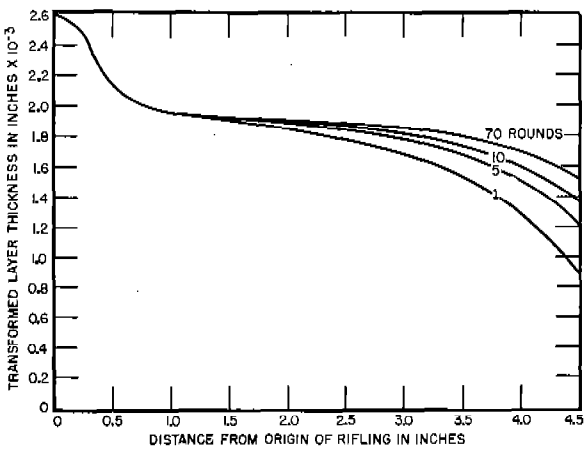


FIGURE 8. Distribution of transformed layer for different numbers of rounds of double-base (40% NG) powder. (This figure has appeared as Plot VI in NDRC Report No. A-452.)

rifling, usually ½, 1, 2, and 4 in., drawing a smooth curve through these points, and extrapolating to the origin itself. Curves of this type are shown in Figure 8.

It was found that the geometry of the projecting lands enhanced the heat transfer so that transformed layers in the lands were thicker and less sensitive to the type of powder than layers in the grooves. The layer thickness most characteristic of the firing of a given powder was therefore taken as the extrapolated thickness in the grooves.

Layer thicknesses determined in this way were found to be independent of the type of bullets or the number of rounds fired. They are tabulated in Table 10.

Rate of Formation of the Transformed Layer. The barrels fired in the series of tests at high ballistic level

TABLE 10. Extrapolated thickness of the transformed layer in the grooves at the origin of rifling of caliber .50 erosion-testing gun.

Powder	Flame temperature (K)	Transformed layer thickness		
		PE bullets* (in.)	AT bullets† (in.)	High level tests (in.)
RDX-5060	2320	0.0010	.....	.....
Cordite N	2469	0.0006	0.0008	.....
FNH/P	2480	.....	0.0008	.....
FNH-M1	2483	0.0009	0.0008	0.00085
RDX-5061	2560	0.0013	.....	.....
NH-M1	2807	0.0011	0.0012	.....
Pyro	2814	0.0012	0.0012	.....
Cordite NQ	2864	0.0012	0.0013	.....
IMR	2938	0.0015	0.0015	0.0015
RDX-5059	3080	.....	0.0011	.....
FNH-M5	3268	0.0019	0.0019	.....
FNH-M2	3564	0.0021	0.0021	0.0022
40% NG	3945	.....	.....	0.0023
60% NG	4300	.....	.....	0.0024

* PE bullets are pre-engraved. (See Section 15.2.1.)
† AT bullets are artillery-type. (See Section 15.2.1.)

were studied at the end of 1, 5, 10, and 70 rounds in order to find the amounts of transformed layer which had formed at these stages. The results showed that the layer had formed during the firing of the first round and that, although very nearly the full thickness was formed at the origin of rifling, somewhat less than full thickness was formed toward the muzzle; thus the distribution of the layer changed somewhat during the firing of subsequent rounds as will be seen in Figure 8, wherein distribution curves are plotted for 1, 5, 10, and 70 rounds fired with pre-engraved bullets and double-base powder containing 40% nitroglycerin.

Full data on the rate of formation of the transformed layer may be obtained from Table 11. Analysis of these data demonstrates the extreme rapidity of the formation of the layer and shows that the region in the barrel throughout which the layer thickness is independent of the number of rounds fired lengthens as the flame temperature of the powder increases. It must be noted that general melting is so pronounced during the firing of the very hot 40% and 60% NG powders, that appreciable material is removed from the surface at the same time that the layer is altering. Accordingly, and as a first approximation, observed layer thicknesses in Table 10 have been corrected by the addition of the observed change in groove radius during the firing of the last round. The correction is entirely negligible in the case of other powders.

TABLE 11. Transformed layer thickness as function of rounds fired at ½, 1, 2, and 4 in. from the origin of rifling in caliber .50 erosion-testing gun.

Powder	Rounds fired	Transformed layer thickness at ½ in.	1 in.	2 in.	4 in.
FNH-M1	1	0.0003+	0.0002	0.0001+	0
	5	0.0004	0.00025	0.00015	0
	10	0.0005+	0.0004	0.0003−	0.0001−
	70	0.0008	0.00075	0.0006	0.00025
IMR	1	0.0008	0.0007	0.0006	0.0005
	5	0.0009+	0.0009	0.0008+	0.0008−
	10	0.0010	0.0010−	0.0009	0.0008
	70	0.0012	0.0011−	0.0010	0.0009
FNH-M2	1	0.0020	0.0018	0.0014	0.0012
	5	0.0020	0.0018	0.0015	0.0013
	10	0.0020	0.0018	0.0017	0.0015
	70	0.0022	0.0021	0.0020	0.0019
40% NG	1	0.0021	0.00195	0.0018	0.0013
	5	0.0021	0.00195	0.0019	0.0015
	10	0.0021	0.00195	0.0019	0.0016
	70	0.0021	0.00195	0.0019	0.0017
60% NG	1	0.0021	0.0019+	0.0017	0.0013−
	5	0.0021	0.0019+	0.0018	0.0016−
	10	0.0021+	0.0020	0.0019	0.0018−
	70	.....	.....	0.0020	0.0020

Relation to Erosion Mechanism. It follows from the fact that a continuous, thick transformed layer forms during the firing of a single round that erosion of a gun steel barrel is really the erosion of a transformed layer. Thus a full knowledge of the nature of the transformed layer is essential if the mechanism of such erosion is to be discovered. The nature of the layer has been discussed in Sections 12.1.2 and 13.2.3. It remains only to reemphasize that the layer defines the region which is rendered austenitic during the firing of any single round and that there is considerable evidence that the hot, austenitic layer has a high chemical reactivity with the constituents of the powder gases.

[15.3.4] Chemical Products on the Bore Surface

The eroded surface of each fired barrel was subjected to x-ray diffraction analysis with the purpose of finding any differences in chemical nature of the surfaces resulting from the firing of different powders, which is discussed at length in Section 12.2. The diffraction patterns were obtained by allowing molybdenum $K\alpha$ radiation to strike the eroded surfaces at small angles.

In addition to ferrite (alpha-iron modification) which was found on each film, four other constituents were found in varying amounts: austenite (gamma-iron modification), cementite (Fe_3C), wüstite (FeO) and the epsilon phase of iron nitride (Fe_2N_x). It was noted that the diffraction lines of the ferrite were often quite broad, particularly in the barrels fired with the double base powders which have the higher flame temperatures. This broadening may actually indicate the presence of distorted-cubic martensite formed by quenching austenite. Austenite itself is never retained by quenching alone, but only if the gamma-iron takes up in solid solution a considerable amount (up to about 0.6%) of carbon or nitrogen or both. Accordingly, the austenite found was probably enriched in carbon or nitrogen or both.

A purely qualitative analysis of the various eroded surfaces is given in Table 12. The designated amounts are only estimates. Evidently, there is an absorption of carbon or nitrogen or both and stabilization, in a superficial layer, of austenite regardless of the powder fired.

In addition, two tendencies may be noted: a tendency toward carburizing and nitriding with the formation of cementite and iron nitride; and a tendency toward oxidizing with the formation of wüstite.

TABLE 12. Qualitative x-ray diffraction analysis of eroded bore surfaces of erosion-testing gun barrels fired with different powders.

Powder	Flame temperature (K)	Austenite (γ-Fe)	Cementite (Fe_3C)	Wüstite (FeO)	Epsilon iron nitride (Fe_2N_x)	Miscellaneous
RDX-5060	2320	Present	Present	Possibly	Present	Pb + *X*
Cordite N	2469	Large	Small	Small	Large	Pb + *X*
FNH-M1	2483	Large	Small	Probably	Large	Pb + *X*
RDX-5061	2560	Present	Probably	Present	Present	Pb + *X*
NH-M1	2807	Large	Present	Probably	Probably	Pb
Pyro	2814	Large	None	Small	Large	...
Cordite NQ	2864	Large	None	Small	Present	Pb
IMR	2938	Large	Present	None	None	Pb
FNH-M5	3268	Large	None	Large	None	...
FNH-M2	3564	Large	None	Large	None	...

[redacted]

High flame temperatures appear to encourage the latter reaction and discourage the former; while low temperatures seem to permit both, although oxidization is not very pronounced.

Metallic lead (Pb) was found on many of the surfaces. Possibly the lead came from lead thiocyanate in the primers and was volatilized in the tests with very hot powders.

Unidentified substances (*X*) were found on several of the surfaces.

15.4 VENT PLUG TESTS

The erosion produced in vent plugs (Section 15.2.2) was measured in terms of the weight loss of each plug tested at the levels of severity afforded by different vent sizes. The measurements were usually made after the firing of 5, 10, and 15 rounds with each of the different powders. Most powders were tested with four different vent sizes: 3/16, 1/8, 3/32, and 1/16 in., but the RDX powders were tested only with three: 3/32, 1/8, and 1/16 in. NH-M1 powder (for 37-mm gun) was tested along with the latter to provide a reference for the comparison of all powders.

A summary of the results in the form of averages of the two runs after 15 rounds are listed in the two parts of Table 13 for all of the powders tested. Erosion was only very small in the largest vents. Hence tests with large vents do not distinguish among the less erosive powders. The more severe conditions in the smaller vents permitted a finer classification.

TABLE 13. Erosion of vents of different sizes expressed in terms of average weight loss after 15 rounds.

Powder	Average weight loss (mg) 3/16-in.	1/8-in.	3/32-in.	1/16-in.
FNH/P	0	14.3	92.2	212.8
FNH-M1	0	23.6	127.8	246.2
NH-M1-3727	0	38.1	120.1	230.8
NH-M1-4974	0	12.2	108.6	210.2
Pyro	1.9	18.3	65.5	212.1
IMR	2.8	35.6	118.1	263.7
FNH-M2	24.8	339.9	512.4	1069.9
	3/32-in.	1/8-in.		1/16-in.
RDX-6079	3.3	34.5		276.6
RDX-6080	7.4	67.4		330.6
NH-M1-3727	2.7	30.5		285.0
RDX-6081	4.1	59.7		317.6
RDX-6082	6.8	67.3		386.1
RDX-6083	18.5	118.1		513.3

15.4.1 Relative Erosiveness of Powders

The powders tested in 1/8-in. and 1/16-in. vents (the only sizes used for both the RDX and the other powders) are listed in Table 14 according to their relative order of erosiveness. In both lists an erosiveness of unity is assigned to NH-M1 powder, lot No. 3727. The numbers used to differentiate the powders of the same types are experimental lot numbers except in the case of NH-M1-3727 which is a standard lot of powder for 37-mm gun, M1916.

TABLE 14. Relative erosiveness of powders tested in 1/8-in. and 1/16-in. vent plugs.

1/8-in. vent Powder	Degree of erosiveness	1/16-in. vent Powder	Degree of erosiveness
NH-M1-4974	0.32	NH-M1-4974	0.91
FNH/P	0.38	Pyro, FNH/P	0.92
Pyro	0.48		
FNH-M1	0.62	RDX-6079	0.97
IMR	0.94	NH-M1-3727	1.00
NH-M1-3727	1.00	FNH-M1	1.06
RDX-6079	1.13	RDX-6081	1.12
RDX-6081	1.96	IMR	1.14
RDX-6080, RDX-6082	2.21	RDX-6080	1.16
		RDX-6082	1.35
RDX-6083	3.87	RDX-6083	1.80
FNH-M2	8.92	FNH-M2	4.62

There is not a one-to-one correspondence between these two orders but in many significant features they are quite similar. By consideration of the partial series determined with the other vent sizes and weighting the results slightly toward low severities so as to approximate better the actual erosive loss found in real guns, it is possible to organize an overall erosiveness series by groups:

NH-M1-4974, FNH/P, Pyro
< NH-M1-3727, RDX-6079 (?)
< FNH-M1 < IMR < RDX-6081
< RDX-6080, RDX-6082
< RDX-6083 < FNH-M2

This series differs in a number of respects from that determined by firings in the caliber .50 erosion-testing gun, as given at the end of Section 15.3.1. It will be noted from a comparison of Tables 2 and 4 that in most cases where RDX powders and single-base powders have nearly the same flame temperature, (that is, RDX-6081, and NH-M1-3727) the former are considerably more erosive than the latter. This fact emphasizes the very great importance of chemical

action by the powder gases in the problem of erosion, for in such cases thermal conditions are closely similar and the only important difference is to be found in the chemical composition of the powder gases. It follows that the overall correlations of erosive effects with temperature which are made below are valid only so long as the chemical compositions of the gases are roughly similar, for example, as they appear to be among the gases from single-base and double-base powders.

15.4.2 Comparison of Erosiveness in Guns and Vents

The significance of these tests is clarified when comparison is made with the erosion rates found by firing the erosion-testing gun (Section 15.3). In Table 15 the various powders are listed in order of increasing erosiveness as determined in the vent plug and in the pre-engraved bullet series in the erosion testing gun. Only the powders tested by both methods are included, except for powders RDX-6079 and RDX-5060, which were nearly the same in composition and flame temperature.

TABLE 15. Order of increasing powder erosiveness as found by tests in the vent plug and in the caliber .50 erosion-testing gun.

Vent plug	Gun
FNH/P	RDX-5060
Pyro	FNH/P
NH-M1	FNH-M1
RDX-6079	NH-M1
FNH-M1	Pyro
IMR	IMR
FNH-M2	FNH-M2

Some rationalization of differences between the two listings is possible. For example, the largest difference is the position of Pyro powder, which was classified in the least erosive group by the vent-plug tests and in an intermediate position by the gun tests. It will be noted that in tests with the largest vent in which erosion is most nearly equivalent in amount to that found in the gun, Pyro was ranked between IMR and the other less erosive powders as it is in the gun listing. It seems possible that had those low-severity tests been able to distinguish among the less erosive powders it might have led to a listing more like that found with the gun and would certainly have brought agreement with respect to Pyro.

The position of RDX-6079 is somewhat uncertain at best. Its present position is only one group removed from that of the matching RDX-5060. The sole other discrepancy is the position of FNH-M1. There seems to be no explanation for the lack of agreement in its case.

In spite of these anomalies it may be concluded that vent plug tests of powders are useful in giving a rough idea of relative erosiveness.

15.5 CORRELATION OF EROSION, THERMAL TRANSFORMATION, HEAT INPUT, AND FLAME TEMPERATURE

15.5.1 Introduction

Throughout this discussion relationships between the rate of erosion as measured by increase in bore diameter, the thermal transformation of the barrel steel, the heat input to the bore surface and the flame temperature of the powder have been implied. A description of these relationships in definite form provides a good summary of the foregoing sections as well as a satisfying demonstration of the intimate connection among these various aspects of gun erosion.

Temperature may be regarded as the key which opens the door to understanding of the nature of gun barrel erosion and in particular to an understanding of erosion as caused by different propellants. The temperature of the bore surface determines the mechanical properties of that surface, the kinds and the rates of chemical reactions which will occur on and in that surface, and the possibility of liquefaction of that surface or of the chemical reaction products that form there. The sum of these effects during firing, discussed in more detail in Chapter 13, embodies the mechanism of gun erosion.

Any correlation of erosive effects with temperature should properly be made with respect to a bore-surface temperature, but such a temperature is not easy to define. First of all, the temperature of the immediate bore surface fluctuates with extreme rapidity and since erosive effects are not instantaneous, some suitable time-average needs to be chosen. Secondly, erosive effects are not two-dimensional but occur within small, albeit, finite volumes. Temperature distribution falls off rapidly inward from the bore surface, so that some suitable space-average needs to be chosen for the reference temperature.

Problems of this sort are not impossible to solve and suitable methods of calculating these average or "effective" temperatures have been worked out.[48] They are, nevertheless, rather laborious.

A simpler approach is to find some easily measured quantity which is related to the bore surface temperature. The adiabatic flame temperature of the powder (Section 2.4.3) is perhaps the most convenient such quantity, although the relation is not a simple one, involving as it does the intermediate relations of gas temperature and heat input. Reliance upon it as a parameter measuring the bore surface temperature is greatly strengthened by the existence of a simple linear relationship between it and the actual measured heat input to the bore which will be demonstrated in Section 15.5.2. It is not unreasonable, then, to attempt to correlate some of the aspects of measured erosion of these barrels against the flame temperature of the powder fired.

15.5.2 Dimensional Erosion Rate versus Flame Temperature

The dimensional erosion rate is, of course, not a function of the flame temperature alone, but depends also on the type of bullets fired and on the loading conditions. The type of bullet is a truly independent factor; the loading condition is probably not truly independent. That is to say, if the loading condition is adjusted to give a higher ballistic level with the same powder, the relation between flame temperature and bore-surface temperature will change so as to raise the latter. The erosion rate and attendant phenomena are therefore increased in magnitude as will be illustrated below. The dimensional erosion rate may be studied with reference to flame temperature, therefore, only if other factors are kept constant or if their influence is quantitatively understood.

The data of Table 8 present the relation between erosion rate and flame temperature for the pre-engraved bullet, the artillery-type bullet, and the high ballistic level series. These data are plotted in Figure 9 where the curve for each series is seen to be similar in shape to an exponential curve. An exponential relationship is strongly implied by the straight lines that result if the same data are plotted on semilogarithmic paper.

For a given change in flame temperature, the erosion rate appears to increase more rapidly at higher flame temperature. Evidently also the use either of engraving type of bullets or of a higher ballistic level increases the erosion rate at all temperatures.

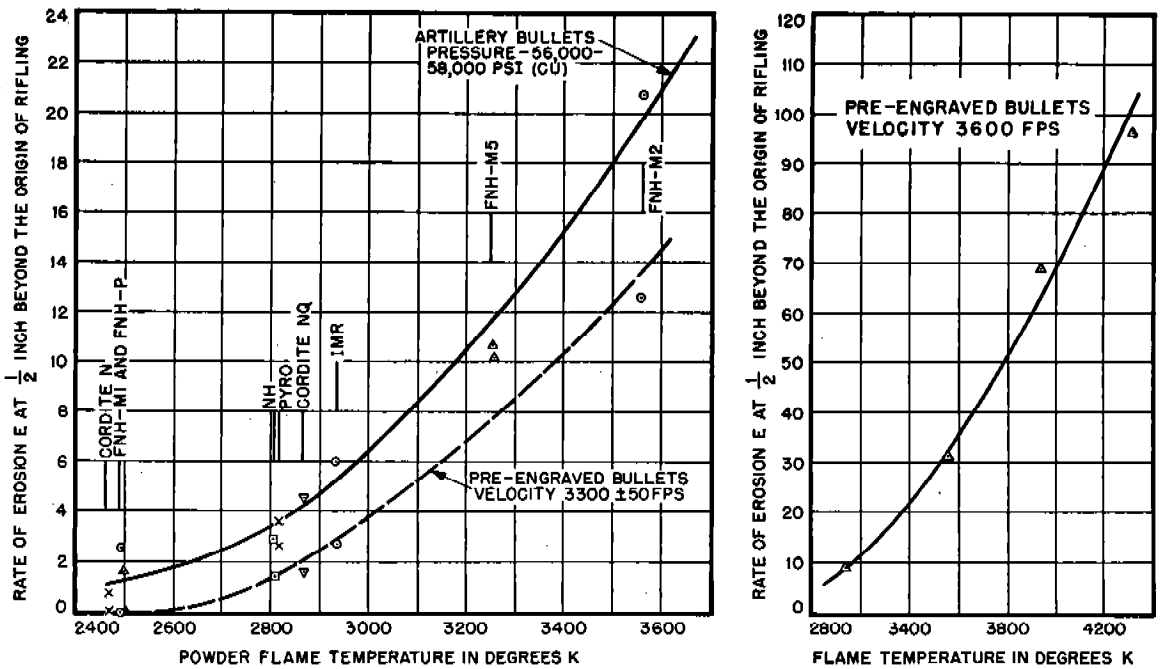


FIGURE 9. Erosion rate (in units of 0.00001 in. per round) versus flame temperature for the pre-engraved bullet, the artillery bullet, and the high ballistic level series. (This figure has appeared as Figures 18 and 20 in NDRC Report No. A-451.)

15.5.3 Heat Input versus Flame Temperature

The data on heat input reported in Table 9 are plotted in Figure 10, where the linear relationship between heat input and flame temperature is evident. It has been suggested that the deviation from linearity at very high flame temperatures is probably the result of absorption of latent heat of fusion during the considerable melting of gun steel that appears to accompany the firing even of a single round.

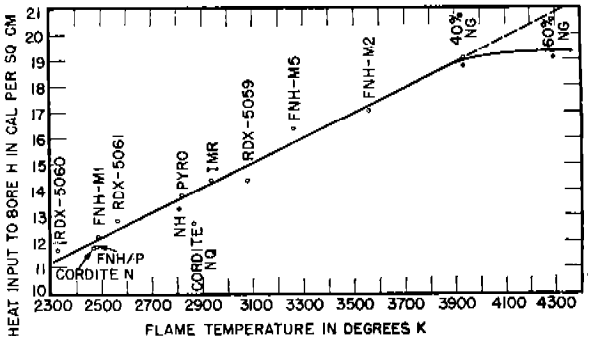


FIGURE 10. Heat input versus flame temperature. (This figure has appeared as Figure 23 in NDRC Report No. A-451.)

Since the heat input should be more directly associated with bore-surface temperature than is the flame temperature, it is reasonable to expect that the plotting of erosion rate versus heat input should give a smoother curve. This deduction is borne out by the facts. If the erosion rate is first plotted against heat input and then the heat input scale is converted to flame temperature by means of the linear relationship of Figure 10, the results of Figure 9 are again obtained with the difference that there is a better fit of the experimental points to the exponential curves showing erosion rate versus flame temperature.

Heat input for a given flame temperature should also increase with the ballistic level. The data now available do not permit an investigation of this point.

15.5.4 Thermal Transformation versus Flame Temperature

By virtue of its rapid rate of formation which permits it to renew itself during each round, the transformed layer presents a characteristic thickness at the origin of rifling which is independent of the type of bullets or the number of rounds fired. This characteristic thickness may be expressed as a function of the flame temperature. As before, the thickness observed with a given flame temperature should increase with the ballistic level, but the available data do not permit an investigation of this point.

The data on thickness of the transformed layer which were presented in Table 10 are plotted versus flame temperature in Figure 11. A straight line may be drawn through points for powders not containing RDX, although at very high flame temperatures the deviations are greater than at low temperatures. Perhaps this is caused by the absorption of the latent heat of fusion having changed the thermal conditions. The distribution of the points for the three RDX powders seems to be random.

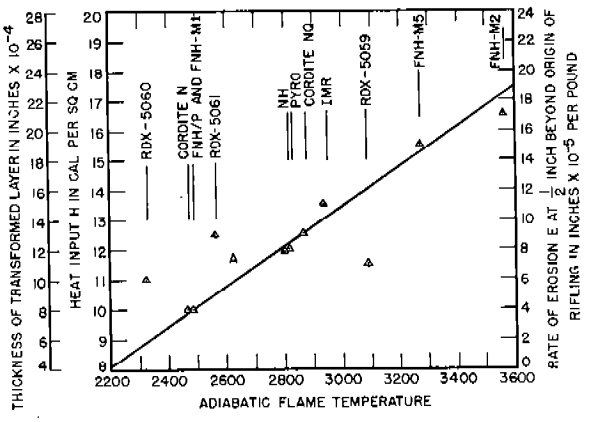


FIGURE 11. Transformed layer thickness versus flame temperature. (This figure has appeared as Figure 64 in NDRC Report No. A-451.)

The mechanism of thermal transformation has been discussed in Section 13.2.3 and a method of calculation has been presented[124] which permits an explanation of the results of Figure 11.

15.6 MODIFICATION OF PROPELLANTS[e]

15.6.1 Introduction

The foregoing section points out the dependence of dimensional erosion rate upon the adiabatic flame temperature of the powder. From this it would seem that a mitigation of erosion might be obtained by developing powders of low flame temperature but with high impetus. This was suggested in Section

[e] An Ad Hoc Committee on Internal Ballistics appointed by the Chairman of the NDRC in 1942, recommended a joint investigation of this subject by the units of NDRC which were subsequently designated as Divisions 1 and 8.[143]

3.5.4 for hypervelocity guns in which erosion with the usual propellants is a limiting factor. It should be noted, however, that the correlation of erosion with flame temperature or heat input holds true only for powders with similar composition. The RDX series of powders[f] must be considered separately from the other powders. In both the studies with vent plugs (Section 15.4.1) and with the caliber .50 erosion-testing gun (Table 8) it was found that RDX powders though cooler than the older standard powders are more erosive. Thus, while it is clear that the temperature of the gases resulting from the combustion of a propellant is probably the most important factor to be considered in the development of less erosive powders, the composition of the gases is also important, and the discussion which follows is warranted.

15.6.2 Variations in Types of Erosion Products

From studies of eroded guns and from the results of laboratory firing tests a great deal has been learned about the effects on gun bores of the various components of the powder gases from different propellants. X-ray- and electron-diffraction examination of steel gun bores, test blocks, and filings exposed to the gases from the usual single- and double-base propellants (Sections 12.2 and 15.3.4) has proved that the nitrocellulose powders (single-base) are carburizing whereas those containing nitroglycerin in addition to nitrocellulose (double-base) are oxidizing. Further evidence of this fact was obtained in the studies of carbon penetration (Section 14.2.5).

Metallographic and chemical studies of the surface layers in eroded guns (Chapter 12) have indicated that the dominant erosion process in guns fired with single-base powders is the removal of partially liquefied material high in carbon and nitrogen, which has resulted from the chemical alteration of the steel by the powder gases. This material has a fusion range about 300 C lower than the melting point of gun steel. On the other hand, liquefaction in guns in which oxidation by the gases from powders containing nitroglycerin takes place is that of unaltered or perhaps only slightly altered steel, as is brought out in Section 13.2.4.

The obvious conclusion from the evidence summarized above is that a less erosive powder might be one that was only a slight modification of the standard nitrocellulose-nitroglycerin type of propellants. It should definitely be less carburizing than the single-base powders so that low-melting products would not be formed on bore surfaces but should not have as high an adiabatic flame temperature as the usual double-base powders which cause melting of the steel itself. Although oxidation does not promote liquefaction to the same extent as carburization, less oxidation than is obtained with the usual, relatively erosive double-base powders would certainly be desirable, since oxide films are presumably readily removed by mechanical forces during firing, and would probably be obtained in the case of a powder that was developed to have a lower flame temperature.

Another modification of powders is suggested in Section 14.4.8 which points out the desirability of decreasing the amount of sulfur in charges.

15.6.3 Thermodynamic Considerations

Single-Base and Double-Base Powders

The same thermodynamic considerations that led to an evaluation of the chemical factors in the causes of erosion, discussed in Section 13.3, may be applied to the problem of finding a less erosive propellant. In the reactions of the powder gases with gun steel the most important components of this gas are carbon monoxide and carbon dioxide. Whether oxidation or carburization of the bore surface occurs depends on the CO/CO_2 ratio in the gases at the effective temperature, for this ratio decreases with the temperature of the gases. Powders containing nitroglycerin have a higher oxygen balance than those containing only nitrocellulose, thus the CO/CO_2 ratios of the former are lower than those of the latter (Figure 9 of Chapter 2) and the gases from double-base powders may be considered more oxidizing or less carburizing. Figures 6 to 8 of Chapter 13 show fields for the ultimate or major products resulting from the interaction of steel and powder gases. In order to obtain boundary conditions so that oxidation and carburization were equal or perhaps even mutually suppressed, an increase in flame temperature and an appreciable decrease in the CO/CO_2 ratio of the gases from a single-base powder would be required. It was suggested[138] that a nitrocellulose powder to which a small amount of nitroglycerin (perhaps 1%) had been added should be investigated.

[redacted]

[f] These powders had been investigated by Division 8, NDRC. They were also among those investigated in Canada[371] during World War II.

RDX Powders

According to the above line of reasoning, RDX powders might be expected to be more erosive than single-base powders of the same flame temperature, which actually is the case. Figure 9 of Chapter 2 shows that the former, because of their higher CO/CO_2 ratios, should be much more carburizing than the latter. The erosivity of these newer propellants, however, does not bear any obvious relationship to their high CO/CO_2 ratios, for studies of carbon penetration with an RDX powder (Section 14.2.5) indicated that the reaction products were not as high in carbon as those obtained from the reaction of a single-base powder at the same bore-surface temperature. It may be that in the case of the RDX powders other reactions besides those of the carbon gases with the steel assume more importance than they do in the case of the nitrocellulose propellants. Indications that this may be true have been found in the few instances in which erosion products resulting from the use of RDX powders have been examined by diffraction techniques.[137]

15.6.4 Experiments with Powders Containing Ferrosilicon

Erosion might be diminished by maintaining a sufficiently high temperature to avoid carburization and nitriding but at the same time preventing oxidation by the addition of a deoxidizer. Gun steel filings, mixed with a charge of double-base powder to which ferrosilicon had also been added, were fired in a caliber .30 rifle according to the technique described in Section 11.2.6.[49] No ferrous oxide (FeO) was identified in the collected products. This compound was always found in these experiments with steel or iron filings when no deoxidizer had been added to the charge. Because of the successful reduction of the oxidation in this case, a firing test was made in the caliber .50 erosion-testing gun (Section 11.2.1) with a 20% nitroglycerin powder to which 5% of ferrosilicon powder had been added. The incomplete test[49] showed a slight reduction of the erosion, particularly in the grooves. Difficulties encountered in deposition of unused ferrosilicon in the grooves and excessive muzzle blast caused the test to be abandoned.

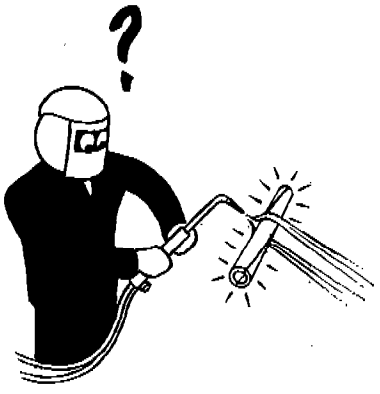
15.6.5 Experiments with Powders Containing Low Percentages of Nitroglycerin

As was pointed out in Section 15.6.3, a nitrocellulose powder to which a small amount of nitroglycerin had been added might be less erosive than one containing nitrocellulose alone. It was planned to test mixtures of a standard single-base and a standard double-base propellant in such proportions that low percentages of nitroglycerin would be obtained. Such mixtures were to be tested first in erosion vent plugs and then in caliber .50 machine gun barrels.

One mixture containing 5% nitroglycerin was tested in the vent-plug apparatus. Because the effect to be studied was essentially chemical in nature, the ⅛-in. vent, which gives reproducible erosion at low severity, was used. This mixture was more erosive than single-base powder. The erosivity of mixtures containing less than 5% nitroglycerin, however, may be worth investigating. The original suggestion, it should be noted, was that only about 1% nitroglycerin should be added. Because of the termination of the Division's activities, further testing was not continued. Only the preliminary control experiments were carried out for the machine gun tests.[110] A continuation of these experiments would be worthwhile; negative results would be of as much value in this case as positive ones.

PART V

EROSION RESISTANT MATERIALS



Fire is the test of gold; adversity of strong men.
—*Seneca*
"De Providentia"

Chapter 16

SELECTION OF EROSION RESISTANT MATERIALS FOR GUN BORES

By *J. F. Schairer*[a]

16.1 EROSION RESISTANT MATERIALS PROGRAM

IN AN EARLY STAGE of the studies of gun erosion at the Geophysical Laboratory for Division 1, NDRC, the conclusion was reached that, because of their lack of resistance to thermal and chemical attack by powder gases during firing, no steels or high-iron alloys showed promise as bore-surface materials under severe firing conditions using conventional propellants. Yet steels are the only materials of adequate strength and ductility that are available in sufficient quantities for gun tubes. Therefore, in order to protect the bore surface of such steel tubes from contact with powder gases (at least near the breech end where powder gas erosion is most severe), attention was concentrated on the development of suitable erosion resistant liners, linings, electroplates, and other coatings.

Laboratory tests showed that of all the 92 elements then recognized, as shown in Figure 1, only the following pure metals[b] were resistant to chemical attack by the powder gases: chromium, molybdenum, tungsten, tantalum, nickel, cobalt, and copper. Only the first four of these have a sufficiently high melting point for severe service under hypervelocity conditions, where melting is an important factor in the failure of a steel gun bore surface. Subsequent tests on pure nickel and high-nickel alloys under less severe laboratory test conditions and firing tests as gun liners showed that these (except nickel-chromium alloys with more than 10% chromium) are subject to severe intergranular attack by powder gases and gave a performance barely equal to or inferior to gun-steel. Copper is quite unsuitable for a gun bore surface material because of its softness and low strength in addition to its low melting point. Other tests showed that in addition to suitable resistance to thermal and chemical attack a bore surface material must have sufficient hardness and strength at temperatures attained during firing to prevent deformation of the rifling by impact of the projectile and must be sufficiently ductile to prevent serious failure by cracking.

In the fall of 1942 efforts were started by Division 1 on the preparation of chromium and molybdenum in form suitable for use as gun liners. By the following summer preliminary tests of molybdenum liners had emphasized the importance of hot hardness as a characteristic of a successful gun liner material. Further study of this phase of the subject led to the discovery that the stellites (Chapter 19), which are cobalt-chromium alloys that have the property of hot-hardness, are erosion resistant as long as the bore-surface temperature is not too high.

By that time the experience of aerial combat during World War II had indicated that erosion was limiting the performance of the caliber .50 aircraft machine gun. Application of the discovery of the erosion resistance of stellites to this problem led to a remarkable increase in the performance level of this gun (Chapter 22). A parallel attack on this same problem led to the development of nitrided, chromium-plated caliber .50 barrels (Chapter 23). Eventually, it was found that an even better barrel was obtained by using a stellite liner with the steel bore chromium-plated ahead of it in such a manner as to constrict the bore at the muzzle (Chapter 24). Furthermore it was found that provided the steel barrel was strengthened by making it slightly heavier (especially at the forward end of the liner) and perhaps by using a special steel having greater strength at high temperatures even better performance could be attained (Chapter 24).

Experience with stellite liners in the caliber .60 machine gun, which has a muzzle velocity of slightly over 3,500 fps, showed that this alloy is "marginal" with respect to its use in a hypervelocity gun. In this particular application a stellite liner lasts long enough to furnish a useful gun barrel life, but when it fails, it does so by melting along surface cracks. That fact coupled with the observation that the surface of a stellite liner melts when fired with double-base powder, even at velocities around 3,000 fps, showed that a material of higher melting point was needed for

[a] Special Assistant, Division 1, NDRC. (Present address: Geophysical Laboratory, Carnegie Institution of Washington.)

[b] There is some evidence (Section 16.4.14) that certain of the metals of the platinum group may be erosion resistant. On account of their scarcity these metals were not seriously considered in the Division 1 program.

	H							
He	Li	Be	B	C	N	O	F	
Ne	Na	Mg	Al	Si	P	S	Cl	
A	K	Ca	Sc	Ti	V	**Cr**	Mn	Fe,Co,Ni
	Cu	Zn	Ga	Ge	As	Se	Br	
Kr	Rb	Sr	Y	Zr	Cb	**Mo**	Ma	Ru, Rh, Pd
	Ag	Cd	In	Sn	Sb	Te	I	
Xe	Cs	Ba	La	Ce				
				Hf	**Ta**	**W**	Re	Os, Ir, Pt
	Au	Hg	Tl	Pb	Bi	Po	Ab	
Rn	Vi	Ra	Ac	Th	Pa	U		

FIGURE 1. Only a few of the 92 elements in the periodic table have been found to be resistant to chemical and thermal attack by the powder gases. The symbols of the rare earth elements have been omitted from this table.

general use in hypervelocity guns, that is, ones fired at muzzle velocities greater than 3,500 fps. Hence the search for such a material was continued at the same time that further efforts were made to extend the application of stellite.

During World War II, caliber .50 gun barrels that had been nitrided and chromium plated and others that had had stellite liners inserted in them were used in combat. Production of stellite-lined barrels of other sizes was ready to start at the time of Japanese surrender. The further application of stellite and other hot-hard alloys to small arms barrels was continued by the Crane Company for the War Department. Continuation of the investigation of chromium electroplates, of duplex electroplates of chromium and other metals, and of alloy electroplates of various pairs of metals (Chapter 20) at the National Bureau of Standards was supported jointly by the War and Navy Departments.

The most promising material for service in hypervelocity guns appears to be a hardened molybdenum (Chapter 18). Sufficient progress was made in its development during the war so that the Navy Department continued to support the efforts of the Westinghouse Electric Company to make this material in a form suitable for large gun liners, following the plans described in Section 33.1.3. Similarly, the War Department, under contract with the Union Carbide and Carbon Research Laboratories, continued the development of chromium-base alloys, which also appear very promising for hypervelocity service (Chapter 17). Vapor-phase plating (Chapter 21) does not appear to be suitable for gun bores, and therefore, its development would not have been continued by Division 1 for this purpose, although it may have industrial applications.

Thus the resistant-materials program of Division 1, NDRC, during the course of 3½ years led to the development of a very successful solution to the erosion problem in machine guns and narrowed the search for bore-surface materials capable of outstanding performance under hypervelocity conditions to three clearly-defined programs, all of which were subsequently pursued by the Armed Services. The present chapter surveys the whole resistant materials program.[c] In so doing, the successful developments, which receive more extended treatment in subsequent chapters (already noted in the foregoing paragraphs), are summarized in order to give proper perspective

[c] The work carried out by the contractors of Division 1, NDRC, in the development of erosion-resistant materials is described in a series of reports listed in the Bibliography.

to the large number of unsuccessful tests of other materials.

16.2 PROPERTIES OF AN IDEAL EROSION RESISTANT MATERIAL

16.2.1 Introduction

Some very definite ideas on the properties of an ideal erosion resistant material have evolved during the course of Division 1's investigation of gun erosion. These concepts are the result of an analysis of the results of laboratory tests of materials and firing tests of gun barrels with and without liners, platings or coatings of special metals or alloys (described in the following sections of this chapter and the remainder of Part V), combined with an analysis and interpretation of the results of ballistic studies, observations on eroded gun bores, and studies of the mechanism of erosion (described in Parts II, III, and IV).

The properties required of a satisfactory bore-surface material depend on the conditions under which it is to be used. The suitability of a given material for use as a bore surface in a particular gun tube is determined by the characteristics required or desired for that weapon with respect to size, rate of fire, muzzle velocity, type of ammunition (design of projectile and choice of propellant), the pressure-temperature-time characteristics of the powder gas, firing schedule, and minimum useful life. Conversely, the ability to attain some of the desired gun characteristics will depend upon obtaining a suitable bore-surface material.

The prime requisites of a satisfactory bore-surface material for any gun tube are resistance to thermal and chemical attack by the powder gas and suitable mechanical properties.

16.2.2 Thermal Resistance[d]

Resistance to thermal attack involves four separate requirements. First, the material must have a combination of high melting point, high specific heat, and high thermal conductivity, such that the maximum temperature attained by the bore surface (Section 5.4) will always be well below the melting point of the material. For hypervelocity guns, the melting point of the bore surface material should be at least 1500 C and preferably very much higher.

[d] See Section 13.2 for a discussion of the thermal factors in the erosion of steel guns.

The second requirement is a high resistance to thermal and chemical shock (Section 13.1.2) as evidenced by a minimum tendency for the surface to crack under a rapid heating and cooling cycle in the presence of chemically active powder gases.

In the third place, the material must undergo no abrupt volume changes as a result of the cyclic changes of temperature and pressure during the firing. In the case of a coating on steel such volume changes may cause poor adhesion and cracking and thus permit attack of the underlying steel by the powder gases, and in the case of a solid liner they may cause either serious cracking or severe constriction of the bore.

As a fourth requirement, the coefficient of thermal expansion should be low so that at elevated temperatures the rotating projectile does not lose engagement with the rifling and fail to attain adequate spin.

16.2.3 Chemical Resistance[e]

Chemical resistance requires either that the material be inert to the powder gases at the temperatures attained by the bore surface in contact with the hot gases, or that, if chemical reaction does take place, a thin adherent protective film be formed. The rate of chemical reaction is involved in chemical resistance: the rate must be so low that no deleterious attack occurs in the short time that hot gases are in contact with hot metal in a particular weapon.

16.2.4 Mechanical Properties[f]

In addition to resistance to thermal and chemical attack by hot powder gases, a satisfactory bore-surface material in any weapon must remain in place during firing, suffer no large permanent change in dimensions, show no permanent deformation or flowage and must not wear excessively or disintegrate by brittle failure after impact. The mechanical properties of the material both at room temperature[g] and at elevated temperatures determine whether a given material with thermochemical resistance to attack by powder gases can meet these additional mechanical

[e] See Section 13.3 for a discussion of the chemical factors in the erosion of steel guns.

[f] See Section 13.4 for a discussion of the mechanical factors in the erosion of steel guns.

[g] In gun barrels for use at high altitudes in aircraft or under severe arctic conditions, some of the low-temperature (down to −100 F) properties of both the barrel steel and special bore surface material are also important.

requirements of a satisfactory bore-surface material.

The strength at elevated temperatures must be high. If engraving-type projectiles are used, this strength is necessary to prevent permanent deformation (swaging) of the rifling by impact of the projectile; however, this requirement can be made less stringent by the use of pre-engraved projectiles (Section 27.3 and Chapter 31). Resistance to swaging, although it is related to hot-hardness and hot-strength, is not determined by these properties alone, but also depends on high-velocity impact resistance, which is difficult to measure.

Resistance to abrasion and wear at high temperatures, which presumably is another corollary of high hot-hardness, must also be high. The ductility of the material and its impact strength both hot and cold, must be great enough to prevent cracking and brittle failure during the severe thermal cycle of repeated firing.

Because most erosion resistant materials are applied as a liner, a lining, or as a bore coating in a gun-steel barrel, it is preferable that the thermal and elastic properties of the material be close to those of gun steel.

16.2.5 Other Properties

In addition to the prime requisites—thermochemical resistance and suitable mechanical properties—just discussed, other desirable properties of a suitable bore-surface material are availability in the quantities desired and ease of application. In order to permit its application in the form of a liner or lining, a substance must be amenable to fabrication in suitable sizes and shapes and must be machineable for boring and rifling or it must be applicable as a relatively thin bore coating.

In the next section of this chapter, the test methods used are described and the results are summarized. Although valuable preliminary information can be gained from laboratory tests of materials and the choice of materials can thereby be narrowed to a few promising substances, the ultimate test of an erosion resistant material is a firing test in the gun in which it is to be used or under conditions as close as possible to this ultimate objective. The specific applications of the newly-acquired knowledge of erosion resistant materials and erosion processes to improvement in the performance of Service weapons and to the design and development of new weapons are described in Parts VI and VII.

16.3 TEST METHODS FOR EVALUATING PROSPECTIVE MATERIALS

16.3.1 Laboratory Explosion Vessels

Important quantitative and qualitative data on the resistance of materials to the erosive action of hot powder gases were obtained by the use of laboratory explosion vessels. The information gained concerned their resistance to melting, chemical attack, and in some cases surface cracking, but did not include their resistance to the mechanical effects of high pressures and deformation or wear by a projectile.

Erosion Vent Plugs

The first device used by Division 1 in evaluating the resistance of metals and alloys to powder-gas erosion was the erosion vent plug.[27] The method of erosion vent-testing previously employed was modified as described in Section 11.2.3. The rate of erosion was made less severe and a better control of the rate of burning of the powder was achieved by closing the muzzle end of the vent plug with a brass rupture disk to release the gases at the same predetermined pressure. The amount of metal removed on successive firings, as determined by change in weight, combined with the results of metallographic examination of the surface of the vent hole after firing was completed, gave a basis for estimating the erosion resistance of the sample.

In the first tests[27] of nearly 100 metals and alloys $\frac{1}{16}$-in. vents and double-base powder were used. Under these relatively severe conditions the amount of metal removed by fusion is much greater than that lost in any other way, and therefore the results suggest what metals have suitable erosion resistance for use under conditions of hypervelocity where bore melting may be a most important factor. Only four metals (tungsten, tantalum, molybdenum, and chromium) showed promise of a marked improvement over gun steels in resistance to thermal and chemical attack under hypervelocity conditions while two others (copper and nickel) showed a less marked improvement.

Nickel and most nickel alloys (except nickel-chromium alloys with more than 10% chromium) are subject to intergranular corrosion when exposed to hot powder gases. This tendency was not detected in the erosion vent-plug test with $\frac{1}{16}$-in. vents because of the removal of metal by fusion. Subsequent vent tests at decreased severity described below and tests

of liners described later (see Sections 16.3.5, 16.3.7, 16.3.8 and 16.4.9) show the complete unsuitability of such materials for a bore surface.

Subsequent experiments indicated that by reducing the severity of attack by the use of an ⅛-in. vent and single-base powder, the microstructures of the bore surface layers became much more like those observed in eroded guns described in Section 12.1.2. The results of these tests were recorded[75] and the results of all vent tests were correlated with erosion rates in medium caliber guns. Under the less severe conditions pure cobalt and high-cobalt alloys including stellite-type alloys are superior in erosion resistance to gun steels while nickel alloys show intergranular attack.

The results of vent-plug tests have only a very limited applicability in the selection of materials to improve the performance of caliber .50 machine gun barrels and other automatic small arms barrels. The reasons for this are discussed and a new testing device is described in Section 16.3.6. Vent-plug tests have been somewhat more successful in the search for materials for the exhaust throats of recoilless guns.[200,203]

Examination of Blocks After Firing in Explosion Vessels

A modified erosion vent-plug apparatus, described in Section 11.2.4, was used to study changes produced in the surface of chromium and molybdenum as well as gun steels by the action of hot powder gases streaming past the flat surface of a block of the material to be tested, which had been set into a recess in the wall of the vessel.[31] Pressure was controlled by the size of a vent plug from which the gases issued after flowing past the D-shaped vents. Flat surfaces made possible ready microscopic and x-ray examination of the blocks between successive firings. The results on gun steel are discussed in Section 12.2.2. The x-ray studies[137] of a chromium block after firing with double-base powder indicated a slight attack by powder gases with the formation of the hitherto unknown compound Cr_3O_4. In the case of molybdenum there was only a slight attack both with single-base and with double-base powders but the resultant products could not be identified.

Tests for Resistance to Surface Cracking

A third type of explosion vessel (Section 11.2.4), similar in general construction to the two types just described, was used to study the types of surface crack patterns formed under simulated gun conditions when hot powder gases flowed across flat surfaces of blocks of polished gun steel and of a number of other metals and alloys.[51] The specimen was examined with a microscope to ascertain the effects produced. Surface cracks formed in pure iron and all steels, more rapidly in high-alloy steels than in gun steels. Intercrystalline cracks formed in pure nickel. No surface cracking occurred with molybdenum, chromium, tantalum or copper under the same conditions of test.

In an attempt to separate as completely as possible the purely thermal effects of erosion from the chemical effects, an electron bombardment apparatus (described in Section 11.3.2) was designed whereby the surface of a small sample of gun steel or other material could be subjected repeatedly to a very high temperature of extremely short duration. The conclusion was reached that thermal action alone does not cause surface cracking, as discussed in Section 13.5.3. This apparatus has been described and the results of tests on gun steel and two other special steels have been recorded.[104] After bombardment a special steel, which was called "TEW alloy" (Ni 30, Cr 20, Mo 4, W 4, Ta 2, C 0.1, balance Fe) showed an expansion of the lattice in one direction. This method of study of erosion resistance might have value if the degree of control could be increased.

16.3.2 Firing of Metal Particles into an Evacuated Tube

Another method to ascertain the resistance of metals and alloys to chemical attack by hot powder gases was devised. It consisted in mixing fine particles (filings) of the sample to be tested with the propellant charge in a caliber .30 cartridge case, after which the cartridge was fired into an evacuated glass tube, the bullet emerging through a port in the forward end of the tube. The advantages of this technique were threefold. Not only did it determine erosion resistance but it was possible to identify the products of such attack and to detect grain growth or inversions that might be the results of exposure to hot powder gases, and thus affect the rate of erosion. The apparatus is described in Section 11.2.6. The residue deposited on the walls of the tube was amenable to removal and examination by means of x-ray powder photographs which were compared with similar pho-

tographs of the original metal particles and other known standards.

This technique was applied to a large number of substances.[79] Excellent resistance to structural and chemical attack by hot powder gases was shown by the pure metals cobalt, tungsten, and tantalum and by the following alloys: an iron-silicon alloy containing 4.85% Si, Stellite No. 21, high-nickel alloys with silicon or aluminum or chromium, and Monel. Most nickel-iron alloys and the nickel steels, however, showed a slight increase in lattice size which may indicate some reaction with the hot gases.

Only a very slight chemical attack was shown by chromium, molybdenum, a chromium-tungsten alloy, K42B, Illium R, Nichrome V and nickel 70-tantalum 30. Gun steels, other steels, pure iron, high-iron alloys, and pure columbium were attacked by the hot powder gases. Powdered ferrosilicon was resistant to chemical attack by single-base powder and was found to retard oxidation of gun steel during firings with double-base powder, as mentioned in Section 15.6.4. Unfortunately all iron-silicon alloys are too brittle to be serviceable as liners or coatings in gun tubes.

16.3.3 Cavitation Erosion Tests

An investigation[38] of the relation of cavitation erosion to gun erosion was made by subjecting some 31 samples of gun steels and other alloys, previously studied as erosion vent plugs (described in Section 16.3.1), to magnetostriction oscillation in air-free water at 8,000 cycles per sec. The degree of correlation between the resistance to cavitation erosion and hardness of the samples was high. There seemed to be no correlation between the resistance to cavitation erosion and erosion caused by hot powder gases as determined in vent-plug tests. Further discussion of these tests is given in Section 11.3.3.

16.3.4 Battelle Laboratory Gun

During the years 1941 to 1943, the Battelle Memorial Institute, under Army contract through Watertown Arsenal, undertook a survey of the resistance of metals and alloys to powder-gas erosion. An apparatus for smooth-bore testing, called the Battelle laboratory gun,[245,552] was developed.

In the apparatus used in early tests, the material to be tested, in the form of a cylindrical tube, 1 in. long and 0.75 in. in inside diameter with a wall thickness of 0.27 in., was in contact with the gases from a propellant for a 37-mm gun for 0.0036 sec at a pressure of about 11,500 psi. A projectile was used in this case with the result that, in effect, the gases streamed through a vent of annular cross section. The part of the projectile that passed through the test specimen was a cylinder ground to have a diametral clearance of 0.005 in. It was screwed to a cast iron weight that slid in a frame and was subjected to a braking action after the projectile had traveled out of the tube. The erosion from the mechanical action of the projectile was insignificant. Therefore a projectile was not used in a later form of the apparatus. Also, instead of using an annular orifice, a rectangular cross section for the passage of the gases was achieved by mounting two flat surfaces of test specimens opposite each other at an optimum distance for the desired testing conditions. In this way a control sample could be fired with the unknown under identical conditions.

When the severity level of the various tests is taken into account, the results obtained with this apparatus were in close agreement with the results obtained with erosion vent plugs described in Section 16.3.1. Since the vent-plug tests are simpler, more rapid and cheaper to make, and since the Battelle gun evaluated mechanical factors only to a slight extent, Division 1, NDRC, did not duplicate it. Instead, attention was concentrated on testing methods (described in the next four sections) which also measured the mechanical suitability of a material as an erosion resistant liner or lining in a rifled gun bore.

16.3.5 Caliber .50 Erosion Testing Gun

The caliber .50 erosion-testing gun,[122] a special hypervelocity gun developed at the Franklin Institute for an accelerated erosion test, has been described in Section 11.2.1.

One of its most important uses was to determine the erosion resistance of a large number of metals and alloys under these hypervelocity conditions. A special form of the gun was developed to permit insertion of a short (8-in.) breech liner at the origin of rifling. Special materials were tested usually as rifled liners or as a plating or coating on the bore of a rifled gun-steel liner. A few full-length monobloc barrels with chromium electroplate applied to the whole bore surface were tested with regular or special projectiles. In most cases, a metallographic examination of the bore surface was made, at Harvard University, on the liner or barrel after firings.



These firing tests[76,77] aided in the evaluation of the materials discussed in Section 16.4, where references are given to other chapters for details about some of the more important ones. Of the materials tested as liners only molybdenum (particularly when hardened by a small amount of alloying with cobalt and by intensive mechanical working), tantalum, and chromium-base alloys gave promise of being sufficiently erosion resistant to withstand hypervelocity conditions. The caliber .50 erosion-testing gun was particularly useful in the development of molybdenum liners.[h] Materials which gave similar promise in the form of coatings were pure chromium electroplates and duplex electroplates with a chromium bore surface and an undercoat of either pure cobalt or a cobalt-tungsten alloy (Section 20.2).

Steels, Monel, and high-nickel alloys showed poor erosion resistance. The bore surface of liners of Stellite No. 21 and Stellite No. 22 melted when double-base powder was used, but showed excellent resistance to both melting and chemical attack with single-base powder. Pure cobalt and cobalt-tungsten alloys applied as electroplates melted with double-base powder and, in some cases, the latter were not sufficiently adherent, although both showed promise as undercoats under chromium electroplate. Copper plate melted; nickel-tungsten alloy electroplates, and Parcolubrite coatings were not erosion resistant; duplex plates of nickel or copper or both under chromium and pyrolytic coatings of molybdenum on Stellite No. 21 or gun steel were mechanically unsatisfactory because of poor adherence or severe deformation.

16.3.6 Short Rifled Caliber .30 Liners

Because of the short duration of contact between powder gases and the bore surface, the high overall barrel temperatures during long bursts, (Section 5.4.2) and the high rate of fire with the resultant severe mechanical effects of projectile impact on the bore surface, the results of erosion vent-plug tests (Section 16.3.1) have only very limited applicability in the selection of materials to improve the performance of caliber .50 machine gun barrels and other automatic small arms barrels. Since the vent plug is not rifled and no projectile is used, the influence of various physical and mechanical properties, such as ductility and hardness, on the durability of a material as a liner in any gun is not evaluated.

To meet these objections a new testing device was developed.[81] In the first model a short rifled liner of the material to be tested served as a barrel and was fitted into the regular erosion vent-plug explosion chamber. Solid copper slugs were fired through the barrel and a rapid erosion rate was obtained by using a large powder charge. Results on the first trials gave excellent results which could be correlated with erosion in a caliber .50 machine gun.

Since firing tests with this arrangement were slow, a new caliber .30 erosion-testing gun, designated Erosion Gun A, was designed. This fired at a much more rapid rate and employed readily available standard caliber .30 AP bullets which were fired through a 6-in. long rifled barrel of the material under test. The barrel was mounted in a 37-mm breech mechanism, chambered for caliber .50 cartridge cases hand-loaded with double-base powder (13% nitroglycerine). Pressures were measured with a piezoelectric gauge threaded into the chamber.

Erosion Gun A was used to test the relative performance of various electroplated coatings particularly chromium plates of various types and thicknesses (Section 16.4.2), and was also used to test a liner bored from a rod of pure swaged cobalt (Section 16.4.7).

16.3.7 Caliber .30 Machine Gun Liners or Barrels

The first tests of possible erosion resistant materials in an actual gun under the erosion program of Division 1, NDRC were made by inserting short liners (some smooth bore and others rifled) of the special materials in the breech end of a caliber .30 machine gun which was then fired with caliber .30 bullets and double-base powder. The barrels were bore-gauged during the firing test and later subjected to metallographic examination. A high-alloy steel, pure nickel (Section 16.4.9) and steel liners with diffused chromium (Section 16.4.2) and with diffused tantalum (Section 16.4.6) bore surfaces were tested.[78] All except the last showed a poorer resistance to erosion than gun steel under comparable conditions.

Two high-alloy steels (Silchrome XCR and XB valve steels) that showed better erosion resistance and better hot hardness than gun steels, were selected for trial as caliber .30 aircraft machine gun barrels, as described in Section 16.4.11.

[h] Under a contract with the Bureau of Ordnance, Navy Department, additional tests in this weapon were carried out by the Franklin Institute in 1946 as part of the program for the further development of molybdenum liners (Section 18.1).

[redacted]

RECEIVED
FEB. 196
ABERDEEN PROVING GROUND, MD.
STEAP-TL

16.3.8 Caliber .50 Heavy or Aircraft Machine Gun Liners or Barrels

The test of materials as short breech liners in caliber .50 machine gun barrels or as electroplates or other bore coatings on short steel breech liners was found to be a very useful, convenient, and rapid method of determining the ability of a material to withstand the combined effect of high temperature, attack by powder gases, and mechanical stresses at the bore surface during the firing of this gun.

A method of liner insertion for the testing of materials was devised at the Geophysical Laboratory.[i] Two caliber .50 heavy machine gun barrels were modified to make one barrel in two sections, a breech section containing the liner and a muzzle section, joined together with a threaded joint as described in Section 11.2.2. The caliber .50 Browning machine gun was selected because this gun could be fired readily and cheaply in a simple, easily constructed firing range under the control of the investigator. The heavy (28-lb, 45-in.) barrel was selected instead of the lighter (10-lb, 36-in.) aircraft barrel for trials of liner insertion because of the heavy barrel walls at the breech end of this barrel.

Later the Crane Company found that the design it had developed for the stellite liner for caliber .50 aircraft machine gun barrels (Chapter 22) was satisfactory for testing other materials. The large number of firing results obtained at the Geophysical Laboratory and at Crane Company in caliber .50 machine gun barrels with liners or with plated bores or with combinations thereof are given in two NDRC reports[80,81] and the results are recorded in this report under the individual materials tested later, in this chapter and in Chapters 17 to 24, inclusive.

Every gun, or at least every class of guns, is to some extent a separate problem with respect to requisite characteristics of its bore surface if erosion is to be minimized and performance enhanced. What would be a great improvement in a caliber .50 machine gun barrel might be no improvement or might be impractical to apply to a large antiaircraft gun or to an 8-in. Naval gun. Nevertheless, fundamental data can be obtained and much of it can be applied to the same size gun fired under any or all of the following conditions: more severe schedules, hypervelocity conditions, higher cyclic rates of fire. Such information can also be applied to larger guns, particularly if the significant differences between types of guns are studied and taken into consideration.

Experiments performed in the development of very superior machine gun barrels showed that the best evaluation of the relative merits of various liner materials could not be obtained if failure occurred by deterioration of the steel barrel into which the liner for test had been inserted. A satisfactory test of the liner material was only obtained when the liner failed before the barrel or when the liner and barrel "wore out" simultaneously. The roles of the liner, the barrel, and of an erosion-resistant electroplate on the steel bore ahead of the liner in the overall performance of machine gun barrels are described in Chapter 24. The flexible CGL firing schedule which has been found so useful for the evaluation of materials and combinations and their performance is described in Section 24.1.3.

16.3.9 Measurements of Thermal and Mechanical Properties

In order to estimate whether there is any possibility or probability that a given chemically resistant material might meet the thermal and mechanical requirements of a bore surface in a specific weapon, or whether the properties of such a material might be altered by metallurgical treatment (for instance, by alloying, mechanical working, or heat-treatment) to enable it to meet some requirement in which it may be deficient, a knowledge of certain thermal properties and of the mechanical properties of the material at room temperature and at elevated temperatures is always desirable and usually necessary. Unfortunately, the part which the absence of or deficiency in a certain property may play in determining behavior and performance of the material in a gun is obscured by the interplay of factors. However, valuable preliminary information can be gained from tests of physical and mechanical properties and the choice of materials for firing tests can be narrowed down to a few promising substances.

Fortunately, many of the thermal and mechanical properties of those pure metals and alloys, which

[redacted]

[i] The program of liner testing in the caliber .50 heavy machine gun barrel undertaken at the Geophysical Laboratory combined three purposes: (1) to find out what happened in a barrel during firing (the mechanism of erosion and dimensional changes in the bore); (2) to obtain quickly some information on the relative erosion resistance and reaction to firing of various materials; and (3) to obtain data which might serve as a basis for predicting how erosion in larger guns might be minimized. (In connection with the latter purpose see the *Introduction* of Section 11.2.2.)

were found to be resistant to chemical attack by hot powder gases, were known. However, many measurements on the most promising of these materials were made by contractors of Division 1, NDRC. These results are summarized in the other chapters of Part V where these specific materials are discussed.

Meltability

Whether or not a particular bore surface material reaches its melting point or softening range depends on the heat input under the particular firing conditions (Section 5.2), the rate of heat conduction away from the bore surface, and the specific heat of the bore-surface material. The relations of these factors have already been discussed in Section 5.4.4. The melting points of all the pure metals and the fusion ranges of most of the alloys were known as were their thermal conductivities and specific heats, and only a few additional measurements[i] were necessary.

Thermal Expansion

The ease or difficulty of satisfactory insertion of a liner of a special material or the adherence of an electroplate or other bore coating depends in part on the relative coefficients of thermal expansion of gun steel and the particular special material as well as the modulus of elasticity and other mechanical properties. For example, major insertion difficulties must be surmounted in the satisfactory insertion of a molybdenum liner, as discussed in Section 26.5.2. Because the coefficient of thermal expansion of molybdenum is only about one-half that of gun steel, a shrunk-in liner is no longer in heavy compression when the gun tube becomes hot and because of the high modulus of elasticity of molybdenum it takes a high proportion of the stress.

The coefficient of thermal expansion of a material for use as the whole or a part of the bore surface of a gun tube should be low so that at the elevated temperatures reached during firing the rotating projectile does not lose engagement with the rifling and fail to attain adequate spin. Poor performance was obtained with special caliber .50 aircraft machine gun barrels of a stainless steel barrel material in which short breech liners of Stellite No. 21 had been inserted, partly as a result of the high coefficient of expansion of such a steel which resulted in inadequate spin and unstable bullets at a much earlier stage than with similar modified gun-steel barrels.

Data on the thermal expansion of most materials were already available. Data on a number of materials were obtained at Crane Company[80] using a recording dilatometer. Measurements were made on chromium-base alloys (Chapter 17) at the University of Michigan for the Climax Molybdenum Company.[87]

Thermal Transformation

Some pure metals or alloys may exist in two or more different crystalline forms. Each such form is stable only over a certain range of temperatures (and pressures) and when the inversion temperature (or inversion range) is reached there is an abrupt polymorphic change accompanied by a volume change. Any abrupt volume change affects erosion resistance and in addition the relative erosion resistance of the several crystalline forms of a given material may be quite different. In the case of a coating on steel such volume changes during the alpha-gamma transformation in the steel or changes in the coating at some inversion in the coating material may cause cracking, poor adhesion, and rapid deterioration of the bore surface. Thermal transformations in gun steels have already been discussed in Section 13.2.3. The inversion temperatures of cubic and hexagonal cobalt and cobalt solid solutions were determined and are discussed in Section 19.3.2. Measurements[80] were made on many materials, using a recording dilatometer, in order to detect inversions and other phase transformations that may occur in the heating and cooling cycle, as well as to measure the thermal expansion.

Change in Properties on Annealing or Heat-Treatment

Permanent changes in the mechanical properties of a bore surface material may result from exposure of such a material to the thermal cycle in a gun bore during firing. Hard chromium electroplate (Section 20.2.2), for example, has a Vickers hardness number [VHN] of about 800 as deposited, and on annealing at elevated temperatures this hardness gradually drops to around 145 VHN. A similar decrease in the hardness of chromium plate occurs in plated guns as a result of annealing during the firing. In stellite and other alloys (see Section 19.3.5) a permanent change

[redacted]

[i] For data on the fusion range and specific heat of Stellite No. 21 and on the fusion range and thermal conductivity of chromium-base alloys, see Sections 19.3.8 and 17.3.1, respectively.

in hardness (precipitation- or age-hardening) may occur during firing, as well as the surface hardening (work-hardening) which may occur as a result of the mechanical working of the bore surface by the projectile. In addition to such changes in hardness and other mechanical properties, grain growth of metals or alloys may also occur as a result of heating and cooling during firing.

Tensile Strength, Ductility, and Modulus of Elasticity

The behavior of erosion resistant metals and alloys as bore-surface materials, particularly when applied as relatively thick sections of metal in the form of gun liners, is dependent upon the strength of these materials especially at elevated temperatures. Unless an erosion resistant material is sufficiently strong to resist the high pressures as well as the high temperatures without a large permanent expansion or brittle failure, and strong enough at elevated temperatures to resist the mechanical forces of engraving of the projectile without permanent displacement of metal by flowage (swaging effect), it will not be a satisfactory bore-surface material. If the ductility of the material is low it will be unable to withstand the stresses that occur during the pressure and temperature cycles in the bore, and also engraving stresses, without brittle failure by surface cracking and cracking in depth. Both the strength and modulus of elasticity of the material as compared with gun steel, as well as the relative coefficients of expansion, determine, in part, the adhesion of an electroplate or other bore coating in a steel bore and the ease or difficulty of insertion of a liner in a steel gun tube.

Attention should be called here to the importance of high-temperature strength in the gun barrel material as well as in the erosion resistant bore-surface material. For use with severe firing schedules at ordinary velocities or for hypervelocity conditions, the poor high-temperature strengths of conventional gun steels limit the performance that might be obtained by use of an erosion resistant liner or bore coating. No such liner or bore coating removes heat from the gun barrel. As described in Section 24.5, caliber .50 aircraft machine gun barrels made of special heat-resisting steels, which also contain a breech liner of Stellite No. 21 and whose bores are chromium-plated ahead of the liner, show greatly improved performance over similar lined and plated barrels made of WD 4150 steel.

The results of measurements of ultimate tensile strength, yield strength, breaking strength, elongation, reduction of area, and modulus of elasticity are summarized in Chapters 17 to 21, where specific erosion resistant materials are discussed.

Notch Impact Tests and High-Velocity Impact Tests[k]

When it is fired, a gun tube is subjected to rapidly applied stresses (Section 7.1), both from sudden large changes in pressure and also from projectile impact on the bore surface. Therefore it is desirable to obtain some estimate of whether an erosion resistant liner material might have sufficient toughness to prevent cracking, fracture, and disintegration under these conditions. For this purpose standard Charpy tests with either keyhole or V notches were made on some materials and the results are summarized under the specific materials in other chapters of Part V. The notch effect is important in determining the life of a material and the nature of its failure. For example, caliber .50 machine gun liners of Stellite No. 6, which (unlike Stellite No. 21) has a low Charpy value, gave excellent performance during initial severe bursts of fire but later, presumably because surface cracking (heat-checking) became severe enough to provide "notches," brittle failure occurred by cracking and propagation of cracks completely through the liner wall.

More attention must be paid to the dynamic physical properties of barrel steels at elevated temperatures, as well as to these properties of special bore-surface materials, in order to utilize more fully the advantages gained by the use of such an erosion resistant bore-surface material in the form of a breech liner or a plated bore. Firing tests, described in Section 24.5, have shown that regular barrel steels deteriorate before an erosion resistant liner or coating shows any severe wear or other failure.

Preliminary investigations were made at the Crane Company (with the apparatus shown in Figure 2) of the properties of steels under high-velocity impact conditions, comparable to the stress propagation conditions obtained during firing. These tests indicated

[k] At Watertown Arsenal[277] a constant-deformation machine has been developed as a testing device for progressive stress damage in 8-in. tubes. It measures qualitatively the mutual influence of ductility of the barrel steel, shape of the stress-raiser, stress, rate of straining and temperature on the tendency of steel to fail by cracking when loaded repeatedly for a relatively small number of times.

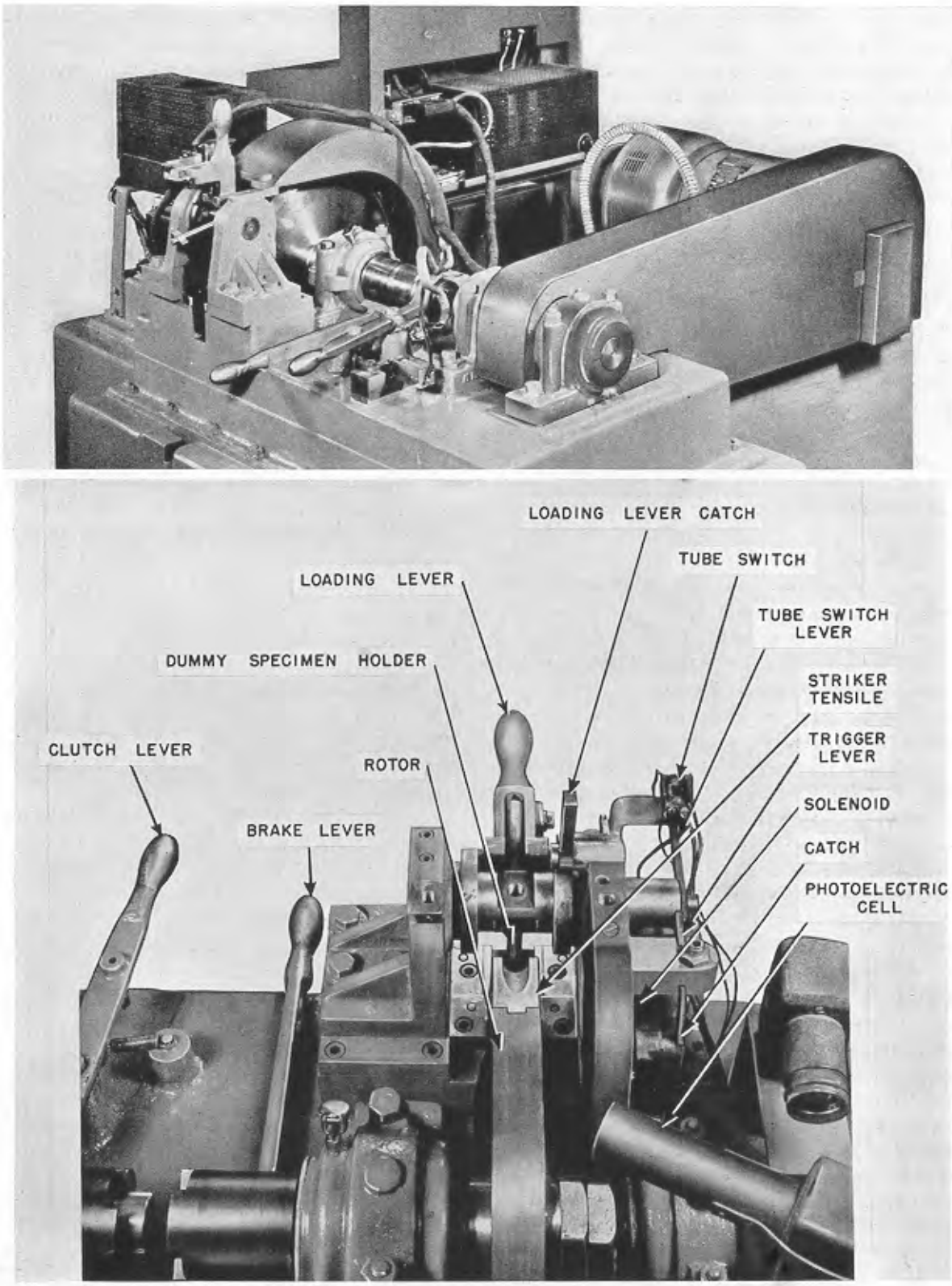


FIGURE 2. Apparatus for high-velocity impact test. (Photographs used by courtesy of the Crane Company.)

CONFIDENTIAL

strength values for metallic materials several times as great as the values accepted for static-design purposes. The mechanism of metallic deformation under conditions of high velocity and elevated temperature is of an essentially different nature than slow deformation.[1] Specifications for gun steels and for erosion resistant materials for liners should, therefore, be based upon the dynamic elevated temperature properties, rather than upon the conventional criteria of chemical composition and static tensile properties at room temperature. Before such specifications can be prepared it must be ascertained which dynamic elevated temperature properties are pertinent to gun barrel performance and suitable apparatus for determining such properties must be adequately developed. It is recommended that such studies be pursued.

Hardness, Hot-Hardness, and Wear Resistance

Firing tests on liners of pure molybdenum in the caliber .50 machine gun barrel (see Section 18.6.1) emphasized the importance of hot-hardness in an erosion-resistant liner material. Even though this soft metal was resistant to chemical attack by powder gases and to melting, early failure occurred by deformation of the rifling and its complete obliteration by swaging impact of the bullets. Subsequent tests on barrels with chromium-plated bores (Section 20.2.3) showed that the erosion resistance of chromium could not be fully utilized because the gun-steel lands beneath the chromium failed by deformation and flowage unless they had been hardened by nitriding or induction-hardening. The rate of loss of hardness (and strength) of the steel bore beneath an erosion-resistant electroplate or other thin bore coating plays an important part in determining the usefulness and permanence of such a bore protection.

The resistance of a material to deformation by the projectile is related to hot-hardness and hot-strength but is not determined by these alone but also by high-velocity impact resistance, mentioned in the preceding subsection. Hot-hardness data for most materials were not available and a large number of measurements were made at the Research Laboratory of the Climax Molybdenum Company for Division 1, NDRC contractors. Most of these results have been presented in several NDRC reports[59,109,110] and a few are summarized for specific materials in other chapters of Part V. In a previous subsection on "Change in Properties on Annealing or Heat Treatment," attention has been called to the effects of the thermal cycle in a gun on the hardness of certain erosion resistant metals or alloys.

A bore-surface material should have good resistance to abrasion and wear at high temperatures. Such resistance is presumably another corollary of high hot-hardness. No measurements of coefficient of friction or wear resistance were made. Measurements of these properties might have been helpful in selecting bore-surface materials. The first problem is that of apparatus, a satisfactory form of which has not yet been devised.

Hydrostatic Tube Testing

A very useful method for determining the mechanical behavior of erosion resistant materials was to test tubes with hydrostatic pressure.[81] By means of the simple apparatus shown in Figure 3 the tensile properties and other properties of a liner material in

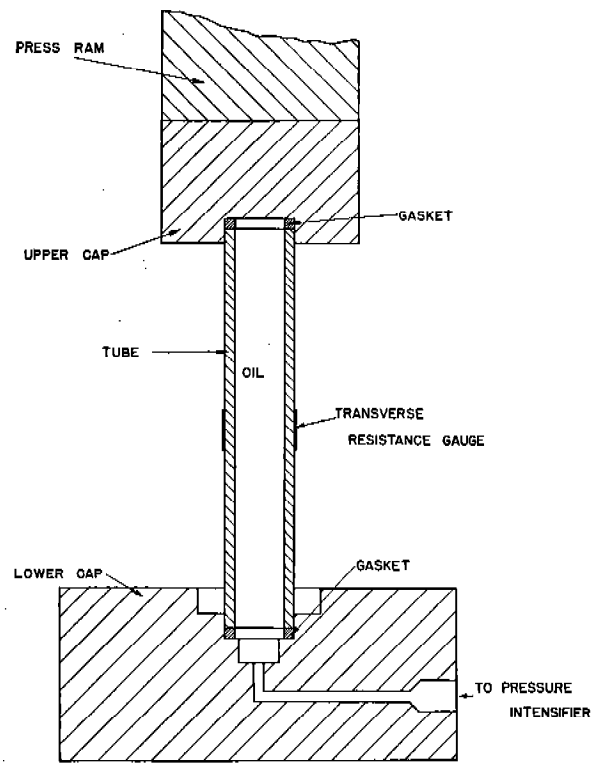


Figure 3. Hydrostatic tube-testing device. (This drawing was obtained by courtesy of the Geophysical Laboratory.)

[1] The influence of impact velocity on the properties of some metals and alloys at *room temperature* has been studied under the auspices of the War Metallurgy Committee (Division 18, NDRC).[558]

the shape of a tube could be determined. By electroplating the inside of steel tubes, subjecting them to hydrostatic pressure of different amounts, and examining them at different stages in the test, the inner fiber stress at which the plate cracked could be found.

This method of testing was also used to detect flaws or lack of strength in individual liners before insertion in the gun barrel for test. A rifled liner was subjected to successively increased hydraulic pressures up to the maximum pressure of the gun barrel. If the liner passed this test but failed in the gun, such failure in all probability was not caused by a flaw in the particular sample. This preliminary nondestructive test that insured the soundness of the liners fired was very helpful in the early stages of the development of molybdenum liners, before the fabrication methods described in Chapter 18 had made it possible to produce samples without flaws.

Adherence Test for Platings or Coatings

To determine the relative adherence of platings or coatings prepared in different ways on steel or other material, a special ring test[93] was developed in which a ring cut from a plated tube was severely deformed by compressing it longitudinally at room temperature.

Bend and Ring-Compression Tests

In addition to the ring-compression test just described for determining the adherence of plates or coatings, similar ring-compression tests[96] were used to evaluate the ductility and strength of various samples of molybdenum fabricated by different methods. During the development of improved fabrication methods for molybdenum described in Section 18.3, it was necessary to have a simpler test so that the strength and ductility of the metal could be determined quickly on a large number of specimens. A simple bend test[95] on a modified tensile and guided bend test machine was developed for this routine testing.

Flaw Detection

In addition to the use of the hydrostatic tube testing method (already described in this section) for the detection of flaws in a metal or alloy, several other methods were employed. Radiographic inspection[80] of castings of Stellite No. 21 was used to detect blowholes, porosity, and refractory inclusions. Cracks in molybdenum[95] were detected either by treating the pieces with aqua regia which caused the cracks to appear as black lines or by the use of the "zyglo" method, where the piece is soaked in thin oil, sprinkled with a fluorescent powder, and then examined under ultraviolet light. Magnetic, electronic, and sonic devices for the detection of flaws in metals and alloys were considered but were not actually used in the erosion-resistant liner program.

Machineability

The machineability of a liner or gun barrel material is an important practical matter. Both tungsten and molybdenum were considered for development as possible liner materials for hypervelocity guns. One reason for rejection of tungsten in favor of molybdenum was the lack of machineability of the former. Some alloys are considered difficult to machine because no one has the "know how." By the use of the proper cutting tools, feeds and speeds, at Crane Company[119] it was easy and practical to bore and rifle liners of Stellite No. 21 and even liners of the much more refractory Stellite No. 6. Similarly, at Climax Molybdenum Company, satisfactory practical methods of boring and rifling liners of chromium-base alloys[87] were developed. The ease with which molybdenum may be machined was improved by studies[96] made at Westinghouse Research Laboratories.

There seems to be little doubt that, if necessary, grinding methods could be successfully developed for handling nonmachineable metals or alloys. Such methods can only be used for rifling gun bores of medium or large caliber. For small bores, such as caliber .30, .50, or .60 (or even 20 mm) grinding methods are probably impossible or at least impractical.

16.4 EVALUATION OF LINER AND COATING MATERIALS

16.4.1 Introduction

By means of the test methods just described in Section 16.3, the possibilities of various metals and alloys as bore surface materials have been evaluated. No substance was found to possess the perfection required in an ideal erosion resistant material as described in Section 16.2. Several metals or alloys were found which, in addition to being resistant to chemical attack by hot powder gases, also met the thermal and mechanical requirements of a bore sur-

face for a specific weapon under severe firing conditions or could be sufficiently changed by metallurgy (alloying, mechanical working, heat-treatment, etc.) to enable them to meet some requirement in which they were somewhat deficient. Before making an appraisal of possible bore-surface materials, a short analysis of the importance of the several factors contributing to failure of such materials will be given. A firing test[49] of a short breech liner of pure unhardened molybdenum in a caliber .50 heavy machine gun barrel showed that, even though there was little or no powder gas erosion (thermal and chemical attack), the lands at the origin of rifling and for some distance beyond were deformed and flattened, with the result that there was a very rapid loss in both velocity and accuracy. A similar result was obtained in regular steel barrels for this same gun, whose unhardened steel bores had been protected from chemical and thermal attack by an erosion-resistant plating (chromium electroplate). The steel beneath the plate deformed and rifling was obliterated, as described in Section 10.5.3. These results emphasized the importance of hot-hardness, resistance to permanent deformation, and wear resistance in a machine gun barrel, even at ordinary velocity.

The hypothesis was advanced that, since the time that powder gases are in contact with the bore surface is very short in the caliber .50 machine gun, possibly hot-hardness and wear resistance rather than resistance to powder gas erosion might play the most important part in determining performance. To test this hypothesis a few materials of known hot-hardness but different composition were selected for test. Liners of high speed steel, two hot die steels, and Stellite No. 6 were prepared and tested.[80] The first three materials all showed poor performance, owing to thermal and chemical attack by powder gases and two of them cracked besides. The liner of Stellite No. 6, on the other hand was resistant to thermochemical attack and to deformation of the rifling. However, ultimate failure occurred by cracking. These results showed that resistance to thermochemical attack was a prime requisite for a bore surface material, even in the caliber .50 barrel at ordinary velocity. It turned out that in the stellite selected for this test, hot-hardness had been overemphasized at the expense of ductility, for later tests of Stellite No. 21 showed that it has adequate hot-hardness and wear resistance combined with excellent ductility. The outstanding success with this material as a machine gun liner, will be outlined later in Section 16.4.8.

The comparative performance of Stellite No. 21 and molybdenum in caliber .50 machine gun barrels and of Stellite No. 21 and molybdenum (both unhardened and hardened) under hypervelocity conditions in the caliber .50 erosion-testing gun showed that resistance to plastic deformation and wear are important qualities of an erosion resistant material but are not sufficient to meet all of the conditions. The deformation of the rifling in liners of pure unhardened molybdenum in both of these guns showed that resistance to powder gas erosion (thermal and chemical attack) is also not a self-sufficient quality. The very promising performance[78] of a liner of hardened molybdenum (Section 18.6.2) in the caliber .50 erosion-testing gun indicated that the combination of thermochemical resistance (no chemical action with or melting by hot powder gases) with high hardness *at the working temperature* of the gun is a sufficient qualification provided, however, that the liner material has sufficient ductility and impact resistance both hot and cold to prevent brittle failure and disintegration. Preliminary firing results[87] with liners of chromium-base alloys (Section 17.4.3) indicated that even relatively brittle materials, which have the other necessary requisites of a bore-surface material, may be utilized if they are so inserted as to maintain them under compression and minimize the possibility of brittle impact failure.

An appraisal of possible bore-surface materials will now be given. Additional details about the most promising ones are given in later chapters of this report. For further information about the others references are given to the reports submitted by the contractors of Division 1.

16.4.2 Chromium Electroplates, Duplex Plates and Other Chromium Coatings

Chromium electroplates show considerable promise as bore-surface materials both at conventional velocities with high rates of fire and under hypervelocity conditions. Pure chromium deposited electrolytically is a brittle metal and quickly develops cracks as a result of firing stresses and some recrystallization during firing. Hot powder gases penetrate these cracks and attack the underlying material (see Section 13.2.3) and possibly the chromium and finally there is failure by undercutting, as described in Section 20.2.1. As a result of the studies of Division 1, NDRC, combined with those undertaken by the Army Ordnance Department, the effectiveness of



chromium plate in resisting erosion and thus improving the life and performance level of automatic, rapid-fire guns has been demonstrated and the effectiveness of chromium plate for service under hypervelocity conditions has been indicated.

The possible advantages of duplex plates and studies of alloy plates are discussed in Chapter 20. The development of improved machine gun barrels by the application of chromium electroplates in conjunction with bore hardening or with liners and other barrel modifications is described in Chapters 23 and 24. The commercial development of the chromium plating of small arms barrels is described in Chapter 25. The success obtained in improving plate utilization, particularly under hypervelocity conditions, by mitigation of the mechanical effects of the engraving of the projectile by the use of pre-engraved projectiles or by the use of the Fisa protector is described in Chapters 31 and 32, respectively.

In addition to the use of hardened steels under chromium electroplate, "hot-hard" liners of Z nickel and of Stellite No. 21 were tried as base material for chromium electroplate. The results were unsatisfactory because of poor adhesion of the plate on these surfaces.

The deposition of chromium pyrolytically from the vapor of its carbonyl was investigated,[74,93] as described in Section 21.6. The method does not appear to be suitable for gun bores. The carbonyl[73] is difficult to prepare. The process of plating is complex and difficult and the metal, which contains some carbon, is hard and very brittle.

A firing test was made in a caliber .30 machine gun[78] on a steel liner with a bore surface of diffused chromium prepared by heating it in an atmosphere of chromium chloride.[322] Serious erosion occurred and performance was inferior to gun steel. Attention is called to the point that a "diffused chromium" surface is not a surface of pure chromium but a graded series of iron-chromium alloys produced by a diffusion or "cementation" process.

As is brought out in Section 20.5, investigation should be continued concerning the chromium electroplating process, types of pure chromium plate, alloy plates and duplex plates, and the properties of such plates, and the effects of gun tube and projectile design on their performance. Studies should be made of the performance in medium-caliber guns of these plates on hardened steel bores and on special full length or partial length thin bore liners or linings of "hot-hard" alloys.

16.4.3 Chromium and Chromium-Base Alloys

Erosion vent-plug tests, other laboratory tests, and examination of worn chromium-plated medium-caliber guns had emphasized the excellent resistance of chromium metal to melting and chemical attack by hot powder gases even under severe conditions. Attempts were made to utilize this metal as a liner material. The outstanding deficiency of chromium is cold ductility. Hence a liner made from chromium electroplate (Section 17.2.2) cracked after having been fired only a few rounds.[49]

Pure chromium, when melted and cast in a vacuum, yielded ingots of soft but brittle metal. Attempts[83] to impart ductility by control of purity, by mechanical working, and by additions of small to moderate amounts of alloying constituents, which are described in Chapter 17, were unsuccessful. Although the metal showed some hot malleability over a limited range of temperatures, it was always brittle when cold.

However, a group of chromium-base alloys[87] (vacuum melted alloys with approximately 60% chromium, 25 to 30% iron, 10 to 15% molybdenum with very low carbon) shows considerable promise. They have very good resistance to thermal and chemical attack under hypervelocity conditions and are strong and hard so that no deformation of the rifling occurs. Their one weakness is their low ductility. In spite of this deficiency, when liners were properly inserted in caliber .50 aircraft machine gun barrels, they showed outstanding performance and did not crack and disintegrate. These alloys and tests are discussed in Chapter 17.

Since both chromium metal and copper have excellent resistance to chemical attack by hot powder gases, an attempt was made to improve the mechanical properties of chromium by preparing powder metallurgy compacts[83] of chromium powder impregnated with an optimum amount of copper with or without subsequent mechanical working by swaging. The best of these compacts showed low weight losses (considerably less than gun steels) in erosion vent-plug tests[49] but not as low as were shown by corresponding compacts made from molybdenum or tungsten powders (Sections 16.4.4 and 16.4.5). Because of the melting out of copper and the low hardness of the compacts, they cannot be considered potentially useful as gun liner materials. Nickel and palladium were tried as impregnating materials for chromium powder but attacked the chromium and formed alloys.

16.4.4 Molybdenum and its Alloys

Pure molybdenum has outstanding resistance to both thermal and chemical attack by powder gases even under the most severe conditions. The melting point (2620 C) is so high as to remove the possibility of bore-surface melting. Firing tests[49,76] showed, however, that as usually fabricated it was not strong enough, not hard enough, and not ductile enough to make a satisfactory liner. Fabrication methods had not been developed to permit preparing the desired shapes and sizes. Furthermore, owing to the large difference in coefficients of thermal expansion and modulus of elasticity between molybdenum and gun steel, liners are difficult to insert.

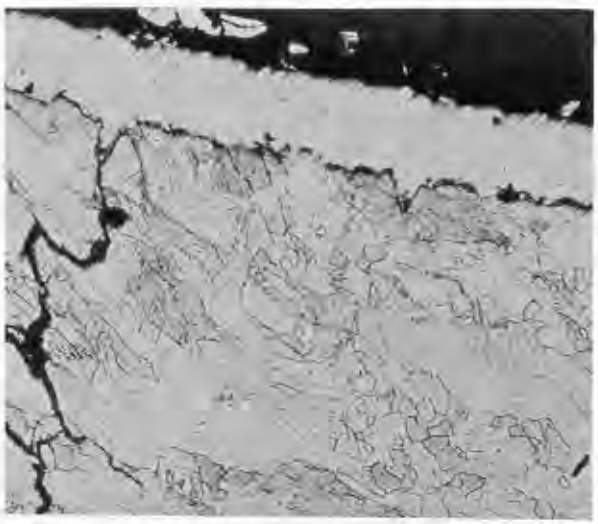


FIGURE 4. Helical two-stave liner of molybdenum containing 0.1 per cent cobalt fired 2,024 rounds with ball bullets, M2 and double-base powder in the caliber .50 erosion-testing gun. Cross section ½ in. beyond origin of rifling. Etched with 10% KOH+10% $K_3Fe(CN)_6$; *100X*. (This figure has appeared as Figure 11 in NDRC Report No. A-405.)

As described in Chapter 18, development[52,95,96] has shown that all three of the mechanical deficiencies can be overcome by alloying with small amounts (about 0.1 to 0.2%) of cobalt or certain other metals and by intensive mechanical working accompanied by proper heating and annealing schedules. Satisfactory fabrication and insertion methods have been developed. Suitably fabricated molybdenum alloy most nearly approaches the properties of the ideal erosion resistant material described in Section 16.2. Figure 4 shows a cross section of a liner of molybdenum containing 0.1 per cent cobalt, which had been fired 2,024 rounds. The bore surface of this same liner is shown in Figure 19 of Chapter 18. Sufficient progress in the development of hardened molybdenum was made under Division 1's auspices, so that the Navy Department continued to support the efforts of the Westinghouse Electric Company to make this material in a form suitable for large gun liners, following plans developed by Division 1, as described in Section 33.1.3.

In addition to fabrication by powder metallurgy methods, studies[97] were made of arc melting, thermit melting, and vacuum melting of molybdenum and high-molybdenum alloys. These methods, which do not seem to offer any advantages over powder metallurgy, are also described in Section 18.7. Pyrolytic plating[98] of molybdenum from the vapor of its carbonyl was investigated and, as described in Section 21.3, does not appear to be suitable for gun bores.

Aqueous electroplating[89] of molybdenum was investigated, but the deposits were impure and poorly adherent. Molybdenum coatings on steel were also made by depositing the suboxide from aqueous solutions and then heat-treating in hydrogen.[95] These plates were brittle and the process was time-consuming and generally unsuitable. Sprayed coatings[99] on steel bores were prepared and shown by firing tests[79] to be brittle and completely unsatisfactory.

In an attempt to avoid fabrication difficulties and improve ductility, powder metallurgy compacts of molybdenum powder and copper (trade name Elkonite) were prepared and tested.[49] They showed excellent resistance to powder gas erosion, nearly comparable to that of pure molybdenum in tests as 1/16-in. erosion vent plugs. However, when one of the best molybdenum-copper Elkonites was tested as a short rifled tube (See Section 16.3.6) using copper slugs as projectiles, the tube split when tested without a steel backing and showed deformation when adequately supported to prevent splitting. These alloys lack the strength and hardness to resist swaging impact by the projectile and show little promise as gun liners.

16.4.5 Tungsten and Its Alloys

Tungsten has the highest melting point of any of the erosion resistant metals. Because its melting point is higher than the adiabatic flame temperatures of conventional propellants, no melting of a tungsten bore surface could occur. All laboratory tests showed that pure tungsten and all tungsten-molybdenum alloys have excellent resistance to chemical attack by

powder gases. In spite of these advantages, no attempt was made to develop tungsten as a liner material because it was short in supply, presented the same fabrication problems (only in a more serious degree) as molybdenum, had the same mechanical deficiencies and difficulties of liner insertion as molybdenum, and besides tungsten (unlike molybdenum) is machineable only with very great difficulty.

Pyrolytic plating[93] of tungsten and of tungsten-molybdenum alloys on steel gun bores was investigated (Section 21.4) and found to be unsuitable because of the formation of brittle intermetallic compounds at the interface between steel and the plate during firing. Sprayed bore coatings[90] of tungsten were prepared. These were brittle and fragile and never subjected to firing tests.

Like the corresponding powder metallurgy compacts of molybdenum or chromium powder and copper, the tungsten-copper Elkonites were found to be resistant to powder gas erosion but even when the copper content was optimum for mechanical properties, they were unsuitable for gun liners because of lack of sufficient strength and hot-hardness to resist the swaging impact of the projectile.

16.4.6 Tantalum and Diffused Tantalum

Of the metals resistant to chemical attack by hot powder gases, only tungsten has a higher melting point than tantalum. However, pure tantalum is very soft—nearly as soft as pure copper—but, unlike copper, it is readily hardened by air, hydrogen, nitrogen, or any gases containing oxygen, nitrogen, hydrogen, or carbon. No hot-hardness data are available on hardened tantalum, and there is some doubt whether its hardness and wear and galling resistance are adequate for rapid-fire guns. Excellent promise for hypervelocity service in guns was confirmed by a firing test[76] on a rifled liner of air-hardened tantalum in the caliber .50 erosion-testing gun. The cross section in Figure 5 shows some cracking but no evidence of powder gas erosion. A liner for a caliber .50 machine gun barrel was prepared but was badly torn during an attempt to rifle it and never reached the test stage.

Tantalum is machineable with some difficulty using carbon tetrachloride as a lubricant but is easily galled or torn. In spite of its promise as a bore-surface material under hypervelocity conditions, no further development of tantalum as a liner material was made by Division 1 because it was so expensive, so short in supply, and so strategic for other war uses.

An attempt was made to plate tantalum on steel from a fused salt bath of potassium fluoride, potassium tantalum fluoride, and tantalum oxide at about 800 C. The results were erratic and no satisfactory plates were produced.

In firing tests[78] in the caliber .30 machine gun, two rifled steel liners with diffused tantalum bore surfaces of different thicknesses (0.0005 in. and 0.001 in.) performed better than gun steel. The thinner coating was more adherent and effective. Attention is called to the nature of diffused tantalum surfaces: such surfaces are not pure tantalum but a graded series of tantalum-iron alloys.

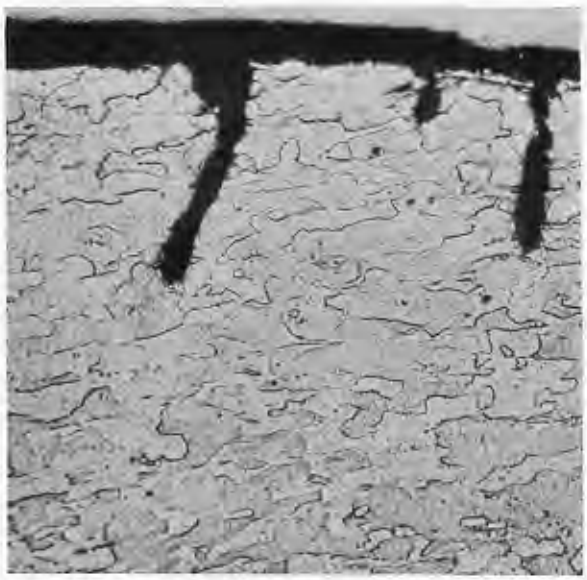


FIGURE 5. Rifled tantalum liner air hardened and fired 150 rounds with ball bullets M2 and double-base powder in the caliber .50 erosion-testing gun. Longitudinal section of a groove about ½ in. from the origin of rifling. The cracks appear wider than they really were, because they became broadened during the polishing of the section. Etched with aqueous solution of 25% H_2F_2 and 25% H_2SO_4; *200X*. (This figure has appeared as Figure 12 in NDRC Report No. A-405.)

16.4.7 Cobalt and High-Cobalt Alloys

Pure cobalt and high-cobalt alloys show excellent resistance to chemical attack by hot powder gases. Unfortunately, their relatively low melting points (1490 C for pure cobalt and lower fusion ranges for the alloys) limit their application under the most severe conditions where bore melting is an important factor in erosion. Pure cobalt has insufficient hot-hardness to resist deformation by swaging impact of

CONFIDENTIAL

the projectile in rapid-fire guns but most of the high-cobalt alloys have adequate hot-hardness and excellent strength and ductility.

Pure cobalt was tested[59] as a short rifled liner in the caliber .30 erosion gun "A" (see Section 16.3.6). Although it showed excellent resistance to chemical attack and melting, deformation of the rifling occurred. A liner of a cobalt alloy containing 7% tungsten tested[81] in a caliber .50 heavy machine gun barrel showed excellent performance, but is probably no better than Stellite No. 21 (see Section 16.4.8), which contains much less cobalt and can be fabricated more easily. A cobalt-base alloy (63 Co, 32 Fe, 4 Cr, 0.02 C) showed better erosion resistance than gun steels in a vent-plug test with 1/8-in. vent and showed good hot-hardness up to 600 C, but its hardness deteriorated very rapidly above this temperature and no further tests of this alloy were made. The results of laboratory tests on iron-cobalt alloys are described in Section 16.4.11.

A gun-steel liner electroplated with pure cobalt 0.005 in. thick was tested[76] in the caliber .50 erosion-testing gun under hypervelocity conditions with double-base powder. Adherence was satisfactory but melting and deformation of the rifling occurred. Cobalt-tungsten alloy plates (see Section 20.4), which can readily be hardened by aging, were deposited on gun-steel liners and tested both in the caliber .50 erosion-testing gun under hypervelocity conditions and in the heavy and aircraft caliber .50 machine gun barrels. Melting occurred under hypervelocity conditions and difficulties with adhesion were encountered in all tests unless the plate had been bonded to steel by a high-temperature diffusion treatment. These plates require more development and show considerable promise as bore-surface materials in medium caliber guns at normal velocities. The promise shown by pure cobalt plates and the alloy plates as undercoatings beneath chromium plate has already been pointed out in Section 16.4.2.

16.4.8 Stellite No. 21 and Other Stellites

The stellites are cobalt-base alloys with 25 to 30% chromium, and with a moderate amount (usually 5%) of molybdenum or tungsten, and small or moderate amounts of one or both of the metals iron and nickel, and with carbon contents varying from 0.2 to slightly over 1%. Stellites, because of their resistance to chemical attack by hot powder gases, hardness, and strength at high temperatures, and excellent wear and abrasion resistance, have shown outstanding performance in applications as short breech liners in machine gun barrels under firing conditions so severe that unmodified steel barrels are unable to withstand such schedules.

A large number of stellites have been tested as liners but, as shown in Chapter 19, none is as satisfactory as Stellite No. 21, which has the optimum combination of mechanical properties (including both hot-hardness and good ductility) for service as a liner material. The outstanding deficiency of the stellites is their low melting ranges (usually 1250 to 1300 C) which limits their application to guns in which bore melting is not an important factor in erosion. In the caliber .50 erosion-testing gun[76] under hypervelocity conditions liners of Stellite No. 21 performed satisfactorily with single-base (IMR) powder but the bores melted when double-base powder was used, as illustrated in the two parts of Figure 6.

Attempts were made to utilize the good ductility and hot-hardness of Stellite No. 21, under hypervelocity conditions or severe firing conditions in machine guns at an increased velocity obtained by the use of double-base powder, by protecting a stellite bore with a high-melting erosion resistant plate. These attempts were unsuccessful. Chromium deposited electrolytically from aqueous solutions had poor adherence and molybdenum applied by pyrolytic plating[93] was unsatisfactory because of the formation of a brittle intermetallic compound at the interface between plate and base material during firing, as described in Section 21.3. Further efforts should be made to deposit chromium by electroplating and then improve adhesion by high temperature bonding. Nitriding had no effect on the performance of liners of Stellite No. 21.

The properties of the stellites (particularly Stellite No. 21), the development of Stellite No. 21 as a liner material, studies of the utilization of this alloy (casting methods, bonding to steel, and the effects of hardness, composition, heat-treatments, method of insertion, liner length and wall thickness on performance), tests of stellites under hypervelocity conditions, applications of Stellite No. 21 to the 37-mm M3 cannon, and tests of other stellites in machine gun barrels are described in Chapter 19. Figure 7 shows a cross section of a Stellite No. 21 liner which had been fired almost 1,100 rounds in a caliber .50 machine gun. The successful insertion of liners of Stellite No. 21 and their application to machine gun barrels, and their

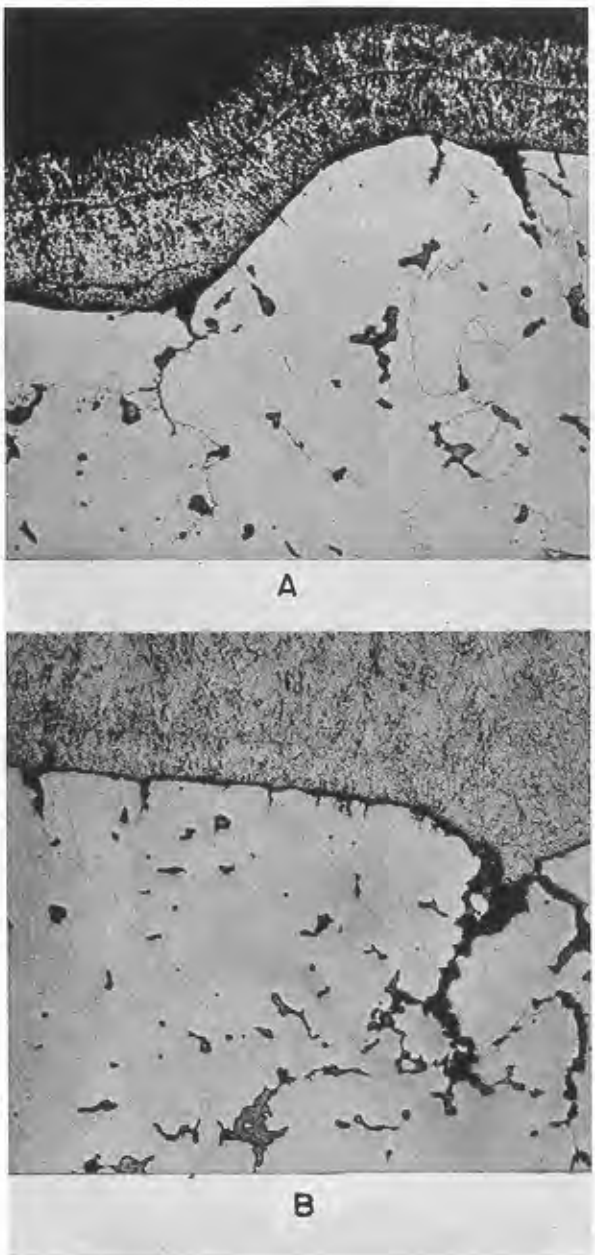


FIGURE 6. Investment cast liners of Stellite No. 21 fired with ball bullets, M2 in the caliber .50 erosion-testing gun; (A) 509 rounds with IMR (single-base) powder; (B) 85 rounds with FNH-M2 (double-base) powder. Cross sections 2 in. from the origin of rifling. The edge of the land in (A) is cracked; whereas the corresponding feature in (B) was melted away. Etched with 10% KOH+10% $K_3Fe(CN)_6$; *150X*. (This figure has appeared as Figures 13 and 14 in NDRC Report No. A-405.)

adoption for Service use are described in Chapter 22. The combination of Stellite No. 21 liner with choked-muzzle chromium plating ahead of the liner and other barrel modifications (weight, contour and composition of barrel steel) to effect even greater increases in performance is described later in Chapter 24.

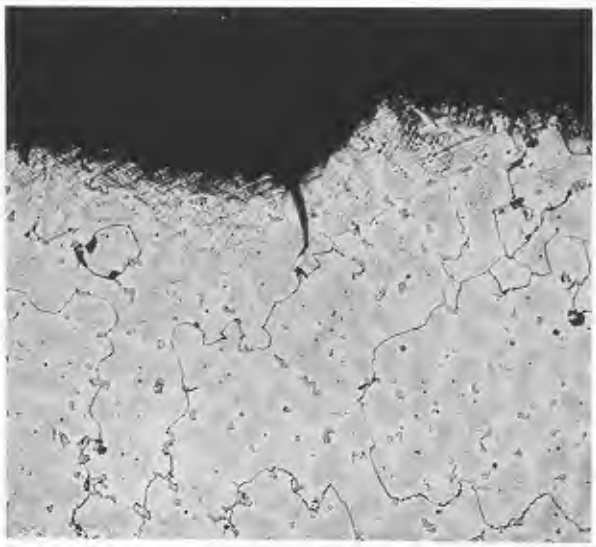


FIGURE 7. Cross section of a nine-inch investment cast Stellite No. 21 liner fired 1,098 rounds in a caliber .50 aircraft machine gun barrel at Purdue University range. Electrolytic aqua regia etch; *100X*. (This figure has appeared in NDRC Report No. A-416.)

16.4.9 Nickel and Nickel Alloys

Pure nickel has too low a melting point (1452 C), is too soft, and is not inert enough chemically for service as a bore-surface material under severe firing conditions. Even when hardened (and certain high-nickel alloys show excellent hot-hardness)[59] the performance is still unsatisfactory. Firing tests on pure nickel and high-nickel alloys, as gun liners and as electroplates, and laboratory tests, showed that these (except nickel-chromium alloys with more than 10% chromium) were subject to severe intergranular attack by powder gases, illustrated in Figure 8, and gave a performance barely equal to or inferior to gun steel.

One supposition[78] was that this intergranular attack was caused by the presence of small amounts of sulfur in the powder gases. It may have been related to a very small increase in the lattice dimensions of fine particles of nickel and some high-nickel alloys that were mixed with the propellant charge and fired into an evacuated tube (see Section 16.3.2). The reason for this increase was not investigated but it seems quite probable that it is caused by the solution of some carbon.[79] Similar experiments disclosed that high-

CONFIDENTIAL

nickel alloys containing silicon, aluminum, chromium, or copper (Monel metal) were unaffected by the hot powder gases. The high-nickel alloys with silicon or aluminum were not tested further and the results on the other alloys when tested as liners are described below.

The nichromes with more than 10% of chromium were resistant to intergranular attack but were too soft to withstand deformation by the projectile and when hardened (for example the Inconels) they lose their erosion resistance. Hastelloy "C" (an alloy with



FIGURE 8. Surface of a rifled nickel liner fired 500 rounds with double-base powder in a caliber .30 barrel. *100X*. (This figure has been taken from a joint progress report on Contracts OEMsr-537 and OEMsr-608.)

about 58% nickel, 17% molybdenum, 15% chromium, 4% tungsten and 6% iron) shows promise[80,126] as a liner material in machine gun barrels or under conditions where bore melting is not an important factor in erosion. The first liner of this alloy tested in the caliber .50 aircraft machine gun barrel was hardened for maximum hardness and failed by cracking. The second liner was tested in the dead soft condition and failed by swaging of the rifling. Termination of the experimental program of Division 1, NDRC, after V-J day prevented further tests at intermediate hardnesses, which should be completed.

Tests of electroplated nickel in the caliber .50 machine gun showed that its erosion resistance was about equal to that of gun steel,[49] which confirmed earlier British experience with medium-caliber guns. A number of nickel-tungsten alloy electroplates were tested in the caliber .50 erosion-testing gun[76] and in the caliber .50 machine gun.[59] All showed poor resistance to powder gas erosion and rapid removal in a few rounds.

An alloy designated "Z" nickel, which contains an unspecified hardening agent, and zirconium-nickel (with about 0.5% zirconium) were tested as liners, both in the caliber .50 erosion-testing gun[76] and in the caliber .50 machine gun,[49] and showed an erosion rate greater than that of gun steel and a characteristic type of erosion (different from gun steel) which was caused by intergranular attack and detachment of grains of metal from the bore. A liner of Monel metal (67.5% nickel, 28.5% copper) showed the same type of attack and poor performance in the caliber .50 erosion-testing gun. It was demonstrated[59] that the alloying elements in these liners just described were not responsible for the erosion by test in a caliber .50 machine gun barrel of a liner of the purest nickel commercially available. In this test the erosion of nickel involved both melting and removal of grains of nickel following weakening along grain boundaries (intergranular attack). A previous test of a liner of pure nickel in the caliber .30 machine gun[78] showed performance inferior to gun steel.

An even more conspicuous failure as a gun liner material was Colmonoy No. 5, a high-nickel alloy (78% nickel) containing some chromium, iron, silicon, and boron, which has been a competitor of stellites for cutting tools and valve seats for high temperature service. When tested[80] as a liner in the caliber .50 heavy machine gun barrel it failed both by cracking and general melting of the bore surface, when fired only 45 rounds. Firing tests[80] in the caliber .50 aircraft machine gun barrel on liners of Hastelloy "A" and Hastelloy "B", which are nickel-molybdenum-iron alloys (with no chromium present), showed that in addition to being too soft they were subject to chemical attack by hot powder gases.

16.4.10

Hardened Iron-Nickel-Cobalt-Chromium Alloys

The remarkable performance of Stellite No. 21 as a liner material in machine gun barrels, which has already been outlined in Section 16.4.8 of this report, focused attention on the hot-hardness of a bore-surface material as an important requisite of such a

material. Because of the possibility of a critical shortage of cobalt in case the war should be of long duration, an attempt was made to find a satisfactory substitute for Stellite No. 21 (which contains about 64% cobalt) with a lower cobalt content or no cobalt. Because of these considerations, in addition to studies of the effect on liner performance of replacing a part of the cobalt of Stellite No. 21 with one or both of the metals nickel and iron, a preliminary reconnaissance was made of the possibilities of cast or wrought iron-nickel-cobalt-chromium alloys with low or moderate carbon contents and any or all of the metals, molybdenum, tungsten, columbium, and tantalum, as hardeners.

Fortunately, about 77 heat-resisting alloys of this series were under investigation and development by the War Metallurgy Committee (Division 18, NDRC), the Navy Department and the National Advisory Committee for Aeronautics for use as blades in gas turbines, in turbosuperchargers and for other important high temperature uses. In order to expedite the preliminary study of the potentialities of these alloys as materials for gun liners, an arbitrary separation into groups was made as follows on the basis of chemical composition:

Group I. Stellite-type alloys: Cobalt-chromium alloys (cobalt-chromium ratio roughly 70 Co–30 Cr) with about 5% of either tungsten or molybdenum and varying carbon content from 0.1 to 0.5%. Part (up to about one-half) of the cobalt may be replaced by nickel.

Group II. K 42-B-type alloys: Low-carbon alloys, approximately Ni 40, Co 25, Cr 20 with Ti and Al as hardening agents.

Group III. Refractaloy-type alloys: Co-Ni-Cr alloys with about 12% of body centered cubic metals (Mo, W, Cb, Ta) and varying carbon contents between 0.05% and 0.5%. (For example: 30 Co, 20 Ni, 20 Cr, 15 Fe, 8 Mo, 4 W, 0.1 C.)

Group IV. N-155-type alloys: Co-Ni-Cr alloys with about 6% of body centered cubic metals (Mo, W, Cb, Ta) and varying carbon contents. (For example: 20 Co, 20 Ni, 20 Cr, 30 Fe, 3 Mo, 2 W, 1 Cb, 0.3 C.)

Group V. S-497-type alloys: Co-Ni-Cr alloys (lower Cr than Refractaloy or N-155-types) with about 12% of body centered cubic metals (Mo, W, Cb) and varying carbon contents between 0.1% and 0.5% (For example: 20 Co, 20 Ni, 14 Cr, 30 Fe, 4 Mo, 4 W, 4 Cb, 0.4 C.)

Group VI. Hardened nickel-chromium alloys: Modified Inconels with hardening agents such as Be, Ti, Al, Mo, W.

Group VII. Hardened stainless steels: Modified 18-8, 25-12 or plain Cr stainless steels with hardening agents such as Ti, Mo, W, Cb, Mn.

Some members of all except the last type show promise as possible gun-liner materials. Most hardened nickel-chromium alloys gave poor test results except Hastelloy "C" (see Section 16.4.9). Of the remainder, K 42-B-type alloys show the least promise for gun liners.

A reconnaissance series of these hot-hard alloys was prepared and cast liners subjected to firing tests in caliber .50 aircraft machine gun barrels. The results are described in Section 19.8.2. The experimental program of Division 1 was terminated before the full potentialities of these materials could be evaluated. The following observations seem warranted by the data available on thermal and mechanical properties of these alloys at both room temperature and elevated temperatures combined with the limited firing results:

1. Some of these alloys besides the stellites show promise for use as liners in machine gun barrels. Further test and development (particularly the effect of heat-treatment on the hardness and properties) should be given to Refractaloy No. 70[92] and to other Refractaloy-type alloys and firing tests should be made on liners of N-155 alloy with about 0.25 or 0.35% carbon.

2. Chromium and cobalt, particularly a combination of both in these alloys, enhances their resistance to chemical attack by powder gases.

3. None of these alloys has a sufficiently high melting point to be used as a bore-surface material in a gun under hypervelocity conditions where melting plays an important part in erosion. Most of them have fusion ranges between 1200 and 1300 C. It might be possible to utilize the excellent hot-hardness and ductility of some of these materials as liners, either under hypervelocity conditions or in machine guns under severe firing conditions at an increased velocity obtained by use of increased powder charges of single-base powder or by the use of double-base powder, if their rifled bores could be protected from melting by the use of a high-melting erosion resistant plate (such as chromium plate) provided that such plate can be made adherent. This possibility should be explored.

4. Trials are warranted of liners of some of these materials in medium caliber guns at conventional

[redacted]

velocities under more severe firing schedules or at regular schedules to obtain longer life. Since some of the alloys are amenable to fabrication as wrought ingots or tubes, they might be more easily applied to such guns than cast alloys.

5. Because of their excellent strength at high temperatures as compared to gun steels, some of the more ductile of these alloys might be considered as gun barrel materials in order to decrease the weight of the gun tube and also to enhance the performance of an erosion resistant liner of a high-melting alloy (for example, a hardened molybdenum or a chromium-base alloy liner) or a high-melting erosion resistant plate (for example chromium electroplate).

16.4.11 Steels and Other Iron Alloys

SUMMARY

No steels or special high-iron alloys tested have shown any outstanding promise as bore-surface materials. The results of laboratory and firing tests described in Section 16.3 and the results of studies of the nature and mechanism of the erosion process and action of propellants on steel gun bores described in Parts III and IV, show that these alloys in general lack thermochemical resistance to powder gas erosion. Laboratory tests and firing tests of specific high-iron alloys as gun liners in machine gun barrels showed chemical attack by hot powder gases. Even when the hot-hardness was sufficient to prevent deformation of the rifling by swaging impact of the bullet and the ductility was adequate to prevent brittle failure, chemical attack, and thermal transformations at the bore surface (usually both) caused ultimate and usually early failure. As an example, a cross section of a Cyclops KL steel liner is shown in Figure 9.

Two aircraft engine valve steels (Silchrome XCR and XB), which show somewhat better erosion resistance than ordinary gun steel, might be used as a barrel material for caliber .30 machine gun barrels under mild firing conditions or as liners or linings in large guns at moderate rates of fire where swaging of the rifling may be a minor factor in performance.



FIGURE 9. Cyclops KL liner fired 645 rounds with standard ball bullets M2 in caliber .50 heavy machine gun barrel. Cross section ½ in. beyond the origin of rifling. Severe gas erosion obliterated the rifling. The light-gray layer at the surface is austenite containing undissolved carbides; below it is a tempered steel layer containing a large number of precipitated carbides. Etched with nital; *100X*. (This figure has been taken from a progress report on Contract OEMsr-537.)

NICKEL AND COBALT STEELS

A liner of unhardened stainless steel (25 Ni, 12 Cr) in a caliber .30 machine gun barrel showed performance[78] inferior to gun steel and evidence of thermochemical attack. A firing test[80] of a liner of a hardened special stainless steel (TEW alloy with 30 Ni, 20 Cr, 4 Mo, 4 W, 2 Ta, 0.1 C, balance iron) in a caliber .50 heavy machine gun barrel showed that this alloy was subject to thermochemical attack by hot powder gases. On the other hand, a similar alloy (Refractaloy No. 70)[92] with 30% cobalt present and lower nickel and iron contents showed promise in this weapon. (See Section 16.4.10.)

An iron-cobalt alloy (50 Fe, 48 Co, 2 V) in the erosion vent-plug test with 1/16-in. vent showed[27] erosion resistance comparable to gun steels for the first few rounds and then weight losses increased more rapidly than with gun steels. It has good hot-hardness[59] up to 600 C. No firing tests in guns were made on this alloy.

TUNGSTEN STEELS

Liners of 18-4-1 high-speed steel (18 W, 4 Cr, 1 V, 0.4 Mo, 0.75 C), Voland No. 2 hot-die steel (9 W, 2.5 Cr, 2.25 Co, 0.34 V, 0.39 C) and Cyclops KL hot-die steel (7 W, 7 Cr, 0.34 C) were subjected to

firing tests[80] in caliber .50 heavy machine gun barrels and in addition to brittle failure all showed chemical interaction with powder gases and formation of an altered surface layer and hence have no promise as bore-surface materials.

Hot-hard steels such as the hot-working die steels do not retain their hardness at elevated temperatures much better than regular WD 4150 gun steel, if they are heat-treated to a hardness of 30 to 35 Rockwell C. At this hardness their machineability is fairly good. When heat-treated to 50 Rockwell C, some of these alloys retain their hardness remarkably well up to about 700 C, but then they are not readily machineable and also ductility and impact resistance are poor, with the result that machine gun liners of these alloys showed brittle failure as well as evidence of chemical attack on firing.

Iron-tungsten electroplates had good hot-hardness but were not resistant to powder gas erosion.

Molybdenum Steels

Monomorphous iron-base alloys (iron with molybdenum up to 20% and very low in carbon), which can be readily hardened by precipitation or aging, when tested as vent plugs showed large weight losses as a result of chemical attack.

A 3% molybdenum steel (0.13–0.18 C) was found to have better erosion resistance than WD 4150 gun steel with single-base powder but, with double-base powder, it resisted erosion no better than the gun steel.

Silicon Steels

As already mentioned in Section 16.3.2, powdered ferrosilicon was resistant to chemical attack by single-base powder and retarded oxidation of gun steel during firings with double-base powder. A liner of a silicon steel (4.7%) tested[76] in the caliber .50 erosion-testing gun disintegrated by brittle failure after a few rounds. Unfortunately all iron-silicon alloys are too brittle to be satisfactory as liners or coatings in gun tubes and in addition their melting points are too low for severe service.

When tested as a liner[81] in the caliber .50 heavy machine gun barrel, an aircraft engine valve steel Silchrome XCR (24 Cr, 5 Ni, 3 Mo, 0.45 C) showed much better resistance to thermochemical attack by powder gases than regular WD 4150 gun steel. In the unhardened condition this steel had excellent tensile properties, hot-hardness, and ductility, but in the hardened condition, elongation dropped from about 22 per cent to around 3 per cent and liners failed by cracking. Silchrome XCR is difficult to prepare clean and free from oxide or carbide segregations which make it difficult to machine. Another similar valve steel Silchrome XB (19.5 Cr, 1.35 Ni, 2.29 Si, 0.76 C) was also being machined into barrels for the caliber .30 machine gun. This steel was believed to have good erosion resistance on the basis of vent-plug data. Termination of the experimental program of Division 1 prevented completion of caliber .30 machine gun barrels of these steels and their testing, which should be completed.

Nitrided Steel

Laboratory tests and firing tests showed that WD 4150 gun steel and Nitralloy when hardened by nitriding or induction hardening of the bore showed no better resistance to powder gas erosion than in the unhardened condition. The use of hardened steel bores protected by an erosion-resistant chromium plating to improve the performance of machine gun barrels is described later in this report (Chapter 23) and the use of special steels with better high temperature properties than gun steels to enhance the performance of erosion resistant liners or plates or combinations thereof is described later in this report. (Chapters 23 and 24.)

16.4.12 Copper and Its Alloys

Pure copper and high-copper alloys show no promise as bore-surface materials in spite of the fact that these materials show excellent resistance to chemical attack by hot powder gases. Even though the melting point of copper is relatively low, because of its high specific heat and excellent thermal conductivity, the melting point of a copper bore surface may not be attained during firing except under very severe conditions. Copper and all hardened copper-base alloys (for example, copper-beryllium alloys, which have excellent room temperature properties) lack, by a large margin, the necessary strength and hardness to resist severe deformation by powder pressures and by the swaging impact of the projectile *at the working temperature* in guns. The unsuccessful attempts to utilize copper in gun liners as one component of powder metallurgy compacts of chromium or molybdenum or tungsten powders with copper was previ-

ously described in this report in Sections 16.4.3, 16.4.4, and 16.4.5, respectively. Copper failed in firing tests[76] as an electroplate or as an undercoat under chromium electroplates (see Sections 16.4.2 and 20.2.4). The severe plastic deformation or even melting of bullet jackets of gilding metal (a high-copper alloy) may be a limiting factor in the performance of improved machine gun barrels under very severe firing conditions as mentioned again later in this report (Chapter 23). A rifled liner of copper hardened by alloying with a small amount of chromium when tested[78] by firing in a caliber .30 machine gun showed no chemical attack, but severe deformation and wear obliterating the rifling.

16.4.13 Surface Coatings and Bore Lubricants

Attempts have been made to find a nonmetallic material that can be applied to a gun steel bore surface to protect it from erosion by the powder gases, or which at least will reduce the frictional component of erosion. The latter purpose has also been extended to include the case of chromium-plated bores. None of the materials tried has been successful.

A liner of WD 4150 gun steel whose rifled bore surface had been specially treated in steam at 1000 F to yield an oxidized bore surface of magnetic oxide of iron showed[76] no improvement in performance over untreated gun steel in the caliber .50 erosion-testing gun.

One of the means suggested for protecting the bore surface was by a renewable film applied to the surface as each round is fired. The material selected for trial was a fluorocarbon, which is a chemically inert compound of high boiling point developed by Division 9, NDRC.

In order to determine the effect of a film of fluorocarbon on the erosion of gun steel, a special type of bullet with a grooved base-cup sealing ring was used. This groove, together with a deep groove in front of the base-cup, was filled with the fluorocarbon in the form of a grease before seating the bullet in the caliber .50 erosion-testing gun. It turned out that the film of fluorocarbon helped seal erosion cracks and thus reduced the customary drop in muzzle velocity,[m] but the degree of erosion was just as severe as that of a control barrel with no protective film.[76]

The bore of a WD 4150 gun steel barrel for the caliber .50 erosion-testing gun was coated with a Parco-Lubrite coating approximately ½-mil thick. This coating consists chiefly of a mixture of iron and manganese phosphates. It was believed that the reduced friction between the bore and the projectile would result in an increased velocity life. A firing test showed no improvement in performance as compared with an untreated steel barrel.[76] It should be noted from Section 31.4.5, however, that a decided improvement in performance is obtained when the preengraved projectiles are Parco-Lubrized.

In firing tests in the caliber .50 erosion-testing gun on barrels or liners with chromium-plated bores, the life of the chromium plate was prolonged and performance improved by the use of cadmium-plated bullets, as mentioned in Section 31.4.5. On the other hand, trials[81] with cadmium-plated AP bullets M2 in nitrided and chromium-plated caliber .50 aircraft machine gun barrels showed no improvement compared with similar barrels fired with the same bullets not plated.

16.4.14 Other Metals and Alloys

In erosion vent-plug tests (see Section 16.3.1) zinc, beryllium, aluminum, and titanium showed[27] such severe thermochemical attack by hot powder gases that no quantitative data could be obtained. Especially in the test of titanium the evolution of much smoke indicated that the action might be largely chemical.

Silver showed poor performance in these same tests. It is not known for sure whether the high weight losses in this case were a result of melting[48] or a combination of melting and chemical attack.

Pure columbium showed thermochemical resistance comparable to gun steels in erosion vent-plug tests[27] but when filings of this metal were mixed with the propellant and fired into an evacuated tube (see Section 16.3.2) interaction with powder gases was observed. The lack of agreement between these two results has not been explained.

Erosion vent-plug tests[75] of an alloy of gold (80%) and palladium (20%) were undertaken as part of the experimental program to evaluate the relative importance of melting and chemical attack in erosion. (See also Section 15.4.1.) This alloy has thermal properties similar to those of gun steel but a slightly lower melting point. When tested under conditions such that the melting points of both the gold-palladium and the steel were exceeded, the former eroded somewhat

[m] This result was later applied to the obturation of preengraved projectiles, as described in Section 31.4.2.

[redacted]

more than the latter. Under milder conditions, however, the order was reversed and the relative amounts of erosion indicated a much higher resistance of the gold-palladium alloy to chemical attack than of gun steel.

Indirect evidence[49] of the resistance of the pure metals rhodium and iridium to chemical attack by powder gases at very high temperatures was obtained when filings of these metals were used in experiments to determine the adiabatic flame temperatures of propellants. When the melting point of the metal was above the flame temperature, the particles remained unaltered. If chemical attack had occurred the observed behavior would not have been realized.

[redacted]

Chapter 17

CHROMIUM AND CHROMIUM-BASE ALLOYS

By *Helen M. Watson*[a]

17.1 INTRODUCTION

17.1.1 Scope of Investigation

CHROMIUM WAS ONE of the first metals considered by Division 1 in the search for a bore-surface material that would solve the erosion problem in guns. It had been found that it possessed resistance to powder-gas erosion and some very desirable physical properties; but early experiments by Division 1 indicated that in order to be useful as a gun-liner material it would have to be prepared in a form stronger and less brittle than then known.

An extensive investigation on the preparation of pure chromium was undertaken for Division 1 at the Westinghouse Research Laboratories in cooperation with the Geophysical Laboratory, C. I. W., and the National Bureau of Standards. No noticeable improvement in ductility could be obtained by control of purity, by addition of small amounts of alloying elements, or by hot-working. Hence it was concluded that it would be unprofitable to continue the effort to develop pure chromium (or a high-chromium alloy) for use as a gun liner.

Later, some of the hot-hard chromium-base alloys that had been developed by the Climax Molybdenum Company for Division 18, NDRC, appeared to offer possibilities as liner materials. The Climax Company, through a contract supervised by Division 1, investigated such applications of the alloys. Two of the alloys (those with the following percentage compositions: chromium 60, iron 25, molybdenum 15; and chromium 60, iron 30, molybdenum 10) were found to be very promising for this purpose. The low ductility of these alloys requires that they be properly supported in the gun barrel, as brought out in Section 26.5.1. In every other respect, particularly by reason of inertness to the erosive action of double-base powder, caliber .50 liners of chromium-base alloys have given superior performance in firing tests. Another desirable feature is the availability of chromium, compared with cobalt and molybdenum, for example. Furthermore, its cost is not prohibitive.

Thus these chromium-base alloys represent one of the three main solutions obtained by Division 1 to the problem of an erosion-resistant bore-surface material. Their potentialities as liners appear to be twofold: for machine guns at high rates of fire, almost without regard to velocity, and for hypervelocity medium-caliber guns. Their further development, especially with respect to increase of ductility, was transferred by Division 1 to the Union Carbide and Carbon Research Laboratories, and then was continued there by the Army Ordnance Department after Division 1's contracts had been terminated.

17.1.2 Preliminary Survey

EXAMINATION OF CHROMIUM-PLATED NAVAL GUNS

It has been the practice for nearly 20 years to apply a plating of chromium to the bore surfaces of Naval guns as a protection against corrosion during periods of inactivity. Microscopic examination of an eroded 5 in./38-cal. chromium-plated gun revealed vestigial areas of the plate that were not perceptibly altered, even though the surrounding regions were severely eroded,[49] as is shown in Figure 2 of Chapter 20.

The plate had failed by cracking, which permitted the powder gases to attack the underlying steel. However, it was evident that the plate itself had withstood the erosive action of the gases, as well as the wear caused by the projectile. This indication of the erosion resistant properties of chromium led to attempts to prepare a liner of pure chromium (Section 17.2.2).

EROSION VENT-PLUG TESTS

Another basis for the belief that chromium might be suitable for an erosion-resistant bore surface was afforded by erosion vent-plug tests (Section 11.2.3). Such tests indicated that chromium is one of the few pure metals that are resistant to powder-gas erosion.[27] When tested with double-base powder in the 1/16-in. diameter erosion vent-plug apparatus, samples of a 50-chromium, 50-iron alloy eroded more than did gun steel, and the erosion rate of a 70-chromium, 30-

[a] Technical Aide, Division 1, NDRC. (Present address: Department of Physics, The Catholic University of America.)

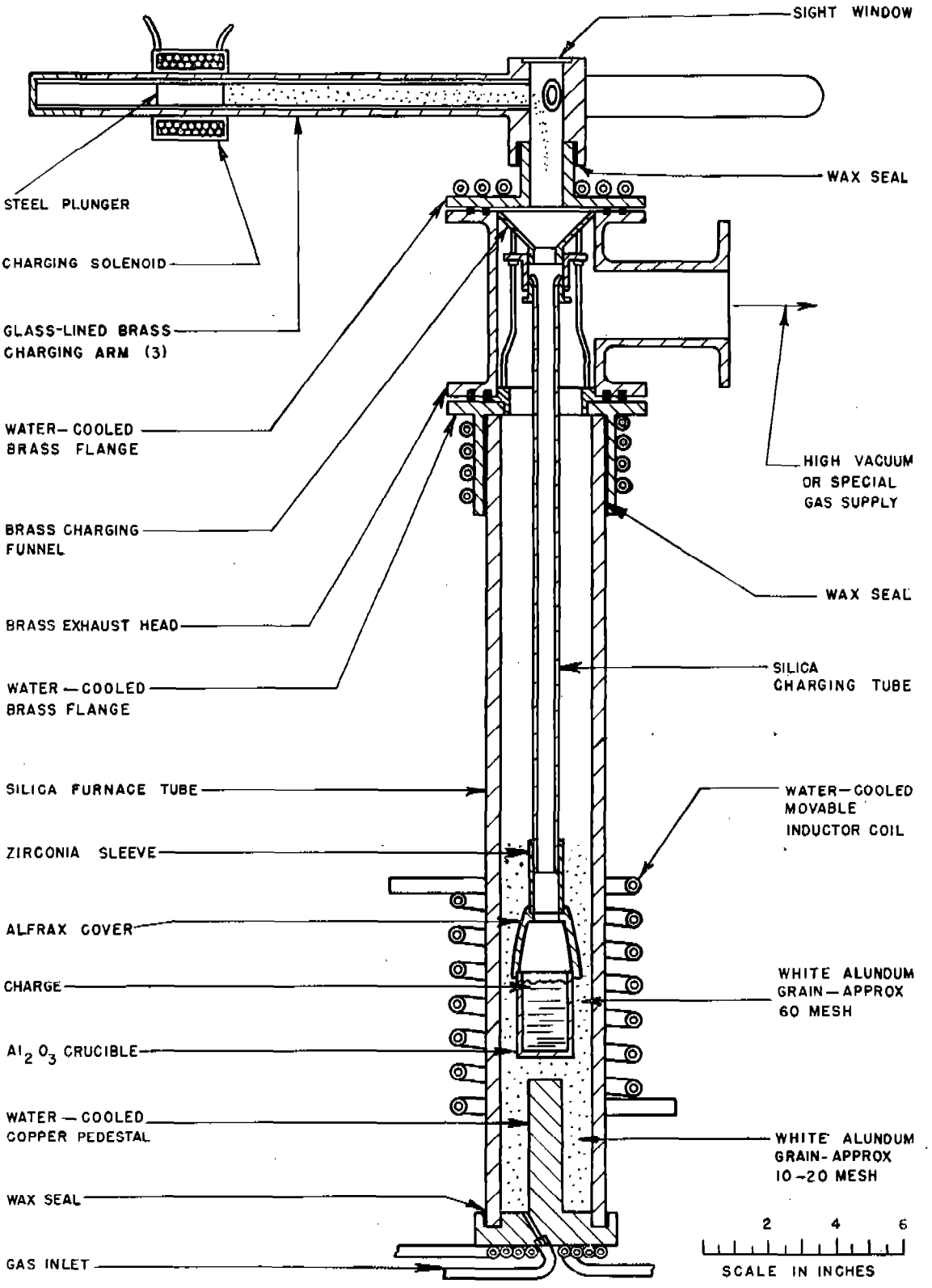


FIGURE 1. Induction-heated vacuum furnace for melting chromium and high-chromium alloys. (This figure has appeared as Figure 2 in NDRC Report A-411.)

tungsten alloy was similar to that of gun steel. Later the vent-plug tests were decreased in severity and their results more nearly approached those obtaining in guns (Section 11.2.3). The latter tests indicated that high-chromium ternary alloys of the chromium-iron-molybdenum and chromium-iron-tungsten series displayed very good erosion resistance.[75]

During the development of these chromium-base alloys,[b] the portions of 13 binary and 9 ternary alloy systems that contained more than 50 per cent chromium were surveyed.[167,168] Two of these systems, the chromium-iron-molybdenum and the chromium-iron-tungsten, were studied in detail. Their selection was based on stress-rupture tests at 870 C (1600 F), in which alloys belonging to the two systems displayed the highest strengths with measurable ductility. The physical properties of such alloys suggested the desirability of applying them to the gun-liner problem.

17.2 METHODS OF PREPARATION

17.2.1 Introduction

Similar methods were employed for the preparation of both the pure chromium and chromium-base alloys, namely, melting and casting high-purity stock under controlled conditions. Since brittleness is characteristic of these materials, care had to be taken that during the melting and casting process they would be kept as free as possible of impurities that would decrease their ductility. It was found that by melting and casting them in vacuum, the oxide-, nitride-, and carbon-contents, which tend to increase their brittleness, were kept at a minimum.

17.2.2 Chromium

Vacuum Melting

A specially designed induction furnace[83] (Figure 1) was constructed after it was found that unsatisfactory melts were formed when the entire charge of chromium chips was placed in a crucible and heated inductively. Chromium metal was "shoveled" gradually from a charging side-arm down the charging chute into a crucible mounted in the furnace tube, at such a rate as to avoid the formation of a crust on the surface of the melt. When melting had been completed, the power was adjusted and, while still in the furnace, the melt was cooled progressively from the bottom upward.

Melting was done in a nearly complete vacuum at first, but it was observed that chromium vapor tended to condense on the cooler surfaces of the melting chamber and block openings that had been provided for sighting and charging. These difficulties were minimized when purified hydrogen or argon, at pressures of a few centimeters of mercury, was introduced into the vacuum chamber during melting. It was important that the melting atmosphere be free of nitrogen, since this element contaminated the melt, as shown in Figure 2, which is to be compared with Figures 3 and 4.

The selection of a nonreactive crucible material was made especially difficult by the relatively high melting point (between 1900 and 2000 C) of chromium. Of the various crucibles tested, those made from pure aluminum oxide, without the use of any siliceous bonding material, proved to be the most satisfactory.

Microexamination of chromium ingots produced in the early experiments revealed the presence of numerous inclusions (Figure 3) which were thought to be



Figure 2. The structure of chromium contaminated by nitrogen. The nitrogen-bearing constituent is indicated at *A*. *250X*. (This figure has appeared as Figure 3 in NDRC Report A-411.)

[b] These alloys had been developed by the Climax Molybdenum Company under an OSRD contract which was supervised by the War Metallurgy Committee of the National Academy of Sciences in a search for heat-resistant metals for gas turbine blades. See Chapter 5 of the Summary Technical Report of Division 18.

GOVERNMENT PROPERTY

chromium oxide (Cr_2O_3). These presumably resulted from either (1) the oxygen known to be present in the electrodeposited chromium used as the source material, or (2) the oxygen picked up from residual gases liberated from the refractories during melting, or both. Zirconium metal was a very effective deoxidizer when added to the melt, as shown by a comparison of the structure shown in Figure 4 with that in Figure 3. Ingots weighing about 300 g were produced.

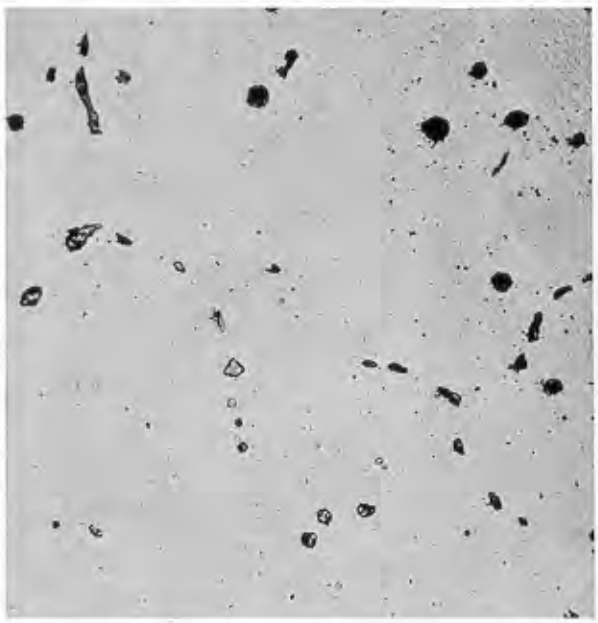


FIGURE 3. A typical section of a pure chromium ingot that had been cooled in the furnace after having been melted in vacuum without a deoxidizer. Oxide inclusions appear along the grain boundaries. *250X*. (This figure has appeared as Figure 4 in NDRC Report A-411.)



FIGURE 4. A typical section of a pure chromium ingot that had been cooled in the furnace after having been melted under a low pressure of argon and deoxidized with zirconium. *250X*. (This figure has appeared as Figure 5 in NDRC Report A-411.)

The chromium used for melting stock was prepared by electrodeposition. It was very pure except for its oxygen content, which was equivalent to 0.1 to 1.5% of chromium oxide (Cr_2O_3). In an attempt to remove the oxygen and thereby effect an increase in ductility, a series of "beneficiation" experiments was carried out. Samples of electrodeposited chromium were heated at temperatures up to their melting points in a current of hydrogen purified by diffusion through palladium. This treatment removed most of the oxygen originally present in the chromium, and improved its cold ductility to a slight extent.

Similar heating in vacuum produced needle-like deposits of condensed chromium, some of which could be bent repeatedly through large angles or, in a few cases, rolled to form thin, irregular plates that would stand some plastic deformation without fracture. The behavior of such crystals was observed microscopically, and it was concluded that whether fracture would result upon the application of compressive forces to the crystal depended upon whether the forces were applied normal to an octahedral plane (no cracking) or to a cubic plane (cracking); and that therefore no significant degree of cold ductility could be expected in polycrystalline masses of pure chromium where the orientation of individual crystallites is random.

Furnace-cooled ingots nearly free of oxide inclusions and otherwise of high purity were obtained starting with "beneficiated" chromium; but their ductility, hardness, and tensile properties were so poor that it was not considered practicable to attempt to make gun liners from such material.

Vacuum Casting

All the furnace-cooled ingots had very coarse grain sizes. It was considered that if chromium having a finer grain structure than is possible with furnace cooling could be prepared, it might possess sufficient ductility. The furnace was redesigned to include a

CONFIDENTIAL

tilting mechanism which permitted the transfer of the molten metal from the crucible to a steel mold without a change in the atmosphere. The two castings of zirconium-deoxidized pure chromium made in this way were quite brittle, and not very strong. They were remarkable for their highly developed radial crystallization patterns (shown in Figure 5) and for the soundness of the metal, except for round shrinkage cavities which extended almost the entire length of the ingot.



FIGURE 5. A vacuum-cast ingot of pure chromium deoxidized with zirconium. It had a well-developed radial crystallization pattern. (This figure has appeared as Figure 9(b) in NDRC Report A-411.)

The chill-cast specimens showed no improvement in malleability at room temperatures compared with those cooled in the furnace. Thereupon the attempts to produce a ductile, pure chromium in appreciable amounts were discontinued.

THERMAL DECOMPOSITION OF IODIDE

A supplementary investigation was undertaken to prepare crystalline metallic chromium of an extremely high order of purity by a method that would minimize the possibility of oxygen contamination. A small amount of crystalline chromium was prepared by thermal decomposition of chromous iodide (CrI_2) on an electrically heated tungsten filament.[8] Considerable cold ductility was exhibited by these crystals, but the method was considered impracticable for large amounts of the metal. Microexamination revealed these crystals to be cubic, and to show octahedral faces. The same observations were made concerning their anisotropy with respect to malleability as were made for the needle-like crystals that resulted from beneficiation experiments described previously.

ELECTRODEPOSITION ON BRASS[c]

An attempt was made, early in the investigation, to prepare chromium liners by electrodepositing chromium on brass tubes to a thickness of $\frac{1}{8}$ inch and then dissolving out the brass.[49] A tube deposited at 75 C with a current density of 100 amp/dm^2 was found to be free of initial cracks, but was exceedingly brittle. Another tube, which had been softened and made more ductile by annealing, was shrunk into a steel tube and rifled. When it was tested as a liner in the heavy barrel of a caliber .50 Browning machine gun (Section 11.2.2), many longitudinal cracks developed after the firing of only a few rounds. No improvement resulted from further experimental work, and it was concluded at that time that mechanical working would be necessary before electrodeposited chromium would have mechanical properties suitable for use as a liner. However, later attempts to improve the properties of chromium by hot-working led to the conclusion that no noticeable benefit could be effected (Section 17.3.2).

17.2.3 Chromium-Base Alloys

VACUUM CASTING

Apparatus used[87] for vacuum-casting chromium-base alloys is shown in Figure 6. As was the case in preparing chromium, particular care had to be taken in choosing the crucible used for melting, to insure that there would be no reaction with the molten material. Alundum crucibles were tried, but it was found that they melted at the high temperatures needed to cast the melt into a mold. Beryllia or zirconia crucibles, wrapped with molybdenum sheet as a resistor, proved to be the most satisfactory.

The alloys were melted by induction heating, and then were transferred through a hole in the bottom of the crucible to a copper casting mold. The metal mold chilled the melt rapidly, and thus produced fine primary grains. However, it was found to be important that the alloy be chilled from the melt at the maximum rate that did not cause cracking or induce unfavorable residual stresses. If chilling was too rapid,

[c] See Chapter 20 for a discussion of electrodeposition on gun-bore surfaces.

CONFIDENTIAL

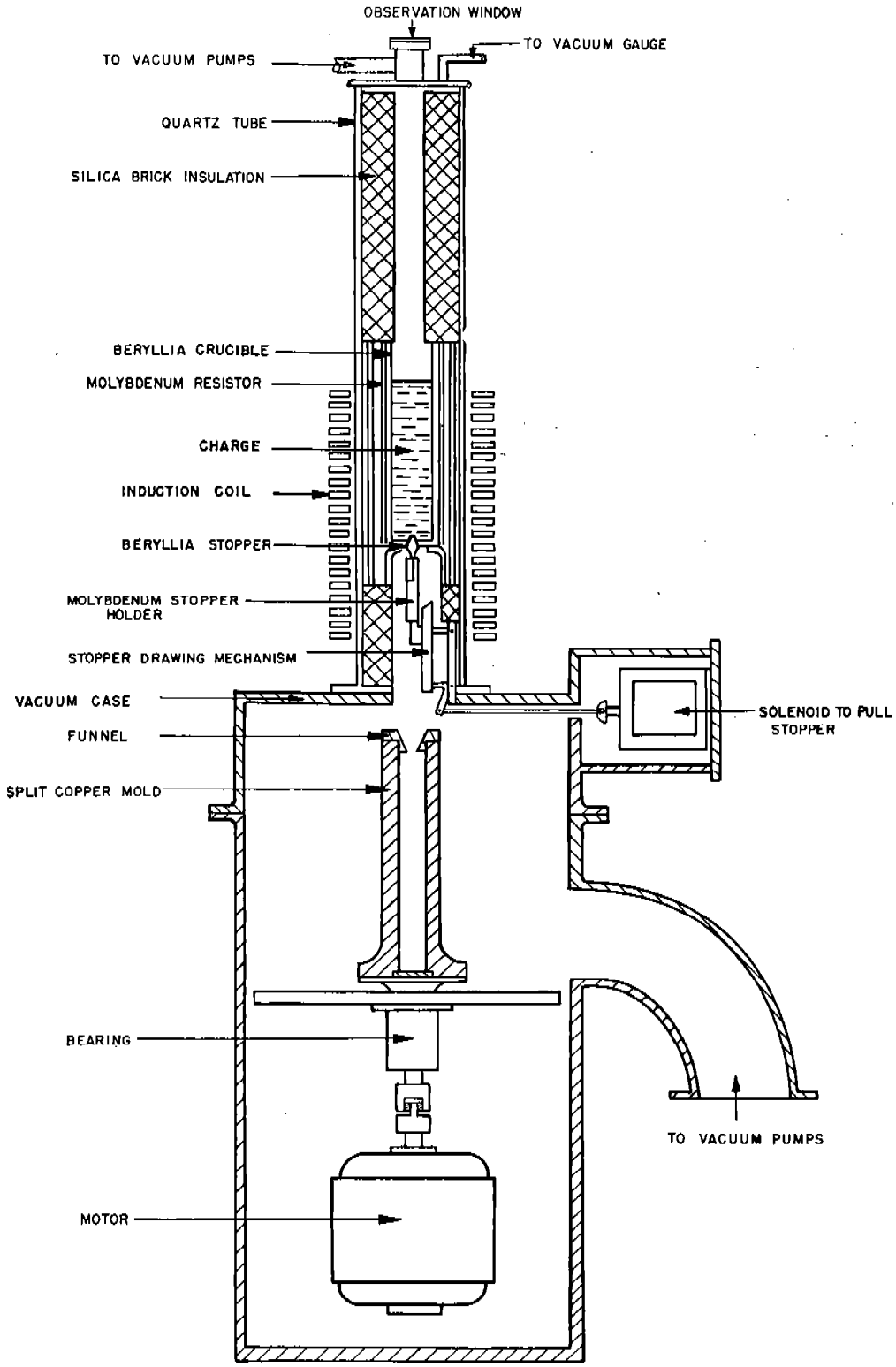


FIGURE 6. Vacuum-casting apparatus for preparation of centrifugally cast caliber .50 gun liners made of chromium-base alloys. (Figure 1 in NDRC Report A-415.)

[redacted]

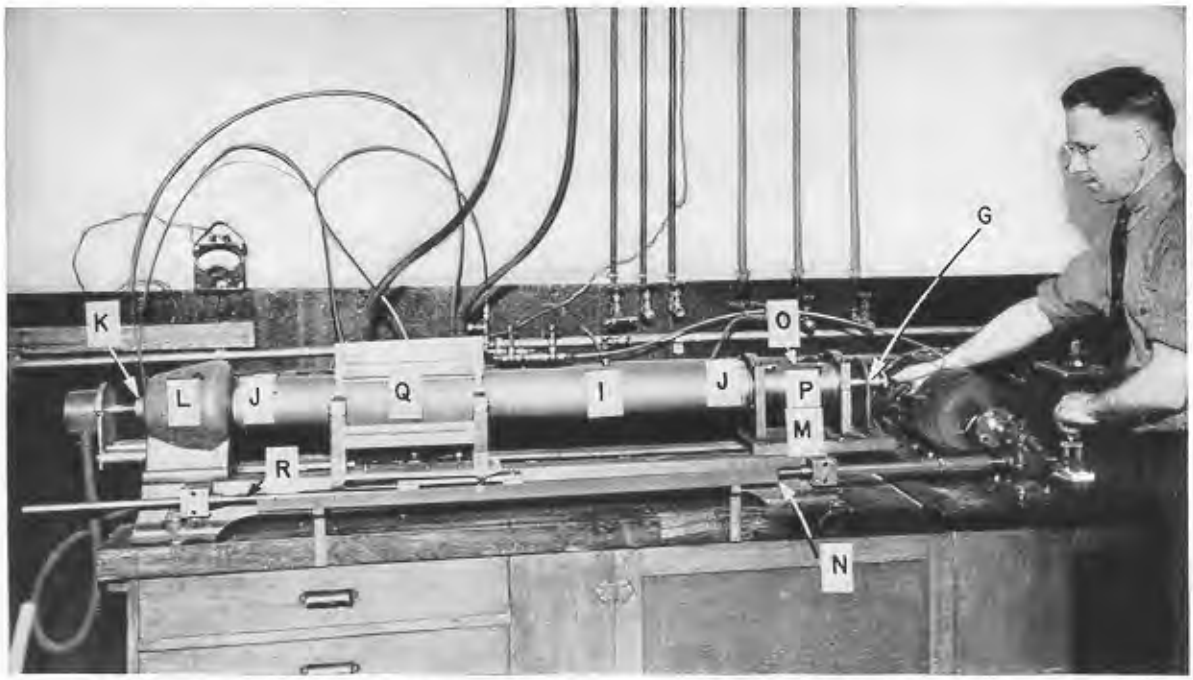


FIGURE 7. Induction-heated apparatus for centrifugal in-melting of chromium-base alloy tubes. (Figure 1 in NDRC Report A-410.)

The Micarta furnace tube *I* contained the powdered charge in a thin-walled carrier tube surrounded by granular refractory in which longitudinal cooling tubes are imbedded. The tapered ends of the furnace tube fit against gasketed chucks *J*, carried by hollow shafts *K*, running in bearings in the head-stock *L* and tail-stock *M* of the lathe *N*. Cooling water is admitted through the inlet tube *G*. Coil springs *O* serve to push the movable bearing shell *P* longitudinally toward the head-stock and thus maintain a tight connection between *I* and *J*. The inductor coil *Q* is moved longitudinally along the ways of the lathe by the lead-screw *R*, which is driven by an adjustable-speed motor.

large temperature gradients, which often caused cracks, resulted.

The copper casting mold was rotated at speeds of from 4,500 to 5,500 rpm, so that tubular castings were produced with parabolic inside surfaces. The diameter of the bore varied from ⅜ in. at the top to ¼ in. at the bottom. About 20 min after they had been poured, the castings were removed from the mold and were placed in an air furnace at 870 C (1600 F), where they were held for a period between 30 and 120 min for relief of casting stresses. The castings were then ready for machining.

This apparatus was capable of melting charges up to 4½ lb. An improved apparatus, designed to melt a 50-lb charge, was constructed but had not been assembled when the investigation under NDRC auspices was discontinued.[d] In addition to the larger charge, the improved design provided for a continuous operation of the apparatus, brought about by the addition of an air lock between the melting and the casting chambers. A tilting mechanism for the crucible, which enabled the melt to be poured over its lip into the casting mold, eliminated bottom pouring.

[d] The improved apparatus was constructed for Climax Molybdenum Company, and at the termination of its contract the equipment was transferred to the Union Carbide and Carbon Research Laboratories where experiments were continued.

CENTRIFUGAL IN-MELTING

A new method of preparing alloy tubes, termed progressive centrifugal in-melting,[82] was tried at Westinghouse Research Laboratories with an alloy of the approximate composition 60-chromium, 35-iron, 5-molybdenum. The melting took place inside a Micarta tube (about 4 in. in diameter and 36 in. long) lined with granular magnesium oxide or aluminum oxide, in the center of which the charge was introduced in the form of metal powder. The tube was evacuated and then rotated at about 1,200 to 1,400 rpm while an inductor coil was moved slowly from one end to the other. In this way successive small portions of the charge were melted and then subsequently frozen while under the influence of centrifugal force. The Micarta tube was protected from the heat of the core by a "squirrel cage," consisting of a system of longitudinal water-cooled copper tubes. The Micarta

CONFIDENTIAL

TABLE 1. Physical properties of chromium and chromium-base alloys compared with those of gun steel.

Property	Chromium	60 Cr—25 Fe—15 Mo	60 Cr—30 Fe—10 Mo	Gun steel*
Density (g/cc)	7.14	7.6	.....	7.83
Melting point (C)	1950 ± 50	ca. 1700	ca. 1650	1450
Specific heat (cal/g/°C)	0.12	.....	.....	0.11
Latent heat of fusion (g-cal/°C @ 15 C)	31.75	.....	.....	.....
Thermal conductivity (cal/cm/sec/°C)	0.165 (15 C)	0.0305 (30 C)	.....	0.102 (50 C)
Coefficient of thermal expansion (/°C)	8.1×10^{-6} (@ 20–300 C)	7.7×10^{-6} (@ 25–315 C)	.....	.....
	.....	8.8×10^{-6} (@ 25–650 C)	10.8×10^{-6} (@ 25–595 C)	13.6×10^{-6} (@ 20–500 C)
Hardness @ 20 C (68 F)	193	480 ± 10	420 ± 15	290‡
(VPN) @ 800 C	.....	.....	.....	36†
@ 870 C (1600 F)	142	198	149	.....
Modulus of elasticity (psi)	.....	33×10^6‡	33×10^6‡	$29–30 \times 10^6$
Tensile strength (psi)§	.....	ca. 100,000 (@ 1350 F)	.....	135,000 (70 F) 45,000 (1200 F)
Stress-rupture strength @ 870 C; (1600 F)				
Stress (psi)	20,000	20,000	20,000	.....
Time for rupture (min)	1	3,000	240	.....
Elongation (%)	3.5	13.0	26.0	.....
Reduction of area (%)	3.7	12.2	24.6	.....

* Oil-quenched and tempered; approximating the composition of SAE 4150 steel.
† From Table 2 of Chapter 19.
‡ Average value obtained from preliminary tests.
§ For other tensile properties of steel see Table 4 of Chapter 19.

furnace tube *I* and the inductor coil *Q* are shown in Figure 7, together with the means employed for operating the furnace.

The experiments had not been carried beyond the exploratory stage by the time the project was terminated. Several sound tubular castings, free from porosity, were obtained; but no metallographic examination was made to find out whether there was much grain-boundary contamination by oxides, carbides, and nitrides. Inasmuch as the method has inherent advantages over casting in the case of large-diameter tubes, it would appear to be worth further investigation as a means of making gun liners of chromium-base alloys.

17.2.4 Chromium Impregnations

The brilliant cleanliness of beneficiated chromium (Section 17.2.2) suggested an investigation of metal-bonded chromium compacts. Several compacts were prepared with copper, nickel, or palladium as impregnants. It was hoped that the resulting composite materials would have the basic properties of chromium, together with the useful mechanical properties of the impregnant.

Tests of copper-bonded chromium showed a tensile strength of 100,000 psi (that of annealed copper is 36,000 psi), but with very poor ductility. When a sample of the compact was tested as an erosion vent-plug[49] it stood up better than gun steel during the first three rounds, but cracked badly on the fourth.

17.3 PHYSICAL PROPERTIES[e]

17.3.1 General Résumé

CHROMIUM

Chromium is a very hard gray metal, resembling iron. Its principal ore is chromite, a complex oxide of iron and chromium containing one-third to one-half chromium oxide (Cr_2O_3). The metal is prepared by reduction of the oxide by aluminum. For some purposes the metal is then purified by electrolysis. Some of the properties of chromium are listed in Table 1.

Among the factors that prompted the investigation of chromium as a material for gun liners was its high melting point. Only nine other metals have higher melting points: rhodium, masurium, iridium, ruthenium, molybdenum, osmium, tantalum, rhenium, and tungsten. The cost of chromium in the pure state is relatively high, not because of any scarcity of ore, but because of the expense in reducing the ore.

[e] The data given in this section are taken from several sources.[83,87,167,168,504,524]

Chromium-Base Alloys

The chromium-base alloys that were considered worth testing as gun liners were those containing from 50 to 60% chromium, from 25 to 45% iron, and from 5 to 15% molybdenum or tungsten. Since alloys with molybdenum displayed greater ductility than those containing tungsten, the latter were soon ruled out, and attention was centered on the chromium-iron-molybdenum system. The two most promising of this ternary alloy system proved to be 60-chromium, 25-iron, 15-molybdenum and 60-chromium, 30-iron, 10-molybdenum.

The chromium's principal contribution was chemical inertness and high melting point; the iron's, ductility; and the molybdenum's, erosion resistance and strength. Since iron is similar to chromium, it does not greatly reduce the high melting point of the latter. Moreover, its presence permits the use of ferrochromium as source material of the chromium.



Figure 8. Typical structure of a chromium-base alloy gun liner before firing. (This figure accompanied the manuscript of NDRC Report A-415, but it was not reproduced in that report.)

Centrifugal cast alloy stress-relieved 2 hr at 870 C, for liner L-123, assembly CX-30. C composition: 60Cr-30Fe-10Mo containing 0.03% C, hardness 407 VPN. Estimated percentage: of carbide, 0.10; of oxide, 0.05. ASTM grain size: 1-3. Electrolytic etch in 10% oxalic acid. *100X*.

Since chromium, iron, and molybdenum all crystallize in the body-centered-cubic arrangement, it was expected that their alloys in the composition range indicated above would possess similar crystalline structures. Nothing that would indicate otherwise has yet been observed. Evidence has been found of an intermetallic compound that is precipitated from the chromium-rich solid solution. It is believed that the compound may be FeCr. When such precipitation occurs, the hardness of the alloy is increased. It is not originally present in chill-cast alloys, but it precipitates on holding the alloy for several hours at 870 C (1600 F).

The melting points of the alloys in the chromium-iron-molybdenum system are not nearly so low as that of steel provided that the percentages of the impurities (carbon, oxygen, nitrogen, and silicon) are low.

Included in Table 1 are some of the physical properties of the two most promising (from the standpoint of hypervelocity-gun liner materials) of the chromium-base alloys investigated: 60-chromium, 25-iron, 15-molybdenum and 60-chromium, 30-iron, 10-molybdenum. Data were not available to complete the table, since only a beginning has been made in the investigation of the properties of chromium-base alloys. In some cases several values were available, but the one given in the table may be considered representative. Figure 8 shows the typical structure of a chromium-base alloy gun liner before firing.

17.3.2 Efforts to Improve Ductility by Hot-Working

Chromium

The principal drawbacks to the use of chromium liners for gun barrels are its lack of ductility and its low strength. Since the former failing is the more serious, an investigation[83] was carried out to determine whether plastic working of chromium at an elevated temperature would so alter the structure of the metal as to bring about some degree of plasticity at ordinary temperatures.

The test assembly consisted of a tube of annealed, electrodeposited chromium fitted into a hollow bar of SAE 4140 steel. Connected to the assembly was a copper tube leading to a hydrogen supply, so that a flow of hydrogen was maintained through the small clearances between the inner and the outer parts of the test piece. The outer part of the assembly was heated in a hydrogen-atmosphere furnace and was

swaged, while hot. This action elongated both the steel and the chromium.

Tests were carried out at several temperatures, ranging from 750 C to 1400 C. With respect to plastic deformation of the chromium, 1200 C was the most favorable temperature. It was observed that at 750 C the chromium was shattered. Only at 1400 C was there any bond formed between the steel and the chromium. When the latter was freed it was found to be still quite brittle, and penetrated by longitudinal or helical radially-disposed cracks.

There was no noticeable improvement in cold ductility of the chromium from the hot-working. These experiments demonstrated quite forcibly the relatively great hot-hardness of chromium compared with that of steel. The chromium had behaved as a somewhat deformable body embedded in another softer and quite plastic one, the steel having flowed past the chromium and dragged it along.

Chromium-Base Alloys

Hot-working experiments[87] were also performed with some chromium-base alloys. The grain size of the alloy is a significant factor in its performance as a gun liner, and forging increases the alloy's ductility by refining the coarse, as-cast grains. Some alloy ingots, from 8 to 9 in. in length, having a 1⅜-in. diameter at the bottom and 1⅝-in. at the top, were inserted in cylindrical hollows in swages made from SAE 4140 steel and from 3%-molybdenum iron. An inductively-heated vacuum furnace was used.

The ease with which the alloy could be swaged decreased as the iron-molybdenum ratio decreased. Ingots of the composition 50Cr-45Fe-5Mo were readily hot-worked at temperatures of from 1260 to 1340 C. A gun liner was forged from an ingot of this composition. At a slightly higher temperature (1370 to 1435 C), ingots of the 60Cr-35Fe-5Mo composition were easily forged, with very few surface cracks. Considerably more difficulty was encountered with 60Cr-30Fe-10Mo ingots for which a forging temperature of from 1435 to 1480 C was required. Circumferential cracks, apparently caused by longitudinal tensile stresses set up at the corners of the swage, were observed.

17.3.3 Fabrication of Chromium-Base Alloys

Because of their higher hardness and greater tendency to tear out, chromium-base alloys whose chromium content is about 60% are, on the whole, less machineable than steel and Stellite No. 21. The machineability was found to be a function of the iron-molybdenum ratio. Alloys of the composition 60Cr-25Fe-15Mo and 60Cr-30Fe-10Mo, in which the ratio is at least 5 to 3, can be machined with high-speed steel tools. Alloys having the ratio less than 5 to 3 but greater than 3 to 5 require cemented-carbide cutting tools, or grinding. Alloys with the ratio less than 3 to 5 can be fabricated only by grinding.[524]

Because of limitations of time and personnel, an exhaustive study of the best method of machining and casting gun liners of chromium-base alloys has not yet been undertaken. The method employed during Division 1's investigation was based on fundamental principles, augmented by techniques that developed as the work progressed. The method[87] that evolved was practicable; although more desirable techniques no doubt would result from a search for the optimum tools and operations.

The danger of nitrogen and oxygen contamination, with resulting increase in brittleness, prevents the welding of chromium-base alloys by the techniques applied to cobalt-, iron-, and nickel-base alloys. Preliminary experiments indicate that an inert atmosphere is necessary, and that the welding rod should be prepared from certain chromium-base alloys.[168]

A very decided advantage of chromium-base alloys over molybdenum as a gun-liner material is that they can be cast as seamless tubes, or perhaps be prepared by centrifugal in-melting (Section 17.2.3).

17.4 FIRING TESTS OF LINERS[87]

17.4.1 Introduction

Liners of nine different alloy compositions were fired in the three types of caliber .50 testing guns described in Sections 11.2.1 and 11.2.2: the erosion-testing gun, the heavy barrel machine gun, and the aircraft machine gun. A strict comparison of the results of the 33 firing tests is not possible, since the attempts to improve the properties of the alloys paralleled experiments on methods of supporting the liner in the barrel. Therefore the later tests represented improvements in all these respects. It was determined that 10% molybdenum was the minimum percentage for adequate erosion resistance and strength, and that when properly supported in the gun barrel, liners of a range of compositions have sufficient ductility to withstand the powder pressure without cracking.

17.4.2 Variation of Composition

The first firing tests were of liners (in heavy barrels) made from alloys of the three compositions that had performed so well in erosion vent-plug tests (Section 17.1.2): 60Cr-25Fe-15W, 55Cr-35Fe-10Mo, and 60Cr-25Fe-15Mo. The results indicated that the alloys possessed good erosion resistance and had sufficiently high hot-hardness and melting points. Cracking of the liners and constriction of the bores were the principal causes of failure. The 60Cr-25Fe-15Mo composition was the best of these three tested in the heavy barrel. This same conclusion was reached in tests in the erosion-testing gun of liners of the compositions 60Cr-25Fe-15Mo, 60Cr-25Fe-15W, and 50Cr-45Fe-5Mo.

Because of their greater ductility, alloys containing molybdenum were selected in preference to the tungsten-bearing ones, and a series of tests to determine the most favorable composition was undertaken. This was determined to lie within the range represented by the compositions 60Cr-30Fe-10Mo and 60Cr-25Fe-15Mo on the basis of the following results of tests:

1. The compositions 60Cr-35Fe-5Mo and 55Cr-43Fe-2Mo (the most ductile of the chromium-base alloys tested) had insufficient erosion resistance and strength.

2. The compositions 55Cr-35Fe-10Mo and 55Cr-30Fe-15Mo had insufficient erosion resistance, although the hardness and strength were nearly satisfactory. The latter alloy had been heat-treated to a hardness of 613 VPN, as contrasted with 454 for the former.

3. The composition 55Cr-25Fe-20Mo had about the same erosion resistance and slightly greater strength than 60Cr-25Fe-15Mo but its machineability was much less than that of the latter.

17.4.3 Assembly Variations

Since the two most promising alloy compositions for gun liners were found to be 60Cr-30Fe-10Mo and 60Cr-25Fe-15Mo, liners prepared from the two alloys were given extensive firing tests. The former composition possesses the greater ductility, but it represents the minimum percentage of molybdenum to impart sufficient erosion resistance and strength.

The principal cause of failure of the liners during the firing tests was longitudinal cracking. A special study[87] was made of the stresses imposed on the liner. Formulas such as those given in Section 26.4.5 were used in computing the stresses produced by shrink-fitting liners in the various types of machine-gun assemblies. Cracking was prevented by imposing an initial hoop stress of from 90,000 to 100,000 psi on the liner. In order to achieve this degree of compression with the relatively thin aircraft barrel, a reinforcing sleeve had to be shrunk on the outside of the barrel. The sleeve was made of Timken No. 17-22A steel, which possesses greater high-temperature strength than ordinary gun steel.

Because of the successful results obtained with two-stave molybdenum liners (Section 18.6), a two-stave assembly of the liner composition 60Cr-25Fe-15Mo was prepared and tested in the caliber .50 erosion-testing gun with double-base powder. The results were disappointing in that longitudinal and circumferential cracks were observed in the fired liner.

In a test to determine what benefits in firing performance would be effected by supporting the liner with a backing material possessing high elevated-temperature strength, an assembly was prepared in which a liner of the composition 60Cr-25Fe-15Mo was supported by a sleeve made from an alloy of the composition 60Cr-30Fe-10Mo, shrunk into the steel retainer. When tested in the caliber .50 erosion-testing gun with double-base powder, a total of 568 rounds was fired. The test was discontinued because of excessive pressure rise caused by slight constriction and roughening of the surface. This represented the greatest number of rounds sustained by a chromium-base alloy assembly in the erosion-testing gun.[76] Upon examination of the fired liner there was no evidence of attack by the powder gases, but cracking and pitting of the bore surface were observed.[77] Some of these effects can be seen in a cross section of the liner, 6 in. beyond the origin of rifling, shown in Figure 9.

Although this test and the one using the stave-type of construction were not successful as far as method of insertion was concerned, they did prove the high order of resistance of these chromium-base alloys to powder gases, even those from double-base powder. The conditions of erosion were so severe in the caliber .50 erosion testing gun that a gun steel barrel was worn out after only 90 rounds.

Preferred Method of Insertion

The foregoing tests of different methods of insertion of chromium-base alloy liners in caliber .50 bar-



FIGURE 9. Cross section of 60Cr-25Fe-15Mo liner, 6 in. beyond origin of rifling, after having been fired 568 rounds with ball bullets and FNH-M2 powder. The surface of the liner had cracked and pitted along the grain boundaries and some pitting had developed. This liner had been supported in a caliber .50 erosion-testing gun tube by a sleeve of 60Cr-30Fe-10Mo. Etched with 10% KOH—10% $K_3Fe(CN)_6$. *100X*. (This figure has appeared as Figure 17 in NDRC Report A-405.)

rels made clear the requirements for a successful assembly. These were that the liner be made cylindrical, that it be restrained by a hoop stress of about 100,000 psi, and that the steel of the barrel have sufficiently good high-temperature strength to maintain this compression even after continued firing (Section 24.5). Furthermore it was desirable that the bore surface of the barrel ahead of the liner be protected from the powder gases in order to utilize fully the great erosion resistance of the liner.[f]

These requirements were met by inserting two liners each of alloys having the compositions that the previous tests had shown were most suitable (60Cr-25Fe-15Mo and 60Cr-30Fe-10Mo) in 13-lb aircraft barrels made of Timken No. 17-22A steel (Section 24.5.3), which had been chromium-plated ahead of the liner recess with choked-muzzle chromium plate (Section 23.1.4). These barrel assemblies were tested in the caliber .50 aircraft machine gun by firing the CGL-350 schedule described in Section 23.1.3. After 3,850 rounds the liners had not failed, but the test was discontinued because of termination of Division 1's contract with the Crane Company,[80] where the firing took place. Numerous surface checks were observed after the initial 350-round burst, and these irregularities in the surface had developed into large pits and cracks of indeterminate depth after the next group of 500 rounds. After that they showed little further change.

The average "cold velocity" (Section 23.1.3) of the barrels containing chromium-base alloy liners increased gradually to a maximum after 3,350 rounds, which indicated that a slight progressive shrinkage of the bore near the origin of rifling took place. The "hot velocity" remained essentially unchanged during the test. The accuracy was poorer than that obtained in the firing of two barrel assemblies similarly prepared containing liners of No. 21 Stellite (Section 24.5.3); but no reason was discovered for the difference. The wear of the bore surface was less for all four chromium-base alloy liners than for the two stellite ones after the same number of rounds. This difference indicated that the chromium-base alloy liners might have lasted longer than the stellite ones, provided that they did not crack or shrink to such an extent that continued firing was impossible.

17.5 POTENTIALITIES OF CHROMIUM-BASE ALLOYS AS LINER MATERIALS

17.5.1 Extent of Suitability

The properties of an ideal erosion resistant material are discussed in Section 16.2. They are reviewed here to see how well chromium-base alloys fulfill the requirements.

THERMAL RESISTANCE

The melting points of the chromium-base alloys have not been determined closely; but presumably they are not a great deal lower than that of pure chromium, since the effects of the iron and molybdenum are in opposite directions. The specific heat is presumably about the same as that of steel whereas the thermal conductivity is only about one-third as

[f] Many of the firing tests in the caliber .50 aircraft barrels had to be discontinued as a result of severe erosion of the steel barrel ahead of the liner, and others were continued long past the stage of "keyholing" caused by erosion there, just to test the endurance of the alloy.

great. Hence the thermal factor ρck in equation (13) of Chapter 5 is also about one-third as great as for gun steel, and consequently the increase in temperature of a very thin layer at the surface after the firing of one round is considerably greater than for gun steel, perhaps as much as 50 per cent.

The consequent thermal stress is also somewhat greater, although the effect of the greater temperature increase is offset somewhat by the lower thermal expansion. This thermal stress applied to a material of low ductility does cause a slight checking of the surface. In this respect these alloys are inferior to stellite, when cool propellants are considered; but on the other hand, since the melting points are high enough to prevent the melting of a surface film when double-base powders are fired, as occurs with stellite, they may be said to be superior to stellite in overall thermal resistance, while inferior to molybdenum in this same respect.

Chemical Resistance

The alloys possess excellent resistance to the chemical action by the powder gases at elevated temperatures.

Mechanical Properties

It is in this category that the alloys display their serious weakness, poor ductility. In spite of this weakness, it has been possible to make successful caliber .50 liners, as described in Section 17.4.3. In other respects they meet the requirements of the ideal material: no large permanent change in dimensions (provided that casting strains are avoided), no permanent deformation or flowage, high strength at elevated temperature (especially in the 60Cr-25Fe-15Mo alloy), and thermal and elastic properties close to those of gun steel, except that the coefficient of thermal expansion is only about two-thirds as great.

Other Properties

The raw material for the alloys is available in sufficient quantity. The process used to prepare the experimental liners was satisfactory, and there is every indication that, with continued development, it ultimately can be adapted to commercial production. The alloys are readily machineable if proper tooling is used.

17.5.2 Recommendations for Further Development

Firing Tests

Since higher potential propellants offer a convenient means of increasing the muzzle velocity of an existing gun, it is suggested that liners of the two chromium-base alloys that have proved to be most promising so far—60Cr-25Fe-15Mo and 60Cr-30Fe-10Mo—be tried in the caliber .50 aircraft machine gun with the experimental double-base powder already developed by the Army Ordnance Department. For such a test the liners might be inserted in a "finned" barrel, such as is described in Section 24.3.3, made of high-strength steel instead of a 13-lb barrel as was used in the tests described at the end of Section 17.4.3. Then the test could be made with the high-speed caliber .50 gun, M3, without sacrifice of cyclic rate.

Improvement of Ductility

Since brittleness is so serious a problem in the extensive application of these alloys, fundamental research should be continued to find a ductile composition. Some experiments[87] at Union Carbide and Carbon Research Laboratories have indicated that the alloy 60Cr-25Fe-15Mo is very susceptible to work hardening. Since iron seems to improve the ductility more than any other alloying element, it may be possible to use a chromium-base alloy with higher iron content and obtain the necessary hardness by work-hardening. It is questionable, however, whether the thermochemical resistance of such an alloy would be sufficient even after hardening.

Another possible way of obtaining a more ductile alloy is by the use of a fourth element. The investigation of the effect of the introduction of different possible fourth components on erosion resistance and liner performance in general would be time consuming. In order to keep to a minimum the number of firing tests, ductility as determined by mechanical tests should be used as the criterion of improvement. A high-temperature impact test, as recommended in Section 16.3.9, under "Notch Impact Tests and High-Velocity Impact Tests" would be ideal for the purpose. When, finally, some more ductile composition has been found, and its erosion resistance is to be evaluated, care should be taken to support it adequately in a barrel made of high-strength steel with the bore surface ahead of the liner protected by chromium

plate or in some other suitable manner as was done in the tests described at the end of Section 17.4.3.

Methods of Production

As a parallel investigation to the continuation of fundamental research on the composition of chromium-base alloys, it is recommended that the development of suitable methods and equipment for the large-scale production of the alloys be continued.

This recommendation is made in anticipation of the time when an alloy possessing the desired properties will have been developed.



Chapter 18

MOLYBDENUM

By *F. Palmer*[a]

18.1 INTRODUCTION

THE SEARCH for an ideal erosion resistant material, discussed in Chapter 16, revealed that molybdenum was one of the few metals that showed great promise in this respect. In particular, it is pre-eminent in its resistance to thermal and chemical attack by the powder gases during the short time of exposure in a gun. At the same time, commercially available molybdenum lacked some of the necessary mechanical properties and could not be produced in the proper size and shape for fabricating gun liners. Extensive investigations have succeeded in showing ways to overcome these deficiencies.

The liners which reacted most favorably to firing tests in a caliber .50 gun were made of an alloy of molybdenum with 0.1 per cent cobalt, which is harder than pure molybdenum. They were fabricated from metal which had been swaged according to a "working schedule" that was developed to obtain the optimum possible strength and ductility for a given reduction in cross section. These liners consisted of two longitudinal segments, or staves, which were twisted so that the seams followed the rifling grooves. After having been fired 2,021 rounds they were still serviceable, whereas gun steel would have failed after 90 rounds under the same hypervelocity conditions of testing.

Because there were still some deficiencies in the design of the best liners mentioned above, further work was planned on other methods of fabricating liners. Also, plans were made to prepare a molybdenum liner for test in a 3-in. Naval gun, as described in Section 33.1.3. The Navy Department subsequently contracted with the Westinghouse Electric Corporation for the use of the facilities set up under its contract with Division 1 and for considerable expansion of them according to plans already developed by the Division.

18.2 COMMERCIAL MOLYBDENUM

18.2.1 Manufacturing Process

The term *powder metallurgy* is used to describe

[a] The Franklin Institute, Philadelphia, Pa.

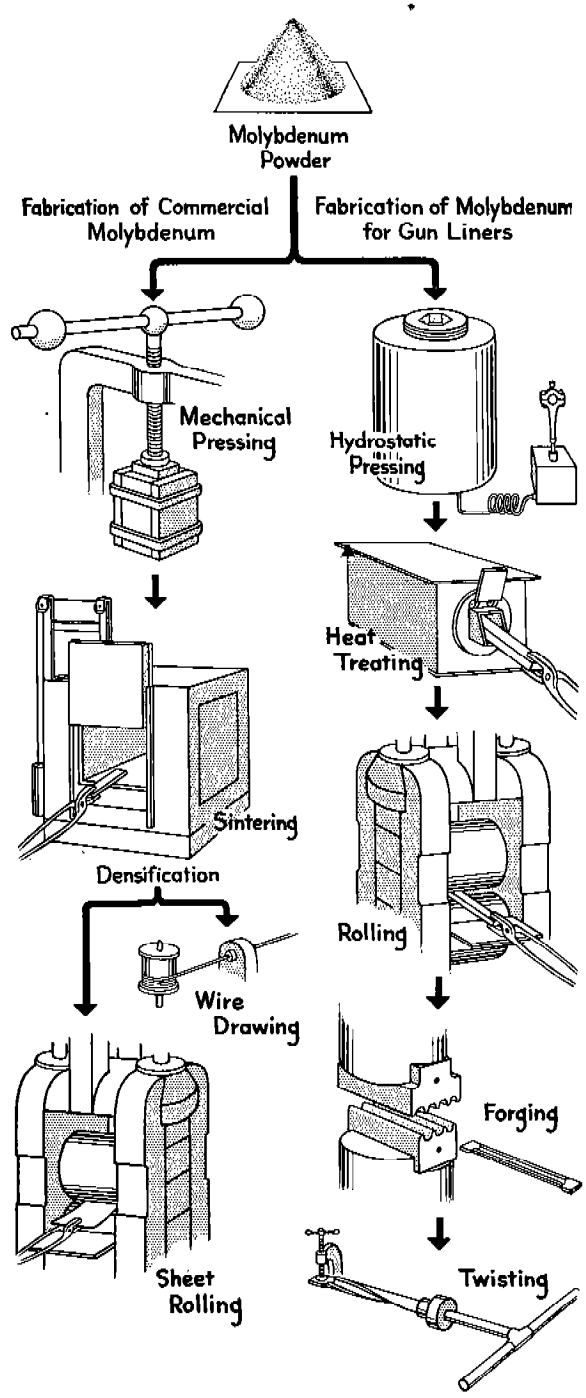


FIGURE 1. The fabrication of molybdenum.

the usual commercial process by which a molybdenum compound, frequently the oxide (MoO_3), is converted into bars of metal. The process starts with the reduction of the compound to a metal powder by heating it in a stream of hydrogen. The successive steps after that are shown in the left-hand column of Figure 1. The metal powder is compressed mechanically in a steel mold so as to form a compact, which is then sintered in hydrogen at a high temperature until the powder particles coalesce somewhat. Further densification is accomplished by heating the sintered molybdenum in hydrogen to a temperature near its melting point (2620 C), so that the powder metallurgy ingot can be subsequently subjected to mechanical working to impart strength and ductility. The principal commercial forms of molybdenum are fine wire and thin sheet. Both are made by working such an ingot first hot (around 1350 C) and then gradually lowering the working temperature as mechanical reduction proceeds. All heatings are made in hydrogen to prevent excessive loss of metal by oxidation. To make wire the bar is swaged in successively smaller dies and finally hot-drawn through other dies. To make sheet or strip (which is a narrow thick sheet) the bar is hot-rolled to the desired thickness.

The more working molybdenum receives the more satisfactory become its physical properties provided working temperatures are properly adjusted. This situation is illustrated in Table 1 for sheet of different thicknesses made from a heat-treated compact of cross section 1x1⅛ inches. During the working process the temperature normally falls below the point of recrystallization (1200 C) with the result that the crystal grains become elongated and interlocked, as shown in Figure 2. This structure in metal which is cold-worked below the recrystallization temperature promotes strength and ductility.

18.2.2 Physical Properties of Molybdenum

Dependence of Mechanical Properties on Amount of Working

The best mechanical properties of molybdenum are obtained only when it is thoroughly worked. The increase in ultimate strength and hardness with continued working, resulting in decreasing thickness, is shown in Table 1. The reduction in thickness of the sheet is roughly proportional to the amount of working.

Table 1. Dependence of physical properties of molybdenum upon hot-working as measured by thickness of sheet.

Thickness (in.)	Hardness (D.P.H.)	Ult. Strength (10^3 psi)	Elong. (2 in.) (per cent)
0.450	227	76.0	slight
0.230	250	88.6	11.0
0.015	270	122.0	4.7

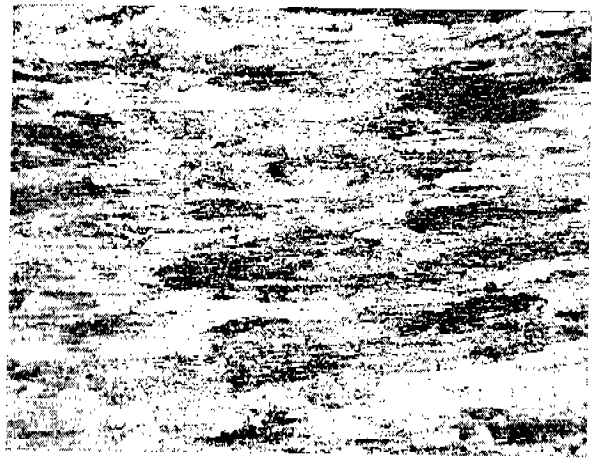


Figure 2. Structure of well-worked, commercial molybdenum (0.126-in. thick). Aqua regia etch, *50 X*. (Figure 4d of NDRC Report No. A-423.)

In the case of wire, the reduction in area is a better measure of amount of working. The results of some early tests on the ultimate tensile strength, in the direction of working of both wire and strip, plotted against cross-sectional area, are shown in Figure 3. Although there is a rather wide scattering of observations on both sides of the mean, the general trend of the curve indicates definitely that the ultimate tensile strength increases as the metal becomes thinner

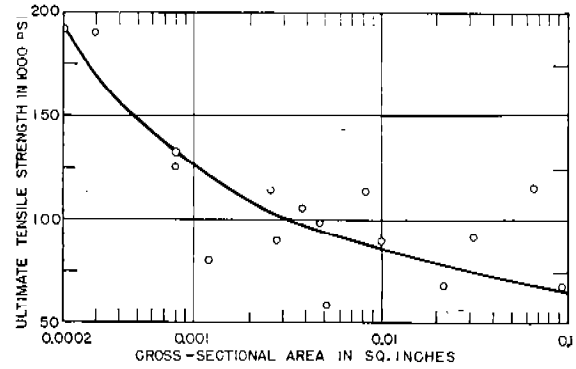


Figure 3. Ultimate tensile strength of commercial molybdenum worked to different cross-sectional areas. (Figure 1 of NDRC Report No. A-423.)

[redacted]

due to the working to which it has been subjected. Scattering of the observations is probably due to the lack of uniformity in the heat-treatment of the bar stock.

It may be inferred from a graph such as that in Figure 4 that the hardness of molybdenum also is related to the amount of working. In spite of the scatter of the observed readings, it is clear that the molybdenum strip became harder the more it was worked.

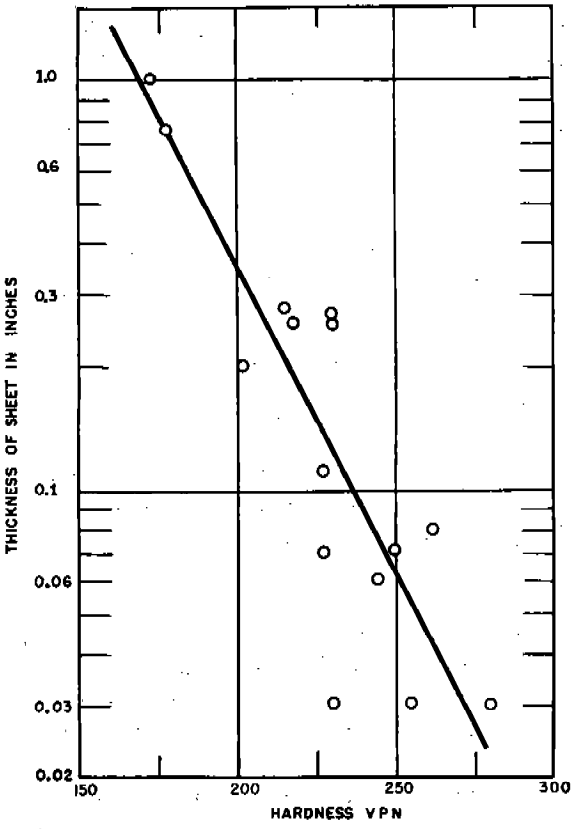


FIGURE 4. Hardness of commercial molybdenum worked to different thicknesses. (Figure 2 of NDRC Report No. A-423.)

RELATION OF PROPERTIES TO ANISOTROPIC STRUCTURE

Although hot-working increases the strength, ductility, and hardness of molybdenum, the worked metal is likely to possess a laminated, anisotropic texture. The tensile strength of rolled molybdenum strip is approximately the same along the direction of working (longitudinal) as across the direction of working (transverse), but in the latter direction the ductility is very small. Hence the strip may be bent without cracking when the crease is transverse, but the metal is brittle and cracks easily when the crease is longitudinal. Microscopic examination of sections etched with aqua regia reveals a progressive change in crystal fabric with amount of working. Unworked molybdenum is fine grained with no definite crystal orientation, as can be seen in Figure 5. When partially worked, there are crystals of various sizes which begin to show the effects of being worked by a tendency toward elongation parallel to the direction of working, as illustrated in Figures 6 and 7. In thoroughly worked material the crystals are all elongated

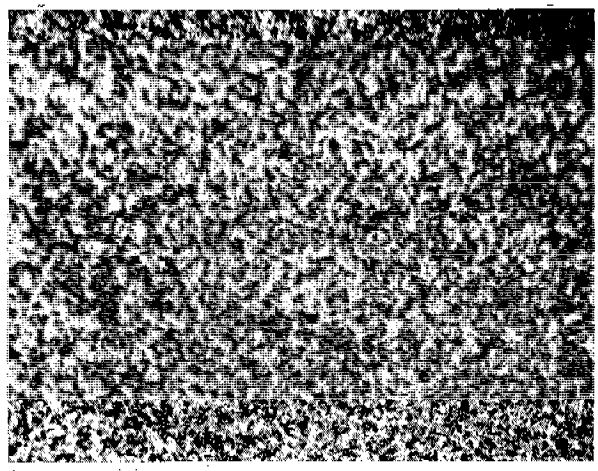


FIGURE 5. Structure of unworked, commercial molybdenum (1.250-in. thick). Aqua regia etch, *50 X*. (Figure 4a of NDRC Report No. A-423.)

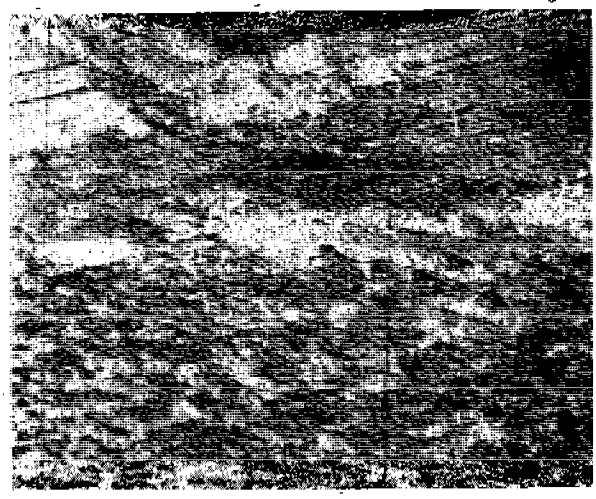


FIGURE 6. Structure of partially worked (laminated) commercial molybdenum (0.430-in. thick). Aqua regia etch, *50 X*. (Figure 4b of NDRC Report No. A-423).

with a fibrous interlocked crystal pattern, which was shown before in Figure 2.

It has been suggested[96] that circumferential ductility might be improved by twisting well-fibered bars of wrought molybdenum so that the axially elongated grains would be turned toward the circumferential direction. When suitable material and equipment become available, the properties of such helically fibered bars should be given careful study.



FIGURE 7. Structure of worked but recrystallized, commercial molybdenum (0.274 in. thick). Aqua regia etch, *50 X*. (Figure 4a of NDRC Report No. A-423.)

UNSUITABILITY OF COMMERCIAL MOLYBDENUM FOR GUN LINERS

Some of the physical properties of molybdenum compared with those of gun steel are given in Table 2. The high melting point and thermal conductivity of molybdenum are advantageous for its use as a bore-surface material. The low strength and ductility of commercial molybdenum are undesirable properties, but, as will be shown in Sections 18.3 and 18.4, means were found for producing molybdenum and molybdenum alloys with a great improvement in these properties. Even then liners had to be designed in such a way that the low thermal expansivity would not prove a major handicap, as discussed in Section 26.5.2.

TABLE 2. Physical properties of commercial molybdenum and gun steel.

Properties	Molybdenum (wrought, ductile)	Gun Steel (oil-quenched and tempered)
Melting point (C)	2535	1450
Thermal expansivity (0–500 C)(%/°C)	5.49×10^{-6}	13.6×10^{-6}
Thermal conductivity (cal/cm/sec/°C)	0.35	0.102
Specific heat (cal/g/°C)	0.065	0.107
Ultimate tensile strength (psi)	$90–100 \times 10^3$	$>130 \times 10^3$
Elongation at rupture (% in 2 in.)	5–20	>16
Hardness at room temperature (VPN)	260–270	280–320

In order to withstand firing stresses of the usual magnitude, the metal of a gun liner must have a thickness of one or two tenths of an inch. On the other hand, sheets of commercial molybdenum that have been worked sufficiently to develop suitable mechanical properties are available only with a thickness of 0.015 in. or less. Hence this material is unsuitable for gun liners.

18.3 PRODUCTION OF DUCTILITY IN THICK SHEET SUITABLE FOR GUN LINERS

18.3.1 Introduction

The first molybdenum liners tested were tubes bored from swaged rods. They all failed after so few rounds that it became evident that molybdenum, in spite of its high melting point and excellent resistance to chemical attack by hot powder gases, would not prove a satisfactory liner material unless its strength and ductility could be largely increased.[49,50] This requirement could be met only by increasing the amount of working (Section 18.2.2).

At the time that Division 1 began the development of molybdenum gun liners, there was no equipment in use that was large enough to work mechanically molybdenum compacts thicker than 1½ in. Furthermore, information was lacking as to how to work thicker bars without cracking them. Hence, it was essential to develop a working schedule which would change a bar of the usual dimensions (⅞x1¼x20 in.) into a strong, ductile sheet thick enough (about ¼ in.) for use as a caliber .50 gun liner. At the same time it was desirable to explore means of preparing and mechanically working bars or ingots of even larger cross section.

18.3.2 Development of a Satisfactory Working Schedule

The investigations[95] that resulted in a satisfactory working schedule may be summarized in terms of two

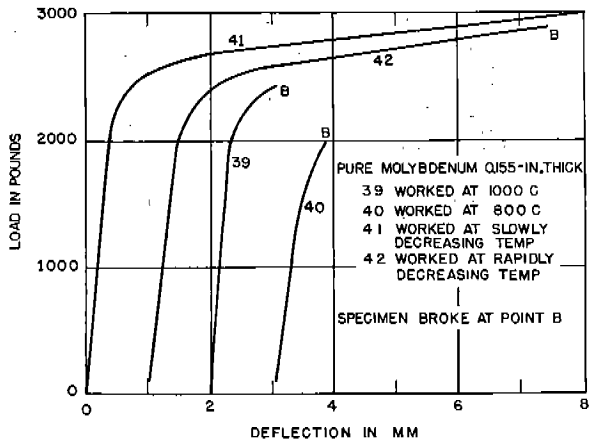


FIGURE 8. Bend strength and yield of samples of pure molybdenum worked at different temperatures. (Figure 14 of NDRC Report A-423.)

principles. These principles are that (1) complete recrystallization *above 1200 C* is essential in order to convert the weak, microcrystalline structure of the treated bars into one with large, uniform grains; and (2) working causes an increase in strength, by elongating and interlocking the large grains, only *below 1200 C*, the temperature at which the metal recrystallizes quickly.

Development of a uniform grain structure is promoted by hot-rolling the bars just the proper amount and reheat-treating them. Since it has been found that crystallization is incomplete with too little working and fine crystals are produced by too much working, the amount of reduction in thickness on the first pass is critical.

Furthermore, edge-cracking and end-splitting are likely to develop in the recrystallized bars unless they, too, are rolled once or twice above 1200 C. Before the temperature is reduced below this point it is apparently necessary to break down the equiaxed grain structure, which can be done only while the metal is plastic. The amount of reduction in thickness on these passes, too, is critical.

The influence on strength and ductility of pure molybdenum worked under different temperature conditions is shown in Figure 8. The letter *B* indicates that the specimen broke at that point. The only specimen which did not break before the termination of the experiment was the one which had been worked at slowly decreasing temperatures. Hence, in a satisfactory working schedule provision has been made for the working to take place while the temperature of the metal is slowly decreased.

TABLE 3. Improved working schedule for alloy of molybdenum with 0.1% cobalt, starting with a bar 1x1¼x24 in.[95]

Pass	Furnace temperature (C)	Reduction of thickness (in.)
Preliminary	1300	0.100
(Reheat-treat to complete recrystallization)		
1	1300	0.200
2	1300	0.150
3	1200	0.100
4	1200	0.100
5	1100	0.075
6	1100	0.075
7	1000	0.075
8	1000	0.050
9	1000	0.050

IMPROVED WORKING SCHEDULE

The best gun liners prepared for test under Division 1's auspices were produced from heat-treated bars of molybdenum plus 0.1% cobalt (Section 18.6), of dimensions about 1x1¼x24 in. These bars were processed according to the schedule shown in Table 3. The preliminary pass served to induce crystallization. The structure after reheat-treatment is shown in Figure 9.

The microstructure of the final product under this working schedule was better at a thickness of 0.250 in. (Figure 10) than that of commercial molybdenum



FIGURE 9. Structure of molybdenum alloy containing 0.1% cobalt, recrystallized according to improved working schedule. Compare Figure 10. Aqua regia etch, *50 X*. (Figure 13a of NDRC Report A-423.)

at different thicknesses (Figures 2 and 7). In addition it had at least 50 per cent greater strength and several times as much ductility as commercial molybdenum of the same thickness.

After the tests of these liners, described in Section 18.6, evidence[76] was found of longitudinal cracking, spalling, and swaging of lands. This result was taken to indicate that even greater reduction in cross section will be necessary to make molybdenum a wholly satisfactory gun liner material, which means that the pressed bar must be considerably thicker than 1¼ in.

18.3.3 Advantage of Hydrostatic Compression

The substitution of hydrostatic pressing for mechanical pressing in the fabrication of the powder compact makes possible the production of thicker bars and also markedly improves the quality of the molybdenum strip. The powder, placed in a rubber tube, is immersed in water in a pressure cylinder and subjected to a hydrostatic pressure of 30,000 to 40,000 psi. The cylinder used had a bore of 8 in., with which bars 3 in. square could be made. A 12-in. cylinder was planned so that 5-in. bars could be made.

The improvement in quality is attributable to the uniformity of the pressing and to the absence of incipient cracks. It was found that the early test liners made from mechanically pressed powder contained incipient cracks which opened up rapidly under firing stresses. The first crack-free liners were made in the form of two staves (Section 18.5) from molybdenum which was hydrostatically pressed.

Later it was found possible to obtain crack-free material by mechanical pressing with special care being taken in the way the molds were filled and handled. It is not certain, however, that equally good results would be obtained from thicker bars. Furthermore, mechanical pressing of large bars requires much more elaborate equipment than does hydrostatic pressing. Hence the latter was to have been used in making molybdenum bars for the 3-in. gun liners described in Section 33.1.3.

18.3.4 Plans for Enlarged Facilities

It had been recognized at the inception of the molybdenum project that in order to fabricate molybdenum for liners larger than small arms much more powerful equipment would be necessary than was then available. The decision to have such equipment installed at the Lamp Division of Westinghouse Electric Company was deferred by NDRC until definitive results were obtained with caliber .50 liners made by means of existing equipment.

New equipment was then planned[95] for the fabrication of molybdenum to be used in the 3-in. gun liner described in Section 33.1.3. It included a 12-in. hydrostatic press, a heavy-duty rolling mill, and a 7,200-ft-lb forging hammer in addition to furnaces and auxiliary equipment. With this equipment,[b] the sequence of operations shown on the right-hand side of Figure 1 could be carried out. The molybdenum powder used as starting material would be "doped" with a small amount of cobalt or other alloying constituent, as described in the next section.



FIGURE 10. Structure of molybdenum alloy containing 0.1% cobalt, reduced to 0.250 in. according to improved working schedule. (Compare Figure 9.) Aqua regia etch *50 X*. (Figure 13b of NDRC Report A-423.)

18.4 HARDENING OF MOLYBDENUM BY ALLOYING

18.4.1 Hardening by Alloying Alone

Molybdenum can be hardened not only by cold-working below the recrystallization temperature but also by alloying with the proper elements. The hardness of some alloys of molybdenum in the unworked condition is given in Table 4. The hardness of pure molybdenum in the same condition is only 175 VPN

[b] The accelerated termination of Contract OEMsr-1205 after V-J Day delayed the purchase of this equipment. It was later installed under a Navy Department contract with the Westinghouse Electric Company.

TABLE 4. Hardness of certain alloys of molybdenum.*

No.	Alloy composition	Hardness (VPN) at 20 C	500 C	600 C
1	Mo + 5% W	213	134	132
2	Mo + 10% W	288	160	153
3	Mo + 15% W	249	196	185
4	Mo + 20% W	268	191	195
5	Mo + 0.01% Ni	223	119	116
6	Mo + 7% Ni	423	372	359
7	48.5 Mo + 48.5 W + 3.0 Ni	494	366	366

* Measurements made by Climax Molybdenum Company, 1943.

at 20 C. These alloys have both higher ultimate strength and higher yield point than pure molybdenum. Unfortunately, the last two alloys in Table 4 are not workable alloys.

18.4.2 Effects of Alloying and Working

More recent observations[95] are plotted in Figure 11 where the hardening effects of both working and alloying with small percentages of cobalt are especially noteworthy. The alloy containing 0.1% cobalt is easily workable and of reasonably satisfactory hardness, hence, in view of the difficulties involved in running a complete reconnaissance series, intensive work was spent largely in the development of this alloy. The improved working schedule given in Table 3 was devised for this particular alloy. For any other alloy a similar working schedule might be developed after a series of trials had been made.

18.4.3 Effect of Temperature on Hardness of Various Alloys

The effects of amount of working and of alloying with other metals are both to be seen in the curves of Figure 11. It will be observed that the hardness at 20 C of unworked pure molybdenum is raised from about 175 VPN to about 240 VPN when worked to a thickness of 0.106 in.; to about 265 VPN when unworked but alloyed with 20% tungsten; and to about 290 VPN when alloyed with 0.1% cobalt and worked to a thickness of 0.25 in. The advantages possessed by molybdenum and its alloys over gun steel (SAE 4150), which is harder than they are at 20 C, are twofold: (1) above 300 C steel loses hardness rapidly with increase in temperature, (2) whereas with the other materials above 300 C the hardness falls off less rapidly and the rate of loss *diminishes* with increase in temperature.

From Figure 11 it is clear that the substitution of an unworked molybdenum liner for one of steel will not eliminate swaging of the lands, for the metal is too soft, as was confirmed by one of the early experiments.[49] Improvement in this respect can be expected only in proportion to the degree of hardening brought about by more efficient working and alloying techniques.

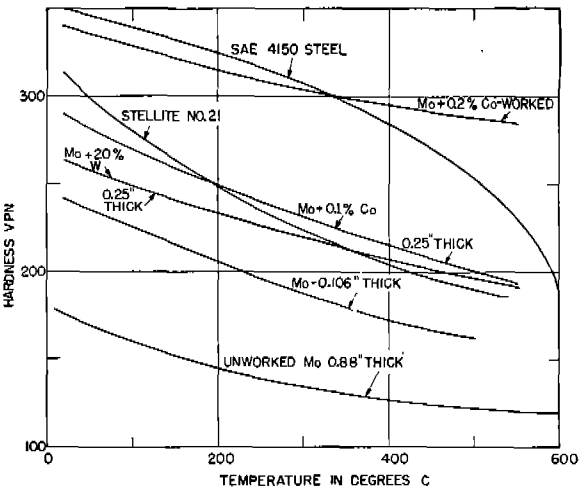


FIGURE 11. Hardness of alloys as a function of temperature—molybdenum containing different amounts of alloying elements compared with Stellite No. 21 and SAE 4150 steel. (Figure 6 of NDRC Report A-423.)

18.4.4 Selection of Best Alloy

ALLOYS OF MOLYBDENUM WITH TUNGSTEN

The first gun liners made of a binary molybdenum alloy contained, respectively, 10%, 15%, and 20% tungsten. When tested in the caliber .50 erosion-testing gun (Section 11.2.1), they all failed after 150 rounds or less. Both longitudinal and transverse cracks occurred, as well as severe spalling. The latter defect was due to their laminated structure of the molybdenum, which, it is now believed (Section 18.2.2), was the result of insufficient working by an improved schedule. Further experiments with tungsten as the alloying element have not been carried out because these alloys were found more difficult to work than others of nearly the same hardness, made at a later date, with small percentages of cobalt or nickel.

ALLOYS OF MOLYBDENUM WITH COBALT OR NICKEL

Molybdenum is hardened to nearly the same extent by the addition of the same small amount of either

cobalt or nickel, though there is evidence that nickel alloys harden somewhat more rapidly than cobalt alloys, and, therefore, are more difficult to fabricate.

The curves of Figure 12 show how the hardness at 20 C of such alloys, both for unworked and worked material, changes with the addition of increasing amounts of either cobalt or nickel. The change in hot-hardness of worked material at 500 C is also shown. Although the results shown here indicate that the hardening effects of cobalt and nickel are the same, other experiments have suggested that nickel is less effective than cobalt. More extensive testing is required. These curves (and those in Figure 11) at least demonstrate that the alloy containing cobalt or nickel is superior to pure molybdenum, even when the latter is well worked. The hot-hardness is still low enough, however, to make the material a not entirely satisfactory one for use in a gun liner.

Nevertheless, two caliber .50 test liners made of an alloy containing 0.1% cobalt gave a remarkable performance, as described in Section 18.6. This alloy does not necessarily represent the best one for the purpose, and therefore further study should be made of the hardening effects of larger percentages of cobalt and of varying amounts of other elements, including nickel, iron, and chromium.

optimum might be used without severe longitudinal cracking during firing. Although the other designs[c] were presumably feasible, some of them were fraught with more difficulties than others, and experiments were finally concentrated on fabricating stave liners.

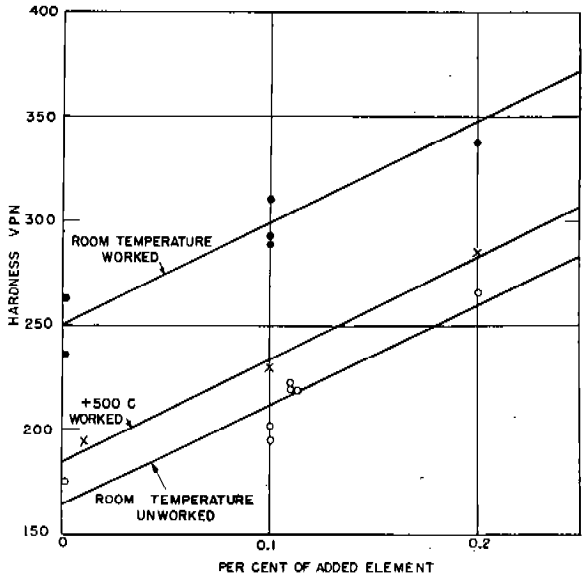


FIGURE 12. Hardening effect of the addition of nickel or cobalt to molybdenum. (Figure 7 of NDRC Report A-423.)

18.5 CONSTRUCTION OF CALIBER .50 LINERS FOR TEST

18.5.1 General Design Considerations

The development of an improved type of molybdenum for gun liners demanded a means of testing the material in an actual gun. The gun selected for the purpose was the caliber .50 erosion-testing gun, described in Section 11.2.1, because with it hypervelocity conditions could be achieved. At the same time the impossibility of obtaining (with the equipment available) molybdenum having adequate physical properties in thick sections increased the difficulty of making even test liners from this material. It was necessary to devise means of making them from well-worked metal of small cross section.

Various designs for molybdenum liners were discussed at the outset of the program.[52] A stave-type liner, that is, one having longitudinal segments, was suggested as a means of transferring much of the load of the powder pressure from the molybdenum liner to the steel carrier. It was hoped that, by doing this, molybdenum of strength and hardness less than the

18.5.2 Stave-Type Liners

STRESSES IN STAVE LINERS

A calculation of the stresses in cylindrical-tube and multiple-stave liners indicated that during the repeated firing of a caliber .50 gun a cylindrical-tube liner would be exposed to stresses considerably higher than the ultimate strength of molybdenum, as is brought out in Section 26.5.3. Hence fatigue failure would be expected after relatively few stress cycles at the assumed explosion pressure (80,000 psi). With a stave-type liner, on the other hand, the stresses would be substantially reduced. The calculation indicated that the greatest reduction would occur for a liner made of four staves, although the reduction for a liner of two staves, in the case of the caliber .50 gun, is nearly as great.

Since the tangential tensile stress at the middle of a stave is nearly proportional to the coefficient of friction between molybdenum and steel,[52] it is evi-

[c] The ones that were tried are mentioned in Section 18.5.3.

TECHNICAL LIBRARY
BLDG. 313
ABERDEEN PROVING GROUND, MD



FIGURE 13. Two-stave straight liner of molybdenum alloy containing 0.1% cobalt after having been fired 442 rounds. (Figure 19b of NDRC Report A-423.)

dent that a reduction in stress can be brought about by proper lubrication of the molybdenum-steel interface. Measurements[96] were made of the coefficient of friction between test pieces of molybdenum and SAE 4150 steel treated with a thin film of lubricating material. Of the lubricants tested, tungsten disulphide was the best, with a coefficient of friction less than one-third that of unlubricated surfaces. It should be pointed out, however, that in firing a lubricated liner, although stresses would be reduced, any tendency toward forward motion and rotation of the liner would probably be increased.

SEAMS OF STAVE LINERS

The first firing tests of two-stave liners[76] gave promise of the eventual success of this type of construction. The principal difficulty was that spalling, a severe case of which is shown in Figure 13, took place. Even though the staves were shrunk into the steel carrier with a large interference, the seams opened up during firing and allowed the hot powder gases to penetrate them and raise the temperature of the edges. An attempt to prevent this by brazing the seams was unsuccessful. Finally, marked improvement was brought about by hot-twisting the staves (1 turn in 15 in.) so that the seams ran down the center of the rifling grooves.[95]

CONSTRUCTION OF TWO-STAVE LINERS FOR TESTING MATERIALS

After preliminary trials had showed that the best means of utilizing the available molybdenum sheet was by a two-stave liner with helical seams, a program was instituted for the trial of several series of such liners, each made from a different alloy. It was started by the test of the alloy containing 0.1% cobalt described in Section 18.4.4. The steps involved in construction of the two-stave liners used in those tests in the caliber .50 erosion-testing gun are shown in Figure 14.[95] The letters given in parentheses refer to the separate parts of this figure.

1. Molybdenum powder containing cobalt was pressed mechanically and heat-treated to form a bar about 1x1¼ in. (Step A.)

2. The bar was subjected to the improved working schedule (Table 3) to produce a strip about 0.22 to 0.25 in. in thickness. (Step B.)

CONFIDENTIAL

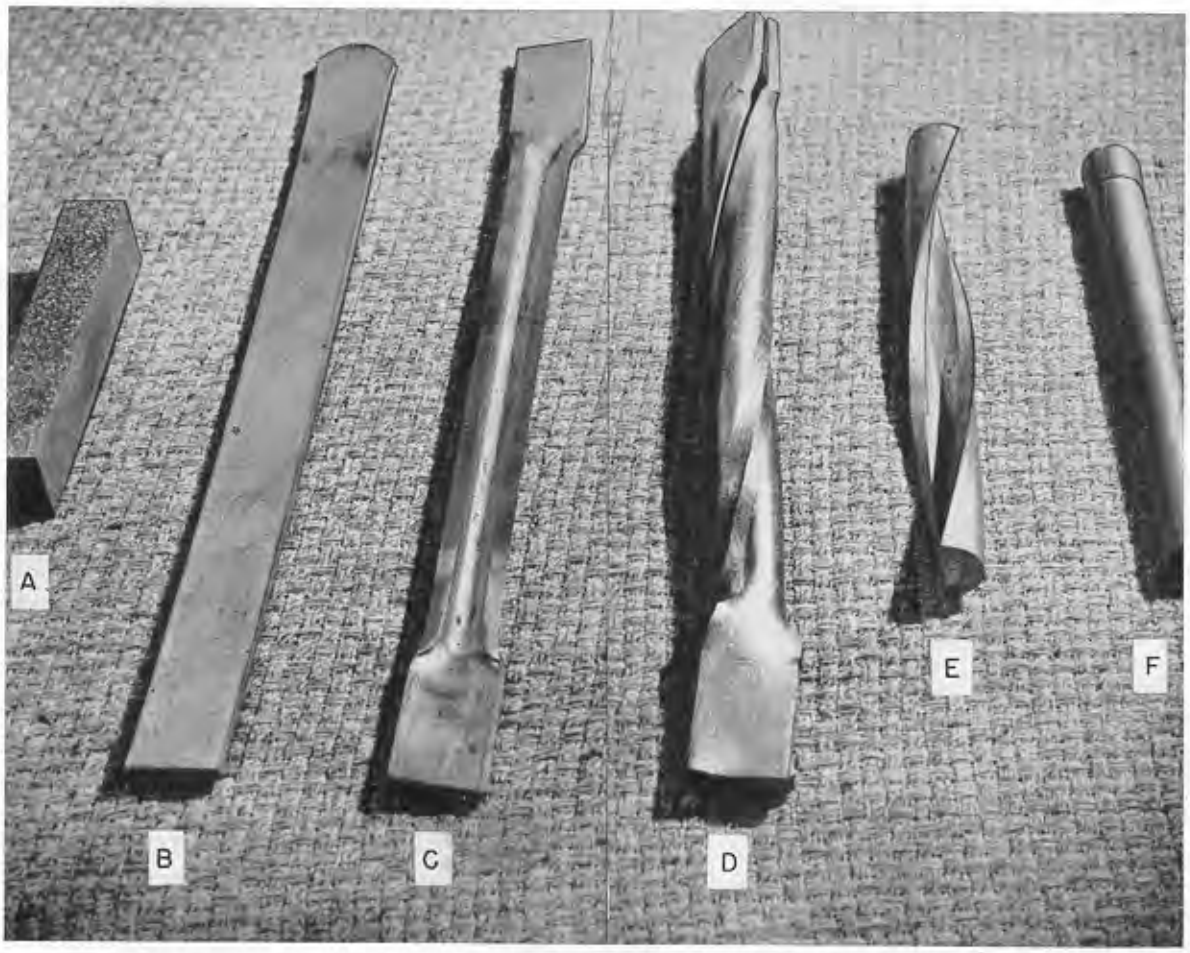


FIGURE 14. Steps in processing a two-stave liner of molybdenum. (Figure 16 of NDRC Report A-423.)

3. The flat strips were troughed in dies in a forging hammer (Figure 15) at about 1000 C. (Step C.)

4. The troughs were tested for cracks by etching with hot aqua regia. Cracked troughs, an example of which is shown in Figure 16, were rejected.

5. Two troughs, fitted together over a tungsten mandrel and held in place by a wrapping of molybdenum wire, were twisted in a hand-twisting machine, illustrated in Figure 17, after having been heated to 1000 C. (Step D.)

6. The ends were trimmed from each twisted trough and the helical mating surfaces were milled as shown in Figure 18.[96] (Step E.)

7. A pair of milled blanks was assembled. The outside surface was rough-machined, and a rough bore was then drilled.

8. The outside surface was ground to final dimensions with the assembly mounted on an arbor so that concentricity of bore and outside surface was attained. The grinding was done so that the outside of the assembled staves had a taper of $\frac{1}{32}$ in. per foot and a shoulder at the breech end $\frac{3}{4}$-in. long with a $\frac{1}{32}$-in. face. Finally the ends were machined and the two-stave assembly was ready for insertion into the steel carrier. (Step F.)

An alternative procedure for step (5) above, known as precision twisting,[96] consisted in mounting the staves, into which a close-fitting core of molybdenum had been slipped, in a segmented retainer which was then placed vertically in a steel mold and heated inductively to a temperature of about 550 C. The twisting was accomplished by hand using a cross bar at the top of the mold. A thin film of Aquadag baked on the working surfaces supplied both protection against oxidation and lubrication. The first staves which had been precision-twisted gave a performance inferior to those which had been hot-twisted, but those results are not necessarily conclusive.

CONFIDENTIAL

Deficiencies in the Design

The foregoing construction of two-stave twisted molybdenum alloy liners for test purposes represents a first step in the utilization of this erosion-resistant material. Disadvantages of this design of liner are: (1) weakness at the seams, where spalling starts, (2) reliance upon the steel carrier to bear most of the pressure load, and (3) movement of the liner.

Seam. The first of these deficiencies is closely related to the fact that the material tested was known to be somewhat inadequate in physical properties, as explained in Section 18.4.4. When a more thoroughly worked molybdenum alloy becomes available, spalling at the seams may cease to be a difficulty. Alternatively, the use of a seamless tube, discussed in Section 18.5.3, would obviate this problem entirely, provided that tubular liners could be made having the necessary tensile properties.

Radial Load. Because the steel carrier that surrounds the stave liner must sustain nearly all the radial load from the combined gas pressure and band pressure (Chapter 7), the outer diameter of the liner is the effective inner diameter of the gun bore. Hence, for a stave liner to be used without reducing the factor of safety, there must be an increase in the wall thickness of the gun in the region of the liner. This change in turn increases the weight of the gun and reduces its maneuverability.

Movement. Some caliber .50 molybdenum liners were observed to move both longitudinally and circumferentially during firing, so that the rear joint opened, constriction of the bore occurred at the forward end, and the rifling of the liner no longer registered with that of the barrel ahead of it. This sort of movement, which was due to insufficient anchorage of the liner in its steel carrier, was corrected by adding a shoulder and increasing the interference of the

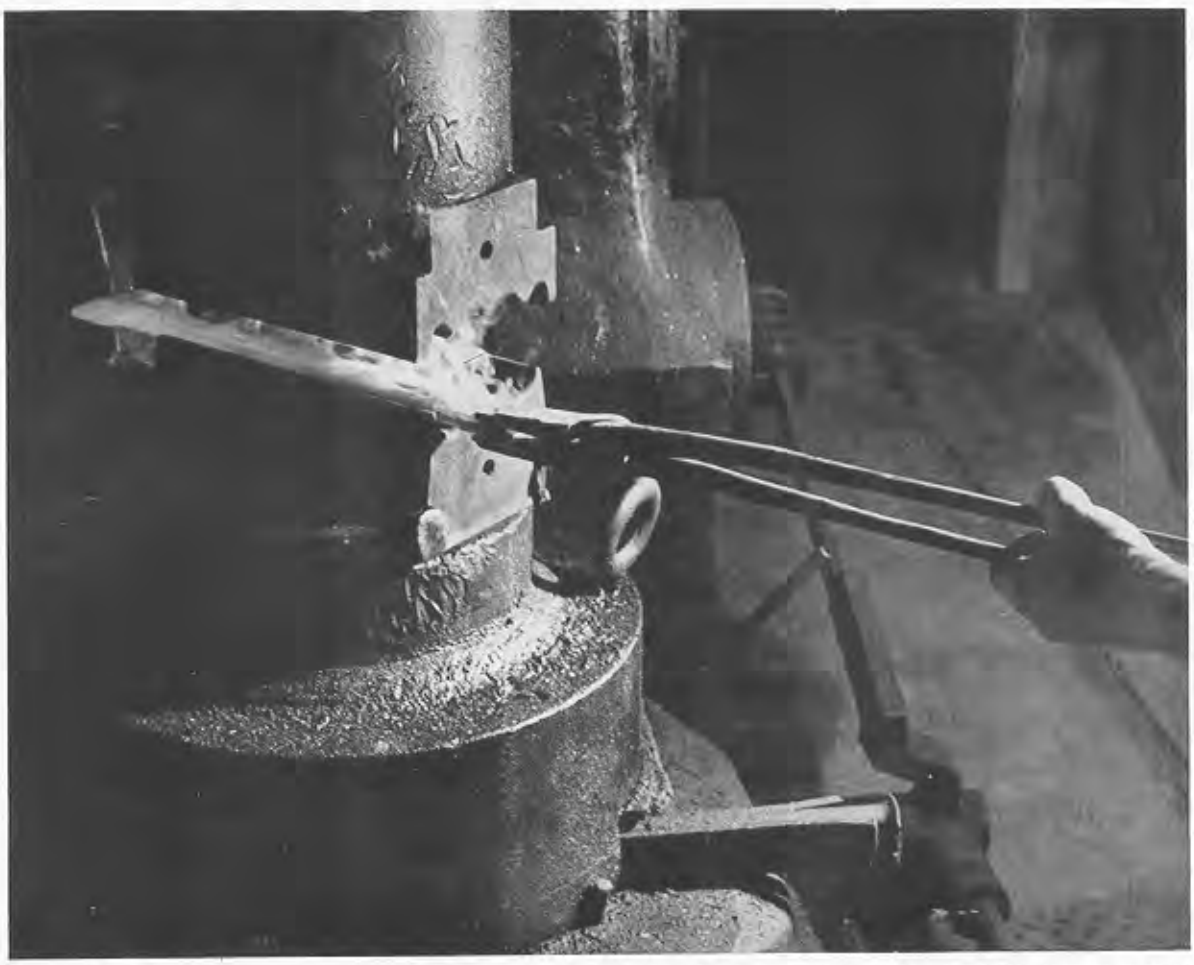


Figure 15. Troughing operation in making a two-stave liner of molybdenum. (Figure 17 of NDRC Report A-423.)

CONFIDENTIAL

shrink-fit. Nevertheless, even the best liners still showed a tendency to forward movement of the liner with consequent constriction of the bore at the forward end. It was not possible to determine from the tests conducted whether this fault would also be eliminated by the use of material of greater strength, although there is a strong a priori assumption that it would be.

18.5.3 Other Designs of Molybdenum Liners[95]

As has already been mentioned, the design of a gun liner to be made from the molybdenum thus far available has had to take into account the lack of strength of the material and its anisotropic character. Although liner design in general is discussed in Chapter 26, it is appropriate to record here the experiments that were made in an effort to develop a practical means of testing molybdenum in the caliber .50 erosion-testing gun and to explore the potentialities of this new gun liner material.

Brazed-in One-seam Tube of Molybdenum Sheet. A test piece was prepared by brazing a lining of 0.025-in. thick molybdenum into an SAE4150 steel carrier with a special copper-base brazing alloy in an atmosphere of Ammogas (NH_3) and heat-treating it. Hydrostatic pressure was applied by filling the bore with Wood's metal held in place by close fitting steel plugs at the ends. Fracture of the lining began after approximately 200 stress cycles, and increased to the end of the test (1,020 cycles). A later circumferential bending test revealed the transverse weakness so characteristic of molybdenum. This method of fabrication merits further study with hardened molybdenum-alloy sheet.

Tube Made from Flat Disks. The disk construction was designed to minimize the radial distortion of the carrier assembly due to firing pressure by having the molybdenum oriented in such a way that its direction of greatest strength opposed the radial stresses. A thick-walled tube was made by brazing a stack of punched disks, machining the outside for a press-fit into the carrier and machining the inside to receive a tapered tubular caliber .50 liner made from a bar of swaged, recrystallized, pure molybdenum. The brazing material, prepared especially for this purpose, was a copper-silver alloy fortified with palladium. The tubular liner, with an interference of 0.003 in., stuck during insertion and defied all attempts to remove it intact. Recovered fragments showed indentations by the edges of the disks caused by the shrink-fit stresses, which would have keyed the liner in position. Another liner of this type should be made for test firing.

Wire-Wrapped Tube. Another method of orienting molybdenum in such a way that the directional characteristic of its strength is made use of consists in wrapping molybdenum wire around a tube made from molybdenum sheet and brazing the wire in place. Some molybdenum wire having a trapezoidal cross section was drawn for this purpose by means of a Turk's head machine, but a liner was not actually constructed. This design also has the drawback that some of its strength would depend on the brazing compound, which might lose strength at gun-operating temperatures.

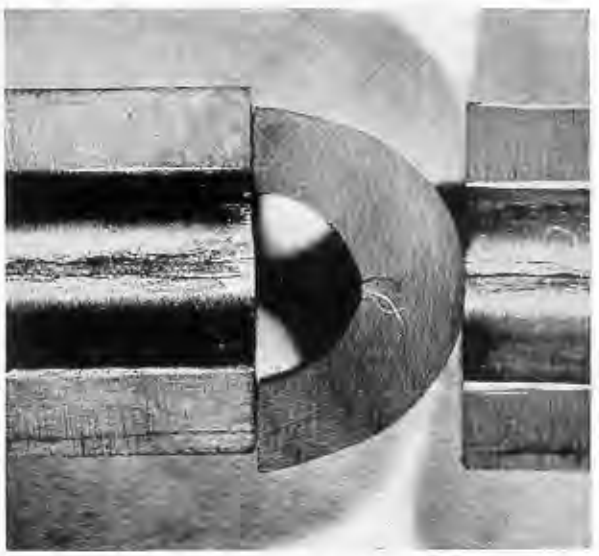


FIGURE 16. Cracks in a molybdenum trough disclosed by hot aqua regia etch. About 2X. (Figure 18 of NDRC Report A-423.)

Cast-Bonded Molybdenum-Steel Strip. Bimetallic slabs were made by casting SAE4150 steel against one face of a flat strip of hot-rolled molybdenum fluxed by painting with a suspension in acetone of finely ground, dehydrated, Easy-Flo flux. Pieces for tension and fatigue tests were made from these composite slabs hot-rolled to about a quarter of their original thickness (final thickness: Mo, 0.015 in.; steel, 0.125 in.). The results of these tests were encouraging so far as resistance to stress was concerned, but the interfacial bond, although apparently complete, showed under the microscope nodules of iron-molybdenum alloy which extended into the molybdenum and acted as stress-raisers. There was also a thin,

CONFIDENTIAL

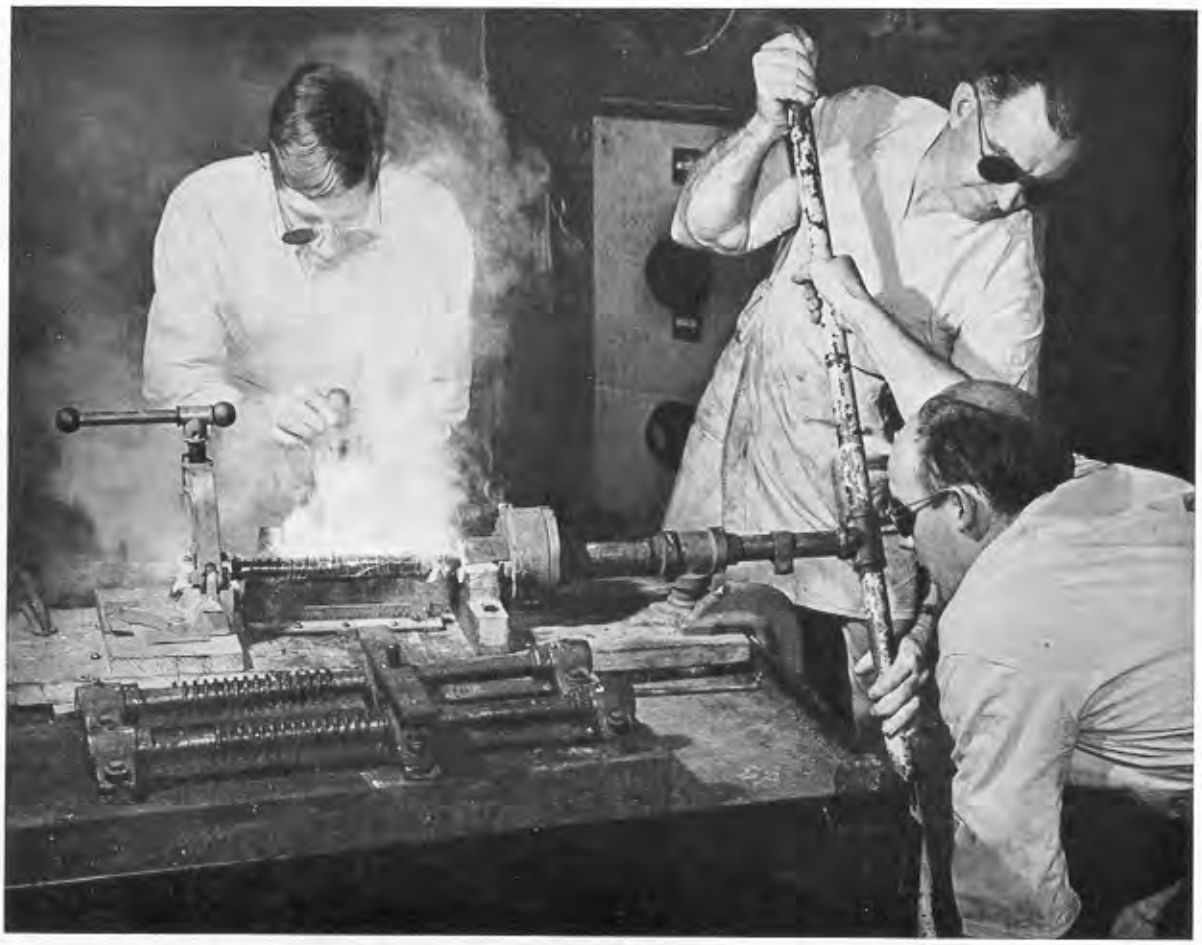


FIGURE 17. Twisting operation in making a two-stave liner of molybdenum. (This figure had accompanied the manuscript of NDRC Report A-423, but it was not reproduced in that report.)

brittle layer between steel and molybdenum that was a definite source of weakness.[d]

Seamless Tube. An experiment was conducted in an effort to evaluate the possibility of making a seamless gun liner of molybdenum. It involved extrusion of hot molybdenum through a die. Although a seamless tube could not actually be made with the equipment available, it was possible to begin extrusion of molybdenum at a temperature of 1200 C. This experiment indicated that pure molybdenum would have to be maintained at that temperature during the extrusion process, which would make it extremely difficult to find suitable dies.

A more promising type of tube-making process is one involving hot-rolling. The plans for continuation of the molybdenum project by the Westinghouse Company under Navy contract included the installation of tube-making equipment.

[d] Perhaps this layer may be the same as that encountered by other observers and described in Sections 18.8.2 and 21.3.3.

18.6 FIRING TESTS OF CALIBER .50 MOLYBDENUM LINERS

18.6.1 Early Liners

The first molybdenum liners tested were fired in a caliber .50 machine gun at the Geophysical Laboratory (Section 11.2.2).[49,50] They were bored from swaged molybdenum rods. Although longitudinal cracking and swaging of the lands caused failure after relatively few rounds, the tests served to demonstrate the remarkable inertness of molybdenum with respect to the powder gases.

Subsequent testing of molybdenum liners was carried out in the caliber .50 erosion-testing gun (Section

CONFIDENTIAL

11.2.1) at the Franklin Institute.[76] The first 24 liners tested failed for mechanical reasons, such as cracking or constriction of the bore, simply because the molybdenum did not have sufficient strength and sufficiently uniform metallographic structure. The tests did confirm the resistance of molybdenum to erosion by powder gases, even those from powder containing 40% nitroglycerin.

Most of this group of liners were of the stave type (Section 18.5.2), including two with four staves and two with ten staves. Although the unsuitability of the material prevented the tests from being definitive, they did furnish clues to improvements in design of test liners, which were incorporated in the design described in Section 18.5.2.

The material used in 13 of these liners was pure molybdenum. Five of them were made from alloys containing 5 to 20% of tungsten. The remainder contained a few hundredths of 1% of nickel as alloying constituent. Because none of this material had been fabricated by the improved working schedule described in Table 3, the possible value of these alloying constituents could not be assayed. After the improved working schedule had been developed, it was planned to make a systematic study of the effect of different alloying constituents.

18.6.2 Liners of Molybdenum Hardened with Cobalt

From the first batch of molybdenum alloy hardened with 0.1% cobalt and fabricated according to the improved working schedule (see Section 18.3.2) four two-stave liners were constructed.[96] The physical properties of the material in these liners is given in Table 5. The measurements were made on test specimens cut from the ends of the strips from which the staves were constructed.

TABLE 5. Physical properties of molybdenum hardened with cobalt used for caliber .50 test liners.[96]

Liner No.	Strength* (%)	Yield† (%)	Hardness‡
BL 33-3	138	.95	241
BL 33-4	150	1.66	235
BL 33-5§	166	3.5	226
BL 33-7§	148	1.08	234

* The ultimate strength compared with that of factory-worked molybdenum of the same gauge thickness as determined by a simple bend test.
† The yield at rupture as determined in the same test.
‡ Vickers pyramid number at room temperature.
§ Helical seams.

Two of the liners had straight seams and two had helical seams. All had a 1/32-in. shoulder, an average

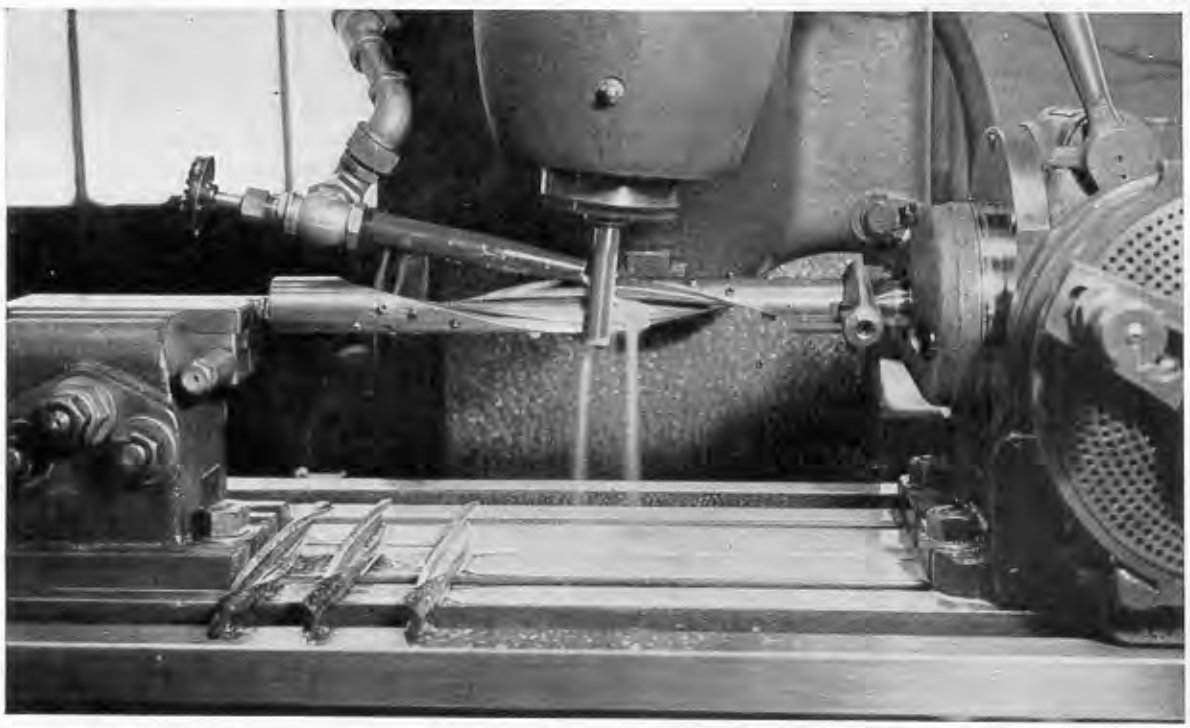


FIGURE 18. Milling the mating surfaces of one stave of a two-stave molybdenum liner. The stave was held in a fixture that was rotated at the same time that it was moved forward. (Figure 73 of NDRC Report A-424.)

CONFIDENTIAL

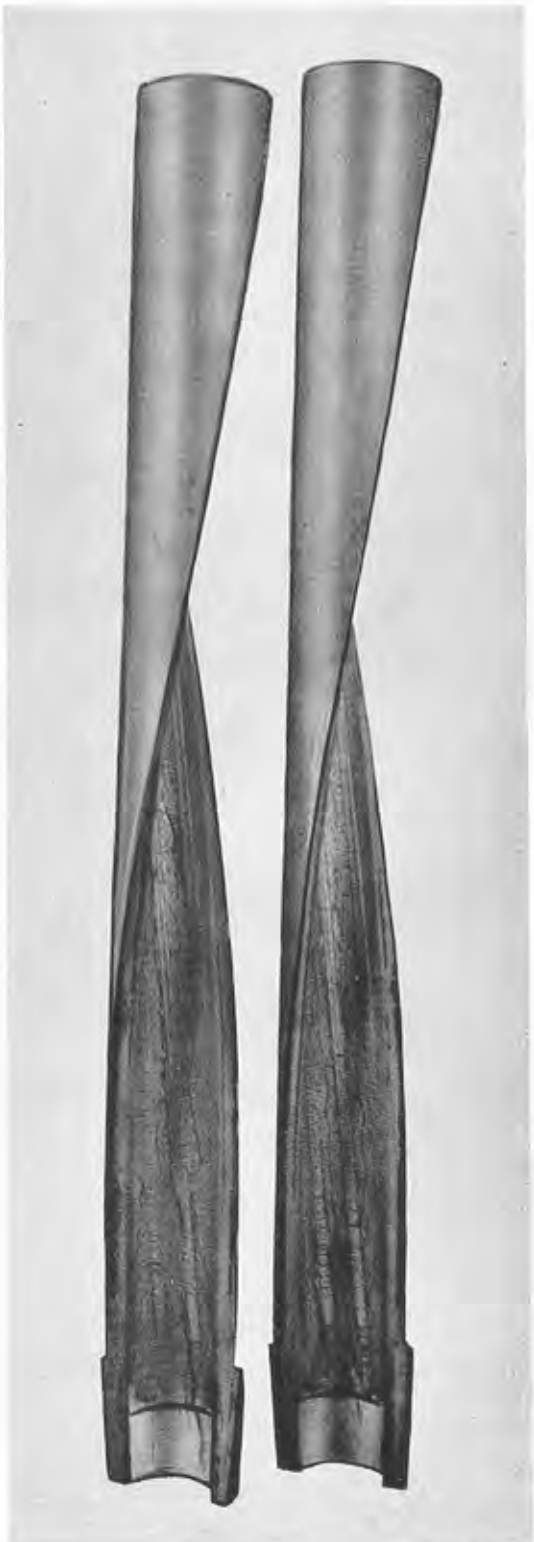


FIGURE 19. Two-stave twisted liner of molybdenum alloy fired 2,024 rounds. See Figure 4 of Chapter 16. (Figure 19a of NDRC Report A-423.)

wall thickness of 0.13 in., and a diametral taper of $\frac{1}{32}$ in. per ft.

These four liners were tested in the caliber .50 erosion-testing gun. Ball bullets were fired at a muzzle velocity of about 3,700 fps, using a double-base powder (20% nitroglycerin) at a maximum pressure of about 57,000 psi.

The results of the tests are summarized in Table 6. They represented a tremendous improvement, for the longest previous test had lasted only 454 rounds. The fact that liner No. BL 33-4 lasted only 152 rounds, however, indicated that the molybdenum was still not as uniform as desired.

TABLE 6. Firing tests in caliber .50 erosion-testing gun of two-stave liners of molybdenum hardened with 0.1% cobalt.[26.35]

Liner No.	Rounds	Cause of failure
BL 33-3	1133	Bore constriction
BL 33-4	152	Spalling
BL 33-5	2022	No failure
BL 33-7	2024	No failure

The tests of liners BL33-5 and BL33-7 were arbitrarily stopped, although the liners were in condition to withstand further firing. There was no evidence of powder gas erosion of the bore surface.

Tests of five other liners made from different batches of molybdenum hardened with 0.1% cobalt were not carried as far as those of liners BL 33-5 and BL 33-7. Some of them were made to test special design features, such as the effect of precision twisting (Section 18.5.2). The overall result of the nine tests of hardened molybdenum liners was that the following types of failure were still present, although to a much smaller degree than with the first group of liners.

Cracking. Longitudinal cracking usually occurred in the center of the grooves after a relatively few rounds. The lack of sufficient transverse strength and ductility permitted the grains, elongated by working, to split apart. This effect was probably aggravated by the smallness of the coefficient of expansion of molybdenum compared with that of steel, for the transverse cracking that took place across the axis of the grain structure would not have occurred if the liner had received proper support from the assembly at all temperatures. Surface checkerwork cracking (seen in Figure 19) was caused by the thermal stresses at the bore surface.

CONFIDENTIAL

Spalling. Spalling occurred along the edges of seams, particularly where the lands crossed straight seams. It often emanated from tool marks and incipient cracks in the surface (Figure 16) which are the result of cleavage fractures in individual crystals under the stresses imposed by the cutting tool. Preliminary experiments[96] have demonstrated the feasibility of reducing both amplitude and asperity of such imperfections by electropolishing, but the problems involved in electropolishing the bore of liners after insertion into the carriers have yet to be solved.

Swaging of Lands. Swaging of the lands increased the land diameter at the origin of rifling and for a short distance beyond. In the case of liners BL 33-5 and BL 33-7 the land height at the origin of rifling was reduced from 0.010 in. to approximately 0.007 in. at the end of the test. This increase in diameter produced a drop in both pressure and velocity. The cause of swaging was a lack of sufficient hot-hardness to withstand engraving stresses. Swaging, however, was reduced to a remarkable degree by the use of the alloy containing 0.1% cobalt.

Liner Movement. Forward movement of the liner opened the joint at the breech end beneath the cartridge case and extrusion of the brass case into this opening sometimes prevented extraction of the case and stopped the test. All liners made without an integral shoulder (Figure 14F) and fired a long time moved forward and opened up at the rear joint.

Plastic flow of metal toward the muzzle end of the liner caused bore constriction which on some occasions terminated the test. In this case, too, the increased hardness of the improved alloy decreased this type of failure.

All these types of failure were influenced if not caused entirely by the fact that the physical properties of the molybdenum were not optimum. The extent to which the design of the liner itself may have contributed has already been considered in Section 18.5.2. These tests, then, represent merely a beginning in the development of molybdenum as a suitable material for gun liners. The program planned by Division 1 and subsequently taken over by the Navy Department envisaged extensive tests of caliber .50 liners for the double purpose of determining whether changes in the fabrication process might give improved material and of trying preliminary design features that might be incorporated in a molybdenum liner for a medium caliber gun, such as that described in Section 33.1.3.

18.7 OTHER METHODS OF FABRICATING LARGE BILLETS OF MOLYBDENUM

18.7.1 Introduction

Some of the foregoing sections of this chapter have told of the need for large presses and furnaces in order to fabricate large billets of molybdenum by the usual powder metallurgy process. Therefore alternative methods were explored by Division 1 for fabricating such billets as starting material for making gun liners. In three of them molybdenum was melted; in the fourth it was merely sintered. The products resulting from the experiments carried out were too brittle for the desired purpose; but there is still a possibility that either vacuum melting or inductive sintering in an atmosphere of hydrogen might be developed to a successful conclusion.

18.7.2 Vacuum Melting in an Electric Arc[e]

In this method of making a large billet of molybdenum an arc is established in vacuo between vertical electrodes made from compressed molybdenum powder. The molybdenum runs down from the upper electrode and collects at the bottom of the furnace in a casting mold that is lined with molybdenum sheet. Although the process involves the liberation of energy at high concentration, it is readily controlled, makes the use of refractories unnecessary, and yields a nearly pure product.

Ingots as large as 25 lb have been cast. Ingots of either molybdenum or molybdenum-base alloys are found to contain fewer nonmetallic inclusions than metal processed in other ways, but they contain many gas pockets, caused by the escape of water vapor, hydrogen, and carbon monoxide which originated in the bar stock. By remelting in a vacuum-arc furnace such an ingot was densified so that the final product had a density of 10.232 g/cu cm, which is nearly that of the maximum theoretical density of

[e]This process was being developed by the Climax Molybdenum Company at its Research Laboratory in Detroit at the time that Division 1, NDRC, entered into Contract OEMsr-1273 for the development of chromium-base alloys (see Chapter 17). The scope of that contract was made to include a study of the vacuum melting of molybdenum in order to determine whether the Climax Company's process might be applicable to the preparation of molybdenum for gun liners. The results of the investigation were described in a series of monthly progress reports. They were summarized in a formal Division 1 report[97] that was drafted but not issued. The Climax Company planned to continue the investigation for its own purposes after the termination of Contract OEMsr-1273.

molybdenum (10.295 g/cu cm), computed from x-ray lattice parameter measurements.

The microstructure of one of these pure molybdenum castings, shown in Figure 20, consists of large, columnar grains similar to those in the recrystallized material made by powder metallurgy technique, shown in Figure 9. The grains of the molybdenum alloy castings are finer and equiaxed, but in both cases the grain size is larger than that of the original compressed and sintered bars. Hence it is not surprising that when an attempt was made to forge this material the ingot split into many rodlike pieces.[95]



FIGURE 20. Structure of molybdenum remelted by the vacuum-arc process. *50 X*. (This figure had appeared in a progress report on Contract OEMsr-1273.)

Molybdenum-base alloys containing tungsten, iron, or cobalt when melted in the vacuum arc are not as hard as similar alloys prepared by powder metallurgy.

18.7.3

Vacuum Melting in an Induction Furnace[96]

MELTING MOLYBDENUM ALLOYS IN A CRUCIBLE OF PURE ALUMINUM OXIDE

A vacuum furnace heated by induction has been used successfully in melting molybdenum-base alloys containing chromium, cobalt, and iron. The details of the furnace may be seen in Figure 21 which is here shown as used in the melting of molybdenum-base alloys with a molybdenum content of 50 to 80%. The Alfrax crucibles, consisting of pure aluminum oxide (Al_2O_3), melt at a temperature in the neighborhood of 2000 C, hence they cannot be used to melt pure molybdenum (melting point, 2620 C). Energy was supplied to the induction coils from a vacuum-tube oscillator generator rated at 20 kw and running at approximately 130 kc.

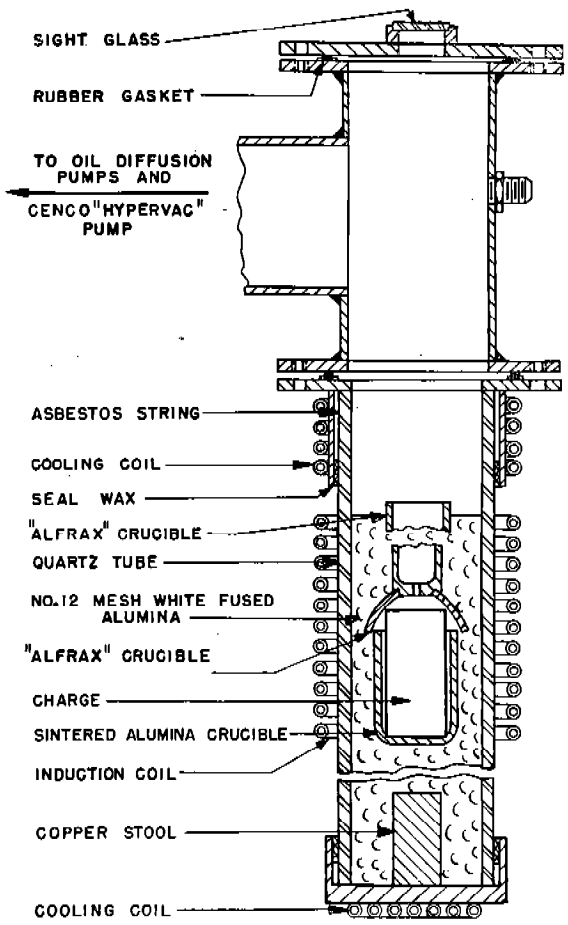


FIGURE 21. Vacuum-melting furnace for molybdenum alloys. (Figure 40 of NDRC Report A-424.)

The compacts (1½ in. x 2 to 3 in.) were melted in about 6 min and allowed to cool in the crucibles. When the melts were removed from the furnace they showed bright untarnished surfaces, but out of about 50 alloys with varying compositions, all but a dozen were too brittle to be of use. The hardness, strength, and malleability of the better ones was not definitely superior to those of molybdenum except in the case of one alloy which, upon analysis, had the following

composition: Mo 79.4%; Cr 8.5%; Co 12.7%. This material, or some similar alloy, might be useful as a gun liner material when adequately supported by the gun tube proper.

Melting Molybdenum in Thorium Oxide Refractories

Test samples of molybdenum alloys have been melted successfully in an inductively heated vacuum furnace having an enclosure of silica glass surrounded by high-temperature thermal insulation of calcined thorium oxide. This hearth material is little affected by temperatures considerably above the melting point of molybdenum. In one test, melting was effected with a 1,100-g charge in a crucible $2\frac{7}{16}$ in. in internal diameter in the field of a coil of 6-in. internal diameter by 10 in. long operated at 800 to 1,000 ampere-turns per inch at a frequency of 9,600 c. In another test, melting was brought about progressively, using the same power supply, in a charge approximately $1\frac{1}{4}$ in. in diameter and 12 in. long formed by stringing drilled blocks of sintered molybdenum on a molybdenum rod to maintain the alignment necessary for subsidence of the column as melting progressed.

Most of the experimental ingots produced by this melting technique were brittle and showed extensive intercrystalline cracking when forged at approximately 1400 C. This may have been due to an observed nonmetallic material of purplish hue and unknown composition[f] which appears to form an extensive intercrystalline network. The crystalline structure of the ingots was coarse and columnar. In one case single crystals about 1 cm in length were detached, and at room temperature were bent repeatedly through an angle of 30 degrees provided the rate of deformation was slow. However, a suddenly applied bending force always caused fracture.

A mixture of molybdenum with thorium oxide (ThO_2), mechanically pressed and sintered at 1000 C, was melted in similar manner. It was thought that the thorium oxide might minimize the grain size in the ingot. The grains were found to be equiaxed, but pronounced grain boundary attack resulted from etching in aqua regia.

[f] This is, perhaps, the same material described in a progress report dated March 27, 1944, by the Climax Molybdenum Company as follows: ". . . a purple tinted material having characteristics between metal and oxide. Its analysis . . . gives it almost exactly the composition of MoO."

18.7.4 Thermit Melting[g]

For some time commercial ferro-molybdenum has been produced by "thermit" melting. In attempting to adapt this technique to the production of ingots of molybdenum of high purity all ferrosilicon was dispensed with and aluminum alone was used to reduce the molybdenum oxide (MoO_3) to the metallic state. Carefully calculated amounts of molybdenum oxide and aluminum were placed in a pot over a form lined with periclase (MgO) and surrounded by a steel shell. After having been baked out both form and shell were buried in a sand pit with the top flush with the sand level.

The charge was ignited with a bomb containing about $\frac{1}{4}$ lb of aluminum and about 2 oz of Solazone (Na_2O_2) which could be lighted with a taper. The reaction began at once and proceeded rapidly, only from 10 to 30 sec having been required for the combustion of about 200 lb of mixture. During the main reaction large volumes of smoke and flames were produced, as shown in Figure 22. This stage was followed by a second, of longer duration, during which the melt bubbled and emitted only a small amount of smoke and flame. After cooling for 24 hr the ingot was removed and, if possible, sawed in two. If it was too hard to saw, it was broken with a sledge hammer.

The characteristics of such ingots are shown in Figure 23 and of the accompanying slags in Figure 24. Mixes Nos. 35, 36, and 38 contained a small amount of iron or iron ore as an oxidizing agent, but No. 37 contained no iron. All four ingots were described as very porous, soft, gassy, and coarse grained. The top of No. 37 was fine grained and contaminated with hard slag. Segregation is seen to be more pronounced in No. 38. Such material is evidently unsuitable for use as a gun liner.

In the experiments performed it was found impossible to obtain a balanced mix which would give a degassed product without an excess of silicon or aluminum or both, elements which tend to make the alloy hard and brittle. Equally unsuccessful was the attempt to find some other material (iron ore, iron, chromium, manganese, copper) which, when added to the mix, would perform the final deoxidation and

[g] This process was investigated by the Climax Molybdenum Company at its plant at Llangeloth, Pennsylvania. The results were described in three reports (dated March 27, July 1, and September 1, 1944) submitted to Division 1, NDRC, under Contract OEMsr-1273. They were summarized in a formal Division 1 report[97] that was drafted but not issued.

leave in the melt a residual element which would not affect its properties adversely.



FIGURE 22. Thermit process in which 100-lb ingot of molybdenum is being prepared by reduction of technical molybdenum oxide with aluminum alone. The picture was taken at 1/2000 sec at *f*11 about 5 sec after start of reaction. (This figure had appeared in a progress report on Contract OEMsr-1273.)

18.7.5

Inductive Sintering in an Atmosphere of Hydrogen[96]

Inductive heating appears to be a practicable means for heating molybdenum or molybdenum alloy (possibly also tungsten) compacts of large cross section to put them into condition for subsequent working. In certain exploratory experiments a $1\frac{1}{2}$x$3\frac{1}{2}$-in. compact was formed by pressing molybdenum powder mixed with 0.1% of Steartex, for lubrication and increased coherence, in a cylindrical die at 30 tons per square inch. The compact was embedded in 40-mesh white fused alumina contained in the quartz tube furnace shown in Figure 21, in which a hydrogen atmosphere was maintained. Temperatures were determined by viewing a cavity in the top of the compact through a sight tube by means of an optical pyrometer. A current of approximately 1,400 ampere-turns per inch at a frequency of 9,600 c was required to raise the temperature of the compact to approximately 2000 C where it was held for about 5 min. The total heating period was about 90 min. Better sintering of the interior of the billets would be obtained by the use of the maximum practicable sintering temperature and an increase in the time the billets are held at such temperature.



FIGURE 23. Sawed and split ingots of molybdenum melted by the thermit process. See Figure 24 for the slag from the same heat. (This figure had appeared in a progress report on Contract OEMsr-1273.)

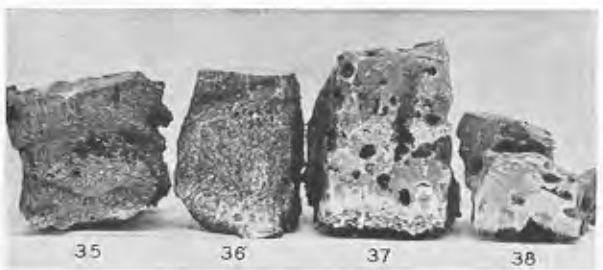


FIGURE 24. Specimens of slag from same four heats from which specimens of molybdenum in Figure 23 were obtained. (This figure had appeared in a progress report on Contract OEMsr-1273.)

After removal from the furnace measurements of the cold sintered billet showed that it had undergone a volume shrinkage of about 40 per cent, and had a density of approximately 9.5 gm/cm^3. It was forgeable, and when worked at temperatures from 900 to 1100 C yielded a sound machinable bar $\frac{3}{8}$x$\frac{3}{8}$x11 in. Such bars were found to be likely to show end-cracking but no other defects. A test of one of the finished pieces at room temperature gave a hardness of 259 VPN. Unlike most metals and alloys, the tensile

CONFIDENTIAL

properties of molybdenum, at room temperature, appear to be highly responsive to variations in the rate of deformation, the higher values of ultimate strength and lower values of ductility accompanying the more rapidly applied stress.

18.8 COATINGS OF MOLYBDENUM

18.8.1 Introduction

Instead of applying molybdenum to the bore surface of a gun in the form of a liner, consideration has been given to the possibility of applying a coating on steel or other base metal. Unsuccessful attempts to obtain satisfactory molybdenum coatings by electrodeposition of metal from aqueous solutions are mentioned in Sections 16.4.4 and 20.1.3. No satisfactory deposits were obtained by aqueous plating of suboxide and subsequent reduction in hydrogen.

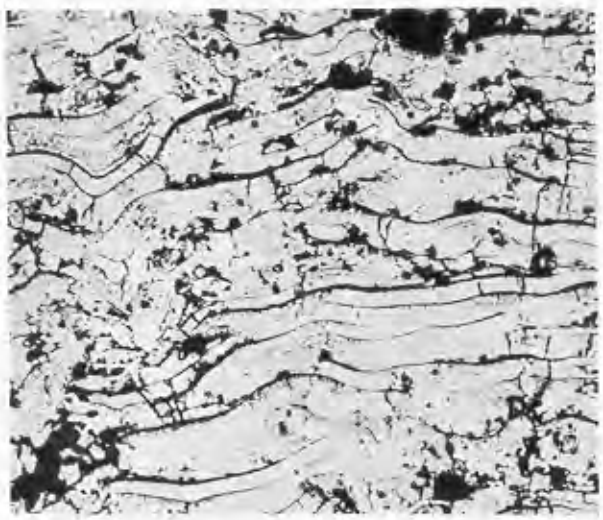


FIGURE 25. Structure of molybdenum coat sprayed on steel with wire gun. The crystals were flattened by spattering. Etched with $KOH + K_3Fe(CN)_6$, *250 X*. (Figure 3 of NDRC Report A-418.)

The exploratory attempts at spray coating are described in the next section. The more extensive experiments with deposition of a coating of molybdenum by pyrolytic plating are described in Chapter 21.

18.8.2 Spray-Coating Molybdenum[90]

Molybdenum coats of different thicknesses can be sprayed on roughened steel, ceramic, graphite, or paper mandrels with a "gun" using 1/8-in. wire and a mixture of oxygen and acetylene under pressure. Such a coating on steel is porous and has a flakelike structure with flattened grains due to plastic deformation during deposition, as shown in Figure 25. Sintering in hydrogen produces only partial densification and the resulting coat is very brittle. Densification by fusion with an atomic hydrogen arc gives rise to coarse-grained coats more brittle still, due to the formation of an intermetallic compound at the interface.[h] Complete densification may be accomplished by spraying on top of the molybdenum a thin top-coat of nickel, or nickel and copper, or stellite, and sintering in hydrogen above the melting point of the top-coat. The coatings so formed have very little ductility.

Densification and improved bonding of the molybdenum to the underlying steel can be accomplished by the use of an electric resistance roller welder. The outside of the steel liner rests upon one roller, while a second roller is pressed against the molybdenum coating inside. When the liner is revolved and a current of several hundred amperes is passed through coat and liner from one roller to the other, the coat is heated and welded to the steel. Figure 26 illustrates the microstructure of a welded coat. No roller-weld coat was made with properties sufficiently good to justify a firing test.



FIGURE 26. Structure of sprayed coat of molybdenum roller-welded to steel. Note heat effects to a depth of 0.1 in. below coat. Nital etch, *200 X*. (Figure 4 of NDRC Report A-418.)

[h] See footnotes (d) and (f).

CONFIDENTIAL

Another method of making a coat of molybdenum on steel is by evaporation from an atomic hydrogen arc, or by projecting the powder into such an arc. The very high temperatures involved in such experiments bring about the formation of intermediate layers of a brittle intermetallic compound which destroys the usefulness of the coat as an erosion-resistant gun lining.



Chapter 19

STELLITES AND OTHER COBALT ALLOYS

By *J. F. Schairer*[a]

19.1 INTRODUCTION

THE SURVEY of erosion-resistant materials given in Chapter 16 mentions that Stellite No. 21, because of its resistance to chemical attack by hot powder gases, hardness and strength at high temperatures, and excellent wear and abrasion resistance, has shown outstanding performance in applications as short breech liners in machine gun barrels under firing conditions so severe that unmodified steel barrels are unable to withstand such schedules. The present chapter describes the metallurgy of Stellite No. 21 and then recounts the tests that have been made with other stellites and other cobalt alloys in an effort to utilize them as gun liner materials. The conclusion[b] from those investigations was that "Stellite No. 21 is an alloy composition that happens to have a nearly unique combination of properties that makes it suitable for use as a gun liner fired with single-base powder."

At the same time, the advantages and limitations of Stellite No. 21 as a liner material should be clearly recognized. Among the advantages are its hot-hardness and hot-strength (to resist deformation of the rifling), its excellent abrasion and wear resistance (to resist wear by the projectile), its good ductility (which prevents serious cracking) and its machinability (which permits satisfactory fabrication). The low thermal conductivity of Stellite No. 21 as compared to gun steel (about ⅓ that of gun steel at 200 C and about ⅔ at 600 C) may be an advantage in some cases for a gun with a stellite liner where the temperature of the steel gun tube limits performance because of lack of strength at high temperatures.

The low melting points (actually fusion ranges) of stellite-type alloys are an outstanding limitation. The melting points of these alloys lie in the range between 1250 and 1350 C while gun steels are in the range of 1400 to 1450 C. There is some evidence (described in Chapters 10 and 13) that erosion, particularly in large guns, is, in part, an actual melting of the bore surface during firing. In all tests of stellite liners in the caliber .50 erosion-testing gun, in machine guns, and in the 37-mm gun, M3, when double-base powder (with a high adiabatic flame temperature) was used, serious melting of the bore surface occurred; while in similar tests using a cooler propellant (IMR or FNH-M1 powder) performance was excellent. Because of their low melting points stellites are not a universal solution to the problem of the erosion of a hypervelocity gun.

19.2 SELECTION OF STELLITE NO. 21 AS A LINER MATERIAL

19.2.1 Vent-Plug Tests of Stellite No. 6

At a very early stage of the studies of gun erosion by Division 1,[c] NDRC, the suggestion was made by C. W. Drury, Chief, Armour Plate Division, Department of Munitions and Supply, Canada, that gun erosion might be mitigated by use of bore-surface material having high hot-hardness. He suggested further that cobalt alloys (for example, the stellites) were the materials to investigate, since cobalt is *the* element that confers this property on an alloy.

As a result of this suggestion, and in spite of criticism of it expressed at a conference[297] with ordnance experts, both Stellite No. 6 and high-speed steel (which also has a certain degree of high hot-hardness) were tested as erosion vent plugs (Section 16.3.1). Both materials showed high weight losses.[27] The evident need for a material with a high melting point to withstand this test was partly the reason that attention was focused on the development of chromium (Chapter 17) and molybdenum (Chapter 18). It was not until later that it was realized that the poor resistance of stellite to "flash" melting in this very severe vent-plug test had masked its resistance to chemical attack by the powder gases, a conclusion that was confirmed by subsequent vent-plug tests of several stellites under less severe conditions.[75]

[a] Special Assistant, Division 1, NDRC. (Present address: Geophysical Laboratory, Carnegie Institution of Washington.)

[b] This conclusion was expressed in the "Report of Stellite Advisory Committee" of Division 1, NDRC, October 5, 1945, after detailed study of the results of the investigations that are summarized in the present chapter.

[c] At that time Section A, Division A of NDRC.

19.2.2 Machine Gun Liner Tests of Stellite No. 6

A firing test on a short breech liner of pure soft molybdenum in the caliber .50 air-cooled, heavy machine gun barrel showed that, even though there was no melting or chemical attack, failure occurred by deformation of the rifling by the swaging impact of the bullets after only a short burst of fire. These test results emphasized the importance of hot-hardness, resistance to permanent deformation, and wear resistance of the bore-surface material in rapid-fire guns even when fired under ordinary velocity conditions.

In order to evaluate the relative importance of hot-hardness and chemical resistivity in controlling the performance of bore-surface materials in a rapid-fire gun, a reconnaissance series of different materials of known hot-hardness was selected for firing tests as short breech liners in the caliber .50 heavy machine gun barrel. Liners of 18-4-1 high speed steel, Voland No. 2 hot-die steel, Cyclops KL hot-die steel,[d] and Stellite No. 6 were tested in the caliber .50 heavy machine gun barrel on a severe firing schedule (500 round groups of 100-round bursts one minute apart). The results[80] on the first three materials were very disappointing. The hot-hardness of these materials could not be utilized because of severe powder gas erosion. Evidence for the thermal alteration at the bore surface of one of the liners of hot-die steel is shown in Figure 9 of Chapter 16. The liner of Stellite No. 6, on the other hand, was resistant both to thermochemical attack by the powder gases and to deformation of the rifling.

Since a test of materials of outstanding hot-hardness was desired, the particular stellite alloy chosen for the test (Stellite No. 6), had been selected because it was the hardest commercial grade of stellite that could be rifled with carbide-tipped cutting tools and because it had an excellent record as a valve-seating material for high-temperature service. After three 500-round groups, the stellite liner showed little or no powder-gas erosion, deformation, or wear. A gun steel barrel in a similar test is nearly worn out after only one such group. However, the liner of Stellite No. 6 showed several deep longitudinal cracks, at least one of which passed completely through the liner wall. Such a liner would be unsafe for Service use. Hot-hardness had been overemphasized at the expense of ductility; moreover, since the liner had moved forward during firing, the insertion problem remained to be solved.

[d] For the compositions of these steels see Section 16.4.11.

19.2.3 Tests of Stellite No. 21

The insertion problem was solved by the use of the flanged liner design described in Section 22.2.1. The problem of cracking was completely solved by changing the composition of the stellite for liner use. Using the same severe firing schedule, a 6-in. length investment-cast liner of Stellite No. 21 was fired 10,900 rounds before it finally wore out.[e] There was no cracking or dangerous failure. This alloy had good hot-hardness, but not as great as that of Stellite No. 6. The ductility of Stellite No. 21, however, is so much greater than that of No. 6 that surface cracks are not propagated in it.

Subsequent firing tests on caliber .50 aircraft machine gun barrels with 9-in. length, flanged-type, investment-cast liners of Stellite No. 21 inserted on a shrink-fit demonstrated outstanding performance of a different order of magnitude from that of standard steel barrels, as is recounted in Chapter 22. Similar results were achieved with other rapid-fire small arms barrels with these liners. Under these conditions, Stellite No. 21 meets the criteria for a satisfactory bore-surface material.

19.3 METALLURGY AND PROPERTIES OF STELLITE

19.3.1 Chemical Composition of Stellites

The stellites are cobalt-base alloys with 25 to 30% chromium, with a moderate amount (usually about 6%) of molybdenum or tungsten, with small or moderate amounts of one or both of the metals iron and nickel, and with carbon contents varying from 0.2 to slightly over 1%. They are commonly cast alloys with manganese and silicon contents of 1 per cent or less. The nominal compositions of some stellites are given in Table 1.

As the nickel or iron content is increased the machinability of the alloy decreases. The stellites that contain molybdenum instead of tungsten are, in general, more ductile and softer than the tungsten-bearing alloys of the same carbon content. When the carbon content of a stellite is high, the alloy is stronger, harder, and more brittle than when the carbon content is low. The effects of the chemical composi-

[e] See Section 22.2.2 for details of this test.

TABLE 1. Nominal percentage composition of stellites.*

	No. 21†	No. 6‡	No. 23	No. X-40	No. 422-19	No. 27
Chromium	28	28	25	25	25	28
Nickel	2	2	2	10	16	32
Tungsten	..	5	5	7	..	..
Molybdenum	6	..	..	..	6	5
Cobalt	Balance (*ca.* 64)	Balance (*ca.* 65)	Balance (*ca.* 68)	Balance (*ca.* 58)	Balance (*ca.* 53)	Balance (*ca.* 35)
Carbon	0.25	0.50	0.40	0.50	0.40	0.40

* All of the cast stellites contain iron (maximum 2.5%), manganese (max 1%), and silicon (max 1%).
† The tentative Army specifications[291] for the composition of investment castings of cobalt-chromium alloy were about the same as this composition.
‡ Stellite No. 22 is rolled Stellite No. 6. Stellite No. 6-2A is similar to Stellite No. 6 only with a lower carbon content.

tion on liner performance are discussed later in this chapter (19.4.5 and 19.6).

19.3.2 Crystallography and Structure of Stellite No. 21

Investment-cast Stellite No. 21 has as its primary phase and matrix, a cobalt-rich, solid solution with a face-centered cubic lattice. The general structure is revealed in the photomicrograph shown as Figure 1. Numerous small, well-distributed areas of binary and ternary eutectic material are present. The binary eutectic is the M_6C, solid solution type, where M may be cobalt, chromium, or molybdenum, and the ternary eutectic includes the phases M_6C, solid solution, and Cr_7C_3 with part of this last carbide transformed to Cr_4C. Small areas of a "pearlitic" constituent (from an analogy to the appearance of pearlite in steels) are present. This is believed to be a eutectoid formed by transformation of the cubic, cobalt-rich, solid solution to a hexagonal form with a simultaneous precipitation of Cr_4C.

The primary, cobalt-rich, solid solution phase of Stellite No. 21 is cubic as cast but can be largely converted into hexagonal metal (with some exsolution of carbides) by heating at 800 C for about 50 hr. The cubic face-centered lattice of the cobalt-rich, solid solution is similar in unit cell size to the cubic modification of pure cobalt which is stable between about 400 C and 1000 C. The effect of the alloying elements chromium and molybdenum apparently raises the lower transition temperature and thus extends the stability range of the low-temperature, hexagonal form to higher temperatures.

METALLOGRAPHIC EXAMINATION[88,110]

After polishing, samples of Stellite No. 21 may be etched in a number of ways for metallographic examination. Two methods have been found particularly useful. An electrolytic etch with dilute aqua regia reveals the general structure of the alloy while an alkaline potassium permanganate solution selectively stains the carbide constituents of the alloy.

The structure varies only slightly from casting to casting and in different parts of the same casting. The

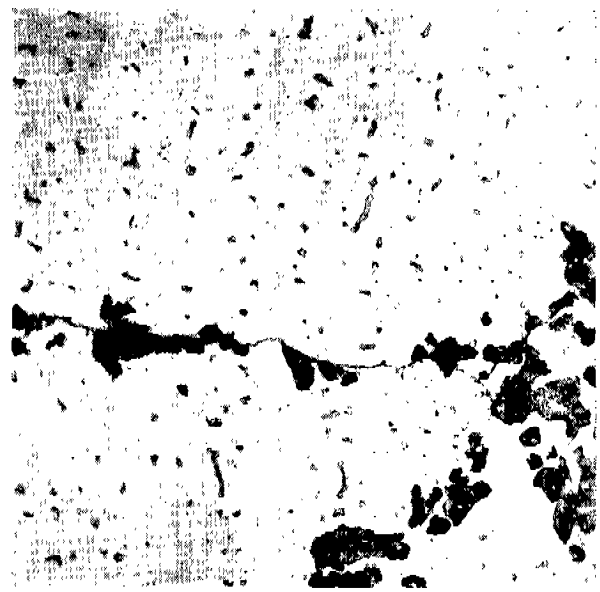


FIGURE 1. As-cast structure of a specimen from a typical investment-cast Stellite No. 21 liner; Electrolytic aqua regia etch; *100X*. (This figure has been taken from NDRC Report A-416.)

rate of cooling during the casting process controls the grain size and the amount of the pearlitic constituent.

A large number of liners of Stellite No. 21 were examined after firing tests. A photomicrograph of a fired liner is shown as Figure 7 in Chapter 16. Little or no change took place as a result of firing except at the immediate bore surface where a large number of surface cracks developed and there was evidence of

age-hardening. Even after a severe firing test the surface cracks, although very numerous, were quite shallow and appeared at random and only occasionally at grain boundaries.

X-Ray Examination[88]

X-ray examinations of Stellite No. 21 were made to see whether there were any peculiarities in the structure of investment-cast liners as compared with that obtained by other casting processes and also to observe any effects of heat-treatment or mechanical working on structure. Examination of liners prepared by investment-casting and by dry and green sand casting showed the investment-cast metal has much larger cubic crystals and that there is more preferential orientation of crystals as a result of this casting process.

Examination of metal at the bore surface of liners after severe firing tests showed cubic metal with a fine particle size. A few very faint lines were present on the x-ray photographs but could not be identified. Thus the essential change at the bore surface as a result of firing was one of crystal size and not one of a chemical nature. The chemical inertness of this alloy towards hot powder gases makes it very erosion-resistant unless loss by melting occurs.

By x-ray studies of samples heated to various temperatures and for various periods of time, the inversion temperature of hexagonal, cobalt-rich solution to cubic, cobalt rich solution in this alloy was found to be approximately 800 C. This inversion is very sluggish; while pulverized metal heated at 800 C transformed in about 2 hours, solid pieces had not entirely transformed in 15 days. Any mechanical working at room temperature, such as cutting, filing, or machining, caused the surface layer to invert to the hexagonal form.

While metallographic techniques do not readily distinguish the hexagonal metal from the cubic, x-ray examination quickly identifies the hexagonal phase.

19.3.3 Effects of Heat Treatment on Structure

Aside from age-hardening, the most noticeable effect of heat treatment on the structure of Stellite No. 21 is a change in the amount of the "pearlite."[88] When specimens of investment-cast metal are heated to 1300 C and held there for 15 minutes the pearlite dissolves. It forms again on cooling from 1300 C to a temperature between about 1050 and 950 C, and the amount formed depends on the cooling rate and consequently on the time the specimen is held in this range.

19.3.4 Effects of Carbon Content on Structure

The effects of variations of carbon content in Stellite No. 21 in the range from 0.08 to 0.58% carbon on the as-cast structure and hardness were studied. In this range both high and low carbon contents surpress the formation of pearlite. Maximum pearlite developed in the alloy with 0.35% carbon.

A similar series with normal carbon content (about 0.25%) but with iron contents ranging from normal (2.5% or less) to as high as 20% were studied. Iron had no effect on the structure in either the as-cast or the heat-treated condition. There was no softening effect on hardness at room temperature, but such additions did decrease the hot-hardness.

19.3.5 Work- and Age-Hardening

The effectiveness of Stellite No. 21 as a liner material results not only from its hot-hardness and resistance to chemical attack by powder gases, but also from its susceptibility to work- and age-hardening and its retention of such added hardness during and after exposure to high temperatures. This conclusion is based on an extensive series of measurements.[88] An intense cold-working of the surface with resultant work-hardening occurs even during the machining operations (boring and rifling) on liners, and additional work- and age-hardness is imposed by firing stresses. Cold-worked Stellite No. 21 age-hardens much more rapidly than the unworked metal and also reaches a higher ultimate hardness.

19.3.6 Volume and Dimensional Stability

Liners of Stellite No. 21 in machine gun barrels have been found to undergo small dimensional changes as a result of firing. With flanged-type liners inserted with a shrink-fit into a recessed caliber .50 aircraft machine gun barrel, the length decreased during firing leaving a small gap at the forward joint, and there was a small decrease in bore diameter with an accompanying increase in muzzle velocity after the first burst of fire. These dimensional changes were probably caused for the most part by stresses during firing, with some slight changes caused by structural

changes in the liner alloy. Such dimensional changes have no deleterious effect on the performance of machine gun barrels.

Past experience with stellite alloys had shown that small dimensional changes resulted from upsetting or plastic deformation when a piece of metal was prevented from expanding freely during heating because of a heavy shrink-fit. Since phase changes in the alloy were known to occur, a series of very careful experiments[88] were made to evaluate volume stability. No measureable changes were found after heating at 700 C. Between 800 C and 1000 C a permanent shrinkage of 0.00086 inches per inch was observed. This change was slow (a matter of an hour or hours depending on the temperature). At 1200 to 1250 C dimensional changes were small and depended much on the previous history of the sample. The changes varied from a small permanent expansion to a small permanent shrinkage. Chilling in liquid air caused no permanent dimensional changes. None of these changes were of great enough magnitude to account for the decrease in liner length during firing; such decrease in liner length must have resulted from bore stresses.

19.3.7 Working Properties for Forging and Rolling

Stellite No. 21 can be hot-forged or hot-rolled. Because of its high-temperature strength, hot-working is much more difficult than with steels or other conventional materials. The essential requirements for the hot-rolling of Stellite No. 21 are the maintenance of a moderately high temperature (about 1190 C) and a comparatively small reduction at each pass. During rolling, numerous reheatings and rolls that can apply high pressures are required, but sheet or strip of limited sizes can be produced in almost any gauge desired. The most desirable temperature range for forging is about 940 to 1070 C. Metal worked by forging or rolling shows the expected amount of grain refinement. Such metal is very hard and usually requires heat-treating (normalizing) at about 1150 C.

Stellite No. 21 cannot be economically pierced and made into seamless tubing. For this reason castings, described in Section 19.4, rather than forgings, were used for liners. To obtain tubes of well-worked metal for tests, however, solid forged bars were drilled to the proper bore diameter. It is likely that welded tubing can be made from rolled strip and experiments on this process were in progress when the experimental work of NDRC was terminated. This process should be investigated further.

19.3.8 Physical and Thermal Properties

The available data on Stellite No. 21 may be summarized as follows:

Hardness and Hot-Hardness. Various samples of Stellite No. 21 from liners showed hardness values between 331 and 387 VPN with 30-kg load at room temperature. Most liners tested about 26 on the Rockwell C scale. Measurements of the hot-hardness of investment-cast Stellite No. 21, with a 10-kg load, and corresponding measurements on WD 4150 machine gun steel are shown in Table 2. This ability to retain a large part of the room-temperature hardness at elevated temperatures is an outstanding property of the stellites.

TABLE 2. Hardness of Stellite No. 21 at different temperatures compared with that of WD 4150 steel.

Temperature (C)	Stellite No. 21 hardness (VPN)	WD 4150 steel hardness (VPN)
20	314	290
500	275	241
600	242	140
700	206	50
800	176	36
20 (after test)	327	202

Specific Gravity and Density. The specific gravity at 20 C is 8.30. Values for density at intervals between 20 C and 800 C are given below under thermal coefficients.

Melting Range. This alloy does not have a sharp melting point but has a fusion range over which liquid and crystals coexist. This fusion range has not been located accurately and is influenced by variations in chemical composition within specification limits for this alloy. The melting and softening ranges probably lie somewhere between about 1280 C and 1350 C. Complete melting may even occur somewhat higher than 1350 C and values as high as 1396 C have been alleged. The melting interval needs further study.

Thermal Coefficients. Temperature distribution in caliber .50 machine gun barrels with and without a stellite liner has already been discussed briefly in Section 5.4.4. The thermal coefficients of Stellite No. 21 as compared with machine gun steel are given here in Table 3. Stellite is a poorer heat conductor than steel.

TABLE 3. Thermal coefficients of Stellite No. 21 and of SAE 4150 steel for comparison (in parentheses).[106]

Temp (C)	Density (gm/cm^3)	Volume specific heat ($cal/cm^3/°C$)	Conductivity ($cal/cm\ sec/°C$)	Diffusivity (cm^2/sec)	Heat conduction constant ($cal/cm^2\ sec^{\frac{1}{2}}/°C$)
20	8.30	0.96	.....	.....	.....
200	8.24 (7.79)	1.00 (0.98)	0.035 (0.100)	0.035 (0.102)	0.19 (0.31)
300	8.20	1.03	0.039	0.038	0.20
400	8.17	1.06	0.043	0.41	0.21
500	8.12	1.09	0.047	0.043	0.23
600	8.09 (7.65)	1.13 (1.35)	0.051 (0.081)	0.045 (0.060)	0.24 (0.33)
800	8.01	1.23	.....	.....	.....

In the case of a single round in a stellite-lined barrel, this results in a lower heat input per round with higher bore-surface temperatures but lower temperatures at depth as compared with a regular steel barrel. A further outcome of this difference in thermal properties is that in a continuous burst the deep swaging temperatures[f] in the region of the liner are not very different than those for a regular steel barrel for 200 rounds. For longer bursts the deep swaging temperatures rise more rapidly in steel than in stellite. Thermal effects in gun barrels during firing are discussed in detail elsewhere.[106]

Dilatometer curves made with an optical, differential dilatometer between room temperature and 1000 C showed no thermal arrests and the heating and cooling curves were nearly identical.[80]

19.3.9 Mechanical Properties

Considerable data on the tensile properties, hardness, impact strength, modulus, and ductility of Stellite No. 21 both at room temperature and at elevated temperature were obtained during the stellite-liner development. The effects of method of casting, heat-treatment and mechanical working on these properties were evaluated.[80] Stellite No. 21 has excellent strength and hardness, as well as reasonably high ductility and impact resistance, both at room temperature and at the elevated temperatures encountered in machine gun barrels during firing. Information on the mechanical properties of the investment-cast metal in the as-cast condition was obtained by mechanical tests. The data for tests at two temperatures are given in Table 4. Data on SAE 4150 steel are given for comparison. The test bars were 1-in. gauge by 0.24-in. Hot-hardness values were given in Table 2.

[f] Temperature at 1/16 in. from bore surface.[106]

Measurements[88] of modulus of elasticity (Young's modulus) showed decided directional properties in investment-cast metal. Because of the very large grain size the entire cross section of a 0.25-in. tensile specimen may consist of a single grain. Moduli ranging from 23 million to 40 million psi were measured. It is interesting to note that such nonuniformity of modulus had no noticeable effect upon life and performance in firing tests. It should be remembered that all cast (and heat-treated) metals, such as steels, brasses, etc., have a rather indefinite elastic modulus, spread over a wide range of experimental values. Only wrought metals have fixed values for their moduli.

19.3.10 Machinability

Stellite No. 21 can be machined readily with proper tooling. In spite of much apprehension on the part of machine gun barrel manufacturers, no serious problems were encountered in the machining of stellite liners in production. By the use of the proper carbide-tipped tools and cuts and feeds[119] determined in the development work,[80] it was found that it was much easier to hold Stellite No. 21 to close tolerances on dimensions than machine gun steel (WD 4150).

19.3.11 Availability

Stellite No. 21 contains more than 60 per cent of cobalt and about 28 per cent of chromium. During the war the supply of both metals was critical. Ferrochrome, which was less critical than pure chromium, was used to supply a part of the chromium.

Only because there was an adequate stock pile of cobalt, were all of the stellite liners needed for machine gun barrels obtained. Practically no cobalt ore is produced in the United States. The world supply comes largely from the Belgian Congo. During times of war, shipping conditions may be such that this supply will

TABLE 4. Results of mechanical tests on investment-cast Stellite No. 21 in as-cast condition* and on SAE 4150 steel.†

Sample	Temp	Tensile strength (psi)	Yield point (psi)	Breaking strength (psi)	Elongation (%)	Reduction of area (%)	Hardness (Rc)
Stellite	Room	90,000	65,000	123,000	23.5	23	29
Steel	Room	135,000	116,000		21	57	
Stellite	1500 F	71,000	45,000	84,000	30	24	
Steel	1200 F	45,000	20,000		38	92	

* Tests made at Crane Co. and results given in Report R on Contract OEMsr-629. The Charpy impact-resistance of this material varies from 9 to 13 ft-lb at 80 F and from 11 to 13 ft-lb at 1000 F.

† Tests made at Crane Co. Results given in letter to Chief, Division 1, August 7, 1944.

not be available. Cobalt occurs as an accessory in the Canadian nickel ores but is usually not extracted because of cost considerations. If stellite is to be used in large amounts for gun liners, attention must be given to an assured, large cobalt supply in wartime or a large stockpile must be available.

19.4 UTILIZATION OF STELLITE NO. 21 AS A LINER OR LINING MATERIAL

19.4.1 Introduction

In order to insure the most effective utilization of the remarkable erosion-resistance and good mechanical properties of Stellite No. 21, it was essential to evaluate the various possible methods of fabricating this alloy and of applying it to gun bores of various sizes with respect to the feasibility of the methods and to the effects of various factors on the performance of machine gun barrels containing stellite liners.

19.4.2 Casting Methods

The first liners of Stellite No. 21 tested were prepared in investment molds. These investment- or precision-castings have proved very satisfactory and nearly one-half of a million liner castings were made for insertion in machine gun barrels of the type described in Chapter 22. This casting method was expensive as compared with certain other ones, but the overall cost was low, because these precision castings required a minimum of grinding and machining operation to complete a liner for insertion.

Firing tests[80] were performed on caliber .50 machine gun liners cast by the following methods: (1) green-sand-mold casting, (2) dry-sand-mold casting, (3) graphite-mold casting, and (4) centrifugal casting in refractory molds. When proper melting and deoxidation techniques were used and the rate of cooling of the castings was controlled to approach the slow rate characteristic of casting in hot investment-molds, liners prepared by dry sand casting and by centrifugal casting in refractory molds were found to be equal in gun performance to those made by investment-casting. However, both of the former types of casting, especially the centrifugal one, require considerably more grinding and machining to finish the liners for insertion. In green sand molds it was difficult to get sound castings, and graphite-mold castings showed a much greater "wear" during firing tests than investment-castings. The centrifugal thermit-casting method[90] and other centrifugal melting techniques[82] were being studied but no liners made by these methods were tested before termination of the experimental program.

One important requirement for any stellite-liner casting is freedom from unsoundness. To insure quality and performance, it was found necessary to radiograph all liner castings in two directions at right angles. Although the soundness of castings could be determined more definitely when radiographed after rough turning and boring, it was found necessary in the interests of speed and economy of production to radiograph before machining. A series of firing tests was conducted to correlate the appearance of the radiographs with firing performance. It has been definitely established that radiographically sound castings insure satisfactory firing performance. In addition, the effects of variations of core materials and changes in the technique of investment casting were correlated with performance on firing. All of these studies insured the reliability of liner performance in Service weapons. In conclusion, it may be stated that investment casting was adopted as the standard method of preparing Stellite No. 21 because of a previously well-established practice. It has been sufficiently well demonstrated, however, that liners prepared from any radiographically sound casting perform satisfactorily; thus, the selection of a casting method depends simply on economic considerations.

19.4.3

Infusion, Incasting, and Torch Deposition

Advantages of Fusion-Bonded Linings

It was expected that if Stellite No. 21 could be attached to steel with a satisfactory fusion- or casting-bond between the two metals, a bore lining of stellite prepared in this way would present the following advantages:

1. It would permit a saving of critical and expensive metal by elimination of the metal of the flange and would also permit the application of thinner layers than is practical with castings. (It is difficult to maintain tolerance during machining and rifling operations in thin-walled castings owing to distortion.)

2. It would eliminate the necessity for a retaining nut behind the breech end of the liner, thus saving machining operations.

3. It would make full-length linings practical. (The preparation and mechanical insertion of full-length liners is very difficult as pointed out in Section 19.4.6.)

4. It would be a practical method of applying a stellite bore surface to the whole or part of the bore of large gun tubes. (It is difficult to make large castings that are sound and free from blow holes, shrinkage cavities, or other imperfections, and the final preparation of the liner casting and recess in the gun tube to receive it involves expensive and time-consuming machine operations.)

Applications of Fusion-Bonded Linings

Stellite No. 21 was applied as full-length or partial-length linings in caliber .50 aircraft machine gun barrels by several methods of infusion and incasting.

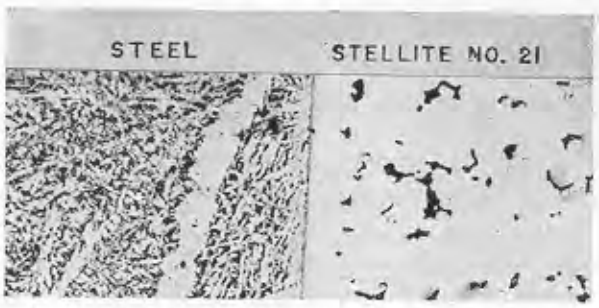


Figure 2. Longitudinal section of Stellite No. 21 rod fused in steel sleeve with steel plug at end of sleeve: Steel etched in nital; Stellite No. 21 etched electrolytically in sodium cyanide solution. (This figure has been taken from a report on Contract OEMsr-629.)

These same methods were used later to prepare replaceable steel liners with a stellite lining for tests in larger gun tubes, as described in Section 33.1.2. Infusion consists of the fusion of a casting in place in a recess in a steel tube. Incasting consists of filling a steel tube (with or without a core) with molten stellite so that the steel and stellite are bonded. A bond produced by infusion is shown in Figure 2.

Composite caliber .50 liners for test purposes were prepared by the several methods listed below and were subjected to firing tests to evaluate the behavior of the bond and the lining material. When suitably prepared, the bond in all cases was found to be excellent according to metallographic evidence and the linings survived all the rigors of firing. Figure 3 shows a fired caliber .50 barrel which had a stellite lining infused by the first method given below.



Figure 3. Caliber .50 barrel, stellite-lined by progressive static infusion and fired 2,008 rounds according to the CGL-350 schedule. (This figure has appeared as Figure 15 of NDRC Report A-417.)

Progressive Static Infusion.[89] A series of short castings was progressively melted in place in a vertical steel tube with a ceramic or other core by use of a moving induction coil. A diagram of the furnace assembly is shown as Figure 4. The apparatus for preparing a lining for a 37-mm gun (Section 33.1.2) by this method is shown in Figure 5.

Centrifugal Infusion or Incasting. Pieces of solid stellite were melted in a spinning steel tube, or molten

CONFIDENTIAL

stellite was poured into a steel tube which was spun until the stellite had solidified.[125] In addition, studies[90] were made of centrifugal, thermit incasting, but no liners for test were prepared by this method before termination of the experimental program.

Cast-Welding.[88] Molten stellite was poured into the space between a heated steel tube and a ceramic or other core.

Vacuum Incasting.[90] Molten stellite was sucked up or down into the evacuated space between a steel tube and a ceramic or other core. A diagram of the mold arranged for down-sucking is shown as Figure 6.

Torch Deposition.[80] A stellite surface was applied as a bore surface on two halves of a flanged, steel caliber .50 liner by torch deposition using an oxyacetylene welding torch. The behavior of the metal and bond during firing was excellent. Torch deposition is not practical for small bores such as caliber .50 but shows much promise for lining large gun tubes.

Three processes of torch deposition were studied; in two, welding was done with oxyacetylene and atomic-hydrogen torches, and the third employed a metallic arc. The atomic-hydrogen-torch welding process appears to be the most practical method of lining large-caliber gun tubes because of the possibility of automatic or semi-automatic application. The oxyacetylene-torch method must be considered unsuitable until a flux is developed which will permit a neutral flame adjustment to yield deposits free from pickup of excess carbon. The metallic-arc welding process appears promising, especially as a means of repairing surface defects in stellite deposits. Studies of these processes should be continued.

Necessary Precautions in Fusion-Bonding

In all of the infusion or incasting methods care was necessary to prevent serious contamination of the stellite by steel, especially in those methods which involved pouring molten metal along a steel surface or centrifugal spinning of molten stellite against steel. The particular problems involved in preparing full-length linings are discussed in Section 19.4.6, and the effects on performance of contamination by steel are discussed in Section 19.4.5.

19.4.4 Other Methods of Applying Stellite

The application of Stellite No. 21 to gun bores as cast liners has already been described in Section 19.4.2, liners bored from forged rods in Section 19.3.7, composite liners or linings prepared by infusion, incasting, or torch deposition in Section 19.4.3, and the possibilities of its application as seamless tubing or welded tubing made from rolled strip has been discussed in Section 19.3.7. In addition to these, three other methods of applying stellite linings or coatings to gun bores were explored as follows:

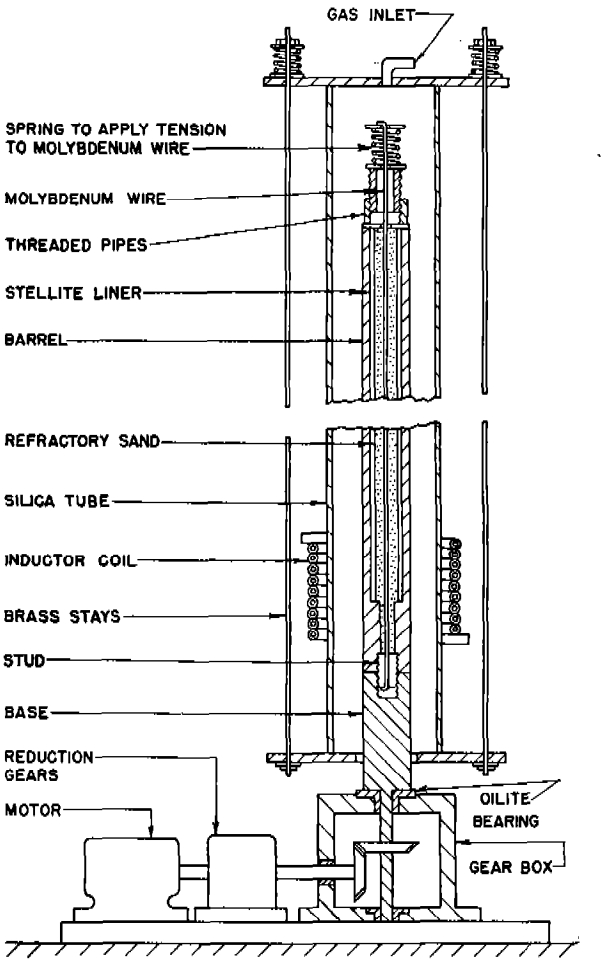


FIGURE 4. Diagram of furnace assembly ready for progressive static infusion of Stellite No. 21. (This figure has appeared as Figure 4 of NDRC Report A-417.)

Sprayed Coatings.[90] Stellite No. 21 was applied to steel surfaces by the use of a "spray-gun." The production of an adherent deposit requires a rough steel surface. In the case of steel tubes with an internal diameter of less than 1½ in., spray methods were impractical. Even the best spray-coats of stellite showed lamination and porosity, and tensile test specimens cut from thick spray coats showed zero elongation and a strength of less than 9,000 psi. The mechanical

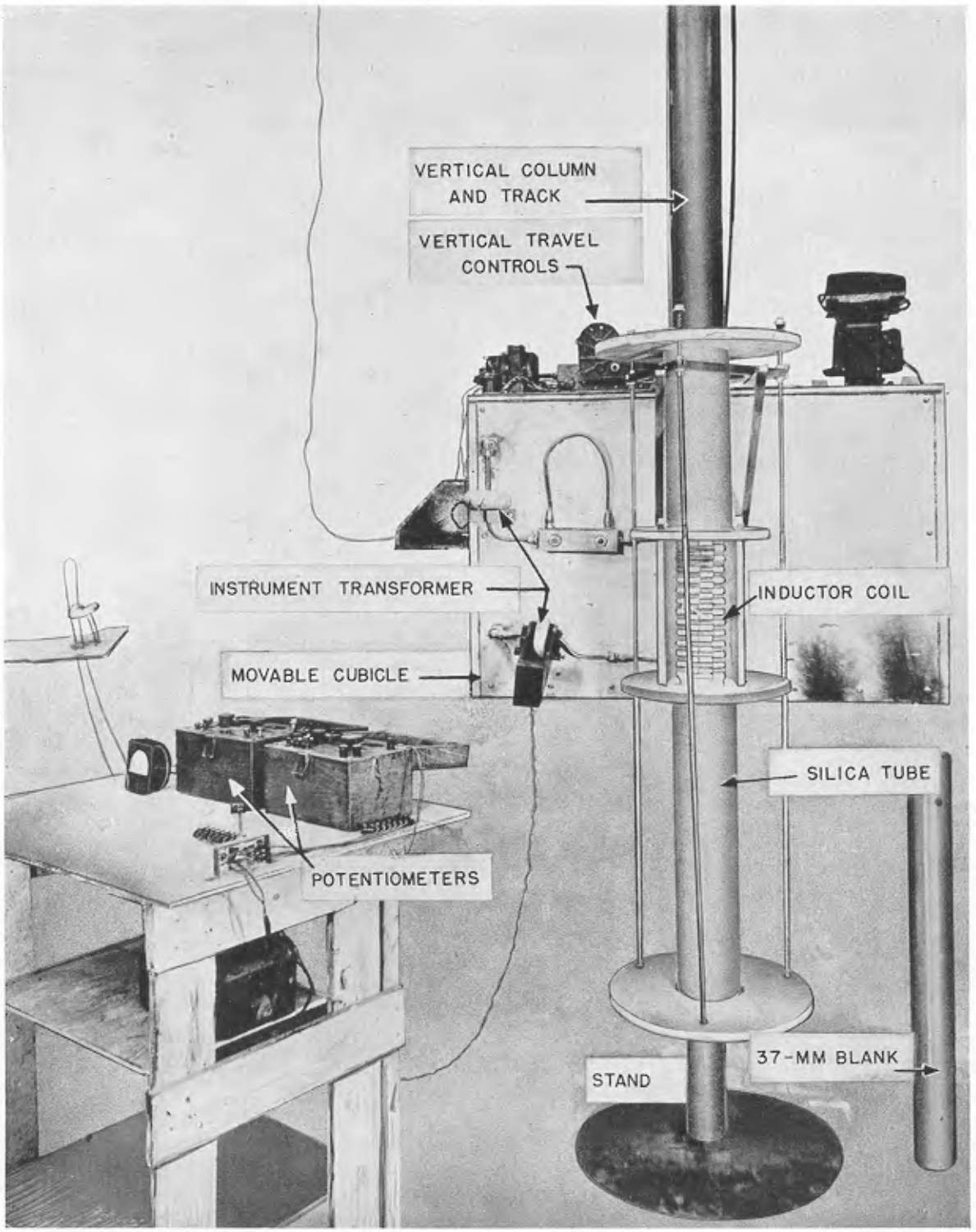


FIGURE 5. Induction-heating furnace for infusing 37-mm blanks. (This figure has appeared as Figure 2 of NDRC Report A-417.)

CONFIDENTIAL

properties of such deposits make them unsuitable as bore-surface materials. Spraying might be used as a method of applying a layer of stellite prior to an infusion or torch-welding process.

Coatings by Thermal Explosion.[88] Metal can be vaporized by heat and such vapor can be deposited to form a coating. Stellite wires were exploded in a vacuum by an electrical discharge and the metal was deposited on the walls of a steel tube. The rate of deposition was extremely slow and the coating was unsatisfactory unless its adherence was improved by a diffusion treatment. The process is expensive and thoroughly impractical.

Electroplating and Diffusion.[88] It is possible to apply the component metals of Stellite No. 21 in the form of a series of thin electrodeposits and then convert these layers into the alloy by a high-temperature diffusion process. It was found that the plates could be applied and subsequently alloyed. These experiments were not carried along far enough to estimate the commercial feasibility of such a method.

19.4.5 Effects of Various Factors on Performance

An extensive series of firing tests[80] was conducted on stellite-lined caliber .50 aircraft machine gun barrels in order to evaluate the importance of the various factors which control the performance of this barrel with a breech liner of Stellite No. 21. In addition to the evaluation of the effects of casting methods and infusion, incasting, and torch deposition methods already described in Sections 19.4.2 and 19.4.3, the effects of the following additional factors were studied.

Hardness

The effects of variations in hardness in regular, 9-in. investment-cast liners was studied. Two thousand liners were checked for hardness and with few exceptions were found to range in hardness from 20 to 30 Rockwell C with an average of 25.8. Two liners with the lowest hardness and two with the highest were selected for test, and performance was comparable to that of liners of normal hardness.

A study of liners with work-hardened bores was in progress, but the experiments were not completed before termination of the program.

Liners with hardened bores produced by the drawrifling processes [135] were subjected to firing tests. The results were inconclusive because the rifling was not of standard dimensions and frequent stoppages occurred during firing.

Nitriding

During the research program to improve further the barrel containing a stellite liner by chromium-plating the steel bore ahead of the liner, which is the

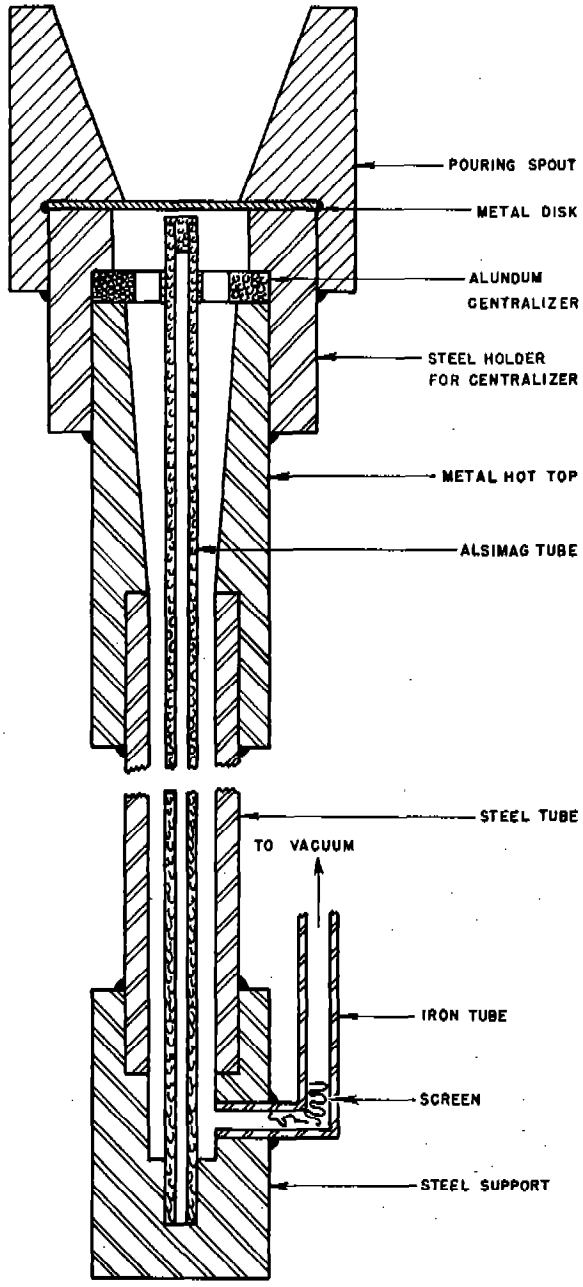


Figure 6. Mold for vacuum incasting of Stellite No. 21. (This figure has appeared as Figure 2 of NDRC Report A-418.)

subject of Chapter 24, nitriding of the steel bore prior to plating was tried. To simplify the procedure the nitriding was performed with the stellite liner in place. Nitriding had little, if any, effect on Stellite No. 21 and when barrels containing stellite liners were nitrided and fired, no difference in performance[81] was noted as compared with regular stellite-lined barrels.

Decarburization

Early in the program it was felt that the presence of eutectoid at the grain boundaries of stellite might be a source of weakness. This material might suffer preferential melting or attack and cause cracking of the bore surface. Several liners were decarburized[88] at 1175 C for 5 hr in dry hydrogen. All of these liners gave inferior performance except one which had been decarburized before machining. This liner gave performance comparable to regular stellite-lined barrels.

Hot-Working

Since much higher strength and hardness and equivalent ductility and better impact resistance were obtained in laboratory tests on metal mechanically worked by rolling or forging, as compared with cast metal, two caliber .50 liners were prepared by boring cast rods which had been forged to the extent that the diameter was decreased from 2 in. to 1 in. Firing tests on these liners showed performance equal to but not superior to that obtained with regular investment-cast liners.

Chemical Composition

Firing tests on stellites other than No. 21, which are described later (Section 19.6), indicated that the chemical composition of the liner alloy was an important factor in determining performance. To insure reliability of performance, exploratory studies of the effects of varying carbon contents, varying iron contents, and varying molybdenum, iron, and carbon contents of Stellite No. 21 were made.

A series of investment-cast liners was prepared with carbon contents varying by steps from 0.08 to 0.58%. Two liners of each composition were subjected to firing tests. The normal carbon content of Stellite No. 21 is 0.20 to 0.35%. The firing tests showed that liners with the normal range of carbon content performed in a very satisfactory manner and that the percentage could be increased to as much as 0.58 without any impairment in performance. When, however, the carbon was as low as 0.08%, performance was distinctly inferior.

The effect of replacing some of the cobalt with iron and thus increasing the iron content beyond the specified maximum of 2.5% was of interest because of a critical shortage of pure chromium, which might require the use of ferrochromium in the production of liner castings, and because increased iron content through pickup from steel is often obtained during the infusion, incasting, and torch deposition methods already described in Section 19.4.3. Firing tests on investment-cast liners prepared with and without ferrochromium and with iron contents varying by steps from 3.3 to 20.15% showed that the maximum iron content that can be tolerated without seriously affecting performance is about 7%.

A few exploratory experiments were made in which two of the constituents were increased and the cobalt decreased. Firing tests on investment-cast liners with the percentages of the constituents varied as follows:

8.60% Fe and 8.90% Mo
9.85% Fe and 0.47% C
7.10% Fe and 0.46% C

showed, respectively, equal, decidedly inferior, and slightly inferior performance as compared with regular liners of Stellite No. 21.

Heat-Treatment

A systematic study was made of the effect of heat treatments on the physical properties, microstructures, and firing performance of both investment-cast and sand-cast Stellite No. 21. All the tensile properties, hot-hardness, and microstructure can be varied by heat-treatment within a rather wide range. A given sample can be made ductile with a relatively low hardness, while another can be made very hard with relatively low ductility and impact resistance. There is no significant difference in physical properties of the metal whether prepared by investment- or sand-casting methods.

A series of investment-cast liners was subjected to selected heat treatments based on the above observations and subjected to firing tests. None of the heat treatments improved the performance over that of the as-cast material. Some heat treatments had no effect while others definitely reduced the performance.

One important observation was that when an investment-casting was subjected to the heat-treat-

ment normally given to gun steel (oil quenching from 1550 F and drawing at 1000 F), there was no effect on its performance. Thus, composite Stellite No. 21-steel assemblies made by infusion or incasting (see Section 19.4.3) can be heat-treated to develop the desired properties in the steel without impairing in any way the performance of the stellite.

Firing tests of investment-cast liners of Stellite No. 21 that had been heat-treated to develop a maximum and a minimum amount of the pearlitic structure showed that neither of these heat treatments was advantageous.

Method of Insertion

In the preparation of cast-stellite liners for insertion in steel machine gun barrels on a production basis, it is desirable to allow as large tolerances as possible on the amount of interference between the liner and barrel recess for a shrink-fit. Too small an interference may allow the liner to rotate during firing, while too large an interference may cause both excessive bore-constriction during firing and difficulties in assembly. Firing tests established a maximum diametrical interference of 0.001 in. on the portion of the liner with small diameter. This may be increased to 0.002 in. on the shoulder or flange of the liner.

There was some evidence that the immersion of liners in liquid nitrogen (either before or after machining or in the process of insertion) slightly enhanced the performance and that liners inserted by heating the barrel only, without cooling the liners, gave somewhat inferior performance. This tentative conclusion should be checked by more comparison-firing data.

Liner Length

Nonplated Steel Ahead of Liner. Six-inch, nine-inch, and twelve-inch (overall length) liners were subjected to firing tests in caliber .50 aircraft machine gun barrels. Severe erosion of the steel bore ahead of a 6-in. liner occurred and seriously affected performance. The 12-in. liner was unsatisfactory because of a dangerous weakening of the barrel near the forward joint after a gap had been produced by a slight shrinkage in liner length during firing. The 9-in. liner gave very satisfactory performance. The problems of full length liners are discussed later in Section 19.4.6.

Plated Steel Ahead of Liner. Chromium-plating of the steel bore ahead of a stellite liner considerably enhances the performance of the machine gun barrel. This combination of a 9-in. liner with plate and its Service applications are described later in Chapter 24. Studies were made of the performance of barrels with 4-in., 6-in., and 9-in. liners of Stellite No. 21 with tapered (choke-muzzle) chromium-plate ahead of the liner. Barrels with a 4-in. liner plus the plate were equivalent in performance to barrels with a 9-in. liner without plate; those with 6-in. liners plus plate were somewhat superior to the latter; and those with 9-in. liners plus plate were very much superior.

Attention should be called at this time to the fact that, in order to get full benefit from a short erosion-resistant liner of Stellite No. 21 with or without an erosion-resistant plate (chromium plate) ahead of the liner, the barrel weight should be increased, the contour (distribution of steel) should be changed, and the composition of the barrel steel should be changed. These matters are taken up fully in Chapter 24.

Wall Thickness of Liners

The $\frac{1}{8}$-in. wall thickness was selected for the liners on the basis of the strength of the liner and its resistance to deformation during handling and during the various grinding, machining, boring and rifling operations necessary to prepare a liner casting for insertion. With considerable care it was possible to prepare two liners with a $\frac{1}{16}$-in. wall thickness. Their firing performance was entirely comparable to regular liners with $\frac{1}{8}$-in. walls. This result is of considerable interest in connection with the performance of stellite when applied to gun bores as thin linings by infusion, incasting, or torch deposition.

Plated Liners

If a bore surface of Stellite No. 21 with its excellent resistance to the swaging impact of projectiles could be protected from surface melting, it might be possible to extend the useful range of application of stellite to hypervelocity conditions with the resultant high bore-surface temperatures. Attempts were made to protect stellite bore surfaces with deposits of the high-melting, erosion-resistant metals chromium, molybdenum, and tungsten. A number of investment-cast caliber .50 liners were rifled oversize to allow for such coatings, and attempts were made to apply satisfactory deposits of chromium by electroplating and of tungsten and molybdenum by pyrolytic plat-

ing, as described in Chapter 21. Electroplated chromium was poorly adherent on stellite surfaces and no firing tests were made. Diffusion bonding to increase adherence of this plate should be studied. Pyrolytic coatings of tungsten and molybdenum on stellite liners were subjected to firing tests and were unable to withstand even a mild schedule without spalling and deformation.

19.4.6 Preparation and Testing of Full-Length Liners or Linings

Linings Prepared by Static Infusion

Caliber .50 aircraft machine gun barrels with partial length and full-length linings of Stellite No. 21 were prepared by the method of progressive static infusion.[89] This method provides barrel blanks with partial or full-length linings ready for finishing as one-piece barrels and eliminates liner insertion and the necessity of the retaining nut behind the liner at the breech end of the barrel. Particular problems were encountered in the preparation of satisfactory full-length linings. Troublesome coring problems were encountered and solved. Preliminary cost analysis studies indicated that it should be possible to manufacture such barrels at substantially lower costs than barrels with inserted 9-in. liners.[125]

When barrels were completed and subjected to firing tests[80] it was found that, unless the stellite lining was of very uniform thickness and was perfectly concentric with the outside diameter of the steel barrel wall, the shot-pattern moved off the target during firing owing to the bimetallic effect and to reversible warping of the composite barrel as a result of heating during firing. Even when the lining was of uniform thickness and concentric, and dispersion was normal, performance was only equivalent to that of barrels with 9-in. long, investment-cast stellite liners inserted on a shrink-fit, and was inferior to that obtained with barrels containing a 9-in. liner plus tapered (choke-muzzle) chromium plate ahead of the liner.

Liners in Series

A 13-lb caliber .50 aircraft machine gun barrel was recessed to receive a nearly full-length bore-surface of Stellite No. 21 by inserting three investment-cast liners.[80] The stellite extended to within 1-in. of the muzzle; the forward two liners had no flanged shoulders. During the firing test, one of the forward liners rotated and a 0.25-in. separation occurred between the forward two liners as a result of shrinkages in length during firing. There was no tendency for the shot-pattern to move off the target as with some of the full-length, infused linings previously described. Overall performance was unsatisfactory.

"In-melted" Liners

Towards the close of the experimental program it was possible to produce full-length liners of Stellite No. 21 which could be shrunk into standard or special caliber .50 aircraft machine gun barrels. They were prepared by a process of remelting a stacked series of short, tubular fillers of investment-cast stellite within an inductively heated, refractory-lined, graphite tube.[89] One of these liners before machining is shown here as Figure 7. Stress-relieving treatments, machining procedures which would preserve the straightness and concentricity of the liners, and a proper insertion procedure were developed. Two barrels with these liners were ready for firing tests, which were not carried out, however, because of the termination of the experimental program.

19.5 APPLICATION OF LINERS OR LININGS OF STELLITE NO. 21 TO GUNS

19.5.1 Improved Machine Gun Barrels

Experience of aircraft combat during the war indicated that erosion was limiting the performance of the caliber .50 aircraft machine gun. The application of short, breech liners of Stellite No. 21 to machine gun barrels led to remarkable increases in the length of life. Barrels containing stellite liners, the subject of Chapter 22, showed outstanding performance under firing conditions so severe that unmodified steel barrels were unable to withstand them.

The combination of the stellite liner with tapered (choke-muzzle) chromium plate ahead of the liner gave further outstanding improvement in performance particularly when the weight of the barrel, contour (distribution of steel) and barrel steel composition were adjusted to enable maximum utilization of the erosion resistance of the liner and plate. The types of barrels that were thus modified and improved are discussed in Chapter 24.

When double-base powder was used in some of the acceptance tests of improved caliber .50 aircraft bar-



FIGURE 7. In-melted, full-length, Stellite No. 21 liner; cast surface except at joints of original fillers. (This figure has appeared as Figure 2 of NDRC Report A-417.)

rels, mentioned in Section 22.3.3, conditions approached those of hypervelocity. The failure of stellite under these conditions is discussed in the next section.

19.5.2 Hypervelocity Guns

Two liners of Stellite No. 21 and two of Stellite No. 22 were tested in the caliber .50 erosion-testing gun (Section 11.2.1) under conditions of hypervelocity at a slow rate of fire.[76,77] For one pair of tests, double-base powder (20% nitroglycerin) was used and for the other pair single-base (IMR) powder. With double-base powder, the bore surface of the stellite liners melted so rapidly that it was impossible to establish full pressure. With single-base powder, with which a muzzle velocity of 3,571 fps was achieved, only a small amount of local melting occurred at the bore surface. The latter tests were discontinued after 500 rounds, at the end of which the rifling of the liners was still in very satisfactory condition. Figure 6 of Chapter 16 shows the contrast between the bore surfaces of liners fired with these two kinds of powder.

Experience with stellite liners in the caliber .60 machine gun barrel showed that this alloy is marginal with respect to its use in hypervelocity guns. This gun, for which liners of Stellite No. 21 are being used regularly, has a muzzle-velocity of slightly over 3,500 fps with IMR powder. In this particular application, a stellite liner, unlike steel, lasts long enough to furnish a useful gun-barrel life. However, metallographic studies have shown that ultimate failure is the result of melting along surface cracks.

These observations showed that an erosion-resistant material of higher melting point than the stellites was required for general use in hypervelocity guns. The development of such materials is described in the other chapters of Part V.

19.5.3 37-mm Cannon

A partial bore lining of Stellite No. 21 has been successfully applied to the 37-mm gun tube, M3. This development is described in Section 33.1.2.

19.6 FIRING RESULTS ON STELLITES OTHER THAN NO. 21

The early firing tests on Stellite No. 6 and the reasons which led to the selection of Stellite No. 21 have already been described in Section 19.2. Firing tests[89] have been made with caliber .50 liners prepared from other stellite-type alloys, the compositions of which are given in Table 1, to determine (1) whether any of these might be superior to Stellite No. 21 as a gun liner, or (2) whether any of them containing less of the critical metal cobalt might be equally suitable. None of the other stellite-type alloys gave performance better than that of Stellite No. 21.

The following tungsten-bearing stellites were tested: No. 6, No. 22, No. 6-2A, No. 23, and No. X40. All showed inferior performance to Stellite No. 21 and greater land "wear" during firing, and all of the liners except the one of Stellite No. 23 exhibited deep cracking and brittle failure at some stage of the firing tests.

Two molybdenum-bearing stellites in which nickel had been substituted for some of the cobalt were tested as liners. Stellite No. 422-19 showed greater land wear. One investment-cast liner of Stellite No. 27 showed performance equal to that of Stellite No. 21, but a duplicate liner from the same casting-heat had no rifling left and the barrel showed a large velocity-drop after one continuous burst of 300 rounds in the caliber .50 aircraft machine gun. When two additional liners of No. 27 were fired later they both showed complete obliteration of the rifling and

a large velocity drop after one long burst of fire. This alloy is very difficult to cast because of shrinkage in the mold and is gummy and difficult to machine.

19.7 COBALT AND HIGH-COBALT ALLOYS AS LINERS

In vent-plug tests (Section 16.3.1) pure cobalt was slightly less resistant to powder-gas erosion (melting and chemical attack) than gun steel under the severe conditions of the 1/16-in. vent test but under the milder conditions of the 1/8-in. vent test it was more resistant.[50] This result was confirmed by a test of a short, rifled caliber .30 liner of pure, swaged cobalt (Section 16.3.6). However, although it exhibited resistance to powder-gas erosion and good ductility, pure cobalt had insufficient hot-hardness to resist deformation of the rifling by swaging impact of the bullets.[59]

In an effort to harden cobalt and if possible to increase its resistance to powder-gas erosion, binary cobalt alloys containing varying amounts of tungsten, molybdenum, or chromium were prepared as ingots and swaged into rods. These alloys eroded less than stellites in vent-plug tests.[59]

The alloy containing 93% cobalt and 7% tungsten showed excellent performance when tested as a liner in the caliber .50 heavy machine gun barrel.[81] Since these alloys contained more critical metal cobalt, were much more difficult to prepare than the easily cast Stellite No. 21, and showed no marked advantage in performance over the latter, their further development as liners was not pursued.

19.8 ALLOYS CONTAINING LESS COBALT THAN MOST STELLITES

19.8.1 Introduction

During the course of the stellite-liner development, difficulties arose because of the shortage of critical materials. Ordnance Department liaison officers urged Division 1, NDRC, to develop substitutes for Stellite No. 21 with less cobalt or if possible without any, in order to save the very critical cobalt, part of which was being obtained from the small stockpile accumulated for war purposes. In an attempt to ease the cobalt situation, nickel-substituted stellites were tested with the unsatisfactory results already described in Section 19.6. In addition, a reconnaissance was made of a series of hot-hard alloys with less cobalt than Stellite No. 21 or with no cobalt. The melting points of these hot-hard alloys are all of the same order of magnitude as the stellites.

19.8.2 Hot-Hard Reconnaissance

Iron, Nickel, Chromium, and Cobalt Alloys

The data for four groups of metals and alloys were examined to determine whether they would be resistant to melting and chemical attack by hot powder gases, resistant to deformation of the rifling by the swaging impact of the projectile, and sufficiently ductile to resist disintegration by brittle failure.

Iron-Base Alloys. High-iron alloys (80% or more of iron) show poor resistance to powder-gas erosion. In the case of gun steel, performance is limited by a combination of chemical attack and flattening (swaging) of the rifling. With special steels or hot-hard, iron-base alloys or with ordinary steel hardened by nitriding or by special hardening techniques, chemical erosion by powder gases is still a serious limitation on performance unless the bore surface is protected by an erosion-resistant plating or coating.

Nickel-Base Alloys. High-nickel alloys (80% or more of nickel), with the exception of binary nickel-chromium alloys, show intergranular attack and disintegration during firing. When the nickel-chromium alloys are hardened by alloying (for example, Inconel-type alloys) their resistance to powder-gas erosion is poor.

Chromium-Base Alloys. Pure chromium and high-chromium alloys are very resistant to chemical attack and melting. However, most of these materials are too brittle for use as gun liners. Certain chromium-base alloys, discussed in Chapter 17, have a high melting point (1650 to 1700 C) and show excellent resistance to powder-gas erosion and very good hot-hardness. Some of these alloys have sufficient ductility to withstand the shock of firing.

Cobalt-Base Alloys. Pure cobalt and cobalt-base alloys (like the stellites) have good hot-hardness and some of them have sufficient ductility for satisfactory use as a gun liner.

Hardened Iron-Nickel-Cobalt-Chromium Alloys

Few data were available on the performance of hardened alloys that contain all four of the above metals. Many such alloys were known to have excellent high-temperature properties including hot-hard-

ness and hot-strength with small to moderate ductility. The extent of their resistance to chemical attack by powder gases was not known. In order to evaluate the possibilities of these alloys, a reconnaissance series of hardened iron-nickel-cobalt-chromium alloys was prepared and tested as liners in the caliber .50 aircraft machine gun barrel.[80,81] The nominal composition of the alloys subjected to firing tests is given in Table 5. They are specific examples of the types briefly described in Section 16.4.10, where their potentialities have been evaluated. The performance of none of these alloys was as good as that of investment-cast Stellite No. 21.

One alloy containing no cobalt (TEW) showed severe chemical attack by powder gases and shows no possibilities. Another alloy (Hastelloy C) containing no cobalt was resistant to powder-gas erosion and shows considerable promise. The Hastelloys have already been discussed in Section 16.4.9. The poor performance of some of the other alloys may have been caused by the poor condition of the specimen tested, owing either to inexperience in casting the particular alloy or to improper choice of hardness, which is dependent on the heat treatment and carbon content. Thus the liner of N155 alloy that was tested was a poor sand-casting. A good, sound investment-casting of this alloy with 0.25% carbon should be tested.

One of the most promising of this group of hot-hard alloys is Refractaloy No. 70.[92] The first liner was bored from a forged and age-hardened bar. It showed very good resistance to powder-gas erosion but cracked during a second burst of 238 rounds after an initial burst of 350 rounds had been fired. Then investment-cast liners were prepared and tested. They were too soft and failed by swaging of the lands. The casting method should be perfected and heat treatment studied to yield liners with optimum hot-hardness and ductility so that the erosion resistance can be utilized.

TABLE 5. Nominal composition of hot-hard alloys (and of Stellites No. 21 and No. 27) used as caliber .50 liners in reconnaissance tests for erosion resistance.

Name	Nominal composition*						
	Co	Ni	Fe	Cr	Mo	W	Other
Stellite No. 21†	62	2	2	28	6	..	C 0.25
S 816‡	45	20	3	20	4	4	Cb 4
Stellite No. 27†	32	32	2	28	5	..	C 0.40
Refractaloy No. 70§	30	20	15	20	8	4	
N 155†	20	20	30	20	3	3	Cb 4
MTB‖	12	30	27	20	4	4	Ta 2
Refractaloy No. 2§	15	40	13	20	5	4	Cb 3
TEW‖	..	30	40	20	4	4	Ta 2
Hastelloy "C"†	..	58	6	15	17	4	
Hastelloy "A"†	..	60	20	..	20	..	
Hastelloy "B"†	..	66	6	..	28		

* All low carbon (usually 0.1%) unless otherwise stated; Mn and Si usually less than 1% each.

† Haynes Stellite Company.

‡ Allegheny Ludlum Steel Corporation.

§ Westinghouse Research Laboratories.

‖ Special alloy similar to some studied in turbine blade research program.[169]

Chapter 20

ELECTROPLATING

By *William Blum*[a]

20.1 GENERAL PRINCIPLES

THIS CHAPTER is confined to the application of electroplated coatings to gun bores to resist erosion. Only incidental references are made to the performance of the plated barrels, more details of which are given in Chapters 23 and 24.

20.1.1 Requirements

Experience and research have shown (Chapter 16) that, to resist erosion, the material of the bore surface should be resistant to chemical attack by the powder gases, have a melting point of at least 1400 C, have high strength, hardness, and ductility at elevated temperatures, and have no abrupt volume changes with temperature.

Because suitable metals are relatively scarce and may not be adaptable to the production of the entire gun tube, a "liner" or coating with the desired properties is advantageous. Such a liner or coating may be produced mechanically, as for example, the molybdenum and stellite liners (Chapters 18 and 19), by electrodeposition, by vaporization, by sputtering, or by chemical decomposition of a vaporized compound (Chapter 21).

20.1.2 Characteristics of Electrodeposited Coatings

The advantages and limitations of electrodeposited coatings to protect gun bores may be summarized as follows.

It is possible to vary the properties of the deposit by control of the conditions used in depositing a given metal. In the case of chromium plate the hardness may range from 400 to 1000 MVn.[b] Other properties such as tensile strength vary over similar ranges. On heating to high temperatures the deposits of a given metal tend to anneal and to reach uniform properties for that metal. By co-depositing two or more metals to form an alloy, it is possible to modify still further the properties of electrodeposits.

The thickness of the electrodeposits can be controlled by regulating the current density and the period of deposition. The deposit follows closely the contour of the base metal, though the thickness is always less in the bottom of the grooves than on the top of the lands. The degree of this difference in thickness depends upon the throwing power of the plating bath employed. In chromium plating, the thickness of the deposit on the lands may be 30 per cent greater than that on the grooves since the chromic acid plating bath has very poor throwing power. In other plating baths the difference is smaller.

With chromium coatings up to 0.01 in. thick, the resultant changes in contour are not important except in artillery bores. The relatively higher and more sharply cornered lands in these bores may cause an undesirable build-up of the deposit on the land corners.

With great care and, in certain cases, with special procedures, a degree of adhesion can be secured such that detachment of the coating removes part of the underlying metal. As no quantitative tests of adhesion are directly applicable to coatings in gun barrels, firing tests must be used as a criterion.

20.1.3 Availability of Electrodeposited Metals

Only a few metals approach in their properties those desired in gun bores, that is high melting points and high hardness and tensile strength at elevated temperatures. The principal ones thus far considered for this purpose, as related in Section 16.1, are chromium, nickel, cobalt, molybdenum, tungsten and tantalum. Of these metals only the first three can be readily electrodeposited in a pure state from aqueous solutions. Available evidence indicates that it is not possible to electrodeposit pure tungsten or molybdenum.

Processes have been described for the electrodeposition of pure tungsten[463] but later published data indicate that deposits reported as tungsten were really alloys and contained at least small amounts of other metals, such as iron, nickel, or cobalt, that were present as impurities in the bath. By intentional ad-

[a] National Bureau of Standards, U. S. Department of Commerce.

[b] Microvickers number: Vickers hardness determined with microhardness testing machine.

ditions of such metals to baths of tungsten or molybdenum it is possible to deposit corresponding alloys.

There are a few reports in the literature on processes for the electrodeposition of pure molybdenum but none of these processes yields satisfactory metallic coatings. A preliminary attempt aimed specifically at the preparation of a molybdenum-plated gun barrel was also unsuccessful because of poor adhesion of the molybdenum to steel.[80]

There are numerous patents on the electrodeposition of tantalum from fused salt baths. The metal obtained is usually in the form of a fine powder, unsuitable to serve as a coating. More recently some attempts have been made without success to prepare an adherent coating from a fused bath consisting of potassium fluoride, potassium tantalum fluoride, and tantalum oxide at about 800 C.[95]

20.2 CHROMIUM PLATING

20.2.1 Previous Experience

More progress was made by Division 1 in the application of chromium than of other electroplates to gun barrels, because some of the properties of chromium approach those desired, and there had been previous experience in the use of chromium coatings to resist abrasion and corrosion.[171] Early attempts to apply it to gun barrels to resist erosion were not very successful. At the Washington Naval Gun Factory during the 1930's chromium coatings less than 0.001 in. thick were applied to the bores of large naval guns. These thin coatings did not greatly increase the useful life of these guns,[86] but they no doubt furnished some protection against corrosion, especially by sea water. Sporadic tests[185] by the Army Ordnance Department of gun barrels chromium plated commercially, and studies[311] at Frankford Arsenal on caliber .30 machine gun barrels, did not indicate any outstanding improvement in gun life.

At the beginning of the Division 1 program, Service guns were carefully examined in order to determine in what manner the chromium plate had failed.[86] The conclusions drawn from these observations were strengthened by later studies of liners that had been fired in caliber .50 machine gun barrels in connection with the development of a technique for applying improved chromium plate to barrels of this caliber.[85]

The sequence of events in erosion of chromium-plated guns was found to be as follows. Microscopic cracks may be present in the plate as deposited (Figure 1), and, because chromium is relatively brittle, additional cracks form during firing. The hot powder gases penetrate the cracks and react with the underlying steel (Section 13.3) which has been thermally altered (Section 13.2). A pocket type of erosion, shown in Figure 1, takes place in the steel at the roots of the cracks in the chromium. The plate on the surface thus undermined, sometimes together with adherent steel, begins to be chipped and torn off by the projectile. This action is initiated most vigorously on the band slope and the adjacent edges of the lands.



FIGURE 1. Surface of chromium plate showing microscopic cracks in the metal as deposited: Unetched; *200X*. (This figure has appeared as Figure 1 in NDRC Report A-414.)

Such erosion progresses forward most rapidly on the tops of the lands, as illustrated in Figure 2. In the grooves, where contact with the projectile is slight, and on the chamber cylinder where no contact occurs, only minute chips of chromium are removed until corrosion along longitudinal cracks has greatly weakened the supporting steel. Swaging of the steel (Section 13.4.2), which may take place beneath the chromium plate, accelerates the cracking, undercutting, spalling, and mechanical removal of plate which has been cracked and pitted.

Once the chromium plate is removed, erosion of a gun bore proceeds as in a nonplated gun. The initial cause of failure just described, however, is related to the mechanical weakness of chromium, which is resistant to thermal and chemical attack by the powder gases. As will be described later, the diminution of the mechanical forces can prolong the life of chromium-plated guns. The use of pre-engraved projectiles (Chapter 31) eliminates engraving stresses and minimizes bore friction, and the Fisa protector (Chapter 32) protects the chromium plate in the region of the origin of rifling.



FIGURE 2. Cross section of eroded 5-in./25-cal., chromium-plated naval gun showing plate mostly in place in the groove but none on the land: Etched with picral; *50X*. (This figure has appeared as a portion of Figure 17 in NDRC Report A-414.)

20.2.2 Conditions of Deposition and Properties of Deposits

Most commercial chromium plating is conducted from solutions containing from 250 to 400 g/l (33 to 55 oz/gal) of chromic acid and 2.5 to 4 g/l of sulfuric acid or an equivalent amount of another sulfate. The baths are usually operated at 40 to 60 C (104 to 140 F) at current densities from 8 to 30 amp/dm^2 (75 to 280 amp/ft^2). Under these conditions a bright, hard coating is produced with a cathode efficiency of about 15 per cent. For ornamental purposes, for example, over nickel on steel automobile parts, the chromium coatings are usually less than 0.00003 in. thick. For wear resistance on gauges and dies, coatings up to 0.005 in. thick may be used.

Types of Chromium Plates

Measurements made in the course of the investigation carried out by Division 1 show that the properties of chromium deposits vary widely with the conditions of deposition. Two rather sharply defined types of chromium exist, to which have been applied the terms "HC" or "high contraction," and "LC" or "low contraction." Both types are included in Table 1. The HC deposits are of the type commonly used for decorative plating and for wear resistance. They are hard and brittle; they contain chromic oxide; and they contract when heated. In contrast the LC deposits are much softer and less brittle (but not actually ductile); they contain little oxide; and they contract only slightly when heated. Because of the lower contraction, the LC deposits are more nearly free from cracks, both as deposited and after having been heated.

Plating Procedures for Different Base Materials

No great difficulty is experienced in obtaining good adhesion of chromium to gun steel, if the customary methods of cleaning and pickling are employed, such as those listed under "Application to Caliber .50 Barrels" in Section 20.2.3.

Attempts to deposit chromium by these methods on stellite or similar alloys usually resulted in poor adhesion of the coatings, probably as a result of passive films on the alloy surface. Plating on chromium and chromium alloys is often accomplished by initial deposition of nickel from an acidified nickel chloride solution. This method did not prove effective on stellite.

Fairly good adhesion of chromium to stellite was obtained by scrubbing the surface first with magnesium oxide and water, followed by pumice and inhibited hydrochloric acid. A very low cathode current density (from 5 to 20 per cent of normal) was then applied for several minutes in the regular chromium plating bath, after which the current was gradually increased to normal during a period of 10 to 15 min. Plating was then conducted as usual. This process represents cathodic pickling in the chromium

CONFIDENTIAL

TABLE 1. Composition and properties of electrolytic chromium deposited from a bath containing 250 g/l CrO_3 and 2.5 g/l SO_4.

Operating conditions			Deposit						
						Hardness (MVn average values) Cooled after heating to:			
Temp C	C.D.* (amp/dm²)	C.E.† (%)	Oxide content (% Cr_2O_3)	Contraction on heating (%)	As deposited	600 C	700 C	800 C	1,000 C
45	25	17	1.4	1.2	850	600	500	400	200
65	30	13	0.7	0.5	800	...	...	...	...
75	50	12	0.2	0.2	500	425‡	...	...	...
85	60	10	0.2	0.2	500	350	300	200	...
100	80	..	...	...	425	...	...	...	...
20§	8	40	4.3	1.8	925	...	...	...	...

* Current density.
† Cathode efficiency.
‡ Measured with Knoop Indentor.
§ From U. S. Bureau of Mines trivalent chromium bath (see Section 20.4.1).

bath. For example, for HC chromium, at 50 C, an initial current density of 1 amp/dm² was gradually increased to 20 amp/dm²; while for LC chromium at 85 C, the current density at the start was 15 amp/dm² and was increased to 80 amp/dm².

One present limitation of plating on stellite liners is that it is difficult to remove stellite uniformly by electropolishing. Until this is accomplished, it will be necessary to machine liners oversize to allow for the thickness of chromium to be deposited.

20.2.3 Applications to Gun Barrels

METHODS

Both types of chromium were applied experimentally to gun barrels, chiefly to the caliber .50, by the National Bureau of Standards for Division 1. These experiments gave direct information regarding the performance of the coatings in small arms.[84] Some similar experiments were carried out at Springfield Armory.[86,318]

In plating the interior of a cylinder such as a gun barrel, a concentric inside anode is used to obtain approximately uniform distribution of the deposit. Typical fittings used to center and insulate the anode and to bring current to it and the cathode (the barrel) are shown in Figures 3 and 4. The longitudinal distribution of the deposit is not usually uniform for the case where the only agitation is the liquid flow caused by upward pumping action of gas discharge, because it varies with the resistance of the anode and the surrounding solution as well as with other factors. By a suitable choice of the metal and the diameter of the anode it is possible to secure a wide range of distribution of deposits in a gun barrel of a given caliber.

Thus it has been found[390] that with a steel anode of a given diameter, for example 3/16 in. in a caliber .50 barrel, and with the anode connection at the top, the

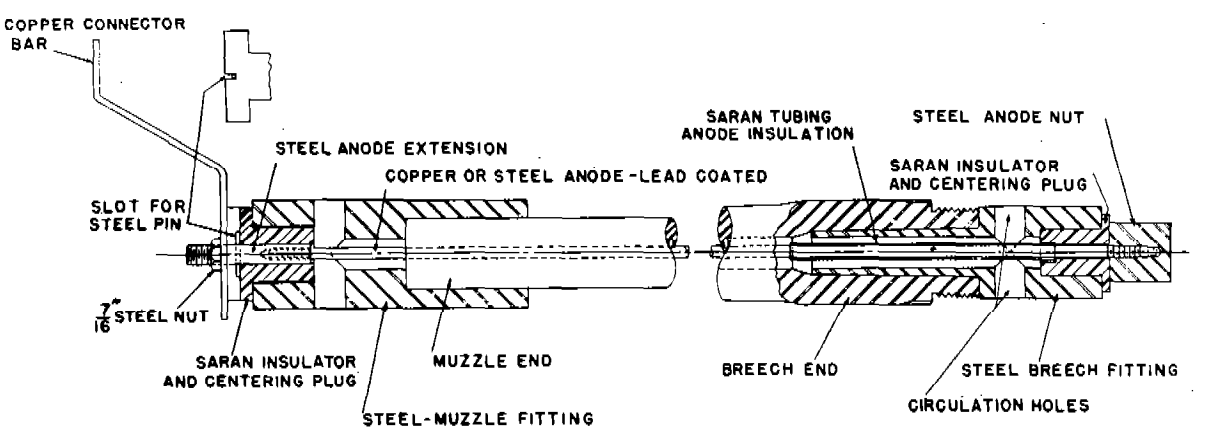


FIGURE 3. Fittings for electroplating caliber .50 aircraft machine gun barrel. (This figure has appeared as Figure 1 in NDRC Report A-412.)

deposit is thicker at the top than at the bottom. This behavior, caused by the high resistance of the steel anode, which reduces the current as it goes through the anode and thus lowers the current density and the thickness of the plate at the bottom, has been used to produce a tapered deposit and a desired "choke" near the muzzle of a caliber .50 aircraft machine-gun barrel. The advantages of the choked muzzle are discussed in Section 23.1.4.

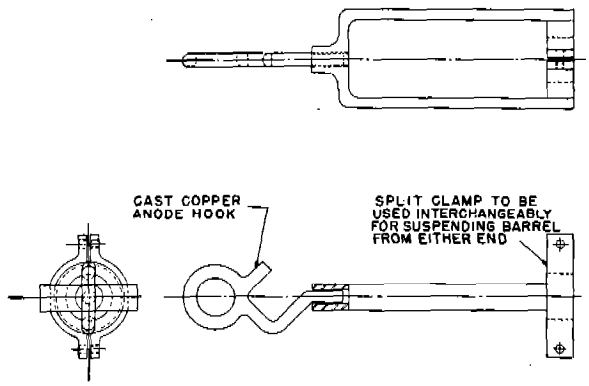


FIGURE 4. Rack for holding caliber .50 machine gun barrel during electroplating. (This figure has appeared as Figure 2 in NDRC Report A-412.)

With a copper anode, which has a lower resistance than the steel anode, the longitudinal distribution is more nearly uniform, and the lower end of the barrel may even receive a thicker deposit than the upper. There are two factors which account for the latter type of uneven distribution. The temperature of the solution within the barrel is slightly higher at the top and this reduces the current efficiency. The gas bubbles formed by the evolution of hydrogen and oxygen accumulate at the top and increase the resistance of the solution, thus reducing the current at this end of the barrel.

Both the steel and copper anodes are plated with lead, or preferably an alloy of lead with about 10% of tin, to prevent attack of the metal of the anode and to foster the reoxidation of trivalent chromium in the bath. At the cathode surface, some of the chromic acid (hexavalent chromium) is partially reduced and forms trivalent chromium, which in turn is reoxidized at the anode until some equilibrium concentration is reached.

The concentration of trivalent chromium affects the taper of the deposit and hence must be controlled. The cathode efficiency increases with an increase in trivalent chromium concentration in such a way that the increase in current efficiency at low current densities is greater than that at higher current densities. Therefore with a steel anode, which produces a lower current density at the bottom than at the top of the barrel, the presence of trivalent chromium results in a higher current efficiency and hence relatively higher plating rate at the bottom than at the top of the barrel.

The deposit taper, that is, the ratio of the thickness at the top to that at the bottom of the bore, therefore decreases with increase in trivalent chromium concentration. In the caliber .50 machine-gun barrel, plated with a $\frac{3}{16}$-in. steel anode, this ratio is approximately 3.0 when the trivalent chromium concentration is nearly zero, and is 1.5 when the trivalent chromium concentration is 15 g/l. The concentration of trivalent chromium can be reduced by electrolysis of the solution in a separate operation with large anodes at a low current density and with small dummy cathodes, preferably surrounded by a porous pot.

In most of the plating experiments at the National Bureau of Standards the gun barrel with the assembled anode and fittings was immersed in a tank containing the plating solution that was maintained at the specified temperature. Holes in the fittings permitted the circulation of the plating solution, induced by a rising stream of gas, consisting of oxygen from the anode and hydrogen from the cathode.

Much of the exploratory plating was done on short steel breech liners, subsequently inserted into the heavy caliber .50 barrels used in rapid-fire tests at the Geophysical Laboratory[81] at normal velocities and in other tests with the hypervelocity erosion-testing gun (Section 11.2.1) at the Franklin Institute.[76] The LC chromium gave approximately 23 per cent greater increase in the life of the barrel fired at normal velocities than did the HC chromium, but conversely, in the aircraft barrels, the HC was superior. This difference illustrates the variation in the nature and degree of erosion in barrels fired under different schedules or having different construction and operation.

The production of a tapered deposit by means of a steel anode as described above, led to a muzzle choke that greatly increased the accuracy life of the aircraft barrels as detailed in Chapter 23. The HC chromium prevented erosion at the muzzle and hence preserved the restricted diameter.

If more than 0.001 in. of chromium is to be applied, especially at the origin of rifling, it is necessary to remove sufficient steel to make room for the chromium. In production of new barrels for plating, this

might be accomplished by reaming and rifling to oversize diameters. Before plating barrels of standard dimensions steel was removed by "electropolishing" (see outline in Section 25.2.1). This process[c] was developed in recent years as a means of producing a bright surface on metals. It depends on the anodic solution of metal in a suitable electrolyte.[d]

The solution finally adopted for gun barrels consists of equal volumes of 96% sulfuric acid and 75% phosphoric acid. The polishing is conducted at 43 C (110 F) and an anodic current density of 27 amp/dm^2 (250 amp/ft^2). The barrel is made anodic, and a copper or steel rod, coated with lead-tin, is used as the cathode. The fittings are similar to those in Figures 1 and 2. In addition to serving as a "taking off tool," electropolishing may be beneficial in improving the surface condition of the steel and fostering good adhesion of the deposits. Electropolishing is a necessary step in the preparation of nitrided steel barrels, from which the outer brittle layer, approximately 0.001 in. thick, must be removed before plating in order to obtain good adhesion of the deposit.

Application to Caliber .50 Barrels

Nitrided Barrels. Firing tests of caliber .50 aircraft barrels that had been plated with chromium directly on gun steel showed that failure of the chromium resulted in part from the swaging of the underlying steel as described in Section 13.4.2. It was then decided to harden the bore surface by nitriding to give a better foundation for the chromium deposit. This resulted in a marked improvement that led to the adoption of the nitrided chromium plated aircraft barrel by the War Department, as described in Chapter 23.

On the basis of firing tests by the Geophysical Laboratory of several hundred nitrided barrels plated at the National Bureau of Standards, specifications were drawn up. These were employed in a pilot plant at the Doehler-Jarvis Corporation in Grand Rapids, Michigan, and minor changes were made before production of plated barrels, described in Chapter 25, was undertaken in a larger unit by that company. The bullet seat must be reamed out to 0.515 + 0.002 in. before nitriding to lead to the specified final dimension. If this is not done, constriction of the bullet seat will result from swaging during firing and will cause jamming of the bullets.

The exact methods and conditions for preparing and plating the barrels were not specified, but the following procedure was recommended and generally followed. (The steps are described in more detail in Section 25.2.1.)

1. Degrease.
2. Decopper (if necessary), rinse, dry.
3. Gauge.
4. Electropolish to remove 0.001 to 0.002 in. of metal with either end up.
5. Rinse.
6. Scrub with pumice and inhibited hydrochloric acid or with pumice and an alkaline cleaner.
7. Dry.
8. Oil (if to be stored).
9. Gauge.
10. Degrease.
11. Scrub with pumice and acid.
12. Rinse.
13. Dry with patch.
14. Etch anodically in chromic acid for 5 min.
15. Plate with chromium, with muzzle end up, using a 3/16-in. steel anode, at 50 C (122 F) and 20 amp/dm^2 (190 amp/ft^2), for the calculated time (about 4 hr).
16. Rinse.
17. Dry.
18. Gauge.
19. Oil for storage.

Stellite Liner Barrels. When it was realized, as described in Section 24.1.1, that aircraft barrels provided with a stellite liner and chromium plate beyond the liner would yield better service than the nitrided plated barrels, development of this "combination" barrel was undertaken and a specification was prepared based on plating and firing tests. The essential requirements were as given in Table 2.

Table 2. Specifications of finished dimensions for chromium plate in caliber .50, 36-in. barrel with 9-in. stellite liner.

Distance from muzzle (in.)	Diameter (in.)
0.5 or 1.5	0.4920 + 0.0045
10	0.4950 + 0.0035
15	0.4955 + 0.0035
23	0.4990 + 0.0020

Thickness of deposit at 23.5 in. from muzzle: 0.0017 ± 0.0007 in.

[c] An extensive bibliography on the subject in reference to types of electrolytes is listed in a paper by Zmeskal.[476]

[d] Valuable information was obtained informally from C. L. Faust of Battelle Memorial Institute.

Several methods were tried for plating liner-barrels. From the plating standpoint, deposition of chromium before liner insertion is preferable; but from the standpoint of production efficiency, plating after inserting the liner is better. The latter method proved difficult because the solutions tended to enter and be retained in the crack at the forward end of the liner and to cause etching of the liner. In the production plating of liner-barrels by the Doehler-Jarvis Corporation (Chapter 25), a dummy steel liner was inserted in the barrel, which was then electropolished and plated under the same conditions as full-length barrels. The dummy liner was counterbored at the forward end to avoid deposition of a sharp edge of chromium there. Further study is required to define the best method of plating liner-barrels.

Heavy Barrels. Only a small number of the 45-inch caliber .50 barrels was plated experimentally. Just as with the plated liners inserted in these barrels, a full-length deposit of LC chromium, about 0.006 in. thick at the origin, yielded the best results. It was not possible, however, to secure the desired longitudinally uniform deposit of LC chromium in these barrels by any variations in the anode size or composition.

Use of a moving anode, regularly employed in chromium plating large naval guns with HC chromium, yielded LC deposits with poor adhesion. Apparently the exposure of part of the bore to the chromic acid bath at the higher temperature caused excessive passivity of the steel so exposed.

The best LC deposits were obtained by "pump plating." With a well-conducting anode, such as of copper, silver, or aluminum, any taper caused by the anode resistance is negligible. Any reverse taper, caused by a difference in the bubble concentration and temperature at the two ends, is avoided by pumping the solution through the bore at a high rate of flow. This procedure reduces the difference in bubble concentration and temperature at the two ends and the higher pressure involved also reduces the bubble volume. The current efficiency is normal at a flow rate of 100 ft/min (30 m/min). By varying the flow rate, the longitudinal distribution of the deposit can be controlled to give either a straight or a choked bore.

To avoid passivating the steel by the hot chromic acid during the change from the 50 C etching solution to the 85 C plating bath, the bore was plated, after etching, with about 0.0002 inch of HC chromium, followed by the LC chromium without current interruption.

Miscellaneous Applications

Firing tests on a small number of caliber .30 barrels plated with HC chromium yielded results parallel to those with the caliber .50 aircraft barrels. A deposit about 0.0025 in. thick at the origin and tapered to effect a muzzle choke of about 0.006 in. in diameter produced a decided increase in life under a severe firing schedule.[81] A few experiments with pump-plating in caliber .30 barrels produced an LC deposit with satisfactory dimensions, but firing tests have not yet been made.

A number of caliber .60 barrels were plated, principally with HC chromium. Firing tests were most promising in barrels plated with from 0.005 to 0.010 in. of HC chromium for several inches from the breech and with only 0.001 to 0.002 in. of plate from there to the muzzle, which was not "choked" in these barrels. The life of this caliber .60 barrel is at least doubled by this type of deposit. More tests are planned, including barrels plated with LC chromium.

In one test of a 20-mm barrel plated with 0.01 in. of HC chromium, the barrel life was approximately doubled. The most favorable thickness and distribution of chromium for this gun barrel have not yet been defined.

Two hypervelocity 37-mm gun barrels, T47, described in Section 31.7, and the 37-mm gun barrel used for tests of the Fisa protector, described in Section 32.5, were plated at the Washington Naval Gun Factory with the cooperation of the National Bureau of Standards. Not enough data were obtained to warrant recommendations for the type or thickness of chromium.

Work done at Battelle Memorial Institute[271,272,276] on 37-mm barrels indicates that there is a continuous improvement in the performance of such barrels plated with HC chromium with increase in deposit thickness up to 0.010 in.

Parts of a 57/40-mm tapered-bore gun, a 4.7-in. recoilless mortar and some 75-mm recoilless rifles were plated at the National Bureau of Standards and tested by different agencies. In general the chromium coating was beneficial, but the results were not sufficiently numerous or consistent to warrant definite recommendations.

As previously noted, most of the plating heretofore applied to large guns was less than 0.001 in. thick. During the past few years several large guns were plated with up to 0.006 in. of HC chromium by the Washington Naval Gun Factory for experimental

firing by the Army Ordnance Department. In one test,[216] a plated 155-mm barrel showed excessive muzzle erosion, and the chromium made no significant improvement. The data on this single test are inconclusive.

While the work described in the foregoing paragraphs was being carried out in the United States, efforts were also being made in Great Britain to improve chromium electroplates for application to gun barrels.[380,385,386] Attention was concentrated especially on plating caliber .50 machine-gun barrels,[389,390,423] with results that compared favorably with those achieved by Division 1. German endeavors in this field did not result in much improvement.[306,391]

20.2.4 Duplex Coatings

The important part played by cracks in the failure of a chromium electroplate on the bore surface of a gun (Section 20.2.1) led to the suggestion that improved performance might be obtained by the use of an undercoat of some other, more ductile material. Duplex coatings consisting of chromium deposited on top of various materials were tested in the caliber .50 erosion-testing gun (Section 11.2.1).

Similar behavior was shown by 1-mil plates of copper and of nickel beneath a 1-mil chromium plate. The undercoat became plastic, whereupon the engraving stresses rubbed the chromium plate off the lands. The copper plate successfully sealed the bore surface from attack by the powder gases, whereas the nickel plate cracked and permitted the powder gases to reach the steel. A combination of a 1-mil plate of nickel on a 1-mil plate of copper under a 1-mil plate of chromium behaved in the same way as the nickel undercoat.

In experiments with the erosion-testing gun, described in Section 31.5, it was found that a thickness of chromium of at least 6 mils on the lands was necessary to prevent thermal alteration of the underlying gun steel.[77] A plate of this thickness would presumably reduce the softening of copper in a duplex plate. The trial of this combination had been considered at one time, but was not carried out because of other more urgent tests. It might be worthwhile to make a systematic study of the effect of varying the proportions of the copper and chromium layers in a duplex coating.

An even more promising type of undercoat for chromium plate, is one of cobalt or of a cobalt-tungsten alloy plate. Three tests were made of chromium-cobalt duplex coatings in the caliber .50 erosion-testing gun. There were 3 mils of chromium on 7 mils of cobalt. Excellent protection of the gun steel surface against powder gas erosion was reported,[76,77] but the cobalt undercoat was swaged, and eventually the plate was removed from the lands for a short distance ahead of the origin of rifling.

Cobalt-tungsten alloy plates of the sort described in Section 20.4.2 are considerably harder than pure cobalt. Therefore, duplex plates were prepared with a 7-mil undercoat of one of these alloys (containing 10% tungsten) under 2 mils of chromium. These duplex plates did not last as long as those containing pure cobalt undercoats; but this result should not be construed as final. The development of these alloy plates is still in a very early stage, and hence it is not certain that the particular ones tested represented the best results possible. There is still the hope that it may be possible to develop one of these alloy plates so that it will have just the right combination of properties to provide the perfect undercoat for chromium plate for the surface of a gun bore.

20.3 NICKEL AND COBALT PLATING

It is possible to electrodeposit nickel and cobalt that have a range of hardness from about 100 to 400 MVn. The nickel and cobalt which have been deposited in gun bores have approximately the same hardness as gun steel (280 to 320 MVn). Therefore no appreciable increase in resistance to abrasion or to swaging should be expected through the use of a surface layer of nickel or cobalt. This assumption is borne out for nickel by the experience of the British Armament Research Department,[367,380,386] which made extensive tests on the use of nickel deposition to salvage worn-out artillery barrels.[379,382,383] By carefully defined technic they secured good adhesion of heavy nickel deposits which, after having been machined and rifled, yielded about the same service as new gun-steel barrels.

Cobalt may be deposited from baths similar to those used for nickel plating. Very satisfactory deposits of cobalt were obtained from a simple solution containing 400 to 500 g/l of cobalt chloride, $CoCl_2 \cdot 6H_2O$. The pH was kept between 3 and 4.5. At room temperature, a current density of 2 to 5 amp/dm^2 was used.

Good adhesion of the cobalt coatings on steel was obtained by first etching the steel anodically in 70% H_2SO_4 for 2 min at 25 amp/dm^2. A "strike" coating

of cobalt was applied for 3 min at 20 amp/dm^2 in a solution containing about 100 g/l of cobalt chloride, kept at a *p*H of 0.5 to 0.7 with HCl. Plating was then conducted from the stronger solution above described.

Electroplated cobalt is usually harder than the electroplated nickel commonly used. Nickel plate softens considerably after annealing at 800 C whereas cobalt retains most of its initial hardness.

Cobalt possesses better erosion resistance than nickel. The firing tests described in Sections 16.3.1 and 16.4.9 have shown that nickel is likely to erode as a result of intergranular corrosion.

A liner was plated with 0.005 in. of cobalt and tested in the caliber .50 erosion-testing gun. (Section 11.2.1). The adherence of the cobalt was good, but its resistance to melting and to swaging was less than that of chromium.[76]

20.4 ALLOY DEPOSITION

A study of the plating of alloys is warranted because, as above noted, such metals as tungsten and molybdenum may be depositable only as alloys; moreover, by the co-deposition of two metals in controlled proportions, certain desired properties may be obtained. While it is possible to co-deposit three or possibly more metals, the definition and control of such processes are much more complicated than for binary alloys.

20.4.1 Chromium Alloys

Because chromium has been found to improve the performance of gun barrels, efforts were made to deposit alloys of chromium that might be less brittle and have less tendency to crack than pure chromium. It is possible to introduce such metals as iron, nickel and cobalt in the form of dichromates into the regular chromic acid baths.[460] It is difficult, however, to co-deposit more than a few tenths of 1 per cent of nickel or cobalt with the chromium and more than a few per cent of iron[461,462] under the conditions for production of either HC or LC chromium. The resultant deposits have essentially the same properties as those of pure chromium deposited under the same conditions.

Relatively soft chromium deposits at 85 C and 21 amp/dm^2 (200 amp/ft^2) were produced in England at first with a low cathode efficiency. The efficiency was then increased by adding 25 g/l of iron or 20 g/l of trivalent chromium to the bath. It is possible to add as much as 45 g/l of iron, but such baths are unstable. Besides increasing the cathode efficiency, addition of 25 g/l or more of iron widens the permissible sulfate range.[384,471]

Thick deposits from the iron-chromic acid baths at 85 C are sounder, that is, less likely to spall or crack, than similar deposits from the chromic acid bath. It is not possible to state whether these differences in behavior result directly from the small iron content of the deposit.

The slight difference in the properties of the plate from the alloy dichromate bath as compared with that from the chromic acid bath under similar conditions did not justify the use of such plating baths in the investigation at the National Bureau of Standards, since they are difficult to prepare and somewhat unstable at high concentrations. It was found that the current efficiency of the chromic acid bath can be more readily increased, particularly at low current densities, either by diluting the bath or by adding hydrofluoric acid instead of sulfuric acid. Neither of these baths has been used in the plating of gun barrels. If the physical and mechanical properties of the deposits from these baths prove to be as good as those from the regular chromium baths, they should be tried in gun barrels.

Alloys of chromium with as much as 1% of tungsten or molybdenum were obtained from chromic acid baths containing added tungstate or molybdate and fluorides or phosphates. The cathode efficiencies were very low.

Efforts were made to co-deposit other metals with chromium from baths containing chromic or chromous salts.[459] Recently the U.S. Bureau of Mines[469,522] developed a process of recovering chromium from its ores by electrolysis of a bath containing chromic and chromous salts and sodium sulfate at a *p*H of 1.8. An insoluble anode was surrounded by a diaphragm. Efficiencies as high as 40 per cent were obtained, but the chromium deposits were dark and brittle and contained as much as 4% of chromic oxide. (See Table 1.) It was not found possible to obtain any promising alloy deposits from baths of this type or from alkaline chromium baths.

Deposits consisting of cobalt with only 1% of chromium were obtained from baths containing 100 g/l of cobalt as sulfate, 50 g/l of chromium as chromic sulfate, and hydroxyacetic acid. The hardness of the deposit was somewhat higher than that of pure cobalt.

From a bath containing tungstate, a ternary

deposit with about 1% of chromium, 5% of tungsten, and the balance cobalt, was obtained. Further work is required to determine whether deposits of this type are practicable and useful for this purpose.

20.4.2 Alloys Containing Tungsten

Between 1930 and 1940 the Tungsten Electrodeposit Corporation patented acidified baths containing fluorides for the deposition of alloys of tungsten with nickel or other metals.[327] Other investigators at the University of Wisconsin published methods for depositing tungsten alloys from both acid and alkaline baths.[464,465,466,467,468] There are Russian publications on deposition of these alloys from ammoniacal baths.[472,473,474]

Experiments[84] at the National Bureau of Standards did not find it possible to produce dense coherent alloy deposits from any of the baths described above. It was then found possible to obtain satisfactory deposits from ammoniacal solutions containing salts of hydroxy-organic acids.

A typical bath for depositing alloys of cobalt and tungsten contains 25 g/l of cobalt (as sulfate or chloride), 10 g/l of tungsten (as sodium tungstate), 400 g/l of Rochelle salt (sodium potassium tartrate) and 50 g/l of ammonium chloride. The *p*H is adjusted with ammonium hydroxide to 8.5, and the bath is operated at 90 to 100 C and at 1 to 5 amp/dm^2.

Deposits containing from 10 to 35% of tungsten and the balance cobalt, nickel, or iron were obtained from baths of this type. Deposits up to 0.05 in. thick were smooth and strong, but brittle. The most promising alloys were the cobalt-tungsten ones, the hardness of which, as deposited, ranges from 500 to 700 MVn. The MVn of iron-tungsten alloys with 50% tungsten is from 700 to 1,000.

When these alloys are heated to 600 C for an hour and cooled, their hardness increases by as much as 100 MVn for cobalt-tungsten or nickel-tungsten, and 200 for iron-tungsten. Heating these alloys to 900 C or higher causes them to soften permanently. The cobalt-tungsten alloys have hot-hardness values that are higher than those of chromium, and unlike chromium, they retain their hardness on cooling.

It is difficult to obtain good adhesion of the cobalt-tungsten alloy directly to gun steel. The procedure finally adopted was to plate a thin layer of cobalt on the steel, treat the cobalt in the alloy bath with an alternating current, and then deposit the alloy. Deposits thus applied to liners had fairly good adherence but in firing tests they showed some flaking near the origin. On heating the plated liner to 900 or 1000 C, the adherence of the alloy was improved, and the deposit was rendered more ductile. This heating, however, tends to crack the alloy layer and to soften the gun steel.

Liners plated with nickel-tungsten and fired in the caliber .50 erosion-testing gun suffered severe gas erosion.[76,77] On the other hand, liners plated with cobalt-tungsten showed[76] better resistance to erosion than gun steel but were inferior to those plated with pure cobalt or chromium. The adhesion of the heat-treated alloy was better than that of chromium. There was less swaging of the lands with the cobalt-tungsten than with cobalt. Efforts are being made to obtain satisfactory adhesion of chromium to the cobalt-tungsten alloy, in order to make possible duplex plates of the sort described in Section 20.2.4.

Much further work, including possible modification of the gun steel, is required to realize the full possibilities for alloys of tungsten with cobalt or other metals. For example, it may be possible to produce by electroforming on a suitable mold, liners having an alloy surface and a body of another metal. Some exploratory trials gave promising results.[84]

20.4.3 Alloys Containing Molybdenum

Much less progress was made in the deposition of alloys of molybdenum. The most promising bath contains 1,000 g/l of potassium carbonate, 15 g/l of cobalt as sulfate or chloride, and 100 g/l of sodium molybdate. At a *p*H of 11, at 100 C and 1 to 5 amp/dm^2, deposits containing up to 35% of molybdenum are produced. They are as hard as the tungsten alloy deposits and harden on heating but are not as strong as the tungsten alloys.

20.5 CONCLUSIONS AND RECOMMENDATIONS

20.5.1 Chromium Deposits

The successful application of HC chromium to caliber .50 aircraft barrels, either previously nitrided (Chapter 23) or provided with a stellite liner (Chapter 24), illustrates the need for study of each type of weapon and condition of service. More experience is required in the plating and firing of different small-caliber guns, including their examination to determine the behavior of each coating at the breech and

muzzle, and the causes of failure. Such information may be valuable not alone in improving the performance of small arms, but also in indicating the most promising materials for artillery, on which the firing tests are necessarily more restricted. Such correlation depends on more complete data on the temperatures, pressures, and erosive conditions involved in each weapon. Such studies should include different types and thicknesses of chromium, applied by methods that may change the adherence, distribution or properties of the deposits.

20.5.2 Duplex Coatings

The use of composite metal coatings, for example, of cobalt or alloys followed by chromium, warrants further study.

20.5.3 Alloy Deposits

The studies thus far conducted at the National Bureau of Standards and elsewhere on the deposition of alloys of tungsten or molybdenum with iron, nickel, or cobalt, are exploratory and valuable in showing that such alloys can be deposited in a dense form and that they possess a wide variety of properties. Much more research is required to define and control favorable conditions for their application to gun bores. They are more likely to prove useful in large than in small guns, because, in the latter, liners of stellite or molybdenum can be inserted. Alloy liners may possibly be produced by electroforming.

20.5.4 Properties of Electrodeposits

Much intensive study is required on the properties of electrodeposited metals and alloys, including the hardness at room and elevated temperatures, and after having been heated; tensile strength, ductility, elastic properties, coefficient of expansion (including permanent expansion or contraction) and resistance to chemical attack by air, water, or powder gases. The existing data on well-known metals, such as chromium, nickel, and cobalt, are fragmentary and in some cases contradictory. Acquisition of more reliable data should lead to more successful applications of deposited metals and alloys for both military and industrial purposes.

20.5.5 Properties of Steel

Further studies on the properties of the steels used in gun barrels are necessary in order to permit the full possibilities of electrodeposited coatings or liners to be realized, as is brought out in Section 24.5. The composition and properties of the steel may affect the adhesion and performance of the coating and may determine what steps, such as heat treatment, may be used to improve the properties or adhesion of the coatings.

Chapter 21

VAPOR-PHASE PLATING OF MOLYBDENUM, TUNGSTEN, AND CHROMIUM[a]

By *Charlotte A. Marsh*[b]

21.1 INTRODUCTION

21.1.1 New Method of Plating Refractory Metals

MOLYBDENUM, TUNGSTEN, AND CHROMIUM have highly desirable erosion-resistant properties. This was demonstrated by tests described in Chapters 16, 17, and 18. The supply of these metals, which is limited in normal times, is especially short in war time because of other large demands of high priority. For this reason it was expedient to consider their application to gun-bore surfaces as thin plates. Moreover, massive molybdenum requires a large amount of mechanical working to provide a suitable liner material, necessitating the elaborate and expensive equipment described in Chapter 18; massive tungsten is virtually unworkable; and massive chromium is brittle, which was learned from the experiments described in Chapter 17.

Thin coats of metals are ordinarily applied by electroplating. Experiments in applying electroplates of these metals are described in Chapter 20. Chromium has proved very successful when applied to steel bore surfaces, but satisfactory electroplates of molybdenum and tungsten have not yet been prepared. Chromium electroplates, however, do not adhere to the surface of stellite or alloys of this type. These alloys, as stated in Chapter 19, have comparatively low melting points, hence their use as erosion resistant liners is somewhat limited by the temperature conditions to be met in firing. The application of a material of higher melting point, such as molybdenum or chromium, to stellite liners may extend their usefulness. This use necessitates the development of a method for applying adherent coatings of these metals to stellite.

It was thought both possible and practical to prepare adherent (to steel or stellite) thin plates of molybdenum, tungsten, and chromium by thermal decomposition of the vapors of their respective carbonyls. To this process, which appears to be novel, the descriptive phrases "vapor-phase plating" and "pyrolytic plating" have been applied. The former is suitable because the metal plate is deposited by decomposition of a vapor, not from solution; the latter because the vapor is decomposed by heat.

21.1.2 Carbonyl Chemistry[447, 448]

Certain of the so-called "heavy metals," notably iron, nickel, cobalt, tungsten, molybdenum, chromium, and the platinum metals, have the property of combining readily with carbon monoxide gas under appropriate conditions to form reasonably stable chemical compounds known as *carbonyls*. These have the general chemical formula $M(CO)_x$, where M is the metal and x is four or greater. The reaction between the metal and carbon monoxide takes place at an appreciable rate only under limited ranges of temperature and pressure, and these vary from metal to metal. Except for iron and nickel, these conditions are not readily obtained, and the other carbonyls are usually prepared by reaction between carbon monoxide and an appropriate compound of the metal.

The carbonyls, when once formed, are stable only within definite, limited ranges of temperature and pressure. When the temperature at a given pressure is raised beyond a specific point, the carbonyl decomposes to reform the metal and carbon monoxide. A secondary reaction may also occur in which carbon and carbon dioxide are formed from the monoxide. The carbon thus released may be deposited on an adjoining surface together with the metal resulting from the decomposition, or it may react with it to form one or more carbides. This secondary reaction is of considerable importance, as will be seen in due course. The amount of carbon or carbide formed may be varied by suitable alteration of the experimental conditions.

[a] This chapter has been based entirely on four Division 1 formal reports,[73,74,93,94] to which reference is made for further details.

[b] Geophysical Laboratory, Carnegie Institution of Washington. (Present address: U. S. Geological Survey, Washington, D.C.)

The formation and decomposition of nickel carbonyl is the basis of the well-known Mond process for the manufacture of pure nickel. The formation and decomposition of iron carbonyl[c] is employed on a laboratory scale for the preparation of small samples of highly pure iron for scientific purposes, and has lately been used for the preparation of pure iron in quantities of several pounds at a time for the manufacture of iron articles by powder metallurgy.

21.1.3 Summary of Recent Progress

The carbonyls of molybdenum, tungsten, and chromium have been known for some years. Surveys of the literature[73,93,94] revealed that they have only been prepared on a laboratory scale and that no attempts have been made hitherto to utilize either the metals or the carbonyls prepared by their decomposition. Improved methods for the preparation of molybdenum and chromium carbonyls have now been developed as described in Sections 21.2 and 21.5, respectively. The considerable work carried out on the vapor-phase plating of molybdenum is summarized in Section 21.3. Only a preliminary investigation on the preparation of tungsten carbonyl, the preparation of plates therefrom, and the properties of these plates has been made, since molybdenum is more readily available. The use of cobalt plates prepared by this method has not been taken up because of the short supply of cobalt, and its higher priority use as an essential constituent of stellite and similar alloys.

None of the plates prepared was satisfactory for the bore surface of a gun, because the high temperature produced during firing weakened the bond between the plate and the underlying material.

The hardness of the plates that are obtained by the method of vapor-phase plating that has been developed can be varied at will. Hence, with a little further investigation, they may have practical application for the hard-surfacing of metals for use where resistance to mechanical wear without severe mechanical shock is involved. If considerably thicker plates of good adherence can be prepared, there is reasonable prospect of success in obtaining resistance to high temperatures.

[c] A detailed study of the reaction between carbon monoxide and iron was carried out[19] preliminary to investigations of the possible importance of the formation of iron carbonyl in gun erosion.[62,63] This work is summarized in Section 14.3.

21.2 PREPARATION OF MOLYBDENUM CARBONYL[94]

21.2.1 Formation of Molybdenum Carbonyl

The method which was developed for the preparation of molybdenum carbonyl in amounts adequate for this program utilized the reaction of carbon monoxide with a reactive form of molybdenum at high pressures. The use of metallic molybdenum as such is not practical, for, no matter how finely divided the metal may be, it reacts too slowly with carbon monoxide. The reason for this is obscure, but is perhaps connected with the presence of a thin film of adsorbed oxygen, which effectively seals off the surface of the metal from reaction.

The reactive form of molybdenum necessary for the reaction with carbon monoxide was produced in the reaction vessel by the reduction of molybdenum pentachloride by a suitable reagent, such as metallic zinc, in the presence of a water-free solvent, such as ether. The two-step process for the formation of carbonyl may be represented by equations (1) and (2).

$$2MoCl_5 + 5Zn \rightarrow 2Mo\ (active) + 5ZnCl_2 \quad (1)$$

$$Mo\ (active) + 6CO \rightarrow Mo(CO)_6. \quad (2)$$

The mechanism of this process and the exact course of the formation of the carbonyl have been the subject of considerable discussion in the chemical literature, but the above reactions seem to fit the observed facts in as simple a way as possible.

21.2.2 Preparation of Anhydrous Molybdenum Chloride

Molybdenum chloride ($MoCl_5$), as was stated above, is one of the principal reagents in the preparation of the carbonyl. Because this reagent was not available in quantity, part of the investigation was perforce the working out of a method for the manufacture of this compound in pound lots or larger quantities.

In the past, anhydrous molybdenum pentachloride, the only stable known chloride of this element, has been prepared in gram quantities by the reaction of a slow current of dry chlorine with finely powdered molybdenum metal, molybdenum oxide (in this instance carbon tetrachloride vapor has sometimes been substituted in part for chlorine), or molybdenum sulfide. The chlorine, which is diluted with an inert gas, is passed over the powdered metal or com-

pound in a hard glass or quartz tube at elevated temperatures. The molybdenum pentachloride has then been removed from the reaction zone, partly by sublimation and partly by the gas stream, and preserved in sealed glass tubes, as it is readily oxidized by moist air.

A new method developed for the preparation of the pentachloride involves directing a jet of chlorine taken from a tank of the commercial gas upon the surface of powdered molybdenum metal. The reaction takes place readily without external heating, and the molybdenum pentachloride melts and can be drawn off through a valve as needed. In practice, the reaction vessel is equipped with an external heating device to sublime the pentachloride from any residual metal or impurities, and it is condensed in a second vessel. Ordinary commercial molybdenum metal powder gives pentachloride of ample purity. The yield is quantitative, and the properties of the product agree with those recorded in the literature.

An apparatus that produced molybdenum pentachloride at the rate of over 2 lb per hour is shown in Figure 1. On the basis of the experience gained in constructing and operating this apparatus, it should prove a simple engineering job to build a continuously operating commercial unit capable of producing molybdenum pentachloride of adequate purity for any purpose in amounts ranging from 10 to 100 lb per hour. However, on the basis of the work so far carried on, no estimate of the cost of molybdenum pentachloride when prepared in large quantities is possible.

21.2.3

Procedure for Producing Molybdenum Carbonyl

Preparation of Crude Product

Molybdenum carbonyl was formed by the reaction of carbon monoxide with the molybdenum resulting from the reduction of anhydrous molybdenum chloride in the presence of a water-free solvent. The preparation of the carbonyl was carried out at high pressure and with constant and effective agitation to provide prolonged contact with the gas and also to provide fresh surfaces for the reaction. After many changes in



Figure 1. Chloridizing apparatus used for improved method of preparing molybdenum pentachloride. Right to left: chlorine tank, safety flasks, asbestos-covered flask containing molybdenum, flasks for trapping fumes, container for pentachloride. (Figure 5 in NDRC Report A-422.)

CONFIDENTIAL

apparatus and operating conditions had been made, the production of purified molybdenum hexacarbonyl in lots of 1 lb or more, with a yield of over 85% of the theoretical, was successfully carried out. The rate of preparation was increased to over 2 lb per hour.

A forged steel autoclave, copper plated on the inside, of 1-gal capacity, shaken in a horizontal plane with a 6-in. stroke by a motor running at 180 rpm was used as a reaction vessel. The autoclave and the horizontal shaker are illustrated in Figure 2.

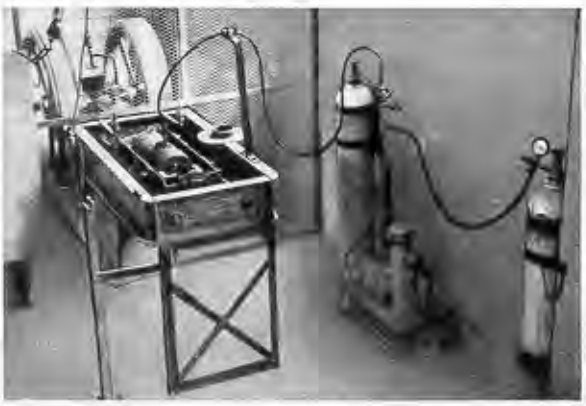


FIGURE 2. One-gallon autoclave in horizontal shaker. (Figure 8 in NDRC Report A-422.)

A discussion of the reagents and the conditions used in the preparation of the carbonyl follows.

The molybdenum pentachloride, the preparation of which was described in Section 21.2.2, was used in the form of irregular, broken lumps, about the size of lump sugar, of material which had been fused. Preliminary brief exposure of this material to the air seems to assist the reaction, probably by allowing excess chlorine to evaporate.

Anhydrous ether was found to be the best solvent. The zinc, in slight excess over the amount theoretically required, was added to the ether solution of the molybdenum pentachloride in the form of a powder fine enough to pass a 30-mesh screen. It was found advisable to add the zinc in one mass, wrapped in paper, so that the reaction would start slowly. If the zinc is added in larger pieces or is placed bare in the pressure vessel, the carbonyl first formed tends to coat its surface, and the reaction nearly stops. Zinc powder of a coarser grain requires a much longer time to complete the reaction than does the 30-mesh powder. Dispersing the zinc on glass wool before introducing it into the container reduces the tendency of the system to seal off the surface of the zinc, but makes it more difficult to distill the product. Aluminum powder, magnesium grains, copper filings, and hydrogen gas were also tried as possible reducing agents, but were less effective than zinc.

A pressure of carbon monoxide of about 700 psi seems to be the most effective. At pressures of 600 to 650 psi the rate of the reaction and hence the yield in a given time are considerably reduced. An increase in pressure to 800 psi seems to have no beneficial effect, but this point needs further study.

A special jacketed 5-gal capacity autoclave, copper plated on the inner surface, equipped with an automatic stirring device capable of running at high and variable speeds, and having charging and discharging vents at top and bottom, was built for further experimental production on a larger scale. It was thought advisable in this case to use a jacketed vessel so that external heating or cooling could be applied to increase or moderate the rates of the reactions and possibly to increase the yield while cutting down the time. In the production of small quantities of the carbonyl, the reactions generate enough heat to maintain a reasonable rate, but not enough to cut down the yield of product by the occurrence of side reactions.

Due to the termination of the program the 5-gal autoclave was not used. On the basis of the production of about 1½ lb of purified carbonyl per successful run of the 1-gal vessel, a production of 6 to 8 lb per run of 5 to 6 hr would be a reasonable expectation on this larger scale.

Removal of Ether

When the reaction was reasonably complete, as shown by the constancy of pressure of carbon monoxide on the gauge over a period of some minutes, the gas was shut off, the pressure vessel opened, and the contents removed. It was found that two phases were present: a liquid phase, consisting of an ether solution of molybdenum carbonyl, zinc chloride, and unreacted molybdenum chloride; and a solid, or more strictly a semisolid phase, which consisted of a mixture of all the above with small lumps of reduced molybdenum metal which had not reacted with the carbon monoxide. In later preparations, where the reaction had gone more nearly to completion, the separation into two phases took place much more slowly, and it was found simpler and quicker to distill the ether from the entire mass without separation.

The contents of the reaction vessel were transferred to a glass flask of suitable size, and the ether distilled

CONFIDENTIAL

off. Water was added dropwise from a funnel with a glass stopcock in the stem, to keep zinc chloride in solution and to permit the removal of the last traces of ether without overheating. If the water is added rapidly, the temperature rises quickly and molybdenum carbonyl is lost.

To prevent loss of carbonyl at the present stage, and also to dry the ether, a reflux condenser, consisting of a wide tube filled with lumps of anhydrous calcium chloride, was attached to the top of the still, and the virtually dry, carbonyl-free ether vapor passing from this was condensed by a water-cooled condenser. This recovered ether, after redistillation through an ordinary reflux condenser, was found to be as effective a solvent for molybdenum pentachloride as was fresh ether. About 85 to 90% of the ether can thus be recovered.

Steam Distillation

The molybdenum carbonyl was separated from the other constituents by steam distillation. In this manner it could be recovered pure, but not dry, without decomposition by overheating. The distillation rate was necessarily slow, about 250 g/hr, since molybdenum carbonyl begins to decompose at about 150 C. The apparatus, shown in Figure 3, was simple. Water was boiled in the flask at the right, the residue from the ether distillation was continuously introduced by a screw-feed device into the center flask, which was equipped with a powerful stirrer as the mass was sticky, and the carbonyl was condensed in the flask at the left, which was cooled in cracked ice. The flask at the extreme left was used to condense any carbonyl vapor that escaped the main condensing flask.

Drying and Sublimation

The molybdenum carbonyl, which carried 35 to 40% water after the steam distillation, had to be carefully and completely dried, before it could be used in the plating experiments described in Section 21.3. The effect of water on the stability of the carbonyl is not great, but the wet mass tended to become sticky and difficult to handle. After considerable experimentation, the following process, which gave a completely dry product with virtually no loss, was devised, using the apparatus shown in Figure 4.

The flask containing the moist carbonyl was inverted to drain off most of the water. It was then placed in an electrically heated oven and the closed end of a wide glass tube of suitable size was passed through the neck of the flask, the joint being made tight by a rubber stopper, through which also passed a smaller tube connected to an effective vacuum pump. The pump was then started, without heating the flask containing the carbonyl, and the remainder of the water was evaporated by the difference in pressure. The water was condensed in a chilled receiver placed between the carbonyl flask and the pump.

After the water had been thus pumped off, a dry receiver was inserted in the line and the carbonyl sublimed onto the walls of the large tube inserted in the flask. This was accomplished by heating the oven to 100-105 C while the pressure was kept at a few millimeters of mercury and the inside of the large



Figure 3. Apparatus for steam distillation of molybdenum carbonyl. (Figure 12 in NDRC Report A-422.)

tube was cooled by a stream of water. The receiver outside the oven was cooled in cracked ice and served as a trap to collect any carbonyl that passed the main condenser. Nearly 700 g of sublimed carbonyl was collected from one lot by this process.

The sublimed molybdenum carbonyl is preserved in glass-stoppered bottles sealed with paraffin wax to exclude all moisture. The product is apparently not sensitive to light, but it is probably well to keep it stored away from direct sunlight.

Properties of Sublimed Product

The properties of molybdenum hexacarbonyl thus prepared may be summarized as follows:

Formula: $Mo(CO)_6$
Molecular weight: 264
White crystalline solid
Specific gravity at 25 C: 1.96

CONFIDENTIAL

On heating in air at 1 atm pressure, decomposes at about 150 C without melting. Sublimes at lower temperatures with little decomposition.

Vapor pressure at 25 C: about 0.1 mm Hg.

Soluble in ethyl ether to the extent of about 2% by weight.

Insoluble in water and mineral acids.

Stable in the presence of water and acids up to about 150 C.

Decomposes in strongly basic solutions in the presence of the halogens.

Little is known as to the toxicity of molybdenum carbonyl. The more highly volatile, liquid or gaseous carbonyls of iron and nickel are extremely active poisons. Molybdenum hexacarbonyl vapor is reported to be relatively nonpoisonous in low concentrations, but this statement needs confirmation. Work on this point is reported to be in progress, but the results are not known to us. The solid appears to be noncorrosive to the skin, but in the present state of our knowledge, it should not be handled without gloves. There is always the possible risk of dermatitis if handled over an extended period. The substance is undoubtedly poisonous if swallowed but the dangerous and lethal doses are not known. It has been reported that an ether solution of molybdenum carbonyl may detonate on standing. There are many precautions to be taken with respect to the various reagents and products involved in the preparation of molybdenum carbonyl.

Summary and Recommendations

A generalized flow sheet for the production of molybdenum carbonyl by the process just described is given is Figure 5.

Much work remains to be done on the most effective means for introducing the reagents into the process and on the most suitable and effective apparatus for carrying out the reactions involved and for purifying the product. Some further experiments on the most effective conditions of temperature and pressure for carrying out the successive steps are required.

Apparatus has been designed and built for the production of molybdenum carbonyl in lots of 5 to 10 lb. Should the development of further applications for the plating of molybdenum by thermal decomposition of the vapor of its carbonyl warrant it, engineering studies leading to the preparation and purification of the carbonyl on a suitable scale should present no undue difficulties, although they may need to be extensive.

21.3 VAPOR-PHASE PLATING OF MOLYBDENUM[93]

21.3.1 General Procedure

Vapor-phase plating of molybdenum is the procedure whereby molybdenum is deposited on a hot surface by the thermal decomposition of molybdenum

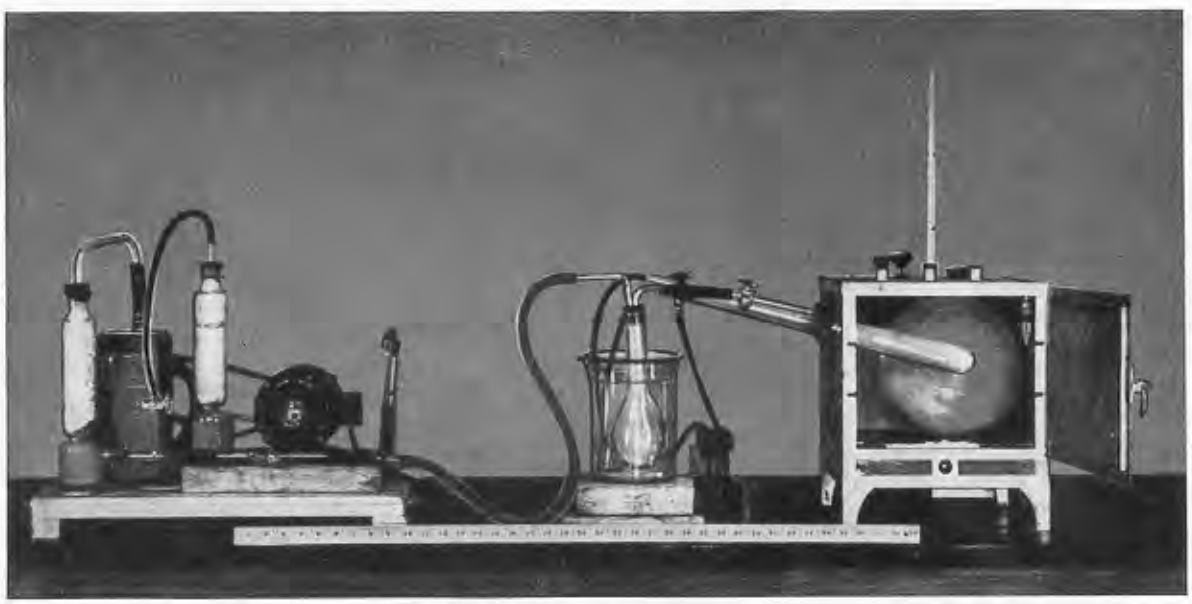


Figure 4. Apparatus for drying and sublimation of molybdenum carbonyl. (Figure 13 in NDRC Report A-422.)

CONFIDENTIAL

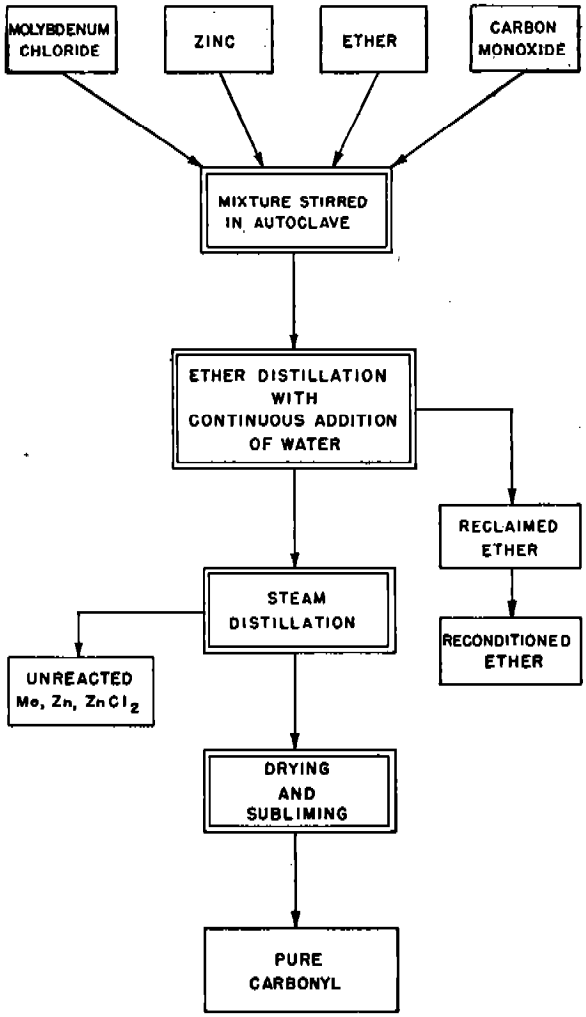


FIGURE 5. Flow-sheet for the production of molybdenum carbonyl. (Figure 14 in NDRC Report A-422.)

carbonyl. An apparatus was developed whereby very pure hydrogen at a low pressure passing over crystalline molybdenum carbonyl held at a constant temperature slightly above room temperature carries molybdenum carbonyl vapor into an electric furnace containing the object to be plated which has been uniformly heated to a predetermined temperature. The carbon monoxide formed by the reaction is removed by pumping at the end of the plating chamber.

Plating may be carried out in the absence of hydrogen; however, there are important advantages in the use of this gas before plating and as a constituent of the plating gas. Heating in dry hydrogen before plating can be effective in removing oxide films from the surfaces to be plated. As a constituent of the plating gas, hydrogen increases the flow of carbonyl with increase in partial pressure of the latter.

The addition of water to the plating gas is beneficial in some cases, as is described later. In order to add water to the hydrogen of the plating gas, only a very simple modification in the apparatus is necessary. A by-pass makes it possible to admit dry hydrogen instead of wet hydrogen to the carbonyl chamber.

A schematic diagram of the apparatus is shown in Figure 6. The small circles on this diagram represent vacuum-tight valves; those which are marked with the letter N are needle valves used for adjustment of the hydrogen flow. In all cases the hydrogen must be very carefully purified, preferably by diffusion through palladium. The carbonyl vapor is released from its chamber at a constant rate, which is determined by the temperature of the chamber and by the rate of flow of the dry or wet hydrogen.

The plating chamber contains means for supporting the specimen, for directing the plating gas to selected areas of the specimen if necessary, and for heating the specimen. The design of the chamber depends on the size and shape of the specimen to be plated. When a gun liner (Section 21.3.4) was being plated, it was held fixed and a water-cooled carbonyl injector moved uniformly within it so that no increase in concentration of the reaction products took place at any point. The plating chamber in this case was a quartz tube and the liner was heated by high-frequency induction. Injector and liner were mounted vertically. Chromel-alumel thermocouples attached to the liner enabled the operator to know its temperature, which had to be carefully controlled.

The pump, which is used to remove the products of the reaction, maintains pressure gradients in the carbonyl and plating chambers and also helps to regulate the pressure in the plating chamber. A McLeod gauge is used to read the pressure behind the injector or at the plating chamber. The reaction products, which are removed from the chamber by pumping, are collected in a liquid air trap, which is designated LA in Figure 6.

21.3.2 Properties of Molybdenum Plates

INTRODUCTION

The properties of a molybdenum plate, of course, depend on the plating conditions. The effects of varying the procedure were studied by means of test specimens. Only after the plates were found to have desirable properties was the procedure used for prac-

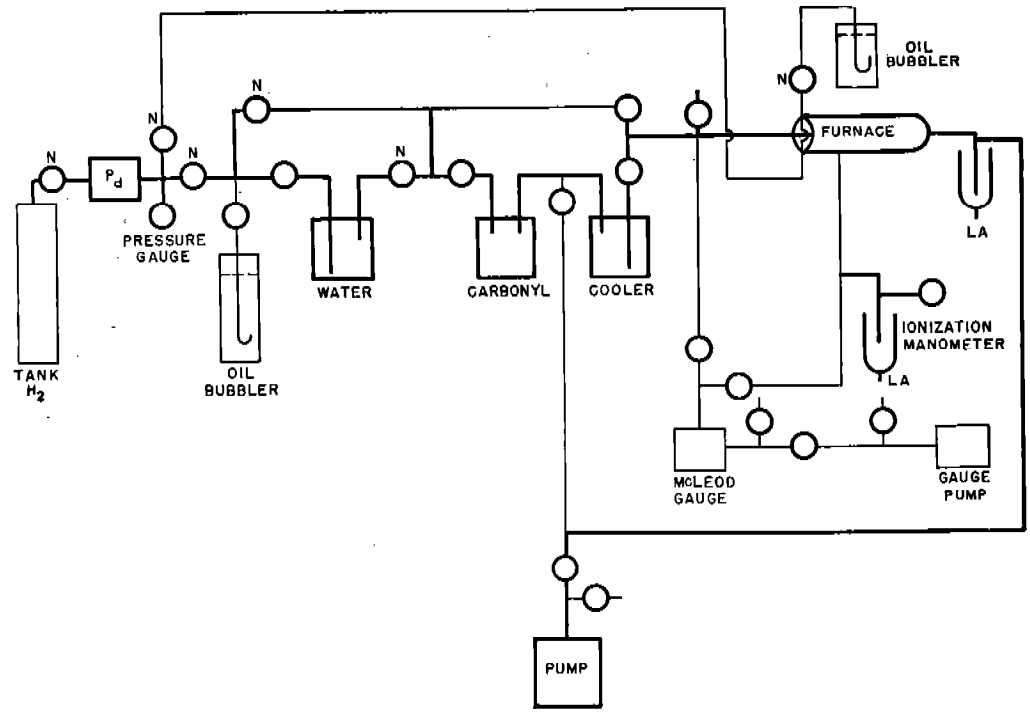


FIGURE 6. Schematic diagram of apparatus for vapor-phase plating of molybdenum. (Figure 5 in NDRC Report A-421.)

tical applications. Most of the experiments discussed here, therefore, are those that were carried out on test specimens.

In a consideration of the properties of a coating or plate deposited on a metal by the thermal decomposition of a carbonyl, distinction must be made between the properties of the coating itself and the nature of the metal-to-plate bond, as with any other coating. In this section only the former are considered. They include:

Chemical composition and crystal structure of the plate;

Mean crystal size and preferred orientation, if any;

Hardness;

Mechanical strength;

Texture, if plate is nonisotropic.

CHEMICAL COMPOSITION OF THE PLATE

The dominant reaction products formed by the decomposition of molybdenum carbonyl are molybdenum and carbon monoxide. As was stated in Section 21.1.2, there are secondary reactions which may take place depending on the plating conditions. The carbon monoxide may decompose to yield carbon and carbon dioxide. The carbon may react with the molybdenum to form a carbide or it may be deposited as interstitial carbon within the coating. The kind of plate produced thus depends on the factors which determine the course of the secondary reactions when the equilibrium is shifted.

Plating experiments in which carbonyl vapor was the only gas admitted to the plating chamber showed how the composition of the plate that was deposited on an iron disk varied with the temperature of the specimen and the pressure of the carbon monoxide from the decomposition of the molybdenum carbonyl. The results are summarized in Table 1. The nature of the plates was determined from x-ray diffraction patterns obtained from the plated surface. Both car-

TABLE 1. Nature of plates deposited from molybdenum carbonyl vapor.

Plating temperature(C)	Low carbon monoxide pressure*	High carbon monoxide pressure*
200–300	Cubic carbide	Cubic carbide
300–400	Cubic carbide	Cubic carbide
400–500	Molybdenum	Cubic carbide
500–800	Molybdenum	Hexagonal carbide

* The pressure range from 0 to about 0.2 mm is described as "low carbon monoxide pressure," and the range from about 0.2 to about 10 mm as "high carbon monoxide pressure."

bides have the formula Mo_2C. It was necessary to determine the empirical formula in the case of the cubic carbide by chemical analyses, for this carbide of molybdenum had not previously been reported. Results of other experiments show that in all cases where any plate at all is deposited, the carbon monoxide enters into the reaction to some extent; that is, all plates carry either some carbide of molybdenum or some interstitial carbon deposited as such in the plate.

The addition of hydrogen to the plating gas greatly assists in reducing oxide coatings on the metal, with a resultant tendency to strengthen the bond. The addition of hydrogen does not tend to lower the carbon content of the plate unless the ratio of hydrogen to carbon monoxide is very large, as is shown in Table 2. The geometry and the temperature of the plating chamber have more effect in this respect.

TABLE 2. Plating conditions at the boundary between molybdenum metal and cubic molybdenum carbide, hydrogen present.

Plating temperature (C)	Partial pressure H_2 (mm)	Partial pressure CO (mm)	Plate formed
425	0.128	0.080	Cubic carbide
400	0.180	0.054	Cubic carbide
325	0.950	0.026	Molybdenum

At high temperatures and at high pressures of residual carbon monoxide and of hydrogen, the mixture of molybdenum and molybdenum carbide forms an unattached, very fine, powdery layer in the chamber, due to decomposition of molybdenum carbonyl in the gas phase. This tendency sets an upper limit to plating rates. By a suitable adjustment of conditions almost any mixture from 100% metallic molybdenum to 100% hexagonal molybdenum carbide can be produced.

If the hydrogen is mixed with water vapor before being passed into the system, lower carbon contents of the plates can be obtained, and the plating rate greatly increased. This effect cannot be obtained by admitting moist air into the system, as oxidation takes place at once, and the plate consists largely of unadherent molybdenum oxide.

Various modifications of the "normal" plating procedure, i.e., molybdenum carbonyl vaporized in a stream of dry or wet hydrogen, were tried. The effect of adding carbon dioxide to the plating gas to decrease the formation of carbon by shifting the equilibrium $2CO \rightleftharpoons C + CO_2$, seems to be very small at 500 C, above which temperature the quality of the plate begins to fall off.

Hydrogen sulfide decreases the formation of carbon more effectively than does hydrogen, at low temperatures, but the adherence of the plate and the quality of the bond suffer greatly. All traces of hydrogen sulfide must be swept most carefully out of the apparatus before a subsequent hydrogen reduction of the metal surface. At low concentrations of hydrogen sulfide (pressures of 0.006–0.0002 mm) the plates formed are of molybdenum metal. When this gas is added in large excess, plates of molybdenum sulfide, MoS_2, are formed. These appear to be adherent, but are, of course, very soft. Molybdenum sulfide in nature is about as soft as natural graphite.

The addition of air plus excess oxygen to pure carbonyl in the correct proportions results in a thin, brittle, adherent plate of molybdenum oxide, MoO_2. Thick deposits of this type cannot be produced, for large amounts of air produce a nonadherent coating.

PHYSICAL CHARACTERISTICS OF THE PLATES

Crystallographic Orientation. Where any degree of adherence is obtained between plate and metal, the plate consists of an interlocking mass of oriented molybdenum crystals. The exact crystallographic orientation seems to vary with the chemical characteristics of the plate and with the plating conditions. In general the softer the plate, the larger and more brilliant are the crystals. Figure 7 shows the large, brilliant crystals typical of a soft plate. The preferred direction of crystal growth appears to be, in nearly all cases, normal to the surface of deposition. This is particularly true when plates of considerable thickness are formed. The tendency towards columnar structure, illustrated in Figure 8, is less in plates with very small individual crystals, which can apparently only be obtained where there is either considerable interstitial carbon but no carbide, or in those plates containing no molybdenum metal but only carbide plus excess carbon.

Hardness. The hardness of the molybdenum plates increases with the carbon content, whether it is present as carbide or as interstitial carbon. Brittleness of the harder plates, on the other hand, increases with an increase in the proportion of carbide. When a hard, but not brittle, plate is desired, therefore, plating conditions should be such that carbon is deposited interstitially and not as carbide. When no carbide is present, the hardness increases with decreasing crystal

TABLE 3. Hardness of certain molybdenum plates.

Plating temperature (C)	Vickers hardness	Percentage composition: Cubic carbide	Percentage composition: Metal	Notes
380	1460	100	0	Large oriented crystals
410	1300	85	15	Large oriented crystals
410	1550	15	85	.....
450	1560	0	100	Very small crystals
540	940	0	100	Small crystals
475	1550	...	...	As plated
475	880	...	...	After 1 hr at 775 C in wet H_2
475	880	...	...	After 1 hr more at 750 C in wet H_2

(same plate)

size, as shown in Table 3, as well as with increasing carbon content. There seems to be no doubt that the presence of interstitial carbon is the cause of both the small crystal size and the hardness.

Below 500 C the use of wet hydrogen has little effect on the hardness; at higher temperatures an increase in water content of the plating gas lowers the hardness considerably because the carbon content of the plate is lowered. The presence of small amounts of water in the plating gas above 500 C shifts the reaction for the formation of carbon from carbon monoxide in the direction of the latter. Removal of precipitated carbon takes place in accordance with the shift in equilibrium when plates are softened by annealing at high temperatures in wet hydrogen as shown in Table 3.

Annealing at high temperatures in dry hydrogen also softens molybdenum plates. A plate with high carbide content, however, is not as effectively softened as one with a low carbide content. It is possible to prepare plates as soft as 200 Vickers by plating in wet hydrogen at 600 C and then giving the plate a high-temperature anneal.

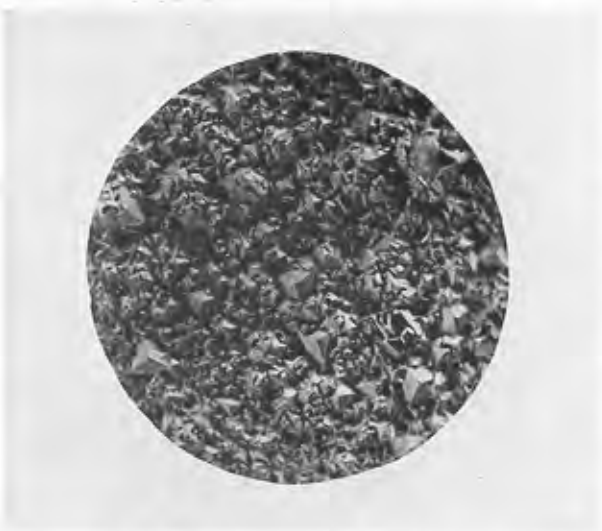


FIGURE 7. Photomicrograph of molybdenum plate consisting of highly oriented crystals showing well developed (100) faces. The (111) planes are parallel to the general surface. (*375X.*) (Figure 8 in NDRC Report A-421.)

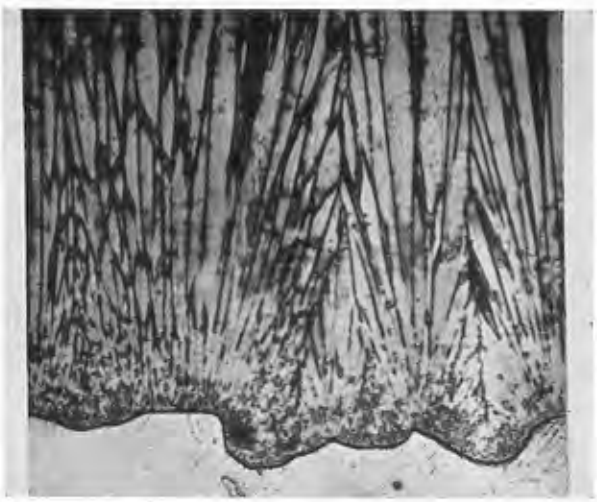


FIGURE 8. Photomicrograph of cross section of a 5-mil molybdenum plate showing large crystals and well-developed columnar structure. (*500X.*) (Figure 9 in NDRC Report A-421.)

21.3.3

Plate-to-Metal Bond

INTRODUCTION

The strength of the bond between metal and plate is especially important in the case of these pyrolytic plates, since the coefficients of expansion of the metals concerned differ widely (steel about 13×10^{-6}; molybdenum, 5.5×10^{-6}; tungsten, 4.5×10^{-6}). Various expedients have been tried to obtain a firm bond, without complete success, but for devices where severe mechanical shock and thermal shock are absent, or are not present simultaneously, the results of experiments to date appear promising.

In general, a good bond requires a metal surface that is perfectly clean, especially free from oxide. The surface must be kept clean until it is adequately protected by plate. For small surfaces, cleaning with very pure abrasive under absolute alcohol can be

CONFIDENTIAL

used, but the best general method appears to be the exposure of the surface to a stream of hydrogen gas at high temperatures in the plating chamber before passing in the plating gas.

The temperature and length of exposure needed depend primarily on the ease of reducibility of the oxide coating. Thus alloy steels and stellite require longer cleaning times and higher temperatures than do pure iron or copper. In some cases it becomes necessary to heat the steel surface to temperatures which are above the transition point for periods that are long enough to change the structure and properties of an underlying layer of measurable thickness, thus making it necessary to heat-treat the article after plating. Stellite surfaces need to be heated to 1000–1100 C for ½ hr for complete deoxidation.

Formation of Good Bonds

The best procedure to give an adequate bond involves a preliminary cleaning operation, followed by hydrogen reduction, after which the plating is started at a lower (but still fairly high) temperature and at a low rate. Conditions to be chosen vary with the chemical nature of the articles to be plated and their geometry.

Testing Bonds

In order to save the time and expense required for full "use" tests of the strength of the plate-to-metal bond, various laboratory tests were developed. A very poor bond fails by spalling when cold, that is, by separating from the underlying metal in flakes as the result of the strains set up on cooling to room temperature. Bonds that withstand this simple test sometimes fail when the article is slightly bent or gently hammered. Failure usually takes place first at a sharp edge.

A test was developed especially for use on specimens prepared for gun barrel liners. In this test a ring ½ in. in inside diameter and ½ in. long, with lands and grooves on the inner surface, was crushed in a compression-type testing machine. It was possible to plate such rings so that the bond would withstand 20 per cent to 30 per cent of axial compression without failure. As the investigation progressed, plates that could withstand 20 per cent axial compression would be regularly prepared, and only articles prepared by techniques that passed this test were subjected to use tests.

A quantitative shear test, using a precision shearing tool actuated by a measured weight attached to a lever arm beyond the tool, and so arranged that the tool always assumed the same angle of shear, was also developed. This device indicated the average value of the strength of the plate perpendicular to the bond (best plates as shown by crushing test) to be 100,000 psi; of the bond, 54,000 psi; and of the hardened and heat-treated steel ring, 87,000 psi.

Effect of Heat Treatment

In the course of these experiments it was shown that heat treating subsequent to plating injures the bond, as evidenced by the severe spalling shown in Figure 9. The damage to the bond was apparently in direct ratio to the length of time of the subsequent heating.

Both heat treating and crushing appear to convert interstitial carbon to the hexagonal carbide, Mo_2C. Furthermore these treatments appear to form a diffusion layer of the carbide at the bond interface. As molybdenum carbide is known to be brittle, this would account for the failure. This diffusion layer is also formed when the use to which an article is put subjects it to similar conditions. It has never shown up in photomicrographs taken of specimens in the "as-plated" condition. Experiments show that 800 C is the maximum temperature that a plate-to-steel bond can safely stand, and about 950 C is the safe maximum for a plate-to-stellite bond.

Other Studies of the Bond

Attempts were made to improve the bond by altering the surface layer of a steel article, and also by applying electroplates of various metals to the steel or stellite surface before the pyrolytic plating. Decarburizing a steel surface to a depth of 30 mils, either with or without subsequent nitriding, had no effect. Electroplating steel specimens with copper, gold, gold on cobalt, gold on nickel, chromium on cobalt, platinum bright on nickel, and palladium on cobalt, did not improve the resistance of the bond to heat treatment at 900 C.

The greatest improvement was shown by molybdenum coatings that were plated on steel specimens which had previously been plated with nickel or with platinum on nickel. However, the improvement shown on flat specimens was not repeated when rifled tube sections were electroplated thus. It may be noted



FIGURE 9. Crushed halves of a molybdenum-plated steel ring. The upper half was crushed 37 per cent without spalling or cracking of the plate. The lower half was heated for 30 minutes at 900 C after plating and was then crushed 12 per cent, which resulted in very severe spalling of the plate. (Magnified 4X.) (Figure 12 in NDRC Report A-421.)

that it is difficult to obtain satisfactory electroplates on such a shape. No other reason for this difficulty is apparent. On stellite surfaces, an undercoat of electroplated nickel gave improvement in resistance to a heat treatment at 900 C, but failed after heating for 1 min at 1100 C.

21.3.4 Application to Gun Liners

By far the greatest amount of time spent on the experimental plating program, after the fundamentals had been worked out, was devoted to the problem of molybdenum-plating short liners of steel and stellite for tests in caliber .50 gun barrels. Many liners were plated and 42 were fired, some in a caliber .50 aircraft barrel and others in the caliber .50 erosion-testing gun. The use of these guns for tests of gun liners is described in Sections 11.2.2 and 11.2.1, respectively.

Plating a bore of such small diameter is a more difficult job than in the case of a larger one, partly due to the greater impedance of the gas flow by walls and partly due to the difficulties of building a "plating-head" or injector that will function in a small tube. For the liners used, the maximum plating rate at which good adherence could be obtained was about 0.18 mil/hr. Calculations indicate that increasing the pumping speed would not increase this rate appreciably, as it appears to be about 75 per cent of the rate possible with a pump of infinite capacity.

Electrolytic polishing of the liner bore under carefully controlled conditions gave a satisfactory surface for plating. This etching process was followed by preliminary reduction of the surface in hydrogen; preliminary heat treatment in hydrogen, to be sure that pure hydrogen was the last thing in contact with the metal before plating; and the application of the first, or bond, layer of plate at a lower rate than for the balance of the plating.

The best performance given by a molybdenum-plated stellite liner fired in the erosion-testing gun was that of a rifled liner with an 8-mil thick, soft-type plate.[76] Wet hydrogen was added to the plating gas to yield this type of plate. This liner was fired 240 rounds at a velocity of about 3,650 fps, a pressure of 58,200 psi, and a rate of 4 to 6 rounds per minute. Ball bullets were used with double-base powder containing 20% nitroglycerin. With IMR powder under approximately the same hypervelocity conditions, the same maximum performance was obtained. The best performance for a steel liner under the hypervelocity conditions noted above was 230 rounds with IMR powder.

In all cases failure was due to spalling of the plate. By far the greatest amount of spalling occurred at

CONFIDENTIAL

the land edges, where the mechanical forces were greatest. Areas where the plate remained intact showed virtually no scoring or powder gas erosion. The facts that failure occurred under hypervelocity conditions at about the same number of rounds for both double-base and single-base powder and that spalling was greatest on land edges indicate that failure was due to mechanical rather than to chemical conditions. From knowledge of the chemical behavior of molybdenum and from the experience with massive molybdenum liners, discussed in Section 18.6, this was to be expected.

There seem to be two dominant causes for the failure of the plates.[d] First, the maximum possible thickness for adherent plates is still not thick enough to keep the bond from being weakened by the heat developed, the bond becoming brittle as the result of the formation of a diffusion layer during firing. Second, the plate tends to split between the parallel-oriented, columnar crystals and thus leaves the basic metal open to attack by the powder gas. The cracks tend to pass down into a steel liner, and pieces of steel "chunk" out. When the hot gases from double-base powder reach a stellite liner, melting starts at once so that flakes of plate are undermined and detached from the surface. Also, the hot powder gases can react with the exposed surface of a steel liner to yield brittle products, described in Chapter 12, which are removed, together with molybdenum plate, by the mechanical action of the projectile. When once the plate fails at a few spots, the action becomes cumulative. The photomicrographic evidence for the cause of the failure of the plate-to-steel bond seems a little clearer than does the evidence of failure for the plate-to-stellite bond.

The effort to make a satisfactory plated gun liner by using a thicker plate had two other difficulties. One was that the plating time became inordinately large. The other was that the rifling lost its definition when the plate was thicker than 10 mils in a caliber .50 liner having rifling 10 mils deep. Some attention was given to the possibility of plating a smooth-bore liner and rifling it after plating. This procedure would have required a softer plate that could subsequently be hardened. Reconnaissance experiments to produce such a plate were unsuccessful.

In summary, then, it may be pointed out that the requirements for a molybdenum plate to be applied to gun liners by the vapor-phase process are as follows: First, a type of plate that is soft enough when deposited so it can be rifled by machining, and then can be hardened by heat treatment or in some other way; second, a type of plate that will have a non-oriented crystallographic structure; and third, a plating rate of at least one mil per hour, so that a plate at least 15 mils thick can be deposited in a reasonable time.

[d] Examinations of the fired liners were carried out at several different places.[76,77,93]

21.3.5 Other Applications

Rocket Nozzles

Rocket nozzles are subject to powder-gas erosion but not to mechanical shock. Since molybdenum has superior resistance to attack by powder gases and, as liners, fails in guns only because of mechanical shock, it was thought worth while to plate rocket nozzles with molybdenum. Several copper and steel nozzles of various designs were plated by the pyrolytic method.[e]

A special plating apparatus had to be designed and built, since the nozzles had tapering orifices and hence the "plater" designed for cylindrical gun liners would not give plates of the desired thicknesses. Plating conditions were worked out, and the nozzles thus plated stood up, in most cases, to the laboratory tests previously described.

On firing, where the duration of a single blast is up to 11 sec and the flame temperature of the powder is 3000 K, the nozzles failed at the metal-to-plate bond. The plate was presumably not thick enough to protect the underlying copper from melting or the underlying steel from being heated above its transition point; in addition to this effect, the formation of a brittle diffusion layer probably occurred during the long-continued heat treatment. The high heat transfer of molybdenum is presumably partly to blame. If much thicker plates could be made adherent, a greater degree of success might be expected.

Recoilless Gun Blocks

Some recoilless gun adjustment blocks were plated with molybdenum.[f] The plates in all cases spalled along the leading edge after about 20 rounds. This

[e] This work was done at the request of the Allegany Ballistics Laboratory of Section H of Division 3, NDRC, and of the Explosives Research Laboratory of Division 8, NDRC.

[f] This work was done at the request of Frankford Arsenal.

was not considered to be satisfactory performance. Heat transfer, accelerated at the leading edge, was the probable cause of failure. A softer and thicker plate might give better performance.

Oxygen Compressor Cylinders[g]

Certain types of oxygen compressor cylinders have to work dry, and the wear of the cylinder against the carbon piston ring is serious. Under the conditions of use it is the friction between the carbon ring and the coating on the inside of the cylinder, rather than the wear resistance of the coating, that is being tested. Previous tests had shown that hard chromium electroplate gave the best performance. A rather soft molybdenum plate lasted 40 hr before wear of the carbon ring became serious. The rate of wear against the molybdenum plate was only about 8 per cent of that against the hard chromium electroplate. No other types of molybdenum pyrolytic plates were tried, but this appears to be a promising field of application of such plates.

Magnetron Anodes

Certain electronic devices, such as magnetron anodes, dissipate large amounts of heat per unit area, the amount increasing with the power radiated. The size of such devices is usually fixed; thus if heat dissipation can be increased while electrical conductivity can be maintained, an increase in power radiated can be obtained. Because of the high rate of heat transfer of molybdenum, it was decided to try the effect of a soft, pure metal plate on the inside of a copper ring which is a portion of the copper anode. It was found that a power increase of at least four times over that possible with an unplated anode took place. The plate remained intact.

Die Surfaces

Another application of great promise is to plate the surface of dies that have to stand hard wear, but not severe shock. A 2-mil molybdenum-molybdenum carbide plate, which probably had a hardness above 1200 Vickers, was applied to a die which consisted of a rod at one end of which was a disk for impressing a convolute in the grid frame of a vacuum tube, the frame being made of molybdenum and tungsten wires. After this die had been used for 50 formings it showed no appreciable signs of scoring. The ordinary die shows serious deterioration after 30 formings and requires refinishing after 100. The test was being continued in 1946 and it was then estimated that the total useful life of the plated die would be many-fold that of the ordinary type.

Another die with a complicated surface, used for drawing copper tubing for coaxial cable, was given a similar plate. The test of this die was still incomplete in 1946, but its performance up to then was much better than that of a nonplated steel die.

Molybdenum Sulfide Plates as Semiconductors

Molybdenum sulfide plates, which are mentioned in Section 21.3.2, appear to present useful possibilities as semiconductors. Only preliminary experiments on such plates were made.

21.3.6 Conclusions and Recommendations

It appears that the fields of use for pyrolytic plates of molybdenum and molybdenum carbide that will most probably repay further investigation are those where resistance to friction or wear, without mechanical shock, is involved. If considerably thicker plates of good adherence can be prepared, there is reasonable prospect of success in obtaining resistance to high temperatures. Such plates would have to be thick enough to protect the underlying metal from melting and thermal transformation. The columnar nature of plates so far prepared increases their lack of resistance to the combination of thermal and mechanical shock. Further research may make it practicable to prepare plates having an unoriented structure, or ones oriented in such a way as to resist the forces that have up to now caused failure.

Inasmuch as a thorough trial had been made of the conceivable ways of maintaining the strength of the bond during firing, it was concluded in the summer of 1945 that the pyrolytic plating process as then developed was not suitable for plating gun liners with molybdenum. Furthermore, the liners of massive molybdenum, described in Chapter 18, had by that time lasted over 2,000 rounds in similar tests. The difficulty of finding a way to match this result by a liner plated with molybdenum by the pyrolytic plating process seemed so great as to make further investigation unwarranted.

[g] This application was tried at the request of Division 11, NDRC, and the tests of the plates were carried out by a Division 11 contractor.

Further study of the present type of pyrolytic plate should not, however, be dropped. In addition to extended tests of the more successful applications, further research should be conducted on means to increase the plating rate and on methods to increase the strength of the plate-to-metal bond, and efforts should be made to define more closely the conditions for preparing a plate of a given hardness, chemical composition, crystal size, or other variable.

21.4 VAPOR-PHASE PLATING OF TUNGSTEN[93]

21.4.1 Preparation and Properties of Tungsten Carbonyl

For reasons stated in Section 21.1.3, the greater part of the efforts on preparing pyrolytic plates for gun bores and other purposes was carried out with molybdenum carbonyl. Consequently, no detailed investigation was made of processes for the large-scale production of tungsten carbonyl or of the raw materials from which to make it. Standard laboratory apparatus and methods were used to prepare an amount of tungsten hexacarbonyl that was sufficient for the experiments that were carried out.

Anhydrous tungsten chloride is obtainable in commerce in quantities adequate for use as a starting material for the production of tungsten hexacarbonyl on a small scale. If it is needed in larger amounts, it can be prepared by the same procedure and with the same type of apparatus, with only minor modifications, as was used for the production of the molybdenum compound (Section 21.2.2).

Tungsten hexacarbonyl is prepared on a laboratory scale in the same fashion as is molybdenum hexacarbonyl described in Section 21.2.3. Tungsten hexachloride is reduced to active tungsten by metallic zinc in an ether suspension, and at the same time the carbonyl is formed by reaction with carbon monoxide under pressure. Upon completion of the reaction, the ether is removed by distillation, and the tungsten carbonyl is removed from the other substances by steam distillation and finally purified by sublimation. No studies have been made to determine the most favorable conditions for obtaining a high yield, but, should it be desired to prepare this compound in amounts larger than 100 g at a time, studies such as those described in Section 21.2.3 concerning the preparation of molybdenum carbonyl should be made.

The properties of tungsten hexacarbonyl are virtually the same as those of the corresponding molybdenum compound, except that its vapor pressure at a given temperature is about one-fifth that of molybdenum carbonyl. Thus at 28.1 C the vapor pressures are 0.037 and 0.156 mm, respectively, and at 35.2 C they are 0.076 and 0.302 mm. The stability of tungsten hexacarbonyl appears to be the same as that of molybdenum hexacarbonyl. The toxicity of its vapor is presumably the same but the risk of handling it a little less because of its slightly lower volatility.

21.4.2 Properties of Tungsten Plates

In general, the investigations on the preparation of tungsten plates by the pyrolytic, or vapor-phase, process stopped at the preliminary stage, since molybdenum plates seemed to show more promise. Tests on improving the bond, on plating tungsten over an intermediate plate of another metal, and on the shear and crushing strength of tungsten plates were not made.

The same apparatus was used as for the vapor-phase plating of molybdenum, as described in Section 21.3.1. When tungsten carbonyl vapor without dry or wet hydrogen is introduced into the plating chamber, the composition of the plate varies as shown in Table 4. It seems to be easier to prepare plates of pure tungsten than of pure molybdenum. The formation of the hexagonal tungsten carbide, W_2C, was never observed in these plating experiments. Although no carbon determinations were made, the cubic compound is considered to be W_2C by analogy with the cubic phase of Mo_2C that was discussed in Section 21.3.2.

TABLE 4. Nature of plates deposited from tungsten carbonyl vapor.

Plating temperature (C)	Low carbon monoxide pressure	High carbon monoxide pressure
200–300	None	None
300–400	Tungsten	Cubic carbide
400–500	Tungsten	Tungsten
500–800	Tungsten	...

In general, the tungsten plates are harder than the molybdenum plates. Hardness varies from 500 Vickers for plates with very low carbon content, to over 2000 Vickers for those with high carbon content. There is a strong tendency, as in the case of molybdenum, for the formation of oriented crystals with the long axis normal to the plated surface.

ALLOY PLATES

Molybdenum-tungsten alloy plates have been prepared by using a finely ground mixture of the two carbonyls in approximately the same mole ratio as the ratio of their vapor pressures [$Mo(CO)_6/W(CO)_6$ is 4.5 at 20 C] in the carbonyl chamber. Such plates prepared at 600 C in wet hydrogen at a moderate rate were quite hard and brittle. Molybdenum plated under these conditions is relatively soft.

21.4.3 Tests of Tungsten Plates

One rifled stellite liner was plated with a 3-mil tungsten coating containing some carbide and fired in a caliber .50 aircraft machine gun barrel with AP-M2 ammunition. The plate was removed completely from the breech third of this 8-in. liner by firing five 50-round bursts at 1-min intervals. This performance was not encouraging.

Tungsten-plated rocket nozzles behaved on test the same as did the molybdenum-plated ones, mentioned in Section 21.3.5.

The performance of tungsten-plated adjustment blocks in a recoilless gun was no better than that of blocks plated with molybdenum (Section 21.3.5).

Two steel compass bearings were plated as follows.[h] One received a plate of tungsten high in interstitial carbon and the other a plate of tungsten carbide. The steel bearings had the shape of a small cylinder with a V-shaped recess ground into one end. The hardness of the plates was about 2200 microvickers, on which scale sapphire is 1800. The ultimate performance was reported to be unsatisfactory, probably due to the thinness of the plate at the bottom of the bearings where the greatest wear would be received.

No increase in the useful life of a high-speed drill was found when a plate of tungsten 1 mil thick was applied.

It should be emphasized that none of the foregoing tungsten plates represented the best product that might be obtained if sufficient study were made of the plating process. Each was a reconnaissance experiment in the early stages of the development of the plating technique, designed to show whether under a wide variety of conditions tungsten plated by the vapor-phase process showed any very great differences as compared with molybdenum so plated. Because none of the tungsten plates was outstandingly better, later efforts were concentrated on molybdenum, as described in Section 21.3.

Before a decision can be reached concerning the relative value of tungsten compared with molybdenum plates deposited pyrolytically, a detailed investigation of the factors affecting the properties of the tungsten plates will have to be carried out, just as has been done with molybdenum. A possible advantage of tungsten plates compared with molybdenum ones is that harder plates of pure tungsten may be prepared more readily than pure molybdenum ones, and possibly at slightly greater plating rates. Also because tungsten carbide may be somewhat harder than molybdenum carbide, it would seem worth while to continue experiments on the preparation of tungsten and tungsten carbide plates for use where extreme hardness is essential. Much work will need to be done before an article of irregular shape, especially one having deep cavities or sharp edges, can be given a fully satisfactory plate of tungsten or of a tungsten compound by this process.

21.5 PREPARATION OF CHROMIUM CARBONYL[73]

21.5.1 Formation of Chromium Carbonyl

Chromium hexacarbonyl, $Cr(CO)_6$, the only stable compound formed between chromium and carbon monoxide, cannot be prepared in the same way as the corresponding molybdenum and tungsten compounds. It can be prepared only by use of a Grignard reagent, which is an organic magnesium bromide in the presence of an organic solvent. The reaction, which involves the formation of an unstable addition compound, may be written as shown in equations (3) and (4).

$$CrCl_3 + C_6H_5MgBr \longrightarrow CrCl_3 \cdot C_6H_5MgBr. \quad (3)$$

$$2CrCl_3 \cdot C_6H_5MgBr + 12CO \longrightarrow 2Cr(CO)_6 + 2C_6H_5MgBr + 3Cl_2. \quad (4)$$

The exact course of the reaction and the possible further steps into which it may be broken down need not concern us here.

The previously published work shows that several experimental procedures have been used in which one or more of the following factors were varied: the compound of chromium, the type of Grignard reagent, the solvent, and the temperature and pressure

[h] They were prepared for and tested by the Bureau of Aeronautics, Navy Department.

at which the reaction was carried out. In all cases the yield of chromium hexacarbonyl was low, the highest reported being 14% of the theoretical, and duplicate experiments seldom gave the same yield. This is a common situation in organic chemistry, where more than one reaction is possible in a given system. The desired product can usually be formed in adequate amount only by a very careful study of the possible variables.

In order to obtain better yields of the carbonyl than had previously been obtained, detailed studies were made of the following points:

1. Chromium compound to be used as starting material. Chromium metal has been included.
2. Composition of Grignard reagent.
3. Solvent.
4. Effect of moisture.
5. Order and mode of addition of reagents.
6. Type of apparatus and materials for its construction.
7. Temperature at which reaction is carried out.
8. Pressure at which reaction is carried out.
9. Effect of stirring or other methods of agitation.
10. Separation of the carbonyl from the reaction mixture.
11. Purification of the carbonyl.
12. Storage of the carbonyl.

As a result of these studies, the yield of pure chromium hexacarbonyl was increased from about 14% to about 64%, when prepared in quantities of 5 g per run using laboratory apparatus. A few experiments on a slightly larger scale gave equal yields. No work has been done on a semicommercial scale, but there are some indications that a continuous process for the manufacture of this substance could be worked out without great difficulty. No estimate of the cost has been made.

21.5.2 Procedure for Producing Chromium Carbonyl

The procedure finally adopted was as follows: Commercial anhydrous chromic chloride was dried at 250 C in nitrogen, and then screened to 40-mesh or finer. Moisture adsorbed here merely required the use of more Grignard reagent and did not seem to decrease the yield. Phenyl magnesium bromide was used as the Grignard reagent. It was prepared, as described in standard laboratory manuals of organic chemistry, by dropping phenyl bromide into a flask containing magnesium turnings and *dry* ether. The container must have an efficient stirrer and be equipped with a reflux condenser. The reagent keeps best in an ether solution.

For most of the experiments 3.08 g of chromic chloride were suspended in 60 cc of dry ether in a container that could be inserted as a tight-fitting liner in a high-pressure vessel. A glass container was used in most cases for convenience, but copper, mild steel, and stainless steel were also used with no adverse effect on the course or yield of the reaction or on the purity of the final product. If elevated temperatures are ever tried in the future, steel should be avoided, as unstable iron carbonyls will be formed by reaction with the carbon monoxide under pressure.

The chromic chloride was kept in suspension by stirring in an atmosphere of nitrogen. The container was cooled to about −70 C, by insertion in a mixture of solid carbon dioxide and acetone, and then a solution of 27 g of phenyl magnesium bromide in 80 cc of dry ether was added slowly, with continuous stirring, during thirty minutes. Much of the Grignard reagent crystallized at this temperature. The container was then removed from the cooling bath, its outside was carefully wiped, and it was placed as quickly as possible in a steel pressure vessel which could be rocked mechanically.

This vessel was then sealed by means of a gas-tight gasket and carbon monoxide was introduced through seamless copper or bronze tubing from a cylinder of the commercial gas. Varying the pressure between 500 and 1,000 psi did not seem to affect the yield of carbonyl. Pressures above 1,000 psi were not tried. The rocking motion was started promptly. The contents of the pressure vessel reached room temperature in about three-fourths of an hour and the reaction seemed to be virtually complete in 2 hr more. The carbon monoxide pressure was then released, the contents of the pressure vessel treated with ice water, 35 cc of dilute (6N) sulfuric acid added, and the brownish to greenish mixture steam-distilled, as described for molybdenum carbonyl in Section 21.2.3.

The ether was thus removed first, and the distillation was continued until no more crystals of chromium carbonyl appeared in the receiver. Enough ether was then added to the receiver to dissolve all the carbonyl and the ether layer separated from the clear aqueous layer. The ether extract was washed with water and dried over anhydrous sodium sulfate. Most of the ether was distilled off through an efficient fractionating column. If adequate fractionation was not obtained, there was loss of chromium carbonyl.

[redacted]

The flask containing the residue was cooled in ice, and the carbonyl was filtered off, washed with a little cold methanol and finally with a little cold dry ether, and dried in air at room temperature. Chromium carbonyl was allowed to stand exposed to the air only long enough for the ether to evaporate. The yield of crude carbonyl in these experiments was between 2.3 and 2.9 g, that is, 53 to 67% of the theoretical.

For further purification, the carbonyl was recrystallized from dry ether in a Soxhlet extractor and sublimed in vacuo. The sublimed material formed large, highly refracting crystals. Analyses for chromium showed the theoretical composition.

21.5.3 Properties of Chromium Carbonyl

Chromium carbonyl is slightly volatile at room temperatures and should be stored in sealed, glass-stoppered, dark-glass bottles. Storage in a dark cupboard is preferable, for traces of impurities make chromium hexacarbonyl much more sensitive to decomposition by light than molybdenum and tungsten carbonyls. The properties of chromium hexacarbonyl resemble those of the molybdenum compound very closely, except for the greater sensitivity to traces of impurities, and the slightly higher vapor pressure of the former. Its solubility, stability in air, and stability in contact with other materials are essentially those of its molybdenum analogue. Accurate values for the constants in question have not yet been obtained.

21.5.4 Pilot-Plant Production

No pilot-plant production of chromium carbonyl has yet been conducted. During the laboratory study of the synthesis, however, attention was paid to possible modifications of procedure that would lead to a convenient and cheap commercial process. The elimination of two features in particular was sought—the use of a Grignard reagent, because of the hazard of working with large quantities of ether, and the use of high pressures, because of the complexity of the procedure. No success was had in a number of attempts to prepare chromium carbonyl by some reaction not involving a Grignard reagent.

At atmospheric pressure the yields of chromium hexacarbonyl by the Grignard reaction are much lower than when the reaction is carried out at high pressures of carbon monoxide. Yields of between 21 and 24% were the best that could be obtained in several experiments. Starting materials other than anhydrous chromic chloride apparently did not react at all, and no carbonyl could be recovered. The yield of carbonyl was not increased by the use of other solvents or of other types of Grignard reagent and was definitely reduced when preliminary temperatures were high.

A few experiments involving the Grignard reaction under pressure on a somewhat larger scale were carried out toward the close of the investigation. A steel autoclave of ½-gal capacity was used, and operations carried out at room temperature. Chromium chloride and ether were placed in this vessel, and the Grignard reagent was introduced gradually through a screw device, while a high pressure of carbon monoxide was maintained in the interior of the autoclave. The subsequent steps were as described above. The yield was 64% of theory. The use of such an apparatus is suggested if it is desired to prepare the carbonyl on this larger scale.

By the use of a specially designed apparatus, with a suitable number of feeding devices, a continuous process for the production of chromium carbonyl could probably be worked out if need be. The subsequent operations are those which have already been carried out on a commercial scale for many years in other types of organic preparations.

21.6 VAPOR-PHASE PLATING OF CHROMIUM[74]

21.6.1 Introduction

Only preliminary experiments on the formation of platings by the thermal decomposition of chromium hexacarbonyl were carried out. Enough work was done to show that plates of different degrees of hardness, which were reasonably adherent at room temperature, could be applied to flat steel surfaces. Temperature limits for the varying hardness of the plates were found. The few plates applied to stellite surfaces were not particularly adherent.

21.6.2 Plating Procedure

The process of plating chromium from the carbonyl was essentially the same as that of plating molybdenum (Section 21.3). A controlled stream of hydrogen passing over the crystalline carbonyl carried carbonyl vapor into the plating chamber where chromium

was deposited on the heated metal object by the decomposition of the carbonyl. The resulting carbon monoxide was removed by continuous pumping. A by-pass was provided in the apparatus so that the hydrogen could be admitted directly to the plating chamber when desired.

The apparatus that was used in the chromium-plating procedure is shown to scale in Figure 10. The Cenco Hypervac 20 vacuum pump, which is run continuously during operations, is connected by a short piece of thick-walled rubber tubing. At the opposite end of the apparatus is a needle valve, through which a small stream of carefully purified hydrogen gas can be admitted. With the exception of these items and of the top of the plating chamber, the apparatus is constructed of Pyrex glass. The trap T_1, in which the unused carbonyl is condensed, is immersed in a bath of solid carbon dioxide and acetone. Traps T_2 and T_3 contain crystals of purified chromium hexacarbonyl; T_2 is surrounded by a constant-temperature bath (not shown), while T_3 is at room temperature. The steel or other disk to be plated is suspended in chamber C by means of the thermocouple leads which are sealed into a ground glass stopper set into the heavy brass top of the chamber. The chamber is surrounded and heated by an induction coil (not shown). Also shown are connections to a McLeod gauge to indicate pressure, to a standard 12-liter volume for calibration of gas flow, and at S_3, to a source of hydrogen sulfide or other gas, which may be used in addition to the hydrogen.

In this apparatus the disk temperature can be varied from room temperature to about 1000 C and carbonyl vapor pressure from 0.040 to 0.220 mm. The hydrogen flow and the proportion of any other gas to hydrogen may be varied at will. The vapor pressure of the carbonyl can be calculated from the temperature of the bath surrounding the carbonyl container T_2 by equation (5),

$$\log p = 10.63 - 3285/T \qquad (5)$$

in which p is expressed in mm of Hg and T in degrees centigrade, provided that the bath has been in position for sufficient time for temperature equilibrium to have been established with the carbonyl.

The procedure preliminary to plating was the same as for molybdenum plating in that the metal surfaces had to be deoxidized by heating in hydrogen at a temperature higher than the plating temperature. When the specimen had cooled to the desired plating temperature, the temperature of the carbonyl supply was adjusted to provide the desired vapor pressure, and the vapor was admitted to the system. After 2 to 4 hr, the carbonyl vapor was cut off, the sample was again heated to the deoxidizing temperature (700 to 800 C), and cooled gradually to anneal the plate.

21.6.3 Characteristics of the Plates with Variations in Procedure

Because the high temperatures involved in this procedure permanently change the characteristics of the steel, some runs were made in which the temperature was never raised above 550 C (well below the alpha-gamma transition point of steel). This resulted in a slight decrease in the strength of the bond be-

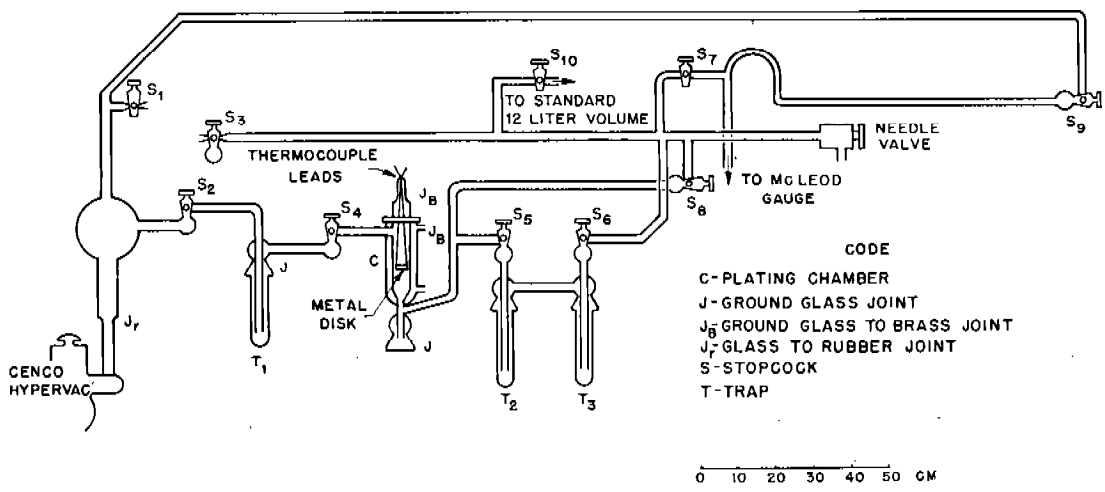


FIGURE 10. Apparatus used in the experiments on the vapor-phase plating of chromium. (Figure 1 in NDRC Report A-402.)

tween steel and plate and also involved a longer time to yield the same plate thickness.

Plates on stellite disks showed poor adherence when the standard procedure was used. This was presumably due to incomplete deoxidation of the stellite surface before plating. Chromium oxide is less readily reduced than is iron oxide, and the experiments with molybdenum plating showed that a good stellite-to-plate bond requires deoxidation for ½ hr at 1100 C. Experiments to confirm this with chromium plates were not carried out.

The composition and hardness of the plate appear to be determined primarily by the disk temperature during the plating process. The results of about 40 experiments on steel disks are summarized in Table 5.

TABLE 5. Composition and hardness of pyrolytically deposited chromium plates.

Plating temperature (C)	Approximate composition (%)	Approximate hardness (Vickers)	Quality of disk-to-plate bond
250–350	50 Cr_2O_3 50 Cr_3C_2	1400	Very poor
400–500	95 Cr 5 Cr_2O_3	1200	Good
500–525	50 Cr 25 Cr_2O_3 25 Unknown	2000	Poor
530–550	50 Cr 50 Cr_2O_3	.....	Very poor
600–650	40 Cr 60 Cr_2O_3 + Cr_3C_2	Very hard (2000)	Good

Identification of the compounds in the plate was by x-ray analysis. The unknown constituent may be a hitherto unknown carbide of chromium.

At plating temperatures of about 400 C a well-bonded, comparatively soft plate is formed, and at about 625 C a very much harder plate with a good bond is formed. A chromium oxide-chromium carbide plate appears to possess poor adherence, while most of the plates carrying metallic chromium appear to adhere better. The presence of oxide in these plates, in contradistinction to the absence of oxides of molybdenum or tungsten in plates of those metals, should be noted. This is presumably due to the much greater ease of formation of chromium oxide and to its greater stability after having been formed.

The plates prepared varied from 0.5 to 5.7 mils in thickness. No relation between thickness and adherence could be noted because of other variables. The plating rate was approximately proportional to the vapor pressure of the carbonyl and, at low rates of flow, to the hydrogen flow. At higher rates of hydrogen flow, the gas was probably not saturated with carbonyl vapor. The disk temperature did not seem to affect the plating rate except at the lowest temperatures. The presence of hydrogen sulfide, added in very small amounts in an attempt to deoxidize the disk surface, decreased the plating rate enormously and ruined the bond. The plate deposited under such conditions is 95% pure chromium with a hardness of only 350 Vickers.

Photomicrographs of four typical plates are shown in Figure 11. In all cases the magnification is 500X. The first etchant used was 5% nital, to show the structure of the steel, followed by a boiling solution of potassium hydroxide and potassium ferricyanide, to show the structure of the plate. The top of each section shows the electroplated surface of iron applied to protect the specimen during cutting and polishing.

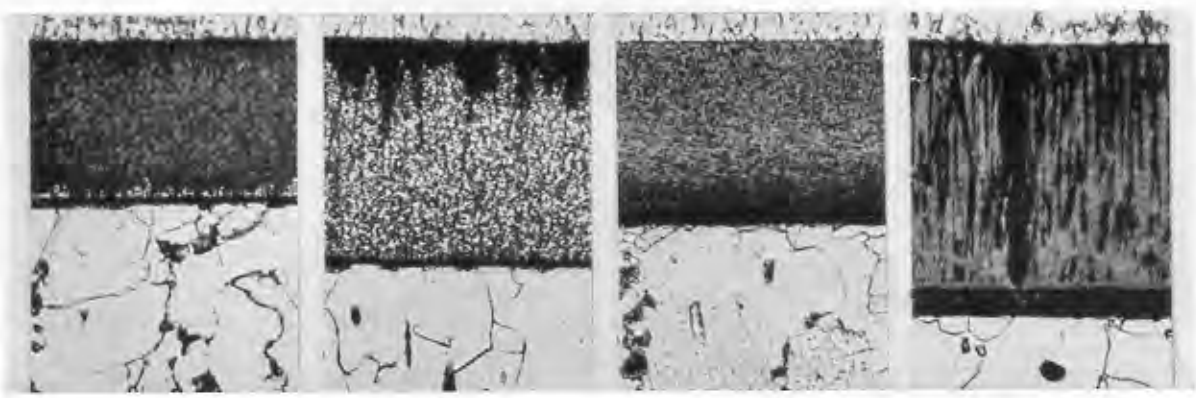


FIGURE 11. Photomicrographs of transverse sections of chromium plates deposited on steel disks by vapor-phase deposition. The structure of the plates varied considerably depending on the temperature of the specimen. (*500X.*) (Portions of Figures 2 and 3 of NDRC Report A-402.)

CONFIDENTIAL

21.6.4 Conclusions and Recommendations

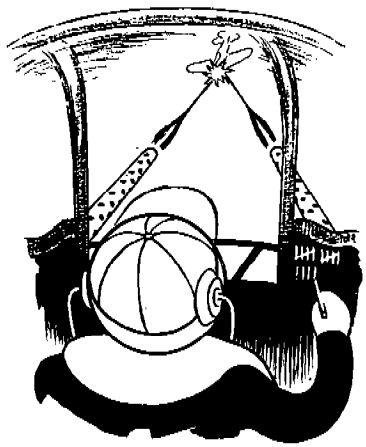
No attempts have been made to apply chromium pyrolytic plates to gun bores or to the inside of smooth tubes. Experience with molybdenum pyrolytic plates makes it appear doubtful if success could be obtained with the expenditure of only a reasonable amount of effort. Moreover, because of the development of alloys (Chapters 17 and 18) that withstand temperatures at which stellite fails, further investigation of chromium pyrolytic plates as a means of extending the usefulness of stellite to hypervelocity guns is not considered worthwhile.

These plates of chromium-chromium oxide-chromium carbide on steel, however, are of considerable general interest. We have here another type of plate that can be applied in an adherent form to a metal surface, the hardness of which can be varied nearly at will throughout remarkably wide limits, and which is (though this needs confirmatory tests) very resistant to corrosion.

Further study should be made of the conditions under which an adherent plate of given properties can be deposited at a reasonable rate. There should also be further study of the firmness of the bond, and of methods to improve it. These plates have promise, it would appear, in the field of extremely hard protective coatings for small articles; also for precision bearing surfaces, or for surfaces subjected to hard wear. The present stage is obviously only a very preliminary one, and extensive research must be done before determining the limits of their application.

PART VI

IMPROVED MACHINE GUN BARRELS



A hit, a very palpable hit.
—*William Shakespeare*
"Hamlet"

Chapter 22

STELLITE-LINED MACHINE GUN BARRELS

By *J. F. Schairer*[a]

22.1 INTRODUCTION

A SHORT BREECH LINER of an erosion resistant material in a gun barrel, which provides a suitable bore surface at and near the origin of rifling where erosion is most severe, is a practical method of decreasing erosion and thus improving gun barrel performance. In order to utilize this method of mitigating erosion in machine gun barrels it was necessary to find and develop a suitable liner material and to insert it in a practical way in a Service weapon. Division 1 has demonstrated that such an erosion-resistant liner material existed, that it could be inserted in a practical manner in a Service weapon, that it would remain in place during firing with no rotation, forward or backward movement, or serious expansion or contraction, and that a gun barrel with such a liner (with the liner joint and discontinuity in the bore surface) would fire accurately and safely and show such outstanding improvement in life and performance as to justify amply the expense and effort required for the modification of regular steel barrels.

The stellites, because of their resistance to chemical attack by hot powder gases, hardness and strength at high temperatures, and excellent wear and abrasion resistance, have shown outstanding performance in machine gun barrels under both mild and severe firing conditions, including schedules so severe that unmodified steel barrels are unable to withstand them. The experiments that led to the selection of Stellite No. 21 as an eminently suitable liner material for machine gun barrels have already been described in Chapters 16 and 19. The development of a practical design for liner insertion in machine gun barrels for production and Service use is described in the present chapter.

22.2 DEVELOPMENT OF THE LINER DESIGN

22.2.1 Insertion of Short Breech Liners

Early in the erosion-resistant materials program of Division 1, NDRC (Section 16.1), the importance of liner insertion for the testing of special materials was realized. Recognizing that the only conclusive test of an erosion resistant material is a firing test in the gun in which it is to be used or under conditions as close as possible to this ultimate objective, the several types of experimental liners described in Sections 16.3 and 26.2 were devised.

All of these designs for liner insertion were developed in order to test liner materials and not overall barrel performance. None of them was intended to be suitable for mass production or for Service use.

In order that an erosion resistant material, once found, could be applied, the Crane Company was asked in August, 1943 to develop a method of inserting short breech liners that would be practical from both the production and Service standpoints. In view of the urgent need for improvement in barrel life and performance of the caliber .50 Browning machine gun, particularly for aircraft combat, all efforts were concentrated initially on barrels of this caliber. Furthermore, it was considered desirable initially to maintain the same external barrel contour in order to utilize guns, mounts, and installations already in Service use and to develop a method for the modification of regular steel barrels already in large supply to permit liner insertion.

Crane Company prepared four designs for liner insertion in caliber .50 machine gun barrels, two for the heavy and two for the aircraft barrel. Three of the designs were similar in that the assembly consisted of three parts—a liner, a chamber section, and a forward section. The liner, which was tapered, was pressed and shrunk into the chamber section and the forward section was then pressed on and the assembly held together with tapered pins. In the fourth design, applied to an aircraft barrel, the liner and chamber sections were integral.

Firing tests were conducted on one heavy barrel assembly made in accordance with what was considered to be the most promising of these designs, using a steel liner for test purposes. After only a few rounds had been fired, the tapered pins sheared and the sections of the barrel separated. Subsequently, another design, similar to this except that a union-ring type of nut rather than tapered pins was used and was

[a] Special Assistant, Division 1, NDRC. (Present address: Geophysical Laboratory, Carnegie Institution of Washington.)

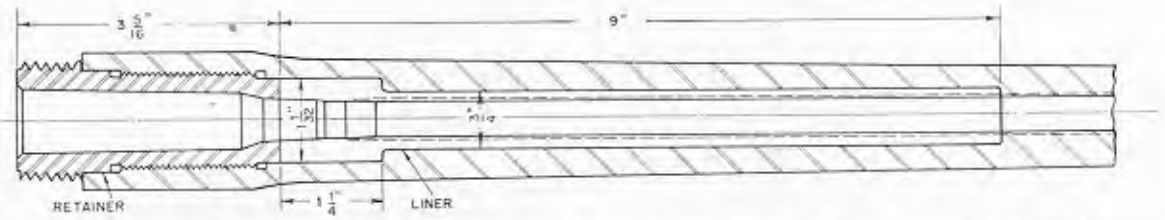


FIGURE 1. Stellite liner 9-inches long inserted in caliber .50 aircraft machine gun barrel according to Crane Company drawing No. 50-35. (Figure 2 of NDRC Report A-408.)

tested with a steel liner with satisfactory results. However, this design was not completely satisfactory as far as production was concerned and could not readily be adapted to the aircraft barrel for which there was the most urgency for improvement.

A new design for the aircraft barrel was developed in which a tapered stellite liner was inserted from the breech end of the barrel and held in place by a threaded retainer screwed into a tapped recess between the breech ends of the liner and barrel. During firing, the tapered stellite liner moved forward, upsetting the steel ahead of the liner and constricting the steel bore. This forward movement occurred as a result of the low coefficient of friction between stellite and steel and dimensional changes in the liner caused by stresses during firing. Increasing the taper or roughening the liner surface by sandblasting were ineffective in preventing the forward movement of the liner.

As a result of these difficulties, the design was further modified to provide for a cylindrical liner with an enlarged shoulder or flange at the breech end to prevent forward movement. The liner was inserted on a diametral shrink-fit by heating a recessed barrel to about 450 or 500 F and cooling the rifled liner in liquid air or nitrogen. Rifling in the liner and barrel were put in alignment during insertion by the use of a rifled mandrel. This design which is shown in Figure 1, entirely eliminated the forward movement of the liner and proved entirely satisfactory and practical for production. The stellite-lined barrel was adopted for Service use in both the caliber .50 aircraft and heavy barrels as described in Sections 22.3.4 and 22.4.2. A stellite-lined caliber .50 aircraft machine gun barrel, disassembled to show the recessed barrel, liner, retaining nut and cartridge, is shown in Figure 2.



FIGURE 2. Caliber .50 stellite-lined aircraft machine gun barrel disassembled to show barrel, liner, and retainer. A complete round of ammunition is also shown. (Figure 3 of NDRC Report A-408.)

22.2.2 Firing Tests on Barrels with Liners of Stellite No. 21

First Firing Test

For the testing of various liner materials to single out those which are markedly superior to gun steel in overall erosion resistance, it was desirable to use a severe firing schedule. Because the heavy walls of the caliber .50 heavy machine gun barrel gave good support to a liner, this barrel was used in initial liner tests. The following severe schedule was used for the testing of the first liner of Stellite No. 21:

Preliminary rounds (total 145)	1 single round 9 single rounds in succession 1 burst of 10 rounds 1 burst of 25 rounds 1 burst of 100 rounds
500-round group	5 bursts of 100 rounds each with 1 min between beginning of each burst.

The 500-round groups were to be repeated as many times as necessary. The barrel was cooled to room

CONFIDENTIAL

temperature, examined, and gauged with a breech-bore gauge after each item of the preliminary schedule and after each 500-round group.

The first liner of Stellite No. 21 tested was an investment-cast liner, 6 in. in overall length. This cylindrical flanged liner was inserted in a caliber .50 heavy machine gun barrel according to a design essentially the same as that shown in Figure 1. After over 6,000 rounds had been fired, the breech-bore gauge had advanced only 0.30 in. (A regular steel barrel is declared worn out after an advance of 2 in. of this gauge.) The liner was still in good condition, but since the liner was too short, the steel bore surface ahead of the liner had eroded considerably. The liner was removed for very careful examination, inserted in a new barrel, and the firing continued. At 10,000 rounds, the breech-bore gauge had not advanced as much as 1 in.; but shortly thereafter the advance became more rapid and the rejection point (2 in.) was reached at 10,900 rounds. The liner[b] had not failed in a dangerous manner by cracking but gradually wore out. Such liner performance was phenomenal. On the same firing schedule a steel barrel was worn out in less than 1,000 rounds.

Firing Tests on Aircraft Barrels

Steps were taken immediately to apply a liner of Stellite No. 21 to the caliber .50 aircraft machine gun barrel and to learn the overall improvement in barrel performance that could be obtained by the use of such a liner. No measurements were available on the effects on accuracy and velocity life of a gun barrel when a short breech liner of an erosion resistant material had been inserted. It was not possible to get such measurements until a suitable liner material had been found and satisfactorily inserted. Division 1 made arrangements with the Sixth Service Command for the Crane Company to utilize an Army firing range at Fort Sheridan near Chicago to make accuracy and velocity firings on stellite-lined barrels.

Two stellite-lined caliber .50 aircraft barrels were to be prepared and compared with two standard barrels on the same moderately severe firing schedule. In the preparation of the lined barrels the liner length was increased to 9 in. This length was a compromise. The firing test in the heavy barrel described above had shown that a 6-in. liner was too short. Owing to practical matters, such as maintenance of tolerance during the recessing of barrels to receive liners and the limitations imposed by the wall thickness of the light aircraft barrel, it was decided to determine the performance of the 9-in. liner.

While the 9-in. investment-cast liners were being prepared, while tooling was in progress for their insertion, and while equipment was being assembled for the accuracy and velocity firings, a composite 7⅛-in.

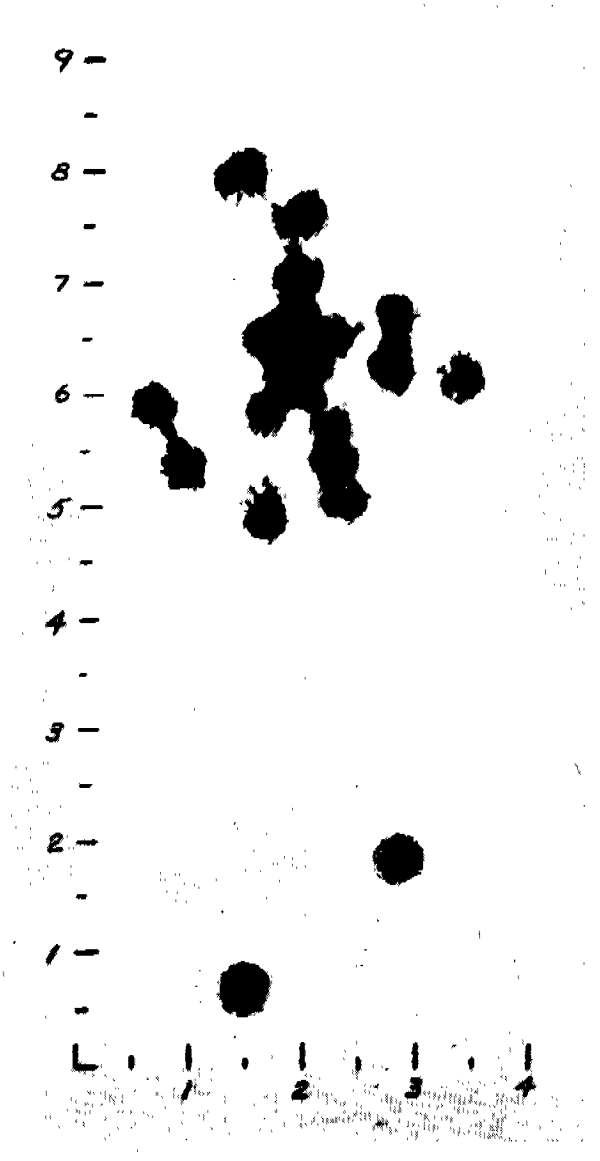


Figure 3. Target sheet for 25-round burst for cold accuracy at 1000 inches during firing test of aircraft barrel No. 5 (fused Stellite No. 21 liner), after 5,084 rounds. Target scale in inches. (Photograph No. 70 in Crane Monthly Report on Contract OEMsr-629 for June 1944.)

[b] Affectionately called "Grandpappy" by those associated with the test.

liner was prepared by casting Stellite No. 21 into a steel sleeve. This liner was inserted in an aircraft barrel and subjected to a firing test. In the light aircraft barrel the same firing schedule as used on the heavy barrel was unsatisfactory. A preliminary test on a steel barrel showed that such a schedule was too severe and that the barrel failed by softening of the steel barrel wall near the muzzle. The schedule adopted for initial tests with lined aircraft barrels, consisted of 250-round groups, with complete cooling between groups, each group consisting of 50-round bursts 1 minute apart. In the firing test (Crane Barrel

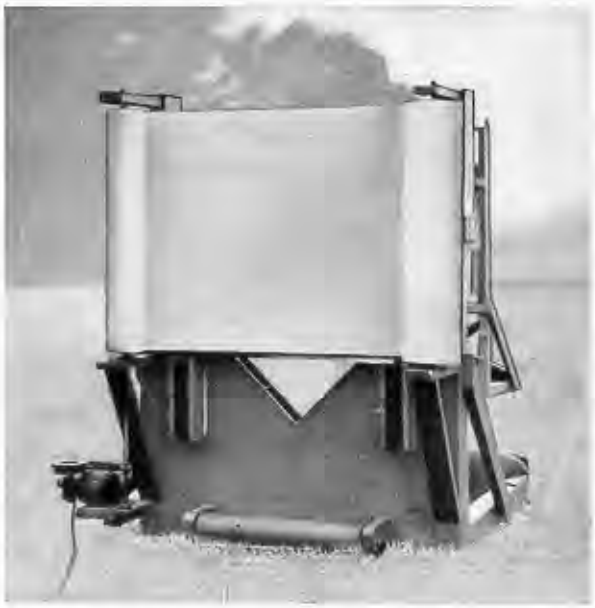


FIGURE 4. Moving target and mechanism for recording burst fire. (Photograph No. 100 in Crane Monthly Report on Contract OEMsr-629 for August 1944.)

No. AC5) on the composite 7-in. liner, the breechbore gauge entered only 0.35 in. after 5,000 rounds on this schedule and the rifling in the liner was still sharp, and the liner bore surface showed only a few small pits and hairline surface cracks. The cold accuracy stationary target sheet after this test is shown in Figure 3.

The accuracy and velocity firings of four caliber .50 aircraft barrels, two with flanged 9-in. investment-cast liners or Stellite No. 21 inserted on a shrink-fit (Figure 1) and two standard steel barrels for comparison, showed the outstanding overall barrel performance of stellite-lined barrels. The firings were conducted with standard ammunition, AP-M2. The initial muzzle velocity of the barrels was about 2,700 fps. In the case of the lined barrels after twelve 250-round groups (3,000 "erosion rounds") no significant velocity drop either hot or cold had occurred. With the standard steel barrels, velocity had decreased to 2,100 fps while hot and 2,500 fps while cold after only two 250-round groups (500 "erosion rounds"). As shown by a moving target (see Figure 4) there was no inaccuracy (keyholing bullets) during the 3,000 erosion rounds with the stellite-lined barrels and the dispersion was not significantly less than the initial value. On the other hand, with the standard steel barrels after only two erosion groups (500 rounds) the bullets covered a target area 40 ft in diameter at 300 yd and all rounds keyholed during the fourth and fifth bursts of the second 250-round group. The firing test on the two stellite-lined barrels was arbitrarily discontinued after 3,000 erosion rounds. This firing schedule was not severe enough to show the full potentialities of these barrels.

22.3 APPLICATION OF STELLITE NO. 21 TO THE CALIBER .50 AIRCRAFT BARREL

22.3.1 Need for Improvement

Experience in aircraft combat by both the Army and Navy Air Forces and those of our British allies had indicated that barrel life and performance of the regular caliber .50 aircraft machine gun barrel were inadequate to meet the needs and requirements of severe combat use. Because of the speed and maneuverability of the target, a high rate of fire and high velocity were required in plane-to-plane combat. Movement of the high-speed target during the time-of-flight of the bullets required the shortest possible time-of-flight. Velocity drop destroyed the accuracy of the computing sights used. The necessity for hitting a target many times before it was destroyed required high velocity, high rate of fire, and longer bursts of fire. The advent of long-range bombing and strafing attacks and night fighting astern of a target located by radar caused a great increase in the length of bursts desired in machine guns. The regular caliber .50 aircraft barrel did not stand up under this abuse and the ability to fire long bursts became an urgent requirement for this weapon.

Barrel erosion was seriously limiting the life and performance of these machine gun barrels. If barrel erosion could be mitigated, vastly more efficient

CONFIDENTIAL

weapons could be placed in the hands of our fighting forces. On the basis of the firing tests on the stellite-lined barrels just described, the utilization of the remarkable erosion resistance of Stellite No. 21 when applied as a short breech liner, showed great promise of yielding a vast improvement in the overall performance and life of this important and critical Service weapon.

22.3.2 Preparation of Lined Barrels for Ordnance Department Tests

As soon as the accuracy and velocity firings on the two stellite-lined caliber .50 aircraft machine gun barrels had proceeded far enough to confirm the expectation of the remarkable increase in overall barrel performance to be obtained by the use of a short erosion-resistant breech liner, Division 1 made plans for the immediate application of these results. Although it was realized that the design and perhaps even the exact liner material might not be as suitable as that which might be revealed by further research, it was felt that the improvement in performance was so outstanding that it would be desirable to freeze the material and the design around that shown in Crane Drawing No. 50-35 (already shown as Figure 1) and furnish barrels for Ordnance Department acceptance tests and immediate Service application, rather than wait for possible further improvements.

Accordingly Division 1 asked Crane Company to prepare 212 barrels just like those which had shown such superior performance in the accuracy and velocity firings. Two hundred of these barrels were for test by the Small Arms Division, Research and Development Service of the Ordnance Department and 12 by the British Air Commission. Crane Company prepared these barrels under Contract OEMsr-629 by the modification of standard steel barrels supplied by the Ordnance Department. The investment-cast liners were supplied by the Haynes Stellite Company (subsidiary of Union Carbide and Carbon Corp.) under Contract OEMsr-1330. With the special tools on hand at Crane Company, it was possible to prepare two barrels per day and deliver them for immediate test. Additional tooling was expedited and soon four barrels per day were available. Because of the long life and superior performance of the stellite-lined barrels, it was possible to supply these barrels faster than they could be tested. In accordance with directions from the Ordnance Department, 150 barrels were sent for test to the Army small arms testing range at Purdue University and 50 to Aberdeen Proving Ground. All of these barrels were made and delivered by October 30, 1944.

The only dimension changed during the course of the preparation of these barrels was that of the bullet seat whose diameter was increased by 0.002 in. This cylinder (32.1 in. from the muzzle) was made slightly larger in stellite-lined[c] barrels than in standard steel barrels because of the slight bore constriction (about 0.002 in. in diameter) as a result of firing. If the bullet seat is too small, stoppages result because of failure of the cartridge to seat. In standard steel barrels, erosion more than keeps pace with constriction.

22.3.3 Test Results

In order to evaluate the relative life and performance of the stellite-lined caliber .50 aircraft machine gun barrels prepared by Division 1, as compared with standard steel barrels under the same firing conditions, the Small Arms Division, Research and Development Service of the Ordnance Department, utilized a series of firing schedules which gave a measure of relative barrel performance under conditions simulating those that might be used in combat. They varied from the very severe conditions of long continuous bursts or moderate length bursts (100 rounds) at frequent intervals (2 min apart) to such mild schedules as 100-round bursts with complete cooling between bursts. The effects on performance were also evaluated for the various types of caliber .50 ammunition, including ball, M2; armor-piercing, M2; armor-piercing incendiary, M8 and M8E1; incendiary, M1; tracer, M1 and M10; and other special experimental ammunition.

Under all conditions, but particularly with long continuous bursts of fire so much desired in severe combat, the stellite-lined barrels showed a very marked superiority to the standard steel barrels. Although the stellite-lined barrels showed a marked improvement in accuracy life over standard steel barrels, the improvement in velocity life was phenomenal. Owing to a small permanent bore contraction in stellite-lined barrels during the first burst of fire, the velocity actually increased and then decreased only very slowly during additional firing. In the case of the tests illustrated by Figure 8, the initial increase amounted to 150 fps.

[c] Also in nitrided and chromium-plated barrels described in Chapter 23.

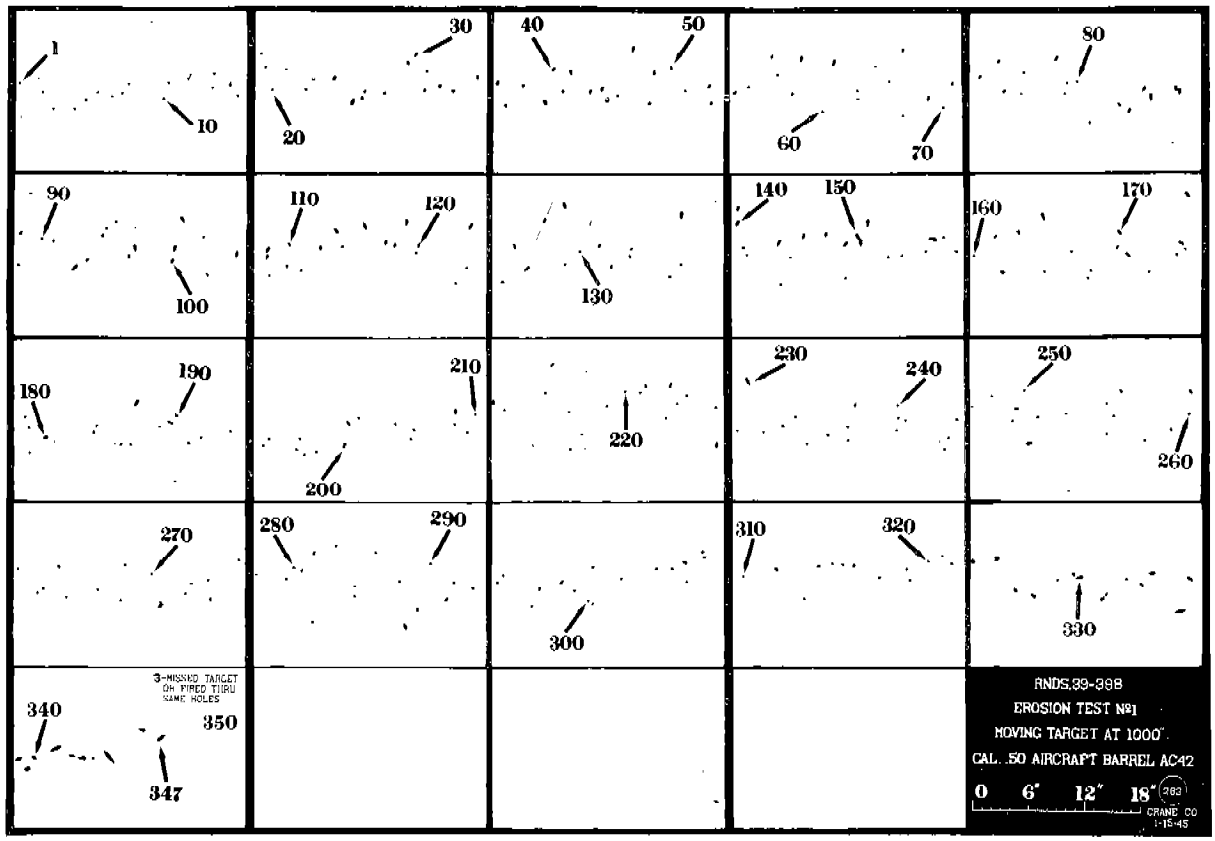


FIGURE 5. Moving target pattern at 1,000 in. for first burst (350 rounds) in test of stellite-lined barrel No. AC42. (Photograph No. 283 in Crane Monthly Report on Contract OEMsr-629 for December 1944.)

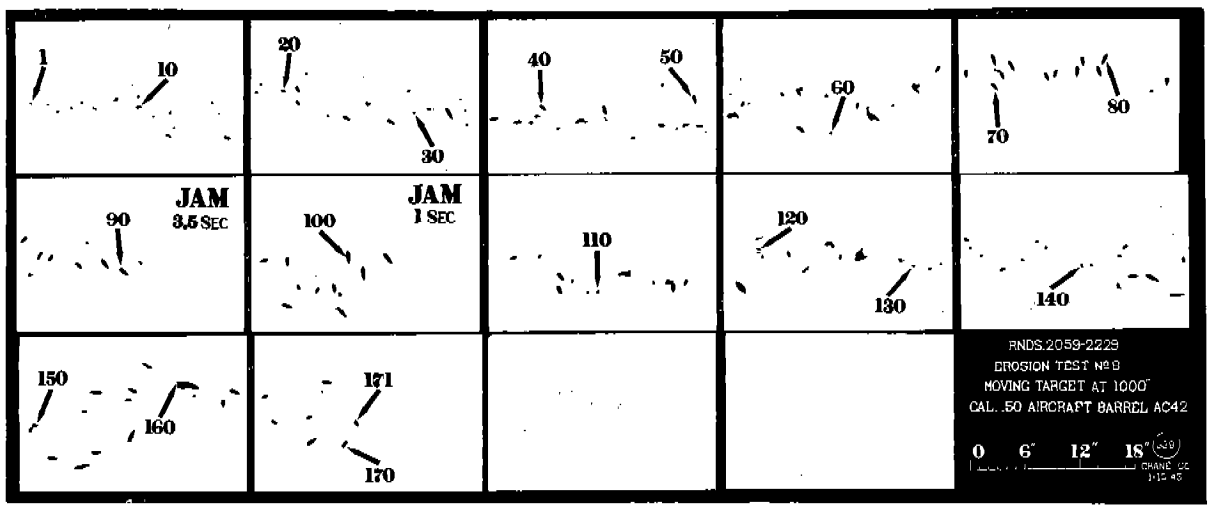


FIGURE 6. Moving target pattern at 1,000 in. for eighth burst (171 rounds) in test of stellite-lined barrel No. AC42. (Photograph No. 338 in Crane Monthly Report on Contract OEMsr-629 for December 1944.)

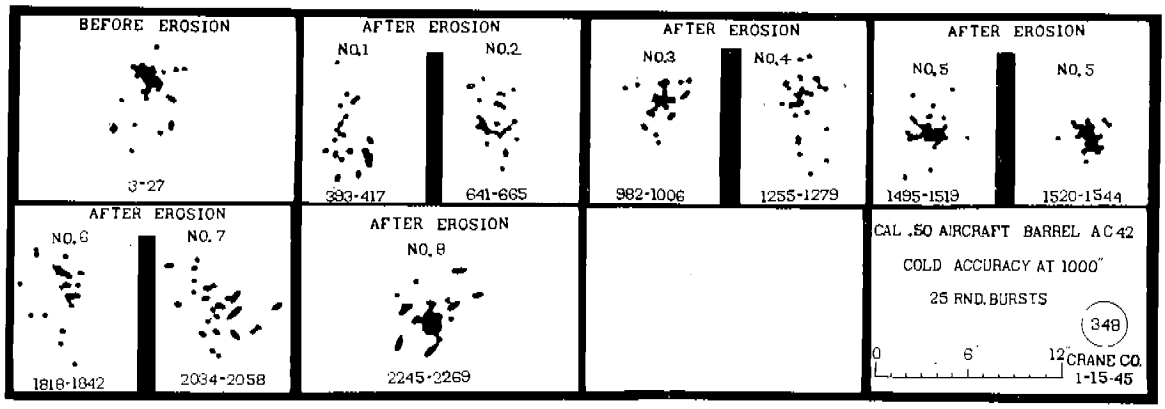


FIGURE 7. Target sheets for 25-round bursts for cold accuracy at 1,000 m. during the course of the firing test on stellite-lined barrel No. AC42. (Photograph No. 348 in Crane Monthly Report on Contract OEMsr-629 for December 1944.)

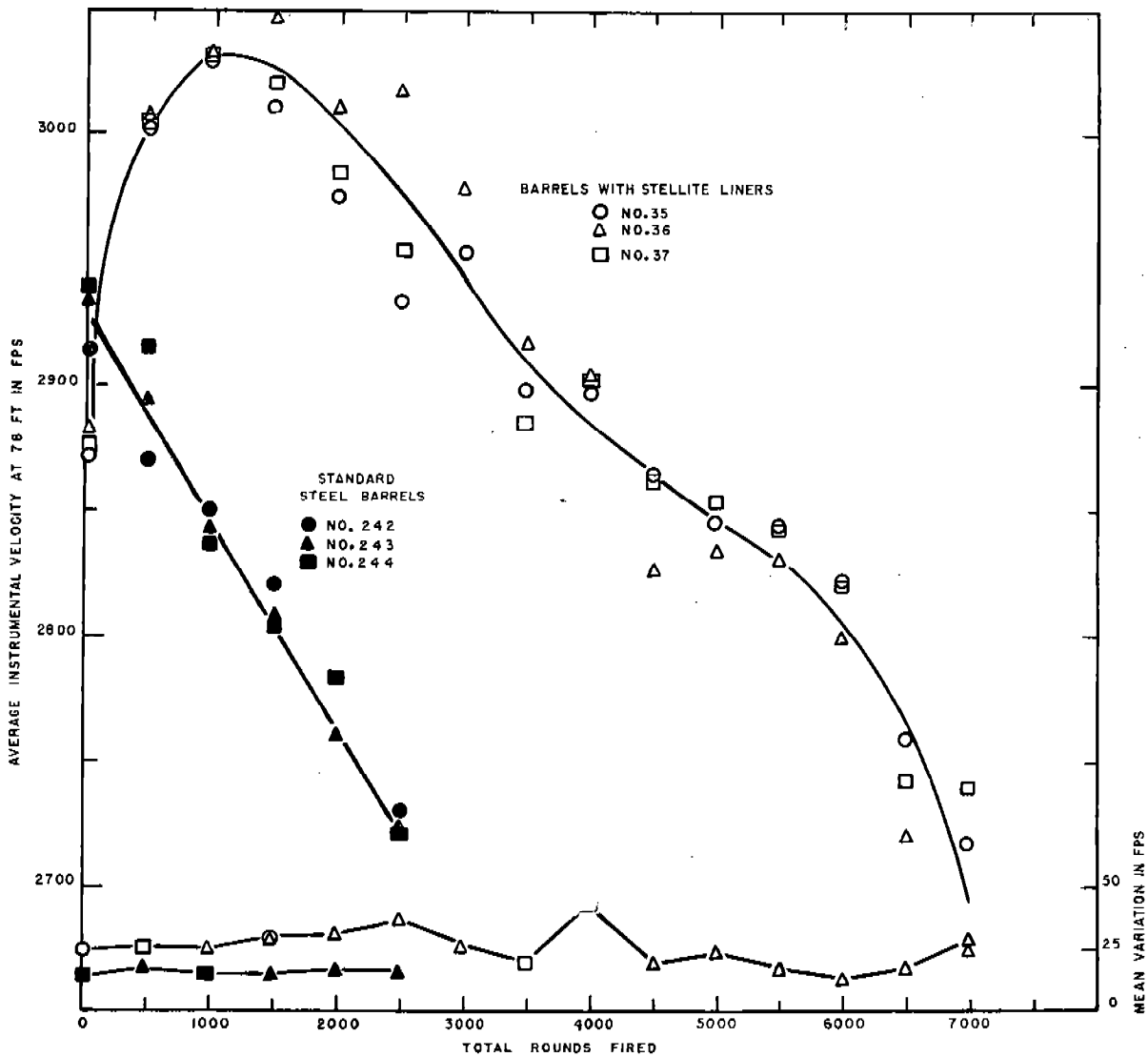


FIGURE 8. Velocity loss in standard steel and stellite-lined caliber .50 aircraft machine gun barrels on the 100-round burst cycle (F-1). (Graph prepared from data in Aberdeen Proving Ground Third Memorandum Report on O.P. 5082.)

[redacted]

The improvement in performance on various test schedules[d] may be summarized as follows:

Continuous Burst Cycle (C—1). In this very severe schedule the barrel is fired in a continuous burst until serious keyholing[e] of the projectile develops. "Cold-velocity" is measured before and after the burst and sometimes "hot-velocity" is measured at the end of the burst. Continuous bursts to serious keyholing are repeated (with complete cooling between bursts) until a drop in cold-velocity of 200 fps occurs and the barrel is rejected for excessive velocity drop. Results on this test schedule show the remarkable superiority of the stellite-lined barrel for use in strafing and by night fighters.

Ordnance Department tests on the steel barrels that were standard in 1943 (Drawing No. D-28272) showed that after a single burst of 167 rounds (mean of ten barrels) nearly complete keyholing occurred and there had been a velocity drop of nearly 200 fps. Thus life was only about 167 rounds. Similar tests were made by the Ordnance Department on seven stellite-lined barrels provided by Division 1. These seven barrels averaged 295 rounds to serious keyholing for the single continuous burst that was fired.[294] No velocity measurements were made on these barrels.

Division 1 conducted more extended tests on regular stellite-lined barrels on the continuous schedule at Crane Company to obtain a standard for comparison with other special barrels being studied in the research program. AP-M2 ammunition was used. Although there was some variation in life and performance of regular[f] stellite-lined barrels, the firing results on barrel No. AC42[80] are representative of what performance was achieved on this schedule. Eight continuous bursts of 350, 212, 301, 233, 200, 247, 176, and 171 rounds, respectively, were fired, plus 379 intermittent rounds for accuracy and velocity measurements, making a total of 2,269 rounds. The cold-velocity dropped only 15 fps after the first burst of 350 rounds. After that it decreased only gradually from its initial value of 2,705 fps to 2,515 fps after the eighth burst. The moving target patterns during the first and eighth bursts are shown in Figures 5 and 6, respectively. The stationary targets for 25-round bursts for cold accuracy at 1,000 in. during the course of the test with this barrel are shown in Figure 7. This stellite-lined barrel not only showed a life of 1,890 rounds as compared with 167 for a standard steel barrel, but in addition it fired an initial burst of twice the length.[g] Even the eighth burst was equal in length to the first and only burst possible with the standard steel barrel.

100-Round Burst Cycle (B—1). In this moderately severe schedule the barrel is fired in 100-round bursts with two-minute cooling intervals until serious keyholing develops or the velocity drop is greater than 200 fps. Ordnance Department tests on 11 standard steel barrels fired with combat ammunition showed an accuracy life of 230 rounds while similar tests on 13 stellite-lined barrels showed an accuracy life of 455 rounds. No velocity measurements were made on the standard steel barrels but the stellite-lined barrels showed a velocity *increase* of 30 fps during the firing. When seven standard steel barrels were fired, with ball M2 ammunition for five 100-round bursts with 2-min cooling intervals, the velocity drop was 533 fps.

100-Round Burst Cycle (F–1). In this mild schedule the barrel is fired in 100-round bursts with complete cooling between bursts. Velocity and accuracy targets are taken during every fifth burst and the cycle is repeated until a 200-fps drop in cold-velocity occurs, or a majority of the rounds fired in a burst produce keyholes.

Three stellite-lined barrels and three steel barrels were fired at Aberdeen Proving Ground on this schedule using combat (API-M8) ammunition.[213] Velocity drop was the cause of end of life in both cases. The standard steel barrels showed a life of 2,500 rounds while the stellite-lined barrels showed a life of 7,000 rounds. Even on this mild schedule stellite-lined barrels showed nearly three times the life of a standard steel barrel. The velocity loss data for these tests is shown graphically as Figure 8.

300-Round Burst Cycle (British Schedule). In this severe schedule the barrel is fired in 300-round bursts with complete cooling between bursts. Cold-velocity measurements are made at the start of the test and

[d] Some of these same firing schedules were used in the testing of nitrided and chromium-plated caliber .50 barrels, as described in Sections 23.1.3 and 23.1.4. Stellite-lined barrels were later tested on the CGL-350 schedule. (See Sections 24.1.3 and 24.4.)

[e] Inaccurate (tumbling) bullets hit the target paper broadside-on (British "B.S.O.") and produce a keyhole-shaped hole in the target paper instead of a round hole.

[f] A "regular" stellite-lined barrel in this report means a caliber .50 steel barrel made to Ordnance Drawing No. D-28272 in which a 9-in. liner (Figure 1) of investment-cast Stellite No. 21 has been inserted by the method developed by the Crane Company[80] (described at the end of Section 22.2.1) or by some equivalent method.

[g] In tests of a large number of barrels at Crane Company the length of the initial continuous burst to serious keyholing varied between 290 rounds and 350 rounds.

after each burst. Accuracy is determined throughout a burst by means of a moving target. Breakdown of accuracy is taken as the stage at which frequent tipping bullets and partial B.S.O.'s (keyholing bullets) commence.

A portion of the stellite-lined barrels prepared by Division 1 for the British Air Commission were tested on this schedule. The results of test[406,413] on two barrels with AP-M2 ammunition showed an accuracy life of 850 and 880 rounds, respectively, as compared with 170 rounds (mean of ten barrels) on standard steel barrels. Firing was continued on the stellite-lined barrels and a 200-fps velocity drop occurred finally after 1,120 and 1,160 rounds, respectively, as compared to about 180 rounds in the standard steel barrels.

Ten 40-Round Bursts (British Schedule). In this test schedule which the British used to indicate suitability of a barrel for improved performance in fighter combat use, ten 40-round bursts are fired at the beginning of each minute. The cycle is repeated following complete cooling after each 400-round group.

A portion of the stellite-lined barrels prepared by Division 1 for the British Air Commission were tested on this schedule.[406,413] The results of test on two barrels with AP-M2 ammunition showed an accuracy life of 3,560 and 4,330 rounds, respectively, as compared with only 190 rounds for the standard steel barrel. Firing was continued on the stellite-lined barrels and a 200-fps velocity drop occurred finally after 4,300 and 5,200 rounds, respectively, as compared to a 400-fps velocity drop in only 240 rounds with a standard steel barrel. Such a marked superiority of roughly 20 to 1 of stellite-lined barrels over standard steel barrels in a test designed to indicate the suitability of a barrel for combat use in fighter planes showed convincingly the remarkable potentialities of the stellite-lined barrel.

22.3.4 Adoption for Service Use

As a result of the very favorable acceptance test results on the 200 stellite-lined barrels prepared by Division 1 on the firing schedules just described, the stellite-lined caliber .50 aircraft machine gun was adopted as standard for Service use. At a meeting of the Ordnance Committee[294] on January 4, 1945 approval was given to recommendations that "Barrel (D-7161580) having a stellite liner be approved for manufacture as the preferred design for use in Gun, Machine, Browning, Caliber .50, M2, Aircraft, Basic; Gun, Machine, Caliber .50, T36, Aircraft, Basic; and Gun, Machine, Caliber .50, T25E3, Aircraft, Basic" and that "The Barrel Assembly presently in manufacture[h] (D-28272) be produced only in such quantity as may be required to balance the Army Supply Program, for the Gun, Machine, Caliber .50, M2, Aircraft, Basic; provided that production of Barrel Assembly (D-28272) shall terminate at such time as requirements can be met by the preferred types."[i]

22.3.5 Pilot Plant Production of Barrels for Extended Service Tests in Combat

The first accuracy and velocity firings on stellite-lined barrels by Division 1 and all subsequent tests by the Ordnance Department[319] were so favorable that it was imperative to develop efficient means of manufacture and to prepare barrels for extended Service tests in combat areas at the earliest possible moment. A very large number of regular steel barrels was available for modification in the fall of 1944. The process of inserting stellite liners in regular steel barrels that had been developed by the Crane Company[80] offered the best opportunity for immediate utilization of these barrels. This process is illustrated in Figure 9. Much of the success achieved was due to the selective fitting of ground liners with recessed barrels, for which careful gauging, such as shown in Figure 10, was required.

The facilities used at the Crane Company (under Contract OEMsr-629) for making the 212 barrels for acceptance tests were expanded and an experimental production line was set up under a separate OSRD contract (OEMsr-1414) to develop efficient means of manufacture and prepare and deliver 2,000 stellite-lined barrels for combat tests. This work was completed in slightly over 2 months on January 13, 1945, and these facilities were then taken over by the Ordnance Department under an Army production contract. The 2,000 barrels were widely distributed to different theaters of operation, especially in the Pacific areas, and tested under combat conditions. Informal reports of these tests confirmed the great superiority of this barrel over the standard steel barrel. Some of the barrels were tested by the Army Air Forces.[299]

[h] The standard steel barrel.

[i] At this same meeting of the Ordnance Committee, the barrel (D-716948) having choked-muzzle chromium plate over a nitrided steel bore (developed by Division 1, as described in Chapter 23) was approved for manufacture as an alternate standard to stellite-lined barrels.

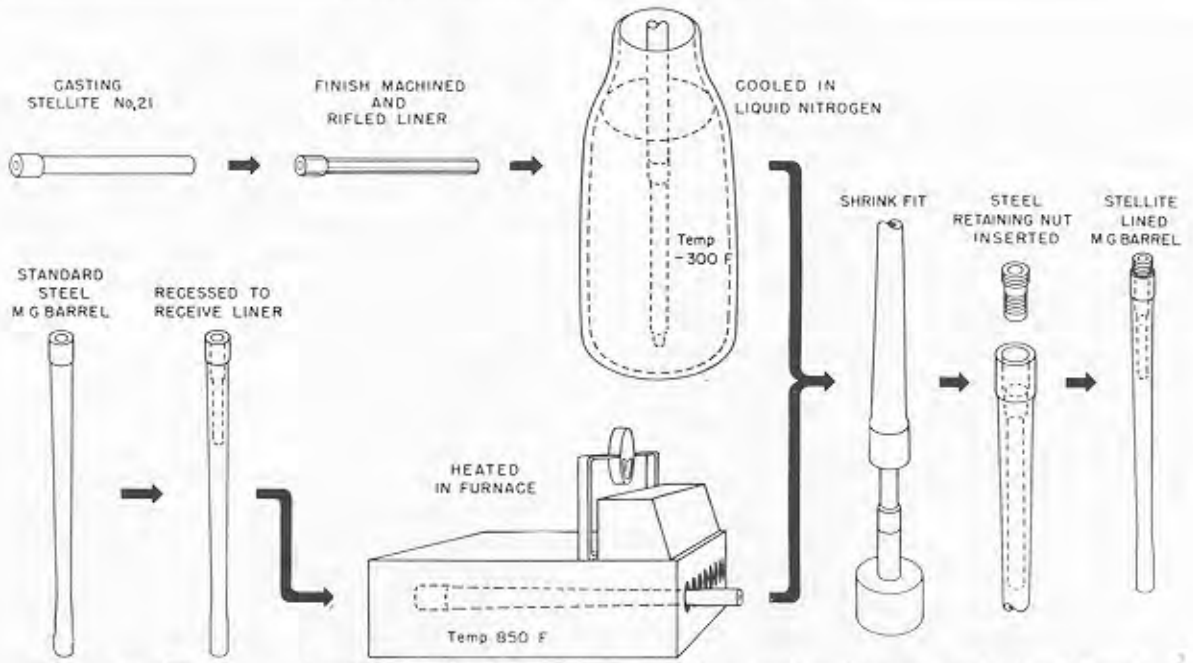


FIGURE 9. The process of making a stellite-lined caliber .50 machine gun barrel from a standard steel barrel.

Very early in the stellite liner development it was recognized by Division 1 that a method of manufacture of stellite-lined barrels starting with barrel forgings was needed. Hence, negotiations with several machine gun barrel manufacturers for development of a suitable means of doing so were initiated soon after the first successful accuracy and velocity firings were made. Before there was time for a contract to be negotiated, the Ordnance Department had decided to undertake this phase of the development. The gun barrel manufacturers, however, were reluctant to try such a radical departure from current manufacturing methods and were dubious concerning the practicability of machining operations on stellite.



FIGURE 10. Gauging of the diameters of rifled stellite liners which have been finish-ground to fit the tube recesses in the caliber .50 machine gun barrels. (Figure 11 of NDRC Report A-447.)

Accordingly, the Ordnance Department arranged a conference on October 10, 1944, at the Philadelphia Office of Division 1 which was attended by representatives of all the prospective manufacturers of stellite-lined barrels. Representatives of the Division 1 staff and the Crane Company described the development of stellite liners and explained the procedures in use at Crane Company for pilot plant production. Further assistance was rendered to the Ordnance Department by having Crane Company supply detailed drawings of the special tools and operations to all prospective Ordnance contractors for stellite-lined barrels and by having representatives of prospective contractors visit and inspect the pilot plant production at Crane Company.

The development of the procedures in use at Crane Company and a statistical analysis of the pilot plant production record on the 2,000 stellite-lined barrels are described in detail in a NDRC Report.[119] This

CONFIDENTIAL

pilot plant production determined the best tools, machines, and sequence of operations for the recessing of steel barrels, boring and rifling of the liners, insertion of liners and alignment of rifling of the liner and rifled steel bore, preparation and chambering of the steel retaining nut, maintenance of tolerances and development of suitable inspection methods at all stages of the process and for the finished barrels. This demonstration at the Crane Company pilot plant of the practicability of manufacture of these barrels was an important contribution to the success of the stellite-lined barrel development.

22.3.6 Studies to Facilitate Manufacturing Methods

In order to facilitate the manufacture of stellite-lined barrels so that significant numbers of these barrels would get into immediate combat use, and also to insure the best utilization of Stellite No. 21 as a bore-surface material, the research and development program of Division 1 included studies of the current manufacturing method and alternate methods of applying this alloy as a liner or lining as well as the effects of various factors, such as variations in chemical composition, casting methods, heat treatment, mechanical-working, liner length, and thickness of liner wall, on the overall performance of lined barrels.

In a few cases (only three were reported) the tack weld, used to prevent the steel retaining nut behind the stellite liner from unscrewing because of the vibration during firing, was brittle and the weld broke. In order to insure the reliability of this weld, studies of the welding process were made[80] which resulted in procedures that gave completely satisfactory welds. Studies were made of the effects of grinding versus reaming on the surface finish of the chamber,[80] of stellite-steel composite liners[89] (to eliminate the need for a retaining nut) and of the pressure bonding of stellite to steel.[89]

The methods for applying Stellite No. 21 to gun barrels by various infusion, incasting, and torch deposition methods have already been described (Section 19.4.3) and alternate methods of liner insertion including swaging into place, brazing, thermit (Al-Fin) bonding, and the Kelsey-Hayes method are described later (Section 26.2) when liner and other design features of gun tubes are discussed. The effects of various metallurgical factors on performance have already been discussed in Section 19.4.5.

22.3.7 Liner Salvage

Because of the possibility of a critical shortage of cobalt, the Ordnance Department informally requested Division 1 to investigate methods for the salvage of stellite liners from worn barrels. Crane Company investigated several methods[80] and found that (1) liners may be readily salvaged by the use of an oxy-acetylene cutting torch to cut the steel surrounding the liner into two sections (properly regulated depth of cut does not damage the liner); (2) pressing-out the liner by means of a hydraulic press at room temperature is unsatisfactory because of the excessive loads required; and (3) heating the outside of the barrel inductively and passing cold water through the bore enables most liners to be removed manually by means of a special extractor. The last method requires further study.

22.4 APPLICATION OF STELLITE LINER TO THE CALIBER .50 HEAVY BARREL

22.4.1 Preparation of Barrels and Test Results

Although the first firing tests of Stellite No. 21 as a liner material were conducted in a caliber .50 heavy machine gun barrel (see Section 22.2.2) major attention was given by Division 1 to the application of this liner material to improve the performance of the caliber .50 aircraft barrel because of the more urgent need for immediate improvement of this light (10 lb) barrel. The high level of performance of stellite-lined aircraft barrels described in Sections 22.3.3 and 22.2.2 made it desirable to ascertain the effects of such a liner on the life and performance of the heavy (28 lb) barrel used with the ground machine gun.

The Ordnance Department received a request from Headquarters, Army Ground Forces, submitted through Headquarters, Army Service Forces, for eight stellite-lined heavy machine gun barrels, four of them for test by the Antiaircraft Artillery Board and four by the Infantry Board. A total of 15 barrels was supplied by Division 1 for these tests and additional tests by the Ordnance Department, Army Service Forces. The results[295] are summarized in Table 1. They showed that inserting a stellite liner in the caliber .50 heavy barrel provides a considerable increase in accuracy life and for all practical purposes under normal firing conditions eliminates velocity drop as a consideration in the life of the heavy machine gun barrel.



TABLE 1. Army erosion tests on caliber .50 heavy machine gun barrels. R: regular steel barrel; L: regular steel barrel containing a 9-in. liner of investment-cast Stellite No. 21.[295]

Schedule		Barrel	Life (rounds)	Reason for end of life	Vel. drop (fps)
Burst (rounds)	Cooling* (min)				
100	2	R	885	Tipping	155
		L	1191	Tipping	26
5 × 100†	1;5	R	1000	Tipping	183
		L	2000	Tipping	1
200	1 or 2	R	1929	Keyholing	142
		L	10554	Keyholing	124
200	Complete	R	3812	Vel. drop and dispersion	199
		L	10225	Dispersion	2

* Cooling in still air between bursts.

† Five 100-round bursts with 1-min cooling between bursts and complete cooling after every 500 rounds.

22.4.2 Adoption for Service Use

As a result of these favorable firing results on barrels prepared by Division 1, the stellite-lined caliber .50 heavy machine gun barrel was adopted for Service use. At a meeting of the Ordnance Committee[295,298] on May 31, 1945, recommendations were approved that "the barrel assembly (D-7161814) having a stellite liner be approved for immediate manufacture as the preferred design for use in Gun, Machine, Browning, Caliber .50, M2, Heavy Barrel, and that these barrels be marked in a distinctive manner," that "the Stellite lined barrel (D-7161814) be placed in production as expeditiously as possible and supersede the Barrel (D 28253-A) presently in manufacture," and that "The Stellite lined barrels (D-7161814) be furnished one for each active caliber .50 M2 HB Gun, plus sufficient spare barrels to cover replacements."

Shortly after its adoption, contracts were awarded by the Ordnance Department to Crane Company and several other barrel manufacturers for the modification of regular steel heavy barrels by the insertion of 9-in. liners of investment-cast Stellite No. 21.

22.4.3 Studies to Obtain Additional Performance

Good evidence is presented later in this report (see Chapter 24) that the performance of aircraft machine gun barrels can be greatly enhanced by combinations of two or more of the following features (1) Stellite No. 21 breech liner, (2) choked-muzzle chromium plating of the steel bore surface ahead of the liner, (3) changes in the weight and external contour (distribution of weight) of the barrel, (4) use of an improved barrel steel with better high-temperature properties than regular WD 4150 machine gun steel, and (5) the use of internal or external barrel cooling methods.

Studies were initiated by Division 1 at Crane Company to evaluate the effects of such combinations on the performance of the caliber .50 heavy machine gun barrel. Thirty regular caliber .50 heavy (28 lb) barrels were modified by the insertion of regular 9-in. liners of investment-cast Stellite No. 21 and 12 additional barrels were prepared with both the liner and choked-muzzle chromium plating ahead of the liner. These barrels were to be used for a study of the effects of plate plus liner with and without variations in the weight and contour. No firing tests were made on these barrels before the termination of the experimental work of Division 1. Crane Company continued these studies under an Ordnance Department research and development contract.

22.5 APPLICATION OF A STELLITE LINER TO CALIBER .30 BARRELS

22.5.1 Development of the Design and Manufacture

As the result of an urgent request from the Army Ground Forces to the Ordnance Department, Division 1 was asked to apply a liner of Stellite No. 21 to caliber .30 machine gun barrels. Crane Company was asked to prepare a design for the application of a stellite liner to the caliber .30 aircraft machine gun barrel, M2, and to prepare a few barrels to test the design. This design was essentially similar to that employed for caliber .50 barrels (see Figure 1). In this case, however, the flanged investment-cast liner was lighter and was 6 inches in overall length. Two barrels tested at the Crane firing range showed that the design was satisfactory and that these stellite-lined barrels were far superior in accuracy and velocity life to standard unlined barrels tested for comparison. Crane Company delivered ten additional barrels for Ordnance Department tests.

It was desirable to supply the Ground Forces for immediate use improved barrels with as low a barrel weight as practical. Test results were needed on three caliber .30 barrels—those used in aircraft M2, the M1919A6 and the M1917A1 guns, with barrel weights of approximately 3.8, 4.5, and 3 lb, respec-

tively. The last barrel is normally used in a water-cooled gun but was to be tested for use without water-cooling in the M1919A6 or M1919A4 gun by means of an adapter. To expedite early Service application if results of test were satisfactory, Division 1 negotiated contracts with two caliber .30 barrel manufacturers (Johnson Automatics Company and Remington Arms Company) to apply a stellite liner "by a practical method" and deliver barrels for test by the Ordnance Department.

Each of the contractors inserted stellite liners supplied by the Haynes Stellite Company in 50 aircraft M2 barrels, 50 M1919A6 barrels, and 25 M1917A1 barrels, and delivered the lined barrels for Ordnance Department tests. Some preliminary testing of barrels was done by each contractor to prove up various new design features and indicate the order of magnitude of the superiority of lined barrels over standard steel barrels. The designs and methods used by these contractors are described later in this report (Sections 26.2.3 and 26.2.4) where liner and design features of gun tubes are discussed more fully.

In addition to the efforts just described, Division 1 cooperated with the Small Arms Division, Research and Development Service of the Ordnance Department in the following ways. Crane Company was asked to insert stellite liners and deliver three barrels for a Garand-type caliber .30 automatic rifle. No information has been received by Division 1 on the results of tests on these barrels. The Johnson Automatics Company was asked to prepare 12 lined barrels for the Johnson light machine gun M1945, 4 lined barrels M1919A6 modified for interchangeable adaption with the M1919A4 gun using the T27 flash hider and muzzle cap, and 6 lined M1919A6 barrels modified by maintaining the maximum dimension at the breech forward to a point 2 in. beyond the liner.

22.5.2 Test Results

The results[127] of firing tests conducted for Division 1 at Johnson Automatics Company on stellite-lined caliber .30 machine gun barrels may be summarized as follows:

M2 Aircraft: In a continuous burst of 500 rounds at 1,200 rounds per minute, the lined barrel was accurate throughout the 500 rounds, whereas the standard steel barrel showed complete keyholing at 360 rounds. In 250-round bursts at 1,200 rpm with 15 min air cooling, the lined barrel lasted 5,000 rounds, the standard barrel 1,200 rounds. In 300-round bursts at 800 rpm with 2 min air cooling, the lined barrels lasted 950 rounds, the standard barrels 450 rounds.

M1919A6: In 250-round bursts at 550 to 600 rpm with 2 min air cooling, the lined barrels lasted 750 to 800 rounds, the standard barrels 350 rounds. In 100-round bursts with 30 sec air cooling, the lined barrel lasted 1,800 rounds, the standard barrel 950 rounds.

M1917A1: When a 3-lb lined barrel was fired in the air-cooled M1919A4 gun with an adapter, on a schedule of 250-round bursts with 2 min cooling in comparison with the 7.5-lb heavy M1919A4 standard steel barrel, each barrel had a life of 600 rounds, but the lined barrel was badly bulged in this test.

M1919A6; Modified Contour: When two lined barrels, further modified by maintaining the largest diameter of the breech to a point 2 in. beyond the liner (additional weight 0.5 lb) were fired in 250-round bursts with 2 min air cooling, they lasted over 1,150 rounds each as compared to 750 to 800 rounds with lined barrels of standard external contour.

Johnson M1945: In continuous fire at a delivered rate of 200 rpm (cyclic rate per 20-shot bursts 750 to 800 rpm) the lined barrel lasted over 700 rounds, the standard steel barrel 350 rounds.

The results[135] of firing tests conducted for Division 1 at Remington Arms Company may be summarized as follows:

M2 Aircraft: In 300-round bursts with 2 min cooling, 13 lined barrels showed an average accuracy life of 1,243 rounds. The poorest barrel had a life of 663 rounds and the best barrels had not lost accuracy when firing was discontinued after 2,000 rounds. In comparison, 11 standard steel barrels averaged 486 rounds accuracy life on this schedule (poorest 400, best 726 rounds).

M1917A1: Seven lined barrels when fired in the M1917A1 water-cooled gun with no water in the jacket on the schedule of 300-round bursts with 2 min cooling gave a life of between 300 and 600 rounds (average 483 rounds). These barrels all failed due to bulging of the barrel at the muzzle end of the liner. The standard steel barrels failed for accuracy between 230 and 440 rounds (average 312). Improved performance (average accuracy life 635 rounds) and no bulging occurred in a test of four lined barrels prepared with a straight cylindrical stellite liner with 0.430-in. outside diameter.

The results of Ordnance Department tests[297,320] on the stellite-lined M1919A6 barrels are given here as Table 2. These data indicate that the stellite-lined caliber .30 barrel has an accuracy life two to three

[redacted]

TABLE 2. Summary of result of Ordnance Department firing tests of stellite-lined caliber .30 machine gun barrels, M1919A6, supplied by Division 1, NDRC, compared with unlined barrels.

Firing cycle Burst (rounds)	Firing cycle Cooling* (sec)	Kind of barrel	Number barrels fired	Accuracy-life† (rounds)	Velocity change (fps)
20	10	Lined	2	1700	+31
		Unlined	3	613	−55
200	120	Lined	2	1080	
		Unlined	3	583	
300	120	Lined	5	759	+46
		Unlined	3	448	−80
400	120	Lined	2	720	
		Unlined	2	380	

* In still air.
† Rounds to serious keyholing.

times as great as that of the regular steel barrel. Furthermore, the lined barrels suffered no permanent loss in velocity but instead an appreciable increase even though the firing schedules used were extremely severe. In all tests the functioning of the guns was normal.

Just as in caliber .50 aircraft machine gun barrels (see Section 22.3.3) caliber .30 barrels with liners show a greater improvement over standard steel barrels on severe firing schedules than on mild schedules, although even on mild schedules the improvement is substantial.

22.5.3 Adoption of Lined M1919A6 Barrel for Service Use

As a result of the very favorable test results on the stellite-lined caliber .30 M1919A6 barrels delivered by Division 1, this barrel was adopted for Service use. At a meeting of the Ordnance Committee[297,298] on July 26, 1945, recommendations were made and approved that "The Barrel Assembly (Drawing No. D-7162295) having a Stellite liner be approved for immediate manufacture as the preferred design for use in Gun, Machine, Caliber .30, Browning, M1919A6, and that these barrels be marked in a distinctive manner, and issued with highest priority to units now in combat," that "The Stellite-lined Barrel (D-7162295) be placed in production as expeditiously as possible and supersede the Barrel[i] (D-54559) presently in manufacture," and that "The Stellite-lined barrels (D-7162295) be furnished one for each active M1919A6 caliber .30 Machine Gun, plus sufficient spare barrels to cover replacements." Plans for large-scale manufacture were initiated but were not carried out owing to cutbacks in the procurement program following V-J Day.

Although the performance of the caliber .30 machine gun barrel, aircraft, M2, was substantially increased by the use of a stellite liner, this weapon was obsolete for aircraft armament and had been supplanted by the caliber .50 aircraft machine gun with its superior fire power. The immediate use of caliber .30 aircraft barrels by Ground Forces would require a modification of mounts and would necessitate a large procurement and supply program for guns, mounts and other accessories and delay the use of improved barrels by Ground Forces in combat. The tests on the very light (3 lb) caliber .30 M1917A1 barrel with a liner had shown failure by bulging due to overheating, aggravated by the thinness of the steel barrel wall at the forward end of the liner.

Studies of the application of the stellite liner to automatic rifles and other caliber .30 barrels was continued by the Ordnance Department at Crane Company after Division 1's contract was terminated.

22.6 APPLICATION OF A STELLITE LINER TO THE CALIBER .60 BARREL

22.6.1 Design and Performance

During World War II, the Ordnance Department was developing a new aircraft machine gun with a caliber .60 bore, a high cyclic rate of fire, and a very high projectile velocity (slightly above 3,500 fps) to deliver more fire power at higher velocities than in any previous aircraft weapons. In early tests the Ordnance Department found that steel barrels would survive only a few hundred rounds owing to severe breech erosion and very rapid loss in velocity life. Since a considerable improvement in barrel life was imperative in order to make the weapon practical, the Ordnance Department requested Division 1 to apply a stellite liner to this barrel.

Crane Company suggested a design for the insertion of a 12-in. length flanged breech liner of Stellite No. 21 on a shrink-fit, a design essentially similar to that successfully used in the caliber .50 aircraft machine gun barrel (see Section 22.2) and prepared some lined barrels. Tests at Aberdeen Proving Ground of the first two lined barrels showed the outstanding performance of these barrels. On the same test schedule as previously used on regular steel barrels for this gun, after 500 rounds (standard

[i] Standard steel barrel for caliber .30 gun M1919A6.

ammunition with IMR powder) a velocity drop of only 30 fps occurred with the lined barrels instead of one of 400 fps which had been encountered with steel barrels. Also on this schedule the lined barrels showed a 200-fps velocity drop only after about 2,000 rounds. No inaccuracy was encountered. Thus the use of a stellite liner in this barrel increased the life about sixfold on a mild schedule and made possible the firing of 50-round bursts, which were entirely too severe for a steel barrel. Crane Company prepared and delivered a total of 70 stellite-lined barrels for this gun, some of them with fluted chambers as described below. The stellite-lined barrel completely supplanted steel barrels for this weapon.

In addition to the regular caliber .60 barrels, Division 1 cooperated with the Ordnance Department by having Crane Company insert stellite liners into six Mann barrels (three of which were provided with cut flutes in the chambers) for tests at Frankford Arsenal to determine the effect of erosion ahead of the liner on the performance of explosive ammunition and on liners inserted in two barrels of an experimental model, caliber .60, T2E4. Difficulties with ammunition prevented the satisfactory testing of these last two barrels.

In view of the success obtained with caliber .50 aircraft barrels by a combination of stellite liner with chromium-plating ahead of the liner (described in Chapter 24), two caliber .60 barrels were prepared with both a stellite liner and chromium plate ahead of the liner, and delivered to the Ordnance Department.

22.6.2 Chamber Fluting

Difficulties with the gun mechanism and ammunition prevented early Service use of caliber .60 barrels with a liner. During the firing of caliber .60 barrels[k] considerable difficulty with extraction of cartridge cases was encountered. The Ordnance Department found it necessary to provide longitudinal flutes in the forward half of the chamber to admit gas behind the cartridge case to aid in releasing it after firing.

[k] All firing tests on caliber .60 barrels were conducted by the Ordnance Department and none were made by Division 1, NDRC, who supplied lined barrels for test.

Fifty-three of the total 70 lined barrels delivered for test by Crane Company just described were fitted with steel retaining nuts made from the fluted chambers of regular steel barrels. The chamber section of the liners in these barrels were fluted by a punch-type of tool, and the retainers of all but the first two barrels were pinned to prevent rotation.

During the testing of lined barrels with fluted chambers, it became evident that the number and depth of flutes then being used were not necessarily the most suitable for the purpose and that there was an urgent need for further tests to determine optimum flute dimensions. Crane Company designed and constructed a special hand-operated fluting tool with which the flute dimensions could be varied at will. In tests at Aberdeen Proving Ground of flutes in ten unlined barrels prepared at Crane Company by the use of this tool, only the barrels with 16 flutes 0.040-in. deep could be extracted without failure. Subsequently lined barrels with similar flutes were sent to the Ordnance Department for test.

22.6.3 Liner with Integral Chamber

Machining difficulties encountered in fluting of composite steel-stellite chambers and difficulties with the erosion that was found to occur in fluted steel chambers led to the design at Crane Company of an integral liner and chamber made of investment-cast Stellite No. 21. In this design the liner flange or shoulder is extended to the breech end of the barrel and no steel retainer is used. This design should have the advantages of easier fluting, no joint in the chamber, erosion-resistant flutes, simplified machining through elimination of the retainer, possibility of precision casting the flutes into the chamber, and the possibility of eliminating the flutes entirely because of the lower coefficient of friction of stellite. Investment-cast liners were prepared by the Haynes Stellite Company under Contract OEMsr-1330 and delivered to Crane Company for insertion into caliber .60 barrels under Contract OEMsr-629. The preparation of the lined barrels was started but not completed before termination of experimental work by Division 1. Some of these barrels should be completed and tested.

Chapter 23

NITRIDED AND CHROMIUM-PLATED MACHINE GUN BARRELS[a]

By *E. F. Osborn*[b]

23.1 DEVELOPMENT OF THE NITRIDED, CHROMIUM-PLATED CALIBER .50 AIRCRAFT BARREL WITH CHOKED MUZZLE

23.1.1 Introduction

DIVISION 1 pursued two parallel problems for the improvement of machine gun barrels by the application of erosion-resistant materials. The development of barrels with a stellite liner has just been described in Chapter 22. Similar success with caliber .50 aircraft barrels was achieved by use of chromium electroplate on a hardened steel bore. The development by the Geophysical Laboratory and the National Bureau of Standards of the nitrided, chromium-plated caliber .50 aircraft barrel with a choked muzzle is described in this chapter. Both barrels were adopted[294,296] at the same time to supersede the regular steel barrel for Service use, the stellite-lined as the preferred barrel and the nitrided and chromium-plated barrel as an alternate. The need of our Air Forces and those of our allies for an improved caliber .50 aircraft barrel which would fire accurately throughout long bursts of rapid fire is discussed in Chapter 22.

As soon as Division 1 became fully aware of this need, which was early in 1944, the development of the two types of improved barrels was initiated and proceeded rapidly as a result of its previous research on the fundamental aspects of erosion of steel and chromium-plated steel guns and on means of mitigating erosion by the use of erosion-resistant materials. Pilot plant production of the improved barrels was undertaken by the W. B. Jarvis Co.,[c] as described in Chapter 25.

Experiments with plated steel liners in the caliber .50 heavy barrel[d] showed that if chromium plate, which has excellent erosion resistance, was to remain near the origin of rifling long enough to improve the velocity-life of this barrel, the metal of the lands under the chromium had to be more resistant to swaging (Section 10.5.3.) than WD 4150 steel.[80,85] Improvement in this respect was obtained by hardening this same steel by nitriding. One big advantage of using WD 4150 steel in the development of improved barrels was that a large stockpile of barrels made of this steel was on hand. By nitriding and properly chromium-plating them, an improved barrel could therefore be obtained through the use of existing stocks.

Experiments with plated steel liners in the heavy barrel had shown that the softer, LC (low contraction) chromium resisted removal better than the hard, HC (high contraction) chromium,[e] as mentioned in Section 16.3.8. Adhesion of this soft plate to steel, however, when applied to the full length of the aircraft barrel, was never consistently good, and it was removed from the bore as rapidly, or often more rapidly, than the hard chromium, which was therefore standardized for the aircraft barrel.

Inasmuch as neither nitriding nor chromium-plating involved critical processes or materials, it was decided to treat the full length of the aircraft barrel rather than use a liner. The principal steps in the process of transforming a standard, steel caliber .50 machine gun barrel into a nitrided and chromium-plated barrel with a choked muzzle are illustrated in Figure 1.

It was found that the main improvement of this aircraft barrel was in accuracy-life, as is brought out in Section 23.1.4. The accuracy-life was improved largely because the muzzle section of the bore was choked and because this choke remained on firing owing to the lack of erosion of the chromium surface. In addition, the velocity-life was improved when severe firing schedules were used because chromium stayed on the bore surface at the origin of rifling long enough to serve as a protection to the steel, and because nitriding of the steel minimized swaging of the lands.

[a] This chapter has been prepared by C. A. Marsh by arrangement of appropriate sections from NDRC Report A-409[81] by E. F. Osborn, following an outline suggested by J. F. Schairer.

[b] Petrologist, Geophysical Laboratory, Carnegie Institution of Washington. (Present address: Department of Earth Sciences, Pennsylvania State College, State College, Pa.)

[c] Now the Jarvis Division of the Doebler-Jarvis Corporation.

[d] "Heavy" and "aircraft" caliber .50 barrels are defined in Section 11.2.2.

[e] For the properties of the different types of chromium plate see Section 20.2.2.



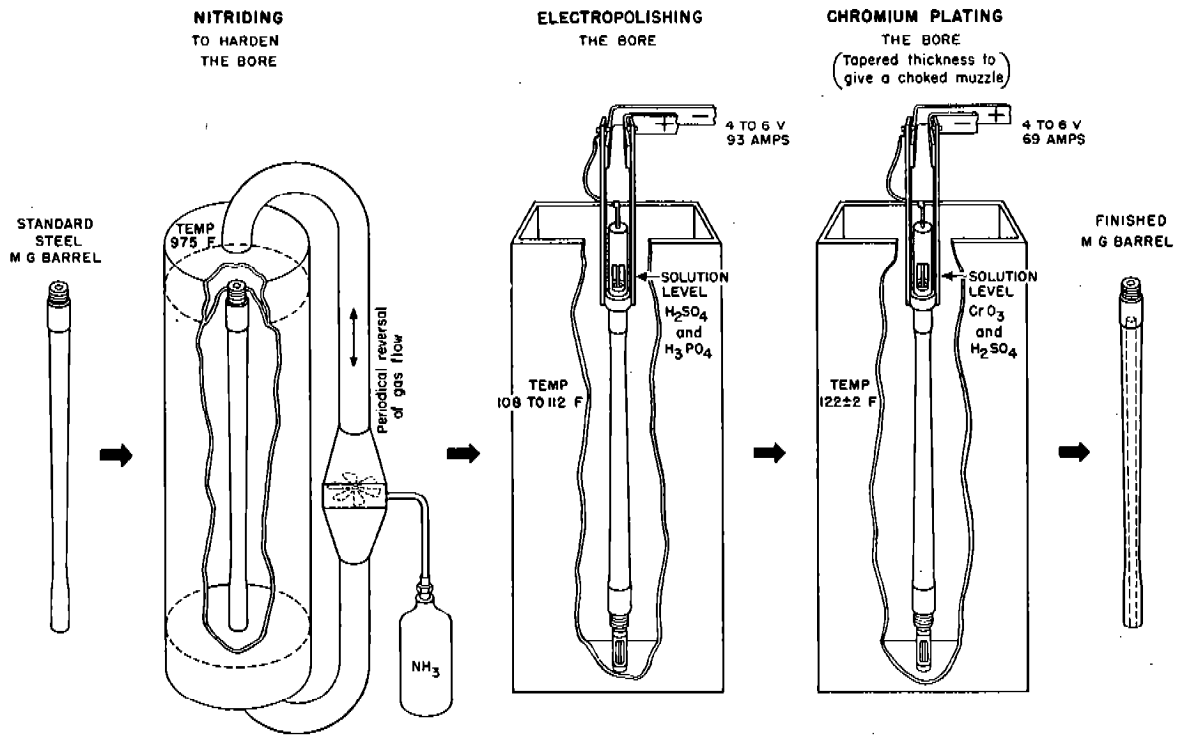


FIGURE 1. The process of making a nitrided and chromium-plated caliber .50 machine gun barrel.

23.1.2 Development of Specifications for Nitrided and Chromium-Plated Barrels

DIMENSIONS

Interior dimensions of the finished nitrided, chromium-plated barrels were continually changed as research continued, the changes being made either to improve the performance of the barrel or to simplify production where the change did not adversely affect performance. The trend of the changes was to decrease the bore diameter at the muzzle and to increase it at the breech, and to increase the tolerance at the muzzle end. The development of the final specifications for dimensions is given in detail in Section 25.2.2.

NITRIDING

Nitriding of the barrels was done by both gas (ammonia) and liquid-immersion methods, the former being used exclusively in production during the war. Research was done on various times and temperatures of nitriding.[109,110] Nitriding, by a cycle common at the Link Belt Company, Philadelphia, was adopted as being satisfactory. The barrels, standing vertically, were held at 950 F for 38 hr. All surfaces of the barrel were nitrided. The hard case on the outside was actually a slight advantage, adding a little strength to the barrel. The incidental nitriding of the breech threads or the chamber was found to be no disadvantage.

Before nitriding, the barrel was cleaned free of grease and decoppered if it had been proof-fired. Later, the barrels to be chromium plated at the pilot plant described in Chapter 25 were also tested for hardness and straightness prior to nitriding; if the hardness on the outside was below 28 Rockwell C, the barrel was not used. In the initial experimental plating a stress-relieving procedure preceding nitriding was used, but this was abandoned when it was found to be of no significant advantage.

Inasmuch as nitriding processes differ somewhat from plant to plant, and the initial hardness and composition of the steel affects the hardness and depth of the case, it was desirable to set up a specification regarding these two characteristics of a case.

In general, the higher the initial, or core, hardness of the steel, the harder is the case, both near the surface and at depth. The carbon content also affects the hardness. For initial hardness of 29 and 36 Rockwell C, the hardness of the case at 0.001 in. below the surface is of the order of 500 and 650 microvickers,

respectively, for WD 4150 steel nitrided 38 hr at 950 F.

Measurements to determine hardness and depth of case were made using the Eberbach microvickers hardness tester.[110] Using a polished cross section of the barrel, a hardness profile of the case was obtained. A typical hardness profile after nitriding 38 hr in ammonia is shown in Figure 2. The tentative specification set up was that the hardness should be a minimum of 500 VPN at a depth of 0.001 to 0.002 in. below the surface, and a minimum of 400 VPN at a depth of 0.010 in.

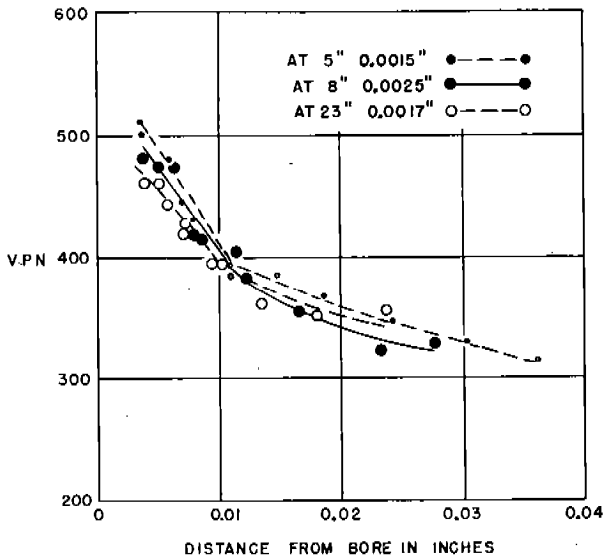


FIGURE 2. Hardness profile of nitrided case in a caliber .50 barrel before firing. Barrel No. L2-J45, nitrided 38 hours in ammonia by Link Belt Company. (This figure had accompanied the manuscript of NDRC Report A-409 but was not reproduced with that report.)

ELECTROPOLISHING AND CHROMIUM-PLATING

The procedure for electropolishing and chromium-plating caliber .50 aircraft barrels to give the bore dimensions and thickness and quality of chromium which were desired was worked out largely by the Electrochemical Section at the National Bureau of Standards[84] and is described in Chapter 20. Improvements were made by the Doehler-Jarvis Corporation during the pilot-plant stage in which an extensive research program was carried out to try to evaluate the importance of various steps in the plating procedure. Before large-scale production got under way with the attendant, necessary freezing of the procedure, it was desirable to eliminate all steps found to be unnecessary, change any of the steps in the direction of improving the adhesion of the chromium, and evaluate the criticalness of the various specifications. On the basis of this research, described in Section 25.2, the final specifications and procedure were established.

23.1.3 Firing Tests

FIRING SCHEDULES[f]

Firing schedules are always a compromise if one wants to obtain all possible information on a barrel. If, for example, one fires a continuous burst to keyholing,[g] he learns only at what stage bullets begin to keyhole. Inasmuch as the test is not interrupted until the barrel is essentially worn out, there is no chance for observing progressive erosion in the barrel and for obtaining other valuable information.

In general, a barrel should be fired in a manner similar to its use in combat. But this is not always practicable or even desirable for several reasons: (1) It is very difficult to decide how a gun is typically fired in combat; the same gun may be fired very differently, for example, on an air-to-ground mission than on an air-to-air mission, or on the same type of mission in different theaters; (2) a testing schedule has to be one that can be executed in a short time; (3) a firing schedule has to be arranged so that observations can be made during the progress of the test, and many of these observations can be made only on the cold barrel.

Consequently, there are valid objections raised to every firing schedule. One has first to decide what it is most necessary to test in a barrel, then by trial find a schedule which will do this reasonably well and at the same time meet the requirements that it not be too far removed from battle practice and that it permit obtaining as much desirable additional information on the performance of the barrel as possible.

In all, 13 different firing schedules were used by the Geophysical Laboratory as the need arose at various times during its program for comparing caliber .50 barrels, and a few other tests such as a 500-round burst were used for special barrels. Each of the firing schedules was given an identifying symbol, such as 5 × 100 (2). The schedules will be briefly described

[f] Some of these same firing schedules were used in the testing of stellite-lined caliber .50 barrels, with the results given in Section 22.3.3.

[g] See footnote (e) in Chapter 22.

below, and then later they will be referred to only by symbol.

GL-135 Schedule. This was the first schedule standardized and it was used only for testing heavy barrels. This schedule was not intended necessarily to bear any relation to the manner in which the caliber .50 heavy barrel gun was fired in combat, but was carried out to obtain information on erosion which might be applicable to large antiaircraft guns. It was desired (1) to have as many of the rounds as feasible pass through the barrel while it was approximately at constant temperature; (2) to wear out a standard steel barrel within a reasonable time, the rejection limit being set at a 200-fps drop in velocity, and (3) to have the rounds fired in several similar groups of bursts so that four or five times during the test the barrel could be cooled for examination and for gauging.

After several firing trials of barrels equipped with thermocouples for measuring the temperature during firing at a point 1/16-in. from the bore surface at the origin of bore, as described in Section 5.3.6, it was decided to fire groups of 400 rounds to a total of 2,000 rounds. Each group consisted of an initial 135-round burst followed by a series of shorter bursts, the length of burst and interval between bursts being established so that in the standard barrel the temperature at the point near the origin of bore would remain, after the initial burst, between 450 and 500 C. Other points in the barrel would not, of course, necessarily remain at a constant temperature. Temperature curves for various points in the barrel during this firing schedule are shown in Figure 3.

5 × 50 (1) Schedule. A 250-round group was fired, consisting of five 50-round bursts, one burst being fired each minute. The barrel was cooled to ambient temperature and the schedule repeated.

5 × 100 (1) Schedule. Same as above except that 100-round bursts were used instead of 50-round bursts.

5 × 120 (1) Schedule. Same as above except 120-round bursts were used. This schedule, used for heavy barrels, is comparable from the standpoint of barrel temperature to the 5 × 100 (2) schedule in an aircraft barrel.

5 × 100 (2) Schedule. Groups of five 100-round bursts were fired with an interval of 2 min between the *end* of each burst and the *beginning* of the next, except that complete cooling to ambient temperature was allowed between groups.

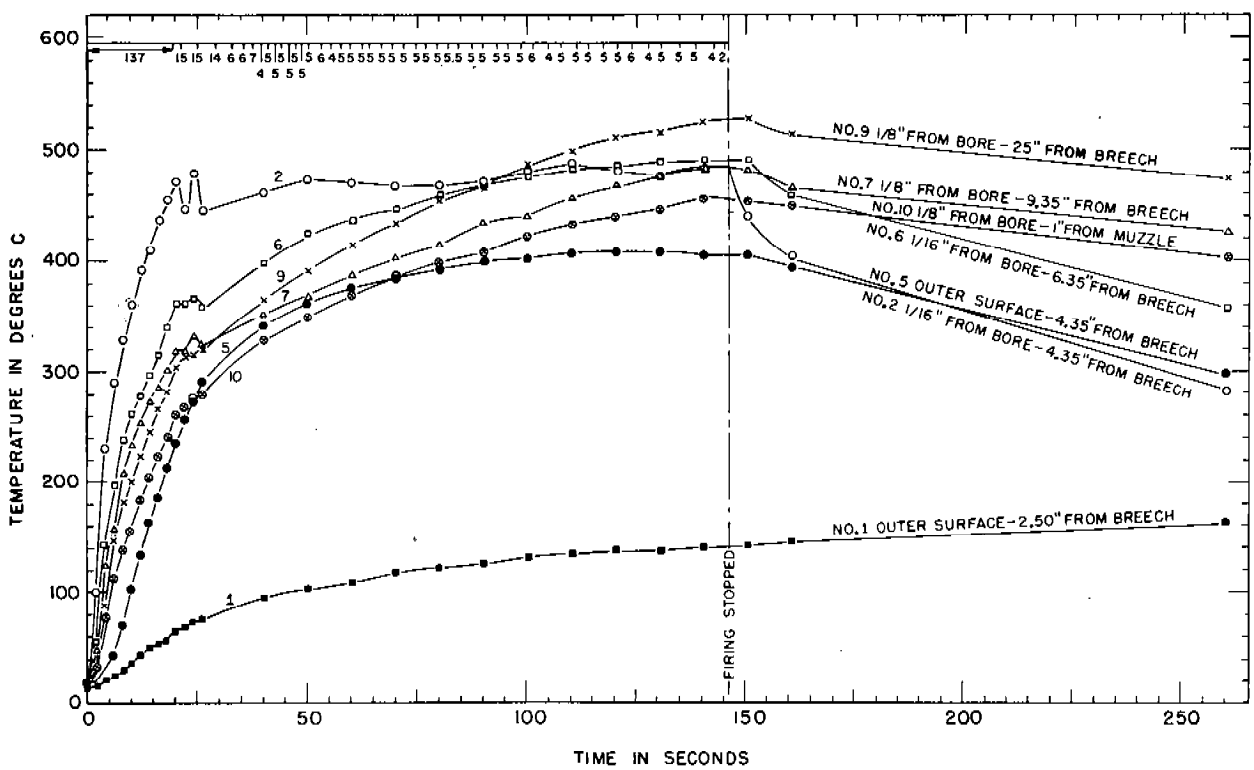


FIGURE 3. Temperature-time curves obtained during firing of GL135 schedule (400 rounds) in a caliber .50 heavy barrel. (*Note:* Number of rounds in a burst shown by scale in upper left of graph.) (Figure 5 in NDRC Report A-409.)

10 × 40 (1) Schedule. In this schedule, used commonly by the British, ten 40-round bursts were fired at 1-min intervals. The barrel was cooled and the schedule repeated.

20 × 25 (3) Schedule. Twenty 25-round bursts were fired at intervals of 3 min. The barrel was cooled to ambient temperature and the schedule repeated.

1 × 300 Schedule. A single 300-round burst was fired, the barrel cooled to ambient temperature, and the burst repeated.

1 × 150 Schedule. Same as above but with a 150-round burst.

1 × 100 Schedule. Same as above, but with a 100-round burst.

CGL-350 Schedule. This schedule consisted of an initial 350-round burst followed, after the barrel was cooled to ambient temperature, by a series of 5 × 100 (2) groups. The "CGL" stands for Crane-Geophysical Laboratory. The schedule, the development of which is described in Section 24.1.3, was used almost exclusively by these two contractors of Division 1 during the last few months of the war in testing the "combination" caliber .50 aircraft barrels described in Chapter 24.

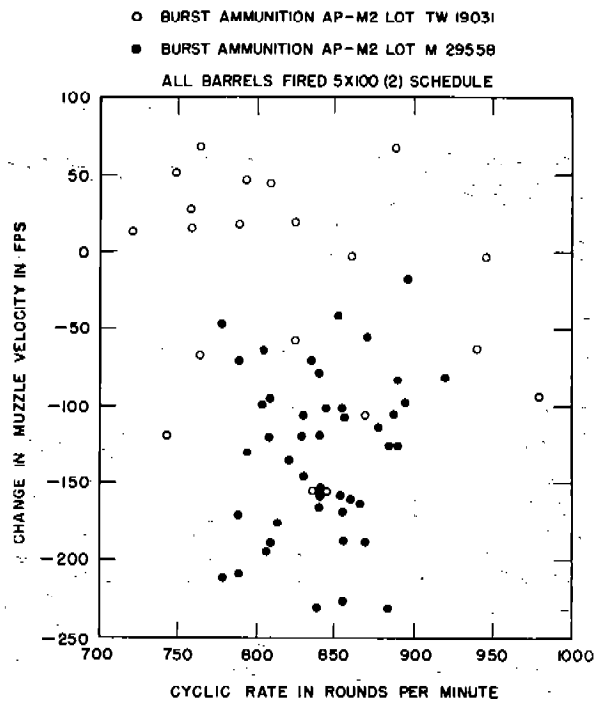


FIGURE 4. Change in muzzle velocity versus cyclic rate for nitrided, chromium-plated caliber .50 aircraft barrels with choked muzzles, fired with two different lots of ammunition. (Figure 19 in NDRC Report A-438.)

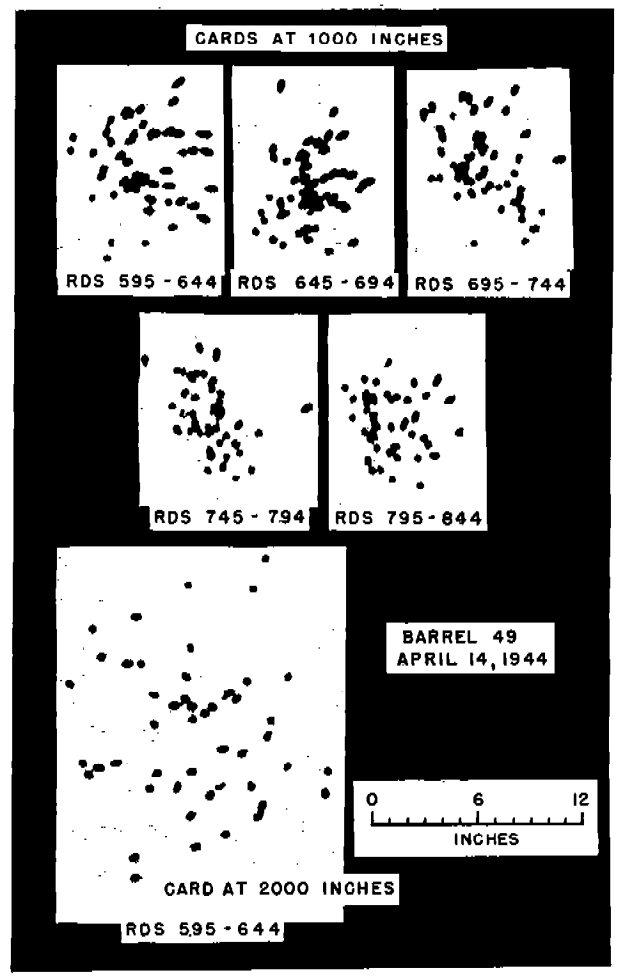


FIGURE 5. Targets for nitrided, chromium-plated caliber .50 aircraft barrel No. 49, during the third erosion group. (This figure had accompanied the manuscript of NDRC Report A-409 but was not reproduced with that report.)

C-1 Schedule.[h] The barrel was fired continuously until serious keyholing of the bullets occurred.

B-1 Schedule.[h] The barrel was fired in 100-round bursts separated by 2-min intervals until serious keyholing of the bullets occurred.

AMMUNITION

The type of caliber .50 ammunition used in testing depended on the object of the test. The following are the standard types that were used: ball-M2; armor piercing, AP-M2; armor piercing incendiary, API-M8 and API-M8E1I; incendiary, I-M1, I-M1E1,

[h] The behavior of standard steel barrels when fired according to this schedule, which is an Army Ordnance Department schedule, is described in Section 22.3.3.

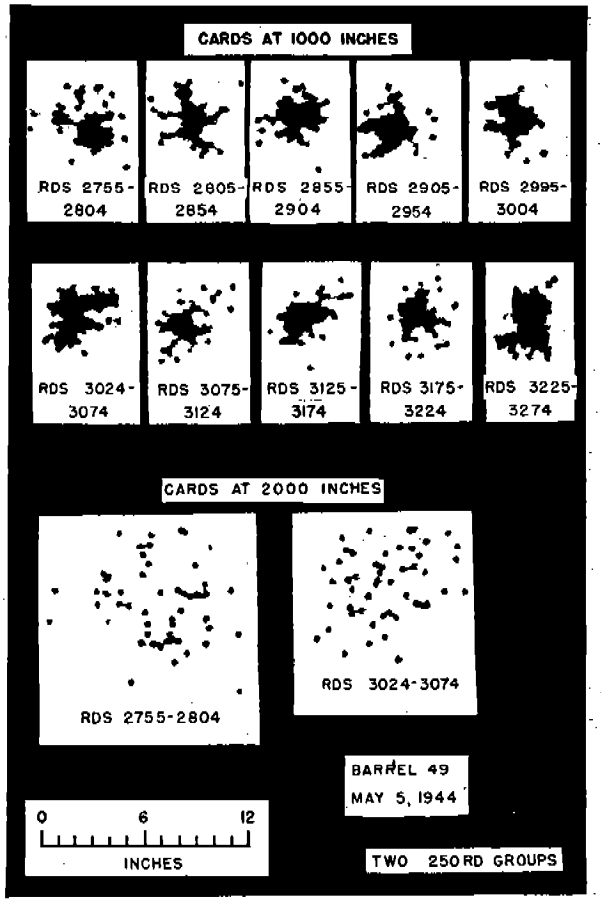


FIGURE 6. Targets for nitrided, chromium-plated caliber .50 aircraft barrel No. 49, during the eleventh and twelfth erosion groups. (This figure had accompanied the manuscript of NDRC Report A-409 but was not reproduced with that report.)

and I-M23 (experimental I-T48) tracer, Tr-M1, Tr-M10, and Tr-M10E1 Rounds designated by the suffix "E1" were loaded with double-base powder containing 20% nitroglycerin, whereas all the others were loaded with a single-base powder, namely IMR 5010, which is less erosive than the double-base powder. Several types of specially loaded ammunition were also used in some tests.

The bullets in these rounds of ammunition have gilding metal jackets, annealed or unannealed. Their different types of construction affect their resistance to engraving, and thus had a perceptible effect on the rate of erosion of the barrels that were tested. The melting and softening of the jackets at the temperatures attained during firing long bursts may definitely limit machine gun performance.

Whenever it is desired to make as accurate as possible a comparison of different barrels, a single type of ammunition and if possible a single lot of that ammunition should be used. A "combat" load, where two or three types of ammunition are used, is not to be recommended. Either ball-M2 or AP-M2 ammunition was used in most of the testing of chromium-plated barrels. Even with AP-M2 ammunition, where one might expect very little variation from lot to lot, considerable variation was found.[110] Figure 4 illustrates the effect of two factors on velocity drop. The plot of cyclic rate against velocity change possibly shows but slight correlation between rate of fire and velocity change. There is, however, a definite correlation between lot of ammunition and velocity drop.

VELOCITY MEASUREMENTS

Velocity measurements were made at the beginning of and at various stages during the firing tests by means of Aberdeen chronographs with screens at 25 and 75 ft from the muzzle. Both hot and cold velocities were determined. The former refer to measurements taken at the end of a burst before the barrel was allowed to cool, while the latter refer to measurements with the barrel at ambient temperature. The rounds used for determining the cold velocities were held at a constant temperature for a minimum of 16 hr preceding the test in order to eliminate the effect of differences in the initial powder temperature on

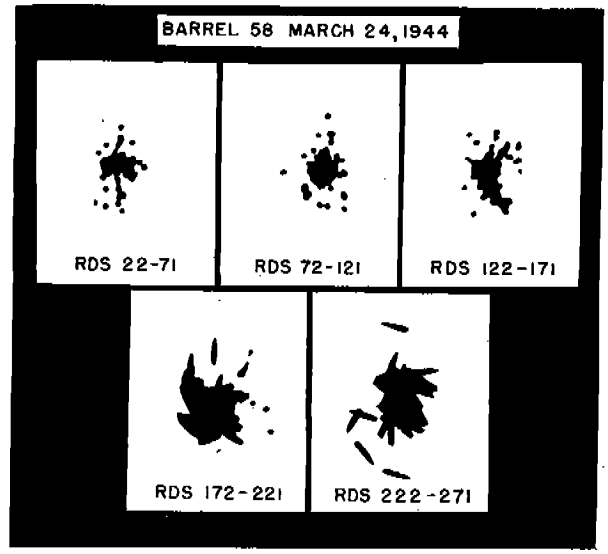


FIGURE 7. Targets for standard, caliber .50 aircraft barrel No. 58, during the first erosion group. (This figure had accompanied the manuscript of NDRC Report A-409 but was not reproduced with that report.)

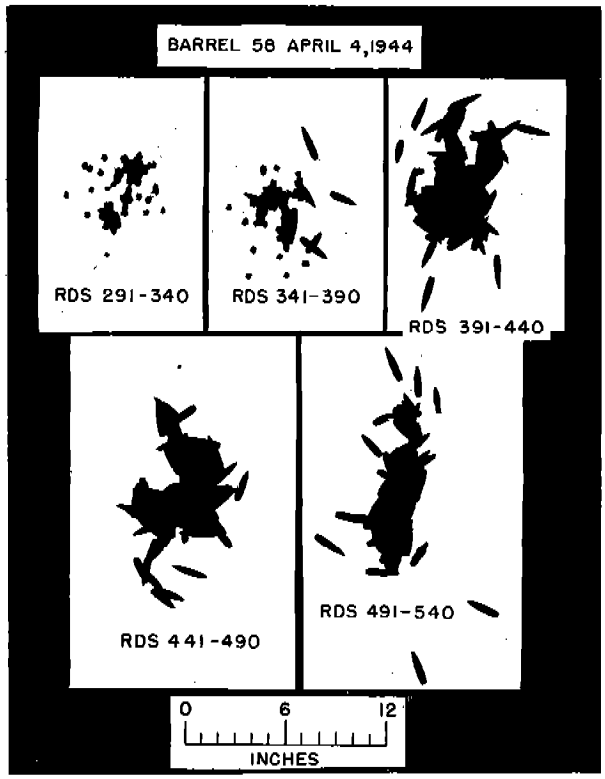


FIGURE 8. Targets for standard caliber .50 aircraft barrel No. 58, during the second erosion group. (This figure had accompanied the manuscript of NDRC Report A-409 but was not reproduced with that report.)

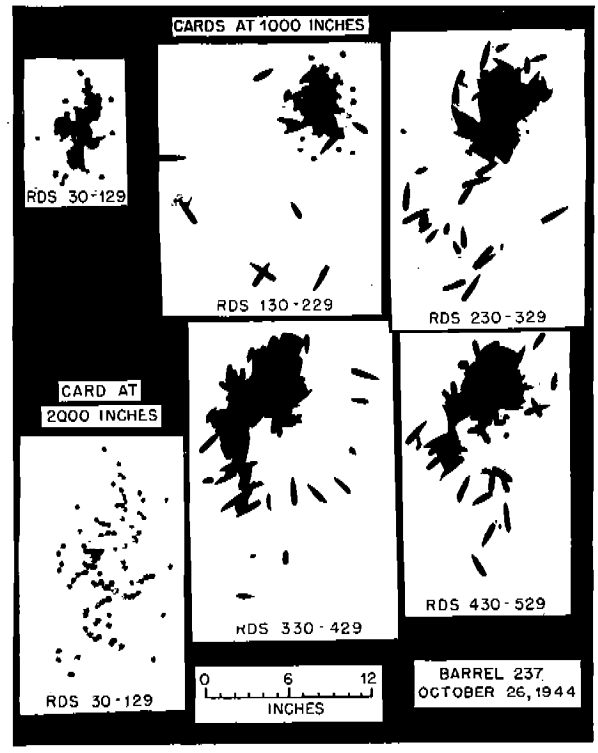


FIGURE 9. Targets for standard caliber .50 aircraft barrel No. 237. Bullets began keyholing in the second 100-round burst. (Figure 6 in NDRC Report A-409.)

velocity of the bullet. They were fired after five warm-up rounds.

ACCURACY MEASUREMENTS

Targets. The two principal measurements were dispersion, or size of target, and yaw of bullets, or angle between axis of bullet and direction of flight. The standard distance from muzzle to target was 1,000 in. A second target was sometimes placed at 2,000 in. For most firing tests, fixed targets were used. Hence, during the firing of schedules like 5 × 50 (1), 5 × 100 (2), and B-1, a new target was set up for each burst. Figures 5 through 10 are photographs of examples of such targets.

A moving screen was used whenever it was desired to know just what rounds in a burst "tipped" or "keyholed." In the recording of data, a yaw of 20 degrees, for which the length of hole is 1 in., was arbitrarily set up as a critical measurement, and the target holes were recorded as being made by bullets having a yaw of either less than or greater than 20 degrees. "Tippers" may have a yaw angle less than this.

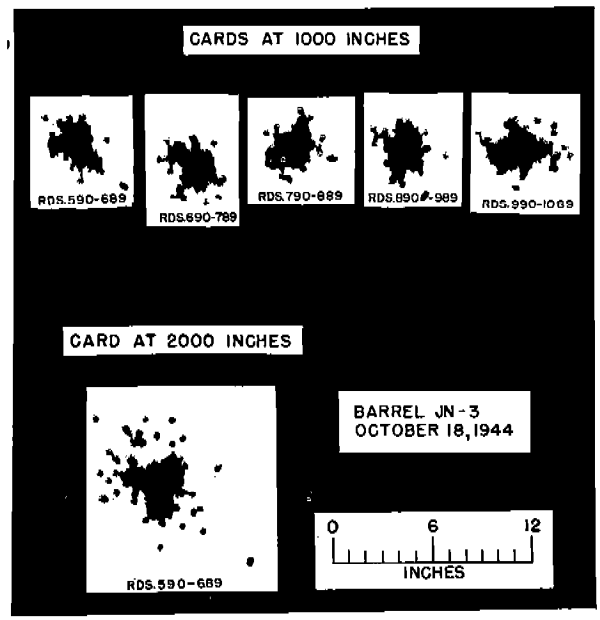


FIGURE 10. Targets for nitrided, chromium-plated caliber .50 aircraft barrel No. JN3. (Figure 7 in NDRC Report A-409.)

Collection of Bullets. A study of engraving on collected bullets often gave information that was not obtainable from target data. The angle of engraving on a bullet gives an indication of the amount of spin and therefore of the stability of the bullet. A bullet having an angle of engraving of 6 degrees (full spin) will normally straighten out even though at 1,000 in. from the muzzle it has a slight yaw. Therefore when a collected bullet has an angle of engraving of 6 degrees, it can reasonably be assumed that it was stable, even if it was yawing at 1,000 in. Examples of collected bullets are shown in Figure 11. Only the first two did not keyhole. The third keyholed even though the angle of engraving was approximately 6 degrees.

23.1.4 Performance of Nitrided and Chromium-Plated Barrels

Hundreds of firing tests were made on the nitrided, chromium-plated barrels with choked muzzles. In very few of these tests, however, were the barrels fired to the end of accuracy-life and ordinarily were not even fired to end of velocity-life, for the firing was done largely to study the effect of some change in the method of producing the barrel on the adhesion of chromium, resistance to swaging of the lands, engraving of the bullet, etc. However, enough barrels were fired to the end of life using various firing schedules that a good picture of the performance of these barrels was obtained. In addition to the barrels fired at the Geophysical Laboratory, some were fired at Aberdeen Proving Ground,[214] a large number of them were fired for the Army Ordnance Department at Purdue University,[319] and some by the British Barrel Life Panel.[406, 414–418]

Accuracy-Life

General Statement. A caliber .50 aircraft machine gun barrel is ordinarily considered to have adequate accuracy if most of the bullets of a burst do not have appreciable yaw. Accuracy-life, therefore, is determined by the point at which "serious keyholing" begins.

The outstanding characteristic of the nitrided, chromium-plated barrels with choked muzzles was their amazingly long accuracy-life. The barrel could be fired until it was red hot on the outside and until the bore from the origin to a foot or so from the muzzle was severely eroded, and still the barrel fired accurately—often firing more accurately toward the end of a long firing program than at the beginning.

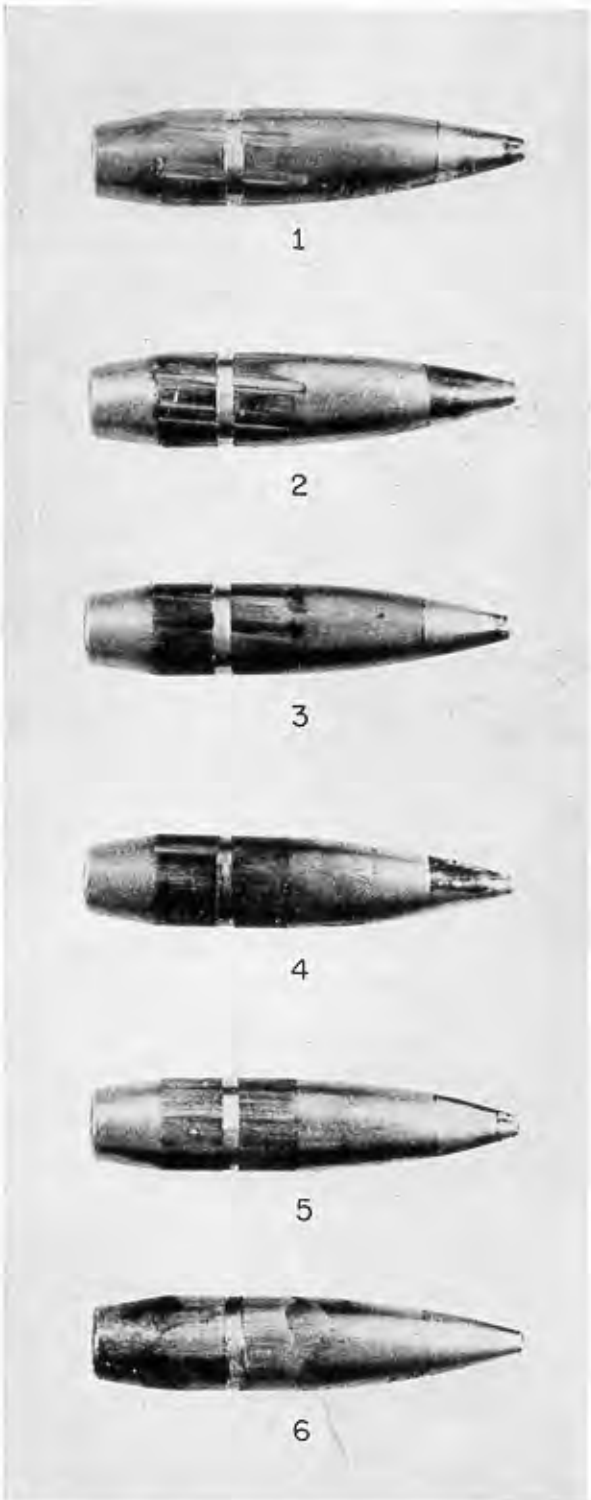


FIGURE 11. Photographs of representative caliber .50 AP-M2 bullets collected in sawdust to show variation in engraving. (Figure 9 in NDRC Report A-409.)

CONFIDENTIAL

Almost as interesting as the long accuracy-life was the consistency of performance of the barrels.

Barrels Fired on Mild Schedule. Barrel No. 49 was the first successful barrel of this type.[i] It was fired on the 5 × 50 (1) schedule approximately 4,000 rounds before it was decided to stop the test. The accuracy of the barrel was better on the last firing than on the first. In comparison, the accuracy of a standard barrel, such as No. 58, broke down at about 180 rounds during the firing of the first group, and at 90 rounds during the firing of the second group. Representative targets of barrels 49 and 58 are shown as follows: Figure 5 is in the third group[j] and Figure 6 in the eleventh and twelfth groups fired in barrel 49. Figure 7 represents the first group, and Figure 8 the second group fired in barrel 58.

Keyholing bullets are those which are unstable because of improper engaging of the lands. This occurs if the land diameter is too great or if the longitudinal profile of the lands has the wrong shape. The land diameter increases permanently by erosion and swaging, and temporarily by thermal expansion as the barrel heats up.

Erosion and swaging were minimized in these barrels by chromium-plating and nitriding, respectively. In Figure 12 are shown star gauge curves of a barrel nitrided and chromium-plated (No. 49), a barrel just chromium-plated (No. 61), and a standard barrel (No. 58), all fired the 5 × 50 (1) schedule. After one group, the land diameter of barrel No. 58 was increased throughout its length. After eight groups, the land diameter of barrel No. 49 was not increased except in the region where the chromium had been removed (breechward of 16 in. from the breech). Furthermore, after firing, the lands in barrel No. 49 reached their full height abruptly, whereas those of No. 58 rose to approximately full height over a long section. An abrupt rise of the lands promotes good engraving of the jacket of the bullet.

Barrels Fired on the Usual More Severe Testing Schedules. In Figures 9 and 10 are shown photographs of typical targets obtained on firing the 5 × 100 (2) schedule. The bullets fired from the standard barrel, No. 237,[109] began keyholing in the second 100-round burst, while the nitrided, chromium-plated barrel with choked muzzle, No. JN3, fired no keyholing rounds in the ten bursts fired.

At the Purdue University range of the Army Ordnance Department, the nitrided, chromium-plated barrels with choked muzzles were fired with "combat ammunition" on the B-1 and C-1 schedules to 100 per cent keyholing[319] and compared with the standard barrel. The results are shown in Table 1.

TABLE 1. Performance of caliber .50 aircraft barrels fired B-1 and C-1 schedules at Purdue University, using combat ammunition.*

Type of barrel	No. of barrels tested	Type of test	Average rounds to 100 per cent keyholing
Standard steel (D28272)†	10	C-1	167
	5	B-1	230
Chromium-plated, with choked muzzle, not nitrided	14	C-1	293
	14	B-1	507
Nitrided, chromium-plated, with choked muzzle (D7162011)†	5	C-1	319
	5	B-1	1098
Stellite-lined near breech (D7161580)†	6	C-1	295
	5	B-1	455

* 2API-M8, 2 I-M1, and 1 Tr-M10 in each five rounds.
† Army drawing number.

Advantage of Choked Muzzle. The effect of thermal expansion in reducing the ability of the lands to engrave the bullet adequately was minimized by the choked muzzle. If a barrel is choked to a diameter of 0.494 in., a temperature of about 800 C is required to expand this bore to the nominal diameter of a caliber .50 barrel—0.500 in. Choking the bore of a caliber .50 barrel over a length of only about a foot at the muzzle is sufficient. A caliber .50 AP-M2 bullet can engage abruptly rising, full-height lands, without serious slipping, when traveling almost at muzzle velocity. Barrels were tried whose bore diameter over the full length was reduced to 0.495 in. by chromium plating. They had no better accuracy-life than those choked only near the muzzle. There was no particular advantage in the taper, as such, but it was a convenient way to get a choked muzzle and at the same time a large enough bore at the breech to prevent the development of excessive pressures.

VELOCITY-LIFE

General Statement. The Army Air Corps uses a drop of 200 fps in cold velocity as a criterion for rejecting a

[redacted]

[i] Detailed data on barrels No. 49 and No. 58 may be found elsewhere.[109]

[j] Warm-up and velocity rounds account for the fact that the total rounds shown on the target photographs are not divisible by 250.

worn barrel. The number of rounds a barrel can fire on a given schedule before its cold velocity has dropped 200 fps is therefore considered its velocity-life.

If the initial velocity is to be maintained, there must be no decrease in the resistance of the bullets to move which would result in inefficient burning of powder and in lower starting pressures. In a chromi-

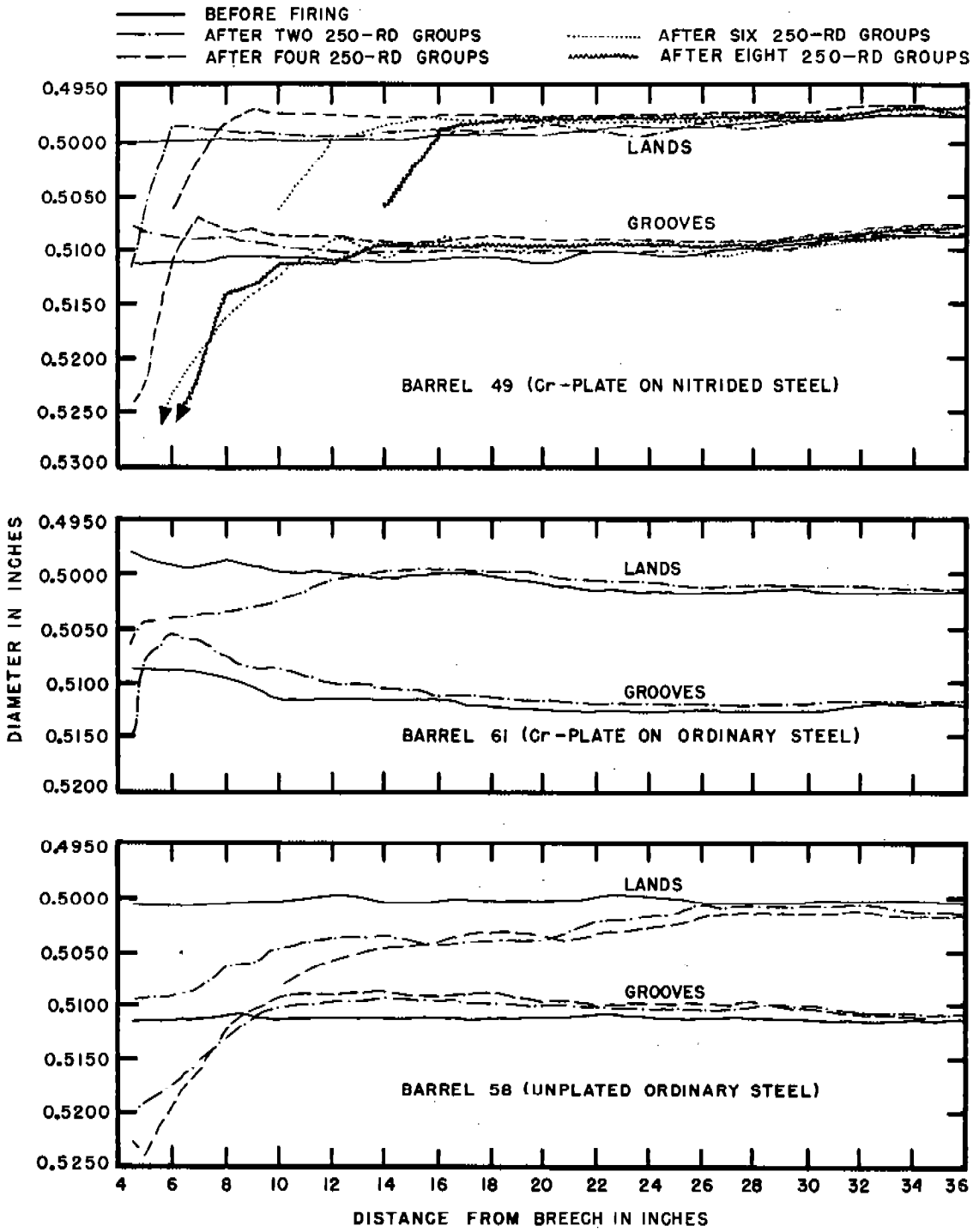


FIGURE 12. Star gauge curves of caliber .50 aircraft barrels fired one or more groups on the 5 × 50 (1) schedule. (This figure had accompanied the manuscript of NDRC Report A-409 but was not reproduced with that report.)

um-plated, caliber .50 aircraft barrel, the starting pressure was essentially maintained as long as the chromium remained on the grooves at the origin of bore, for as the chromium was removed from the lands at this point, constriction of the grooves and swaging of the lands tended to produce a smooth bore with cold diameter of 0.505 in., and this constriction offered sufficient resistance to the start of the bullet so that the cold velocity dropped very little or actually increased.[k] Eventually the cold velocity dropped as the chromium was progressively removed from the grooves, the removal starting at the origin of bore and progressing muzzleward.

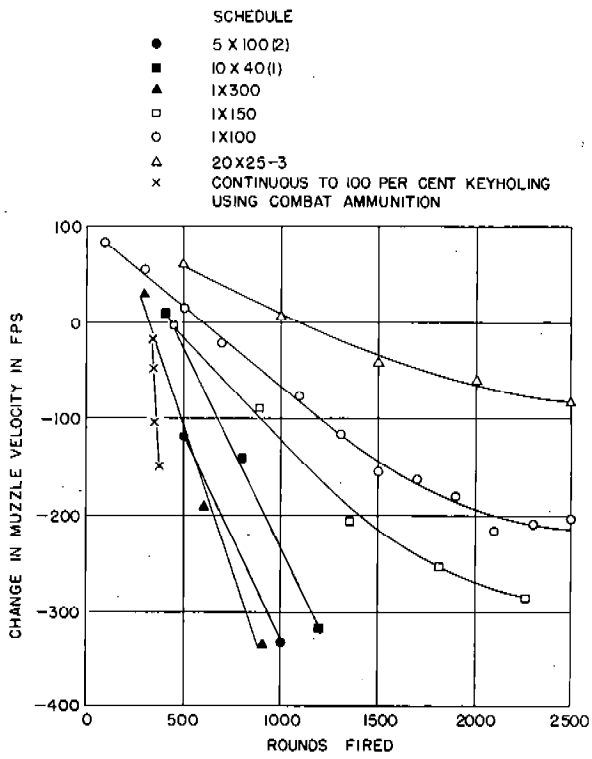


FIGURE 13. Average velocity of nitrided, chromium-plated caliber .50 aircraft barrels with choked muzzles plotted against rounds fired according to seven different schedules. (This figure had accompanied the manuscript of NDRC Report A-409 but was not reproduced with that report.)

Velocity-Life of Nitrided, Plated Barrels. The velocity of the nitrided, chromium-plated barrels increased at first as the grooves constricted and caused slightly higher gas pressures; then as the chromium was gradually removed from the vicinity of the origin of rifling and the steel eroded, the velocity fell off rather regularly. In Figure 13 is shown a plot of velocity versus rounds fired on seven different schedules. For a mild schedule such as 1 × 100 or 20 × 25 (3), the velocity-life was not much different from that of a standard barrel. On the more severe schedules, however, the velocity-life was much better than that of a standard barrel. For example, on firing one 500-round group on the 5 × 100 (2) schedule, the velocity of a standard barrel dropped 400 to 500 fps as compared with a drop of about 100 fps for the nitrided, chromium-plated barrel.

Gauge for Indicating Rejection Point of Barrels. No matter how good a barrel is, it will reach a point, if fired long enough, at which it should be discarded. An important problem with all barrels is the finding of a suitable field method for determining this rejection point. In general, caliber .50 aircraft barrels should be rejected if on the next short burst they would be firing bullets with a large yaw or the velocity drop would be more than 200 fps. The problem of a gauge for indicating the rejection point of a nitrided, chromium-plated barrel with a choked muzzle is resolved into a single problem of a method for indicating velocity-drop, since the accuracy-life is much longer than the velocity-life.

A gauge which is a very good indicator of the velocity-drop of this barrel was developed. A drawing of it is shown in Figure 14, and a curve of velocity-drop versus gauge-advance is shown in Figure 15.

The gauge is of the plug type, described in Section 10.2.2, with a head 0.507 in. in diameter. It is entered from the breech end of a barrel, and the amount of its forward run beyond the zero point is observed. Then the velocity-drop of the barrel can be read from Figure 15.

CAUSE OF EARLY APPEARANCE OF "TIPPERS" IN SOME BARRELS

After the nitrided, chromium-plated barrels with choked muzzles were in production (800 barrels a day) accuracy acceptance tests showed that some were being manufactured that had a poor accuracy. In the acceptance test a 300-round burst of AP-M2 ammunition was fired. Bullets with a yaw of as much as 20 degrees (tippers) were appearing in the first few rounds. The barrels, however, did not fire keyholing rounds at an early stage, nor did the point of 100 per cent keyholes appear earlier than usual.

Nothing could be found wrong with the barrels on routine inspection. After a detailed investigation it

[k] A fuller discussion of the causes of velocity changes in barrels may be found elsewhere.[110]

[redacted]

was found that the poor performance was caused by roughness of the bore.[110] The roughness was in the originally machined steel surface, which remained rough after electropolishing. The plating, if anything, accentuated the roughness.

Another possible explanation of the poorer accuracy of some plated barrels over others is in the difference in the methods used in manufacturing the barrels. It was shown that chromium-plated barrels and stellite-lined barrels which had a separate muzzle bearing had greater dispersion, because of a higher percentage of tippers, than the same types of barrels with an integral muzzle bearing. Several manufacturing procedures were varied in both cases so it was not possible to determine what factor caused the difference in behavior.

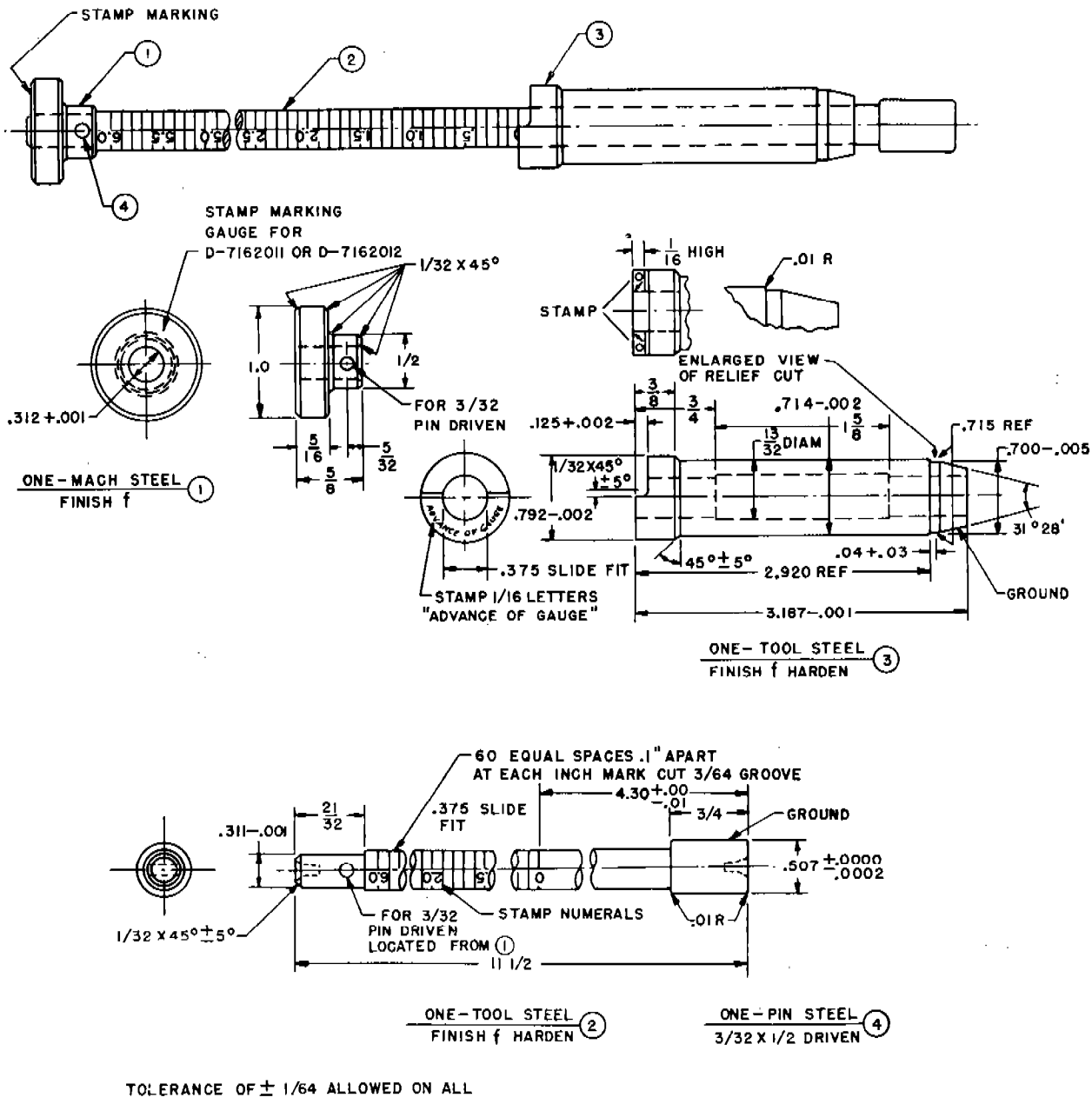


FIGURE 14. Drawing of 0.507-in. plug gauge for determining rejection point of nitrided, chromium-plated, caliber .50 aircraft barrels with choked muzzles. (Figure 21 in NDRC Report A-409.)

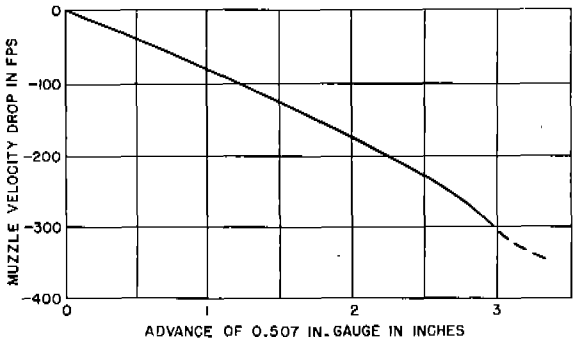


FIGURE 15. Curve showing drop in muzzle velocity corresponding to advance of the 0.507-in. plug gauge in eroded, nitrided, chromium-plated, caliber .50 aircraft barrels with choked muzzles. (Figure 22 in NDRC Report A-490.)

23.2 OTHER MODIFICATIONS OF MACHINE GUN BARRELS

23.2.1 Caliber .50 Aircraft Barrels

CHROMIUM-PLATED BARRELS NOT NITRIDED

In Section 23.1 was discussed the nitrided, chromium-plated caliber .50 aircraft barrel with choked muzzle. A few words should be said about barrels identical to these except that they were not nitrided. In addition, the steel to be replaced by chromium was removed from some of these nonhardened barrels by machining rather than by electropolishing. These barrels were made before the facilities for large-scale nitriding had been found.

Even without the nitriding, the chromium-plated barrel with choked muzzle was much superior in accuracy-life to the standard barrel, and in fact was as good in this respect as the barrel containing a stellite liner (Chapter 22), according to firing tests. The data are recorded in Table 1. Although superior to standard barrels, the nonhardened barrels, whether machined or electropolished prior to plating, were not as good with respect either to accuracy-life or to velocity-life as similar barrels that were nitrided; therefore, nitriding was adopted and facilities for large-scale nitriding were easily found.

CHROMIUM-PLATED BARRELS OF OTHER STEELS WITH HARDENED BORES

The improved caliber .50 aircraft barrels described in Section 23.1 were made of WD 4150 steel. Research on special steels was carried out, as described in Section 16.4.11, to find an improved type of steel for machine gun barrels. For barrels that were to be plated with an erosion-resistant material such as chromium, it was not as important to have a steel that resisted attack by the powder gases as it was to have one with better high temperature properties than nitrided WD 4150 steel. The search for these superior steels was narrowed down to a few which would develop, upon hardening, a tough case that had good hardness at temperatures approaching 800 C and good resistance to tempering.

The following steels[1] were made into caliber .50 aircraft barrels, which after bore-hardening were to be chromium-plated and tested:

Nitralloy, obtained from A. Milne and Company, New York. Analysis: 0.43 C, 0.56 Mg, 0.017 P, 0.018 S, 0.30 Si, 1.58 Cr, 0.35 Mo, 1.04 Al.

Molybdenum Steel, obtained from Ford Motor Company. Analysis: 3 Mo, 0.13 C.

Molybdenum Steel, made to order by Allegheny-Ludlum Steel Corporation. Analysis (average of 4 heats): 0.33 C, 0.45 Mn, 0.20 P, 0.015 S, 0.29 Si, 2.05 Mo, 0.10 Ni, 0.03 Cr.

Chro-mow, obtained from the Crucible Steel Company. Analysis: 5 Cr, 1.35 Mo, 1.25 W, 1 Si, 0.30 C.

Potomac Die-Steel, obtained from the Allegheny-Ludlum Steel Corporation. Analysis: 5 Cr, 1.7 Mo, 1.3 W, 1 Si, 0.33 C.

Only the first three of these steels were tested as barrels. There was not time to conclude the work on barrels of the Chro-mow and Potomac hot-die steels, although barrels were made up and two of the Chro-mow barrels were nitrided.

Nitrided Nitralloy has a very hard case, its hardness near the surface being of the order of 1000 VPN. The hot hardness of the case is excellent. Aircraft barrels of this steel were nitrided, electropolished, and chromium-plated, and subjected to firing tests. The lands near the origin of bore stood up very well. The adherence of the chromium to the steel and the resistance to swaging of the lands were better than in nitrided WD 4150 steel barrels. But the barrels failed near the muzzle end, where sections of lands broke out. The case is apparently too brittle for strains near the muzzle of this barrel.

The bore-surface of barrels of both the molybdenum steels were induction-hardened, electropolished, and chromium-plated. They performed better than chromium plated barrels of WD 4150 steel but

[1] Some of these same steels were made into barrels for stellite liners, as described in Section 24.5.3.

were not superior to those of WD 4150 steel nitrided and chromium-plated.

Studies of "Free-Run" Barrels

As discussed in Section 23.1.4, the nitrided, chromium-plated caliber .50 aircraft barrel with choked muzzle had a very long accuracy-life compared with its velocity-life. Such a barrel could be eroded to a smooth bore condition over the section extending from the origin of bore to within about a foot of the muzzle and still fire accurately, but with the barrel in this condition the muzzle velocity was several hundred feet per second lower than in a new barrel.

The web of the powder was such that it burned efficiently and built up the proper pressure only when the bullet had an adequate starting pressure. When there were no lands at the origin of bore or no constriction to resist movement of the bullet, the powder pressure did not reach the required high peak.

In view of these considerations, it was thought that a barrel with a longer velocity-life and adequate accuracy-life would result, without giving excessive initial pressure, if a barrel were reamed to give a few inches of free run to the bullet. A powder which would burn fast enough to develop the required pressure in a smooth-bore barrel would have to be used. Possibly the barrel could then be eroded for a considerable distance ahead of the origin of bore without greatly affecting the muzzle velocity.

Single-base powders having a smaller web than is usual for caliber .50 ammunition were loaded into cartridge cases and bullets crimped in. They were fired in steel barrels having various lengths of free run and chamber pressures were measured by means of a copper ball crusher gauge. A "free-run" of 1½ in. and 244 grains of M1 powder of one particular experimental lot were found to be about the optimum conditions.[109,110]

Using the components of AP-M2 ammunition, except for the powder, Frankford Arsenal then loaded 10,000 rounds containing the lot of powder that was found best. Chromium-plated, free-run, aircraft barrels, with choked muzzles, were made. Some of the barrels were nitrided prior to plating. In the firing tests, using the 5 × 100 (2) schedule and the special ammunition, the velocity-drop was considerable, probably because of severe erosion in the free-run zone.

It was thought that this erosion could be considerably lessened by experimenting to find the optimum diameter of the free-run cylinder and a better bore-surface coating. Because of the fact that the project was never given a high priority, the contract terminated before this program could be rounded out.

23.2.2 Nitrided, Chromium-Plated Caliber .50 Heavy Barrels With Choked Muzzles

Although the first experiments with liners were made using the caliber .50 heavy barrel,[m] research with the explicit object of improving this particular barrel was postponed until the major work on the aircraft barrel was completed. The standard monobloc steel, heavy barrel has a good life as is, but it is obvious that its life can be improved considerably by inserting a liner of Stellite No. 21 (Section 22.4) or properly chromium-plating the bore, or both.

Nitrided, chromium-plated heavy barrels with choked muzzles were made. Both hard and soft chromium plates were applied. They were fired according to the 5 × 100 (1) schedule.[110] It was found that modifying barrels in this manner would give a large increase in accuracy-life and, when this firing schedule was used, would increase somewhat the velocity-life. On the more mild schedules, the velocity-life would probably not be significantly improved.

23.2.3 Caliber .30 and Caliber .60 Barrels

General Statement

Inasmuch as the problems connected with caliber .30 and caliber .60 machine gun barrels are very similar to those of the caliber .50 barrels, little further research was required to improve them.

Nitrided and Chromium-Plated Caliber .30 Aircraft Barrels with Choked Muzzles

Caliber .30 aircraft barrels were tested in the aircraft gun which fires 1,200 to 1,300 rounds per minute. Two firing schedules were used with armor-piercing ammunition: (1) A series of 300-round bursts with complete cooling after each burst—1 × 300 schedule, and (2) three 300-round bursts with 2 minutes between bursts—3 × 300 (2) schedule.

The barrels which were tested were chromium-plated to give a choked muzzle of 0.292 + 0.004-in.

[m] See footnote (c) of Chapter 11.

bore diameter. Some of these were nitrided prior to plating.

The following conclusions were drawn from this investigation: (1) As in the case of the caliber .50 barrels, the more severe the firing schedule, the greater was the advantage of nitriding and taper-chromium-plating the bore. When the 1 × 300 schedule was employed, the accuracy-life of the chromium-plated barrels with choked muzzles was considerably better than that of a standard barrel, and the velocity-life was about 25 per cent better. With the 3 × 300 (2) schedule, both accuracy-life and velocity-life were much better for the modified than for the standard barrel. (2) The soft type of chromium appeared to be no better in this barrel than the hard chromium. Nitriding the bore, in addition to plating it, was advantageous.

Nitrided and Chromium-Plated Caliber .60 Barrels

Caliber .60 barrels, a few of which had been nitrided, were chromium-plated. It was particularly important in the chromium-plated barrels for this gun to have the cylindrical section lying between the forward end of the cartridge case and the run-out of rifling sufficiently large to eliminate the possibility of excessive pressures. Moreover, barrels performed in general better when the bore diameter near the origin was on the large side of the tolerance. Some barrels with choked muzzles were tested, but no conclusive results were obtained.

The firing schedule used to test these barrels at Aberdeen Proving Ground [215] was supposed to consist of six 50-round bursts separated by 2 min intervals. Malfunctioning of the gun and ammunition, and the necessary replacement of parts during the test usually prevented this schedule from being followed. Consequently, it was difficult to compare barrels made in different ways.

In general, it can be said that chromium-plating the bore of a caliber .60 barrel, with or without prior nitriding, could be expected to increase its life by a factor of at least 2 or 3 when fired on a schedule which would wear out the standard steel barrel in 200 to 300 rounds.[110] Therefore, the investigation should be continued when a more reliable gun mechanism is available.

Chapter 24

BARRELS BOTH STELLITE-LINED AND CHROMIUM-PLATED

By *J. F. Schairer*[a]

24.1 DEVELOPMENT AND PERFORMANCE OF "COMBINATION" CALIBER .50 AIRCRAFT BARRELS

WHILE THE TWO TYPES of improved caliber .50 aircraft machine gun barrels, stellite-lined (described in Chapter 22), and nitrided and chromium-plated (described in Chapter 23) were being developed by Division 1, NDRC, at Crane Company and Geophysical Laboratory respectively, their advantages and disadvantages were noted. It soon became evident that a third and still better barrel should result from a combination of the stellite liner with choked-muzzle chromium plate on the steel bore ahead of the liner. Thereupon, the development of the stellite-lined and chromium-plated barrel with choked muzzle (or "combination" barrel) was initiated at Geophysical Laboratory and developed by the cooperative efforts of this laboratory, the Crane Company, and the National Bureau of Standards.

24.1.1 Accuracy- and Velocity-Life of Improved Machine Gun Barrels

Although the stellite-lined barrel showed a marked improvement in accuracy-life over steel barrels with no liner, as described in Section 22.2.2, the most outstanding characteristic of the lined barrel was the vast improvement in velocity-life. This long velocity-life is the result of the phenomenal resistance of the liner material to bore enlargement by either powder gas erosion (chemical attack or melting or both) or by the swaging impact of the bullets. In fact, a small constriction of both land and groove diameters occurs during the first burst of fire resulting in a velocity increase and during additional firing bore enlargement and velocity decrease only take place very slowly.

When one of the more severe firing schedules is used (Section 23.1.3), the cold muzzle velocity will be little if any below the initial velocity and the liner is relatively new and unworn when the barrel is rejected for inaccuracy. The relatively short accuracy-life, as compared to velocity-life, is largely the result of bore enlargement ahead of the liner by erosion of steel and of the thermal expansion of the barrel at the high temperatures (Section 5.6.3) attained in severe firing with the resultant failure of the bullets to engage the rifling properly and attain adequate spin for stable flight.

In contrast, although nitrided and choked-muzzle, chromium-plated barrels showed (see Section 23.1.4) a marked improvement in velocity-life over non-plated steel barrels, their most outstanding characteristic was a vast improvement in accuracy-life. The long accuracy-life of this barrel is largely the result of the erosion-resistant choked-muzzle, which is responsible for maintaining stability of bullets throughout long bursts (as already discussed more fully in Section 23.1.4), and barrels were rejected for excessive velocity drop long before they fired any inaccurate bullets.

Thus, the performances of the two types of improved machine gun barrels, stellite-lined, and nitrided and chromium-plated, were complementary, the former showing a very large improvement in velocity-life, the latter in accuracy-life, over unmodified steel barrels.

24.1.2 Preparation and Testing of "Combination" Barrels

The studies at the Geophysical Laboratory of the cause of failure of caliber .50 barrels made it clear that a barrel having a combination of a short breech liner of Stellite No. 21 and tapered-chromium-plate on the steel bore ahead of this liner should have a longer overall life than either the stellite-lined or nitrided and chromium-plated barrel alone. After this advantage had been demonstrated by the Geophysical Laboratory a cooperative program for the preparation and testing of "combination" barrels was arranged between Geophysical Laboratory (and its subcontractor for plating, the Doehler-Jarvis Corporation) and Crane Company. An additional advantage hoped for from the use of chromium plate ahead of the liner was a saving of strategic stellite by using a much shorter liner.

[a] Special Assistant, Division 1, NDRC. (Present address: Geophysical Laboratory, Carnegie Institution of Washington.)

Fourteen 10-lb caliber .50 aircraft barrels for each of three liner lengths were prepared with the steel bores chromium-plated ahead of investment-cast Stellite No. 21 liners of 4-in., 6-in., and 9-in. lengths. Machining and insertion was performed by Crane Company and the bore was electropolished and plated by the Doehler-Jarvis Corporation before liner insertion (Section 25.2.3). The procedure developed for the chromium plating of the bore ahead of a stellite liner was, with only slight modification, the same as used for full-length barrel plating.

Four of each of the "combination" barrels with the liners of the various lengths were subjected to firing tests at Geophysical Laboratory[81] and two of each at Crane Company.[80] Concordant data were obtained and the remainder of the satisfactory barrels were delivered to the Ordnance Department for preliminary tests. As a result of all these tests, 80 additional similar "combination" barrels with 9-in. length liners were delivered to the Ordnance Department for test.

To evaluate the effects of bore hardening (by nitriding) beneath the chromium plate ahead of 4-in., 6-in., and 9-in. length stellite liners, two of each of these barrels were prepared for test by Division 1. Firing tests showed that bore hardening ahead of the liner had but little effect on performance and that this manufacturing complication was unnecessary.[81]

24.1.3 Development of the CGL Firing Schedule

During the development of the "combination" barrels just described and in the development of barrels showing even further improvements in performance (achieved by methods described later in this chapter in Sections 24.2, 24.3, and 24.5) it was necessary to increase the severity of the firing-test schedule. These caliber .50 aircraft machine gun barrels were so far superior in life and performance to anything previously known that a stepped-up firing schedule was required to give an adequate comparison of barrel performance and to indicate the full potentialities of these barrels. One requirement for such a schedule was that it yield a maximum of desired information on a barrel and that barrels could be fired to end of life in a reasonable time. Two contractors of Division 1 (Crane Company and Geophysical Laboratory) collaborated in the development of the new firing-test schedule, hence the name "CGL" schedule.

Several things were considered in the choosing of this schedule:

1. The Air Forces required a barrel that is capable of firing a long continuous burst or bursts and closely spaced long intermittent bursts.

2. Any schedule requiring the firing of a very long continuous burst or closely spaced long intermittent bursts which overheat and distort the barrel, because of the lack of high-temperature strength of gun steel, does not permit the evaluation of the relative merits of different liner materials.

3. If too moderate a schedule is selected, it will require a long firing test, besides not simulating extreme combat conditions.

4. If possible, the schedule should be flexible, to provide for an evaluation of somewhat inferior materials that might be used as substitutes, as well as for very superior materials and combinations.

5. The same ammunition should be used in firing all special barrels to make the results comparable.

Two schedules were seriously considered—one employing a series of continuous bursts of arbitrarily fixed and diminishing length—the other a continuous burst of fixed length followed by a series of intermittent bursts. A schedule of the latter type was adopted as the firing-test schedule in the development of superior machine gun barrels and in the test of promising materials and combinations. This initial burst gives an indication of performance under the severe conditions of prolonged continuous fire and the subsequent repeated groups indicate performance under the severe conditions of moderate length bursts at frequent intervals.

The CGL schedule[80,81] calls for a long continuous burst of predetermined duration (usually 350 rounds) followed by 500-round groups fired in five bursts of 100 rounds each with a 2-minute cooling interval between bursts, such groups being repeated until end of life from inaccuracy (50-per cent keyholing bullets), excessive velocity drop (greater than 200 fps), excessive muzzle blast, or any dangerous condition of the barrel. After the long continuous burst and after each 500-round group the barrel is cooled to room temperature. Accuracy during bursts is observed by means of a moving target. Cold- and hot-velocity measurements are taken at stated intervals. Figure 1 shows a data sheet for a caliber .50 aircraft barrel fired on the CGL-350 schedule. To provide a flexible base to evaluate inferior barrels as well as very superior barrels, the length of the long continuous burst can be varied. A suffix thus (CGL-400, CGL-350, CGL-300, etc.)

Data sheet for caliber .50 aircraft barrel No. AC155 fired on CGL-350 schedule. All targets at 1,000 in. Total rounds fired: erosion 1,350; all others 150. Instrumental velocity at 78 ft. (This figure is based on one in progress report on Contract OEMsr-629.)

Test No.	Instr. vel. (fps) Cold	Hot	20-rd cold accuracy 90% of rd EHD*	EVD†	No. rds >20° yaw	100-rd burst accuracy 95% of rd EHD*	EVD†	No. rds >20° yaw	Max. bore dia.	Cyclic rate, rpm	Remarks
0. Initial	2640		5.5	4.5	0	Continuous Burst Accuracy					Appearance satisfactory.
1. Cont. burst (350 rounds)	2650	2420	7.4	3.6	0	First rd with yaw 20: 337 No. rounds with yaw 50: 0 Number of yawers: 2				818	Muzzle flash severe last 50 rds. Mild erosion ahead of the liner; slight wear in liner; rifling clearly defined throughout.
2. 500-rd group											Muzzle flash severe during last 2 bursts.
Burst 1		2625				4.5	6.5	0		820	
Burst 2		2600				4.5	6.7	0		820	The barrel is eroded ahead of
Burst 3		2465				6.8	8.5	10		820	the liner for about 3 in.
Burst 4		2360				10.8	10.5	25		820	Rifling is clearly defined
Burst 5	2670	2330	5.5	5.5	0	11.2	12.6	Approx. 100		820	but worn in the center of the barrel. The liner is slightly worn.
3. 500-rd group											3 sec stoppage in burst 1 and
Burst 1		2570				9.3	9.7	6		780	2.5 sec stoppage in burst 3.
Burst 2		2360				14	14.5	Approx. 36		780	
Burst 3		2265				10.2	14.3	Approx. 100		780	
Burst 4		None				9	11	Approx. 100		780	
Burst 5	2415	2030	10	10	20	11.3	11.8	Approx. 100		780	
4. 500-rd group											
Burst 1											
Burst 2											
Burst 3											
Burst 4											
Burst 5											

* EHD = Extreme horizontal dispersion (in.). † EVD Extreme vertical dispersion (in.).

FIGURE 1

indicates the length of the long continuous burst which in all cases is followed by the regular 500-round groups of intermittent fire. All of the very superior barrels whose development is described in this chapter were tested on the CGL-350 schedule, using AP-M2 ammunition. The results are summarized later (Figure 6).

24.1.4 Performance of "Combination" Barrels

Initial firing tests by Division 1 on "combination" caliber .50 aircraft barrels with 4-in., 6-in., and 9-in. length investment-cast liners of Stellite No. 21 and choked-muzzle chromium plate on the steel bore ahead of the liner were made on the continuous-to-keyholing (C—1) schedule[b] and on an intermittent (B—2) schedule.[c] The plated barrels with 4- and 6-in. liners were approximately equivalent in performance to a barrel with a 9-in. liner but no plate ahead of the liner. The plated barrel with 9-in. liner was far superior to either the regular stellite-lined barrel (Chapter 22) or the nitrided and chromium-plated barrel (Chapter 23) particularly on the intermittent schedule. The Air Corps wanted only the best barrels, so attention was concentrated in further tests on the "combination" barrel with a 9-in. liner with plate ahead of the liner. Besides the very severe CGL-350 firing schedule used in further tests by Division 1, a

[b] Defined in Chapter 22.3.3.

[c] On the B—2 schedule a barrel is fired in 500-round groups consisting of five bursts of 100 rounds each with a 2-min cooling interval between bursts and complete cooling after each 500-round group. Such groups are repeated to end of life of the barrel. This schedule is designated "5 × 100 (2)" in Chapter 23.

variety of schedules was used in tests by the Ordnance Department on barrels delivered by Division 1.

As a result of the firing tests on very severe schedules one serious defect of "combination" barrels was discovered. Their long accuracy and velocity lives permitted firing of such duration and severity that many of the barrels failed in a dangerous manner by rupturing longitudinally near the muzzle end of the barrel. Such failure can be eliminated by reinforcement of the barrel, which is considered in the next section.

24.2 EXTERNAL REINFORCING SLEEVE FOR BARRELS

On a severe firing schedule, such as the CGL-350 schedule, end of life of a "combination" barrel is brought about by a permanent expansion of the barrel in the region of the forward end of the liner. The sequence of events in the weakening of the barrel wall caused by the high temperatures during the firing of long bursts is given in Section 5.6.4. Figure 16 of Chapter 5 shows two caliber .50 aircraft barrels distorted during firing. It should be noted that distortion was principally in one plane. Stellite-lined barels (with no plate ahead of the liner) will also blow out in the same manner if the firing of long bursts is continued long enough. Because of the much shorter accuracy life of this barrel as compared to the "combination" barrel, however, firing is usually stopped before the barrel can rupture.

The expansion of various parts of the barrel was estimated[81] on the basis of star gauge data and outside diameter measurements made before and after firing on a number of "combination" and other barrels. After firing the 350-round burst on the CGL-350 schedule, "combination" barrels showed permanent expansion (cold) of the bore at 8 to 10 in. from the breech, that is, 2 to 4 in. behind the end of the liner. The average for seventeen barrels measured was 0.0043 in. (range from 0.000 to 0.015 in.). Just ahead of the liner the expansion was about the same. Forward of this the amount of expansion tapered off. Clearly, this expansion had to be prevented if the best use of either or both the liner and chromium plate was to be made.

A simple method of reinforcing the barrel in this weak region was found to be highly successful, essentially eliminating the permanent expansion and greatly increasing the life of the "combination" barrel as well as making it a safe barrel. A thin cylindrical steel sleeve or collar, 6-in. long, was shrunk on the outside of the barrel, after it had been turned to a cylinder over the weakest section. It was located so that the region embraced by the forward 5 in. of the liner and 1 in. ahead of the liner was externally reinforced. The weight of the sleeve had to be kept at a minimum because increase in barrel weight would have decreased the cyclic rate of fire of the gun. This matter is discussed more fully later in Section 24.3.2.

The experiments on barrel reinforcement at Geophysical Laboratory indicated that, (1) a reinforcing sleeve should start at about 7½ in. from the breech and extend to 13½ in. from the breech, (2) sleeves made of WD 4150 steel or of NE 8630 steel tubing are satisfactory, (3) wire winding of the barrel ahead of the sleeve is advantageous, but may not give enough improvement to justify the extra time, cost, and weight, and (4) external sleeves should be fixed in place, as by a spot weld at the forward end of the collar, to eliminate any possibility of their slipping. The experiments with "special contour" barrels described in Section 24.3.1 suggested that most of the benefit of an external reinforcing sleeve might be provided by machining the barrel to have outside dimensions the same as those of a barrel with a shrunk-on external sleeve. Two alternative designs for "combination" barrels with integral reinforcement were prepared at Geophysical Laboratory and some barrels were made according to these designs which are designated as "GLA" and "GLB" in Figure 2. It was not possible to make the firing tests before termination of the experimental program of Division 1. The barrels were turned over to the Ordnance Department with the recommendation that these tests be made.

Firing tests[80] by Division 1, according to both the CGL-350 and CGL-400 schedules made on stellite-lined barrels without plate ahead of the liner but with reinforcing sleeves showed that such barrels gave considerably improved performance over regular stellite-lined barrels. Accordingly a few thousand such barrels for Service trials and use were to have been produced at Crane Company in the late summer of 1945 under an Ordnance Department contract. Substantial production of "combination" barrels with reinforcing sleeves also was planned. Although the expedient of adding reinforcing sleeves was satisfactory in principle for the utilization of barrels in stock, the machine gun barrel manufacturers preferred to manufacture new barrels with integral steel reinforcement rather than to shrink-on external sleeves.

[redacted]

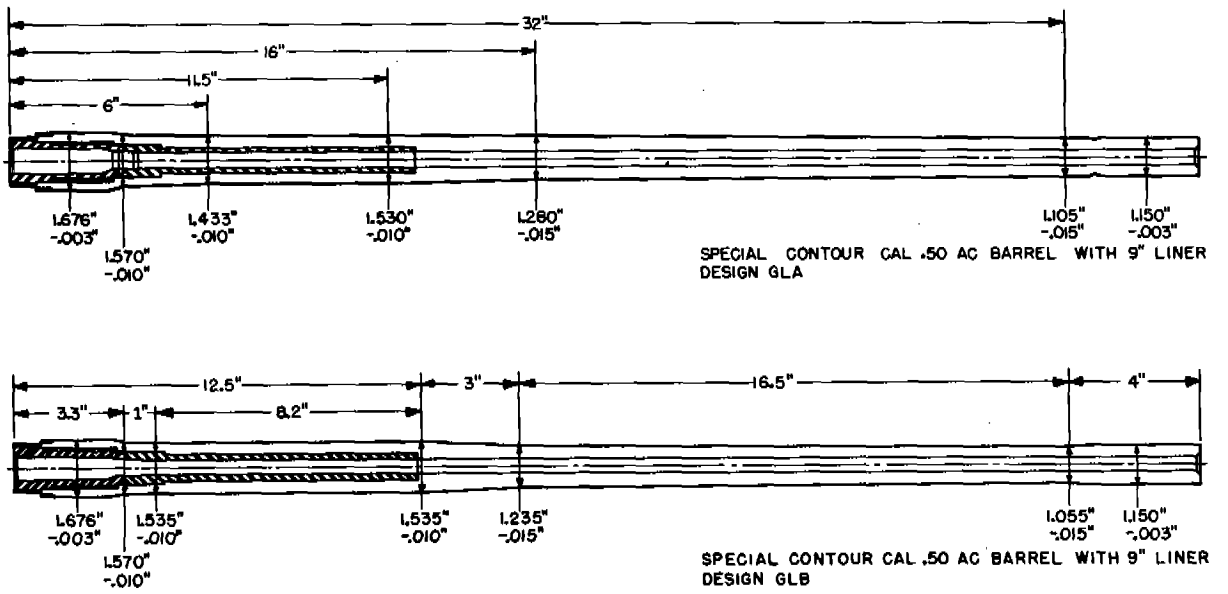


FIGURE 2. Designs for "combination" caliber .50 aircraft machine gun barrels with integral reinforcement at the forward end of the stellite liner. (Figure 24 in NDRC Report A-409.)

The remarkable results of the studies by Division 1 on barrel reinforcement in general and other changes in external contour of barrels are described in the next section (Section 24.3). Regular and special caliber .50 aircraft barrels are pictured in Figure 3. The relative performance of all superior barrels including both "combination" barrels and stellite-lined barrels with an external reinforcing sleeve is shown later in Figure 6. Before new barrel forgings could be obtained the Army production contracts were canceled immediately after V-J Day.

24.3 CHANGE IN WEIGHT AND CONTOUR OF LINED AND "COMBINATION" BARRELS

24.3.1 Effects of Barrel Weight on Performance

Even before the external reinforcing sleeve had been added to stellite-lined barrels at the Geophysical Laboratory, a different approach to the same problem had been started at the Crane Company, another Divison 1 contractor.

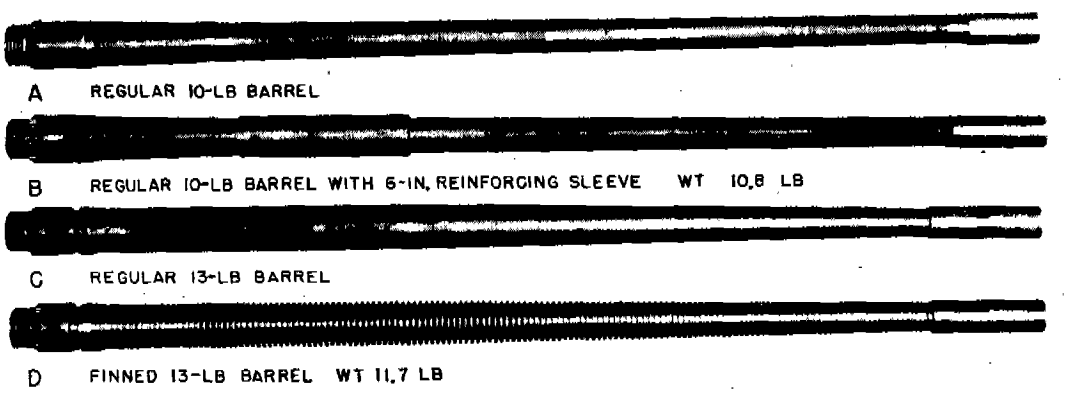


FIGURE 3. Photographs of regular and special caliber .50 aircraft barrels. (Figure 6 in NDRC Report A-408.)

To evaluate the effects of barrel weight on the performance of stellite-lined caliber .50 aircraft machine gun barrels, regular 9-in. liners of investment-cast Stellite No. 21 were inserted in two 13-lb caliber .50 aircraft barrels (Figure 4B). This 13-lb barrel (36-in. long) was an obsolete barrel that had been replaced for Service use by the regular 10-lb barrel having the same length (Figure 4A.)

Firing tests on the stellite-lined 13-lb barrels on the severe CGL-350 schedule showed a remarkable increase in life. Whereas the life of the regular 10-lb stellite-lined barrel on this schedule averages about 750 rounds, the lined 13-lb barrels showed a life of about 3,500 rounds. In both cases rejection was caused by inaccuracy while velocity drop had been very slight. In contrast, a change in weight from 10 lb to 13 lb results in only a very slight increase in life with regular steel barrels without the liner, the total life on the same schedule being 170 and 220 rounds, respectively.

24.3.2 Effects of Barrel Weight on Cyclic Rate of Gun

Because of the Air Forces' requirement for a high cyclic rate of fire in aircraft combat, it is important to note the effects of barrel weight on the cyclic rate of fire of aircraft machine guns. When a 13-lb barrel was fired at Crane Company in the Browning aircraft machine gun, M2, the cyclic rate was only 700 to 800 rpm even with all of the oil removed from the buffer, whereas the cyclic rate with a 10-lb barrel in this gun can be adjusted to approximately 750 rpm with oil in the buffer and to about 1,000 rpm with the oil removed.

Firing tests were made by the Ordnance Department on a series of barrels of different weights supplied by Division 1, using the newly adopted high-speed gun (M3). This gun has a rated cyclic rate of 1,250 rpm with a 10-lb barrel. In the test firings in which all barrels were fired in the same gun, the 13-lb barrel reduced the rate by 200 rpm and an 11.75-lb barrel reduced it by only 70 rpm. These data suggested that, unless delays could be tolerated while the gun mechanism was modified, efforts should be concentrated on the development of the best barrel with a weight not much in excess of 11.5 lb.

24.3.3 Effects of Distribution of Weight on Performance

The remarkable results of firing tests on stellite-lined 13-lb caliber .50 aircraft barrels were described in Section 24.3.1. Similar results were obtained on the CGL-350 schedule on special contour 13-lb barrels of design suggested by the Ordnance Department. These special contour barrels had a heavy cylindrical section extending from the breech end of the barrel to a point somewhat beyond the liner. The barrels were prepared at Springfield Armory and subjected to firing tests at Crane Company as a part of a broad study of the effects of distribution of weight (changes in exterior contour of barrels) on the performance of stellite-lined and "combination" barrels.

In view of the limitations imposed on barrel weight by the effects of increased weight on cyclic rate of fire of the gun (see Section 24.3.2), Crane Company prepared and tested barrels the weight of which was reduced by machining steel from 13-lb barrels to decrease the diameter in selected areas. All of these tests were conducted with the M2 gun (no M3 guns were available at this time) at a cyclic rate of 750 rpm. Two lined barrels were prepared for each of 8 special designs shown in Figure 4.

Another design (not shown in Figure 4) was similar in external contour to the barrel with a 6-in. external reinforcing sleeve (Figures 3B and 4J) except that the section of increased diameter was integral with the barrel and the weight was 10.9 lb. The performance of the barrel with an integral sleeve was somewhat superior to that of the barrel with the shrunk-on sleeve. The best performance per unit of weight was obtained from lined 13-lb barrels into which circumferential grooves had been cut so that the contour at the root of the groove was the same as that of the standard 10-lb barrel. The result was a barrel (Figures 3D and 4C) having integral, transverse fins, with a weight of about 11.7 lb. The performance of this barrel was equivalent to that of the lined 13-lb barrel without fins (Figure 4B) and represents an outstanding improvement in performance over stellite-lined 10-lb barrels with only a very slight reduction in the cyclic rate of fire. Such fins provide a maximum of barrel reinforcement and cooling surface with a minimum of additional barrel weight.

The two designs described in the preceding paragraph were selected for test with choked-muzzle chromium plating ahead of the liner. Two barrels of each design were prepared. The performance of the plated barrel with the integral reinforcing sleeve (weight 10.9 lb) was equivalent to that of the lined 13-lb barrel described above with fins (weight 11.7 lb) but with no plate ahead of the liner.

[redacted]

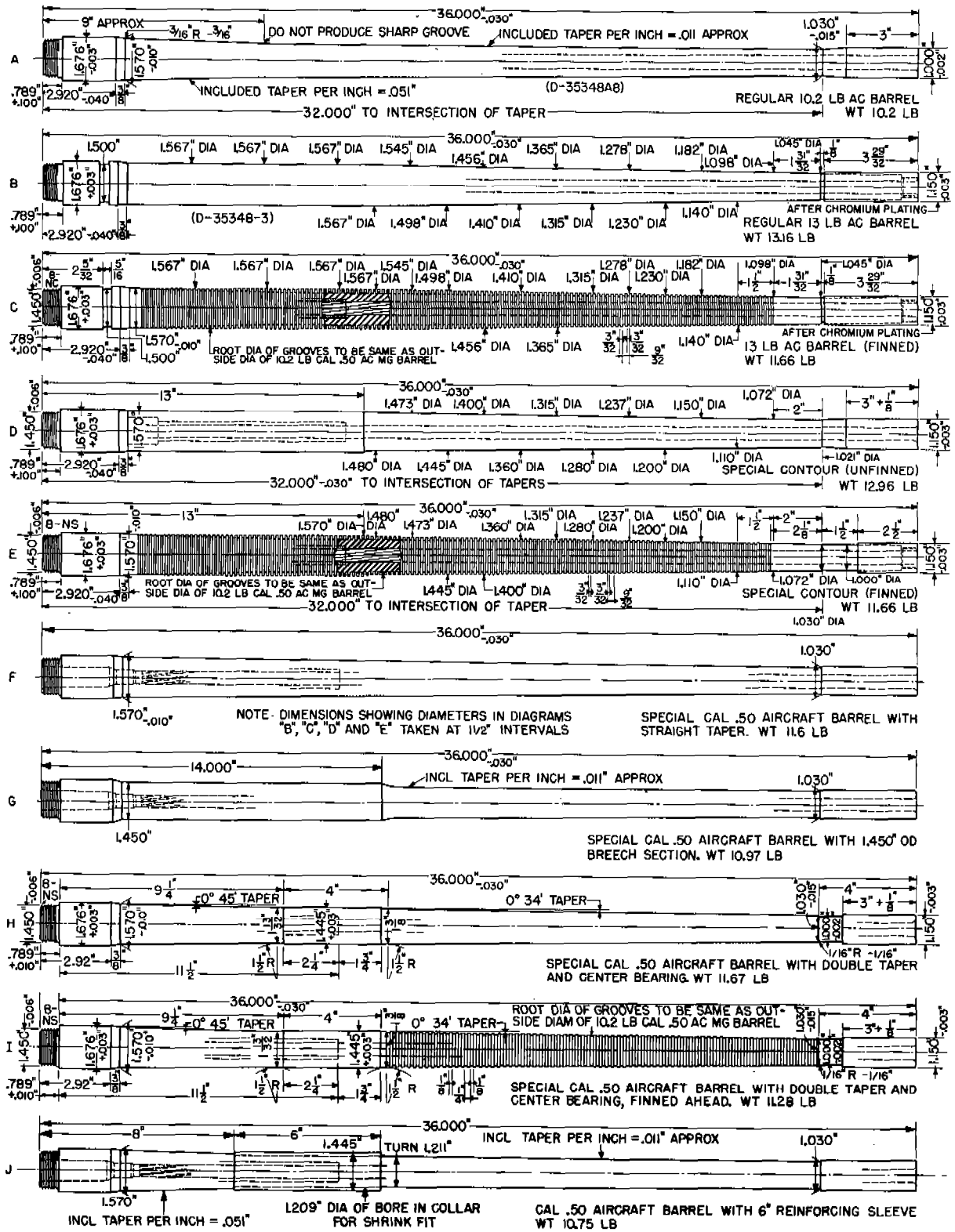


FIGURE 4. Eight designs of caliber .50 aircraft machine gun barrels having special contours. (Drawing submitted by Crane Company with interim report on Contract OEMsr-629.)

The finned barrel with both liner and plate (weight 11.7 lb) was far superior to any other aircraft barrel tested and showed a life of about 5,000 rounds on the severe CGL-350 schedule. This barrel life approximately is equal to the life of the gun mechanism and both gun and barrel can be discarded as a unit. One of the lined and plated finned barrels was rejected after 5,000 rounds because of a 200-fps velocity drop. The other burst near the muzzle after more than 5,000 rounds had been fired. The use of a barrel steel having better high temperature properties than the WD 4150 steel regularly used for machine gun barrels would prevent such rupture. (This question of choice of barrel steel is discussed later in Section 24.5.)

In the stellite-lined and chromium-plated finned barrel, the full usefulness of the erosion resistant liner is attained and liner and barrel wear out at about the same time. Preparations for procurement of the necessary barrel forgings for the production of these very superior barrels were in progress by the Ordnance Department when the procurement program was curtailed after V-J Day.

24.3.4 Aluminum-Clad Barrels

In order to evaluate the effects on performance that might be achieved by the external cladding of regular steel barrels with a lightweight metal of high thermal conductivity, regular 10-lb aircraft barrels were clad at the Al-Fin Corporation with aluminum muffs by the Al-Fin Thermit process.[559] These barrels were machined at Crane Company to yield a barrel (Figure 5) with circumferential fins, and stellite liners were inserted in some of these barrels. The total barrel weight was 11.5 lb. Firing tests on unlined barrels showed some improvement in performance over 10-lb steel barrels with no aluminum muff but severe powder gas erosion and flattening of the lands by the swaging impact of the projectile terminated life at an early stage. When the stellite-lined, aluminum clad, finned barrels were tested on the CGL-350 schedule, the performance was better than that of stellite-lined barrels without muffs, but the aluminum melted and dripped from the hot barrel.

Thereupon, two more lined barrels with solid aluminum muffs were encased in a thin steel tube to hold in place any aluminum which might melt and to take advantage of the heat of fusion of aluminum to cool the barrel. These barrels, which weighed about 13.5 lb, showed a performance somewhat superior to that of the unplated and lined 13-lb steel barrels described in Section 24.3.1, but the weight was so great as to make this barrel impractical.

Although it might have been possible to obtain comparable performance with reduced weight more suitably distributed, it was felt that lined and chromium-plated barrels with integral steel fins were more promising for immediate Service application. Therefore, no further work was done on aluminum clad barrels. Some preliminary tests on copper clad barrels were made by the Ordnance Department as a result of these studies by Division 1, NDRC, on aluminum clad barrels.

24.4 PERFORMANCE OF VARIOUS IMPROVED CALIBER .50 AIRCRAFT BARRELS

In order to show clearly the remarkable degree of improvement in firing performance of caliber .50 aircraft machine gun barrels that it has been possible to make, the pertinent data are summarized in Figure 6, where comparison is made on the very severe CGL-350 schedule already described in Section 24 1.3. All firings were made with AP-M2 ammunition and all barrels were made of regular WD 4150 machine gun steel. In each case the number of rounds of total life is a representative value. In most cases it is an average from firings on ten or more barrels. In all cases at least two barrels were fired and gave closely agreeing test data.

24.5 CHANGE OF BARREL STEEL TO ENHANCE PERFORMANCE

24.5.1 Barrel Heating During Firing

The high overall barrel temperatures attained during severe firing (Section 5.4.2) limit the life and performance of machine gun barrels in terms of both the length of continuous bursts and the length and frequency of intermittent bursts. This situation is not corrected by the use of an erosion resistant liner or plate, and therefore it prevents their complete utilization.

Temperatures as high as 900 C at a point 4.35 in. from the breech and 0.068 in. from the bore of a 10-lb caliber .50 aircraft barrel were recorded during the firing of severe schedules, as described in Section 5.5.1. A temporary increase in bore diameter results from the thermal expansion of the barrel steel at these

high temperatures and such expansion tends to prevent engagement of the bullets in the rifling and the attainment of proper spin for stable flight. Fortunately, erosion-resistant choked-muzzle chromium plating overcomes this difficulty in large part.

The lack of high-temperature strength and hardness of the barrel steel is a more serious limitation. A barrel that distorts or "wilts" cannot be expected to fire accurately and safely. This difficulty can be mitigated in lined and plated barrels by (1) changing the weight (amount) and distribution (contour) of steel in a barrel, (2) by cooling (internal or external), and (3) by a change in barrel steel composition. The use of the first of these methods to secure vastly enhanced performance was just described in Section 24.3. The second method is discussed in Section 5.7.

There is good evidence from firing tests summarized later in this chapter that moderate to substantial improvement in performance can be achieved in machine gun barrels with a stellite liner, with or without choked-muzzle chromium plate ahead of the liner, by the use of a barrel steel having better high-temperature strength and short-time tensile properties than ordinary WD 4150 machine gun barrel steel to prevent permanent expansion.

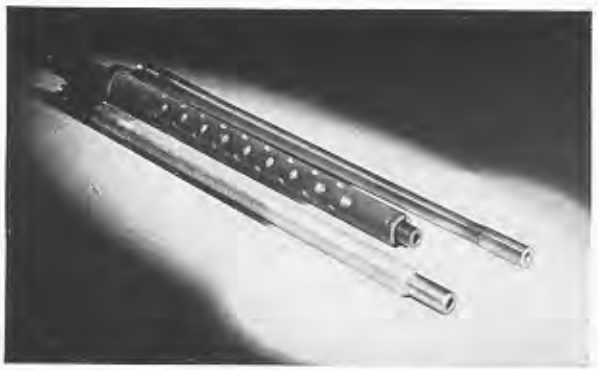


FIGURE 5. Aluminum clad caliber .50 machine gun barrel with circumferential fins and a regular barrel for comparison. (This figure was taken from a progress report by Crane Company on Contract OEMsr-629.)

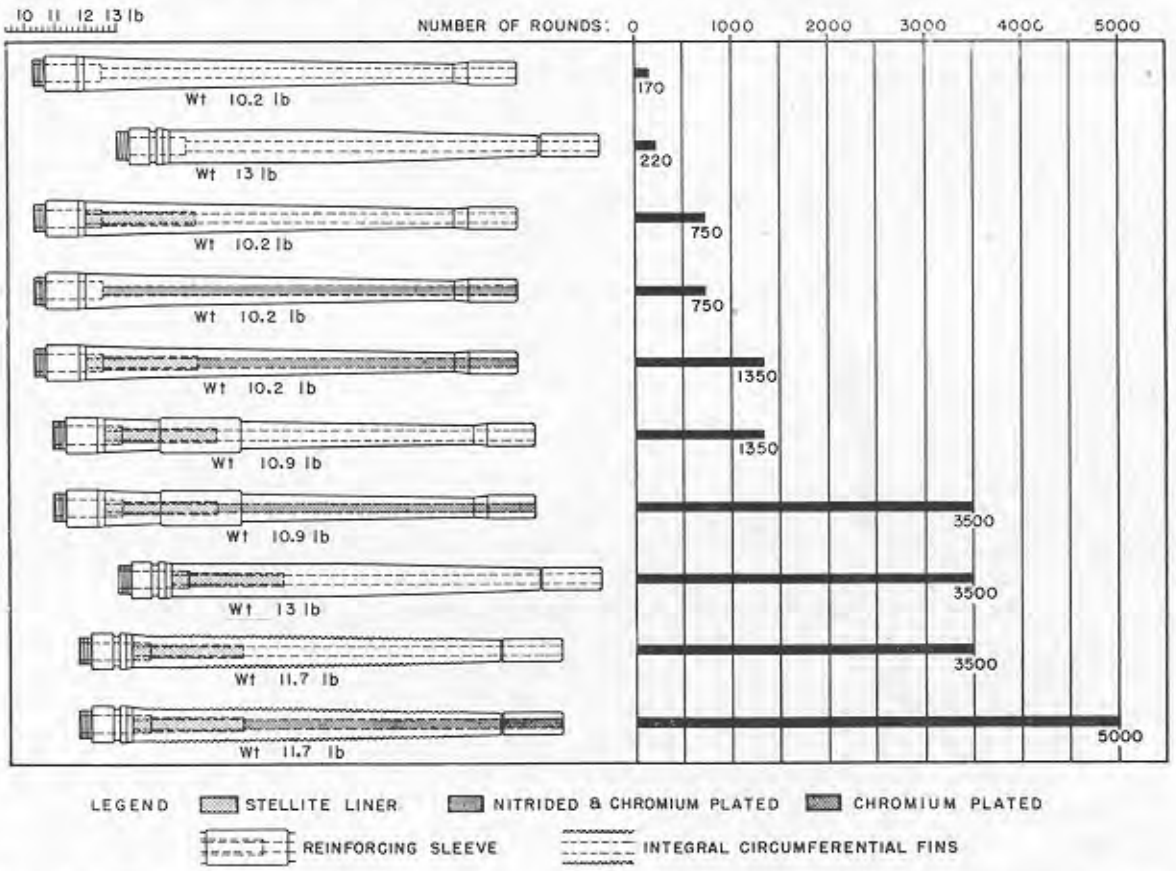


FIGURE 6. The increase in life of caliber .50 machine gun barrels that has resulted from the use of a stellite liner, chromium plating, and the combination of these two modifications.

CONFIDENTIAL

24.5.2 Special Alloy Steels for Gun Barrels

The possible use of various steels and special high-iron alloys as bore-surface materials has already been discussed in Section 16.4.11. The conclusion was reached that because of their lack of resistance to powder gas erosion, no steels or high-iron alloys tested have shown any outstanding promise as bore-surface materials under severe firing conditions. Trials of special barrel steels as a base for choked-muzzle chromium plate on a hardened steel bore and of methods of hardening steel bores before plating have already been described in Section 23.2.1. These steels were selected for their good hot-hardness and low rate of loss of hardness with time when heated in the range of temperatures attained by caliber .50 aircraft barrels during severe firing schedules. Of the steels tested, only barrels of molybdenum steel (Mo, 3.0%; C, 0.13%), whose bores had been induction hardened and then plated with choked-muzzle chromium plate, showed performance equal to or slightly better than nitrided and similarly plated barrels of regular WD 4150 machine gun barrel steel.

In contrast, the use of a barrel steel with better high-temperature properties than WD 4150 gun steel gave moderate to substantial improvements in performance when machine gun barrels with a stellite liner, with or without choked-muzzle chromium plate ahead of the liner, were subjected to firing tests. Before termination of the experimental program of Division 1 there was time for only a reconnaissance of the effects of change of composition and properties of barrel steel on the performance of stellite-lined and chromium-plated machine gun barrels. Enough special steel barrels were made and firing tests completed to indicate that by change of barrel steel at least a doubling of life could be obtained on severe schedules and that longer bursts of fire were possible and feasible without serious impairment of barrel life. Under the stress of war conditions, only a few readily available special steels that could be obtained as bar stock or forgings of the proper size and which were machinable by conventional methods could be tested as barrels.[d] It is strongly recommended that more systematic and extensive studies of the effect of barrel steels on the life and performance of stellite-lined barrels (with and without other features, such as plate ahead of the liner and special weight and contours) be pursued.

[d] The Ordnance Department was very much interested in these reconnaissance studies and cooperated by having a portion of the special barrels prepared at Springfield Armory from steels supplied by contractors of Division 1 who had encountered difficulties in getting special barrels made promptly by the machine gun barrel manufacturers.

24.5.3 Tests of Stellite-Lined Barrels Made of Special Steels

Low-Alloy Steels

The results of tests, extent of testing, and progress on preparation for test of barrels of low-alloy steels containing stellite liners[e] may be summarized as follows:

Templex Steel. Firing tests on four caliber .50 aircraft barrels of Templex steel (ASTM Specification A 193-44 T Grade B 14, a vanadium bearing SAE 4140-type steel) with a 9-in. liner of Stellite No. 21 showed that it is possible to fire a continuous burst of 425 rounds without serious inaccuracy and with little warping or wilting of the barrel. On control tests with similar lined barrels of WD 4150 gun steel the barrels distorted and the barrel blew out in an attempt to fire such a long continuous burst. Thus use of the special steel gives a safety factor when emergency combat conditions necessitate a very long burst of fire.

3% Molybdenum Steel. A firing test on a caliber .50 aircraft barrel of a 3% molybdenum steel containing 0.13% carbon with a 9-in. liner of Stellite No. 21 showed that the accuracy-life and velocity-life obtained from this barrel were superior to those obtained with similar lined barrels of WD 4150 gun steel when fired on the same severe schedule (CGL-350 schedule).

2% Molybdenum Steel. Fifteen caliber .50 aircraft barrels were prepared for test from a steel having the composition: 2.05% Mo, 0.45% Mn, 0.10% Ni, 0.03% Cr, 0.29% Si, 0.20% P, 0.015% Si, and 0.33% C. Five barrels had 9-in. liners of Stellite No. 21 inserted. Two were fired and three were delivered to the Ordnance Department for its tests. The two barrels fired showed no improvement over WD 4150 steel because the steel was not hardened. Five barrels with 9-in. liners of Stellite No. 21 were induction hardened on both the outside diameter and on the bore and were delivered to the Ordnance Department for test.

[e] All these stellite liners were of the design shown in Figure 1 of Chapter 22.

The hardening on the outside diameter was performed to test the strengthening effect of such a hardened layer in preventing barrel expansion under very severe firing conditions. Five barrels recessed to receive 9-in. liners of Stellite No. 21 and induction hardened on the outside diameter and on the bore were chromium plated ahead of the liner recess. After this operation liners were inserted and the barrels delivered to the Ordnance Department for test. The results of the Ordnance Department tests of these several groups of barrels were not available when this summary was written.

Timken 1722A Steel. Springfield Armory prepared for Division 1 six 13-lb caliber .50 aircraft machine gun barrels from Timken 1722A steel, which is a low-alloy steel somewhat similar to ordinary WD 4150 gun steel but with superior high-temperature strength. Liners of special chromium-base alloys were inserted in four barrels (Section 17.4.3) and stellite liners in two barrels. All barrels were fired 5,000 rounds on the severe CGL-350 schedule with no failure. Firing should be continued.

High-Alloy Steels

The results of tests, extent of testing and progress on preparation for test barrels of high-alloy steels are summarized below.

All of the high-alloy steels were difficult to machine and there is some doubt as to whether it would be practical to manufacture barrels for this reason. Another serious question is whether during war time sufficient critical alloying elements would be available to permit the manufacture of a large number of barrels from such high-alloy steels.

Chro-mow Steel Barrels. Two barrels of Chro-mow steel (5 Cr, 1.35 Mo, 1.25 W, 1 Si, 0.30 C) from the Crucible Steel Company, with 9-in. liners of Stellite No. 21 were subjected to firing tests. The results were somewhat inconclusive because the barrels had been bored oversize for chromium plating, but no plate was applied. After severe firing both the steel and liner showed good resistance to erosion but the barrel was inaccurate owing to the oversize bore.

Peerless A Steel. Four barrels of Peerless A steel (9 W, 3.25 Cr, 0.25 V, 0.28 C) from the Crucible Steel Co., with 9-in. liners of Stellite No. 21 were tested. They had double the life of similar barrels of WD 4150 gun steel on the CGL-350 schedule.

Silchrome XCR Steel. Silchrome XCR steel (24 Cr, 5 Ni, 3 Mo, 0.45 C) from the Allegheny-Ludlum Steel Corp. has better high-temperature properties than gun steel and when tested as a liner in the caliber .50 heavy machine gun barrel showed better erosion resistance than WD 4150 gun steel. Thirty-two bars of this steel were sent to Springfield Armory by Division 1 for the preparation of special barrels. Twenty special caliber .50 aircraft barrels (some regular 10-lb and some special 13-lb barrels with 9-in. liners of Stellite No. 21) were to be prepared as well as six caliber .30 aircraft barrels with no liner. It was found impossible to drill or machine this steel because of hard spots in the steel supplied.

Potomac Grade 81 Steel. Springfield Armory prepared three 13-lb caliber .50 aircraft barrels of Potomac Grade 81 steel (4.8 Cr, 1.28 W, 1.3 Mo, 0.20 V, 0.32 C) from the Allegheny-Ludlum Steel Corp. These barrels, which contained 9-in. liners of Stellite No. 21 were sent to Crane Company for test. After termination of the NDRC contract at Crane, they were transferred to the Ordnance Department for test.

HIA Grade 160 Steel. Springfield Armory prepared three 13-lb caliber .50 aircraft barrels of HIA Grade 160 steel (4.9 Cr, 4 Mo, 1.8 Ni, 0.44 C) from the Allegheny-Ludlum Steel Corporation. These barrels, which contained 9-in. liners of Stellite No. 21 were sent to Crane Company for test. After termination of the NDRC contract at Crane, they were delivered to the Ordnance Department for test.

Grade 1084 Steel. Springfield Armory attempted to prepare three 13-lb caliber .50 aircraft barrels from Grade 1084 steel (9 Cr, 1 Mo, 0.26 C) from the Allegheny-Ludlum Steel Corp. Two barrels were spoiled owing to the poor machinability of this steel. One barrel was completed and sent to Crane Co. for test. Owing to termination of the NDRC contract at Crane, this barrel was transferred to the Ordnance Department for test.

Grade 1093 Steel. Crane Company obtained from the Allegheny-Ludlum Steel Corp. several bars of Grade 1093 steel. They intended to send them to Springfield Armory, which was to prepare 13-lb caliber .50 aircraft barrels. Owing to the termination of the NDRC contract at Crane Company, this steel was never sent to the Armory.

XB Valve Steel. Geophysical Laboratory sent several bars of XB valve steel from the Allegheny-Ludlum Steel Corp. to Springfield Armory. This steel has the composition 19.5 Cr, 1.35 Ni, 2.29 Si, 0.76 C. Two regular caliber .50 aircraft barrels with 9-in. liners of Stellite No. 21 were made and retained by the Ord-

nance Department after termination of the experimental program of Division 1.

Exelloy Steel. Three regular 10-lb caliber .50 aircraft barrels of this steel were made for Crane Company by Springfield Armory from Exelloy steel, which is a Crane Company steel containing 13% Cr, 0.5% Ni, 0.11% C. One barrel without a liner gave a performance inferior to that of a regular WD 4150 steel barrel. Regular Stellite No. 21 liners were to have been inserted in the other two barrels, but one barrel was spoiled in processing. A 6-in. external reinforcing sleeve (Section 24.2) of Templex steel (see above) was fitted on the other barrel with a liner and it was subjected to a firing test. Its performance was comparable to a similarly reinforced WD 4150 steel barrel with a liner except that the Exelloy steel barrel ruptured, terminating the test. The resistance of this steel to impact from the bullets apparently is very poor.

Potomac Hot Die Steel. Six regular 10-lb caliber .50 aircraft barrels of Potomac Hot Die Steel (5 Cr, 1.7 Mo, 1.3 W, 1 Si, 0.33 C) from the Allegheny-Ludlum Steel Corp. were made for Geophysical Laboratory by Springfield Armory. These barrels were for use in bore hardening prior to chromium plating but similar barrels could be used with liners. This steel is very similar to the Chro-mow steel already discussed.

TK Hot Die Steel. Two regular 10-lb caliber .50 aircraft barrels of TK Hot Die Steel (10 W, 3.8 Cr, 0.22 Cb, 0.1 Mo, 0.06 V, 0.34 C) from the Carpenter Steel Co. were made for Geophysical Laboratory by Springfield Armory. The steel was first heat treated to about 35 Rockwell C. Both barrels were defective and were not fired. Pieces of this steel, which has good high-temperature properties, were used at Geophysical Laboratory to make the external reinforcing sleeves for regular WD 4150 steel barrels with stellite liners described in Section 24.2.

24.6 OPTIMUM COMBINATION FOR BEST PERFORMANCE

In summary we may say that to obtain the best caliber .50 aircraft machine gun barrel performance[f] the following features should be combined:

(1) Breech liner of Stellite No. 21, 9 in. long;

(2) Choked-muzzle chromium plate ahead of the liner;

(3) Proper change in weight and external contour of the barrel (total weight and distribution of metal consistent with cyclic rate of fire desired and maximum permissible weight).

(4) Barrel made from special heat-resisting steel with better elevated temperature properties than conventional machine gun barrel steel.

(5) External or internal barrel cooling, a subject discussed in Section 5.7. The cooperation of the Air Forces working hand in hand with the developers of gun barrels, guns, and gun mounts will be necessary in order to combine effectively external barrel cooling with the other improvements.

Attention is called here to some very suggestive firing tests (Section 17.4.3) of 13-lb caliber .50 aircraft barrels of a special steel containing liners of two different chromium-base alloys. Because of their higher melting temperatures the chromium-base alloy liners, unlike those of stellite (Section 19.5.2), should perform well in firings with higher velocity ammunition using double-base powder. Further development and tests of the chromium-base alloy liners should be made to evaluate their potentialities in machine gun barrels under hypervelocity conditions.

[f] Melting or at least softening of the bullet jacket from frictional heat (Section 6.1.2) may impose an additional limitation on gun performance when the present gilding metal jacket is used. No material having greater strength at elevated temperatures has been suggested that would not increase the frictional wear on the barrel.

[redacted]

Chapter 25

PILOT PLANTS FOR CHROMIUM-PLATING CALIBER .50 BARRELS[a]

By *V. Wichum*[b] and *C. A. Marsh*[c]

25.1 DEVELOPMENT OF IMPROVED BARRELS

THE RATHER RAPID DEVELOPMENT of the improved caliber .50 aircraft machine gun barrels described in Chapters 23 and 24 was made possible by the setting-up of pilot plants for small-scale production after other essentials of design had been determined by laboratory experiments. A brief chronological account of the development which led to the adoption by Army Ordnance of these improved barrels to supersede the formerly standard steel barrel is deemed worth while in order to evaluate the success of the pilot-plant projects.

The nitrided, chromium-plated caliber .50 aircraft barrel with choked muzzle was designed as a result of experiments to find a suitable hot-hard material to resist swaging and an adherent erosion-resistant plating to prevent powder-gas erosion of the bore.[81] The choked muzzle was to increase the accuracy-life of the barrel. The plating and electropolishing procedures (described in Chapter 20) were worked out at the National Bureau of Standards in collaboration with the Geophysical Laboratory, Carnegie Institution of Washington, where firing tests and examination of fired barrels were carried out to serve as a basis for specifications, as described in Section 23.1.2.

The techniques employed by the National Bureau of Standards were not necessarily practical for large-scale production. To prove the practicability of chromium-plating large quantities of caliber .50 barrels, a commercial plating company, the W. B. Jarvis Company[d] was chosen in July 1944 to carry out pilot-plant operations resulting in limited production of barrels for testing purposes, under a subcontract with the Geophysical Laboratory. Necessary changes in the recommended procedure were made in order to conform to production methods.

An extensive research program was carried out by the Geophysical Laboratory and the Jarvis Company to evaluate the importance of various steps in the plating procedure. On the basis of this research, final specifications and the procedure outlined in Section 25.2.1 were established.[81]

Thereupon, several hundred barrels plated by the Doehler-Jarvis Corporation were delivered by Division 1 to the Army Ordnance Department for test. This barrel was finally adopted for Service use in January 1945.[294]

The need for immediately starting production of chromium-plated barrels led the Ordnance Department to request the assistance of Division 1 in guiding prospective Ordnance contractors. Thereupon, early in 1945 a contract was arranged with the Chrome Gage Corporation for an additional pilot plant to serve specifically as a control for Ordnance production contracts.

During the setting-up of the latter pilot plant, the Doehler-Jarvis Corporation continued to produce barrels for test at the Geophysical Laboratory and for the Services. In April 1945, production was started under a separate Ordnance contract with this company. During the last two months of its operation, Doehler-Jarvis was chromium plating almost 700 barrels daily on that contract.

By the time that a small number of barrels had been produced by the Chrome Gage Corporation successful experiments with the "combination" barrel (Chapter 24) led the Ordnance Department to cancel orders in June 1945 for the nitrided, chromium-plated barrel with choked muzzle and to request production of the "combination" barrel. This barrel, which contained a 9-in. liner of Stellite No. 21 and which was chromium-plated ahead of the liner to give a choked-muzzle, was found to have both a long accuracy-life and a long velocity-life. In spite of the necessity for developing new plating techniques for the "combination" barrel, several hundred barrels

[a] This chapter is based largely on an informal report submitted on November 29, 1945, to the National Bureau of Standards by the Doehler-Jarvis Corporation and on the final report[142] from the Chrome Gage Corporation on Contract OEMsr-1444. The former report has not been distributed; and the latter has had a very limited distribution.

[b] Engineer, Division 1, NDRC. (Present address: New York, N. Y.)

[c] Geophysical Laboratory, Carnegie Institution of Washington. (Present address: U. S. Geological Survey, Washington, D. C.)

[d] Later, the Jarvis Division of the Doehler-Jarvis Corporation.

were plated both by Chrome Gage and Doehler-Jarvis before the surrender of Japan brought about the closing of both pilot plants.

25.2 PILOT PLANT OF THE DOEHLER-JARVIS CORPORATION

25.2.1 Plating Procedure for Nitrided Barrels

The chromium-plating procedure recommended by the National Bureau of Standards, as given in Section 20.2.3, is essentially the one followed by Doehler-Jarvis. Some changes were made as a result of firing tests on several lots of barrels that were plated, with variations in the procedures.[110] About 50 different experimental lots of barrels were plated, there being one to five barrels in a lot. The type of anode, the trivalent chromium content of the bath, times of plating, current density, longitudinal distribution of chromium, length of reversal of current prior to plating, method of scrubbing the bore, and so on, were varied independently. The barrels were tested by firing and carefully examined. The resulting preferred procedure is listed below together with appropriate notes on the various steps. Also the changes that were made from time to time are noted. A diagram of the three principal steps in the process of producing the improved barrel from a standard barrel is shown as Figure 1 of Chapter 23.

Decoppering was one of the steps listed in Section 20.2.3. This was done, in the case of the nitrided barrels, before nitriding and so it is not included here. Also for a discussion of the nitriding and tests prior to plating, the reader is referred to Section 23.1.2.

Outline of Procedure

The steps in the procedure will not only be listed but will be grouped as follows:

1. Receive, unpack, check quantity and type.
2. Buff muzzle bearing to remove chromium plate.
3. Number, giving lot number, Doehler-Jarvis identification "J," and serial number, (Example—L2-J20).
4. Paint barrel with stop-off lacquer.
5. Clean barrel.
   a. Swab with solvent (Triad).
   b. Scrub with inhibited hydrochloric acid and pumice.
   c. Scrub with alkaline cleaner and pumice.
   d. Boroscope.
   e. Rinse and dry.
   f. Oil lightly.
6. Gauge.
   a. Make out Record Sheet for each barrel and enter all information up to this point.
   b. Gauge lands and grooves at designated points and gauge centering cylinder.
   c. Enter above information on Record Sheet.
   d. Determine time for electropolishing and enter on Sheet.
7. Clean barrel.
   a. Same as Step No. 5 except that boroscoping and final oiling is unnecessary.
8. Rack for electropolish.
   a. Assemble fittings and anode, making sure fittings are clean, insulators are in good repair, and that anode is clean and straight. Use Saran tube over anode when inserting in barrel. This tube must be wiped with solvent each time before use. Anode must be checked for tension.
   b. Assemble hanger with above assembly, making sure that all contacting points are clean and that the barrel hangs straight.
9. Electropolish (see Figure 1 of Chapter 23).
   a. Check temperature of solution (108–112 F) and see that agitation is constant and adequate.
   b. Place barrel in tank and make connections.
   c. Apply current, starting with 9-10 volts. Amperage will drop after a short time. When this occurs, adjust current to 90 amp.
   d. Electropolish for designated time. Operator should place tag on hanger showing "Time In" and "Time Out." Also a record of this operation is to be made on sheet provided for this purpose.
10. Clean and unrack.
    a. Rinse with spent CrO_3 solution.
    b. Rinse with water.
    c. Unrack.
    d. Rinse.
    e. Scrub with pumice and cleaner.
    f. Rinse and dry.
    g. Oil lightly.
11. Gauge.
    a. Gauge lands and grooves at designated points and record on Record Sheet.
    b. Calculate and enter amount removed on Sheet.

c. Calculate plating time and enter on Record Sheet.

12. Clean.
    a. Same as Step No. 7.
13. Rack for plating.
    a. Same procedure and precautions as under Step No. 8.
14. Pretreat (anodic etch in chromic acid).
    a. Check temperature of pretreat tank (125 F) and check agitation.
    b. Place barrel in tank, make connections, and apply current for 5 min at 70 amp.
15. Plate (See Figure 1 of Chapter 23).
    a. Check temperature of plating tank (122-123 F) twice a shift and check agitation.
    b. Remove barrel from reversing bar (in pretreat tank) and place on plating bar. Make connections and apply current at 70 amp for designated time. Tagging and recording as in Step No. 9.
16. Clean and unrack.
    a. Same as Step No. 10 except that rinsing before unracking is done with water only. First cold and then hot water is used.
17. Gauge.
    a. Read lands and grooves at designated points and centering cylinder.
    b. Calculate and record thickness of plate.
    c. Calculate ratio for thickness at breech and muzzle and plating speed.
    d. Place all barrels, O.K. and rejects, in box or truck for removal to Final Inspection.
    e. Transfer Record Sheets to Final Inspection.
18. Inspect finally.
    a. Boroscope.
    b. Check gauging records for completeness and compliance with specific dimensions and tolerances.
    c Place O.K. barrels in space provided.
    d. Send rejected barrels back for stripping and replating or place with scrap barrels.
    e. Make proper disposition of *all* Record Sheets.
    f. Enter information on *all* Record Sheets on "Disposition" sheet. This sheet must show status of each barrel plated.
19. Remove paint and prepare for shipment.
    a. List O.K. barrels according to lot and barrel number.
    b. Remove paint and thoroughly clean barrel inside and out. Clean threads and flutes at breech end with a wire brush to remove rust, scale, and chemical deposits.
    c. Paint an olive drab band 4 in. wide around each barrel 2 in. behind front muzzle bearing.
    d. Dip barrel in rust-proofing oil, wrap in paper and pack. Check lot and serial number against list.

Cleaning Operations

Degreasing. During intervals when the barrels were not being treated in some one of the various solutions, it was necessary to keep them oiled to prevent rusting. The grease or oil had to be removed prior to some of the steps of the procedure. This was done by swabbing the bore with Triad.

Scrubbing. Before gauging the nitrided barrels prior to electropolishing it was necessary to scrub the bore to remove the brittle iron nitride layer. This operation was performed with a tightly fitting patch or a wire brush on a cleaning rod, using powdered pumice and a dilute, inhibited hydrochloric acid solution; 50 per cent concentrated HCl by volume plus 10 ml per liter of "Rodine" inhibitor. A boroscope was used to differentiate between a well-scrubbed bore and one with a nitride layer.

A scrub with alkaline cleaner was always employed after one with hydrochloric acid. Other scrubbing operations when acid was not used were usually carried out with the cleaner plus powdered pumice. The solution contained 8 oz/gal of a commercial cleaner.

Rinsing. Thorough rinsing was always necessary after the barrels had been subjected to scrubbing, polishing, or plating solutions. After the electropolishing, the bores were rinsed with a small amount of spent chromic acid plating solution to avoid etching by sulfuric acid which occurs when the polishing solution is diluted. After the electroplating, a hot rinse was used to facilitate the drying which had to be done as quickly as possible. A cold rinse was employed first to remove the bulk of the plating solution so the hot rinsing tank would not become contaminated.

Oiling. As was stated above, oiling was necessary between some steps to prevent rusting. Finger print removing oil was applied lightly.

Gauging Operations

The gauging before electropolishing and electroplating was carried out with a Sheffield Precisionaire

gauge. This served not only as a routine check on the barrels during processing but enabled the operator to calculate the times the barrels should remain in the solutions in order to obtain dimensions that were within the specified tolerances.

Preliminary gauging after chromium-plating to determine the diameter of the centering cylinder was done by means of plug gauges. The first of the final gauging operations made use of the Sheffield Precisionaire gauge. If the barrels were found to be within the dimensional tolerances, they were taken to the next operations (Nos. 18 and 19). If not satisfactory, they were regauged with a Federal Star Gauge. As a result of this step they were either accepted or rejected or put into the "merit" classification.

Electropolishing

To remove sufficient metal from the bore to accommodate the chromium plate that was to be added and to remove burrs and sharp corners, the bores of the barrels were electropolished using the solution described in Section 20.2.3. The solution, kept at 108-112 F, contained 50% by volume each of concentrated (96%) sulfuric acid and concentrated (75%) phosphoric acid. Its specific gravity was maintained between 1.68 and 1.76 by adding or evaporating water. A $\frac{3}{16}$-in. diameter copper rod plated with a lead-tin alloy (0.005 in. thick) was used as a cathode. The initial current applied was higher than the correct operating current (93 amp, which gave a current density of 250 amp per sq ft). If the initial current was low, followed by an increase, the bore might be etched instead of polished. Vigorous air agitation was necessary to prevent a taper.

With the above procedure, the polishing rate was about 0.001 in. on the diameter in 10 min. The time usually required was slightly more than ten minutes.

Anodic Etch Prior to Plating

After the barrels were assembled in the plating bath a reversal of current prior to plating was applied for 5 min, a time determined by experimental work. This procedure, which cleaned the bore surface and gave it a slight etch, was found to improve the adhesion of the chromium plate to the steel.

Electroplating

The barrels were plated with HC chromium (see Section 20.2.2) in such a manner that the deposit was thicker at the muzzle end than near the breech. This taper was automatically obtained when the procedure given below was followed. The conditions which affect the amount of taper are discussed in Section 20.2.3.

The solution, kept at 122 ± 2 F, contained 250 ± 10 g chromic acid (CrO_3) and 2.5 g ±0.1 anhydrous sulfuric acid per liter. During continuous use of the tanks, the amount of chromium reduced to the trivalent state increased with a resultant substantial increase in the plating speed so that corrections in the plating time had to be made. Also, tapered anodes ($\frac{3}{16}$ in. at the muzzle end and $\frac{1}{8}$ in. at the breech end) were tried when, as a result of operation, the amount of trivalent chromium in the bath affected the taper. The anode to be used when the solutions were new was a $\frac{3}{16}$-in. steel rod plated with a lead-tin alloy (0.005 in. thick). Either a $\frac{1}{8}$-in. or $\frac{5}{32}$-in. anode was used depending on the age of the bath. The plating current was 69 amp, which gave a current density of 190 amp per sq ft. Air agitation insured a uniform temperature and bath composition.

The assembling of the barrels, anodes, and fittings for plating was essentially the same as for electropolishing. The barrels were plated with the muzzle end up and the current connection was made at the top of the anode. It was necessary to stop-off the first $3\frac{1}{4}$ in. at the breech end of the coated steel anode with Saran tubing so that the corresponding section of the chamber would not be plated.

The plating rate for a new bath was about 0.001 in. per hour on the diameter at $31\frac{1}{4}$ in. from the muzzle, which is just ahead of the origin of rifling.

The finished bore surface was to have a continuous bright plate that was free from nodules, blisters, flaking, or other surface imperfections.

Fittings used to center and insulate the anodes and the current connections are shown in Figures 3 and 4 in Chapter 20.

Simplified Procedure

A simplified procedure, in which several steps were omitted, was tried on one lot of barrels after the Ordnance Department had approved some barrels plated by the above procedure. It was found to be satisfactory.

The major changes were the omission of lacquering (Step 4 of Section 25.2.1), and the omission of the scrubbing and gauging prior to electropolishing (Steps 5, 6, and 7 of Section 25.2.1), since the latter

removes the nitride layer equally well. The barrels were merely degreased before being polished. The rinse with spent chromic acid solution after electropolishing (Step 10a) was also omitted in the final procedure.

25.2.2

Dimensions of Nitrided, Plated Barrels with Choked Muzzles

The diameter of the bore across the lands at both breech and muzzle ends of the regular, steel barrels from which the improved type of barrel was made by nitriding and chromium-plating was between 0.4990 and 0.5010 in. In the latter type of barrel, however, a taper of bore diameter from the origin of rifling to the muzzle was found to be the feature essentially responsible for the very great prolongment of accuracy-life.

The bore dimensions after plating had to be held within specified limits for optimum performance. On the basis of research up to October 1944, which was prior to operations by Doehler-Jarvis, the dimensions[81] were specified to be as shown in the second column of Table 1.

TABLE 1. Final specifications for nitrided, chromium-plated caliber .50 aircraft barrels.

Distance from muzzle (in.)	Specified diameter (in.) Oct. 1944	June 1945
1½	0.4950 + .0015	0.4920 + .0040
10	0.4980 (max.)	0.4950 + .0030
15	0.4985 (max.)	0.4960 + .0030
31¼	0.4985 + .0015	0.4985 + .0025
32.1	0.512 + .002	0.513 + .002

The maximum value for the diameter at the muzzle was set at 0.4965 in. after it had been found that the muzzle had to be choked to at least this extent to obtain optimum performance. At the origin of rifling the diameter could not be less than 0.4985 in. because the excessive gas pressures which would develop when the bore in this region was smaller than this might cause primers to be blown. Between both ends of the rifled portion of the barrel a uniform taper was desirable, but limiting dimensions were not set for positions at equal distances throughout the bore. It was important, however, that there should not be a sharp taper right at the muzzle, hence maximum diameters were specified for positions at 10 and 15 in. from the muzzle end.



FIGURE 1. Varying thickness of chromium plate at different positions along the bore of a nitrided and chromium-plated caliber .50 barrel with choked muzzle. (From a Doehler-Jarvis report to Geophysical Lab.)

CONFIDENTIAL

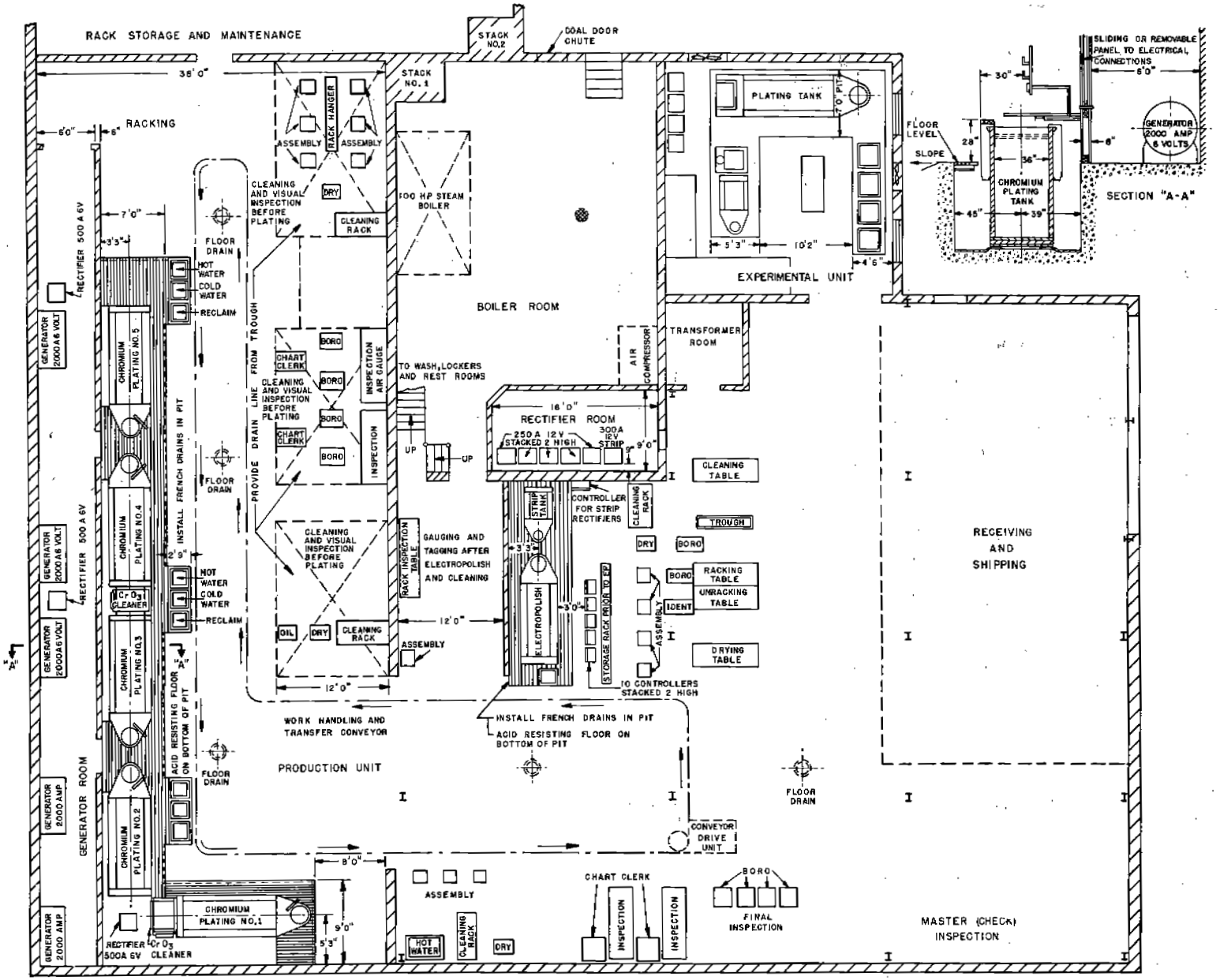


FIGURE 2. Floor plan of pilot plant set up by Chrome Gage Corporation for chromium plating caliber .50 machine gun barrels. (From OSRD Report No. 6517.)

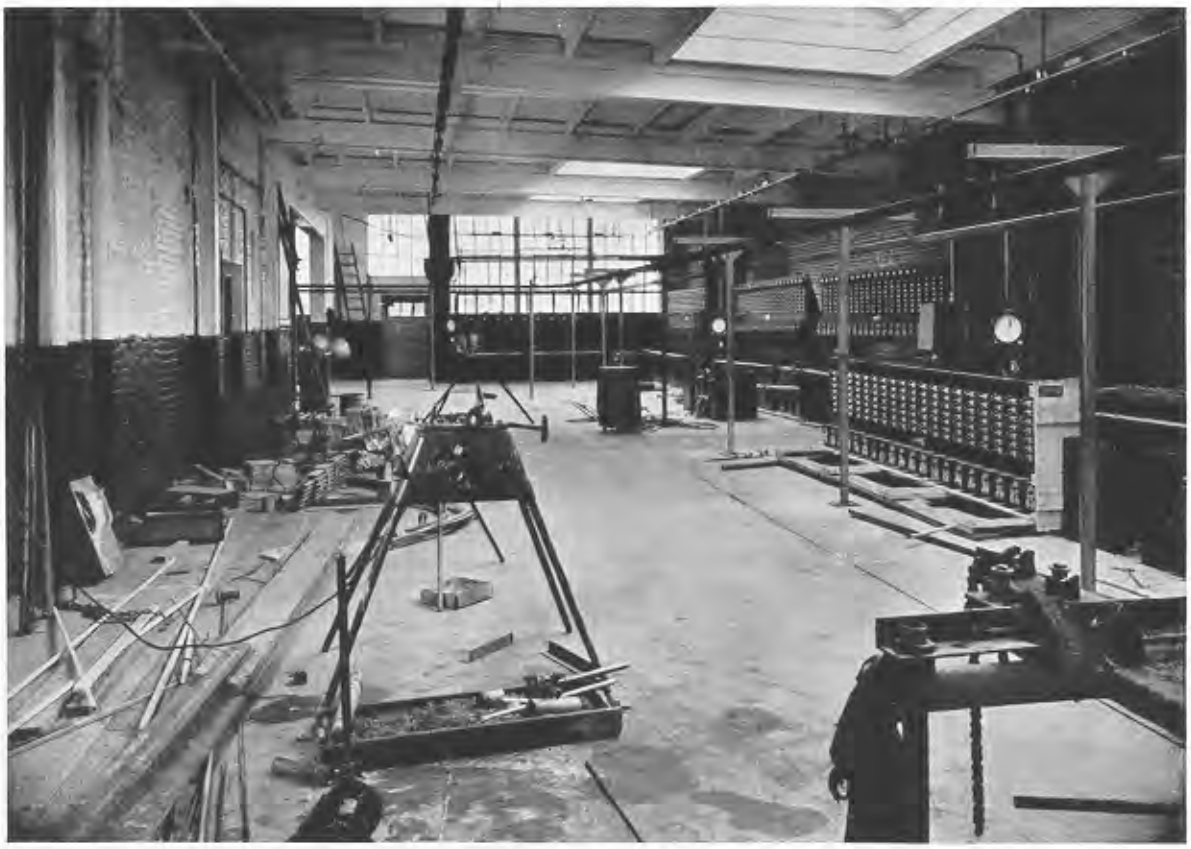


FIGURE 3. Production unit in Chrome Gage pilot plant. (From OSRD Report No. 6517.)

During the course of the work at Doehler-Jarvis, these specifications were modified slightly, on the basis of experience gained in the testing of plated barrels. The final specifications as of June 6, 1945, the date the orders for these barrels were canceled because of the development of the stellite-lined, chromium-plated barrel, described in Chapter 24, are given in the third column of Table 1. A comparison of this column with the second one shows the greatest change in specified diameters was at the muzzle. It was found that better barrel performance was favored with smaller diameters than 0.4950 in. This dimension could be even less than 0.4920 in. but in this case plating time would be too much longer than was justified by the increase in barrel performance.

The taper was obtained by chromium-plating the bore under carefully controlled conditions so that the deposit was thicker at the muzzle than at the breech. Figure 1 shows the variation in thickness from muzzle to breech in a typical barrel. The minimum thickness was the only one specified; thus, on any land at the origin of rifling it was to be 0.0020 $\pm$ 0.0005 in.

The large amount of heat input (Section 13.2.5) to the steel in the cylinder of the caliber .50 machine gun barrel causes a decrease in diameter of about 0.002 in. When the cylinder becomes constricted, stoppages may occur as a result of the failure of the cartridges to seat. In a regular steel barrel, constriction is not a problem because the unprotected steel is subject to erosion by the powder gases when the barrel is first fired, but in chromium-plated barrels the cylinder has to be made larger. The stock barrels, therefore, were reamed out before nitriding and plating. As can be seen from Table 1, the diameter (32.1 in. from muzzle) specified in October 1944 was not large enough.

25.2.3 "Combination" Barrels

Changes had to be made in the procedure described above for nitrided barrels when caliber .50 aircraft barrels that were to contain a stellite liner were chromium-plated. Only the portion ahead of the liner was to be plated. These barrels were not nitrided.

CONFIDENTIAL

If they had been proof-fired, it was necessary to decopper them before the standard plating procedure was applied. Not enough work was done before the termination of the program to determine the best production method of plating these barrels. The difficulties encountered are discussed in Section 20.2.3.

25.2.4 Accomplishments of the Dochler-Jarvis Pilot Plant

The operation of the Doehler-Jarvis pilot plant made at least three important contributions to the project.

1. It provided the several hundred barrels necessary for testing by the interested Army and Navy Services, prior to acceptance of such barrels for production.

2. It made possible the testing on an adequate scale of the large number of variables involved in preparing and plating the barrels, thus permitting choice of the most effective methods.

3. It demonstrated that a well-managed and efficiently operated plant could carry out on a production scale the relatively complex and precise plating operations involved, with uniformly good results, a very low percentage of rejections, and at reasonable costs.

25.3 PILOT PLANT OF THE CHROME GAGE CORPORATION

25.3.1 Description of Project

When Army Ordnance had outlined a program for the large-scale production of improved caliber .50 aircraft machine gun barrels, the Chrome Gage Corporation of Philadelphia was chosen as the commercial plant to confirm or improve the plating technique developed at the pilot plant of the Doehler-Jarvis Corporation, and to operate a commercial plant.

Under the terms of the contract 10,000 caliber .50 aircraft machine gun barrels were to be nitrided and chromium-plated, the nitriding to be done by a subcontractor. A pilot plant was to be installed to develop methods which would be better suited to quantity production than the existing ones, would yield more uniform results, and would substantially reduce the cost of plating caliber .50 gun barrels with hard chromium. The following program was set up.

1. Design and equip an experimental plant or unit having a capacity of plating twenty barrels simultaneously under varying conditions.

2. Design and equip a pilot production plant or unit having a capacity of plating 100 barrels simultaneously.

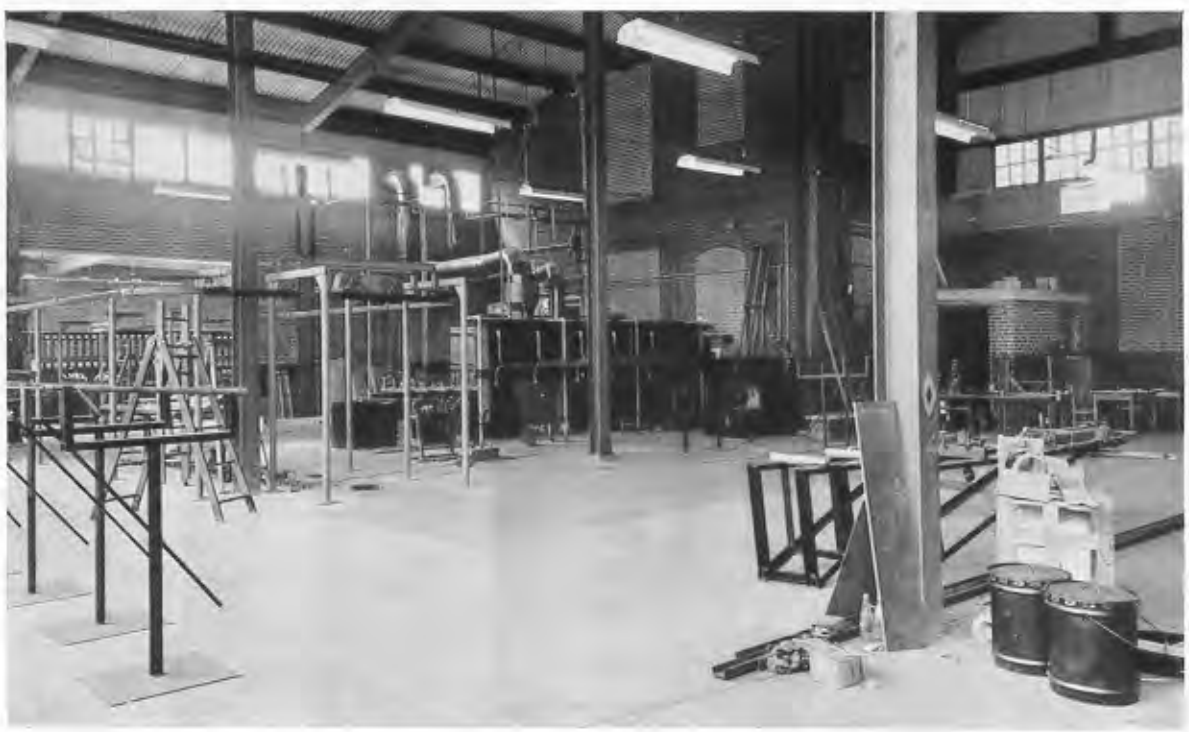


FIGURE 4. Receiving, shipping, and final inspection areas of Chrome Gage pilot plant. (From OSRD Report No. 6517.)

CONFIDENTIAL

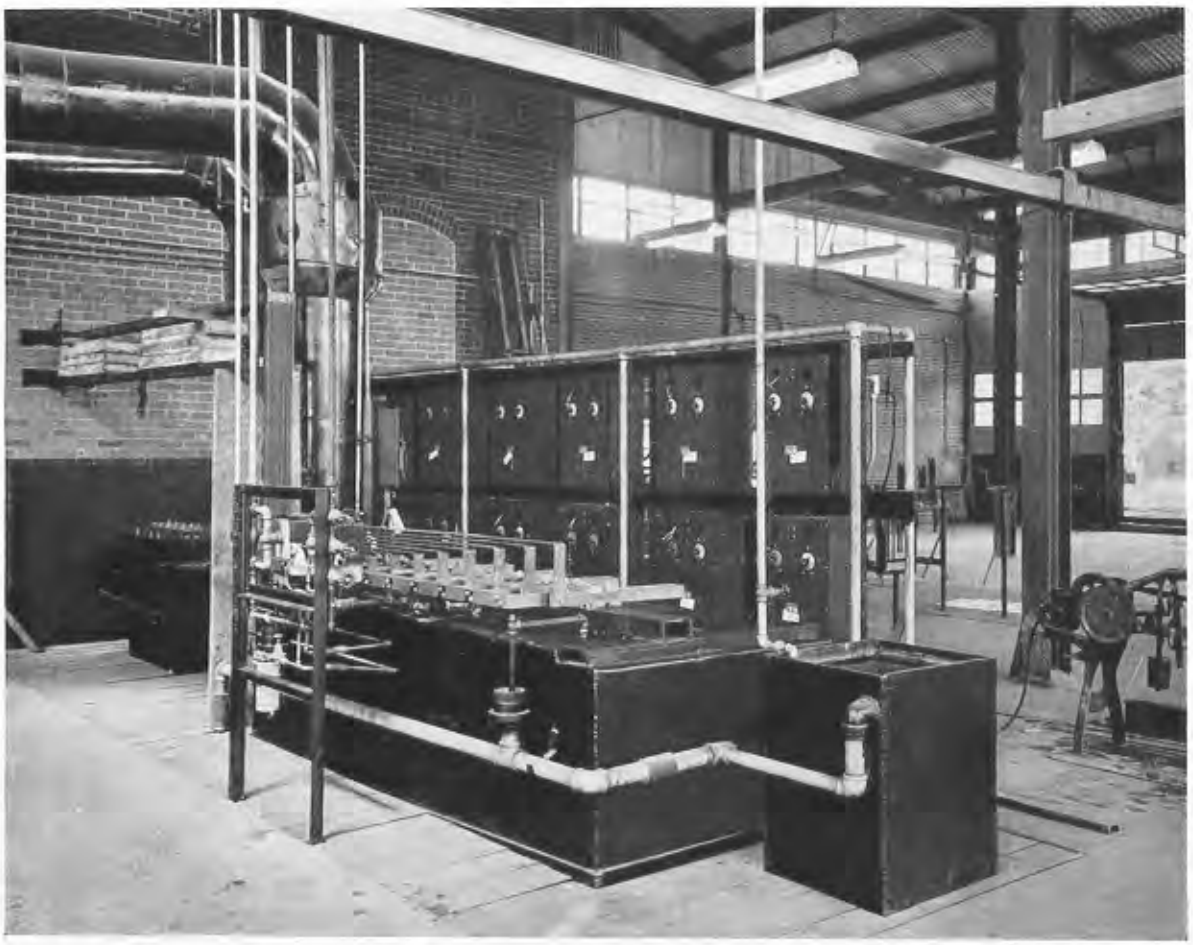


FIGURE 5. Electropolishing tank of production unit in Chrome Gage pilot plant. (From OSRD Report No. 6517.)

3. Develop testing methods, inspection procedure, and specifications for all stages of processing from the time barrels were received until they were test fired.

4. Explore possible improvements in testing and processing through research and development, and try same in the experimental unit before adoption in production manufacture.

5. Evolve methods of handling in production with the least expense of labor.

6. Provide methods of checking and inspection, which would prevent faulty processing and furnish the necessary information by which results might be analyzed.

7. Carry on experimental plating operations.

The net result of this program was to be a check on the practicality of the tentative specifications[292] issued by the Ordnance Department for nitrided and chromium-plated caliber .50 aircraft machine gun barrels with choked muzzle (Chapter 23). Those specifications had been based on the experience of the Doehler-Jarvis Corporation. Before production could get under way, the scope of the project was expanded to include the plating of the chromium-plated caliber .50 barrels with stellite liners at the breech end (Chapter 24), also in accordance with tentative Ordnance Department specifications.

25.3.2

Plant Installation

When a termination order was received on August 17, 1945, the production line of the pilot plant was not quite completed. It had been designed to handle 500 barrels a day. An old dye house had been extensively remodeled in accordance with the floor plan shown in Figure 2. Two views of the partially completed installations are shown in Figures 3 and 4. The electropolishing unit, which was complete except for some minor electrical work, is shown in Figure 5.

CONFIDENTIAL

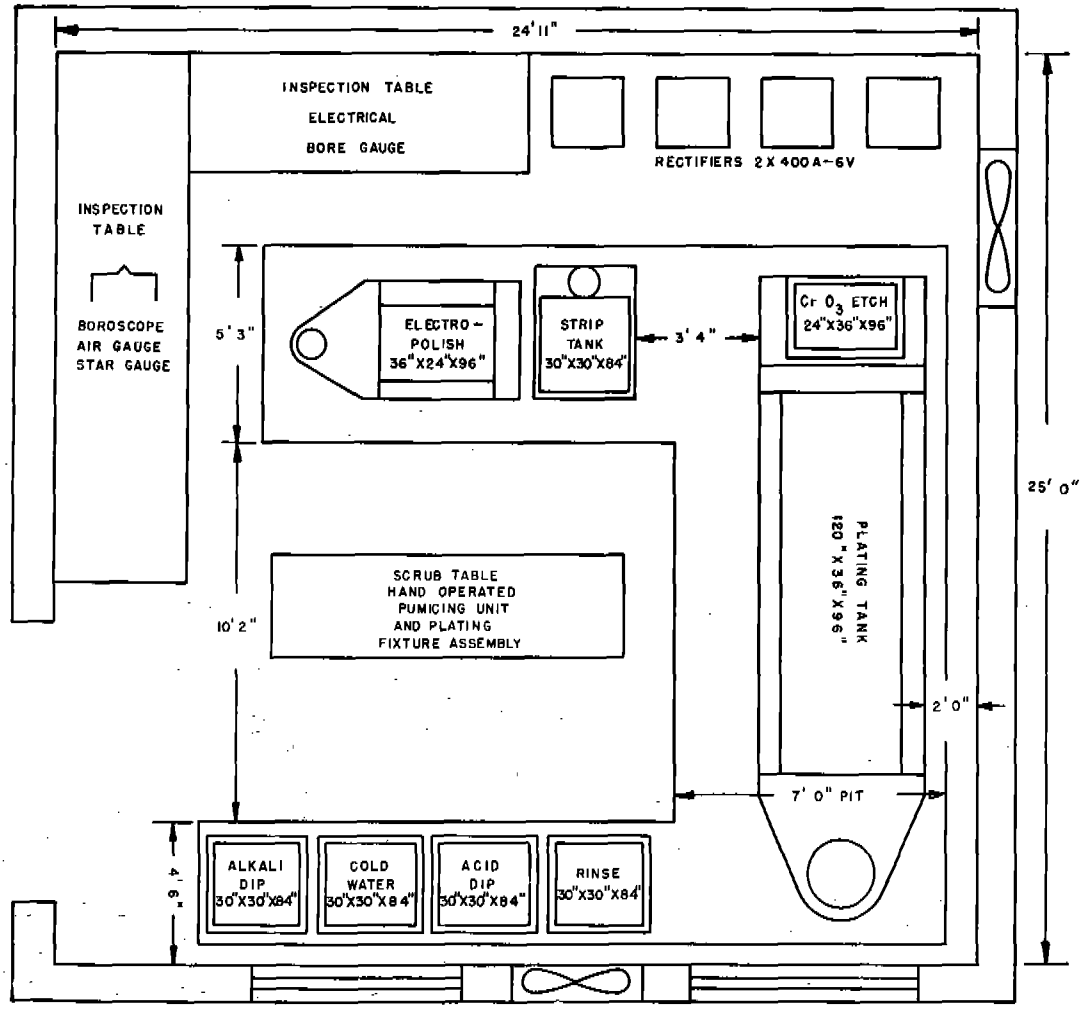


FIGURE 6. Floor plan of experimental plating unit in Chrome Gage pilot plant. (From OSRD Report No. 6517.)

An experimental plating unit suitable for a large range of work had been in operation slightly over 3 months. Its floor plan is shown in Figure 6 and an interior view of it in Figure 7.

Noteworthy among the designs of equipment were ones for the following: a plating fixture and clamp for the gun barrel to provide for concentricity of anode, good electrical contact, and ease of assembly and handling; an efficient pneumatic pumicing unit for scrubbing the bores; a boroscope inspection unit; an improved star gauge; and an electrical bore gauge involving a new application of a strain gauge, as is described in Section 25.3.5. Groups of barrels were handled by the overhead conveyor shown in Figure 8.

Interpretation of test results was facilitated by the recording methods devised. Samples of Form CGC No. 1, "Barrel Inspection Before Plating" and of Form CGC No. 2, "Gauging Record" are shown in Figures 9 and 10, respectively, with appropriate data filled in for actual barrels. These two forms were to be used for all barrels put through the production line, as well as for experimental barrels.

In addition a "Graphic Record" was maintained on Form CGC No. 3 (Figure 11) for each barrel in the experimental plating unit to show the bore diameter through the length of the barrel initially, after electropolishing, after plating, and after a firing test. The conditions for electropolishing and electroplating were recorded on the same form. Two other forms were also used for the experimental barrels to record the details of the firing test and the appearance of the bore surface as shown by a boroscope examination after the test.

25.3.3 Barrels Handled and Processed

Nearly 1,300 barrels were handled in one or more stages of the plating process, either in the experimental unit or in preliminary trials of the production line.

Of these barrels, which had been nitrided and were to be chromium-plated, 382 were rejected before electropolishing, 330 were rejected after electropolishing, and 266 after plating. Finally, 308 barrels were accepted, based on dimensions and appearance. Some barrels had also been rejected before nitriding for the following reasons: (1) did not pass straightness test, (2) had rough or torn bullet seats, and (3) showed poor machining in rifling. Many doubtful barrels however, were considered acceptable, which accounts for the large number of rejections in further processing. Those rejected before electropolishing showed defects which it was not possible to remove by the scrubbing or cleaning operation. Similarly, most of those showing machining defects which had not been removed by either scrubbing or electropolishing were rejected, while a small number failed to meet dimensional requirements.

Those rejected after plating fell into four categories, namely (1) failed dimensionally, (2) showed stains and miscellaneous irregularities, (3) had small pits, and (4) had lands rippled by machining marks.

About 100 barrels with a liner recess were plated. Most of this plating, however, was carried out in order to develop a technique for the production line. Only 20 of these barrels were processed according to production methods. Eighteen were considered to be satisfactorily plated.

25.3.4 Plating Procedure

The procedure for chromium-plating the nitrided

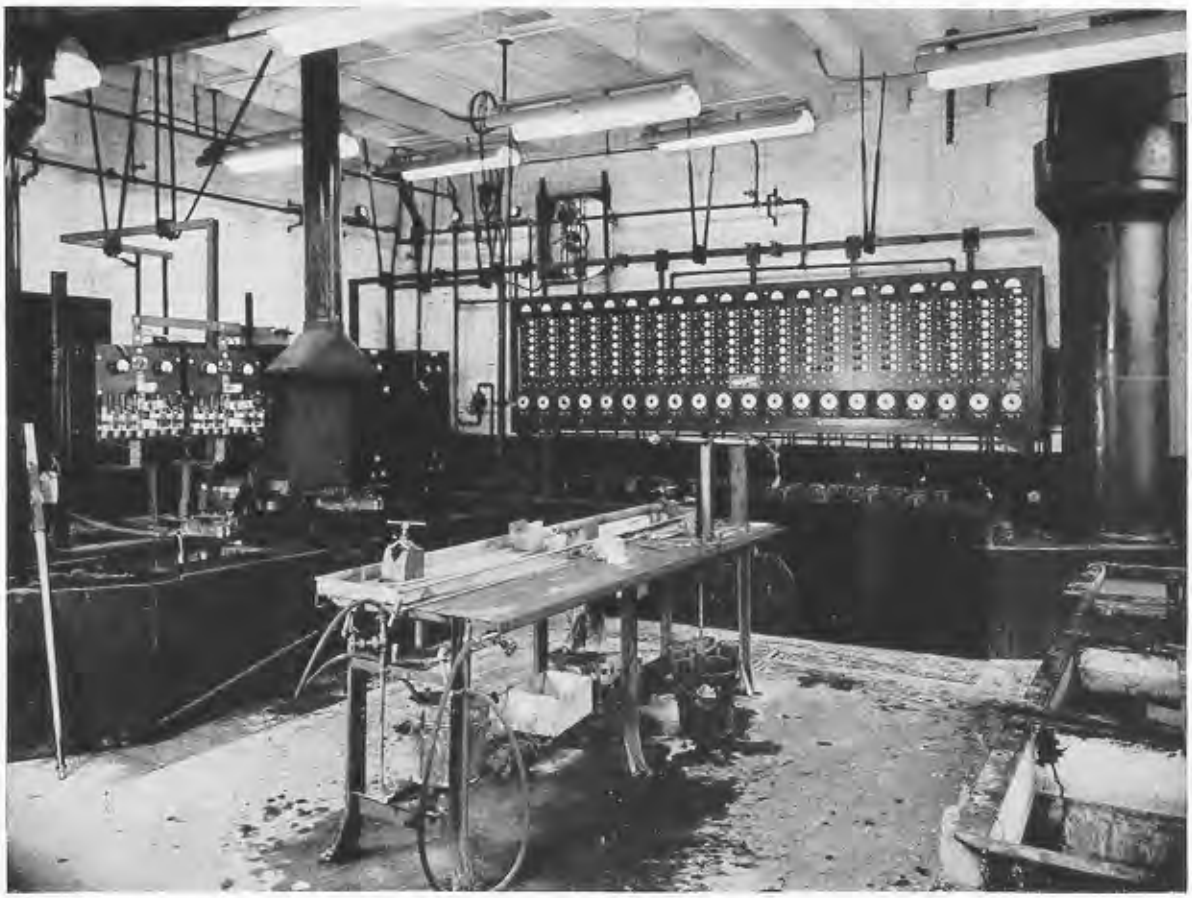


FIGURE 7. Experimental plating unit in Chrome Gage pilot plant, showing electropolishing and strip tanks in the left foreground, scrubbing table in center foreground, rinsing tank in right foreground, and plating tank in background. (From OSRD Report No. 6517.)

CONFIDENTIAL

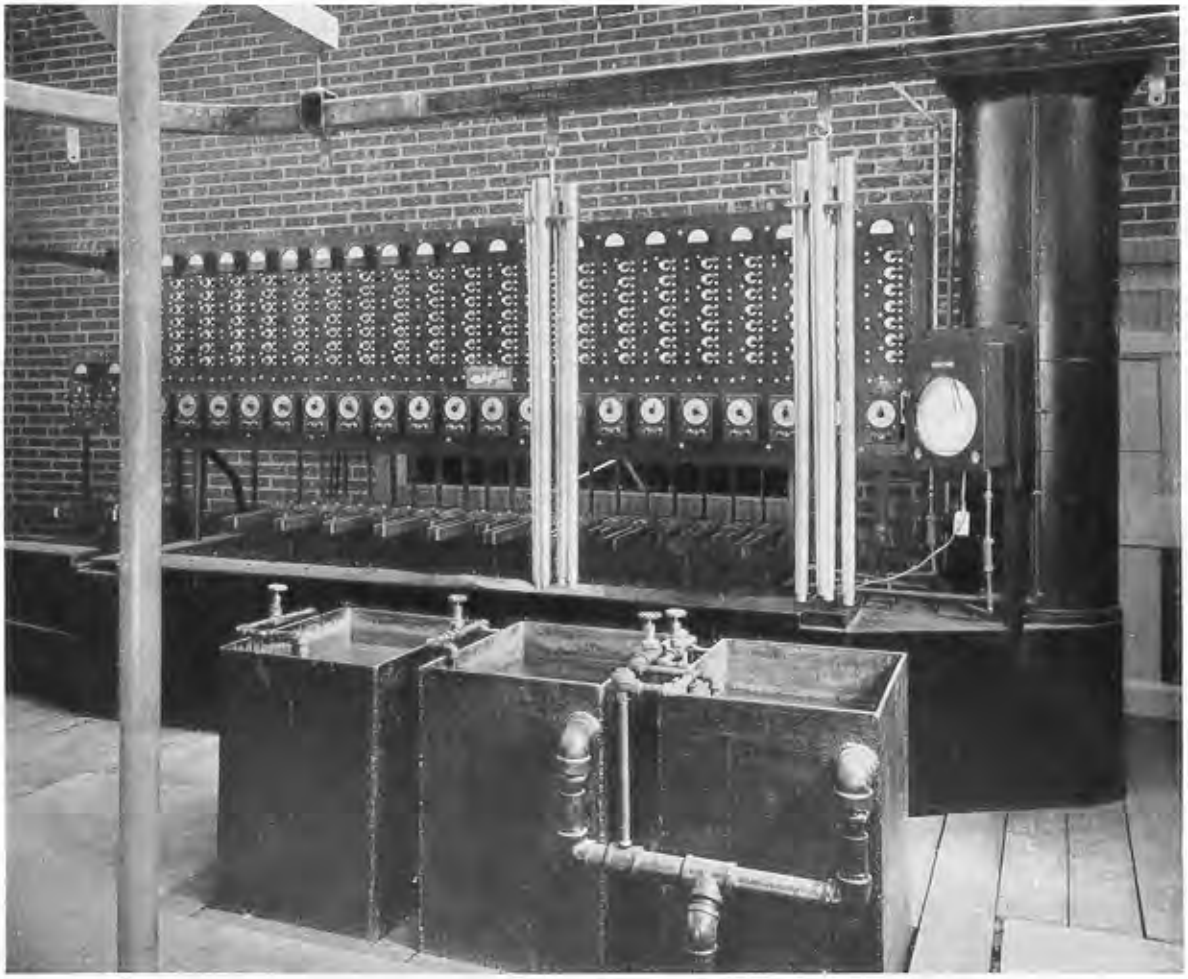


FIGURE 8. Caliber .50 gun barrels suspended from overhead conveyor in Chrome Gage pilot plant, with rinsing tanks in foreground and plating tank in background. (From OSRD Report No. 6517.)

barrels was essentially the same as that used by Doehler-Jarvis, involving the steps given in Section 25.2.1. As had been done at the Doehler-Jarvis pilot plant, an effort was made in the experimental unit of the Chrome Gage plant to determine ways in which the procedure might be altered in order to increase production economically while maintaining or increasing the good performance of the barrels produced.

A rather extensive program was carried out to determine the feasibility of plating a group of barrels with only one current control device. In the original setup a separate one was needed for each barrel. The conclusions drawn from these experiments were that equal division of current could not be expected unless the surface resistance of each barrel was identical, which could not be achieved without a rigid control over the cleaning and degreasing of the barrels.

In the processing of some barrels, the scrubbing operations prior to plating were omitted, and in the case of others the electropolishing was omitted. In the absence of firing tests of those barrels no conclusions could be drawn.

In plating a barrel that was to receive a stellite liner, a dummy steel liner usually was inserted in the liner recess according to the method used by Doehler-Jarvis, which is described in Section 20.2.3. Experiments were performed in order to improve the plating at the junction of the liner and the steel bore, but no improvement resulted. Finally plating was carried out without the dummy liner. The anode was stopped off opposite the portion of the barrel that was not to be plated. These barrels were not test fired, but there

CONFIDENTIAL

CGC No. 1

Date July 22, 1945

BARREL INSPECTION BEFORE PLATING

Type M3; Test A

Barrel Manufacturer Savage Arms Corp. Barrel No. 14

Barrel Drawing 7181530 ~~Nitrided by~~ Hardness R15N

~~Decoppered~~: Yes No

~~Reamed Bullet Seat and Origin of Rifling~~ O. K. Reject

Reasons for Rejection:
- Burrs on Origin of Rifling
- Rough Surface
- Deep Tool Marks
- Chattered
- Wrong Dimension
- Actual Dimension

Condition of Chamber: O. K. Reject

Reasons for Rejection:
- Rough Surface
- Deep Tool Marks
- Chattered

Bore Straightness: O. K. X Reject

~~Bore Diameter at Muzzle~~

Boroscope Examination: O. K. Reject X

Reasons for Rejection:
- Defective Machining X
- Imperfect Lands
- Excessive Pits
- Cracks, Checks, Etc.

Remarks:

INITIAL: Chatter marks on lands up to about 2 in. from junction; burrs at junction; excessive rough and raised chamfer (larger than 1/32 in.)

PLATED: Build up; nodules near junction 7.22.45

Chrome Gage Corporation, Phila., Pa. Inspected by R. Wirt

CGC No. 1

FIGURE 9. Chrome Gage Corp. Form No. 1, "Barrel Inspection Before Plating."

CGC No. 2

Date July 22, 1945

GAGING RECORD

Type of Gage for Recording Dimensions Star Gage.

MEASUREMENTS
INCHES FROM MUZZLE

Test A
C 7 - Bbl. #14

	23½	15	10	1.5	~~Bullet Seat~~ 32.1
Lands, Initial:					
Vertical Diameter					
Horizontal Diameter	.50175	.5015	.5015	.50175	
(a) Average Diameter					
Lands, After Polishing					
Vertical Diameter					
Horizontal Diameter	.50275	.502	.502	.5025	
(b) Average Diameter					
Amount Removed by Electropolishing (b) minus (a)	.001	.0005	.0005	.00075	
Lands, After Plating:					
Vertical Diameter					
Horizontal Diameter	.499	.4976	.4962	.4953	
(c) Average Diameter					
Plate Thickness (b) minus (c) / 2	.0019	.0022	.0029	.0046	

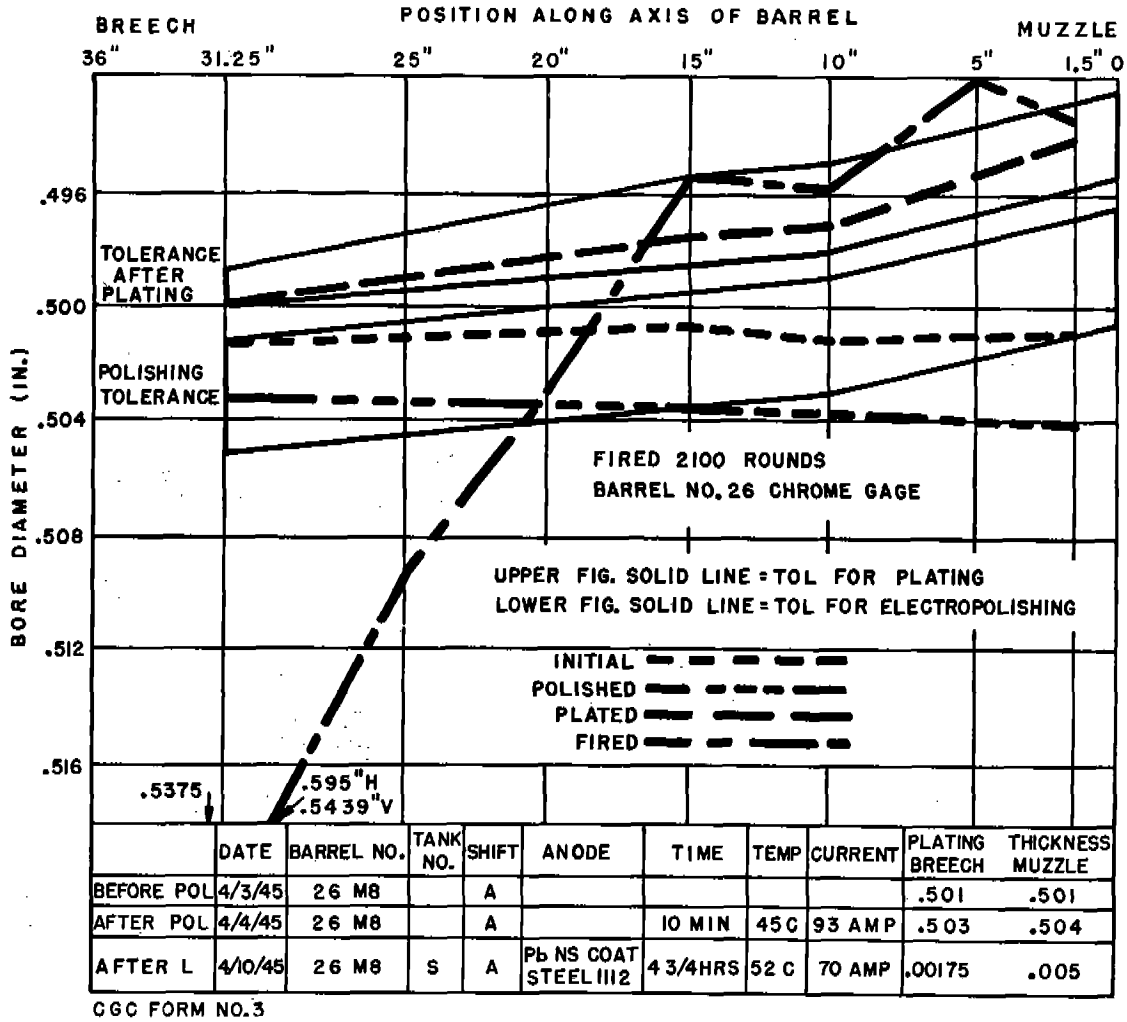
	23½	20	15	10	5	1.5	~~Bullet Seat~~ 32.1	~~Bullet Seat~~ 32.1
Land Diameter After Performance Test	.5097	.5043	.4955	.4953	.4945	.4948		

Measurer R. Wirt Report Approved by

Recorder K. Bennett Chrome Gage Corporation, Philadelphia, Pa.

CGC No. 2

FIGURE 10. Chrome Gage Corp. Form No. 2, "Gaging Record."



	DATE	BARREL NO.	TANK NO.	SHIFT	ANODE	TIME	TEMP	CURRENT	PLATING THICKNESS BREECH	MUZZLE
BEFORE POL	4/3/45	26 M8		A					.501	.501
AFTER POL	4/4/45	26 M8		A		10 MIN	45C	93 AMP	.503	.504
AFTER L	4/10/45	26 M8	S	A	Pb NS COAT STEEL 1112	4 3/4 HRS	52 C	70 AMP	.00175	.005

CGC FORM NO. 3

FIGURE 11. CGC Form No. 3, "Graphic Record," showing bore diameter of caliber .50 barrel initially, after electropolishing, after plating, and after having been test fired.

were definite indications that it would be possible to plate barrels without dummy liners and obtain satisfactory plating results.

In all these experiments on the barrels to contain liners, the barrels were electropolished with the breech end up so that the slight taper produced would be in the same direction as the taper produced later by the plating operation and thus the amount of plating necessary to offset a reverse taper, produced by polishing with the muzzle end up, would not be required.

CURRENT DISTRIBUTION ALONG A CYLINDRICAL ANODE

A formula for the distribution of the current along the anode, assuming a uniform resistance of both anode and solution, was developed. Equations (1), (2), and (3) express the current and voltage across the solution and the current through a section of the anode, in terms of the geometry shown in Figure 12.

$$I_x = I_0 \frac{\sinh \alpha(l - x)}{\sinh \alpha l}. \tag{1}$$

$$i_x = \frac{\alpha I_0}{\pi d} \frac{\cosh \alpha(l - x)}{\sinh \alpha l}. \tag{2}$$

$$E_x = E_P + \rho \alpha I_0 \frac{\cosh \alpha(l - x)}{\sinh \alpha l}. \tag{3}$$

In these equations I is the current, i the current density, E the voltage across the solution, E_P the voltage of polarization, l the length (in cm) of exposed anode, d diameter of bore, α^2 the ratio r/ρ (where r is the resistance per unit length of the anode and ρ the

resistance of a ring of solution 1 cm long), and x the distance in centimeters along the tube measured from the end where the current enters. However, the experience in plating caliber .50 barrels at the National Bureau of Standards, as described in Chapter 20, casts doubt on the validity of the assumption of uniform resistance of the solution. Perhaps in "pump plating" the solution resistance may be sufficiently

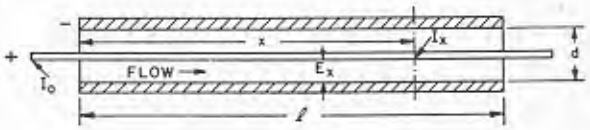


FIGURE 12. Geometrical relations in a gun barrel being plated with a cylindrical anode. (From OSRD Report No. 6517.)

uniform for the analysis to apply. In plating without circulation of the solution, differences in temperature between the bottom and top of the barrel cause changes in both the solution resistance and cathode efficiency that tend to compensate each other as far as their effects on the current density are concerned, but the extent of compensation in any particular case is not predictable.

25.3.5 Electrical Bore Gauge

An electrical bore gauge, which was a type of strain gauge, was developed to permit the gauging of rifled and tapered bores with greater accuracy than is possible with other types of gauges. The range of the instrument was great enough so that it could be used to gauge eroded barrels as well as new ones.



FIGURE 13. Top view of strain gauge beam removed from head of electrical bore gauge (magnified 4X). (From OSRD Report No. 6517.)

This gauge makes use of a cantilever beam, shown in Figure 13, containing a sensitive electrical strain gauge that records the amount of motion of a feeler point on its end. This feeler point makes contact with another feeler supported by a spring fastened to the cover. The spring is three-pronged, the ends of the prongs on either side being curved so as to engage the grooves of the rifling and to center the feeler point on the land. On either side of the gauge head body is a fixed contact point.

The gauge head is mounted in the end of a tube mounted on ball-bearings on a vertically adjustable support, which slides on a base on which are also mounted the vertically adjustable gun barrel rest, as shown in Figure 14. After calibration the gauge head



FIGURE 14. Head of electrical bore gauge in position for insertion in a barrel. (From OSRD Report No. 6517.)

is moved inside the bore, following the rifling. The gauge is connected to a potentiometric voltage indicator, on the dial of which is given a practically instantaneous measurement of the bore diameter at any point in the bore. The 30-in. scale is uniformly graduated in one thousandths of an inch, and each thousandth has 20 subdivisions, each representing 0.00005 in. Thus the magnification is approximately 1,250 to 1, for a gauging range of 0.025 in. Over this entire range the gauge will duplicate readings to within 0.0001 in.

It was planned eventually to use the electrical bore gauge in connection with a potentiometric recorder. Then a continuous written record of the diameter of the bore could be obtained in a few seconds for the whole length of a caliber .50 barrel from the centering cylinder to the muzzle.

25.4 RECOMMENDATIONS

Future operation of a pilot plant for the chromium plating of machine gun barrels calls for four principal activities, as follows:

1. Experiments to develop a technique for plating

CONFIDENTIAL

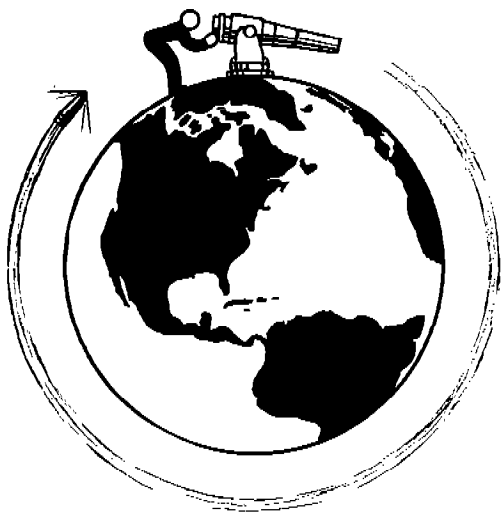
"combination" barrels with stellite or other erosion resistant liner already inserted;

2. Experiments looking toward simplification of the plating procedure;

3. Development of a reasonably reliable gauge for measuring the thickness of the plate, in order to solve the problem of checking the concentricity of the plate with the bore.

PART VII

HYPERVELOCITY GUNS AND PROJECTILES



When men are arrived at the goal, they should not turn back.
—*Plutarch*
"Of the Training of Children"

Chapter 26

SHORT LINERS AND OTHER DESIGN FEATURES OF GUN TUBES

By *William H. Shallenberger*[a]

26.1 INTRODUCTION

EROSION-RESISTANT MATERIALS have been developed to increase the life of gun barrels, as described in Chapter 16. For various reasons, however, it is not practical to construct complete barrels of such materials. Therefore gun barrels and tubes still need to be made of steel into which short erosion-resistant liners are inserted at the breech end. In general, the insertion of such liners introduces problems not encountered in tubes of monobloc construction or in ones containing full-length steel liners. (Figure 1.)

The improvements made in machine gun barrels by the use of stellite liners have been discussed in Chapter 22. One of the purposes of the present chapter is to describe various methods that have been used to insert stellite liners in machine gun barrels as illustrations of how the general methods in use for designing gun tubes need to be modified to utilize erosion-resistant materials. The experiments already conducted by Division 1 with replaceable steel liners (Section 26.3) point the way toward one means of utilizing erosion-resistant materials in medium caliber guns.

The specific designs suggested for a molybdenum liner for a 3-in./70-cal. gun are described in Section 33.1.3. One of the special features of them is the stave-type of construction, already described in Section 18.5.2. An analysis of the stresses in these liners is presented in Section 26.4, following a review of the usual formulas for the stresses in shrunk-in liners. Consideration is also given to the effect on liner insertion of a difference between the coefficient of thermal expansion of steel and the liner material, such as molybdenum.

The stress distribution in liners may also be influenced by the design of rifling and the use of pre-engraved projectiles, as discussed in Section 26.6.

[a] Engineer, Engineering and Transition Office, NDRC. (Present address: Granada Hill, San Fernando, California.) While this chapter was being edited, which was after Mr. Shallenberger had left NDRC, several small additions were made to it, in order to take care of related subjects not treated elsewhere in the volume: Section 26.3 was expanded by Dr. J. F. Schairer; Sections 26.5.1 and 26.5.2 were added by the Editor; and Section 26.6.3 was prepared by Miss C. A. Marsh. (Editor's note.)

26.2 MEANS OF HOLDING RESISTANT LINERS IN PLACE

26.2.1 General Résumé

When a liner is inserted into a gun barrel it is necessary that the liner be held rigidly in place. The action of the projectile, in being accelerated down the bore, applies forces on the liner tending to move it forward and to rotate it. If the liner moves forward, the liner and the barrel at the forward joint become upset and constrict the bore, while rotation of the liner moves the rifling out of alignment and causes double-engraving of the projectile.

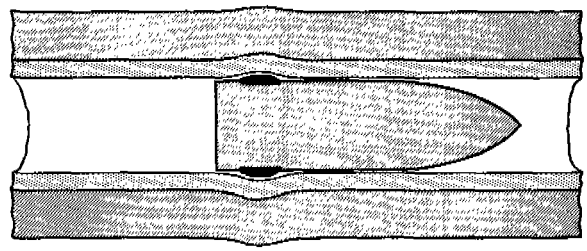


FIGURE 1. A successful gun liner must follow the momentary changes in dimensions of the whole gun tube caused by passage of the projectile without undergoing permanent set and without cracking.

Various methods are used to secure the liner in the tube. Two of these methods produce an interference fit between the tube and liner, so that a high radial pressure exists at the interface. In the case of machine gun barrels movement has been prevented mechanically. Also it has been proposed to hold the liner by bonding it to the tube. The insertion of erosion-resistant liners for test purposes has already been described in Section 11.2.2.

26.2.2 Shrink-Fit of Tube and Liner

The means developed by the Crane Company for Division 1 for inserting and securing stellite liners in caliber .50 machine gun barrels was subsequently

used for nearly all production of these barrels during World War II. This method, as described in Section 22.2.1, consisted essentially of boring out a recess at the breech end of the barrel extending approximately 8 in. forward of the origin of rifling, and shrink-fitting a rifled cylindrical liner into the recess. A shoulder near the breech end of the liner butted against a corresponding shoulder in the barrel to prevent forward motion of the liner. Figure 1 of Chapter 22 shows the assembly of this type of caliber .50 liner and barrel.

The Savage Arms Corporation, on a production contract with the Ordnance Department, employed an assembly method similar to that of the Crane Company, with a few exceptions. Rifling of the barrel was done after assembly, using the rifled liner as a guide for the rifling tool. When it was decided to chromium-plate the barrel ahead of the liner (Chapter 24) it became necessary to rifle the barrel before plating and assembly, and use an indexing arbor during assembly to align the rifling. Instead of tack-welding the retainer to the barrel to prevent unscrewing, the threads of the retainer were silver-soldered to the threads in the barrel.

26.2.3 Expansion of the Liner by Draw Rifling

Interference between the barrel and liner was used[135] to prevent movement of the liner, but this method produced the interference after assembly rather than before. To obtain the desired interference, the liner was expanded sufficiently to give it a permanent set by forcing a plug through it. The exterior of this plug was so shaped that at the same time it expanded the barrel, it also formed the rifling. Two types of liner assemblies were prepared in this way by Remington Arms for the caliber .30 Browning machine gun, M2-AC, M1917A1, and M1919A6.[b] The first was copied from the Crane design for caliber .30 (Section 22.5.1) except that the rifling and chambering operations were not performed prior to assembly, nor were interference fits used. After assembly the threaded breech end was screwed into a face plate on a La Pointe hydraulic push broach. The tungsten-carbide rifling plug or "button," pushed through the barrel with a rotary motion, required about 5 sec to pass through the barrel. To reduce friction and prevent galling during rifling, the bore surface was given a light plating of copper or indium. This plating was, of course, removed after rifling.

Helical grooves on the outside of the plug formed the desired rifling by a swaging action. Displacement of metal caused the liner and retainer to take a permanent expansion, thus locking them securely in the barrel. Since the amount of expansion and elastic recovery are dependent upon the wall thickness, it was necessary that the barrel contour be cylindrical before rifling, to prevent a taper in the finished bore. The outside of the barrel was machined to the desired contour after rifling.

It was felt that the high interface pressure resulting from swage-rifling would be sufficient to prevent forward motion of the liner and that the shoulder could be eliminated. Therefore, an alternate design was made as shown in Figure 2. Cylindrical bar stock was bored through with a diameter of 0.300 in. and then counterbored at one end to a diameter of 0.430 in. for the liner. The liner and a steel ring were also bored through and turned to an outside diameter of 0.430 in. After inserting the liner and retainer ring and plating the inside surface, the assembly was swage-rifled, as described previously. The chamber was then reamed in the normal manner. The steel retainer ring could have been eliminated, but was used to reduce the amount of stellite required and to prevent the stellite from coming to a feather edge, which might break off easily.

This method of assembly is very inexpensive on account of the small amount of machining required, and also effects considerable savings in stellite by eliminating the flange at the end. One serious disadvantage of swage-rifling the entire assembly is that it does not permit chromium-plating the barrel before assembly, because the plate would not withstand the rifling process. As described in Chapter 24, such plate ahead of the liner more than doubles the useful life of a stellite-lined caliber .50 machine gun barrel. Its value for the caliber .30 barrels was not determined by Division 1. Because of the reduced severity of erosion in this gun, compared with the caliber .50, it is questionable whether chromium plate ahead of the stellite liner is necessary.

26.2.4 Mechanical Retention of the Liner

The methods of inserting and retaining stellite liners in caliber .30 machine gun barrels previously discussed relied upon interference between the liner and the barrel. Mechanical methods of holding the

[b] Experimental work along the same lines was also done on caliber .50 machine gun barrels but did not progress as far as that on the caliber .30.[135]

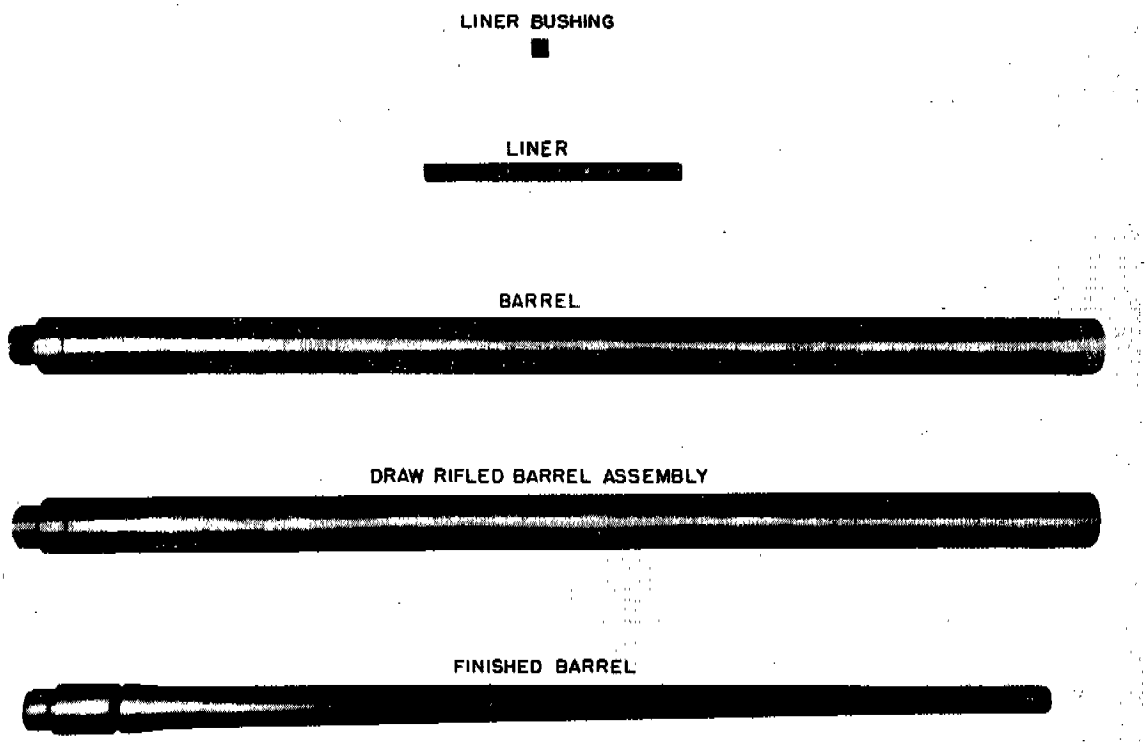


FIGURE 2. Caliber .30 Browning machine gun barrel assembly, M1917A1-R1, with straight liner of Stellite No. 21; Remington design. (This figure was taken from NDRC Report No. A-463.)

liner were also developed.[127] By avoiding shrink-fits, it was felt that larger machining tolerances could be used, thus simplifying and speeding production.

One promising design, shown in Figure 3, consisted of counterboring the breech end of the barrel to the depth necessary to accommodate the liner. A flangeless liner was inserted in the recess and retained by a simple set screw. Rifling of the liner and barrel could be done separately before assembly, or the liner could be rifled before assembly and used to guide the rifling bar for rifling the barrel. Although this method performed satisfactorily when using a steel liner, it was not tried with a stellite liner, because of the possibility of crumbling of the feather edge at the breech end of the stellite. Subsequently, the Kelsey-Hayes Wheel Company, on a production contract for caliber .50 barrels, adopted a design using such a feather-edge without difficulty. Hence the design presumably would be practical for stellite.

To avoid this feather-edge the design shown in Figure 4 was devised. In this design, the barrel and liner were pre-rifled and the liner inserted with a loose

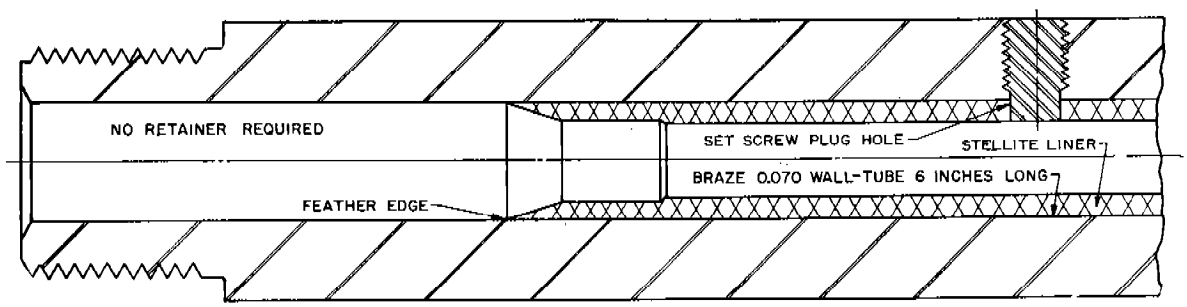


FIGURE 3. Caliber .30 Browning machine gun barrel assembly with flangeless liner; Johnson design. (This figure has appeared as Figure 2 in NDRC Report No. A-455.)

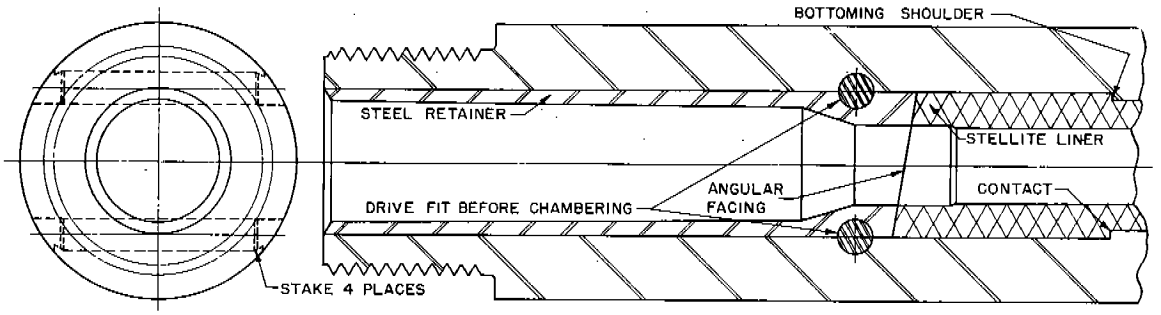


FIGURE 4. Caliber .30 Browning machine gun barrel assembly, M2, with stellite liner staked with pins; Johnson design. (This figure has appeared as Figure 4 in NDRC Report No. A-455.)

or light press-fit. To determine what tolerances were required, several assemblies were made with different clearances over a range of several thousandths of an inch. All performed satisfactorily, indicating that close tolerances were not required. Forward motion of the liner was prevented by a shoulder on the liner, which seated on a corresponding shoulder in the barrel. To prevent rotation of the liner, the breech end of the liner was faced at an angle and the forward end of the chamber piece was faced at a corresponding angle. The chamber piece was held in place and prevented from rotating by two tapered pins that secured it to the barrel.

26.2.5 Bonding of Liner to Barrel

Various methods of bonding a stellite liner to a machine gun barrel were proposed. Samples of stellite copper-brazed to gun steel prepared by salt-bath brazing showed satisfactory bond strength.[c] Therefore designs were made and a program formulated for the experimental production of stellite-lined caliber .50 barrels assembled by brazing. Two types were to be built and tested. One type was to be brazed over the entire length of the liner and separate chamber piece. In the other type, the stellite was to be bonded (by casting) to a steel end and this steel end to be brazed to the barrel. After assembly, the liner and barrel were to be swage-rifled by the process described in Section 26.2.3. It is recommended that this unfinished project be completed.

In other experiments stellite was bonded to steel by the process commonly known as the Al-Fin process.[d] This process has been used very successfully to bond aluminum muffs or finned surfaces to steel cylinders for aircraft engines.[559] However, tests showed serious weakening of the joint at high temperatures, in the case of the stellite-steel assembly.

Stellite has been successfully bonded to steel by centrifugal casting into steel tubes.[125] These tubes with their stellite linings were experimentally assembled into caliber .50 barrels by standard insertion methods. The firing tests[80] showed that a stellite lining prepared in this way gave a performance equivalent to that of an investment-cast liner. Attempts were to have been made to cast stellite centrifugally directly into barrel forgings bored out to receive it, either as short breech linings or as full-length linings. On account of termination of Division 1's experimental program in 1945, this project was not completed. It is recommended that the Services undertake to finish it.

26.3 INSERTION OF A REPLACEABLE STEEL LINER

26.3.1 Purpose of a Replaceable Steel Liner

The erosion of steel gun tubes as described in Chapter 10 is particularly severe at and near the origin of rifling; but significant erosion also occurs for several calibers ahead of this region. This enlargement of the bore by causing a rapid and undesirable drop in muzzle velocity and in some cases malfunctioning of the ammunition limits the useful life of the gun tube.

[c] This work was carried out by the A. F. Holden Co. under Contract OEMsr-1473. Because the work under that contract did not progress much beyond the planning stage, the final report contained few details. Therefore it has not been issued as a formal NDRC report.

[d] This work was carried out by the Al-Fin Corporation under Contract OEMsr-1494. Because the work under that contract did not progress much beyond the planning stage, the final report contained few details. Therefore it has not been issued as a formal NDRC report.

In 1942, before the erosion-resistant metals and alloys described in Chapter 16 had been developed, it was felt that the life of steel gun tubes, particularly under severe conditions of firing, might be extended considerably by the use of a series of short, interchangeable, replaceable, steel breech-liners. The German 88-mm antitank gun was so constructed that its liner could be removed in three sections.[225,246] The development of a successful design and tests of liners of this type are described in the next two sections of this chapter. A modification of such a replaceable steel liner was used as a means of testing erosion-resistant materials in cannon tubes. For this purpose the erosion-resistant material may be applied as a bore lining or liner within the steel liner. Stellite was thus tested in a 37-mm gun, as described in Section 33.1.2.

25.3.2 Development of the Liner Design

For the initial experimental work on the design of a replaceable steel liner, the 75-mm gun was chosen because of its ready availability. Three types of liners, 10 calibers long and about 0.5-in. average thickness, were designed and constructed at Crane Company,[80] and were tested at Aberdeen Proving Ground.[231]

The first two types were elliptical in cross section to prevent rotation. This involved difficult and expensive machining operations. The first type failed by permanent expansion at the forward end, which was too thin, and by moving backward slightly upon firing. A ring of "copper" formed at the forward joint, and the liner could not be replaced until the copper had been machined out. The second type failed by radial expansion of the chamber section during the firing of five rounds. Removal of the liner in the field was impossible.

The third and successful type of liner was of circular cross section over the entire length, and had an external taper except for a thick flange at the breech end, which had the same outside diameter as the tube. The liner was secured to the tube by socket-head cap screws set into counterbored holes in the flange and tapped into the rear face of the tube. Removal was easily accomplished by inserting the screws into tapped holes in the flange and using them to back the liner out of the tube.

A 75-mm liner assembly, made according to this design, was proof-fired and immediately subjected to a series of 50 service rounds. A second series of 300 service rounds was then fired at a rate of 1 round per min. After each firing the liner was easily removed by one man in 10 min. Some of the screws had started to move slightly and their threads were flattened. New screws of harder material, equipped with lock washers, were procured, and a third series of 300 service rounds was fired without incident. These tests demonstrated that the basic design of replaceable steel liner was sound.

26.3.3 Successful 90-mm Liner

Preparation of Liner Assemblies

With the experience gained in design development just described, a series of three interchangeable, replaceable, steel liners was designed and constructed for the 90-mm gun, M1. This gun has extensive tactical use, and, since its tube life under certain service conditions was quite short, the use of replaceable liners would materially ease the problem of supply and transportation. The possibility of extending the



Figure 5. 90-mm gun tube, T19, with replaceable steel liner, before firing. Top: Breech-end view of tube and liner. Bottom: Forward end of liner, showing gas sealing lip. (By courtesy of Aberdeen Proving Ground.)

CONFIDENTIAL

life in this way was of especial interest in the spring of 1944, when consideration was being given by the Army to firing this gun with double-base powder in order to increase its muzzle velocity.[220]

The liner shown in Figure 5 was 64 in. long, and weighed about 250 lb, in contrast to the weight of the 90-mm gun tube, M1, which is 1,465 lb. This same figure shows the breech end of the recessed tube and the gas sealing lip on the forward end of the liner.

For the purpose of saving time, a liner was machined from a tube which had muzzle defects but a perfect breech end, the chamber of which was retained in the liner. The main tube into which the liner was inserted had defective rifling at the origin but otherwise was perfect. In recessing for the liner, this defect was, of course, removed. In the fabrication of the three liners, the tube was used as a pattern in order to avoid preparing gauges.

A liner can be assembled and disassembled by two men in about 20 min, which is much less than the time required for unscrewing the tube from the breech ring or for dismounting the tube and the breech ring. No difficulties were experienced in removing a liner after firing as many as 553 rounds. A ring of "copper" about 0.01 in. thick formed at the joint ahead of the liner, but always adhered to the liner when it was withdrawn.

Results of Firing Tests

The assembly with a 90-mm M1 tube and interchangeable, replaceable steel liners was designated by the Ordnance Department as 90-mm Gun, T19, and was tested for Division 1 at Aberdeen Proving Ground. All tests so far have been successful. Three liners have been fired from the same tube. Nearly all rounds were fired with FNH-M2 (double-base) powder and APC ammunition. Firing was at normal rates in groups of 25 or 32 rounds.

The first liner was fired 321 rounds and then replaced by a second. The liner had not worn excessively but was replaced on account of an increase in diameter of about 0.010 in. in the tube ahead of the liner. Star-gauge readings during the course of the test had indicated that wear of the forward end of the liner would approximately equal that of the barrel just ahead of it when the latter had become 0.010 in., so this figure was chosen as a criterion to indicate the time to change liners. Actually performance was satisfactory at this stage of erosion.

Introduction of the second liner restored the gun to approximately new tube performance. This restoration of performance in terms of velocity is shown very well by the results presented in Figure 6.

The second liner was fired 553 rounds, at which stage malfunctioning of the ammunition occurred

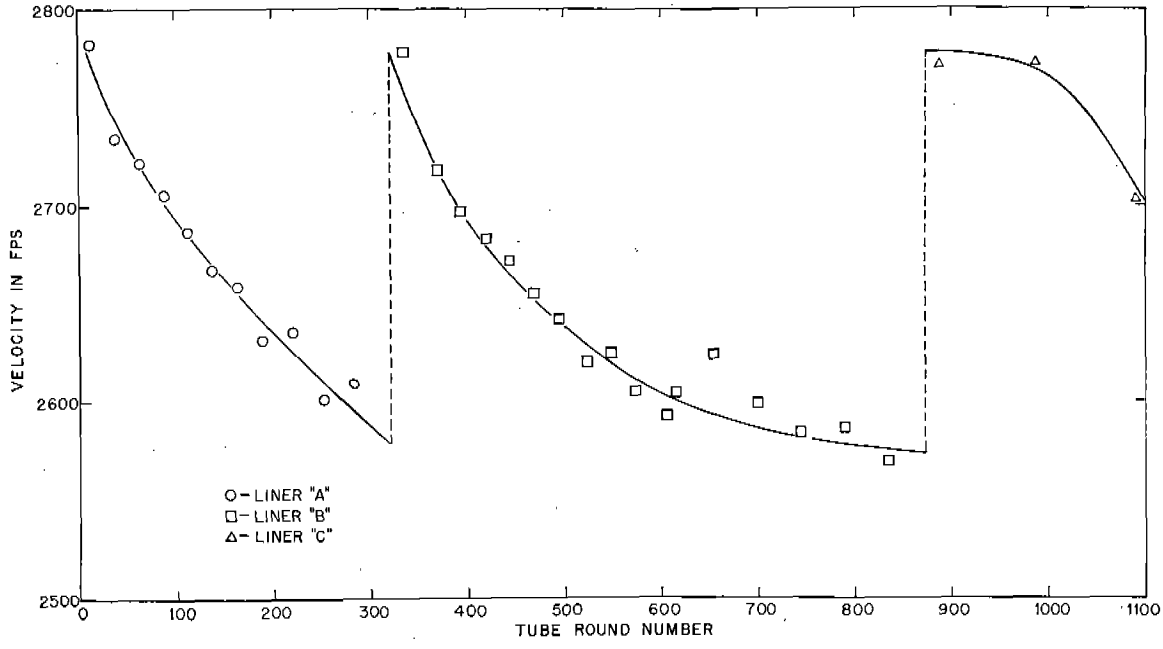


Figure 6. Velocity loss with replaceable steel liners "A," "B," and "C" fired in 90-mm gun, T19. (Aberdeen Proving Ground Memo Reports, O.P. 6102.)

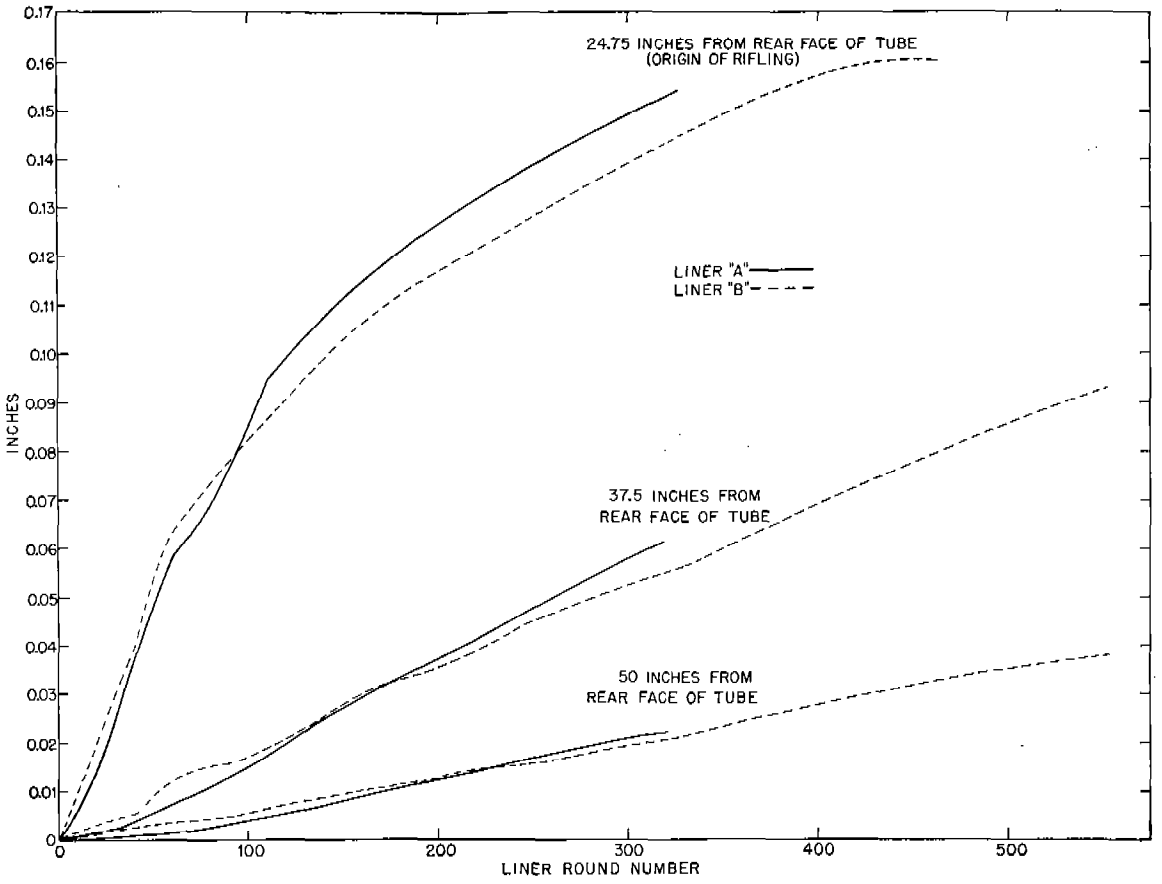


FIGURE 7. Land erosion of replaceable steel liners "A" and "B" fired in 90-mm gun tube, T19. (This graph is based on data given in Aberdeen Proving Ground Memo Reports, O.P. 6102.)

and the test was discontinued. Its rate of erosion was the same as that of the first liner, as shown in Figure 7. The third liner has been fired several hundred rounds. No difficulties with interchangeability or replaceability have been encountered.

In order to evaluate the potential usefulness of a replaceable steel liner, two further steps are needed. The first is to continue the firing tests already made, using as many additional liners as would be required to render the main tube unfit for further service. The end of its life presumably would occur because of the erosion ahead of the liner. The rate of this erosion is independent of the condition of the tube at the origin of rifling, for a graph of this erosion as a function of the total number of rounds fired in the tube, shown in Figure 8, does not reflect the replacement of liner "A" after round 321. A similar comparison after the insertion of liner "C" was not possible because the bore diameter of the tube proper decreased instead of increased, presumably because of coppering. No information is available by which to form an estimate of how much erosion in this region can be tolerated without either seriously weakening the tube or causing malfunctioning of the ammunition.

After the true end of life had been determined in terms of the number N of liners that could be inserted in the same tube, the next step would be to find out whether the use of these liners was economical. The cost of manufacturing, and shipping to a theater of war, one recessed tube plus N liners should be compared with the total cost of manufacturing and shipping N monobloc tubes. A fairly rigorous comparison could be made on the basis of an engineering study of the manufacturing operation. The tolerances that must be maintained are very close, being of the order of one thousandth of an inch on the diameters of the liner and of the recessed hole in the tube. If there is more play than this small amount, the liner expands excessively, and then is not readily removable, as was found with the second design of 75-mm liner. With modern manufacturing methods the necessary tolerances can be achieved in production.

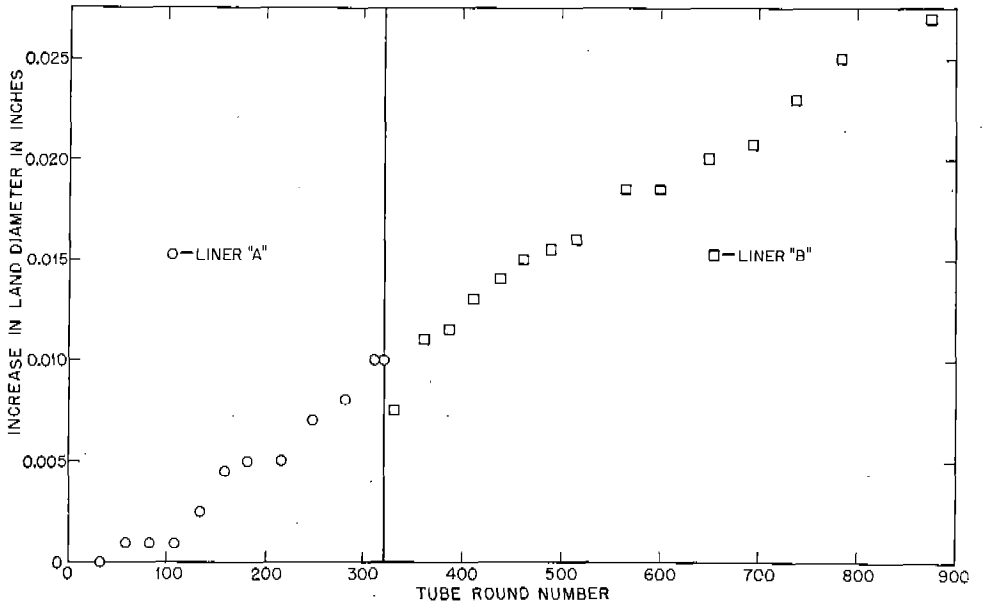


FIGURE 8. Land erosion of 90-mm gun tube, T19 just beyond junction of tube and replaceable steel liner, when fired with liners "A" and "B." (This graph is based on data given in Aberdeen Proving Ground Memo Reports, O.P. 6102.)

26.4 APPLICATION OF THEORY OF TUBE STRESSES[c]

26.4.1 Introduction

While many approximate and exact theories of tube stresses have been formulated, the resulting equations (some of which are presented in Chapter 7) are in general too unwieldy for use in routine design work. For this reason, except where great accuracy is required, many assumptions are made, which result in simple equations having an accuracy usually as good as the fundamental data. It is the purpose of this section to discuss and illustrate the application of these simplified equations to the design of hypervelocity gun tubes, especially those containing liners.

There are four basic assumptions made: (1) that the section being considered is a small section of a thick-wall tube having infinite length and constant contour, (2) that the internal pressure is equally distributed and acts only radially so that there are no longitudinal stresses, (3) that the Lamé formula expresses the radial distribution of tangential stresses, and (4) that the material is at all times in the elastic state.

[c]A review[563] of some phases of this subject, based on work carried out by Massachusetts Institute of Technology for the Navy Bureau of Ordnance during the war, has been published recently. (Editor's note in proof.)

26.4.2 Theories of Failure

A simple tensile or compression member can usually be considered to have failed when the simple stress in that member reaches or exceeds the yield strength (or elastic limit) of the material as measured in the usual tension or compression test. However, for members subjected to more than one principal stress, this theory does not yield satisfactory results. For example, in a gun tube, failure might occur before any of the principal stresses reached the yield strength.

Two theories of failure of gun tubes have been extensively used. Until recently, the gun designers of the Army and Navy used the "maximum strain theory" (St. Venant). This theory states that failure occurs when any part is strained beyond the strain corresponding to the yield strength as determined by the usual tensile test. This criterion of failure has been superseded by the "shear-energy theory" (Mises-Hencky) (also called "distortion-energy"), which states that failure may be considered to occur when the shear-energy in a unit volume of the material exceeds the shear-energy per unit volume at the yield point in the usual tensile test. This might also be expressed by stating that failure occurs when the "equivalent" stress exceeds the yield strength. The equivalent stress is calculated by equation (1), which is the same as equation (4) of Chapter 7. In this

equation σ_e = equivalent stress; σ_t = tangential stress; σ_r = radial stress; and σ_z = longitudinal stress.

$$\sigma_e = \frac{1}{\sqrt{2}}\sqrt{(\sigma_t - \sigma_r)^2 + (\sigma_r - \sigma_z)^2 + (\sigma_z - \sigma_t)^2} \quad (1)$$

26.4.3 Stress Distribution in a Thick-Wall Tube

When a thick-wall tube is subjected to both internal and external pressures, the stresses throughout the wall are not constant but vary from the inner to the outer surface, as a function of the radius. This distribution of the stresses is given by equations (2a, b, and c), which are the so-called Lamé formula presented in a different notation in equations (1), (2), and (3) of Chapter 7. Here μ = Poisson's ratio (usually taken as 0.3 for gun steel); p_a = internal pressure; p_b = external pressure; r_a = internal radius; r_b = external radius; r = radius to any section.

$$\sigma_t = \left(\frac{r_b^2 p_b - r_a^2 p_a}{r_b^2 - r_a^2}\right) + \left(\frac{r_a^2 r_b^2 (p_b - p_a)}{r_b^2 - r_a^2}\right)\frac{1}{r^2}. \quad (2a)$$

$$\sigma_r = \left(\frac{r_b^2 p_b - r_a^2 p_a}{r_b^2 - r_a^2}\right) - \left(\frac{r_a^2 r_b^2 (p_b - p_a)}{r_b^2 - r_a^2}\right)\frac{1}{r^2}. \quad (2b)$$

$$\sigma_z = -\mu(\sigma_t + \sigma_r) = -2\mu\left(\frac{r_b^2 p_b - r_a^2 p_a}{r_b^2 - r_a^2}\right). \quad (2c)$$

For a gun tube, which is subjected to internal pressure only, equations (2) reduce to equations (3),

$$\sigma_t = -p_a\frac{r_a^2 + r_b^2}{r_b^2 - r_a^2} = -p_a\frac{W^2 + 1}{W^2 - 1}. \quad (3a)$$

$$\sigma_r = p_a. \quad (3b)$$

$$\sigma_z = p_a\frac{2\mu r_a^2}{r_b^2 - r_a^2} = p_a\frac{2\mu}{W^2 - 1}. \quad (3c)$$

in which W, the wall ratio, is defined as r_b/r_a or d_b/d_a. Tensile stresses are considered positive, while compressive stresses and pressures are considered negative.

As an example, consider a tube having an internal pressure of 60,000 psi; inside diameter, 3 in.; and outside diameter, 6 in. From equation (3) the three principal stresses are calculated as:

$$\sigma_t = 80{,}000 \text{ psi}$$
$$\sigma_r = -60{,}000 \text{ psi}$$
$$\sigma_z = -12{,}000 \text{ psi}.$$

Substituting these values in equation (1) yields a value of 123,200 psi for the equivalent stress.

In order to prevent failure therefore, the material of which the tube is made must have a yield strength of at least 123,200 psi. This calculation does not take account of any safety factors, conversion from copper to true pressure, or proof pressure, these having presumably been considered in arriving at the maximum pressure of 60,000 psi.

26.4.4 Design Procedure for Cannon Tubes

The Ordnance Department of the Army has developed a procedure to be followed in the design of cannon tubes, other than auto-frettaged tubes.[293] In the use of this method the stress equations (3) have been simplified to equation (4),

$$Y = \frac{P}{W^2 - 1}\sqrt{3W^4 + 1}. \quad (4)$$

for Y, the stress in pounds per square inch at which yielding occurs, in terms of P, the actual internal (powder) pressure (in pounds per square inch) and W, the wall ratio of the tube, defined as above. For a given yield strength, the tangential resistance (maximum pressure without stressing beyond the yield strength) will be R, which is defined by equation (5).

$$R = \frac{Y(W^2 - 1)}{\sqrt{3W^4 + 1}}. \quad (5)$$

$$R' = P' \times 1.2 \times 1.15 \times \text{F.S.} \quad (6)$$

This tangential resistance must be not less than R', defined by equation (6) in which P' = rated maximum powder pressure (copper); 1.2 = conversion from copper gauge to actual pressure; 1.15 = ratio of proof pressure to rated maximum; and F.S. = factor of safety.

The factor of safety should be as high as is consistent with dimensional restrictions of the gun, and in no case less than 1.05 over the region of expected maximum pressure. Factors of safety at the muzzle (not considering muzzle bells) will normally be about 3.

The yield strength measured at 0.1 per cent offset, as specified by U. S. Army Specification 57-106A, is approximately 10,000 psi higher than the true elastic strength of the steel.[290] Therefore the yield strength to be used in the above calculations for tangential resistance must be 10,000 psi less than that measured at 0.1 per cent offset.

A report[327] has been written recently as an aid in the designing of guns. It contains an excellent set of equations, tables, and graphs covering a wide range

of wall ratios, with good explanations of the methods of finding the combined effects of band and gas pressures. There is also a well-outlined method of separating the localized uniform band pressure from that of the traveling wave. The fundamentals of gun design have been discussed in two other reports, in one[307] of which particular attention is paid to radial vibrations and in the other[310] to longitudinal stresses.

26.4.5 Stresses in Shrunk-In Liners

For many years both the Army and the Navy have made medium- and large-caliber guns of the "built-up" type, in which a full-length liner is shrunk into the tube. In general, the use of shrunk tubes and liners tends to reduce maximum stresses, making the assembly capable of withstanding higher powder pressures without failure than can the ordinary monobloc tube. Therefore in some models an additional jacket is shrunk on the outside of the tube over the rear portion that is exposed to the maximum powder pressure.

This same method is useful for preventing movement of an erosion-resistant liner, as has been mentioned in Section 26.2.2.

Since actual interference does not exist after the parts have been shrunk together, there is a high pressure between the tube and liner. This pressure creates stresses in the tube and liner, even with the gun at rest. To these stresses should be added algebraically the stresses produced in a monobloc tube by the powder pressure, in order to obtain the pressure at any point during firing.

In the discussion that follows, the assumptions are made that (1) the radial external pressure on the liner is equal to the radial internal pressure on the tube, (2) no shear forces exist between the tube and liner, and (3) the external radial deformation of the liner plus the internal radial deformation of the tube is equal to the radial interference.

For a liner with uniform external pressure, according to equations (2), the simple stresses at the outside surface are given by equations (7a and b), and the unit tangential strain by equation (7c).

$$\sigma_t = \left[\frac{r_b^2 + r_a^2}{r_b^2 - r_a^2}\right] p_b. \tag{7a}$$

$$\sigma_r = p_b. \tag{7b}$$

$$e_t = \frac{1}{E}(\sigma_t - \mu\sigma_r) = \frac{p_b}{E}\left(\frac{r_b^2 + r_a^2}{r_b^2 - r_a^2} - \mu\right), \tag{7c}$$

in which E is the modulus of elasticity. Then the change in outside diameter of the liner is given by equation (8).

$$\Delta D_L = 2r_b e_t = \frac{2P_b r_b}{E_L}\left(\frac{r_b^2 + r_a^2}{r_b^2 - r_a^2} - \mu_L\right). \tag{8}$$

Similarly, for the tube (inside radius $= r_b$, outside radius $= r_c$ and internal pressure $= p_b$) the change in outside diameter is given by equation (9).

$$\Delta D_T = -\frac{2p_b r_b}{E_T}\left(\frac{r_c^2 + r_b^2}{r_c^2 - r_b^2} - \mu_T\right) \tag{9}$$

The diametral interference I between the liner and tube will be determined in general by equation (10).

$$I = \Delta D_T - \Delta D_L$$

$$= 2p_b r_b\left[\frac{1}{E_T}\left(\frac{r_c^2 + r_b^2}{r_c^2 - r_b^2} - \mu_T\right) + \frac{1}{E_L}\left(\frac{r_b^2 + r_a^2}{r_b^2 - r_a^2} - \mu_L\right)\right] \tag{10}$$

If both the tube and liner have the same modulus of elasticity, E, and Poisson's ratio, μ, equation (10) reduces to equation (11).

$$I = \frac{2r_b}{E}\left[\frac{r_c^2 + r_b^2}{r_c^2 - r_b^2} + \frac{r_b^2 + r_a^2}{r_b^2 - r_a^2} - 2\mu\right] p_b. \tag{11}$$

From this equation the shrinkage pressure caused by any given shrink-fit interference may be computed. Thus, if a liner having 0.50 in. ID, 0.75 in. OD, $E = 50{,}000{,}000$ psi, $\mu = 0.3$, is shrunk in a tube having 0.75 in. ID, 1.3 in. OD, $E = 30{,}000{,}000$ psi, $\mu = 0.3$, an interference of 0.001 in. between the tube and liner will cause a shrinkage pressure of 14,800 psi.

At the bore surface of the liner, the tangential stress produced by the shrinkage pressure is given by equation (12), which is derived from equation (2a) by substitution of the boundary conditions $r = r_a$ and $p_b = 0$. This stress will be negative, indicating that the surface is in compression. When powder pressure is applied

$$\sigma_\theta\Big|_{r=r_a} = \frac{-2pr_b^2}{r_b^2 - r_a^2} \tag{12}$$

this surface is in tension. Thus the shrinkage pressure tends to reduce the stress produced by the gas pressure, and higher gas pressures may be used than if the barrel had been of monobloc construction.

26.5 SPECIAL PROBLEMS IN INSERTION OF EROSION-RESISTANT LINERS

26.5.1 Support of Brittle Liner Materials

The insertion of stellite liners described in Section 26.2 was simplified by the fact that Stellite No. 21 has yield strength and ductility closely approaching those of gun steel, as may be seen by examination of Table 4 in Chapter 19. This is true both at room temperature and at the elevated temperatures that occur in gun barrels during firing. Also the modulus of elasticity and the coefficient of thermal expansion of Stellite No. 21 do not differ greatly from those of gun steel. Because of this similarity in properties the stress distribution in a stellite liner is not greatly different from that in a similar steel liner.

For a liner of a brittle material, however, a much less favorable situation exists. A single application of the powder pressure will crack such a liner inserted in the ways described in Section 26.2. The situation expressed by equation (12) suggests a way of circumventing this difficulty. By putting the liner under strong compression initially, it is possible to counterbalance the powder pressure so that even during firing the liner remains in slight compression. In this way it was possible to prevent longitudinal cracking of caliber .50 liners of the brittle chromium-base alloy described in Chapter 17. A compressive hoop stress of from 90,000 to 100,000 psi was imposed on the liner by a severe shrink-fit.

26.5.2 Effect of Differences in Thermal Properties

The successful use of a large compressive hoop stress in preventing cracking of a brittle liner requires that the coefficient of thermal expansion of the liner material should be not too much smaller than that of the steel in which it is inserted. Otherwise during firing, especially in a machine gun barrel, the barrel is likely to expand away from the liner.

One of the difficulties of the utilization of molybdenum as a gun liner material is that it has a low coefficient of thermal expansion. As may be seen from the two curves in Figure 9, steel expands linearly more than twice as much as molybdenum. The problem is further complicated by its high modulus of elasticity which causes it to bear an undue proportion of the internal pressure in the gun tube. With such a tube the heat exchange between the powder gases, the molybdenum liner, and the steel container depends in large measure on the ratio of the thermal constants of molybdenum and steel. Roughly speaking, the specific heat of molybdenum is one-half that of steel, the thermal conductivity is twice as great, and the thermal expansion one-third as large. Therefore, if a given amount of heat is applied to a given insulated mass of molybdenum its temperature increase is nearly twice as great as that of a similar mass of steel under the same conditions. For a molybdenum liner contained in a steel jacket and

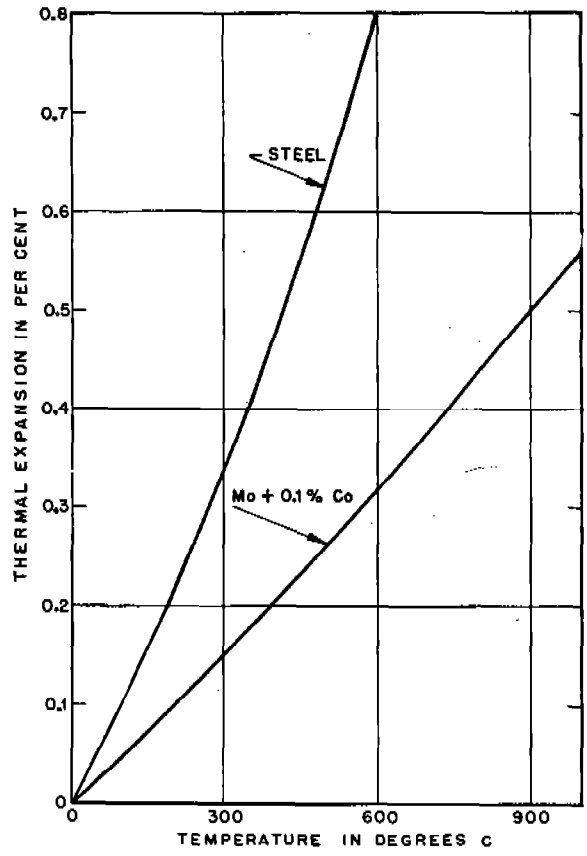


FIGURE 9. Thermal expansion of steel and of molybdenum containing 0.1 per cent cobalt. (This figure has appeared as Figure 3 in NDRC Report No. A-423.)

subjected to the hot powder gases in a gun bore, the temperature does not at first rise as high as if it were insulated, since the heat it receives is rapidly conducted to the steel jacket. The consequent heating of the steel jacket may cause it to expand so much more than the molybdenum liner that the latter is left unsupported.

In the meantime continuing flow of heat into the molybdenum from the powder gases will raise its temperature and increase its expansion. The inter-

ruption of heat flow into the steel jacket would permit it to cool and contract until the steel and molybdenum surfaces come into contact again, after which the process would be repeated. This cycle of heating and cooling might cause thermal stresses in molybdenum which would cause disastrous cracking.

In the first tests of molybdenum liners, this difficulty was prevented by shrinking and brazing the molybdenum tube into a sleeve of an iron-nickel-cobalt-titanium alloy, designated as Ti-Kovar. This alloy has the lowest coefficient of linear expansion in the range 20 to 500 degrees centigrade of any alloy that has both high strength and good elongation. The use of the Ti-Kovar sleeve made it possible to fire a 100-round burst through one of these molybdenum liners inserted in a caliber .50 heavy machine gun barrel without cracking.[49] The ultimate tangential strength of the molybdenum had been measured as 84,000 psi.

Its ductility was probably less than that of the molybdenum prepared later by the improved working schedule described in Section 18.3.2.

An answer to the question of whether the foregoing situation will be of real importance in the use of a seamless molybdenum liner cannot be given until a sample of molybdenum having superior physical properties has been prepared. It may well be that molybdenum having an ultimate tangential strength of say 120,000 psi and slight ductility will be able to resist successfully the deformation just described. Molybdenum with this high a tensile strength would also have a correspondingly high compressive strength and would therefore stand a rather severe shrink-fit. Hence, it does not seem unreasonable to expect that given a seamless molybdenum tube having the properties just mentioned, it can be successfully inserted as a gun liner by shrink-fitting alone.

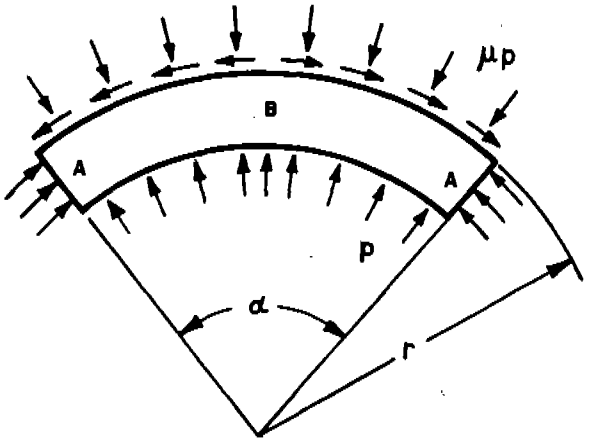


FIGURE 10. Cross section of a longitudinal segment or "stave" of a four-stave gun liner, showing the forces acting on it. (This figure has appeared as Figure 16 in NDRC Report No. A-273.)

26.5.3 Stresses in Stave-Type Liners

Another means that has been successful in virtually eliminating longitudinal cracking in a molybdenum liner is the stave type of construction described in Section 18.5.2. With this arrangement the tangential stresses tending to produce tensile failure merely open up the seams between staves. The stress produced in such stave-type liners has been analyzed in the following terms.[52]

A cross section of a stave or longitudinal segment for a four-stave liner is shown in Figure 10. Assuming that the liner fits loosely, it is acted upon by normal forces over the entire outside surface equal to the explosion pressure p and by frictional forces μp set up on the outside surface by sliding of the stave in the barrel as the barrel expands. Neglecting bending moments, the tensile stress at B, the center line of the outside of the stave, is given by equation (13),

$$\sigma_t = p\left(\frac{\mu\alpha r}{2h} - 1\right), \tag{13}$$

where p is the explosion pressure, μ the coefficient of friction, α the segment angle (radians), r the radius to the outside of the segment, h the thickness of the segment. To determine the equivalent stress, zero axial extension was assumed so that $\sigma_z = 0.3(\sigma_t - p)$. Since $\sigma_r = -p$, the equivalent stress, based on equation (1), is given by equation (14).

$$\sigma_e = 0.89p\sqrt{\frac{\sigma_t^2}{p^2} + 1.8\frac{\sigma_t}{p} + 1}, \tag{14}$$

which may be transformed to equation (15) by combination with equation (13).

$$\sigma_e = 0.44p\sqrt{(\mu\alpha r/h)^2 - 0.4(\mu\alpha r/h) + 0.8} \tag{15}$$

This equation shows that both the simple and equivalent stresses (for a given gas pressure) are a function of the nondimensional ratio $(\mu\alpha r/h)$ alone, and that as this ratio increases the stresses likewise increase. Obviously, then, it is desirable to make this ratio small by (1) lubricating the surface between the stave and barrel, (2) using a large number of staves, and (3) using thick-walled staves.

Table 1 shows the stresses in a stave-type liner for

TABLE 1. Calculated stresses in stave-type liners for caliber .50 gun at explosion pressure of 80,000 psi.[52]

Thickness of liner h (in.)	Coefficient of friction μ	Four-stave ($\alpha = \pi/2$) σ_t (psi)	Four-stave ($\alpha = \pi/2$) σ_e* (psi)	Two-stave ($\alpha = \pi$) σ_t (psi)	Two-stave ($\alpha = \pi$) σ_e* (psi)
3/16	0.2	− 51,000	36,400	− 21,000	54,700
	.4	− 22,000	54,000	37,000	101,500
	.6	8,000	77,500	96,000	152,000
	.8	37,000	101,500	106,000†	162,000†
3/32	0.2	− 34,000	46,000	12,000	80,700
	.4	12,000	80,700	105,000†	160,000†
	.6	58,000	119,500	106,000†	162,000†
	.8	105,000	160,000†	106,000†	162,000†

* Equivalent stress based on shear-energy theory, Equation 15. Negative signs indicate compression. Axial stress taken as $0.3(\sigma_t - p)$ corresponding to zero axial extension.

† These values are practically the same as for a seamless liner.

a caliber .50 gun at explosion pressures of 80,000 psi, computed by equation (15) for two different liner thicknesses, two different values of α, and four different values of μ.

An important conclusion from equation (13) is that, under the assumptions made, the tangential stress in liners of a given number of staves in guns of different calibers will be the same provided that the wall ratio and the coefficient of friction remain constant.

Increasing the number of staves to decrease the tangential stress in each one introduces the problem of restraining the staves. Brazing has been successfully used[95] for ten-stave liners fired a relatively few rounds in the caliber .50 erosion-testing gun (Section 11.2.1). For larger caliber guns brazing would be considerably more difficult and might be less successful.

A mechanical scheme for keying the staves of a multistave liner in place has been suggested. Each stave is machined with a tongue on its back surface to fit into a corresponding groove in a steel jacket. The tongues should be shaped as shown in the plane section perpendicular to the axis represented by Figure 11 so that their tightness may not be affected by the different thermal expansion of the stave and the steel jacket. In general, the back of a stave is bounded by four planes having a common line of intersection, and similar plane surfaces form the grooves and thrust bearing surfaces in the jacket. Because of the mechanical difficulties inherent in this design, it has not yet been tried.

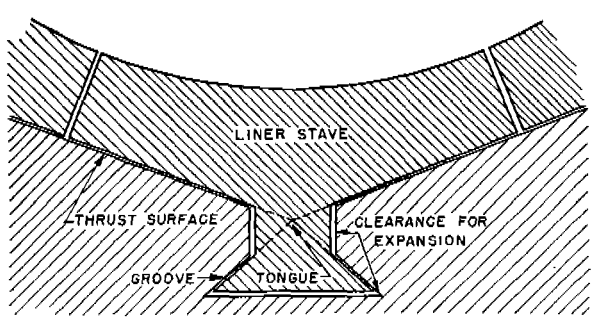


FIGURE 11. Proposed method of keying the staves of a liner into a steel gun barrel. (This figure was taken from a monthly progress report from the Geophysical Laboratory on Contract OEMsr-51.)

26.6 DESIGN OF RIFLING

26.6.1 Rifling Requirements of Hypervelocity Guns

The hypervelocity guns to which Division 1 has given consideration have been ones for firing spin-stabilized projectiles.[f] Hence the bore surface of the gun tube is rifled with helical grooves in order to impart spin to the projectile by engagement with a soft metal jacket on bullets or a soft metal rotating band on artillery projectiles.

The rotational velocity of a projectile is directly proportional to the muzzle velocity when it is fired from guns having the same twist of rifling. Fortunately the stability relations, discussed in Chapter 8, are such that if the projectile is stable at one velocity it is stable at all velocities. Therefore the twist of rifling of a hypervelocity gun needs to be no different from that of a lower velocity gun in order to make the projectile stable.

[f] The stabilization of projectiles by means of fins or in other ways was not investigated. It may be noted in passing, however, that the erosion-resistant materials developed by the Division would be just as useful for hypervelocity smooth-bore guns. Also the absence of rifling would increase the ease of application and would permit the utilization of relatively thick, hard coatings that are not practical for rifled gun tubes.

The torsional moment exerted on the engraved projectile band by the rifling increases as the square of the velocity. The strength of the band material cannot be increased indefinitely without seriously increasing the band pressure (Chapter 7). Therefore the strength of the band appears to be a serious limitation to the use of jacketed or banded projectiles at velocities in excess of about 4,000 fps. An answer to this problem is to be found in the use of pre-engraved projectiles, as discussed in Section 27.3.

Regardless of whether banded or pre-engraved projectiles are fired, the form of the rifling of a hypervelocity gun should be modified slightly in order to strengthen it, for the torque exerted on the rifling by the projectile also increases as the square of the velocity.

26.6.2 Factors Affecting the Strength of Rifling

For a given torque on the projectile, the bearing pressure between the rifling and the projectile is inversely proportional to the depth of the grooves, the width of the rotating band, and the number of lands and grooves. It is obviously desirable to keep this pressure as low as possible to prevent wear.

Depth of Grooves

Increasing the groove depth in the caliber .50 erosion-testing gun (Section 11.2.1) from 0.005 in. to 0.010 in. gave increased velocity-life at muzzle velocities of 4,000 fps. Naturally, engraving stresses and radial bore pressures were increased when using engraving-type bullets, but the resulting wear was not proportional. Obviously a compromise must be made to prevent introduction of one problem by eliminating another.

Firing tests indicated that pre-engraved projectiles (Section 27.3.3), having engraving twice as deep as normal, showed only 1 to 2 per cent greater drag than a smooth projectile and that depth of rifling had so little effect that deep rifling is not detrimental to exterior ballistics. Furthermore fewer and wider lands decrease drag by reducing the frontal area of the projectile, thus favoring this design.

Number of Lands and Grooves

The use of a large number of lands and grooves for high-velocity guns has been known to be undesirable because of erosion, since the narrow lands are easily crushed or worn by the engraving bullet and melted by the gas blast. To be sure, an increased number of lands and grooves increases bearing area and decreases bearing stresses, but increased area can be better obtained by other means.

Width of Lands and Grooves

When deeper grooves are used, it appears desirable to make the lands wider. This reduces the bending stresses at the roots of the lands, and also reduces shearing stresses in the lands. It must be remembered that as the width of lands is increased, the width of splines engraved on the rotating band is decreased and may lead to excessive shearing stresses there. When using jacketed or banded projectiles wide lands require high engraving pressures and may require additional strength in the gun tube. This need not be considered with pre-engraved projectiles.

Wide lands have a further advantage in that they reduce the possibility of body engraving, by giving a larger area of support to the projectile. It appears desirable, when using pre-engraved projectiles, to have the rifling as much as two to four times as deep and the lands two or three times as wide as is used in conventional guns. It is also suggested that not more than 12 lands and grooves should be used in guns over about 3 inches caliber and a fewer number on smaller sizes.

Wide lands improve launching conditions by giving better support to the projectile while in the bore. It is easier to maintain accurate bore dimensions with fewer and wider lands and the effect of bore clearance is reduced. This is particularly important in minimizing yawing and balloting in the larger bore sizes, where the inertia of the moving mass is very great and the pounding produces deep and often irregular wear, such as has been described in Section 10.4.10.

Angle of Twist

A high angle of twist is desirable for exterior ballistics but introduces higher side forces on the rifling, particularly at high gas pressures. For this reason, some guns have been designed with an increasing angle of twist toward the muzzle. This arrangement tends to relieve bearing stresses at the breech end but increases them at the muzzle. Decrease in length of

bearing, as the projectile goes through an increasing angle of twist, further increases bearing stresses.

If exterior ballistics will permit, it is desirable, as far as wear is concerned, to reduce the angle of twist.

A high velocity of rotation may also adversely affect launching conditions. If the projectile is unbalanced or if there is appreciable clearance between the projectile and the bore, centrifugal forces introduce an initial yaw in the projectile. Since these centrifugal forces are proportional to the square of the angular velocity, the value of a low angle of twist is apparent.

26.6.3 R.D. System of Rifling and Banding

A special design of rifling and a projectile to match it was proposed by Colonel G.O.C. Probert and his colleagues at the Research Department of Woolwich Arsenal.[16] This has been called the Probert system, or preferably the R.D. [Research Department] system. The purpose of this design was to simulate the bore profile of a somewhat eroded barrel and thus to minimize the effects of erosion and increase the barrel life. The design of projectile and barrel was such that the initial resistance of the former to movement was as small as possible in a new gun and that the proportional decrease of resistance with increasing wear was also as small as possible. The use of this system in several British 3.7-in. guns proved successful. A trial[122] was made in the caliber .50 erosion-testing gun (Section 11.2.1). The projectile was made with two copper bands, the rear one of which had a larger diameter than the forward one. The rear band sealed the bore while the forward one was being engraved. The forcing cone was extended and its slope made as small as possible. After an erosion test of 150 rounds at an initial muzzle velocity of 3,650 fps using double-base powder, the increase in land diameter was not much less than that with ball M2, or artillery-type bullets, but the velocity drop was much less (170 fps, as compared with 320 fps). With pre-engraved bullets, however, the corresponding velocity drop was only 125 fps; consequently, no further work was done by Division 1 on the development of this system for use in hypervelocity guns. This system, however, has been used by the Bureau of Ordnance of the Navy Department in its new 3-in./70-cal. gun.

Chapter 27

DESIGN FEATURES OF PROJECTILES

By *F. R. Simpson*[a] and *H. L. Black*[b]

27.1 INTRODUCTION

HYPERVELOCITY GUNS require projectiles suitable for withstanding higher stresses during their passage down the gun bore and during flight. This is particularly true in the case of hollow, high-explosive shells. The second section of the present chapter summarizes what has been done in determining the stresses in shells and analyzing their effects on the design of the projectile. The most important stresses in the mantle of a shell are those due to band pressures caused by engraving during the rifling process (see Chapter 7), and those due to gas pressure around the shell body behind the band. The former, which usually are of greatest intensity over a short section, give higher local stress beneath the band at the inner radius of the shell than the latter.

Two methods for reducing the radial stresses resulting from the band pressure on the shell beneath it have been investigated. The first method, described in Section 27.3, eliminates virtually all the radial compressive load by using a pre-engraved rotating band on the body of the shell of such design that it fits the gun bore and rifling snugly. This band gives the projectile suitable spin and satisfactory obturation, and leaves only the stress resulting from gas pressure to be resisted by the shell wall. The second method, described in Section 27.4, is the use of a low-stress rotating band of high torsional shear strength, with low radial compressive resistance and reduced surface friction in the gun bore.

The use of either method of reducing the radial load due to engraving allows either the use of higher gas pressure, with a corresponding increase in muzzle velocity, or a reduction in gun weight by decreasing the wall thickness and retaining the same gas pressure and velocity. In addition, the contribution of frictional wear to erosion is reduced, especially by the use of pre-engraved projectiles. The consequent large increase in barrel life resulting from the combination of pre-engraved projectiles and a chromium-plated gun bore is described in Chapter 31.

Special types of projectiles—such as the sabot-projectiles and those for use in tapered-bore guns—which attain higher velocities through a reduction in mass of the projectile, have their peculiar problems of stress analysis. They are described in Chapters 29 and 30.

Although the testing of shell forgings for leakage through the base is not the immediate concern of the projectile designer, defects in the forging material which permit such leakage are serious, since premature explosion in the gun may result. Two testing methods for revealing certain types of imperfections in shell bases are described in Section 27.5.

27.2 STRESSES IN SHELLS

27.2.1 Introduction

The Applied Mathematics Panel of NDRC, at the request of Division 1, prepared a review[147] in early 1944 of the work done in this country and in England[369,373] on the strength features of the design of high-explosive shells.[c] Much of the general analysis in that report is still pertinent, and therefore it is quoted with a few editorial changes (to adapt it to the present report) in the remaining paragraphs of this section and in Sections 27.2.2 and 27.2.3. In the latter section a paragraph has been added to bring the subject up to date.

It would seem that very little consideration had been given to the design of projectiles for strength until a few years ago. Apparently the failure of certain shells upon passage through the guns (with consequent premature bursts) led to some attention being paid to the problem. It is not particularly difficult to make the thickness of the shell walls so great that no failure would occur, but it is desirable in most cases to make the shells rather thin in order that the

[a] Ordnance Research Engineer, The Franklin Institute, Philadelphia, Pa.

[b] Technical Aide, Division 1, NDRC. (Present address: Department of Mathematics, Michigan State College, East Lansing, Michigan.)

[c] This review was prepared by Dr. J. J. Stoker, a research mathematician of the Applied Mathematics Panel, following visits to the persons in this country working on the problem and a study of their reports and those from British investigators.

explosive charge carried may be as large as possible and also in order that proper fragmentation characteristics are obtained. In other words, a shell design is wanted which provides just sufficient strength to prevent failure of the shell in the gun and not much more.[d]

The problem could be treated either experimentally or theoretically or by a combination of both methods. It has been suggested that one might design a series of shells of decreasing thickness, fire and retrieve them and then make measurements of permanent deformations in order to arrive at the optimum design. There is much to be said for such a plan, but it would be rather costly and would require rather elaborate statistical controls, since the number of variables which enter into the problem is large. The problem has therefore been considered hitherto in the main as a problem in the theory of elasticity or strength of materials in which the stresses are to be calculated in the shell on the assumption of perfectly elastic behavior of the material, with a view to basing the design on the stresses thus determined.

27.2.2 General Discussion of the Shell Design Problem[e]

Types of Stress on a Typical Shell

A study of the stresses developed in a shell during its passage through the gun requires, to begin with, a knowledge of the external forces exerted on it. In Figure 1 we indicate schematically a fairly typical design of a high-explosive shell. It is essentially a hollow cylinder with rather thin walls which taper to a roughly conical nose at the forward end. The shell is closed at the rear by a base which is generally thicker and heavier than the side walls. The base may be rounded on the inside of the shell; in some cases it is an integral part of the shell, in others it is screwed into the shell.

Shrunk into a groove cut from the outer shell wall is a rotating band of soft metal (copper or gilding metal, for example), the main purpose of which is to engage the rifling in the gun so that the shell will be set into rapid rotation about its axis as it passes down the gun barrel. The rotating band has an outside diameter greater than the bore of the gun—an excess of metal is provided to ensure rotation of the shell and also to provide a seal which prevents the propellant gases back of the shell from escaping between the shell walls and the gun. Apart from the rotating band, the outside diameter of the shell is kept appreciably smaller than the bore of the gun except at a portion toward the nose of the shell (called the "bourrelet") which is turned to fit rather snugly inside the gun. The shell is thus centered in the gun at the bourrelet and the rotating band. The interior hollow portion of the shell may be filled with various explosive substances, liquid or solid.

It is useful to consider in a descriptive way what happens to the shell when the gun is fired. At the instant of firing the very high gas pressure P_g developed in the chamber back of the shell gives the shell a very high acceleration forward. The rotating band

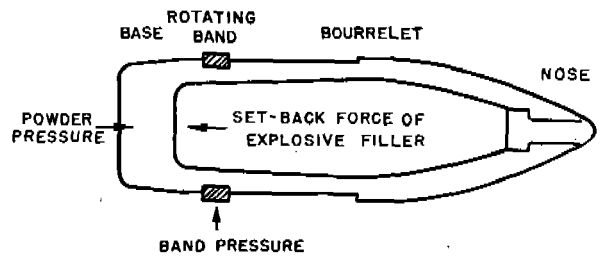


Figure 1. Schematic diagram of a typical high-explosive shell, showing the forces acting on it in the bore. (This figure is based on Figure 1 in AMP Report No. 75.1)

is "engraved" by the rifling of the gun, as described in Section 7.3.5, which sets up a very high mutual pressure, the so-called "band-pressure," P_b, in the radial direction between the rotating band and the gun barrel as well as between the rotating band and the shell.[f] As the shell proceeds down the barrel of the gun, its angular velocity of rotation increases until a maximum is attained at the muzzle of the gun. The gas pressure decreases during projectile travel while the band pressure may or may not decrease after engraving has been completed.

From this description of what occurs during passage of the shell through the gun, one sees that the external forces exerted on the shell might be classified into the following three types:

1. The gas pressure P_g which acts on the base of the shell and also on that portion of the outer shell mantle which lies back of the rotating band.

[d] Shells for armor-piercing purposes are an exception to this statement, at least as far as the forward part of the shell is concerned.

[e] Quoted from p. 4 to 12, inclusive, of AMP Report No. 75.1[47] [See footnote (c).]

[f] The band pressure is considered in detail in Chapter 7.

2. The band pressure P_b which is exerted over a rather narrow ring around the shell mantle.

3. Inertia forces of various sorts arising from the high accelerations imparted to various parts of the shell as well as to the liquid or solid filling in the hollow portion of the shell.[g] These forces of dynamical origin can be further subdivided into those due to forward acceleration under the action of the gas pressure P_f and those arising from the angular acceleration and angular velocity imparted to the shell by the rifling of the gun.

Analysis of Shell Stresses

Various methods are available for determining the stresses in shells. It will be helpful for our later discussion to indicate in a general way how a few of the estimates for the stresses are made. This is perhaps the best way to become acquainted with the difficulties and complexities peculiar to the problem.

Stresses in the Base. Let us consider, for example, how the stresses in the base of the shell are analyzed. The base is subjected on its rear face to the gas pressure P_g and to a pressure P_f on the interior face which arises from the inertia of the filler inside the shell. The latter pressure is readily computed once the forward acceleration of the shell is known. This acceleration is found from the total mass of the shell and filling through the assumption that the unbalanced force on the shell is that due to the gas pressure P_g, retarding forces arising from the driving band being ignored. The radial stresses in the base are then computed from the theory of bending of thin circular plates, the net pressure causing bending being given by $-P_g - P_f$.

Stresses in the Walls. In the more or less cylindrical side walls of the shell the stresses are calculated as follows. First of all there is a compressive stress on any plane section perpendicular to the axis of the shell which is found at any section by dividing the inertia force arising from the mass of that part of the shell (as well as the fuze, adapter, etc.), which lies in front of the section by the area of the cross section. In addition there are radial and circumferential stresses in the shell walls due to inertia forces arising from the rotation of the shell and from a liquid filling (if present). These forces act radially outward from the axis of the shell. The stresses arising from this source are calculated from the Lamé formulas for stresses in thick cylinders of uniform thickness, which are given by equations (1), (2), and (3) in Chapter 7.

Combination of Stresses. Once the stresses on all the faces of a rectangular volume element at any point have been determined, it is necessary to judge their significance in causing a possible plastic deformation or even a rupture. The different criteria of failure are discussed in Section 27.2.4.

It might be noted that the stresses arising from the various types of load do not have their maxima at the same times: the gas and band pressures are in general largest during engraving, while the stresses due to rotation of the shell are largest at the muzzle of the gun.

Limitations of the Theory

The theory of bending of thin plates and the Lamé theory of thick-walled cylinders are based on assumptions which are not fulfilled in the problems considered here. The base of the shell is generally so thick in comparison with its diameter that the theory of bending of thin plates is not strictly applicable. In addition, the boundary condition to be imposed at the edge of the base is rather uncertain. The Lamé formulas are also not strictly applicable to the problem of determining the stresses in the walls of the shell, since these formulas are derived under the assumptions that the cylinder is uniform in thickness, infinitely long, and subjected to loads which are the same over the entire length of the cylinder.

In view of the complexity of the problem when treated as one in the exact theory of elasticity, approximation formulas are the only practical ones to be used in carrying out stress analyses for shells, as discussed in Section 27.2.3. Investigators both in Britain[349,351,355,357,359] and in this country[34] have carried out a few analyses according to the exact theory, and compared the results with those obtained by using approximate methods. A fairly good agreement was obtained. The approximate methods tend to give lower values of the stresses.

At the Catholic University a method was developed of determining the stresses in a thick-walled cylindrical shell due to normal pressures on a rotating band of normal width.[34] The Ordnance Department extended the development by a method of applying the numerical results found for a given band width to the determination of stresses from another band, of

[g] The forces arising from these sources are referred to by ordnance engineers as forces due to "setback," in graphic analogy with what happens to a passenger seated in a streetcar when the car starts up quickly.

any arbitrary width, provided that the wall ratio (the ratio of the outer shell radius to the inner) remained unchanged.[546]

27.2.3 Practical Formulas for Shell Design

U. S. Army Practice

The Army Ordnance Department has devised means of estimating the stresses in a shell which, roughly speaking, consist in making use of the available formulas (from the theory of elasticity or strength of materials) for the stresses in the various portions of the shell which fit the circumstances as well as possible.

The principal improvement in these methods of calculating shell stresses, made as a result of investigations at Catholic University for Division 1, has been to take into account the effect of the band seat in the body of the shell, which acts like a notch as far as the stress distribution is concerned. The stresses in this case were calculated by the use of new approximation formulas.[17] It was assumed that a uniform radial pressure due to the band was applied over the notch and a uniform radial pressure due to the powder gas was applied to the mantle of the shell behind the notch, as illustrated by Figure 2. For the boundary conditions at the shoulder of the notch, radial displacements and their axial derivatives were fitted exactly; but it was not possible to calculate stress concentrations at the corner. The hoop stress and the axial stress on the inner and outer walls were expressed in terms of the wall ratio of the shell, the width of the pressure band,[h] and a series of empirical coefficients, as shown at the end of the next section.

Relaxation Methods[i]

The British have devised a set of formulas for the approximate analysis of the stresses in shells, and they have compared the results obtained by these formulas with those obtained by making use of the exact theory of elasticity. As a consequence the problem then becomes a complicated boundary value problem associated with a pair of linear partial differential equations of second order. The fact that the mathematical problem is of this character and that the body to which it is to be applied is so complicated in shape explains why it is impossible to expect to obtain a set of formulas for the stresses applicable to shells of any dimensions which would be at once simple and exact.

The phrase relaxation methods used so frequently in the British reports refers to an iteration scheme for solving the linear equations which arise when the solution of the boundary value problem is obtained approximately by means of the method of finite differences. These computations are very laborious and require a considerable amount of skill and experience to carry out. In addition, the solutions must be carried through numerically for each different shell design. The intention was to analyze a sufficient number of different shells covering a fairly wide range of designs in order to obtain information which can be used in the practical design of shells.[336,338,343,344,347,361]

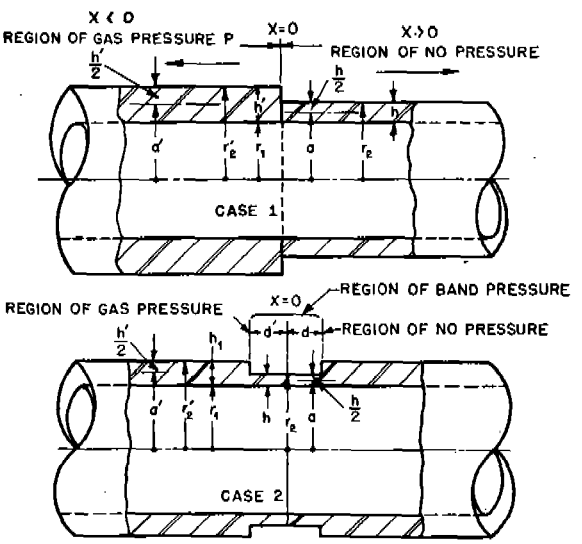


FIGURE 2. The band seat in a shell acts like a notch, and separates the shell into three regions of stress.

The relaxation methods make it possible to analyze the effect of the band pressure on the stresses in the shell. In the cases analyzed it was found that the band pressure has, for example, a quite considerable effect on the stresses in the base at the regions where the stresses are largest.[362] The band pressure tends to bend the base in such a way as to relieve stresses caused by other loads; the reduction may amount to almost 50 per cent in some cases. This is probably due largely to the fact that the cases selected were ones in which the rotating band was located in part di-

[h] The static experiments described in Section 7.3 showed that the width of the pressure band is slightly less than the width of the rotating band.

[i] Quoted from p. 18 and 19 of AMP Report No. 75.1.[147] [See footnote (c).]

rectly above the base. If the band were located a distance of a band width or two in front of the base, it is unlikely that such large effects of the band pressure on the stresses in the base would be found. Again it should be noted that such an analysis leads only to the stress distribution in a particular design and not to formulas for the stresses valid for any design.

In their desire to design shells with a minimum factor of safety the British have carried out a few actual firing tests with shells designed to have abnormally low factors of safety. The trials (for 2-pounder shells) indicated that the factor of safety might be reduced quite considerably below the customary value without the risk of causing premature bursts.[363]

27.2.4 Criterion of Failure of a Shell[117]

It is recognized that the best criterion of plastic flow is that of Mises and Hencky.[514] This criterion has the additional advantage that its application does not require a determination of the principal axes of stress, but that any direction of axes can be used.

According to the Mises-Hencky theory, plastic flow occurs if the equivalent stress, S_e, which is given by equation (1), is larger than the yield point of the material in the usual tension test.

$$S_e^2 = \tfrac{1}{2}[(\widehat{\theta\theta}-\widehat{rr})^2 + (\widehat{rr}-\widehat{xx})^2 + (\widehat{xx}-\widehat{\theta\theta})^2 + 4\widehat{rx}^2]. \quad (1)$$

In this equation $\widehat{\theta\theta}$ represents circumferential or "hoop" stress, $\widehat{rr}$ radial stress, $\widehat{xx}$ axial stress, and $\widehat{rx}$ shear stress.

Equation (1) can be simplified for cases where the stress is transmitted to the shell by the rotating band. From symmetry, the shear stress is zero under the middle of the band where S_e is largest. Except for very narrow bands, the largest equivalent stress occurs on the inner surface of the shell, where the radial and shear stresses are zero. Equation (1) is then reduced to equation (2).

$$S_e^2 = \widehat{\theta\theta}^2 - \widehat{\theta\theta}\,\widehat{xx} + \widehat{xx}^2 = (\widehat{\theta\theta}-\widehat{xx})^2 + \widehat{\theta\theta}\,\widehat{xx}. \quad (2)$$

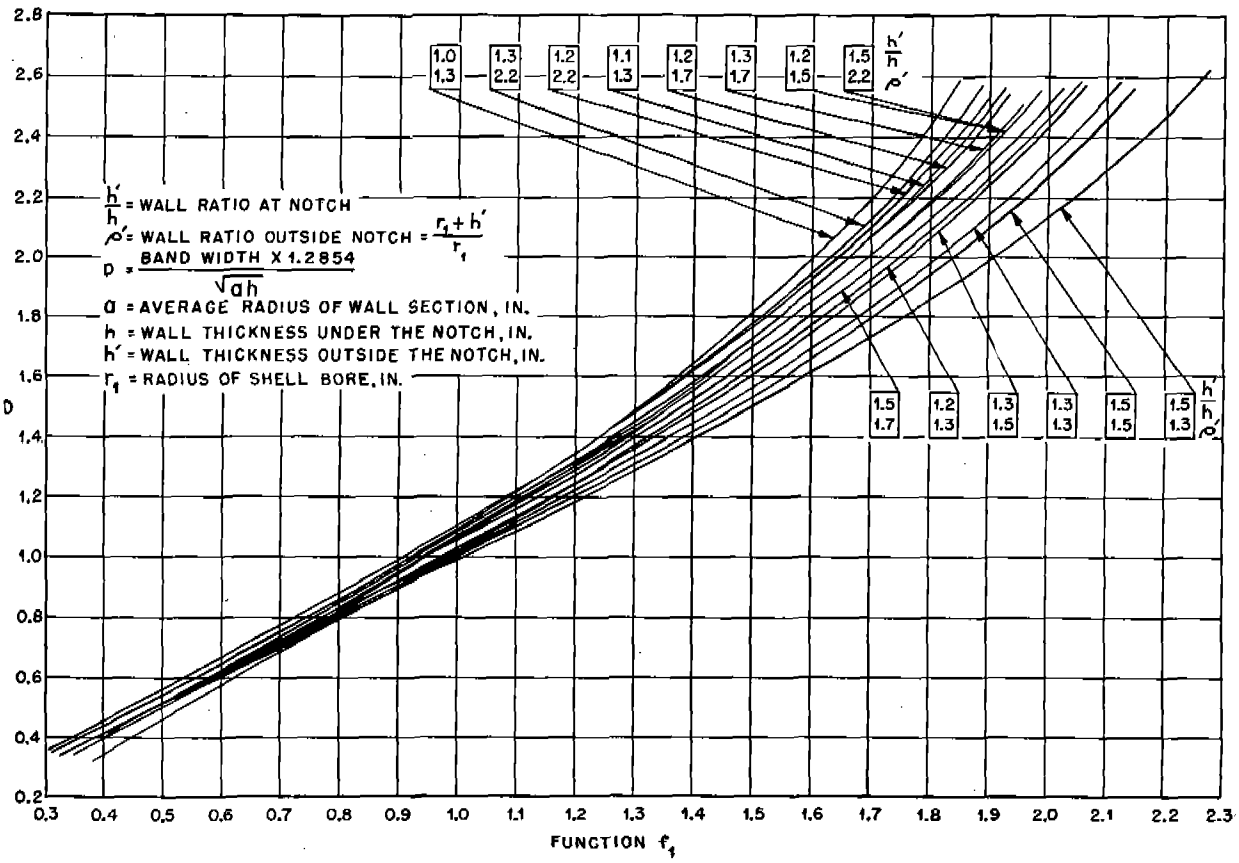


FIGURE 3. Empirical function f_1 for computing the tangential stress at the inner wall of a shell under the rotating band. (This figure has been prepared from Table I in NDRC Report No. A-281.)

Summary of Method for Calculating Stresses in a Shell

The procedure for calculating the stresses in a shell can be summarized briefly as follows.[j]

1. Calculate the average band pressure P_b as described in Section 7.3.3 by the use of P/EAI.

2. Obtain the hoop stresses $\widehat{\theta\theta}_1$ and $\widehat{\theta\theta}_2$ at the inner wall, corresponding to the two cases of Figure 2, by the use of equations (3) and (4).

$$\widehat{\theta\theta}_1 = -\frac{\rho'^2}{\rho'^2 - 1} P_g f_2 \tag{3}$$

$$\widehat{\theta\theta}_2 = -\frac{\rho'^2}{\rho'^2 - 1} P_b f_1 \tag{4}$$

In these equations ρ' is the wall ratio (ration of outer to inner diameter) of the shell beyond the band seat, P_g is the gas pressure, P_b is the band pressure, and the values of the empirical coefficients f_1 and f_2 are given in Figures 3 and 4, respectively. The hoop stress at the outer wall is given by equation (5),

$$\widehat{\theta\theta}_e = \widehat{\theta\theta}_i \left(\frac{\rho'^2 + 1}{2\rho'^2}\right) \tag{5}$$

in which $\widehat{\theta\theta}_i$, the combined hoop stress at the inner wall, is given by the sum of equations (3) and (4).

3. In similar manner obtain the axial stresses at the inner and outer walls by means of equations (6), (7), and (8).

$$\widehat{xx}_1 = -\frac{\rho'^2}{(\rho'^2 - 1)(\rho' + 1)} P_g f_4 . \tag{6}$$

$$\widehat{xx}_2 = -\frac{\rho'^2}{(\rho'^2 - 1)(\rho' + 1)} P_b f_3 . \tag{7}$$

$$\widehat{xx}_e = \widehat{xx}_i \tfrac{1}{2}[(1 - \mu)\rho' + (1 + \mu)/\rho']. \tag{8}$$

The coefficients f_3 and f_4 are given in Figures 5 and 6, respectively. In equation (8) the value of Poisson's ratio μ is taken as 0.3 for steel.

4. Substitute these stresses in equation (2) to obtain separate values of the equivalent stress at the inner and outer walls. Compare these stresses with the actual tensile strength at the yield point of the material used. If the stresses at the inner and outer walls are both below the yield point, there should be no failure of the shell in firing. If the stress at the inner wall is above but that at the outer wall below the yield point, the shell should ordinarily still be satisfactory. If both are below the yield point, the design should be changed to give added strength.

[j] The derivation of the equations listed in this section is given in NDRC Report A-281.[56]

27.3 PRE-ENGRAVING OF PROJECTILES[120]

27.3.1 Design Features of Pre-Engraved Projectiles

The most promising method of reducing radial load on the shell resulting from band pressure is by removing the usual band and replacing it with pre-engraved teeth or splines on the outside to fit the rifling. By thus eliminating the usual bore friction and the resulting abrasion of the bore surface, the life of the barrel may be increased several-fold, especially in the case of a chromium-plated bore surface, as is described in Chapter 31. The many advantages of this type of projectile outweigh the few disadvantages, such as alignment in the gun for automatic fire and the precision required for engraving the teeth, both of which problems have been overcome in actual tests.

Many design features of pre-engraved projectiles were investigated in a comprehensive ballistic research program undertaken by The Franklin Institute in cooperation with the Ballistic Research Laboratory, Aberdeen Proving Ground, where the firings were made.

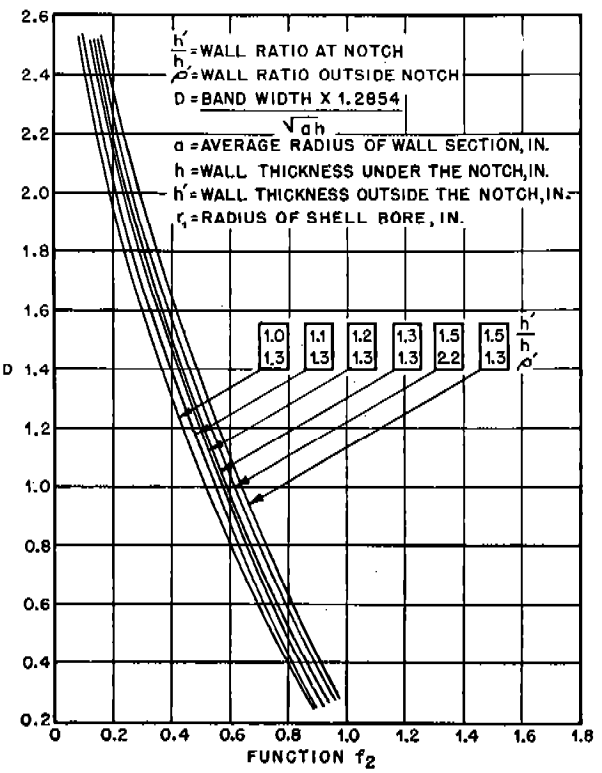


Figure 4. Empirical function f_2 for computing the tangential stress at the inner wall of a shell due to powder pressure alone. (This figure has been prepared from Table II in NDRC Report No. A-281.)

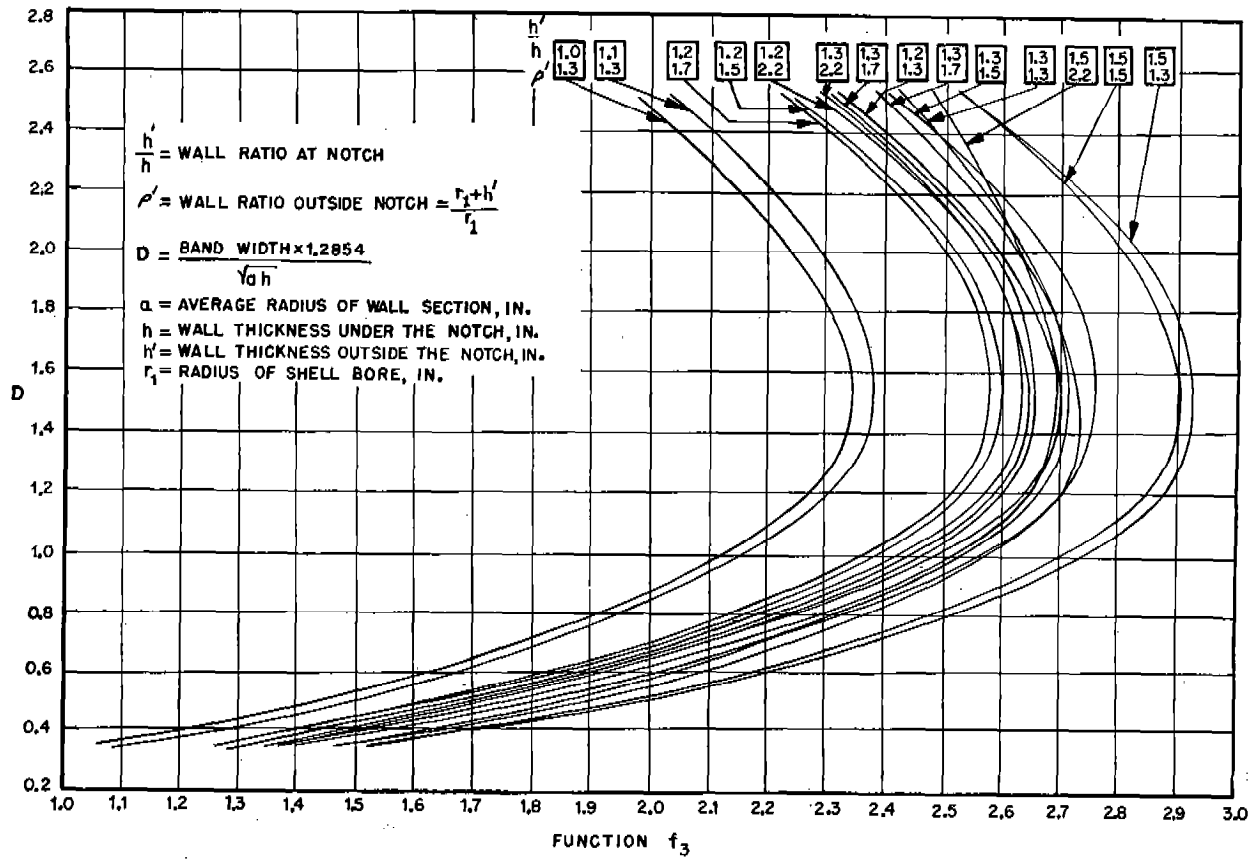


FIGURE 5. Empirical function f_3 for computing the longitudinal stress at the inner wall of a shell under the rotating band. (This figure has been prepared from Table III in NDRC Report No. A-281.)

The program was made extensive enough to include a number of controversial points in projectile design that had to be settled before the use of pre-engraved projectiles could be justified.

It is evident that the flight of any projectile is greatly affected by its launching condition as well as by its performance in the air. For example, a projectile with excellent exterior characteristics, such as low drag, will show a large dispersion if its launching is incorrect, thereby discounting the advantages obtained from its design. As indicated by the analyses of the experimental results set forth in Sections 27.3.2 and 27.3.3, certain definite trends in performance are associated with the action of the projectile within the gun, and other trends are associated with its action in free flight.

RECOMMENDATIONS

The analysis of the results of those firing tests, which are discussed briefly in Sections 27.3.2 and 27.3.3, led to the following recommendations concerning the design of pre-engraved projectiles.

1. The driving teeth should be reduced to a minimum number and their height increased to 4 or 5 times the depth of engraving now used on standard banded projectiles. It is believed that the number of teeth on a projectile should not exceed 12 for all projectiles above 3 in. in diameter and be not less than 4 for smaller sizes. (See Section 26.6.2 for the corresponding recommendation with respect to the number and width of the grooves in the gun tube.)

2. The front end of the driving teeth should be kept sharp radially, should be pointed circumferentially at an angle of about 30 degrees to the projectile axis, and should be flush with the body and the bottom of the grooves.

3. A centering cylinder should be provided between the back of the ogive and the front end of the driving teeth for aligning the projectile axially in the gun.

4. The origin of rifling in the gun should be just beyond a short centering cylinder in the bore. The ends

of the lands should be normal to the axis and pointed circumferentially at the same angle as the points on the projectile, in order to facilitate engagement of the projectile with the rifling during chambering.

5. The front end of the driving teeth should be placed as far forward as possible to give engagement in the rifling for as long as possible, as the origin of rifling advances with erosion.

6. The length of the driving teeth should be made sufficient to withstand the driving torque at the highest muzzle velocity required with the minimum engagement expected in a worn barrel.

7. A smooth, narrow rear bourrelet should be provided just forward of the boat-tail to give a close fit in the gun bore and thus insure accurate guiding.

8. A good method of obturating should be provided, such as a base cup of rubber, Lucite, or other material, or a narrow sealing ring of some soft material, such as copper, that offers very little resistance to engraving and consequent bore friction.

9. For greatest accuracy and consistent performance, an ogive of not less than 8 nor more than 10 calibers should be used to give a minimum drag coefficient with good stability.

10. The center of gravity of the projectile should be kept well forward to give greatest stability. This arrangement, with the band placed well forward, brings the driving teeth approximately over the center of gravity so that the yawing tendency is reduced to a minimum in the gun and in flight.

27.3.2

Interior Ballistics of Pre-Engraved Projectiles

Among the factors affecting the motion of a projectile within a gun, the following seem to have the greatest effect. (Compare Figure 14 in Chapter 10.)

1. Yawing and balloting of the projectile within the bore.

2. Radial gas thrust against the projectile.

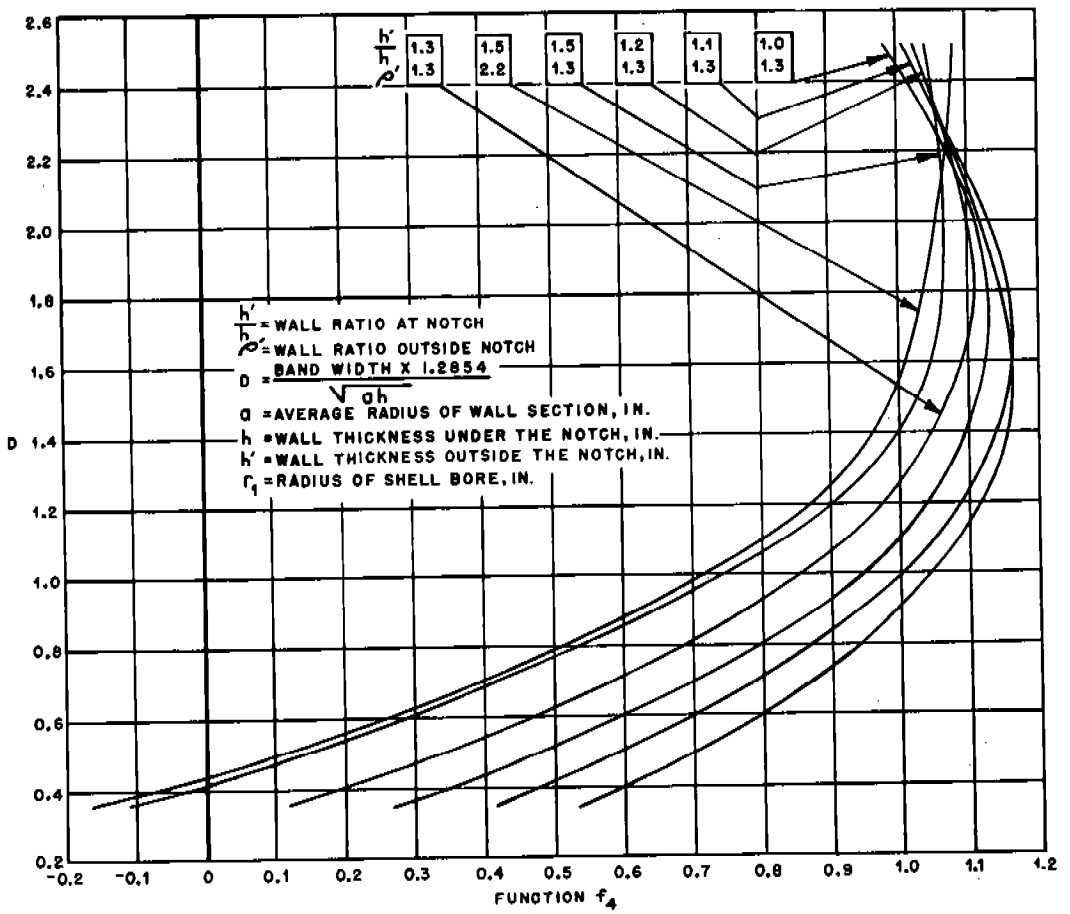


FIGURE 6. Empirical function f_4 for computing the longitudinal stress at the inner wall of a shell due to powder pressure alone. (This figure has been prepared from Table IV in NDRC Report No. A-281.)

3. Launching conditions.

Yawing and Balloting. Excessive angular motion of the projectile within the gun bore is detrimental to its accuracy, as evidenced by the results obtained when firing an eroded gun with its large bore clearance and consequently greater freedom of radial movement. In tests with an accurate gun, for which bore and projectile dimensions were closely controlled, measurements were made by spark photographs of the actual average external yaw angle for various designs of projectiles. The effect of different lengths of bearing between projectile and gun and of different bore clearances—which are the most important factors affecting the internal yaw angle and resulting flight performance of a projectile—have been determined from results of these tests.

Figure 7 shows the type of action that may take place near the muzzle of a gun at the time of launching. As the projectile emerges from the bore, it may quickly develop yaw, resulting from a combination of unbalanced gas pressure around the projectile, unbalanced masses under the action of the centrifugal force caused by the spin, and friction forces.

Examination of the recovered projectiles confirmed this action. There were rifling marks on the bourrelet on one side and on the rear guide on the other side. This indicates that the projectile followed a certain set of lands spirally down the bore in a yawing position. As shown in Figure 8, there is good agreement among the "jump ratios" (the ratio between the average external yaw angle and the calculated internal yaw angle) for the different designs.

A low inherent drag coefficient, KD_0 reduced to zero yaw, does not seem to keep a projectile from yawing. Conditions of launching must, therefore, be the principal factor influencing muzzle jump and flight yawing. Since with the equipment available for these tests, the muzzle jump could be compared only qualitatively, only the average yaw angles of the various projectiles observed can be compared. At time of

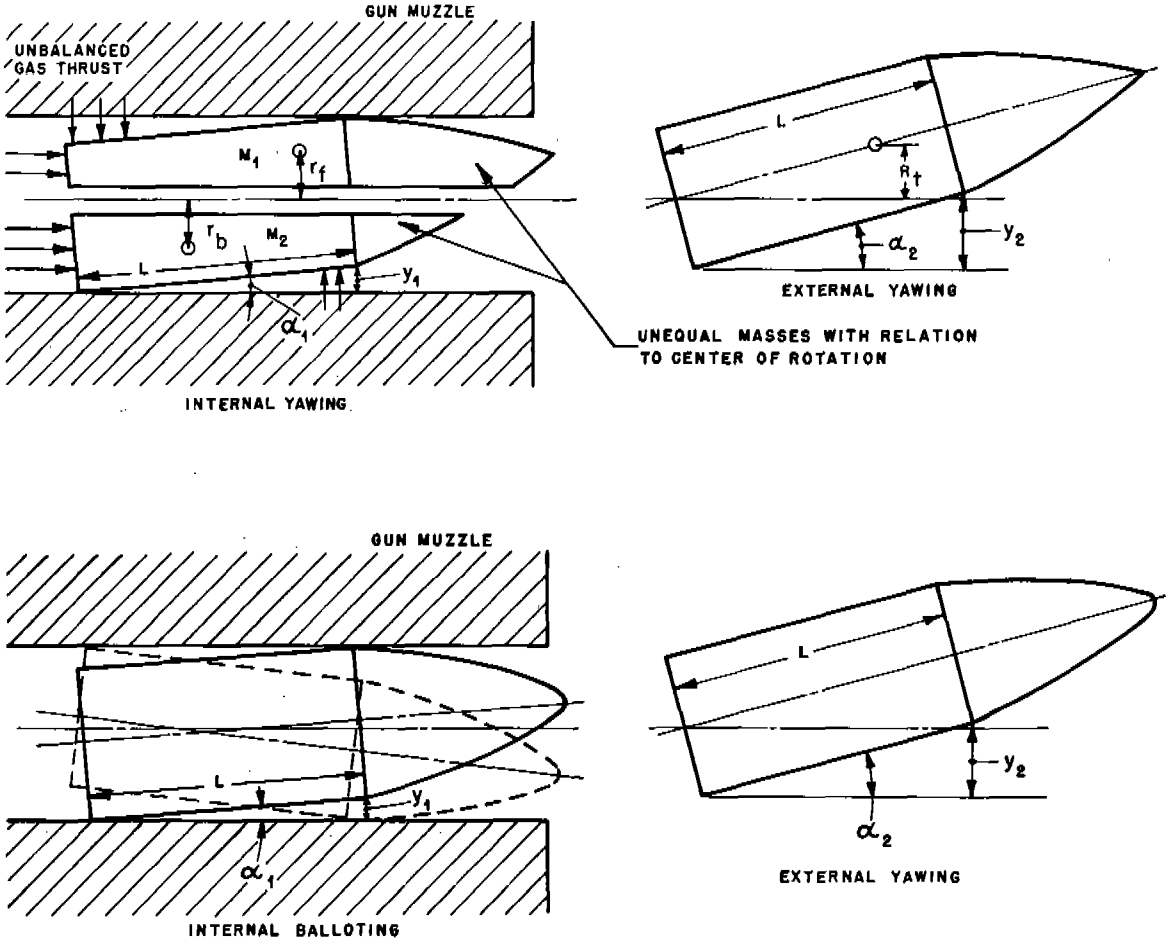


FIGURE 7. Relation of internal action to yawing of projectile in flight.

EFFECT OF PE BULLET DESIGN ON ITS INTERIOR BALLISTICS ARRANGED ACCORDING TO LEAST YAW ANGLE (EXTERNAL)(ALL FIRINGS RESOLVED TO 3.2 MACH NUMBER).50 CAL TESTS

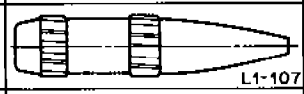
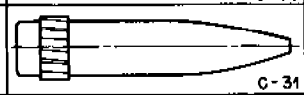
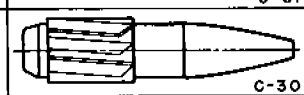
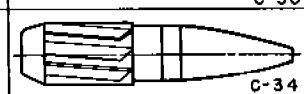
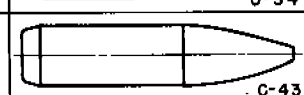
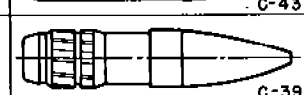
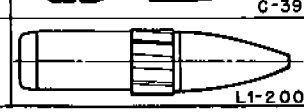
NO.	DESIGN	TYPE	α_2 ACTUAL AVERAGE EXTERNAL YAW ANGLE IN DEGREES	L ACTUAL BEARING LENGTH IN INCHES	y TOTAL BORE CLEARANCE OFFSET IN INCHES	SINE OF INTERNAL YAW ANGLE	α_1 CALCULATED INTERNAL YAW ANGLE IN DEGREES	$\frac{\alpha_2}{\alpha_1}$ JUMP RATIO	TYPE OF LAUNCHING ACTION
1	 L1-107	TWO-BANDED PE	1.45	1.150	.002	.00170	.0980	14.8	NORMAL PE
2	 C-33	NARROW REAR BAND BOAT-TAILED PE	1.76	1.113	.003	.00270	.1548	11.5	NORMAL PE
3	 C-31	NARROW REAR BAND FLAT BASE PE	1.98	1.173	.003	.00256	.1456	13.6	NORMAL PE
4	 C-30	WIDE REAR BAND BOAT-TAILED SOLID STEEL PE	2.01	1.173	.003	.00256	.1456	13.8	NORMAL PE
5	 C-34	WIDE REAR BAND BOAT-TAILED ALUMINUM HEAD PE	2.15	1.173	.003	.00256	.1456	14.7	NORMAL PE
6	 C-43	BANDLESS BOAT-TAILED SMOOTH	2.22	1.235	.004	.00324	.1850	12.0	SMOOTHEST POSSIBLE ACTION
7	 C-39	ARTILLERY TYPE PE	3.15	1.177	.003	.00256	.1456	21.6	SMALL LAUNCHING FRICTION AND GAS THRUST DISTURBS FLIGHT
8	 L1-200	NARROW FORWARD BAND BOAT-TAILED PE	4.59	1.210	.003	.00248	.1421	32.3	GAS THRUST DISTURBS FLIGHT (OBTURATE)

FIGURE 8. Relation of interior to exterior yaw.

launching, there is about a thirteen-fold increase in yaw angle for most pre-engraved projectiles, as compared with a twenty-fold increase for artillery type, and a thirty-fold increase for one with a narrow forward band.

Gas Thrust. The behavior of the forward-banded type of projectiles represented by design No. 8, Figure 8, indicated that an unbalanced radial thrust from the pressure of the powder gas takes place in the gun bore, pushing the base or even the whole projectile against the rifling on one side. Because of the large pressure area on the base of this type projectile, there must be an excessive gas kick at the instant the bullet leaves the muzzle. A certain amount of rear guiding and obturation probably would reduce the muzzle jump and exterior yaw, and at the same time give excellent flight characteristics to the bullet, similar to those exhibited by design No. 1.

Launching Conditions. Results of firing the artillery-type projectile (design No. 7, Figure 8) indicate that this type has a greater average exterior yaw than the pre-engraved type. An explanation of this is hard to make. While the form factors and drag are similar, the conditions at time of launching may be such that there is excessive disturbance at the muzzle due to the large gas pressure drop around the projectile causing high velocity gas jets that develop unbalanced forces when they hit any bullet irregularity. Design No. 7 has a cannelure in the band and a slight change in contour near the bourrelet, both of which are not present in design No. 3. In design No. 1 with the two bands there is a sealing effect around the body of the projectile caused by the presence of an expansion chamber, as it were, between the front and rear bands. This cuts down the jet effect because of the lower pressure-drop and reduces the muzzle disturbance, since there are no irregularities forward of the gas jets. Irregular friction forces at launching of design No. 7 may also account for some of the additional yaw.

27.3.3

Exterior Ballistics of Pre-Engraved Projectiles

The exterior ballistics of pre-engraved projectiles were carefully investigated to make certain that no feature of their design would be detrimental to their flight. Careful checks were made of each design variable by changing only one feature at a time. Extreme care was used during the firing tests to duplicate firing conditions, spark photographs, and analysis of performance. The consistency of the results shows that they are dependable to within about 1 per cent.

The following design variables were checked with groups of similar projectiles and the observed data were evaluated.

Number of Rotating Bands. (Group 1, Figure 9.) From a comparison of the three projectile types in this group it has been possible to evaluate the effect of adding each band or circular obstruction to a high-velocity projectile. Comparison of the drag of the single-banded projectile with the smooth one shows an increase of 4 per cent, while the addition of another band, even though its sharp, front edge is at the point of tangency of the ogive, adds only 1.7 per cent additional drag. Spark photographs of this projectile (L1-107) in flight confirmed this result. The extent to which the drag of the rear band is greater than that of the front band indicates that the region between the base of the ogive and a point back of the center of gravity is not so sensitive to drag as is the base or boat-tail region, particularly on a projectile of this type with a short ogive radius.

Position of Bands. (Group 2, Figure 9.) The conclusions reached from a study of group 1 with regard to the relative effect of changes made on the base portion of the projectile and on the portion just back of the ogive, were confirmed by results from group 2 although they were not so pronounced. This probably can be accounted for by the absence of the low-pressure region in either type, with a general lessening of disturbances to the boundary layer. In this connection, group 7 of Figure 9 should be noted because of its comparison of a boat-tailed and a flat-base projectile. There the effect of changes is more pronounced, both because of the increased moment of the disturbance and because of the re-entrant stream lines being more effective in producing disturbances.

Width of Bands. (Group 3, Figure 9.) In this series, the rear edge of all the driving bands was kept in the same position with reference to the boat-tail and the band was widened by adding to the front portion. Again there is indicated a tendency for the front edge of the driving band to have less effect on the drag as it is placed closer to the ogive. But what is perhaps more important with reference to pre-engraved projectiles is a complete absence of any indication that the deep engraving (0.010 in. is twice the standard depth of 0.005 in.) on a wide band has any noticeable effect on the drag. It indicates that there is plenty of opportunity to increase the depth of the engraving to give very low unit pressure on the sides of the rifling in a gun without appreciably affecting the drag, as advocated in Section 26.6.2. This will allow greatly increased muzzle velocities with increased accuracy-life of the gun.

Leading Edge of Bands. (Group 4, Figure 9.) In order to find the effect of pointing the leading edge of the splines on pre-engraved projectiles, which is one way of indexing them for automatic firing (Section 28.4), a comparison test was made of the drag with the front edges of the bands square, conical, and pointed circumferentially. As was expected, the square edge at the ogive used on the L1-107 type gave the highest resistance, but when the splines were pointed and the front edge set slightly back of the ogive, the drag became exactly the same as that of a narrow band whose front edge was even further back and cut conical. It is desirable to have the front edge of the driving bands on pre-engraved projectiles square in order to center them when entering the bore. The fact that pointing of the lands cuts down the drag as much as 3 per cent indicates that the proposed design of pre-engraved projectiles should have excellent flight characteristics.

Radius of Ogive. (Group 5, Figure 9.) The effect of lengthening the radius of ogive is clearly demonstrated in group 5. The projectile with a 19-caliber radius of ogive shows a drag coefficient less than half that for the one with a 5-caliber radius. However, both these designs show a dangerously low stability factor, while the bullet with an intermediate radius shows good stability although a higher drag than the one with the long radius of ogive. This indicates the importance of balancing all the factors so that a high-velocity projectile will give low drag but, at the same time, be dependable in flight. This bullet had a low yaw angle and was otherwise quite dependable, even with a flat base which might have been boat-tailed to reduce further the drag.

While it is desirable to have a long nose radius, it is important that the length of guide of the body of the projectile shall not be shortened so much as to handi-

cap the launching. This might also throw the center of gravity too far back from the nose of the projectile, resulting in poor stability.

Location of Center of Gravity. (Group 6, Figure 9.) The effect of changing the location of the center of gravity of a projectile is shown by the three examples in group 6. In one the center of gravity is located well forward in the smooth projectile, C-43; at an intermediate point in a wide-banded projectile, C-30; and well back in the third one, C-34. The stability factor is high with the first type and very low for the last, but the form factors are reversed accordingly.

Types C-30 and C-34, with the same drag factor 0.132 and same contour, show the effect on the form factor of moving the center of gravity toward the rear a distance of 0.212 in. This was accomplished by making the nose of the C-34 projectile of aluminum. Their general performance was much the same but the second was less reliable in flight.

Boat-Tailing. (Group 7, Figure 9.) A good indication of the effect of boat-tailing a flat-based bullet is shown in group 7 by comparison of two otherwise identical projectiles: C-33 (boat-tailed) and C-31 (flat-based). Here the change from a flat base to a boat-tail reduced the drag by more than 2 per cent. At the same time the yaw in flight was also reduced by this streamlining, indicating a tendency of the boat-tail to stabilize the flight.

Figure 10, which illustrates the effect of various design factors on the reduction of drag, relates this tendency to the thickness of the boundary layer within the streamlines surrounding the projectile and leading to vortices set up at the corner of the flat base. It indicates that, for high velocities and long radii of ogive, a boat-tailed base is very important as is any change that will make the rear portion as smooth as possible. Here, as in air-foil design, any tear-drop section such as the Joukowsky profile is an excellent one for obtaining low drag.

Degree of Smoothness or Reynold's Number. (Group 8, Figure 9.) The three projectiles in this group, all having nearly the same form factor and physical dimensions, demonstrate the reduction in drag that can be obtained by removing roughness of any kind that tends to interfere with the laminar flow of the streamlines around the projectile, as visualized in Figure 10. The removal of one of the two bands from projectile L1-107 gives the single-banded type C-39, with a 3 per cent lower drag. Removal of the single band to give a perfectly smooth projectile, C-43, reduces the drag 2½ per cent more.

The photographs of these three projectiles in flight showed that the one with two bands, L1-107, had a heavy shock wave coming from the front and rear edges of each band, in addition to the head wave. The second, C-39, had the front band removed; the heavy wave from the front edge of the first band disappeared but a light wave still persisted from a shoulder 0.002 in. high radially near a point at which the rear of the front band was located in L1-107. The waves at the rear band were about the same as before but, due to a chamfer on the front edge, the shock wave was flattened out smoothly.

Lastly, the smooth projectile C-43 showed no heavy shock wave except that at the head. This should, therefore, be the source of most of the drag.

As far as an actual change in the surface smoothness or Reynold's number is concerned, it is difficult to obtain much of an improvement in drag simply by polishing a bullet, although tool marks and surface irregularities must be avoided as much as possible.

The "paddle-wheel" action of the deeper driving splines used on pre-engraved projectiles gives no indication, in the spark photographs, of causing any appreciable drag, because their action probably takes place in a region of turbulence and recirculation created by the front edge of the band. Consequently, the effects of fringing at the rear edge of a self-engraving band should not increase the drag greatly unless it is near the boat-tail. Irregular fringing, however, will tend to cause rotary unbalance of the bullet in flight, with resulting large dispersion.

Conclusion. The splines on pre-engraved, high-velocity projectiles are no more detrimental to the flight of a projectile than on any standard banded type. Furthermore, their location can be placed well forward of the base of the projectile to give a decided ballistic advantage and prolong the engagement life of a gun.

It is interesting to note that reducing all the roughnesses and obstructions on L1-107 (group No. 8) reduced the drag factor from 0.136 to 0.129, whereas changing the radius of ogive from 5 calibers to 19 calibers (group No. 5) reduced the drag coefficient from 0.132 to 0.065. This fact indicates that rotating bands and pre-engraving of projectiles affect the drag very little in comparison with the shape of the ogive.

27.3.4 Manufacturing Techniques

The pre-engraved caliber .50 projectiles used by Division 1 have been made by forcing soft steel

[redacted]

EFFECT OF PE BULLET DESIGN ON ITS EXTERIOR BALLISTICS GROUPED ACCORDING TO DESIGN PARAMETERS (ALL FIRINGS RESOLVED TO 3.2 MACH NO.).50 CAL TESTS

GROUP NO.	TEST PURPOSE	TYPE	DRAG FACTOR K_{D_0}	FORM FACTOR K_M	A BASE TO BAND IN INCHES	B BAND WIDTH IN INCHES	C RAD OF OGIVE IN INCHES	D BASE TO ℄ BEARING IN INCHES	E BASE TO CG(ACT) IN INCHES	L LENGTH OF GUIDE IN INCHES	S STABILITY FACTOR	RELATIVE STABILITY	ACTUAL YAW ANGLE IN DEGREES	DRAG EFFECT
1	NUMBER OF BANDS													
	C-43	NO BANDS	.129	1.22	—	—	2.500	.631	1.018	1.235	1.765	FAIR	2.20	LOW
	E, D, CENTER OF GRAVITY, C, L, CENTER LINE OF BEARING, A, B — C-33	SINGLE BAND	.134	1.18	.200	.250	2.500	.756	1.00	1.113	1.550	GOOD	1.78	1ST BAND (+4%)
	L1-107	TWO BANDS	.136	1.20	.200	.250	2.500	.775	.977	1.150	1.362	GOOD	1.45	2ND BAND (+1.7% MORE)
2	POSITION OF BANDS													
	C-33	NARROW REAR BAND	.134	1.18	.200	.250	2.500	.756	1.00	1.113	1.550	GOOD	1.78	LITTLE CHANGE
	L1-200	NARROW FRONT BAND	.133	1.20	.972	.375	2.600	.742	1.013	1.210	2.225	POOR BECAUSE OF LAUGHING	4.59	LITTLE CHANGE
3	WIDTH OF BANDS													
	C-33	NARROW BAND	.134	1.18	.200	.250	2.500	.756	1.00	1.113	1.550	GOOD	1.78	HIGH
	C-39	MEDIUM BAND ARTILLERY TYPE	.132	1.20	.200	.500	2.500	.788	.994	1.117	1.463	POOR	3.15	HIGH
	C-30	WIDE BAND	.132	1.20	.200	.750	2.500	.786	.992	1.173	1.520	FAIR	2.01	HIGH
4	LEADING EDGE OF BANDS													
	L1-107	SQUARE	.136	1.20	.200	.250	2.500	.775	.977	1.150	1.362	GOOD	1.45	HIGH DRAG
	C-39	TAPERED OR CONICAL	.132	1.20	.200	.500	2.500	.788	.994	1.177	1.463	POOR	3.15	GOOD DRAG
	C-30	POINTED	.132	1.20	.200	.750	2.500	.786	.992	1.173	1.520	FAIR	2.01	GOOD DRAG

FIGURE 9. Effects of design on exterior ballistics of pre-engraved, caliber .50 bullets grouped according to design parameters.

[redacted]

EFFECT OF PE BULLET DESIGN ON ITS EXTERIOR BALLISTICS
GROUPED ACCORDING TO DESIGN PARAMETERS
(ALL FIRINGS RESOLVED TO 3.2 MACH NO.) .50 CAL TESTS

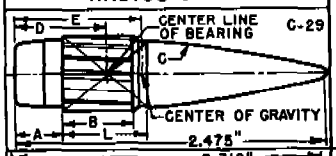
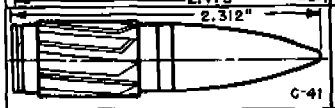
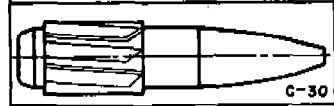
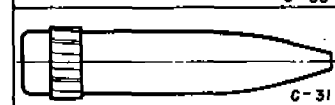
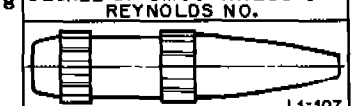
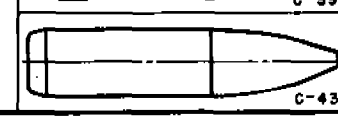
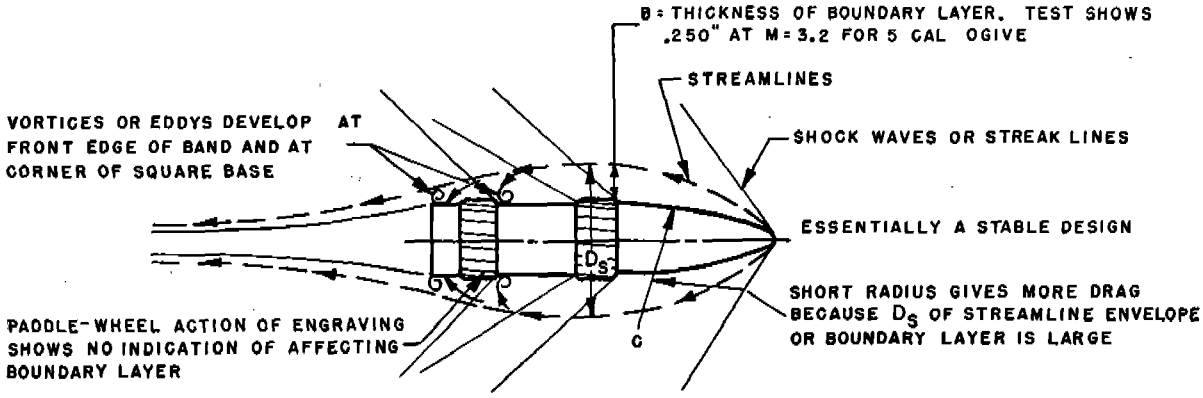
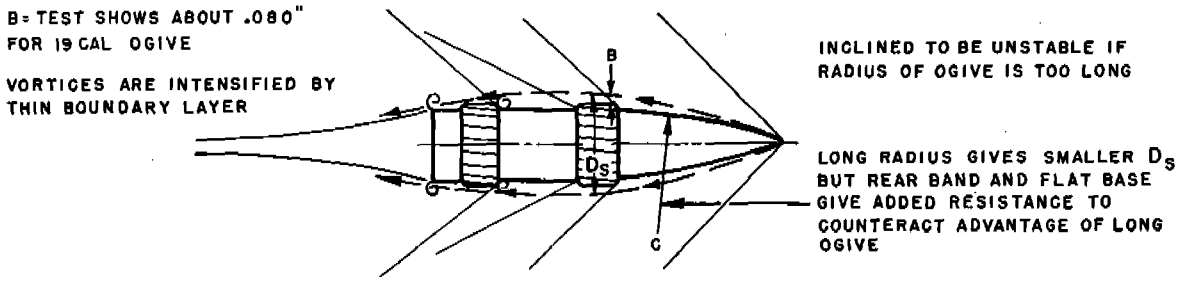
GROUP NO.	TEST PURPOSE	TYPE	DRAG FACTOR K_{D_0}	FORM FACTOR K_M	A BASE TO BAND IN INCHES	B BAND WIDTH IN INCHES	C RAD OF OGIVE IN INCHES	D BASE TO ℄ BEARING IN INCHES	E BASE TO CG (ACT) IN INCHES	L LENGTH OF GUIDE IN INCHES	S STABILITY FACTOR	RELATIVE STABILITY	ACTUAL YAW ANGLE IN DEGREES	DRAG EFFECT
5	RADIUS OF OGIVE													
		LONG RADIUS OGIVE 19 CAL	.065	1.00	3.68	.587	9.25	.645	.905	.800	1.565	FAIR	1.20	LOW
		MEDIUM RADIUS OGIVE 9 CAL	.098	1.036	.200	.750	4.33	.475	.883	.950	2.290	GOOD	0.97	MEDIUM
		SHORT RADIUS OGIVE 5 CAL	.132	1.20	.200	.750	2.500	.786	.992	1.173	1.520	FAIR	2.01	HIGH
6	LOCATION OF CENTER OF GRAVITY													
		CG FORWARD	.129	1.22	—	—	2.500	.631	1.018	1.235	1.765	FAIR	2.22	GOOD
		CG INTER-MEDIATE	.132	1.20	.200	.750	2.500	.786	.992	1.173	1.520	FAIR	2.01	FAIR
		CG BACK	.132	1.70	.200	.750	2.500	.756	.780	1.235	1.180	FAIR	2.15	FAIR
7	BOAT-TAILING													
		BOAT-TAILED	.134	1.18	.200	.250	2.500	.756	1.00	1.113	1.550	GOOD	1.78	HIGH
		FLAT BASE	.137	1.15	.200	.250	2.500	.786	1.02	1.173	2.02	FAIR	1.98	HIGH
8	DEGREE OF SMOOTHNESS OR REYNOLDS NO.													
		TWO BANDS	.136	1.20	.200	.250	2.500	.775	.977	1.150	1.362	GOOD	1.45	HIGH
		MEDIUM BAND AT	.132	1.20	.200	.500	2.500	.786	.944	1.117	1.463	POOR	3.15	HIGH
		SMOOTH	.129	1.22	—	—	2.500	.631	1.018	1.235	1.550	FAIR	2.20	LOW

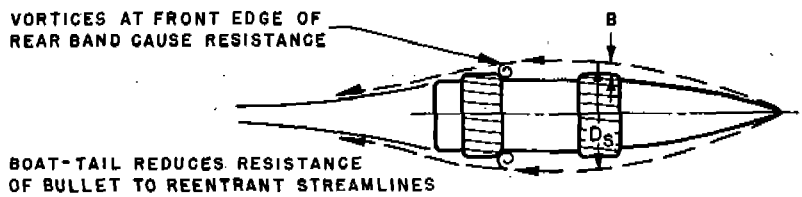
FIGURE 9. *(Continued)*



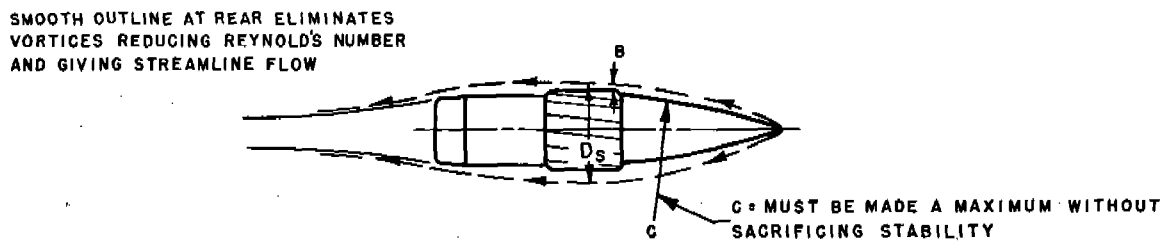
FLAT-BASED TWO-BANDED SHORT RADIUS OF OGIVE



FLAT-BASED TWO-BANDED LONG RADIUS OF OGIVE



BOAT-TAILED TWO-BANDED LONG RADIUS OF OGIVE



BOAT-TAILED AND WITHOUT REAR BAND

FIGURE 10. Design factors in the reduction of drag for pre-engraved bullets at hypervelocity.

blanks through a stepped series of dies, used either individually in a punch press or in series in a special, long-stroke broaching machine. These dies make a series of grooves in the band which are accurately concentric with the bourrelet and rear guide, have the same twist as the rifling, and are of the correct size to fill all the grooves completely. To obtain this accuracy, it is necessary to use guides that center the band on the projectile blank when it enters each cutting die.

After engraving, all the teeth are pointed simultaneously on the front end in one operation using a special machine that has been developed for generating by a helix the proper cylindrical surface, accurately centered and matched to the engraving within 0.001 in. There is no doubt that this can be done commercially on a large scale. By Parco-Lubrizing[k] these steel projectiles, rusting is avoided and a low friction means is provided for sliding through the gun.

By using a special adapter, a portion of the pointing machine is also used in pointing the rifling in the gun. This requires changing to another type of cutter and, by using the same machine, the same angle of pointing is generated so that there is plane contact with the points on the projectile. The ratchet grooves in the breech of the barrel are cut in a jig to position the rifling accurately in relation to the firing mechanism. The relative cost of these changes on the gun barrel are slight, but are proportionately greater on the projectiles.

The manufacturing techniques for the 37-mm gun, T47 and projectiles (see Section 31.7) were essentially the same as those for the caliber .50, except that everything was done on a larger scale. Larger dies were required and consequently a heavier press had to be used. A bigger machine was necessary for the greater amount of metal removed from the teeth in the pointing operation, although the amount of cut could be adjusted. The essential differences consisted in more machining being required on the base of the cases and in necessary alterations to the firing mechanism. The latter changes are described in Section 28.4.4.

27.4 LOW-STRESS ROTATING BANDS

If pre-engraved projectiles are not to be used, it is very desirable to design rotating bands giving low stresses. Accordingly, studies for this purpose were made at The Franklin Institute, the Leeds and Northrup Company, and the Catholic University of America.

27.4.1 Caliber .50 Projectiles

FIRING TESTS

Banded caliber .50 bullets of the seven classes listed below were tested to determine the effect of rotating-band design on the force required for engraving.

1. Regular artillery-type (see Figure 3 of Chapter 11).

2. Artillery-type with obturating ring of 0.530 in. diameter, and with band diameters varying from 0.493 to 0.510 in.

3. Artillery-type with radial holes, 0.055 in. in diameter drilled in rotating band.

4. Artillery-type having all-steel rotating band with six circumferential grooves 0.0155 in. in depth. (Figure 11).

5. Types 3 and 4 with holes or grooves filled with solder.

6. Several of foregoing types with cadmium plate 0.003 in. thick on the band.

7. Pre-engraved, double-banded steel (see Figure 3 of Chapter 11.)

The erosion-testing gun, described in Section 11.2.1, was used in these tests.[122] The barrel was of monobloc gun steel construction with grooves 0.010 in. in depth. Precautions were taken to eliminate as far as possible all variables that would affect the maximum powder pressure, except the band design itself; the average maximum pressure attained on firing 6 rounds was then taken as a measure of the engraving force.

Reduction of the band diameter (class 2) gave a consistent decrease in powder pressure; the smallest band noted, of diameter 0.493 in., gave a pressure of 41,590 psi as compared with 53,950 psi given by a 0.510-in. band; this represents a pressure decrease of 23 per cent.

Little improvement, only about 5 per cent in the case of 81 holes, resulted from drilling holes in the band (class 3). However, when these were filled with solder (class 5), the reduction in pressure was of the order of 9 per cent for bands with either 54 or 81 holes.

The grooved steel projectile, either plain (class 4), or with cadmium plating (class 6), or filled with solder and cadmium-plated (class 6), diminished the powder pressure by approximately 7 per cent.

[k] Parco-Lubrizing is a trade-marked process (Parker Rust Proof Company, Detroit, Michigan) for applying to steel a wear-resistant coating that consists chiefly of an admixture of iron and manganese phosphates.

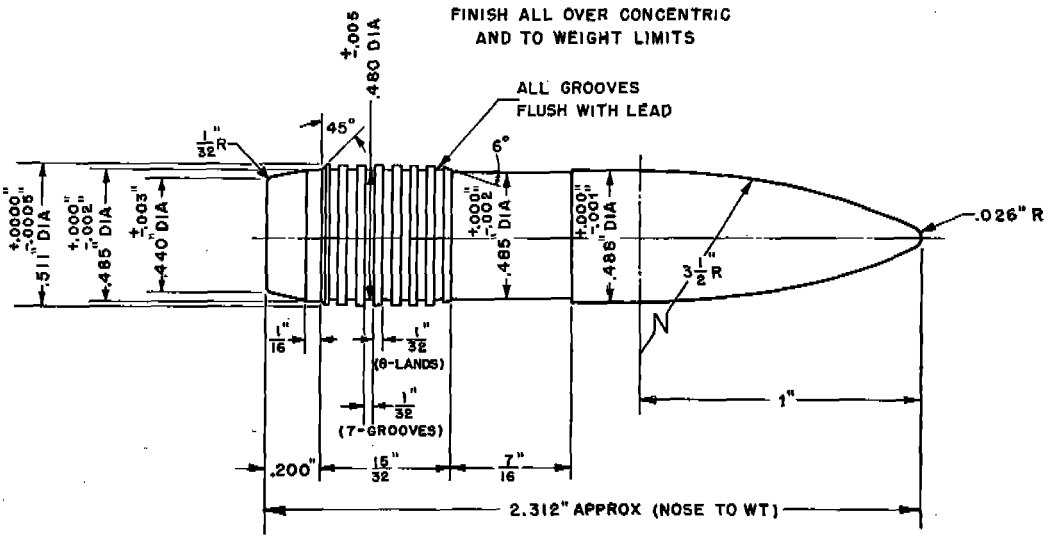


FIGURE 11. Drawing of artillery-type, caliber .50 bullet having an all-steel rotating band with six circumferential grooves.

The completely pre-engraved bullet (class 7) gave by far the best results, with pressures reduced by a third (see section 27.3).

STATIC TESTS

In addition to the firing tests, static tests were conducted to determine the force required to engrave several of the projectiles listed above. It was found that little reduction was brought about by the use of plain bands with drilled holes, but when the holes were solder-filled the force required was diminished by 70 per cent. Cadmium plating diminished the static load by 25 per cent.

EROSION TEST OF PROJECTILES WITH GROOVED STEEL BANDS

Particular interest was attached to the grooved steel-banded projectile (class 4) because it could be converted readily from standard-type bullets already in production. From the point of view of lowered radial stresses only, these projectiles should have been better without the solder filling. However the rather narrow circumferential fins would have been subjected to large bending moments. The lead-tin alloy which filled the grooves served to reinforce the fins and also to form a lubricant "in situ." The entire bullet was then cadmium-plated to reduce friction. Static tests had indicated a 50 per cent reduction of engraving force from that required for the standard artillery type.

This design, shown in Figure 11, seemed very promising, and a number of these projectiles were fired in an erosion test. It was found that land and groove erosion at the origin of rifling, and also muzzle-velocity drop, were no greater than those observed with a copper-banded bullet. Land erosion from 10 in. beyond the origin of rifling was, however, greater. Recovered bullets, shown in Figure 12, illustrate normal engraving and failure to engrave caused by wear in the gun.

27.4.2 Larger Projectiles[114]

While the stresses can be lowered by making either the width or the diameter of the band smaller, the functions of the band set lower limits on these quantities, particularly in the case of a worn gun. In order to impart spin to the projectile, a minimum area of band metal must be in contact with the driving face of the lands; and similarly, satisfactory obturation demands sufficient metal to fill the grooves.

37-MM PROJECTILES

Effect of Cannelures. A natural approach to the problem of reducing stresses is to consider the effects of grooves, or cannelures, in the band. The Service design for the 37-mm shot, M51, has a cannelure approximately 0.1 in. wide and 0.022 in. deep. This depth is great enough so that the lands of the gun should not touch the bottom of the cannelure. After engraving, however, enough metal is found to have

been pushed into the cannelure to fill it to the level of the rest of the engraved portion. This metal increases the radial and axial loads without helping support the side thrust necessary to cause rotation. The addition of a number of similar cannelures would in effect only shorten the band; the limits would still apply; and the overall result would be to add metal without increasing the effectiveness of the band.

If instead the band groove is deepened, the result of plastic flow will be to force metal into the bottom of the cannelure, out of contact with the gun lands, thus decreasing the radial load and friction. Addition of other cannelures of this type will further reduce stresses.

It has been shown[54,114,372] that the extruded fringes of band metal increase radial load without contributing to the lateral bearing surface between the face of the gun lands and the projectile grooves. The projectile body has a groove adjoining the rear of the rotating band which, however, is not large enough to prevent the formation of fringes. To correct this the body groove was enlarged.

Experimental Tests. The theory was then subjected to experimental check by the method described in Section 7.3. The original cannelure of depth 0.022 in. was first replaced by one of 0.040 in. with marked improvement. There was evidence that even deeper cannelures were desirable, and the final tests were performed on bands with a cannelure depth of 0.065 in. The groove in the body back of the band was of such a depth (approximately 0.03 in.) that the bottom of it was level with the bottoms of the cannelures. With a single such cannelure and the body groove, both radial and axial loads are reduced to about 70 per cent. Addition of a second deep cannelure cut the loads to about half their normal value for a band of this size. Since the effective length of the band has been diminished, the second cannelure need not be deep to cause a further reduction in stress. The resistance to side thrust would in the latter case be reduced by approximately 20 per cent. These reductions have been confirmed in firing tests at Aberdeen Proving Ground.

In the estimates made for radial loads in the various designs of bands, the theory of Effective Area of Interference [EAI] developed in Chapter 7 was used. The method was readily applicable in the earlier tests. With deeper cannelures, however, it was necessary to introduce negative terms for the portions of the cannelures and body grooves having smaller diameter than the gun lands. The calculated negative contributions turned out to be about twice too large; this indicates that the space provided to accomodate the extruded metal is only half used.

Cadmium Plating. Further experiments were conducted to study the effect of cadmium plating of the band. The plate applied was 0.002 in. thick. The radial load was not affected, but the axial load was reduced by a factor 2 or 3. The overall effect of the new design, with cadmium plating, was to produce a band which has a radial load about half and an axial load about one-fifth to one-sixth of the loads for a normal band of the same dimensions.

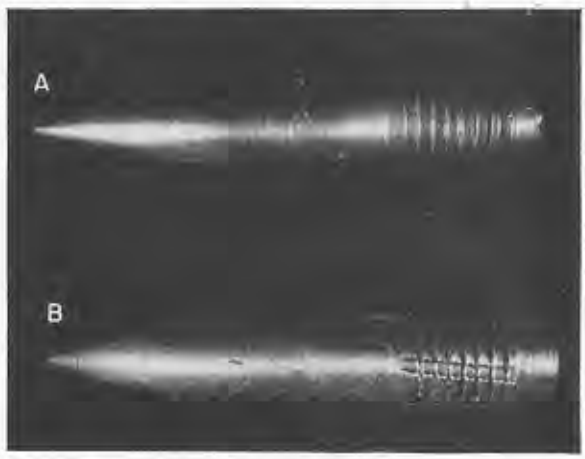


FIGURE 12. Normal engraving and failure to engrave; shown by collected artillery-type caliber .50 bullets with all steel rotating bands. (A) Round #156: Bullets skidded along bore; band diameter reduced to 0.492 in. (B) Round #83: Normal band engraving.

75-MM PROJECTILES

A 75-mm AP projectile, M72, with the rotating band modified by a cannelure 0.098 in. wide and 0.070 in. deep was tested for radial load. This gave 20,600 lb/in. circumference in a tube section of wall ratio 1.75 with French-type rifling, in which the corners of the lands are rounded. If the band had been of equivalent length, without a cannelure, a radial load of about 40,000 lb/in. circumference would have been expected; for an unmodified Service-design band, the load would have been about 53,000 lb/in. circumference.

A comparison of band stresses during firing was made for a 75-mm, AA gun T22 at Aberdeen Proving Ground. This gun has rectangular rifling, as contrasted with the French-type rifling used in the gun mentioned in the previous paragraph. HE shells were used. The Service-type band has an overall length of

CONFIDENTIAL

0.86 in., the forward 0.14 of which tapers at 8°30′. The modified band has a cannelure of width 0.1 in. and depth 0.05 in. near the center of the flat section. As determined by a gauge about 25 in. toward the muzzle from the origin of rifling, the radial load averaged 43,200 lb/in. circumference for the standard bands, and 34,700 lb/in. circumference for those with a cannelure. The corresponding values of P/EAI are 40.5 and 40.4. The agreement is remarkable.

It would appear desirable to carry out firing tests that have been suggested[117] to gain further information about the effects of deep cannelures of rectangular cross section. In particular, it should be determined whether erosion is decreased and whether bands that have been so modified seal satisfactorily in eroded tubes.

British Investigations[1]

The British have carried out experimental and theoretical studies on the subject of the proper design of the rotating band itself.[362,372,388,556] One of their ideas is to separate the two functions of the band, i.e., that of causing rotation of the projectile and that of acting as a seal to prevent the escape of the propellant gases past the shell. Since these are two very different functions, it is not at all unlikely that a design which separates the two might lead to a band which would cause a much smaller band pressure. One very interesting experiment was carried out with a double band on a 17-pounder shell; the front band was turned down so that there was no excess copper and the rear band was modified so that a seal would be ensured. The strain gauge readings on the gun when the shell was fired indicated that the band pressure was negligible. In addition, the stresses in an experimental band design have been calculated using relaxation methods.[359]

27.5 METHODS FOR DETECTING DEFECTS IN SHELLS

Emphasis on accurate determination of the stresses in a shell mantle is important to allow the designer to provide sufficient metal in the walls to prevent yielding. But it is also necessary that the metal used be homogeneous and free of slag inclusions, pipes, cracks, or other defects that may cause failure in service by the hot gases seeping through the base or the walls of the shell and igniting the explosive within. For this purpose, two methods have been developed for testing the finished shells to detect defective openings.

27.5.1 First Testing Method

Ammoniated water is used as a testing medium. The liquid is forced against the base of a shell forging under a pressure somewhat greater than maximum gas pressure that will be encountered in a gun. An indicator, such as moist litmus paper, is placed inside the shell cavity. Defective openings in the base of the shell are revealed by a change in color of the indicator caused by fumes from the ammoniated water.

The apparatus used in this first method employs a special pressure plate for a hydraulic press. In this plate the base of the shell fits tightly around the rim, sealing a cavity beneath, which connects to a high-pressure tank and compressor. Inside the shell is a steel form against which the ram of this quick-acting hydraulic press applies the necessary load for sealing the base. The valve from the compression chamber is then opened for a brief time, after which it is closed and the ram lifted. If there is a defect in the shell base that would allow the slightest amount of gas to get through, the indicator changes color.

This method is very fast and suitable for production line testing. However, there are certain disadvantages, one of which is the presence of ammonia fumes in the air surrounding the equipment that may affect the operators and the surrounding equipment. However, this disadvantage can be offset, to a large extent, by the use of a greased-paper seal at the top of the forging, and by the use of ventilating fans in the room. Another objection is the fact that this equipment is more expensive than the second method described below, although its cost is not high when it is considered that one set of equipment would take care of several production lines that were located in the same or nearby buildings.

27.5.2 Second Testing Method

Another method is a self-contained apparatus for use under a hydraulic press. It consists of a stationary piston in a movable cylinder supported on springs, sufficiently powerful to hold a seal on the base of the shell before compression of the liquid begins. The apparatus is contained in a guide cylinder on which an indicator is mounted for measuring the relative travel of the moving cylinder carrying the shell. The

[1] This paragraph is quoted from p. 20 of AMP Report No. 75.1.[147] [See footnote (c).]

space above the top of the piston and surrounded by the movable cylinder is completely filled with liquid, such as water or Varsol (a high-grade kerosene).

This method is slower and less sensitive than the first method and, therefore, is not capable of such fast production. It is well suited for use in a shop where chemical fumes are not desirable.

Several sets of tests were conducted on 75-mm and 3-in. shells, with Varsol used as the liquid. The results indicated that a shell will be satisfactory and without defects through the base up to about 2.35-mm deflection of the indicator. From 2.35 to 3.00-mm deflection the shells are doubtful and above that value they must be rejected.

Chapter 28

AUTOMATIC GUN MECHANISM

By *William H. Shallenberger*[a]

28.1 INTRODUCTION

IN ADDITION to making hypervelocity guns practical by the control of erosion, considerable work is required to make them practical from a mechanical standpoint. That is, a mechanism designed for medium-velocity weapons may not be entirely suited to hypervelocity guns.

One project undertaken by Division 1, NDRC, was the development of a 20-mm automatic aircraft cannon. Although this gun was designed to use standard ammunition rather than special hypervelocity ammunition, it had certain characteristics that made it particularly suited for use with pre-engraved projectiles (Chapter 31) and hypervelocity ammunition in general. Therefore, discussion of that particular gun makes up a major portion of this chapter (Section 28.2). It describes in a general way the difficulties encountered in operation and means whereby the difficulties were overcome, and presents certain conclusions and recommendations for the use of future designers of such weapons. Section 28.3 treats of some of the problems involved in designing an automatic gun mechanism for use with hypervelocity ammunition. Loading and indexing mechanisms for pre-engraved projectiles are discussed in Section 28.4.

The information for this chapter is taken largely from published NDRC reports, which cover the work in more detail than can be given here. Some of the ideas presented herein, however, have not been published elsewhere, to the author's knowledge.

28.2 JOHNSON 20-mm GUN[b]

28.2.1 Introduction

In the summer of 1942, the Navy desired to increase the firepower of aircraft by replacing the caliber .50 Browning machine gun with the 20-mm AN-M2 (Hispano-Suiza) automatic cannon. The Navy Department requested Division 1, NDRC, to develop an integral belt-feed for this gun, but a preliminary examination of the problem indicated that it would be preferable to develop an entirely new gun than to try to make the necessary modifications in an existing gun. To this end, Division 1, NDRC, undertook Project NO-124 to design and build a firing model of a 20-mm automatic aircraft cannon having an integral belt-feed. Under this project[c] three models were designed.

The first model, known as Model I, was designed and built to test the basic mechanism and did not incorporate all of the requirements of the Navy specifications (Section 28.2.2). The second model was designed to overcome certain structural defects encountered in Model I, but, before it was built, it was decided to proceed with a design that would satisfy the Navy requirements. Therefore Model III was designed, built, and tested. Basically, both firing models were similar in that they were gas-operated, with blowback assist, but they differed considerably in the details of operation. Model III represented considerable improvement in design over Model I, in that it more nearly satisfied the Navy requirements and eliminated certain features of Model I that gave trouble in operation. These two models fired a total of approximately 6,000 rounds of Oerlikon and Hispano-Suiza 20-mm ammunition and also some special high-velocity caliber .50 ammunition.

28.2.2 Navy Specifications for 20-mm Automatic Aircraft Guns

Certain broad and general specifications were supplied by the Bureau of Ordnance, Navy Department, after the project had been undertaken. These specifications were supplemented by more detailed requirements to guide the design of the third model.[329] The most important of them are summarized herewith, by quotation in part from that specification.

1. Materials difficult to obtain or to fabricate should not be specified. The gun and all accessories should be

[a] Engineer, Engineering and Transition Office, NDRC. (Present address: Granada Hill, San Fernando, California.)

[b] This section has been condensed from an NDRC report[126] by the same author.

[c] The work was carried out principally by Johnson Automatics, Inc., under Contract OEMsr-746. The kinematic analyses described in Section 28.2.5 were performed by the University of California under Contract OEMsr-1375.

of a design suitable for mass production and interchangeability of parts.

2. The gun shall be fully automatic in operation, no outside power being required except for the firing solenoid and charger.

3. The gun shall be capable of firing standard 20-mm ammunition. It shall also be capable of satisfactory operation with ammunition whose overall length is as much as ¼ in. longer or shorter than standard, and with ammunition so belted that the position of the bases of the rounds varies by as much as 1/16 in.

4. With the gun mounted in an airplane wing, the barrel or barrel assembly shall be capable of being quickly and easily replaced without removing other parts of the gun.

5. The feed mechanism shall be an integral part of the gun and energy for actuation shall be derived from the gun. The feed shall be interchangeable from right to left hand by merely exchanging components. The feed opening or feed tray shall be stationary with respect to the mounting.

6. Cases shall be ejected downward, and links ejected at any angle between horizontal and downward, through openings to which chutes may be attached.

7. The maximum cross section of the gun with all accessories shall not exceed that of a rectangle 8 in. high and 10 in. wide. The overall length using the full length AN-M2 barrel shall not exceed 85 in. and the weight with all accessories shall not exceed 110 lb. (In conversation, Navy representatives indicated consideration would be given to modification of length and weight requirements if superior performance made such changes desirable.)

8. The gun shall be capable of firing at a rate of at least 700 rounds per minute under service conditions. It shall operate satisfactorily under accelerations of $5g$ in any direction or $7g$ vertically, whichever has the greater effect on operation. It shall be capable of feeding a belt of ammunition equivalent to at least 15 rounds suspended vertically when subjected to $7g$ in the vertical direction.

9. Except for barrel erosion, parts should be capable of withstanding 5,000 firing cycles without requiring replacement.

Even though the guns built on this project did not satisfy all the Navy's specifications, these models were useful as prototypes to test the mechanism. When they were constructed it was recognized that they were subject to certain revisions to bring them within the specifications.

28.2.3 Operation of Models I and III

For a better understanding of the sections to follow, a detailed discussion of the sequence of operation of the two firing models is given herewith.

Model I

The lower part of Figure 1 is a vertical cross section through the main operating portion of Model I. Also shown is a top view of the breech block, breech slide and breech slide lever, and the principal dimensions of the breech slide cam path. As the bullet proceeds down the barrel (A), it uncovers the gas port (B), admitting gas at high pressure into the gas cylinder (C). This gas forces the piston (D) rearward, which in turn drives the operating shaft (E) back against the driving spring (F). Attached to the rear end of the operating shaft is the locking platform (G). A forward extension on the locking platform holds the rear edge of the lock (H) downward against a locking abutment on the stationary locking key (I). The forward edge of the lock engages a cylindrical surface on the bottom of the breech block (J), locking it in the closed position, until the locking platform is moved rearward sufficiently to allow the lock to rotate upward out of engagement with the locking key. This upward rotation of the lock is produced by the chamber pressure pushing rearward and having the locking abutment of such an angle (30 degrees to the vertical) that disengagement tends to take place.

As the locking platform moves rearward, an extension on its top surface engages a lug on the bottom of the striker (K) and draws it back against the striker spring (L). Just as the lock is released from the locking key, the locking platform strikes a lug at the lower rear end of the breech block. This impact, aided by residual pressure in the chamber, drives the breech block rearward. As the lock comes out of engagement with the locking key, it moves upward against the forward end of the locking platform, thus holding the breech block, striker, lock, and locking platform in fixed relative positions. In this manner they all move rearward together, being decelerated somewhat by the driving spring, until the breech block strikes the buffer spring (not shown). When this occurs, the moving parts are rapidly brought to a stop, and the energy stored in the buffer and driving springs drives these parts forward again.

This forward motion continues until the forward end of the breech block strikes the barrel collar (N),

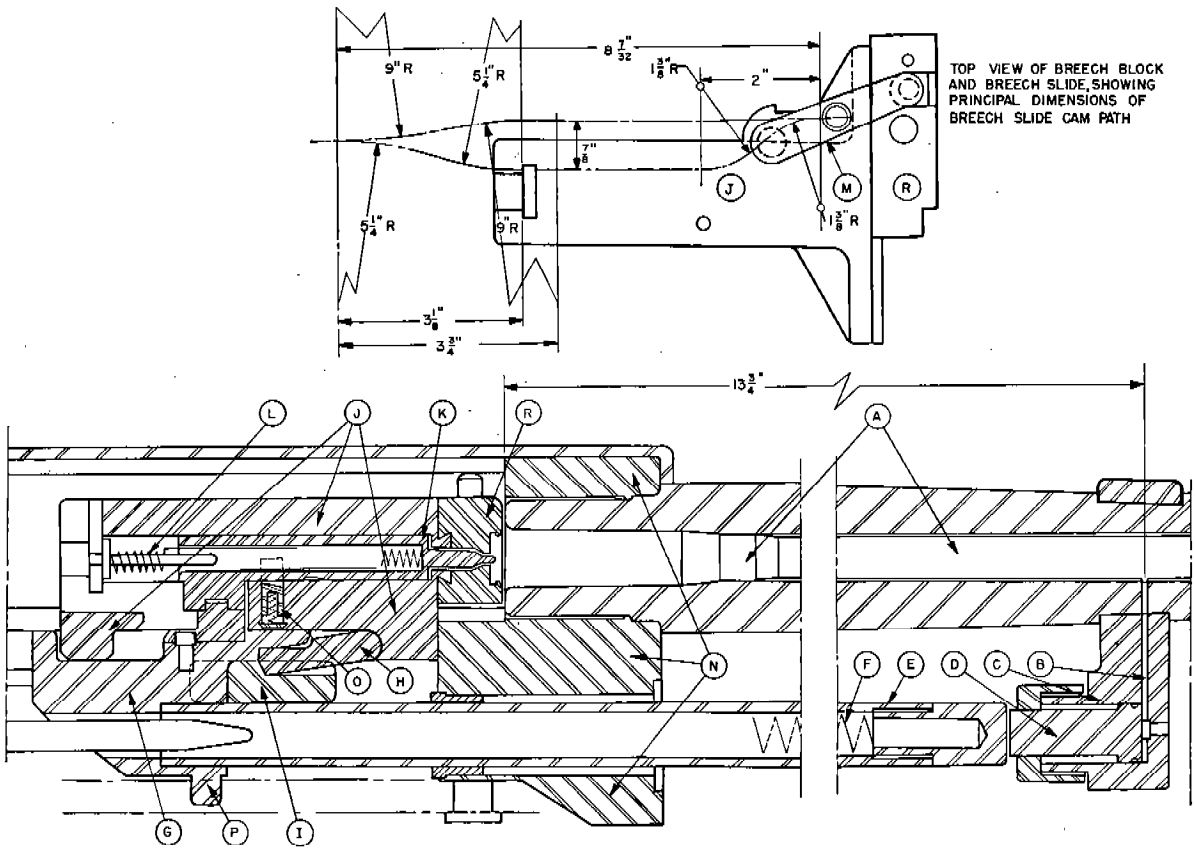


FIGURE 1. Mechanism of 20-mm gun, Model I. (This figure has appeared as Figure 1 in NDRC No. Report A-454.)

and it is brought to a sudden stop. At the same time, the lock is free to move downward against the locking key. If the sear (O) is held down by the trigger (not shown), the striker is free to move forward with the locking platform and operating shaft, under the force of the striker and driving springs. As the locking platform moves forward, its forward projection holds the lock in the locked position until gas pressure again moves the shaft and platform to the rear.

If the trigger is released, the sear is free to move upward and engage the sear notch in the striker. Thus, when the breech block, and its associated parts move forward, the striker, locking platform and operating shaft are held to the rear of their extreme forward position by the sear in the sear notch, until the sear is pushed downward by the trigger, allowing these parts to move forward again.

Ammunition for the gun is supplied from a closed-loop belt of disintegrating steel links, and is fed from the left-hand side (not shown). The feed tray is rigidly attached to the barrel and receiver and moves with them in recoil and counter-recoil, and is not interchangeable from side to side. In these respects this model does not satisfy the Navy requirements, but since this model was constructed only to test the mechanism, this feature should not be considered a fault of the design. It was corrected in Model III.

Power for feeding the belt is derived from the motion of the locking platform. A stud (P) on the bottom of the locking platform fits in a curved groove in the feed lever. As the platform moves back and forth, the lever is caused to swing to the right and left. A pawl attached to the forward end of the lever feeds the belt to such a position that the round to be fed lies parallel to the chamber and 1⅞ in. to the left. The feed lever is of such shape that the belt is fed during the closing stroke of the locking platform, and the lever is positioned prior to feeding by the opening stroke of the platform. Since the details of the feed tray are not unlike those of other belt-fed weapons, no further description of them is necessary.

To extract the fed round from the belt and translate it from its position 1⅞ in. to the left of the chamber to its position in the chamber, a breech slide

(R) is used. The breech slide is attached to the breech block by a dovetail in such a manner that it is free to slide to the right and left with respect to the breech block, and, of course, moving back and forth with the breech block. A cam in the top of the receiver actuates a lever (M), causing the breech slide to move right or left according to the position of the breech block.

On the forward face of the breech slide is a T slot. At the left end of the breech slide are two spring-loaded extractor claws, giving, in effect, an extension of the T slot. A third extractor at the end closes the T slot. As the breech block and slide move forward into battery, the three extractor claws grip the round to be extracted from the belt, on three sides of the extractor groove. The fourth side is gripped by an angular face pin projecting from the forward face of the breech slide. Thus held securely in the breech slide, the round is extracted from the belt as the breech block moves rearward. The cam is so designed that lateral motion does not begin until the round is free of the feed tray. Part of the lateral motion takes place on the opening stroke and the remainder on the closing stroke. When the projectile is about halfway in the chamber, the cam begins to return the breech slide to its initial position. This motion is completed when the breech block is about ¼ in. from the battery position. Thus the breech slide is moving forward when it engages a new round in the feed tray.

The motion of the empty case being removed from the chamber is similar to that of the round being fed. The lateral acceleration of the breech slide is sufficient to throw the empty case out of the open end of the T slot, so the empty case is ejected forward and to the right of the gun at an angle of 30-45 degrees to the axis of the barrel.

Model III

Figure 2 is a vertical cross section through a portion of the receiver of the Model III gun. The lower view

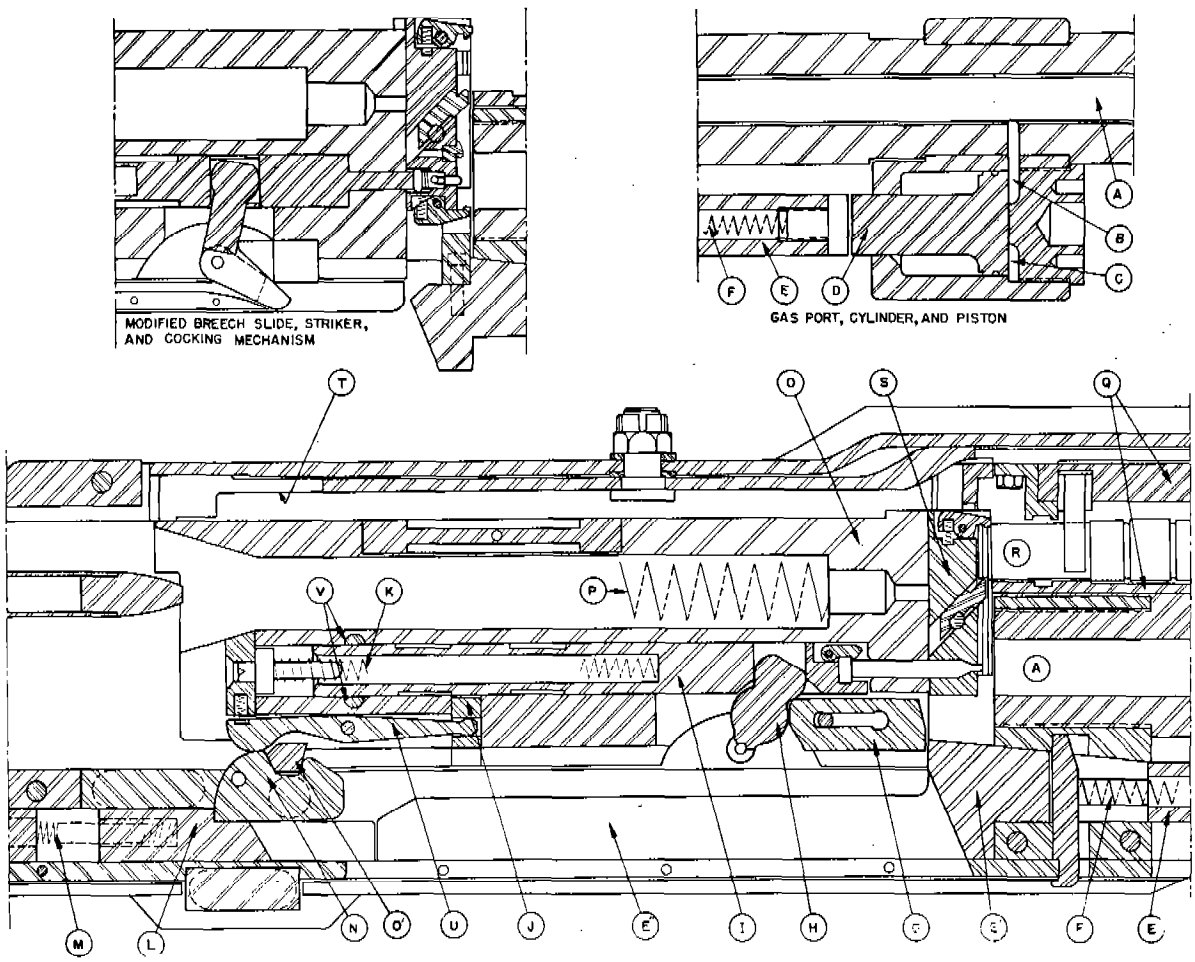


Figure 2. Mechanism of 20-mm gun, Model III. (This figure has appeared as Figure 2 in NDRC Report No. A-454.)

shows the parts in the receiver as originally designed and built. The figure at the upper right shows the gas port, cylinder and piston, and that at the upper left shows the modifications made in the cocking mechanism, breech slide, and operating shaft to overcome difficulties encountered in operation. (See Section 28.2.4.)

As the bullet proceeds down the barrel (A), it uncovers the gas port (B), admitting gas at high pressure into the gas cylinder (C). This gas forces the piston (D) rearward, which in turn drives the operating shaft (E) back against the spring (F).

As the operating shaft moves rearward ½ in., a raised portion (E′) forces the cocking slide (G) rearward, which, through a two-to-one cocking lever (H), cocks the striker (I) a distance of 1 in. This permits the sear (J) to move upward into a sear notch in the striker, holding it cocked against the firing spring (K). While the operating shaft is cocking the striker, its forked rear end (E″) pushes the locking platform (L) rearward against its springs (M), until the lock (N) is free to rotate counterclockwise. The slope at the rear end of the forked operating shaft forces the lock to rotate.

When the lock has rotated sufficiently, it comes out of engagement with a section (O′) of the breech block (O), and the breech block is free to move rearward against the driving spring (P).

At the instant the lock becomes disengaged, the raised portion (E′) of the operating shaft strikes the forward face of the breech block. This impact, plus the residual chamber pressure, imparts sufficient energy to the breech block to drive it to the rear against the driving spring, until it strikes the buffer spring (not shown). All of the energy for feeding the belt and chambering the round is taken from the kinetic energy of the breech block and the potential energy of the buffer and driving springs.

Removal from the feed tray (A) of the round to be fed (R) is by means of a breech slide (S) similar to that in the Model I. The main difference is that in the Model III the feed tray is above the chamber to permit feeding from either side, so the motion of the round is downward, instead of from left to right.

The belt feed mechanism and feed tray are similar to the same components in the Browning caliber .50 machine guns. The feed tray in Model III is attached to the mount instead of the receiver, to prevent feed tray motion when the gun recoils. Belt feed is interchangeable from one side to the other, thus satisfying certain Navy requirements not complied with in Model I.

Ignition of the round in the chamber is by means of the striker, the cocking of which was previously described. When the breech block closes, the lock (N) is rotated to the locked position, permitting the locking platform (L) to be forced under the rear of the lock by the springs (M). When the locking platform has moved forward a distance sufficient to assure positive locking, a small projection on the locking platform strikes a lever in the lock. Neither the projection on the locking platform nor the lever in the lock is shown in Figure 2. The lever in the lock pushes the rear end of the sear lever (U) upward, so its forward end draws the sear (J) downward, allowing the firing spring to push the striker forward to ignite the primer of the chambered round. Release of the striker cannot occur until the locking platform is well under the lock, thus preventing premature ignition with an unlocked breech. Manual control of firing is obtained by means of another sear (V), which is moved horizontally by an electric solenoid. When this sear is in its sear notch, the striker cannot move forward to strike the primer.

In both the Model I and Model III, the round being fed is tightly gripped in the breech slide by the three extractor claws and the angular face pin from the time it is extracted from the belt until it enters the chamber. There is no opportunity for rotation during this period, and the round enters the chamber in the same angular position it had in the belt. Thus the guns are well suited to firing pre-engraved ammunition, if the rounds are properly oriented in the belt, as is brought out in Section 28.4.

28.2.4 Problems Encountered and Corrective Measures Applied

It would be too much to expect that the prototype of any mechanism as complex as an automatic cannon would operate satisfactorily when first fired. Numerous failures occurred, and in most cases these were overcome by modifications in the mechanism itself. Some difficulties encountered would require either a change in the ammunition or a radical change in the mechanism. Insofar as possible, problems encountered with Model I were solved by changes in design introduced with Model III.

It is quite possible that under service conditions other difficulties might have occurred as a result of conditions not encountered during testing, such as extremes of temperature and high acceleration of the gun as a whole. Space does not permit a full discussion of all of the problems encountered, only the most

important being discussed here. These and others are covered more fully in the report[126] previously referred to.

"Pulled" Projectiles

The most serious difficulty encountered, and the only one which was not corrected, either by improved design or by temporary modifications, was failure of the round to enter the chamber, when the guns were fired at cyclic rates in excess of 500 rpm. There were two types of failure of this nature. First, when the round was removed from the feed tray, the projectile was pulled from the case and left in the tray. Second, the nose of the projectile, instead of entering the chamber, would strike the breech face and jam the mechanism.

Since these failures occurred only at high cyclic rates, it was evident that they resulted from dynamic rather than static conditions. The problem was analyzed by means of high-speed motion pictures, from which kinematic analyses were made. These analyses showed that the breech block undergoes very high accelerations (680 g at 561 rpm) when operating normally. Tests were made of the ammunition to determine what forces were required to pull the projectiles from the cases. It was found that a force of 295 lb would remove the projectile completely, and 200 lb would loosen it badly. The acceleration force is of the order of 215 lb under normal conditions, so it might be expected that the projectiles would always be loosened, and under abnormal conditions would be pulled out completely.

To analyze the failure of rounds to enter the chamber, kinematic analyses were made of the lateral accelerations and resulting bending moments, which would swing the nose of the projectile to one side or the other of the chamber. It was found that these bending moments were insufficient to cause jamming under normal conditions, if the projectile was tight in the case, but if the projectile had been loosened on removal from the feed tray the bending moments were sufficient.

To correct these difficulties, special ammunition was made up which had a tighter crimp than normal. This functioned satisfactorily except for a few rounds in which the case was torn by the resulting sharp edge of the crimping groove. It was understood that ammunition with a stronger crimp would be available from the Navy Department, so further corrective measures were not tried. However, none of the new ammunition was forthcoming, so the feeding problem persisted for the life of the project.

Rebound of Impacting Parts

When two elastic pieces come together in impact, they tend to separate at approximately the same relative velocities at which they came together. This rebound tendency had two serious effects, "shuttling" and "breakage" in Model I, and reduced cyclic rate in Model III.

It will be recalled from the sequence of operation of Model I, that when the locking platform [(G) in Figure 1] has moved back far enough for unlocking to occur, it strikes a lug at the lower rear of the breech block, and the block and locking platform move rearward together, held in fixed relative positions by the lock. Thus any rebound taking place after impact occurs by elastic deformation of the parts. Kinematic analysis (Section 28.2.5) showed a relative motion, known as "shuttling," in which separation takes place by elastic deformation, to be followed by another impact and separation. Shuttling occurred until the energy of the initial rebound was absorbed by hysteresis or plastic deformation of the affected parts. This frequently resulted in breakage of the lug at the lower rear of the breech block, and also in loss of energy which might have been used to increase the cyclic rate. This could not be corrected in Model I but was avoided in the design of Model III.

Closure of the breech in Model III was completed by impact on the barrel collar. The locking mechanism was not quick enough to prevent rebound after this impact, with the result that the breech block bounced back a distance of approximately 2.7 in., increasing the time for the cycle by as much as 40 msec. Several methods were proposed to eliminate this difficulty. The method finally adopted was to bring the breech block to a low velocity just before impact. This was done by holding the operating shaft to the rear until the breech block was about ⅛ in. from its battery position. Thus the breech block, just before going into battery, would strike the operating shaft and transfer most of its kinetic energy. Thus it had a very low velocity when striking the barrel collar and the lock had sufficient time to prevent rebound.

Parts Breakage

Structural failure of parts is always a source of annoyance and frequently a serious danger. Fortunately

breakage of parts in either model never resulted in danger to personnel or other equipment, but it frequently did cause serious delays in the program.

One of these failures was breakage of the breech block in Model I, due to "shuttling," as previously discussed. The other serious failure occurred in the receiver plates of Model III. This was analyzed and found to be the result of high stresses during firing, applied at sections where stress concentrations and residual heat-treating stresses were likely to occur. Furthermore, the steel originally specified (SAE 4650) was not available in the desired sizes and shapes and a higher carbon steel was used. The impact strength of this steel was found to be quite low, which was probably an important factor in the failure. It was possible to make temporary repairs by bolting an auxiliary plate to the receiver plate to carry the load. Later, it was decided to prepare new receiver plates of the proper carbon content and give closer supervision to the heat-treatment to avoid brittleness. Insofar as possible, stress concentration was avoided in the redesign of the plates.

Several other breakages occurred, but they were usually the result of abnormal stresses caused by some other failure, and would not have occurred under normal operation.

Cocking Failure in Model III

One of the first difficulties encountered in operation of Model III was failure of the cocking mechanism to operate. It was found that a pressure wave from the gas piston traveled down the operating shaft and caused the locking platform to bound away with a "billiard ball" effect. Thus unlocking was completed almost instantaneously and the breech block would move rearward without cocking the striker.

This was overcome by making cocking dependent upon breech block travel, rather than on motion of the operating shaft. The changes made in the striker and cocking mechanism are shown in Figure 2.

Case Ejection in Model III

In Model I, ejection of empty cases was accomplished by the lateral acceleration of the breech slide, which was sufficient to throw the empty case out of the T slot. It was expected that this would occur also with Model III, but the breech slide accelerations were reduced in Model III to improve chambering, and were insufficient to provide positive disengagement of the case from the T slot. The presence of the empty case in the T slot during the closing stroke would cause jamming of the mechanism.

This difficulty was overcome by cutting away the T slot at its lower end and providing extraction by an extractor claw at the lower end of the breech slide. Two spring-loaded plungers, set in the face of the breech slide, pressed against the base of the case near its upper edge, tending to rotate the case in a clockwise direction about the extractor claw. A small platform was bolted to the top of the operating shaft to support the front of the case until it was far enough out of the chamber that it would not strike the operating shaft during ejection. These changes in the breech slide are shown in Figure 2.

With the exception of "pulled" projectiles, all operational difficulties encountered in testing these guns were overcome. It is believed that problems of feeding can be overcome only by a radical redesign of the mechanism or by a tighter crimp on the ammunition.

28.2.5 Kinematic Analyses

Certain difficulties in the operation of Model I indicated the desirability of knowing in more detail the actual movements of the component parts. This was particularly important in analyzing failures due to "pulled" projectiles, which were described in Section 28.2.4.

Kinematic analyses were made from high-speed motion pictures taken at 1,000 frames per second, by plotting displacement-time curves. Using a standard method of graphical differentiation, velocity and acceleration curves were drawn.[508] Figure 3 shows a typical kinematic analysis of Model I when firing at a cyclic rate of 561 rpm. It is noted that during the opening stroke, the velocity of the breech block is about 300 in./sec, and about 200 in./sec during the closing stroke. "Shuttling" of the breech block and locking platform appears as ripples on the velocity and acceleration curves in the region of +4 to +18 msec. Ripples on the velocity curve during the closing stroke are the result of transfer of kinetic energy to and from the breech slide.

The high acceleration of the breech block, as a result of impact from the locking platform, is shown at +3 msec, when it has a value of 262,000 in./sec^2. Values of very high accelerations of short duration cannot be determined accurately, because the exposures at every millisecond interval do not indicate the actual movement during that interval but only

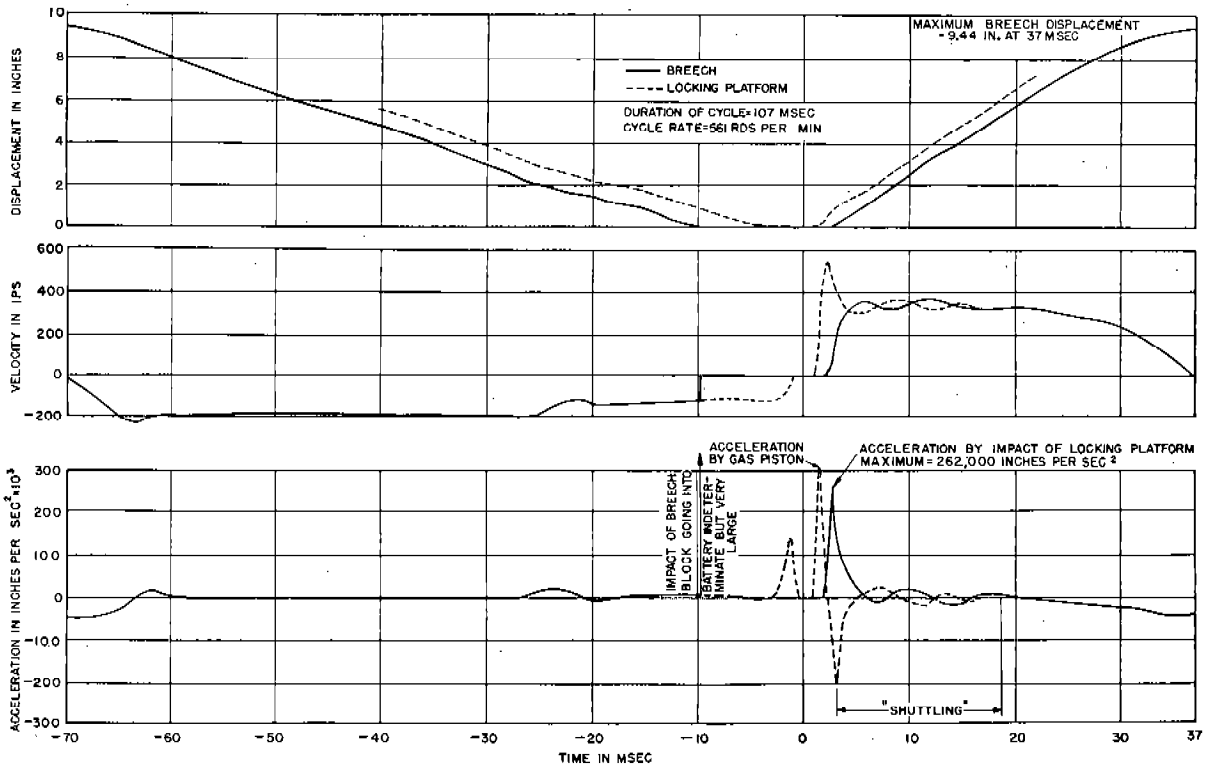


FIGURE 3. Kinematic analysis of firing cycle, 20-mm gun, Model I. (This figure has appeared as Figure 5 in NDRC Report No. A-454.)

the net displacement and hence the average velocity. However, the values so obtained are useful in giving a clue to operational difficulties.

By combining the data of Figure 3 with the drawings of the breech slide cam path, it was possible to determine the transverse accelerations of the breech slide. They produced bending moments tending to bend the projectile out of the case and the round as a whole out of the T slot. Curves of these bending moments are shown in Figure 4. These curves show that during the transverse movement of the breech slide, the moment on the complete round varies from about 50 to 150 lb-in., and the moment on the projectile about the crimping groove varies from about 9 to 24 lb-in. The nose of the projectile enters the chamber at a breech block displacement of about 7 in. on the closing stroke, at which time the bending moments on the round and projectile are approximately 70 and 12 lb-in., respectively. If the projectile were tight in the case, these moments would not be sufficient to prevent chambering, but it must be remembered that the projectile was previously loosened by the acceleration on removal from the feed tray.

The kinematic analysis was useful in determining the energy of the system. It was found that the total energy of the breech block and driving spring increased during the early part of the opening stroke, partially as a result of blowback. During the closing stroke, the energy dropped rapidly, shortly after leaving the buffer spring, due to the absorption of energy by the belt feeding mechanism, thus giving a slow closing stroke. If energy for belt feeding had been taken near the end of the closing stroke, instead of at the beginning, a considerably higher cyclic rate would have been obtained.

There was insufficient time to make complete kinematic analyses of Model III. However, the analyses did show a very high acceleration (900,000 in./sec²) resulting from impact of the operating shaft. These curves were similar to those for Model I, except for the presence of rebound at the end of the closing stroke, and the absence of "shuttling."

The kinematic analyses were probably the most important factor in locating and eliminating sources of trouble in operation of the guns.

28.2.6 Prediction of Firing Rate

During the design period of Model III, it was felt desirable to predict the firing rate, in order that spring

constants and other factors might be given optimum values before completion of the design. Unfortunately the time available was too short to incorporate the results of the calculations into the design, or to make a complete calculation of the final design. Hence the calculations shown herein apply only to a hypothetical gun having the same general characteristics as the Model III gun.

Briefly the method of calculation consisted of setting up a differential equation of motion for each part of the cycle, determining the time for that part, and taking the sum of the times as the total for the cycle. For some parts of the cycle the time was known or estimated, some could be calculated directly, and others had to be calculated by a step-by-step method.

The cycle was considered to start at the instant the sear released the striker. The results of the computations are summarized in Table 1. The bases on which they were made are indicated in the following paragraphs, which are numbered to correspond to the successive time intervals.

1. The striker had simple harmonic motion, being a simple spring-mass system for which the mass weighed 1.02 lb and the spring had a constant of 30 lb/in. The natural frequency ω of the system was evaluated by equation (1)

$$\omega = \sqrt{\frac{k}{m}}, \tag{1}$$

in which k is the elastic constant of the spring and m

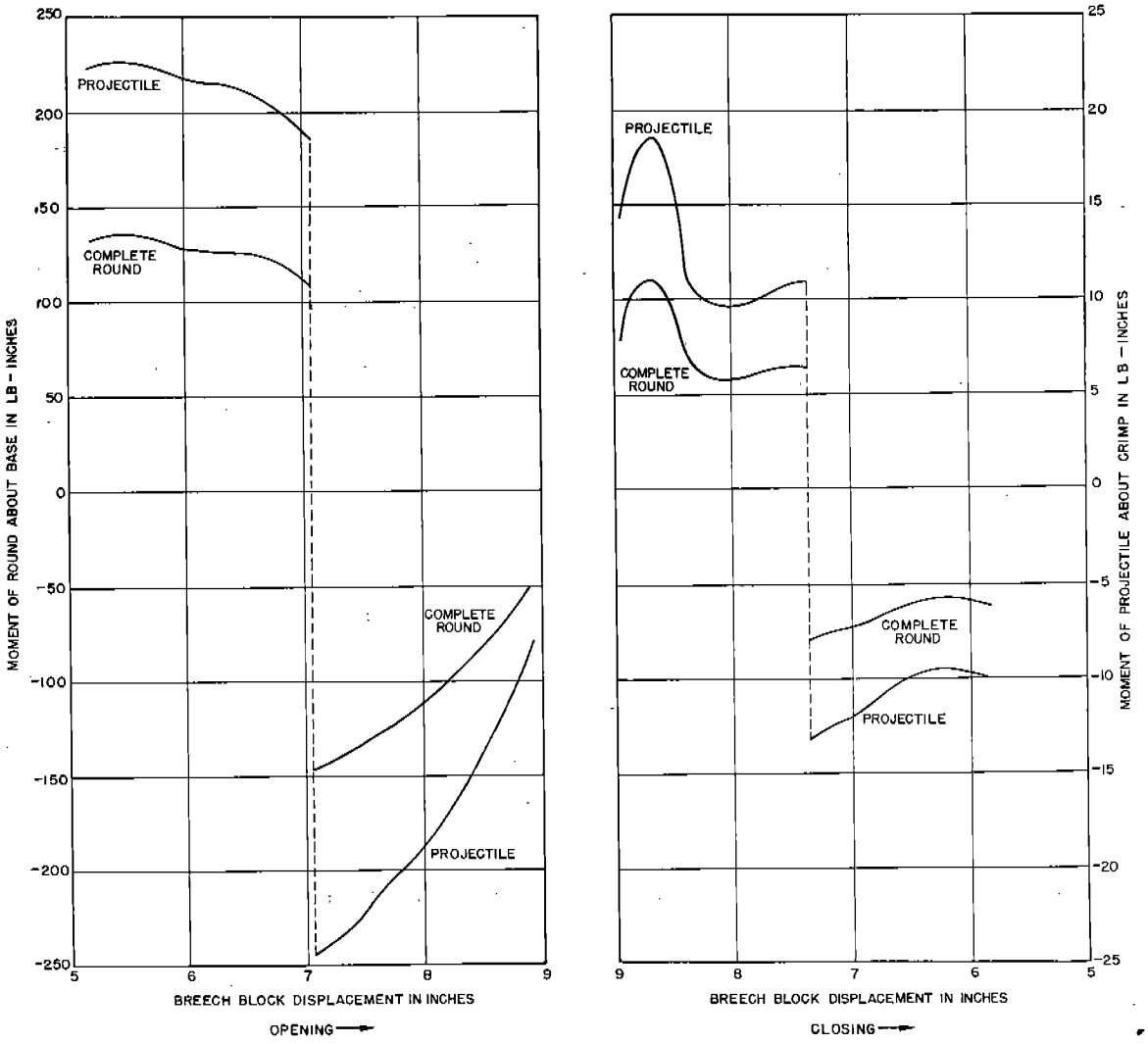


FIGURE 4. Bending moment on round due to breech slide acceleration, 20-mm gun, Model I. (This figure has appeared as Figure 6 in NDRC Report No. A-454.)

TABLE 1. Calculated time for each interval in the firing cycle of 20-mm automatic cannon.

Interval*	Event	Time (sec)
$t_1 - t_0$	Striker motion	0.0125
$t_2 - t_1$	Projectile to pass port	0.0016
$t_3 - t_2$	Operating shaft motion	0.0015
$t_4 - t_3$	Primary extraction	0.0002
$t_5 - t_4$	Impact	0.0002
$t_6 - t_5$	Blowback	0.0067
$t_7 - t_6$	Motion of breech block from the end of blowback until engagement with buffer	0.0134
$t_8 - t_7$	Compression of buffer	0.0074
$t_9 - t_8$	Decompression of buffer	0.0074
$t_{10} - t_9$	Buffer to battery	0.0380
$t_{11} - t_{10}$	Locking platform motion	0.0096
	Total	0.0985
	Equivalent firing rate: 609 rpm	

* The cycle is considered to start at the instant the scar releases the striker.

is its mass. The time for the first interval of the cycle is then given by equation (2),

$$t_1 - t_0 = \frac{1}{\omega} \cos^{-1} \frac{x_1}{x_0} \tag{2}$$

in which x_0 and x_1 are the compressions of the spring before release and after striking the primer.

2. Interior ballistic data for the ammunition fired showed that the time $t_2 - t_1$ for the projectile to move 11 in. after the primer was struck was 0.00159 sec.

3. After the gas port had been uncovered, high pressure gases flowed into the cylinder and drove the piston and operating shaft rearward. Equation (3) is the general equation of motion.

$$m\ddot{x} + kx = F, \tag{3}$$

where F is the force on the piston and x its displacement. This force is a function of the pressure in the barrel (which varies with time) and of the volume in the cylinder (which varies with x). Inasmuch as it is impractical to use an analytical function of F, the motion was solved by a step-by-step process, using time intervals of 0.0001 sec to find the time required to move 0.5 in.

4. During the next ⅛-in. movement of the operating shaft, it cammed the lock out of engagement with the breech block and imparted some initial energy to the breech block. This "primary extraction" process was most easily solved by an energy balance, making assumptions regarding friction and taking into account the effect of blowback.

5. The laws of impulse and momentum were used to estimate the velocity of the breech block after impact.

6. During the early part of the opening stroke of the breech block, the motion was aided by blowback and retarded somewhat by friction. The equation of motion is similar to equation (3), but, of course, has different constants. Since the blowback force was not a constant or a simple function of x or t, a step-by-step process was used. Friction was estimated at 50 lb and the blowback pressure p at any instant was calculated[48] by equation (4)

$$p = \frac{p_0}{(1 + at')^\gamma} \tag{4}$$

in which p_0 is the barrel pressure when the projectile leaves the muzzle, a is the ratio of the muzzle velocity to the barrel length, γ is the ratio of the specific heats of the powder gas, and the time t' is measured from the instant the bullet leaves the muzzle.

7. The motion of the breech block from the end of blowback until it struck the buffer spring was similar to that during blowback except the blowback force was zero.

8. The required constants of a buffer spring to be compressed 2 in. were calculated, and the new value of k substituted in equation (3) for calculation of the period of buffer spring compression.

9. It was assumed that decompression of the buffer spring required the same time as compression.

10. The time for the closing stroke of the breech block was calculated in two different ways; first, by application of the principles of a spring-mass system taking into account the energy required for belt feeding, and, second, by assuming that the closing stroke required about 65 per cent longer than the opening stroke. The value obtained by the latter method was used.

11. After the breech block went into battery the locking platform had to move under the lock. Again the process involved a simple spring-mass system.

The total calculated time for the cycle was 0.0985 sec, so that the calculated firing rate was 609 rounds per minute.

Two possible ways of increasing the firing rate without affecting breech block motion are by shortening the time for the striker to move and by using an instantaneous locking device. The first of these was actually done to correct another fault (cocking difficulties—see Section 28.2.4), and the time for striker motion reduced to 0.005 sec, which would increase the calculated firing rate to 659 rpm. The use of an in-

stantaneous lock such as a toggle link would reduce the time for the cycle by a further 0.0096 sec, raising the calculated firing rate to 737 rpm.

28.2.7

Conclusions

As a result of the experimental work and theoretical analyses performed on this 20-mm gun project, certain conclusions may be drawn.

1. Both models that were built and fired performed satisfactorily within limits.

2. All of the problems encountered, with the exception of "pulled" projectiles, were overcome by changes in the gun mechanism itself.

3. Neither of the guns built completely satisfied the Navy requirements with respect to weight and length.

4. The standard Navy ammunition used is not satisfactory for this type of mechanism, without modifying the mechanism to reduce acceleration forces and bending moments.

5. The kinematic analyses were of great importance in determining causes of failure and in correcting them.

6. Both models had remarkable belt-pulling ability.

7. Impacts resulting in "shuttling" or rebound cause parts failure and low cyclic rates.

8. More information on the action of gas cylinders and blowback is needed.

9. During the design stages, the results of theoretical kinematic analyses (calculation of firing rate, etc.) would be helpful in choosing correct springs and weights.

10. Quick-acting locking devices are useful to increase cyclic rate.

11. High breech block weights require more energy for the same cyclic rate.

12. Long travel for parts reduces cyclic rates if velocities and accelerations are to be kept to a minimum.

13. Maximum blowback power is obtained with early breech opening. This is limited, however, by the ability of the case to resist rupture with high internal pressure.

14. The gun mechanism is adaptable to pre-engraved projectiles.

28.2.8

Recommendations

In order to make the experience of this project of most effective use to future designers, there are presented herewith certain recommendations which the author believes will minimize difficulties if they are adopted. Some of these recommendations are very broad while others are specific, some relate to design and others to further lines of investigation, and some concern the gun alone while others concern the ammunition in relation to the gun.

1. The rounds should be moved with accelerations as low as possible to avoid inertia forces and couples that tend to loosen projectiles in the case and make chambering difficult. This applies to belt feeding, removal from belt and translation to the axis of the chamber. This might be accomplished by the use of buffer springs to limit maximum accelerations.

2. To take maximum advantage of blowback power, the breech should be opened as early as practicable. There are some limitations to this expedient however. Extraction of energy for blowback may result in loss of muzzle energy, and early extraction subjects the empty case to high internal pressures which might rupture it and make extraction difficult.

3. The ammunition should be designed for the gun. This design should include sufficient crimping to prevent loosened projectiles, and sufficient wall strength of the case to permit early extraction. This recommendation is closely allied to recommendations 1 and 2.

4. For maximum cyclic rate, the breech block opening and closing strokes should be at as high a velocity as practicable. For limited total energy of the block, the weight should be low and the driving spring only stiff enough to assure breech block closure under the worst conditions.

5. Energy for auxiliary functions, such as cocking and belt feeding, should be extracted as near the end of the breech closing stroke as possible, to maintain a high kinetic energy in the breech block. This has the added advantage of reducing the breech block velocity as it goes into battery and helps eliminate rebound.

6. For better analysis of gas-operated weapons, an analytical study should be made of the action of gas ports and pistons.

7. The time required for events in the cycle that occur between the time the breech block closes and the striker hits the primer should be as short as possible, to get high cyclic rates. Instantaneous locking devices and short stroke strikers will shorten this time considerably.

8. The weights of the operating shaft and the breech block should be so proportioned that the maximum



amount of energy is transferred from the shaft to the breech block at the instant of impact.

9. Rebound of the breech block, when going into battery, can be eliminated by having it impact against some mass, such as the operating shaft, thus losing kinetic energy before the impact with the barrel collar or other stationary mass.

10. Careful dynamic studies should be made during design, to avoid faults that would result in low cyclic rate or failure to operate under conditions of high acceleration.

11. To keep the gun as short and light as possible, the length and travel of the breech block should be kept short. This will also raise the cyclic rate.

12. Insofar as possible, locking stresses should be limited to the forward part of the receiver, or preferably kept free of the receiver. In this way the weight of the receiver can be materially reduced.

13. If locking devices, driving and buffer springs, and the weight distribution of the breech block are symmetrical about the axis of the chamber, friction forces and lateral stresses could be minimized and the weights of parts reduced.

14. The charger and trigger solenoid should be mounted inside the receiver, so that right- and left-hand interchangeability is not required. This would reduce the number of openings required in the receiver and the stress concentrations resulting therefrom.

15. Snap catches, etc., that have to act immediately should be avoided, because they tend to engage on very small surfaces and rapid wear occurs.

16. Buffer springs between impacting surfaces might be used to reduce impact stresses and high accelerations resulting from impact.

17. Spring-actuated parts should have springs of sufficient strength to prevent undesired motion of these parts under high "g" conditions.

18. Ejection ports should be sufficiently large and free of obstructions to prevent jamming of empty cases and links. It must be remembered that complete rounds must frequently be ejected in case of misfire.

19. Large flat plates for the receiver or other parts should be avoided, because they are difficult to heat-treat without distortion.

20. The parts should be designed so they can be easily machined from bar, tube, or plate stock without removal of too much material. If necessary, forgings or castings could be used, but the use of stock material is preferable from the procurement standpoint.

21. Parts requiring high tensile strength should not be subjected to impacts and should be designed to avoid stress concentration and residual heat-treatment stresses. Likewise parts subjected to impacts should not be required to carry high stresses. This is necessary to avoid the use of special alloys having both high tensile and high impact strengths.

22. Consideration should be given to modification of the power linkage by the use of multiple-drive units, one gas cylinder being used to produce fore-and-aft movements and another to produce movements of the belt and other parts moving at a right angle to the axis of the barrel. In this way a higher cyclic rate could be obtained without putting undue stress on the moving parts.[d]

28.3 PROBLEMS IN DESIGNING AUTOMATIC MECHANISM FOR HYPERVELOCITY AMMUNITION

28.3.1 Introduction

Higher velocity of a given projectile may be obtained by increasing the mean net force acting on the base of the projectile, or by increasing the distance over which that force works. The distance over which the force acts can readily be increased by lengthening the barrel of the gun. The mean net force acting depends upon the height and shape of the pressure-travel curve, and can be increased by increasing the maximum gas pressure, decreasing retarding forces (friction), or by maintaining a larger proportion of the curve at or near its maximum value.

There are objections to the use of any of these methods of increasing muzzle velocity, so a compromise is usually made of the various factors. Longer barrels result in heavier guns that require more power for the elevating and traversing mechanism. Increased maximum gas pressures mean that the walls of the barrels must be thicker (and heavier) or made of higher strength materials. Little can be gained by reducing friction, as this force is only a small fraction of the total propelling force. In order to maintain a

[d] This recommendation is taken from a postscript written for NDRC Report A-454[126] by Mr. J. A. TenBrook, formerly Head of the Engineering and Development Branch, Division 1, NDRC. In that position he had supervision of the contract under which the Johnson 20-mm gun was being developed. (Editor's note.)

larger proportion of the pressure curve at or near its maximum value, that is, to increase the ratio

$$\frac{\text{mean effective pressure}}{\text{maximum pressure}},$$

a larger quantity of slower burning powder is required. This increases heat transfer to the barrel, gives higher muzzle pressures, and increases muzzle flash. An increased powder charge usually requires a larger cartridge case. This may be obtained by increasing its length, diameter, or both.

The tactical disadvantages of the methods of obtaining higher muzzle velocities have been mentioned. These methods also introduce serious problems in the design of the gun mechanism itself.

The remarks to follow relate only to weapons using normal weight projectiles,[c] in which high velocities are obtained by increased pressure, longer barrel and increased powder charge. They are not concerned with the use of "half-weight," sabot or deformable projectiles.

28.3.2 Recoil

The maximum velocity of the recoiling parts in free recoil V_f is given[509] by equation (5),

$$V_f = \frac{MV + 4700C}{W}, \tag{5}$$

in which M is the weight of the projectile, V is the muzzle velocity of the projectile, C is the weight of powder, 4700 is the assumed mass-mean velocity of the powder gas, and W is the weight of recoiling parts. If the gun is to be operated as a hypervelocity gun, V and C would be increased and the mass-mean velocity of the gas would probably be increased somewhat due to higher muzzle pressures and temperatures. The weight of the gun would probably be somewhat greater to give greater strength or longer travel, but in general the numerator of equation (5) would increase faster than the denominator. Therefore the velocity of free recoil would be higher at hypervelocities than at normal velocities. This would necessitate a redesign of the recoil mechanism to absorb greater energy, permit longer travel or exert greater retardation. In the case of recoil-operated guns, such as the Browning machine gun, hypervelocity ammunition and the greater recoil velocity (with normal weight projectiles) would probably give increased cyclic rate.

[c] That is, projectiles for which the ratio of the weight M to the cube of the diameter d is approximately 0.5 lb/in.^{3}.

28.3.3 Barrel Design

Needless to say, the use of higher chamber pressures to secure higher velocities necessitates heavier walls or higher strength materials. Dynamic stresses resulting from increased recoil accelerations would have to be given consideration, as would bending stresses due to barrel whip if the length were increased. Barrel temperatures would be somewhat higher (see Chapter 5), so the effect of temperature on strength would be important and provisions for adequate cooling might be required.

28.3.4 Breech Lock or Breech Ring

Inasmuch as high muzzle velocities are usually obtained by the use of higher chamber pressures the strength of the breech lock must be increased. This condition is further aggravated by the fact that the cartridge case is of larger diameter giving an additional increase of total force on the breech block. If a sliding breech block is used, these remarks apply to the breech ring.

28.3.5 Breech Block

Sliding breech blocks frequently have an insert on the forward face to facilitate assembly of the striker mechanism. High chamber pressures and setback of the cartridge case occasionally produce enough deformation of the breech block and insert to interfere with opening of the breech. Therefore consideration must be given to the strength of the breech block to avoid this condition.

To accommodate the larger powder charges required for hypervelocity, the cartridge cases are usually increased in length and diameter. Therefore to handle the longer round, recoiling breech blocks must travel a greater distance and the receiver and mechanism contained therein must be modified accordingly.

28.3.6 Feed Mechanism

Since the total weight of the complete hypervelocity round is somewhat greater than that for normal velocity, the feed mechanism must be somewhat stronger, and the mechanism will require larger quantities of powder for satisfactory operation.



28.4 LOADING AND INDEXING MECHANISMS FOR PRE-ENGRAVED PROJECTILES

28.4.1 Introduction

Pre-engraved projectiles in chromium-plated barrels are useful in prolonging barrel life, as is shown in Chapter 31. In order for such projectiles to be practical, there must be some means of indexing them positively, to make certain that the splines or teeth on the projectile will engage the rifling of the barrel during chambering of the round. If proper orientation is not obtained, the splines will jam on the lands and result in excessive powder pressure and rapid wear at the origin of rifling.

Tests[120] made on existing loading mechanisms showed how much angular rotation of the projectile took place in moving from the belt or clip or other ammunition supply until it was seated in the chamber. By pointing the lands and splines with matching 30-degree slopes a certain amount of misalignment could be tolerated, but it would be preferable to have accurate alignment.

The Browning caliber .50 machine gun showed a case rotation of ±20 degrees, which would be satisfactory for a four-land barrel. Large and irregular rotation of the cartridge case was found in the 37-mm AA gun, M1A2 and in the 40-mm AA gun, M1 (Bofors). About half the shells were inserted unfavorably in hand loading and in power loading a 90-mm gun, M1, at 22 rounds per minute. These tests indicated that changes in the projectile, origin of rifling, and feeding mechanism were required to chamber the pre-engraved round satisfactorily.

The following guns and ammunition were modified to fire pre-engraved ammunition: (1) Caliber .50 Browning machine gun, (2) 40-mm Bofors gun, and (3) 20-mm Johnson gun, Model III.

28.4.2 Browning Caliber .50 Machine Gun

Several changes were made in the gun and ammunition to make possible the chambering of pre-engraved ammunition, as follows:

(1) Four rifling grooves in the barrel instead of eight.

(2) Groove depth 0.020 in. instead of 0.005 in.

(3) Pre-engraved steel bullet with four integral splines 0.020 in. high, instead of soft jacket.

(4) Splines on bullet pointed with 30° slope.

(5) Lands at origin of rifling pointed with 30° slope.

(6) Indexing slot on base of cartridge case.

The splines on the projectile were properly oriented with respect to the indexing slot, which in turn was given a definite angular position in the belt. These two steps were easily taken by modification of the cartridge and belt loading mechanisms. Thus the projectiles were so aligned in the belt that, if no rotation took place in going from the belt to the chamber, all rounds would occupy the same angular position in the chamber. Only four ratchet notches are milled at the rear of the barrel, so the barrel would have to be in one of the four desirable angular positions. Previous tests had shown a maximum angular displacement of the round of only ±20 degrees in going from the belt to the chamber. This is well within the allow-

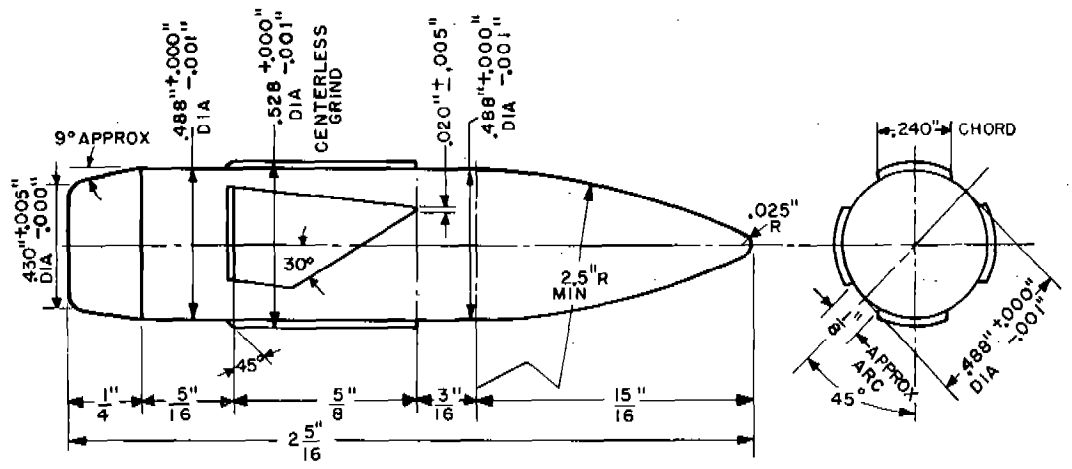


FIGURE 5. Caliber .50 pre-engraved projectile for test of automatic fire in Browning machine gun. (This figure has appeared as Figure 30 in NDRC Report No. A-448.)

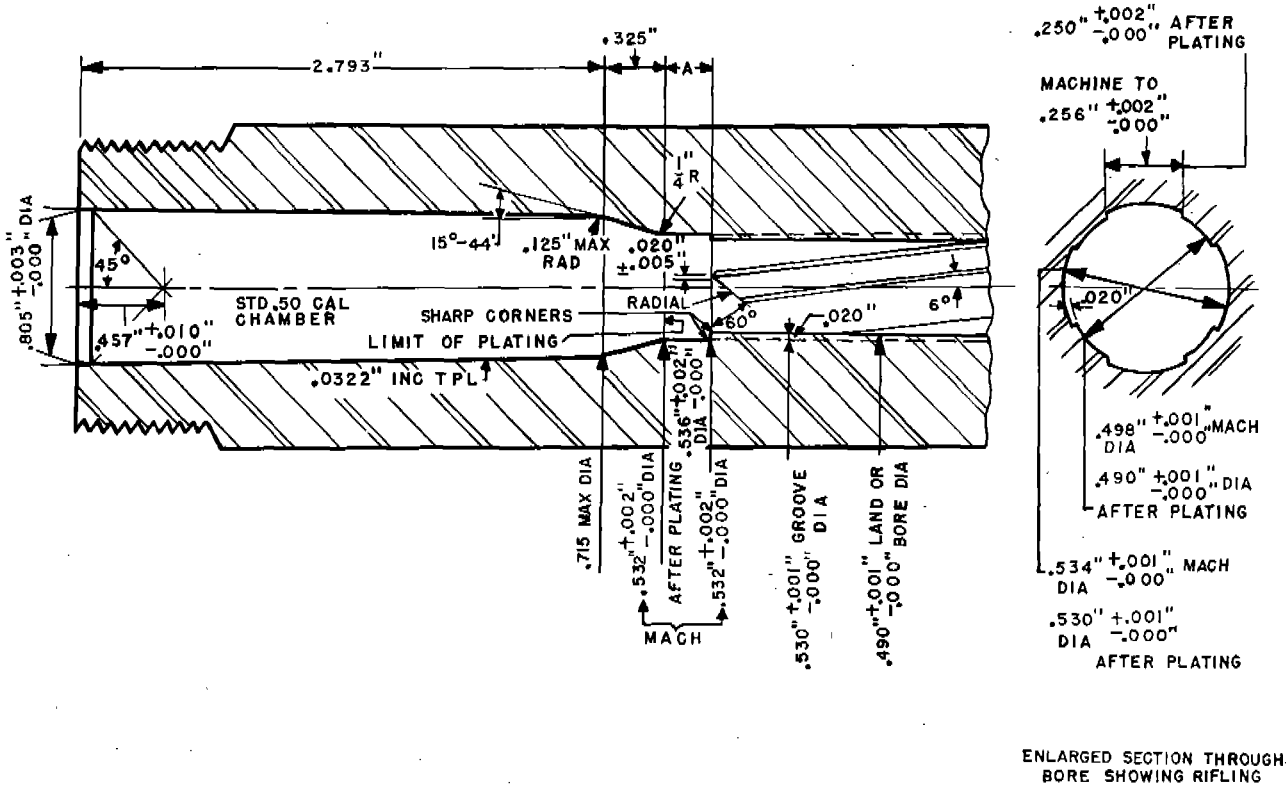


FIGURE 6. Chamber details of caliber .50 machine gun barrel modified to permit firing the pre-engraved projectile shown in Figure 5. (This figure has appeared as Figure 34 in NDRC Report No. A-448.)

able limits to prevent "hang-ups" in a four-groove barrel, with pointed lands and splines.

In firing 600 rounds of pre-engraved ammunition in this gun, there were no malfunctions in entering the rifling and no hang-ups at the origin of rifling, indicating that this method of indexing is satisfactory at rates of 500-550 rpm.

The pre-engraved projectile is shown in Figure 5, and the chamber details of the modified barrel in Figure 6.

28.4.3 Johnson 20-mm Automatic Aircraft Guns

The Model I and Model III guns, described in Section 28.2.3, were adapted to fire high-velocity caliber .50 ammunition. These guns employ a novel feeding system whereby the round is positively held in the breech slide from the time it is drawn from the belt until it is well in the chamber, with no opportunity for rotation about its axis. Thus, if the round is properly indexed in the belt, it will be properly oriented in the barrel.

The tests in the Model I gun were simply to determine whether or not such orientation was actually obtained. They consisted of putting a scratch on each case and loading the rounds in the belt so the scratches were at the 12 o'clock position. A corresponding groove was cut in the 12 o'clock position in the chamber, so the high chamber pressure of firing would leave an indicating mark on the case. This could be compared with the scratch previously made to indicate the amount of rotation, if any. The ammunition consisted of a caliber .50 ball bullet, M2, loaded into a 20-mm case necked down to fit the caliber .50 projectile. A charge of approximately 476 grains of double-base powder was used to give a pressure of 56,000 to 58,000 psi and a velocity of 3,600 to 3,700 fps. In tests at 560 to 570 rpm, it was found that very little, if any, rotational displacement of the rounds took place, indicating that this mechanism would be suitable for pre-engraved ammunition.

The Model III gun was fired with caliber .50 pre-engraved high-velocity ammunition. This was similar to that used in Model I, except that pre-engraved projectiles with pointed lands were used as had been

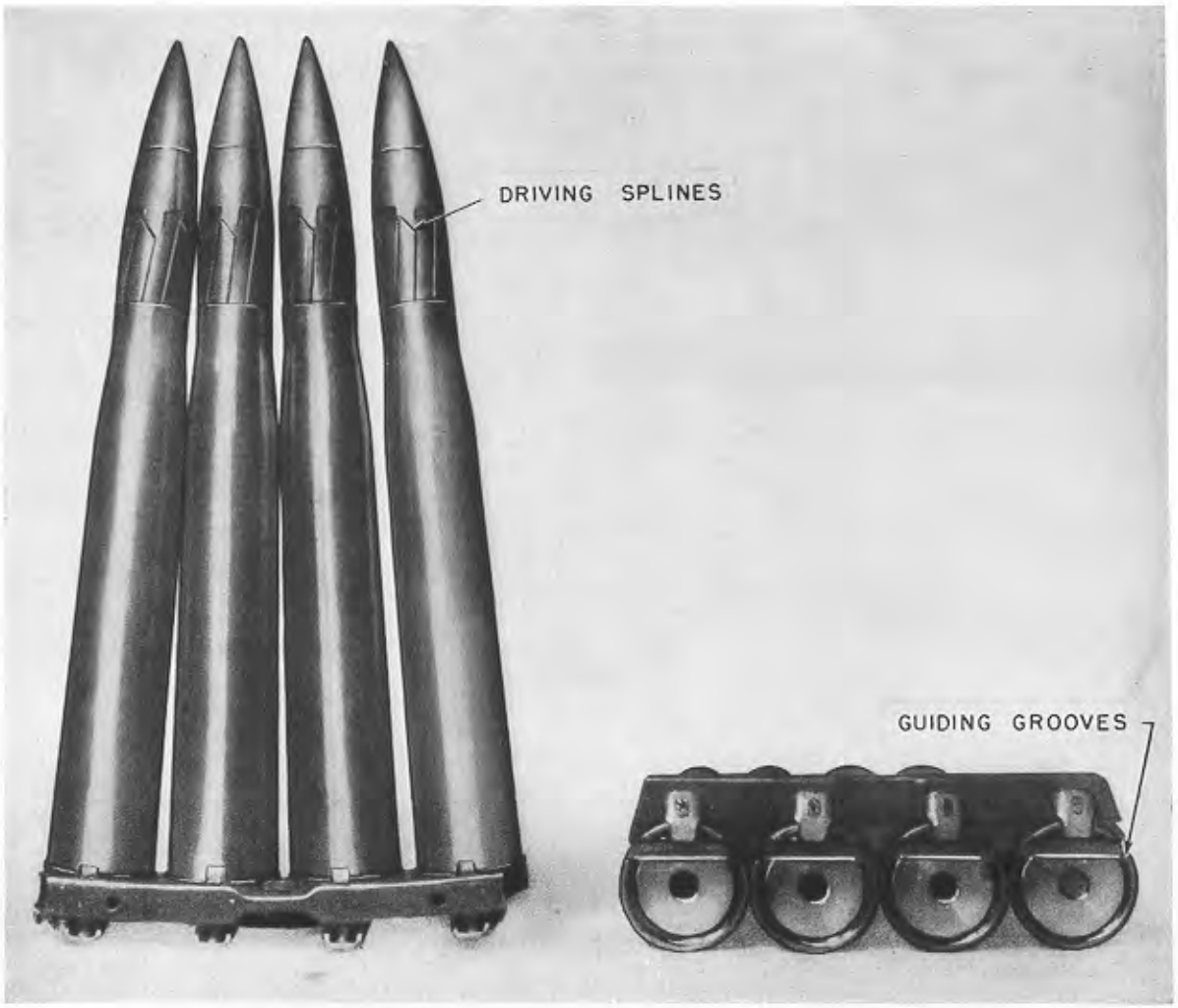


FIGURE 7. Complete rounds of 37-mm pre-engraved ammunition assembled in clip ready for loading into 37-mm gun. (This figure has appeared as Figure 38 in NDRC Report No. A-448.)

done in the Browning caliber .50 barrel. In the 50 pre-engraved rounds fired, the rotation of the assembled rounds was negligible. In fact, it was found that even with random indexing in the belt, the pointed lands and splines were sufficient to give correct orientation in the chamber.

28.4.4 Modified Bofors 40-mm Mechanism

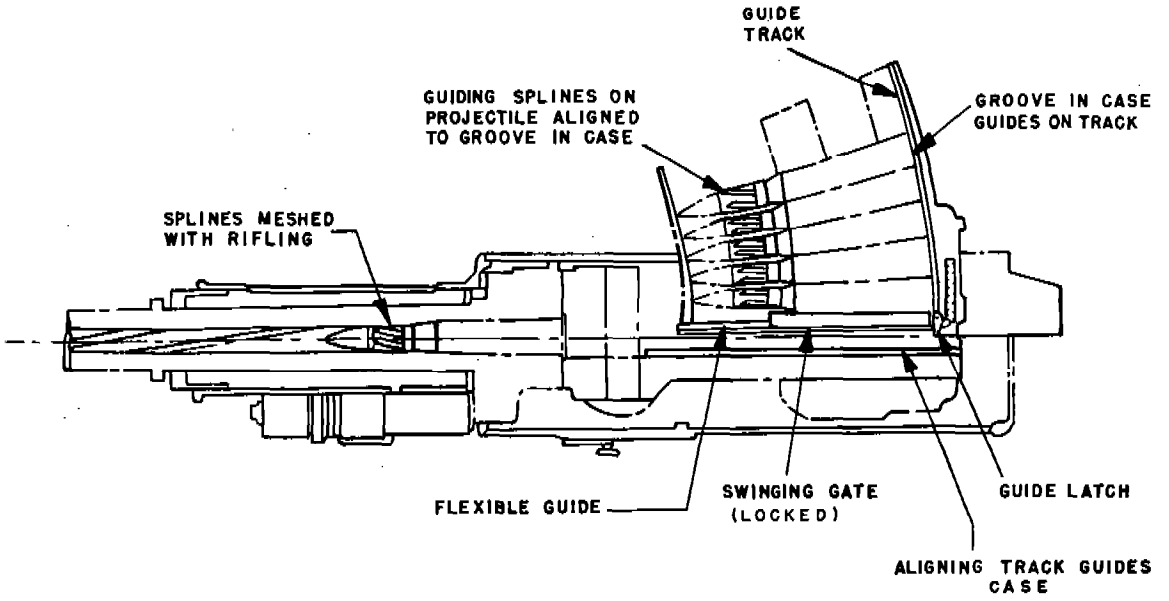
This gun was modified to fire 37-mm pre-engraved ammunition by using six grooves of 0.030-in. depth, with the lands pointed on a 30-degree slope at the origin of rifling and by changing the feeding mechanism to prevent rotation of the previously indexed round. The projectile had six corresponding splines pointed with a 30-degree slope to match the lands. They were aligned in the case so that proper indexing of the case would automatically index the round. The case was the standard 40-mm case, necked to fit the 37-mm pre-engraved projectile. A guiding groove was cut in the base to guide the case on a vertical aligning track. An extension of this groove was cut in the edge of the flange to guide the case along a horizontal track in the tray. The complete rounds[f] assembled in the clip are shown in Figure 7.

The feed mechanism was modified by insertion of guiding tracks to maintain alignment of the rounds. A vertical track was mounted on the base guide to engage the slot milled in the base of the case, as it

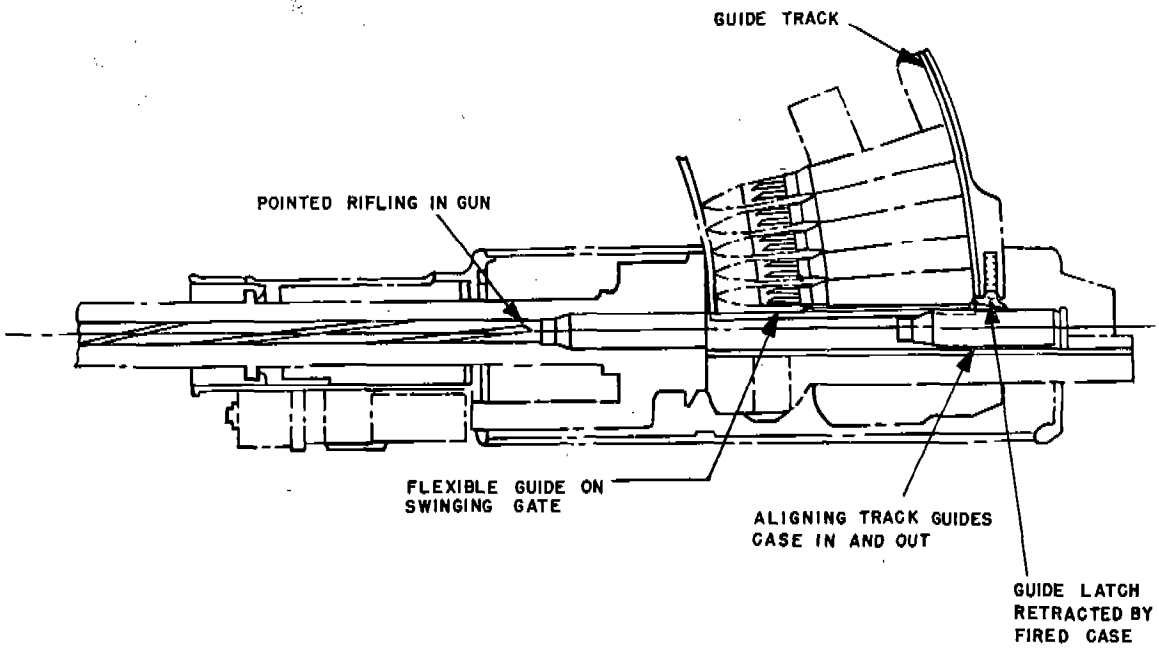
[f] A single round and separate projectile are pictured in Chapter 31 (Figure 18).

CONFIDENTIAL

FOR AUTOMATIC FIRING OF PRE-ENGRAVED PROJECTILES IN 40-MM MOUNT



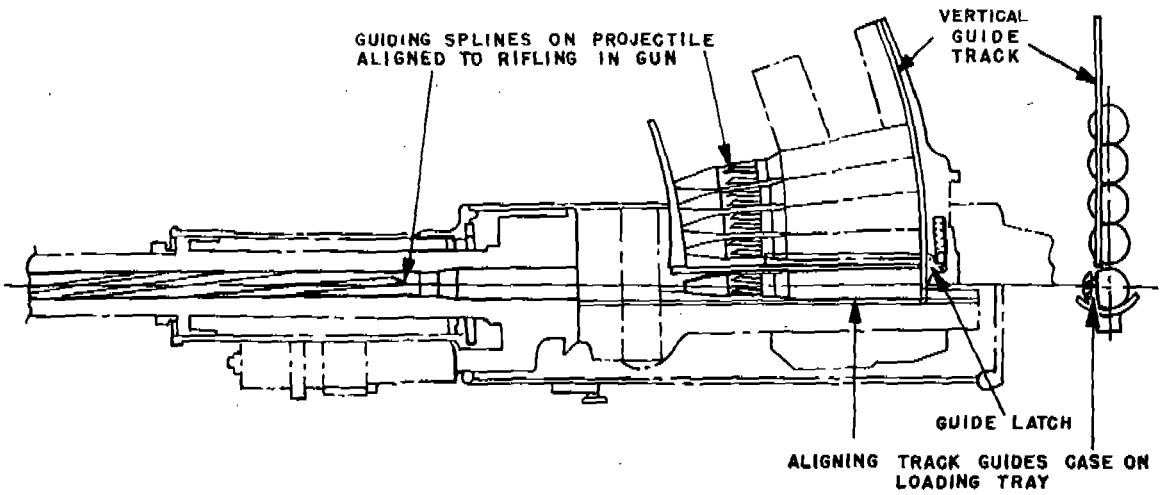
FIRST STAGE – GUN LOADED



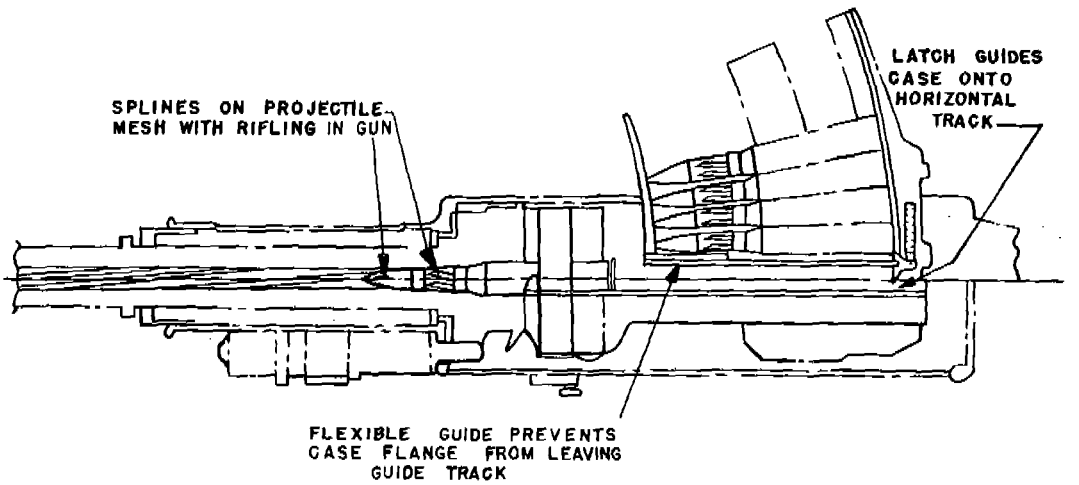
SECOND STAGE-CASE BEING EJECTED

FIGURE 8A. First two stages in the operation of the automatic loading mechanism for 37-mm pre-engraved ammunition. (This figure has appeared as Figure 41 in NDRC Report No. A-448.)

moved downward. A similar track was mounted on the feed tray and extended in sections on the breech ring and breech block to engage the groove in the edge of the flange. Thus while the round was moving vertically to the feed tray it was guided by one track and groove, and by another track and groove while moving horizontally. A spring-loaded guide latch acted as an extension of the vertical track to align the case during the transition from the vertical to the horizontal track. While the round was being rammed



THIRD STAGE – CARTRIDGE ON LOADING TRAY



FOURTH STAGE – CARTRIDGE BEING RAMMED

FIGURE 8B. Last two stages in the operation of the automatic loading mechanism for 37-mm pre-engraved ammunition. (This figure has appeared as Figure 41 in NDRC Report No. A-448.)

by the feed rollers, a flexible guide above the case prevented the case flange from leaving the horizontal guide track. Figure 8 shows four stages in the firing, ejection of an empty case, and chambering of a new round.

This work was not completed under NDRC auspices. It was continued during 1946 on an Army contract[5] with the plan that the mechanism will be tested for functioning of pre-engraved ammunition under automatic firing conditions.

[5] Contract W-36-034-7380 with the Franklin Institute.

Chapter 29

SABOT-PROJECTILES[a]

By *J. S. Burlew*[b]

29.1 THE SABOT PRINCIPLE

29.1.1 Introduction

THE DEVELOPMENT of sabot-projectiles was one of several projects undertaken by Division 1 in its endeavor to attain higher useful muzzle velocities than were attainable with conventional projectiles fired from conventional guns. A sabot-projectile may be fired from a standard gun interchangeably with standard rounds without alteration to the gun or change in the normal powder pressure. It was this feature of sabot-projectiles that made their development seem especially worth while at the beginning of this country's participation in World War II. The use of heavier armor by the Germans, as has been brought out in Chapter 1, had created a need for higher velocity armor-piercing projectiles, in order to increase the penetration at battle ranges of existing guns.

The hope that this need might be met most quickly by firing sabot-projectiles from existing guns led NDRC to focus attention on their development. Although these projectiles were not developed in time to be used by American forces during the war, the latest tests indicated that a 90-mm sabot-projectile could be made so that its accuracy would be as great as that of the standard projectile, while at the same time it would have greater armor penetration because of its higher velocity.

29.1.2 General Description

A sabot-projectile is one that separates into two or more parts after leaving the muzzle of the gun. One or more parts comprising the *sabot* are discarded, while the projectile proper (referred to as the *subcaliber projectile*) proceeds along its trajectory.[c] Figure 1 is an exploded view of the individual parts of a sabot-projectile of the same general design as that described in Section 29.3.4.

The muzzle velocity of a sabot-projectile is greater than that of the projectile of normal weight for the same caliber gun, when the powder charge is the same, because of the reduced mass of the projectile. The mere attainment of increased muzzle velocity is not particularly difficult, but by itself it is of no practical value. In order for the hypervelocity sabot-projectile to be useful, it must have a good form factor and satisfactory stability, so that it retains a higher velocity all the way to the target. Therefore the first step in the program for the development of sabot-projectiles by Division 1 was a study (described in Section 29.2.2) to determine the design limitations for the subcaliber projectile in order that satisfactory stability might be attained when it is fired from existing guns having standard twist of rifling.

29.1.3 Advantages and Disadvantages of Sabot-Projectiles[190]

VALUE FOR ARMOR PENETRATION

The application of the sabots with which Division 1 was concerned for the most part was intended to increase the armor penetration obtainable with guns already in service use.[100] Even though a considerable portion of the energy of a sabot-projectile is lost be-

[a] As originally planned, this chapter was to have been a critical analysis of the problem of designing sabot-projectiles, illustrated by examples drawn from the experience of Division 1 contractors. It was not possible to find an author who had the time to do this, and therefore the Editor has supplied merely a résumé of what Division 1 did in this field, with references to the formal NDRC reports in which further details may be found. He is indebted to Mr. J. McG. Millar (formerly Assistant Physicist, Geophysical Laboratory, Carnegie Institution of Washington) and to Mr. Edmund Bainbridge (formerly Engineer, NDRC Engineering and Transition Office) for helpful suggestions concerning the material in Section 29.1 and to Mr. Millar for a draft of Section 29.2.2.

[b] Technical Aide, Division 1, NDRC. (Present address: Geophysical Laboratory, Carnegie Institution of Washington.)

[c] In many reports dealing with sabot-projectiles the caliber of the subcaliber projectile has been included in the designation of the caliber of the projectile, as for instance: "11–20 mm," "75–57 mm," and "105–75 mm." No standard designation has been established. In the present chapter such designations have not been used, for in the light of the later development work on sabot-projectiles it does not seem necessary to place special emphasis on the diameter of the subcaliber projectile. It is no more fundamental a property than some other characteristics, such as the weight, which are not included in the designation. Furthermore, to refer to a sabot-projectile simply as a 90-mm one, instead of as a "90–56 mm" one, for example, emphasizes the important point that as far as use is concerned the sabot-projectile is interchangeable with other rounds for the same gun.

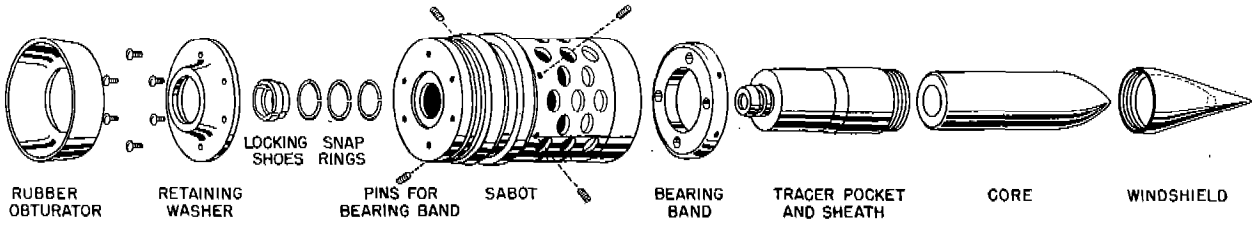


FIGURE 1. Exploded view showing the separation of the various parts of a sabot-projectile, based on the design of the 90-mm projectile shown in Figures 7 and 8.

cause of the high ratio of charge to projectile weight[37] and because of the nonpenetrating parts of the sabot, the remaining energy is concentrated over a much smaller area of the armor plate.

A steel subcaliber projectile does not show a large advantage for armor penetration.[14,42] By the proper choice of diameter of the subcaliber projectile in a gun with favorable twist, an increase in armor penetration of about 20 per cent over the standard projectile is obtainable, provided that shatter (Section 9.2) does not decrease its effectiveness.

As is pointed out in Section 9.2, the properties of good tungsten carbide are such that it is superior to steel for armor penetration, especially at hypervelocities. The optimum size core depends on a multitude of factors, such as the best length of core relative to the diameter, the weight of the sabot, the twist of rifling of the gun, and the range at which the maximum amount of armor penetration is desired.[14] Some of these factors are discussed in Section 33.2.4.

OTHER ADVANTAGES

There are several other uses of sabot-projectiles which have been considered by Division 1 in a preliminary fashion. One of these is to effect an increase in the maximum range of the projectile over that of the standard projectile for a given gun.[42] Thus it has been computed that shooting a 10-in. projectile from a 16-in. gun would increase the range of this gun at least 12,000 yd, that is, from 49,000 to 61,000 yd.

Another advantage is the possibility of shortening times of flight of medium-caliber projectiles at long ranges. By the use of fin stabilization it has been computed that times of flight at ranges of the order of 30,000 yd could be reduced by 30 to 40 per cent. Although the projectile proposed would probably be effective for direct hits, there might be no advantage in shells with proximity or time fuzes because of the reduced high explosive charge.[41] In this connection see Section 33.2.3.

In addition, a sabot may make possible the use of a lighter gun for firing a given projectile at a given velocity. This advantage would of course be especially important for aircraft armament or for airborne equipment.[d] A complex calculation[205,551] involving ballistics, strengths of materials, and carriage weight, among other factors, would be required for its evaluation for any particular use.

EFFECT ON EROSION

So far there have not been enough sabot-projectiles tested to determine the rate of erosion of a gun firing such ammunition; but analysis[48] of its ballistics indicates that the erosion might be less than that of a gun firing conventional ammunition. Another possibility is that of shooting fin-stabilized projectiles from a smooth bore gun (Section 29.2.2). The latter feature might simplify construction of the gun and decrease the erosion.

DISADVANTAGES

There are of course disadvantages to a sabot-projectile. The principal one is the danger to friendly troops. If a sabot is a centrifugal type (Section 29.2.3), the parts fly off in a cone with an apex angle determined in large part by the twist of rifling. It is approximately 14 degrees for a twist of 1:25. Although their range is short, there is still a distinct possibility that the fragments will hit friendly troops. The danger from the axial type (Section 29.2.3) is less since all parts travel in a line parallel to the trajectory, but on hitting the ground ricochets at any angle are possible. However, for use in tanks and airplanes (especially jet-propelled ones) these objections might be minor.

[d] This objective was achieved to a limited extent in the design of a sabot for firing the 57-mm projectile, M86, from the 105-mm howitzer M3, as described in Section 29.3.5. The 57-mm gun, M1, mounted on a field carriage weighs 2,700 lb, whereas the 105-mm howitzer, M3, on its mount weighs only 2,495 lb.

In comparison with a skirted projectile fired from a tapered bore gun, it is brought out in Section 33.2 that a sabot-projectile has the disadvantage of losing some of its energy in the discarded sabot parts. This disadvantage is counterbalanced by the fact that a sabot-projectile can be fired from a standard gun interchangeably with regular ammunition. Hence each type of subcaliber projectile is likely to have its own field of usefulness in the future.

29.2 DESIGN OF SABOT-PROJECTILES

29.2.1 General Requirements

A complete sabot-projectile must combine a subcaliber projectile suited to its purpose (either armor penetration or high-explosive use) with a sabot that will make it possible to fire the subcaliber projectile from the gun as effectively as possible. One important feature is stability (discussed in the next section), the neglect of which seems to have been responsible for the lack of success with the previous attempts to develop sabot-projectiles.

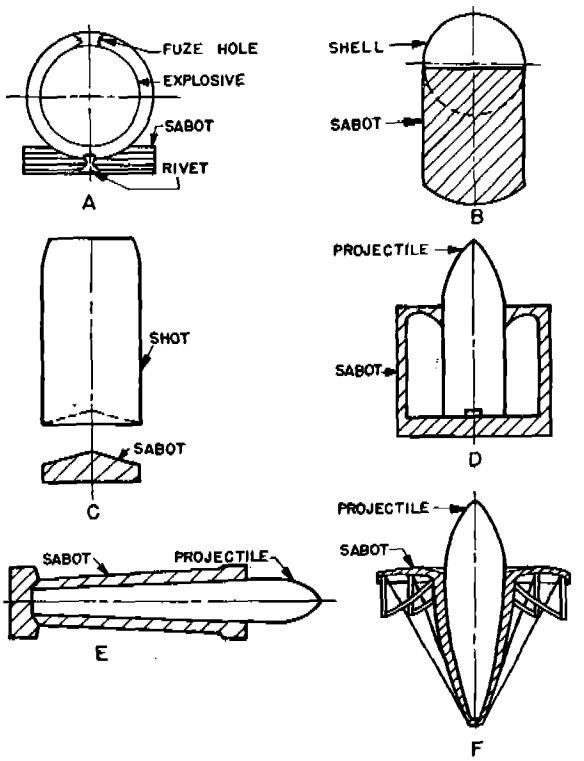


FIGURE 2. Early sabot-projectiles. (This figure has appeared as Figure 1 of NDRC Report No. A-234.)

A number of patents[212] on sabots for subcaliber projectiles have been granted. Although detailed specifications are in general lacking, the representative projectiles illustrated in Figure 2 indicate a complete disregard for the principles of interior and exterior ballistics.[42]

The sabot itself must be so designed that:[41] (1) it is light in weight; (2) it is strong enough to accelerate the projectile without breaking up in the bore, even when fired from a worn gun; (3) it is gas tight; (4) it communicates sufficient angular momentum to the projectile to give it full spin; (5) it is disengaged from the subcaliber projectile with negligible influence on the trajectory; (6) it holds the projectile firmly, for convenience in handling the ammunition; and (7) it can be manufactured easily and at a reasonable cost.

29.2.2 Stability of Sabot-Projectiles[14,42]

The theory of the stability of subcaliber projectiles in general is presented in Section 8.3. As pointed out there, it is desirable that the stability factor be at least 1.5 in order to allow for variations in atmospheric conditions and to provide adequate damping of the yaw. If a gun is to be designed for shooting a particular projectile by means of a sabot, the twist of rifling can be adjusted so as to give the necessary stability; but if a sabot-projectile is to be shot from an existing gun, the stability requirements imposed by the twist of rifling restrict the diameter and design of the subcaliber projectile.

Figure 3 shows the relationship between the diameter of the subcaliber projectile and the twist of rifling of the gun when the stability factor of the pro-

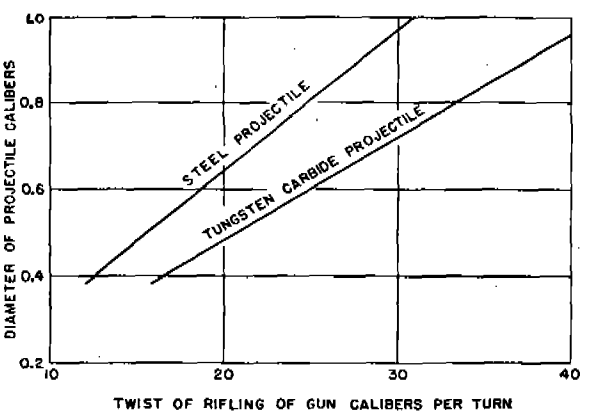


FIGURE 3. Relationship between the diameter of a subcaliber projectile and the twist of rifling of a gun for a stability factor of 1.5. The design of the projectile is similar to that of a standard armor-piercing one.

jectile is 1.5 and its design is similar to that of a standard armor-piercing projectile. This figure is based on the 57-mm APC projectile, M86, and would be correct only if the various sizes of subcaliber projectiles were exactly scaled models of this particular projectile and if the velocities were all 2,800 fps. If another such graph were based on an armor-piercing projectile of similar design, or if account were taken of the higher velocities obtainable with the subcaliber projectiles, the differences would be relatively minor.

If the subcaliber projectile is made of a much denser material, such as tungsten carbide, but is otherwise similar to standard armor-piercing projectiles, a much greater reduction of diameter is possible than with a steel subcaliber projectile. In practice, the subcaliber projectiles using tungsten carbide have had steel sheaths around a tungsten carbide core. (For example, see Figure 8). Thus it has proved practicable to obtain only a part of this advantage with respect to stability.

If a standard-shaped projectile of a particular diameter would be unstable when fired from a given gun by means of a sabot, it may possibly be made stable in this use by changing its center of gravity. This change can be effected by changing the shape of the windshield, by shortening the body of the projectile, or (in the case of tungsten carbide cored projectiles) by moving the core forward. However, the first two solutions result in greater retardation while the last is restricted by the geometry.

Another possible way of increasing the stability of such a combination is the use of fins canted parallel to the rifling of the gun. This method would be especially applicable in a sabot-projectile since there would be room in the sabot for the fins. In a few preliminary tests by Division 1 trouble was encountered in holding the fins on the projectile and so the results were inconclusive.[41] The Germans tried finned sabot-projectiles[305,387,392] during World War II, but their effectiveness has not yet been evaluated.

Designs of subcaliber projectiles suitable to be fitted with sabots and fired from 76-mm and 90-mm guns with a twist of 1:32 were prepared at the Ballistic Research Laboratory, Aberdeen Proving Ground.[209]

29.2.3 Types of Sabot Release

Disengagement of the sabot from the subcaliber projectile requires the application of a differential force at about the time the projectile leaves the muzzle of the gun. Three different types of force have been used: the centrifugal force of the rotating sabot itself, the propulsion of high-pressure gas in a cavity at the base of the projectile, and the resistance of the atmosphere acting on the sabot. Two essentials are that the applied force not disturb the flight of the projectile to such an extent that its accuracy is impaired and that the disengagement always takes place sufficiently close to the same point in the trajectory that the range of the projectile is not affected. If the gun is fitted with a muzzle brake, an added requirement is that the disengagement occur in such a manner that there is no interference with the brake. In practice this meant that it be delayed until after the sabot-projectile had cleared the brake, for the U. S. Ordnance Department was unwilling to increase the clearance between the projectile and the baffles in the brake (which would decrease the efficiency), as was done by the British.[394]

A theoretical analysis of types of sabot release at the beginning of Division 1's interest in the subject led to the conclusion[41] that the use of centrifugal force to disengage the sabot was preferable. It was considered that it was less likely to cause perturbation of the trajectory because it could be applied symmetrically in a radial direction, whereas the other two forces, applied along the axis of the projectile, would exaggerate any yaw that happened to be present when separation occurred. Firings with 20-mm projectiles confirmed this hypothesis;[41] but later experience with larger caliber ones showed that satisfactory accuracy could be achieved with axial release under certain conditions, as described below.

Centrifugal Release

The sabots that were released centrifugally were made of two principal parts: the sabot body and the base. It happened that the early models made both by the Geophysical Laboratory[41] and by the University of New Mexico[42] had plastic bodies and metal bases. The plastic body, which was usually just a sleeve that fitted tightly over the subcaliber projectile, was weakened by longitudinal slots, in order that it would break apart after the projectile left the gun. In the 20-mm size (Section 29.3.1) the base was a solid Dural plate to which the body was threaded, whereas in the 75-mm sabots (Section 29.3.2) and the 105-mm sabots (Section 29.3.5) the base was a steel ring screwed on the rear end of the subcaliber projectile and it had radial slots so that it too was broken into several pieces by centrifugal force.

[redacted]

When it was found desirable to substitute a light-alloy for plastic in the body of the 75-mm and 105-mm sabots (see Section 29.2.4), the body was made in four segments that were held together by a steel ring at the forward end, termed a bourrelet band. This ring was of such strength that it was broken by centrifugal force, and thus the segments of the body were released.

A serious difficulty with the simple type of centrifugal release just described was that the sabot began to disintegrate as soon as it emerged from the muzzle, and hence would interfere with a muzzle brake. In an effort to prevent this action with an all-metal sabot for the 76-mm gun, which used a muzzle brake, several types of delayed centrifugal release were tried. In the simplest, the segments of the sabot body were held in place by a ring at the rear that was just strong enough to expand slowly by centrifugal action after it had cleared the muzzle brake, until finally it broke and released the segments. A preferable arrangement, which was adopted for the 76-mm sabot-projectile Model 3-76-EH described in Section 29.3.3, is described in the paragraph "Combined Axial and Centrifugal Release."

Release by Gas Pressure

A sabot may be blown off the subcaliber projectile by means of compressed gas confined in a space between the rear face of the projectile and the base of the sabot. In some experiments[100,133] this gas was some of the propellant gas itself, which entered the space through a small hole while the gas pressure was near its maximum value; and in other experiments[41] it was obtained by the explosion of a small charge of black powder placed in the space and ignited by the powder gases. Neither of these methods was tried extensively, because the preliminary trials were unpromising, the projectiles having been very inaccurate. Inasmuch as the first trials of axial release sabots made at about the same time gave equally unsatisfactory results, whereas later efforts were successful, this method would seem to deserve further consideration. It was used successfully in combination with the method of axial release in a sabot designed in Canada for both the British 6-pounder[394] and 17-pounder guns.[100]

Axial Release

In the method of release just described the sabot separates from the subcaliber projectile by movement along their common axis, but the term axial release has been reserved for the type of release that makes use of air resistance to separate them. In order to make this type of release practical there must be some provision for locking the two parts together to prevent separation both during handling prior to firing and also during passage down the bore of the gun.

One type of lock consisted of a series of shear pins extending through the sabot body into the subcaliber projectile, so designed that they broke under setback.[133] A more satisfactory method of locking the sabot to the subcaliber projectile was to have a tracer pocket on the latter extend through the center of the steel base plate of the sabot and then to attach some sort of retaining ring to this projection. First tried on a 105-mm sabot-projectile,[236] this locking means was later applied to other sizes and types.

Of the different retaining rings tried, the most satisfactory was a split steel ring designed to open under the influence of centrifugal force. This type of retaining device was used for both the 76-mm sabot-projectiles of Design 3-76J (Section 29.3.3) and the "deep-cup" 90-mm sabot-projectile (Section 29.3.4). Thus, although the final separation of such a sabot from its subcaliber projectile is caused by differential air resistance, the unlocking is centrifugal.

Earlier experiments with deep-cup sabots for 20-mm projectiles[41] and for 57-mm ones[42,100] were unsuccessful, because of large yaw after separation, whereas cup-type sabots developed for a 90-mm gun (Section 29.3.4) separated successfully. The reason for this difference in behavior is not clear from the record.

Combined Axial and Centrifugal Release

In one type of 76-mm sabot-projectile intended to be fired through a muzzle brake, separation occurred in two stages.[100] First, axial drag caused the base plate of the sabot to move rearward with respect to the sabot body, which was made of segments of light alloy. These segments were held at their forward ends under a bourrelet band of steel, which was strong enough to resist the centrifugal thrust until the rear ends of the segments were released. Then the added thrust that occurred when the rear ends were moved outward by centrifugal force broke the bourrelet band.

With this design also the initial locking of the sabot to the subcaliber projectile was very important. As is brought out in Section 29.3.3, 76-mm projectiles made

[redacted]

according to University of New Mexico designs performed satisfactorily when fired at Aberdeen Proving Ground,[223] whereas another group made by the Remington Arms Company and also fired at Aberdeen[223] failed, in some cases by breaking up in the bore. The only difference in the design of the two lots was the substitution of a garter spring of closely coiled piano wire for a split steel ring threaded to the exterior of the tracer pocket. The spring, which was a less secure type of locking arrangement, apparently permitted separation of the parts at the time of loading or the start of travel, with consequent break-up of the projectile in the bore. This cause of failure was not recognized at the time,[133] because of other doubtful factors that subsequently were better understood.[100]

29.2.4 Materials for Sabot Construction

All the successful designs of medium-caliber projectiles (See Section 29.3) have used steel bases for the sabots. In addition steel was used for the entire sabot of the cup-type developed for the 90-mm gun, as described in Section 29.3.4. This sabot-projectile has a very low ratio of weight of subcaliber projectile to that of the entire projectile (see Table 1, p. 567). It would seem, therefore, that an extensive re-evaluation of design factors is necessary before it can be certain that an all-steel sabot can be made as light as those of other materials.

Light Alloys

Both Dural (aluminum alloy) and Dowmetal (magnesium alloy) have been used successfully for the body of a sabot-projectile in the 76-mm size.[100] Dural was also used for the base of the sabot for 20-mm projectiles.[41]

These alloys are easily eroded by hot powder gases, and therefore it is essential that streaming of the powder gases over them be prevented by proper obturation. Furthermore, these alloys are not strong and hard enough to resist engraving at the bourrelet. To prevent it, sabots of these alloys need to have steel bourrelet bands, such as used with the 76-mm projectiles (Section 29.3.3).[100]

Plastics

An examination of the properties of materials of construction led to the conclusion[54] in 1943 that organic thermosetting plastics were the only nonmetallic materials having sufficient strength to be used for sabots. Sabot bodies made of this kind of plastic have given satisfactory performance when fired soon enough after manufacture so that no dimensional change of the plastic took place.[41,42] After exposure to a humid atmosphere, however, the plastics used for 75-mm and 105-mm sabot-projectiles swelled to such an extent that the rounds could not be fired.[100]

Tests were made at the Geophysical Laboratory of a number of phenol-formaldehyde plastics with fiber or paper filling preparatory to using them for some 20-mm sabots. Exposure for 3 months to extremes of humidity (1% and 90%) at a temperature of 104 F caused linear dimensional changes of about $\pm$ 0.3 per cent. For a 90-mm sabot this would correspond to a change in diameter of $\pm$ 0.01 in., which is larger than the tolerance permitted. The sliding bourrelet mentioned in Section 29.3.1 might be a means of allowing for such a change in diameter.

Experimental all-plastic sabots of various designs were fired from both a 57-mm and a 75-mm gun. Most of them were machined and threaded on the subcaliber projectile, but a few of them were molded directly on it. The results were erratic, only a few rounds having shown satisfactory flight.[54] A critical examination of the work has led to the conclusion that "it appears improbable that these [laminated] plastics are strong enough to be used in all-plastic sabots for spin-stabilized projectiles to be fired from present day guns."[100]

29.2.5 Obturation

The experience gained during the development of a sabot-projectile for the 90-mm gun, M1A2 (Section 29.3.4) confirmed the earlier experience of the British in the development of a sabot for the 6-pounder gun[394] that effective obturation is very important in promoting the best accuracy. If parts of the sabot are made of Dural or Dowmetal, obturation is also essential to prevent gas-washing of those parts with consequent failure of the projectile in the bore.

29.3 SABOT-PROJECTILES DEVELOPED BY DIVISION 1

29.3.1 Sabot-Projectiles for 20-mm Gun

The final design of sabot-projectile developed by the Geophysical Laboratory[41] in tests with the 20-mm Hispano-Suiza gun was of the centrifugal release type



(Section 29.2.3). The plastic body, which was a close fit on the core, was screwed to the Dural base. Type CW6, shown in Figure 4, had an 11-mm subcaliber projectile of heavy alloy (to simulate tungsten carbide). In another type the subcaliber projectile was steel. A special feature of these projectiles was the sliding bourrelet, which was found to be essential for accuracy. In the early models it had been on the outside, but the arrangement shown in Figure 4 has the advantage that it avoids having an exterior groove in which dirt might collect. Handmade projectiles of these designs performed reasonably well when fired single shot. A muzzle velocity of 4,130 fps was attained with the tungsten carbide core. The dispersion of the best rounds was about 40 per cent greater than that of standard ammunition fired from the same gun.

The original objective of this program had been to work out a satisfactory sabot mechanism in the 20-mm size and then to adapt it to larger caliber guns for use against tanks. Accordingly, this design was adapted to a sabot with which to fire the 57-mm APC projectile, M86, from a 3-inch gun. These sabot-projectiles were used in firings at Aberdeen Proving Ground to test the armor penetration of the M86 projectile at high velocities,[235,242] after preliminary firings[206,232,233] had demonstrated the feasibility of this plan. Another adaptation of the 20-mm design was used for the first design of a 105-mm sabot-projectile with a 75-mm subcaliber projectile.[e] Partially satisfactory results were obtained in preliminary firings[236] at Aberdeen Proving Ground.

An attempt was made to develop a design of 20-mm sabot-projectile that could be manufactured by mass production methods, for possible use in the 20-mm Hispano-Suiza gun. The subcaliber projectile was the 15-mm steel core for the caliber .60 ammunition then under development by Frankford Arsenal. For the sake of simplifying the manufacture of the plastic sabot body no sliding bourrelet was used. It was not possible to mold the plastic body with a small enough tolerance, and difficulty was experienced in fitting the Dural bases to the sabot bodies. Nevertheless a small lot of these projectiles (Model C5b) were prepared for preliminary firing tests at Aberdeen Proving Ground to determine the exterior ballistics[207,237] of these projectiles and the interior ballistics[234] of the gun firing them. It was concluded that the poor efficiency in armor penetration that was observed was due to slippage between the subcaliber projectile and the base. Furthermore, as mentioned in Section 29.2.4, considerable variation in dimensions was observed when various plastics (intended for the sabot body) were exposed to different conditions of humidity.[100] Thereupon this project was abandoned.

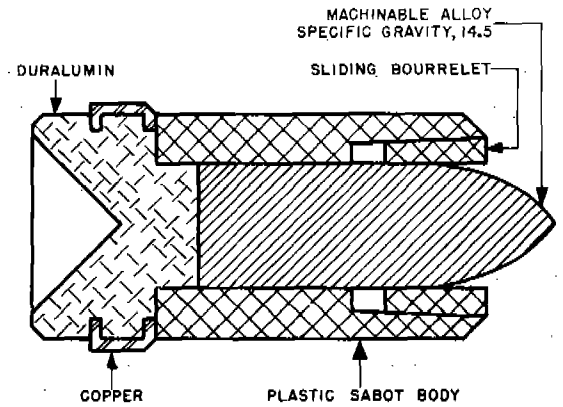


FIGURE 4. 20-mm sabot-projectile, Model CW6, with sliding plastic bourrelet and dense core, employing centrifugal release. (This figure has appeared as part of Figure 9 in NDRC Report No. A-233.)

29.3.2 Sabot-Projectiles for 75-mm Gun and Howitzer

The sabot-projectiles for the 75-mm tank gun, M3, also were of the centrifugal-release type (Section 29.2.3) with a plastic body that was a press-fit on the subcaliber projectile. The base of the sabot was a steel ring screwed to the base of the subcaliber projectile. These projectiles were developed by the University of New Mexico[42,100] following preliminary experiments with sabot-projectiles fired from a Navy 6-pounder gun (caliber: 57 mm).

The core of Model 28-75D, shown in Figure 5, was a slightly modified 57-mm APC projectile, M86, weighing 7 lb. A lot of these projectiles was fired at Aberdeen Proving Ground[238] at a muzzle velocity of about 2,800 fps compared with 2,030 fps for the standard 75-mm APC projectile, M61. Although the accuracy and other features of performance were satisfactory, the using Services decided that at that time (just after the Normandy invasion) there was no tactical use for this projectile for the 75-mm gun, especially in view of the expectation that tanks would soon be equipped with 76-mm guns having a muzzle velocity of about 2,600 fps for a 15-lb projectile.[100]

[e] These projectiles were supplied by the Geophysical Laboratory. Because better facilities for an extensive development existed at the University of New Mexico, the 105-mm project was continued there, with the results described in Section 29.3.5.

About 6 months later a slight modification of this design was prepared for use in the 75-mm pack howitzers, M1A1, M2, and M3. Preliminary firings were made at Aberdeen Proving Ground (July 1944) with satisfactory results. A number of these projectiles were forwarded to the Armored Board, Fort Knox, Kentucky, for test in comparison with standard ammunition. By that time it had been learned that plastic sabots for the 105-mm howitzer (Section 29.3.5) had swelled from exposure to a humid atmosphere, and this 75-mm ammunition was examined. It also had



FIGURE 5. 75-mm sabot-projectile, Model 28-75D, with plastic sabot body and steel sabot base ring that separate centrifugally. (This figure appeared in a progress report from the University of New Mexico on Contract OEMsr-668.)

swelled to such an extent that it could not be loaded in the gun. Drawings were made of a modified design in which light alloy would be substituted for the plastic,[100] but these projectiles were not constructed.

Previously an entirely different type of all-metal 75-mm sabot-projectile using the 57-mm projectile, M86, for the subcaliber part had been made for Division 1 by the Budd Wheel Company and three rounds had been fired at Aberdeen Proving Ground.[239] The test was inconclusive and no further development was made.

29.3.3 Sabot-Projectiles for 76-mm Gun

When the Army Ordnance Department requested Division 1 to develop a sabot-projectile with tungsten carbide core for the 76-mm gun, M1A2, it was decided to make this sabot an all-metal one. The design was complicated by the fact that the projectile had to pass through a muzzle brake with only a slight clearance.

In order to satisfy the latter requirement, the design finally developed at the University of New Mexico,[100] which is shown in Figure 6, employed the delayed centrifugal release described at the end of Section 29.2.3. The core was a tungsten carbide one similar to that used by the British in a sabot-projectile for the 17-pounder gun (caliber: 3 in.). Determinations of velocity vs time of flight and of range vs time of flight were made at the New Mexico proving ground by the method of tracer photography[57] described in Section 8.6.

A first lot of these projectiles (Design 3-76EH) was fired at Aberdeen Proving Ground with satisfactory results[223] at muzzle velocities slightly above 3,600 fps. X-ray photographs[210] were made of some rounds to study the separation of the sabot from the subcaliber projectile. The design was modified in a number of minor details, the most important of which was the substitution of a steel retaining ring (Section 29.2.3) for a Dowmetal one. Projectiles of this design (3-76J) were also fired at Aberdeen Proving Ground with satisfactory results.[223]

Subsequently the Remington Arms Company modified the design in an attempt to develop a model suitable for mass production.[100,133] As mentioned in Section 29.2.3, this model when fired at Aberdeen Proving Ground[223] (where it was designated "76-mm, T23") failed in the bore, presumably because the garter spring that had been substituted for the steel retaining ring did not hold the parts together at the beginning of travel. Although a number of successive modifications were fired at Aberdeen Proving Ground,[223] in none of them was this fault corrected, and all were erratic in their behavior.

An entirely different design (76-48-R2) was tried later.[343] Although it was patterned after the later designs of 90-mm deep-cup sabots (Section 29.3.4), it was inaccurate. The reason was not determined.

29.3.4 Sabot-Projectiles for 90-mm Gun

The experience gained with the 76-mm sabot-projectile (Section 29.3.3) was applied to the development of a sabot-projectile for the 90-mm gun, M1A2, which also used a muzzle brake. The first such projectile, constructed by the Remington Arms Company[133] from a design prepared by the University of New Mexico,[100] was similar to the latter's

76-mm projectile described in the previous section, in that it had a segmented sabot body of Dowmetal. To it was fitted a copper obturator. This model failed when fired at Aberdeen Proving Ground,[222] as did a number of successive modifications of it,[222] which were designated as the "90-mm, T32 series." The reason for these failures was later discovered to be the separation of the sabot from the subcaliber projectile in the bore at the beginning of travel, as had happened also with the Remington 76-mm models.[100,133]

An entirely different type of sabot (the "deep-cup" type described in Section 29.2.3) was then developed for this gun by the Remington Arms Co.[133] At first the firings were carried out at Aberdeen Proving Ground,[222] where these projectiles were designated as the "90-mm, T38 series," and later at a private range at Pine Camp, N. Y.

The final design (90-56-R13), shown in Figures 7 and 8, used a subcaliber projectile that consisted of a 6-lb tungsten carbide core contained in a steel sheath. Reference should also be made to Figure 1, which is a schematic representation of this design. On the basis of a single shoot of 5 rounds from a new gun, this was by far the most accurate sabot-projectile of any size developed by Division 1. The five shots, which had a muzzle velocity of 3,383 fps, struck within a rectangle 1.3 ft wide and 0.8 ft high at 1,000 yd. This accuracy is essentially the same as that obtained with standard 90-mm ammunition. A corresponding model (90-58-R84) was made up with an 8-lb core, but there was time to fire only two such projectiles before the close of the project. Their performance was satisfactory.[133]

The high degree of accuracy achieved with these 90-mm projectiles was attributed to several features of the design:

1. The sabot was long enough relative to its diameter to avoid any tendency toward cocking in the bore.

2. An effective rubber obturator prevented escape of powder gases past the sabot at the beginning of travel, which might have heated and thereby weakened the bourrelet or which might have pushed the projectile out of line with the axis of the bore.

3. A pair of sintered iron rotating bands had adequate strength to spin the projectile. (It should be noted, however, that there was no opportunity to test this final model in a worn gun tube.)

4. The subcaliber projectile was firmly attached to the sabot, which prevented lateral movement during loading and during the beginning of travel and which also insured that full spin was imparted to the subcaliber projectile.

5. The middle bearing (which was just to the rear of the center of gravity) in conjunction with the bourrelet ring maintained concentricity of the subcaliber projectile with respect to the sabot and hence with respect to the axis of the gun.

6. When separation did occur, considerable clearance resulted from only ½ in. of relative motion along the axis; and hence there was no appreciable



FIGURE 6. 76-mm sabot-projectile, Design 3-76EH, with light-alloy sabot body and steel base plate that separate by axial and delayed centrifugal release. (This figure has appeared in NDRC Report No. A-461.)

CONFIDENTIAL

interaction between the sabot and the subcaliber projectile.

During the design and construction of the successive models of 90-mm sabot-projectiles attention was paid to production engineering. As a result, at the end of the project it was possible to make recommendations for the equipment and manpower required to produce these projectiles at a rate of 2,000 a day.[134]



FIGURE 7. 90-mm all-steel sabot-projectile, Model 90-56-R13, with tungsten carbide core, employing axial release. (This photograph has appeared in NDRC Report No. A-461.)

29.3.5 Sabot-Projectiles for 105-mm Howitzer

The 105-mm howitzer, M3, is a lightweight weapon developed for the use of airborne troops. Ordinarily it fires a 33-lb HE shell at a muzzle velocity of 1,020 fps or less, depending on the range desired. The use of a sabot-projectile seemed to offer an opportunity to provide a moderately high-velocity AP shot for the same gun and also a smaller HE shell having a high enough muzzle velocity to be usable against "point" targets.

The two sabot-projectiles developed at the University of New Mexico for this howitzer were of the same general design and differed chiefly in the subcaliber projectiles.[f] One was the 57-mm APC projectile, M86; the other was the 3-in. HE shell, M42A1. For the former it was necessary to determine the stability factor, using the experimental method currently in use by the Ballistic Research Laboratory, Aberdeen Proving Ground,[177] and then to shorten the windshield on the projectile in order to increase the stability factor to a value of 1.5.[100]

The sabot used for these projectiles was similar to that of the 75-mm Model 28-75D (Figure 5). Both the AP projectiles (Model 2-105R) and the HE projectiles (Model 3-105B) were fired at Aberdeen Proving Ground with satisfactory results.[224] Then about 100 of each type were sent to the Infantry Board, Fort Benning, Georgia, for Service acceptance tests. There difficulty was encountered in loading the projectiles in the gun because of swelling of the plastic sabot bodies. After the excess material had been removed by machining, some of the projectiles were fired. The results were satisfactory, except that the gun hop was excessive. Some AP rounds were also fired from the heavier howitzer, M2. On the basis of all these tests it was decided that there was no further interest in the 105-mm sabot-projectile that used the 3-in. HE shell for its subcaliber projectile. There was some interest in the substitution of light alloy for plastic in the 57-105-mm combination, but the development of sabot-projectiles for the 76- and 90-mm guns pre-empted the available facilities.

29.4 CONCLUSION

The investigation of sabot-projectiles by Division 1 has involved experiments with a wide variety of designs. Whereas this field previously had been regarded by ordnance specialists as unprofitable, these experiments have demonstrated the great potential usefulness of sabot-projectiles. Although none of them reached the final stage of test under combat conditions, there has been accumulated a wealth of basic design data. The outstanding conclusions of the work have been summarized in this chapter; in ad-

[f] A different type of sabot-projectile for the 105-mm howitzer is described in Section 29.3.1.

CONFIDENTIAL

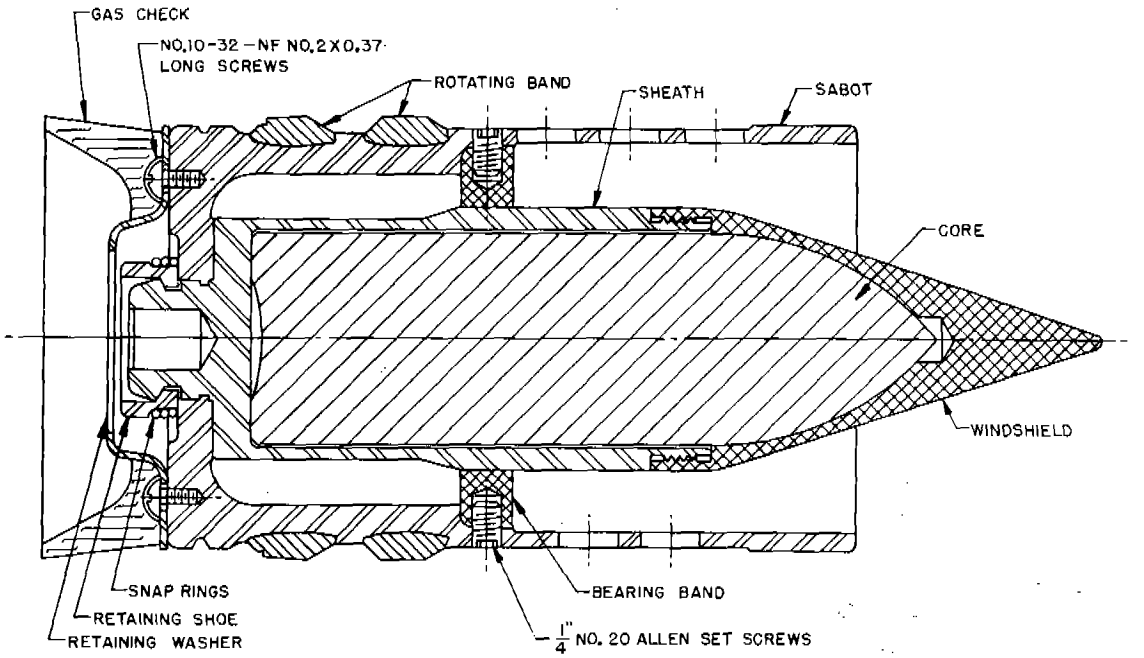


FIGURE 8. 90-mm all-steel sabot-projectile, Model 90-56-R13, with tungsten carbide core, employing axial release. (This drawing has appeared in NDRC Report No. A-461.)

dition to which there are many useful details in the original reports cited.

The characteristics of the final designs of sabot-projectiles of different sizes, which have been discussed in Section 29.3, are given in Table 1. The best accuracy was achieved with the 90-mm one. None of these projectiles was constructed and fired in sufficiently large quantities to determine how serious would be the variation in performance caused by variations in the dimensions of the projectiles from large-scale production. One of the chief purposes of the pilot-plant operations planned for the 90-mm sabot-projectiles was to make available a quantity of projectiles for such tests. This phase of the work was not carried out because of the demobilization of OSRD.

Each of the projectile designs listed in Table 1 has one or more features that is worth further study. Thus the delayed centrifugal release mechanism of the

TABLE 1. Characteristics of final designs of sabot-projectiles developed by Division 1 contractors.

Caliber (mm)	20	75	76	90	105	105
Subcaliber diam. (mm)	15	57	55.9	55.9	57	76
Core diameter (mm)	15	57 (M86)	38.1	45.0	57 (M86)	76 (M42A1)
Core material*	S	S	WC	WC	S	S
Projectile model	C5b	28-75D	3-76EII	90-56-R13	2-105R	3-105B
Gun model	M1A2	M3†	M1A2	M1A2	How, M3	How, M3
Type of release‡	C	C	A-C	A	C	C
Weight of subcal. (lb)	0.147	7.00	5.77	8.06	7.207	12.7
Total weight (lb)	0.207	8.38	7.97	12.50	11.1	15.6
Weight ratio	0.71	0.84	0.72	0.64	0.66	0.81
Muzzle velocity (fps)	3,310	2,800	3,650	3,880	2,660	1,980
MV stand. proj. (fps)	2,615	2,030	2,600	2,650	1,020	1,020
Wt. stand. proj. (lb)	0.36	14.96	15.44	24.11	33.00	33.00
Chamber pr.§ (psi)	48,000	36,000	43,000	38,000	30,000	30,000
Twist of rifling	1:25.58	1:25.58	1:32	1:32	1:20	1:20
Number rounds fired	ca. 50	69	8	5	10	10
Bibliographic ref.	207	41, 100	100, 223	133	100, 224	100, 224

* S = steel; WC = tungsten carbide.

† This projectile was also fired from the 75-mm pack howitzer.

‡ C = centrifugal release; A = axial release; A-C = axial and delayed centrifugal release.

§ Rated maximum pressure for the gun.

76-mm projectile, if used in conjunction with a good obturator (such as was used later in the 90-mm projectile) and adequate means to hold the parts together, might be very effective for projectiles that need to pass through a muzzle brake. For projectiles that do not need to pass through a muzzle brake, the simple Design 28-75D with light alloy substituted for plastic in the sabot body should be satisfactory, especially if an obturator is added.

If at some time in the future a plastic is developed that has greater dimensional stability than those tried, it would be worth while to reopen the question of the use of plastics in sabots. Perhaps the sliding bourrelet of the 20-mm projectile added to Design 28-75D would increase the accuracy of this type.

Because the energy imparted to the discarded parts of a sabot-projectile is wasted, it is desirable to keep the weight of the sabot to a minimum. By making use of the total experience with sabot-projectiles that is now available, it should be possible to develop designs by which this can be accomplished without sacrificing reliability of performance.

Chapter 30

TAPERED-BORE GUNS AND SKIRTED PROJECTILES[a, b]

By *Edwin L. Rose*[c]

30.1 INTRODUCTION

THE TAPERED-BORE GUN, firing a skirted projectile, offers one of several means for the attainment of hypervelocity without exceeding currently existing limits on powder-gas pressures and temperatures. It produces this hypervelocity by driving a projectile of reduced mass with the same force as that applied by the powder gas to the base of a standard weight projectile. In common with the standard-bore gun firing a sabot-projectile (Chapter 29) this combination offers a marked advantage over the standard gun firing a lightweight projectile of equal weight but of standard caliber, since the retardation in flight of the special projectiles is less by a factor which is roughly the square of the ratio of the diameters. The combination of tapered-bore gun and skirted projectile possesses an appreciable advantage over the sabot arrangement in that all the parts are attached to the projectile so that the entire muzzle momentum is available for overcoming air resistance. The importance of these advantages is shown strikingly in Section 33.2 where the relative performances of different types of hypervelocity guns, in various types of service, is analyzed in some detail.

In the light of the recently developed facts, it appears that the use of tapered-bore guns is not merely an expedient for the attainment of hypervelocity with standard pressures, but that regardless of future improvements in the velocity of projectiles of standard caliber *important gains will always be attainable from the addition of the tapered bore feature.* This observation is in direct opposition to military consensus. It therefore requires critical consideration in order to check its validity and to make sure that an opportunity for a substantial improvement in the effectiveness of weapons is not overlooked until too late.

The development of a 57/40-mm tapered-bore gun and skirted projectile was originally undertaken by Division 1, NDRC, for the purpose of making available to our Armed Forces designs, manufacturing equipment, and methods[d] for producing tapered-bore guns and ammunition of the Gehrlich type.[e] Soon after the work was undertaken it appeared that the production of such guns was unnecessarily tedious and expensive in the consumption of man-hours of critical labor. It was thought that if suitable projectiles designed to withstand the shock of extremely rapid deformation could be devised, the Janacek type of gun, which uses a standard tube with a short tapered adaptor attached to the muzzle, would be much more practical. In addition to simplifying the problem of manufacture its use would open the way to conversion of existing guns for the firing of skirted projectiles.

Tests on a number of tubes both rifled and unrifled, with tapers of different lengths, showed that it was practicable to drive a suitably designed projectile through an 8-in. long taper and thereby reduce the diameter of the fins from 57 mm to 40 mm at a velocity in excess of 5,000 fps. It was further found that with this short taper the rifling could be limited to the standard bore section without appreciable loss of

[a] The term "skirted" is used here in lieu of "deformable" to avoid confusion with the prior use of the term in connection with terminal ballistics to designate soft or plastic projectiles as distinguished from rigid, nonplastic, or hard projectiles.

[b] The tapered-bore gun described in this chapter was developed for Division 1, NDRC, by the Jones and Lamson Machine Company under Contract OEMsr-467. The development of the skirted projectiles for this gun was first undertaken by the Bryant Chucking Grinder Company under Contract OEMsr-534, and was later continued by the Jones and Lamson Machine Company. This chapter is based on the combined final report[128] under those two contracts. The history of the development of tapered-bore guns had been covered in an earlier report.[2]

[c] Member, Division 1. (Present address: Consulting Engineer, Jones and Lamson Machine Company, and Bryant Chucking Grinder Company, Springfield, Vt.)

[d] A suggestion[528] of a method for rifling tapered bores, considered in the early studies of this project, came from V. Bush.

[e] Earlier, the Division had sponsored some work at the National Bureau of Standards on a method of static testing skirted projectiles.[4] Those tests had led to the design of a series of 37/28-mm skirted projectiles of a so-called hour-glass shape, which were fired at Aberdeen Proving Ground from a 37-mm gun, M3, to which a Littlejohn adaptor of the British design[425] had been added. Those firings were made by the Army Ordnance Department as part of its own program[218] on the development of hypervelocity projectiles for firing from existing guns. The results[217,218,219,227,228,229,230] were communicated to the Jones and Lamson and Bryant companies and were useful in the early planning of the 57/40-mm project. (Editor's note.)

spin of the projectile before emergence. All doubts as to the preferability of the Janecek adaptor were thus eliminated and this design was adopted.

In order to carry through a completed design, the work was concentrated on the development of a tungsten carbide-cored projectile suitable for antitank use. The high-explosive projectile was entirely neglected. Nevertheless some of the greatest potentialities of the tapered-bore gun and skirted projectile lie in their use against rapidly moving, maneuvering targets where higher velocity greatly increases the probability of an effective hit. The problem of producing a satisfactory skirted projectile has been solved in a manner applicable to either armor-piercing or high-explosive use. The main problems remaining to be solved for skirted high-explosive projectiles are the achievement of suitable stability in flight (to insure accurate flight characteristics), and the attainment of good fragmentation characteristics. These problems are hardly more difficult than those encountered in the case of the armor-piercing projectile and they do not appear to present any insurmountable obstacles.

The work done on the 57/40-mm development appears to provide a satisfactory basis for the design of tapered adaptors and skirted projectiles suited to any velocities readily attainable with guns and powders available within the visible future. Projectiles of the type developed have been successfully fired at velocities as high as 5,200 fps. It seems quite reasonable to expect that the methods outlined herein may produce matériel capable of successful firing at velocities approaching 10,000 fps. The attainment of this end must, however, await the full application of what we have learned regarding erosion control. It is further dependent upon additional improvements in structural design to take advantage of improved erosion control.

30.2 57/40-MM TAPERED-BORE GUN AND SKIRTED PROJECTILE

As finally developed, the 57/40-mm tapered-bore gun comprises a tapered muzzle adaptor attached by a screw thread to the muzzle end of a Canadian Mk III 57-mm gun. The overall length of the adaptor is 34 in.; the tapered section is 8⅝ in.; the straight muzzle section, of 40-mm diameter, is 21 in.; and the remainder is taken up by the attachment section. Figure 1 is a photograph of a complete 57-mm Mk III mount with the tapered muzzle adaptor in place on the gun. This figure also shows two pieces of assembled ammunition at the side of the gun. The details of the adaptor are shown in Figure 2. The principal



FIGURE 1. 57/40-mm hypervelocity tapered-bore gun, Jones and Lamson final design, on standard 57-mm field carriage. (This figure has appeared as Figure 54 in NDRC Report No. A-456.)

CONFIDENTIAL

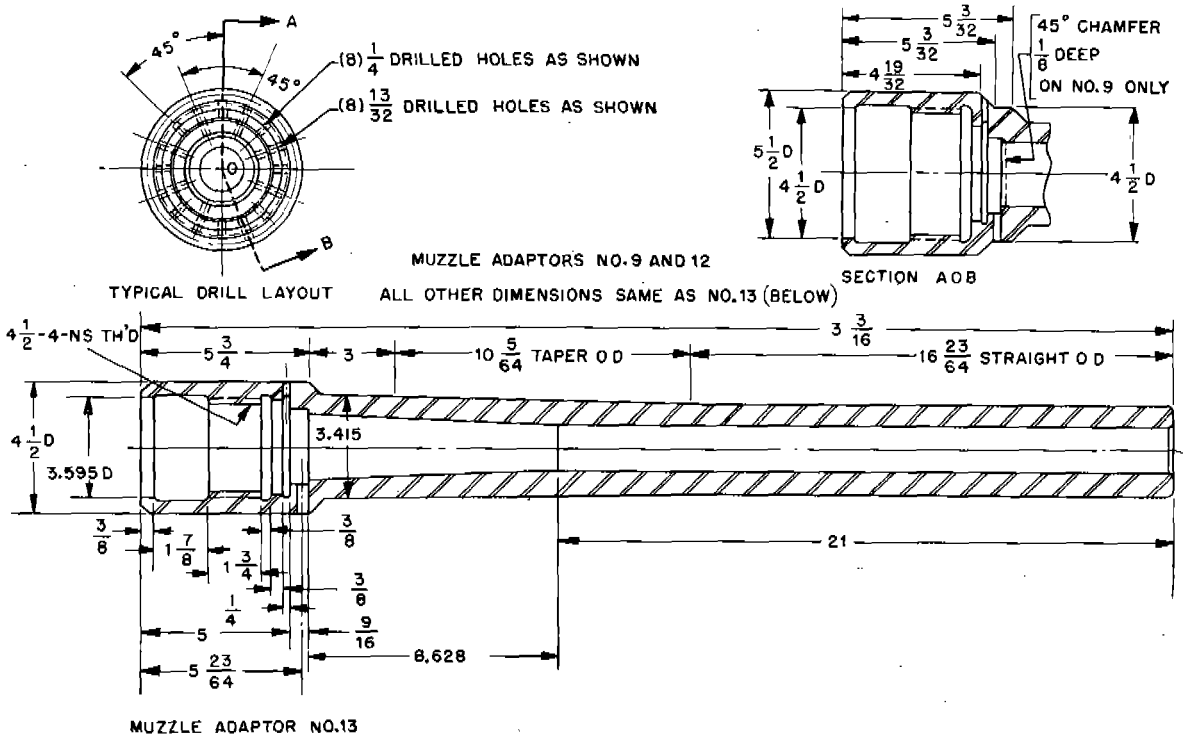


FIGURE 2. Muzzle adaptors for 57/40-mm tapered-bore gun. (This figure has appeared as Figure 12 in NDRC Report No. A-456.)

features of this design are the means of attachment, the tapered transition from initial to emergent caliber, the straight minor-caliber muzzle section, and the vent holes at the base of the taper. The vent holes serve to suppress the powder-gas shock wave which tends to form when the projectile enters the taper, and which, if unsuppressed, causes destruction of the cartridge case.

The taper acts as a squeezing die, reducing the diameter of the projectile to its emergent size as it travels through this section. The straight section serves to set the final dimension of the projectile, to center its geometrical and spin axes, and to keep down the yaw at the instant the projectile leaves the gun.

The attachment section is provided with a thread for securing the adaptor to the gun and with bearing surfaces to center its axis with the axis of the gun. There are also a seal surface and vent holes to keep the powder pressure from developing its full value in the clearance space between the end face of the gun tube and the base of the adaptor, thereby reducing the necessary strength of the securing thread. The securing thread is a left-hand thread. It is necessary only to screw the adaptor on by hand since the spin friction tightens it. Surprisingly, the adaptor can generally be removed by hand after firing numerous shots.

The 57/40-mm skirted projectile is a tungsten carbide-cored, armor-piercing projectile, consisting of six parts. It is provided with a front flange or skirt to center the front end in the bore, and with a rear skirt to serve as an obturator, sealing the bore and transmitting the powder force to the projectile, and centering the base of the projectile in the bore.

Figure 3 is a photograph of a cut-open assembled projectile, while Figure 4 is an exploded view of the projectile with the various parts identified. The nose point is an aluminum or magnesium part providing a sharp point for minimizing the shock air wave resistance, and a body of soft material to minimize the impulse tending to deflect the projectile at the instant of impact against inclined armor.

The windshield has a smooth ogival exterior contour to keep down air resistance. It is made of steel and together with the carrier helps to support the core against fracture on impact against inclined armor.

The nose pad is of aluminum. It is machined with projecting corners where it bears on the nose of the core to permit some plastic flow when the windshield is screwed tightly against the core. The nose pad



FIGURE 3. 57/40-mm skirted projectile, Jones and Lamson final design: Quarter sectioned; two-thirds actual size. (This figure has appeared as Figure 62 in NDRC Report No. A-456.)

serves the dual purpose of insuring a tight assembly, in which the core does not shift as it experiences the accelerations which occur in the gun, and of "softening" the impact when the core strikes armor. The actual nature of this latter function is not understood, but it is an observed fact that armor-piercing cores show less tendency to shatter when fitted with such a pad. The container, and the skirts which form an integral part of it, are critical features of design. Success of a skirted projectile design depends on the choice of suitable material and suitable contours and proportions of its parts. The skirts are deformed from their initial to their final shapes in a time of the order of one to two ten-thousandths of a second. At the rates of strain which this deformation involves, almost all materials show some degree of brittleness. The strain work at fracture is greatly reduced. Ductile materials must be used, sharp corners must be avoided, and parts subjected to bending must be curved and proportioned so that bending strain is distributed over substantial linear intervals.

The design of the rear skirts presents a difficult compromise between providing enough material to support the powder pressure and keeping thickness of material down so as to minimize deformation forces and friction. Figure 5 shows a fully deformed, skirted projectile in flight.

Since small guns, especially those in antitank service, are seldom provided with director control, the use of tracer ammunition is generally required. The tracer pocket devised for the skirted projectile is simple, but seems to possess advantages and novel features which warrant its adoption for other ordnance use.

30.3 DESIGN THEORY FOR TAPERED GUNS AND SKIRTED PROJECTILES

30.3.1 Design of Skirts

Early deformable projectiles were provided with conical skirts machined integrally with the body of the projectile. The line of junction between the outer surfaces of the skirt and projectile was a point of strain concentration during the final stages of the deformation process. At high rates of strain even the ductile, low-carbon steels show a large reduction of elongation and a consequent trend toward brittleness. Beyond a certain critical muzzle velocity the skirts showed a tendency to separate from the body at this

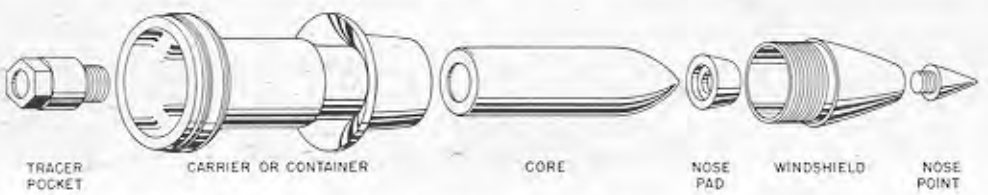


FIGURE 4. Exploded view of skirted projectile containing a tungsten carbide core to be fired from a tapered-bore gun.

CONFIDENTIAL

region of high strain. This is undoubtedly a manifestation of the reduced elongation.

To avoid separation, skirts should be designed with a curved cross section. The tangent to the neutral axis of the section, at the point of juncture with the body, should be parallel to the axis of the projectile. If this design is followed, and if the arc of curvature is of suitable radius, the bending strains developed during deformation is distributed and conditions conducive to fracture are avoided.

In addition to centering the projectile in the bore, the rear skirt serves as an obturator and must support the powder pressure. The curved section which serves to distribute strain also helps to reduce the skirt thickness necessary to support the pressure, by subjecting the material to nearly pure compression and eliminating bending stress. In this regard the ideal section is one in which the curvature increases from the base of the projectile to the point of bearing on the bore. However, the gains to be made by this further refinement do not compensate for the increased difficulty of tooling.

The skirt sections visible in Figure 2 are the result of extensive trial and error design, guided by the considerations outlined above.

30.3.2 Stresses in Skirts

In addition to the stresses developed by the powder pressure and by the deformation process, the skirts are subject to other tensile stresses induced by deformation forces, by friction, and by shock as the projectile enters the taper. The deformation is for the most part by plastic compression and does not produce tension. However, since the skirts are pulled through the taper by the body of the projectile, the work of deformation of the skirt material and the work in overcoming friction are developed by a tensile force. Furthermore, the skirts experience change of velocity on entering and leaving the tapered bore. There is first a loss of momentum on impact and a recovery when leaving the taper. The recovered momentum is supplied by a tensile force. This force appears to be the controlling one in determining design.

The bending stresses resulting from the deformation process have been satisfactorily controlled by the curved skirt design outlined in Section 30.3.1. The remaining tensile stresses, developed by the work of plastic deformation, by friction, and by shock, appear to be determined almost entirely by the design of the gun tube. To the extent that they can be modified by projectile design, the effects are minor.

Tensile stresses in skirts induced by the work of deformation and by friction have been subjected to an approximate analysis and the shock stresses have been estimated. The analysis is based on the following assumptions:

1. Impact between skirt and wall of taper is inelastic.
2. Portions of skirt which have not engaged wall retain their original contour.
3. Portions of skirt which have engaged wall conform to wall.

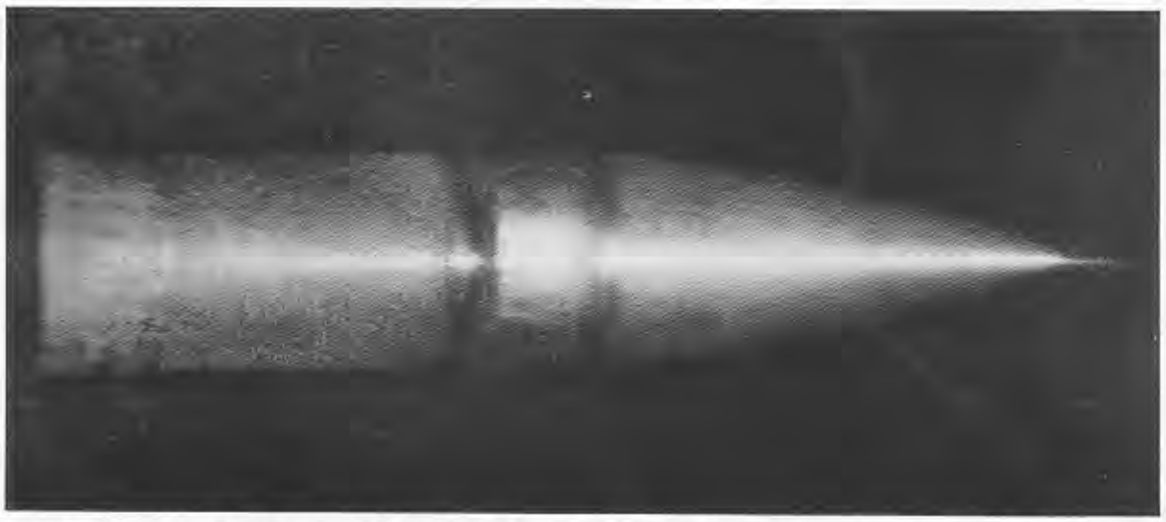


FIGURE 5. Projectile No. 451 after deformation: Taken in flight, using microflash unit; velocity 4,650 fps. (This figure has appeared as Figure 20 in NDRC Report No. A-456.)

CONFIDENTIAL

4. No portion of skirt suffers compressive or tensile deformation parallel to the neutral axis of its section.

On the basis of these assumptions, higher stress values were obtained than would result from any actual process of deformation.

If the skirt is given any initial contour in an axial plane, subject to the limitation that at all points the tangent to the neutral axis of the section of the skirt makes a greater angle with the projectile axis than does the tangent to the tapered bore, then, when the skirt engages the taper, it moves over the surface of the taper with a sliding velocity, V_s. This velocity is given by equation (1),

$$V_s = V_0(\cos\beta - \sin\beta \tan\alpha), \tag{1}$$

in which V_0 is the velocity of the projectile, α is the angle of intersection of the skirt surface with the bore surface, and β is the angle between the axis and the tangent to the taper at the same point.

In the case where α and β are constant, V_s is constant from the start of engagement until the base of the skirt enters the throat of the taper. V_s is always less than V_0 if α is positive. Consequently, when the skirt enters the throat its velocity must be abruptly increased from V_s to V_0 and a wave of stress supplying the necessary change in momentum of the skirt starts at the base and moves toward the rear of the skirt. The propagation of this wave is complicated by the nonuniform transverse section of the skirts and by surface friction. However, a lower limit to its magnitude can be calculated by assuming a uniform section and neglecting friction. The change of velocity ΔV occurring at the throat is given by equation (2).

$$\Delta V = V_0 - V_s = V_0(1 - \cos\beta + \sin\beta \tan\alpha). \tag{2}$$

It can readily be shown that this sudden change of velocity is accompanied by a tensile stress wave of amplitude T_s, expressed by equation (3),

$$T_s = \Delta V\sqrt{\frac{E\delta}{g}} = V_0\sqrt{\frac{E\delta}{g}}(1 - \cos\beta + \sin\beta \tan\alpha), \tag{3}$$

in which E is Young's modulus for the material, δ its density and g the acceleration of gravity. If T_0 is the tensile strength of the material, the allowable change of velocity ΔV_0 is given by equation (4),

$$\Delta V_0 < T_0\sqrt{\frac{g}{E\delta}}, \tag{4}$$

and the critical limits on taper and skirt angles are given by equation (5),

$$1 - \cos\beta + \sin\beta \tan\alpha < \frac{T_0}{V_0}\sqrt{\frac{g}{E\delta}}, \tag{5}$$

which for small values of β and α reduces to the approximate form of equation (6).

$$\sin\beta\left(\frac{\sin\beta}{2} + \sin\alpha\right) < \frac{T_0}{V_0}\sqrt{\frac{g}{E\delta}}. \tag{6}$$

In tests with 57/40-mm skirted projectiles, fired through tapered tubes of different lengths of taper, it was found that, at a muzzle velocity of 4,500 fps, projectiles could be fired successfully through an adaptor which tapered from 57 mm to 40 mm in 8 in. of length, but that the skirts separated in an adaptor with a 4-in. taper. The half angles of these two cones are respectively 0.04 radians and 0.08 radians. For the above velocity, and a skirt material having $T_0 = 100{,}000$, $\delta = 0.28$, $E = 30{,}000{,}000$, the left-hand side of expression (6) becomes <0.13.

$$\sin\beta\left(\frac{\sin\beta}{2} + \sin\alpha\right) < \frac{100{,}000}{4{,}500 \times 12}\sqrt{\frac{32.2 \times 12}{3 \times 10^7 \times 0.28}} < 0.13.$$

The value of α is not known for these tests. However it was small. For $\alpha = 0$ the limiting value of β is 0.16 and for $\alpha = \beta$ the limiting value is 0.09. When it is remembered that friction and the work of plastic deformation have been omitted in this computation the discrepancy is seen to be in the right direction. It is possible that α was more of the order of 2β, in which case the limiting value of β would be 0.07 radian. This value is between the 0.04-radian and 0.08-radian values indicated above.

The tensile stress at the base of the skirt, resulting from friction and plastic working as the skirt enters the throat, is given by equation (7)

$$T_{fw} = \frac{PtL(\sin\beta + \phi\cos\beta)}{r(1 - \phi\sin\beta)} \tag{7}$$

in which T_{fw} is the tensile stress in question, P is the compressive stress for plastic working, r is the radius of the throat, t is the thickness of the skirt, L the length of skirt, and ϕ the coefficient of friction. This stress at the instant of shock is determined from equation (3), and the total stress is given by the sum of equations (3) and (7). For the materials used in the present designs, P is in the neighborhood of 100,000 psi, t is about 0.125 in. for the front skirt and 0.250 in. for the rear skirt, and L is about 0.7 in. for the front

skirt, and 1.14 in. for the rear skirt. For $\beta = 0.08$ radian and with a coefficient of friction of 0.05, T_{fw} = approx. 1,500 psi for front skirt; T_{fw} = approx. 6,000 psi for rear skirt. These values are of the order 1.5 per cent to 6 per cent of the shock stress computed above, and can therefore have little influence on the critical angle. Apparently the shock stress is all important in determining the limiting velocity of a tapered-bore gun.

Since α is limited to positive values, it is apparent that little can be done to the design of the skirt to change the velocity limit. The only effective control is by the adjustment of β. Small values of β produce low shock tension. However, if β is too small, the length of the adaptor becomes excessive. The solution to the elimination of shock stress appears to be in the more careful detailed design of the adaptor.

30.3.3 Design of Tapered Contour for Adaptor

Because of certain aspects of the tooling problem, the designs for the 57/40-mm tapered-bore gun embodied a straight conical transition. It is now clear that a continuously curving transition contour is much better adapted to deform the projectile with minimum tensile stress. If the transition curve is made tangent to the straight muzzle bore section, the acceleration of the skirt from its minimum velocity is over a finite distance, and there is no tensile shock stress. In particular, if the transition contour and that of the skirt are both circular arcs, a very favorable condition obtains.

Letting s represent distance measured along the axis of the transition section from the throat forward, d the overall length of the transition, L the length of the section of skirt instantaneously in contact with the bore, and B_0 the entering slope of the section, the instantaneous acceleration of the sliding velocity is given by equation (8), which is obtained by differentiating equation (1).

$$\frac{dV_s}{dt} = V_0[-\sin\beta - \sin(\beta + \alpha)]\frac{d\beta}{ds}\frac{ds}{dt}. \quad (8)$$

With sufficient approximation,

$$L = L_0\frac{s}{d}, \quad \frac{d\beta}{ds} = \frac{\beta_0}{d}, \quad \frac{ds}{dt} = V_0, \quad (9)$$

and

$$T_s = L\delta\frac{dV_s}{dt} = \left[\frac{L_0\delta\beta_0V_0^2s}{gd^3}\right]\left[\sin\beta_0\frac{d-s}{d} + \sin\left(\alpha + \beta_0\frac{d-s}{d}\right)\right]. \quad (10)$$

In all practical situations β is small enough to permit the use of β for $\sin\beta$ with sufficient accuracy. Furthermore, for the geometrical arrangement specified, α is approximately a constant m times β. Hence, letting $\alpha = m\beta$ and using the approximation $\sin(\alpha + \beta) = (m + 1)\beta$, the tensile stress T_s is represented by equation (11).

$$T_s = \frac{L_0V_0^2\beta_0^2\delta(2 + \beta)(d - s)s}{gd^3}. \quad (11)$$

Its maximum value is given by equation (12)

$$T_m = (2 + m)\frac{L_0V_0^2\beta_0^2}{4gd}. \quad (12)$$

The effect of this change on shock stress is strikingly shown by considering the case of a 57/40-mm gun with a 4-in. long transition. If we let $T_s = T_0$ = 100,000 psi; $L_0 = 0.6$ in.; $\delta = 0.28$; $d = 4$ in.; $m = 9$ (90 degree arc); $\beta_0 = 0.17$ radian—the situation will apply to a projectile of the type developed and the limiting velocity is represented by equation (13)

$$V_0 = \sqrt{\frac{4gdT_0}{L_0\beta_0^2\delta(2 + m)}} = 9{,}000 \text{ fps}. \quad (13)$$

With an 8 in. long arcuate transition, the limiting velocity increases to about 25,000 fps.

By this change, the safe velocity has been more than doubled for a 4-in. taper, which tests showed would not pass a projectile at a velocity of 4,500 fps. The maximum safe velocity of an 8-in. taper having a continuously curving transition contour would thus be above the theoretical limit attainable with a gun of infinite length, which is assumed to be 20,000 fps (Section 3.5.2). Thus no practical limit to velocity appears to be imposed by the use of a tapered adaptor. In fact, furtherance of the development would present opportunities to reduce the length of adaptors while retaining a net gain in performance. There are good reasons to believe that, with the adoption of the smooth, horn shape for the transition, the length of the straight muzzle section may be materially reduced. This is particularly true if means for controlling wear are adopted. There appears to be no reason why the length of this section should exceed twice the bearing length of the projectile, if the need for an excessive length allowance for wear is eliminated. In the case of the 57/40-mm adaptor, reduction of the working length from 30 in. to approximately 10 in. appears to be a reasonable possibility.

Theoretically it is possible to design the transition to develop substantially constant tensile stress in the

skirt, throughout the travel period, but such an improvement seems to have no practical importance. A decrease in horn length of only one-third could be effected, and this reduction is relatively insignificant in view of the more significant decrease in length resulting from the use of a circular contour.

30.3.4 Muzzle Velocity and Velocity Limits

When the muzzle velocity of the standard projectile is known the velocity of the corresponding subcaliber projectile can be estimated with reasonable approximation by equation (14), in which

$$V' = V_0 \left(\frac{W_0 + \frac{1}{4}W_p}{W' + \frac{1}{4}W_p} \right)^{1/2} \qquad (14)$$

V' is the new velocity, V_0 the standard velocity, W' the new weight, W_0 the standard weight and W_p the weight of powder. In the case of skirted projectiles, the preliminary estimates for a new design can be made from equation (15).

$$V' = V_0 \left(\frac{\delta_0}{\delta'} \right)^{1/2} \left(\frac{1 + \frac{1}{4}\frac{W_p}{W_0}}{1 + \rho^3/4\frac{W_p}{W_0}} \right)^{1/2} \qquad (15)$$

Here ρ is the ratio of new caliber to standard caliber, δ' is the mean density of the new projectile material, and δ_0 the standard density.

For estimating purposes, these approximations appear to be quite satisfactory for velocities up to 5,000 fps in spite of a substantial increase in the kinetic energy imparted to the powder gases at these velocities. In the case of the 57/40-mm development, the standard projectile weight was 6 lb and its velocity was 3,000 fps. The final design of carbide-cored, skirted projectile weighed 53 oz and attained a velocity of 4,100 fps when the powder was adjusted to give a maximum pressure equal to the standard pressure. This measured velocity compares well with a velocity of 4,050 fps calculated by equation (14). A skirted solid steel shot attained a velocity of 5,200 fps, when fired with a powder charge of 45 oz at the rated maximum pressure for the gun (52,000 psi). This compares with 5,100 fps calculated by equation (15).

For more exact computations, the methods outlined in Chapter 3 are applicable. According to the analysis given there, the theoretical limiting velocity for an ideal, infinitely long gun is about 36,000 fps. If friction and heat losses are taken into consideration, with a high ratio of charge to projectile mass the limiting muzzle velocity is more likely to be of the order of 20,000 fps (Section 3.5.2). Tests with an 8-mm, 125-caliber gun, carried out several years ago by Langweiler, [26,198] indicated a limit of about 14,000 fps. Since, in such a small gun, heat and friction losses would be relatively high, the attainment of a somewhat greater velocity would be expected from the use of larger guns and guns in which is used some means of reducing friction, such as pre-engraved projectiles (Section 27.3).

The length of the 57/40-mm tapered-bore gun is 50 calibers (with respect to the larger diameter). In spite of the fact that Langweiler's gun was a little over twice as long (125 calibers, as compared with 50) and that finely pulverized powder was used for its tests, velocities obtained with the tapered-bore gun firing skirted projectiles correspond to Langweiler's results to within a few per cent. The charge-to-mass ratio ranged from 0.85 to 44. For a ratio of 10, the velocity is about 8,000 fps, which is 60 per cent of the indicated maximum of 14,000 fps. With higher ratios of charge to projectile, the velocity gain is slight; for a change in ratio from 10 to 20, the velocity increases by about 800 fps. It appears reasonable, therefore, to consider a velocity of 8,000 fps as representing rather closely the practical limit to velocity attainable with present powders. Minor increases may be obtained by an increase in gun length, by recourse to measures designed to reduce friction, and by the development of higher potential propellants.

In comparison with Langweiler's gun, it is apparent that the lower efficiency of the tapered-bore gun, which results from its shorter barrel length and the relatively high friction of the skirted projectile, is compensated for by its lower heat loss. Analyses of deformation stresses indicate that no difficulty should be experienced in the construction of tapered-bore guns and skirted projectiles which would attain a velocity of about 8,000 fps.

30.3.5 Venting to Suppress Gas Pressure Shock Wave at Base of Taper

During early tests of the 57/40-mm gun, frequent difficulty was experienced with collapse and burning of powder-case necks. Since this prevented re-use of the cases, a remedy was sought. It was found that the phenomenon was generally absent when the projectiles were fired with the adaptor off, and that for each adaptor there was a velocity below which case failure did not occur. It was further found that the velocity

(or powder pressure) at which failure occurred was lower the shorter the taper. A typical burned case is shown in Figure 6.

These observations led to the conclusion that collapse of the cases was caused by a shock wave set up when the projectile reached the base of the taper. This wave was a wave of pressure traveling toward the breech. Upon reaching the neck of the powder case it encountered an expansion from the bore diameter to the chamber diameter and experienced a partial reversal. If the amplitude of the shock wave was high enough, this reversal resulted in a pressure drop in the throat so that gases trapped between the neck and the bore caused collapse of the neck. Subsequent rapid escape of the gas in the chamber caused destruction by burning. British investigators who had encountered the same difficulty assumed that it was caused by the compression of air and gas between the skirts of the projectile.[402]

Further consideration of the situation led to a realization that the shock wave started at the adaptor could conceivably attain such amplitude as possibly to exceed the strength of the muzzle section of the gun. This leads to the question as to how much the amplitude of the shock wave may be.

When a compressible fluid moving with relative velocity V_0 strikes an obstacle, the stagnation pressure P_s is given by equation (16).

$$P_s = P_0\left(1-\frac{K-1}{2}N_m\right)^{K/K-1}, \qquad (16)$$

in which P_0 is the initial pressure, K the gas constant, and N_m, the Mach number corresponding to the relative velocity.

With the tapered-bore gun, the velocity of sound C in the gas at the base of the projectile as the projectile enters the straight muzzle bore is about 3,000 fps. The projectile velocity may be assumed to be 4,200 fps. N_m is therefore of the order of 1.4. A limiting value of P_s, for the case of a zero-length taper, is given by the relations expressed in equation (17).

$$\begin{aligned}\Delta V &= V_0\left(1-\frac{1}{p^2}\right) = \Delta N_m = \frac{V_0}{C}\left(1-\frac{1}{p^2}\right)\\ &= \frac{4{,}200}{3{,}000}\left[1-\left(\frac{40}{57}\right)^2\right] = 0.7, \qquad (17)\\ P_s &= P_0\left(1+\frac{1.4-1}{2}\times 0.7^2\right)^{1.4/0.4} = 1.4P_0.\end{aligned}$$

The pressure P_0 at the base of the projectile is roughly 12,000 psi so the shock pressure will be around $P_s = 1.4 \times 12{,}000 = 17{,}000$ psi. This figure agrees reasonably well with a measured pressure of about 20,000 psi.

To soften this shock wave, it is necessary to "bleed off" gas through vent holes at the base of the taper. The ideal way would be to provide vents having a capacity equal to the differential of projectile displacement between the major and minor calibers. However, tests showed case failure occurred only above a critical velocity which was different for each taper. Only partial venting is therefore necessary.



FIGURE 6. On the right, type of cartridge case failure experienced when used with unvented tapered-bore gun tube. Undamaged case on left. (This figure has appeared as Figure 5 in NDRC Report No. A-456.)

In the case of the 57/40-mm projectile at a velocity of 4,200 fps, the differential displacement is 58 cu ft/sec, the density of the gas is about 7 lb per cu ft, and the mass displacement is therefore 400 lb per sec. The flow through a sharp edged orifice is given by

$$W = \frac{0.53aP}{\sqrt{T}}, \qquad (18)$$

CONFIDENTIAL

in which W is mass, in lb/sec; a the orifice area, in sq in.; P the pressure, in lb/in.^{2}; and T the gas temperature, in degrees Fahrenheit on the absolute temperature scale. In the present instance P is about 12,000 psi, T about 4000 F and, W, 400 lb/sec. Hence, the required vent area a is 4.2 sq in.

It is interesting to note that in practice about 3 sq in. of vent holes were found necessary to prevent case failure. Four square inches was the area provided in the final designs.

It was found that venting caused numerous gas-erosion grooves and gouges in the bore around the vent holes. These appeared to contribute to skirt breakage. The condition was rectified in later designs by machining a groove around the inside of the barrel just before the start of the taper. The vent holes were terminated in this groove.

Figure 7 shows that nearly equal volumes of powder gas were discharged through the vents and from the muzzle of the gun.

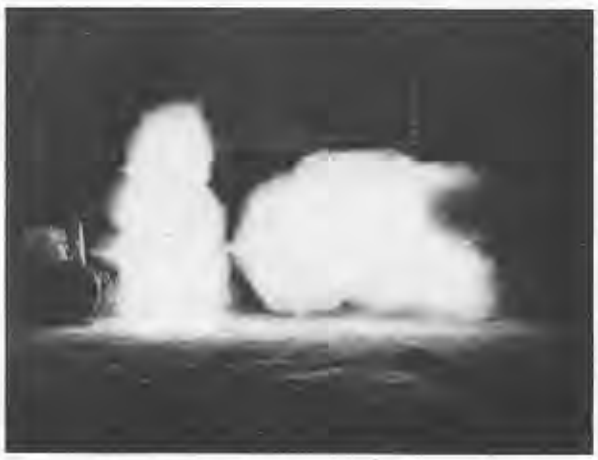


FIGURE 7. Effect of vents in tapered-bore gun tube on muzzle blast. (This figure has appeared as Figure 7 in NDRC Report No. A-456.)

30.4 GUN DEVELOPMENT TESTS

30.4.1 General Testing

In order to choose the optimum length of taper for deforming a two-skirted projectile, eight different tubes were designed and built. All had an overall length of 115 in. and a 40-mm section length of 7 in. In machining these tubes use was made of a thread collocating gauge designed for the purpose,[11] by means of which it is possible to locate the axial plane of a transverse center line across the threaded end of a tube such that the axial plane of this line bears a desired relation to the axial plane of a point on the face of the thread.

The rate of taper used in changing the bore diameter from 57 mm to 40 mm varied from ¼ in. per ft to 2 in., giving taper lengths of 32, 16, 8, and 4 in. One gun of each taper was rifled its full length and one of each left smooth in the taper. All of these tubes were rifled in the 57-mm section with 12 helical grooves having a pitch of 25 calibers. The selection of this rifling pitch was based on calculations. Later experience with another tube showed that a pitch of 17.5 calibers was too great. Although in general, a 25-caliber pitch performed satisfactorily, it was not used in the final design because the standard pitch (30 calibers) was found to give the carbide-cored skirted projectile enough angular velocity for more than sufficient flight stability.

For the smooth-taper barrels, skirt breakage was observed at a limiting maximum pressure of between 25,000 and 37,000 psi copper, for taper lengths of 4 and 8 in. Fired from the rifled, 16-in. taper barrel at copper pressures ranging from 46,000 to 52,000 psi, six shots remained intact. Satisfactory results were obtained with both the rifled and smooth-bored 32-in. taper, in tests at pressures as high as 40,000 psi.

At the outset of the development, consideration of the motion of the projectile down the bore led to the conclusion that if the tapered and muzzle sections could be made short enough they could be left unrifled, with negligible loss of spin and consequent satisfactory ballistic performance. Both ballistic tests and measurement of the pitch of scratches made on the smooth bore of various tubes showed that in all, except possibly the tube with the 32-in. long taper, the loss of spin was truly negligible.

With the need for rifling in the tapered section thus eliminated, the last pretense of the necessity of single-piece construction was removed. Experience with the single-piece tapered-bore guns showed that the use of short smooth-bored tapers was practicable without sacrifice of performance. It therefore became obvious that the only practical construction for a tapered-bore gun was the use of a standard straight-bore gun with a smooth tapered-bore adaptor. This adaptor should differ from the Janacek adaptor in having a short, straight section of bore at the muzzle. It should also differ in having a curved transition section in place of a straight sided cone. Work was then concentrated on the development of a suitable, properly secured adaptor.

30.4.2

Testing of Adaptors

The lightweight adaptor shown in Figure 2, weighs 45 lb. Several experimental types were made to determine the optimum lengths of taper and 40-mm straight section. These results more or less substantiated the previous work on the one-piece tapered gun tubes. The short 4-in. taper caused breakups and was itself badly eroded after nine rounds. Tapers of 8, 16, and 32 in. in length performed satisfactorily with all-steel projectiles. The heavier tungsten carbide-cored projectiles were found to perform satisfactorily with the 8-in. taper. An 8-in. taper was therefore considered to be the shortest practical length.

Wear in the adaptors was fairly rapid. Adaptors were manufactured with a 40-mm bore section as short as 8 in. and as long as 22 in. The 21-in. length was decided upon not only because of the greater accuracy resulting from it, in comparison with the short lengths, but also because the life of the adaptor was increased. As can be seen in Figure 8, the wear on the adaptors was greatest near the end of the taper and decreased in the direction of the muzzle. In effect, the 40-mm section after some use assumed the form of a slow taper. Hence, the longer the 40-mm bore can be made, the greater the number of shots which can be fired while maintaining complete deformation of the projectile.

Strain gauge measurements were made to determine the safety factor which could be expected from the adaptor. In one case the measurements of circumferential stress showed a total of 60,000 psi at the beginning of the taper, 44,000 psi at the end of the taper, and 49,000 psi in the middle of the straight section. These stresses all had the same general characteristics. There was a short period of high stress which lasted while the skirts were passing the gauges and then a relatively long period of stress caused by pressure decay in the gases. Skirt pressure stress started out at about 12,000 psi at the beginning of the taper, increased to 16,500 psi at the end of the taper, and jumped to 22,000 psi in the middle of the straight section. The gas pressure, on the other hand, dropped from 48,000 psi at the beginning of the taper to 27,500 psi at the end of the taper, and 27,000 psi in the middle of the 40-mm straight section. These stresses are not excessive in consideration of the fact that the elastic limit of the adaptor steel is 110,000 psi.

When these adaptors were attached to the standard 57-mm Canadian Mk III gun of 87-in. length, the assembly was "muzzle heavy." In order to produce a balanced gun, the Canadian Mk III was turned down to the outside dimensions of a standard U.S. Mk V 57-mm gun.

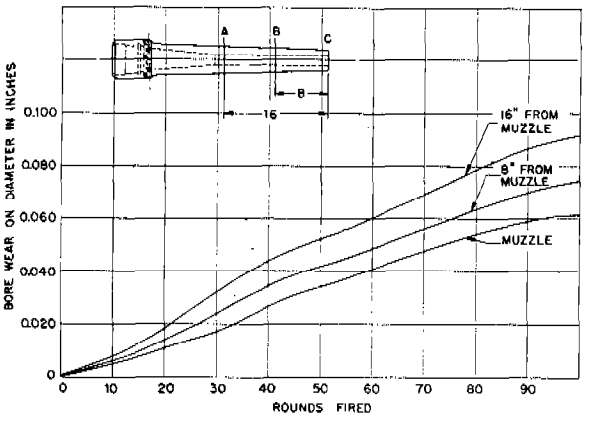


FIGURE 8. Wear on tapered-bore adaptor No. 8 as a function of rounds fired. (This figure has appeared as Figure 16 in NDRC Report No. A-456.)

30.4.3

Gun Wear Tests

The wear in the guns tested was fairly high both in the adaptor and in the main bore at the origin of rifling. This was to be expected. In the first place, the powder pressure exerts a substantial radial bearing component against the exposed area of the skirt. In the second place, the skirt is made of low carbon steel and it is a known fact soft steel bearing on steel under heavy bearing pressure produces a high rate of wear. When this frictional wear is added to the normal erosion wear at the origin of rifling, the observed high rate is not surprising.

An attempt was made to silver-solder a pressed and sintered carbonyl iron band to the rear skirt, but the design of this application was not satisfactory.

With the skirted-type projectile, wear occurred both in the grooves and in the lands. Projectile breakups noticed in worn tubes are probably caused by dislocation of the loosely fitting projectile in the enlarged section near the breech end at the moment of firing. Some gun tube data for wear on the lands are given in Figure 9. The fact that the muzzle wear is relatively slow compared with main tube wear correlates nicely with the fact that tube wear dies out much more rapidly along the bore than does the powder pressure which controls the skirt bearing pressure.

During the early travel gas pressure is high, so the bearing pressure is high. Furthermore, at low speeds the coefficient of friction is high. As the speed builds up a surface film on the projectile apparently melts,

and wear on the bore drops off rapidly. In this type of gun, the increased wear near the origin of rifling, can be explained by the fact that the reduced gas erosion, (resulting from a shorter time of travel) is offset by the increased mechanical friction in this region. Evidence of low friction at high velocity derives in part from the fact that the loss of spin in the taper is substantially less than can be obtained from calculations based on coefficients of friction at normal velocities.

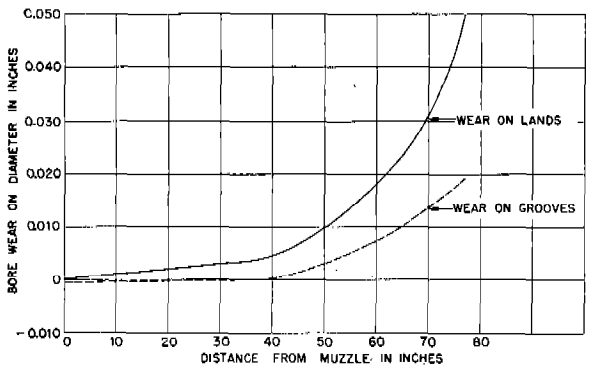


FIGURE 9. Wear on 57/40-mm gun tube No. 16 after 80 rounds. (This figure has appeared as Figure 15 in NDRC Report No. A-456.)

30.4.4 Attempts to Reduce Wear

Various methods were attempted to increase the wear resistance of the adaptors by surface treatment, but these were, in general, unsuccessful or inconclusive. The first adaptor was made of NE 8713 steel, and gas carburized to a hardness of Rockwell C63 on the outer edge of the case. Cross sectioning and metallographic examination of the muzzle end after six rounds had been fired through this adaptor showed surface cracks to a depth of approximately 0.035 in.

On the basis of these results, later designs called for heat treating NE 8749 steel and drawing to Rockwell C30. These were more successful, although in the test of one adaptor, slight checking at the muzzle was observed after 103 rounds had been fired. No checking or scuffing was noticeable on any of the other adaptors heat treated in this manner.

Another was chromium-plated to a thickness of 0.003 in. at the National Bureau of Standards. After 40 rounds no measurable wear was observed with gauges. However, at a distance of about 7 in. from the beginning of the taper there was a region where the surface was checked or scuffed. Also, in the straight section about an inch from the end of the taper, the chromium plate appeared to have flaked off of the surface. Chromium plate with its low coefficient of friction appears to offer good possibilities of increasing the life of these muzzle adaptors, if flaking can be controlled.

Wear tests were made with a stellite liner (Chapter 19) in a 57-mm muzzle adaptor. Twenty-six rounds of skirted projectiles, followed by 20 rounds of standard 57-mm test projectiles, were fired through this liner with no apparent wear. There was a slight cracking observed. This was presumably caused by the liner being out of round and not fitting tightly at all points in the adaptor. It is still to be hoped that a gun of the Janacek type with a stellite liner extending 12 to 15 calibers forward from the origin of rifling, and with a stellite-lined muzzle adaptor would have a long life.

30.5 PROJECTILE DEVELOPMENT TESTS

30.5.1 Projectile Skirt Tests

REAR SKIRTS

A number of rounds was fired with steel-bodied projectiles to determine optimum rear-skirt thickness. The thicknesses tested varied between $\frac{1}{8}$ in. and $\frac{5}{16}$ in. All showed good results at pressures up to 40,000 psi in the unsegmented vented tube with a 16-in. taper. These projectiles weighed about 33 oz. Other lightweight projectiles performed well with a $\frac{3}{16}$-in. thick rear skirt. However it was found, by tests with the tungsten carbide-cored type projectile (which weighed about 50 oz), that the minimum thickness that would stand up under firing was $\frac{7}{32}$ in.

Microflash pictures showed that the rear skirt had a slight tendency to balloon at high velocity under the action of the propulsive charge. A series of tests was undertaken to determine the effects on the skirts of high pressures. Slight flaring of the rear skirt, as observed from the size of the holes in cardboard screens, occurred between pressures of 45,000 and 55,000 psi (copper pressure). Breakage of the skirts was observed in one round at as low a pressure as 44,670 psi. No observable flaring was observed at a pressure as high as 50,900 psi.

It can be concluded that the skirt-breakage limit for the recommended projectile skirt design is very close to the maximum pressure recommended by the Army for use with this type of gun. At pressures of 45,000 psi the muzzle velocity of the final design of the 53-oz armor-piercing projectile is estimated to be about 4,200 fps.

Front Skirts

The front skirt presented more of a problem. After trying a conical front skirt a number of experiments were made on skirts with a double curvature. None of these performed very well, and as far as could be seen from recovered pieces, the failures were in the front skirt. It was noted, however, that the thinner front skirts performed better than the thicker. One type had a $\frac{3}{16}$-in tapered front skirt with a straight outline on the outside and a curvature at its base. However, wear measurements on this type indicated that the projectile was not deforming readily. It was therefore decided to revert to the uniformly curved-type front skirt. The thickness was standardized at $\frac{1}{8}$ in. This type of front skirt has since performed quite satisfactorily.

Skirt Position

Not much attention was paid in earlier designs to the relative position of the front and rear skirts. Actual practice indicated that this is a very important factor in the stability of the projectile both inside and outside the gun. The front skirt should be ahead of the center of gravity of the projectile at all times during deformation, to prevent the shell from careening inside the tube. In many of the later types of projectile, which were nose heavy as a result of the use of steel ballistic caps or high-density nose tips, an abnormal amount of yaw was observed.

A great deal of the wind resistance of the projectile is caused by the rear skirt and it, hence, has a large effect upon the center of pressure.

The tendency has been in later designs, to keep the rear skirt as far back of the center of gravity as possible by moving the core forward. In the recommended design type, the front skirt has been moved as far forward as possible without interfering with the contour of the ogive and the threaded section which receives the windshield.

Skirt Material Tests

The first skirt material used was SAE 1020 steel. Though this was satisfactory as far as could be determined from the firings, it was decided to use SAE 1120 steel because of its better machining qualities, a relative lack of ingot pattern, and its freedom from inclusions. SAE 3240, which had an original hardness of Rockwell B87–95, was found to be superior to both the other types with regard to breakage, but less satisfactory with respect to gun wear. During armor-piercing tests it was found that many projectiles made of SAE 1120 were breaking up under 45,000 psi maximum pressure. Steps were taken to strengthen the sheath in the thin region beneath the front skirt. Additional attempts were made to induction-harden the thin-walled section of the sheath. Tests showed that this method was not very satisfactory, and it was finally decided to resort to the heat treatment of the whole container to a hardness of Rockwell B84 to B90. Satisfactory results were obtained and this method was adopted.

Windshield Design Tests

The armor-plate penetration tests showed that the windshield design is extremely important at high angles of obliquity. There are apparently three primary factors to be considered:

1. To use an ogive with a long enough radius to prevent serious retardation in flight.
2. To support the tungsten carbide core and prevent "shattering" upon impact.
3. To prevent the projectile from "scooping" the armor plate at high angles of obliquity.

Tests with one type projectile showed both "shatter" and excessive "scooping" for angles at which, judging from results of other high-velocity tungsten carbide-cored projectiles such as the 2-pounder Mk I "Littlejohns,"[154] there should have been perforation with no "shatter." By redesign of the windshield this performance was met.

30.5.2 Test of Flight Characteristics

There was some fear that the angular velocity produced by a rifling of one turn in 30 calibers might not be enough to provide external flight stability for a skirted-type projectile. It was believed that frictional forces developed during passage through the taper section of the gun might retard the projectile considerably.

The exterior-angular frequency F of a skirted projectile can be obtained from yaw-card measurements of the rate of precession ϕ' from equation (19),

$$F = \frac{\pi A}{B\phi'}, \tag{19}$$

in which A is the axial moment of inertia and B is the transverse moment of inertia.

[redacted]

The moments of inertia of the projectile were obtained from the measurements of the frequency of oscillation of the projectile, suspended from a wire, about the axis of each required moment of inertia. The moment of inertia I about the suspension axis is derived from equation (20).

$$I = \frac{T^2 \mu a^4}{8\pi h}, \tag{20}$$

in which h is the length of wire, μ is the shear modulus of the wire material, a is the radius of the wire, and T is the measured time for a full oscillation. The ratio of moments of inertia is readily computed from equation (21)

$$\frac{A}{B} = \left(\frac{T_A}{T_B}\right)^2, \tag{21}$$

if the two times are measured with the projectile suspended from the same wire. By the same method the ratio of the axial moments of inertia before and after deformation can be obtained.



FIGURE 10. Wave front of skirted projectile No. 451: Taken in flight; using microflash unit; velocity approximately 4,500 fps. (This figure has appeared as Figure 21 in NDRC Report No. A-456.)

These methods were employed to determine the following angular frequencies for one type projectile (No. 524):

	Angular Frequency
1. New tube, no deformation, no friction	67-in./turn (theoretical)
2. New tube, deformation, no friction	50-in./turn (theoretical)
3. New tube (76 rounds) from measurements of ϕ'	53-in./turn (observed)
4. Old tube (189 rounds) from measurements of ϕ'	67-in./turn (observed).

In order to check these results an adaptor which had been used with a worn tube was cross-sectioned. Measurements made on the rifling imprints on this adaptor showed, as closely as could be determined, an angular frequency of one turn in 67 in.

From these results it can be concluded that because of the decrease in the moment of inertia after deformation, the angular velocity for this type projectile should increase by about 35 per cent after passing through the taper section of the gun. Actually, observations showed an increase of about 25 per cent, the remaining 10 per cent being accounted for by frictional losses occurring during deformation. It can also be seen from these results that the projectile angular velocity decreases as the tube wear increases. Because of the increased angular velocity observed in a skirted projectile, it may be possible to tolerate more tube wear than in the standard gun and still maintain flight stability.

Stability factors were calculated on the basis of data obtained from yaw cards spaced at 10-ft intervals along 200 ft of the firing range. From these the rate of precession, ϕ', and the length of one period of yaw, L, were measured. The stability factor S.F. is given by equation (22):[287]

$$\text{S. F.} = \frac{\left(\frac{L\phi'}{\pi}\right)^2}{\left(\frac{L\phi'}{\pi}\right)^2 - 1}. \tag{22}$$

Calculations based on the results of the firings of the Type 524 projectile gave a stability factor of 1.8. In successive rounds, three types of projectiles which differed in the location of the tungsten carbide core were fired. The results are given in Table 2 of Chapter 8. The core position of Type No. 1936 was used in the final design.

Shadow pictures of projectiles in flight were obtained with the use of the Microflash equipment. The projectile velocities were approximately 4,400 fps. One of these pictures, shown in Figure 10, indicates very little distortion of the main wave front emanating from the nose of the projectile. There are secondary waves from the region of the interface of the container and the ballistic cap and from the forward and back edges of the front and rear skirts. There is quite a bit of turbulence observable along the sides of the projectile in the region in back of the front skirt. A large amount of turbulent wake is discernible in the rear of the projectile. From an analysis of the performance

CONFIDENTIAL

data of the 57/40-mm skirted projectile, its ballistic coefficient was determined to be 1.0 for a form factor of 1.24.

30.5.3 Windshield Testing

Magnesium windshields were tried in early projectile models, but this material was later discarded in favor of aluminum, mainly because of greater ease of machining. In firing tests against armor plate there was evidence that at high angles, a long aluminum windshield tends to swerve the core away from the normal to the plate, producing a "scoop" shot. This is treated more thoroughly in Section 30.6.3.

Several projectiles were designed with steel ballistic caps. They performed slightly better than the aluminum-capped type.

Other projectiles were made with "soft steel" ballistic caps of various designs. There were usually only one or two projectiles manufactured of each of these designs and they were nearly all fired at 3-in plate at 55 degrees. It is difficult to tell, therefore, which type of steel was more satisfactory. The main intent in using a steel ballistic cap is to help prevent the nose of the core from shattering upon impact. This purpose seemed to be realized. Compounded windshields of various materials were tried and were found to be the most efficient in the prevention of core shatter.

Some projectiles had an elkonite nose tip and others were manufactured with elkonite nose pads. Elkonite is a powder metallurgy product composed of tungsten and copper. It has a density of 14.5 g/cc, approximately that of tungsten carbide, but unlike tungsten carbide, it is readily machinable. Its hardness ranges from 95 to 100 Rockwell B. Projectiles in which this material was placed ahead of the brittle tungsten carbide core were quite successful in preventing shatter at high angles of obliquity. Elkonite, however, is a relatively scarce and expensive material and was not used in the final design. The desired results were obtained with a steel ballistic cap with an aluminum pad and tip.

30.5.4 Testing of Cores

General

The core diameter was made 1.1 in. to conform to the core size of the Littlejohn 6-pounder skirted projectiles and the British 6-pounder sabot-projectile. Some armor plate tests were made with projectiles which had finish-ground cores of the British design. Later unground cores were used. These were similar to the ground one except for a 2.2-in. radius ogive on the radius instead of the original 1.54-in. radius ogive. Projectiles were also manufactured with cores having a flat core nose tip. No significant variation in performance could be detected in tests against armor plate at high angles of obliquity. This seems to substantiate the results of Division 2, NDRC.[156]

Physical Testing of Cores

Cores of the following composition were used: 89-87% tungsten carbide, and 11 to 13% cobalt.

Hardness measurements were made on 10 cylindrical ground cores and unground cylindrical cores. These, chosen at random from a larger lot, gave readings averaging 88.0 VDS Rockwell A. There was no significant difference in hardness between the ground and unground samples. Rockwell A88 converted into Vickers reading is 1350 DPH. This is considerably more than the minimum of 950 DPH required by British Ordnance for cores of these same specifications.

The transverse rupture strengths of 14 tungsten carbide cores were determined. Eight unground cores measured had an average transverse rupture strength of 139,300 psi with a minimum of 111,700 psi and a maximum of 200,900 psi. Six unground cores measured had an average transverse rupture strength of 181,900 psi with a minimum of 144,600 psi and a maximum of 215,700 psi. The minimum specification for British 2-pounder SV Mk II unground cores is 156,800 psi. Two out of six unground cores failed to meet these specifications. Moreover, seven out of eight ground cores were found to have transverse rupture strengths below 156,800 psi. These results signify that the cores are measurably weakened when ground, probably due to thermal stresses impressed in the material by the operation.

Transverse rupture-strength tests were made. Three tungsten carbide cores were used to apply the load to the core under test. The cores usually broke transversely into two main pieces. Considerable chipping was observable on the surface in the region of the fracture.

There is no conclusive evidence gathered during the tests against armor plate to prove that the unground core performs noticeably better than the ground core. It is mainly on the basis of the transverse rupture strength tests that the unground core (Type 1499) is recommended for the final design.

30.6 PERFORMANCE TESTING OF 57/40-MM TAPERED-BORE GUN AND SKIRTED PROJECTILE

30.6.1 General

In an effort to stimulate interest of the Services in the potentialities of the tapered-bore gun, the experimentation and testing were carried considerably beyond that necessary to establish the basis of design. In the course of this work the quality of performance of the gun was improved beyond the demands of practical necessity. The tests and the refinements developed during their conduct have shown results for the skirted projectile, in both accuracy and armor penetration, which are noticeably superior to either the sabot-projectile or the lightweight standard caliber projectile, of equal core size, when fired from the same gun. This advantage improves with the range.

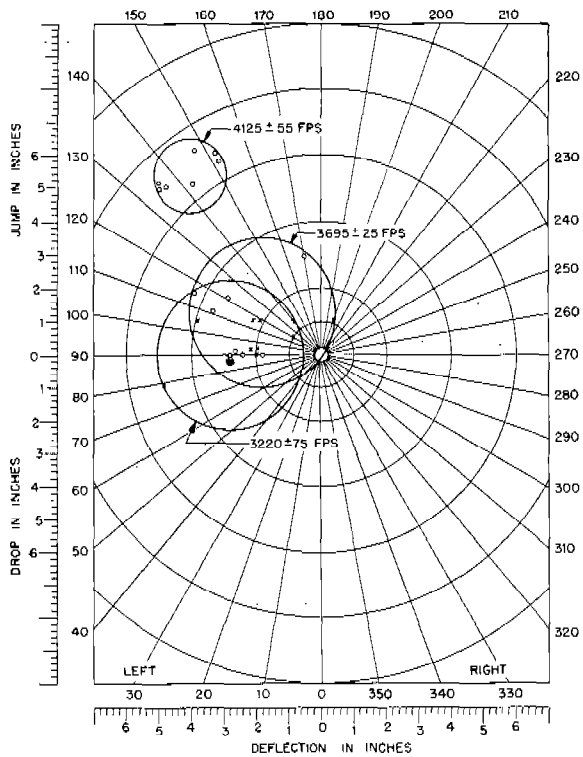


FIGURE 11. Accuracy of skirted projectile J&L 860 at three velocities: Rounds 440 to 496. (This figure has appeared as Figure 31 in NDRC Report No. A-456.)

30.6.2 Accuracy Tests

Limitations on space available made it necessary to conduct most tests at a range of 100 yd. It is realized that a direct comparison between results at this range and at longer ranges is only approximate. However, experience indicates that the initial yaw with a skirted projectile in a tapered bore is small. For this reason the extrapolation should be fairly satisfactory. Furthermore, the stability factor in the case of the armor-piercing projectile with a tungsten carbide core was rather high. It is therefore to be expected that the good results obtained should be fairly closely duplicated, under equally well-controlled conditions at longer range.

The accuracy of the gun at 100 yd appears to depend on the type of projectile as well as the particular tube and adaptor which was used. Consequently, the accuracy chart shown in Figure 11 was based upon firing in which these factors were constant. It was also found that the position of the shot groups relative to the bore sight depended upon the muzzle velocity. The scatter circles are drawn to include all shots of each of the three ranges of velocity. It can be noted that the accuracy of the projectile tested appears to improve as the velocity is increased. This may signify a more uniform deformation of the projectile at greater speeds or greater stability due to relatively less loss of spin in the adaptor.

The probable error circle at 100 yd was computed for a projectile with a muzzle velocity of 4,200 to 3,900 fps on the basis of the points shown in Figure 11. This circle is shown in Figure 12. The probable error circle for the British 6-pounder sabot-projectile shown in the same figure, was obtained from nine shots fired in the standard 57-mm tube at muzzle velocities from 3,900 to 4,200 fps. Assuming a normal distribution, this circle represents the area into which 50 per cent of the shots are expected to fall. If the dispersion be assumed to be proportional to the range the radius of the probable error circle would be 7 in. at 1,000 yd for the skirted projectile, while it would be over 3 ft at this distance for the sabot-projectile. The superior accuracy of the skirted projectile is probably due, in part, to the very low value of initial yaw and to a somewhat higher stability resulting from a more favorable location of center of gravity. It is, of course, possible that the low accuracy of the sabot-projectile is due in part to disturbance of it in flight by the discarding elements.

Firings were later conducted at Aberdeen Proving Ground.[540] The gun was mounted in a Scout car and firings were made against a 12 ft by 12 ft target at a range of 1,717.63 ft. The average instrumental velocity for 20 rounds was 3,950 fps.

The radius of the probable error circle under these conditions was 12 in. at the above mentioned range

or 21 in. at 1,000 yd, assuming, again, that the trajectory is a straight line.

This dispersion was somewhat greater than was to be expected on the basis of firings at the Jones and Lamson range. The discrepancy may be caused either by the two different types of gun mountings used, or by the fact that an unground core was supplied with the projectile type fired at the Proving Ground, while a ground core was used in the other projectile.

30.6.3 Armor Penetration Tests

Preliminary Tests

Aberdeen Proving Ground was supplied with the tubes and adaptors and with two types of skirted projectiles. These were used to conduct a series of tests[560] to determine the performance of the tapered-bore gun against 4- and 6-in. armor plate at 30 degrees obliquity, and 3-in. armor at 55 degrees. Members of the Princeton University Station, Division 2, NDRC, analyzed these firings and compared the results with those of other tungsten carbide-cored projectiles.[154] The performance of the skirted projectile was much worse than was to be expected. It was concluded at this time, after a study of the results, that the unsatisfactory behavior was probably due to a disintegration of the tungsten carbide core at the moment of impact. The Jones and Lamson Research Department in cooperation with members of Division 2, NDRC, undertook a program of armor-plate tests to determine the ballistic limit of the skirted projectile, and to devise an improved design in which the core would not shatter upon impact.

Design Changes to Improve Penetration

A number of design changes was made to attempt to prevent core shatter. Of these the following are most noteworthy.

1. An aluminum nose pad was added. This did not prevent shatter when used alone, but seemed to be advantageous in conjunction with a steel ballistic cap.
2. A steel windshield was substituted for the aluminum windshield.
3. An unground core was substituted for the ground core.

In addition to the problem of core shatter it was noticed that the length of the distance from the core nose to the tip of the ballistic cap had an important effect on the performance at high angles of obliquity. The plate results showed that the long aluminum ballistic cap of the projectile was deflecting the core, before it hit the plate, to such an extent as to produce "scooping." To counteract this effect the windshield was shortened and the steel tip replaced with an aluminum tip. This type of tip not only increases the stability inside of the gun by shifting the center of gravity backwards, but also provides a soft nose point which produces less swerving away from the normal to the armor plate at the moment of impact.

Several other minor changes were made. A radius of curvature was added to the section under the front skirt to replace the sharp angle where container breakage was observed. In addition the container was hardened overall to Rockwell B84 to B90. Later tests showed that, with this treatment, the skirts would not break at 45,000 psi (copper pressure), the rated pressure of the gun.

Ballistic Limits of Skirted Projectile and of British Sabot-Projectile

The ballistic or perforation limit of any particular type of projectile depends upon the following

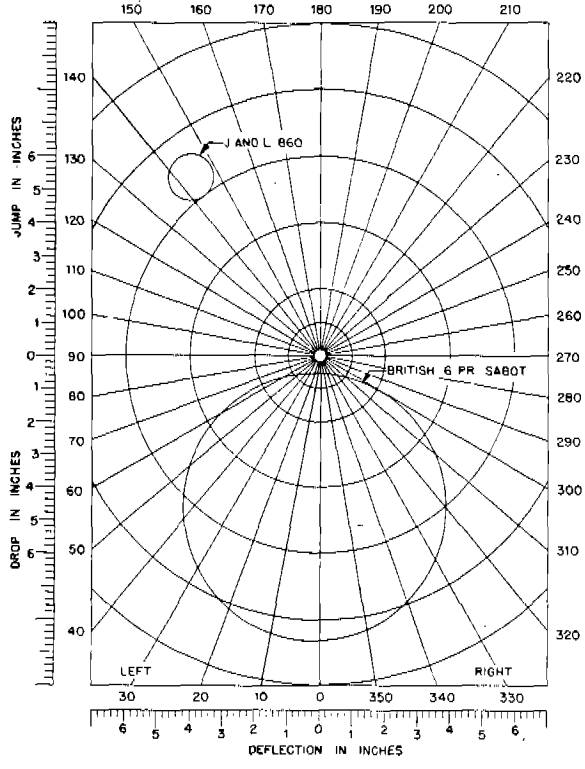


Figure 12. Probable error circles at 1000 yds for skirted projectile J&L 860 and British 6-pounder sabot-projectile: Velocity 4,020 ± 160 fps. (This figure has appeared as Figure 32 in NDRC Report No. A-456.)

three factors:

1. The striking velocity of the projectile.
2. The angle of obliquity of the armor plate.
3. The thickness of the plate.

Firings were made against 2-in., 3-in., 4-in., and 6-in. homogeneous armor plate supplied by Aberdeen Proving Ground. Three levels of projectile velocity were used; 3,200 fps, 3,700 fps, and 4,150 fps. The plate was set at 5-degree intervals and an attempt was made to bracket the ballistic limit with two shots on either side at each of the velocity levels. From the

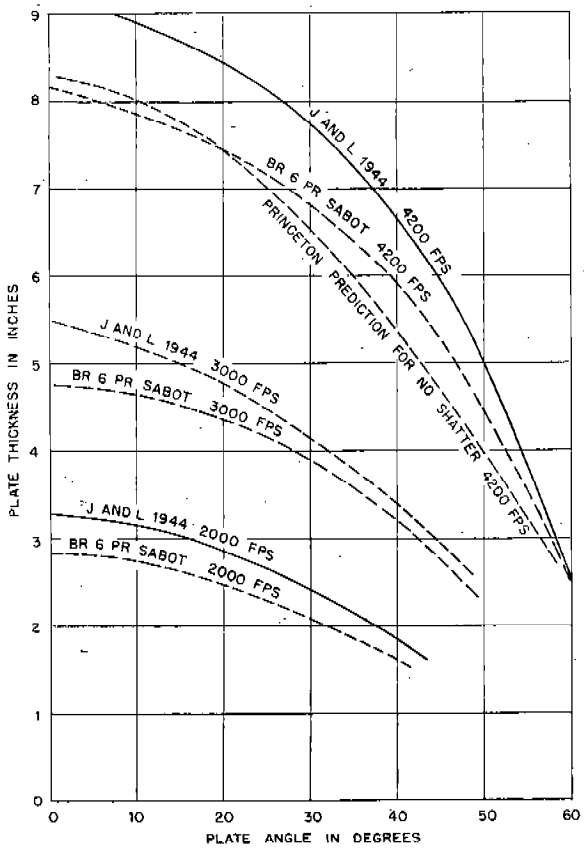


FIGURE 13. Ballistic limit as a function of plate thickness and plate angle. (This figure has appeared as Figure 35 in NDRC Report No. A-456.)

size of the holes made when perforation occurred, observation of recovered material and from gammagraphs and exographs it was evident that above certain angles and velocities the skirted projectile completely shattered on impact. The minimum velocity at which shatter occurred was, in general, between 2,500 and 3,000 fps. It occurred at angles of obliquity which varied with the thickness of the armor plate. With 2-in. armor plate one type of skirted projectile shattered at angles roughly greater than 50 degrees; for 3-in. plate at angles greater than 35 degrees; for 4-in. plate at angles greater than 25 degrees, and for 6-in. plate at angles greater than 10 degrees. Forty British 6-pounder discarding sabots with 1.1-in. tungsten carbide cores were made available for firing at the Jones and Lamson range. Firings made at the same plates used for the skirted projectiles offered a means of comparing the relative performance of the three types.

One type of skirted projectile and the British sabot-projectile performed much better than the other type at high angles of obliquity, mainly because of the absence of core shatter. A third type of skirted projectile (No. 1949) which is identical to the final design except for an insignificant detail in the container, penetrated 3 in. of armor at an obliquity angle of 55 degrees. It has been noted that the performance of the skirted projectile is better than that of the sabot-projectile at low angles of obliquity. This is apparently due, in part, to the greater weight of parts of the sheath in relation to the weight of corresponding parts of the British projectile. The weights of the two types of skirted projectile are approximately 48 and 50 oz, respectively, while the weight of the sabot-projectile is only 37 oz. The greater weight results in higher residual velocity at impact and in higher effective mass at impact. However, as the angle of obliquity of the armor plate is increased the sabot-projectile gradually overcomes this initial disadvantage. Two reasons are advanced to explain this action. In the first place, the distance from the core nose to the point of the ballistic cap is only 1.00 in. in the sabot-projectile design, while it is 1.31 in. in the design of the skirted projectile. In the second place, the subcaliber sheath diameter of the sabot-projectile is only 1.45 in., as opposed to a sheath diameter of 1.58 in. in the case of the skirted projectile.

In Figure 13 the ballistic limit is shown as a function of plate thickness and plate angle for three different velocities. Curves for Type No. 1944 skirted projectile seem to converge at an angle of approximately 70 degrees. Above this angle, the projectile would be expected to ricochet regardless of projectile velocity or plate thickness. The "ricocheting angle" for the sabot-projectile appears to be about 65 degrees, which is reasonable in view of the fact that the projectile is somewhat lighter. The maximum thickness which Type No. 1944 would be expected to penetrate would be about 9.4 in. of armor at normal, while the sabot-projectile would be expected to penetrate approximately 8 in. at normal.[157] Figures 14



FIGURE 14. Perforation produced by projectile 1949 in 3-in. armor plate at an angle of 55-degree obliquity: Front of plate 3G; two-thirds actual size. (This figure has been taken from a Division 2 report.)

and 15 illustrate the absence of core shatter from the firing of a Type No. 1949 skirted projectile at a velocity of 4,200 fps, and an angle of obliquity of 55 degrees.

DE MARRE FORMULA

An attempt was made to fit the penetration results of the skirted projectile to the De Marre formula,

$$\alpha\left(\frac{e}{d}\right)^{\beta} = \frac{WV^2\cos^2\theta}{d^3}. \qquad (23)$$

This gives the penetration, e (in.), of a projectile in terms of the striking velocity V (fps), angle of obliquity θ degrees projectile weight W (lb), and projectile diameter d (in.). This application is discussed in Section 9.2. These results are shown in Figure 16 for the cases of 0, 30, and 50-degree angles of obliquity. Both α and the constant β varied with the impact angle according to data in the following table.

Angle (degrees)	$\text{Log}_{10}\,\alpha$	β
0	5.88	1.60
30	6.04	1.45
50	6.19	1.26

For steel projectiles equation (25) was found[564] to be quite accurate with $\beta = 1.43$ and $\log_{10}\alpha = 6.15$.

The British find that with tungsten carbide cores, the constant $\log_{10}\alpha$ varies with the angle of attack as was observed in the case of the skirted projectile.

CONFIDENTIAL

Using a core of 0.653-in. diameter and 0.42-lb weight against 80-mm and 100-mm homogeneous armor at striking velocities between 3,000 and 3,500 fps, the following values of $\log_{10}\alpha$ were observed; at 0 degree, $\log_{10}\alpha = 5.965$; at 30 degrees, $\log_{10}\alpha = 6.117 - 0.017(e/d - 1)$. The observations made at the J&L range appear to be in very good agreement with these results. Figure 16 shows that carbide cores will average about three times the penetrating power of steel cores.

Perforation Range Comparisons

Using the data supplied by Princeton University Station, Division 2, NDRC, and those of the British[301] in conjunction with the results of the firings at the J&L range, the perforation range of the J&L 1944 and the British sabot were determined. The retardation of the J&L Type 1944 was assumed to be the same as the retardation of the J&L Type 860. The perforation-range curve of the sabot given by the British is for armor plate at 30-degree angle. In order to obtain the retardation of the sabot the following procedure was used. From the curves for the ballistic limit as a function of striking velocity and angle of obliquity for 3-in., 4-in., and 6-in. plate, the 30-degree line for the British sabot was drawn on Figure 17. As can be seen, this is in close agreement with the datum point taken from the perforation range curves for 6-pounder projectiles supplied by the British. Conse-



Figure 15. Perforation produced by projectile 1949 in 3-in. armor plate at an angle of 55-degree obliquity: Rear of plate 3G; two-thirds actual size. (This figure has been taken from a Division 2 report.)

CONFIDENTIAL

quently, this line was used in conjunction with the British data to obtain the retardation curve for the British sabot. Using the retardation for the British sabot and the J&L projectiles, and the ballistic limit curves for 3-in. and 6-in. armor plate, the perforation range as a function of the obliquity angle was determined for J&L projectile Type 1944 and the British sabot against these two thicknesses. These curves show plainly that while the British sabot is slightly more effective than the J&L 1944 at short ranges, it rapidly loses its advantage at distances greater than 400 or 500 yd. This is even more strikingly apparent in the case of the 6-in. plate than in the case of the 3-in. plate. There are apparently two reasons for this behavior. In the first place the subcaliber sabot, being only about 75 per cent as heavy as the J&L Type 1944, loses velocity at a more rapid rate. In the second place, the greater amount of energy at the moment of impact, due to the greater mass as well as the higher velocity, acts in favor of the J&L Type 1944 projectile.

Using the ballistic limit curves, it was possible to obtain the specific limit energies for the J&L projectile, at various plate angles up to 55 degrees, as a function of the plate thickness in core calibers. In these calculations the weight and diameter of the core has been used. The remainder of the projectile was neglected. The average performance for each angle was approximated by straight lines on a logarithmic plot. On the basis of this graph, predictions have been made of the ballistic limits, against 3- and

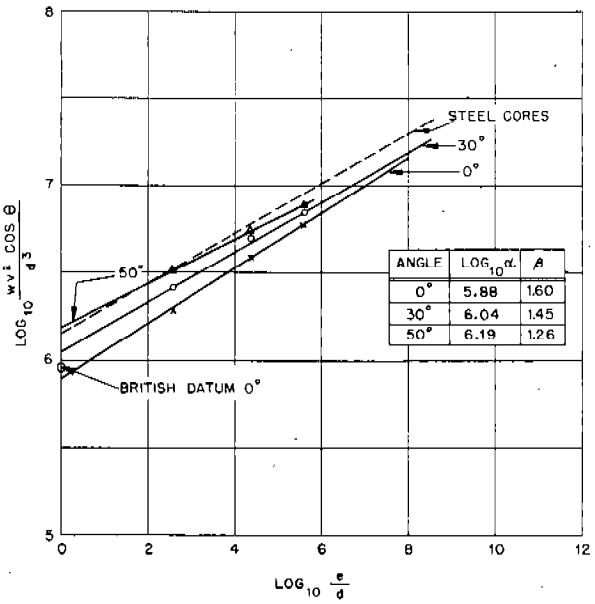


FIGURE 16. Determination of constants in DeMarre formula for tungsten carbide cores against armor plate at impact angles of 0 degree, 30 degrees, and 50 degrees, and comparison with values for steel cores. (This figure has appeared as Figure 44B in NDRC Report No. A-456.)

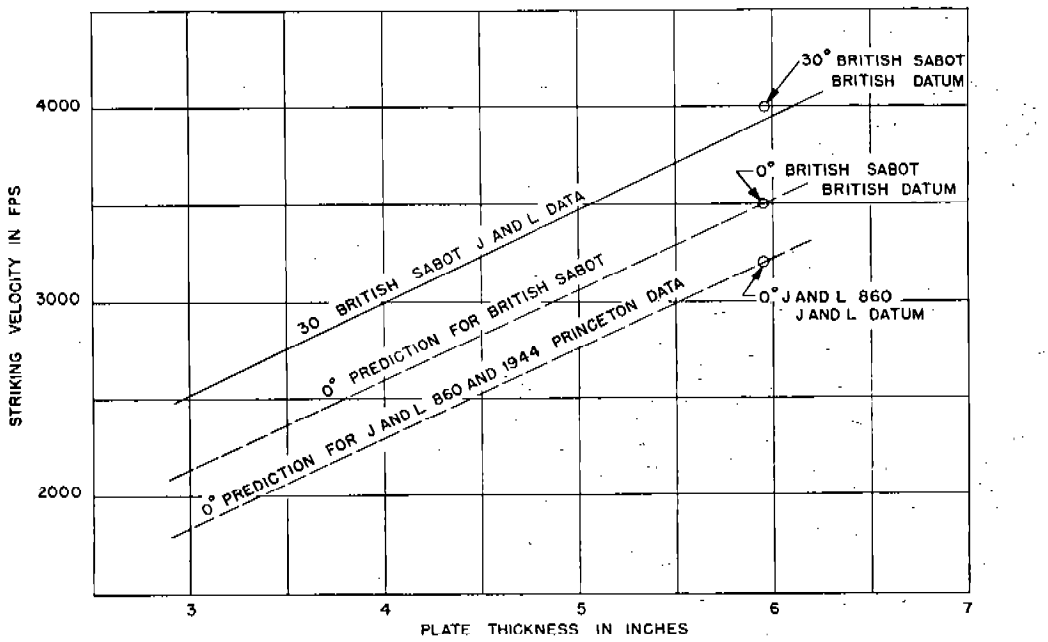


FIGURE 17. Ballistic limit as a function of striking velocity and plate thickness. (This figure has appeared as Figure 44C in NDRC Report No. A-456.)

[redacted]

6-in. plate, for a 90/63-mm skirted projectile, which had been scaled up from the 57/40-mm projectile dimensions. These calculations were made on the basis of a core weight of 6.04 lb and a core diameter of 1.75 in. for the enlarged projectile.

A prediction of the perforation range for a 90/63-mm projectile against 3- and 6-in. armor plate is shown in Figure 18. The retardation for this prediction was considered to be inversely proportional to the projectile weight.

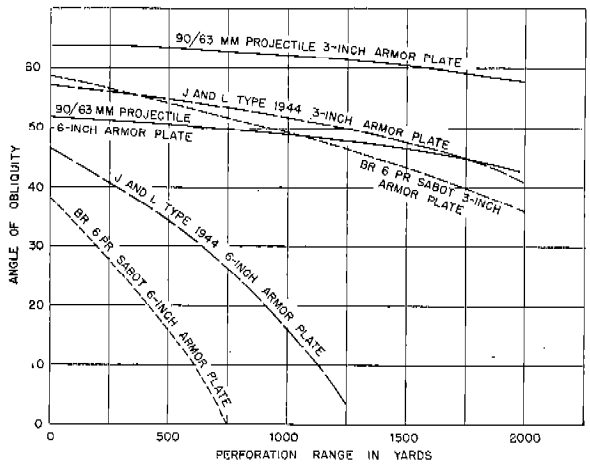


FIGURE 18. Perforation range as a function of angle of obliquity for J&L Type 944 and British 6-pounder sabot: Muzzle velocity, 4,150 fps. (This figure has appeared as Figure 44E in NDRC Report No. A-456.)

30.7 SUGGESTIONS FOR FUTURE DEVELOPMENT

Any plans for future development of tapered-bore guns and skirted projectiles should include attention to the following:

1. Application of a thin layer of bronze or other bearing material on the bearing surfaces of the skirts of projectiles: This should greatly improve the wear and accuracy life of gun tubes and tapered adaptors for the observed wear therein is predominantly through friction.

2. Application of wear resistant liners of such material as stellite in gun tubes and adaptors: With suitable bearing material coatings on projectiles and wear resistant surfaces in gun tubes and adaptors the life of tapered-bore guns fired at present pressures should equal or exceed the life of standard guns.

3. Development of a suitable high-explosive type skirted projectile for antiaircraft use: The potential advantages of subcaliber projectiles in this service are tremendous.

4. Detailed analysis of the shock stresses, plastic deformation, and friction effects in projectile skirts: It appears most likely that improvements in maximum velocity without breakage and reduction in length of tapered bore and straight section of adaptors may result from such studies.

Chapter 31

PRE-ENGRAVED PROJECTILE WITH CHROMIUM-PLATED BORE

By *Nicol H. Smith*[a]

31.1 INTRODUCTION[b]

IN THE EARLY WORK with the caliber .50 erosion-testing gun described in Section 11.2.1, it was soon realized that for hypervelocities the standard caliber .50 gun barrel and bullet were not satisfactory. The gilding metal jacket was too weak to withstand the rotational stresses due to the high velocity as long as the depth of the grooves was as small as it is in this barrel. This deficiency was partly overcome by using a banded projectile with a copper rotating band, but it needed to be excessively wide for satisfactory performance.

In addition, there was little or no exact information concerning (1) the relative effect on gun erosion of wear produced by the engraving and rubbing of the projectile and (2) the influence of gas leakage (and obturation) on gun erosion. These questions could be answered by experimental firings of pre-engraved projectiles in the caliber .50 erosion-testing gun. With this end in view, work on pre-engraved projectiles (hereafter referred to as PE) was started at The Franklin Institute in January 1943.

The use of PE projectiles makes possible the reduction to a minimum of engraving stresses and bullet friction, properties inherent in projectiles which are not pre-engraved. Thus it is possible to eliminate these factors as contributing causes of gun erosion and isolate that which may be attributed to powder gases alone.

Hence, the purpose of this investigation became threefold.

1. To determine the effect of PE projectiles upon gun erosion, pressure, velocity, and accuracy;
2. To examine the exterior ballistics of PE projectiles of different design; and
3. To see how such projectiles can be adapted to firing in existing guns of different caliber.

Early work on PE projectiles had been done in England and France, especially by Charbonnier during World War I. Reference is made to the more complete report[120] for a historical sketch of PE projectiles. They were used by the Germans in World War II for at least one gun, a 28-cm railway gun.[303,304]

31.2 CONCLUSIONS

The use of PE projectiles has enabled one to determine the relative effect of the components affecting gun erosion. Results have shown that (1) the engraving of the rotating band and the abrasion produced by the friction of the bullet are important factors contributing to the erosion of both gun steel and chromium plate; (2) gas leakage is not a direct cause in initiating gun erosion; and (3) reduction of engraving stresses and bullet abrasion reduces the wear of gun steel and chromium-plated gun bores. The use of PE projectiles in determining the erosiveness of different propellants is described in Section 15.3.

The reduction of bullet wear results in an increase in the velocity life of the gun. This increase is about twofold to fivefold in gun steel bores and twentyfold in chromium-plated bores.

PE projectiles permit the use of high-strength steel bands, thereby resulting in a very material improvement in the accuracy of the projectile.

Experiments with the caliber .50 Browning machine gun mechanism have shown that PE projectiles properly indexed can be fired in a gun having a high cyclic rate of fire without hang-ups or any malfunction of the gun attributable to the PE projectile, as described in Section 28.4.

The use of the steel-banded PE projectile chromium-plated bore combination makes it possible to obtain a hypervelocity gun having a greater velocity- and accuracy-life.

31.3 METHODS OF TESTING AND MEASUREMENT

The caliber .50 erosion-testing gun (Section 11.2.1) was used as the tool in the preliminary tests of the PE bullets. In most tests double-base powder containing 20 per cent nitroglycerin was used.

[a] Associate Director, The Franklin Institute, Philadelphia, Pa.

[b] Sections 31.1 to 31.7 have been based on NDRC Report A-448[120] by the same author, to which reference should be made for further details. All the tables except No. 12 and all the figures except No. 19 have been taken from that report.

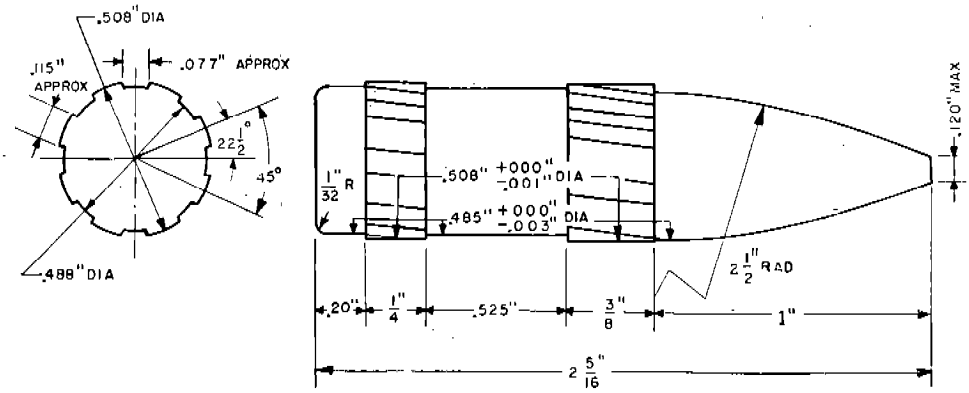


FIGURE 1. Caliber .50 PE projectile (soft steel).

The PE bullet shown in Figure 1 was adopted as the standard steel-banded PE projectile for test purposes. Conditions of loading were chosen in establishing the powder charge to give a maximum powder pressure of 56,000 to 58,000 psi (copper). The web of the powder was adjusted by mixing a "fast" powder (small web) with a complementary part of a "slow" powder (large web) so that a charge of 476 grains gave the desired pressure and a velocity of about 3,700 fps in a 45-in. barrel.

Velocity and pressure measurements were obtained at intervals to determine the velocity-life of the gun. Plug gauge and star gauge measurements were made at intervals to determine the distribution and progress of erosion of the lands and grooves. Accuracy measurements were taken at 100 ft to determine the accuracy-life of the gun.

The gun was considered to have failed when: (1) the velocity had dropped 200 fps, or (2) the mean radius of dispersion at 100 ft had increased to three times its initial value or keyholing bullets were observed.

31.4 CALIBER .50 EROSION-TESTING GUN EXPERIMENTS

31.4.1 Introduction

PE projectiles were fired in gun barrels having a steel surface and a chromium-plated surface. In both cases the effect of PE projectiles on the following was studied.

1. Progress and distribution of land and groove erosion.
2. Pressure and velocity performance.
3. Accuracy performance.

In addition, using PE projectiles as a tool, the effects of the following factors on the erosion of gun steel and of chromium plate were studied.

1. Gas leakage and obturation.
2. Type of projectile.
3. Thickness of chromium plate.

The results and conclusions of these tests are given in the following sections.

31.4.2 Effect of Gas Leakage and Improved Obturation on the Erosion of Gun Steel

Since the standard PE projectile has a clearance of 0.002 to 0.003 in. across the lands and grooves in the bore, the first question which is presented is: "What effect will this gas leakage have on erosion?" To answer this question, the following tests were fired.

1. Standard PE projectiles for 0.005-in. rifling which gave a calculated leakage area of 0.0028 sq in.
2. PE projectiles having two slots 0.020-in. deep milled diametrically opposite, which gave a calculated leakage area of 0.0078 sq in.
3. PE projectiles having two slots 0.030-in. deep milled diametrically opposite which gave a calculated leakage area of 0.0103 sq in.
4. Standard PE projectiles with cellulose obturating wads saturated with liquid fluorocarbon.
5. Standard PE projectiles with solid fluorocarbon obturating wads.

Liquid fluorocarbon is a very stable organic compound (polymerized polyfluorethylene derivative) which under the conditions of firing does not foul the bore by its decomposition products. This material has the consistency of heavy molasses. Cellulose wads were saturated with the heated liquid and attached to the base of the PE projectile.

The solid fluorocarbon was the same basic material but polymerized further to the solid condition. Wads were cut to fit the neck of the cartridge case and attached to the base of the projectiles. The fluorocarbons were obtained from Division 8, NDRC.

When making the firing test the successive rounds were so chambered that the slots in the projectile were progressively rotated one barrel groove per round, thus insuring equal presentation of the slot around the circumference of the bore.

In order to keep the pressure and powder charge constant at 56,000 to 58,000 psi (copper) and 476 grains, respectively, it was necessary to increase the percentage of fast powder as the leakage area was increased.

A summary of the firing conditions and the observed increase in land and groove diameters at 0.5 in. beyond the origin of rifling are given in Table 1. The latter data are shown graphically in Figures 2 and 3.

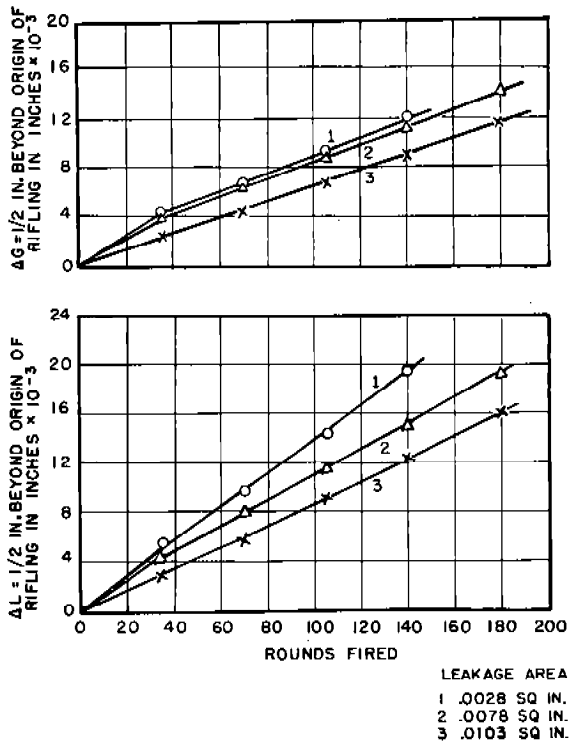


FIGURE 2. Effect of projectile clearance on land and groove erosion, for PE projectiles fired in the caliber .50 erosion-testing gun.

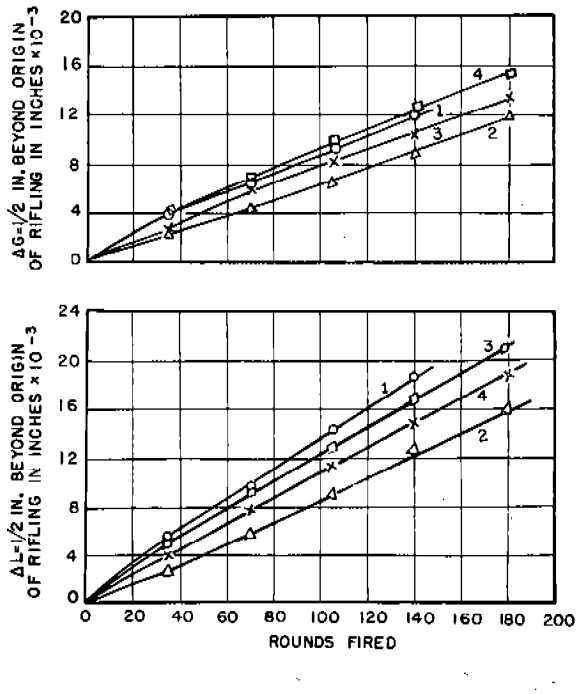


FIGURE 3. Effect of obturation of PE projectiles on land and groove erosion of a steel barrel in the caliber .50 erosion-testing gun.

TABLE 1. Firing conditions and land and groove erosion for gas leakage tests with caliber .50 pre-engraved projectiles after 35, 70, 105, 140, and 180 rounds.

Test	Leakage area (in.)	Pressure* (psi)	Velocity (fps)	Increase in land diameter, ΔL in in. × 10^{-3}					Increase in groove diameter, ΔG in in. × 10^{-3}				
				35	70	105	140	180	35	70	105	140	180
L1(F4)	0.0028	57,200	3,753	5.6	9.6	14.4	18.7	....	4.2	6.5	9.3	12.0	....
F(F4)	0.0078	54,900	3,630	4.4	8.2	11.6	15.0	19.3	4.0	6.3	8.8	11.1	14.1
F(F5)	0.0103	57,500	3,678	2.8	5.7	9.1	12.5	15.8	2.3	4.5	6.6	8.8	11.7
F(F3)	0†	56,700	3,705	4.0	7.6	11.2	14.8	18.8	2.6	6.0	8.2	10.5	13.5
F(F6)	0§	55,800	3,701	5.0	9.2	13.0	16.7	21.0	4.0	6.4	9.9	12.5	15.4

* All tests fired with 476 grains double-base powder of two granulations.
†Cellulose wads.
§Fluorocarbon wads.

These results show that the increase in land and groove diameter is least for the greatest gas leakage area. The data for ΔL and ΔG fall in the following order:

ΔL 0.0028 in.^{2} > 0.0078 in.^{2} > 0.0103 in.^{2} leakage area.

ΔG 0.0028 in.^{2} > 0.0078 in.^{2}> 0.0103 in.^{2} leakage area.

ΔL Solid fluorocarbon wad > cellulose-liquid fluorocarbon wad > 0.0103 in.^{2} leakage area.

ΔG Solid fluorocarbon wad > cellulose-liquid fluorocarbon wad > 0.0103 in.^{2} leakage area.

The land erosion observed with both types of obturating wads was slightly less than observed with the standard PE projectile (0.0078 sq in. leakage area). However, in both cases the erosion was greater than observed with the projectiles having the greatest leakage area (0.0103 sq in. leakage area).

These test data show that for a caliber .50 PE projectile the clearance between the projectile and the bore neither initiates nor accelerates gun erosion. In fact, with increasing leakage area it was found that the measured land and groove erosion decreased. It is believed that this reduction in erosion is caused by the increasing percentage of fast powder. An increase in the percentage of fast powder would result in a shorter duration of maximum pressure and hence maximum temperature.

Since the PE projectile is free moving in the bore of the gun, any gas leakage past the projectile would only expose one particular area of the bore to the blast of hot gas for a very short time. This is contrary to the situation with the regular engraving-type projectile, which is momentarily slowed up in its travel during the engraving process. Any gas leakage past the *engraving bullet* would accelerate gun erosion because of the "blow torch" action discussed in Section 5.4.4 of the gases for a much longer time on a localized area of the bore.

Serious effects due to gas leakage with PE projectiles might be experienced in a larger caliber gun, where the time required to start the projectile moving might be unusually long. In this case the product of duration (time) × heat (cal/cm^2) might be great enough to increase erosion. In this case it would be necessary to use some practical method for obturating the PE projectile.

31.4.3 Effect of Pre-Engraving on Pressure and Velocity Performance

Starting Resistance and Powder Pressure

The manner in which a given propellant burns, which determines the maximum powder pressure, is dependent mainly upon the resistance to starting the projectile. In a conventional type of gun using banded ammunition, this starting resistance can be attributed to: (1) force to overcome the inertia of the projectile, (2) force to unseat bullet from case, and (3) force to engrave the rotating band.

As the starting resistance decreases, the burning characteristics of the powder are so changed as to affect seriously the maximum powder pressure. Using PE projectiles the force to engrave is completely eliminated, with the result that the powder pressure obtained with the same granulation of propellant as used for an engraving bullet is very much less.

The effect of decreasing the force to engrave is clearly shown in Table 2. The force to engrave was gradually decreased by reducing the band diameters and finally eliminated by pre-engraving the projectiles. A pressure drop of 17,900 psi and a velocity drop of 292 fps were observed.

In order to keep the pressure at the level observed with an engraving-type bullet, keeping the powder charge the same, it is necessary to use a powder with

Table 2. Effect of engraving force on pressure and velocity of caliber .50 projectiles.

Band dia. (in.)	Land dia. (in.)	Band/Land interference (in.)	Pressure* (psi)	Pressure change	Velocity (fps)	Velocity change
0.510	0.490	0.020	54,000	.....	3,452	.....
0.509	0.490	0.019	54,200	+ 200	3,405	− 47
0.508	0.490	0.018	52,700	− 1,300	3,380	− 72
0.503	0.490	0.013	49,100	− 4,900	3,330	−122
0.498	0.490	0.008	44,800	− 9,200	3,280	−172
0.493	0.490	0.003	41,600	−12,400	3,233	−219
(PE)	0.490	.....	36,100	−17,900	3,160	−292

* All firings made with a charge of 465 grains IMR powder, web thickness 0.0338 in.

[redacted]

a smaller web thickness ("faster" powder). In the experiments just referred to, the same charge of a powder having a web thickness of 0.0285 in. gave the same pressure and a greater velocity than the engraving-type bullet. The relationship between type of projectile, web thickness, pressure and velocity is shown in Table 3.

TABLE 3. Relationship between web thickness, pressure, and velocity for banded (AT) and pre-engraved (PE) caliber .50 projectiles.

Bullet	Powder charge (grains)	Web thickness (in.)	Pressure (psi)	Velocity (fps)
AT	465 IMR	0.0338	54,000	3,452
PE	465 IMR	0.0338	36,100	3,160
PE	465 IMR	0.0285	53,900	3,520

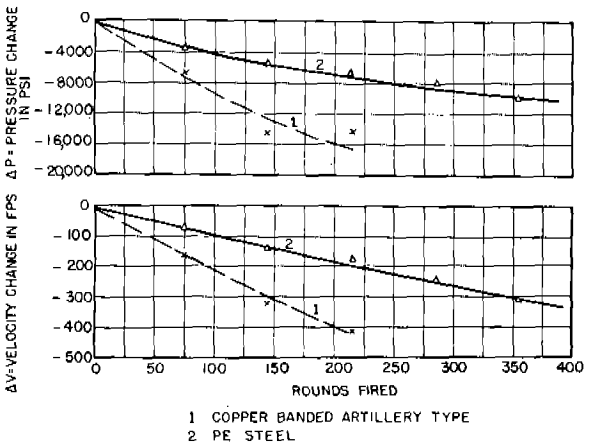


FIGURE 4. Comparison of pressure and velocity change for artillery banded and PE steel projectiles, fired in the caliber .50 erosion-testing gun with double-base powder at a muzzle velocity of 3,700 fps.

PRESSURE-VELOCITY CHANGE AND BORE ENLARGEMENT

Any change in the forcing cone or other area of the bore close to the origin of rifling affects the starting resistance of an engraving-type bullet. This consequently affects the pressure and the velocity. However, the engraving component of the starting resistance has been completely eliminated when using PE bullets. This means that the pressure and the velocity of a PE projectile are little affected by any enlargement at the origin of rifling.

Experiments have shown that this is not actually true. As the bore enlarges due to gas erosion, the amount of gas leaking past the bullet increases. During the early stages of the burning of the powder, the rate of burning is seriously affected by any change in the amount of gas that might leak past the bullet and thus affect the pressure over the powder. For this reason, as the bore enlarges there is a gradual decrease in pressure and velocity. The use of obturating devices to prevent this gas leakage and maintain a more uniform pressure and velocity level is described in a later paragraph of this section.

A comparison of the pressure and velocity performance with artillery-type bullets having copper rotating bands (designated as AT) and PE bullets is shown in Figure 4. These data are an average of two tests. From these curves it may be seen that a velocity drop of 200 fps occurred much sooner with the engraving-type bullets and the pressure drop corresponding to that velocity change was 8,800 psi instead of 7,200 psi.

EFFECT OF DOUBLE ENGRAVING ON POWDER PRESSURE

As the lands at the origin of rifling erode and the point of engagement with the PE projectile advances towards the muzzle there comes a time when the PE projectile does not mesh with the rifling and engraving of the steel band might occur. Since the powder web and load were adjusted for *no engraving resistance* there was a very good chance of obtaining excessively high pressures and producing damaging effects if double engraving occurred. However, examination of the curve of pressure versus rounds fired in Figure 4 shows a continuous drop in pressure, even though double engraving of the steel band occurred between rounds 215 and 285. It is believed that the gas leakage which occurred due to the increase in bore dimensions caused by erosion acted as a safety valve when the bullet was momentarily retarded while being double engraved.

EFFECT OF OBTURATION ON VELOCITY PERFORMANCE

To determine the effect of various means of obturation on velocity performance of PE projectiles the following obturated caliber .50 PE projectiles shown in Figure 5 were tested:

1. Standard steel PE projectile.
2. Standard PE projectile with copper obturating ring behind rear PE band.
3. Standard PE projectile with a cellulose acetate (plastic) obturating cup attached to the base of the projectile.

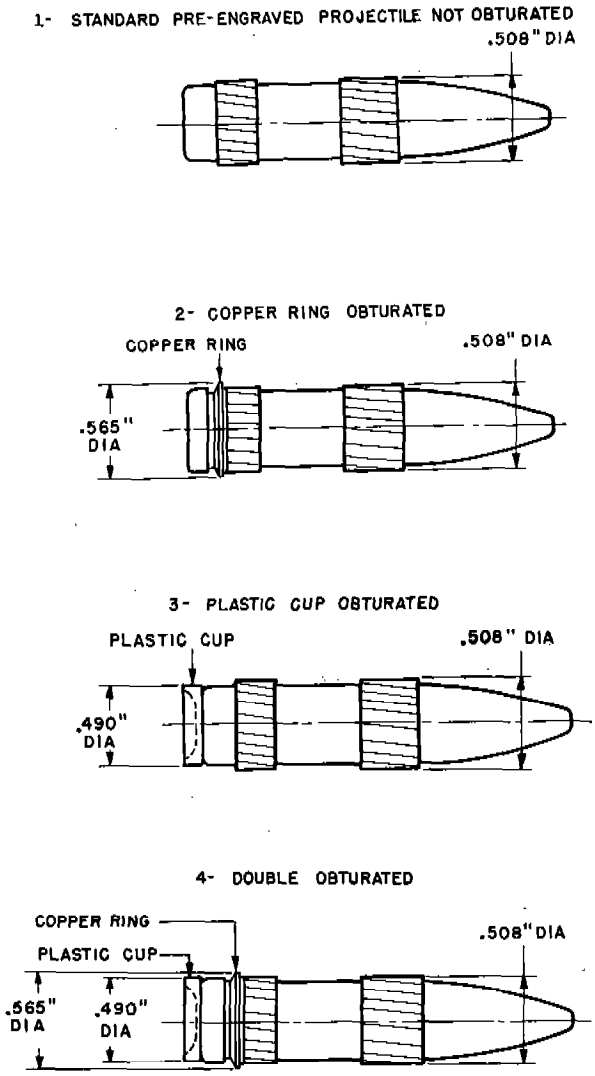


FIGURE 5. Types of obturated PE projectiles used in tests with the caliber .50 erosion-testing gun.

4. Standard PE projectile combining the copper obturating ring with the plastic obturating cup.

To test the effectiveness of the obturating devices velocity measurements were taken at various stages in the life of the gun. The erosion rounds during the test using Firing Schedule II were standard PE bullets (No. 1 in Figure 5). The initial firing conditions are given in Table 4, and the velocity changes at various stages of bore erosion are shown in Figure 6. In all instances the obturating devices increased the number of rounds fired for a velocity drop of 200 fps.

These data show that the velocity performance can be improved and maintained at a more uniform level by using obturating devices with PE projectiles. The best obturating device was that used with projectile No. 4. The copper obturating ring was effective at low powder pressure and the plastic base cup became effective as the powder pressure reached its maximum.

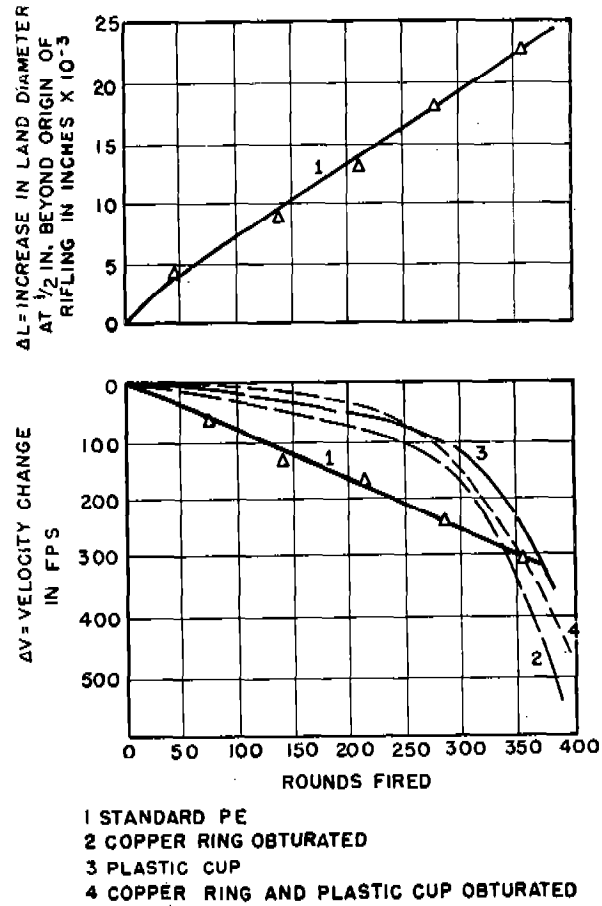


FIGURE 6. Velocity performance of the obturated PE projectiles shown in Figure 5, fired at a muzzle velocity of 3,650 fps.

TABLE 4. Comparison of velocity change with obturated caliber .50 PE projectiles.

Bullet No. Powder (476 grains)	1 30 Per cent slow 70 Per cent fast	2 75 Per cent slow 25 Per cent fast	3 75 Per cent slow 25 Per cent fast	4 75 Per cent slow 25 Per cent fast
Initial pressure (psi)	56,700	53,800	47,700	56,200
Initial velocity (fps)	3,645	3,650	3,440	3,673
Velocity after 355 rd (fps)	3,340	3,295	3,180	3,363

[redacted]

31.4.4 Effect of Pre-Engraving on Accuracy

The superior performance of the PE steel projectiles in a new and eroded barrel is due entirely to the high strength of the material in the band. Equally good accuracy has been obtained with a bullet having a steel band which has to be engraved in the gun. In the latter case, however, severe abrasion of the barrel occurred due to the high friction and engraving stresses of the steel band.

A comparison of the accuracy of ball bullets, M2, copper-banded artillery-type bullets and PE steel bullets fired for a range of velocities in new and eroded caliber .50 barrels is shown in Table 5. These data are shown graphically in Figures 7 and 8. These results show that: (1) ball bullets, M2, are not satisfactory for high velocity; (2) a banded artillery-type projectile is intermediate in accuracy between the ball and PE projectile and its accuracy is affected by erosion of the bore; (3) a PE steel projectile is the most accurate of these bullet types, and its accuracy is not affected by erosion of the bore.

TABLE 5. Accuracy of different types of caliber .50 bullets.

Velocity (fps)	Mean radius of dispersion (in.) at 100 ft		
	Ball, M2	Banded artillery type	PE
		(a) In new barrel	
2,900 ± 50	0.4	0.5	0.45
3,300 ± 50	1.2	1.0	0.8
3,700 ± 50	7.9	1.1	0.7
		(b) In eroded barrel	
2,900 ± 50	1.2	0.75	0.45
3,500 ± 50	10.9	1.45	0.45

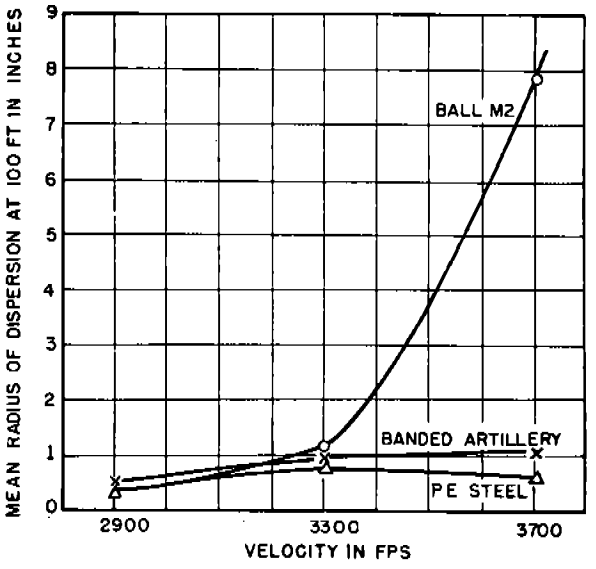


FIGURE 7. Dispersion of ball, M2, banded AT and PE projectiles for various velocities fired in the caliber .50 erosion-testing gun using a new steel barrel.

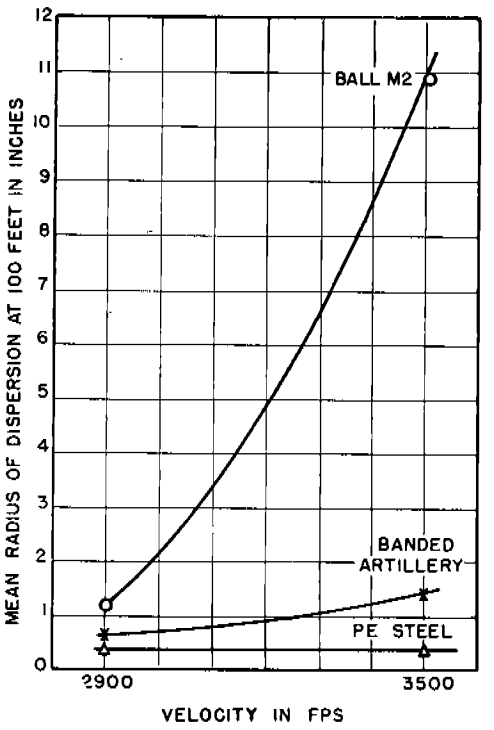


FIGURE 8. Dispersion of ball, M2, banded AT and PE projectiles for various velocities fired in the caliber .50 erosion-testing gun using an eroded barrel.

In firing gun steel barrels with PE bullets until accuracy failure occurs the accuracy of the PE bullet remains practically unchanged until engagement of the teeth on the bullet with the rifling in the barrel is lost. When misalignment occurs, the steel PE bullet is double engraved, and severe wear of the lands occurs. During this period the accuracy remains the same until a bore diameter is reached when the bearing area in contact with the lands is greatly overloaded and shearing of the steel band occurs.

This behavior results in a very uniform, good accuracy pattern throughout the accuracy-life of the gun, after which it suddenly becomes very bad. This is shown clearly in Table 6. The targets in Figure 9 illustrate the progress of accuracy failure. It is readily seen that (1) the accuracy is uniformly maintained throughout the life of the gun, (2) there is no gradually increased dispersion, and (3) accuracy failure is very bad when it does occur.

31.4.5

Effect of Band Material on Projectile Performance

The strength of the band material and the type of surface riding on the bore surface are important factors in the performance of a PE projectile. The strength of the band material (strength factor) is usually the determining factor in the accuracy-life of the gun, and the type of surface on the PE band and bourrelet (friction factor) is an important factor in decreasing the wear of the lands and grooves and thereby increasing the velocity-life of the gun.

Strength Factor. A comparison of the test data, such as shown in Figure 10, obtained by firing steel-banded PE and gilding metal-banded PE projectiles, shows a reduction in the land and groove wear when using gilding metal PE projectiles. The pressure and velocity drop caused by gilding metal-banded PE projectiles, however, are identical with those caused by the steel PE projectiles.

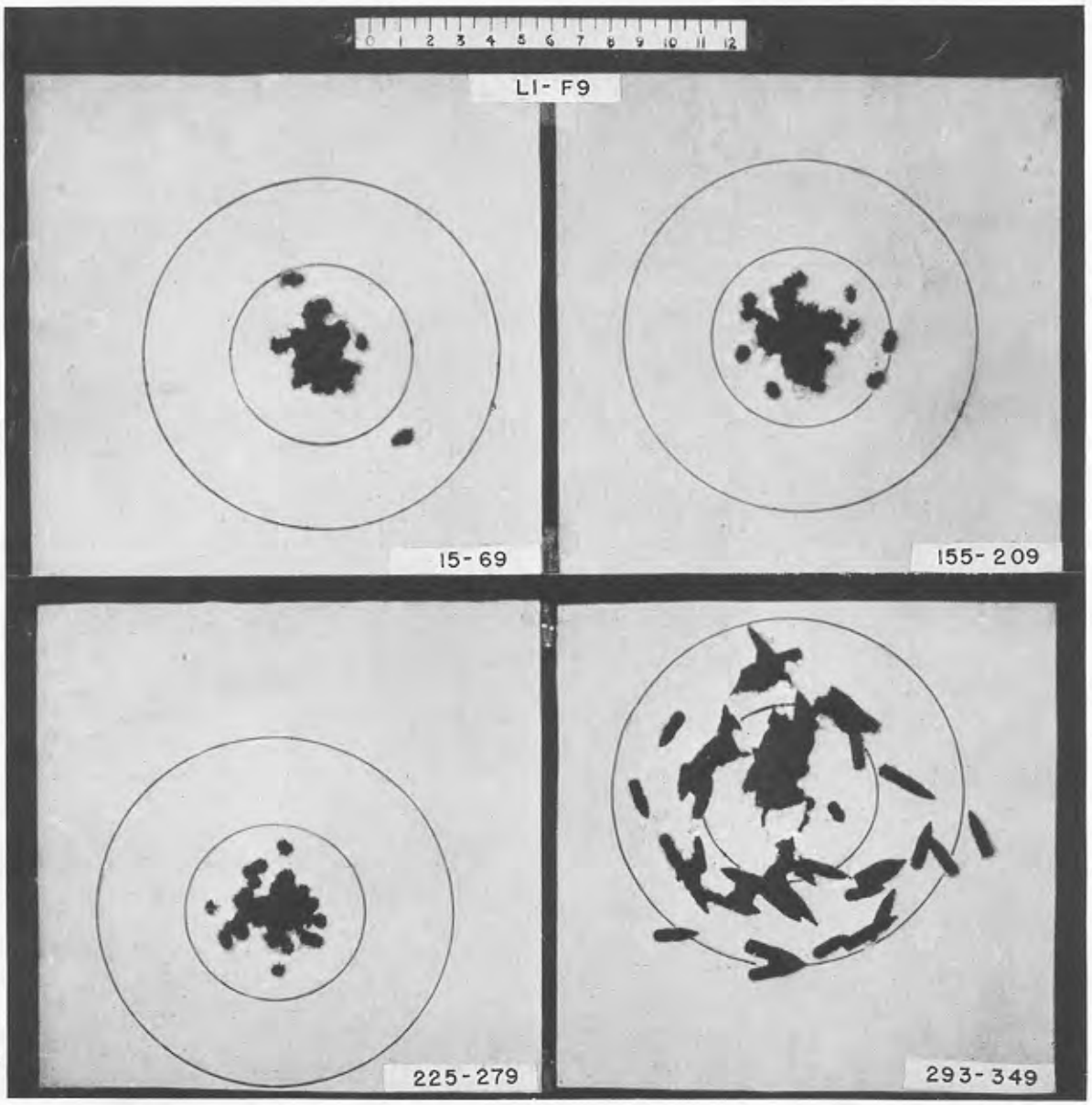


FIGURE 9. Accuracy targets for caliber .50 PE projectiles at 100 feet, during the firing of 54-round groups at four stages in the life of a steel barrel in the erosion-testing gun. The barrel reached the end of accuracy-life during the last group.

CONFIDENTIAL

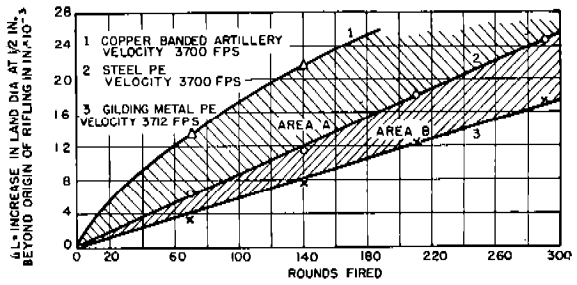


FIGURE 10. Comparison of land wear for banded artillery-type, steel PE, and gilding metal PE projectiles fired in the caliber .50 erosion-testing gun at a muzzle velocity of 3,700 fps.

A comparison of the accuracy measurements of artillery banded, steel PE, and Parco-Lubrized steel PE projectiles during the erosion life of a gun steel barrel is given in Table 6.

TABLE 6. Increase in accuracy of caliber .50 pre-engraved projectiles compared with copper banded artillery type fired at 3,700 fps from a new barrel.

	Mean radius of dispersion (in in.) at 100 ft			
Rounds	Artillery type	Gilding metal PE	Steel PE	Parco-Lubrized steel PE
1– 10	1.0	...	0.85	1.0
11– 65	2.4	1.4	1.1	1.0
81–135	3.3	1.6	1.1	0.9
151–205	...	2.1	1.1	1.0
221–275	...	4.0	1.1	1.0
291–345	...	...	3-2*	1.0
370–424	...	...	....	0.7
440–494	...	...	....	2.6*

* Keyholing bullets.

Keyholing bullets occurred after 280–290 rounds for the steel PE projectiles, and after 425–435 rounds for the Parco-Lubrized steel PE projectiles, thereby showing a one and one-half increase in accuracy life.

It is clearly seen that the progressive failure of the gilding metal band as erosion increases is due entirely to the lower strength of the band material. For this reason gilding metal is not recommended as a band material when fired under hypervelocity conditions.

Friction Factor. The decrease in land wear due to a change in coefficient of friction from steel against steel to gilding metal against steel is shown in Figure 10. Curve 1 gives the land enlargement for the engraving copper-banded projectiles. Curve 2 gives the same for the steel PE projectiles. Therefore, the area *A* between curves 1 and 2 represents the amount of land wear caused by the engraving of the rotating band.

Curve 3 gives the land enlargement for the gilding metal PE projectiles. Therefore, the area *B* between curves 2 and 3 represents the amount of land wear contributed by the friction of the steel-banded PE projectile.

In another pair of tests, steel PE projectiles were (1) cadmium plated, and (2) Parco-Lubrized[c] with oil treatment and then tested for accuracy and velocity performance and reduction in land and groove erosion.

Compared with the plain steel PE projectiles less land wear was observed with the cadmium-plated and Parco-Lubrized bullets. However, best all-around performance was observed with the Parco-Lubrized and oil-treated projectiles.

The comparison of land wear between banded artillery-type, steel PE and Parco-Lubrized PE projectiles is shown in Figure 11 and Table 7. Area *A* between curves 2 and 3 represents the amount of land wear at 0.5 in. from the origin of rifling contributed by the friction of the steel-banded PE projectile.

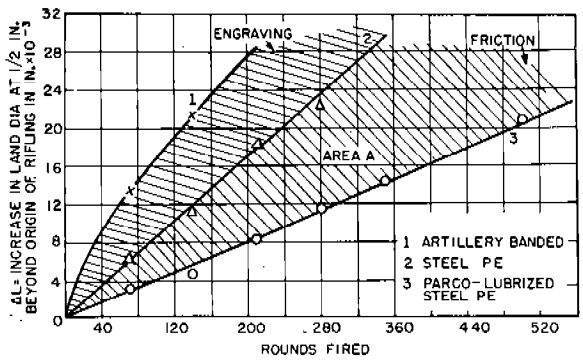


FIGURE 11. Comparison of land wear for banded artillery-type, steel PE, and Parco-Lubrized PE projectiles fired in the caliber .50 erosion-testing gun at a muzzle velocity of 3,650-3,700 fps.

The reduction in wear of the lands and grooves is reflected in the increase in velocity-life observed with barrels fired with Parco-Lubrized steel PE projectiles. The observed velocity changes at various stages of erosion, compared with those for banded artillery-type projectiles, are shown graphically in Figure 12. Using a 200-fps drop in velocity as the criterion for the velocity-life of the gun, these results, which are summarized in Table 8, show a twofold increase in velocity-life by Parco-Lubrizing the steel PE projectiles. The same increase in velocity-life of a chromium-plated bore surface was also observed.

[c] Defined in footnote (k) in Section 27.3.4.

TABLE 7. Land wear of caliber .50 barrels fired with pre-engraved projectiles at 3,650 to 3,700 fps (see Figure 11).

Bullet	Distance from O.R. (in.)	Increase in land diameter (10^{-3} in.) After rounds 70	140	210	280	350	500
Steel PE	0.5	6.4	11.4	18.1	22.5	....	....
Steel PE	2.0	3.1	7.8	14.4	18.8	....	....
Parco-Lubrized PE	0.5	3.3	4.9	8.1	11.5	14.5	20.5
Parco-Lubrized PE	2.0	2.9	3.3	6.8	10.0	12.5	18.2

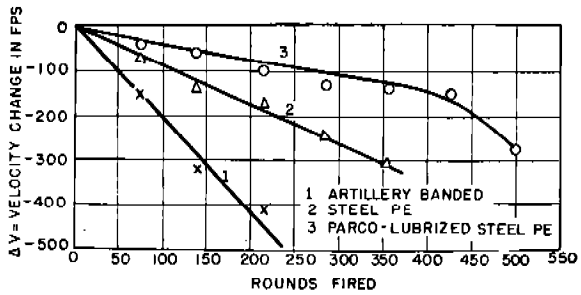


FIGURE 12. Comparison of velocity change for banded artillery-type, steel PE, Parco-Lubrized steel PE projectiles fired in the caliber .50 erosion-testing gun at a muzzle velocity of 3,650-3,700 fps.

TABLE 8. Velocity life of caliber .50 steel barrels fired with bullets having rotating bands of different materials.

Bullet	Initial velocity (fps)	Velocity-life* (rounds)	(relative)
Artillery-type (copper banded)	3,657	95	1.0
Gilding metal banded, PE	3,712	215	2.3
Steel, PE	3,703	225	2.4
Steel, PE, Parco-Lubrized	3,646	455	4.8

* Number of rounds at which velocity drop equaled 200 fps.

31.4.6 Effect of Type of Powder

In the determination of the erosiveness of propellants, which is described in Chapter 15, PE projectiles played an important role. By comparing the results obtained when they were fired with those when banded artillery-type projectiles were fired, it was possible to distinguish between the amount of wear of the lands contributed by engraving of the band and friction of the band. As shown in Figure 9 of Chapter 15, discussed in Section 15.5.2, this amount is proportionately much higher for propellants having low flame temperatures, for the powder gas erosion becomes the predominating factor with the hotter propellants.

31.5 OPTIMUM THICKNESS OF CHROMIUM PLATE

Altered layers, similar to those formed in unprotected steel (Section 12.1.2), are observed in the steel underlying thin chromium plates. Since the formation of the altered layer is a thermal effect, the thickness of the altered layer produced is a function of the plate thickness and of the temperature and heat content of the powder gases. Experimental data, obtained with caliber .50 and 37-mm guns, suggest that there is a definite chromium plate thickness for each gun that will give the maximum performance of PE projectiles. This critical chromium plate thickness is determined by the heat input to the bore surface. In other words, guns having a high heat input per unit area require a thicker chromium plate than guns having a low heat input.

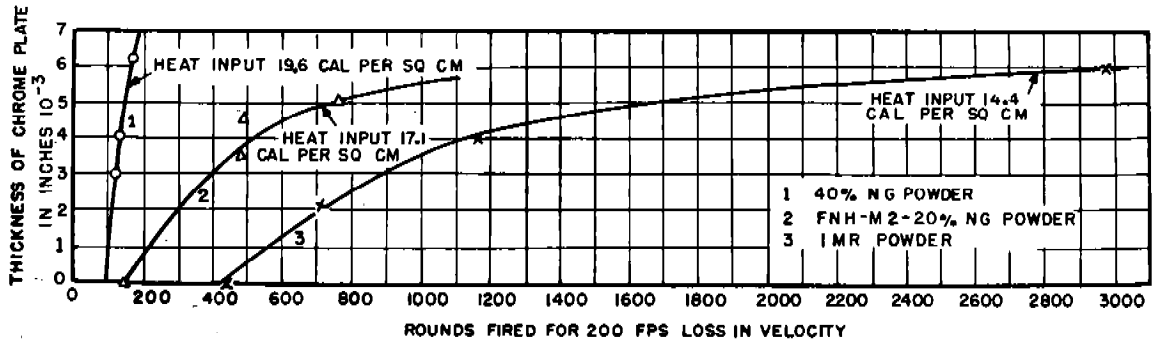


FIGURE 13. Effect of powder type and chromium-plate thickness on performance of PE projectiles fired in the caliber .50 erosion-testing gun.

[redacted]

In order to vary the heat input per unit area in the caliber .50 erosion-testing gun, powders of different flame temperature were used. The thickness of the chromium plate was varied from 0.002 to 0.006 in. In all tests the same ballistic level was maintained; namely, a pressure of 56,000 to 58,000 psi (copper) and a velocity of 3,600 to 3,650 fps. The powders used were (1) IMR type, flame temperature 2940 K; (2) FNH-M2, flame temperature 3560 K; (3) a double-base powder containing 40% nitroglycerin, flame temperature 3945 K.

Standard steel-banded PE projectiles (Figure 1) were used in the tests. The barrels were fired until a drop in velocity of 200 fps was observed. The velocity-life of the barrels having the various chromium plate thicknesses and fired with the different powders is summarized in Table 9.

TABLE 9. Velocity-life of caliber .50 barrels firing PE projectiles as a function of chromium plate thickness and powder.

Thickness of Cr plate (in.)	Rounds fired for a velocity drop of 200 fps
(a) Powder: 40% (nitroglycerin content) double-base; heat input, 19.6 cal/cm².	
0	90
0.003	120
0.004	130
0.00625	180
(b) Powder: FNH-M2 (double-base containing 20% nitroglycerin); heat input, 17.1 cal/cm².	
0	146
0.0035	470
0.0045	490
0.005	765
(c) Powder: IMR (single-base); heat input, 14.4 cal/cm².	
0	362
0.00225	710
0.004	1,165
0.006	2,970

The above data are shown graphically in Figure 13. These curves show that when the heat input is above 19 cal/cm², a chromium plate thickness greater than 0.006 in. is necessary in order to obtain the best velocity performance of PE projectiles. When the heat input is between 14 and 15 cal/cm² the best velocity performance is observed with 0.006-in. chromium plate thickness. When the heat input is about 17 cal/cm², good performance is observed with 0.005-in. chromium plate, but considerably better performance would have been observed if the plate thickness were between 0.007 in. and 0.008 in.

It has been shown[76] in the testing of various chromium plate thicknesses that there is a limit to the thickness that will perform satisfactorily due to the brittle nature of chromium. Above 0.008-in. thickness, chromium plate fired with PE bullets breaks away on the lands and exposes gun steel or leaves a thin layer of plate, both of which are very susceptible to gas erosion.

A thick cobalt undercoat (0.007 to 0.010 in.) next to the steel followed by a thinner chromium layer (0.003 in.) performed very satisfactorily in some preliminary firing tests under hypervelocity conditions, using PE projectiles, as described in Section 20.2.4.

It is recommended, therefore, that when calculations of heat input in a particular gun are very high and show the need of a chromium plate thicker than 0.008 in., that a thick cobalt-chromium duplex plate be tried.

31.6 INCREASE IN LIFE OF CHROMIUM-PLATED BORES

In the early firings of chromium-plated bores with the usual engraving-type projectiles it was soon recognized that engraving stresses and friction were a major factor in the failure of the chromium plate. Detailed description of the progress of chromium plate failure under hypervelocity conditions is given in the final report on coatings.[76] The process of erosion in chromium-plated Service guns is described in Section 20.2.1.

In general, the failure of a chromium-plated surface is due to (1) engraving stresses, (2) bullet friction, and (3) thermal changes at the gun steel-chromium interface. The first two items are effective chiefly because of the lack of ductility of the chromium.

The features of chromium plate failure usually observed are: (1) cracking of the plate in a block or checkerwork pattern; (2) curling up of the edges of the blocks which gives the surface a wrinkled appearance; (3) pitting, or removal of small crack-isolated blocks of chromium; (4) spalling or removal of large areas due to undercutting; and (5), in the case of plates thinner than the critical thickness, the formation of an altered steel layer beneath the plate.

As mentioned in Section 31.4.4, the wear and friction factors in the erosion of gun steel were greatly reduced by the use of PE projectiles. Since chromium plate, because of its high melting point (about 1950 C), possesses excellent resistance to powder gas erosion, the combination of a chromium-plated bore and PE

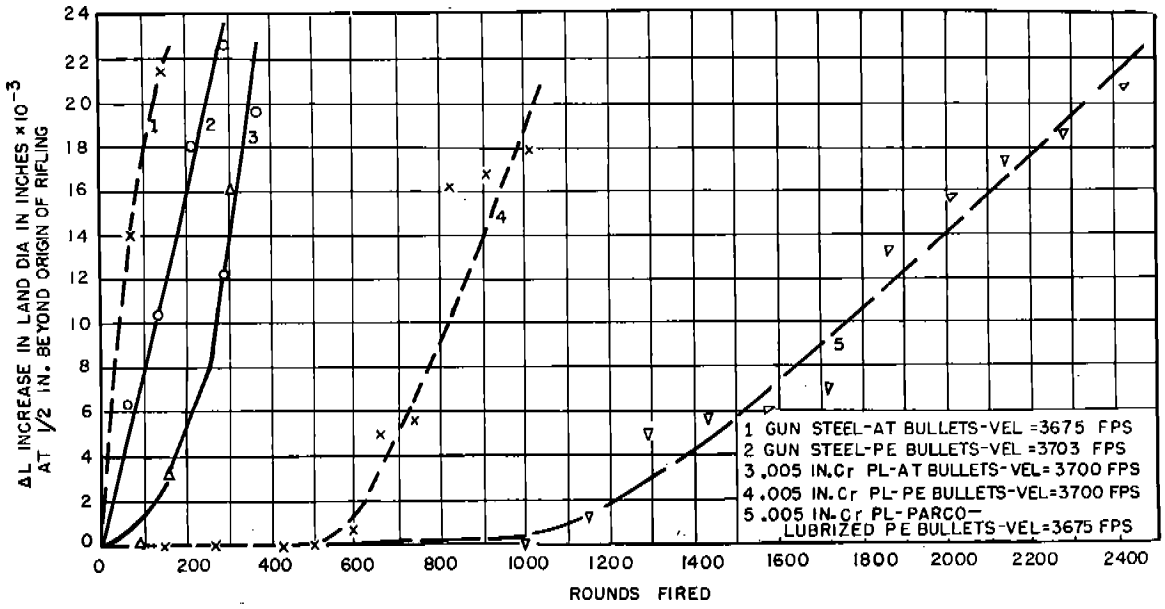


FIGURE 14. Progress of land erosion of plain steel and chromium-plated steel barrels in the caliber .50 erosion-testing gun fired with banded artillery-type, steel PE, and Parco-Lubrized PE projectiles at a muzzle velocity of 3,675 to 3,700 fps.

Parco-Lubrized steel projectiles gives excellent performance.

31.6.1 Effect on Land Erosion

In the following tests double-base powder was used to give a velocity of 3,650 to 3,700 fps in a 45-in. barrel. The observed increase in land diameter at 0.5 in. beyond the origin of rifling for gun steel and 0.005-in. chromium plate using banded artillery-type and steel PE projectiles is shown graphically in Figure 14. The results show that the chromium plate protects the steel surface for a definite period. This period of protection is much shorter for the banded artillery-type bullets. As soon as gun steel is exposed to the erosive effects of the powder gases, the rate of erosion increases very rapidly. Parco-Lubrized PE bullets give the longest protection period and the lowest erosion rate after the gun steel has been exposed.

31.6.2 Effect on Velocity Performance

The velocity change observed with banded and PE projectiles fired in gun steel and chromium-plated bores is summarized in Figure 15.

Using a drop in velocity of 200-fps as the criterion for the velocity-life of the gun, it is readily seen that Parco-Lubrized PE bullets combined with a chromium-plated bore improves the velocity performance of the gun. The performance is shown in Table 10.

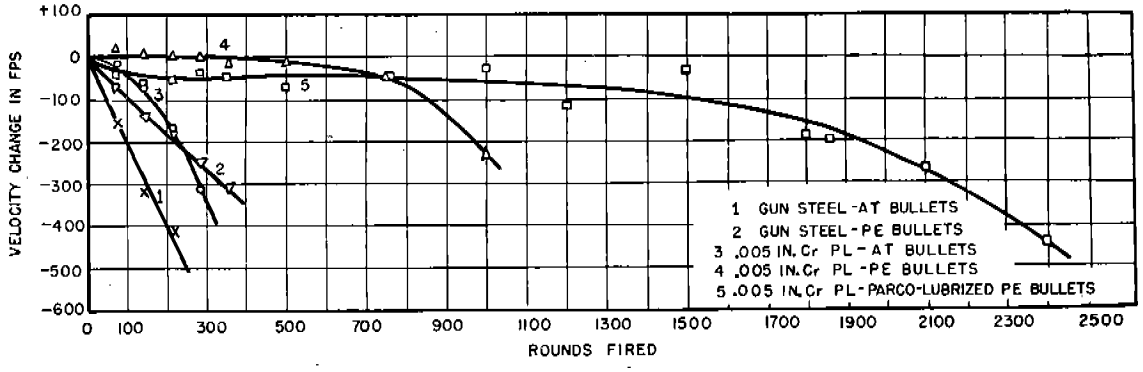


FIGURE 15. Comparison of velocity change for banded artillery-type, steel PE and Parco-Lubrized PE projectiles fired from plain steel and chromium-plated steel barrels in the caliber .50 erosion-testing gun at a muzzle velocity of 3,675-3,700 fps.

[redacted]

TABLE 10. Comparison of velocity performance.

Bore surface	Bullet	Initial velocity (fps)	Rounds fired for $\Delta V = -200$ fps	Relative velocity-life
Gun steel	Artillery banded	3,675	95	1.0
Gun steel	PE	3,703	225	2.4
0.005-in. Cr plate	Artillery banded	3,700	220	2.3
0.005-in. Cr plate	PE	3,700	975	10.0
0.005-in. Cr plate	Parco-Lubrized PE	3,675	1,875	20.0

The decrease in wear and friction of the Parco-Lubrized bullets on a chromium-plated bore is shown in the increase in velocity-life of the gun. These results show that in order to obtain the maximum performance with PE projectiles it is necessary to (1) Parco-Lubrize all parts of the projectile that rub on the bore, and (2) use a chromium-plated bore having a chromium-plate thickness greater than the critical thickness necessary to prevent formation of an altered steel layer at the steel-chromium interface.

31.6.3 Effect on Accuracy Performance

In one test, Parco-Lubrized PE bullets were fired in a chromium-plated bore (0.005-in. chromium plate) until keyholing bullets were observed at 100 ft from the muzzle. This did not happen until 2,775 rounds had been fired, whereas with a gun-steel bore and steel PE bullets, keyholing started after 248–322 rounds had been fired. Thus the combination of chromium plate and Parco-Lubrized steel PE bullets increased the accuracy-life by 8.5 to 10 times.

31.7 DESIGN AND TEST OF THE 37-MM GUN, T47

31.7.1 General Plan

It has been shown in the preceeding sections that a large increase in velocity-life could be obtained in a hypervelocity gun by using Parco-Lubrized steel PE projectiles in combination with a chromium-plated bore. The thickness of the chromium plate should be such that the temperature at the chromium-gun steel interface is below the transition temperature of the steel in order to prevent the formation of an altered layer.

In the caliber .50 erosion-testing gun, twentyfold increase in velocity-life was observed. Although the increase in velocity-life would not necessarily be of the same order for larger caliber guns, it was felt that it would be substantial.

As a preliminary to the design of a hypervelocity 90-mm gun (Section 31.8), it was decided to make a hypervelocity 37-mm gun and observe the performance of the PE chromium plate combination in this gun. With this end in view the following specifications for the gun tube were set up.

1. A 40-mm Bofors gun forging (Navy specification) length: 88.58 in.
2. Chambered for 40-mm case necked down to 37-mm. (Chamber capacity 29.9 cu in.)
3. Bored and reamed for a 37-mm projectile.
4. Rifled for 6 grooves of 0.0030-in. depth, with lands and grooves of equal width.
5. Lands at the origin of rifling pointed with a 30-degree slope to eliminate "hang-ups."
6. Plated with 0.006-in. standard chromium.

By firing a normal weight pre-engraved projectile at a pressure of 50,000 psi (copper), it was expected that a muzzle velocity of 3,500 fps would be achieved.

31.7.2 Gun Tube

The 40-mm gun forging was chambered, bored, and rifled according to the dimensions shown in Figure 16.

The constants for the 37-mm gun, T47, are as follows:

Length	88.58 in.
Chamber capacity	29.9 in.^{3}
Travel of projectile	76.58 in.
Number of grooves	6
Depth of grooves	0.030 in.
Twist	1 in 25 calibers
Ratio: width of groove/shelling width of land	1
Land diameter (after plating)	1.457+.002 in.
Groove diameter (after plating)	1.517+.002 in.
Groove width (after plating)	0.375+.005 in.

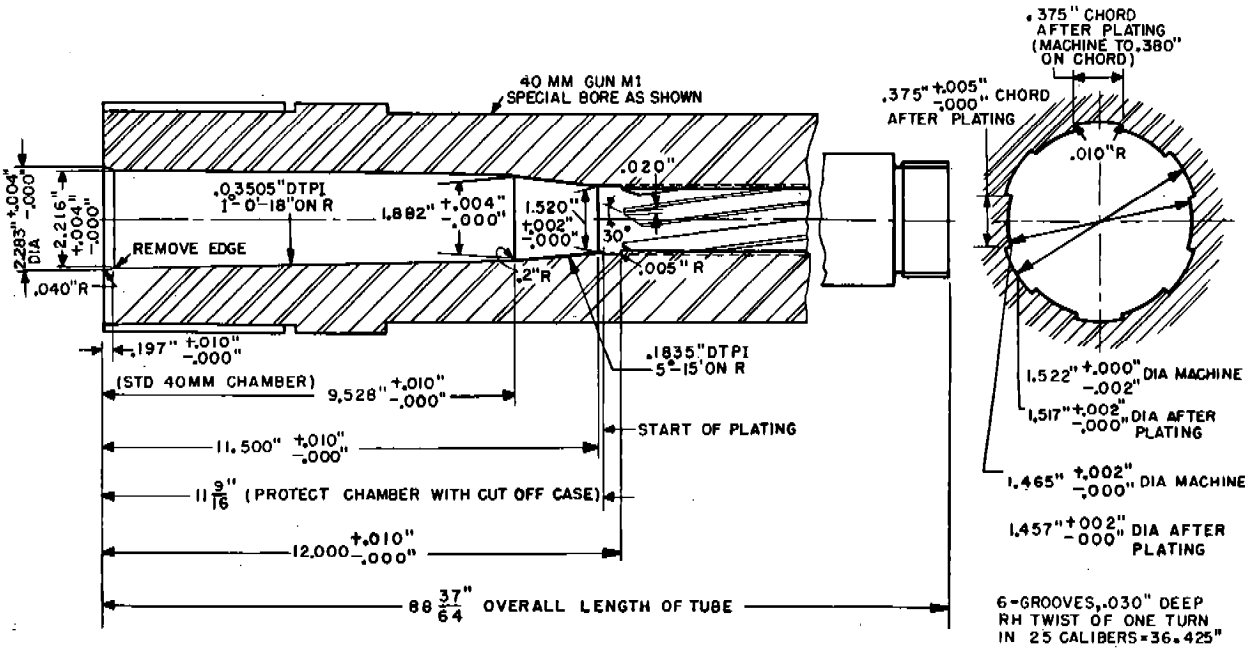


FIGURE 16. Chamber and rifling of a 40-mm forging used for the 37-mm gun, T47, to fire PE projectiles.

Stress calculations were made for the chamber, which was the critical section of the tube. The results showed that the pressures to be used in firing were dangerously near the yield point of the steel. However, since PE projectiles were being used, the time of maximum pressure was reduced and the radial load due to engraving was also eliminated; therefore it was felt that the gun tube was strong enough to withstand 50,000 psi (copper). Two gun tubes were later proof-fired at 62,000 psi (copper) with no serious trouble.

Chromium plating of the bore surface was to start at a point 11 9/16 in. from the breech face and proceed to the muzzle. Allowance in the land dimensions was made so that after machining, 0.002 in. on the radius was to be removed by electropolishing, to give a final land diameter before plating of 1.469 (+.002) in. The application of 0.006-in. chromium plate would then give the specified land diameter for the finished tube. Allowance in the groove dimensions was made for a 25 per cent less distribution of the plate thickness than was to be deposited on the lands.

The groove dimension was made smaller because it was expected that less chromium would be deposited on the groove surface than on the land surface. This difference in plate distribution was believed due to the difference in distances from the anode. Previous experience indicated that when 0.006-in. chromium was deposited on the land surface, about 0.0045-in. chromium was deposited on the groove surface. The application of 0.0045-in. chromium plate on the grooves would give a finished groove diameter of 1.517 in. (+.002 in.)

After plating, the gun tubes were found to be constricted in the grooves. The grooves were lapped to 1.516-in. diameter so that a PE projectile, whose maximum diameter across the teeth was 1.513 in., easily passed through the bore. The final plate thickness was found by gauging to be only 0.0045 to 0.0055 in. on the lands and 0.0030 to 0.0035 in. on the grooves.

31.7.3 Ammunition

Special ammunition components were also required. A PE projectile weighing 1.62 lb and made according to Figure 17 was used as the standard projectile to obtain a velocity of 3,500 fps. Other projectiles weighing 1.34 lb and 1.92 lb were also made. The standard projectile and assembled round are shown in Figure 18.

The standard 40-mm cartridge case, M22A1, was resized at the neck and shoulder so that a 37-mm PE projectile would fit.

Firings to establish the powder granulation and load were made at the Ordnance Research Center, Aberdeen Proving Ground.[240] The results of these firings are given in Table 11.

TABLE 11. Powder granulation and load for 37-mm gun, T47.[240]

Proj. wt. (lb)	Powder				Muzzle velocity (fps)			Pressure (psi)		
	Lot	Type	Web (in.)	Charge (oz)	Mean	Max. var.	Mean dev.	Mean	Max. var.	Mean dev.
1.34	13231	M5	0.0400	12.10	3,486	22	5.9	35,100	3,300	700
1.34	13231	M5	0.0400	12.82	3,668	24	8.7	40,900	2,200	600
1.62	13225	M5	0.0400	13.10	3,493	17	4.0	43,300	3,900	1,000
1.62	13231	M5	0.0400	12.82	3,495	62	13.7	44,200	3,300	900
1.62*	13231	M5	0.0400	12.54	3,451	34	6.7	43,900	2,600	700
1.62*	13231	M5	0.0400	12.82	3,525	20	5.3	47,700	5,400	1,200
1.62	14822	M1	0.0231	13.25	3,378	45	11.9	49,800	2,900	900
1.92	Pilot 299	M2	0.0425	12.00	3,284	..	....	49,800	....	....
1.92	13231	M5	0.0400	12.82	3,344	28	7.9	52,400	2,800	700

* Projectile with obturating disk.

The results of these tests showed that a powder having the M5 composition and a web of approximately 0.0400 in. was suitable as a propellant to yield a muzzle velocity of 3,500 fps within a pressure limit of 50,000 psi (copper) when using 1.34- and 1.62-lb projectiles, with or without an obturating disk.

31.7.4

Erosion Test

One of the two 37-mm gun tubes, T47, was mounted on a modified 57-mm carriage and sent to Aberdeen Proving Ground for an erosion test. The other one, similarly mounted, was sent to Division 1, NDRC

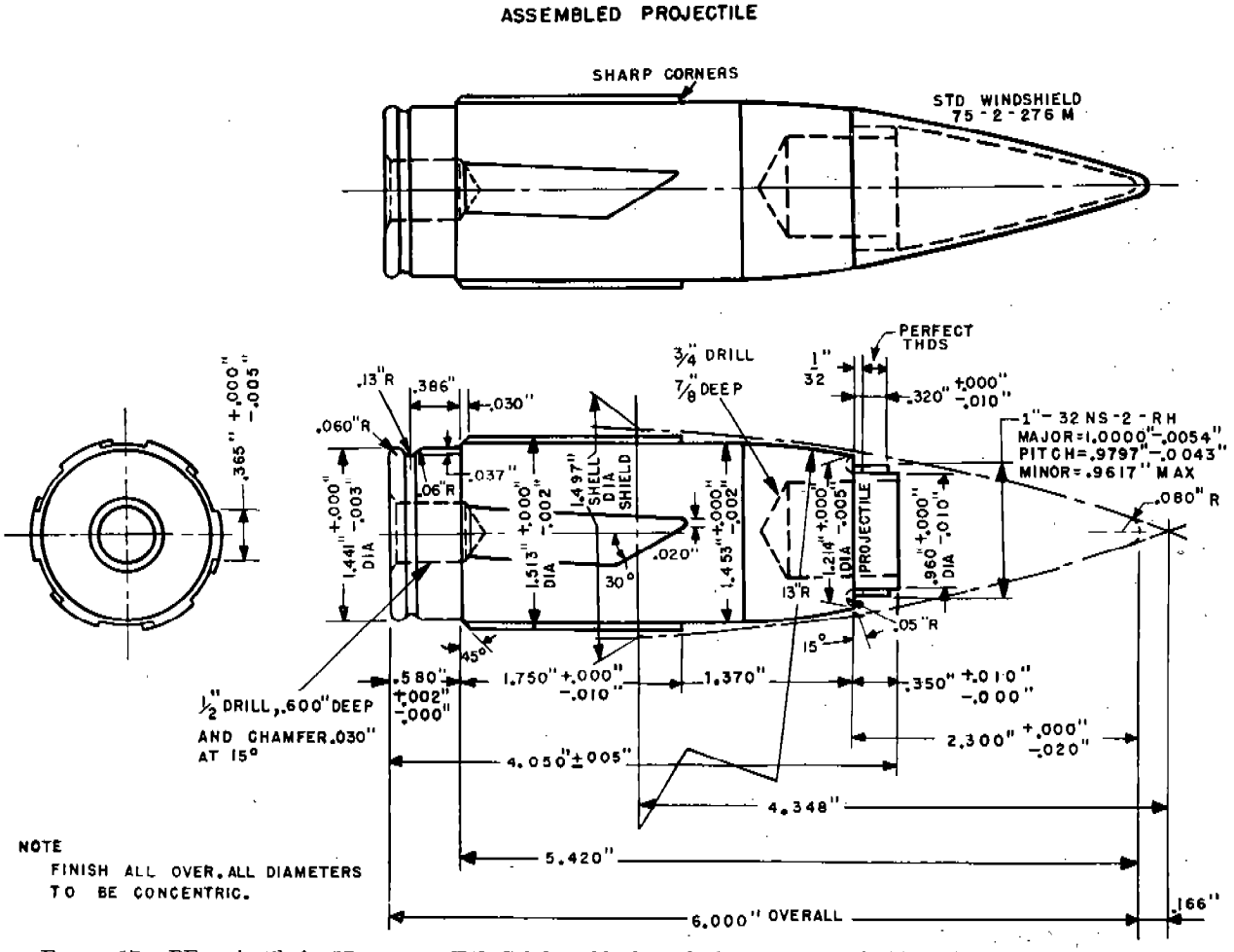


FIGURE 17. PE projectile for 37-mm gun, T47: Solid steel body with aluminum windshield, unobturated, weight 1.62 lb.

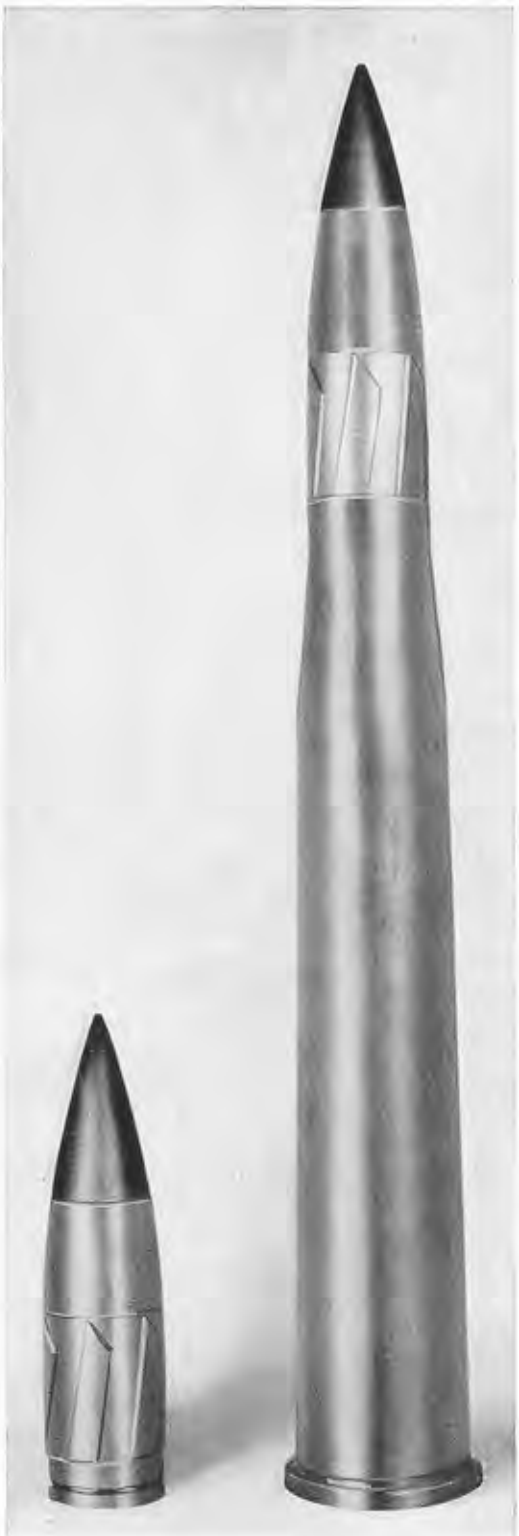


FIGURE 18. 37-mm PE projectile and assembled round.

ballistic firing range at Carderock, Maryland, for the ballistic tests summarized in Chapter 4.

For the erosion test, a charge of 12.85 oz of FNH-M5 powder was established to give a velocity of 3,500 fps with a pressure of 43,500 psi (copper) using 1.62-lb PE projectiles. Erosion rounds were fired in groups of 50 rounds at a rate of fire of 5 to 6 rounds per minute.

Failure of the plate occurred in the grooves and the subsequent stripping of the plate and erosion of the exposed gun steel caused a drop in velocity of 200 fps after 541 rounds. This failure of the chromium plate can be attributed to too thin a plate (less than 0.006 in. on both lands and grooves—see Section 31.7.2) to prevent alteration of the steel at the chromium plate-steel interface. It has been shown in Section 31.5 that chromium plate thickness is the determining factor in obtaining long gun life, when PE projectiles are fired from a chromium-plated bore.

It is, therefore, recommended that another 37-mm gun tube T47 be plated with the proper thickness (0.006 in.) of chromium plate on the lands and grooves to insure thermal protection of the steel at the interface.

31.8 DESIGN OF CHROMIUM-PLATED HYPERVELOCITY 90-MM GUN TO FIRE PRE-ENGRAVED PROJECTILES[d]

31.8.1 General Plan

By the time that Division 1 had made considerable progress in the development of erosion-resistant materials, it was realized that their eventual application to hypervelocity guns of medium caliber would require testing them in an experimental hypervelocity gun. Such a gun would also give an opportunity to explore directly some of the ballistic factors believed to be important in connection with the design of a hypervelocity gun—especially by the use of very high densities of loading.

The project for the development of this gun was termed the A-Z project, because it was expected that all phases of the Division's program ("from A to Z") would be drawn upon as it grew. Thus in the end the series of A-Z guns would be the embodiment of the Division's accomplishments. The material selected for the first trial was chromium electroplate, to be used in conjunction with pre-engraved projectiles. It

[d] This section has been added by the Editor to round out the subject of this chapter. It is based on an NDRC report.[118]

CONFIDENTIAL

was understood that as other materials became available, other tubes would be prepared to test them in a gun of this size, and of the same general design.

As a guide to the choice of specifications for this gun, an extensive series of ballistic calculations was made with the Division 1 system; the results are described in Section 3.5.5. The choice was finally narrowed down to a gun having a muzzle velocity slightly in excess of 4,000 fps and an overall length of not more than 90 calibers.

31.8.2

Gun Tube Design

Further ballistic calculations led to adoption of the specifications listed in Table 12. From them a strength curve was calculated in the usual way (Section 26.4.4), with the results shown in Figure 19.

TABLE 12. Basic specifications for 90-mm gun, A-Z.

Bore diameter (90-mm)	3.524 in.
Length of gun	88 calibers
Weight of projectile	23.8 lb
Muzzle velocity	4,200 fps
Maximum powder pressure	60,000 psi
Volume of chamber	760 cu in.
Density of loading	0.80
Powder type (7-perforate)	FNH-M1
Travel of projectile	281.0 in.

One requirement determining the choice of specifications for the tube was that in the experimental firing the 120-mm gun mount, M1 be used in order to save the time required to make a special mount. Also, consideration was given to the possibility that the 120-mm breech ring and breech block be used with minor modifications.

The design of the chamber involved several compromises. Its total volume was fixed by the basic specifications. A long slender case was preferable as far as strength of the tube was concerned, and, in fact, the requirement that the 120-mm breech ring be used imposed an upper limit on the diameter of the chamber at the rear. As far as ease of fabrication of the cartridge case and ease of manipulation by an automatic loading mechanism were concerned, a short case was favored. The compromise made between these two competing requirements led to a chamber that was 34 in. long and 6.0 in. in diameter at the rear. This diameter corresponds to a wall ratio of 2.6.

It was decided to make the cartridge case of brass, because of uncertainties regarding the likelihood of steel cases being made with the high strength neces-

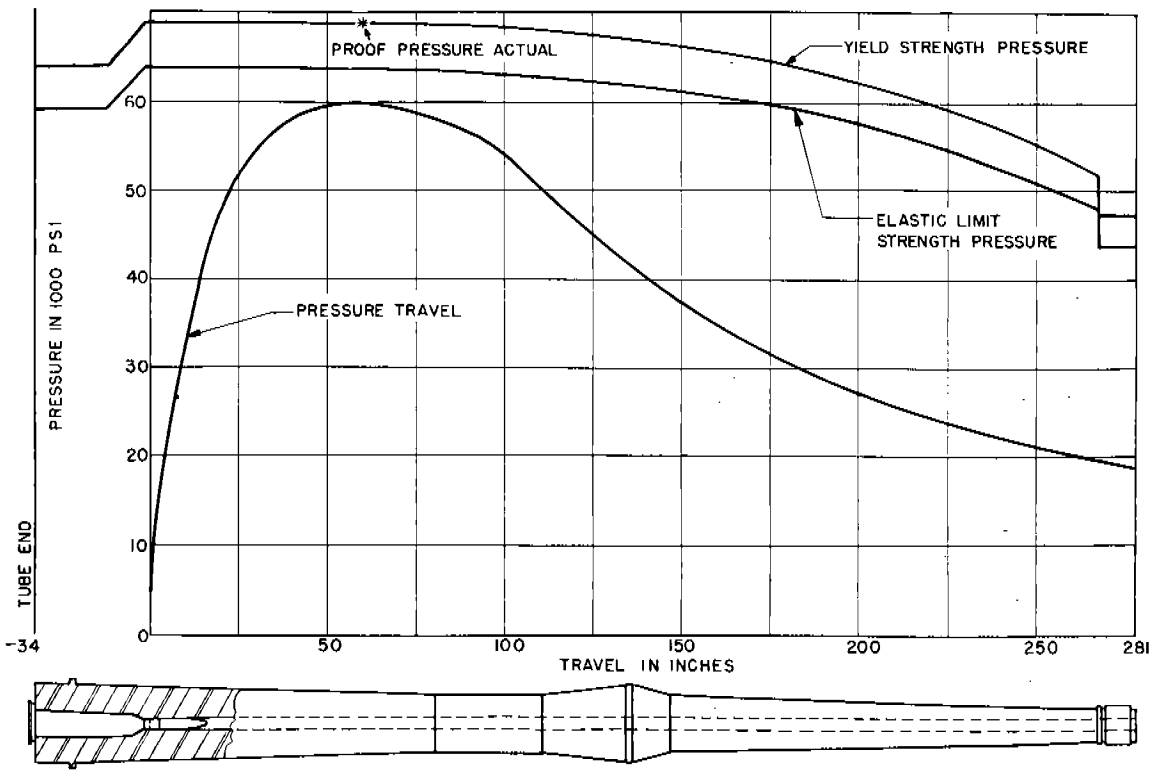


FIGURE 19. Strength curve and pressure-travel curve for tube of 90-mm gun, A-Z.

sary to avoid sticking. Special attention was given in the design to the avoidance of cracking close to the inside corner of the base.

The forging design adopted was a modification of the forging for the 120-mm gun tube. The finished exterior dimensions at the rear were made identical with those for the 120-mm tube, so that the tube would fit the mount. The entire tube was somewhat longer (315.0 in. instead of 283.5 in.) than the 120-mm, and the forward end was made with a smaller external diameter. With this design the maximum strain in the tube at the origin of rifling was 0.0028 in. per in. and it was 0.0031 in. per in. at the large chamber cone. These values of strain are close to that which separates a critically stressed tube from a normally stressed one.

31.8.3

Gun Tubes

The A-Z project was halted by the termination of Division 1's activities. The preparation of the tube forgings, however, was far enough along so that it seemed expedient to finish them. Six forging blanks had been cast from an alloy steel containing nearly 3% nickel, about 0.9% chromium, about 0.5% molybdenum, and about 0.1% vanadium. The minimum yield strength specified was 130,000 psi.

During machining of the heat-treated forgings, cracks in the steel were discovered in four of them, and they had to be rejected. In one case the cracks were not disclosed until the final honing operation. A study of the test data, including the examination of microstructure, suggested that the reason for this high percentage of rejections was poor melting practice, which resulted in steel with too high an inclusion rating to give the requisite degree of finished-surface continuity.

The machining of two tubes was completed as far as the exterior, the chamber, and a smooth bore were concerned. These tubes, ready for rifling, were sent to Watervliet Arsenal in April 1946, after an agreement had been reached with the Army Ordnance Department that it would complete their manufacture and test them. The Naval Gun Factory had agreed to chromium-plate them with the cooperation of the Electrochemistry Section of the National Bureau of Standards. The original design of these tubes had called for pointed lands; but in view of the results with the 37-mm gun, T47, described in Section 31.7.4, this decision needs to be reconsidered.



Chapter 32

THE FISA PROTECTOR AND CHROMIUM-PLATED BORE[a]

By *Nicol H. Smith*[b]

32.1 INTRODUCTION

AMONG THE MEANS of preventing erosion of a steel gun barrel, one of the simplest in principle is to cover the area of the bore surface just ahead of the origin of rifling in order to protect it from the action of the hot powder gases. The Fisa protector[c] is a device for accomplishing this purpose. Its development followed information[300] received from abroad in 1942 that plans for a new Bofors 57-mm AA gun included the use of a thin metal sleeve on the projectile as a means of controlling erosion.

The Fisa protector is a very thin, slightly tapered sleeve of soft steel that is slipped over a complete round of ammunition, the larger end of the sleeve snugly fitting the neck of the cartridge case up to the shoulder, and the remainder covering the projectile almost to the bourrelet. Figure 1 shows a Fisa sleeve before and after firing. During firing the sleeve is locked to the cartridge case by the expansion of the neck of the case, which is extruded by the powder pressure into several rectangular holes cut through the rearward end of the sleeve, thus insuring the withdrawal of the sleeve with the case. Thus the Fisa protector in effect is a replaceable steel liner (Section 26.3) that is replaced after each round fired.

The gun from which ammunition equipped with a Fisa protector is to be fired must be modified slightly in order to allow the round to be chambered. The diameters of the centering cylinder and of the bore as far forward as the front of the sleeve must be enlarged by almost twice the thickness of the sleeve. Grooves of standard depth are then cut in the enlarged bore to re-establish the rifling.

Preliminary tests showed that the Fisa protector was not effective in increasing the life of a plain steel hypervelocity caliber .50 gun barrel, because of excessive erosion of the unprotected part of the bore ahead of the sleeve. Further development dealt with the combination of a Fisa protector and a chromium-plated bore surface. The sleeve protects the chromium plate from some of the engraving stresses that are so detrimental to it (see Section 20.2.1), and hence lengthens the life of the gun barrel. In this respect, its function is similar to that of a pre-engraved projectile, described in Chapter 31. Although the latter is more effective in eliminating engraving stresses, the former has the advantage that the round of ammunition does not need to be indexed before being chambered.



FIGURE 1. Components, assembled round, and fired round for caliber .60 Fisa protector. (This figure has appeared as Figure 29 in NDRC Report No. A-449.)

Tests in the caliber .50 erosion-testing gun, which are described in Section 32.3, showed that the Fisa protector nearly doubled the velocity-life. Tests in a

[a] This chapter is based on a formal Division 1 report[331] by the same author, to which reference is made for further details.

[b] The Franklin Institute, Philadelphia, Pennsylvania.

[c] The term Fisa is a coined word made up of the initial letters of the phrase "Franklin Institute, Section A." At the time that The Franklin Institute was asked to develop this device as part of the work under Contract OEMsr-533, that contract was being supervised by Section A of Division A, NDRC (later Division 1).

37-mm gun, M3, revealed that the Fisa protector cannot be used with the present standard ammunition for that gun because of excessive interference between the rotating band and the grooves in the gun. These tests are described in Section 32.5 and some preliminary ones with a caliber .60 barrel in Section 32.4.

32.2 DESIGN OF THE FISA PROTECTOR

32.2.1 Analysis of the Functions of the Fisa

The most difficult aspect of the development of the Fisa protector was the proportioning of the different parts. The final design for the caliber .60 size, which is shown in Figure 2, includes those tapers and shoulders that were found to reduce to a minimum the various types of failure that were observed during preliminary firing tests. The design may be comprehended most easily by analyzing the function of each of the four sections of the sleeve, which are designated in Figure 3.

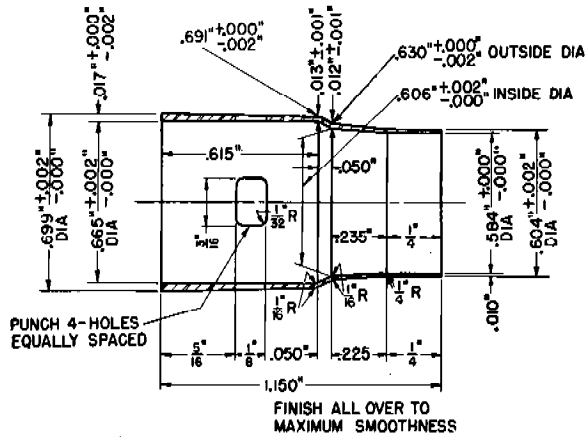


FIGURE 2. Fisa protector for caliber .60 barrel, dimensioned drawing. (This figure has appeared as Figure 30 in NDRC Report No. A-449.)

SECTION G

This part of the sleeve fits over the case neck. It is tapered to facilitate extraction from the chamber after firing. Four rectangular holes are punched in this section to lock the sleeve to the case during firing. The extrusion of the brass into these holes by the powder pressure performs the locking operation. Tapering the external dimension of this section also allows for a thicker section in the sleeve and thereby aids in a more positive locking action.

In order to prevent failure to extract, it was found necessary to crimp the sleeve to the case, using the same crimp that is used on the projectile. This gives positive action at low powder pressures when the extrusion of the brass does not occur fast enough to lock the sleeve to the case in a satisfactory manner. Another feature that was found essential to prevent failure to extract was to have a carefully controlled clearance between section G and the centering cylinder of the barrel.

SECTION F

The purpose of this shoulder is to prevent the sleeve from moving forward during the engraving operation. This short section is also tapered to facilitate extraction of the fired cartridge case and sleeve assembly.

SECTION E

Sections E and D are the parts of the sleeve that are engraved. The passage of the projectile through this zone forces the metal in the sleeve into the rifling and the rotating band is thus engraved through the sleeve.

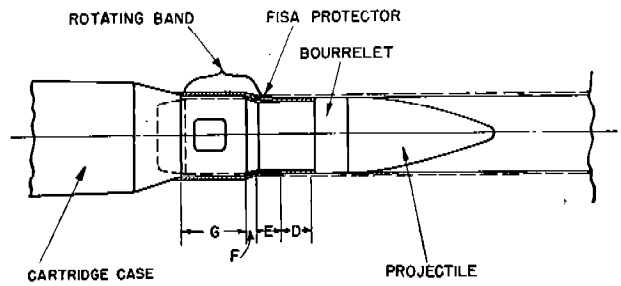


FIGURE 3. The Fisa protector, schematic drawing. (This figure has appeared as Figure 5 in NDRC Report No. A-449.)

The external dimension of section E is tapered rearward to give a thicker section having greater strength and also to facilitate extraction of the case and sleeve assembly from the chamber. The internal dimension of section E is also tapered in order to distribute the engraving stresses over a greater area.

SECTION D

This section is straight and serves as a die to finish the engraving operation. The purpose of this section was to engrave the rotating band completely so that the projectile would emerge from the sleeve as a fully pre-engraved projectile having 0.001- to 0.002-in. clearance between the engraved band and the rifling

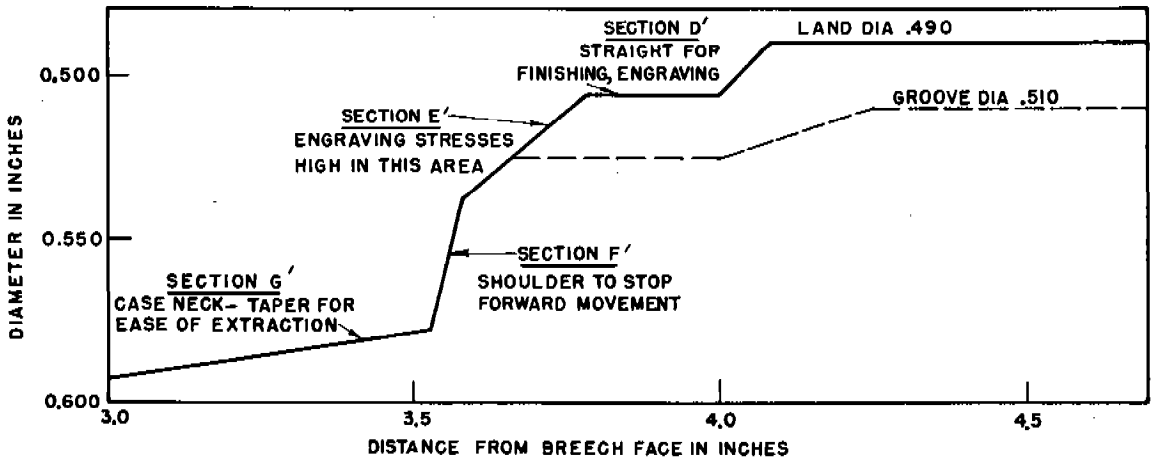


FIGURE 4. Profile of caliber .50 barrel in region of origin of rifling, modified to accommodate Fisa protector. (This figure has appeared as Figure 6 in NDRC Report No. A-449.)

beyond the sleeve. With regular rifling and ammunition it is not possible to attain this ideal condition.

TEARING OF THE SLEEVE

Tearing of the engraving parts of the sleeve (sections D and E) was the most troublesome type of failure encountered. It was found that it could be minimized by:

1. Increasing the ultimate strength of the metal in the sleeve. (This remedy makes fabrication by the deep drawing process almost impossible.)
2. Increasing the thickness of the metal in sections D and E.
3. Reducing the forward component of force from the moving projectile to a value below the yield point of the metal in sections D and E by Parco-Lubrizing or cadmium plating the inner surface of the sleeve.
4. Reducing the radial load on the sleeve during engraving by eliminating the interference between the rotating band and the grooves and providing additional and deeper cannelures in the band, in accordance with the experiments described in Section 27.4.2.

32.2.2 Extent of Engraving

To determine the amount of engraving done through the sleeve, a caliber .50 barrel was rifled for a distance equal to the length of the sleeve and made smooth bore beyond the sleeve to the muzzle. The thickness of the metal in a series of sleeves and the inside diameters were varied. The recovered bullets showed that to obtain maximum engraving of the band it was necessary to:

1. Keep the thickness of the metal at 0.010 in. in order for the engraving to be sharp, and
2. Reduce the inside diameter of the sleeve to the diameter of the body of the projectile so that it would have to be forced over the bourrelet.

Even by making the inside diameter of the sleeve for a caliber .50 bullet 0.003 in. smaller than the bourrelet diameter and the thickness of the sleeve 0.010 in. it was possible to obtain only 75 to 80 per cent of complete engraving. This meant that additional engraving of the band would occur beyond the sleeve, thereby subjecting the chromium-plated lands in that area to slight engraving stresses and friction.[d]

32.2.3 Modification of the Rifling

In order that the assembled round with the sleeve can be chambered properly, it is necessary to remove metal from the chamber and origin of rifling area to allow for the thickness of the sleeve. A profile of the origin of rifling modified for the caliber .50 sleeve is shown in Figure 4. The various sections shown match the sections on the sleeve (Figure 3).

[d] The experience with chromium-plated caliber .50 aircraft machine gun barrels, described in Chapter 23, demonstrated that for accuracy in firing long bursts with that gun it is essential to have the muzzle of the barrel slightly constricted. Hence it would seem undesirable to have a projectile for a machine gun, such as the caliber .60, completely engraved by the Fisa protector. On the other hand, the greater depth of rifling necessary with the Fisa protector might make continuation of engraving all the way down the bore unnecessary. In this connection it should be noted that in the only test of a Fisa protector in automatic fire (Section 32.3.4) the caliber .50 barrel had tapered chromium plate. (Editor's note.)

32.2.4 Manufacture of the Fisa

The first sleeves that were tested were machined from soft steel bar stock. Examination of the finished sleeves under a low-power microscope showed shallow grooves produced by the tools. When the thickness of the sleeve was reduced to 0.010 in., these grooves produced areas of weakness which resulted in tearing of the sleeves.

A more satisfactory method of manufacture was then used to produce a better quality sleeve in greater quantity. The sleeves were drawn from a copper-coated, soft drawing steel (SAE 1010) having the proper thickness to give the required metal thickness in the finished sleeve. The copper coating prevented galling in the dies during the drawing operation. The method of manufacture was the same for the caliber .50, caliber .60, and 37-mm Fisas, although the number of steps in the fabrication of the sleeves was different. Figure 5 shows the steps in the fabrication of a 37-mm Fisa protector and may be taken as representative of the manufacture of the sleeves in general.

32.3 CALIBER .50 EXPERIMENTS

32.3.1 Methods of Testing and Measurement

The caliber .50 erosion-testing gun (Section 11.2.1) was used as the tool in the preliminary tests of the Fisa protector, at a velocity of 3,500 fps with a slow rate of fire. The behavior of the sleeves was first tested in a gun steel bore and later in chromium-plated bores. Subsequently, they were tested in the Browning machine gun at a velocity of 2,900 fps and a cyclic rate of fire of about 600 rpm.

All the tests in the erosion-testing gun were fired with double-base powder containing 20% nitroglycerin and copper-banded, artillery-type bullets (Figure 3 of Chapter 11). The charge was adjusted to give a maximum powder pressure of 50,000 to 52,000 psi (copper) for a velocity of 3,500 fps.



FIGURE 5. Operations in the fabrication of a drawn 37-mm Fisa protector. (This figure has appeared as Figure 34 in NDRC Report No. A-449.)

CONFIDENTIAL

The gun was considered to have failed when (1) the velocity had dropped 200 fps (end of velocity-life), or (2) the mean radius of dispersion at 100 ft had increased to three times its initial value or keyholing bullets were observed (end of accuracy-life).

Plug gauge and star gauge measurements were taken at intervals to determine the distribution and progress of erosion of the lands and grooves.

32.3.2 Gun Steel Bores

The results of the tests with gun steel bores showed that the sleeve protected the origin of rifling against erosion by the powder gases, but that the erosion beyond the origin of rifling was greater than would be observed normally without the use of the sleeve. This increased erosion beyond the sleeve is probably caused by increased turbulence of the powder gases produced by the discontinuity of the bore surface.

Although the decrease in powder pressure was slight, because of the protection of the origin of rifling by the sleeve, there was a considerable increase in dispersion due to the severely eroded lands beyond the sleeve. This resulted in an accuracy failure of the gun after 55 rounds. Without the sleeve the control tests gave an accuracy failure of 125 rounds.[122]

32.3.3 Chromium-Plated Bores

When the bore beyond the sleeve was protected by chromium plate, the accuracy failure mentioned in the preceding section was postponed. The gun barrel was plated with 0.005- to 0.006-in. standard chromium plate (Section 20.2.2) after electropolishing to remove this thickness of steel. The plate started at the shoulder at the breech end of section G (see Figure 3) and was continuous to the muzzle.

During the life of the gun the area near the origin of rifling was completely protected by being beneath the sleeve. Failure occurred beyond the end of the sleeve, although the rate of erosion was much slower than that observed in the gun steel bore. The use of the sleeve in a chromium-plated bore increased the velocity-life of the gun four times compared with gun steel without the sleeve, as shown in Table 1 and in Figure 6.

32.3.4 Browning Machine Gun Tests

The purpose of the tests with the Browning machine gun action was to observe the behavior of the sleeve used with banded artillery-type projectiles under conditions of rapid fire. A special barrel was used that had the same external contour as the standard caliber .50 aircraft machine gun barrel. The rifling was made 0.010-in. deep, the origin of rifling was modified to accommodate the sleeve, and the bore was plated[84] with chromium 0.0038-in. thick at the breech end and 0.0045-in. thick at the muzzle.

In the final test of cadmium-plated sleeves the gun was fired with a standard charge of IMR powder to give a muzzle velocity of 2,800 fps. A control test was fired with a plain steel barrel and ball bullets, M2. Each barrel was fired 750 rounds in three groups of 250 rounds, each group consisting of five 50-round bursts fired at 1-min intervals [the 5×50 (1) schedule as defined in Section 23.1.3] at a cyclic rate of 600 to 640 rounds a minute.

At the end of 750 rounds (three groups) the chromium-plated barrel used with the Fisa protectors showed no drop in velocity and no change in dimensions at the origin of rifling. The gun steel barrel after the same number of rounds showed a velocity drop of 139 fps and an increase in land diameter of 0.0108 in. at the origin of rifling. Furthermore, some of the bullets from this barrel keyholed in each 250-round group, whereas none of the bullets fired from the barrel with Fisa protectors keyholed.

TABLE 1. Increase of velocity-life of caliber .50 barrel obtained by use of Fisa protector with chromium-plated bore.

	Velocity life* (rounds)
Gun steel bore—control	90
0.005 in. chromium-plated bore—no Fisa	225
0.005 in. chromium-plated bore—Fisa protector	400

* Number of rounds fired for a velocity loss of 200 fps.

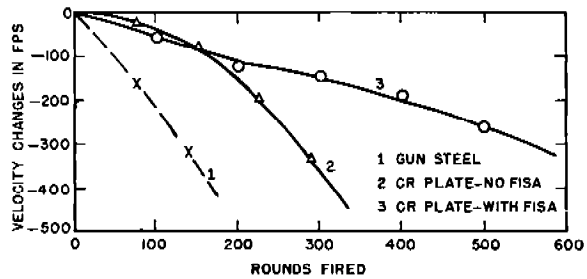


FIGURE 6. Velocity loss of caliber .50 barrels fired at an initial muzzle velocity of 3,500 fps: (1) unprotected gun steel barrel; (2) chromium-plated barrel; and (3) chromium-plated barrel with Fisa protector. (This figure has appeared as Figure 23 in NDRC Report No. A-449.)

Although slight tearing of the sleeves was observed during the test, this did not interfere with the functioning or performance of the gun.

32.4 CALIBER .60 EXPERIMENTS

A caliber .60 barrel, Ordnance Drawing No. 7160408, was modified for the sleeve designated as A-104 shown in Figure 2. The barrel was electropolished and chromium-plated.[84] The sleeves were drawn from copper-coated, flat sheet steel and cadmium plated to reduce the friction between the band and the sleeve during the engraving operation.

It was necessary to modify the caliber .60 projectile, T32 (then undergoing test by the Ordnance Department), by reducing the diameter of the body back of the bourrelet by 0.008 in. This was done so that the diameter of the sleeve could be reduced in sections D and E (see Figure 3) and the lands could be deeper in the areas designated as D′ and E′ in Figure 4. This was necessary to obtain deeper engraving of the rotating band of the projectile. The components of the assembled round, the assembled round, and a fired round are shown in Figure 1.

A total of 80 rounds was fired. All sleeves were extracted from the chamber and there was no stretching or tearing of the sleeves. The chromium plate failed along the bore on account of a poor bond, and firing was discontinued.

32.5 37-MM FIRING TESTS

A 37-mm gun tube, M3 was step rifled for the Fisa protector and chromium plated after electropolishing. A thickness of 0.0055- to 0.0060-in. chromium plate was applied. The sleeves were drawn from copper-coated, flat sheet steel. In assembling the round the standard M51B1 and M51B2, projectiles were used with the 37-mm cartridge case, M16. Double-base powder (FNH-M2) was used in all the tests.

Preliminary firing tests showed that a crimp was necessary to lock the sleeve to the cartridge case strongly enough to insure satisfactory extraction of the sleeve with the case after firing, in particular at low pressures (30,000 to 40,000 psi-copper).

In order to reduce the coefficient of friction between the sleeve and the band the sleeves were coated with various low-friction coatings. The following sleeves were tested:

1. Cadmium-plated—as drawn.
2. Cadmium-plated—annealed sleeves.
3. Chromium-plated—as drawn.
4. Parco-Lubrized—as drawn.
5. Parco-Lubrized—annealed.
6. Steel—as drawn.
7. Brass—machined.

Results of tests fired at 50,000-psi pressure (copper) and a velocity of 2,900 fps showed (1) all the brass sleeves were torn; (2) the cadmium-plated and Parco-Lubrized sleeves performed better than the steel sleeves as drawn; (3) the annealed sleeves were no better than the sleeves as drawn; and (4) Parco-Lubrizing the sleeve surface was slightly better than cadmium plating it.

It was hoped that the sleeve could be slipped over existing assembled rounds without any change to the ammunition. Because of the excessive interference between the sleeve and the band in the grooves, however, a small percentage of the sleeves were torn during engraving.

A total of 162 rounds was fired in the chromium-plated 37-mm barrel. Excessive erosion of the chromium plate occurred at the maximum height of the lands and in the grooves just beyond the end of the sleeve. This has been attributed to improper application of chromium plate. As mentioned in Chapter 20, there has not yet been sufficient experience in applying thick chromium plates to this size gun tube to give assurance of success in every plating job.

It is recommended that further tests of 37-mm Fisa protectors be made, using a newly plated tube and projectiles having a reduced band diameter so that there is no interference in the grooves. The radial load might also be further reduced by increasing and deepening the cannelures, as described in Section 27.4.2.



Chapter 33

PRACTICAL HYPERVELOCITY GUNS

By *L. H. Adams*,[a] *J. S. Burlew*,[b] *and E. L. Rose*[c]

33.1 PRESENT STATUS OF THE DEVELOPMENT

33.1.1 Understanding of the Erosion Process

THE control of gun erosion has been the crux of the hypervelocity problem, as was brought out in Chapter 1. The studies of the mechanism of erosion conducted by Division 1 have led to an understanding of the part that different factors play in that process, as described in Chapter 13. Guided by this knowledge the search for erosion-resistant materials, described in Chapter 16, was focused on a few metals and their alloys. The need for fabricating these materials in forms suitable for application to gun bores led to a large number of metallurgical investigations, described in Chapters 17, 18, 19, and 20.

Success in this development work has already been attained as far as stellite liners for machine gun barrels and chromium plating of such barrels are concerned, as is recounted in Chapters 22, 23, 24, and 25. The application of these same materials to cannon, however, has not yet been realized. Because of the larger size, the problem is considerably more difficult. The first attempt to apply chromium electroplate to a cannon tube in conjunction with pre-engraved projectiles is described in Section 31.7. The preliminary efforts that have been made to apply stellite and molybdenum as liners for cannon are described in the next two sections of this chapter.

33.1.2 Stellite Liners for Cannon

Breech liners and linings of Stellite No. 21 have been applied experimentally to 37-mm gun tubes, but exhaustive tests have not been completed. Plans for this work were started by Division 1 at the informal suggestion of the Ordnance Department, as soon as the first successful tests of a liner of Stellite No. 21 had been made in a caliber .50 aircraft machine gun barrel, as related in Section 22.2.2. At that time experience in making large "investment castings" of Stellite No. 21 was so slight that preparation of liners was undertaken by other methods also. Because of delays in machining the liners made by the other methods, an investment-cast liner also was completed in time to be included in the group tested.

Test Assemblies

Two 37-mm gun tubes, M3, containing bore surfaces of Stellite No. 21 for 20.8 in. forward from the origin of rifling were prepared.[80] One tube contained a flanged investment-cast liner of stellite shrunk directly into the breech end of the tube and held in place by a steel breech nut containing a portion of the chamber. This design is essentially the same as that employed in the insertion of investment-cast liners for machine gun barrels, shown in Figure 1 of Chapter 22, except that in proportion to its caliber, the wall thickness of the 37-mm liner is less.

The second tube was provided with two interchangeable, replaceable steel liners, similar in design to the replaceable liners for the 90-mm gun described in Section 26.3. These two steel liners had been given a lining of stellite, applied to the bore surface by the process of progressive static infusion[89] described in Section 19.4.3. These two liners were prepared in the same way, except that one of them was heat-treated after the infusion process to increase the strength of the steel.

Firing Tests

The three liners were fired at the Ordnance Research Center, Aberdeen Proving Ground.[221] The investment-cast liner and the static-infused, heat-treated liner were each fired 104 rounds with single-base powder. After 12 rounds for the establishment of charge and proof had been fired, the liners were fired at excess pressure (averaging 42,000 psi, copper) for

[a] Chief, Division 1, NDRC. (Present address: Geophysical Laboratory, Carnegie Institution of Washington.) Author of Section 33.3.

[b] Technical Aide, Division 1, NDRC. (Present address: Geophysical Laboratory, Carnegie Institution of Washington.) Author of Section 33.1.

[c] Member, Division 1, NDRC. (Present address: Consulting Engineer, Jones & Lamson Machine Company and Bryant Chucking Grinder Company, Springfield, Vermont.) Author of Section 33.2

7 rounds, followed by a total of 85 rapid-fire rounds (6 rounds a minute), at an average muzzle velocity of 2,575 fps for the investment-cast liner, and 2,540 fps for the other. After the first 19 rounds there was some expansion of the bore diameter, which was greatest at and near the origin of rifling. Since no significant changes in bore dimensions resulted from the firing of the remaining rounds, it was concluded that the early increase in diameter represented irreversible expansion of the liner, caused by both band pressure and powder pressure. As a result of a small decrease in liner length, an opening appeared at the breech end of the liner, permitting the cartridge case to expand into this opening, thus causing difficulties in extraction. The opening was observed after 29 rounds had been fired and increased in width during the firing of the remaining 75 rounds.

To determine whether melting of the stellite would take place, the investment-cast liner was then fired 43 rounds with double-base powder (FNH, M2, which contained 20% nitroglycerin). In order to obtain a muzzle velocity of about 2,900 fps, the pressure was increased to 50,000 psi (copper). Eight proof rounds were followed by 10 rounds at an average rate of 4 rounds a minute. A boroscope examination showed a marked change in the appearance of the bore surface at the origin of rifling, indicating that fusion of the surface had taken place. An additional 25 rounds (at a rate of about 6 a minute) were fired later.

The third liner—a static-infused liner that had not been heat-treated after the infusion process—was to have been fired with single-base powder at a higher pressure than that used for the other two liners. There was difficulty in achieving the desired pressure with the powders available at the Proving Ground. After 29 rounds had been fired, examination of the liner indicated that lack of heat treatment of the steel caused no difficulty.

These firing tests demonstrated that stellite withstands the action of single-base powder in a 37-mm gun fired at normal velocities, but that it is melted when double-base powder is fired at a slightly higher velocity. They also showed that the stellite is not cracked by the stresses of firing in this gun. Application of stellite to the bore surface by static infusion seems preferable to the use of an investment casting, because of a change in dimensions or movement of the liner, which opens a crack at the rear of the liner. These tests were not carried far enough with single-base powder to determine how much better Stellite No. 21 resists erosion in a 37-mm gun than does steel.

Future Possibilities

The surface melting of the 37-mm stellite liner when fired with double-base powder had been predicted by calculations of the bore-surface temperature by the Hobstetter method described in Section 5.4.1. Calculations for other guns fired at hypervelocities, even with single-base powder, indicate that surface melting of stellite will occur in general in medium- and large-caliber guns. Hence stellite as such cannot be regarded as the complete solution to the hypervelocity problem.

One possible way of circumventing this difficulty would be to coat the stellite with a material of higher melting point, such as chromium or molybdenum. This possibility had been the motivation behind the efforts to plate molybdenum or chromium on stellite by the carbonyl process, as described in Sections 21.3 and 21.6. Although success was not achieved, future discoveries in connection with the carbonyl process or some other plating process might make this possibility a reality.

Even though the tests of 37-mm stellite liners did not result in a demonstration of wide applicability of this material to cannon, the investigation was well worth while. The experience gained in it is helpful in planning uses for other erosion-resistant materials. Thus the chromium-base alloys described in Chapter 17 are potentially very important as bore-surface materials for cannon. As soon as a casting of suitable properties has been prepared, it will be a straightforward job to make it into a liner for trial with assurance that the design of the liner itself would be satisfactory. As mentioned in the next section, some of this experience has also been helpful in planning a molybdenum liner for a medium-caliber gun.

33.1.3 Plans for Molybdenum Liner for 3-in. Gun

The firing tests of caliber .50 molybdenum liners described in Section 18.6 showed that considerable progress had been made in improving the properties of molybdenum so that it would be suitable for use as a gun liner. The next step was to try a molybdenum liner in a medium-caliber gun, preferably of higher than conventional velocity. At the suggestion of the Bureau of Ordnance the Navy's new 3-in./70-cal. gun was selected for this purpose in the spring of 1945. This gun, just then in process of development, was designed as a high-velocity weapon firing automati-

cally for antiaircraft use. The muzzle velocity is 3,400 fps at a maximum true pressure of 60,000 psi. The gun is intended to be fired at a rate of 90 rounds a minute for as long as one minute. The heating of the barrel under these conditions is discussed in Section 5.5.3.

Liner Designs

Arrangements were made to expand the facilities of the Westinghouse Lamp Division to make possible the fabrication of larger pieces of molybdenum, as described in Section 18.3.4. Then a planning conference was held in the office of Division 1 on August 15, 1945 (the day after V-J Day), at which a number of Division 1 contractors[d] considered various means of inserting liners of both molybdenum and chromium-base alloy in the 3-in./70-cal. gun.

One design of molybdenum liner proposed was similar to the investment-cast stellite liners. The molybdenum, which might be fabricated in several staves (Section 18.5.2) or as a seamless tube (Section 18.5.3), would be shrunk into the recessed gun tube and then held in place by a short steel chamber liner.

A simpler way of handling a multistave liner would be to shrink the staves into a steel carrier and then insert this composite liner into the recessed gun tube, in the same way the composite stellite liner was inserted in a 37-mm tube (Section 33.1.2).

Both the foregoing designs would involve recessing the gun tube from the breech end, which would make it necessary also to line the chamber. A way of avoiding this is to make the gun tube in two longitudinal segments held together by a locking ring. The rear segment, which contains the chamber, is recessed rearward from its front end to receive the liner. The front segment is turned down to fit into the forward end of this recess and make a seal with the front end of the liner. This design is a modification of those used by the Geophysical Laboratory (Section 11.2.2) and by The Franklin Institute (Section 11.2.1) in caliber .50 guns for testing materials for erosion resistance. Another advantage of this design is that by using a relatively short muzzle section it is simpler to chromium-plate the steel bore surface ahead of the molybdenum liner.

[d] No formal report of this conference has been issued. It was attended by representatives of the following contractors in addition to Division 1 and Navy Bureau of Ordnance personnel: Crane Company, The Franklin Institute, Union Carbide and Carbon Research Laboratories, Westinghouse Lamp Division, and Westinghouse Research Laboratories.

Continuation of Project

After termination of Division 1's contracts the Navy Bureau of Ordnance contracted with the Westinghouse Electric Corporation to continue the development of molybdenum liners. Following further tests of caliber .50 models, using molybdenum fabricated with the enlarged facilities mentioned in Section 18.3.4, it is planned to make preliminary tests with a 40-mm liner of the two-segment design described in the previous paragraph. The first liners will be two-stave ones, but it is hoped that eventually tube-making experiments will result in a successful seamless liner. Eventually it may be possible to utilize molybdenum in the form of a seamless liner the whole length of the gun, as shown in Figure 1. This design might be the most economical.

33.1.4 Plans for A-Z Gun

As a culmination of Division 1's investigation of erosion-resistant materials, the A-Z project was undertaken, whose ultimate purpose was the development of a gun tube for an entirely new weapon which would embody the best features of erosion control developed by the Division. It was hoped that the project would result in a gun whose velocity was the highest practicable. By the introduction of liners or other means of erosion control, surface cracking in the structural portion of the gun tube would be eliminated. The way would then be open to work the gun materials at a higher stress and to use materials of higher strength and lower elongation than is permissible in existing weapons. The gun was to be designed to fire both high-explosive and armor-piercing projectiles, so that a decision as to its eventual application could be made later.

As a first step, plans were formulated for an experimental, medium-caliber hypervelocity gun which could be used as a testing gun for three types of experiments: insertion of an erosion-resistant bore-surface material; trial of a high-strength gun steel; and ignition of powder at high densities of loading, possibly leading to the development of a higher density powder grain.

The design of a 90-mm gun, having a muzzle velocity of 4,200 fps and a maximum powder pressure of 60,000 psi, was decided upon. The basic specifications for the gun are given in Table 12 of Chapter 31. The first trial was to have been with a chromium-plated tube, fired with pre-engraved projectiles (Section



FIGURE 1. The hypervelocity gun of the future may well be one containing a full-length liner of hardened molybdenum alloy.

31.8). Additional rifled tubes, counterbored to receive liners, were to be prepared so that as erosion-resistant materials became available their performance as breech liners could be evaluated. When Division 1's investigations were terminated, tube forgings for the A-Z gun were being prepared. Two of them were completed to the stage of smooth-boring and chambering, and were turned over to the Army Ordnance Department for experimental use.

33.2 EVALUATION OF MILITARY IMPORTANCE OF HYPERVELOCITY GUNS FIRING SUBCALIBER PROJECTILES

33.2.1 General Observations

MILITARY ECONOMICS

Many arguments favor the use of hypervelocity guns, but verbal argumentation leads to no conclusions regarding the relative merits of military weapons. This is partly because of the many points of view from which the problem of evaluation can be approached. There appear to be two extreme approaches between which the many alternatives lie.

In the military emergency where failure means incalculable loss, the cost of attack or defense, however figured, is no consideration. The sole questions of importance are what to do and what is within reach to do with. It is too late for planning and economic study to contribute to the solution and the only argument which avails anything comes as the post-mortem where successes and errors are unearthed, discussed, and recorded for the benefit of future generations.

In broad-gauge military planning, during times of peace, the evaluation of weapons is an economic problem. It is concerned both with the economics of production in time of peace, and with the economics of production and use in time of war. In time of peace the economy is a dollar economy; in time of war it is controlled by the use of critical labor and critical material. The labor includes all the labor from the harvesting of raw materials, through manufacture of matériel, manufacture of transport equipment, labor of transport, labor of use, and labor of maintenance and repair. Little can be accomplished in the attempt to design equipment for the unpredictable emergency. Much can be accomplished toward reducing the probability of the emergency by advance planning of the economical conduct of war so as to make available manpower and materials most effective for the purpose.

The most effective weapon is the one which involves the minimum cost for a given damage to the enemy. The relative evaluation of cost and damage is involved in questions of military economics and strategy. In general, the problem is beyond the scope of this report. However, when the destructiveness of a given weapon can be increased many fold without additional cost, there is no question regarding its economics, military or otherwise. It is from this standpoint that we approach the evaluation of guns of established design, firing subcaliber projectiles at hypervelocity. Such projectiles include both sabot-projectiles (Chapter 29) and skirted projectiles (Chapter 30).

CONFIDENTIAL

The evaluation of the actual overall military economy of this accomplishment is a matter deserving further careful and extended study. It is to be hoped that the simple approach to the problem outlined here may point the way for the conduct of more elaborate studies of weapons in general.

Pros and Cons of Subcaliber Projectiles

Many valuable weapons have been neglected because, in the absence of simple methods for analytical evaluation, resort has been to opinion or to limited or inconclusive experience in judging their usefulness. The use of subcaliber projectiles in standard-bore guns has suffered this fate. It has long been known that muzzle velocities could be increased by use of subcaliber projectiles.[190] But it has also been known that reducing the caliber of projectiles reduces the effective radius of burst of the high-explosive projectile and the relative armor penetration of the armor-piercing projectile. It has also been known that a reduction in caliber increases the retardation of the projectile and therefore its loss of velocity over a given range.

These arguments have been aimed against the use of the subcaliber projectile without any attempt at a quantitative determination of the point of diminishing returns, the point at which the sacrifices offset the gains. The fact that there is a considerable region within which the net gains are substantial in spite of apparent disadvantages has been completely passed over. The fundamental reason behind this has been the fact that the method of handling the ballistic computation necessary in evaluating guns has been cumbersome and the computations too laborious for the extensive studies necessary.

The methods outlined in this report are not exact. However, their application to problems with known solutions shows results within an accuracy of a few per cent. Furthermore, the accuracy is completely obscured by the manyfold gains indicated so that there is no question as to the validity of conclusions except, possibly, under extreme conditions which lie outside of the present region of practical importance. The same methods could undoubtedly be applied to many other problems concerned with the evaluation of guns.

Increased Projectile Velocity

Raising the velocity of the projectile fired from a gun increases the effectiveness of the gun in one or more of several ways, depending on the use. These may be summarized as follows.

1. In unaided (no director) fire aimed at a stationary or moving target, it increases the allowable error in estimating range without reducing the probability of hitting.

2. In unaided fire aimed at a moving target, it reduces the necessary lead angle. Since the allowable absolute error in lead angle is independent of the lead and since the absolute accuracy of estimating lead is better the smaller the lead, the probability of hitting is improved.

3. In director-controlled fire against a maneuvering target, the probability of hitting increases more rapidly than the velocity[164] since the region into which the target can maneuver in the time of flight is diminished in volume. The probability of hitting is greatly increased by attaining an increase in velocity.

4. The thickness of armor that can be penetrated at a given range increases with velocity up to a critical velocity[205] at which the projectile breaks up; and the range at which a given thickness can be penetrated increases with velocity.

When subcaliber ammunition is used to increase velocity, there is a net gain in effectiveness in spite of the reduced relative effectiveness of the smaller projectile. The overall effectiveness may be considered as the product of the probability of a damaging hit and the measure of effectiveness of the hit. As the size of the subcaliber projectile is varied downward this product, for each situation, increases for some range of caliber reduction, reaches a maximum, and then diminishes. The only situations in which this is not true are those in which the probability of hitting is not affected by velocity (for instance in director-controlled fire against a fixed target or against a target moving on a definitely fixed and predictable course); or those in which the power of the standard projectile is just sufficient to destroy the target and any reduction of caliber decreases the destructive effect.

In attacks against armor, the effectiveness of a projectile which has insufficient energy to penetrate, is always increased by the use of a subcaliber projectile, provided that (1) the velocity required for penetration by the subcaliber projectile is not above its shatter value (see Section 33.2.4), and (2) the range is not so great that air-resistance velocity attenuation wipes out the potential gain. In antiaircraft use, where the high-explosive projectile has a finite range

[redacted]

of effectiveness of fragmentation, the gains by the use of subcaliber projectiles are always very striking, over a large range of target distances and with standard-caliber velocities as high as 6,000 fps. It does not appear that any velocity for the standard-caliber projectile attainable with a practicable gun design is so high that the effectiveness of the gun in antiaircraft service may not be materially improved by the use of a subcaliber projectile.

There are three methods for increasing the muzzle velocity for a given gun and powder charge.

1. Use of lightweight, standard-caliber projectile.
2. Use of a subcaliber projectile with discarding sabot in a standard-bore gun. (See Chapter 29.)
3. Use of a subcaliber, skirted projectile in a standard-bore gun fitted with a tapered muzzle adaptor, or in a one-piece tapered-bore gun. (See Chapter 30.)

Both types of subcaliber projectiles have a considerable advantage over the standard projectile of equal weight in that they suffer less velocity loss for a given muzzle velocity, over a given range. The skirted projectile has a definite advantage over the sabot-type projectile of the same weight, in that the entire initial momentum of the skirted projectile is available for sustaining velocity against air resistance, whereas the momentum of the sabot is lost at the muzzle of the gun. This fact shows up quite strikingly in some of the comparisons which follow. Furthermore, since the skirted projectile fits the bore tightly throughout its travel, it leaves the bore with less yaw and its accuracy is measurably superior.

Tungsten Carbide Cores

The development of the use of tungsten carbide cores in armor-piercing projectiles has gone hand-in-hand with the development of subcaliber projectiles and guns for firing them. This is not because of any unique advantage deriving from the combination, for the use of carbide cores in standard-caliber projectiles possesses similar advantages. However, since the purpose of the subcaliber development has been the attainment of the utmost in penetration, the adoption of the tungsten carbide core has been a natural accompaniment.

The gain from the use of tungsten carbide cores derives particularly from the high density of the material, which increases the energy density over the impact area, with a given velocity and from the high hardness which keeps down the deformation of the projectile on impact. The gain in penetration is also influenced, probably in a minor way, by the low coefficient of friction of tungsten carbide on steel. Furthermore, tungsten carbide of suitable cobalt content shows some increase in shatter velocity over steel.

All these factors combine to produce a very substantial gain in armor penetration through the use of tungsten carbide, and future attempts to develop projectiles of increased armor penetration should include a concentrated effort to improve the methods of using tungsten carbide. Such efforts should, in part, be directed at the development of a tungsten carbide head for a high-explosive, armor-piercing projectile. When used as a subcaliber projectile in a hypervelocity gun, such a projectile should have great effectiveness.

33.2.2 Velocity Gains From the Use of Subcaliber Projectiles

Limiting Effect of Powder Gas Kinetic Energy

Several years ago Langweiler fired an 8-mm/125-caliber gun with a fixed charge of pulverized nitrocellulose powder and with projectiles varying in weight from 1.18 times the charge weight to $^1/_{44}$ the charge weight. Results of these firings[26,493] show quite strikingly the effect of kinetic energy of the powder gas in limiting the velocity of the projectile. In particular they show that the velocity-charge function can be estimated with good accuracy by assuming approximately one-fourth of the charge weight added to the projectile weight and treating the kinetic energy of this combination as proportional to the powder energy. [See equation (4) in Section 3.2.2.]

Figure 2 is a graph of the Langweiler values of the velocity plotted against ratios of charge to projectile mass. The curve was drawn through points calculated from equation (1),

$$V = \frac{V_k}{\left(\frac{M}{C} + \frac{1}{a}\right)^{\frac{1}{2}}} \qquad (1)$$

in which V is the calculated velocity, M is the projectile mass, and C is mass of charge. The assumption is made that a fraction $1/a$ of the powder gas mass moves with the projectile. V_k is a constant with the dimensions of velocity, equal to V when $M/C = (1 - 1/a)$.

The value of a was determined from the experimental data in Table 1. In this table, also, calculated

TABLE 1. Experimental data from firing of 8-mm/125-cal. gun[498]

C/M	V_{exp} fps	V_{calc} fps	ΔV per cent
0.85	3,970	4,000	0.8
3.20	6,365	6,365	0
5.80	7,380	7,480	1.4
11.00	7,970	8,280	4.2
22.00	8,950	8,900	0.6
44.00	9,150	9,150	0

values of velocity are compared with experimental values. Fitting the curve to the points where $C/M = 44$ and $C/M = 3.2$, a is found to be 0.247 and V_0 is 4,780 fps. The approximation is quite good enough for our purpose.

Also plotted on Figure 2 are points of velocity versus C/M from data obtained at Carderock with the 3-in./50-cal. Navy gun (Section 4.2.2). These points are seen to fit the curve almost perfectly. Also plotted are a number of points obtained with a large variety of projectile designs and with various powder grain sizes, from firings with the 57/40-mm tapered-bore gun with skirted projectiles (Chapter 30). It is to be noted that for low values of C/M these latter points tend to lie below the Langweiler curve while for higher values they tend to lie above it. However, the highest value attained lies on the curve. There are several reasons for this behavior.

1. The friction in the tapered-bore gun is high and tends to displace the point of zero velocity to the right.

2. The friction at low velocities is substantially constant and it becomes less important as the powder charge increases so the two curves approach each other.

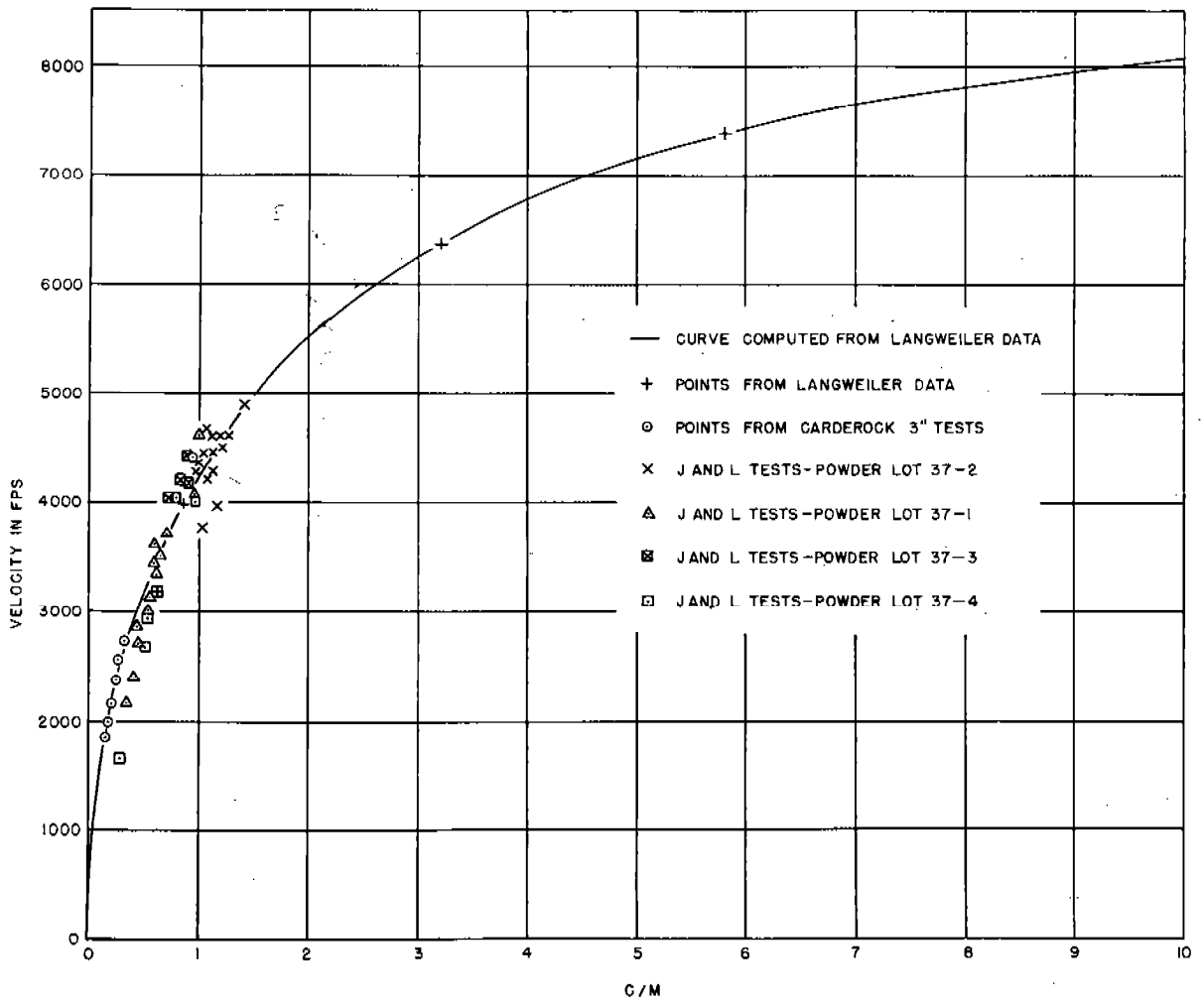


FIGURE 2. Velocity vs ratio of charge to projectile.

3. The Langweiler curve was taken with constant charge while the 57/40-mm data were taken with varying charge and nearly fixed projectile mass.

4. As the velocity of the projectile increases, surface friction apparently begins to melt the projectile surface material and the lubricating effect of this molten material reduces the friction; all indications are that the coefficient of friction at 4,000 fps is less than 1 per cent.

5. The relative heat loss, from powder gas to walls, decreases as the size of the gun increases. The thermal efficiency of the larger gun is therefore higher.

6. The horizontal spread of points is due to variation of powder temperature and to variation in projectile friction from one design to another. Gun wear also contributes to this spread.

The improvement in efficiency for higher charge and the greater efficiency of the larger gun cause the 57/40-mm curve to cross the Langweiler curve. The 57-mm standard load is a 6.28-lb projectile propelled by 36.5 oz of powder. The muzzle velocity is 2,800 fps and the charge-projectile mass ratio is 0.37. This point lies on the Langweiler curve as do skirted projectiles fired with 36.5 oz of powder. It is therefore clear that the skirted projectiles fired from a tapered-bore gun closely follow the performance indicated by Langweiler's curve. The velocity performance of the tapered-bore gun or of the gun firing a sabot-projectile can be computed from equation (2)

$$V_s = V_0\left[\frac{1 + 0.25(C/W_0)}{W_s/W_0 + 0.25(C/W_0)}\right]^{1/2} \qquad (2)$$

in which V_0 is the velocity for the standard gun and C is the standard charge, for the standard projectile of weight W_0. V_s is the velocity that would be obtained from the subcaliber projectile of weight W_s. If the charge is to be varied, additional data are necessary to introduce the effect of friction and cooling of the powder gas. Equation (2) provides a simple expression for use in determining subcaliber projectile velocities for the purpose of approximate analyses.

Effect of Gun Caliber on Muzzle Velocity

When an homologous series of projectile designs has been prepared the weights of the projectiles will vary with the cube of the caliber. However, when subcaliber projectiles are fired, additional parts are necessary to fill the bore, serving to support the powder pressure and to guide the projectile down the bore. These parts add weight. A rough analysis indicates that the gross weight of a subcaliber projectile can be related to the weight of the standard projectile by equation (3)

$$\frac{W_s}{W_0} = \rho^3 + \sigma(1 - \rho)^2(1 + \rho + \beta), \qquad (3)$$

in which W_s is the weight of the subcaliber projectile, W_0 is the weight of the standard projectile, ρ is the ratio of subcaliber to standard caliber, and σ and β are design constants. For a skirted projectile, σ is approximately 0.16 and $\beta = 0$. For sabot-type projectiles, σ is substantially the same and $\beta = 3$.

By combining equations (2) and (3), the muzzle velocity V_{ms} of a subcaliber projectile is given by equation (4).

$$V_{ms} = V_0 \cdot \left[\frac{1 + 0.25(C/W_0)}{\rho^3 + \sigma(1 - \rho)^2(1 + \rho + \beta) + 0.25(C/W_0)}\right]^{1/2} \qquad (4)$$

Effect of Range on Velocity and Time of Flight of Subcaliber Projectiles

As indicated above, the analytical treatment of the relative effectiveness of different types and sizes of guns has always been complicated by the traditional empirical handling of the ballistic aspects of the problem. In general it has not been practicable to effect a valid comparison without constructing and firing actual full-sized models. It is quite obvious that this fact has had an adverse effect on the cost of developing ordnance and on the interest taken in the consideration of the potentialities of new weapons.

Fortunately, when the field of hypervelocity is entered, the situation becomes greatly simplified. In unpublished studies of ballistic tables it has been found that the ballistic performance of projectiles of good aerodyamic design can be treated with sufficient accuracy for all purposes except actual fire control in service, by very simple functions, for a considerable range of velocities above that of sound. For guns with high velocities the accuracy is good throughout the range of target distances for which tables are generally computed.

Over a considerable range of velocities above that of sound, with good aerodynamic projectile design, the resistance force varies closely with the three-halves power of the velocity. In Chapter 8 closer approximations effective over a limited range of velocity are indicated. The three-halves power law is quite sufficiently accurate for many purposes up to Mach numbers approaching 10.

When the muzzle velocity is above, say, 2,600 fps, the range tables show a maximum variation of range for constant time of flight, with varying elevation, of only a few per cent. In the case of the 120-mm gun, M1, this variation is of the order of only 1 per cent. This fact is due to the compensating effects of reduced air resistance at high altitudes in balancing loss of velocity due to gravity. In view of these facts very good analytical approximations can be made by neglecting altitude-density effects and the effect of gravity on the flight of the projectile. Under these circumstances the differential equation of projectile motion along the line of sight may be written in the form of equation (5),

$$\frac{d^2r}{dt^2} = -K\left(\frac{dr}{dt}\right)^{3/2} \tag{5}$$

in which r is the distance along the line of sight, t is the time of flight, and K is the aerodynamic retardation constant. The solution of equation (5) may be written in the forms (6), (7), and (8),

$$r = \frac{ut}{1 + \frac{K\sqrt{ut}}{2}}, \tag{6}$$

$$t = \frac{r/u}{1 - \frac{Kr}{2\sqrt{u}}}, \tag{7}$$

$$V_r = u\left(1 - \frac{Kr}{2\sqrt{u}}\right)^2, \tag{8}$$

where u is the initial velocity of the projectile, and V_r is velocity at range r.

The 120-mm gun, M1, is a high-velocity (3,150 fps) gun with a good projectile design. Ballistic computations based on the three-halves power resistance law fit its ballistic table quite well. For instance, for 25 sec time of flight the range on a horizontal line of sight is 14,200 yd. For these conditions calculation shows that $u = 3{,}000$ fps; $Kr/2\sqrt{u} = 0.432$; $K/2\sqrt{u} = 0.0000304$; $K = 0.00191$. Calculations of t by means of equation (7) deviate only slightly (between 1 and 2 per cent) from corresponding values of t given in the range tables.

When the projectile size is varied while maintaining constant aerodynamical design, K varies directly with the cross-sectional area of the projectile and inversely with its mass. Furthermore K depends primarily on the nose design and changes in length affect it little. For subcaliber projectiles we may therefore write equation (9),

$$K = K_0\rho^2\frac{W_0}{W_s} = K_0\frac{\rho^2}{\rho^3 + \sigma(1-\rho)^2(1+\rho+\beta)} \tag{9}$$

in which K_0 and K are the constants for the standard and subcaliber projectiles respectively.

In using this relation we must bear in mind that, in the case of the sabot-projectile, the sabot parts are discarded at the muzzle. Hence σ and β become zero for the sabot-projectile in flight. In the case of the skirted projectile, β is 0. We therefore obtain equations (10) and (11).

$$K_{(\text{skirted})} = K_0\frac{\rho^2}{\rho^3 + \sigma(1-\rho)^2(1+\rho)}. \tag{10}$$

$$K_{(\text{sabot})} = \frac{1}{\rho}K_0. \tag{11}$$

By making use of equations (4) to (11) we may now write, for the velocity at any range, equations (12) and (13).

For values of ρ close to unity, equations (12) and (13) can be approximated by equation (14).

$$V_{r\,(\text{skirted})} = V_0\left\{\frac{1 + 0.25(C/W_0)}{\rho^3 + \sigma(1-\rho)^2(1+\rho) + 0.25(C/W_0)}\right\}^{1/2} \cdot \left\{1 - \frac{K_0\rho^2[\rho^3 + \sigma(1-\rho)^2(1+\rho) + 0.25(C/W_0)]^{1/4}}{2\sqrt{V_0}[1 + 0.25(C/W_0)]^{1/4}[\rho^3 + \sigma(1-\rho)^2(1+\rho)]}\right\}^2. \tag{12}$$

$$V_{r\,(\text{sabot})} = V_0\left\{\frac{1 + 0.25(C/W_0)}{\rho^3 + \sigma(1-\rho)^2(1+\rho+\beta) + 0.25(C/W_0)}\right\}^{1/2} \cdot \left\{1 - \frac{K_0[\rho^3 + \sigma(1-\rho)^2(1+\rho+\beta) + 0.25(C/W_0)]^{1/4}}{2\rho\sqrt{V_0}[1 + 0.25(C/W_0)]^{1/4}}\right\}^2. \tag{13}$$

$$V_{r\,(\text{skirted})} = V_{r\,(\text{sabot})} = V_r = V_0\left[\frac{1 + 0.25(C/W_0)}{\rho^3 + 0.25(C/W)}\right]^{1/2}\left\{1 - \frac{K_0}{2\rho\sqrt{V_0}}[\rho^3 + 0.25(C/W_0)]^{1/4}\right\}^2. \tag{14}$$

[redacted]

It is apparent from inspection of this relation that while decreasing the projectile caliber always reduces the range at which the velocity reaches zero, there is still always a finite range of target distance within which striking velocity is increased by reducing caliber.

33.2.3 Gains in Effectiveness of Fire against Moving Targets Resulting from Use of Subcaliber Projectiles

Reduction of Time of Flight

From equation (7) and the expressions for K and W/W_0, the time of flight t of a subcaliber projectile is found to be given by equations (15) and (16).

For a standard diameter projectile of reduced weight equal to that of the skirted projectile, the time of flight is given by equation (17).

Table 2. Ratios of times of flight for various types of projectiles.

	10,000-yd range			15,000-yd range		
ρ	t_d/t_0	t_s/t_0	t_l/t_0	t_d/t_0	t_s/t_0	t_l/t_0
1.0	1.00	1.00	1.00	1.00	1.00	1.00
0.9	0.90	0.90	0.92	0.90	0.91	1.12
0.8	0.76	0.81	1.06	0.81	0.82	1.60
0.7	0.70	0.73	1.37	0.69	0.82	∞
0.6	0.59	0.66	2.30	0.60	0.89	....
0.5	0.52	0.65	∞	0.61	1.20	....
0.4	0.44	0.78	....	0.72	3.50	....

$$t_{a\ (\text{skirted})} = \frac{r}{V_0} \frac{[\rho^3 + \sigma(1-\rho)^2(1+\rho) + 0.25(C/W_0)]^{1/2}}{[1 + 0.25(C/W_0)]^{1/2} \left\{1 - \frac{K_0 r}{2\sqrt{V_0}} \frac{\rho^2[\rho^3 + \sigma(1-\rho)^2(1+\rho) + 0.25(C/W_0)]^{1/4}}{(\rho^3 + \sigma[1-\rho]^2[1+\rho]^{3/4}[1 + (0.25C/W]^{1/4}}\right\}}. \tag{15}$$

$$t_{s\ (\text{sabot})} = \frac{r}{V_0} \frac{[\rho^3 + \sigma(1-\rho)^2(1+\rho+\beta) + 0.25(C/W_0)]^{1/2}}{[1 + 0.25(C/W_0)] \left\{1 - \frac{K_0 r}{2\sqrt{V_0}} \frac{[\rho^3 + \sigma(1-\rho)^2(1+\rho+\beta) + 0.25(C/W_0)]^{1/4}}{\rho[1 + 0.25(C/W_0)]^{1/4}}\right\}}. \tag{16}$$

$$t_{l\ (\text{lightweight})} = \frac{r}{V_0} \frac{[\rho^3 + \sigma(1-\rho)^2(1+\rho) + 0.25(C/W_0)]^{1/2}}{[1 + 0.25(C/W_0)]^{1/2}[1 - \frac{K_0 r}{2\sqrt{V_0}} \frac{[\rho^3 + 0.25(1-\rho)^2(1+\rho) + 0.25(C/W_0)]^{1/4}}{[1 + 0.25(C/W_0)]^{1/4}[\rho^3 + \sigma(1-\rho)^2(1+\rho)]}}. \tag{17}$$

For purposes of numerical comparison the 120-mm gun, M1, has been chosen as it has a good projectile design and the normal muzzle velocity is high enough so that the approximate analysis applies throughout the range of uses. For this gun $C/4W_0$ has the value 0.11. Table 2 shows a comparison of times of flight for 10,000-yd range and 15,000-yd range of skirted and sabot-projectiles fired from this gun for varying values of ρ. It is not practicable to reduce ρ below 0.5 and values of 0.6 and 0.7 are more practical. The value of 0.4 has been included only to show the trend. There have also been included columns of time of flight t for lightweight, full-caliber projectiles having the same weight as the skirted projectile. The values shown in the table are the ratios of the time of flight of the reduced projectile to that (t_0) of the standard projectile.

Table 2 shows a substantial reduction in time of flight through the use of a subcaliber projectile. However, this is at the cost of a reduction in the damage power of the projectile itself. It is important to consider the situation from the standpoint of overall gain. The probability of a direct hit is greatly increased with the subcaliber projectile, but the damage depends on the power of the hit. When the size of a high-explosive shell is reduced, its radius of effectiveness may be considered to be proportional to its diameter down to the point where the fragments become too small to effect critical damage.

The superior performance of the skirted projectile results from the fact that no mass is discarded so that all the initial momentum is available for overcoming resistance. It is to be noted that the relative performance of either subcaliber projectile is not greatly affected by range for values of ρ of 0.6 and above. The effect will, however, become more pronounced at greater ranges. The standard-caliber lightweight projectile is obviously of little value except at relatively short range.

Effect of Subcaliber on Probability of Damaging Hit

The probability of an effective hit is a function of the number of shells which must be thrown into the space of future positions of the target to insure such a hit. This in turn depends on the dimensions of

[redacted]

the vulnerable portion of the target and the radius of effectiveness of the burst. Numerically it is the reciprocal of the number of bursts spaced on some regular pattern of minimum density, sufficient for the purpose, modified by a coefficient which introduces the statistical aspects of the problem. For simplicity, a fair approximation can be made by treating both the target and the burst as spheres of radii R_t and R_b respectively. There are good reasons why this gives substantially as good an approximation as a more complicated analysis. If the bursts are placed at the corners of a cubical lattice having diagonal length of $2(R_t + R_b)$ and if V_t is the volume of future positions of the target, the bursts per hit is expressed by equation (18),

$$N_h = \frac{3V_t}{8s(R_t + R_b)^3}. \tag{18}$$

The probability of a hit is given by equation (19).

$$P_h = \frac{8}{3}\frac{s(R_t + R_b)^3}{V_t}. \tag{19}$$

With a target subject to three-dimensional accelerations and moving at speed and with radial acceleration such that the change of course is 90 degrees or less in the time of flight of the projectile, the volume V_t is approximately proportional to the sixth power of the time of flight t. The higher the velocity of the target the more closely this condition is met. We may therefore write equation (20).

$$P_{hs} = P_0 R_b^3 \frac{(a + \rho)^3}{t^6}. \tag{20}$$

Here P_0 is a statistical coefficient, $1/a$ is the ratio of the radius of a normal burst to that of the target, and R_b is the ratio of the diameter of a subcaliber projectile to that of the normal projectile.

The relative probability of a damaging hit with a subcaliber projectile as compared with that of a normal projectile is given by equation (21).

$$p_R = \frac{P_{hs}}{P_{hn}} = \frac{(a + \rho)^3}{(a + 1)^3}\left(\frac{t_n}{t_s}\right)^6. \tag{21}$$

It is clear from this equation that the probability of a damaging hit is highest for the projectile with the shortest time of flight when ρ and a are constant. An analysis of the data shows that of the various forms of lightweight projectiles of equal power, fired from the same gun, the skirted projectile has the shortest time of flight. In an attack against a maneuvering target, there are very great advantages in the use of subcaliber projectiles, particularly those of the skirted type, in spite of the effect of reduced caliber in diminishing the radius of effectiveness of the high-explosive burst. For the sabot-projectile the relative effectiveness at $\rho = 0.6$, near the point of greatest probability, is only about one-half that of the skirted projectile. This advantage of subcaliber projectiles persists into the region where practical considerations prevents further reduction of projectile caliber.

The design of a deformable, high-explosive projectile presents certain difficulties which become more serious with decreasing values of ρ. Although the theoretical probability of damage is maximum in the neighborhood of $\rho = 0.6$ for a range of 10,000 yd, and for lower values of ρ at shorter ranges, the region $\rho = 0.7$ to $\rho = 0.8$ is that to which practical considerations limit design. There is, however, an obviously substantial advantage to be gained even though we are limited to working in this region. Figure 3 illustrates graphically the advantages of subcaliber projectiles.

While present design considerations tend to restrict the caliber ratio to values of 0.7 and 0.8, Figure 3 shows the great theoretical advantages to be gained by further decreasing ρ, down to values in the neighborhood of 0.55. In fact, in the least favorable

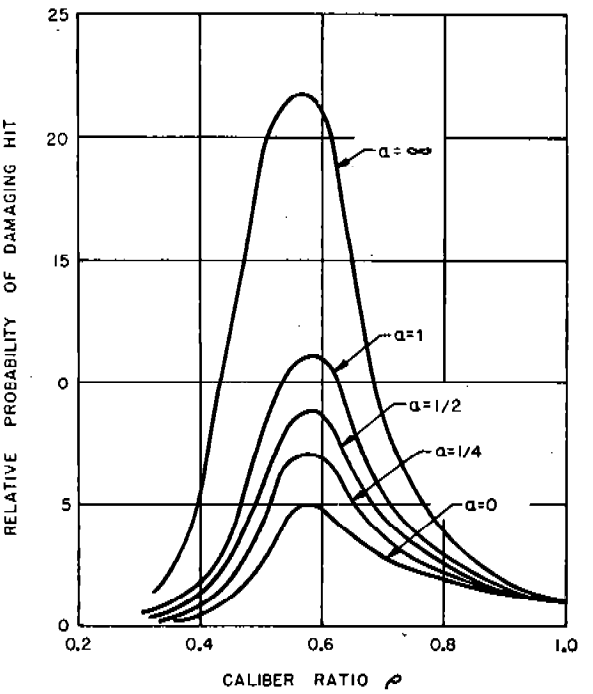


FIGURE 3. Theoretical advantages of subcaliber projectiles in increasing probability of damaging hit.

case ($a = 0$), there is a gain of the order of 2 to 1 in going from $\rho = 0.7$ to $\rho = 0.55$. This fact creates a great opportunity for further gain by efforts to bridge this gap in design. The ultimate lower limit is that prescribed by the space available in the emergent bore for accommodation of the deformed rear skirt. For powder pressures in the neighborhood of 45,000 psi, this limit is approximately at $\rho = 0.5$. For higher pressures the value is larger. The use of higher strength material is indicated. This, however, introduces a wear problem and demands development of wear-resistant liners. In the case of high-explosive projectiles, the weight of the rear skirt becomes important in influencing the stability of flight. For designs developed to date it would probably be difficult to maintain stability for ρ less than 0.75, except by greatly increased rate of spin. However, this matter has not yet been thoroughly analyzed.

For small values of ρ an excessive portion of the available space is taken up by the front skirt. When this occurs the space available for the high explosive is insufficient and the fragmentation of the projectile is apt to be unsatisfactory. New studies may lead to a better method for supporting the front end of the projectile. Even in the face of these difficulties the gains to be made by extending the range of ρ toward 0.5 are such that even though the relative effectiveness be substantially reduced by the sacrifice of good design there may still be a net gain in increased probability of damage. This aspect of the design study is worthy of exhaustive treatment. Further consideration needs also to be given to effect of size on damage and the point at which the fragmentation is such as to produce ineffective bursts against the target.

In the above analysis the standard powder case and charge are assumed, with only the projectile weight varying. A gain in the probability of a damaging hit is indicated throughout the range of practicable caliber ratios. For a standard burst-to-target ratio of unity, which is in the neighborhood of service conditions, the maximum probability is about 11.0 times normal, and the probability at the present limit of caliber ratios (0.7) is 5.5 times normal. This gain in chance of damage is obtained at no increase in ammunition cost but at a probable actual reduction in cost. In other words, the ammunition cost per hit will be reduced to less than one-fifth of the present cost. By the same token, the same ammunition cost can attain damage under much more difficult conditions.

At the present time the life of the gun is reduced to about one-third its normal value. By the use of stellite liners (Chapter 19) this can undoubtedly be returned to normal for some guns, or actually increased. In other words, almost the entire saving in ammunition cost can be made effective by such design. The most important aspect of the situation is, however, that a given battery of guns, its directors, auxilliary equipment, its whole personnel and the equipment, personnel, and personnel and fuel used in transporting it to its point of use, are rendered five or more times as effective. The material advantages, when viewed from this standpoint, are very impressive.

Limitations on Gains

While the evaluation of the precise conditions is not within the scope of the present discourse, it should be pointed out that there is a range for any gun beyond which use of a subcaliber projectile will not reduce the time of flight. Furthermore, there is a shorter range beyond which reduction of caliber does not increase the probability of a damaging hit. These limitations require thorough analysis in connection with any further studies along these lines.

33.2.4 Gains in Armor Penetration by Use of Subcaliber Projectiles

The de Marre formula for penetration of armor plate by steel projectiles is given by equation (22),

$$e = d\left(\frac{WV^2\cos^2\theta}{\alpha d^3}\right)^{1/\beta}, \tag{22}$$

in which e is the thickness of plate penetrated, d is the diameter of the projectile, W is its weight, θ the angle of impact relative to normal, V the striking velocity, and α and β are constants. For nondeformable projectiles, $\log \alpha = 6.15$ and $\beta = 1.43$. Hence equation (22) reduces to equation (23).

$$e = \frac{1}{d^{1.1}}\left(\frac{WV^2\cos^2\theta}{\alpha}\right)^{1/1.43}. \tag{23}$$

If the projectile energy is kept constant while its diameter is varied, the penetration improves as the diameter diminishes. This improvement continues until the impact velocity reaches the shatter value.

When tungsten carbide is used as a projectile material, α and β both diminish, and the relative penetration is increased. The constants are now, however, not independent of θ and there is a region of θ wherein

the advantage of tungsten carbide is not so great. On the average, tungsten carbide is in the neighborhood of 2.5 to 3.5 times as effective as steel in armor penetration. This gain is due in part to the fact that the values of α and β are more favorable but also to the fact that for a given value of projectile mass, the tungsten carbide projectile diameter is only about three-fourths that of the steel projectile.

In view of the higher density, a carbide projectile of given diameter has lower velocity than the corresponding steel projectile for given penetration, and since it also has a higher shatter velocity, it can strike armor plate with much more energy than can a steel projectile of the same size.

The shatter velocity of tungsten carbide is roughly three-halves that of steel so a projectile of given energy should, on this basis alone, have about two and one-half times the penetration of steel. The more advantageous values of α and β produce the additional improvement.

From equation (23) it is apparent that reduction of caliber, while retaining projectile energy, improves penetration. However, in an actual gun, the powder energy is fixed and, as pointed out in Section 2.2, a part of this energy is delivered as kinetic energy of the powder gas. In view of this, the energy of the projectile diminishes as the caliber is reduced. Furthermore, because of less favorable ballistic conditions, the projectile strikes the plate with a further reduction in relative energy and the advantages of subcaliber projectiles for armor penetration are thereby modified. There is, however, a region of advantage in which gains in armor-piercing effectiveness are actually attained by the use of subcaliber projectiles.

In order to simplify the present analysis, we neglect the mass of skirts and sabots. This is not strictly allowable, but the optimum conditions occur in a region of values of ρ for which the error is not serious. When this is done, the striking velocity is given by equation (24).

$$V_s = V_0 \left[\frac{1 + 0.25(C/W_0)}{\rho^3 + 0.25(C/W_0)}\right]^{1/2} \cdot \left\{1 - \frac{K_0 r}{2\rho\sqrt{V_0}} \left[\frac{\rho^3 + 0.25(C/W_0)}{1 + 0.25(C/W_0)}\right]^{1/4}\right\}^2. \quad (24)$$

Inserting this value for V in equation (23), and dividing by equation (25),

$$e_0 = \frac{1}{d_0^{1.1}} \left(\frac{W_0 V_0^2 \cos^2\theta}{\alpha}\right)^{1/1.43}, \quad (25)$$

equation (26) for the relative penetration is obtained.

$$\frac{e}{e_0} = \rho \left[\frac{1 + 0.25(C/W_0)}{\rho^3 + 0.25(C/W_0)}\right]^{1/1.43} \cdot \left\{\frac{1 - \frac{K_0 r}{2\rho\sqrt{V_0}} \left[\frac{\rho^3 + 0.25(C/W_0)}{1 + 0.25(C/W_0)}\right]^{1/4}}{1 - \frac{K_0 r}{2\sqrt{V_0}}}\right\}^{4/1.43}. \quad (26)$$

For values of ρ near unity, the expression $1 - \Delta$ may be substituted for ρ. Upon expansion, and with neglect of higher powers of Δ, equation (26) reduces to equation (27).

$$\frac{e}{e_0} = 1 + \Delta \left\{\frac{3}{1.43(1 + 0.25(C/W_0)} - 1 + \frac{4}{1.43}\left(\frac{3}{4}\frac{1}{1 + 0.25(C/W_0)} - \Delta\right) \cdot \frac{K_0 r/2\sqrt{V_0}}{1 - \frac{K_0 r}{2\sqrt{V_0}}}\right\}. \quad (27)$$

It is clear that there is a set of conditions for which e/e_0 is not increased by changing the caliber ratio ρ. These conditions are given by equation (28).

$$\frac{3}{1.43[1 + 0.25(C/W_0)]} - 1 = \left(\frac{4}{1.43} - 1\right)\frac{K_0 r}{2\sqrt{V_0}}. \quad (28)$$

When C/W_0 is fixed, the range at which no increase in penetration results from a reduction of caliber is given by equation (29),

$$r_1 = \frac{[2.1/1 + 0.25(C/W_0)] - 1}{1.8}, \qquad r_0 = 1.16 r_0 \left[\frac{0.152 - .12(C/W_0)}{1 + 0.25(C/W_0)}\right], \quad (29)$$

in which $r_0 = 2\sqrt{V_0}/K_0$. For the 120-mm gun, C/W_0 is approximately 0.45, so the range is 17,000 yd.

It is thus apparent that gains in armor penetration may be accomplished out to ranges which are well beyond those at which there would be likely use of a gun of this size for the purpose of making direct hits against armor.

The order of magnitude of the gains resulting from the use of subcaliber projectiles without change of material is indicated in Table 3, which has been prepared for steel projectiles at zero range, for the 120-mm gun with standard powder load.

TABLE 3. Relative armor penetration from subcaliber and standard steel projectiles fired from 120-mm gun at zero range.

ρ	e/e_0
1.0	1.0
0.8	1.16
0.7	1.28
0.6	1.34
0.5	1.40
0.4	1.28

While the gains are not so striking as those resulting from the use of tungsten carbide projectiles, they are sufficient to be interesting.

When the diameter of a tungsten carbide projectile is 75 per cent that of the standard projectile, its weight is substantially the same, so the muzzle velocity does not change. Under these circumstances the retardation of the carbide projectile is only of the order of half that of the steel projectile. The relative penetration is given by equation (30).

$$\frac{e_c}{e_0} = 1.4 \left[\frac{1-(K_0 r/4\sqrt{V_0}}{1-(K_0 r/2V_0)}\right]^4. \qquad (30)$$

Thus we have the remarkable condition that not only is the initial penetration of the tungsten carbide greater, but it improves materially with range. In the case of the 120-mm gun, with an equal weight tungsten carbide projectile the relative penetration for different ranges is given in Table 4. The absolute limit

TABLE 4. Relative armor penetration from tungsten carbide-cored subcaliber projectiles and standard projectiles fired from 120-mm gun.

r (yd)	e/e_0
0	1.4
5,000	2.0
10,000	3.0
15,000	5.7
20,000	13.0

of range for this gun is about 30,000 yd with the steel projectile, and double that with the carbide projectile. The normal ballistic tables extend to about 17,000 yd. This is perhaps as striking an indication of the advantage of the combination of subcaliber and tungsten carbide in projectile design as can be given, for it combines the effects of increased normal penetration and improved ballistics.

As the weight of the tungsten carbide projectile is further reduced, the initial penetration increases and for a while there is a continued increase all down the line. Ultimately, a point is reached where the ratio of tungsten carbide velocity to steel velocity is constant throughout the range of travel, and under this condition the penetration ratio is constant. This occurs, however, at a value of ρ less than 0.2 which is well below the practical limit.

In some respects absolute values of penetration are more significant than relative values. From this standpoint it is worth noting that, in the case of the 120-mm gun, the equal-weight subcaliber projectile has, at a range of about 2,800 yd, the same penetration as the steel projectile at zero yd. At 5,000 yd the tungsten carbide penetration is 85 per cent that for steel at zero range, while at 10,000 yd it is 72 per cent, and at 15,000 yd 53 per cent. At 15,000 yd the penetration for steel is only 9 per cent of that at zero range.

33.3 WHAT OF THE FUTURE?

33.3.1 Continuation of Fundamental Research

Although Division 1, by its intensive effort during a period of five years, made gratifying progress toward the understanding of erosion and the practical solution of the hypervelocity problem, it cannot be claimed that the problem is completely solved. The investigations uncovered a number of new problems interesting in themselves and of fundamental importance in connection with further improvements in gun design. Nearly all parts of the broad program of Division 1 could be carried further profitably by the Army or Navy or by an independent organization operating in conjunction with the Armed Services. In the future, great emphasis should continue to be placed upon basic research. The accomplishments of Division 1 have resulted mainly from an understanding of the fundamentals and not from a mere "polishing up" of previously existing devices. Developing and testing are of course essential, but substantial improvements depend on the new ideas that evolve as the result of research. Some of the fields on which it appears emphasis should be placed in future investigations are mentioned below.

33.3.2 Interior Ballistics

Although important advances have been made recently in this field, additional information is needed. In particular, an effort should be made to secure

simplified relations between the various factors involved. Furthermore, hypervelocity gun design would be facilitated by improvement of ignition and insurance of uniform ballistics even at very high densities of loading and correspondingly high pressures.

33.3.3 Heating of Guns

Much additional work needs to be done before we have a complete knowledge of the temperatures in various parts of a gun barrel under varying conditions of firing. Further investigations should include both experimental determinations and mathematical analyses. It is essential to know more completely the temperatures at the bore surface of guns of various sizes under various conditions of firing, in order to deal intelligently with all aspects of gun erosion; and it is desirable to have full knowledge of the temperatures at points in the wall in order to predict the behavior of new designs of gun barrels. Such information is important also in connection with the determination of the value of cooling devices.

33.3.4 Erosion

Although we now have a fairly satisfactory picture of gun erosion, further studies would be worth while. Laboratory apparatus that would separate properly the various phenomena involved is desirable. For example, an improvement in the electron bombardment technique (Section 11.3.2) for producing thermal effects that may be completely free from chemical ones would be useful. It is interesting to note that although many kinds of laboratory tests relating to erosion have been devised, we still do not have the means of duplicating at will in a simple laboratory apparatus the erosion that takes place in an actual gun. So long as it continues to be necessary to test erosion-resistant materials, there will be a need for laboratory apparatus by which we may avoid part or all of the cumbersome and expensive testing that now must be carried out with guns, which for the larger sizes involves very considerable cost in money and time.

33.3.5 Bore Friction

Much effort would be justified in an attempt to secure more complete information on bore friction in various types and sizes of guns. This investigation might well be carried forward as a part of a long-range research program of investigations in interior ballistics, using all possible experimental and theoretical approaches. Rapid and convenient techniques for measuring bore friction would facilitate the development of improved rifling and banding and in general of methods for reducing friction, which is the direct or indirect source of various difficulties with hypervelocity guns. Further data would be useful in developing methods for reducing friction by improved band design or otherwise.

33.3.6 Liners and Coatings

Recent results on the selection and application of liners and coatings of erosion-resistant materials are encouraging and justify further studies. Adequate firing tests should be made of materials such as hardened molybdenum, chromium-base alloys, and electroplated duplex coatings or alloy coatings especially of cobalt and tungsten. Although the low fusion point of stellite appears to limit its utility to small guns and moderate muzzle velocities, some further tests would be worth while. The theoretical possibilities of a hot-hard alloy such as stellite coated with a refractory material like molybdenum or chromium are so attractive that this particular development should be continued until it is determined whether or not this combination will afford a universal solution of the hypervelocity problem, by preventing both erosion and flattening of the lands under the most severe conditions. In this group of projects may also be placed further studies on the Fisa protector (Chapter 32), the advantages of which, either alone or in combination with other features, have not been fully evaluated.

33.3.7 Improved Propellants

It appears quite obvious that it would be well worth while to attempt to develop propellants that either by low flame temperature or favorable chemical composition will be less erosive (in proportion to energy) than existing propellants. Furthermore, adequate tests should be made on mixtures of single-base and double-base propellants having an approximately "neutral" chemical action, that is, ones in which the carburization of the bore is reduced without excessive increase of flame temperature (Section 15.6). There remains a possibility that by minimizing chemical action and the production of low-melting compounds on the bore surface, the erosion-resistance of gun steel

could be significantly improved. Further investigations using an adiabatic compression apparatus (Section 11.3.1) might provide a useful clue as to desired compositions for nonerosive propellants.

33.3.8 Special Projectiles

Sabot-projectiles (Chapter 29) have been developed that have satisfactory accuracy and meet the requirement of firing through a muzzle brake; but further improvements are desirable, and additional studies should be made so as to determine the best types for various uses. The utility of tapered-bore guns and skirted projectiles (Chapter 30) is worthy of further evaluation as emphasized in Section 33.2. The pre-engraved projectile in combination with a chromium-plated barrel (Chapter 31), which tests in a small-caliber gun indicate is a remarkably effective method for reducing gun erosion and thus making hypervelocity practical, should be studied further in order to ascertain what conditions of plating are necessary for large guns and to find the most suitable projectile designs. In this connection, it is vital to develop simple and convenient loading and indexing mechanisms (Section 28.4) in order to utilize fully the advantages of pre-engraved projectiles for various types of guns. Another item that would justify critical evaluation is the "booster" projectile, especially the type which near the end of its flight receives an additional impulse from a rocket-like mechanism.[c]

[c] A similar suggestion is given by Division 8 in its section of the History of OSRD.

33.3.9 High-Strength Steels for Gun Barrels

The use of much higher pressures for hypervelocity guns is an interesting possibility. This would simplify the design of such guns, but would serve to emphasize the desirability of making gun tubes of steel having a strength much higher than that of ordinary gun steel. There is good reason to believe that the avoidance of damage to the bore surface through erosion would greatly increase the probability of favorable behavior with steels of high strength.

33.3.10 "Economics" of Gun Fire

From a broad point of view, the overall advantage of hypervelocity is to be judged by performance in relation to weight, cost, and mobility. It is vital, therefore, to make a careful determination of the optimum conditions for hypervelocity guns so as to find the combination of factors that involves the minimum consumption of labor and critical material per unit of damage. As a result of the new knowledge accumulated in the last five years, there can remain little doubt that the guns of the future will operate at velocities higher than in the past. Hypervelocity is advantageous and it is practicable. A practical limitation on muzzle velocity is now imposed not by physics, but rather by economics. Whether the limit beyond which it will be unprofitable to increase the velocity is generally at 4,000 or 4,500 fps or much higher is to be determined by future assessment and balancing of all the relevant factors.

GLOSSARY

ACCURACY LIFE. The number of rounds that can be fired from a gun before it becomes inaccurate because of erosion. The criterion for accuracy-life varies from gun to gun. Cf. *velocity life*. (See Section 23.1.4.)

AIRCRAFT BARREL, caliber .50. A 36-in. caliber .50 machine gun barrel made according to Ordnance Department Drawing D35348A or D28272.

ALTERED LAYER. A thin layer of steel at the bore surface of a gun, the chemical and physical nature of which differs from that of the underlying steel because of changes that have taken place during firing. (See Section 12.1.1.)

AUSTENITE. A solid solution of carbon in the high-temperature form of iron, called gamma-iron. Cf. *ferrite*. (See Section 12.2.1.)

BALLISTIC LEVEL. The charge and pressure at which a gun is fired.

BODY ENGRAVING. A mark or marks on the bourrelet or body of a projectile caused by contact with the lands of the gun. (See Sections 6.1.2, 10.4.10.)

BORE PROFILE. A graph in which is plotted either the bore diameter or the change in bore diameter of a gun as a function of the position along the axis of the bore. (See Section 10.2.1.)

CANNELURE. A circumferential groove in a projectile.

CEMENTITE. Iron carbide, one of the constituents of steel, which is sometimes formed on the bore surface of a gun during firing. (See Section 12.5.2.)

CLOCK POSITION. A position on the circumference of the bore of a gun designated by analogy with the position of the hour hand on the face of a clock.

COOK-OFF. The premature explosion of the powder charge in a gun chamber or of the high-explosive filler in a shell or fuze caused by the heat of the gun when the round is left in the chamber. (See Section 5.6.2.)

COVOLUME. A correction factor in the equation of state of the powder gases which takes into account the space occupied by the gas molecules themselves. (See Section 2.4.2.)

CYCLONITE. A high explosive that has been used experimentally as the active ingredient in a propellant by dispersing the crystals of the compound in a nitrocellulose matrix.

DPH. "Diamond pyramid hardness," which is measured by means of a Vickers hardness tester.

DOUBLE-BASE POWDER. A powder containing nitroglycerine and nitrocellulose as its active ingredients.

DUPLEX PLATE. An electroplate consisting of two or more separate electroplates deposited one on top of the other. (See Section 20.2.4.)

ESR. "Equivalent Service Rounds," that is, the number of full-charge rounds that is considered equivalent to a larger number of rounds fired at a reduced charge. (See Section 10.3.3.)

FERRITE. A solid solution of not more than 0.06% carbon in the low-temperature form of iron, called alpha-iron. Cf. *austenite*. (See Section 12.2.1.)

FISA PROTECTOR. A device for protecting the bore of a gun from erosion. (See Chapter 32.)

HEAVY BARREL, CALIBER .50. A 45-in. caliber .50 machine gun barrel made according to one of the following Ordnance Department drawings: D28253-11, D28253A, D28253A3, or D28269-8X.

HC PLATE. "High contraction plate," a type of chromium plate. (See Section 20.2.2.)

HYPERVELOCITY. A projectile velocity greater than those commonly used, arbitrarily taken by Division 1 as one in excess of 3,500 fps. (See Section 1.1.3.)

LC PLATE. "Low contraction plate," type of chromium plate. (See Section 20.2.2.)

MICROFLASH. A high-intensity light source of very short duration used for photographing moving objects, manufactured by the General Radio Company after a design developed by H. E. Edgerton.

NC. Nitrocellulose.

NG. Nitroglycerine.

NITAL. A solution of nitric acid in ethyl alcohol used to etch steel specimens prior to metallographic examination.

OBTURATION. Sealing of a gun bore against escape of the powder gases, either through the breech or past the projectile.

PARCO-LUBRIZING. A trade-marked process (Parker Rust Proof Company, Detroit, Michigan) for applying to steel a wear-resistant coating that consists chiefly of an admixture of iron and manganese phosphates. It was found advantageous to use it on pre-engraved projectiles.

PEBBLING. The roughness that appears on the bore surface of a gun that has been liquefied by the powder gases. (See Section 13.5.3.)

RDX. A code name for cyclonite, the active ingredient of some propellants.

RPM. Rounds per minute.

VELOCITY LIFE. The number of rounds that can be fired from a gun before its muzzle velocity decreases a predetermined amount because of erosion. A value of 200 fps was adopted for this velocity drop for the caliber .50 aircraft barrel during World War II. Cf. *accuracy life*. (See Section 23.1.4.)

BIBLIOGRAPHY

Numbers such as Div. 1-540-M1 indicate that the document listed has been microfilmed and that its title appears in the microfilm index printed in a separate volume. For access to the index volume and to the microfilm, consult the Army or Navy agency listed on the reverse of the half-title page.

Some abbreviations are used in identifying the source of reports. They include the following:

CIW	Carnegie Institution of Washington
NBS	National Bureau of Standards
MIT	Massachusetts Institute of Technology
BTL	Bell Telephone Laboratories, Inc.
BRL-APG	Ballistic Research Laboratory, Aberdeen Proving Ground
WA	Watertown Arsenal
OCO	Office of the Chief of Ordnance
AC	Advisory Council on Scientific and Technical Development
ADD	Armament Design Department
ARD	Armament Research Department
RD	Research Department

The number prefixed by the letter "A" following the OSRD number is the number assigned by the Technical Reports Section, NDRC (formerly in the office of Division A, NDRC) at the time the report was edited and prepared for duplication by that office. A number of these reports had not been duplicated by the time the office of Division A was closed. Manuscript copies were supplied for microfilming.

FORMAL REPORTS ISSUED BY DIVISION 1, NDRC

1. *Methods for Detecting Defects in the Base of a Shell Forging*, R. W. Goranson, OSRD 373, Report A-31, CIW, Feb. 6, 1942. Div. 1-540-M1
2. *A Brief History of Tapered Bore Guns*, J. S. Burlew, OSRD 515 Preliminary Report A-43, Geophysical Lab., CIW, Apr. 17, 1942. Div. 1-330-M1
3. *The Measurement of Large Transient Stresses*, R. W. Goranson, W. Garten, Jr., and J. A. Crocker, OSRD 498, Progress Report A-45, Geophysical Lab., CIW, Apr. 10, 1942. Div. 1-210.1-M1
4. *A Method of Investigating the Deformation of Deformable Projectiles*, H. L. Whittemore and L. R. Sweetman, OSRD 631, Memorandum A-36M, NBS, July 16, 1942. Div. 1-540-M2
5. *The Piezoelectric Projectile Accelerometer and a Bore-Friction Gage*, N. M. Smith, Jr., OSRD 808, Progress Report A-59, Geophysical Lab., CIW, Aug. 17, 1942. Div. 1-210.31-M1
6. *Simple Calculation of Thermochemical Properties for Use in Ballistics*, Addenda to NDRC Report A-101, J. O. Hirschfelder and J. H. Sherman, OSRD 1300, Memoranda A-67M to A-70M, Geophysical Lab., CIW March 1943. Div. 1-210.2-M4
7. *A Vertical Step-sweep Circuit for the Cathode-Ray Oscillograph*, N. M. Smith, Jr., OSRD 2081, Memorandum A-77M, Geophysical Lab., CIW, November 1943. Div. 1-620-M1
8. *The Preparation of Chromium by the Thermal Decomposition of Chromium Iodide*, D. R. Mosher, OSRD 2082, Memorandum A-78M, Westinghouse Electric and Manufacturing Co., Inc., November 1943. Div. 1-420.33-M1
9. *Thermodynamic Properties of British Flashless and Cordite MD Powders*, F. T. McClure, D. W. Osborne, and J. O. Hirschfelder, OSRD 817, Progress Report A-82, Geophysical Lab., CIW, Aug. 24, 1942. Div. 1-210.2-M1
10. *A Theorem on Radial Deformation in Thick Tubes*, K. F. Herzfeld, OSRD 3209, Memorandum A-83M, Catholic University of America, January 1944. Div. 1-320-M1
11. *A New Thread Collocating Gage*, F. E. Blake and D. F. Ringie, OSRD 3287, Memorandum A-85M, Jones & Lamson Machine Co., February 1944. Div. 1-620-M2
12. *Heat Conduction, Gas Flow, and Heat Transfer in Guns*, J. O. Hirschfelder, W. Garten, Jr., and O. Hougen, OSRD 863, Progress Report A-87, Geophysical Lab., CIW, Sept. 1, 1942. Div. 1-310-M1
13. *On Longitudinal Stresses in Guns*, K. F. Herzfeld, OSRD 3421, Memorandum A-87M, Catholic University of America, March 1944. Div. 1-320-M2
14. *Stability of Subcaliber Projectiles*, C. L. Critchfield, OSRD 870, Progress Report A-88, Geophysical Lab., CIW, Sept. 8, 1942. Div. 1-510-M1
15. *The Erosion of Guns, Part I*, J. S. Burlew, OSRD 882, Progress Report A-90, Geophysical Lab., CIW, Sept. 15, 1942. Div. 1-400-M2
16. *An Improved Approximation Formula for Stresses in Cylinders*, K. F. Herzfeld, OSRD 3465, Memorandum A-90M, Catholic University of America, April 1944. Div. 1-320-M3
17. *A Comparison of Ballistic Systems*, J. O. Hirschfelder, R. B. Kershner, C. F. Curtiss, J. Sherman, R. E. Johnson, N. L. Johnson, J. W. Wrench, Jr., E. Harmon, and M. G. Aldrich, OSRD 3556, Memorandum A-91M, Geophysical Lab., CIW, April 1944. Div. 1-210.1-M6
18. *Interaction of Carbon Monoxide and Iron*, J. C. W. Frazer and F. H. Horn, OSRD 873, Progress Report A-92, Johns Hopkins University, Sept. 12, 1942. Div. 1-410.1-M1

19. *Apparatus for Collecting Solid Particles Discharged from a Rifle. A Simple Optical Sighting Device*, J. L. England, OSRD 3753, Memoranda A-93M & A-94M, Geophysical Lab., CIW, May 1944. Div. 1-420.23-M2

20. *Notes on the Potentiometric Titration of Iron*, E. Jensen, OSRD 3869, Memorandum A-95M, Geophysical Lab., CIW, July 1944. Div. 1-650-M1

21. *The Erosion of Guns, Part II*. J. S. Burlew, OSRD 982, Progress Report A-91, Geophysical Lab., CIW, Nov. 4, 1942. Div. 1-400-M3

22. *Anodic Polishing for the Removal of Very Thin Layers from Steel Surfaces*, W. D. Urry and E. Jensen, OSRD 3968, Memorandum A-96M, Geophysical Lab., CIW, July 1944. Div. 1-650-M2

23. *Simple Calculation of Thermochemical Properties for Use in Ballistics*, J. O. Hirschfelder and J. Sherman, OSRD 935, Progress Report A-101, Geophysical Lab., CIW, Oct. 14, 1942. Div. 1-210.2-M2

24. [a]*Thermodynamic Properties of Propellant Gases*, J. O. Hirschfelder, F. T. McClure, C. F. Curtiss, and D. W. Osborne, OSRD 1087, Progress Report A-116, Geophysical Lab., CIW, Nov. 25, 1942. Div. 1-210.2-M3

25. *The Drag Coefficient for a Cone Moving with High Velocity*, W. Karush and C. L. Critchfield, OSRD 1104, Report No. A-126, Geophysical Lab., CIW, Dec. 21, 1942. Div. 1-220.1-M1

26. *Interior Ballistics [Part I]*, J. O. Hirschfelder, R. B. Kershner, and C. F. Curtiss, OSRD 1236, Report No. A-142, Geophysical Lab., CIW, February 1943. Div. 1-210.1-M2

27. *Metals Tested as Erosion Vent Plugs*, O. H. Loeffler, G. Phair, and H. S. Jcrabek, OSRD 1249, Report No. A-148, Geophysical Lab., CIW, Feb. 19, 1943. Div. 1-420.21-M1

28. *A Physico-Chemical Study of Gun Erosion*, E. Posnjak, OSRD 1311, Report No. A-161, Geophysical Lab., CIW, March 1943. Div. 1-410.1-M2

29. *Velocity and Pressure during Free Run-Up of a Projectile*, C. F. Curtiss, OSRD 1430, Report No. A-179, Geophysical Lab., CIW, April 1943. Div. 1-210.1-M3

30. *Interior Ballistics [Part II]*, J. O. Hirschfelder, R. B. Kershner, C. F. Curtiss and J. Sherman, OSRD 1435, Report No. A-180, Geophysical Lab., CIW, April 1943. Div. 1-210.1-M2

31. *A Study by Means of Electron and X-Ray Diffraction of the Alteration of Steel by Hot Powder Gases*, L. H. Germer, J. J. Lander, G. Tunell, and P. N. Metzelaar, OSRD 1659, Report No. A-199, Bell Telephone Laboratories, Inc., and Geophysical Lab., CIW, July 1943. Div. 1-410.1-M4

32. *The Temperature of the Bore Surface of Guns*, G. S. Fulcher (editor), OSRD 1666, Report No. A-201, Geophysical Lab., CIW, July 1943. Div. 1-310-M2

33. *Interior Ballistics [Part III]*, J. O. Hirschfelder, R. B. Kershner, and J. H. Sherman, OSRD 1677, Report No. A-204, Geophysical Lab., CIW, July 1943. Div. 1-210.1-M2

34. *Exact Theory of the Stress Distribution in a Shell Due to Engraving*, H. A. Jordan, K. F. Herzfeld, and V. O. McBrien, OSRD 1714, Report No. A-207, Catholic University of America, July 1943. Div. 1-520-M1

35. *Interior Ballistics [Part IV]*, C. F. Curtiss and R. E. Johnson, OSRD 1740, Report No. A-208, Geophysical Lab., CIW, August 1943. Div. 1-210.1-M2

36. *Interior Ballistics of Recoilless Guns*, J. O. Hirschfelder, R. B. Kershner, C. F. Curtiss, and R. E. Johnson, OSRD 1801, Report No. A-215, Geophysical Lab., CIW, September 1943. Div. 1-210.1-M4

37. *Interior Ballistics [Part V], The Performance of High-Velocity Guns*, J. O. Hirschfelder, R. B. Kershner, C. F. Curtiss, and R. E. Johnson, OSRD 1916, Report No. A-222, Geophysical Lab., CIW, October 1943. Div. 1-210.1-M5

38. *Metals Tested for Resistance to Cavitation Erosion*, G. E. Ziegler and L. E. Line, OSRD 1917, Report No. A-223, Armour Research Foundation, October 1943. Div. 1-420.23-M1

39. *Report on Firing of First Eleven Rounds in 3-In. Gun at David W. Taylor Model Basin during May, June, July 1943*, OSRD 2019, Report No. A-229, NBS and Geophysical Lab., CIW, November 1943. Div. 1-210.3-M1

40. *Carbon and Nitrogen in Gun Erosion*, J. F. Schairer and E. G. Zies, OSRD 2042, Report No. A-230, Geophysical Lab., CIW, November 1943. Div. 1-410.1-M5

41. *Development of Subcaliber Projectiles for the Hispano-Suiza Gun*, C. L. Critchfield and J. McG. Millar, OSRD 2067, Report No. A-233, Geophysical Lab., CIW, November 1943. Div. 1-510-M2

42. *Sabot-Projectiles for Cannon*, W. D. Crozier, H. F. Dunlap, C. E. Hablutzel, L. Lepaz, and D. T. MacRoberts, OSRD 3010, Report No. A-234, University of New Mexico, December 1943. Div. 1-510.1-M1

43. *A Method of Obtaining the State and Composition of the Powder Gas at Shot Ejection with Tables for Pyro Powder*, R. E. Johnson, OSRD 3239, Report No. A-248, Geophysical Lab., CIW, February 1944. Div. 1-210.2-M5

44. *An Experimental Study of Powder Gas Radiation and Temperature*, F. C. Kracek and W. S. Benedict, OSRD 3291, Report No. A-252, Geophysical Lab., CIW, February 1944. Div. 1-210.2-M6

45. *On the Heating of Rotating Bands*, C. L. Critchfield, OSRD 3329, Report No. A-256, Geophysical Lab., CIW, February 1944. Div. 1-530-M1

46. *Measurement of Various Ballistic Quantities on a Projectile Moving in the Bore of a Gun*, N. M. Smith, Jr., and J. A. Crocker, OSRD 3376, Report No. A-259, Geophysical Lab., CIW, March 1944. Div. 1-210.3-M2

47. *The Pressure on a Cone Moving with Small Yaw at High Velocity*, W. Karush and C. L. Critchfield, OSRD 3397

[a]A previous edition of this report had been designated as Report A-48 (OSRD 547).

Report No. A-260, Geophysical Lab., CIW, March 1944. Div. 1-220.1-M2

48. *Thermal Effects of Propellent Gases in Erosion Vents and in Guns*, L. W. Nordheim, H. Soodak, and G. Nordheim, OSRD 3447, Report No. A-262, Duke University, May 1944. Div. 1-310-M3

49. *Investigation of Gun Erosion at the Geophysical Laboratory, Vol. 1, July 1941 to July 1943*, OSRD 3448, Report No. A-263, Geophysical Lab., CIW, March 1944. Div. 1-400-M1

50. *Investigation of Gun Erosion at the Geophysical Laboratory, Vol. II, July 1943 to December 1943*, OSRD 3449, Report No. A-264, Geophysical Lab., CIW, April 1944. Div. 1-400-M1

51. *A Method for Testing Resistance of Metals to Surface Cracking under Conditions Similar to Those Obtaining in Guns*, E. Ingerson, OSRD 3628, Report No. A-271, Geophysical Lab., CIW, May 1944. Div. 1-410.3-M1

52. *Preliminary Report on Molybdenum as a Material for an Erosion-Resistant Gun Liner*, P. H. Brace and J. W. Marden, OSRD 3700, Report No. A-273, Westinghouse Electric and Manufacturing Co., Inc., May 1944. Div. 1-420.32-M1

53. *The Effect of Sulfur and Other Components of Black Powder on the Erosion of Gun Steel*, W. D. Urry and E. Ingerson, OSRD 3811, Report No. A-276, Geophysical Lab., CIW, June 1944. Div. 1-410.1-M6

54. *Molding Sabots for Projectiles*, OSRD 3832, Report No. A-278, Arthur D. Little, Inc., June 1944. Div. 1-510.1-M2

55. *Interior Ballistics [Part VI], Pressure Travel Curves, with an Addendum to Interior Ballistics, I.*, R. E. Johnson, C. F. Curtiss, and R. B. Kershner, OSRD 3855 Report No. A-279, Geophysical Lab., CIW, June 1944. Div. 1-210.1-M7

56. *Deduction of Practical Formulas for the Stress in the Mantle of a Shell Due to Band Pressure and Powder-Gas Pressure*, K. F. Herzfeld and V. Griffing, OSRD 3868, Report No. A-281, Catholic University of America, June 1944. Div. 1-530-M2

57. *Trajectory Determination by Tracer Photography*, W. D. Crozier, OSRD 3890, Report No. A-283, University of New Mexico July 1944. Div. 1-220.2-M1

58. *Formulae for Strains in a Thick-Walled Tube near the Projectile*, C. Snow, OSRD 4320, Report No. A-298, NBS, November 1944. Div. 1-320-M4

59. *Investigation of Gun Erosion at the Geophysical Laboratory, Vol. III, January 1944 to July 1944*, OSRD 4345, Report No. A-300, Geophysical Lab., CIW, November 1944. Div. 1-400-M1

60. *Chemical Thermodynamics of Gun Erosion*, C. F. Curtiss and N. L. Johnson, OSRD 4363, Report No. A-301, Geophysical Lab., CIW, November 1944. Div. 1-410.1-M8

61. *The State of Equilibrium among the Carbon Atoms of a Propellant Gas*, W. D. Urry and P. J. Hannan, OSRD 4461, Report No. A-303, Geophysical Lab., CIW, December 1944. Div. 1-210.2-M7

62. *Vent Plug Erosion by the CO-CO_2 Gas System*, J. C. W. Frazer, F. H. Horn, and R. C. Evans, OSRD 6327, Report No. A-310, Johns Hopkins University, Oct. 31, 1944. Div. 1-420.21-M2

63. *Iron-Carbonyl Formation as a Mechanism Contributing to Gun Erosion*, J. C. W. Frazer, F. H. Horn, and R. C. Evans, OSRD 6328, Final Report No. A-311, Johns Hopkins University, Oct. 31, 1944. Div. 1-410.1-M7

64. *Static Band Pressures in 37-MM Projectiles [Part I]*, F. A. Biberstein, Jr., R. Brown, V. Griffing, K. F. Herzfeld, J. M. Krafft, and W. T. Whelan, OSRD 4550, Report No. A-312, Catholic University of America, January 1945. Div. 1-530-M3

65. *Second Report on Firings in 3-In. Gun at David W. Taylor Model Basin, October 1943 to May 1944*, OSRD 4986, Report No. A-323, NBS and Geophysical Lab., CIW, Mar. 25, 1945. Div. 1-210.3-M3

66. *Interior Ballistics [Part VII], Numerical Methods of Solution of the Ordinary Problems of Interior Ballistics*, R. E. Johnson, N. L. Johnson, and J. W. Wrench, Jr., OSRD 6231, Report No. A-348, Geophysical Lab., CIW, Oct. 1, 1945. Div. 1-210.1-M9

67. *The Erosion of Guns at the Muzzle*, L. E. Line, Jr., OSRD 6322, Report No. A-357, Aug. 23, 1945. Div. 1-430-M2

68. *The Aerodynamics of a Slightly Yawing Supersonic Cone*, A. H. Stone, OSRD 6306, Report No. A-358, Geophysical Lab., CIW, July 10, 1945. Div. 1-220.1-M3

69. *Interior Ballistics, A Consolidation and Revision of Previous Reports, Interior Ballistics [Parts I to VII, Inclusive]*, C. F. Curtiss and J. W. Wrench, Jr., OSRD 6468, Report No. A-397, Geophysical Lab., CIW, July 15, 1945. Div. 1-210.1-M8

70. *The Penetration of Nitrogen into Steel Rifle Barrels as Measured by a Tracer Method*, G. L. Davis, OSRD 6469, Report No. A-398, Geophysical Lab., CIW, Nov. 30, 1945. Div. 1-410.1-M10

71. *Measurement of Heat Input to the Bore Surface of Caliber .50 Gun Barrels*, E. L. Armi, J. L. Johnson, R. C. Machler, and N. E. Polster, OSRD 6470, Report No. A-399, Leeds & Northrup Co., July 23, 1945. Div. 1-310-M4

72. *Measurement of Frictional Heat Input in Gun Barrels and of Frictional Bullet-Bore Interface Temperatures*, E. L. Armi, J. L. Johnson, R. C. Machler, and N. E. Polster, OSRD 6471, Report No. A-400, Leeds & Northrup Co., Sept. 27, 1945. Div. 1-310-M5

73. *The Synthesis of Chromium Hexacarbonyl*, B. B. Owen, OSRD 6472, Report No. A-401, Yale University, Sept. 17, 1945. Div. 1-630-M1

74. *Pyrolytic Plating of Chromium from the Vapor of Chromium Hexacarbonyl*, B. B. Owen, OSRD 6473, Report No. A-402, Yale University, Oct. 8, 1945. Div. 1-630-M1

75. *The Results of Erosion Vent-Plug Tests Particularly under Conditions of Decreased Severity and Their Application to the Erosion of Guns*, H. S. Jerabek, G. Phair, D. Enagonio, and C. A. MacQuaid, OSRD 6474, Report No. A-403, Geophysical Lab., CIW, Dec. 5, 1945. Div. 1-420.21-M3

76. *The Behavior of Gun Liners and Coatings Tested under Conditions of Hypervelocity*, N. H. Smith, OSRD 6475, Report No. A-404, Franklin Institute, Oct. 2, 1945. Div. 1-340-M1

77. *Metallographic Examination of Gun Liners and Coatings Tested under Conditions of Hypervelocity*, J. N. Hobstetter, OSRD 6476, Report No. A-405, Harvard University, Oct. 30, 1945. Div. 1-340-M2

78. *Erosion Tests of Materials in the Form of Short Liners in a Caliber .30 Machine-Gun Barrel*, J. Wulff, OSRD 6477, Report No. A-406, Johnson Automatics, Inc., Apr. 12, 1944. Div. 1-420.3-M1

79. *Search for Erosion-Resistant Materials for Guns by Firing Particles of Metal and Alloys into Vacuum to Determine Their Structural and Chemical Behavior*, E. Posjnak, OSRD 6478, Report No. A-407, Geophysical Lab., CIW, Dec. 4, 1945. Div. 1-420.23-M3

80. *Gun-Barrel Liners—Materials, Insertion, and Testing*, F. D. Cotterman, N. A. Ziegler, and J. P. Magos, OSRD 6479, Report No. A-408, Crane Company, Jan. 16, 1946. Div. 1-420.3-M2

81. *The Testing of Erosion-Resistant Materials and the Development of Improved Machine-Gun Barrels*, E. F. Osborn, OSRD 6480, Report No. A-409, Geophysical Lab., CIW, Nov. 29, 1945. Div. 1-420.2-M1

82. *Progressive Centrifugal Inmelting for the Preparation of Alloy Tubes*, P. H. Brace, OSRD 6481, Report No. A-410, Westinghouse Electric and Manufacturing Co., Inc., Apr. 8, 1946. Div. 1-640-M1

83. *Chromium and Chromium-Base Alloys as Materials for Gun Liners*, P. H. Brace, J. F. Schairer, and N. A. Ziegler, OSRD 6482, Report No. A-411, Westinghouse Electric and Manufacturing Co., Inc., Jan. 5, 1946. Div. 1-420.33-M2

84. *Experimental Electroplating of Gun Barrels*, W. Blum, A. Brenner, and V. A. Lamb, OSRD 6483, Report No. A-412, NBS, Dec. 21, 1945. Div. 1-420.4-M3

85. *An Illustrated Study of the Effects of Firing on Chromium-Plated Bores of Caliber .50 Machine Guns*, H. E. Merwin and M. Sullivan, OSRD 6484, Report No. A-413, Geophysical Lab., CIW, December 1945. Div. 1-420.4-M2

86. *Symposium on Chromium-Plating, Washington, D. C., May 14, 1943*, Division One, NDRC, OSRD 6485, Report No. A-414. Div. 1-420.4-M1

87. *Development of Chromium-Base Hot-Hard Alloys as Gun Liner Materials*, R. M. Parke and F. P. Bens, OSRD 6486, Report No. A-415, Climax Molybdenum Co., Jan. 21, 1946. Div. 1-420.33-M3

88. *Stellite No. 21 as a Material for Gun Liners—Metallurgy and Properties*, W. A. Wissler, OSRD 6487, Report No. A-416, Union Carbide & Carbon Research Laboratories, Inc., Jan. 17, 1946. Div. 1-420.31-M7

89. *Studies of the Application of Stellite No. 21 to Gun Bores*, T. H. Gray and D. R. Mosher, OSRD 6488, Report No. A-417, Westinghouse Electric and Manufacturing Co., Inc., Nov. 12, 1945. Div. 1-420.31-M5

90. *Investigation of Certain Methods for Making Gun Linings of Stellite and Other Erosion-Resistant Materials*, J. Wulff, OSRD 6489, Report No. A-418, MIT, Sept. 28, 1945. Div. 1-420.31-M1

91. *Preparation and Testing of 37-mm Stellite Liners*, J. S. Burlew, OSRD 6490, Report No. A-419, CIW. Div. 1-420.31-M8

92. *Refractaloy 70 as a Liner Material for Caliber .50 Barrels*, T. H. Gray, OSRD 6491, Report No. A-420, Westinghouse Electric and Manufacturing Co. Inc., Jan. 10, 1946. Div. 1-420.35-M1

93. *Pyrolytic Plating from the Carbonyls of Molybdenum, Tungsten, and Chromium*, L. H. Germer and J. J. Lander, OSRD 6492, Report No. A-421, BTL, Nov. 30, 1945. Div. 1-630-M2

94. *The Semicommercial Preparation of Molybdenum Carbonyl*, A. L. McCoy, OSRD 6493, Report No. A-422, Climax Molybdenum Co., July 20, 1945. Div. 1-420.32-M2

95. *Fabrication of Molybdenum for Use as a Gun-Liner Material*, J. W. Marden, OSRD 6494, Final Report No. A-423, Westinghouse Electric and Manufacturing Co., Inc., Oct. 31, 1945. Div. 1-420.32-M3

96. *Development of Molybdenum for Gun Liners*, P. H. Brace, OSRD 6495, Report No. A-424, Westinghouse Electric and Manufacturing Co., Inc., Feb. 1, 1946. Div. 1-420.32-M4

97. *Experiments on the Melting of Molybdenum*, F. Palmer, OSRD 6496, Report No. A-425, Climax Molybdenum Co., and Westinghouse Electric and Manufacturing Co., Inc., February 1946. Div. 1-420.32-M5

98. *Studies of Erosion Products of Gun-Bore Surfaces*, E. G. Zies and C. A. Marsh, OSRD 6497, Report No. A-426, Geophysical Lab., CIW, Mar. 9, 1945. Div. 1-410.1-M13

99. *The Penetration of Carbon into Gun-Bore Surfaces*, W. D. Urry, E. Jensen, and P. J. Hannan, OSRD 6498, Report No. A-427, Geophysical Lab., CIW, Nov. 20, 1945. Div. 1-410.1-M9

100. *Work on Sabot-Projectiles by the University of New Mexico under Contract OEMsr-668 and Supplements, 1942-1944*, J. W. Greig, OSRD 6499, Report No. A-428, University of New Mexico, October 1946. Div. 1-510.1-M5

101. *Study of Erosion by Adiabatically Compressed Gases*, W. Garten, Jr., and Gordon L. Davis, OSRD 6500, Report No. A-429, Geophysical Lab., CIW, Dec. 21, 1945. Div. 1-410.1-M12

102. *Statistical Study of Muzzle Erosion Data at the Naval Proving Ground*, G. Cresson, E. Frankel, and G. Kovsky, OSRD 6501, Report No. A-430, Geophysical Lab., CIW, June 21, 1945. Div. 1-430-M1

103. *An Experiment to Determine the Effects of Stress on Gun Erosion*, R. W. Goranson and W. Garten, Jr., OSRD 6502, Report No. A-431, Geophysical Lab., CIW, Nov. 26, 1945. Div. 1-410.3-M2

104. *Transient Thermal Action on Gun Steel Induced by Electron Bombardment*, W. Garten Jr. and Gordon L. Davis, OSRD 6503, Report No. A-432, Geophysical Lab., CIW, Feb. 15, 1946. Div. 1-410.2-M3

105. *A Method for the Determination of the Melting Temperatures of Gun Erosion Products*, E. Jensen, OSRD 6504, Report No. A-433, Geophysical Lab., CIW, Jan. 11, 1946. Div. 1-410.2-M2

106. *Temperature Distribution in Gun Barrels*, G. Comenetz and V. Schwab, OSRD 6505, Report No. A-434, Geophysical Lab., CIW, March 1946. Div. 1-310-M6

107. *The Quenching of Powder Gas Reactions*, F. C. Kracek and P. J. Hannan, OSRD 6506, Report No. A-435, Geophysical Lab., CIW, Mar. 9, 1946. Div. 1-210.2-M8

108. *Microwave Techniques for Interior Ballistic Measurements*, H. S. Roberts, OSRD 6507, Report No. A-436, Geophysical Lab., CIW, December 1945. Div. 1-210.31-M2

109. *Investigation of Gun Erosion at the Geophysical Laboratory, Volume IV—July to December 1944*, P. R. Heyl, OSRD 6508, Report No. A-437, Geophysical Lab., CIW, February 1946. Div. 1-400-M1

110. *Investigation of Gun Erosion at the Geophysical Laboratory, Volume V—January to September 1945*, P. R. Heyl, OSRD 6509, Report No. A-438, Geophysical Lab., CIW, April 1946. Div. 1-400-M1

111. *The Second Approximation for a Yawing Supersonic Cone*, A. H. Stone, OSRD 6510, Report No. A-439, Geophysical Lab., CIW, Nov. 26, 1945. Div. 1-220.1-M4

112. *Illustrations and Descriptions of Surface Features of Eroded Gun Bores*, H. E. Merwin and M. Sullivan, OSRD 6511, Report No. A-440, Geophysical Lab., CIW, January 1946. Div. 1-400-M4

113. *Comparisons of Interior Ballistic Theory and Experiment—3-In. and 37-MM Guns Fired at David W. Taylor Model Basin*, W. S. Benedict, OSRD 6512, Report No. A-441, Geophysical Lab., CIW, March 1946. Div. 1-210.3-M6

114. *Static Band Pressure in 37-mm Projectiles [Part II]*, F. A. Biberstein, Jr., R. Brown, V. Griffing, K. F. Herzfeld, J. M. Krafft, and W. T. Whelan, OSRD 6513, Report No. A-442, Catholic University of America, Aug. 28, 1945. Div. 1-530-M3

115. *Static Band Pressures in 37-mm Projectiles [Part III]*, F. A. Biberstein, Jr., R. Brown, V. Griffing, K. F. Herzfeld, J. M. Krafft, and W. T. Whelan, OSRD 6514, Report No. A-443, Catholic University of America, December 1945. Div. 1-530-M3

116. *Interior Ballistics of the 3-In. Gun Fired at David W. Taylor Model Basin with a Critical Examination of Certain Assumptions of the Hirschfelder System of Interior Ballistics*, R. E. Johnson, J. W. Wrench, Jr., O. Kracek, and K. F. Herzfeld, OSRD 6515, Report No. A-444, Catholic University of America, Nov. 10, 1945. Div. 1-210.1-M10

117. *Stresses in Shells Due to Band Pressure*, K. F. Herzfeld, OSRD 6516, Final Report No. A-445, Catholic University of America, Dec. 28, 1945. Div. 1-530-M4

118. *Design and Construction of Tubes for a Hyper-Velocity 90-mm Gun*, J. H. Billings, OSRD 6539, Report No. A-446, Drexel Institute of Technology, February 1946. Div. 1-340-M3

119. *Pilot Plant for Production of Modified Caliber .50 Machine Gun Barrels with Stellite Liners*, R. A. Mueller, F. D. Cotterman, and J. P. Magos, OSRD 6518, Report No. A-447, Crane Co., Oct. 17, 1945. Div. 1-420.31-M4

120. *Pre-Engraved Projectiles*, N. H. Smith, OSRD 6519, Report No. A-448, The Franklin Institute, Dec. 6, 1945. Div. 1-520-M2

121. *Fisa Protectors—Design, Production, and Tests*, N. H. Smith, OSRD 6520, Report No. A-449, The Franklin Institute, Nov. 20, 1945. Div. 1-420.5-M1

122. *The Caliber .50 Erosion Testing Gun*, N. H. Smith, OSRD 6521, Report No. A-450, The Franklin Institute, Jan. 7, 1946. Div. 1-420.22-M1

123. *Comparison of the Erosiveness of Propellant Powders*, N. H. Smith, OSRD 6522, Report No. A-451, The Franklin Institute, Oct. 12, 1945. Div. 1-420.1-M1

124. *Application of Heat Transfer Theory to Metallographic Evidences of Gun Erosion*, J. N. Hobstetter, OSRD 6523, Report No. A-452, Harvard University, Dec. 20, 1945. Div. 1-410.2-M1

125. *Production of Stellite Liners by Centrifugal Casting*, W. H. Shallenberger, OSRD 6524, Report No. A-453, Industrial Research Laboratories, Inc., December 1945. Div. 1-420.31-M6

126. *Development of 20-mm Automatic Aircraft Cannon*, W. H. Shallenberger, OSRD 6525, Report No. A-454, Johnson Automatics, Inc., and University of California, Dec. 18, 1945. Div. 1-610-M1

127. *Production of Modified Caliber .30 Machine-Gun Barrels with Stellite Liners*, M. M. Johnson, Jr., OSRD 6526, Final Report No. A-455, Johnson Automatics, Inc., Sept. 28, 1945. Div. 1-420.31-M2

128. *57/40-mm Tapered-Bore Gun Tubes and Deformable Projectiles*, OSRD 6527, Report No. A-456, Jones & Lamson Machine Co., and Bryant Chucking Co., Oct. 24, 1945. Div. 1-330-M2

129. *Contributions to the Development of Erosion-Resistant Materials for Gun Liners and Linings*, P. H. Brace, OSRD 6528, Report No. A-457, Westinghouse Electric and Manufacturing Co., Inc., June 24, 1946. Div. 1-420.3-M3

130. *Studies of Worn Muzzle Sections of Guns by Laboratory Techniques*, L. E. Line, Jr., J. N. Hobstetter, and Members of the Staff of the Geophysical Laboratory, CIW, OSRD 6529, Report No. A-458, Harvard University and Geophysical Lab., CIW, Jan. 28, 1946. Div. 1-430-M3

131. *Report on Firings of 37-mm, Gun T47, at David W. Taylor Model Basin,* OSRD 6530, Report No. A-459, NBS and Geophysical Lab., CIW, Oct. 22, 1945. Div. 1-210.3-M4

132. *Third Report on Ballistic Firings with 3-In. Gun at David W. Taylor Model Basin,* OSRD 6531, Report No. A-460, NBS and Geophysical Lab., CIW, Mar. 25, 1946. Div. 1-210.3-M5

133. *Development of an All-Metal Type of Sabot-Projectile,* OSRD 6532, Report No. A-461, Remington Arms Co., Oct. 12, 1945. Div. 1-510.1-M3

134. *A Production Process for the Manufacture of an All-Metal Type of Sabot-Projectile,* OSRD 6533, Report No. A-462, Remington Arms Co., Oct. 12, 1945. Div. 1-510.1-M4

135. *Production of Modified Machine-Gun Barrels with Stellite Liners Including Studies of Draw Rifling,* OSRD 6534, Report No. A-463, Remington Arms Co., Oct. 3, 1945. Div. 1-420.31-M3

136. *Hastelloy C as a Liner Material for Machine-Gun Barrels,* F. S. Badger and W. A. Wissler, OSRD 6535, Report No. A-464, Union Carbide and Carbon Research Laboratories, Inc., May 16, 1946. Div. 1-420.34-M1

137 *Electron and X-Ray Diffraction Studies of Gun Erosion Products,* F. E. Haworth, OSRD 6536, Report No. A-465, BTL, Dec. 6, 1945. Div. 1-410.1-M11

138. *Chemical Thermodynamics of Gun Erosion,* J. J. Lander, OSRD 6537, Report No. A-466, BTL, Apr. 14, 1943. Div. 1-410.1-M3

139. *Investigation of the Control of Erosion in Guns and the Improvement of Gun Performance,* P. R. Heyl, OSRD 6538, Report No. A-467, Geophysical Lab., CIW, June 1946, Revised July 31, 1946. Div. 1-400-M5

140. *Ballistic Research, Project Summaries for Division 1, as of October 1, 1945,* Report No. A-383, Oct. 8, 1945. Div. 1-100-M1

141. *Determination of the Linear Burning Rates of Propellants from Pressure Measurements in the Closed Chamber,* L. G. Bonner, OSRD 4382, Duke University (for Divisions 1 and 3, NDRC), Nov. 30, 1944.

142. *Pilot Plant for Hard Chromium Plating Caliber .50 Machine Gun Barrels,* Arnold Weisselberg, Chrome Gage Corporation, OSRD 6517, Nov. 16, 1945.

OTHER REPORTS ISSUED BY OSRD[b]

143. *Report of the Ad Hoc Committee on Internal Ballistics of the National Defense Research Committee,* Sept. 29, 1942.

144. *Cranz's Textbook of Ballistics: Vol. II, Interior Ballistics and Vol. III, Experimental Ballistics,* translated by C. C. Bramble and Henry Bluestone, translation revised and edited by J. D. Elder and Duane Roller, Technical Reports Section, NDRC, May 6, 1944 and Apr. 9, 1945. (See Item 505.) Div. 3-220-M3

145. *The Effect of Hyper-Velocity on the Probability of Hitting Tanks,* E. J. Moulton, W. Weaver, OEMsr-1007 Report No. 26.1, Applied Mathematics Panel, July 1, 1943. Div. AMP-901.1-M1

146. *Comment on the Memorandum "Aircraft Machine Guns, the Evaluation of Hyper-Velocity Types of, for Naval Aircraft, Dated March 18, 1943, and Prepared by the Special Board of Naval Ordnance,"* Memorandum No. 53.1, Applied Mathematics Panel, NDRC, July 12, 1943. (See Item 325 for Navy Memorandum.) Div. AMP-504.1-M10

147. *The Shell Design Problem,* AMP Report No. 75.1, OEMsr-1007, Applied Mathematics Panel, February 1944. Div. AMP-903.1-M3

148. *A Report of the Kinematic and Dynamic Analysis of the Johnson 20-mm Automatic Cannon, Model I,* L. M. K. Boelter, R. C. Martinelli, F. E. Romie, F. M. Hamaker, and N. W. Snyder, University of California (for OSRD Engineering Office), January 1945.

149. *Stress Analysis of Breech Mechanism of the Johnson 20-mm Automatic Cannon, Model III,* L. M. K. Boelter, F. M. Hamaker, and F. E. Romie, University of California (for OSRD Engineering Office), Jan. 1, 1945.

150. *Firing Rate Analysis of the Johnson 20-mm Automatic Cannon, Model III,* L. M. K. Boelter, F. M. Hamaker, N. W. Snyder, and F. E. Romie, University of California (for OSRD Engineering Office), Jan. 1, 1945.

151. *Analysis of Thermal and Pressure Stresses in Caliber .50 Light Aircraft Machine Gun Barrel,* L. M. K. Boelter, N. W. Snyder, R. Bromberg, and L. M. Grossman, (Report to OSRD), University of California, January 1945.

152. *Terminal Ballistic Performance of Non-deforming Projectiles with Special Reference to High Velocities,* C. W. Curtis, Princeton Technical Memorandum No. 11, Division 2, NDRC, Mar. 18, 1944.

153. *High Velocity Performance of Tungsten Carbide Projectiles,* Princeton Technical Memorandum No. 17, Division 2, NDRC, Mar. 18, 1944.

154. *Plating Trials of 57/40-mm Deformable Projectile,* C. W. Curtis and R. J. Emrich, Princeton Technical Memorandum No. 81, Division 2, NDRC, November 1944.

155. *Transverse Rupture Strength Measurement of Tungsten Carbide Cores for 57/40 mm Deformable Projectile,* R. J. Emrich, Princeton Technical Memorandum No. 95, Division 2, NDRC, Jan. 9, 1945.

156. *Terminal Ballistics of Tungsten Carbide Projectiles: Survey and Nose-Shape Tests,* C. W. Curtis, R. J. Emrich, and J. R. Sproule, OSRD 4720b, Report No. OTB-7b, Feb. 15, 1945.

157. *Terminal Ballistics of Tungsten Carbide Projectiles: Effect of Carrier, Part I,* E. R. Jones, C. W. Curtis, and R. J. Emrich, OSRD 5350a, Report No. OTB-12a, July 15, 1945.

[b]Items 539 and 547 in *Additional References* of this Bibliography pertain to this section.

158. *Perforation Limits for Nonshattering Projectile Against Thick Homogeneous Armor at Normal Incidence*, C. W. Curtis and R. L. Kramer, OSRD 6464, Report No. A-393, December 1945.

159. *Effect of Pressure and Temperature on the Rate of Burning of Double-Base Powders of Different Compositions*, W. H. Avery and R. E. Hunt, OSRD-1993, NDRC Report No. A-225, Jet Propulsion Research Laboratory, Indian Head, Md., October 1943.

160. *The Mechanism of Powder Burning*, Farrington Daniels and collaborators, OSRD-3206, NDRC Report A-243. University of Wisconsin, January 1944.

161. *Observations on the Burning of Double-Base Powders*, B. L. Crawford, Jr., C. Huggett, and J. J. McBrady, OSRD-3544, NDRC Report A-268, University of Minnesota, April 1944.

162. *Minutes of the Third Meeting of the Sub-Group on Burning Rates and Related Problems Held at the Ballistic Research Laboratory, Aberdeen Proving Ground, Aberdeen, Maryland, April 28–29, 1944*, OSRD 3711, Rocket Propellant Panel of the Joint Committee on New Weapons and Equipment.

163. *Rocket Fundamentals*, OSRD-3992, Report No. ABL-SR4, Section H, Division 3, NDRC, George Washington University, Dec. 26, 1944.

164. *The Way Muzzle Velocity Affects the Probability of Hitting Aircraft by A-A Fire*, Section D-2, NDRC (Memorandum), Apr. 1, 1942.

165. *Measurements of Fluid Friction Loss in 0.50 Caliber Rifled and Unrifled Gun Barrels*, Robert T. Knapp, OSRD 2001, California Institute of Technology, July 16, 1943.

166. *Firing Strains in a 37-MM Field Gun*, A. V. deForest, Contract OEMsr-155 (Extra Progress Report), Massachusetts Institute of Technology, Feb. 16, 1942.

167. *Heat-Resisting Metals for Gas Turbine Parts (N-102): Chromium-Base Alloys*, R. M. Parke, OSRD 5044, Progress Report M-510, Climax Molybdenum Co., May 7, 1945. Div. 18-502.11-M1

168. *Heat-Resisting Metals for Gas Turbine Parts (N-102): Chromium-Base Alloys*, R. M. Parke and A. J. Herzig, OSRD 6547, Final Report M-656, Climax Molybdenum Co., Jan. 21, 1946. Div. 18-502.11-M2

169. *Final Report on Heat-Resisting Metals for Gas Turbine Parts (N-102)*, H. C. Cross and W. F. Simmons, OSRD 6563, Final Report M-636, Battelle Memorial Institute, American Brake Shoe and Foundry Co., and others, Jan. 21, 1946. Div. 18-502.1-M11

170. *Prevention of Cracking in Gun Tubes*, R. F. Mehl, Cyril Wells, Irwin Broverman, J. W. Spretnak, C. F. Sawyer, and C. C. Busby, OSRD 5383, Final Report M-555, Carnegie Institute of Technology, July 30, 1945. Div. 18-302.5-M3

171. *Industrial Applications of Chromium Plating: A Review*, M. Kolodney, OSRD 1074, Advisory Report M-26, National Academy of Sciences, Nov. 27, 1942. Div. 18-900-M1

REPORTS ISSUED BY ABERDEEN PROVING GROUND[c]

172. *Form Factors of Projectiles*, H. P. Hitchcock, BRL-APG, June 24, 1942. (Revised later by addition of new tables.)

173. *The Equation of State of the Powder Gas*, J. P. Vinti, Report No. 288, BRL-APG, July 8, 1942

174. *The Effect of Cross Wind on the Yaw of Projectiles*, R. H. Kent and H. P. Hitchcock, Report A-IV-31, BRL-APG, Feb. 24, 1928.

175. *The Rate of Erosion of the Browning Caliber .30 Tank Type Machine Gun as Dependent on the Temperature of the Gun and Other Factors*, N. A. Tolch, Report No. 13, BRL-APG, July 8, 1935.

176. *Resistance Functions of Various Types of Projectiles*, H. P. Hitchcock, Report No. 27, BRL-APG, June 1935.

177. *Stability Factors of Projectiles*, H. P. Hitchcock, Report No. 30, BRL-APG (revised) Sept. 30, 1940.

178. *Heating Effects and Endurance Properties of the 105-mm A.A. Gun, M1, as Determined by Rapid Fire Tests*, N. A. Tolch, Report No. 35, BRL-APG, Feb. 12, 1936.

179. *Heating Effects and Endurance Properties of the 3-In. A. A. Gun, M3, as Determined by Rapid Fire Tests*, N. A. Tolch, Report No. 39, BRL-APG, Mar. 2, 1936.

180. *Roggla's Equation and its Application to Interior Ballistic Problems*, R. H. Kent, Report No. 48, BRL-APG, (revised) July 3, 1941.

181. *Study of the Heating and Cooling of the Bore of the 75-mm Gun, M1897 E3*, W. D. Dickinson, Report No. 49, BRL-APG, Apr. 22, 1936.

182. *Heating Effects and Distribution of the Energy of the Charge of the Caliber .50, M2 Machine Gun, Heavy Barrel*, N. A. Tolch, Report No. 61, BRL-APG, Oct. 1, 1936.

183. *Heating Effects and Distribution of the Energy of the Charge of the Caliber .50 Machine Gun, M2, Water-Cooled Type*, N. A. Tolch, Report No. 74, BRL-APG, Apr. 5, 1937.

184. *An Elementary Treatment of the Motion of a Spinning Projectile about its Center of Gravity*, R. H. Kent, Report No. 85, BRL-APG, Aug. 16, 1937. (See Report No. 459 for revision.)

185. *Development of Chrome Plating of Guns*, T. K. Vincent, Report No. 87, BRL-APG, Nov. 3, 1937.

186. *Heating of Guns*, J. R. Lane, Report No. 104, BRL-APG, May 20, 1938.

187. *The Cooling of Guns*, J. R. Lane, Report No. 146, BRL-APG, Apr. 26, 1939.

188. *A Study of Form Factors of Spinning Projectiles*, H. P. Hitchcock, Report No. 166, BRL-APG, Dec. 8, 1939.

[c]The following items in *Additional References* of this Bibliography pertain to this section: 540, 543, 548, 549, 550, 551, 552, 554, 555, 558, 560, 561, and 562.

189. *Drag on Conical Heads*, H. P. Hitchcock, Report No. 240, BRL-APG, July 14, 1941.

190. *The Performance of Sub-caliber Projectiles Compared with that of Conventional Types*, R. H. Kent, Report No. 265, BRL-APG, Jan. 9, 1942.

191. *Cooling Corrections for Closed Chamber Firings*, R. H. Kent and J. P. Vinti, Report No. 281, BRL-APG, Sept. 7, 1942.

192. *The Motion of the Axis of a Spinning Shell Inside the Bore of the Gun*, F. V. Reno, Report No. 320, BRL-APG, Feb. 27, 1943. (See Item 201 for a treatment of this subject based on a different assumption.)

193. *The Effect of Yaw Upon Aircraft Gunfire Trajectories*, T. C. Sterne, Report No. 345, BRL-APG, June 11, 1943.

194. *Report on the Temperature Dependence of Rocket Behavior*, J. H. Frazer, J. H. Wiegand, J. E. Mayer, J. W. Perry, C. Fennimore, and H. D. Burnham, Report No. 353, BRL-APG, May 1, 1943.

195. *Firing Strain Measurements on 76-mm Gun, M1E2*, V. H. McNeilly, Report No. 362, BRL-APG, June 1, 1943.

196. *Simplified Equations of Interior Ballistics*, J. E. Mayer, Report No. 388, BRL-APG, Aug. 4, 1943.

197. *On the Motion of a Projectile with Small or Slowly Changing Yaw*, J. L. Kelley and E. J. McShane, Report No. 446, BRL-APG, Jan. 29, 1944.

198. *Evidence of a Stepwise Mechanism of Powder Burning from Closed Chamber Firings*, H. D. Burnham, Report No. 456, BRL-APG, Mar. 28, 1944.

199. *An Elementary Treatment of the Motion of a Spinning Projectile about its Center of Gravity*, R. H. Kent and E. J. McShane, Report No. 459, BRL-APG, Apr. 11, 1944. (A revision of Report No. 85.)

200. *Erosion in Vent Plugs*, J. H. Wiegand, Report No. 520, BRL-APG, Jan. 25, 1945. (See Report No. 578 for continuation.)

201. *The Motion of the Axis of a Spinning Shell Inside the Bore of the Gun*, L. H. Thomas, Report No. 544, BRL-APG, May 8, 1945. (See Item 192 for a treatment of this subject based on a different assumption.)

202. *A Method for Computation of the Pressure on the Head of a Pointed High-Speed Projectile*, I. E. Segal, Report No. 571, BRL-APG, Aug. 31, 1945.

203. *Erosion in Vent Plugs, II. The Effects of Vent Shape and of Metal*, J. H. Wiegand, Report No. 578, BRL-APG, Jan. 25, 1946.

204. *The Dependence of Muzzle Velocity on the Potential and the Force of the Powder*, J. P. Vinti and J. Chernick, Report No. 583, BRL-APG, Oct. 26, 1945.

205. *Notes on Increasing the Penetration of the Medium Tank Gun*, S. J. Zaroodny, Memorandum Report No. 111, BRL-APG, Dec. 26, 1941.

206. *Yaw of 3-In./57-mm Sabot Type Projectile Fired from British 17-Pounder Gun*, H. P. Hitchcock, Memorandum Report No. 171, BRL-APG, June 1, 1943.

207. *Ballistics of NDRC 20-mm Sabot Type Projectiles*, A. P. Alexander and H. P. Hitchcock, Memorandum Report No. 251, BRL-APG, Nov. 27, 1943.

208. *The Observed and Computed Deflections of Bullets Fired Sidewise from an Airplane*, T. E. Sterne, Memorandum Report No. 273, BRL-APG, Feb. 19, 1944.

209. *Designs of Sub-Caliber Projectiles*, H. P. Hitchcock, Memorandum Report No. 302, BRL-APG, June 17, 1944.

210. *Flash Radiographs of 76-mm Sabot-Projectile*, J. C. Clark, Memorandum Report No. 330, BRL-APG, Sept. 14, 1944.

211. *Effects upon the Moment and Drag Coefficient of an Increase in Width of the Driving Band*, W. A. Siljander, Memorandum Report No. 365, BRL-APG, Apr. 30, 1945.

212. *Experimental Subcaliber A. P. Projectile for the 37-mm Aircraft Gun, M4*, S. J. Zaroodny, Report No. 323, BRL-APG, Jan. 8, 1943.

213. *Test of Aircraft Machine Gun Barrels, Caliber .50, with Stellite Liners*, 1st and 3rd Memorandum Reports on F. R. No. S-42589, Ordnance Program No. 5082, APG, Sept. 14, and Nov. 11, 1944.

214. *Test of Chromium Plated Caliber .50 Aircraft Machine Gun Barrels, Lot No. 2*, 4th Memorandum Report on Firing Record S-42762, Ordnance Program No. 5082, APG, Mar. 16, 1945.

215. *Test of Gun, Machine, Caliber .60, T17E3, Aircraft [Using Chromium-Plated Barrels Furnished by Division One]*, 12th, 13th, and 14th Memorandum Reports on Firing Record S-42900, Ordnance Program No. 5082, APG, Apr. 24, 25, 26, 1945.

216. *First Report in Connection with the Test of the Accuracy Life of the 155-mm Gun, M1A1E1, No. 3052; and Thirty-first Report on 155-mm Gun—8-inch Howitzer Matériel*, Ordnance Program No. 5084, (2 Vols), APG, Sept. 6, 1944.

217. *Test of Special High-Velocity "Hour Glass" Type 37/28-mm Projectile by NDRC*, Memorandum Report On Ordnance Program No. 5364, APG, July 11, 1942.

218. *The Second Report on the 37/28-mm and 37-mm High Velocity Armor Piercing Projectiles and Twenty-second Report on Ordnance Program No. 5364*, APG, July 19, 1942.

219. *Form Factor, Yaw Recovery, and Breech Pressure Firings of 37/28-mm NDRC (N.B.S. Type G) Projectiles*, Firing Record No. S-20960, Ordnance Program No. 5364, APG, Feb. 3, 1943.

220. *First Report in Connection with the Test of the Accuracy Life of Tubes, 90-mm Gun, M3E2 (Chromium-Plated) and Sixth Report on Ordnance Program No. 5412*, APG, Apr. 27, 1945.

221. *Test of 37-mm Tube, Stellite Liners A, B, and C*, 3rd Memorandum Report, Firing Records Nos. M-46044, M-46045, M-46269, Ordnance Program No. 5426, APG, Sept. 9, 1945.

222. *First Report on Test of Projectile, Hyper-Velocity Armor Piercing (Sabot), 90-mm T32 and T38 Series, First Report on Ordnance Program No. 5757, and First Report on Ordnance Program No. 5962*, APG, Oct. 2, 1945.

223. *First Report on the Projectile H.V.A.P. (Sabot), 76-mm 3-76EII (University of New Mexico), T23 and T23EI (Remington Arms Company), and Second Report on Ordnance Program No. 5962*, APG, Oct. 2, 1945.

224. *Firing Test to Determine Ballistic and Functioning Characteristics of 105-mm/3-inch and 105-mm/57-mm Sabot-Projectiles (University of New Mexico Design)* Firing Record No. P-31518, Ordnance Program No. 5762, APG, June 7, 8, 1944.

225. *Second and Final Report on 8.8 cm Anti-Tank Gun Pak 43/41, German*, Memorandum Report on Ordnance Program No. 5772, APG, Aug. 3, 1945.

226. *Data Relative to the Erosion Resisting Quality of Chromium-plated Caliber .50 Aircraft Barrels*, Firing Record No. S-33346, Ordnance Program No. 5800, APG, Dec. 22, 1943 to Feb. 4, 1944.

227. *Test of 37/28-mm Hour Glass Projectiles by NDRC*, Firing Record No. S-14020, Ordnance Program No. 5829, APG, July 6 to Nov. 14, 1942.

228. *Practicability of Design of NDRC 37/28-mm Projectiles*, Firing Record No. S-18216, Ordnance Program No. 5829, APG, Dec. 15, 1942.

229. *Test of 37/28-mm NDRC Projectiles (N.B.S. Type G with Various Deviations)*, Memorandum Report on Ordnance Program No. 5829, APG, Mar. 22, 1943.

230. *Firing Test to Determine by Spark and Micro-Flash Photography which of Two 37/28-mm NDRC (NBS Type G with .238" and .100" Base Skirts) Projectiles has the Better Contour Characteristics in Flight*, Firing Record No. S-23635, Ordnance Program No. 5829, APG, Apr. 14, 1943.

231. *Tests of Replaceable Liner for 75-mm Gun, M3*, First through Thirteenth Memorandum Reports on Ordnance Program No. 5834, APG, Apr. 22, 1943 to May 25, 1944.

232. *Firing Test to Determine Stability of 3" Sabot-Type Projectile when Fired from 3" Gun, M1918M1, at Chamber Pressure of 40,000 p.s.i.*, Firing Record No. P-20826, Ordnance Program No. 5867, APG, Apr. 14, 1943.

233. *Firing Test to Determine Suitability and Stability of Experimental 3" Sabot-Type Projectiles*, Firing Record No. P-21895, Ordnance Program No. 5867, APG, Apr. 29, 30, 1943.

234. *Determination of Pressure and Velocity Relationship of 20 mm Subcaliber Projectiles for NDRC*, Firing Record No. S-22190, Ordnance Program No. 5945, APG, Mar. 10, 1943.

235. *Firing Tests of 3-in./57mm Sabot-Projectile (Critchfield Design) Fired in British 17-Pounder (3-in.) Gun, Mk. I*, Firing Records Nos. M-23473 (Ordnance Program No. 5954) and M-22798 (Ordnance Program No. 5965), APG, May and June 1943.

236. *Firing Tests of 105/75-mm Sabot-Projectile, Critchfield Design*, Firing Records Nos. M-23342 and M-24905. Ordnance Program No. 5954, APG, June and July 1943.

237. *Stability Firing Program on the 20-mm Sabot-Type Projectile for the Ballistic Research Laboratory*, Firing Record No. S-31707, Ordnance Program No. 5962, APG, June 7, Sept. 8, 9, 25, 27, and Oct. 5, 1943.

238. *Firing Tests of 75/57-mm Sabot-Type Projectiles, University of New Mexico, Design 28-75D*, Firing Records Nos. M-24862, M-25496, M-28120, and M-28827, Ordnance Program No. 5962, APG, July 12 to Dec. 23, 1943.

239. *Firing Test to Obtain Micro-Flash Pictures of 75-mm Eksergian Sabot-Type Projectiles in Flight*, Firing Record No. M-24957, Ordnance Program No. 5962, APG, July, 19, 21, 1943.

240. *Proof Firing of 37-mm Tubes, T47 and Establishment of Charge for 37-mm Experimental Pre-Engraved Projectiles in 37-mm Gun, T47*, Firing Record No. P-37989, Ordnance Program No. 5996, APG, June 6 to 21, 1945.

241. *First Report on Development Test of 90-mm Gun, T19, with a Removable Liner and First Report on Ordnance Program No. 6102*, APG, July 9, 1945.

242. *Test of 3-in./57-mm Sabot-Type Projectile (Critchfield Design) Fired Against Armor*, Projectile Test, Report No. AD-P99, APG, Aug. 29 to Nov. 18, 1943.

243. *The Action of p-Phenylenediamine on Nitrocellulose*, C. P. Fennimore, Report No. 612, BRL-APG, June 25, 1946.

REPORTS ISSUED BY WATERTOWN ARSENAL[d]

244. *Report of Conference on Gun Erosion*, WA, Watertown, Mass., Oct. 15, 1941.

245. *Erosion in Gun Barrels* (Monthly Progress Reports to Watertown Arsenal on War Department Contract), H. W. Russell, Battelle Memorial Institute, February 12, 1941 to June 30, 1942, pages 1 to 430, incl.; July 1, 1942 to December 31, 1942, pages 1 to 82, incl.; January 31, 1943 to ———.

246. *Metallurgical Tests of German 8.8 cm. Gun*, First, Second, and Third Partial Reports, WA File Nos. 386.3/22, 386.3/23, 386.3/28, WA, May 14, 27, June 12, 1943.

247. *Metallurgical Examination of Three 76-mm Gun Tubes, Two After Endurance Firing and One After Proof Firing*, N. L. Reed, Experimental Report No. WAL 730/56, WA, July 17, 1944.

248. *Examination of 76-mm Gun Tube M1, No. 52, which was Fired 2220 Rounds at Aberdeen Proving Ground*, A. M. White, Experimental Report No. WAL 730/65, WA, Nov. 13, 1943.

249. *Stresses in Gun Tubes: Band Pressure Characteristics of 37-mm, M3 Gun No. 770, Tube No. 2928*, R. Beeuwkes,

[d]Items 541, 557, and 563 in *Additional References* of this Bibliography pertain to this section.

Jr., Experimental Report No. 730/95, WA, Apr. 21, 1944.

250. *Strains in Gun Tubes: Calculation of Pressure Expansion Curves of Circular Cylinders*, R. Beeuwkes, Jr., J. H. Laning, Jr., Experimental Report No. WAL 730/111, WA, Mar. 8, 1944.

251. *Stresses in Guns under Combined Band and Gas Pressures*, J. H. Laning, Jr., Memorandum Report No. WAL 730/118, WA, Mar. 25, 1944.

252. *Firing Strains in Guns Arising from Passive Resistances*, J. H. Laning, Jr., Memorandum Report No. WAL 730/123, WA, Apr. 5, 1944.

253. *Stresses in Guns under Combined Band and Gas Pressures, Part 1*, J. H. Laning, Jr., Experimental Report No. WAL 730/137, WA, Apr. 28, 1944.

254. *Stresses in Guns Under Combined Band and Gas Pressures. Part 2. Elastic Strains at the Outer Surface for Internal Radial Pressures, Basic Data*, O. L. Bowie, J. H. Laning, Jr., Experimental Report No. WAL 730/137-1, WA, Mar. 22, 1945.

255. *Stresses in Guns under Combined Band and Gas Pressures. Part 3. Elastic Strains at the Outer Surface for Internal Frictional Forces, Basic Data*, O. L. Bowie, J. H. Laning, Jr., Experimental Report No. WAL 730/137-2, WA, May 18, 1945.

256. *Stresses in Guns under Combined Band and Gas Pressures. Part 4. Maximum Equivalent Tensile Stress at the Bore Surface*, O. L. Bowie, J. H. Laning, Jr., Experimental Report No. WAL 730/137-3, WA, Aug. 31, 1945.

257. *Centrifugal Casting: Metallurgical Examination of 76-mm M1A1 Gun Tube No. 1025 After Extended Firing Test*, P. A. G. Carbonare, Experimental Report No. WAL 730/144, WA, Oct. 5, 1944. (See Appendix, Report No. WAL 731/69-5, Item 267.)

258. *Methods for Computation of Plastic Stresses in Guns Under Combined Band and Gas Pressures*, J. H. Laning, Jr., Memorandum Report No. WAL 730/166, WA, July 6, 1944.

259. *Metallurgical Examination of 76-mm Gun Tubes M1A1 No. 1441 and M1E6 No. 1033 after Extended Firing Tests and Detonation Tests at Aberdeen Proving Ground*, A. M. Burghardt, Experimental Report No. WAL 730/197, WA, Oct. 24, 1944.

260. *Erosion II. Plug Erosion Tests*, P. R. Kosting, Report No. 731/37, WA, June 15, 1938.

261. *The Effect of Service upon 75-mm Gun M1897 No. 1587*, P. R. Kosting, Report No. 731/44, WA, Aug. 29, 1939.

262. *37-mm Browning Automatic Gun M1, No. 1 Barrel*, P. R. Kosting, Report No. 731/45, WA, Oct. 17, 1940.

263. *Erosion of Guns: Chromium Plated 37-mm Gun Tube M1, No. 4 (C-4557)*, R. E. Peterson, Report No. 731/63, WA, Dec. 21, 1942.

264. *Erosion and Progressive Stress-Damage in 76-mm Gun Tube M1, No. 341*, P. R. Kosting, Memorandum Report No. WAL 731/69, WA, Nov. 15, 1943.

265. *The Extent of Progressive Stress-Damage and of Erosion in 76-mm Gun Tube M1A1, No. 1425*, P. R. Kosting and R. H. Patterson, Memorandum Report No. WAL 731/69-3, WA, Jan. 14, 1944.

266. *Erosion and Progressive Stress-Damage in 76-mm Gun Tubes, Including T1 No. 2*, P. R. Kosting, Memorandum Report No. WAL 731/69-4, WA, July 8, 1944.

267. *Progressive Stress-Damage and Erosion in Centrifugally Cast and Cold Worked 76-mm Gun Tube M1A1 No. 1025*, P. R. Kosting and J. A. Kornatowski, Memorandum Report No. WAL 731/69-5, WA, Sept. 11, 1944. (Appendix to Report No. WAL 730/144, Item 257.)

268. *Spectroscopic Analysis of Bore Interface of 76-mm Gun Tubes M1 No. 52 and M1A1 No. 1425*, P. R. Kosting, Memorandum Report No. 731/69-6, WA, Nov. 7, 1944.

269. *Erosion and Progressive Stress-Damage of Guns: 76-mm, M1E2, Tube No. 1105*, P. R. Kosting and R. H. Patterson, Memorandum Report No. 731/69-7, WA, Dec. 18, 1944.

270. *Erosion of Metals, Alloys, Nitrided Steel, and Metallic Coatings on Steel*, P. R. Kosting, Experimental Report No. WAL 731/72-1, WA, Mar. 24, 1944.

271. *The Chromium Plating and Firing Tests on Seven 37-mm, M3 Gun Tubes*, (Report to Watertown Arsenal on War Department Contract), H. W. Russell, L. R. Jackson, E. J. Ramaley, and C. L. Faust, (Watertown File No. 731/75-8), Battelle Memorial Institute, Feb. 15, 1944.

272. *Memorandum Concerning Chromium Plating for Erosion Resistance by Battelle Memorial Institute*, L. R. Jackson, Battelle Memorial Institute, Report No. WAL 731/75-12, WA, Apr. 14, 1944.

273. *Comparison of Rotating Bands of 37-mm, 75-mm, 3-inch, 90-mm, 105-mm, and 155-mm Projectiles*, P. R. Kosting and H. E. Squires, Memorandum Report No. WAL 731/90-1, WA, Jan. 26, 1945.

274. *Erosion and Progressive Stress-Damage of Guns: 90-mm, M1, Tube No. 7*, P. R. Kosting, Memorandum Report No. WAL 731/90-2, WA, Jan. 29, 1945.

275. *Erosion and Progressive Stress-Damage of Cannon*, M. Flynn, R. H. Patterson, and P. R. Kosting, Memorandum Report No. WAL 731/90-4, WA, Dec. 13, 1945.

276. *The Chromium Plating of Six 37-mm Gun Tubes and Four Special 15-inch Sections of 37-mm Gun Tubes*, (Report to Watertown Arsenal on War Department Contract), L. R. Jackson, C. L. Faust, and E. L. Combs, (Watertown File No. 731/94-1), Battelle Memorial Institute, Nov. 1, 1944.

277. *Progressive Stress-Damage of Gun Tubes, First Partial Report*, P. R. Kosting, Experimental Report No. WAL 731/95, WA, May 2, 1944.

278. *Progressive Stress-Damage of Gun Tubes, Second Partial Report*, P. R. Kosting, Experimental Report No. WAL 731/95-1, WA, Oct. 2, 1944.

279. *Film in Chromium Electroplate*, J. B. Cohen, Experimental Report No. WAL 731/99, WA, June 3, 1944.

280. *Progressive Stress-Damage in 37-mm, M3 Tubes, No. 1500 and No. 4040*, J. A. Kornatowski and P. R. Kosting, Experimental Report No. WAL 731/102, WA, May 30, 1944.

281. *Progressive Stress-Damage in 37-mm, M6 Tube No. 102770 (NDRC-CIT Test)*, J. A. Kornatowski and P. R. Kosting, Experimental Report No. WAL 731/111, WA, July 11, 1944.

282. *The Erosion of 37-mm M1A2 Gun Tubes, Including the Effect of Propellant Powders FNH-M1 and FNH-M2 and of Band Diameter*, P. R. Kosting, Experimental Report No. 731/115, WA, Aug. 7, 1944.

283. *Investigation of 75-mm Gun Tube T13E1 No. 36209 After 3608 Rounds at Normal Pressure*, P. R. Kosting and J. A. Kornatowski, Experimental Report No. WAL 731/126, WA, Nov. 17, 1944.

284. *Investigation of 155-mm Gun Tube M1A1 No. 98 Which was Returned from the European Theater of War*, P. R. Kosting and Mildred D. Flynn, Experimental Report No. WAL 731/133, WA, Dec. 22, 1944.

285. *A Detailed Study of the Bore Interface of Chromium Plated Tube No. 1521 from 155-mm Gun M1A1E1 No. 3052 after 2353 Rounds*, J. B. Cohen and J. A. Kornatowski, Experimental Report No. WAL 731/173, WA, Sept. 11, 1944.

OTHER REPORTS ISSUED BY THE WAR DEPARTMENT[c]

286. *High and Low Temperature Ballistic Research: First Progress Report on Firings in 76-mm Gun, M1*, Technical Division, OCO, July 3, 1943.

287. *Stability and Resistance Firings*, Ordnance Proof Manual No. 15-10, OCO, Aug. 7, 1943.

288. *Proof Technique: Inspection of Cannon and Measurement of Significant Dimensions*, Ordnance Proof Manual No. 40-15, OCO, Feb. 26, 1943.

289. *Velocity Measurements of Projectiles*, Ordnance Proof Manual No. 40-17, OCO, Dec. 21, 1942.

290. *Steel Forgings for Cannon Tubes*, U. S. Army Specification No. 57-106A, War Department Manual, Jan. 1, 1945.

291. *Cobalt-Chromium-Alloy; Castings, Investment*, Ordnance Department Tentative Specification, AXS-1494, Jan. 11, 1945.

292. *Procedure and Final Detail Physical, Dimensional, and Performance Requirements for Nitrided and Chromium Plated Caliber .50 AC Machine Gun Barrels*, 2nd Ed., OCO, Feb. 10, 1945.

293. *Design Procedure for Cannon Tubes*, Memorandum No. 7, Cannon Branch, Armament Development Division, Research and Development Service, OCO, 1945.

294. *Barrel, Gun, Machine, Caliber .50, Improvement in Accuracy Life—Status of Project for*, Ordnance Committee Minute 26230, OCO, (Approved) Jan. 4, 1945.

295. *Barrel (D-7161814) for Gun, Machine, Browning, Caliber .50, M2, Heavy Barrel—Recommended for Adoption*, Ordnance Committee Minute 27817, OCO, (Approved) May 31, 1945.

296. *Barrels, Machine Gun, with Chromium-plated Bores—Change in Security Classification Recommended*, Ordnance Committee Minute 28357, OCO, (Approved) July 12, 1945.

297. *Barrel (D-7162295) for Gun, Machine, Caliber .30, Browning, M1919A6—Recommended for Adoption*, Ordnance Committee Minute 28510, OCO, (Approved) July 26, 1945.

298. *Barrel (D-7162295) for Gun, Machine, Caliber .30, Browning, M1919A6—Recommendation for Adoption Approved; Barrel (D-7161814) for Gun, Machine, Browning, Caliber .50, M2, Heavy Barrel—Recommendation for Adoption Approved*, Ordnance Committee Minute 28893, (read for record) OCO, Aug. 30, 1945.

299. *Test of Stellite Lined Caliber .50 Machine Gun Barrels*, Report on Project No. 4238C472.91, Army Air Forces Board, Orlando, Fla., June 28, 1945.

300. *Bofors 57-mm A-A Gun*, Military Attaché Stockholm Report No. 1421, Military Intelligence Division, War Department, Oct. 30, 1941.

301. *Penetration Range Curves for 6 Pr. Projectiles, A.R.D./T.H.V. No.-218*, Inclosure to Military Attaché London Report No. 64056, Military Intelligence Division, War Department, Dec. 29, 1943.

302. *N.A.F.D.U. Cooling System for Cal. .50 Aircraft Machine Guns*, Military Attaché London Report No. R174-45, Military Intelligence Division, War Department, Jan. 8, 1945.

303. *Report on 28-cm Projectile*, G-2 Report 196, File No. 0.0. 386.3/1542, Incl. 1, OCO, Apr. 12, 1944.

304. *German 28-cm Railway Gun*, H. M. Loewy, Ordnance Intelligence Unit (D), APO 464, U. S. Army, June 12, 1944.

305. *German Sabot Projectiles*, H. L. Karsch and Purcell, Ordnance Technical Intelligence, Hq. Com Z, USFET.

306. *Chrome Plating of Barrels by the Heinrich Reining, G.m.b.H.*, J. M. Crews, A. E. Kramer, CIOS Target Nos. 2/722 and 21/503, Artillery and Weapons Metallurgy, Combined Intelligence Objectives Sub-Committee, G-2 Division, SHAEF (Rear) APO 413, June 1945.

307. *Radial Vibrations of Gun Tube*, G. C. Evans, T.D.B.S. Report No. 15, OCO, Sept. 22, 1943.

308. *Use of Tables to Calculate Band Pressures from Strain Gauge Data*, G. C. Evans, T.D.B.S. Report No. 30, OCO, Apr. 4, 1944.

309. *Criteria for Dimensions of Rotating Bands*, G. C. Evans, T.D.B.S. Report No. 32, OCO, June 7, 1944.

[c]Items 538, 545, 546, and 553 in *Additional References* of this Bibliography pertain to this section.

310. *Notes on Gun Design,* G. C. Evans, T.D.B.S. Report No. 36, OCO, June 5, 1944.

311. *Engineering Report on Chromium Plating Various Small Arms Barrels,* A. Willink, Frankford Arsenal, July 28, 1931.

312. *Caliber .50 Interior Ballistic Data,* E. R. Thilo, Report No. T-1401, Ordnance Laboratory, Frankford Arsenal, Nov. 25, 1942.

313. *Development of a Standard Erosion Gage Weapon and a Standardized Erosion Test,* W. J. Kroeger and C. W. Musser, Report No. R-268, 1st Report, Research Item 1004.0, Ordnance Laboratory, Frankford Arsenal, January 1943.

314. *An Accelerated Erosion Test in the Erosion Gage,* W. J. Kroeger and S. Fernbach, Report No. R-269, 2nd Partial Report, Research Item No. 1004.0, Ordnance Laboratory, Frankford Arsenal, January 1943.

315. *A Reproducibility Test of the Caliber .30 Erosion Gage,* W. J. Kroeger and S. D. Rolle, Report No. R-331, 3rd Partial Report, Research Item 1004.0, Ordnance Laboratory, Frankford Arsenal, May 1943.

316. *Determination of Quickness of Standard Pyro and FNH Powders,* Technical Reports Nos. 966, 1017, 1050, Chemical Department, Technical Group, Picatinny Arsenal, May 17, 1939, Jan. 3, 1940, and July 26, 1940.

317. *Thermochemical and Physical Tests of Nitro-guanidine Powders,* Technical Report No. 1336, Chemical Department, Technical Group, Picatinny Arsenal, Sept. 6, 1943.

318. *Investigation of Erosion in Caliber .50 M2 AC BMG Barrels,* Partial Technical Reports on S.A. W.O. 311, Engineering Department, Experimental Division, Springfield Armory, Nov. 12, 1943, Mar. 1, 1944, and June 6, 1944.

319. *Reports on Tests of Special Aircraft Caliber .50 Machine-Gun Barrels (Prepared by Division One, NDRC),* Reports Nos. 29, 34, 36, 37, 42, 47, 48, 50, 52, 54, 58, 60, 63, 64, 65, 66, 67, 68, 75, 76, 77, 81, 82, 87, 94, 95, 98, 108 (each report has an individual title), Purdue University, Engineering Experiment Station, Small Arms Ordnance Research, (under contract with War Department), August 1944—May 1945.

320. *Reports on Tests of Special Caliber .30 Machine-Gun Barrels (Prepared by Division One, NDRC),* Reports Nos. 72, 77, 91, 102, 103, 107 (each report has an individual title), Purdue University, Engineering Experiment Station, Small Arms Ordnance Research (under contract with War Department), January 1945—May 1945.

321. [*Apparatus for Measuring Bore-Surface Temperatures*], Report 26B, Purdue University, Engineering Experiment Station, Small Arms Ordnance Research (Final Report Covering the Artillery Research Work under Contract W-11-022-ORD-4266), June 30, 1946.

REPORTS ISSUED BY NAVY DEPARTMENT

322. *Partial Report on Chromizing of Steels,* NRL Report No. M-1822, Navy Department, Dec. 16, 1941.

323. *Reports from Special Board on Naval Ordnance, October 1 and 15, 1926, Concerning 3-in./105-Caliber Gun,* quoted in letter ED1(Re5a) from Capt. G. L. Schuyler to J. S. Burlew, NDRC, Mar. 28, 1942.

324. *"Probert" Gun and Projectile Design,* Naval Attaché London Report Serial No. 838, Naval Intelligence Division, Navy Department, April 1942.

325. *Aircraft Machine Guns, the Evaluation of Hyper-Velocity Types of, for Naval Aircraft,* Memorandum from the Special Board on Naval Ordnance, Navy Department, Mar. 18, 1943.

326. *Thermal Deformation of Gun Bores,* C. W. MacGregor and L. F. Coffin, Jr., Report to the Chief of the Bureau of Ordnance, Navy Contract No. NOrd-470, MIT, Sept. 20, 1943.

327. *The Effect of Projectile Bands on the Strength of Gun Barrels,* C. W. MacGregor and L. F. Coffin, Jr., Report to the Chief of the Bureau of Ordnance, Navy Contract No. NOrd-470, MIT, Sept. 20, 1943.

328. *Equipment and Procedures for Chrome Plating 3"/50 Cal., 5"/25 Cal., 5"/38 Cal., 6"/47 Cal., 5"/51 Cal., 6"/53 Cal., 8"/55 Cal., 12"/50 Cal., 14"/45 Cal., 14"/50 Cal., 16"/45 Cal., and 16"/50 Cal. Guns,* Informal Report, Naval Gun Factory, 1943.

329. *20-mm Aircraft Automatic Gun (Design),* Navord Ordnance Specifications, NAVORD OS 3380, Navy Department, June, 23, 1944.

330. *Strain Gauge Measurements on 3"/50 Guns,* Report No. 5-45, U. S. Naval Proving Ground, Dahlgren, Virginia, Mar. 20, 1945.

331. *Supersonic Flow around Yawing Cones,* Z. Kopal, MIT, Report No. 186 (Informal) to Bureau of Ordnance, Navy Department, 1945.

332. *Technical Conference on Supersonic Flow and Shock Waves,* Z. Kopal, NAVORD Report No. 203-45, Navy Department, 1945.

REPORTS ISSUED BY BRITISH MINISTRY OF SUPPLY[f,g]

333. *Temperature Measurements in Guns,* AC 1099/Gn.38, Met. Report 38 3/41, Aug. 11, 1941.

334. *The Structure of the Reaction Zone in the Burning of Colloidal Propellant,* S. F. Boys and J. Corner, AC 1139/IB.8, (WA-66-49), August 1941.

[f]Following the abbreviations AC, ADD, ARD, and RD, the file number of the report in the OSRD Liaison Office is given.

[g]Item 556, in *Additional References* of this Bibliography pertains to this section.

335. *Thermal Decomposition of S. C. Cordite* (Interim Report), C. E. H. Bawn and R. F. J. Freeman, AC 1398/IB.42, (W-112-8), November 1941.

336. *Note on Application of Results Obtained by Relaxation Methods*, F. Smithies, AC 1553/Gn.81, (II-5-842), January 1942.

337. *Preliminary Trial to Establish the Possibility of Electric Communication with the Projectile along the Bore*, A. J. Garratt, AC 1578/Gn.86 (RD/Ball. Report 8/41), (II-5-1036), January 1942.

338. *Further Note on Application of Results Obtained by Relaxation Methods*, F. Smithies, AC 1648/Gn.91, (OB-1-15-1), January 1942.

339. *Strains in a Gun Barrel near the Driving Barrel [Band] of a Moving Projectile*, G. I. Taylor, AC 1851/GN.104, (II-5-1065), March 1942.

340. *Thermochemical Data for the Products of Propellant Explosion*, AC 1862 IB/FP.20, (WA-252-52), March 1942.

341. *Preliminary Calculations on Stresses in Shell*, R. V. Southwell, AC 2201/Gn.127, (WA-177-43), June 1942.

342. *The Measurement of Shot Resistance in the Bore of a Gun*, R. E. Kutterer, AC 2244/IB.107, (WA-183-25).

343. *Stresses in H. E. Shell: Results Obtained by Relaxation Methods*, 2nd Report, AC 2457/Gn.153, (WA-259-47), August 1942.

344. *Stresses in Shell: Comparison of Approximate and Relaxation Methods*, D. G. Sopwith, AC 2680/Gn.170 (WA-260-15), September 1942.

345. *The Thermal Sensitivity of Explosives, Seventh Report*, A. J. B. Robertson, AC 2789/S.E.76, (WA-315-10), October 1942.

346. *Application of Relaxation Methods to Calculation of Stresses in Shell*, R. V. Southwell, AC 2797/Gn.180, (WA-315-3), October 1942.

347. *Stresses in H. E. Shell: Comparison of Approximate and Relaxation Methods*—II, D. G. Sopwith, AC 3066/Gn. 198, (WA-384-12), November 1942.

348. *The Heating of a Gun Barrel by the Propellant Gases*, E. P. Hicks and C. K. Thornhill, AC 3119/IB.146, (WA-507-1), December 1942.

349. *Stresses in Shell*, AC 3136/Gn.200, (WA-384-18), December 1942.

350. *A Method for the Oscillographic Study of Rapid Pressure Changes; Thermal Decomposition of R.D.X. and Ignition of Nitrocellulose*, A. J. B. Robertson, Eighth Report on the Thermal Sensitivity of Explosives, AC 3264/SE.108, (WA-436-11), Dec. 22, 1942.

351. *Stresses in Shell*, D. N. de G. Allen, AC 3276/Gn.208, (WA-403-5), December 1942.

352. *Spectrum of Cordite Burning in an Inert Atmosphere*, (Interim Report), W. C. Price and R. W. G. Norrish, AC 3410/IB.FP.133, (WA-334-14), January 1943.

353. *The Methods of Internal Ballistic Calculation in Use in the Armament Research Department, Part 1. The Present Working Method*, S. W. Coppack, AC 3605/IB.161 (ARD/Ball. Report 82/42, December 1942), (WA-532-6), March 1943.

354. *The Methods of Internal Ballistic Calculation in Use in the Armament Research Department. Part 2. Some Developments towards Greater Theoretical Completeness*, S. W. Coppack, AC 3606/IB.162, (ARD/Ball. Report 82/42, December 1942), (WA-532-7), March 1943.

355. *Stresses in Shell*, D. N. de G. Allen, AC 3632/Gn.236, (WA-542-13), March 1943.

356. *Stresses in Shells*, AC 3867/Gn.246, (WA-620-11), April 1943.

357. *Stresses in Shell*, D. N. de G. Allen, AC 3883/Gn.247, (WA-620-12), April 1943.

358. *A Spectroscopic Study of the Light Emitted by Cordite Burning in Closed and Vented Vessels*, W. C. Price and A. R. Philpotts, AC 4031/IB./FP.167, (WA-656-15).

359. *Stresses in Shell*, D. N. de G. Allen, AC 4032/Gn.253, (WA-708-4), May 1943.

360. *Abstracts of N.D.R.C. Reports Nos. A-91 and A-161*, AC 4144/Gn.259, (WA-708-7), June 1943.

361. *Stresses in H.E. Shell: Comparison of Approximate and Relaxation Methods—III*, D. G. Sopwith, AC 4252/Gn. 262, (WA-746-7), June 1943.

362. *Stresses in H.E. Shell: Effect of Driving Band Pressure—II*, D. G. Sopwith, AC 4254/Gn.263, (WA-746-8), June 1943.

363. *Stresses in H.E. Shell: Firing Trials in 2 Pr. H.E. Shells with Reduced Factors of Safety*, D. G. Sopwith, AC 4412/Gn.275, (WA-791-6), July 1943.

364. *Interim Report on the Thermal Decomposition and Burning of S.C. Cordite at Ordinary Pressure*, C. E. H. Bawn, AC 4658/PRP.35, (WA-940-10), Aug. 24, 1943.

365. *The Examination of Eroded Metal Surfaces by Means of Replica Films*, J. F. Allen and P. L. Willmore, AC 5341/Gn.317, (WA-1490-16), December 1943.

366. *Stresses in Guns*, D. N. de G. Allen, AC 5342/Gn.318, (WA-1490-17), December 1943.

367. *Review of Work Carried out in 1943 in the Armament Research Department, Metallurgical Branch*, AC 5467/Met. 184, (WA-1484-8), January 1944.

368. *Determination of the Coefficients of Friction of Steel on Steel at High Velocities*, G. Grotsch and E. Plake, AC 5912/Gn.340 Ball. 161, (RD Translation No. 898), (WA-3135-2A), March 1944. (See Item 493.)

369. *Stresses in Thin-Walled Shells*, W. E. A. Acum and D. N. de G. Allen, AC 5997/Gn.344, (WA-2057-14), March 1944.

370. *Note on Longitudinal Strain in Gun Tubes*, J. W. Graggs and C. J. Tranter, AC 6930/Gn.376, (WA-2961-12), September 1944.

371. *A Review of Some Recent Canadian Work on Gun Propellants*, K. J. Laidler, AC 6867/Bal.200, (WA-3005-5), September 1944.

372. *The Design of Driving Bands*, R. Beeching, AC 7199/Gn.389 (ADD Tech. Report 32/44), (WA-3145-6), September 1944.

373. *Stresses in Thin-Walled Shells*, W. E. A. Acum and D. N. de G. Allen, AC 7586/Gn.401, (WA-3822-14), December 1944.

374. *Tabulation of the Hunt and Hinds System of Internal Ballistics*, M. M. Nicolsen, AC 8335/Ball.281, (WA-5173-7), June 1945.

375. *The Choice of Calibre for Bomber and Fighter Aircraft*, RD Armament Report 1, (WA-3208-1a), September 1944.

376. *The Firing Stresses in the Q.F. 17-Pr. Gun*, G. H. Weston and J. B. Goode, ARD Ballistics Report 7/45, (WA-3830-6), January 1945.

377. *The Firing Stresses in the Q.F. 2-Pr. Mark 10 Gun* K. V. Hyde and J. B. Goode, ARD Ballistics Report 9/45, (WA-3830-7), January 1945.

378. *The Firing Stresses in the Q.F. 6-Pr. 6Cwt. Mk. 3*, G. H. Weston and J. B. Goode, ARD Ballistics Report 11/45, (WA-4104-1), February 1945.

379. *Notes on the Salvage and Recovery of Overmachined Steel Parts by Electrodeposition*, ARD Electrodeposition Memorandum No. 1, (WA-3767-4), January 1944.

380. *Notes on the Inspection of Heavy Electrodeposits of Nickel and Chromium*, ARD Electrodeposition Memorandum No. 5, (WA-3767-4C), May 1943.

381. *Report on Exudation and Cook-Off of Cordite Loaded Ammunition in Browning M.G.*, ARD Explosives Report 111/42, (II-5-3425), May 1942.

382. *Repair of Worn or Over-Machined Steel Components by Electrodeposition of Nickel*, RD Met. Report 205/41, (II-5-1686), April 1941.

383. *Plant for Repair of Gun Barrels of Chambers by Electrodeposition of Nickel*, RD Met. Report 458/41, (II-5-1830), September 1941.

384. *Improvements in the Electrodeposition of Chromium: Production of Machinable Chromium Deposits*, G. E. Gardam, RD Met. Report 465/41, (WA-776-7c), September 1941. (See Item 471.)

385. *Electrodeposition of Chromium in Gun Barrels; Summary of Present Position of Knowledge of the Control of the Hardness and Structure of Electrodeposited Chromium*, G. E. Gardam, RD Met. Report 400/42, (WA-171-1a), July 1942.

386. *Notes on the Inspection of Heavy Electrodeposits of Nickel and Chromium*, ARD Met. Report 235/43, (WA-1258-14), October 1943.

387. *German 10.5 "Sabot" Type H.E. Shell*, ARD Met. Report 26/44, (WA-1630-8), February 1944.

388. *Compression Properties of Driving Band Copper*, ARD Met. Report 90/44 (AC 6257/Gn.354) (WA-2136-12), April 1944.

389. *Method of Chromium Plating 0.5 inch Browning Barrels: Preliminary Process Specification*, ARD Met. Report 159/44, July 1944 [II-5-6092(s)]; (WA-4283-12), Revised April 1945.

390. *Firing Trials with .5 inch Browning M/G Barrels with Chromium Plated Bores*, ARD Met. Report 206/44, (WA-2926-7H), September 1944.

391. *Examination of Chromium Plated German Machine Gun and Breech Mechanism*, ARD Met. Report 221/44, (WA-3054 and WA-3524-1), October 1944 and Addendum, November 1944.

392. *Examination of a 7.5-cm Sabot Type A.P. Projectile*, ARD Met. Report 253/44, (WA-3650-4), November 1944.

393. *A Spectroscopic Investigation of the Light Emitted (1) in the Burning of Calcium Free Cordite and (2) in Secondary Gun Flashes Obtained with the Cordite*, W. C. Price and H. R. Philpotts, A. C. 3870.

394. *The 6 Pdr. Sabot Projectile*, G. S. Sanders, ARD Tech. Report 2/45, (WA-4153-2), January 1945.

395. *Notes on the Principles and Present Position of Hyper-Velocity Guns and Projectiles*, G. O. C. Probert, ARD Terminal Ballistic Report 22/44, (WA-2905-5A), July 1944.

396. *Theories of the Burning of Colloidal Propellants*, J. Corner, ARD Theoretical Research Report 2/43, (WA-1297-5), October 1943.

397. *Some Theoretical Considerations of the Problem of Gun Erosion*, C. K. Thornhill, ARD Theoretical Research Report 7/43, (WA-1424-2), December 1943.

398. *The Heating of a Gun Barrel by the Propellant Gases, II. Comparison between Theoretical and Experimental Values of Heat Transfer in Small Arms Weapons*, C. K. Thornhill and H. N. Ware, ARD Theoretical Research Report 29/44 (AC 7091/Gn.384/Ball.-209), (WA-3005-11), July 1944. (See Item 403 for revision).

399. *The Stresses in a Film of Fluid Lubricant on the Bore Surface of a Gun Barrel during Shot Travel*, E. P. Hicks, ARD Theoretical Research Report 48/44, (WA-3695-2), December 1944.

400. *Report on a Visit to the United States, February–April 1945, in Connection with Work on Gun Erosion*, ARD Theoretical Research Report 14/45, (WA-5071-3), June 1945.

401. *An Estimate of the Heating of a 3-in. Gun during Firing at 90 R.P.M.*, C. K. Thornhill and E. P. Hicks, ARD Theoretical Research Memorandum 15/45, May 1945.

402. *The Pressure of Air and Gas between the Bands of a Littlejohn Projectile*, J. Corner, ARD Theoretical Research Memorandum 20/44, (AC 6932/Gn.377) (WA-2870-11), August 1944.

403. *Notes on the Continuous Heating of a Gun Barrel during Successive Firings, with Revision of Experimental Results Derived in ARD Theoretical Research Report No. 29/44*, ARD Theoretical Research Memorandum 3/45, [WA-2792-2a(1)], January 1945. (See Item 398.)

404. *The Life of Gun Barrels,* ARD Theoretical Research Translation 2/44, (WA-3065-9), September 1944.

405. *Barrel Wear of a .5-in. Cal. Browning Machine Gun for Aircraft; a Review of the Principal Proceedings of the Ordnance Board, 1940–March 1944,* A. F. Burstall, ADD Technical Report 5/44, (I-A-243), July 1944.

406. *The Life of the .50" Browning Barrel,* C. F. Austin and R. Beeching, ADD Technical Report 10/45 (First Report of the Barrel Life Panel of the Armament Design and Research Departments), April 1945 (WA-4517-11). Addendum, B. C. Brookes, Report 10a/45, (WA-5635-4), December 1945.

407. *Barrel Wear of .5-in. Cal. Browning Machine Gun for Aircraft: A Review of Items of Special Interest to the Panel on Barrel Life of Machine Guns Taken from the Recent Reports of Division 1 of the National Defense Research Committee (N.D.R.C.), U.S.A.,* A. F. Burstall, ADD Technical Report 12/44, (WA-2177-7b), March 1944.

408. *Summary from Geophysical Laboratory (U.S.A.) Report, May 1944 N.D.R.C. Div. 1—320; Chromium Plated and Nitrided Liners and 9½ lb. Barrels,* Barrel Life Panel B.R. 561, (WA-3506-1d), July 1944.

409. *Summary of American Work (N.D.R.C. Div. 1) Relevant to Erosion and .50-in. Browning Barrel Life; January–March, part April and May, 1944,* C. F. Austin, Barrel Life Panel B.R. 578, (WA-3506-1b), August 1944. (Continuation of ADD Tech. Report 12/44, Item 407.)

410. *Summary of American Work (N.D.R.C. Div. 1) Relevant to Erosion and .50 in. Browning Barrel Life, March—June 30th, 1944,* C. F. Austin, Barrel Life Panel B.R. 659, (WA-3506-1c), September 1944.

411. *Note on the Cooling of .500" Browning Barrels,* Barrel Life Panel S.A. 2542, (II-5-6319), March 1944.

412. *Results of Trials on .5-in. Cal. Browning Barrels, Temperature Indicating Paints and their Use in Barrel Rejection,* Barrel Life Panel S.A. 2542/38R, [WA-2534–11g (1)], July 1944.

413. *Results of Trial on .5-in. Cal. Browning Barrels. Accuracy, Velocity and Bore Wear when Firing Various Cycles of A.P.M2 through Barrels Having Stellite Liners,* Barrel Life Panel S.A. 2542/82R, (WA-3750-5B), December 1944.

414. *.50" Barrels Nitrided and Chromium Plated in USA,* Barrel Life Panel S.A. 2542/108R, [II-5-7025(s)], April 1945.

415. *.50" Cadmium Plated Barrels [Bullets],* Barrel Life Panel S.A. 2542/112R, (WA-4545–3M), May 1945.

416. *.50" Chromium Plated Barrels from U. S.A. (B.A.C. Lot 1),* Barrel Life Panel S.A. 2542/115R, (WA-5432-2), June 1945.

417. *.50" Barrels Nitrided and Chromium Plated in U.S.A. (B.A.C. Lot 2),* Barrel Life Panel S.A. 2542/119R, (WA-5432-6), August 1945.

418. *Nitrided and Chromium Plated Barrels,* Barrel Life Panel S.A. 2542/127R, (WA-5658-8), November 1945.

419. *0.50-inch Browning Chromium Plated Barrel Life, Incorporating the Effect of Cooling by Air Flow, with the Use of Cooling Ducts Designed by N.A.F.D.U.,* Pendine Report 112/45, (WA-5164-5), July 1945.

420. *0.50-inch Browning Barrel Life, Incorporating the Effect of Cooling by Air Flow, with the Use of Ducts Designed by N.A.F.D.U.,* Pendine Report 290/44, [II-5-7017(s)], April 1945.

421. *The Nitrogen Content and Constitution of the Hard "White Layer" in Eroded Guns,* Brynmor Jones, University College, Cardiff, Research Dept. (Woolwich), Extra-Mural Report No. 8, (II-5-2042), 1942.

422. *The Engravement of Shell on Firing and its Possible Relation to Wear in Guns,* J. F. Allen, S.R.I. (FRG) Reports, (WA-2877-3A), (AC 6971/Gn.381 Ball. 202, October 1944).

423. *Chromium Plating of Bores of 0.5-inch Browning Barrels,* Informal Communication from A. W. Hothersall (Armament Research Department) to British Central Scientific Office, (II-5-6295), October 1944.

424. *Stresses and Strains in Thick and Thin Tubes with Semi-Infinite Pressure Distribution,* D. G. Sopwith, Eng. Div. Report 116/45 (AC 8130/Gn.428), (WA-4334-12), March 1945.

REPORTS ISSUED BY OTHER BRITISH GOVERNMENT OFFICES[h]

425. *High-Velocity Guns on the Gerlich and Smoothbore Principles,* Ordnance Board (Gr. Brit.), Proceeding No. 11379, Mar. 13, 1941.

426. *German 28/20-mm A/T Gun (Model 41): Pressures in Petrol Tanks Due to the Impact of Projectiles,* Ordnance Board (Gr. Brit.), Proceeding No. 15,750, (W-137-47), Jan. 9, 1942.

427. *Q. F. 3.7-inch gun Mark VI: (i) Mechanical Break-down to be Expected in Prolonged Firing; (ii) Possibility of "Cook-off",* Ordnance Board (Gr. Brit.), Proceeding No. 27,604, (WA-2140-23), May 12, 1944.

428. *20-mm Hispano: "Cook-off" in Hot Guns: (i) Results of Trials; (ii) Explosions in Lips of Belt Feed Mechanism,* Ordnance Board (Gr. Brit.), Proceeding No. 30,417, (WA-3980-12), Feb. 26, 1945.

429. *"Effect of Increased Temperature on Firing", B. L. 16-inch Mark IV Gun for Naval Service,* Ordnance Board (Gr. Brit.), Proceeding No. Q 3617, Appendix, Sec. 30, (WA-5099-4).

430. *Cooling of .50" Browning Guns in Naval Aircraft,* Preliminary Report, Reports Nos. 2, 4 to 8 incl., NAFDU/40/39 Arm.; Report No. 3, NAFDU/40/73 Arm., [II-5-6431(s) to II-5-6438(s), incl.], August–October 1944. (See Item 302 for summary of these reports.)

[h]Item 544 in *Additional References* of this Bibliography pertains to this section.

431. *A System of Internal Ballistics*, F. R. W. Hunt and G. H. Hinds, revised by C. J. Tranter, Military College of Science Publication, G. M. II, H. M. Stationery Office, (WA-4515-2), 1941.

432. *Temperature Indicating Materials*, Post Office Engineering Department, Radio Report No. 1298, (WA-4566-7), February 1945.

433. *Some Notes on the Calibration of Thermindex Paints*, Informal report submitted with letter January 10, 1945 from L. C. Tyte to G. Comenetz, Geophysical Laboratory, Carnegie Institution of Washington (WA-3679-6A,B).

JOURNAL ARTICLES (UNCLASSIFIED)[1]

434. "Supersonic Flow over an Inclined Body of Revolution," H. S. Tsien, *J. Aeronaut. Sci.*, Vol. 12, 1938, p. 480.

435. "A Contribution to the Thermodynamical Theory of Explosions," J. B. Henderson, H. P. Hasse, *Proc. Roy. Soc. (London)*, Vol. A100, 1922, p. 461.

436. Proudman, *Proc. Roy. Soc.* 100A, 289 (1922).

437. "The Air Pressure on a Cone Moving at High Speeds," G. I. Taylor, J. W. Maccoll, *Proc. Roy. Soc. (London)*, Vol. A139, 1933, p. 278.

438. "The Conical Shock Wave Formed by a Cone Moving at a High Speed," J. W. Maccoll, *Proc. Roy. Soc. (London)*, Vol. A159, 1937, p. 459.

439. Mansell, *Trans. Roy. Soc. (London)*, 207A, 243 (1907).

440. "On the Equation of State of Propellant Gases," A. D. Crow, W. E. Grimshaw, *Trans. Roy. Soc. (London)*, Vol. A230, 1931, p. 39.

441. "Combustion of Colloidal Propellants," A. D. Crow, W. E. Grimshaw, *Trans. Roy. Soc. (London)*, Vol. A230, 1931, p. 387.

442. "Researches on Explosives," A. Noble, F. A. Abel, *Trans. Roy. Soc. (London)*, Vol. A ——, 1875, p. 122. Reprinted in *Artillery and Explosives*, 1906, p. 99.

443. "Researches on Explosives," A. Noble, *Trans. Roy. Soc. (London)*, Vol. A205, 1905, p. 201.

444. "The Aerodynamics of a Spinning Shell," R. H. Fowler, E. G. Gallop, G. N. H. Lock, H. W. Richmond, *Trans. Roy. Soc. (London)*, Vol. A221, 1920, p. 296.

445. "Campo Aerodinamico a Velocita Iperacustica Attorno a un Solido di Rivoluzione a Prora Acuminata," C. Ferrari, *L'Aerotecnica*, Vol. 16, No. 2, 1936, p. 121.

446. "Campi di Corrente Impersonora Attorno a Solidi di Rivoluzione," C. Ferrari, *L'Aerotecnica*, Vol. 17, No. 6, 1937, p. 507.

447. "Valence Relations Among the Metal Carbonyls," A. A. Blanchard, *Chem. Rev.*, Vol. 26, No. 3, June 1940, p. 409.

448. "The Metal Carbonyls," A. A. Blanchard, *Science*, Vol. 94, No. 2440, Oct. 3, 1941, p. 311.

449. "Die Bildung von Eisen-, Kobalt- und Nickelcarbonyl durch Hochdrucksnythese aus Halogeniden in vergleichen der Darstellung," H. Hieber, H. Behrens, U. Teller, *A. anorg. allgem. Chem.*, Vol. 249, 1942, p. 26.

450. "Arbeitsbilanz beim Schuss aus einem Gewehr," C. Cranz, R. Rothe, *Z. ges. Schiess-u. Sprengstoffw.*, Vol. 3, 1908, pp. 301, 327, 474.

451. "Decomposition, Heat of Combustion and Temperature of Explosion of Explosives," O. Poppenberg and E. Stephan, *Z. ges. Schiess-u. Sprengstoffw.*, Vol. 4, 1909, p. 281.

452. "Decomposition of Powder in Guns during Firing," O. Poppenberg, E. Stephan, *Z. ges. Schiess-u. Sprengstoffw.*, Vol. 4, 1909, p. 388.

453. "Beitrage zur thermodynamischen Behandlung explosibler Vorgänge, I," A. Schmidt, *Z. ges. Schiess-u. Sprengstoffw.*, Vol. 24, No. 2, 1929, p. 41.

454. "Intermolecular Forces and the Properties of Gases," J. O. Hirschfelder, W. E. Roseveare, *J. Phys. Chem.*, Vol. 43, 1939, p. 15.

455. J. O. Hirschfelder, R. B. Ewell, J. R. Roebuck, *J. Chem. Phys.*, Vol. 6, 1938, p. 205.

456. J. O. Hirschfelder, F. T. McClure, I. F. Weeks, *J. Chem. Phys.*, Vol. 10, 1942, p. 201.

457. "Decomposition of Nitrocellulose," R. Robertson, S. S. Napier, *J. Chem. Soc.*, 1907, p. 761.

458. "Decomposition of Nitroglycerine," R. Robertson, *J. Chem. Soc.*, 1909, p. 1241.

459. "The Deposition of Chromium from Solutions of Chromic and Chromous Salts," Charles Kasper, *J. Research Natl. Bur. Standards*, Vol. 11, 1933, p. 515.

460. "Mechanism of Chromium Deposition from the Chromic Acid Bath," Charles Kasper, *J. Research Natl. Bur. Standards*, Vol. 14, 1935, p. 700.

461. "Cathodic Deposition of Chromium Nickel Alloy," M. F. Skalozubov, A. S. Vlasova, *Chem. Abs.*, Vol. 35, 1941, p. 1323.

462. "Cathodic Deposition of Iron-Chromium-Nickel Alloy," M. F. Skalozubov, I. A. Goncharova, *Chem. Abs.*, Vol. 35, 1941, p. 1323.

463. "The Electrodeposition of Tungsten from Aqueous Solutions," C. G. Fink, F. L. Jones, *Trans. Electrochem. Soc.*, Vol. 59, 1931, p. 461.

464. "The Co-deposition of Tungsten and Iron from Aqueous Solutions," M. L. Holt, *Trans. Electrochem. Soc.*, Vol. 66, 1934, p. 453.

465. "Metals Co-deposited with Tungsten from the Alkaline Tungsten Plating Bath," M. L. Holt, *Trans. Electrochem. Soc.*, Vol. 71, 1937, p. 301.

466. "Electrodeposition of Nickel-Tungsten Alloys from an Acid Plating Bath," M. L. Holt, M. L. Nielsen, *Trans. Electrochem. Soc.*, Vol. 82, 1942, p. 193.

[1]The following items in *Additional References* of this Bibliography pertain to items 534, 536, 537, 542, and 559 of this section.

467. "Electrodeposition of Iron-Tungsten Alloys from an Acid Plating Bath," M. L. Holt, R. E. Black, *Trans. Electrochem. Soc.*, Vol. 82, 1942, p. 205.

468. "Electrodeposition of Cobalt-Tungsten Alloys from an Acid Plating Bath," M. L. Holt, R. E. Black, P. F. Hoglund, *Trans. Electrochem. Soc.*, Vol. 84, 1943, p. 353.

469. "The Electrowinning of Chromium from Trivalent Salt Solutions," R. R. Lloyd, W. T. Rawles, R. G. Feeney, *Trans. Electrochem. Soc.*, Vol. 89, (Preprint No. 20), April 1946. (See Item 522.)

470. "Electrolytic Polishing of Stainless Steel and Other Metals," O. Zmeskal, *Metal Finishing*, Vol. 43, 1945, p. 280.

471. "The Production of Machineable Chromium Deposits," G. E. Gardam, *J. Electrodepositors' Tech. Soc.*, Vol. 20, 1945, p. 69.

472. "Electrolytic Deposition of Alloys of Tungsten, Nickel, and Copper from Water Solutions," L. N. Goltz, Z. N. Kahrlamov, *J. Applied Chem. (U.S.S.R.)*, Vol. 9, 1936, p. 640.

473. "Electrolytic Deposition of Tungsten and its Practical Utilization," S. I. Sklyarenko, O. S. Druzhinia, M. M. Masal'tseva, *J. Applied Chem. (U.S.S.R.)*, Vol. 13, 1940, p. 1926.

474. "Electroplating with Tungsten and Molybdenum," P. P. Belyaev, A. I. Lipovetskaya, *Korroziya i Borba s Nei*, Vol. 6, No. 247, 1940.

475. "The Erosion of Gun Tubes and Heat Phenomena in the Bore of a Gun," H. J. Jones, *Engineer*, Vol. III, 1911, p. 294.

476. "The Erosion of Guns," H. M. Howe, *Trans. Am. Inst. Min. Met. Engrs.*, Vol. 58, 1918, p. 513.

477. "Nitrogen in Steel and the Erosion of Guns," H. E. Wheeler, *Trans. Am. Inst. Min. Met. Engrs.*, Vol. 67, 1922, p. 257.

478. "Some Notes on the Effect of Nitrogen on Steel," O. A. Knight, H. B. Northrup, *Chem. & Met. Eng.* Vol. 23, 1920, p. 1107.

479. "The Erosion of Guns," R. H. Greaves, H. H. Abram, S. H. Rees, *J. Iron and Steel Inst.*, Vol. 119, 1929, p. 113.

480. "La Température de Combustion de la Poudre sans Fumée en Fonction de sa Composition Chimique," Part I, A. L. Th. Moesveld; Parts II and III, G. de Bruin, P. F. de Pauw; *Comm. de la Ste. Anme. Fabrique Neerlandaises d'Explosifs*, Nos. 7, 8, 9, 1928, 1929.

481. "Carburization as a Factor in the Erosion of Machine Gun Barrels," W. W. deSveshnikoff, *Army Ordnance*, Vol. 5, 1925, p. 794.

482. "[White Layer] Symposium," *Army Ordnance*, Vol. 5, 1925, p. 797. (This symposium included the following five papers: "The Cause of the White Layer," Henry Fay; "Erosion of Machine Gun Barrels," W. T. Gorton; "Additional Tests Needed to Determine Value of Various Steels," J. S. Vanick; "The Nitrogen Theory of Erosion," H. E. Wheeler; "Old and New Theories in Gun Erosion," A. G. Zimmermann.)

483. "The White Layer in Gun Tubes and its Relation to the Case of Nitrided Chromium-Aluminum Steel," H. H. Lester, *Trans. Am. Soc. Steel Treating*, Vol. 16, No. 5, 1929.

484. "The Sulfides of Zinc, Cadmium, and Mercury; Their Crystalline Forms and Genetic Conditions," E. T. Allen, J. L. Crenshaw, H. E. Merwin, *Am. J. Sci.*, Vol. 34, 1912, p. 341.

485. "Resistance of Slender Bodies Moving with Supersonic Velocities with Special Reference to Projectiles," T. von Karman, N. B. Moore, *Trans. Am. Soc. Mech. Engrs.*, Vol. 54, 1932, p. 303.

486. "Neuere Ergebnisse der Funkenkinematographie," H. Schardin, W. Struth, *Z. Tech. Physik*, Vol. 18, No. 11, November 1937. Translation: "Recent Results in Spark Cinematography," Translation No. 107, David W. Taylor Model Basin, Navy Dept., December 1942.

487. "Combustion of Explosives in Closed Vessels. Comparison of Experimental and Calculated Temperature and Pressure," H. Muraour, G. Aunis, *Chaleur et Ind.*, Vol. 20, 1939, p. 31.

488. "Notes de balistique intérieure," H. Muraour, *Mém. artillerie française*, Vol. 4, 1925, p. 455.

489. "Pre-engraved Projectiles," ("Les obus rayés") P. Charbonnier, *Mém. artillerie française*, Vol. 6, 1927, p. 3.

490. "The Wear of Rifle and Automatic Arms Barrels and their Metallographic Analysis," ("Usure des canons d'armes portatives et automatiques, et leur analyse metallographique"), P. Felsztyn, S. Spiewak, *Mém. artillerie française*, Vol. 17, 1938, p. 283.

491. "Resistance de forcement des projectiles dans le canon et son étude par le calcul," M. C. Spetzler, *Mém. artillerie française*, Vol. 17, No. 68, 1938, p. 869.

492. "Ein Verfahren zur Messung schnellveränderlicher Oberflächentemperaturen und seine Anwendung in Schusswaffenläufen," P. Hackemann, *Luftfahrtforschungsanstalt Hermann Göring*, (E. V. Braunschweig), Jan. 27, 1941. (Translation: "A Method for Measurement of Fast Changing Surface Temperature and its Application for Small Arms Barrels," Ordnance Technical Intelligence Branch, OTIB No. 1243.)

493. "Bestimmung des Reibungskoeffizienten bei hohen Geschwindigkeiten für Stahl auf Stahl," G. Grotsch, E. Plake, *Jahrbuch 1938 der deutschen Luftfahrt-Forsch*, p. 345. (See Item 368.)

494. R. Sauer, *Luftfahrt-Forsch.*, Vol. 19, 1942, p. 148.

495. Busemann, *Luftfahrt-Forsch.*, Vol. 19, 1942, p. 137.

496. "Flow in a Smooth Straight Pipe at Velocities above and below the Velocity of Sound," W. Frossel, *Forschung auf dem Gebiete des Ingenieurwesens*, Vol. 7, March–April 1936. (Translation: Tech. Memo. No. 844, National Advisory Council for Aeronautics, 1938.)

497. H. Muraour, *Bull. Soc. Chim. Mém.* Vol. 41, 1927, p. 1451.

498. H. Langweiler, *Z. Physik*, Vol. 19, 1938, p. 416.

499. A. Mittasch, *Z. angew Chem.*, Vol. 41, 1928, p. 827.

500. R. H. Kent, *Physics*, Vol. 7, 1936, p. 319.

501. J. E. Lennard-Jones, *Physica*, Vol. 4, 1937, p. 941.

502. "Apparatus for Optical Studies at High Pressure," T. Poulter, *Phys. Rev.* Vol. 40, 1932, p. 860.

BOOKS (UNCLASSIFIED)[i]

503. *Metals Handbook*, American Society for Metals; Cleveland, Ohio, 1939, pp. 368, 390.

504. *Handbook of Chemistry and Physics*, 25th ed,; Chemical Rubber Publishing Co., Cleveland, Ohio, 1941.

505. *Lehrbuch der Ballistik*, C. Cranz, Edwards Brothers, Ann Arbor, Mich., 1943. (Cf. Item 144).

506. *Statistical Thermodynamics*, R. H. Fowler, E. A. Guggenheim, Cambridge University Press, 1939, Chapter 7.

507. *Modern Developments in Fluid Dynamics*, Vol. II, S. Goldstein, Oxford-Clarendon Press, 1938.

508. *Kinematics of Machines*, George L. Guillet, 4th ed., John Wiley and Sons, 1940.

509. *Elements of Ordnance*, T. J. Hayes, John Wiley and Sons, 1938.

510. *Automatic Arms: Their History, Development and Use*, M. M. Johnson, Jr., C. T. Haven, Morrow and Co., 1941.

511. *Thermodynamics and Free Energy*, G. N. Lewis, M. Randall, McGraw-Hill Book Co., 1923.

512. *A Treatise on the Mathematical Theory of Elasticity*, A. E. H. Love, 4th ed., Cambridge University Press, 1934, pp. 274-277.

513. *Heat Transmissions*, W. H. McAdams, 2nd ed., McGraw-Hill Book Co., 1942.

514. *Plasticity*, A. Nadai, McGraw-Hill Book Co., 1931, Chapter 13.

515. *Naval Ordnance* (A textbook prepared for the use of midshipmen at the U. S. Naval Academy), Officers of the U. S. Navy, Annapolis, U. S. Naval Institute, 1939.

516. *Principes de Thermodynamique*, Saint Robert, Turin, 1870, p. 251 ff.

517. *Friction*, Stanton, London, 1923, p. 149.

518. *Theory of Elasticity*, S. Timoshenko, McGraw-Hill Book Co.

519. *Theory of Plates and Shells*, S. Timoshenko, McGraw-Hill Book Co., 1940.

520. *Text-Book of Ordnance and Gunnery*, W. H. Tschappat, 1st ed., John Wiley and Sons, 1917.

521. *Chemical Computations and Errors*, Crumplet and Yoe, p. 232.

[i]Item 535 in *Additional References* of this Bibliography pertains to this section.

MISCELLANEOUS DOCUMENTS

522. *The Electrowinning of Chromium*, R. S. Dean, Annual Report of Metallurgical Division, Fiscal Year 1941, U. S. Bureau of Mines Report Investigations 3600, 1941. (See Item 469.)

523. *A Digest of Ballistic Data on Large Naval Guns Obtained for the Bureau of Ordnance, Navy Department*, National Bureau of Standards, October 1924.

524. *Chromium-Base Alloys*, R. M. Parke, F. P. Bens, Climax Molybdenum Company, Mar. 15, 1945. (Report submitted to War and Navy Departments for clearance prior to publication.)

525. *Performance and Design Criteria for .50 Caliber Gun Barrel Coolers for Aircraft*, J. A. Broadston, Report No. NA-8568, North American Aviation, Inc., 1945.

526. *Report on Gun Barrel Cooling Tests for Mustang Aeroplanes*, J. A. Broadston, North American Aviation, Inc.

527. [*Fluoride Baths for Electroplating*], Armstrong, Menefee, U. S. Patents: 2,145,241; 2,145,745; 2,145,746; 2,160,-321; 2,160,322.

528. *Machine for Rifling Guns*, V. Bush, U. S. Patent No. 2,319,206, Jan. 23, 1942.

529. *Improvements in the Manufacture and Production of Coloured Coatings Capable of Indicating Temperatures*, Patent Specification (British) 478,140, Jan. 10, 1938.

530. *Thermetric Colours*, Dyestuffs Division, Imperial Chemical Industries, Ltd.

531. *Temperature Indicating Paints*, F. G. Nicholls, Australian and New Zealand Scientific Research Liaison (London) Report No. 156, (II-5-2397), August 1942.

532. *The Friction of the Driving Bands of Shells, Part II*, Lubrication and Friction Report No. 34, Council for Scientific and Industrial Research, Australia, (A.C. 5847/Gn.337, March 1944), (WA-1977-15), November 1943.

533. *The Mathematical Analysis of dp/dt–p–t Curves Obtained from Closed Vessel Firings*, N. S. Mendelshon, IBRL Report No. 5, Internal Ballistics Research Laboratory, Valcartier, Quebec.

ADDITIONAL REFERENCES

534. G. Jaeger, *Wiener Sitzber*, Vol. 105, 1896, p. 15.

535. *Gastheorie, II*, L. Boltzmann, 1898, sec. 51-61.

536. J. D. van der Waals, Jr., *Versl. K. Akad. Amst*, Vol. 10, 1902, p. 640.

537. H. Happell, *Ann. d. Phys.*, Vol. 21, 1906, p. 342.

538. *Calorific Values of Smokeless Powders as Affected by Variations in Composition, Granulation*, etc., C. G. Dunkle and N. T. Volsk, Picatinny Arsenal Tech. Reports Nos. 231, 620, June 1932, April 1935.

539. *Thermochemical Examination of a Number of Commercial and Experimental Propellants*, J. F. Kincaid, OSRD 1578, Division 8, NDRC.

540. [*Tests to Determine Ballistic Characteristics of Projectile, A.P., 57/40-mm, J&L A-1944*], Firing Records Nos. P-35551, P-35549, Ordnance Program No. 5829, APG, July 5, 10, 11, 1945.

541. P. R. Kosting and R. E. Peterson, WA Report WAL 731/59.

542. "Some Two-Dimensional Problems in Conduction of Heat with Circular Symmetry," H. S. Carslaw and J. C. Jaeger, *Proc. Lond. Math. Soc.*, Vol. 46, 1939-40, p. 361.

543. *Test of 76-mm Sabot-Projectile*, Firing Record No. P-35485, APG, Mar. 14, 1945.

544. Ordnance Board (Gr. Brit.), Proceedings No. 30,047.

545. [*Report on Breech Injection Devices*], Purdue University.

546. *Stresses in Shell with Wall Ratio 1.5*, G. C. Evans, T.D.B.S. Report No. 20, OCO, January 1944.

547. *Direct Measurement of Burning Rates by an Electric Timing Method*, B. L. Crawford, Jr., and C. Huggett, OSRD-4009, NRDC Report A 286, Univ. of Minnesota, August 1945.

548. *The Final Reactions of the Burning of Nitrocellulose*, C. P. Fennimore, Report No. 464, BRL-APG, Apr. 29, 1944.

549. *Experiments on Ignition of Nitrocellulose*, C. P. Fennimore and J. H. Frazer, Report No. 465, BRL-APG, May 12, 1944.

550. *A Comparison of Antiaircraft Guns of Various Calibers*, R. H. Kent, Report No. 125, BRL-APG, Dec. 1, 1938.

551. *Means of Obtaining Greater Armor Penetration from Antitank Guns*, R. H. Kent, Report No. 214, BRG-APG, Jan. 8, 1941.

552. *Gun Erosion: Development of Standardized Erosion Tests*, P. R. Kosting, Experimental Report No. WAL 731/72, WA, Nov. 15, 1943.

553. *Tables for Interior Ballistics*, A. A. Bennett, Document No. 2039, OCO, Washington, D. C., April 1921.

554. *Project for a New Table for Interior Ballistics for Multiperforated Powder*, J. P. Vinti, Report No. 402, BRL-APG.

555. *Some Comments on Effect of Adding Length to the Afterbody of a Square-Based, Conical-Headed Projectile*, R. N. Thomas, Report No. 543, BRL-APG, Apr. 23, 1945.

556. *An Investigation into the Behaviour of the Shell Driving Band from the Aspect of Gun Design*, K. V. Hyde and G. H. Weston, A.C. 4758/Gn.294 (ARD Ball. Report 67/43), (WA-1019-4), September 1943.

557. *Gun Tubes—Stresses and Deformations of Circular Cylinders. Part I: Mathematical Analysis for Cylinders Under Uniform Pressure*, R. Beeuwkes, Jr., and J. H. Laning, Jr., Report No. WAL 660/16, WA.

558. *Progress Report on Behavior of Metals Under Dynamic Conditions, (NS-109): The Influence of Impact Velocity on the Tensile Properties of Some Metals and Alloys*, D. S. Clark and P. E. Duwez, California Institute of Technology, OSRD 3837 (War Metallurgy Division M-288), June 19, 1944.

559. "Al-Fin Process," *Metals and Alloys*, 1945.

560. *Firing Tests to Determine the Armor Plate Penetrating Characteristics of Projectile, A.P., 57/40-mm. Dwg. J&L A-1944*, Firing Record No. P-35543, Ordnance Program No. 5829, APG, June 29–July 4, 1945.

OSRD APPOINTEES

DIVISION 1

Chief

L. H. ADAMS

Deputy Chief

H. B. ALLEN

Members

W. BLEAKNEY
L. J. BRIGGS
R. EKSERGIAN
C. E. MACQUIGG
E. L. ROSE
E. R. WEIDLEIN

Secretary

J. S. BURLEW

Special Assistants

J. W. GREIG[a]
J. P. MARBLE
J. F. SCHAIRER
J. A. TENBROOK

Engineers[b]

E. BAINBRIDGE
W. H. SHALLENBERGER
V. WICHUM

Technical Aides

H. L. BLACK
J. S. BURLEW
GRACE L. HART
O. H. KNEEN
L. E. LINE, JR.
J. P. MARBLE
RITA G. SCHUBERT
N. H. SMITH
HELEN M. WATSON

[a]Title of appointment was "Consultant," but functions were those of a Special Assistant.

[b]Because of the emphasis placed upon the engineering phases of the Division's activities at the time of the reorganization of Division 1, on October 1, 1944 the personnel was supplemented by engineers, two of whom were assigned by the Engineering and Transitions Office, NDRC.

Contract No.	*Contractor*	*Subject*
OEMsr- 51	Carnegie Institution of Washington, Geophysical Laboratory, Washington, D. C.	Investigation of gun erosion and other ordnance problems.
OEMsr- 430	Western Electric Company, Inc., Bell Telephone Laboratories, Murray Hill, N. J.	Electron diffraction studies of altered layers on steel and ferrous alloy specimens.
OEMsr- 463[a]	The Johns Hopkins University, Baltimore, Maryland	Determination of the effect of carbon monoxide and other gases on gun steel.
OEMsr- 465	Johnson Automatics, Inc., Boston, Mass.	Development of erosion-resistant liners and coatings in guns, and methods of testing such materials in the form of short liners.
OEMsr- 467	Jones and Lamson Machine Co., Springfield, Vt.	Development, design, and construction of rifled gun barrels and related equipment.
OEMsr- 516[b]	The Catholic University of America, Washington, D. C.	Theoretical interior ballistic investigations, and the development of experimental methods for determining stresses in projectiles and in gun tubes.
OEMsr- 533[a]	The Franklin Institute of the State of Pennsylvania, Philadelphia, Penna.	Investigation of gun erosion and other ordnance problems.
OEMsr- 534	Bryant Chucking Grinder Co., Springfield, Vt.	Design, development, and construction of special projectiles.[c]
OEMsr- 536	Leeds & Northrup Company, Philadelphia, Penna.	Development of methods and equipment for recording temperature-time measurements in gun barrels.
OEMsr- 537	President and Fellows of Harvard College, Cambridge, Mass.	Metallurgical studies of erosion effects on alloy specimens.
OEMsr- 598	The Rector and Visitors of the University of Virginia, Charlottesville, Va.	Investigation of centrifugal effects in projectiles.
OEMsr- 608	Massachusetts Institute of Technology, Cambridge, Mass.	Development of test specimens of erosion-resistant metallic coatings by various techniques.
OEMsr- 613	Armour Research Foundation, Chicago, Ill.	Performance of supersonic cavitation erosion tests.
OEMsr- 629[a]	Crane Co. Chicago, Ill.	Design, development, construction, and testing of gun barrel liners.
OEMsr- 668	The University of New Mexico, Albuquerque, N. M.	Design, development, and construction of subcaliber projectiles.

[a]Contract continued by Office of the Chief of Ordnance, War Department.
[b]Contract continued by Bureau of Ordnance, Navy Department.
[c]Beginning January 1, 1944, this work was continued under Contract OEMsr-467.

Contract No.	*Contractor*	*Subject*
OEMsr- 733[d]	Duke University, Durham, N. C.	Studies of the burning rates of propellant powders.
OEMsr- 746	Johnson Automatics, Inc. Boston, Mass.	Development of a belt-fed 20-mm automatic cannon for aircraft installation.
OEMsr- 865	General Electric Company, Lamp Department, Cleveland, Ohio	Preparation of short liners of erosion-resistant materials.
OEMsr- 886	Arthur D. Little, Inc. Cambridge, Mass.	Development of lightweight materials and methods of their fabrication for use in subcaliber projectiles.
OEMsr- 915[b]	Westinghouse Electric Corp., Research Laboratories, E. Pittsburgh, Penn.	Development of erosion-resistant materials for use as gun liners.
OEMsr-1038	Duke University, Durham, N. C.	Theoretical investigations of the thermal effects in gun erosion.
OEMsr-1184	Western Electric Company, Inc., Bell Telephone Laboratories, Murray Hill, N. J.	Investigation of vapor-phase plating of erosion-resistant materials from metal carbonyls.
OEMsr-1205	Westinghouse Electric Corporation, Lamp Division, Bloomfield, N. J.	Development of molybdenum for use as gun liners; investigation of erosion-resistant, electrodeposited tantalum.
OEMsr-1273	Climax Molybdenum Company, Detroit, Michigan	Development of erosion-resistant materials, and preparation of gun liners of such materials.
OEMsr-1318	Yale University, New Haven, Conn.	Preparation of chromium carbonyl and of carbonyl-deposited chromium plates.
OEMsr-1320	Climax Molybdenum Company, New York, N. Y.	Development of methods for semicommercial preparation of molybdenum and tungsten carbonyls.
OEMsr-1330[b]	Union Carbide & Carbon Research Laboratories, Inc. Niagara Falls, N. Y.	Development of hot-hard alloys suitable for gun liners.
OEMsr-1368	Remington Arms Company, Inc. Ilion, N. Y.	Development of sabot-projectiles.
OEMsr-1414	Crane Co., Chicago, Ill.	Preparation of 2,250 stellite-lined caliber .50 aircraft machine gun barrels.
OEMsr-1424	Industrial Research Laboratories, Ltd. Los Angeles, Cal.	Development of erosion-resistant, centrifugal-cast liners for gun tubes.
OEMsr-1433	Johnson Automatics, Inc. Boston, Mass.	Production of machine gun barrels with erosion-resistant liners.
OEMsr-1438	Remington Arms Company, Inc. Ilion, N. Y.	Production of machine gun barrels with erosion-resistant liners, including application of draw rifling to this purpose.

[b]Contract continued by Bureau of Ordnance, Navy Department.
[d]Transferred to Section H, Division 3.



Contract No.	*Contractor*	*Subject*
OEMsr-1444	Chrome Gage Corporation, Philadelphia, Penn.	Development of pilot plant for chromium plating caliber .50 machine gun barrels and production of not more than 10,000 such barrels.
OEMsr-1473	The A. F. Holden Company, New Haven, Conn.	Investigation of the bonding of hot-hard liners in gun tubes, and of heat-treating composite barrels.
OEMsr-1494	Al-Fin Corporation, Jamaica, N. Y.	Application of thermite-welding process to securing of erosion-resistant liners in machine gun barrels.
OEMsr-1499	Midvale Company, Philadelphia, Penn.	Manufacture of six special 90-mm gun tubes (under purchase agreement).
OEMsr-1499[e]	National Bureau of Standards, Electrochemical Section, Washington, D. C.	Improvement in plating processes, and their application to gun tubes.
OEMsr-1499[e]	National Bureau of Standards, Inductance and Capacitance Section, Washington, D. C.	Experimental investigation of bore friction and other phases of interior ballistics.

[e]Several transfers of funds from OSRD; work continued after 10/31/45 by a transfer of funds from the Navy Department.

SERVICE PROJECT NUMBERS

The projects listed below were transmitted to the Office of the Executive Secretary, OSRD, from the War or Navy Department through either the War Department Liaison Officer for NDRC or the Office of Research and Inventions (formerly the Coordinator of Research and Development), Navy Department.

Service Project No.	*Title*
	Army Projects
OD-32	Hydrostatic Testing of Shells.
OD-42	Investigation of Methods for the Calculation of the Stresses in the Bases of High-Explosive Shell.
OD-52	Gun Erosion, Including Hypervelocity Gun Studies.
OD-52 Ext.	Stellite Liner for Caliber .60 Machine Gun Barrels.
OD-52 Ext.	Stellite Liner for Caliber .30 Machine Gun Barrels.
OD-52 Ext.	Development of a Satisfactory Production Process for Nitriding and Chromium Plating Caliber .50 Aircraft Machine Gun Barrels.
OD-52 Ext.	Chromium Plating of Caliber .60 T17E3 Machine Gun Barrels.
OD-52 Ext.	Study of the Problem of Excessive Bore Erosion in High Velocity Aircraft Weapons.[a]
OD-154	Theory and Design of Muzzle Brakes.[b]
	Navy Projects
NO-21	Shell Stresses.
NO-23	Gun Erosion.
NO-23 Ext.	Development of Erosion-Resistant Short Liners for the Proposed 3-In./70-Cal. Naval Gun.
NO-26	Hypervelocity Guns and Projectiles.
NO-26 Ext.	Advisory Service in Regard to the Heating and Cooling Problems Connected with the 3-In./70-Cal. Rapid-Fire Gun.
NO-124	Development of an Improved 20-mm Aircraft Cannon to Replace the Hispano-Suiza, AN-M2.
NO-202	Ballistic Calculations.

[a]Division 1 served only in an advisory capacity to the Ordnance Department.

[b]This project was transferred to Division 2, NDRC, at an early stage.



INDEX

The subject indexes of all STR volumes are combined in a master index printed in a separate volume. For access to the index volume consult the Army or Navy Agency listed on the reverse of the half-title page.

Acceleration of projectiles, 79, 133–134
Accelerometers
  capacitance-resistance type, 90
  crystal, 80, 90
  differentiators for velocimeter, 89–90
  mutual-inductance type, 89–90
Accuracy-life of caliber .50 gun barrels, 450–451
  chromium-plated, 458, 464–466, 473, 478
  stellite-lined, 450–451, 473, 478
Acetylene in quenched powder gas, 32
Adaptors for tapered-bore guns
  chromium-plated, 580
  design, 575–576
  for 57/40-mm gun, 571
  tests, 579
  wear after firing, 579
Adiabatic compression of gases
  apparatus, 231–232, 306–307
  maximum temperature and pressure, 305
  pressure as function of time, 306
  studies on powder gas reactions with steel, 305–307
Adiabatic flame temperature of powders, 324–325
  see also Powder gas, temperature calculation, 38–39
  correlation with erosiveness of powder, 324
  correlation with heat input, 318–319, 324
  effect on gun barrel heating, 325
  energy released during burning, 38
ADP crystal (ammonium diphenyl phosphate), 90
Air blasts for cooling guns, 121, 126–127
Air-cooled guns
  cook-off tests, 121
  effect on performance, 127
Aircraft machine gun barrels
  caliber .30; 471–472
  caliber .50; 458, 470–471
  chromium-plated, 458–500
  nitrided, 458–472
  stellite-lined, 445–453, 473–484
Alabandite (gun erosion product), 236
Al-Fin Corporation, aluminum-clad gun barrels, 480
Alloys
  chromium, 360–365, 367–369, 406–407, 416–417
  cobalt, 370, 376–377, 391–407
  electroplated coatings, 416–417
  hot hard, 406
    see also Stellite, metallurgy and properties
  iron, 406–407
    see also Steel
  molybdenum, 374–377, 383–387
  nickel, 351, 376–377, 406–407
  stellite, 391–413, 443–457, 473–484
  TEW, 335, 352, 407
  tungsten, 376, 417, 434
Alpha iron, definition, 248
Altered layers on gun bores
  see Bore surface, thermal transformation; Erosion of guns, bore-surface reactions; Erosion products in gun bores
Aluminum
  gun barrels, 480-481
  thermochemical resistance, 354
  windshields for projectiles, 583
Alundum crucibles for melting molybdenum alloys, 386–387
Ammonia
  for decoppering, 234–235
  in powder gases, 272, 301–302
  reaction with carbon monoxide, 293
Ammoniated water, use in detecting defective projectile shells, 536
Ammonium diphenyl phosphate crystal, 90
AN-M2 gun
  see Johnson 20-mm gun
Antiaircraft guns, 118–119, 124, 133
Armor-piercing projectiles, 189–192
  advantages of hypervelocity projectiles, 9–10
  cap, 191
  deformable projectiles, 191
  De Marre formula, 587–588, 626
  muzzle velocity, 192
  nondeformable projectile, 191–192
  projectile material, 192
  sabot-projectiles, 170, 557–558
  scale effect, 189
  skirted projectiles, 585–590
  specific limit energy, 189–191
  steel, 191
  subcaliber, 192, 626–628
  tests with 57/40-mm tapered-bore gun, 585–590
  tungsten carbide cored, 190, 192
Artillery-type projectiles for erosion-testing gun
  comparison with pre-engraved projectiles, 595
  erosion distribution curves, 313, 315
  progress of erosion, 316
Austenite in eroded guns
  as solvent for carbon and nitrogen, 264, 268
  decomposition, 264
  definition, 248
  detection by electron bombardment, 277
  development, 262–263
  diffraction patterns, 253
  mechanical segregation, 254
  reactivity, 263–264
  removal technique, 257–258
  white layer on gun bores, 247, 264
Automatic gun mechanism, 538–556
  design for hypervelocity ammunition, 549–550
  Johnson 20-mm gun, 538–549, 552–553
  pre-engraved projectiles, 551–556
Axial stresses in shells, 523
A-Z hypervelocity gun, 74–75, 606–608, 617–618

Baldwin-Southwark strain gauge, 90
Ballistic coefficient, formula, 164
Ballistic pendulum, water, 184–185
Ballistics of guns, interior, 54–162
  see also Ballistics of hypervelocity guns, interior
  3-in. gun, 78–94, 135–144
  37-mm gun, 144–148
  band pressure and stress, 152–162
  bore friction, 129–151
  density of loading of powders, 63, 69–70
  heating of guns during firing, 98–128
  instrumentation for experimental firings, 76–97
  methods of calculation, 62–66
  powder gas, 21–53
  pre-engraved projectiles, 525–527
  research recommendations, 628–629
  tapered-bore guns, 75
Ballistics of guns, interior, equations, 55–62
  basic processes, 55
  burning rates of powders, 62
  equation of energy, 57
  equation of motion, 55–57
  equation of state, 36–38, 57–58
  heat and friction losses, 61–62
  interval after burning, 59–60
  interval of burning, 58–59

powder constants, 61
solution, 58–60
Ballistics of guns, interior, firing test measurements, 78–83
bore friction, 133–135
ejection of projectile, 82
firing pin striking primer, 78
gun recoil, 78, 80
jump of gun, 82
muzzle velocity, 79
photographs of muzzle smoke and flash, 82–83
powder gas pressure, 78, 80–82
powder gas temperature, 80, 82
projectile acceleration in gun, 79
projectile deceleration on range, 79
projectile travel in gun, 63, 78–79, 130, 133
radiation from powder gas, 78
strain on gun, 82
Ballistics of guns, interior, instrumentation, 76–97
accelerometers, 89–90
Carderock range, 76–77
comparator for distance measurements on films, 94
flashmeter, 83, 94
gauges, 82, 90–92, 95–97
guns, 77–78
high-speed cameras, 93–94
microflash equipment, 83, 94
microwave interferometer, 92–93, 133
optical ejection indicator, 93
photography, 82–83, 93–94, 274
projectile gauges, 95–97, 133
protractor for differentiating curves, 94–95
radiation pyrometer, 92, 94
recoilmeters, 80, 86–87
recording apparatus, 83–86
solenoids for projectile velocity, 91
strain gauges, 82, 90–91
velocimeters, 80, 86–90
Ballistics of hypervelocity guns, interior, 66–75
design considerations, 70–74
gun length and muzzle velocity, 74
limit to muzzle velocity, 67–68, 619
means of increasing muzzle velocity, 66
90-mm gun, 74–75
optimum conditions, 68–70
pre-engraved projectiles, 525–527
research recommendations, 628–629
sabot-projectiles, 75, 619–624
subcaliber projectiles, 75, 619–624
Ballistics of hypervelocity projectiles, exterior, 163–179
comparison with standard projectiles, 163
deceleration on range, 79, 624
drag coefficient for a cone moving with high velocity, 175–177
firings of caliber .50 projectiles, 179
flight characteristics, 163–165
formula for drag force, 163
motion of a slightly yawing cone at supersonic speeds, 170–175
photographs of projectiles in flight, 83
pre-engraved projectiles, 528–532
shock waves in air, 83, 170
stability of subcaliber projectiles, 165–170
trajectory determination by tracer photography, 177–179
velocity, 79, 179
Ballistics of hypervelocity projectiles, terminal, 180–192
armor perforation, 189–192, 626–628
disruption of a liquid by projectile, 180–189
Band, projectile
see Projectile bands, rotating
Band pressure of gun tubes, 152–162
band-to-bore friction, 129–130
cause of gun erosion, 275
correlation with bore friction, 153–154
dynamic measurements, 159–162
evaluation, 135, 157, 522–523
high-speed strain-recording equipment, 161
measurements with 37-mm projectiles, 156–159, 161–162
prediction, 157
radial stress, 152
relation to erosion, 159
static measurements, 156–159
theory, 152–154
wear of band, 159
Barrels (gun)
aircraft machine gun, 446–453, 458–500
aluminum-clad, 480–481
cannon, 511–512
centering cylinder, 266
cooling methods, 121, 124–128
Fisa protector, 609–614
free-run, 471
heating, 102, 104, 121, 323–325, 466
heavy machine gun, 223–224, 338, 414, 453–454
machine gun, 443–500
nitralloy, 470
nitrided, 413, 458–472, 486–491
special contour, 478
stellite-lined, 155, 413–414, 443–457, 473–484
thermal stresses, 154–156
velocity measurements, 463
X-ray examination of erosion, 251
Barrels, caliber .30; 454–456
chromium-plated, 471–472
design and manufacture, 454–455
erosion-testing gun, 337
M1919A6 barrel, 455–456
nitrided and chromium-plated, 471–472
stellite-lined, 454–456, 471–472
test results, 455–456
Barrels, caliber .50
see also Erosion-testing gun
air-cooling devices, 127
aircraft, 446–453, 458–500
band pressure measurements, 162
chromium-plated, 216, 413–414, 458–484
erosion tests, 223–224, 454
Fisa protector, 611
heating rate, 116–117
heavy barrels, 338, 453–454, 471
need for improvement, 446–447
nitrided, 458–472
Ordnance department tests, 447–451
pilot plant production, 451–453, 485–500
pre-engraved projectiles, 592, 598–599
rotating projectile bands, 533–534
stellite-lined, 446–454, 473–484
thermal stress, 155
velocity loss, 449
Barrels, caliber .60
chromium-plated, 472
Fisa protector, 609–610, 614
nitrided, 456–457, 472
stellite-lined, 456–457
Barrels, chromium-plated
see Chromium-plated gun barrels
Barrels, design, 503–517, 615–617, 630
erosion-resistant liners, 503–506, 513–515
hypervelocity gun, 615–617, 630
replaceable steel liner, 506–509
rifling, 515–517
Barrels, liners for
see Liners for gun barrels
Barrels, steel
see Steel for gun barrels
Barrels, stresses in
see Stress in gun barrels
Battelle laboratory gun, 336
Beryllium, thermochemical erosion resistance, 354
Beta-rays, measurement, 242
Black powder in guns
effect on cracking of steel, 299
effect on gun erosion, 297, 299
Body engraving, 130, 210–212, 516–517
Bofors 40-mm gun mechanism, modifications for firing pre-engraved projectiles, 553, 555–556

Bore friction, 129–151
body engraving, 129
component forces, 129–130
definitive equation, 129
determination from band pressure, 153–154
distribution of energy of the powder, 61–62, 148–151
effect of powder gas pressure, 130
effect of temperature, 99–100
friction coefficient, 157
friction factor, 599–600
friction-time curves, 130–131
heating effect, 100–101, 104, 116–118, 135, 318–319
importance, 129
pre-engraved projectiles, 594
reduction, 275, 523
research recommendations, 629
Bore friction, determination, 130–135
average friction, 135
falling weight tests, 132–133
from ballistic firings, 133–135
from band pressure, 153–154
integration method, 134–135, 147
measurements in T-47 gun, 144–148
measurements in 3-in. gun, 135–144
microwave interferometer, 133
projectile acceleration, 133–134
projectile gauges, 133
static push tests and strain measurements, 132
summary of methods, 130–132
Bore gauge, electrical, 499
Bore lubricant, 354, 533
Bore profile, 197
Bore softening by heat, 261–264
development of martensite, 263
heating process, 261–262
liquefaction of surface, 213–216, 258, 264, 266, 277
rapid-fire guns, 123, 262, 475
single-shot guns, 261–262
Bore surface, coppering, 217–218
decoppering methods, 218, 234–235
definition, 195
erosion products, 251–254
friction, 130
Bore surface, cracking, 276–279, 319
apparatus for studying, 277
causes, 274, 276–279
chromo-plated guns, 213, 410
entrapped erosion products, 227–228
patterns, 212–213
pitting of surface, 277
plaques, 236
powder gas erosion, 274, 276–277
reaction of sulfur gases with gun steel, 299–300
resistance, 335
shearing of lands, 277
stress erosion, 277, 279
Bore surface, erosion
see Bore surface, cracking; Erosion of guns; Erosion products in gun bores
Bore surface, materials
see Erosion-resistant materials; Steel for gun barrels; Stellite, metallurgy and properties
Bore surface, penetration
see Carbon penetration into gun steel; Nitrogen penetration into gun steel
Bore surface, thermal transformation
cracking, 277, 279
critical temperature of steel, 262–263
distribution of transformed layer, 319–320
effect of hydrogen sulfide, 271–272
martensitic layer, 246
metallographic examination, 244–246
rate of formation of transformed layer, 320
relation to erosion, 321, 323–325
softening of bore, 261–263
thickness of transformed layer, 320–321
troostite band, 247
Bore-surface temperature, 105–115
continued fire, 112–113
control during firing tests, 224, 286–287, 303, 461
correlation with erosion rate of gun steel, 323
effect of bore-surface material, 114–115
effect of gas leakage, 115, 123
effect of preheating, 114
effect on reaction of powder gases with gun steel, 250, 269–272, 286–287, 303, 305–306
maximum, 118, 121
melting, 113–114, 257, 333
Bore-surface temperature, methods of determining, 107–112
comparison of methods, 112
Fulcher method, 108
fusion temperature of erosion products, 113–114
Hicks, Thornhill, and Ware method, 111
Hirschfelder, Kershner, and Curtiss method, 108–109
Hobstetter method, 111–112
Nordheim method, 109–111
thermocouples, 105–106, 113
British research
bore-surface temperature, 111
heating of gun barrels, 102, 119
projectile design, 522, 536
sabot-projectile, 585–587
Browning machine guns
see also Barrels, caliber .30; Barrels, caliber .50
cook-off tests, 121
modifications for firing pre-engraved projectiles, 551–552
performance, 446
tests with Fisa protector, 613–614
Bullets
see Projectiles
Burning of powder, 21–28, 58–60
burning constants, 27, 64
effect of pressure, 35
effect of radiation, 27–28
energy released, 38
equation, 58
firings in closed vessels, 48-51
interval after burning, 59–60
interval of burning, 58–59
mechanism, 23–24
pressure-travel curves, 63–65
rate, 24–28, 62
stages, 24

Cadmium-plated projectiles, 354, 535, 599
Caliber of guns
see also Barrels, caliber .30; Barrels, caliber .50; Barrels, caliber .60; Guns, specific calibers
effect on heat input to barrels, 99
effect on muzzle erosion, 206
effect on muzzle velocity, 622
effect on origin erosion, 200
Calorimetric methods of measuring gun heating, 102–104
Cameras, high-speed, 82–83, 93–94, 544
Cannon, automatic (20-mm)
see Johnson 20-mm gun
Cannon tubes
see Barrels (gun)
Capacitance-resistance accelerometer, 90
Carbides, 253–258
chromium, 256–257, 438
formation, 272
iron, 235–236, 253–257, 268
molybdenum, 429
nickel, 257–258
tungsten, 190–192, 433, 572, 583, 620
Carbon, radioactive, 33–35, 285
Carbon equilibrium in powder gas, 33–35, 285
Carbon monoxide, reaction with gun steel, 289–296
ammonia and hydrogen in the charge, 293
isolation and identification of iron carbonyl, 293–296

sulfur in the charge, 291–293
weight losses, 290–291
X-ray analysis of eroded specimens, 291
Carbon penetration into gun steel, 267–269, 284–289
austenite as solvent, 264, 268
bore-surface temperature, 286–287
comparison with surface reactions, 267
compounds, 284–285
conditions for penetration, 268
effect of number of rounds, 288
effect of propellant, 288–289
effects of temperature, 286–288
formation of white layers, 269
iron-carbon system, 267-268
method of determining, 285–286
Carbonaceous materials in eroded gun bores, 254
Carbonyls, 419–424
chemistry of, 419–420
chromium, 434–436
iron, 225, 227, 293–296, 419–420
molybdenum, 420–425
nickel, 419–420
tungsten, 433
Carburization
see Carbon penetration into gun steel
Carderock firing range, 76–77
Carnegie Institution of Washington
combination stellite-lined and chromium-plated gun barrels, 473–484
experimental ballistic firings, 76–97, 159–162, 180–189
gun barrel liner, 223–224, 338
nitrided, chromium-plated caliber .50 aircraft barrel, 458–472
Casting, methods
centrifugal, 362
for stellite, 397, 398, 506
investment, 397
vacuum, 359
Cavitation erosion
apparatus for studying, 233–234
tests, 336
Cementite in eroded guns, 253–257
disengagement by attacking steel, 235–236, 255–257
eutectic temperature, 268
mechanical segregation, 254
Centrifugal in-melting, 362–363, 397–398, 506
CGL firing schedule for erosion-testing machine gun barrels, 462, 474–475
Chalcocite, detection in eroded guns, 252
Chemical alteration of bore surface
see Erosion products in gun bores
Chloridizing apparatus for preparing molybdenum pentachloride, 421
Chrome Gage Corporation, pilot plant for chromium-plating, 492-499
barrels handled and processed, 495
description of project, 492–493
electrical bore gauge, 499
electropolishing tank, 493
plant installation, 493–494
plating procedure, 495–499
Chromium, erosion resistance, 331, 345, 356, 358
Chromium, methods of preparation, 358–363
contaminated by nitrogen, 358
deoxidized with zirconium, 359–360
electro-deposition, 344, 359–360, 417–418
impregnations, 363
inclusions, 358–359
induction-heated vacuum furnace, 357
thermal decomposition of iodide, 360
vacuum casting, 359–360
vacuum melting, 358–359
Chromium, physical properties, 363–365
comparison with gun steel, 363
ductility, 364–365
erosion vent-plug tests, 345, 356, 358
melting point, 331, 358
Chromium alloys, 360–365
cobalt, 406
electroplated coatings, 416–417
machineability, 365
nickel-chromium alloys, 351
physical properties, 363–365
preparation, 357, 360–363
research recommendations, 368–369, 484
thermochemical erosion resistance, 345, 367–368, 406–407
Chromium alloys, gun liners, 364–369
advantages, 365
chemical resistance, 368
disadvantages, 364
firing tests, 365–367
mechanical properties, 368
research recommendations, 368–369
resistance to powder gas erosion, 344–345, 351, 367–368
thermal resistance, 367–368
Chromium carbide in eroded guns, 256–257
Chromium carbonyl
formation, 434–436
Grignard reagent, 434–435
properties, 436
Chromium plate, 408–415, 434–439
see also Electroplated coatings
annealing, 339, 411
composition and properties
duplex coatings, 415, 417
failure in gun bores, 344, 38[illegible] 410, 601
hardness, 408
plating procedures for different base materials, 410–411
research recommendations, 417–418
surface cracks, 277, 409
thickness limitations, 408, 600
types, 410
vapor-phase deposition, 434–439
Chromium-plated adaptors for tapered-bore guns, 580
Chromium-plated gun barrels, 411–415, 458–500
caliber .30; 471
caliber .50; 413–414, 458–471
caliber .60; 472
disadvantages, 213
effect of thickness with pre-engraved projectiles, 600–601
electropolishing, 413
erosion, 213, 216–217, 245, 263–264, 276–277
fired with pre-engraved projectiles, 600–603, 606
heavy machine gun barrels, 414, 471
high- and low-contraction chromium, 412
methods of plating, 411–413, 459, 488, 495–499
naval guns, 356
90-mm, 606–608, 617–618
nitrided barrels, 413, 459–460, 465–471, 486–491, 495
pump plating, 414
specifications, 413, 460, 491
stellite-lined, 413, 471–484, 491
temperature-time curves, 461
thermally-altered surface layer, 245
Chromium-plated gun barrels, firing tests, 460–465
accuracy measurements, 463–465
ammunition, 462–463
firing schedules, 460–462
Fisa protector, 613
increase in muzzle velocity and cyclic rate, 462
pre-engraved projectiles, 592, 601, 603
targets, 462–464
temperature-time curves, 461
velocity measurements, 463
Chromium-plated gun barrels, performance, 465–470
accuracy-life, 465–466
advantage of choked muzzle, 466
gauges, 468
keyholing bullets, 466
projectile engraving, 465
star gauge curves, 467

tippers, 468–469
velocity-life, 466–468
Chromium-plated gun barrels, pilot plants, 485–500
Chrome Gage Corporation, 492–499
Doehler-Jarvis Corporation, 485–492
recommendations, 499–500
Chromium-plated gun barrels, stellite-lined
see Stellite-lined and chromium-plated gun barrels
Chro-mow steel gun barrels, 470, 483
Chronograph, Aberdeen, 223, 309, 463
Circumferential strain in gun barrels, 155–156
Climax Molybdenum Company
chromium-base alloys for gun liners, 356
molybdenum carbonyl preparation, 420–425
thermit melting of molybdenum, 386–387
vacuum melting of molybdenum, 385–386
Coatings, erosion-resistant
see Electroplated coatings; Erosion-resistant materials; Vapor-phase plating
Cobalt alloys, 351–357
see also Stellite, metallurgy and properties
hardened iron-nickel-cobalt-chromium alloys, 351–352, 406–407
molybdenum, 370, 376–377, 383–385
resistance to powder gas erosion, 347–348, 351
steel, 352
Cobalt gun liners, 347–348, 406
Cobalt plating, 415–416
Cobalt-chromium alloy gun liners
see Stellite gun liners
Colmonoy gun liner, 350
Columbium, thermochemical erosion resistance, 354
Comparator for distance measurements on films, 94
Compression of gases, adiabatic
apparatus, 231–232, 306–307
maximum temperature and pressure, 305
pressure as function of time, 306
reactions with steel, 305–307
Contact printing for study of erosion products, 240, 252
Continuous recoilmeter, 87
Cook-off in guns, 117, 121
Cooling of gun barrels, 124–128, 481, 484
see also Heating of gun barrel during firing
air blasts, 121, 126–127
convection, 126
coolants, 127
devices, 125
injection sprays, 127–128
radiation, 126
rates of cooling, 117, 124, 126
water jackets, 127
Copper crusher gauge, use in erosion-testing gun, 309
Copper for gun barrels, 353–354
Copper potassium chloride for removal of erosion products, 235, 255
Copper sulfides (gun erosion product), 252–253
Coppering of gun bores
decoppering methods, 218, 234–236
definition, 195
entrapped erosion products, 235, 251–254
friction, 100, 130, 135
Corrosion of bore surface
see Bore surface, thermal transformation
Cracking of bore surface
see Bore surface, cracking
Crane Company
gun liners for testing materials, 224, 338, 443–444
means of inserting resistant gun liners, 443–446, 503–504, 615
pilot plant for manufacturing stellite-lined barrels, 451–453
replaceable steel liner, 507–512
Crystal accelerometer, 80, 90
Crystal gauges, piezoelectric, 96–97
Cyanides in eroded guns, 249, 253
Cyanogen in powder gases, 272
Cyclonite (propellant), 21
erosiveness, 322, 327
reaction products, 289
Cyclops KL gun liners, 352

Decoppering of gun bores, 218, 234–235
Deformable projectiles
see also Skirted projectiles
armor penetration, 191
De Marre formula for projectile penetration of armor, 190, 587–588, 626
Die surfaces, molybdenum-plated, 432
Diffraction techniques for studying gun erosion
see Electron diffraction, gun erosion studies; X-ray diffraction in gun erosion studies
Disks, rupture, 225, 228, 310
Doehler-Jarvis Corporation, pilot plant for chromium-plating, 485–492
dimensions of nitrided-plated barrels with choked muzzles, 489–491
procedure for nitrided barrels, 486–489
stellite-lined gun barrels, 491–492
Double-base powders, erosiveness
see Powders, double-base, erosiveness
Dowmetal sabot-projectiles, 562
Drag coefficient, 175–177
conical-headed projectile, 176
drag function, 176
effect of body engraving, 211
effect of yaw, 175–176
formula, 163
function of Mach number, 175
reduction of drag, 532
suggestions for further research, 176–177
Draw rifling process for gun tubes, 504
Duplex coatings, 345, 415, 428
Dural sabot-projectiles, 562

E6 thermindex paint, 107
Eberbach Microvickers hardness tester, 460
8-in. howitzer, Mark VII, 124
Ejection indicator for gun tubes, 82, 93
Electrical bore gauge, 499
Electron bombardment, gun erosion studies
apparatus, 232–233
cracking of bore surface, 277, 335
formation of austenite, 277
thermal shock, 277
Electron diffraction, gun erosion studies, 237–239
comparison with X-ray diffraction, 237
detection of cyanides, 249, 253
detection of magnetite, 270
diffraction patterns, 237
erosion products from different powders, 249
erosion products from sulfur, 298–299
limitations, 237–238
microplow, 238–239
test blocks exposed to powder gases, 249
unidentified lines, 239
vent plugs, 228, 230
Electronic pulsers, 86
Electroplated coatings, 408–418
see also Chromium plate; Vapor-phase plating
alloy deposition, 416–417
availability of electrodeposited metals, 408–409
characteristics, 408, 418
cobalt, 415–416
current distribution during plating, 498–499

gun barrels, 411–415, 458–500
molybdenum, 409, 417
nickel, 350, 415–416
pump plating, 414
requirements, 408
research recommendations, 417–418
tantalum, 409
tungsten, 417
Electropolishing tank for chromium-plating, 413, 488, 493
Elkonite
projectile nose tips, 583
resistance to powder gas erosion, 346
Energy distribution of gun powder, 148–151
average temperature, 148
energy balance during burning, 38, 149
energy equation, 148
heat, 148–149
kinetic energy, 148, 620–622
Energy of projectiles
equation, 57
in water, 186–187
kinetic, 148
loss during flight, 163–164
loss in gun firing, 61–62, 98–99, 163
specific limit energy for armor perforation, 189–191
Engraving of projectiles
see Pre-engraved projectiles; Projectile engraving
Epsilon iron nitride in eroded guns, 255–256
detection, 249
mechanical segregation, 255
nitrogen content, 268
stability, 253
surface layers, 256
Equations of interior ballistics
see Ballistics of guns, interior, equations
Equivalent stress in gun tubes, 511
Erosion of guns, 195–327
asymmetry, 201, 207–208
correlation with thermal transformation, 323–325
definition, 195
groove erosion, 195, 198, 203
hypervelocity guns, 11, 13, 16, 615, 629
land erosion, 195, 198, 203, 277, 602
liner joint, 202–203, 255, 274, 403, 476, 508
measurement, 197–198
muzzle erosion, 195, 203–212
origin erosion, 195, 198–203, 207
powder gas erosion, 272–275, 283–327
pre-engraved projectiles, 313–317
relation to muzzle velocity, 10, 200–201, 206
research recommendations, 629
scoring, 274
swaging of rifling, 123, 216, 275–276, 458–459
Erosion of guns, bore-surface reactions, 267–272
see also Bore surface, cracking; Coppering of gun bores
carbon penetration, 264, 267–269, 284–289
equilibrium curves, 271
hydrogen sulfide, 271–272, 294
liquefaction of bore surface, 213–216, 264, 266, 277
nitrogen compounds, 267–269, 272, 300–304
oxidation, 267, 269–270, 283
pebbling of surface, 215, 278–279, 319
softening of the bore, 213–216, 261–264, 266, 277
thermal transformation, 262–264, 319–325
water gas components, 269–271
white layers, 247, 256, 264, 269
Erosion of guns, causes, 244, 260–279
bore design, 276
bore friction, 275
chemical factors, 260, 267–272, 333
cracking of bore surface, 276–279
distortion of rifling, 216–217
effect of chromium-plate, 263–264, 410
gas leakage, 273–274, 592–594
inclusions, 215
liquefaction of bore surface, 213–216, 264, 266, 277
mechanical, 272–276, 333–334
mushrooming, 263
powder composition, 297, 299–300, 307, 326–327
principal factors, 260–261
projectile, 558
stress, 230, 279
sulfur, 296–300
thermal factors, 120–121, 154–156, 261–267, 277, 513–514
Erosion of guns, laboratory studies, 219–243
see also Erosion products in gun bores
apparatus for cavitation erosion, 233–234, 336
caliber .30 barrel, 286, 294–295, 297, 302
caliber .50 erosion-testing gun, 220–223, 309–310, 336–337
caliber .50 machine guns, 223–224
chemical analysis, 239–240
collection of particles and gases discharged from gun barrels, 230–231
determination of the melting temperatures of erosion products, 240
electron bombardment apparatus, 232–233, 277, 335
electron diffraction, 228–230, 237–239, 249, 270, 298–299
firing tests, 220–231
gauges, 197–198, 222–223, 225
isotopic tracers, 240–243, 285, 297
metallographic examination of eroded surfaces, 236–237, 244–246, 319–321
vent plugs, 224–232, 310–311, 322–323, 334–335
visual examination of eroded surfaces, 236–237
X-ray diffraction, 237–239, 248–251, 291, 301
Erosion of guns, mitigation
see also Liners for gun barrels
electroplated coatings, 408–418, 460, 488
Fisa protector, 609–614
modification of powders, 283, 300, 307, 325–327
pre-engraved projectiles, 591–608
requirements, 408
test of ferrosilicon, 327
thermodynamic considerations, 326–327
Erosion products in gun bores, 244–259, 321–322
collection of gases and particles, 230, 249, 301, 335
comparison of single- and double-base powders, 248–251
entrapped in the coppering, 251–254
fusion temperature, 113–114, 240, 258
melting, 257
vinylite coatings for examination, 236
Erosion products in gun bores, removal techniques, 234–236, 254–258
by attacking the steel, 235–236
chemical removal, 255–258
copper potassium chloride solution, 235, 255
coppering and entrapped products, 234–235, 251–254
degreasing of test specimens, 234
fractionation of erosion products, 236
mechanical removal, 234, 254–255
Erosion products in gun bores, specific substances
alabandite, 236
austenite, 247–249, 253–254, 257–258, 262–264

cementite, 235–236, 253–257, 268
chromium carbide, 256–257
cyanides, 249, 253
epsilon iron nitride, 249, 253, 255–256, 268
ferrite, 248–249
galena, 252
iron carbides, 253–257, 268
iron carbonyl, 225, 227, 293–296, 419–420
iron nitrides, 253, 255–256, 268
iron oxides, 273
lead, 252
magnetite, 254, 270, 306
martensite, 263
nickel carbide, 257–258
nitrides, 255–256, 268
potassium sulfate, 252
pyrrohotite, 254
sphalerite, 253
wüstite, 249, 253
Erosion products in gun bores, surface layers, 244–248, 255–258
austenite-rich layers, 257, 262–264
cementite-rich layers, 256
characteristics, 244
chromium-plated guns, 245
constituents, 255
effect of single-base powders, 247
inner and outer white layer, 244, 247–248, 258, 264
liquefaction of bore surface, 213–216, 258, 264, 266, 277
martensite layer, 246, 263
techniques of studying, 234–240, 244
thermally-altered layer, 245–246, 258–259, 261–264
troostite band, 247
Erosion studies in vents, 220–232
see also Erosion vent-plug tests
apparatus, 228, 230
D-shaped cross section, 227–230
method, 230, 334–335
results of studies, 249, 272–275, 277–279, 299–300
rifled barrel as vent, 225–227, 294
stressed vents, 230, 272–275
studies of cracking, 227–228
use of oxygen and carbon monoxide mixtures, 227
Erosion vent-plug tests, 224–230
apparatus, 224–225
carbon monoxide reactions, 290–293
chromium, 334, 345, 356, 358
detection of iron carbonyl, 225, 227, 294
powders, 310–311, 322–323
resistance of metals and alloys, 334–335
rupture disks, 225, 228, 310
subjected to adiabatically compressed gases, 231–232, 305–307
X-ray diffraction examination, 228, 230
Erosion-resistant materials, 331–439
applications, 343–355, 440–506, 513–515
chemical resistance, 333
chromium and alloys, 263–264, 344–345, 351–352, 356–369, 416–417
cobalt alloys, 391–407
desirable properties, 333–334
electrodeposited coatings, 408–418
evaluation, 343–355
fluorocarbon coating, 354
machineability, 343, 371, 396
melting points, 333
molybdenum, 334, 370–390
nickel alloys, 334, 349–351, 406–407
parco-lubrite coating, 354
research program, 331–332
research recommendations, 629
steels, 337
stellite, 334, 391–407
tantalum, 334, 347
thermal properties, 333, 338–340, 513–514
tungsten, 334
types, 331
vapor-phase plating, 419–439
Erosion-resistant materials, mechanical properties, 340–343
adherence of coatings, 343
flaw detection, 343
hardness, hot-hardness, and wear resistance, 342
machineability, 343
requirements, 333–334
tensile strength, ductility, and modulus of elasticity, 340
Erosion-resistant materials, test methods, 334–343
Battelle laboratory gun, 336
bend and ring-compression tests, 343
caliber .30 machine gun liners, 337
caliber .50 erosion-testing gun, 336–337
caliber .50 machine gun liners, 338
cavitation erosion tests, 336
erosion vent plugs, 334–335
firing of metal particles into an evacuated tube, 335–336
hydrostatic tube testing, 342–343
notch impact tests and high velocity impact tests, 340–342
resistance to surface cracking, 335
Erosion-testing gun, caliber .30; 337
Erosion-testing gun, caliber .50; 219–223
applications, 219, 222–223, 336–337
design, 220, 309, 336–337
limitations, 223
molybdenum liners, 377–385
tests on Fisa protector, 612–614
tests using pre-engraved projectiles, 313–317, 592–600
use of gauges, 222, 309
X-ray examination of barrels, 251, 310, 321
Erosion-testing gun, propellant tests, 313–322
artillery-type bullets, 313, 317
chemical products on the bore surface, 321–322
conditions of test, 309
distribution of erosion, 313–315
erosion rate, 317–318
heat input to the barrel, 318–319
measurements, 309–310
metallographic changes accompanying firing, 319–321
pre-engraved bullets, 313–317
progress of erosion, 313, 316–317
X-ray diffraction examination of barrels, 251, 310, 321
Erosive action of powders
see Powders, erosiveness
Exelloy gun steel, 484
Explosion vessel for vent-plug tests, 224–225
Explosives for propellants, 21
Exterior ballistics of projectiles
see Ballistics of hypervelocity projectiles, exterior

Falling weight apparatus for determining bore friction, 100, 132–133
Ferrite (erosion product), 248
Ferrosilicon
reduction of gun erosion, 327
resistance to chemical attack, 336
.50 caliber guns
see Barrels, caliber .50
57-mm gun, erosion products, 255
57/40-mm tapered-bore guns
accuracy tests, 584–585
design, 570–572
design of skirted projectile, 572
muzzle adaptor, 571
wear after firing, 580
57/40-mm tapered-bore guns, armor penetration tests, 585–590
ballistic limits of projectiles, 585–587
DeMarre formula, 587–588
design changes to improve penetration, 585
perforation range comparisons, 588–590
Firing schedules for testing gun barrels, 309, 460–462, 474–475
Fisa protector for gun barrels, 609–614
caliber .50; 612–613

caliber .60; 609, 614
design, 14, 610–612
effect on velocity-life, 609
extent of engraving, 611
manufacture, 612
tests, 612–614
37-mm, 614
5-in. gun, 253
Flame temperature of powders
see Adiabatic flame temperature of powders
Flashmeter, measurement of muzzle flash intensity, 83, 94
Flight characteristics of hypervelocity projectiles, 163–165
ballistic coefficient, 164
range and time of flight at high speeds, 164–165, 624–626
subcaliber projectiles, 165, 619–626
velocity and energy loss, 163–164, 619–623
Fluorocarbon for coating gun bores, 354
FNH-M1 gun powder
effect on gun erosion, 250
erosion products, 270
temperature of powder gas, 122
FNH-M2 gun powder, erosiveness, 250, 270, 289
Forcing cone, 158, 198, 595
Formulas
ballistic coefficient of projectile, 164
burning of gun powder, 58
De Marre formula for projectile penetration of armor, 190, 587–588, 626
drag coefficient of projectile, 163
energy distribution of gun powder, 148
energy of projectile, 57
Lamé formulas for gun tube stresses, 152, 511
moment coefficient of projectile, 167
motion of projectile, 55-57
muzzle velocity, 63, 67–68, 620–624
projectile design, 521–522
stability of subcaliber projectiles, 168
stresses in gun barrels, 511
4.7-in. gun
origin erosion, 199
star-gauge curves, 196
14-in. gun, 203, 212, 253
40-mm guns, 118, 121, 553–556
Franklin Institute
caliber .50 erosion-testing gun, 220–223, 336–337, 377–385
Fisa protector, 609–614
"Free-run" machine gun barrels, 471
Friction in guns
see Bore friction
G8-type projectile, 163–164
Galena, detection in eroded guns, 252
Gamma iron, 248
see also Austenite in eroded guns
Gamma-prime iron nitride in eroded guns, 255–256, 268
Gas compression, adiabatic
apparatus, 231–232, 306–307
maximum temperature and pressure, 305
pressure as function of time, 306
studies on powder gas reaction with steel, 305–307
Gas leakage in guns, 592–596
bore surface temperature, 115, 123
causes, 115
erosive effect, 273–274, 562, 592–594
pre-engraved projectiles, 596
pressure, 202
sabot-projectile, 562
swaging of rifling, 123
velocity performance, 202, 595–596
Gas pressure shock waves, suppression in guns, 576–578
Gas turbulence in guns, 53, 266, 273, 613
Gas-operated machine gun
see Johnson 20-mm gun
Gauges
electrical bore gauge, 499
erosion gauge, 196–198, 222–223, 225
liner rejection gauge, 468
plug, 198, 222, 309–310, 469–470
Sheffield Precisionaire gauge, 487
star gauge, 196–198, 222, 467
thread-collocating gauge for machining gun tubes, 578
use in production of chromium-plated gun barrels, 486–488, 499
Gauges for ballistic measurements, 90–92, 95–97
bore friction measurements, 133
copper crusher, 225, 309
piezoelectric, 96–97
pressure, 91–92, 309
projectile gauges, 95–97, 133
resistance, 91–92
strain, 82, 90–91
Geiger-Mueller counters, 240–242, 296–297
detection of radioactive carbon, 285
detection of sulfur in eroded guns, 240–241, 296
gun erosion studies, 242
use of rifle barrel, 297
Geophysical Laboratory, C.I.W.
combination stellite-lined and chromium-plated gun barrels, 473–484
experimental ballistic firings, 76–97, 159–162, 180–189
gun barrel liner, 223–224, 338
nitrided, chromium-plated caliber .50 aircraft barrel, 458–472
GL-135 firing schedule for testing heavy barrels, 461
Gold-palladium alloy, thermochemical erosion resistance, 354–355
Greenough stereoscopic microscope, 236
Grignard reagent for producing chromium carbonyl, 434–436
Groove erosion in gun bores
at muzzle, 203
at origin of rifling, 198
definition, 195
Gun ballistics
see Ballistics of guns
Gun barrels
see Barrels (gun)
Gun bores
see Bore friction; Bore softening by heat; Bore surface; Heat input to bore surface
Gun chamber
fluting, 457
integral with liner, 457
Gun erosion
see Erosion of guns
Gun firing, thermal effects, 98–128
see also Bore-surface temperature; Cooling of gun barrels; Heat input to bore surface; Heating of gun barrel during firing; Thermal stresses in gun barrels
accuracy drop, 121–122
ballistics, 121–123
bore friction, 99–100
burning rate of powders, 27
erosion, 120–121, 308
expansion of bore, 123, 466, 476–477, 480
pressure and velocity changes, 122–123
softening of bore surface, 213–218, 234–235, 251–254, 261–264, 276–279
weakening of barrel wall, 123–124, 476–477, 480
Gun friction
see Bore friction
Gun liners
see Liners for gun barrels
Gun mechanism, automatic, 538–556
design for hypervelocity ammunition, 549–550
Johnson 20-mm gun, 538–549
pre-engraved projectiles, 551–556
Gun powders
see Powders
Gun recoil measurements
accelerometers, 80, 89–90
ballistic firing tests, 78, 80

displacement of gun, 80
pressure in recoil cylinders, 82
recoilless gun blocks, 431–432
recoilmeters, 80, 86–87
starting time, 78
velocimeters, 80, 88–89
Gun steel
see Steel for gun barrels
Gun tubes
see Barrels (gun)
Guns, coppering
decoppering methods, 218, 234–236
definition, 195
entrapped erosion products, 235, 251–254
friction, 100, 130, 135
Guns, general types
air-cooled, 121, 127
antiaircraft, 124
for firing pre-engraved projectiles, 551–553, 555–556, 591–608
howitzers, 124, 563–564, 566
tapered-bore, 15, 75, 569–590
water-cooled, 121, 127
Guns, pressures in
see Pressure in guns
Guns, rifling design
see Rifling of guns
Guns, specific calibers
see also Erosion-testing gun
.30 caliber, 337, 454–456, 471–472
.50 caliber; *see* Barrels, caliber .50
.60 caliber, 456–457, 472, 609–610, 614
3-in.; *see* 3-in. gun
3.7-in., 119, 121, 249
4.7-in., 196, 199
5-in., 253
8-in., 124
14-in., 203, 212, 253
20-mm Hispano-Suiza, 118, 121, 133
20-mm Johnson automatic, 123, 538–549
37-mm; *see* 37-mm guns
40-mm, 118, 121
57-mm, 255
57/40-mm tapered-bore, 570–572, 580, 584–590
75-mm, 119, 156–159, 535–536, 563–564
76-mm, 122, 214, 564–565
90-mm, 74–75, 507–510, 564–567, 606–608, 617–618
105-mm, 118–119, 124, 566
155-mm, 128, 201, 210
Bofors, 40-mm, 553, 555–556
Browning machine gun, 121, 212, 551–552, 613–614
Hispano-Suiza, 118, 121, 133
Johnson M1945; 455
Hastelloys
gun liners, 350
thermochemical erosion resistance, 407
Haynes Stellite Company, investment-cast stellite liners, 447
Heat input to bore surface
see also Bore-surface temperature; Heating of gun barrel during firing
bore friction as source of heat, 61, 100-101, 104, 116–118, 318–319
correlation with erosiveness of powder, 324
correlation with flame temperature of powder, 318–319, 324
powder gases as source of heat, 62, 99, 101-102, 149
radiation as source of heat, 99
37-mm gun, T47; 101
3-in. gun, Mark 3; 101
variation with caliber, 109
Heat input to bore surface, methods of measurement, 102–107
calorimetric methods, 102–104
embedded thermocouple, 105–106, 113
heating by firing at steady rate, 102–103
strain measurements, 82, 106
surface-temperature measurements, 104–105
thermal analyzer, 107
Heat losses in guns, 61–62
Heat of explosion of powder gas
see Powder gas, thermodynamics
Heat transfer coefficient, 100
Heating of gun barrel during firing
see also Bore-surface temperature; Cooling of gun barrels; Heat input to bore surface; Thermal stresses in gun barrels
ballistic equations, 61–62
effects, 120–124, 216
rate of heating, 115–120
temperature-time curves for machine-gun barrels, 116–117, 461
Heavy machine gun barrel
caliber .50; 338, 453–454, 471
chromium-plated, 414
liners for, 223–224
HIA grade 160 gun steel, 483
High-speed cameras, 82–83, 93–94
High-speed machine gun, 478
Hispano-Suiza gun
bore-friction measurements, 133
improvement, 538
Mark V (20-mm), 118, 121
sabot-projectiles, 562–563
Hoop stress in shells, 152, 523
Howitzers
8-in. Mark VII, 124
75-mm, 563–564
105-mm, 566
Hydraulic obturator, 96
Hydrocyanic acid in powder gases, 272
Hydrogen in eroded guns
reaction with carbon monoxide, 293
reaction with steel, 274–275
Hydrogen sulfide, 292–294
effect on bore surface, 271–272
effect on erosiveness of carbon mixtures, 292–293
effect on gun erosion, 294
molybdenum sulfide plates, 427
reaction with steel, 296
Hydrostatic tube-testing device, 342–343
Hypervelocity guns
automatic mechanism, 549–556
A-Z gun, 74–75, 606–608, 617–618
definition of hypervelocity, 8
erosion, 11, 615
erosion-resistant liners and coatings, 14
Fisa protector, 14, 609–614
gun tube design, 503–517, 630
interior ballistics, 66–75, 628–629
molybdenum liners, 382–385, 616–617
replaceable steel liners, 14, 507
research recommendations, 628–630
rifling design, 515–516
stellite liners, 405, 615–616
summary of volume, 1–4
tapered-bore, 15, 75, 569–590
Hypervelocity guns, ballistic design considerations, 70–74
choice of powder, 73–74
limiting density of loading, 70–71
limiting pressure, 71–72
90-mm gun, 74
preferred volume ratio, 72
Hypervelocity projectiles, 9–15, 163–170, 557–608
see also Projectiles
advantages, 9–10, 618–628
comparison with standard, 163
drag coefficient, 175–177
flight characteristics, 163–165
limitations, 10–12
pre-engraved, 313–317, 523–533, 551–556, 591–608, 630
range, 9, 164–165, 202
sabot, 169–170, 557–568, 585–587, 630
skirted, 569–590, 620, 630
subcaliber, 165–170, 618–628
summary of volume, 1–4
tungsten carbide-cored, *see* Tungsten carbide-cored projectiles

Hypervelocity projectiles, armor perforation
see Armor-piercing projectiles
Hypervelocity projectiles, ballistics
see Ballistics of hypervelocity projectiles
Hypervelocity projectiles, design, 518–537
British, 522, 536
core, 572, 583
low-stress rotating bands, 533–536
materials used, 192
methods for detecting defects in shells, 536–537
pre-engraved, 523–525
sabot, 559–562
stresses in shells, 518–524
Hypervelocity projectiles, effect of yaw, 170–175
drag coefficient, 175–176
normal force and center of pressure, 172–174
normal head force coefficient and yaw ratio, 174–175
ratio of shock yaw to projectile yaw, 173–174
recommendations for future research, 177
theory, 170–172
Hypervelocity projectiles, liquid penetration, 180–189
effect of velocity, 180
firings into cans of liquid, 180–181
motion pictures of jets during disruption, 181–183
pressures in water, 184–187
research recommendations, 187
shock waves, 181–183, 187–188
transfer of momenta, 188–189

Injection sprays for cooling gun barrels, 127–128
Interferometer, microwave, 92–93, 133
Interior ballistics
see Ballistics of guns, interior; Ballistics of hypervelocity guns, interior
Iridium, thermochemical erosion resistance, 355
Iron alloys
see also Steel
thermochemical erosion resistance, 331, 406–407
Iron carbide in eroded guns, 253–257
disengagement by attacking steel, 235–236, 255–257
eutectic temperature, 268
mechanical segregation, 254
Iron carbonyl from eroded guns, detection, 293–296
chemistry of, 419–420
effect of hydrogen sulfide, 294
experimental method, 293
formation, 225, 227
gas mixture in caliber .30 barrels, 294
location of erosion products, 293–294
solid iron-bearing deposits, 295–296
vent plugs, 225, 227, 294
Iron nitrides in eroded guns
epsilon iron nitride, 249, 253, 256, 268
formation, 268
gamma-prime iron nitride, 255–256, 268
mechanical segregation, 255
resistance, 253
Iron oxides in eroded guns, 273
Iron sulfide in eroded guns, 254
Iron-carbon system, 267–268
Iron-nitrogen system, 268
Isothermal transformation diagram for steel, 275
Isotopic tracers, gun erosion studies, 240–243, 285, 296
demonstration of carbon equilibrium, 240–241
Geiger-Mueller counters, 242
sampling, 241–242
temperature of specimen, 242–243

Jet propulsion motor, radiation and temperature of gases, 51–52
Johnson 20-mm gun, 538–549
automatic chambering mechanism, 540–541, 552–553
case ejection and cocking failure, 544
description of models, 539–542
firing rate, 545–549
kinematic analyses, 544–545
Navy specifications, 538–539
parts breakage, 543–544
"pulled" projectiles, 543
rebound of impacting parts, 543
recommendations, 548–549
Jump ratio of projectiles, 526

Keyholing projectiles, 450, 466
Kinetic energy of projectiles, 148

Lamé formulas for gun tube stresses, 152, 511
Land erosion in gun bores
at muzzle, 203
at origin of rifling, 198
definition, 195
effect on gun life, 602
shearing of lands, 277
Lead in eroded guns, detection, 252
Leeds and Northrup Company, heat measurements for guns, 104
Linear velocimeter, 89
Liners for gun barrels, 440–457
Cyclops KL steel liners, 352
erosion, 202–203, 255, 274, 403, 509
investment-cast stellite, 397, 447, 615
90-mm gun, 507–510
protrusion of, 124
replaceable steel liners, 14, 507–510
Liners for gun barrels, design, 503–509
bonding of liner to barrel, 506
Crane Company liner, 224, 338, 443–444
effect of differences in thermal properties, 513–514
expansion of the liner by draw rifling, 504
Geophysical Laboratory liner, 223–224, 338, 473–484
mechanical retention of the liner, 504–506
methods of inserting, 366–367, 443, 503–509
research recommendations, 368–369, 484, 616–617, 629
shrink fit of tube and liner, 503–504, 512
stresses in, 512–515
support of brittle liner materials, 513
Liners for gun barrels, materials tested, 343–355
characteristics, 331, 351
chromium and alloys, 344–345, 351–352, 364–369
cobalt and alloys, 347–348, 351–352, 391–407
copper and alloys, 353–354
evaluation, 351–352
hardened alloys, 350–351
molybdenum, 345–346, 370–390, 616–617
monel-metal, 350
nickel and alloys, 349–352, 406–407
Refractaloy No. 70; 351–352
requirements, 344
research recommendations, 617, 629
steel, 14, 351–353, 506–509, 513
stellite, 351, 391–407, 443–457, 473–484
tantalum, 347
TEW alloy, 335, 352, 407
tungsten, 346–347
Link-Belt Company, nitriding of steel, 459–460
Longitudinal stresses in shells, 153, 524–525
Lubrication of gun bore, 354, 533

Mach number, relation to drag coefficient, 175
Machine guns
see Browning machine guns; Guns
Magnetite in eroded guns
detection by electron diffraction, 270

formation, 306
mechanical segregation, 254
Magnetron anodes, molybdenum-plated, 432
Martensite in eroded guns, 263
Martensitic layer, 246
Massachusetts Institute of Technology, strain-recording equipment, 161
Metals, plating
see Electroplated coatings; Vapor-phase plating
Metals, thermochemical erosion resistance
see Thermochemical erosion resistance of metals and alloys
Methane in quenched powder gas, 32
Microflash equipment, 83, 94
Microplow for electron diffraction measurements, 237–239
Microscope, stereoscopic, 236
Microwave interferometer, 92–93, 133
Mises-Hencky theory, 152, 510, 522
Molybdenum, 370–390
bend strength and yield, 374
carbides, 429
chloride, 420–421
coatings, 388–390, 409, 420–433
commercial, 370–373
effect of temperature on hardness, 376
hardening by alloying, 375–376
Molybdenum, methods of preparation, 385–389
commercial process, 370–371
hydrostatic compression test, 375
inductive sintering in an atmosphere of hydrogen, 388–389
melting in thorium oxide refractories, 387
thermit meltings, 387–388
vacuum melting in an electric arc, 385–386
vacuum melting in an induction furnace, 386–387
working schedule, 373–375
Molybdenum, vapor-phase plating, 420–433
apparatus, 426
applications, 430–432
general procedure, 424–425
plate-to-metal bond, 428–430
properties of plates, 425–428
recommendations, 432–433
sulfide plates, 427, 432
Molybdenum alloys, 374–377, 383–387
cobalt, 370, 376–377, 383–385
electroplated coatings, 417
hardness, 376
melting alloys in aluminum oxide crucible, 386–387
nickel, 376–377
tungsten, 376, 434
vacuum-melting furnace, 385–386
working schedule, 374
Molybdenum carbonyl, 420–425
drying and sublimation, 423–424
flow-sheet for production, 425
formation, 420
preparation of anhydrous molybdenum chloride, 420–421
preparation of crude product, 421–422
properties of sublimed product, 423–424
recommendations, 424
removal of ether, 422–423
steam distillation, 423
Molybdenum gun liners
alloy with cobalt, 383–385
caliber .50 erosion-testing gun, 377–385
causes of failure in tests, 382–385
commercial molybdenum, 373
firing tests, 382–385
insertion, 514
requirements, 431
suitability of alloys, 346
thermal properties, 513–514
3-in. gun, 616–617
Molybdenum gun liners, method of fabrication
brazed-in one-seam tube, 381
cast-bonded molybdenum-steel strip, 381–382
design considerations, 377
for caliber .50 erosion-testing gun, 377–385
seamless tube, 382
tube made from flat disks, 381
wire-wrapped tube, 381
Molybdenum gun liners, stave-type, 377–381
construction, 378–379
deficiencies in design, 380–381
milling operation, 383
precision twisting, 379, 382, 384
seams, 378
stresses, 377–378, 514–515
troughing operation, 380
Molybdenum pentachloride, apparatus for preparing, 421
Molybdenum steel for machine gun barrels, 353, 381–382, 470, 482–483
Molybdenum-tungsten alloy plates, 434
Moment coefficient, formula, 167
Monel-metal gun liners, 350
Motion of projectile, equation, 55–57
Mushrooming (pocketlike erosion), 263
Muzzle adaptors for 57/40-mm tapered-bore guns, 571, 575–580
chromium-plated, 580
design, 575–576
tests, 579
vents, 578
wear after firing, 579
Muzzle blast
effect of gun length, 72
photography of flash, 82–83
Muzzle erosion, 203–212
asymmetry of erosion, 207–208
correlation with body engraving, 210–212
correlation with origin erosion, 207
definition, 195
dependence on caliber, 206
dependence on muzzle velocity, 206
development with firing, 204–206
effect on gun performance, 208–211
effect on projectile yaw, 211
land and groove erosion, 203
variation along the bore, 203–204
Muzzle flash
effect of gun length, 72
photography, 82–83, 93–94
Muzzle velocity
dependence on gun caliber, 622
effect of gun length, 74
effect on armor perforation, 192
formula, 63
means of increasing, 66, 549–550
measurement, 79
relation to erosion, 200–201, 206
subcaliber projectiles, 622
upper limit, 67–68, 619

National Bureau of Standards
experimental ballistic firings, 76–97, 159–162
nitrided, chromium-plated caliber .50 aircraft barrel, 458–472
Nickel
alloys, 350–352, 376–377, 406–407
carbide, 257–258
carbonyl, 419–420
gun liners, 349–352
plating, 350, 415–416
90-mm guns
chromium-plated, 606–608
cooling, 128
design, 74–75, 606–608
erosion, 249, 509–510
molybdenum liner, 616–617
replaceable steel liner, 507–509
sabot-projectiles, 564–567
Nitralloy for machine gun barrels, 470
Nitric oxide in quenched powder gas, 32
Nitrided and chromium-plated gun barrels, 458–472
accuracy and velocity-life, 458
caliber .60; 456–457, 472
hardness profile, 460

method of nitriding, 413, 459–460
nitralloy, 470
specifications, 459–460
stellite-lined and chromium-plated, 401–402, 491–492
temperature-time curves, 461
velocity-life, 458, 466–468
Nitrided and chromium-plated gun barrels, firing tests, 460–465
accuracy measurements, 463–465
ammunition, 462–463
change in muzzle velocity versus cyclic rate, 462
firing schedules, 460–462
targets, 462–464
temperature-time curves, 461
velocity measurements, 463
Nitrided and chromium-plated gun barrels, performance, 465–470
accuracy-life, 465–466
advantage of choked muzzle, 466
appearance of "tippers", 468–469
gauge for indicating rejection point, 469–470
keyholing bullets, 466
projectile engraving, 465
star gauge curves, 467
velocity-life, 466–468
Nitrided and chromium-plated gun barrels, plating process, 413, 486–491
anodic etch prior to plating, 488
caliber .50 heavy barrels, 471
cleaning operations, 487
electroplating, 488
electropolishing, 488
gauging operations, 487–488
plating procedure, 486–487
with choked muzzles, 489–491
Nitrided gun liners, 353, 401–402
Nitrides in eroded guns
epsilon iron nitride, 249, 253, 255–256, 268
formation, 268, 272, 301–303
gamma-prime iron nitride, 255–256, 268
mechanical segregation, 255
Nitroaustenite, 268
see also Austenite in eroded guns
Nitrocellulose, thermal decomposition, 23–24
Nitrogen penetration into gun steel, 267–269, 300–304
austenite as solvent, 268
bore-surface temperatures, 303
comparison with surface reactions, 267
conditions for penetration, 268
cracking, 300
effect of ammonia, 301
formation of nitrides, 272, 301–303
formation of white layers, 269
iron-nitrogen system, 268
method of determining, 303
nitrogen content of reaction products, 304
Nitroglycerin
in gun powders, 327
thermal decomposition, 23–24

Obturation
see Gas leakage in guns
Obturator, hydraulic, 96
Occlusion of gases, 274–275
105-mm guns
antiaircraft, 124
heating rates, 118–119
105-mm howitzer, 566
155-mm guns, 128, 201, 210
Optical ejection indicator, 93
Origin erosion in gun bores, 198–203
asymmetry of erosion, 201
correlation with muzzle erosion, 207
definition, 195
dependence on caliber, 200
dependence on muzzle velocity, 200–201
development with firing, 199–200
effect on gun performance, 201–202
rate, 201
variation along the bore, 199
Oscillograph for ballistic measurements, 83–86
Oxygen, reaction with steel, 269–271
Oxygen compressor cylinders, molybdenum-plated, 432

Paints, temperature-indicating, 106–107
Palladium-gold alloy, thermochemical erosion resistance, 354–355
Parco-Lubrite for coating gun bores, 354
Parco-lubrized projectiles, 275, 599
Parco-lubrizing process, 533
PE projectiles
see Pre-engraved projectiles
Pebbling of gun bore surface, 215, 278–279, 319
Peerless A gun steel, 483
Pendulum, water ballistic, 184–185
Phenyl magnesium bromide, use in producing chromium carbonyl, 434–436
Photoelectric pyrometer
apparatus, 46–47
design principles, 46
3-in. gun measurements, 92, 94
Photography in ballistics
gas leakage, 274
high-speed cameras, 82–83, 93–94
muzzle flash, 82–83, 93–94
muzzle smoke, 82–83
projectile disruption of water, 181–183
projectile in flight, 83, 177–179
Piezoelectric crystal gauges, 96–97
Pilot plants for chromium-plating of gun barrels, 485–500
Chrome Gage Corporation, 492–499
Doehler-Jarvis Corporation, 485–492
recommendations, 499–500
Pilot plants for stellite-lined gun barrels, 451–453
Plaques for studying cracks in gun bores, 236
Plastics for sabot-projectiles, 562
Plating
see Chromium plate; Electroplated coatings; Vapor-phase plating
Plug gauges
erosion measurements, 198, 222, 309–310
indicating rejection point of gun barrels, 469–470
Potassium sulfate in eroded guns, 252
Potomac die-steel for machine gun barrels, 470, 483–484
Powder gas, 21–53
see also Gas
covolume, 36, 57
heat transfer to gun, 62, 99–102, 149
molecular constituents, 37
turbulence, 53, 266
Powder gas, chemical equilibrium, 28–35
carbon atoms, 33–35
CO/CO_2 ratio, 32–33
composition, 32–33
during burning, 24
quenching, 30–32
reactions during cooling, 22, 28–30
water gas reaction, 29, 32–33, 35
Powder gas, erosive effects, 272–277, 283–307
see also Erosion products in gun bores
apparatus for studying, 306–307
carbon gases, 284–296
cracking of bore surface, 274, 276–277
gas leakage, 273–274, 562, 592–594
gun liner joint, 274
individual powder gas constituents, 305–307
mitigation, 300, 307, 325–327
nitrogen, 300–304
occlusion of gases, 274–275
removal of material from bore, 272–273
scouring action, 273
sulfur gases, 271–272, 296–300

temperature and pressure, 274, 305–306
Powder gas, pressure, 36–37, 41
effect of pre-engraved projectiles, 594–596
effect on bore friction, 130
erosive effects, 274, 305–306
method of measuring, 80–81, 91–92
peak pressure, 22
quenching experiments, 31–32
resistance gauge for measuring, 91–92
starting time, 78
Powder gas, radiation, 42–53
absorption, 53
characteristics, 45
effect on burning rate, 27–28
effect on gun temperature, 99
peak radiation, 22
photoelectric pyrometer, 46–47, 92, 94
spectral characteristics, 43–45
starting time, 78
temperature determinations from radiation measurements, 42–43
Powder gas, temperature, 48–53
composition as a function of temperature, 37–38
determination from radiation measurements, 42-43
erosive effects, 251, 274, 305–306
firings in a jet propulsion motor, 51–52
firings in closed vessels, 48
firings in 3-in. gun, 48–51
measurement, 46–47, 80, 82, 92, 94
temperature gradient, 53
Powder gas, thermodynamics, 35–42
adiabatic flame temperature, 35, 38–39
change of internal energy with density, 37
energy released, 35–36
enthalpy and entropy, 40
equation of state, 36–38
heat of explosion, 36, 41–42
pressure, 36–37, 41
specific heats, 40
Powder metallurgy
chromium, 345
elkonite, 346
molybdenum compounds, 346, 370–371
Powders
see also Powder gas
adiabatic flame temperature, 38–39, 312, 324–325
characteristics of powders tested, 312
density of loading, 63, 69, 71
distribution of energy, 148–151
equation of burning, 58
explosives, 21
FNH-M1; 122, 250, 270
FNH-M2; 250, 270, 289
granulation, 73–74
impetus, 57, 73
parameters, 61
pyro powder, 323
RDX, 289, 322, 327
research recommendations, 327, 629–630
Powders, burning process
see Burning of powder
Powders, composition
changes in nitroglycerin content, 327
changes to mitigate erosion, 283, 300, 307, 325–327
effect on burning rate, 27
effect on gun erosion, 297, 299–300, 307, 326–327
ferrosilicons, 327
Powders, double-base, erosiveness
comparison with single-base, 308, 326
electron diffraction examinations of eroded specimens, 249
erosion products, 248–251, 267
FNH-M2 powder, 250, 270, 289
liquefaction of bore surface, 266
thermodynamic considerations, 250–251, 326
X-ray examination of eroded specimens, 248–251, 310
Powders, erosiveness, 288–289, 308–327
black powder, 297, 299
caliber .50 tests, 309–310, 313–322
dependence on gas temperature, 251
dimensional erosion rate vs flame temperature and heat input, 324–325
effect of composition, 251
erosion rate, 324
erosion vent plug tests, 310–311, 322–323
heat input versus flame temperature, 325
mitigation, 283, 300, 307, 325–327
pre-engraved projectiles, 600
RDX powders, 322, 327
thermal transformation vs. flame temperature, 325
types of powder tested, 311–313
Powders, single-base, erosiveness
carbon penetration into gun steel, 288
comparison with double-base, 308, 326
electron diffraction examination of eroded specimens, 249
erosion products, 247–251, 267
FNH-M1 powder, 250, 270
liquefaction of bore surface, 266
outer white layer, 247
thermodynamic considerations, 250–251, 326
X-ray examination of eroded specimens, 248–251, 310
Pre-engraved projectiles, 523–533, 591–608
accuracy, 597
band material, 598–600
bore friction, 145–147
cadmium-plated, 599
design, 14, 523–525
double engraving, 595
effect on powder gas pressure, 594–596
erosion, 313–317, 595, 600–603, 606
exterior ballistics, 528–532
interior ballistics, 525–527
manufacturing techniques, 529, 533
parco-lubrized, 275, 599
powders for, 600
research recommendations, 630
yaw, 526–527
Pre-engraved projectiles, guns for firing, 591–608
.50 caliber, 592, 598–599, 601
37-mm gun, T 47; 603–606
90-mm gun, 606–608
chromium-plated bores, 600–603
Pre-engraved projectiles, loading and indexing mechanism, 551–556
Browning caliber .50 machine gun, 551–552
Johnson 20-mm automatic aircraft guns, 552–553
modification of guns, 551–552
modified Bofors 40-mm mechanism, 553, 555–556
Pre-engraved projectiles, tests, 591–600
effect of band material, 598–600
effect of gas leakage on erosion of gun steel, 592–594
effect of type of powder, 600
effect on accuracy, 597
erosion studies, 313–317
methods of testing and measurement, 591–592
pressure and velocity, 594–596
T47 gun, 603–606
Pressure in guns
effect of gas leakage, 202
effect of temperature, 122–123
effect on burning rate of powder, 35
gauges for measurement, 91–92
in recoil cylinders, 82
in water penetrated by a projectile, 184–187
powder gas, 31–32, 80–81, 91–92, 305–306
pre-engraved projectiles, 594–596
pressure-time curves, 81, 136–137, 145

pressure-travel curves, 63–65, 68, 138–139, 607
rotating gun-bands, 129–130, 152–162, 521–523
Probert system of gun rifling and projectile banding, 517
Progressive stress-damage, 260, 279
Projectile bands, rotating
37-mm, 534–535
75-mm, 535–536
caliber .50 projectiles, 533–534
design, 533–536
effect of cadmium plating, 535
engraving, 158–159
erosion tests, 534
low-stress types, 533–536
melting, 100, 130, 135, 484
pre-engraving; *see* Pre-engraved projectiles
shearing, 202
Projectile engraving
see also Pre-engraved projectiles
bore friction, 129–130
effect of Fisa protector, 611
force required, 129, 533–534
heat, 99–100, 318–319
indication of stability, 465
process, 158–159
relation to erosion, 275
relation to powder pressure, 594
stresses, 275
Projectiles
see also Hypervelocity projectiles
abrasive action, 275, 591
acceleration, 79, 133–134
center of pressure, 173
characteristics, 176–179
comparison of standard and hypervelocity, 163
deceleration, 79
design, 518–536
energy; *see* Energy of projectiles
erosive effects, 275–276
finned, 169
head shapes, 176
jump ratio, 526
normal force, 174
parco-lubrized, 275, 599
research recommendations, 630
rotating bands; *see* Projectile bands, rotating
shatter, 189–191
stability, 169–170, 176–177, 515, 559–560
trajectory, 63, 78–79, 83, 130, 133, 177–179
velocity, 91, 515, 594–596, 619–624
yaw; *see* Yaw of projectiles
Projectiles, stresses, 518–523
axial stress, 523
band pressure, 521–522
British method of investigation, 522, 536
criterion of failure of a shell, 522–523
detection of defects, 536–537
external forces, 519
formulas for shell design, 521-522
high-explosive, 519
hoop stress, 152,523
limitations of theory, 520–521
longitudinal stress, 153, 524–525
method of calculating, 523
Mises-Hencky theory, 522
shear, 522
skirted projectiles, 573–575
stresses in base and walls, 520
tangential stress, 515, 523
types, 519–520
yield strength, 523
Projectiles, types
armor-piercing, 9–10, 189–192, 557–558, 585–590, 626-628
artillery-type for erosion-testing gun, 313, 315–316, 595
cadmium-plated, 354, 535, 599
conical-headed, 175–177
deformable, 169, 191
nondeformable, 191–192
pre-engraved, 313–317, 523–533, 551–556, 591–608
sabot, 169–170, 557–568, 585–587
skirted, 569–590, 620
spin-stabilized, 510, 515
subcaliber, 165–170, 618–628
tungsten carbide-cored; *see* Tungsten carbide-cored projectiles
Propellants
see Powders
Protractor for differentiating curves, 94–95
Pulsers, electronic, 86
Pump plating of gun barrels, 414
Pyro powder, erosiveness of, 323
Pyrolitic plating, 418–439
see also Electroplated coatings
carbonyl chemistry, 419–420
chromium, 434–439
molybdenum, 420–433
refractory metals, 418
tungsten, 433–434
Pyrometer, photoelectric
apparatus, 46–47
design principles, 46
radiation pyrometer, 92,94
Pyrrhotite in eroded guns, 254

Radial stress from projectile bands, 152
Radial-deflection scanner, 156–157
Radiation
effect on burning rate of powders, 27–28
effect on cooling of guns, 126
effect on heating of guns, 99
from powder gas; *see* Powder gas, radiation
Radiation pyrometer, 46–47, 92, 94
Radioactive carbon, 33–35, 285
Radioactive sulfur, experiments on erosion in guns, 296
Radioactive tracers, gun erosion studies, 240–243
demonstration of equilibrium,240-241
Geiger-Mueller counters, 242
sampling, 241–242
temperature of specimen, 242–243
Range of hypervelocity projectiles, 9, 164–165, 202
R.D. system of gun rifling and projectile banding, 517
RDX powder
erosiveness, 322, 327
reaction products, 289
Recoil of gun
see Gun recoil measurements
Recoilmeters, 80, 86–87
Recommendations for future research
see Research recommendations
Recording apparatus for ballistic measurements, 83–86
oscillograph and recorder, 83–85
oscillograph calibrators, 85–86
pulsers, 86
timing and developing of film, 86
Refractaloy No. 70
gun liners, 351–352
thermochemical erosion resistance, 407
Research recommendations
bore friction, 629
drag coefficient, 176–177
electroplated coatings, 417–418
erosion in guns, 629
gun liners, 368–369, 484, 629
gun propellants, 629–630
gun steel, 418, 482, 630
hypervelocity guns, 628–630
interior ballistics of guns, 628–629
Johnson 20-mm gun, 548–549
molybdenum carbonyl, 424
pilot plants for chromium-plating of gun barrels, 499–500
pre-engraved projectiles, 630
sabot-projectiles, 630
stability of projectiles, 176–177
tapered-bore gun and skirted projectiles, 590
vapor-phase plating, 432–433, 439
water penetration by hypervelocity projectiles, 187

yaw of hypervelocity projectiles, 177
Resistance gauge for powder-pressure measurements, 91–92
Reynold's number, pre-engraved projectiles, 529
Rhodium, thermochemical erosion resistance, 355
Rifling of guns, 515–517
  draw rifling, 504
  modification for Fisa protector, 611
  pre-engraved projectiles, 551–556
  Probert system, 517
  R.D. system, 517
  requirements of hypervelocity guns, 515–516
  strength factors, 516–517
  swaging, 216–217, 275–276, 458–459, 504
  torque on rifling, 516
Rocket nozzles, molybdenum-plated, 431
Rotating projectile band
  see Projectile bands, rotating
Rupture disks in erosion vent plugs, 225, 228, 310

Sabot-projectiles, 557–568
  ballistic limits, 585–587
  characteristics, 567
  comparison with skirted projectiles, 586, 620
  conditions for optimum armor penetration, 170
  description, 557
  evaluation, 557–559
  interior ballistics, 75
  plastic, 562
  requirements, 557
  research recommendations, 568, 630
  stability, 169–170, 559–560
  time of flight, 165
Sabot-projectiles, design, 15, 559–562
  materials, 562
  obturation, 562
  requirements, 559
  stability, 559–560
Sabot-projectiles, release methods, 560–562
  axial release, 561, 565–567
  centrifugal release, 560–561, 563–565
  combined axial and centrifugal release, 561–562, 564, 568
  gas pressure, 561
Sabot-projectiles, sizes, 562–567
  20-mm gun, 562–563
  75-mm gun and howitzer, 563–564
  76-mm gun, 564–565
  90-mm gun, 564–567
  105-mm howitzer, 566
St. Venant maximum strain theory, 510
Savage Arms Corporation, insertion of gun liners, 504
Scanner, radial-deflection, 156–157
Scoring by powder gas, 274
75-mm guns
  band pressure measurements, 156–159
  projectile design, 535–536
  sabot-projectiles, 563–564
76-mm guns, 122, 214, 564–565
Shear-energy theory, 510
Sheffield Precisionaire gauge, 487
Shell stresses
  see Projectiles, stresses
Shock waves, 83
  conical, 171
  in water penetrated by a bullet, 181–183, 187–188
  pressure as function of bullet velocity, 186
  suppression, 576–578
Silichrome gun steel, 337, 352–353, 483
Silicon steel for gun liners, 353
Silver, thermochemical erosion resistance, 354
Single-base powders
  see Powders, single-base, erosiveness
Skirted projectiles, 569–590
  advantages over sabot-type, 586, 620
  armor penetration tests, 585–590
  deformation, 573
  design, 572–573
  research recommendations, 590
  stresses, 573–575
  tungsten carbide core, 572
  use in 57/40-mm gun, 570–572, 584–590
  velocity limits, 576
Skirted projectiles, tests, 579–585
  accuracy tests, 584–585
  cores, 583
  flight characteristics, 581–583
  front skirts, 581
  material, 581
  rear skirts, 580
  skirt position, 581
  windshield, 581, 583
Sleeves for gun barrels, reinforcing, 476–477
  see also Fisa protector for gun barrels
Solenoids for determining projectile velocity, 91
Specifications
  chromium-plated machine gun barrels, 413, 460
  Johnson 20-mm gun, 538–539
  nitrided machine gun barrels, 459–460
  stellite-lined gun barrels, 413
Spectral characteristics of powder gas, 43–45
Sphalerite in eroded guns, 253
Spin-stabilized projectiles, 515
SR-4 strain gauge, 90
Stability of projectiles
  see also Subcaliber projectiles, stability
  deformable projectiles, 169
  effect of yaw, 168
  effect on muzzle erosion, 12
  recommendations for future research, 176–177
  sabot-projectile, 169–170, 559–560
  spin-stabilized, 515
Star gauges, 196–198
  curves, 196–197, 467
  erosion tests, 222
  two- and three-point gauges, 197
Stave-type gun liners
  see Molybdenum gun liners, stave-type
Steel, diffusion of elements through, 267–272, 284–296
  carbon, 264, 267–271, 284–296
  hydrogen, 274–275, 296
  nitrogen, 264, 267–269, 272, 300–304
  oxygen, 269–271
  sulfur, 296–300
Steel, effect of powder gas
  see Powder gas, erosive effects
Steel for gun barrels, 418, 480–484
  Chro-mow, 483
  critical temperature, 262–263
  Exelloy, 484
  HIA grade 160; 483
  isothermal transformation diagram, 275
  microstructural constituents, 265
  molybdenum steels, 353, 381–382, 482
  nickel and cobalt steels, 352
  nitralloy, 476
  nitrided steel, 353, 401–402, 459–460
  Peerless A, 483
  physical properties, 275, 363, 373, 418
  Potomac die-steel, 470, 483–484
  research recommendations, 482, 630
  Silichrome, 337, 352, 483
  silicon, 353
  stainless, 351
  Temples, 482
  thermal expansion, 513
  Timken 1722A, 483
  TK hot die steel, 484
  tungsten steels, 352–353
  XB valve steel, 483–484
Steel for projectiles, 191, 557, 581
Steel gun liners, replaceable, 506–509
  design, 14, 507
  lined with stellite, 615
  90-mm liner, 507–509
  purpose, 506–507

Stellite, metallurgy and properties, 391–397, 401–404
availability, 396–397
carbon content, effect on structure, 394
chemical composition, 392–393, 402, 407
decarburization, 402
ductility, 392
hardness, 395, 401
heat treatment, effect on structure, 394, 402
hot working, 402
machinability, 396
mechanical properties, 396
melting ranges, 331, 348, 396
metallographic examination, 393–394
nitriding, 401
specific gravity and density, 395
strength at high temperatures, 395
thermal coefficients, 395–396
thermochemical resistance, 391
volume and dimensional stability, 394–395
work- and age-hardening, 394
working properties for forging and rolling, 395
X-ray examination, 394
Stellite gun liners, 351, 397–406, 443–457
coating methods, 397–398
design, 398–399, 404–405, 443–446, 503–509
erosion, 124, 348–349
for caliber .30 barrels, 454–456
for caliber .50 barrels, 404, 446–454, 473–484
for caliber .60 barrels, 456–457
for cannon, 405, 615–616
infusion and incasting, 398, 404
inmelting, 404
insertion, 403, 443–446, 503–508
integral chamber, 457
length, 403, 473, 475
liners in series, 404
manufacturing methods, 451–454
pilot plants, 451–453
plating of barrels; *see* Stellite-lined and chromium-plated gun barrels
salvage, 453
sprayed coatings, 399–401
steel barrels, special, 482–484
stresses in, 155, 513
thickness, 155, 403
torch deposition, 399
velocity-life, 473
Stellite-lined and chromium-plated gun barrels, 473–484
accuracy- and velocity-life, 473, 478
barrel steel, 480–484
caliber .30; 471–472
CGL firing schedule, 474–475
design, 477, 479, 484
effects of barrel weight, 477–480
external reinforcing sleeve, 476–477
performance, 403–404, 465–469, 473–478
plating procedure, 410–411, 414, 486–491, 495–499
specifications, 413, 459, 491
tests, 473, 475–476
Stereoscopic microscope, 236
Strain gauges for measuring projectile displacement, 90–91
Baldwin-Southwark gauge, 90
SR-4; 90
types of measurements, 82
Strain measurements
circumferential strain in gun barrel, 155–156
determination of bore friction, 132
firing tests, 82, 106
Strain-recording equipment, 161
Stress, erosive effects, 230, 277, 279, 510
Stress in gun barrels, 510–515
see also Band pressure of gun tubes
caliber .50; 162
circumferential, 155–156
compressive, 511, 513
design procedure for cannon tubes, 511–512
equations, 511
equivalent stress, 511
failure, 510–511
integrated stresses, 153
Lamé formula, 152, 511
land erosion, 510
liner stresses, 512–515
longitudinal, 153, 524–525
Mises-Hencky theory, 510
progressive stress-damage, 279
radial stress, 152
St. Venant theory, 510
shrunk-in liners, 512
stave-type liner, 515
stress distribution in a thick-wall tube, 511
tangential, 152, 511
tensile, 511
thermal stress, 154–156, 277, 279, 513–514
Stress in projectiles
see Projectiles, stresses
Stress measurements of projectile bands
see Band pressure of gun tubes
Stress raisers in guns, 279
Stressed erosion-vent apparatus, 230, 272–275
Subcaliber projectiles, 618–628
see also Sabot-projectiles; Skirted projectiles
armor penetration, 192, 626–628
ballistic coefficient, 165
effectiveness of fire, 624–626
flight characteristics, 165
interior ballistics, 75
military economics, 618–619
pros and cons of subcaliber projectiles, 619–620
tungsten carbide cores, 165, 572, 583, 585–587, 620
velocity gains 619–624
Subcaliber projectiles, stability, 165–170
deformable projectiles, 169
effect of yaw, 168
formula, 168
methods of obtaining stability, 168–169
moment coefficient, 167
over long arcs of the trajectory, 167
projectile fired from a plane, 168
sabot-projectiles, 169–170, 559–560
theory, 165-166
Subcaliber projectiles, velocity gains, 619–624
effect of gun caliber, 622
effect of range, 622–624
limiting effect of powder gas kinetic energy, 620–622
Sulfides
copper and zinc, 252–253
hydrogen, 271–272, 292–294, 296, 427
identification in eroded guns, 240, 252–253, 298–299
Sulfur
compounds, 252–253, 299
effect on erosion, 240–241, 252, 296, 299
penetration into steel, 299
radioactive, 296
reaction with carbon monoxide, 291–293
reaction with gun steel, 296–300
Sulfur prints, 298–299
Supersonic cone, motion of, 170–179
Swaging of rifling, 216–217, 275–276, 458–459, 504

Tangential resistance in gun tubes, 511
Tangential stress
projectiles, 523
stave-type liners, 515
Tantalum
electrodeposition from fused salt baths, 409
gun liners, 347
Tapered-bore guns, 569–590
adaptors, 571, 575–576, 579–580

design, 15, 575–576
57/40-mm, 570–572, 580, 584–590
interior ballistics, 75
suggestions for future development, 590
tests, 578–580
venting, 576–578
wear of gun, 579–580
Target patterns, moving, 448–449
Temperature, effect on gun performance
see Gun firing, thermal effects
Temperature-indicating paints, 106–107
Temperature-time curves for machine gun barrels, 116–117, 461
Templex gun steel, advantages, 482
Terminal ballistics of hypervelocity projectiles, 180–192
armor perforation, 189–192
disruption of a liquid by projectile, 180–189
TEW steel alloy
gun liners, 352
resistance to surface cracking, 335
thermochemical erosion resistance, 407
Thermal alteration of bore surface
see Bore surface, thermal transformation
Thermal analyzer, 107
Thermal effects of gun firing
see Gun firing, thermal effects
Thermal shock, factor in gun erosion, 261, 277
Thermal softening of gun bores, 261–263
development of martensite, 263
heating process, 261–262
mushrooming, 263
single-shot guns, 261–262
Thermal stresses in gun barrels, 154–156
circumferential strain at outer surface, 155–156
cracking of bore surface, 277, 279
liner insertion, 513-514
stresses at a point, 154–155
Thermindex paint E6; 107
Thermochemical erosion resistance of metals and alloys, 343–355
aluminum, 354
beryllium, 354
chromium-base alloys, 406–407
cobalt, 347–348
columbium, 354
gold-palladium, 354–355
hastelloys, 407
iridium, 355
iron-base alloys, 406–407
nickel-base alloys, 406–407
Refractaloy No. 70; 407
rhodium, 355
silver, 354
stellite No. 6; 391–392
stellite No. 21; 391
TEW steel alloy, 407
titanium, 354
zinc, 354
Thermocouples for measuring gun temperature, 105–106, 113
Thermodynamics of powder gas
see Powder gas, thermodynamics
37-mm gun, T47
ballistic firings, 78
bore friction measurements, 144–148
burning-rate constants for powders, 27
design, 603–605
energy distribution of gun powder, 151
erosion test with pre-engraved projectiles, 606
heat input to bore surface, 101
pressure-time curves, 145
37-mm guns
design of projectiles, 534–535
tests with Fisa protector, 614
37-mm guns, band pressure measurements, 156–159, 161–162
apparatus and method, 156–157
band pressure per inch circumference, 157
effective area of interference (EAI), 157
friction coefficient, 157
prediction of band pressures, 157
pressure-time curves, 145
process of engraving, 158–159
radial deformation, 156
Thorium oxide refractories for melting molybdenum, 387
Thread-collocating gauge for machining gun tubes, 578
3-in. gun
antiaircraft, 124
bore friction measurements, 135-144
energy balance during firing, 149-151
liners, 249, 616–617
Mark 3; 77–78, 101
powder gas temperature measurements, 48–51
pressure and friction curves, 131
pressure-time curves, 81, 136–137
pressure-travel curves, 68, 138–139
70 caliber, 119–120
3-in. gun, band pressure measurements, 159–161
axial strain, 154
graphical determination, 160–161
tangential strain, 153
3.7-in. gun, 119, 121, 249
Ti-Kovar (alloy) for gun tube sleeves, 514
Timing-pulse generator, 86
Timken 1722A gun steel, performance, 483
Titanium, thermochemical erosion resistance, 354
TK hot die steel, 484
Tracer isotopes, gun erosion studies, 240–243
demonstration of equilibrium, 240–241
Geiger-Mueller counters, 242
sampling, 241–242
temperature of specimen, 242–243
Tracer photography, 83, 177–179
Trajectory of projectiles, determination from photography, 83, 177–179
Transformation of surface layers
see Bore surface, thermal transformation
Trivalent chromium, 412
Troostite band in gun bore surfaces, 247
Tube stresses
see Stress in gun barrels
Tungsten
alloys, 376, 417, 434
carbonyl, 433
chloride, 433
gun liners, 346–347, 352–353
vapor-phase plating, 433–434
Tungsten carbide-cored projectiles
armor perforation, 190, 192, 628
skirted projectiles, 572
strength, 583
subcaliber projectiles, 165, 620, 628
Tungsten Electrodeposit Corporation, tungsten alloy deposition, 417
Turbulent flow, 53, 266, 273, 613
20-mm guns
Hispano-Suiza, AN-M2; 118, 121, 123, 133
Johnson, 538-549
projectiles, 171, 562–563

University of California, thermal analyzer, 107

Vapor-phase plating, 418–439
see also Electroplated coatings
carbonyl chemistry, 419–420
chromium, 434–439
molybdenum, 420–433
refractory metals, 418
research recommendations, 432–433, 439
tungsten, 433–434
Velocimeters, 86–90
differentiators for, 89–90
linear, 89

measurement of gun velocity in recoil, 80, 88–89
rotary, 88–89
Velocity, muzzle
see Muzzle velocity
Velocity measurements on gun barrels
see also Velocity-life of caliber .50 gun barrels
effect of chromium-plated bores, 458, 463, 469, 602–603
gun in recoil, 80
velocity-drop, 202, 508, 595–596
Velocity of projectiles
effect on armor perforation, 192
means of increasing, 66, 549–550, 619–620
pre-engraved projectiles, 594–596
solenoids for determining, 91
spin-stabilized, 515
subcaliber, 619–624
Velocity-life of caliber .50 gun barrels
chromium-plated, 458, 466–468, 473, 478
stellite-lined, 450–451, 473, 478
Vent plugs, erosion
see Erosion vent-plug tests
Vinylite coatings for studying eroded gun bore surfaces, 236

Water ballistic pendulum, 184–185
Water gas reaction, 29, 32–33, 35, 269–271
Water-cooled guns
cook-off tests, 121
disadvantages, 127
water jackets, 127
Weapons, gas-operated
see Johnson 20-mm gun
White layer on eroded gun bores
austenite, 247, 264
carbon, 269
removal technique, 256
single-base powders, 247
Windshields for projectiles, 583
Wire-in-bore technique of interior ballistic measurements, 95–96
Wüstite in eroded gun, 249, 253

XB valve steel for gun barrels, 483–484
X-ray diffraction in gun erosion studies, 237–239, 248–251
bore surfaces, 248–249
carbon monoxide reactions, 291
comparison with electron diffraction, 237
erosion-testing gun barrels, 251, 310, 321
fired metal particles, 249–250
identification of reaction products, 247–249, 291, 301
Stellite No. 21; 394
test blocks exposed to powder gases, 249
unidentified lines, 239, 254
use of different wavelengths, 238
vent plugs, 228, 230

Yaw of projectiles
effect of muzzle erosion, 211
effect on drag coefficient, 175–176
effect on hypervelocity projectiles, 170–175
effect on stability, 168, 463
pre-engraved, 526–527
research recommendations, 177
within gun bore, 526–527

Zinc, thermochemical erosion resistance, 354
Zinc sulfides (gun erosion product), 252
Zirconium, deoxidizer for chromium, 359–360
Zirconium-nickel gun liners, 350